NISTIR XXXX Draft

Face Recognition Technology Evaluation (FRTE)

Part 1: Verification

Patrick Grother
Mei Ngan
Kayee Hanaoka
Joyce C. Yang
Austin Hom

Information Access Division
Information Technology Laboratory

This publication is available free of charge from:
https://www.nist.gov/programs-projects/face-recognition-vendor-test-frvt-ongoing

2024/03/27

ACKNOWLEDGMENTS

The authors are grateful for the long-standing support and collaboration of the the Department of Homeland Security's Science & Technology Directorate (S&T) and the Office of Biometric Identity Management (OBIM).

Additionally, the authors are grateful to staff in the NIST Biometrics Research Laboratory for infrastructure supporting rapid evaluation of algorithms.

DISCLAIMER

Specific hardware and software products identified in this report were used in order to perform the evaluations described in this document. In no case does identification of any commercial product, trade name, or vendor, imply recommendation or endorsement by the National Institute of Standards and Technology, nor does it imply that the products and equipment identified are necessarily the best available for the purpose.

INSTITUTIONAL REVIEW BOARD

The National Institute of Standards and Technology's Research Protections Office reviewed the protocol for this project and determined it is not human subjects research as defined in Department of Commerce Regulations, 15 CFR 27, also known as the Common Rule for the Protection of Human Subjects (45 CFR 46, Subpart A).

FNMR(T) "False non-match rate"
FMR(T) "False match rate"

FRTE STATUS

This report is a draft NIST Interagency Report, and is open for comment. It is the thirty sixth edition of the report since the first was published in June 2017. Prior editions of this report are maintained on the FRTE website, and may contain useful information about older algorithms and datasets no longer used in FRTE.

FRTE remains open: All tracks of the FRTE are open to new algorithm submissions.

2024-03-26 changes since 2024-02-21:

- We have added results for first algorithms from six developers: FaceLocate, FPT Education, FPT Information System, Kogniza Technology, i2v Systems, and Seamfix.
- We have added results for new algorithms from eleven returning developers: AFR Engine, Aware, Beijing Hisign Technology, Cu-Face, Dactionable Technologies, First Credit Bureau Kazakhstan, Innovatrics, Nominder, Securif AI, Veridium, and Viettel Cyberspace Center.
- We have retired results for nine algorithms per our policy to only list results for two algorithms per developer. Results for retired algorithms appear in prior versions of this report in the archive.

2024-02-21 changes since 2024-01-22:

- We discontinued the visa-visa benchmark in FRTE since Feburary 14th 2024. For highly performing algorithms, the only remaining false negative error in that set were in babies and in a few greyscale poor quality half-tone scans of paper photos.
- We have added results for first algorithms from four developers: Online Mobile Services JSC, Openedge Technologies, TNI Technoology, and Yoti.
- We have added results for new algorithms from nine returning developers: CMC Institute of Science and Technology, City and County of Honolulu, Dermalog, Euronovate SA, Maxvision Technology, Megvii/Face++, Neurotechnology, Toshiba, useB, and Universidade de Coimbra.
- We have retired results for nine algorithms per our policy to only list results for two algorithms per developer. Results for retired algorithms appear in prior versions of this report in the archive.

2024-01-22 changes since 2023-12-15:

- We have added results for first algorithms from six developer: GPS Vietnam Trading, iCOMM Media & Tech, PAPIL11 S.R.O., QazSmartVision.AI, Sparsh CCTV, and VNIS Joint Stock.
- We have added results for new algorithms from eight returning developers: Cyberlink Corp, Intellivision, Hangzhuo AIlu Network Information Technology, Lebentech Biometrics, Momentum Digital, Regular Biometrics Solutions, ROC, and Via Technologies Inc.
- We have retired results for six algorithms per our policy to only list results for two algorithms per developer. Results for retired algorithms appear in prior versions of this report in the archive.

2023-12-15 changes since 2023-11-21:

- We have added results for first algorithms from five developer: CMC University, Element System Solutions Company, Fraud.com, Techainer, and Vietnam Payment Solutions.

FNMR(T) "False non-match rate"
FMR(T) "False match rate"

- ▷ We have added results for new algorithms from thirteen returning developers: Accurascan, Adera Global, Alchera, Aware, Clearview AI, Cognitec Systems, Incode Technologies Inc, Inspur (Beijing) Electronic Information, IntelliVIX, ioNetworks, NHN Corp, PT Autentika Digital Indonesia, and Qnap Security.
- ▷ We have retired results for twelve algorithms per our policy to only list results for two algorithms per developer. Results for retired algorithms appear in prior versions of this report in the archive.

2023-11-21 changes since 2023-10-27:

- ▷ We have added results for new algorithms from ten returning developers: Coretech Knowledge Inc, Beijing DeepSense Technologies, General Interface Solutions Holding Ltd, Glory, Kakao Brain, Nominder, Smarvist Teknoloji, STCON LLC, Suprema AI Inc, and Yuan High-Tech Development
- ▷ We have retired results for eight algorithms per our policy to only list results for two algorithms per developer. Results for retired algorithms appear in prior versions of this report in the archive.

2023-10-27 changes since 2023-09-29:

- ▷ We have added results for first algorithms from two developer: Authme and Dactionable Technologies.
- ▷ We have added results for new algorithms from twelve returning developers: Intel Research Group, Guangzhou Pixel Solutions, Kasikorn Labs, Kakao Bank, Luxand, Megvii/Face++, Panasonic R+D Center Singapore, Private Identity LLC, Recognito, Seventh Sense Artificial Intelligence, UNICC-Solution Architecture Section, and Universidade de Coimbra.
- ▷ We have retired results for eight algorithms per our policy to only list results for two algorithms per developer. Results for retired algorithms appear in prior versions of this report in the archive.

2023-09-29 changes since 2023-09-09:

- ▷ We have added results for first algorithms from one developer: Intozi Tech.
- ▷ We have added results for new algorithms from seven returning developers: Euronovate, Maxvision Technology, Miaxis Biometrics, Mukh Technologies, Toshiba, University of Surrey-CVSSP, and useB.
- ▷ We have retired results for six algorithms per our policy to only list results for two algorithms per developer. Results for retired algorithms appear in prior versions of this report in the archive.

2023-09-09 changes since 2023-08-16:

- ▷ We have renamed and split FRVT into two sets of technology evaluations: The Face Recognition Technology Evaluation (FRTE) is the umbrella for the ongoing 1:1, 1:N and twins disambiguation tracks; the Face Analysis Technology Evaluation (FATE) holds the morph and attacked detection tracks, the quality assessment tracks, and the new age estimation tracks.
- ▷ We have added results for first algorithms from two developers: Facehawk and Regular Biometrics Solutions.
- ▷ We have added results for new algorithms from eight returning developers: CMC Institute of Science and Technology, Canon, Cu-Face, EI Networks, ICM Airport Technics, Securif AI, Securifai, Vietnam Posts and Telecommunications Group, and Vision Intelligence Center of Meituan

FNMR(T) "False non-match rate"
FMR(T) "False match rate"

- We have retired results for six algorithms per our policy to only list results for two algorithms per developer. Results for retired algorithms appear in prior versions of this report in the archive.

2023-08-16 changes since 2023-07-21:

- We have added results for first algorithms from one developers: Facia.ai.
- We have added results for new algorithms from fifteen returning developers: Accurascan, Alchera, FOO, Hangzhuo AIlu Network Information Technology, HyperVerge, ioNetworks, Innovatrics, Nominder, Rank One Computing, Neurotechnology, Tech5, Tripleize, Unissey, UX Labs, and Verigram.
- We have retired results for ten algorithms per our policy to only list results for two algorithms per developer. Results for retired algorithms appear in prior versions of this report in the archive.

2023-07-21 changes since 2023-06-16:

- We have added results for first algorithms from five developers: DeCloak Intellegences, Innominds Software SEZ India, Trust Stamp, Vcortex Labs, and Viettel Cyberspace Center
- We have added results for new algorithms from fourteen returning developers: AFR Engine, Alice Biometrics, Euronovate SA, IMDS Software, Idemia, IntelliVIX, Intellivision, NHN, Pangiam, STCON, Samtech InfoNet, Veridium, VinBigData, and Vision-Box
- We have retired results for eleven algorithms per our policy to only list results for two algorithms per developer. Results for retired algorithms appear in prior versions of this report in the archive.
- We have stopped using wild images in FRVT since May 1st 2023. All results for that set have been removed from the website, and will be removed from future PDF reports.

2023-06-16 changes since 2023-04-20:

- We have added results for first algorithms from seven developers: EI Networks Private Ltd, General Interface Solutions Holding Ltd, Recognito, Serendipity Ltd, ST Engineering, and useB.
- We have added results for new algorithms from eighteen returning developers: Advance.AI, AYF Technology, Cyberlink Corp, Incode Technologies Inc, Intel Research Group, Intellibrain Technological Projects, Maxvision Technology, Megvii/Face++, Omnigarde Ltd, Paravision, Qnap Security, Seventh Sense Artificial Intelligence, Shanghai Jiao Tong University, Veridas Digital Authentication Solutions S.L., Universidade de Coimbra, Yuan High-Tech Development, UNICC-Solution Architecture Section, and Verihubs,verihubs-inteligensia.
- We have retired results for 15 algorithms per our policy to only list results for two algorithms per developer. Results for retired algorithms appear in prior versions of this report in the archive.

2023-04-20 changes since 2023-04-04:

- We have added results for first algorithms from one developers: IDENTY.
- We have added results for new algorithms from three returning developers: Metsakuur, Autentika Digital Indonesia, and Verigram.
- FRVT will re-open 2023-05-01.
- We have retired results for 3 algorithms per our policy to only list results for two algorithms per developer. Results for retired algorithms appear in prior versions of this report in the archive.

2023-04-04 changes since 2023-03-09:

- ▷ We have added results for first algorithms from six developers: Aratek Biometrics City and County of Honolulu, FOO, Intelligent Control Technology NCS, and Swsam Solutions.
- ▷ We have added results for new algorithms from nine returning developers: Cubox, Glory, InsightFace AI, Miaxis Biometrics, Mukh Technologies, Turkcell Technology, Samsung S1, Via Technologies, and Vision Intelligence Center of Meituan
- ▷ We have retired results for 7 algorithms per our policy to only list results for two algorithms per developer. Results for retired algorithms appear in prior versions of this report in the archive.

2023-03-09 changes since 2023-02-01:

- ▷ We have added results for first algorithms from eight developers: Biometric LLC (biometric.vision) KZ, Candour Biometrics, Fast Enterprises, KakaoBank, Mitek Systems, Nominder, Private Identity, and UNICC-Solution Architecture Section.
- ▷ We have added results for new algorithms from 22 returning developers: AFR Engine, Biocube Matrics, CMC Institute of Science and Technology, Cloudwalk - Moontime Smart Technology, Cyberlink Corp, Beijing DeepSense Technologies, First Credit Bureau Kazakhstan, Enface, Hangzhuo AIlu Network Information Technology, Herta Security, IMDS Software, Inspur (Beijing) Electronic Information Industry Co, Intellivision, MicroFocus, Neurotechnology, Pangiam, NSENSE Corp, STCON LLC, Touchless ID, University of Surrey-CVSSP, Vision-Box, and YooniK.
- ▷ We have retired results for 14 algorithms per our policy to only list results for two algorithms per developer. Results for retired algorithms appear in prior versions of this report in the archive.
- ▷ We have introduced new set of non-frontal portrait to border comparisons. The new images are described in section 2.3 and their use in seciton 3.2.

2023-02-01 changes since 2022-12-15:

- ▷ We have added results for first algorithms from four developers: CU-Face, Korea ID, Onfido, and TrueID-VNG.
- ▷ We have added results for new algorithms from 21 returning developers: Alchera, Armatura, Cogent-Thales, Dermalog, Didi ChuXing Global Face, Gorilla, Hyperverge, Innovatrics, Intel Research, IntelliVIX, Intema-LGL, Kasikorn Labs, Paravision, Rank One Computing, Sensetime Group, Suprema AI, Tech5, Unissey, U. Coimbra Visteam, Vixvizion (Imagus), and Yuan High-Tech Development.
- ▷ We have retired results for 20 algorithms per our policy to only list results for two algorithms per developer. Results for retired algorithms appear in prior versions of this report in the archive.
- ▷ We have introduced new set of non-frontal portrait to border comparisons. The new images are described in section 2.3 and their use in seciton 3.2.

2022-12-15 changes since 2022-11-06:

- ▷ We have added results for first algorithms from four developers: Miaxis Biometrics, PT Autentika Digital Indonesia, PT Qlue Performa Indonesia, and STCON.

FNMR(T) "False non-match rate"
FMR(T) "False match rate"

- ▷ We have added results for new algorithms from 14 returning developers: Adera Global, Aiseemu Technology, Chunghwa Telecom,chtface, FRP, Griaule, Line Corporation, Maxvision Technology, Mukh Technologies, Papilon Savunma, Qnap Security, Realnetworks, Securif AI, SQIsoft, and Veridium.
- ▷ We have retired results for 10 algorithms per our policy to only list results for two algorithms per developer. Results for retired algorithms appear in prior versions of this report in the archive.

2022-11-06 changes since 2022-09-26:

- ▷ We have added results for first algorithms from six developers: AFR Engine, CMC Institute of Science and Technology, Saga Densan Center, Turkcell Technology, UXLabs, and Wise AI SDN BHD.
- ▷ We have added results for new algorithms from 14 returning developers: Coretech Knowledge, Cloudwalk - Moontime, Cloudmatrix, Deepglint, Guangzhou Pixel Solutions, Hangzhuo AIlu Network Information Technology, NEO Systems, One More Security, Palit Microsystems, Panasonic R+D Center Singapore, Samsung S1, Seventh Sense Artificial Intelligence, Touchless ID, and Veridas Digital Authentication Solutions S.L.
- ▷ We have retired results for 10 algorithms per our policy to only list results for two algorithms per developer. Results for retired algorithms appear in prior versions of this report in the archive.

2022-09-26 changes since 2022-08-30:

- ▷ We have added results for first algorithms from three developers: Codeline, First Credit Bureau Kazakhstan, and InfoCert.
- ▷ We have added results for new algorithms from 14 returning developers: Advancegroup, Armatura LLC, Beijing Hisign Technology, Cybercore, Cyberlink Corp, Herta Security, ICM Airport Technics, InsightFace AI, Metsakuur, NSENSE Corp, Samsung-SDS, Videmo Intelligente Videoanalyse, Vietnam Posts and Telecommunications Group, and Vision Intelligence Center of Meituan.
- ▷ We have retired results for 11 algorithms per our policy to only list results for two algorithms per developer. Results for retired algorithms appear in prior versions of this report in the archive.

2022-08-30 changes since 2022-07-29:

- ▷ We have added results for first algorithms from two developers: Aximetria, Intellibrain Technological Projects
- ▷ We have added results for new algorithms from twelve returning developers: Alchera Inc, Dermalog, Idemia, Incode Technologies Inc, Intellivision, Kasikorn Labs, Megvii/Face++, Techsign, TuringTech.vip, Universidade de Coimbra, Verijelais, Vixvizon
- ▷ We have retired results for six algorithms per our policy to only list results for two algorithms per developer. Results for retired algorithms appear in prior versions of this report in the archive.

2022-07-29 changes since 2022-06-27:

- ▷ We have added results for first algorithms from seven developers: FRP LLC (Hawaii), IMDS Software, Inspur (Beijing) Electronic Information Industry, Intema - LGL Group, PAPAGO, Qaz Biometric Systems, and VIDA-Digital Identity

- We have added results for new algorithms from nine returning developers: Cyberextruder, Glory, Maxvision Technology, Rank One Computing, Securif AI, Suprema AI, Suprema ID, Toshiba, and Yuan High-Tech Development.
- We have retired results for nine algorithms per our policy to only list results for two algorithms per developer. Results for retired algorithms appear in prior versions of this report in the archive.

2022-07-29 changes since 2022-06-27:

- We have added results for first algorithms from seven developers: FRP LLC (Hawaii), IMDS Software, Inspur (Beijing) Electronic Information Industry, Intema - LGL Group, PAPAGO, Qaz Biometric Systems, and VIDA-Digital Identity
- We have added results for new algorithms from nine returning developers: Cyberextruder, Glory, Maxvision Technology, Rank One Computing, Securif AI, Suprema AI, Suprema ID, Toshiba, and Yuan High-Tech Development.
- We have retired results for nine algorithms per our policy to only list results for two algorithms per developer. Results for retired algorithms appear in prior versions of this report in the archive.

2022-06-27 changes since 2022-06-03:

- We have added results for first algorithms from two developers: Krungthai Bank, and Smartbiometrik.
- We have added results for new algorithms from thirteen returning developers: Aiseemu, Corsight, Digidata, Griaule, Guangzhou Pixel Solutions, Hangzhuo AI Network Information Technology, Neurotechnology, Real Networks, Samsung S1, Sensetime Group, Smart Engines, Verihubs Inteligensia, and VinBigData.
- We have retired results for eight algorithms per our policy to only list results for two algorithms per developer. Results for retired algorithms appear in prior versions of this report in the archive.

2022-06-03 changes since 2022-05-05:

- We have added results for first algorithms from seven developers: Jaak IT, Metsakuur, Palit Microsystems, Smarvist Teknoloji, and Touchless ID.
- We have added results for new algorithms from sixteen returning developers: Cyberlink, FaceOnLive, Kakao Enterprise, Line Corporation (Line Clova), Multi-Modality Intelligence, NEO Systems, and Unissey
- We have retired results for four algorithms per our policy to only list results for two algorithms per developer. Results for retired algorithms appear in prior versions of this report in the archive.
- We have moved the results for the twenty human-difficult pairs used in the May 2018 paper *Face recognition accuracy of forensic examiners, superrecognizers, and face recognition algorithms* by Phillips et al. [1]. to the algorithm-specific report cards (example: PDF).
- Likewise, we have added figures showing impostor distribution shifts across demographics to the report card.

2022-05-05 changes since 2022-03-18:

- ▷ We have added results for first algorithms from seven developers: Accurascan, DICIO, FacePhi, Pangiam, University of Surrey-CVSSP, and Veridium.
- ▷ We have added results for new algorithms from sixteen returning developers: ACI Software, Canon Inc, Cloudwalk - Moontime Smart Technology, Cybercore,

2022-05-05 changes since 2022-03-18:

- ▷ We have added results for first algorithms from seven developers: Accurascan, DICIO, FacePhi, Pangiam, University of Surrey-CVSSP, and Veridium.
- ▷ We have added results for new algorithms from sixteen returning developers: ACI Software, Canon Inc, Cloudwalk - Moontime Smart Technology, Cybercore, Cyberextruder, Gemalto Cogent, HyperVerge Inc, KuKe3D Technology, Megvii/Face++, Mobbeel Solutions, Panasonic R+D Center Singapore, Qnap Security, Samsung-SDS, Vietnam Posts and Telecommunications Group, Viettel Group, and Vision Intelligence Center of Meituan.
- ▷ We have retired results for 12 algorithms per our policy to only list results for two algorithms per developer. Results for retired algorithms appear in prior versions of this report in the archive.

2022-03-18 changes since 2022-02-23:

- ▷ We have added support for the detection of multiple people in a single image (see Section 1.2). Specifically the API allows an algorithm to extract features from one or more faces it detects in an image. NIST scores such cases as a correct match when any detected face matches the reference photo, and as a false positive when either face matches a non-mated reference photo. The expected effect of doing this will be to improve reported false non-match rates, and to minimally elevate false match rates. This technique was only applied to images of type "border" and "kiosk".
- ▷ We have added results for first algorithms from four developers: IntelliVIX, Kasikorn Labs, Lebentech Biometrics, and Wicket.
- ▷ We have added results for new algorithms from 10 returning developers: Chunghwa Telecom, Cloudmatrix, Beijing DeepSense Technologies, FarBar Inc, Imagus Technology Pty, Intellivision, Maxvision Technology, NHN Corp, Seventh Sense Artificial Intelligence, and Verigram.
- ▷ We have retired results for 4 algorithms per our policy to only list results for two algorithms per developer. Results for retired algorithms appear in prior versions of this report in the archive.

2022-02-23 changes since 2022-01-24:

- ▷ We have added results for first algorithms from four developers: AFIS and Biometrics Consulting, Digidata, Graymatics, Hangzhuo AIlu Network Information Technology, KnowUTech LLC, Sukshi Technology Innovation, T4iSB, and TuringTech.vip
- ▷ We have added results for new algorithms from 18 returning developers: Cognitec Systems GmbH, GeoVision Inc, Glory, Herta Security, Intel Research Group, InsightFace AI, Kakao Enterprise, N-Tech Lab, Omnigarde Ltd, Papilon Savunma, Paravision, Realnetworks Inc, Reveal Media Ltd, Shenzhen Inst Adv Integrated Tech CAS, Suprema AI Inc, Toshiba, Universidade de Coimbra, and Yuan High-Tech Development
- ▷ We have retired results for 14 algorithms per our policy to only list results for two algorithms per developer. Results for retired algorithms appear in prior versions of this report in the archive.

FNMR(T) "False non-match rate"
FMR(T) "False match rate"

2022-01-24 changes since 2022-01-20:

- ▷ We have added results for new algorithms from one returning developer: Vocord.

2022-01-20 changes since 2021-12-18:

- ▷ We have added results for first algorithms from four developers: Armatura, Beyne.AI, One More Security, and VinBigData
- ▷ We have added results for new algorithms from 19 returning developers: AuthenMetric, BOE Technology Group, Cybercore, Cyberlink, Dahua Technology, FaceTag Co, Innovatrics, Megvii, Mobbeel Solutions, Neurotechnology, Oz Forensics, Rank One Computing, Regula Forensics, Samsung S1, Securif AI, Sensetime Group, TigerIT Americas, Videmo Intelligente Videoanalyse, and YooniK.
- ▷ We have retired results for 14 algorithms per our policy to only list results for two algorithms per developer. Results for retired algorithms appear in prior versions of this report in the archive.

: **2021-12-16** changes since 2021-11-22:

- ▷ We have added results for first algorithms from five developers: Alfabeta, Cloudmatrix, Euronovate SA, FaceOnLive Inc, and Mobipin Technology.
- ▷ We have added results for new algorithms from ten returning developers: ACI Software, ITMO University, NEO Systems, Guangzhou Pixel Solutions, Panasonic R+D Center Singapore, Qnap Security, Scanovate, Tevian, Unissey, and Vietnam Posts and Telecommunications Group.
- ▷ We have retired results for eight algorithms per our policy to only list results for two algorithms per developer. Results for retired algorithms appear in prior versions of this report in the archive.
- ▷ We have revamped the figure showing performance on 20 pairs of open-source images. It now color-codes false negatives and postives against a default threshold value.

2021-11-22 changes since 2021-10-28:

- ▷ We have added results to the website for kiosk-collected images where the design and geometry configuration mean that many images have considerable downward pitch angle. In some images, the face is partially cropped. Some images have other background faces.
- ▷ We have stopped using child exploitation images in FRVT, as we lost access to the imagery. All results for that set have been removed from the website, and will be removed from future PDF reports.
- ▷ We have added results for first algorithms from seven new developers: CUDO Communication, Daon, KuKe3D Technology, Mantra Softech India, Maxvision Technology, Multi-Modality Intelligence, and Samsung-SDS.
- ▷ We have added results for new algorithms from seven returning developers: Acer Incorporated, Cloudwalk-Moontime Smart Technology, Gorilla Technology, ID3 Technology, Incode Technologies, NSENSE Corp., and SQIsoft.
- ▷ We have retired results for six algorithms per our policy to only list results for two algorithms per developer. Results for retired algorithms appear in prior versions of this report in the archive.

FNMR(T) "False non-match rate"
FMR(T) "False match rate"

2021-10-28 changes since 2021-09-08:

- ▷ We have substantially revised the algorithm-specific report cards that are linked from the FRVT results page. (Example: HTML).
- ▷ We have added results for first algorithms from eight new developers: Beijing Mendaxia Technology, Beijing Hisign Technology, Biocube Matrics, Clearview AI, Reveal Media, Toppan ID Gate, Verigram, and Viettel High Technology.
- ▷ We have added results for new algorithms from thirty returning developers: 20Face, 3divi, Canon Inc Chunghwa Telecom, Corsight, Decatur Industries, Deepglint, Dermalog, FaceTag, Fiberhome Telecommunication Technologies, GeoVision, ICM Airport Technics, Imagus Technology, InsightFace AI, Kakao Enterprise, Kookmin University, Line Corporation, N-Tech Lab, NotionTag Technologies, Realnetworks, Suprema ID, Taiwan-Certificate Authority, Toshiba, Tripleize, Trueface.ai, Veridas Digital Authentication, Visidon, VisionLabs, YooniK, and Yuan High-Tech Development.
- ▷ We have retired results for twenty algorithms per our policy to only list results for two algorithms per developer. Results for retired algorithms appear in prior versions of this report in the archive.

2021-09-08 changes since 2021-08-02:

- ▷ We have added results for first algorithms from seven new developers: Griaule, SQIsoft, Qnap Security, Techsign, Smart Engines, Verihubs, and Wuhan Tianyu Information Industry.
- ▷ We have added results for new algorithms from sixteen returning developers: ADVANCE.AI, AuthenMetric, CloudSmart Consulting, Code Everest Pvt, Cognitec Systems, Thales Gemalto Cogent, Intel Research Group, Omnigarde, Oz Forensics, Rank One Computing, Samsung S1 Corp, Securif AI, Tevian, TigerIT Americas, Universidade de Coimbra, and Vigilant Solutions
- ▷ We have retired results for eleven algorithms per our policy to only list results for two algorithms per developer. Results for retired algorithms appear in prior versions of this report in the archive.

2021-08-02 changes since 2021-06-25:

- ▷ We have added results for first algorithms from eight new developers: Bee the Data, Closeli Inc, Coretech Knowledge Inc, Deepsense (France), ioNetworks Inc, Kakao Pay Corp, Seventh Sense Artificial Intelligence, and SK Telecom.
- ▷ We have added results for new algorithms from fifteen returning developers: Alchera Inc, Adera Global PTE, Aware, Bresee Technology, Cyberlink Corp, Expasoft LLC, Fujitsu Research and Development Center, Gorilla Technology, Idemia, Neurotechnology, NEO Systems, NHN Corp, Paravision, Panasonic R+D Center Singapore, and Shenzhen University-Macau University of Science and Technology.
- ▷ We have retired results for twelve algorithms per our policy to only list results for two algorithms per developer. Results for retired algorithms appear in prior versions of this report in the archive.

2021-06-25 changes since 2021-05-21:

- ▷ We have added results for first algorithms from six new developers: Alice Biometrics, BOE Technology Group, Fincore, Neosecu, Sodec App, and Yuntu Data and Technology.

FNMR(T) "False non-match rate"
FMR(T) "False match rate"

- ▷ We have added results for new algorithms from seven returning developers: Incode Technologies, HyperVerge, Mobbeel Solutions, Guangzhou Pixel Solutions, Remark Holdings, Sensetime, and Vietnam Posts and Telecommunications Group.
- ▷ We have retired results for four algorithms per our policy to only list results for two algorithms per developer. Results for retired algorithms appear in prior versions of this report in the archive.

2021-05-21 changes since 2021-04-26:

- ▷ We have added results for first algorithms from five new developers: Ekin Smart City Technologies, Suprema ID, Tripleize, Taiwan-Certificate Authority, and Vision Intelligence Center of Meituan.
- ▷ We have added results for new algorithms from eight returning developers: ID3 Technology, Imagus Technology, Momentum Digital, N-Tech Lab, NSENSE, Shanghai Jiao Tong University, Vision-Box, and Yuan High-Tech Development
- ▷ We have retired results for seven algorithms per our policy to only list results for two algorithms per developer. Results for retired algorithms appear in prior versions of this report in the archive.

2021-04-26 changes since 2021-04-16:

- ▷ We have added results for first algorithms from three new developers: Quantasoft, Rendip, and NEO Systems.
- ▷ We have added results for new algorithms from four returning developers: 3Divi, Realnetworks, Veridas Digital Authentication Solutions, and Universidade de Coimbra.
- ▷ We have retired results for three algorithms per our policy to only list results for two algorithms per developer. Results for retired algorithms appear in prior versions of this report in the archive.

2021-04-16 changes since 2021-03-19:

- ▷ We have added results for first algorithms from six new developers: 20Face, Beijing DeepSense Technologies, BitCenter UK, Enface, FaceTag, InsightFace AI, Line Corporation, Lema Labs, Nanjing Kiwi Network Technology, Omnigarde, Regula Forensics, and Suprema.
- ▷ We have added results for new algorithms from ten returning developers: CloudSmart Consulting, Dermalog, GeoVision, Neurotechnology, Panasonic R+D Center Singapore, Samsung S1, Securif AI, Trueface.ai, Vigilant Solutions, and Visidon.
- ▷ We have retired results for ten algorithms per our policy to only list results for two algorithms per developer. Results for retired algorithms appear in prior versions of this report in the archive.

2021-03-19 changes since 2021-03-05:

- ▷ We have added results for first algorithms from six new developers: Ajou University, AuthenMetric, Code Everest, Corsight, Papilon Savunma, and NHN Corp
- ▷ We have added results for new algorithms from seven returning developers: Alchera, Deepglint, Fiberhome Telecommunication Technologies, Kakao Enterprise, Kookmin University, Megvii/Face++, and NotionTag Technologies.

FNMR(T) "False non-match rate"
FMR(T) "False match rate"

- We have updated many of the hyperlinked HTML report-cards to include seven figures on demographic dependence. Figures of this kind first appeared, and are documented in, the December 2019 document, NIST Interagency Report 8280 on demographic differentials in face recognition. The figures quantify false negative dependence on demographics using "visa-border" comparisons, and false positive dependence using comparisons of "application" photos that uniformly of quality and similar to visa photos.

2021-03-05 changes since 2021-01-19:

- We have added results for first algorithms from three new developers: IVA Cognitive, Mobbeel, and MoreDian Technology.
- We have added results for new algorithms from returning developers: Ability Enterprise - Andro Video, ACI Software, Adera Global, AnyVision, BioID Technologies, China Electronics Import-Export, Cognitec Systems, Fujitsu Research and Development Center, Glory, Guangzhou Pixel Solutions, Hengrui AI Technology, Incode Technologies, Intel Research, iQIYI, Mobai, Oz Forensics, Paravision, VisionLabs, and Xforward AI Technology.
- We have added a new "resources" tab to the main webpage. It includes sortable columns for data related to speed, model size, storage, and memory consumption.
- We have retired results for 13 algorithms per our policy to only list results for two algorithms per developer. Results for retired algorithms appear in prior versions of this report in the archive.

2021-01-19 changes since 2020-12-18:

- This report adds results for first algorithms from four developers: Herta Security, Irex AI, Shenzhen University-Macau University of Science and Technology, and Vietnam Posts and Telecommunications Group. See Table 9 for more information.
- The report also includes results for thirteen developers who have previously submitted algorithms: Bresee Technology, Canon (previously Canon Information Technology (Beijing)), Cyberlink, CSA IntelliCloud Technology, Dahua Technology, ID3 Technology, Imagus Technology (Vixvizion), Moontime Smart Technology, N-Tech Lab, Thales Cogent, Veridas Digital Authentication Solutions, Vocord, and Yuan High-Tech Development.
- We have retired results for ten algorithms per our policy to only list results for two algorithms per developer. Results for retired algorithms appear in prior versions of this report in the archive.

2020-12-18 changes since 2020-10-09:

- This report adds results for first algorithms from ten developers: BitCenter UK, CloudSmart Consulting, Cubox, Institute of Computing Technology, Naver Corp, Minivision, NSENSE Corp, Viettel Group, Visage Technologies, and Xiamen University. See Table 9 for more information.
- The report also includes results for eighteen developers who have previously submitted algorithms: ADVANCE.AI, Awidit Systems, Chosun University, Dermalog, GeoVision, ICM Airport Technics, Idemia, Institute of Information Technologies, Kakao Enterprise, Neurotechnology, Panasonic R+D Center Singapore, Rank One Computing, Sensetime Group, Shanghai Jiao Tong University, TigerIT Americas LLC, Vigilant Solutions, Winsense, and YooniK

- We have retired results for twelve algorithms per our policy to only list results for two algorithms per developer. Results for retired algorithms appear in prior versions of this report in the archive.

Changes since September 18, 2020:

- This report adds results for first algorithms from five developers: Aigen, Cortica, Kookmin University, Securif AI and Vinai.
- The report also includes results for three developers who have previously submitted algorithms: Fujitsu Laboratories, Hengrui AI, and X-Forward AI.
- In the per-algorithm report-cards linked from tables and the main webpage, we have added a chart to showing reduction in error rates over the course of FRVT i.e. from 2017 onwards for all algorithms supplied by that developer. Similarly we have added a chart showing error rate reductions for our test of protective face mask verification.
- We plan to continue evaluating algorithms on various mask datasets. We hold that algorithms should be capable of detecting masks and verifying identity of all combinations of masked and unmasked faces. We have accordingly increased the amount to time allowed to extract those features from 1.0 to 1.5 seconds.

Changes since August 25, 2020:

- This report adds results for first algorithms from eight new developers. Akurat Satu Indonesia, Cybercore, Decatur Industries, Innef Labs, Satellite Innovation/Eocortex, Expasoft, and Mobai.
- The report includes results for seven developers who have previously submitted algorithms: 3Divi, BioID Technologies, Incode Technologies, Innovatrics, iSAP Solution, Synology, and Tevian.
- We have retired results for five algorithms per our policy to only list results for two algorithms per developer. Results for retired algorithms appear in prior versions of this report in the archive.

Changes since July 27, 2020:

- We have introduced per-algorithm report sheets. These are HTML documents linked from the accuracy tables in this report (i.e. Table 35) and on the FRVT 1:1 homepage. The sheets contain interactive graphics allowing, for example, mouseover exploration of FNMR(T) and FMR(T). Some of their content had previously appeared in this document.
- This report adds results for algorithms from six new developers. ACI Software, Bresee Technology, Fiberhome Telecommunication Technologies, Imageware Systems, Oz Forensics, and Pensees.
- The report includes results for thirteen developers who have previously submitted algorithms: Canon Information Technology (Beijing), Cyberlink, Dahua Technology, Gorilla Technology, ID3 Technology, Intel Research Group, iQIYI Inc, Momentum Digital, Netbridge Technology, Tech5 SA, Shenzhen AiMall Tech, Vigilant Solutions, and VisionLabs.
- We have retired results for nine algorithms per our policy to only list results for two algorithms per developer. Results for retired algorithms appear in prior versions of this report in the archive.

Changes since May 18, 2020:

- The report is the first FRVT update since the pandemic closed it from March to June 2020.

FNMR(T) "False non-match rate"
FMR(T) "False match rate"

- This report includes results for algorithms from nine new developers: GeoVision Inc, Su Zhou NaZhi-TianDi Intelligent Technology, YooniK, AYF Technology, PXL Vision AG, Yuan High-Tech Development, Beihang University-ERCACAT, ICM Airport Technics, and Staqu Technologies
- This report includes results for algorithms from 15 returning developers Acer Incorporated, Antheus Technologia, Chosun University, Chunghwa Telecom, Idemia, Moontime Smart Technology, Neurotechnology, Guangzhou Pixel Solutions, Panasonic R+D Center Singapore, Rank One Computing, Scanovate, Shanghai Universiy - Shanghai Film Academy, Synesis, Trueface.ai, and Veridas Digital Authentication Solutions
- We have retired results for ten algorithms per our policy to only list results for two algorithms per developer. Results for retired algorithms appear in prior versions of this report in the archive.
- We separated timing and other resource consumption from the main participation table. The new Table 22 includes template generation durations for four kinds of images, not just mugshots.
- We have published a separate report, NIST Interagency Report 8311 on accuracy of pre-pandemic algorithms on subjects wearing face masks. We plan to track improvements in accuracy on masked images going forward. In particular, we invite submission of algorithms that can detect whether a person is wearing a mask, extract features from the full face or the exposed periocular region, and do appropriate comparison. We do not intend to evaluate algorithms that assume 100% of images will be of masked individuals.

Changes since March 25, 2020:

- The report is a maintenance release - it does not add any new algorithms, and FRVT has been closed to new algorithms since mid March 2020.
- We modified the primary accuracy summary, Table 35, as follows:
  - For visa images, the column for FNMR at FMR = 0.0001 has been removed. The visa images are so highly controlled that the error rates for the most accurate algorithms are dominated by false rejection of very young children and by the presence of a few noisy greyscale images. For now, two visa columns remain: FNMR at FMR= 10^{-6} and, for matched covariates, FNMR at FMR= 10^{-4}.
  - We have inserted a new column labelled "BORDER" giving accuracy for comparison of moderately poor webcam border-crossing photos that exhibit pose variations, poor compression, and low contrast due to strong background illumination. The accuracies are the worst from all cooperative image datasets used in FRVT.
- Accordingly, we updated the failure-to-template rates in Table 45.
- We withdrew a figure showing how false matches are concentrated in certain visa images used in cross-comparison, because it didn't attempt to include demographic information.

Changes since February 27, 2020:

- The report adds results algorithms from two new developers: Beijing Alleyes Technology, and the Chinese University of Hong Kong. Results for newly submitted algorithms from two other developers will appear in the next report.
- The report adds results for algorithms from thirteen returning developers: ASUSTek Computer, Aware, Cyberlink Corp, Gorilla Technology, Innovative Technology, Kakao Enterprise, Lomonosov Moscow State University, Panasonic R+D Center Singapore, Shenzhen AiMall Technology, Shenzhen Intellifusion Technologies, Synology, Tech5 SA, and Via Technologies.

- Per policy to only list results for two algorithms per developer, we have dropped results for algorithms from Aware, Cyberlink, Gorilla Technology, Kakao Enterprise, Lomonosov Moscow State University, Panasonic R+D Center Singapore, and Tech5 SA.

Changes since January 20, 2020:

- The report adds results for five new developers: Ability Enterprise (Andro Video), Chosun University, Fujitsu Research and Development Center, University of Coimbra, and Xforward AI Technology.
- The report adds results for algorithms from six returning developers: AlphaSSTG, Incode Technologies, Kneron. Shanghai Jiao Tong University, Vocord, and X-Laboratory.
- We have corrected template comparison timing numbers for algorithms submitted September 2019 to January 2020. The values reported previously were slower due to a software bug.
- We have dropped results for algorithms from Vocord and Incode per policy to only list results for two algorithms per developer.
- The FRVT 1:1 homepage has been updated with latest accuracy results.
- The FRVT 1:N homepage now includes an update to the September 2019 NIST Interagency Report 8271. The new report adds results for one-to-many search algorithms submitted to NIST from June 2019 to January 2020.

Changes since January 6, 2020:

- Section 2 has been updated to better describe the Visa and Border images. The caption for Table 35 has been updated to better relate the accuracy values to particular image comparisons.
- The report adds results for five new developers: Acer, Advance.AI, Expasoft, Netbridge Technology, and Videmo Intelligente Videoanalyse.
- The report adds results for algorithms from 7 returning developers: China Electronics Import-Export Corp, Intel Research Group, ITMO University, Neurotechnology, N-Tech Lab, Rokid, and VisionLabs.
- We have dropped results from this edition of the report per policy to only list results for two algorithms per developer: N-Tech Lab, Neurotechnology, ITMO, Visionlabs, and CEIEC.
- The FRVT homepage has been updated with latest accuracy results.

Changes since November 11, 2019:

- Table 22 has been updated to include runtime memory usage. This is the first time such a quantity has been reported. The value is the peak size of the resident set size logged during enrollment of single images.
- We have migrated summary results table to a new platform that supports sortable tables: https://pages.nist.gov/frvt/html/frvt11.html
- The report adds results for four new developers: Antheus Technologia, BioID Technologies SA, Canon Information Tech. (Beijing), Samsung S1 (listed in the tables as S1), and Taiwan AI Labs.
- The report adds results for algorithms from 13 returning developers: Anke Investments, Chunghwa Telecom, Deepglint, Institute of Information Technologies, iQIYI, Kneron, Ping An Technology, Paravision, KanKan Ai, Rokid Corporation, Shanghai Universiy - Shanghai Film Academy, Veridas Digital Authentication Solutions, and Videonetics Technology.

FNMR(T) "False non-match rate"
FMR(T) "False match rate"

- We have dropped results from this edition of the report per policy to only list results for two algorithms per developer: remarkai-000, veridas-001, sensetime-001, iit-000, anke-003, and everai-002. Results for these are available in prior editions of this report linked from the FRVT page.
- We issued NIST Interagency Report 8280: FRVT Part 3: Demographics on 2019-12-19. It includes results for many of the algorithms covered by this report.

Changes since October 16, 2019:

- The report adds results for ten new developers: Ai-Union Technology, ASUSTek Computer, DiDi ChuXing Technology, Innovative Technology, Luxand, MVision, Pyramid Cyber Security + Forensic, Scanovate, Shenzhen AiMall Tech, and TUPU Technology.
- The report adds results for 12 returning developers: CTBC Bank Glory Gorilla Technology Guangzhou Pixel Solutions Imagus Technology Incode Technologies Lomonosov Moscow State University Rank One Computing Samtech InfoNet Shanghai Ulucu Electronics Technology Synesis, and Winsense.
- We have dropped results from this edition of the report per policy to only list results for two algorithms per developer: glory-000, gorilla-002, incode-003, rankone-006, and synesis-004.
- Results for five recently submitted algorithms will appear in the next report.

Changes since September 11, 2019:

- The report adds results for five new participants: Awidit Systems (Awiros), Momemtum Digital (Sertis), Trueface AI, Shanghai Jiao Tong University, and X-Laboratory.
- The reports adds results for five new algorithms from returning developers: Cyberlink, Hengrui AI Technology, Idemia, Panasonic R+D Singapore, and Tevian. This causes three algorithm, to be de-listed from the report per policy to list results for two algorithms per developer.

Changes since July 31 2019:

- The HTML table on the FRVT 1:1 homepage has been updated to include a column for cross-domain Visa-Border verification. Results for this new dataset appeared in the July 29 report under the name "CrossEV" - these are now renamed "Visa-Border".
- The FRVT 1:1 homepage lists algorithms according to lowest mean rank accuracy:
  $\text{Rank}(\text{FNMR}_{\text{VISA}}$ at FMR = 0.000001) +
  $\text{Rank}(\text{FNMR}_{\text{VISA-BORDER}}$ at FMR = 0.000001) +
  $\text{Rank}(\text{FNMR}_{\text{MUGSHOT}}$ at FMR = 0.00001 after 14 years) +
  $\text{Rank}(\text{FNMR}_{\text{WILD}}$ at FMR = 0.00001)
  This ordering rewards high accuracy across all datasets.
- The main results in Table 35 is now in landscape format to accomodate extra columns for the Visa-Border set, and mugshot comparisons after at least 12 years.
- The report adds results for nine new participants: Alpha SSTG, Intel Research, ULSee, Chungwa Telecon, iSAP Solution, Rokid, Shenzhen EI Networks, CSA Intellicloud, Shenzhen Intellifusion Technologies.
- The reports adds results for six new algorithms from returning developers: Innovatrics, Dahua Technology, Tech5 SA, Intellivision, Nodeflux and Imperial College, London. One algorithm, from Imperial has been retired, per policy to list results for two algorithms per developer.
- The cross-country false match rate heatmaps have been replotted to reveal more structure by listing countries by region instead of alphabetically.

FNMR(T) "False non-match rate"
FMR(T) "False match rate"

- The next version of this report will be posted around October 18, 2019.

Changes since July 3 2019:

- The HTML table on the FRVT 1:1 homepage has been updated to list the 20 most accurate developers rather than algorithms, choosing the most accurate algorithm from each developer based on visa and mugshot results. Also, the algorithms are ordered in terms of lowest mean rank across mugshot, visa and wild datasets, rewarding broad accuracy over a good result on one particular dataset.
- This report includes results for a new dataset - see the column labelled "visa-border" in Table 5. It compares a new set of high quality visa-like portraits with a set webcam border-crossing photos that exhibit moderately poor pose variations and background illumination. The two new sets are described in sections 2.2 and 2.4. The comparisons are "cross-domain" in that the algorithm must compare "visa" and "wild" images. Results for other algorithms will be added in future reports as they become available.
- This report adds results for algorithms from 9 developers submitted in early July 2019. These are from 3DiVi, Camvi, EverAI-Paravision, Facesoft, Farbar (F8), Institute of Information Technologies, Shanghai U. Film Academy, Via Technologies, and Ulucu Electronics Tech. Six of these are new participants.
- Several other algorithms have been submitted and are being evaluated. Results will be released in the next report, scheduled for September 5. That report will include results for new datasets.
- Older algorithms from Everai, Camvi and 3DiVi, have been retired, per the policy to list only two algorithms per developer.

Changes since June 20 2019:

- This report adds results for algorithms from 18 developers submitted in early June 2019. These are from CTBC Bank, Deep Glint, Thales Cogent, Ever AI Paravision, Gorilla Technology, Imagus, Incode, Kneron, N-Tech Lab, Neurotechnology, Notiontag Technologies, Star Hybrid, Videonetics, Vigilant Solutions, Winsense, Anke Investments, CEIEC, and DSK. Nine of these are new participants.
- Several other algorithms have been submitted and are being evaluated. Results will be released in the next report, scheduled for August 1.
- Older algorithms from Everai, Thales Cogent, Gorilla Technology, Incode, Neurotechnology, N-Tech Lab and Vigilant Solutions have been retired, per the policy to list only two algorithms per developer.

Changes since April 2019:

- This report adds results for nine algorithms from nine developers submitted in early June 2019. These are from Tencent Deepsea, Hengrui, Kedacom, Moontime, Guangzhou Pixel, Rank One Computing, Synesis, Sensetime and Vocord.
- Another 23 algorithms have been submitted and are being evaluated. Results will be released in the next report, scheduled for July 3.
- Older algorithms for Rank One, Synesis, and Vocord have been retired, per the policy to list only two algorithms per developer.

Changes since February 2019:

- This report adds results for 49 algorithms from 42 developers submitted in early March 2019.
- This report omits results for algorithms that we retired. We retired for three reasons: 1. The developer submitted a new algorithm, and we only list two. 2. The algorithm needs a GPU, and we no longer allow GPU-based algorithms. 3. Inoperable algorithms.
- Previous results for retired algorithms are available in older editions of this report linked here.
- The mugshot database used from February 2017 to January 2019 has been replaced with an extract of the mugshot database documented in NIST Interagency Report 8238, November 2018. The new mugshot set is described in section 2.5 and is adopted because:

FNMR(T) "False non-match rate"
FMR(T) "False match rate"

- ▷▷ It has much better identity label integrity, so that false non-match rates are substantially lower than those reported in FRVT 1:1 reports to date - see Figure 135.
- ▷▷ It includes images collected over a 17 year period such that ageing can be much better characterized - - see Figure 368.

- ▷ Using the new mugshot database, Figure 368 shows accuracy for four demographic groups identified in the biographic metadata that accompanies the data: black females, black males, white females and white males.
- ▷ The report added a figure (now moved to web) with results for the twenty human-difficult pairs used in the May 2018 paper *Face recognition accuracy of forensic examiners, superrecognizers, and face recognition algorithms* by Phillips et al. [1].
- ▷ The report uses an update to the wild image database that corrects some ground truth labels.
- ▷ Some results for the child exploitation database are not complete. They are typically updated less frequently than for other image sets.

FNMR(T) "False non-match rate"
FMR(T) "False match rate"

Contents

List of Tables

FNMR(T) "False non-match rate"
FMR(T) "False match rate"

List of Figures

FNMR(T) "False non-match rate"
FMR(T) "False match rate"

FNMR(T) "False non-match rate"
FMR(T) "False match rate"

FNMR(T) "False non-match rate"
FMR(T) "False match rate"

FNMR(T) "False non-match rate"
FMR(T) "False match rate"

FNMR(T) "False non-match rate"
FMR(T) "False match rate"

FNMR(T) "False non-match rate"
FMR(T) "False match rate"

FNMR(T) "False non-match rate"
FMR(T) "False match rate"

FNMR(T) "False non-match rate"
FMR(T) "False match rate"

	Location	Developer Name	Short Name	Seq. Num.	Validation Date
1	NL	20Face	20face-000	000	2021-04-12
2	NL	20Face	20face-001	001	2021-09-29
3	US	3Divi	3divi-006	006	2021-04-14
4	US	3Divi	3divi-007	007	2021-09-27
5	TH	ACI Software	acisw-007	007	2021-11-15
6	TH	ACI Software	acisw-008	008	2022-03-22
7	US	AFIS and Biometrics Consulting	afisbiometrics-000	000	2022-01-27
8	US	AFR Engine	afrengine-002	002	2023-06-27
9	US	AFR Engine	afrengine-003	003	2024-03-15
10	TW	ASUSTek Computer Inc	asusaics-000	000	2019-10-24
11	TW	ASUSTek Computer Inc	asusaics-001	001	2020-02-25
12	CN	AYF Technology	ayftech-001	001	2020-07-06
13	CN	AYF Technology	ayftech-003	003	2023-05-15
14	TW	Ability Enterprise - Andro Video	androvideo-000	000	2021-01-25
15	IN	Accurascan	accurascan-002	002	2023-08-01
16	IN	Accurascan	accurascan-003	003	2023-12-06
17	TW	Acer Incorporated	acer-001	001	2020-06-30
18	TW	Acer Incorporated	acer-002	002	2021-11-10
19	SG	Adera Global PTE	adera-004	004	2022-11-14
20	SG	Adera Global PTE	adera-005	005	2023-11-17
21	SG	Advance.AI	advance-004	004	2022-09-06
22	SG	Advance.AI	advance-005	005	2023-05-25
23	TH	Ai First	aifirst-001	001	2019-11-21
24	TW	AiUnion Technology	aiunionface-000	000	2019-10-22
25	TH	Aigen	aigen-001	001	2020-10-06
26	TH	Aigen	aigen-002	002	2021-03-15
27	CN	Aiseemu Technology	aiseemu-001	001	2022-06-16
28	CN	Aiseemu Technology	aiseemu-002	002	2022-11-18
29	KR	Ajou University	ajou-001	001	2021-03-08
30	ID	Akurat Satu Indonesia	ptakuratsatu-000	000	2020-09-11
31	KR	Alchera Inc	alchera-006	006	2023-07-18
32	KR	Alchera Inc	alchera-007	007	2023-11-22
33	ID	Alfabeta	alfabeta-001	001	2021-12-02
34	ES	Alice Biometrics	alice-000	000	2021-06-15
35	ES	Alice Biometrics	alice-001	001	2023-07-05
36	RU	Alivia / Innovation Sys	isystems-001	001	2018-06-12
37	RU	Alivia / Innovation Sys	isystems-002	002	2018-10-18
38	IN	AllGoVision	allgovision-000	000	2019-03-01
39	CN	AlphaSSTG	alphaface-001	001	2019-09-03
40	CN	AlphaSSTG	alphaface-002	002	2020-02-20
41	GB	Amplified Group	amplifiedgroup-001	001	2019-03-01
42	CN	Anke Investments	anke-004	004	2019-06-27
43	CN	Anke Investments	anke-005	005	2019-11-21
44	BR	Antheus Technologia	antheus-000	000	2019-12-05
45	BR	Antheus Technologia	antheus-001	001	2020-06-25
46	GB	AnyVision	anyvision-004	004	2018-06-15
47	GB	AnyVision	anyvision-005	005	2021-02-03
48	CN	Aratek Biometrics Co Ltd	aratek-001	001	2023-03-27
49	US	Armatura LLC	armatura-001	001	2022-01-04
50	US	Armatura LLC	armatura-003	003	2023-01-13
51	CN	AuthenMetric	authenmetric-003	003	2021-08-09
52	CN	AuthenMetric	authenmetric-004	004	2022-01-03
53	TW	Authme	authme-001	001	2023-10-17
54	US	Aware	aware-007	007	2023-11-15
55	US	Aware	aware-008	008	2024-03-15
56	IN	Awidit Systems	awiros-001	001	2019-09-23
57	IN	Awidit Systems	awiros-002	002	2020-10-28
58	CH	Aximetria	aximetria-001	001	2022-08-10
59	JP	Ayonix	ayonix-000	000	2017-06-22
60	CN	BOE Technology Group	boetech-001	001	2021-06-22
61	CN	BOE Technology Group	boetech-002	002	2021-12-21
62	ES	Bee the Data	beethedata-000	000	2021-07-26
63	CN	Beihang University-ERCACAT	ercacat-001	001	2020-07-06
64	CN	Beijing Alleyes Technology	alleyes-000	000	2020-03-09
65	CN	Beijing DeepSense Technologies	deepsense-002	002	2023-02-22
66	CN	Beijing DeepSense Technologies	deepsense-003	003	2023-10-23
67	CN	Beijing Hisign Technology	hisign-002	002	2022-09-09
68	CN	Beijing Hisign Technology	hisign-003	003	2024-03-15
69	CN	Beijing Mendaxia Technology	mendaxiatech-000	000	2021-09-15
70	CN	Beijing Vion Technology Inc	vion-000	000	2018-10-19

Table 1: Summary of participant information included in this report.

FNMR(T) "False non-match rate"
FMR(T) "False match rate"

	Location	Developer Name	Short Name	Seq. Num.	Validation Date
71	KZ	Beyne.AI	beyneai-000	000	2022-01-03
72	CH	BioID Technologies SA	bioidtechswiss-001	001	2020-08-28
73	CH	BioID Technologies SA	bioidtechswiss-002	002	2021-02-17
74	IN	Biocube Matrics	biocube-001	001	2021-09-08
75	IN	Biocube Matrics	biocube-002	002	2023-02-09
76	KZ	Biometric LLC	biometric-vision-000	000	2023-01-25
77	UK	BitCenter UK	farfaces-001	001	2021-04-09
78	CN	Bitmain	bm-001	001	2018-10-17
79	CN	Bresee Technology	bresee-001	001	2020-12-30
80	CN	Bresee Technology	bresee-002	002	2021-06-30
81	VN	CMC Institute of Science and Technology	cist-003	003	2023-08-14
82	VN	CMC Institute of Science and Technology	cist-004	004	2024-02-15
83	VN	CMC Univerisity	cmcuni-001	001	2023-12-05
84	CN	CSA IntelliCloud Technology	intellicloudai-001	001	2019-08-13
85	CN	CSA IntelliCloud Technology	intellicloudai-002	002	2020-12-17
86	TW	CTBC Bank	ctbcbank-000	000	2019-06-28
87	TW	CTBC Bank	ctbcbank-001	001	2019-10-28
88	KR	CUDO Communication	cudocommunication-001	001	2021-10-20
89	US	Camvi Technologies	camvi-002	002	2018-10-19
90	US	Camvi Technologies	camvi-004	004	2019-07-12
91	FI	Candour Biometrics	candour-001	001	2023-02-10
92	JP	Canon Inc	canon-004	004	2022-04-25
93	JP	Canon Inc	canon-005	005	2023-09-05
94	CN	China Electronics Import-Export Corp	ceiec-003	003	2020-01-06
95	CN	China Electronics Import-Export Corp	ceiec-004	004	2021-01-18
96	CN	China University of Petroleum	upc-001	001	2019-06-05
97	CN	Chinese University of Hong Kong	cuhkee-001	001	2020-03-18
98	KR	Chosun University	chosun-001	001	2020-07-01
99	KR	Chosun University	chosun-002	002	2020-11-25
100	TW	Chunghwa Telecom	chtface-005	005	2022-03-09
101	TW	Chunghwa Telecom	chtface-006	006	2022-11-03
102	US	City and County of Honolulu	cchonolulu-000	000	2023-03-27
103	US	City and County of Honolulu	cchonolulu-001	001	2024-01-18
104	US	Clearview AI Inc	clearviewai-000	000	2021-09-22
105	US	Clearview AI Inc	clearviewai-001	001	2023-12-05
106	CN	Closeli Inc	closeli-001	001	2021-07-15
107	US	CloudSmart Consulting LLC	csc-002	002	2021-03-24
108	US	CloudSmart Consulting LLC	csc-003	003	2021-08-26
109	TW	Cloudmatrix	cloudmatrix-001	001	2022-02-16
110	TW	Cloudmatrix	cloudmatrix-002	002	2022-10-17
111	CN	Cloudwalk - Hengrui AI Technology	cloudwalk-hr-003	003	2020-09-25
112	CN	Cloudwalk - Hengrui AI Technology	cloudwalk-hr-004	004	2021-02-10
113	CN	Cloudwalk - Moontime Smart Technology	cloudwalk-mt-006	006	2022-10-20
114	CN	Cloudwalk - Moontime Smart Technology	cloudwalk-mt-007	007	2023-02-21
115	IN	Code Everest Pvt	facex-001	001	2021-03-08
116	IN	Code Everest Pvt	facex-002	002	2021-08-24
117	KR	Codeline	codeline-000	000	2022-09-13
118	DE	Cognitec Systems GmbH	cognitec-004	004	2022-02-10
119	DE	Cognitec Systems GmbH	cognitec-005	005	2023-12-01
120	TW	Coretech Knowledge Inc	coretech-001	001	2022-09-29
121	TW	Coretech Knowledge Inc	coretech-002	002	2023-11-02
122	IL	Corsight	corsight-002	002	2021-09-01
123	IL	Corsight	corsight-003	003	2022-06-09
124	IL	Cortica	cor-001	001	2020-09-24
125	TW	Cu-Face	cu-face-003	003	2023-08-28
126	TW	Cu-Face	cu-face-004	004	2024-03-13
127	KR	Cubox	cubox-002	002	2021-08-24
128	KR	Cubox	cubox-003	003	2023-03-07
129	JP	Cybercore	cybercore-002	002	2022-04-25
130	JP	Cybercore	cybercore-003	003	2022-08-31
131	US	Cyberextruder	cyberextruder-003	003	2022-03-16
132	US	Cyberextruder	cyberextruder-004	004	2022-07-20
133	TW	Cyberlink Corp	cyberlink-012	012	2023-06-02
134	TW	Cyberlink Corp	cyberlink-013	013	2023-12-15
135	MX	DICIO	dicio-001	001	2022-03-22
136	CN	DSK	dsk-000	000	2019-06-28
137	VN	Dactionable Technologies	datech-000	000	2023-10-16
138	VN	Dactionable Technologies	datech-001	001	2024-02-21
139	CN	Dahua Technology	dahua-006	006	2020-12-30
140	CN	Dahua Technology	dahua-007	007	2021-12-20

Table 2: Summary of participant information included in this report.

FNMR(T) "False non-match rate"
FMR(T) "False match rate"

	Location	Developer Name	Short Name	Seq. Num.	Validation Date
141	IE	Daon	daon-000	000	2021-11-03
142	TW	DeCloak Intellegences	decloakface-001	001	2023-06-13
143	US	Decatur Industries Inc	decatur-000	000	2020-08-18
144	US	Decatur Industries Inc	decatur-001	001	2021-09-27
145	CN	Deepglint	deepglint-004	004	2021-09-17
146	CN	Deepglint	deepglint-005	005	2022-10-17
147	FR	Deepsense	dps-000	000	2021-07-16
148	DE	Dermalog	dermalog-011	011	2022-12-12
149	DE	Dermalog	dermalog-012	012	2024-01-19
150	CN	DiDi ChuXing Technology	didiglobalface-001	001	2019-10-23
151	CN	DiDi ChuXing Technology	didiglobalface-002	002	2023-01-09
152	IN	Digidata	digidata-000	000	2022-01-27
153	IN	Digidata	digidata-001	001	2022-06-10
154	GB	Digital Barriers	digitalbarriers-002	002	2019-03-01
155	IN	EI Networks Private Ltd	einetworksindia-000	000	2023-05-03
156	IN	EI Networks Private Ltd	einetworksindia-001	001	2023-09-05
157	TR	Ekin Smart City Technologies	ekin-002	002	2021-05-04
158	TH	Element System Solutions Company Ltd	element-000	000	2023-11-14
159	AE	Enface	enface-001	001	2021-12-17
160	AE	Enface	enface-002	002	2023-02-27
161	CH	Euronovate SA	euronovate-003	003	2023-09-19
162	CH	Euronovate SA	euronovate-004	004	2024-01-19
163	RU	Expasoft LLC	expasoft-001	001	2020-09-03
164	RU	Expasoft LLC	expasoft-002	002	2021-07-26
165	LB	FOO	foomobi-001	001	2023-03-13
166	LB	FOO	foomobi-002	002	2023-08-07
167	VN	FPT Education	fedu-001	001	2024-03-15
168	VN	FPT Information System	fpt-000	000	2024-02-26
169	US	FRP LLC	frpkauai-001	001	2022-07-18
170	US	FRP LLC	frpkauai-002	002	2022-11-21
171	CA	FaceLocate	facelocate-001	001	2024-02-22
172	DE	FaceOnLive Inc	faceonlive-001	001	2021-11-23
173	DE	FaceOnLive Inc	faceonlive-002	002	2022-04-11
174	ES	FacePhi	facephi-000	000	2022-04-06
175	GB	FaceSoft	facesoft-000	000	2019-07-10
176	KR	FaceTag Co	facetag-000	000	2021-03-22
177	KR	FaceTag Co	facetag-002	002	2022-01-06
178	UK	Facehawk Ltd	facehawk-000	000	2023-08-22
179	UK	Facia.ai	facia-001	001	2023-07-21
180	TW	FarBar Inc	f8-001	001	2019-07-11
181	TW	FarBar Inc	f8-002	002	2022-03-02
182	US	Fast Enterprises	fastenterprises-000	000	2023-03-01
183	CN	Fiberhome Telecommunication Technologies	fiberhome-nanjing-003	003	2021-03-12
184	CN	Fiberhome Telecommunication Technologies	fiberhome-nanjing-004	004	2021-09-14
185	UK	Fincore Ltd	fincore-000	000	2021-06-07
186	KZ	First Credit Bureau Kazakhstan	firstcreditkz-002	002	2023-02-21
187	KZ	First Credit Bureau Kazakhstan	firstcreditkz-003	003	2024-02-20
188	UK	Fraud.com	fraudcom-000	000	2023-12-01
189	CN	Fujitsu Research and Development Center	fujitsulab-002	002	2021-02-24
190	CN	Fujitsu Research and Development Center	fujitsulab-003	003	2021-07-12
191	VN	GPS Vietnam Trading	gpstechvn-000	000	2024-01-02
192	US	Gemalto Cogent	cogent-007	007	2022-04-11
193	US	Gemalto Cogent	cogent-008	008	2023-01-03
194	TW	General Interface Solutions Holding Ltd	gistouch-000	000	2023-05-08
195	TW	General Interface Solutions Holding Ltd	gistouch-001	001	2023-11-09
196	TW	GeoVision Inc	geo-002	002	2021-04-01
197	TW	GeoVision Inc	geo-004	004	2022-02-10
198	JP	Glory	glory-006	006	2023-03-23
199	JP	Glory	glory-007	007	2023-11-10
200	TW	Gorilla Technology	gorilla-008	008	2021-11-08
201	TW	Gorilla Technology	gorilla-009	009	2022-12-14
202	US	Graymatics	graymatics-001	001	2022-01-13
203	US	Griaule	griaule-001	001	2022-05-31
204	US	Griaule	griaule-002	002	2022-12-02
205	CN	Guangzhou Pixel Solutions	pixelall-009	009	2022-10-26
206	CN	Guangzhou Pixel Solutions	pixelall-010	010	2023-10-18
207	CN	Hangzhuo AIlu Network Information Technology	hzailu-005	005	2023-08-10
208	CN	Hangzhuo AIlu Network Information Technology	hzailu-006	006	2023-12-28
209	ES	Herta Security	hertasecurity-002	002	2022-09-02
210	ES	Herta Security	hertasecurity-003	003	2023-01-27

Table 3: Summary of participant information included in this report.

FNMR(T) "False non-match rate"
FMR(T) "False match rate"

	Location	Developer Name	Short Name	Seq. Num.	Validation Date
211	CN	Hikvision Research Institute	hik-001	001	2019-03-01
212	IN	HyperVerge Inc	hyperverge-003	003	2022-04-11
213	IN	HyperVerge Inc	hyperverge-005	005	2023-08-08
214	AU	ICM Airport Technics	icm-004	004	2022-09-07
215	AU	ICM Airport Technics	icm-005	005	2023-09-05
216	FR	ID3 Technology	id3-006	006	2020-12-17
217	FR	ID3 Technology	id3-008	008	2021-11-10
218	UK	IDENTY	identy-000	000	2023-04-04
219	CA	IMDS Software	imds-software-002	002	2023-02-10
220	CA	IMDS Software	imds-software-003	003	2023-06-20
221	RU	ITMO University	itmo-007	007	2020-01-06
222	RU	ITMO University	itmo-008	008	2021-11-19
223	RU	IVA Cognitive	ivacognitive-001	001	2021-01-29
224	FR	Idemia	idemia-009	009	2022-07-27
225	FR	Idemia	idemia-010	010	2023-06-30
226	US	Imageware Systems	iws-000	000	2020-08-12
227	GB	Imperial College London	imperial-000	000	2019-03-01
228	GB	Imperial College London	imperial-002	002	2019-08-28
229	US	Incode Technologies Inc	incode-009	009	2021-06-22
230	US	Incode Technologies Inc	incode-013	013	2023-12-08
231	IT	InfoCert	infocert-001	001	2022-09-08
232	IN	Innef Labs	innefulabs-000	000	2020-09-04
233	IN	Innominds Software SEZ India Pvt	innominds-001	001	2023-06-23
234	GB	Innovative Technology	innovativetechnologyltd-001	001	2019-10-22
235	GB	Innovative Technology	innovativetechnologyltd-002	002	2020-02-26
236	SK	Innovatrics	innovatrics-010	010	2023-08-03
237	SK	Innovatrics	innovatrics-011	011	2024-03-08
238	CN	InsightFace AI	insightface-003	003	2022-08-23
239	CN	InsightFace AI	insightface-004	004	2023-03-31
240	CN	Inspur (Beijing) Electronic Information Industry Co	inspur-001	001	2023-02-24
241	CN	Inspur (Beijing) Electronic Information Industry Co	inspur-002	002	2023-12-08
242	CN	Institute of Computing Technology	icthtc-000	000	2020-11-29
243	RU	Institute of Information Technologies	iit-002	002	2019-12-04
244	RU	Institute of Information Technologies	iit-003	003	2020-12-01
245	IS	Intel Research Group	intelresearch-007	007	2023-05-30
246	IS	Intel Research Group	intelresearch-008	008	2023-10-03
247	KR	IntelliVIX	intellivix-004	004	2023-06-21
248	KR	IntelliVIX	intellivix-005	005	2023-11-14
249	AE	Intellibrain Technological Projects	g42-intellibrain-001	001	2022-07-27
250	AE	Intellibrain Technological Projects	g42-intellibrain-002	002	2023-05-10
251	CN	Intelligent Control Technology Co Ltd - IGearx	igearx-face-000	000	2023-03-28
252	US	Intellivision	intellivision-006	006	2023-07-14
253	US	Intellivision	intellivision-007	007	2023-12-19
254	LU	Intema-LGL Group	intema-000	000	2022-07-15
255	LU	Intema-LGL Group	intema-001	001	2023-01-11
256	IN	Intozi Tech Pvt Ltd	intozi-001	001	2023-09-25
257	US	IrexAI	irex-000	000	2020-12-17
258	IL	Is It You	isityou-000	000	2017-06-26
259	MX	Jaak IT	jaakit-001	001	2022-05-20
260	KR	Kakao Bank	kakaobank-000	000	2023-02-27
261	KR	Kakao Bank	kakaobank-001	001	2023-10-10
262	KR	Kakao Brain	kakao-008	008	2022-05-12
263	KR	Kakao Brain	kakao-009	009	2023-11-07
264	KR	Kakao Pay Corp	kakaopay-001	001	2021-07-06
265	TH	Kasikorn Labs	kasikornlabs-002	002	2022-12-13
266	TH	Kasikorn Labs	kasikornlabs-003	003	2023-10-05
267	SG	Kedacom International Pte	kedacom-000	000	2019-06-03
268	US	Kneron Inc	kneron-003	003	2019-07-01
269	US	Kneron Inc	kneron-005	005	2020-02-21
270	US	KnowUTech LLC	knowutech-000	000	2022-02-13
271	US	Kogniza Technology	kogniza-001	001	2024-03-01
272	KR	Kookmin University	kookmin-002	002	2021-03-05
273	KR	Korea Identification Inc	koreaid-001	001	2022-12-12
274	TH	Krungthai	krungthai-002	002	2022-06-21
275	CN	KuKe3D Technology	kuke3d-001	001	2021-10-28
276	CN	KuKe3D Technology	kuke3d-002	002	2022-04-14
277	MX	Lebentech Biometrics	lebentech-000	000	2022-02-16
278	MX	Lebentech Biometrics	lebentech-001	001	2023-12-12
279	IN	Lema Labs	lemalabs-001	001	2021-04-13
280	JP	Line Corporation	lineclova-002	002	2022-05-18

Table 4: Summary of participant information included in this report.

FNMR(T) "False non-match rate"
FMR(T) "False match rate"

	Location	Developer Name	Short Name	Seq. Num.	Validation Date
281	JP	Line Corporation	lineclova-003	003	2022-11-28
282	RU	Lomonosov Moscow State University	intsysmsu-001	001	2019-10-22
283	RU	Lomonosov Moscow State University	intsysmsu-002	002	2020-03-12
284	IN	Lookman Electroplast Industries	lookman-002	002	2018-06-13
285	IN	Lookman Electroplast Industries	lookman-004	004	2019-06-03
286	US	Luxand Inc	luxand-000	000	2019-11-07
287	US	Luxand Inc	luxand-001	001	2023-10-17
288	RU	MVision	mvision-001	001	2019-11-12
289	IN	Mantra Softech India	mantra-000	000	2021-10-28
290	CN	Maxvision Technology	maxvision-005	005	2023-09-21
291	CN	Maxvision Technology	maxvision-006	006	2024-01-19
292	CN	Megvii/Face++	megvii-008	008	2023-10-12
293	CN	Megvii/Face++	megvii-009	009	2024-02-12
294	KR	Metsakuur	metsakuurcompany-002	002	2022-09-14
295	KR	Metsakuur	metsakuurcompany-003	003	2023-04-04
296	CN	Miaxis Biometrics	miaxis-002	002	2023-03-22
297	CN	Miaxis Biometrics	miaxis-003	003	2023-09-19
298	GB	MicroFocus	microfocus-002	002	2018-10-17
299	GB	MicroFocus	microfocus-003	003	2023-02-23
300	CN	Minivision	minivision-000	000	2020-10-28
301	UK	Mitek Systems	mitek-000	000	2023-01-27
302	NO	Mobai	mobai-000	000	2020-08-26
303	NO	Mobai	mobai-001	001	2021-02-17
304	ES	Mobbeel Solutions	mobbl-001	001	2021-06-16
305	ES	Mobbeel Solutions	mobbl-003	003	2022-04-19
306	KR	Mobipin Technology	mobipintech-000	000	2021-11-23
307	TH	Momentum Digital	sertis-002	002	2021-05-13
308	TH	Momentum Digital	sertis-003	003	2023-12-27
309	CN	MoreDian Technology	moredian-000	000	2021-02-24
310	US	Mukh Technologies	mukh-003	003	2023-03-15
311	US	Mukh Technologies	mukh-004	004	2023-09-13
312	CN	Multi-Modality Intelligence	multimodality-000	000	2021-10-19
313	CN	Multi-Modality Intelligence	multimodality-001	001	2022-05-16
314	RU	N-Tech Lab	ntechlab-011	011	2021-09-13
315	RU	N-Tech Lab	ntechlab-012	012	2022-01-20
316	SG	NCS Pte Ltd	ncssg-001	001	2023-03-24
317	CA	NEO Systems	neosystems-004	004	2022-05-02
318	KR	NHN Corp	nhn-004	004	2023-06-26
319	KR	NHN Corp	nhn-005	005	2023-12-06
320	KR	NSENSE Corp	nsensecorp-004	004	2022-09-08
321	KR	NSENSE Corp	nsensecorp-005	005	2023-02-08
322	CN	Nanjing Kiwi Network Technology	kiwitech-000	000	2021-03-19
323	KR	Neosecu Co	openface-001	001	2021-06-15
324	TW	Netbridge Technology Incoporation	netbridgetech-001	001	2020-01-08
325	TW	Netbridge Technology Incoporation	netbridgetech-002	002	2020-08-11
326	LT	Neurotechnology	neurotechnology-017	017	2023-07-28
327	LT	Neurotechnology	neurotechnology-018	018	2024-02-09
328	ID	Nodeflux	nodeflux-002	002	2019-08-13
329	LT	Nominder	nominder-002	002	2023-11-04
330	LT	Nominder	nominder-003	003	2024-03-06
331	IN	NotionTag Technologies Private Limited	notiontag-001	001	2021-03-04
332	IN	NotionTag Technologies Private Limited	notiontag-002	002	2021-09-17
333	US	Omnigarde Ltd	omnigarde-002	002	2022-01-19
334	US	Omnigarde Ltd	omnigarde-003	003	2023-05-10
335	KR	One More Security	omface-000	000	2021-12-15
336	KR	One More Security	omface-001	001	2022-10-21
337	UK	Onfido	onfido-000	000	2022-12-13
338	VN	Online Mobile Services JSC	momovn-001	001	2024-01-26
339		Openedge Technologies Pvt	openedge-000	000	2024-01-29
340	RU	Oz Forensics LLC	oz-003	003	2021-08-09
341	RU	Oz Forensics LLC	oz-004	004	2021-12-13
342	TW	PAPAGO Inc	papago-001	001	2022-07-19
343	CZ	PAPIL11 S.R.O.	papil11-000	000	2024-01-04
344	ID	PT Autentika Digital Indonesia	autentika-001	001	2023-04-05
345	ID	PT Autentika Digital Indonesia	autentika-002	002	2023-11-21
346	ID	PT Qlue Performa Indonesia	qluevision-001	001	2022-11-15
347	CH	PXL Vision AG	pxl-001	001	2020-06-30
348	TW	Palit Microsystems	palit-000	000	2022-05-16
349	TW	Palit Microsystems	palit-001	001	2022-09-26
350	SG	Panasonic R+D Center Singapore	psl-011	011	2022-10-06

Table 5: Summary of participant information included in this report.

FNMR(T) "False non-match rate"
FMR(T) "False match rate"

	Location	Developer Name	Short Name	Seq. Num.	Validation Date
351	SG	Panasonic R+D Center Singapore	psl-012	012	2023-10-13
352	US	Pangiam	pangiam-001	001	2023-02-21
353	US	Pangiam	pangiam-002	002	2023-06-21
354	TR	Papilon Savunma	papsav1923-002	002	2022-01-20
355	TR	Papilon Savunma	papsav1923-003	003	2022-11-25
356	US	Paravision	paravision-013	013	2023-05-08
357	US	Paravision (EverAI)	paravision-011	011	2022-12-12
358	SG	Pensees Pte	pensees-001	001	2020-08-17
359	US	Private Identity LLC	privid-001	001	2023-02-06
360	US	Private Identity LLC	privid-002	002	2023-10-03
361	IN	Pyramid Cyber Security + Forensic (P)	pyramid-000	000	2019-11-04
362	KZ	Qaz Biometric Systems	qazbs-000	000	2022-06-22
363		QazSmartVision.AI	qazsmartvisionai-000	000	2024-01-11
364	TW	Qnap Security	qnap-004	004	2023-05-05
365	TW	Qnap Security	qnap-005	005	2023-11-16
366	CZ	Quantasoft	quantasoft-003	003	2021-04-19
367	US	ROC	rankone-015	015	2023-07-20
368	US	ROC	roc-016	016	2023-12-19
369	US	Realnetworks Inc	realnetworks-007	007	2022-06-14
370	US	Realnetworks Inc	realnetworks-008	008	2022-11-10
371	AE	Recognito	recognito-000	000	2023-05-24
372	AE	Recognito	recognito-001	001	2023-09-27
373	US	Regula Forensics	regula-000	000	2021-04-13
374	US	Regula Forensics	regula-001	001	2021-12-14
375	AM	Regular Biometrics Solutions	rebs-000	000	2023-08-22
376	AM	Regular Biometrics Solutions	rebs-001	001	2023-12-22
377	CN	Remark Holdings	remarkai-001	001	2019-03-01
378	CN	Remark Holdings	remarkai-003	003	2021-06-22
379	SG	Rendip	rendip-000	000	2021-04-19
380	UK	Reveal Media Ltd	revealmedia-005	005	2021-09-24
381	UK	Reveal Media Ltd	revealmedia-006	006	2022-01-26
382	CN	Rokid Corporation	rokid-000	000	2019-08-01
383	CN	Rokid Corporation	rokid-001	001	2019-12-13
384	KR	SK Telecom	sktelecom-000	000	2021-07-09
385	KR	SQIsoft	sqisoft-002	002	2021-11-03
386	KR	SQIsoft	sqisoft-003	003	2022-10-26
387	SG	ST Engineering	stengg-000	000	2023-06-06
388	SA	STCON LLC	stcon-002	002	2023-07-05
389	SA	STCON LLC	stcon-003	003	2023-11-07
390	DE	Saffe	saffe-001	001	2018-10-19
391	DE	Saffe	saffe-002	002	2019-03-01
392	JP	Saga Densan Center Co Ltd	sdc-000	000	2022-10-18
393	KR	Samsung S1 Corp	s1-005	005	2022-06-17
394	KR	Samsung S1 Corp	s1-007	007	2023-03-20
395	KR	Samsung-SDS	samsungsds-001	001	2022-04-18
396	KR	Samsung-SDS	samsungsds-002	002	2022-09-16
397	IN	Samtech InfoNet Limited	samtech-001	001	2019-10-15
398	IN	Samtech InfoNet Limited	samtech-002	002	2023-07-06
399	RU	Satellite Innovation/Eocortex	eocortex-000	000	2020-08-26
400	IL	Scanovate	scanovate-002	002	2020-06-26
401	IL	Scanovate	scanovate-003	003	2021-11-15
402	NG	Seamfix	seamfix-001	001	2024-03-08
403	RO	Securif AI	securifai-007	007	2023-08-17
404	RO	Securif AI	securifai-008	008	2024-02-26
405	CN	Sensetime Group	sensetime-007	007	2022-06-17
406	CN	Sensetime Group	sensetime-008	008	2023-01-04
407	UZ	Serendipity Ltd	serendipity-000	000	2023-05-31
408	SG	Seventh Sense Artificial Intelligence	seventhsense-003	003	2023-05-31
409	SG	Seventh Sense Artificial Intelligence	seventhsense-005	005	2023-10-05
410	US	Shaman Software	shaman-000	000	2017-12-05
411	US	Shaman Software	shaman-001	001	2018-01-13
412	CN	Shanghai Jiao Tong University	sjtu-004	004	2021-05-13
413	CN	Shanghai Jiao Tong University	sjtu-005	005	2023-05-05
414	CN	Shanghai Ulucu Electronics Technology	uluface-002	002	2019-07-10
415	CN	Shanghai Ulucu Electronics Technology	uluface-003	003	2019-11-12
416	CN	Shanghai University - Shanghai Film Academy	shu-002	002	2019-12-10
417	CN	Shanghai University - Shanghai Film Academy	shu-003	003	2020-06-24
418	CN	Shanghai Yitu Technology	yitu-003	003	2019-03-01
419	CN	Shenzhen AiMall Tech	aimall-002	002	2020-03-12
420	CN	Shenzhen AiMall Tech	aimall-003	003	2020-08-12

Table 6: Summary of participant information included in this report.

FNMR(T) "False non-match rate"
FMR(T) "False match rate"

	Location	Developer Name	Short Name	Seq. Num.	Validation Date
421	CN	Shenzhen EI Networks	einetworks-000	000	2019-08-13
422	CN	Shenzhen Inst Adv Integrated Tech CAS	siat-002	002	2018-06-13
423	CN	Shenzhen Inst Adv Integrated Tech CAS	siat-005	005	2022-02-08
424	CN	Shenzhen Intellifusion Technologies	intellifusion-001	001	2019-08-22
425	CN	Shenzhen Intellifusion Technologies	intellifusion-002	002	2020-03-18
426	CN	Shenzhen University-Macau University of Science and Technology	sztu-000	000	2020-12-17
427	CN	Shenzhen University-Macau University of Science and Technology	sztu-001	001	2021-07-13
428	RU	Smart Engines	smartengines-000	000	2021-08-25
429	RU	Smart Engines	smartengines-001	001	2022-05-31
430	ES	Smartbiometrik	smartbiometrik-001	001	2022-05-16
431	TR	Smarvist Teknoloji	smartvist-000	000	2022-05-10
432	TR	Smarvist Teknoloji	smartvist-001	001	2023-11-02
433	DE	Smilart	smilart-002	002	2018-02-06
434	DE	Smilart	smilart-003	003	2019-03-01
435	TR	Sodec App Inc	sodec-000	000	2021-06-02
436		Sparsh CCTV	sparsh-001	001	2024-01-02
437	IN	Staqu Technologies	staqu-000	000	2020-07-15
438	CN	Star Hybrid Limited	starhybrid-001	001	2019-06-19
439	CN	Su Zhou NaZhiTianDi intelligent technology	nazhiai-000	000	2020-06-25
440	IN	Sukshi Technology Innovation	sukshi-000	000	2022-02-13
441	KR	Suprema AI Inc	suprema-004	004	2023-01-09
442	KR	Suprema AI Inc	suprema-005	005	2023-10-25
443	KR	Suprema ID Inc	supremaid-001	001	2021-05-04
444	KR	Suprema ID Inc	supremaid-002	002	2022-06-24
445	UK	Swsam Solutions	swsam-001	001	2023-03-13
446	RU	Synesis	synesis-006	006	2019-10-10
447	RU	Synesis	synesis-007	007	2020-06-24
448	TW	Synology Inc	synology-000	000	2019-10-23
449	TW	Synology Inc	synology-002	002	2020-08-20
450	BR	T4iSB	t4isb-000	000	2022-01-28
451	VN	TNI Tech Co	tnitech-000	000	2024-02-05
452	CN	TUPU Technology	tuputech-000	000	2019-10-11
453	TW	Taiwan AI Labs	ailabs-001	001	2019-12-18
454	TW	Taiwan-Certificate Authority Incorporation	twface-000	000	2021-05-14
455	TW	Taiwan-Certificate Authority Incorporation	twface-001	001	2021-09-14
456	CH	Tech5 SA	tech5-007	007	2022-12-30
457	CH	Tech5 SA	tech5-008	008	2023-08-11
458	VN	Techainer	techainer-001	001	2023-11-30
459	TR	Techsign	techsign-000	000	2021-08-25
460	TR	Techsign	techsign-001	001	2022-07-01
461	CN	Tencent Deepsea Lab	deepsea-001	001	2019-06-03
462	RU	Tevian	tevian-007	007	2021-08-06
463	RU	Tevian	tevian-008	008	2021-12-06
464	US	TigerIT Americas LLC	tiger-005	005	2021-07-29
465	US	TigerIT Americas LLC	tiger-006	006	2021-12-13
466	RU	Tinkoff Bank	tinkoff-001	001	2021-05-13
467	CN	TongYi Transportation Technology	tongyi-005	005	2019-06-12
468	TW	Toppan ID Gate	toppanidgate-000	000	2021-09-28
469	JP	Toshiba	toshiba-007	007	2023-09-13
470	JP	Toshiba	toshiba-008	008	2024-02-01
471	ES	Touchless ID	touchlessid-002	002	2023-01-23
472	ES	Touchless ID	touchlessid-003	003	2023-07-12
473	JP	Tripleize	aize-002	002	2021-10-08
474	JP	Tripleize	aize-003	003	2023-08-10
475	VN	TrueID-VNG	trueidvng-001	001	2023-01-05
476	US	Trueface.ai	trueface-002	002	2021-03-29
477	US	Trueface.ai	trueface-003	003	2021-09-30
478	UK	Trust Stamp	truststamp-001	001	2023-07-14
479	CN	TuringTech.vip	turingtechvip-001	001	2022-02-03
480	CN	TuringTech.vip	turingtechvip-002	002	2022-07-27
481	TR	Turkcell Technology	turkcell-000	000	2022-10-11
482	TR	Turkcell Technology	turkcell-001	001	2023-03-15
483	CN	ULSee Inc	ulsee-001	001	2019-07-31
484	UN	UNICC-Solution Architecture Section	unicc-002	002	2023-06-07
485	UN	UNICC-Solution Architecture Section	unicc-003	003	2023-10-16
486	TW	UXLabs	uxlabs-001	001	2022-09-19
487	TW	UXLabs	uxlabs-003	003	2023-07-28
488	FR	Unissey	unissey-003	003	2022-12-19
489	FR	Unissey	unissey-004	004	2023-07-19
490	PT	Universidade de Coimbra	visteam-007	007	2023-10-18

Table 7: Summary of participant information included in this report.

FNMR(T) "False non-match rate"
FMR(T) "False match rate"

	Location	Developer Name	Short Name	Seq. Num.	Validation Date
491	PT	Universidade de Coimbra	visteam-008	008	2024-02-06
492	UK	University of Surrey-CVSSP	surrey-cvssp-002	002	2023-02-16
493	UK	University of Surrey-CVSSP	surrey-cvssp-003	003	2023-09-13
494	US	VCognition	vcog-002	002	2017-06-12
495	VN	VNIS Joint Stock	vnis-000	000	2024-01-08
496	US	Vcortex Labs	vcortex-001	001	2023-06-14
497	ES	Veridas Digital Authentication Solutions S.L.	veridas-008	008	2022-10-17
498	ES	Veridas Digital Authentication Solutions S.L.	veridas-009	009	2023-05-08
499	UK	Veridium	veridium-002	002	2023-06-30
500	UK	Veridium	veridium-003	003	2024-02-21
501	KZ	Verigram	verigram-001	001	2022-03-09
502	KZ	Verigram	verigram-003	003	2023-08-09
503	ID	Verihubs	verihubs-inteligensia-001	001	2022-06-16
504	ID	Verihubs	verihubs-inteligensia-002	002	2023-06-07
505	ID	Verijelas	verijelas-000	000	2022-08-01
506	TW	Via Technologies Inc	via-004	004	2023-02-23
507	TW	Via Technologies Inc	via-005	005	2023-12-26
508	AE	Viante.AI	viante-000	000	2023-06-09
509	DE	Videmo Intelligente Videoanalyse	videmo-001	001	2021-12-22
510	DE	Videmo Intelligente Videoanalyse	videmo-002	002	2022-08-31
511	IN	Videonetics Technology Pvt	videonetics-001	001	2019-06-19
512	IN	Videonetics Technology Pvt	videonetics-002	002	2019-11-21
513	VN	Vietnam Payment Solution	vnpay-000	000	2023-12-05
514	VN	Vietnam Posts and Telecommunications Group	vnpt-005	005	2022-08-24
515	VN	Vietnam Posts and Telecommunications Group	vnpt-006	006	2023-08-18
516	VN	Viettel Cyberspace Center	vtcc-000	000	2023-06-26
517	VN	Viettel Cyberspace Center	vtcc-001	001	2023-11-20
518	VN	Viettel Group	vts-000	000	2020-11-04
519	VN	Viettel Group	vts-001	001	2022-04-20
520	VN	Viettel High Technology	viettelhightech-000	000	2021-08-04
521	US	Vigilant Solutions	vigilantsolutions-010	010	2021-04-07
522	US	Vigilant Solutions	vigilantsolutions-011	011	2021-08-07
523	VN	VinAI Research VietNam	vinai-000	000	2020-09-24
524	VN	VinBigData	vinbigdata-002	002	2022-06-07
525	VN	VinBigData	vinbigdata-003	003	2023-06-23
526	SE	Visage Technologies	visage-000	000	2020-12-09
527	FI	Visidon	vd-002	002	2021-04-12
528	FI	Visidon	vd-003	003	2021-10-12
529	CN	Vision Intelligence Center of Meituan	meituan-003	003	2023-03-06
530	CN	Vision Intelligence Center of Meituan	meituan-004	004	2023-08-16
531	PT	Vision-Box	visionbox-003	003	2023-02-01
532	PT	Vision-Box	visionbox-004	004	2023-06-30
533	RU	VisionLabs	visionlabs-010	010	2021-01-25
534	RU	VisionLabs	visionlabs-011	011	2021-10-13
535	AU	Vixvizon	vixvizion-006	006	2022-08-11
536	AU	Vixvizon	vixvizion-007	007	2023-01-17
537	RU	Vocord	vocord-009	009	2020-12-28
538	RU	Vocord	vocord-010	010	2021-12-20
539	US	Wicket	wicket-000	000	2022-02-14
540	CN	Winsense	winsense-001	001	2019-10-16
541	CN	Winsense	winsense-002	002	2020-11-20
542	MY	Wise AI SDN BHD	wiseai-001	001	2022-10-25
543	CN	Wuhan Tianyu Information Industry	wuhantianyu-001	001	2021-08-05
544	CN	X-Laboratory	x-laboratory-000	000	2019-09-03
545	CN	X-Laboratory	x-laboratory-001	001	2020-01-21
546	CN	Xforward AI Technology	xforwardai-001	001	2020-09-25
547	CN	Xforward AI Technology	xforwardai-002	002	2021-02-10
548	CN	Xiamen Meiya Pico Information	meiya-001	001	2019-03-01
549	CN	Xiamen University	xm-000	000	2020-10-19
550	PT	YooniK	yoonik-003	003	2022-01-06
551	PT	YooniK	yoonik-004	004	2023-02-10
552	UK	Yoti	yoti-001	001	2024-02-13
553	TW	Yuan High-Tech Development	yuan-005	005	2022-06-22
554	TW	Yuan High-Tech Development	yuan-008	008	2023-11-06
555	CN	Yuntu Data and Technology	ytu-000	000	2021-06-16
556	CN	Zhuhai Yisheng Electronics Technology	yisheng-004	004	2018-06-12
557	IN	i2v Systems	i2v-001	001	2024-03-11
558	VN	iCOMM Media and Tech	icomm-000	000	2023-12-26
559	CN	iQIYI Inc	iqface-000	000	2019-06-04
560	CN	iQIYI Inc	iqface-003	003	2021-02-23

Table 8: Summary of participant information included in this report.

FNMR(T) "False non-match rate"
FMR(T) "False match rate"

	Location	Developer Name	Short Name	Seq. Num.	Validation Date
561	TW	iSAP Solution Corporation	isap-001	001	2019-08-07
562	TW	iSAP Solution Corporation	isap-002	002	2020-09-01
563	TW	ioNetworks Inc	ionetworks-001	001	2023-08-01
564	TW	ioNetworks Inc	ionetworks-002	002	2023-12-08
565	KR	useB	useb-001	001	2023-09-12
566	KR	useB	useb-002	002	2024-01-19

Table 9: Summary of participant information included in this report.

FNMR(T) "False non-match rate"
FMR(T) "False match rate"

	ALGORITHM	CONFIG	LIBRARY	TEMPLATE						COMPARISON[4]	
	NAME	DATA	DATA	MEMORY	SIZE	GENERATION TIME (ms)[4]				TIME (ns)[5]	
		(KB)[1]	(KB)[2]	(MB)[3]	(B)	MUGSHOT	480x720	960x1440	1600x2400	3000x4500	GENUINE	IMPOSTOR
1	20face-000	117155	324083	344 1417	149 2048 ± 0	56 232 ± 1	44 223 ± 1	39 226 ± 4	30 222 ± 1	20 224 ± 1	540 44880 ± 134	538 44462 ± 163
2	20face-001	226824	324119	357 1512	497 4096 ± 0	69 279 ± 2	53 266 ± 1	45 266 ± 1	40 267 ± 1	30 267 ± 0	410 5553 ± 54	407 5541 ± 65
3	3divi-006	273866	52656	311 1252	143 2048 ± 0	276 654 ± 1	245 651 ± 0	226 660 ± 1	208 678 ± 2	205 759 ± 13	130 775 ± 19	128 770 ± 22
4	3divi-007	483115	24723	319 1288	218 2048 ± 0	253 615 ± 1	220 616 ± 1	203 623 ± 1	190 644 ± 1	192 727 ± 5	118 707 ± 31	119 712 ± 25
5	accurascan-002	14057	24437	240 945	28 512 ± 0	30 173 ± 23	33 188 ± 14	29 191 ± 14	25 208 ± 16	35 317 ± 14	474 12255 ± 69	473 12231 ± 72
6	accurascan-003	998397	27018	420 1996	113 2048 ± 0	290 676 ± 1	259 677 ± 7	250 700 ± 8	243 751 ± 16	271 950 ± 47	56 540 ± 10	57 536 ± 10
7	acer-001	36650	66086	87 417	32 512 ± 0	48 199 ± 0	47 237 ± 28	41 229 ± 26	37 242 ± 37	26 259 ± 21	308 2453 ± 44	309 2461 ± 62
8	acer-002	43922	624858	47 192	157 2048 ± 0	38 184 ± 0	30 184 ± 0	23 185 ± 0	19 185 ± 0	15 186 ± 0	358 3370 ± 47	358 3350 ± 54
9	acisw-007	267619	36111	60 287	193 2048 ± 0	74 283 ± 0	65 293 ± 3	89 414 ± 0	81 404 ± 0	83 484 ± 1	195 1316 ± 22	194 1297 ± 23
10	acisw-008	171703	39359	279 1102	329 2048 ± 0	130 400 ± 1	87 362 ± 28	72 369 ± 9	48 300 ± 2	40 336 ± 5	196 1327 ± 19	197 1337 ± 32
11	adera-004	0	959123	392 1748	549 6144 ± 0	506 1246 ± 1	456 1204 ± 1	454 1230 ± 2	412 1207 ± 2	363 1254 ± 1	250 1840 ± 34	249 1828 ± 31
12	adera-005	0	959113	388 1734	548 6144 ± 0	396 914 ± 1	338 879 ± 3	319 880 ± 2	293 886 ± 2	259 910 ± 2	260 1896 ± 14	257 1874 ± 20
13	advance-004	803133	954494	162 681	357 2048 ± 0	463 1099 ± 20	431 1107 ± 15	411 1093 ± 21	374 1103 ± 21	335 1138 ± 21	265 1935 ± 35	266 1936 ± 32
14	advance-005	277607	126218	151 624	163 2048 ± 0	221 573 ± 1	197 574 ± 2	172 573 ± 2	151 574 ± 2	130 601 ± 2	219 1517 ± 16	219 1518 ± 26
15	afisbiometrics-000	545886	32882	273 1085	31 512 ± 0	495 1219 ± 1	439 1135 ± 1	427 1137 ± 2	389 1137 ± 1	337 1147 ± 1	203 1400 ± 29	199 1357 ± 32
16	afrengine-002	579618	239125	254 1018	198 2048 ± 0	374 851 ± 3	417 1065 ± 16	372 993 ± 7	282 855 ± 5	241 857 ± 9	188 1259 ± 13	191 1270 ± 23
17	afrengine-003	579563	239117	253 1017	206 2048 ± 0	460 1088 ± 1	352 911 ± 15	404 1067 ± 5	273 833 ± 3	284 989 ± 2	192 1294 ± 48	193 1284 ± 29
18	aifirst-001	224157	808777	105 485	152 2048 ± 0	230 587 ± 2	194 568 ± 2	181 584 ± 3	164 601 ± 6	203 755 ± 5	169 1099 ± 14	170 1087 ± 45
19	aigen-001	256958	595227	290 1154	380 2048 ± 0	553 1448 ± 9	523 1451 ± 8	529 1759 ± 6	523 2594 ± 4	513 5691 ± 44	376 3772 ± 57	374 3736 ± 56
20	aigen-002	205300	1316138	230 896	140 2048 ± 0	228 586 ± 24	203 582 ± 4	331 920 ± 4	507 1758 ± 5	512 5427 ± 17	372 3678 ± 44	371 3646 ± 48
21	ailabs-001	1054663	338989	310 1252	345 2048 ± 0	282 664 ± 4	298 774 ± 50	430 1145 ± 12	514 1972 ± 74	509 5205 ± 272	559 104034 ± 661	559 103415 ± 7722
22	aimall-002	370156	25210	368 1576	372 2048 ± 0	336 776 ± 4	363 927 ± 27	340 940 ± 21	318 955 ± 34	289 1003 ± 75	557 72811 ± 7399	554 71216 ± 6286
23	aimall-003	504324	171935	410 1913	76 1024 ± 0	279 662 ± 1	288 740 ± 51	270 752 ± 62	240 741 ± 46	221 807 ± 47	529 34565 ± 93	529 34598 ± 118
24	aiseemu-001	0	1005354	475 2701	516 4096 ± 0	432 1001 ± 1	398 1017 ± 0	383 1014 ± 5	350 1022 ± 2	312 1059 ± 4	399 4864 ± 25	398 4855 ± 32
25	aiseemu-002	0	1216980	506 3453	479 4096 ± 0	519 1298 ± 5	484 1303 ± 4	476 1313 ± 2	448 1329 ± 0	393 1348 ± 2	402 4917 ± 37	399 4916 ± 37
26	aiunionface-000	241642	840295	82 402	164 2048 ± 0	266 637 ± 13	294 754 ± 41	385 1025 ± 28	402 1179 ± 29	452 1639 ± 47	163 1072 ± 19	167 1080 ± 47
27	aize-002	257106	182517	136 586	284 2048 ± 0	164 467 ± 1	144 479 ± 1	272 756 ± 1	492 1477 ± 1	505 4617 ± 41	70 597 ± 16	78 598 ± 14
28	aize-003	257130	33045	128 546	123 2048 ± 0	41 187 ± 0	32 188 ± 0	22 182 ± 0	18 183 ± 0	17 195 ± 0	90 621 ± 37	72 592 ± 1
29	ajou-001	363257	31734	94 442	240 2048 ± 0	194 530 ± 0	174 536 ± 0	153 535 ± 0	140 549 ± 0	121 577 ± 0	73 597 ± 19	76 596 ± 13
30	alchera-006	1000967	493456	347 1426	332 2048 ± 0	192 522 ± 2	177 540 ± 3	160 544 ± 2	148 569 ± 3	196 739 ± 3	289 2233 ± 38	290 2253 ± 77
31	alchera-007	1000948	493456	349 1430	362 2048 ± 0	196 530 ± 2	188 556 ± 2	168 566 ± 2	153 581 ± 2	206 762 ± 4	284 2178 ± 35	284 2169 ± 44
32	alfabeta-001	128232	21780	13 74	42 512 ± 0	66 271 ± 0	59 276 ± 0	113 459 ± 2	296 886 ± 2	483 2547 ± 9	48 470 ± 25	49 458 ± 20
33	alice-000	1741293	19355	504 3329	518 4096 ± 0	414 950 ± 2	365 933 ± 1	346 949 ± 1	348 1011 ± 3	366 1264 ± 8	486 14975 ± 201	485 14890 ± 229
34	alice-001	1428001	17074	165 690	350 2048 ± 0	458 1080 ± 1	418 1075 ± 0	415 1095 ± 1	392 1143 ± 1	415 1435 ± 1	512 21885 ± 278	511 21921 ± 265
35	alleyes-000	507636	997090	221 857	214 2048 ± 0	339 784 ± 1	378 970 ± 61	357 974 ± 62	314 943 ± 69	309 1057 ± 23	193 1298 ± 34	196 1303 ± 51
36	allgovision-000	172509	155862	132 561	139 2048 ± 0	122 384 ± 8	103 395 ± 17	87 413 ± 14	106 471 ± 14	181 710 ± 21	524 29903 ± 406	523 29735 ± 194
37	alphaface-001	259849	81636	121 527	318 2048 ± 0	251 612 ± 1	216 613 ± 3	196 612 ± 1	176 619 ± 1	148 640 ± 2	155 1008 ± 10	155 1002 ± 19
38	alphaface-002	768995	70692	350 1434	269 2048 ± 0	260 628 ± 2	290 746 ± 19	267 751 ± 18	252 779 ± 22	229 828 ± 40	148 945 ± 25	149 935 ± 17
39	amplifiedgroup-001	0	47053	15 81	72 866 ± 2	15 93 ± 0	-	-	-	-	549 57803 ± 4210	547 56365 ± 1196
40	androvideo-000	174847	585063	84 405	220 2048 ± 0	67 277 ± 0	62 285 ± 0	55 314 ± 0	68 372 ± 1	137 620 ± 0	332 2860 ± 28	330 2847 ± 22
41	anke-004	349388	410776	168 706	432 2056 ± 0	259 625 ± 1	229 627 ± 2	214 635 ± 3	194 653 ± 2	281 982 ± 8	99 633 ± 22	97 632 ± 34
42	anke-005	328553	429160	286 1134	427 2056 ± 0	232 590 ± 2	209 594 ± 5	190 601 ± 3	187 638 ± 4	226 821 ± 24	111 685 ± 19	114 687 ± 26
43	antheus-000	119453	41994	23 116	56 520 ± 0	18 109 ± 1	31 187 ± 1	27 189 ± 1	21 195 ± 1	22 236 ± 2	432 6901 ± 268	431 6936 ± 103
44	antheus-001	119453	41962	24 118	57 520 ± 0	22 120 ± 1	52 265 ± 13	122 468 ± 22	417 1223 ± 27	485 2660 ± 87	424 6218 ± 47	421 6216 ± 45

Notes	
1	The configuration size does not capture static data included in libraries.
2	The library size is the combined total of all files provided in the submission lib folder. These libraries e.g. OpenCV may or may not be installed on any end user's platform natively and would not need to be installed with the algorithm. Some developers put neural network models in their libraries.
3	The memory usage is the peak resident set size reported by the ps system call during template generation.
4	The median template creation times are measured on Intel®Xeon®CPU E5-2630 v4 @ 2.20GHz processors.
5	The comparison durations, in nanoseconds, are estimated using std::chrono::high_resolution_clock which on the machine in (2) counts 1ns clock ticks. Precision is somewhat worse than that however. The ± value is the median absolute deviation times 1.48 for Normal consistency.

Table 10: Summary of algorithms and properties included in this report. The red superscripts give ranking for the quantity in that column.

	ALGORITHM	CONFIG	LIBRARY	TEMPLATE							COMPARISON[4]	
	NAME	DATA	DATA	MEMORY	SIZE	GENERATION TIME (ms)[4]					TIME (ns)[5]	
		(KB)[1]	(KB)[2]	(MB)[3]	(B)	MUGSHOT	480x720	960x1440	1600x2400	3000x4500	GENUINE	IMPOSTOR
45	anyvision-004	401001	630797	280 1102	88 1024 ± 0	103 355 ± 1	-	-	-	-	259 1891 ± 51	250 1829 ± 85
46	anyvision-005	190979	116595	263 1048	83 1024 ± 0	426 985 ± 1	392 997 ± 1	380 1004 ± 1	332 995 ± 1	286 995 ± 1	123 733 ± 14	123 733 ± 16
47	aratek-001	254521	15993	435 2135	228 2048 ± 0	61 251 ± 1	58 275 ± 0	44 252 ± 0	42 278 ± 0	33 286 ± 0	244 1776 ± 20	241 1744 ± 38
48	armatura-001	0	374608	510 3518	196 2048 ± 0	301 688 ± 1	266 689 ± 1	244 693 ± 1	224 708 ± 3	204 756 ± 13	29 270 ± 17	31 268 ± 11
49	armatura-003	0	836082	367 1572	550 6144 ± 0	446 1028 ± 1	406 1032 ± 1	387 1027 ± 0	353 1036 ± 1	301 1041 ± 3	548 51850 ± 56	546 51835 ± 48
50	asusaics-000	257418	245320	143 605	217 2048 ± 0	174 484 ± 13	162 506 ± 21	303 850 ± 26	510 1789 ± 61	514 6305 ± 188	408 5455 ± 78	406 5422 ± 112
51	asusaics-001	257418	245330	139 595	503 4096 ± 0	370 842 ± 17	397 1008 ± 20	494 1377 ± 28	521 2423 ± 90	518 7284 ± 277	449 8618 ± 42	448 8638 ± 136
52	autentika-001	0	3198534	376 1650	227 2048 ± 0	296 683 ± 2	353 912 ± 4	327 908 ± 3	304 919 ± 3	253 893 ± 4	555 71804 ± 600	553 70747 ± 582
53	autentika-002	0	3198136	380 1676	348 2048 ± 0	115 374 ± 1	164 511 ± 1	150 528 ± 1	130 534 ± 1	108 546 ± 1	543 46941 ± 1172	540 46351 ± 822
54	authenmetric-003	293599	39492	223 866	280 2048 ± 0	431 992 ± 1	396 1006 ± 1	378 1003 ± 2	340 1002 ± 1	300 1036 ± 1	242 1757 ± 19	242 1755 ± 19
55	authenmetric-004	381165	39492	305 1214	299 2048 ± 0	393 910 ± 1	351 909 ± 1	328 915 ± 1	305 921 ± 2	270 950 ± 1	237 1724 ± 14	235 1691 ± 29
56	authme-001	1015124	37791	431 2097	487 4096 ± 0	412 949 ± 1	376 969 ± 7	353 960 ± 6	321 961 ± 1	275 966 ± 4	328 2836 ± 34	328 2827 ± 54
57	aware-007	135312	18711	81 388	20 480 ± 0	316 713 ± 1	281 716 ± 1	261 731 ± 3	254 785 ± 8	287 999 ± 30	160 1058 ± 23	171 1091 ± 37
58	aware-008	135312	18715	80 387	21 480 ± 0	328 751 ± 1	287 737 ± 0	264 739 ± 3	272 825 ± 9	291 1007 ± 27	173 1120 ± 25	181 1152 ± 35
59	awiros-001	15499	87480	18 88	43 512 ± 0	16 97 ± 6	13 98 ± 4	16 138 ± 6	32 225 ± 7	115 556 ± 8	166 1079 ± 44	163 1050 ± 45
60	awiros-002	289016	203723	130 556	294 2048 ± 0	171 479 ± 0	157 500 ± 0	152 534 ± 0	175 618 ± 0	268 946 ± 1	268 1966 ± 31	268 1957 ± 25
61	aximetria-001	408902	487912	462 2539	302 2048 ± 0	440 1013 ± 1	400 1023 ± 21	388 1029 ± 5	336 999 ± 2	320 1091 ± 5	391 4401 ± 94	388 4490 ± 80
62	ayftech-001	195423	43580	182 731	34 512 ± 0	137 408 ± 23	142 476 ± 52	287 814 ± 108	512 1827 ± 384	511 5412 ± 1029	86 615 ± 16	143 885 ± 44
63	ayftech-003	526164	127257	373 1640	204 2048 ± 0	434 1003 ± 5	399 1017 ± 6	382 1006 ± 6	346 1009 ± 7	314 1063 ± 5	194 1301 ± 20	195 1300 ± 25
64	ayonix-000	58505	5252	10 69	95 1036 ± 0	2 18 ± 2	-	-	-	-	91 621 ± 23	94 620 ± 26
65	beethedata-000	227849	1087592	131 557	303 2048 ± 0	162 465 ± 0	141 467 ± 0	120 468 ± 0	104 467 ± 0	77 467 ± 0	278 2121 ± 34	279 2110 ± 38
66	beyneai-000	256958	591433	421 1998	334 2048 ± 0	155 451 ± 8	131 449 ± 1	274 767 ± 7	504 1603 ± 25	506 4669 ± 124	373 3730 ± 57	372 3668 ± 54
67	biocube-001	25030	6192987	98 457	519 4096 ± 0	73 282 ± 22	64 292 ± 24	148 521 ± 57	211 684 ± 59	373 1282 ± 68	511 21787 ± 96	510 21812 ± 109
68	biocube-002	69898	10651580	102 468	517 4096 ± 0	363 826 ± 4	319 838 ± 4	437 1175 ± 4	526 2933 ± 1074	521 9144 ± 1090	515 23074 ± 94	513 23036 ± 99
69	bioidtechswiss-001	1178769	120811	352 1455	39 512 ± 0	418 966 ± 4	473 1270 ± 270	468 1294 ± 96	474 1409 ± 157	464 1793 ± 79	316 2610 ± 25	316 2624 ± 32
70	bioidtechswiss-002	744786	114842	248 990	41 512 ± 0	400 917 ± 2	364 930 ± 2	347 952 ± 2	315 947 ± 3	310 1058 ± 11	283 2177 ± 29	285 2170 ± 31
71	biometric-vision-000	445487	72132	235 915	298 2048 ± 0	367 836 ± 3	318 831 ± 3	310 869 ± 5	319 955 ± 8	398 1370 ± 19	481 14437 ± 161	479 14325 ± 167
72	bm-001	287734	38076	33 148	1 64 ± 0	152 444 ± 88	-	-	-	-	258 1887 ± 31	258 1877 ± 26
73	boetech-001	261376	88710	513 3658	187 2048 ± 0	65 271 ± 1	55 268 ± 1	46 273 ± 0	43 286 ± 1	36 318 ± 1	553 68519 ± 1921	551 67648 ± 822
74	boetech-002	294347	88710	425 2057	268 2048 ± 0	86 305 ± 4	69 296 ± 1	49 302 ± 1	50 313 ± 1	45 348 ± 2	554 68921 ± 2137	552 69473 ± 2104
75	bresee-001	287880	23227	307 1223	355 2048 ± 0	498 1223 ± 3	461 1216 ± 1	480 1331 ± 1	419 1227 ± 1	396 1360 ± 1	533 37240 ± 655	532 37167 ± 584
76	bresee-002	313627	30902	414 1951	346 2048 ± 0	326 743 ± 4	441 1143 ± 2	431 1146 ± 2	393 1148 ± 2	346 1176 ± 2	245 1778 ± 22	244 1775 ± 23
77	camvi-002	236278	225285	184 737	82 1024 ± 0	292 677 ± 7	285 726 ± 36	311 869 ± 28	385 1129 ± 43	491 2785 ± 113	85 612 ± 26	83 603 ± 20
78	camvi-004	280733	615819	236 919	311 2048 ± 0	330 759 ± 10	329 861 ± 17	364 986 ± 34	433 1279 ± 51	493 2891 ± 158	149 948 ± 40	150 963 ± 31
79	candour-001	150086	97632	104 477	238 2048 ± 0	544 1400 ± 1	508 1396 ± 1	505 1408 ± 1	473 1407 ± 1	424 1464 ± 1	465 10725 ± 133	464 10712 ± 127
80	canon-004	2399160	114188	551 7037	553 6200 ± 0	411 948 ± 4	373 955 ± 3	352 959 ± 3	325 977 ± 3	315 1064 ± 2	436 7172 ± 63	434 7169 ± 51
81	canon-005	2521818	80309	548 6700	536 4148 ± 0	497 1223 ± 21	464 1221 ± 2	453 1230 ± 4	421 1234 ± 5	390 1329 ± 3	423 6142 ± 99	422 6226 ± 146
82	cchonolulu-000	727461	37284	86 416	44 512 ± 0	24 123 ± 13	18 126 ± 10	15 129 ± 10	14 134 ± 10	19 223 ± 10	238 1726 ± 35	236 1697 ± 35
83	cchonolulu-001	733744	37284	90 426	327 2048 ± 0	27 162 ± 21	35 197 ± 23	142 513 ± 96	377 1118 ± 267	474 2142 ± 584	392 4418 ± 37	386 4361 ± 35
84	ceiec-003	260371	88707	91 430	170 2048 ± 0	355 817 ± 4	341 883 ± 57	320 897 ± 60	299 899 ± 72	266 944 ± 72	291 2256 ± 38	289 2241 ± 54
85	ceiec-004	263476	67011	85 408	176 2048 ± 0	444 1024 ± 1	403 1027 ± 1	386 1027 ± 1	352 1030 ± 1	306 1055 ± 1	252 1844 ± 26	252 1836 ± 20
86	chosun-001	765615	707	109 491	188 2048 ± 0	337 783 ± 2	314 826 ± 4	528 1662 ± 13	529 3679 ± 67	527 11694 ± 243	152 998 ± 25	161 1035 ± 11
87	chosun-002	234001	31875	96 451	200 2048 ± 0	60 248 ± 3	56 273 ± 3	525 1495 ± 14	532 7920 ± 90	531 80302 ± 1349	92 623 ± 17	100 634 ± 13
88	chtface-005	408364	311100	342 1415	130 2048 ± 0	93 322 ± 0	74 316 ± 1	59 325 ± 2	56 324 ± 1	63 411 ± 2	262 1907 ± 19	260 1898 ± 23

Notes	
1	The configuration size does not capture static data included in libraries.
2	The library size is the combined total of all files provided in the submission lib folder. These libraries e.g. OpenCV may or may not be installed on any end user's platform natively and would not need to be installed with the algorithm. Some developers put neural network models in their libraries.
3	The memory usage is the peak resident set size reported by the ps system call during template generation.
4	The median template creation times are measured on Intel®Xeon®CPU E5-2630 v4 @ 2.20GHz processors.
5	The comparison durations, in nanoseconds, are estimated using std::chrono::high_resolution_clock which on the machine in (2) counts 1ns clock ticks. Precision is somewhat worse than that however. The ± value is the median absolute deviation times 1.48 for Normal consistency.

Table 11: Summary of algorithms and properties included in this report. The red superscripts give ranking for the quantity in that column.

	ALGORITHM	CONFIG	LIBRARY	TEMPLATE							COMPARISON[4]	
	NAME	DATA	DATA	MEMORY	SIZE	GENERATION TIME (ms)[4]					TIME (ns)[5]	
		(KB)[1]	(KB)[2]	(MB)[3]	(B)	MUGSHOT	480x720	960x1440	1600x2400	3000x4500	GENUINE	IMPOSTOR
89	chtface-006	733645	610439	453 2424	172 2048 ± 0	191 522 ± 1	166 514 ± 1	154 536 ± 2	144 561 ± 1	174 693 ± 2	273 2034 ± 41	275 2049 ± 29
90	cist-003	0	1267350	476 2706	546 5248 ± 0	517 1291 ± 1	483 1300 ± 1	488 1352 ± 3	436 1287 ± 2	382 1313 ± 1	441 7838 ± 63	440 7823 ± 40
91	cist-004	0	1603990	463 2563	547 5248 ± 0	504 1243 ± 1	474 1271 ± 1	461 1264 ± 3	424 1252 ± 1	374 1287 ± 1	355 3216 ± 25	355 3220 ± 32
92	clearviewai-000	342491	211852	480 2745	257 2048 ± 0	545 1402 ± 1	510 1403 ± 1	507 1412 ± 1	477 1420 ± 1	408 1418 ± 1	222 1592 ± 37	222 1561 ± 37
93	clearviewai-001	613532	511807	332 1353	390 2048 ± 0	265 635 ± 2	241 642 ± 1	225 659 ± 1	198 664 ± 1	166 674 ± 1	137 827 ± 10	138 829 ± 20
94	closeli-001	420342	9851	194 773	501 4096 ± 0	369 839 ± 1	321 843 ± 1	299 841 ± 1	277 845 ± 1	244 865 ± 1	407 5404 ± 17	405 5400 ± 25
95	cloudmatrix-001	10390	542121	52 249	360 2048 ± 0	20 114 ± 1	15 117 ± 0	13 118 ± 0	13 123 ± 1	12 169 ± 1	546 50263 ± 212	544 50243 ± 237
96	cloudmatrix-002	256635	693318	262 1036	185 2048 ± 0	126 395 ± 1	105 398 ± 1	83 399 ± 1	78 402 ± 1	69 437 ± 20	545 49578 ± 120	543 49602 ± 180
97	cloudwalk-hr-003	383739	144263	245 983	445 2057 ± 0	244 606 ± 0	206 588 ± 0	186 594 ± 0	169 612 ± 1	109 547 ± 2	433 6982 ± 80	432 6972 ± 84
98	cloudwalk-hr-004	502916	520169	340 1399	394 2049 ± 0	382 873 ± 1	337 877 ± 1	316 876 ± 1	289 879 ± 1	258 902 ± 3	471 11652 ± 127	470 11608 ± 123
99	cloudwalk-mt-006	563322	480071	508 3499	208 2048 ± 0	537 1385 ± 0	506 1392 ± 1	500 1398 ± 1	469 1397 ± 4	420 1444 ± 2	357 3364 ± 96	356 3324 ± 83
100	cloudwalk-mt-007	563322	480071	509 3499	199 2048 ± 0	535 1379 ± 2	516 1425 ± 7	510 1427 ± 6	476 1417 ± 2	418 1443 ± 7	344 3000 ± 68	341 2971 ± 74
101	cmcuni-001	0	604227	294 1177	236 2048 ± 0	478 1161 ± 1	453 1187 ± 1	444 1194 ± 5	410 1200 ± 1	353 1207 ± 1	353 3153 ± 22	352 3158 ± 26
102	codeline-000	361659	138388	301 1194	254 2048 ± 0	554 1453 ± 0	525 1456 ± 2	519 1456 ± 0	485 1457 ± 0	430 1483 ± 1	281 2171 ± 69	286 2194 ± 84
103	cogent-007	621565	72316	408 1888	65 550 ± 0	528 1329 ± 2	496 1333 ± 5	483 1337 ± 4	453 1353 ± 5	403 1390 ± 4	38 355 ± 8	39 367 ± 14
104	cogent-008	856817	73587	439 2176	66 550 ± 0	548 1412 ± 1	515 1419 ± 2	509 1426 ± 3	480 1437 ± 3	429 1476 ± 1	44 436 ± 14	44 441 ± 23
105	cognitec-004	705645	62678	134 580	408 2052 ± 0	160 463 ± 9	154 497 ± 9	137 504 ± 10	125 521 ± 10	141 631 ± 12	347 3028 ± 197	347 3059 ± 238
106	cognitec-005	326804	198231	207 819	399 2052 ± 0	88 311 ± 10	88 364 ± 12	73 370 ± 10	70 390 ± 10	90 498 ± 16	298 2332 ± 48	300 2330 ± 40
107	cor-001	1194948	11240	309 1249	447 2060 ± 0	313 699 ± 3	330 863 ± 76	309 865 ± 80	285 872 ± 89	272 952 ± 39	562 270145 ± 2259	562 282686 ± 11788
108	coretech-001	235361	305490	358 1523	270 2048 ± 0	302 688 ± 7	270 695 ± 7	312 870 ± 17	290 879 ± 15	249 877 ± 15	93 625 ± 25	105 641 ± 25
109	coretech-002	339881	296194	502 3300	347 2048 ± 0	158 459 ± 1	132 451 ± 1	304 851 ± 1	286 875 ± 2	280 980 ± 2	307 2443 ± 17	304 2436 ± 13
110	corsight-002	1474921	32093	409 1892	450 2080 ± 0	516 1290 ± 1	479 1287 ± 1	466 1290 ± 1	438 1307 ± 2	402 1388 ± 4	518 24953 ± 637	515 24263 ± 578
111	corsight-003	1413063	32198	374 1642	452 2080 ± 0	491 1202 ± 2	455 1190 ± 5	446 1199 ± 3	422 1236 ± 3	395 1349 ± 7	523 28754 ± 434	522 28279 ± 446
112	csc-002	0	519768	3 30	62 544 ± 0	168 473 ± 0	153 494 ± 0	126 481 ± 1	113 490 ± 1	96 514 ± 5	40 367 ± 11	40 371 ± 10
113	csc-003	0	400435	4 31	61 544 ± 0	181 499 ± 0	158 500 ± 1	136 502 ± 0	122 508 ± 1	104 535 ± 4	43 393 ± 8	42 397 ± 7
114	ctbcbank-000	257208	599238	133 570	328 2048 ± 0	216 568 ± 43	213 606 ± 38	243 690 ± 53	227 711 ± 50	231 831 ± 51	366 3551 ± 87	395 4805 ± 209
115	ctbcbank-001	275511	599238	140 603	232 2048 ± 0	272 652 ± 35	301 781 ± 30	315 875 ± 43	298 898 ± 51	298 1030 ± 47	379 3926 ± 45	378 3924 ± 56
116	cu-face-003	1015124	37791	432 2116	495 4096 ± 0	410 945 ± 1	372 955 ± 3	350 957 ± 2	317 949 ± 3	273 963 ± 2	323 2769 ± 19	324 2782 ± 41
117	cu-face-004	1016682	37791	427 2083	499 4096 ± 0	442 1022 ± 1	404 1031 ± 1	375 998 ± 3	366 1070 ± 1	295 1021 ± 2	334 2884 ± 38	333 2864 ± 48
118	cubox-002	542254	90975	417 1966	116 2048 ± 0	401 921 ± 1	358 921 ± 1	334 922 ± 1	309 933 ± 1	290 1003 ± 1	271 2008 ± 72	270 1969 ± 57
119	cubox-003	1694397	209684	507 3491	191 2048 ± 0	482 1179 ± 0	454 1189 ± 0	445 1198 ± 0	413 1208 ± 0	367 1264 ± 1	295 2289 ± 112	295 2297 ± 68
120	cudocommunication-001	385258	341277	272 1080	282 2048 ± 0	403 925 ± 1	360 923 ± 1	337 928 ± 1	308 932 ± 0	274 964 ± 1	313 2534 ± 20	315 2537 ± 20
121	cuhkee-001	787853	74917	461 2515	416 2052 ± 0	423 977 ± 31	-	-	-	-	319 2719 ± 60	325 2783 ± 56
122	cybercore-002	166096	7374	464 2565	310 2048 ± 0	177 489 ± 1	156 500 ± 4	135 500 ± 1	118 499 ± 2	102 528 ± 1	475 12389 ± 123	474 12352 ± 112
123	cybercore-003	289176	7969	527 4311	513 4096 ± 0	371 844 ± 2	327 855 ± 4	308 864 ± 4	284 862 ± 4	250 878 ± 2	415 5744 ± 41	415 5737 ± 31
124	cyberextruder-003	253300	12354	95 444	47 512 ± 0	125 390 ± 1	100 388 ± 1	82 393 ± 1	76 399 ± 1	66 435 ± 1	19 198 ± 4	18 189 ± 8
125	cyberextruder-004	169301	12354	69 302	4 128 ± 0	50 206 ± 0	40 208 ± 0	33 209 ± 0	35 229 ± 0	25 249 ± 1	9 145 ± 14	11 155 ± 14
126	cyberlink-012	1200318	102281	484 2789	554 6212 ± 0	240 601 ± 1	223 621 ± 5	195 610 ± 2	171 614 ± 2	155 649 ± 5	301 2343 ± 26	302 2377 ± 34
127	cyberlink-013	893519	102285	415 1964	555 6212 ± 0	242 603 ± 1	211 602 ± 2	193 606 ± 2	170 613 ± 2	150 642 ± 1	34 307 ± 7	34 306 ± 5
128	dahua-006	831641	119261	535 5068	159 2048 ± 0	543 1398 ± 2	509 1397 ± 1	504 1404 ± 1	470 1402 ± 1	405 1402 ± 1	27 249 ± 13	28 250 ± 11
129	dahua-007	1578737	119418	553 7237	475 4096 ± 0	542 1393 ± 2	502 1373 ± 1	496 1378 ± 1	462 1378 ± 1	400 1379 ± 2	41 367 ± 102	43 434 ± 108
130	daon-000	280726	2307	423 2010	448 2065 ± 0	214 562 ± 3	202 581 ± 5	276 791 ± 9	274 838 ± 15	305 1055 ± 32	495 16052 ± 88	494 16041 ± 85
131	datech-000	617605	139575	540 5599	481 4096 ± 0	220 573 ± 32	204 583 ± 44	185 593 ± 37	534 14123 ± 9564	529 15514 ± 2343	442 7857 ± 29	441 7852 ± 25
132	datech-001	835404	139615	552 7179	478 4096 ± 0	441 1017 ± 83	411 1057 ± 65	401 1062 ± 88	375 1109 ± 81	378 1299 ± 92	443 7944 ± 31	442 7981 ± 56

Notes	
1	The configuration size does not capture static data included in libraries.
2	The library size is the combined total of all files provided in the submission lib folder. These libraries e.g. OpenCV may or may not be installed on any end user's platform natively and would not need to be installed with the algorithm. Some developers put neural network models in their libraries.
3	The memory usage is the peak resident set size reported by the ps system call during template generation.
4	The median template creation times are measured on Intel®Xeon®CPU E5-2630 v4 @ 2.20GHz processors.
5	The comparison durations, in nanoseconds, are estimated using std::chrono::high_resolution_clock which on the machine in (2) counts 1ns clock ticks. Precision is somewhat worse than that however. The ± value is the median absolute deviation times 1.48 for Normal consistency.

Table 12: Summary of algorithms and properties included in this report. The red superscripts give ranking for the quantity in that column.

	ALGORITHM	CONFIG	LIBRARY	TEMPLATE						COMPARISON[4]	
	NAME	DATA	DATA	MEMORY	SIZE	GENERATION TIME (ms)[4]				TIME (ns)[5]	
		(KB)[1]	(KB)[2]	(MB)[3]	(B)	MUGSHOT	480x720	960x1440	1600x2400	3000x4500	GENUINE	IMPOSTOR
133	decatur-000	350495	171271	232 907	526 4100 ± 0	443 1024 ± 2	-	-	-	-	469 11439 ± 80	468 11418 ± 112
134	decatur-001	342866	253734	356 1508	398 2052 ± 0	465 1103 ± 2	415 1064 ± 2	402 1063 ± 2	362 1067 ± 2	317 1084 ± 2	82 610 ± 19	81 602 ± 8
135	decloakface-001	29693	170719	77 368	307 2048 ± 0	45 196 ± 58	37 201 ± 52	40 229 ± 53	47 298 ± 60	103 532 ± 61	395 4638 ± 19	392 4646 ± 22
136	deepglint-004	1073382	261571	498 3116	297 2048 ± 0	557 1470 ± 1	529 1474 ± 1	524 1485 ± 1	490 1474 ± 1	434 1492 ± 2	421 5961 ± 34	420 5955 ± 29
137	deepglint-005	960326	213877	494 2991	383 2048 ± 0	547 1408 ± 1	518 1431 ± 2	508 1424 ± 3	478 1424 ± 3	421 1446 ± 2	430 6765 ± 38	428 6765 ± 40
138	deepsea-001	147497	336250	74 358	89 1024 ± 0	261 630 ± 7	293 752 ± 37	265 746 ± 30	233 727 ± 32	224 820 ± 32	204 1401 ± 37	211 1467 ± 50
139	deepsense-002	73173	1266131	536 5280	74 896 ± 0	531 1350 ± 1	482 1299 ± 8	477 1324 ± 0	452 1348 ± 0	427 1474 ± 4	364 3505 ± 32	366 3515 ± 40
140	deepsense-003	73173	1359497	545 6555	75 901 ± 0	366 832 ± 2	366 940 ± 2	301 845 ± 4	328 983 ± 1	279 976 ± 7	247 1797 ± 25	247 1795 ± 19
141	dermalog-011	0	278395	173 716	2 128 ± 0	100 343 ± 0	82 345 ± 0	64 347 ± 0	61 351 ± 0	50 363 ± 0	32 299 ± 19	29 253 ± 14
142	dermalog-012	0	293431	175 723	3 128 ± 0	36 181 ± 0	24 179 ± 0	21 182 ± 0	20 186 ± 0	24 242 ± 0	11 163 ± 10	20 196 ± 16
143	dicio-001	61751	119517	17 84	58 520 ± 0	201 538 ± 0	191 563 ± 10	329 915 ± 3	511 1800 ± 7	510 5286 ± 30	325 2818 ± 20	326 2807 ± 31
144	didiglobalface-001	259849	70680	120 527	296 2048 ± 0	250 612 ± 1	237 633 ± 3	213 634 ± 3	192 650 ± 15	162 666 ± 4	150 973 ± 20	152 988 ± 20
145	didiglobalface-002	260054	161508	204 812	309 2048 ± 0	257 622 ± 1	236 633 ± 1	219 642 ± 2	196 659 ± 4	191 726 ± 15	61 560 ± 10	65 567 ± 13
146	digidata-000	133370	30249	55 259	145 2048 ± 0	108 361 ± 0	85 360 ± 0	69 361 ± 0	64 363 ± 0	53 380 ± 0	277 2084 ± 37	273 2039 ± 42
147	digidata-001	254564	33036	75 367	226 2048 ± 0	211 559 ± 1	189 561 ± 1	167 562 ± 1	145 564 ± 1	131 602 ± 1	463 10308 ± 102	462 10301 ± 121
148	digitalbarriers-002	83002	598577	412 1930	420 2056 ± 0	51 209 ± 11	49 250 ± 19	86 411 ± 37	260 808 ± 72	475 2236 ± 123	477 13409 ± 228	476 13267 ± 206
149	dps-000	0	2211812	341 1405	484 4096 ± 0	379 868 ± 2	344 893 ± 6	516 1445 ± 9	525 2910 ± 38	522 9345 ± 17	212 1473 ± 37	213 1479 ± 37
150	dsk-000	11967	782905	54 252	36 512 ± 0	84 304 ± 47	76 317 ± 33	376 1001 ± 96	524 2660 ± 170	525 10451 ± 832	435 7152 ± 115	433 7134 ± 111
151	einetworks-000	372608	219883	225 880	424 2056 ± 0	270 645 ± 3	-	-	-	-	400 4876 ± 66	401 5156 ± 77
152	einetworksindia-000	372375	479472	328 1322	422 2056 ± 0	116 378 ± 1	96 382 ± 1	78 383 ± 1	75 397 ± 0	74 456 ± 3	491 15171 ± 41	489 15138 ± 62
153	einetworksindia-001	562398	481792	398 1808	434 2056 ± 0	169 479 ± 0	146 481 ± 1	128 485 ± 1	116 494 ± 1	107 541 ± 1	489 15147 ± 63	488 15134 ± 74
154	ekin-002	51434	278	28 139	464 3072 ± 0	487 1186 ± 13	450 1180 ± 12	440 1181 ± 11	408 1191 ± 11	352 1207 ± 8	388 4294 ± 80	409 5569 ± 112
155	element-000	721679	24895	317 1287	305 2048 ± 0	129 399 ± 1	114 417 ± 1	97 428 ± 9	108 478 ± 14	171 688 ± 45	67 583 ± 10	68 585 ± 13
156	enface-001	370710	173609	160 669	84 1024 ± 0	208 550 ± 4	187 555 ± 3	231 668 ± 7	326 981 ± 15	480 2416 ± 59	429 6734 ± 68	429 6766 ± 69
157	enface-002	858356	98741	556 9004	90 1024 ± 0	445 1026 ± 1	408 1038 ± 3	398 1057 ± 7	380 1123 ± 4	391 1338 ± 8	221 1529 ± 23	220 1530 ± 35
158	eocortex-000	255937	59432	49 224	120 2048 ± 0	85 305 ± 22	81 341 ± 25	104 440 ± 47	103 464 ± 45	95 513 ± 44	147 923 ± 11	148 918 ± 11
159	ercacat-001	811623	58012	486 2816	403 2052 ± 0	451 1052 ± 3	-	-	-	-	315 2551 ± 62	312 2501 ± 81
160	euronovate-003	0	5637394	300 1193	458 2201 ± 0	83 300 ± 0	71 300 ± 0	50 303 ± 0	49 310 ± 0	42 340 ± 0	534 37908 ± 968	533 38285 ± 938
161	euronovate-004	0	1335993	264 1049	457 2201 ± 0	75 290 ± 0	66 294 ± 0	47 294 ± 0	45 295 ± 0	34 294 ± 0	541 46290 ± 490	539 46199 ± 484
162	expasoft-001	39057	983064	30 142	364 2048 ± 0	11 70 ± 0	9 74 ± 0	8 77 ± 0	7 73 ± 0	6 74 ± 0	231 1660 ± 35	232 1676 ± 48
163	expasoft-002	38760	59825	39 170	265 2048 ± 0	8 34 ± 0	5 34 ± 0	5 34 ± 0	4 34 ± 0	2 34 ± 0	451 8870 ± 78	450 8838 ± 77
164	f8-001	272977	19668	315 1276	376 2048 ± 0	361 822 ± 39	-	-	-	-	494 15262 ± 139	493 15277 ± 212
165	f8-002	28278	215616	16 84	387 2048 ± 0	9 39 ± 0	7 41 ± 0	7 75 ± 0	24 197 ± 1	176 702 ± 1	485 14765 ± 131	484 14790 ± 133
166	facehawk-000	120009	7737	26 129	71 776 ± 1	128 399 ± 0	108 402 ± 0	88 414 ± 1	73 391 ± 2	70 440 ± 3	467 10931 ± 155	466 10915 ± 149
167	facelocate-001	4739	11106	459 2449	5 168 ± 0	7 34 ± 1	6 38 ± 0	11 84 ± 1	11 112 ± 4	18 206 ± 13	455 9565 ± 91	456 9629 ± 131
168	faceonlive-001	0	71529	64 300	423 2056 ± 0	34 179 ± 0	25 179 ± 0	28 190 ± 0	29 217 ± 0	43 343 ± 1	161 1064 ± 37	160 1033 ± 35
169	faceonlive-002	155220	141019	249 997	243 2048 ± 0	338 783 ± 1	306 797 ± 2	279 794 ± 2	261 809 ± 3	257 901 ± 2	478 13798 ± 197	477 13743 ± 127
170	facephi-000	148904	5219	561 20248	366 2048 ± 0	381 871 ± 2	339 881 ± 3	318 880 ± 4	297 888 ± 4	269 949 ± 12	383 4067 ± 53	383 4047 ± 53
171	facesoft-000	370120	10612	200 796	256 2048 ± 0	289 675 ± 18	250 669 ± 3	239 686 ± 3	205 675 ± 5	169 687 ± 2	290 2239 ± 28	293 2277 ± 96
172	facetag-000	1232331	4022	241 965	69 684 ± 0	102 355 ± 17	92 369 ± 8	367 989 ± 33	520 2408 ± 91	519 7930 ± 316	556 72003 ± 625	555 71912 ± 612
173	facetag-002	819806	4021	169 706	150 2048 ± 0	204 544 ± 1	182 544 ± 0	158 542 ± 0	137 545 ± 0	114 554 ± 0	239 1730 ± 25	238 1733 ± 25
174	facex-001	305074	930372	505 3336	338 2048 ± 0	143 422 ± 4	125 434 ± 4	147 520 ± 7	239 737 ± 13	455 1670 ± 27	256 1871 ± 23	254 1846 ± 29
175	facex-002	305074	928334	495 3011	171 2048 ± 0	144 426 ± 5	121 429 ± 4	144 516 ± 8	235 730 ± 12	461 1738 ± 36	96 631 ± 25	92 614 ± 19
176	facia-001	296496	745403	228 889	295 2048 ± 0	464 1099 ± 1	433 1109 ± 0	422 1113 ± 0	381 1125 ± 3	361 1250 ± 1	552 62245 ± 397	550 62249 ± 496

Notes	
1	The configuration size does not capture static data included in libraries.
2	The library size is the combined total of all files provided in the submission lib folder. These libraries e.g. OpenCV may or may not be installed on any end user's platform natively and would not need to be installed with the algorithm. Some developers put neural network models in their libraries.
3	The memory usage is the peak resident set size reported by the ps system call during template generation.
4	The median template creation times are measured on Intel®Xeon®CPU E5-2630 v4 @ 2.20GHz processors.
5	The comparison durations, in nanoseconds, are estimated using std::chrono::high_resolution_clock which on the machine in (2) counts 1ns clock ticks. Precision is somewhat worse than that however. The ± value is the median absolute deviation times 1.48 for Normal consistency.

Table 13: Summary of algorithms and properties included in this report. The red superscripts give ranking for the quantity in that column.

	ALGORITHM	CONFIG	LIBRARY	TEMPLATE						COMPARISON[4]	
	NAME	DATA	DATA	MEMORY	SIZE	GENERATION TIME (ms)[4]				TIME (ns)[5]	
		(KB)[1]	(KB)[2]	(MB)[3]	(B)	MUGSHOT	480x720	960x1440	1600x2400	3000x4500	GENUINE	IMPOSTOR
177	farfaces-001	346494	44581	56 262	37 512 ± 0	484 1179 ± 1	451 1180 ± 1	439 1180 ± 0	404 1185 ± 1	355 1209 ± 2	141 855 ± 25	140 860 ± 31
178	fastenterprises-000	273365	235899	256 1030	264 2048 ± 0	280 662 ± 1	251 671 ± 0	229 664 ± 0	204 673 ± 3	170 688 ± 5	377 3806 ± 96	527 32064 ± 185
179	fedu-001	466605	496375	364 1557	202 2048 ± 0	235 592 ± 1	224 623 ± 1	205 624 ± 0	179 623 ± 0	152 647 ± 0	302 2362 ± 13	301 2361 ± 22
180	fiberhome-nanjing-003	352895	1482309	222 859	260 2048 ± 0	474 1136 ± 7	438 1134 ± 4	425 1132 ± 3	390 1139 ± 3	339 1154 ± 5	168 1097 ± 38	168 1083 ± 42
181	fiberhome-nanjing-004	443779	1482313	270 1077	473 4096 ± 0	525 1321 ± 5	486 1304 ± 3	474 1307 ± 2	440 1308 ± 3	388 1326 ± 5	190 1276 ± 40	190 1265 ± 38
182	fincore-000	256615	19409	125 536	274 2048 ± 0	187 508 ± 3	161 505 ± 0	139 508 ± 1	124 513 ± 2	105 535 ± 1	243 1765 ± 31	243 1763 ± 22
183	firstcreditkz-002	977538	24879	413 1951	300 2048 ± 0	509 1265 ± 1	475 1275 ± 4	472 1299 ± 7	451 1341 ± 17	438 1515 ± 40	128 761 ± 28	129 774 ± 32
184	firstcreditkz-003	1145884	24907	437 2144	215 2048 ± 0	489 1188 ± 79	531 1492 ± 77	532 2566 ± 293	531 4939 ± 888	528 14753 ± 3518	87 616 ± 10	91 613 ± 16
185	foomobi-001	0	219961	43 189	324 2048 ± 0	105 357 ± 0	99 388 ± 2	428 1138 ± 1	527 2974 ± 10	523 10101 ± 10	544 47409 ± 453	542 47413 ± 421
186	foomobi-002	0	219961	42 189	131 2048 ± 0	82 299 ± 0	77 323 ± 0	351 957 ± 1	522 2496 ± 2	520 8549 ± 7	525 30257 ± 724	524 30010 ± 320
187	fpt-000	19013	170633	48 219	359 2048 ± 0	21 118 ± 0	17 122 ± 1	14 122 ± 0	12 120 ± 0	14 178 ± 2	378 3871 ± 31	377 3883 ± 29
188	fraudcom-000	354020	561861	242 966	409 2052 ± 0	212 561 ± 2	176 539 ± 2	156 541 ± 1	142 557 ± 5	125 594 ± 6	292 2258 ± 10	291 2256 ± 29
189	frpkauai-001	507771	24807	525 4143	353 2048 ± 0	306 689 ± 1	269 691 ± 0	247 697 ± 2	230 714 ± 6	213 775 ± 31	126 752 ± 29	127 764 ± 23
190	frpkauai-002	519141	24803	282 1113	289 2048 ± 0	347 799 ± 0	387 987 ± 0	395 1046 ± 1	397 1163 ± 2	463 1769 ± 4	144 907 ± 20	144 886 ± 28
191	fujitsulab-002	0	1088887	381 1685	531 4104 ± 0	501 1237 ± 2	465 1222 ± 2	455 1236 ± 1	423 1251 ± 2	389 1327 ± 2	327 2836 ± 25	327 2809 ± 44
192	fujitsulab-003	662263	318209	547 6691	530 4104 ± 0	415 951 ± 20	367 941 ± 19	348 952 ± 19	323 971 ± 20	302 1045 ± 21	331 2855 ± 16	331 2849 ± 19
193	g42-intellibrain-001	1031335	235521	564 25154	14 269 ± 0	422 976 ± 6	379 975 ± 1	374 997 ± 2	364 1068 ± 3	397 1362 ± 8	418 5878 ± 96	418 5865 ± 71
194	g42-intellibrain-002	1043920	132389	560 19747	13 269 ± 0	397 915 ± 2	356 920 ± 2	344 946 ± 2	334 998 ± 4	359 1224 ± 8	483 14703 ± 56	483 14658 ± 97
195	geo-002	369903	98667	255 1021	261 2048 ± 0	341 791 ± 1	305 793 ± 0	278 794 ± 0	256 795 ± 1	219 803 ± 1	361 3407 ± 45	362 3422 ± 65
196	geo-004	168980	107714	318 1287	385 2048 ± 0	510 1268 ± 1	477 1279 ± 1	462 1274 ± 0	428 1259 ± 1	377 1296 ± 1	156 1023 ± 20	158 1028 ± 22
197	gistouch-000	155338	444582	127 541	335 2048 ± 0	95 325 ± 1	79 326 ± 1	63 337 ± 1	62 354 ± 1	89 495 ± 1	454 9505 ± 604	451 9443 ± 388
198	gistouch-001	426635	444545	377 1651	291 2048 ± 0	405 930 ± 3	355 919 ± 3	339 937 ± 4	322 966 ± 2	327 1113 ± 1	447 8475 ± 133	446 8460 ± 173
199	glory-006	0	1004784	456 2438	537 4182 ± 0	314 704 ± 1	299 774 ± 0	356 968 ± 2	518 2286 ± 18	524 10381 ± 151	417 5853 ± 77	417 5819 ± 74
200	glory-007	0	1004846	457 2442	538 4182 ± 0	124 385 ± 0	122 431 ± 0	175 575 ± 14	487 1464 ± 24	515 6782 ± 62	365 3506 ± 51	365 3489 ± 66
201	gorilla-008	450175	707000	400 1812	562 8338 ± 0	238 595 ± 1	207 590 ± 0	189 600 ± 1	178 621 ± 2	188 720 ± 9	394 4530 ± 44	390 4524 ± 38
202	gorilla-009	329584	297395	325 1304	540 4242 ± 0	391 899 ± 2	359 922 ± 1	323 901 ± 3	306 924 ± 4	299 1032 ± 12	297 2294 ± 74	297 2301 ± 66
203	gpstechvn-000	108365	345975	468 2646	377 2048 ± 0	81 296 ± 1	70 297 ± 1	51 304 ± 0	51 316 ± 0	54 382 ± 0	306 2442 ± 11	306 2440 ± 16
204	graymatics-001	13095	70406	25 128	485 4096 ± 0	42 191 ± 1	38 203 ± 1	184 592 ± 5	506 1698 ± 9	517 7150 ± 34	537 39874 ± 309	535 39762 ± 295
205	griaule-001	0	412061	314 1271	406 2052 ± 0	479 1164 ± 1	428 1096 ± 5	417 1099 ± 4	388 1136 ± 2	436 1509 ± 2	380 3948 ± 23	381 3957 ± 32
206	griaule-002	0	1320474	406 1870	397 2052 ± 0	359 822 ± 1	361 924 ± 4	326 907 ± 1	356 1038 ± 21	412 1430 ± 9	382 4005 ± 32	382 4012 ± 31
207	hertasecurity-002	0	944582	296 1182	25 512 ± 0	175 484 ± 7	143 478 ± 3	124 480 ± 3	117 495 ± 3	100 520 ± 3	294 2289 ± 40	292 2267 ± 48
208	hertasecurity-003	0	944583	295 1181	24 512 ± 0	180 495 ± 7	145 480 ± 3	129 486 ± 3	114 491 ± 3	99 520 ± 4	439 7619 ± 65	438 7597 ± 94
209	hik-001	667866	9290	546 6597	102 1408 ± 0	271 651 ± 0	249 667 ± 8	235 677 ± 16	212 686 ± 13	195 737 ± 12	51 488 ± 19	52 477 ± 22
210	hisign-002	1014906	102652	434 2131	453 2080 ± 0	346 797 ± 0	307 800 ± 5	281 800 ± 0	257 801 ± 0	218 803 ± 1	26 232 ± 11	22 207 ± 11
211	hisign-003	2232829	156367	370 1599	451 2080 ± 0	449 1040 ± 5	420 1083 ± 4	407 1085 ± 4	371 1088 ± 4	321 1093 ± 4	12 167 ± 8	10 150 ± 10
212	hyperverge-003	1167779	282156	471 2687	80 1024 ± 0	559 1477 ± 2	532 1503 ± 3	526 1520 ± 3	499 1525 ± 4	447 1565 ± 3	63 566 ± 11	63 561 ± 8
213	hyperverge-005	3413303	284050	470 2686	85 1024 ± 0	304 689 ± 0	268 690 ± 0	245 693 ± 0	222 702 ± 6	201 752 ± 5	47 465 ± 2	50 464 ± 10
214	hzailu-005	1573726	275643	501 3292	545 5128 ± 0	299 684 ± 10	254 673 ± 7	202 622 ± 1	209 682 ± 6	184 715 ± 2	254 1853 ± 51	251 1829 ± 34
215	hzailu-006	2996729	275643	544 6070	556 7176 ± 0	565 1498 ± 11	530 1483 ± 15	512 1439 ± 8	482 1441 ± 10	446 1564 ± 40	304 2434 ± 19	307 2452 ± 32
216	i2v-001	276820	26600	206 815	388 2048 ± 0	320 721 ± 0	286 729 ± 0	260 731 ± 0	237 731 ± 0	208 764 ± 0	470 11523 ± 176	469 11533 ± 142
217	icm-004	2012129	1089	265 1052	166 2048 ± 0	142 419 ± 6	110 407 ± 6	111 454 ± 15	165 603 ± 51	441 1527 ± 235	484 14730 ± 154	482 14521 ± 152
218	icm-005	877530	1097	283 1116	219 2048 ± 0	39 185 ± 3	28 181 ± 3	32 208 ± 9	54 321 ± 36	293 1014 ± 185	461 10245 ± 65	461 10245 ± 69
219	icomm-000	807818	139431	549 6728	472 4096 ± 0	243 605 ± 26	215 610 ± 30	192 605 ± 27	168 610 ± 23	149 641 ± 32	448 8507 ± 25	447 8516 ± 26
220	icthtc-000	172459	1471004	292 1165	319 2048 ± 0	99 338 ± 11	80 338 ± 9	100 437 ± 16	223 705 ± 24	460 1719 ± 44	406 5284 ± 63	404 5290 ± 54

Notes	
1	The configuration size does not capture static data included in libraries.
2	The library size is the combined total of all files provided in the submission lib folder. These libraries e.g. OpenCV may or may not be installed on any end user's platform natively and would not need to be installed with the algorithm. Some developers put neural network models in their libraries.
3	The memory usage is the peak resident set size reported by the ps system call during template generation.
4	The median template creation times are measured on Intel®Xeon®CPU E5-2630 v4 @ 2.20GHz processors.
5	The comparison durations, in nanoseconds, are estimated using std::chrono::high_resolution_clock which on the machine in (2) counts 1ns clock ticks. Precision is somewhat worse than that however. The ± value is the median absolute deviation times 1.48 for Normal consistency.

Table 14: Summary of algorithms and properties included in this report. The red superscripts give ranking for the quantity in that column.

	ALGORITHM	CONFIG	LIBRARY	TEMPLATE						COMPARISON[4]	
	NAME	DATA	DATA	MEMORY	SIZE	GENERATION TIME (ms)[4]				TIME (ns)[5]	
		(KB)[1]	(KB)[2]	(MB)[3]	(B)	MUGSHOT	480x720	960x1440	1600x2400	3000x4500	GENUINE	IMPOSTOR
221	id3-006	210116	7706	[246]984	[59]520 ± 0	[298]683 ± 0	[422]1088 ± 1	[442]1192 ± 1	[414]1209 ± 1	[370]1270 ± 1	[409]5547 ± 34	[408]5563 ± 34
222	id3-008	242416	8151	[266]1059	[12]264 ± 0	[357]819 ± 0	[458]1209 ± 2	[471]1297 ± 2	[449]1329 ± 1	[413]1433 ± 1	[413]5658 ± 44	[413]5624 ± 40
223	idemia-009	1066728	70572	[474]2700	[68]636 ± 0	[492]1207 ± 1	[462]1218 ± 1	[451]1222 ± 2	[416]1222 ± 3	[371]1280 ± 10	[414]5664 ± 84	[411]5597 ± 90
224	idemia-010	996690	66244	[448]2306	[19]412 ± 0	[239]596 ± 1	[235]632 ± 22	[204]624 ± 18	[183]633 ± 7	[186]719 ± 5	[235]1699 ± 37	[237]1703 ± 38
225	identy-000	271397	14217	[103]474	[127]2048 ± 0	[305]689 ± 0	[273]702 ± 0	[253]712 ± 3	[244]757 ± 0	[277]970 ± 1	[105]655 ± 25	[103]637 ± 23
226	igearx-face-000	665623	298245	[227]885	[136]2048 ± 0	[377]860 ± 1	[328]855 ± 4	[300]844 ± 0	[291]881 ± 0	[264]924 ± 3	[226]1628 ± 45	[230]1657 ± 41
227	iit-002	259579	52070	[181]731	[374]2048 ± 0	[189]514 ± 1	[170]531 ± 2	[162]547 ± 1	[156]583 ± 1	[193]733 ± 2	[157]1023 ± 7	[156]1011 ± 66
228	iit-003	261288	53791	[209]821	[151]2048 ± 0	[172]482 ± 0	[151]493 ± 0	[140]509 ± 0	[135]541 ± 0	[158]661 ± 0	[35]324 ± 17	[36]326 ± 8
229	imds-software-002	373632	352627	[212]833	[275]2048 ± 0	[166]469 ± 1	[371]954 ± 2	[413]1094 ± 5	[361]1064 ± 4	[338]1153 ± 4	[468]11100 ± 155	[467]11090 ± 145
230	imds-software-003	373648	352628	[192]769	[180]2048 ± 0	[91]317 ± 5	[246]654 ± 4	[277]793 ± 6	[249]770 ± 4	[240]848 ± 2	[428]6624 ± 66	[427]6603 ± 77
231	imperial-000	370120	10623	[201]796	[325]2048 ± 0	[284]669 ± 1	[257]675 ± 3	[238]683 ± 17	[207]676 ± 2	[172]689 ± 2	[279]2130 ± 32	[276]2052 ± 100
232	imperial-002	472327	16134	[401]1826	[279]2048 ± 0	[218]569 ± 1	[201]581 ± 15	[174]575 ± 5	[152]576 ± 2	[123]588 ± 3	[293]2278 ± 90	[280]2131 ± 44
233	incode-009	266103	21014	-	[223]2048 ± 0	[183]503 ± 0	[150]490 ± 1	[133]498 ± 0	[121]505 ± 0	[106]537 ± 0	[170]1102 ± 28	[173]1113 ± 29
234	incode-013	483720	41434	[375]1647	[382]2048 ± 0	[200]535 ± 1	[186]548 ± 1	[165]555 ± 4	[139]545 ± 1	[136]618 ± 1	[181]1152 ± 37	[182]1154 ± 41
235	infocert-001	1204340	38972	[355]1490	[111]2048 ± 0	[384]874 ± 1	[342]891 ± 1	[396]1050 ± 5	[489]1473 ± 2	[498]3174 ± 8	[403]5055 ± 108	[400]5008 ± 100
236	innefulabs-000	370588	162172	[93]439	[381]2048 ± 0	[437]1006 ± 3	[401]1025 ± 3	[389]1030 ± 4	[358]1041 ± 2	[334]1135 ± 3	[416]5782 ± 41	[416]5741 ± 45
237	innominds-001	102207	777689	[284]1124	[207]2048 ± 0	[96]333 ± 21	[83]350 ± 19	[62]335 ± 16	[59]339 ± 17	[44]346 ± 18	[311]2482 ± 23	[311]2491 ± 29
238	innovativetechnologyltd-001	177232	335757	[71]341	[110]2048 ± 0	[148]433 ± 7	[130]446 ± 8	[102]439 ± 4	[92]452 ± 4	[85]485 ± 7	[257]1877 ± 42	[263]1924 ± 97
239	innovativetechnologyltd-002	173939	372324	[233]912	[144]2048 ± 0	[278]661 ± 2	[284]726 ± 4	[360]981 ± 27	[333]997 ± 40	[209]766 ± 3	[251]1841 ± 50	[255]1857 ± 59
240	innovatrics-010	604731	111234	[384]1715	[534]4136 ± 0	[247]611 ± 3	[233]632 ± 2	[257]723 ± 1	[236]730 ± 1	[211]768 ± 6	[384]4077 ± 42	[376]3857 ± 65
241	innovatrics-011	643997	50017	[390]1745	[539]4184 ± 0	[329]754 ± 2	[295]767 ± 3	[273]765 ± 3	[253]783 ± 4	[245]867 ± 3	[385]4135 ± 57	[379]3937 ± 91
242	insightface-003	1016917	26668	[363]1550	[134]2048 ± 0	[457]1073 ± 0	[425]1092 ± 2	[405]1070 ± 1	[370]1082 ± 1	[323]1101 ± 1	[72]597 ± 16	[75]595 ± 17
243	insightface-004	928816	26668	[396]1800	[333]2048 ± 0	[520]1298 ± 1	[497]1356 ± 2	[475]1313 ± 1	[442]1311 ± 0	[394]1349 ± 1	[62]565 ± 7	[61]559 ± 5
244	inspur-001	364862	91934	[213]833	[112]2048 ± 0	[538]1385 ± 1	[499]1361 ± 4	[502]1401 ± 2	[497]1495 ± 1	[468]1891 ± 1	[412]5641 ± 42	[412]5622 ± 40
245	inspur-002	447948	91934	[252]1009	[253]2048 ± 0	[453]1056 ± 5	[410]1056 ± 7	[416]1096 ± 7	[509]1776 ± 23	[419]1444 ± 12	[393]4504 ± 32	[389]4515 ± 35
246	intellicloudai-001	220831	868246	[157]655	[317]2048 ± 0	[165]468 ± 2	[136]456 ± 1	[118]466 ± 3	[115]492 ± 1	[142]632 ± 2	[159]1056 ± 4	[164]1051 ± 72
247	intellicloudai-002	259047	58559	[511]3585	[524]4100 ± 0	[372]847 ± 1	[323]847 ± 2	[302]849 ± 1	[279]853 ± 1	[251]878 ± 4	[136]822 ± 28	[135]818 ± 23
248	intellifusion-001	271872	289387	[190]762	[255]2048 ± 0	[331]764 ± 38	[297]774 ± 39	[280]797 ± 42	[258]803 ± 34	[220]805 ± 33	[171]1112 ± 28	[174]1128 ± 41
249	intellifusion-002	762731	385841	[239]941	[515]4096 ± 0	[413]950 ± 2	[430]1096 ± 42	[409]1088 ± 33	[399]1168 ± 31	[343]1171 ± 10	[236]1713 ± 57	[231]1665 ± 87
250	intellivision-006	287736	262742	[174]723	[443]2056 ± 0	[53]214 ± 0	[42]214 ± 0	[37]221 ± 0	[41]272 ± 0	[46]357 ± 1	[490]15153 ± 32	[490]15142 ± 38
251	intellivision-007	192454	262742	[88]419	[430]2056 ± 0	[25]148 ± 0	[20]157 ± 0	[19]166 ± 0	[17]180 ± 0	[29]265 ± 0	[487]15100 ± 50	[486]15095 ± 45
252	intellivix-004	361668	128097	[299]1189	[133]2048 ± 0	[145]427 ± 0	[127]437 ± 0	[107]444 ± 0	[98]461 ± 0	[119]565 ± 2	[217]1498 ± 37	[212]1478 ± 16
253	intellivix-005	774405	128093	[515]3692	[132]2048 ± 0	[285]673 ± 1	[242]643 ± 3	[223]654 ± 3	[202]666 ± 3	[212]769 ± 5	[213]1481 ± 65	[210]1451 ± 26
254	intelresearch-007	523218	101150	[303]1197	[114]2048 ± 0	[233]590 ± 1	[205]585 ± 1	[182]588 ± 1	[166]603 ± 4	[164]668 ± 6	[374]3738 ± 42	[375]3752 ± 53
255	intelresearch-008	523218	101214	[302]1196	[351]2048 ± 0	[263]634 ± 1	[230]630 ± 1	[210]632 ± 1	[184]635 ± 2	[182]711 ± 4	[371]3661 ± 34	[370]3641 ± 44
256	intema-000	1532392	19488	[275]1088	[50]513 ± 0	[439]1010 ± 0	[394]1001 ± 4	[373]994 ± 0	[331]993 ± 5	[308]1056 ± 1	[145]910 ± 29	[146]906 ± 32
257	intema-001	1122562	19536	[353]1458	[51]513 ± 0	[532]1354 ± 1	[490]1318 ± 5	[482]1336 ± 4	[447]1328 ± 2	[399]1375 ± 0	[151]977 ± 31	[151]980 ± 31
258	intozi-001	21863	74210	[29]140	[336]2048 ± 0	[13]85 ± 0	[12]86 ± 0	[12]86 ± 0	[9]87 ± 0	[7]87 ± 0	[456]9579 ± 252	[453]9530 ± 167
259	intsysmsu-001	384409	172480	[198]789	[138]2048 ± 0	[252]614 ± 2	[219]615 ± 2	[220]642 ± 2	[241]750 ± 3	[341]1159 ± 4	[89]621 ± 8	[87]611 ± 31
260	intsysmsu-002	765921	172298	[197]786	[86]1024 ± 0	[236]593 ± 1	[304]793 ± 2	[292]827 ± 1	[287]875 ± 104	[376]1293 ± 3	[57]549 ± 25	[60]548 ± 29
261	ionetworks-001	39860	333205	[62]298	[344]2048 ± 0	[150]439 ± 2	[123]433 ± 2	[116]461 ± 2	[93]454 ± 2	[86]488 ± 2	[425]6335 ± 103	[424]6358 ± 91
262	ionetworks-002	337801	73038	[391]1746	[209]2048 ± 0	[303]689 ± 1	[253]672 ± 5	[230]665 ± 3	[203]669 ± 3	[159]664 ± 6	[431]6884 ± 154	[430]6808 ± 102
263	iqface-000	268819	596337	[167]704	[543]4750 ± 32	[203]538 ± 26	[152]494 ± 2	[159]543 ± 3	[238]734 ± 4	[404]1393 ± 4	[565]636433 ± 38446	[565]632654 ± 85615
264	iqface-003	370803	963398	[210]821	[544]4763 ± 37	[193]529 ± 1	[171]532 ± 2	[188]599 ± 8	[278]850 ± 2	[456]1694 ± 2	[564]575924 ± 2601	[564]576653 ± 2051

Notes	
1	The configuration size does not capture static data included in libraries.
2	The library size is the combined total of all files provided in the submission lib folder. These libraries e.g. OpenCV may or may not be installed on any end user's platform natively and would not need to be installed with the algorithm. Some developers put neural network models in their libraries.
3	The memory usage is the peak resident set size reported by the ps system call during template generation.
4	The median template creation times are measured on Intel®Xeon®CPU E5-2630 v4 @ 2.20GHz processors.
5	The comparison durations, in nanoseconds, are estimated using std::chrono::high_resolution_clock which on the machine in (2) counts 1ns clock ticks. Precision is somewhat worse than that however. The ± value is the median absolute deviation times 1.48 for Normal consistency.

Table 15: Summary of algorithms and properties included in this report. The red superscripts give ranking for the quantity in that column.

	ALGORITHM	CONFIG	LIBRARY	TEMPLATE						COMPARISON[4]	
	NAME	DATA	DATA	MEMORY	SIZE	GENERATION TIME (ms)[4]				TIME (ns)[5]	
		(KB)[1]	(KB)[2]	(MB)[3]	(B)	MUGSHOT	480x720	960x1440	1600x2400	3000x4500	GENUINE	IMPOSTOR
265	irex-000	741899	47419	429 2090	466 3080 ± 0	375 852 ± 2	325 850 ± 1	314 874 ± 2	313 939 ± 1	360 1249 ± 5	22 201 ± 11	23 208 ± 8
266	isap-001	99049	204201	1 18	511 4096 ± 0	1 0 ± 0	-	-	-	-	46 459 ± 17	48 456 ± 11
267	isap-002	256765	49931	61 288	371 2048 ± 0	334 769 ± 3	402 1027 ± 2	317 877 ± 2	246 761 ± 1	260 912 ± 2	348 3045 ± 94	342 2973 ± 66
268	isityou-000	48010	36621	20 110	563 19200 ± 0	19 113 ± 5	-	-	-	-	561 237517 ± 1318	561 237374 ± 1279
269	isystems-001	274621	639268	278 1091	370 2048 ± 0	76 291 ± 9	-	-	-	-	59 557 ± 16	64 564 ± 22
270	isystems-002	358984	803389	369 1595	356 2048 ± 0	360 822 ± 8	-	-	-	-	125 749 ± 31	99 632 ± 28
271	itmo-007	415979	245376	443 2199	155 2048 ± 0	325 741 ± 2	-	-	-	-	314 2551 ± 50	314 2529 ± 80
272	itmo-008	726866	318238	338 1376	486 4096 ± 0	455 1060 ± 1	412 1058 ± 1	399 1059 ± 1	367 1072 ± 4	325 1104 ± 1	368 3578 ± 25	369 3580 ± 28
273	ivacognitive-001	256958	62791	243 975	119 2048 ± 0	518 1292 ± 3	480 1289 ± 4	467 1292 ± 4	437 1292 ± 3	385 1321 ± 4	386 4228 ± 41	384 4226 ± 41
274	iws-000	30875	3063	14 77	48 512 ± 0	68 277 ± 5	61 283 ± 1	131 494 ± 3	329 984 ± 3	494 2987 ± 39	153 999 ± 40	153 992 ± 22
275	jaakit-001	99024	24754	53 251	29 512 ± 0	12 76 ± 0	10 77 ± 0	9 79 ± 0	8 81 ± 0	9 93 ± 0	310 2466 ± 57	310 2465 ± 66
276	kakao-008	734583	104820	520 3879	115 2048 ± 0	473 1135 ± 3	443 1148 ± 3	432 1150 ± 3	394 1156 ± 1	345 1175 ± 1	124 736 ± 23	121 727 ± 22
277	kakao-009	766989	104820	524 4042	281 2048 ± 0	237 593 ± 1	212 603 ± 4	198 613 ± 2	174 617 ± 2	145 636 ± 4	45 457 ± 20	46 448 ± 17
278	kakaobank-000	570796	98479	472 2690	506 4096 ± 0	499 1234 ± 1	470 1254 ± 7	456 1248 ± 3	466 1389 ± 3	466 1843 ± 11	397 4790 ± 35	394 4803 ± 35
279	kakaobank-001	780621	98829	442 2189	190 2048 ± 0	226 584 ± 0	214 608 ± 1	194 607 ± 5	210 684 ± 1	263 922 ± 2	522 27092 ± 174	521 27065 ± 158
280	kakaopay-001	397864	179869	164 685	500 4096 ± 0	153 448 ± 0	178 542 ± 0	157 542 ± 0	136 542 ± 0	112 553 ± 0	97 633 ± 22	96 630 ± 22
281	kasikornlabs-002	256431	61063	146 613	162 2048 ± 0	399 917 ± 35	350 907 ± 13	354 963 ± 13	443 1320 ± 45	484 2629 ± 178	526 31025 ± 180	525 31054 ± 186
282	kasikornlabs-003	256442	61063	187 751	177 2048 ± 0	273 652 ± 5	247 656 ± 5	271 755 ± 11	344 1007 ± 27	476 2240 ± 168	517 24022 ± 121	514 23998 ± 97
283	kedacom-000	245292	37401	563 23574	17 292 ± 0	185 506 ± 3	185 547 ± 10	201 614 ± 9	158 588 ± 10	161 665 ± 24	110 684 ± 14	111 682 ± 16
284	kiwitech-000	369711	21375	215 841	276 2048 ± 0	234 591 ± 0	208 594 ± 0	187 595 ± 1	163 596 ± 0	132 609 ± 0	241 1755 ± 20	239 1734 ± 16
285	kneron-003	58366	1747	41 188	363 2048 ± 0	71 281 ± 3	60 280 ± 1	56 315 ± 13	66 365 ± 7	358 1224 ± 30	405 5237 ± 63	403 5274 ± 99
286	kneron-005	375374	13633	99 457	330 2048 ± 0	190 518 ± 2	168 522 ± 4	166 556 ± 5	245 757 ± 19	462 1760 ± 25	264 1922 ± 11	264 1926 ± 20
287	knowutech-000	808045	32886	326 1312	103 1536 ± 0	549 1419 ± 2	501 1372 ± 1	495 1377 ± 1	463 1382 ± 2	401 1386 ± 2	375 3743 ± 31	373 3693 ± 38
288	kogniza-001	0	394421	320 1288	104 1536 ± 0	515 1285 ± 2	485 1304 ± 4	465 1280 ± 2	432 1278 ± 2	387 1326 ± 2	341 2968 ± 37	340 2971 ± 20
289	kookmin-002	371771	30734	211 827	147 2048 ± 0	448 1038 ± 2	409 1047 ± 1	394 1045 ± 1	360 1061 ± 1	328 1116 ± 1	103 638 ± 19	102 636 ± 20
290	koreaid-001	256261	20152	399 1810	379 2048 ± 0	123 384 ± 2	101 390 ± 1	106 444 ± 2	141 556 ± 6	217 795 ± 5	101 636 ± 11	101 636 ± 10
291	krungthai-002	2360957	15033	297 1185	225 2048 ± 0	87 308 ± 0	72 314 ± 5	53 309 ± 0	52 319 ± 0	49 362 ± 0	345 3014 ± 20	343 2980 ± 22
292	kuke3d-001	403462	68786	123 530	477 4096 ± 0	354 814 ± 2	309 811 ± 2	286 814 ± 2	262 814 ± 1	235 834 ± 1	426 6412 ± 57	425 6413 ± 51
293	kuke3d-002	270544	1227855	208 820	154 2048 ± 0	184 504 ± 3	160 504 ± 1	141 511 ± 1	127 523 ± 2	122 585 ± 1	340 2943 ± 22	339 2966 ± 38
294	lebentech-000	0	10360	21 110	27 512 ± 0	3 22 ± 0	1 22 ± 0	1 22 ± 0	1 23 ± 0	1 23 ± 0	134 801 ± 42	136 825 ± 51
295	lebentech-001	0	144456	365 1567	306 2048 ± 0	32 174 ± 0	23 175 ± 0	30 200 ± 1	33 227 ± 9	60 397 ± 20	50 485 ± 17	51 473 ± 28
296	lemalabs-001	748400	198794	481 2745	337 2048 ± 0	351 810 ± 0	310 812 ± 0	285 813 ± 0	266 819 ± 0	239 844 ± 1	473 11930 ± 35	472 11913 ± 37
297	lineclova-002	475779	406756	330 1352	183 2048 ± 0	513 1284 ± 1	476 1275 ± 2	463 1275 ± 1	431 1273 ± 2	372 1281 ± 2	322 2765 ± 10	321 2767 ± 31
298	lineclova-003	585149	410482	386 1725	194 2048 ± 0	552 1444 ± 1	520 1438 ± 1	513 1439 ± 2	481 1440 ± 1	422 1446 ± 2	335 2890 ± 23	336 2899 ± 29
299	lookman-002	138200	25410	559 16518	64 548 ± 0	31 173 ± 1	-	-	-	-	83 610 ± 19	89 612 ± 22
300	lookman-004	244775	37401	562 23548	63 548 ± 0	186 507 ± 5	183 545 ± 12	200 613 ± 12	160 590 ± 11	156 656 ± 16	142 871 ± 29	142 878 ± 29
301	luxand-000	0	57908	336 1366	96 1040 ± 0	134 407 ± 23	124 433 ± 11	108 444 ± 14	102 464 ± 14	117 562 ± 25	138 828 ± 28	137 828 ± 32
302	luxand-001	85194	72189	152 636	273 2048 ± 0	147 431 ± 0	128 443 ± 0	105 443 ± 2	91 448 ± 0	98 519 ± 0	207 1433 ± 16	208 1433 ± 16
303	mantra-000	471458	62566	186 749	400 2052 ± 0	139 413 ± 18	149 487 ± 19	132 494 ± 18	123 511 ± 18	127 598 ± 19	352 3151 ± 51	350 3127 ± 63
304	maxvision-005	309326	61739	436 2138	146 2048 ± 0	438 1007 ± 1	468 1245 ± 5	384 1017 ± 1	357 1040 ± 4	379 1299 ± 3	267 1950 ± 38	267 1948 ± 34
305	maxvision-006	315987	61739	500 3172	178 2048 ± 0	507 1247 ± 3	457 1208 ± 3	450 1211 ± 5	415 1215 ± 1	368 1268 ± 4	266 1938 ± 17	265 1929 ± 35
306	megvii-008	1644071	44035	428 2086	393 2049 ± 0	524 1313 ± 1	512 1404 ± 4	489 1363 ± 2	456 1362 ± 3	409 1420 ± 2	507 20059 ± 1598	508 20448 ± 1633
307	megvii-009	1644071	44039	447 2294	395 2049 ± 0	526 1322 ± 1	495 1328 ± 1	484 1339 ± 3	517 2075 ± 3	406 1404 ± 4	508 20081 ± 1621	507 20260 ± 1577
308	meituan-003	860010	244091	483 2772	514 4096 ± 0	563 1487 ± 1	533 1518 ± 0	521 1469 ± 6	493 1478 ± 0	426 1471 ± 7	172 1112 ± 16	172 1097 ± 20

Notes	
1	The configuration size does not capture static data included in libraries.
2	The library size is the combined total of all files provided in the submission lib folder. These libraries e.g. OpenCV may or may not be installed on any end user's platform natively and would not need to be installed with the algorithm. Some developers put neural network models in their libraries.
3	The memory usage is the peak resident set size reported by the ps system call during template generation.
4	The median template creation times are measured on Intel®Xeon®CPU E5-2630 v4 @ 2.20GHz processors.
5	The comparison durations, in nanoseconds, are estimated using std::chrono::high_resolution_clock which on the machine in (2) counts 1ns clock ticks. Precision is somewhat worse than that however. The ± value is the median absolute deviation times 1.48 for Normal consistency.

Table 16: Summary of algorithms and properties included in this report. The red superscripts give ranking for the quantity in that column.

	ALGORITHM	CONFIG	LIBRARY	TEMPLATE						COMPARISON[4]	
	NAME	DATA	DATA	MEMORY	SIZE	GENERATION TIME (ms)[4]				TIME (ns)[5]	
		(KB)[1]	(KB)[2]	(MB)[3]	(B)	MUGSHOT	480x720	960x1440	1600x2400	3000x4500	GENUINE	IMPOSTOR
309	meituan-004	850507	244091	482 2759	494 4096 ± 0	344 796 ± 1	313 822 ± 0	290 820 ± 11	263 815 ± 11	227 824 ± 0	176 1149 ± 10	179 1148 ± 5
310	meiya-001	280055	264913	114 507	396 2049 ± 0	256 622 ± 12	-	-	-	-	445 8356 ± 615	444 8134 ± 97
311	mendaxiatech-000	1941475	45484	530 4397	520 4097 ± 0	503 1243 ± 2	471 1255 ± 1	492 1373 ± 2	503 1598 ± 3	486 2689 ± 8	542 46906 ± 275	541 46872 ± 217
312	metsakuurcompany-002	0	957558	244 980	438 2056 ± 0	425 980 ± 1	382 978 ± 1	358 976 ± 2	342 1005 ± 1	324 1103 ± 2	450 8766 ± 326	449 8786 ± 324
313	metsakuurcompany-003	0	957562	251 1004	433 2056 ± 0	417 965 ± 2	377 970 ± 5	400 1060 ± 12	343 1005 ± 6	331 1121 ± 1	444 8234 ± 145	443 8111 ± 280
314	miaxis-002	0	216484	68 328	26 512 ± 0	77 292 ± 0	63 290 ± 1	48 297 ± 0	46 298 ± 0	47 359 ± 1	162 1065 ± 48	162 1040 ± 54
315	miaxis-003	0	439726	141 604	304 2048 ± 0	264 634 ± 0	225 624 ± 2	199 613 ± 0	128 524 ± 0	160 665 ± 0	275 2053 ± 20	274 2048 ± 28
316	microfocus-002	96288	27362	40 176	6 256 ± 0	63 259 ± 18	-	-	-	-	36 337 ± 34	27 230 ± 25
317	microfocus-003	169603	27689	115 507	8 256 ± 0	178 490 ± 19	167 517 ± 30	269 752 ± 55	383 1126 ± 121	487 2713 ± 345	7 121 ± 5	7 117 ± 5
318	minivision-000	836697	16597	526 4263	509 4096 ± 0	447 1035 ± 1	407 1033 ± 2	391 1035 ± 1	355 1037 ± 1	311 1059 ± 2	309 2466 ± 26	308 2460 ± 25
319	mitek-000	105584	44643	58 277	78 1024 ± 0	62 256 ± 21	51 265 ± 10	74 375 ± 24	138 545 ± 42	322 1098 ± 124	329 2846 ± 88	322 2777 ± 74
320	mobai-000	365451	80573	196 786	551 6144 ± 0	333 766 ± 8	333 869 ± 6	448 1205 ± 31	513 1867 ± 45	502 3549 ± 190	496 16458 ± 333	495 16423 ± 1473
321	mobai-001	265297	60164	124 534	341 2048 ± 0	249 612 ± 3	218 614 ± 3	240 687 ± 9	295 886 ± 31	459 1707 ± 103	200 1386 ± 25	201 1377 ± 26
322	mobbl-001	231160	58706	50 226	267 2048 ± 0	37 183 ± 32	29 184 ± 25	68 354 ± 76	269 823 ± 396	490 2781 ± 1166	472 11832 ± 109	471 11851 ± 88
323	mobbl-003	172248	60960	59 282	221 2048 ± 0	281 664 ± 6	248 661 ± 5	228 663 ± 5	199 665 ± 6	173 691 ± 5	476 12506 ± 111	475 12509 ± 100
324	mobipintech-000	370514	303291	293 1173	326 2048 ± 0	505 1245 ± 1	466 1234 ± 1	460 1264 ± 1	454 1360 ± 1	458 1707 ± 1	482 14506 ± 214	481 14433 ± 197
325	momovn-001	246938	1013076	193 769	375 2048 ± 0	57 237 ± 1	54 268 ± 7	52 308 ± 10	44 293 ± 5	56 390 ± 3	209 1438 ± 13	209 1443 ± 13
326	moredian-000	525259	21374	261 1035	233 2048 ± 0	311 694 ± 0	272 698 ± 0	249 699 ± 0	220 700 ± 0	183 713 ± 1	248 1803 ± 11	246 1779 ± 23
327	mukh-003	556405	180996	404 1853	316 2048 ± 0	566 1896 ± 3	534 1948 ± 1	531 2003 ± 0	515 1981 ± 0	470 2016 ± 0	71 597 ± 13	84 604 ± 16
328	mukh-004	405118	181085	331 1353	262 2048 ± 0	210 558 ± 1	193 567 ± 1	170 569 ± 1	149 569 ± 3	124 593 ± 1	116 704 ± 1	116 703 ± 2
329	multimodality-000	0	503924	343 1417	339 2048 ± 0	141 416 ± 0	117 420 ± 0	94 423 ± 0	88 427 ± 0	76 463 ± 0	140 848 ± 25	133 800 ± 28
330	multimodality-001	185719	545045	339 1390	492 4096 ± 0	490 1190 ± 2	445 1169 ± 2	435 1165 ± 2	398 1167 ± 2	347 1177 ± 2	206 1424 ± 35	203 1384 ± 42
331	mvision-001	227502	149531	176 723	23 512 ± 0	308 691 ± 21	274 702 ± 19	248 697 ± 24	225 708 ± 29	180 710 ± 27	174 1123 ± 40	183 1154 ± 38
332	nazhiai-000	547484	16141	477 2716	165 2048 ± 0	297 683 ± 3	265 687 ± 2	297 835 ± 27	276 840 ± 31	236 834 ± 34	288 2230 ± 34	281 2133 ± 81
333	ncssg-001	148743	490151	218 847	210 2048 ± 0	406 936 ± 2	370 946 ± 3	343 944 ± 2	312 938 ± 5	278 972 ± 2	369 3579 ± 50	363 3459 ± 34
334	neosystems-004	243546	352623	122 529	272 2048 ± 0	94 324 ± 0	279 711 ± 3	291 827 ± 7	281 854 ± 2	261 916 ± 2	480 14437 ± 176	480 14355 ± 173
335	netbridgetech-001	133108	205875	116 508	505 4096 ± 0	14 85 ± 1	11 83 ± 0	10 84 ± 0	10 92 ± 0	10 113 ± 4	452 9280 ± 74	452 9446 ± 512
336	netbridgetech-002	257687	49931	63 299	174 2048 ± 0	368 838 ± 6	320 838 ± 2	298 839 ± 1	275 839 ± 3	242 859 ± 3	336 2893 ± 65	346 3050 ± 123
337	neurotechnology-017	371650	98242	451 2385	7 256 ± 0	188 508 ± 2	165 513 ± 0	146 519 ± 1	129 533 ± 1	138 622 ± 15	1 80 ± 1	1 79 ± 1
338	neurotechnology-018	698669	98271	528 4367	53 515 ± 0	322 725 ± 1	291 747 ± 1	266 747 ± 4	248 769 ± 2	234 833 ± 22	2 85 ± 2	3 87 ± 7
339	nhn-004	931648	432753	489 2864	474 4096 ± 0	248 612 ± 0	234 632 ± 0	215 636 ± 0	206 676 ± 6	225 820 ± 0	498 17323 ± 99	497 17334 ± 133
340	nhn-005	1278729	432776	490 2890	510 4096 ± 0	352 811 ± 0	252 671 ± 13	222 652 ± 0	232 726 ± 12	252 890 ± 3	499 18123 ± 400	499 18214 ± 250
341	nodeflux-002	774668	690213	101 466	349 2048 ± 0	315 708 ± 4	278 709 ± 4	254 716 ± 5	231 716 ± 7	194 736 ± 3	363 3475 ± 62	361 3408 ± 143
342	nominder-002	249049	116931	403 1852	9 258 ± 0	133 405 ± 1	118 425 ± 2	96 424 ± 1	90 434 ± 0	93 505 ± 0	4 101 ± 11	4 102 ± 14
343	nominder-003	249964	116931	452 2417	10 258 ± 0	288 675 ± 2	264 683 ± 5	234 677 ± 2	221 701 ± 3	214 775 ± 3	3 87 ± 4	2 84 ± 4
344	notiontag-001	92753	427967	155 642	67 584 ± 0	404 929 ± 35	424 1092 ± 39	533 3709 ± 81	533 10233 ± 180	530 31181 ± 521	538 43636 ± 286	536 43724 ± 330
345	notiontag-002	271987	967207	493 2965	456 2120 ± 0	156 453 ± 2	134 453 ± 3	110 453 ± 3	94 458 ± 2	79 471 ± 3	509 20278 ± 194	506 20195 ± 186
346	nsensecorp-004	513276	139178	379 1675	378 2048 ± 0	551 1433 ± 0	521 1445 ± 7	518 1450 ± 3	496 1487 ± 5	-	303 2388 ± 42	303 2385 ± 63
347	nsensecorp-005	411845	138437	308 1240	121 2048 ± 0	555 1455 ± 0	524 1453 ± 0	517 1449 ± 0	484 1457 ± 2	433 1490 ± 4	280 2131 ± 51	283 2165 ± 66
348	ntechlab-011	786933	209458	550 6867	101 1280 ± 0	476 1148 ± 2	440 1142 ± 1	434 1159 ± 1	403 1185 ± 1	375 1290 ± 3	13 179 ± 11	15 173 ± 11
349	ntechlab-012	570796	212350	537 5450	461 2560 ± 0	523 1309 ± 1	491 1323 ± 1	479 1331 ± 1	455 1360 ± 1	423 1460 ± 3	24 211 ± 8	25 211 ± 7
350	omface-000	45945	844976	34 154	87 1024 ± 0	40 185 ± 1	39 206 ± 2	31 203 ± 1	22 195 ± 1	16 193 ± 1	49 481 ± 42	47 456 ± 20
351	omface-001	146370	1799745	32 145	81 1024 ± 0	43 194 ± 2	43 222 ± 2	35 209 ± 0	27 216 ± 1	21 233 ± 1	502 18369 ± 19	501 18366 ± 32
352	omnigarde-002	368860	32882	189 760	79 1024 ± 0	521 1303 ± 1	469 1246 ± 1	458 1249 ± 1	426 1253 ± 1	365 1261 ± 1	321 2727 ± 34	319 2686 ± 32

Notes	
1	The configuration size does not capture static data included in libraries.
2	The library size is the combined total of all files provided in the submission lib folder. These libraries e.g. OpenCV may or may not be installed on any end user's platform natively and would not need to be installed with the algorithm. Some developers put neural network models in their libraries.
3	The memory usage is the peak resident set size reported by the ps system call during template generation.
4	The median template creation times are measured on Intel®Xeon®CPU E5-2630 v4 @ 2.20GHz processors.
5	The comparison durations, in nanoseconds, are estimated using std::chrono::high_resolution_clock which on the machine in (2) counts 1ns clock ticks. Precision is somewhat worse than that however. The ± value is the median absolute deviation times 1.48 for Normal consistency.

Table 17: Summary of algorithms and properties included in this report. The red superscripts give ranking for the quantity in that column.

	ALGORITHM	CONFIG	LIBRARY	TEMPLATE						COMPARISON[4]	
	NAME	DATA	DATA	MEMORY	SIZE	GENERATION TIME (ms)[4]				TIME (ns)[5]	
		(KB)[1]	(KB)[2]	(MB)[3]	(B)	MUGSHOT	480x720	960x1440	1600x2400	3000x4500	GENUINE	IMPOSTOR
353	omnigarde-003	427751	35153	188 756	55 517 ± 0	286 673 ± 0	231 631 ± 1	212 633 ± 1	186 637 ± 1	151 647 ± 1	187 1259 ± 22	188 1244 ± 16
354	onfido-000	273478	959781	234 914	323 2048 ± 0	157 459 ± 17	133 451 ± 15	109 451 ± 14	99 462 ± 15	92 505 ± 18	225 1617 ± 50	226 1637 ± 53
355	openedge-000	447048	272235	337 1376	428 2056 ± 0	111 367 ± 0	109 404 ± 1	66 352 ± 1	60 350 ± 0	55 385 ± 0	488 15122 ± 41	487 15110 ± 48
356	openface-001	0	40111	19 100	292 2048 ± 0	26 148 ± 1	19 154 ± 0	70 365 ± 3	83 409 ± 9	134 616 ± 31	80 608 ± 14	85 604 ± 13
357	oz-003	484147	519652	558 11575	417 2053 ± 0	534 1375 ± 12	503 1388 ± 3	530 1773 ± 16	516 2039 ± 6	499 3209 ± 5	558 73905 ± 456	557 73892 ± 444
358	oz-004	373982	1075452	554 7845	418 2053 ± 0	365 832 ± 7	335 871 ± 6	322 899 ± 10	369 1078 ± 12	450 1608 ± 10	551 61654 ± 418	549 61749 ± 450
359	palit-000	428754	144958	334 1360	488 4096 ± 0	219 570 ± 1	199 578 ± 1	177 576 ± 3	155 583 ± 1	133 614 ± 1	286 2227 ± 16	288 2226 ± 16
360	palit-001	173886	145564	137 587	122 2048 ± 0	54 227 ± 0	45 224 ± 1	38 224 ± 1	34 229 ± 3	28 262 ± 2	177 1150 ± 16	175 1135 ± 23
361	pangiam-001	1015455	37259	366 1569	179 2048 ± 0	420 972 ± 1	385 982 ± 3	361 981 ± 2	330 990 ± 7	304 1052 ± 2	8 136 ± 11	8 139 ± 13
362	pangiam-002	486035	39834	304 1205	391 2048 ± 0	90 316 ± 0	73 316 ± 0	57 317 ± 0	53 319 ± 1	37 326 ± 2	6 111 ± 13	5 103 ± 2
363	papago-001	669274	52817	449 2341	237 2048 ± 0	511 1272 ± 6	481 1296 ± 7	470 1295 ± 6	434 1281 ± 3	392 1345 ± 3	493 15236 ± 169	491 15184 ± 142
364	papil11-000	1146378	24895	441 2184	312 2048 ± 0	407 942 ± 3	432 1108 ± 2	447 1204 ± 6	460 1369 ± 10	471 2033 ± 35	84 612 ± 7	90 613 ± 11
365	papsav1923-002	491185	24727	287 1139	414 2052 ± 0	342 792 ± 1	383 978 ± 1	392 1042 ± 1	395 1158 ± 1	453 1641 ± 19	184 1209 ± 29	186 1206 ± 38
366	papsav1923-003	515576	24803	281 1113	137 2048 ± 0	345 797 ± 0	388 987 ± 1	393 1043 ± 1	401 1178 ± 1	465 1809 ± 7	143 903 ± 26	145 905 ± 34
367	paravision-011	781138	95589	454 2424	529 4100 ± 0	376 852 ± 0	334 871 ± 1	307 858 ± 1	280 854 ± 0	248 873 ± 1	224 1608 ± 35	224 1625 ± 32
368	paravision-013	1537125	95602	533 4648	527 4100 ± 0	429 991 ± 9	391 993 ± 5	371 992 ± 4	339 1002 ± 5	288 1002 ± 7	214 1481 ± 26	216 1490 ± 25
369	pensees-001	1619431	408932	411 1922	560 8200 ± 0	467 1108 ± 3	522 1448 ± 17	511 1439 ± 10	488 1464 ± 5	444 1546 ± 9	351 3151 ± 34	351 3143 ± 25
370	pixelall-009	0	1009114	387 1732	557 8192 ± 0	562 1484 ± 3	507 1395 ± 3	501 1400 ± 4	467 1391 ± 3	414 1433 ± 3	253 1848 ± 13	253 1842 ± 19
371	pixelall-010	0	1469903	473 2693	559 8192 ± 0	477 1153 ± 3	421 1084 ± 4	419 1103 ± 4	372 1093 ± 3	330 1118 ± 4	261 1906 ± 13	259 1898 ± 29
372	privid-001	0	76008	31 143	564 30720 ± 0	154 450 ± 0	135 454 ± 0	119 467 ± 1	107 472 ± 1	91 504 ± 1	497 17041 ± 74	496 17053 ± 100
373	privid-002	0	219733	258 1031	251 2048 ± 0	508 1261 ± 3	444 1156 ± 4	433 1155 ± 2	396 1162 ± 3	381 1302 ± 4	112 686 ± 22	109 680 ± 20
374	psl-011	814579	606050	534 4959	561 8248 ± 0	527 1324 ± 2	492 1323 ± 8	478 1326 ± 8	445 1324 ± 8	386 1322 ± 4	233 1680 ± 37	234 1688 ± 40
375	psl-012	1318147	622004	532 4535	535 4144 ± 0	470 1111 ± 2	436 1122 ± 2	421 1104 ± 2	378 1119 ± 1	329 1117 ± 1	66 583 ± 17	70 589 ± 17
376	ptakuratsatu-000	0	585434	329 1347	60 538 ± 0	385 875 ± 3	331 863 ± 48	338 928 ± 9	320 958 ± 17	316 1066 ± 26	420 5900 ± 103	414 5687 ± 167
377	pxl-001	110116	78231	36 168	45 512 ± 0	17 101 ± 5	14 104 ± 5	26 189 ± 12	82 408 ± 27	425 1470 ± 144	411 5598 ± 45	410 5590 ± 68
378	pyramid-000	372608	219883	202 804	419 2056 ± 0	223 583 ± 2	-	-	-	-	434 7147 ± 59	437 7586 ± 425
379	qazbs-000	362015	805258	259 1034	234 2048 ± 0	522 1307 ± 1	467 1243 ± 0	457 1248 ± 9	425 1253 ± 1	369 1270 ± 0	404 5181 ± 62	402 5167 ± 93
380	qazsmartvisionai-000	560570	99515	450 2371	35 512 ± 0	310 694 ± 1	277 708 ± 7	255 717 ± 5	226 711 ± 5	190 723 ± 7	133 795 ± 29	130 781 ± 34
381	qluevision-001	173605	205230	78 376	558 8192 ± 0	55 229 ± 1	46 230 ± 1	42 231 ± 1	36 233 ± 1	23 239 ± 1	359 3374 ± 38	359 3365 ± 41
382	qnap-004	371274	61422	250 1002	361 2048 ± 0	109 365 ± 0	89 365 ± 1	71 367 ± 0	67 368 ± 0	52 375 ± 3	107 681 ± 7	110 682 ± 13
383	qnap-005	977818	61429	487 2828	258 2048 ± 0	419 969 ± 5	389 988 ± 8	369 992 ± 6	338 1000 ± 7	292 1008 ± 6	98 633 ± 1	98 632 ± 13
384	quantasoft-003	370518	211354	267 1063	314 2048 ± 0	262 632 ± 2	239 634 ± 0	209 632 ± 0	182 631 ± 1	144 634 ± 0	20 201 ± 7	21 203 ± 8
385	rankone-015	0	289078	44 190	11 261 ± 0	206 547 ± 5	180 543 ± 6	178 578 ± 2	180 629 ± 7	254 894 ± 9	21 201 ± 19	14 172 ± 16
386	realnetworks-007	570797	101527	499 3145	429 2056 ± 0	530 1348 ± 2	498 1358 ± 11	490 1363 ± 10	464 1386 ± 9	439 1517 ± 6	60 559 ± 31	58 539 ± 35
387	realnetworks-008	73346	75421	83 402	439 2056 ± 0	80 296 ± 3	67 294 ± 3	67 353 ± 4	63 361 ± 5	84 485 ± 5	55 539 ± 31	59 543 ± 29
388	rebs-000	1375350	62664	492 2934	483 4096 ± 0	258 623 ± 0	238 633 ± 10	207 626 ± 10	173 616 ± 1	135 617 ± 0	178 1150 ± 1	180 1150 ± 2
389	rebs-001	2038561	62673	466 2582	525 4100 ± 0	348 802 ± 1	311 812 ± 8	294 829 ± 1	259 807 ± 2	222 811 ± 4	180 1151 ± 8	178 1145 ± 4
390	recognito-000	549308	247223	542 5903	463 2564 ± 0	459 1086 ± 2	429 1096 ± 1	418 1102 ± 2	391 1142 ± 3	356 1219 ± 7	16 193 ± 8	19 190 ± 16
391	recognito-001	517547	62334	517 3833	462 2564 ± 0	456 1072 ± 1	423 1089 ± 1	414 1095 ± 4	376 1112 ± 2	351 1205 ± 4	14 183 ± 10	16 183 ± 7
392	regula-000	262444	29384	145 610	169 2048 ± 0	488 1187 ± 1	437 1126 ± 1	424 1129 ± 0	387 1132 ± 1	342 1159 ± 1	53 491 ± 16	54 500 ± 22
393	regula-001	256075	25980	247 987	248 2048 ± 0	514 1284 ± 1	463 1220 ± 1	452 1222 ± 1	418 1226 ± 1	364 1255 ± 1	39 361 ± 10	37 342 ± 25
394	remarkai-001	241857	868314	179 730	405 2052 ± 0	364 831 ± 6	324 849 ± 18	397 1055 ± 25	409 1198 ± 34	440 1519 ± 38	186 1229 ± 20	134 805 ± 56
395	remarkai-003	280516	58559	521 3909	521 4100 ± 0	427 986 ± 1	390 993 ± 1	370 992 ± 1	335 999 ± 3	294 1019 ± 2	132 787 ± 20	131 793 ± 22
396	rendip-000	0	437653	183 735	197 2048 ± 0	161 464 ± 2	137 458 ± 0	123 473 ± 0	110 483 ± 1	116 556 ± 4	64 576 ± 13	66 573 ± 11

Notes	
1	The configuration size does not capture static data included in libraries.
2	The library size is the combined total of all files provided in the submission lib folder. These libraries e.g. OpenCV may or may not be installed on any end user's platform natively and would not need to be installed with the algorithm. Some developers put neural network models in their libraries.
3	The memory usage is the peak resident set size reported by the ps system call during template generation.
4	The median template creation times are measured on Intel®Xeon®CPU E5-2630 v4 @ 2.20GHz processors.
5	The comparison durations, in nanoseconds, are estimated using std::chrono::high_resolution_clock which on the machine in (2) counts 1ns clock ticks. Precision is somewhat worse than that however. The ± value is the median absolute deviation times 1.48 for Normal consistency.

Table 18: Summary of algorithms and properties included in this report. The red superscripts give ranking for the quantity in that column.

	ALGORITHM	CONFIG	LIBRARY	TEMPLATE							COMPARISON[4]	
	NAME	DATA	DATA	MEMORY	SIZE	GENERATION TIME (ms)[4]					TIME (ns)[5]	
		(KB)[1]	(KB)[2]	(MB)[3]	(B)	MUGSHOT	480x720	960x1440	1600x2400	3000x4500	GENUINE	IMPOSTOR
397	revealmedia-005	293933	202465	191 767	528 4100 ± 0	146 428 ± 0	120 428 ± 0	99 430 ± 0	89 433 ± 0	71 442 ± 0	272 2023 ± 38	271 2009 ± 26
398	revealmedia-006	293933	200912	185 745	402 2052 ± 0	119 381 ± 0	95 381 ± 0	77 382 ± 0	69 384 ± 0	58 394 ± 0	95 626 ± 35	80 600 ± 2
399	roc-016	0	674869	45 191	18 392 ± 0	213 562 ± 1	181 543 ± 2	164 553 ± 2	146 564 ± 2	139 626 ± 2	17 194 ± 8	12 161 ± 26
400	rokid-000	258612	396624	306 1218	441 2056 ± 0	205 546 ± 3	179 542 ± 2	161 545 ± 1	126 522 ± 3	118 563 ± 4	362 3457 ± 62	364 3463 ± 77
401	rokid-001	641223	413733	269 1071	446 2060 ± 0	394 911 ± 2	346 901 ± 5	321 899 ± 2	300 900 ± 3	256 901 ± 3	356 3345 ± 50	357 3346 ± 149
402	s1-005	482369	95685	289 1146	286 2048 ± 0	433 1001 ± 0	395 1002 ± 0	379 1004 ± 0	345 1008 ± 0	297 1029 ± 2	94 626 ± 74	69 589 ± 14
403	s1-007	482385	59657	288 1144	245 2048 ± 0	428 988 ± 1	374 965 ± 0	355 966 ± 0	324 972 ± 0	285 991 ± 0	104 648 ± 26	107 658 ± 25
404	saffe-001	85973	62488	37 168	99 1280 ± 0	70 281 ± 1	-	-	-	-	189 1274 ± 19	192 1277 ± 26
405	saffe-002	260622	28285	220 855	290 2048 ± 0	356 817 ± 11	308 805 ± 15	284 809 ± 19	264 815 ± 29	223 813 ± 23	120 717 ± 7	120 714 ± 29
406	samsungsds-001	1189592	147444	523 3922	507 4096 ± 0	475 1140 ± 3	442 1145 ± 4	485 1344 ± 5	459 1366 ± 5	437 1514 ± 7	547 51559 ± 773	545 51721 ± 1003
407	samsungsds-002	1040732	147475	503 3321	431 2056 ± 0	471 1118 ± 1	447 1175 ± 12	491 1372 ± 6	446 1324 ± 2	432 1489 ± 4	531 35803 ± 266	531 36181 ± 674
408	samtech-001	288082	219883	142 605	426 2056 ± 0	79 294 ± 3	-	-	-	-	440 7694 ± 59	439 7678 ± 91
409	samtech-002	192220	474779	172 714	440 2056 ± 0	52 212 ± 0	41 212 ± 0	36 215 ± 0	31 225 ± 0	32 285 ± 1	492 15231 ± 50	492 15215 ± 59
410	scanovate-002	256986	457227	219 850	117 2048 ± 0	312 696 ± 32	280 713 ± 33	263 738 ± 28	251 779 ± 32	344 1172 ± 53	346 3021 ± 38	349 3120 ± 163
411	scanovate-003	135585	89469	203 805	189 2048 ± 0	227 585 ± 1	217 613 ± 12	183 591 ± 1	167 610 ± 2	167 684 ± 1	339 2926 ± 22	338 2925 ± 20
412	sdc-000	256814	481583	195 784	230 2048 ± 0	395 913 ± 14	349 906 ± 9	429 1142 ± 19	508 1774 ± 45	507 4719 ± 222	528 32645 ± 93	528 32653 ± 112
413	seamfix-001	429267	86391	67 320	156 2048 ± 0	319 718 ± 8	276 707 ± 25	345 947 ± 18	498 1521 ± 55	503 4179 ± 226	419 5897 ± 118	419 5867 ± 123
414	securifai-007	94589	88169	135 583	222 2048 ± 0	182 500 ± 0	163 506 ± 0	134 499 ± 1	119 501 ± 1	94 505 ± 1	215 1484 ± 11	214 1483 ± 13
415	securifai-008	111759	84658	170 711	277 2048 ± 0	268 641 ± 4	243 647 ± 3	227 663 ± 3	191 645 ± 3	154 649 ± 1	216 1498 ± 11	215 1487 ± 13
416	sensetime-007	765353	37533	543 5950	91 1028 ± 0	539 1386 ± 41	493 1323 ± 2	487 1347 ± 2	457 1366 ± 2	449 1593 ± 8	210 1460 ± 29	207 1425 ± 26
417	sensetime-008	1176483	60067	541 5882	92 1028 ± 0	561 1479 ± 31	519 1436 ± 4	523 1482 ± 4	500 1525 ± 5	454 1669 ± 2	191 1283 ± 51	187 1240 ± 47
418	serendipity-000	0	346443	100 462	242 2048 ± 0	392 900 ± 8	347 901 ± 3	335 922 ± 2	311 936 ± 1	283 987 ± 2	79 602 ± 1	86 607 ± 10
419	sertis-002	460790	68929	159 660	321 2048 ± 0	486 1181 ± 1	448 1178 ± 0	441 1183 ± 0	406 1187 ± 0	357 1221 ± 0	167 1086 ± 32	165 1076 ± 31
420	sertis-003	0	451507	416 1965	192 2048 ± 0	151 441 ± 0	126 436 ± 2	117 461 ± 2	100 463 ± 1	81 473 ± 4	146 915 ± 10	147 917 ± 8
421	seventhsense-003	603091	453847	277 1090	411 2052 ± 0	435 1003 ± 2	381 977 ± 0	293 828 ± 1	265 817 ± 1	228 826 ± 2	220 1523 ± 25	221 1530 ± 22
422	seventhsense-005	4000865	453775	465 2581	522 4100 ± 0	472 1119 ± 1	435 1120 ± 1	426 1134 ± 4	386 1131 ± 2	336 1144 ± 1	324 2787 ± 28	323 2777 ± 22
423	shaman-000	0	120033	113 507	493 4096 ± 0	274 653 ± 16	-	-	-	-	42 380 ± 25	41 379 ± 31
424	shaman-001	0	174446	118 511	470 4096 ± 0	78 294 ± 2	-	-	-	-	100 635 ± 19	45 441 ± 25
425	shu-002	731250	148309	229 890	498 4096 ± 0	327 751 ± 2	296 769 ± 4	333 922 ± 4	479 1431 ± 9	501 3489 ± 47	566 2930763 ± 47355	566 2929759 ± 39149
426	shu-003	428774	146940	117 511	211 2048 ± 0	358 820 ± 6	315 828 ± 3	341 941 ± 9	439 1308 ± 15	495 3045 ± 44	312 2506 ± 26	313 2512 ± 38
427	siat-002	486842	7738	455 2434	401 2052 ± 0	222 579 ± 0	-	-	-	-	129 769 ± 13	125 750 ± 13
428	siat-005	380936	16935	323 1299	250 2048 ± 0	132 403 ± 0	107 400 ± 0	84 401 ± 0	80 403 ± 1	65 422 ± 7	65 577 ± 13	67 580 ± 17
429	sjtu-004	1953267	241108	479 2741	541 4608 ± 0	500 1236 ± 2	459 1209 ± 2	469 1294 ± 4	502 1554 ± 5	489 2738 ± 8	349 3057 ± 14	348 3070 ± 20
430	sjtu-005	1953267	241151	478 2734	542 4608 ± 0	241 601 ± 1	221 617 ± 1	258 724 ± 2	384 1127 ± 3	492 2855 ± 11	337 2898 ± 4	337 2900 ± 4
431	sktelecom-000	527132	298496	327 1321	105 1536 ± 0	469 1110 ± 1	434 1113 ± 1	423 1114 ± 1	379 1120 ± 1	340 1155 ± 1	521 26583 ± 128	518 26508 ± 126
432	smartbiometrik-001	30875	92620	11 72	22 512 ± 0	255 620 ± 7	227 625 ± 7	218 640 ± 4	234 728 ± 6	303 1047 ± 8	115 703 ± 31	117 710 ± 40
433	smartengines-000	1711	3025	8 50	16 288 ± 0	29 168 ± 7	26 180 ± 1	23 188 ± 3	28 217 ± 3	31 275 ± 1	18 197 ± 5	13 167 ± 11
434	smartengines-001	7095	4601	7 47	15 288 ± 0	97 333 ± 89	111 408 ± 1	95 423 ± 1	96 460 ± 2	113 553 ± 5	10 153 ± 11	9 143 ± 13
435	smartvist-000	5959	134084	38 169	46 512 ± 0	10 59 ± 0	8 56 ± 0	6 56 ± 0	6 58 ± 0	8 90 ± 1	208 1435 ± 31	206 1422 ± 48
436	smartvist-001	349219	25644	231 904	125 2048 ± 0	113 370 ± 0	93 374 ± 0	75 377 ± 1	85 422 ± 0	73 445 ± 0	326 2835 ± 99	329 2836 ± 80
437	smilart-002	111826	87805	57 263	77 1024 ± 0	33 176 ± 16	-	-	-	-	503 18784 ± 136	503 18795 ± 151
438	smilart-003	67339	91670	46 192	38 512 ± 0	35 180 ± 12	27 181 ± 10	54 313 ± 22	201 665 ± 49	477 2299 ± 196	201 1395 ± 74	157 1027 ± 66
439	sodec-000	836592	13142	491 2902	512 4096 ± 0	450 1041 ± 2	405 1032 ± 1	390 1035 ± 1	354 1037 ± 2	313 1061 ± 2	246 1794 ± 37	245 1775 ± 23
440	sparsh-001	0	366290	531 4525	287 2048 ± 0	294 680 ± 2	244 648 ± 1	216 638 ± 0	189 642 ± 0	185 717 ± 0	457 9600 ± 275	454 9601 ± 290

Notes	
1	The configuration size does not capture static data included in libraries.
2	The library size is the combined total of all files provided in the submission lib folder. These libraries e.g. OpenCV may or may not be installed on any end user's platform natively and would not need to be installed with the algorithm. Some developers put neural network models in their libraries.
3	The memory usage is the peak resident set size reported by the ps system call during template generation.
4	The median template creation times are measured on Intel®Xeon®CPU E5-2630 v4 @ 2.20GHz processors.
5	The comparison durations, in nanoseconds, are estimated using std::chrono::high_resolution_clock which on the machine in (2) counts 1ns clock ticks. Precision is somewhat worse than that however. The ± value is the median absolute deviation times 1.48 for Normal consistency.

Table 19: Summary of algorithms and properties included in this report. The red superscripts give ranking for the quantity in that column.

	ALGORITHM	CONFIG	LIBRARY	TEMPLATE						COMPARISON[4]	
	NAME	DATA	DATA	MEMORY	SIZE	GENERATION TIME (ms)[4]				TIME (ns)[5]	
		(KB)[1]	(KB)[2]	(MB)[3]	(B)	MUGSHOT	480x720	960x1440	1600x2400	3000x4500	GENUINE	IMPOSTOR
441	sqisoft-002	278039	386291	161 675	425 2056 ± 0	163 466 ± 8	140 466 ± 2	121 468 ± 11	97 461 ± 6	80 472 ± 4	127 758 ± 11	126 760 ± 23
442	sqisoft-003	362737	607964	205 812	444 2056 ± 0	267 638 ± 2	255 674 ± 7	256 718 ± 17	200 665 ± 6	187 720 ± 6	139 844 ± 11	139 844 ± 23
443	staqu-000	879661	624676	268 1064	508 4096 ± 0	353 813 ± 25	-	-	-	-	342 2979 ± 31	345 3007 ± 75
444	starhybrid-001	100509	289356	217 845	142 2048 ± 0	106 358 ± 82	84 355 ± 49	76 379 ± 58	77 401 ± 79	57 393 ± 67	165 1075 ± 51	166 1078 ± 53
445	stcon-002	1255490	62667	430 2095	502 4096 ± 0	225 583 ± 0	195 570 ± 2	173 574 ± 2	154 582 ± 1	140 630 ± 0	175 1143 ± 2	176 1142 ± 4
446	stcon-003	2119710	62673	518 3862	523 4100 ± 0	362 823 ± 0	312 821 ± 1	295 831 ± 3	268 823 ± 1	237 838 ± 2	179 1151 ± 5	184 1157 ± 5
447	stengg-000	361104	34674	177 724	367 2048 ± 0	350 809 ± 1	357 921 ± 2	377 1002 ± 1	255 794 ± 1	473 2130 ± 5	270 2005 ± 22	272 2011 ± 34
448	sukshi-000	94035	688738	79 382	565 32768 ± 0	135 407 ± 11	112 413 ± 8	138 504 ± 8	213 689 ± 11	448 1574 ± 28	459 9817 ± 50	457 9787 ± 62
449	suprema-004	1430475	116085	497 3096	489 4096 ± 0	560 1478 ± 2	527 1472 ± 2	522 1469 ± 1	491 1476 ± 1	435 1496 ± 1	354 3201 ± 14	354 3202 ± 22
450	suprema-005	1430177	116089	496 3093	491 4096 ± 0	343 794 ± 1	332 863 ± 1	283 808 ± 5	292 883 ± 1	230 830 ± 5	381 3950 ± 7	380 3948 ± 4
451	supremaid-001	258193	23479	126 541	386 2048 ± 0	170 479 ± 1	147 481 ± 0	125 481 ± 0	112 490 ± 0	101 522 ± 0	117 704 ± 19	106 652 ± 19
452	supremaid-002	256273	23899	70 334	158 2048 ± 0	173 483 ± 0	159 501 ± 0	130 488 ± 0	120 503 ± 0	120 565 ± 0	269 1990 ± 19	262 1923 ± 29
453	surrey-cvssp-002	903493	87776	385 1720	389 2048 ± 0	493 1213 ± 1	460 1211 ± 1	464 1279 ± 0	435 1282 ± 0	380 1300 ± 0	460 9906 ± 120	458 9911 ± 167
454	surrey-cvssp-003	1013099	109557	444 2208	181 2048 ± 0	340 789 ± 1	322 846 ± 1	306 854 ± 1	420 1234 ± 2	500 3283 ± 3	437 7358 ± 130	435 7336 ± 93
455	swsam-001	265887	95072	154 642	160 2048 ± 0	454 1058 ± 34	419 1079 ± 31	410 1091 ± 35	368 1076 ± 9	326 1109 ± 45	338 2902 ± 31	335 2892 ± 32
456	synesis-006	731941	21817	354 1472	532 4104 ± 0	207 549 ± 1	184 546 ± 1	163 552 ± 1	143 558 ± 2	147 639 ± 28	114 697 ± 32	115 688 ± 31
457	synesis-007	1442961	24145	458 2443	467 3080 ± 0	494 1215 ± 5	472 1268 ± 30	473 1306 ± 67	441 1311 ± 58	410 1423 ± 52	108 684 ± 32	113 686 ± 25
458	synology-000	221021	25809	97 453	283 2048 ± 0	136 407 ± 14	113 415 ± 14	246 694 ± 31	468 1396 ± 58	504 4568 ± 211	506 19720 ± 203	504 19767 ± 379
459	synology-002	256713	25943	108 488	186 2048 ± 0	390 886 ± 4	343 892 ± 3	332 920 ± 2	337 1000 ± 5	383 1317 ± 12	211 1466 ± 32	217 1496 ± 45
460	sztu-000	338637	15871	322 1298	249 2048 ± 0	197 531 ± 0	172 532 ± 0	151 533 ± 0	132 537 ± 0	110 548 ± 0	68 585 ± 11	74 592 ± 13
461	sztu-001	338650	15871	324 1299	352 2048 ± 0	199 535 ± 0	175 537 ± 0	155 538 ± 0	134 540 ± 0	111 553 ± 0	75 599 ± 10	79 598 ± 10
462	t4isb-000	234227	115237	73 345	358 2048 ± 0	436 1006 ± 5	393 1001 ± 1	381 1006 ± 1	347 1009 ± 1	296 1022 ± 2	370 3586 ± 34	367 3534 ± 34
463	tech5-007	0	340324	469 2647	33 512 ± 0	533 1360 ± 0	500 1366 ± 0	493 1376 ± 0	461 1373 ± 0	417 1438 ± 6	54 538 ± 19	55 516 ± 22
464	tech5-008	0	365877	539 5567	322 2048 ± 0	277 655 ± 3	226 624 ± 11	206 625 ± 11	181 631 ± 11	179 710 ± 12	438 7371 ± 81	436 7367 ± 99
465	techainer-001	198738	703687	419 1977	153 2048 ± 0	120 381 ± 9	102 391 ± 5	85 402 ± 5	74 391 ± 1	75 461 ± 5	466 10726 ± 189	465 10714 ± 243
466	techsign-000	0	1101622	418 1969	244 2048 ± 0	110 366 ± 1	106 398 ± 1	436 1172 ± 3	528 3065 ± 18	526 10460 ± 65	396 4758 ± 112	393 4789 ± 93
467	techsign-001	0	586983	407 1881	118 2048 ± 0	335 772 ± 35	303 788 ± 23	282 802 ± 42	316 949 ± 10	407 1409 ± 26	69 592 ± 11	73 592 ± 13
468	tevian-007	779934	19523	383 1712	93 1032 ± 0	224 583 ± 1	200 579 ± 0	180 580 ± 0	159 588 ± 1	146 636 ± 0	401 4894 ± 65	397 4841 ± 83
469	tevian-008	847177	19519	512 3610	94 1032 ± 0	388 884 ± 2	348 903 ± 1	324 903 ± 1	302 911 ± 1	267 946 ± 1	398 4828 ± 40	396 4811 ± 41
470	tiger-005	342866	253734	361 1532	415 2052 ± 0	461 1097 ± 2	416 1065 ± 2	403 1066 ± 2	363 1067 ± 3	319 1088 ± 3	88 620 ± 19	93 615 ± 16
471	tiger-006	421186	394688	171 714	407 2052 ± 0	541 1392 ± 16	514 1411 ± 10	515 1444 ± 10	501 1531 ± 11	467 1848 ± 10	249 1810 ± 20	248 1801 ± 13
472	tinkoff-001	274660	389272	148 616	167 2048 ± 0	481 1176 ± 3	449 1179 ± 3	438 1178 ± 3	400 1169 ± 2	350 1203 ± 3	390 4361 ± 74	387 4364 ± 75
473	tnitech-000	234032	13976	538 5471	229 2048 ± 0	140 415 ± 1	119 427 ± 1	92 419 ± 4	87 427 ± 3	67 436 ± 2	305 2438 ± 14	305 2436 ± 19
474	tongyi-005	1140701	138919	433 2121	455 2089 ± 0	28 165 ± 1	-	-	-	-	504 18924 ± 65	505 20158 ± 103
475	toppanidgate-000	671181	711850	395 1798	476 4096 ± 0	398 915 ± 1	354 916 ± 1	330 916 ± 1	303 917 ± 1	262 917 ± 1	519 25262 ± 84	516 25264 ± 97
476	toshiba-007	547545	76675	321 1297	421 2056 ± 0	321 722 ± 1	302 784 ± 0	275 777 ± 4	247 766 ± 2	233 832 ± 15	119 709 ± 22	118 712 ± 26
477	toshiba-008	707290	76687	394 1791	436 2056 ± 0	424 979 ± 1	380 976 ± 0	365 986 ± 3	341 1005 ± 2	307 1056 ± 14	106 674 ± 68	112 683 ± 71
478	touchlessid-002	255586	14284	76 367	259 2048 ± 0	114 371 ± 1	94 375 ± 1	101 438 ± 3	188 640 ± 10	445 1548 ± 57	263 1915 ± 41	256 1871 ± 38
479	touchlessid-003	271397	14226	119 512	231 2048 ± 0	138 410 ± 0	116 419 ± 0	98 429 ± 0	109 479 ± 1	168 685 ± 6	81 608 ± 17	77 596 ± 1
480	trueface-002	253947	123116	107 486	109 2000 ± 0	107 360 ± 0	86 361 ± 0	93 423 ± 0	161 590 ± 1	-	15 192 ± 14	17 186 ± 19
481	trueface-003	346530	24308	522 3916	285 2048 ± 0	466 1107 ± 22	258 677 ± 3	262 732 ± 7	301 905 ± 5	-	5 103 ± 11	6 112 ± 29
482	trueidvng-001	766071	37721	393 1781	552 6144 ± 0	421 975 ± 1	386 985 ± 1	368 989 ± 1	349 1016 ± 1	333 1128 ± 2	532 37129 ± 216	556 72067 ± 305
483	truststamp-001	1795742	275073	359 1524	70 768 ± 0	44 194 ± 0	34 191 ± 0	24 187 ± 0	26 210 ± 1	41 338 ± 8	446 8415 ± 66	445 8392 ± 71
484	tuputech-000	11476	17185	6 33	252 2048 ± 0	23 122 ± 4	16 120 ± 1	17 142 ± 2	23 196 ± 5	62 411 ± 14	516 23893 ± 406	517 25279 ± 406

Notes	
1	The configuration size does not capture static data included in libraries.
2	The library size is the combined total of all files provided in the submission lib folder. These libraries e.g. OpenCV may or may not be installed on any end user's platform natively and would not need to be installed with the algorithm. Some developers put neural network models in their libraries.
3	The memory usage is the peak resident set size reported by the ps system call during template generation.
4	The median template creation times are measured on Intel®Xeon®CPU E5-2630 v4 @ 2.20GHz processors.
5	The comparison durations, in nanoseconds, are estimated using std::chrono::high_resolution_clock which on the machine in (2) counts 1ns clock ticks. Precision is somewhat worse than that however. The ± value is the median absolute deviation times 1.48 for Normal consistency.

Table 20: Summary of algorithms and properties included in this report. The red superscripts give ranking for the quantity in that column.

	ALGORITHM	CONFIG	LIBRARY	TEMPLATE						COMPARISON[4]	
	NAME	DATA	DATA	MEMORY	SIZE	GENERATION TIME (ms)[4]				TIME (ns)[5]	
		(KB)[1]	(KB)[2]	(MB)[3]	(B)	MUGSHOT	480x720	960x1440	1600x2400	3000x4500	GENUINE	IMPOSTOR
485	turingtechvip-001	399874	54535	147 615	343 2048 ± 0	536 1384 ± 4	505 1391 ± 1	499 1393 ± 1	475 1411 ± 1	428 1476 ± 2	240 1733 ± 19	240 1734 ± 20
486	turingtechvip-002	167556	140995	224 877	161 2048 ± 0	564 1493 ± 2	487 1306 ± 1	497 1382 ± 1	450 1337 ± 1	411 1426 ± 3	479 13819 ± 103	478 13807 ± 137
487	turkcell-000	271083	133553	153 636	175 2048 ± 0	468 1110 ± 1	426 1094 ± 0	420 1103 ± 0	382 1126 ± 1	348 1201 ± 1	333 2866 ± 23	334 2873 ± 40
488	turkcell-001	287616	133870	158 657	195 2048 ± 0	295 682 ± 0	271 695 ± 0	242 688 ± 1	215 692 ± 0	177 702 ± 0	389 4342 ± 71	385 4310 ± 72
489	twface-000	661735	11782	485 2796	216 2048 ± 0	380 871 ± 1	336 873 ± 1	313 873 ± 2	288 876 ± 2	255 898 ± 1	218 1504 ± 29	218 1510 ± 34
490	twface-001	671511	11782	488 2851	201 2048 ± 0	402 923 ± 1	362 925 ± 2	336 926 ± 1	307 929 ± 2	265 940 ± 2	202 1400 ± 32	204 1402 ± 37
491	ulsee-001	370519	57261	-	128 2048 ± 0	275 654 ± 2	-	-	-	-	422 6065 ± 94	423 6228 ± 77
492	uluface-002	0	480761	276 1088	278 2048 ± 0	383 873 ± 42	326 855 ± 9	359 978 ± 24	430 1271 ± 40	478 2333 ± 68	505 19207 ± 1114	502 18501 ± 274
493	uluface-003	97357	529422	313 1264	465 3072 ± 0	416 965 ± 11	375 968 ± 10	408 1087 ± 20	465 1387 ± 36	482 2469 ± 86	520 26057 ± 195	520 26865 ± 566
494	unicc-002	277015	1705310	378 1673	235 2048 ± 0	245 609 ± 1	222 620 ± 1	197 612 ± 0	197 660 ± 2	207 763 ± 3	296 2289 ± 13	294 2295 ± 22
495	unicc-003	361274	1737967	397 1806	368 2048 ± 0	529 1343 ± 3	494 1328 ± 1	486 1345 ± 1	458 1366 ± 1	431 1484 ± 6	300 2339 ± 74	299 2327 ± 29
496	unissey-003	0	814526	156 650	490 4096 ± 0	318 718 ± 1	289 744 ± 0	349 956 ± 1	472 1403 ± 1	496 3055 ± 2	223 1594 ± 20	223 1570 ± 44
497	unissey-004	1	1065839	257 1030	471 4096 ± 0	101 354 ± 2	90 366 ± 0	90 416 ± 0	84 417 ± 0	61 409 ± 0	387 4261 ± 124	391 4557 ± 480
498	upc-001	0	89914	271 1077	97 1052 ± 0	209 551 ± 15	275 703 ± 56	259 724 ± 51	242 751 ± 49	243 863 ± 33	350 3114 ± 44	353 3165 ± 97
499	useb-001	1000960	493816	348 1429	384 2048 ± 0	287 673 ± 4	198 577 ± 4	179 579 ± 8	162 596 ± 9	210 768 ± 2	287 2230 ± 65	296 2299 ± 90
500	useb-002	1000967	493456	346 1423	173 2048 ± 0	198 532 ± 2	300 778 ± 2	224 657 ± 4	195 657 ± 2	238 843 ± 3	299 2336 ± 47	298 2323 ± 60
501	uxlabs-001	291127	39378	166 700	496 4096 ± 0	127 395 ± 0	98 387 ± 0	80 388 ± 0	72 390 ± 0	59 396 ± 0	255 1863 ± 31	261 1921 ± 45
502	uxlabs-003	1051837	37767	372 1638	469 4096 ± 0	540 1390 ± 1	513 1410 ± 5	498 1391 ± 3	471 1402 ± 6	416 1435 ± 1	230 1645 ± 10	227 1641 ± 37
503	vcog-002	3229434	118946	514 3666	566 61504 ± 5	104 357 ± 25	-	-	-	-	563 296154 ± 3077	563 296436 ± 4183
504	vcortex-001	105305	55240	111 502	73 896 ± 0	49 201 ± 2	36 197 ± 0	34 209 ± 3	38 244 ± 6	51 371 ± 19	30 279 ± 4	32 277 ± 4
505	vd-002	254498	34389	5 31	54 516 ± 0	300 684 ± 5	261 679 ± 4	232 676 ± 5	216 693 ± 5	202 754 ± 5	33 300 ± 14	35 319 ± 32
506	vd-003	254505	44051	2 29	413 2052 ± 0	309 691 ± 5	267 690 ± 5	237 683 ± 4	214 691 ± 5	189 722 ± 5	154 1003 ± 11	154 1001 ± 7
507	veridas-008	1100495	1190915	555 8633	141 2048 ± 0	408 944 ± 12	369 945 ± 11	481 1334 ± 27	519 2382 ± 48	516 6959 ± 172	121 723 ± 14	122 731 ± 16
508	veridas-009	1100503	625120	557 9163	288 2048 ± 0	231 589 ± 6	192 565 ± 5	176 576 ± 5	157 583 ± 5	163 666 ± 6	102 638 ± 5	104 638 ± 16
509	veridium-002	0	52482	35 161	459 2486 ± 0	4 25 ± 0	3 25 ± 0	3 29 ± 0	3 30 ± 0	3 51 ± 0	539 43891 ± 177	537 43918 ± 167
510	veridium-003	0	25975	27 136	460 2490 ± 0	5 27 ± 0	2 25 ± 0	2 28 ± 0	2 30 ± 0	4 53 ± 0	530 34755 ± 140	530 34828 ± 177
511	verigram-001	282155	11773	467 2638	340 2048 ± 0	283 664 ± 2	256 675 ± 2	296 833 ± 4	411 1202 ± 7	488 2733 ± 32	232 1664 ± 60	228 1648 ± 56
512	verigram-003	1590775	20692	424 2052	482 4096 ± 0	307 691 ± 4	260 677 ± 1	233 677 ± 1	217 694 ± 1	200 746 ± 1	535 38843 ± 1140	534 38665 ± 1071
513	verihubs-inteligensia-001	216524	51916	92 437	224 2048 ± 0	215 564 ± 0	190 562 ± 0	169 566 ± 1	147 566 ± 0	128 600 ± 0	510 21770 ± 84	509 21735 ± 102
514	verihubs-inteligensia-002	361105	17045	178 727	182 2048 ± 0	167 471 ± 0	138 458 ± 0	114 459 ± 0	101 463 ± 1	78 471 ± 0	500 18131 ± 558	498 17851 ± 197
515	verijelas-000	254540	10322	389 1736	331 2048 ± 0	92 321 ± 0	78 325 ± 1	61 329 ± 0	58 335 ± 5	48 360 ± 0	462 10267 ± 143	460 10218 ± 109
516	via-004	530941	93634	335 1361	263 2048 ± 0	112 368 ± 0	104 397 ± 1	65 352 ± 1	65 364 ± 2	87 490 ± 1	28 255 ± 7	30 255 ± 8
517	via-005	510729	93629	446 2257	354 2048 ± 0	202 538 ± 0	169 528 ± 0	149 525 ± 1	131 535 ± 2	129 601 ± 1	25 223 ± 2	26 222 ± 7
518	viante-000	1244225	19718	362 1532	435 2056 ± 0	452 1054 ± 0	414 1059 ± 1	406 1075 ± 1	365 1070 ± 4	318 1087 ± 1	427 6461 ± 44	426 6424 ± 32
519	videmo-001	212051	95063	66 309	205 2048 ± 0	47 199 ± 0	21 164 ± 0	18 164 ± 0	15 164 ± 0	11 165 ± 0	31 296 ± 17	33 288 ± 16
520	videmo-002	212053	32963	69 333	184 2048 ± 0	46 199 ± 0	22 169 ± 0	20 169 ± 0	16 170 ± 0	13 170 ± 0	23 209 ± 7	24 208 ± 8
521	videonetics-001	30875	5963	9 61	30 512 ± 0	64 262 ± 3	57 273 ± 1	103 439 ± 3	267 820 ± 3	479 2393 ± 43	182 1153 ± 38	177 1142 ± 65
522	videonetics-002	121981	6289	22 115	412 2052 ± 0	72 282 ± 5	68 295 ± 1	143 513 ± 4	351 1029 ± 3	497 3151 ± 46	185 1219 ± 57	189 1262 ± 56
523	viettelhightech-000	259471	215557	89 421	266 2048 ± 0	159 461 ± 1	139 461 ± 2	115 461 ± 1	105 467 ± 2	88 494 ± 0	74 599 ± 11	71 591 ± 13
524	vigilantsolutions-010	348798	49973	214 841	106 1548 ± 0	254 615 ± 0	232 631 ± 0	211 632 ± 0	185 636 ± 0	157 659 ± 0	52 490 ± 13	53 488 ± 11
525	vigilantsolutions-011	255661	49973	138 591	107 1548 ± 0	131 402 ± 0	115 418 ± 0	91 418 ± 0	86 422 ± 0	72 445 ± 0	37 339 ± 20	38 366 ± 37
526	vinai-000	402391	866522	260 1034	241 2048 ± 0	462 1099 ± 1	427 1095 ± 1	412 1093 ± 1	373 1099 ± 1	332 1126 ± 1	343 2996 ± 20	344 2993 ± 26
527	vinbigdata-002	256322	138864	144 607	135 2048 ± 0	217 569 ± 2	196 572 ± 1	171 571 ± 1	150 572 ± 1	126 596 ± 1	282 2175 ± 44	282 2160 ± 53
528	vinbigdata-003	259968	183557	72 342	213 2048 ± 0	373 849 ± 6	488 1312 ± 1	305 853 ± 2	444 1321 ± 2	232 832 ± 2	164 1074 ± 37	169 1086 ± 40

Notes	
1	The configuration size does not capture static data included in libraries.
2	The library size is the combined total of all files provided in the submission lib folder. These libraries e.g. OpenCV may or may not be installed on any end user's platform natively and would not need to be installed with the algorithm. Some developers put neural network models in their libraries.
3	The memory usage is the peak resident set size reported by the ps system call during template generation.
4	The median template creation times are measured on Intel®Xeon®CPU E5-2630 v4 @ 2.20GHz processors.
5	The comparison durations, in nanoseconds, are estimated using std::chrono::high_resolution_clock which on the machine in (2) counts 1ns clock ticks. Precision is somewhat worse than that however. The ± value is the median absolute deviation times 1.48 for Normal consistency.

Table 21: Summary of algorithms and properties included in this report. The red superscripts give ranking for the quantity in that column.

	ALGORITHM	CONFIG	LIBRARY	TEMPLATE						COMPARISON[4]	
	NAME	DATA	DATA	MEMORY	SIZE	GENERATION TIME (ms)[4]				TIME (ns)[5]	
		(KB)[1]	(KB)[2]	(MB)[3]	(B)	MUGSHOT	480x720	960x1440	1600x2400	3000x4500	GENUINE	IMPOSTOR
529	vion-000	228219	7533	110 498	410 2052 ± 0	98 333 ± 1	-	-	-	-	536 39839 ± 3561	519 26830 ± 2241
530	visage-000	49218	70150	12 72	40 512 ± 0	6 27 ± 0	4 27 ± 0	4 31 ± 0	5 38 ± 0	5 63 ± 0	285 2220 ± 14	287 2218 ± 14
531	visionbox-003	259542	156891	312 1263	449 2068 ± 0	293 678 ± 2	262 682 ± 1	236 682 ± 2	219 695 ± 2	198 739 ± 5	229 1643 ± 56	229 1649 ± 66
532	visionbox-004	309730	154797	345 1422	533 4116 ± 0	117 378 ± 1	91 369 ± 0	81 389 ± 5	79 402 ± 2	68 437 ± 4	276 2071 ± 31	278 2076 ± 41
533	visionlabs-010	1067280	19357	226 883	52 513 ± 0	323 730 ± 0	282 717 ± 1	251 709 ± 0	228 713 ± 1	197 739 ± 0	76 600 ± 41	95 626 ± 35
534	visionlabs-011	1067280	19353	238 923	49 513 ± 0	324 731 ± 1	283 717 ± 1	252 710 ± 1	229 714 ± 1	199 741 ± 1	58 556 ± 26	62 559 ± 25
535	visteam-007	331673	264832	106 485	239 2048 ± 0	246 611 ± 1	228 625 ± 1	208 626 ± 1	172 615 ± 1	153 647 ± 0	318 2704 ± 38	320 2732 ± 54
536	visteam-008	582800	264832	180 731	246 2048 ± 0	483 1179 ± 1	446 1173 ± 1	449 1210 ± 1	407 1190 ± 3	354 1208 ± 1	317 2632 ± 28	317 2647 ± 42
537	vixvizion-006	594053	396294	333 1359	212 2048 ± 0	386 876 ± 9	316 828 ± 3	289 817 ± 1	271 825 ± 2	247 871 ± 1	77 600 ± 23	88 611 ± 25
538	vixvizion-007	594053	470119	351 1435	247 2048 ± 0	389 885 ± 35	317 828 ± 1	288 816 ± 1	270 825 ± 1	246 870 ± 1	78 600 ± 28	82 602 ± 34
539	vnis-000	285395	1404886	129 546	301 2048 ± 0	149 437 ± 1	129 443 ± 1	112 456 ± 2	95 458 ± 2	82 477 ± 2	199 1386 ± 10	202 1382 ± 16
540	vnpay-000	258919	1404844	112 504	293 2048 ± 0	58 239 ± 1	48 248 ± 0	43 252 ± 0	39 249 ± 0	27 260 ± 0	197 1353 ± 11	198 1353 ± 23
541	vnpt-005	560630	240888	291 1157	315 2048 ± 0	546 1403 ± 0	511 1404 ± 6	503 1403 ± 6	483 1456 ± 0	451 1630 ± 10	367 3562 ± 23	368 3554 ± 29
542	vnpt-006	1114807	360198	445 2245	369 2048 ± 0	512 1277 ± 2	504 1390 ± 19	506 1410 ± 14	494 1481 ± 30	457 1703 ± 69	360 3400 ± 20	360 3393 ± 22
543	vocord-009	1380132	201560	529 4372	108 1920 ± 0	558 1472 ± 2	528 1472 ± 1	527 1549 ± 1	505 1667 ± 2	472 2064 ± 2	274 2052 ± 50	277 2056 ± 39
544	vocord-010	902552	206873	519 3866	98 1088 ± 0	556 1459 ± 2	526 1459 ± 1	520 1463 ± 2	495 1484 ± 1	442 1535 ± 3	320 2724 ± 31	318 2653 ± 45
545	vtcc-000	284612	132031	149 619	124 2048 ± 0	89 315 ± 0	75 317 ± 0	58 321 ± 0	55 322 ± 0	39 334 ± 1	513 22074 ± 112	512 22173 ± 163
546	vtcc-001	528186	132058	298 1189	168 2048 ± 0	317 715 ± 1	-	-	-	-	514 22740 ± 167	558 86287 ± 1073
547	vts-000	256589	169760	382 1697	373 2048 ± 0	176 486 ± 1	148 481 ± 0	127 484 ± 0	111 485 ± 1	97 517 ± 0	560 124209 ± 352	560 123652 ± 358
548	vts-001	293000	475743	150 622	148 2048 ± 0	291 676 ± 1	263 683 ± 6	241 687 ± 3	218 695 ± 2	178 709 ± 2	458 9620 ± 44	455 9618 ± 54
549	wicket-000	826392	641802	426 2071	308 2048 ± 0	550 1419 ± 2	517 1429 ± 3	514 1444 ± 4	486 1460 ± 3	443 1537 ± 6	550 60976 ± 232	548 61096 ± 323
550	winsense-001	264428	32035	237 922	100 1280 ± 0	332 766 ± 7	413 1058 ± 47	362 983 ± 97	359 1053 ± 119	384 1320 ± 84	227 1631 ± 28	269 1964 ± 171
551	winsense-002	281379	25780	405 1855	271 2048 ± 0	179 494 ± 2	155 498 ± 1	145 519 ± 1	133 537 ± 1	143 634 ± 1	234 1683 ± 8	233 1685 ± 7
552	wiseai-001	189467	60781	51 245	392 2048 ± 0	59 240 ± 0	50 251 ± 0	60 328 ± 1	57 327 ± 0	38 332 ± 0	330 2850 ± 29	332 2852 ± 31
553	wuhantianyu-001	465118	66457	274 1086	320 2048 ± 0	269 642 ± 1	240 642 ± 1	221 644 ± 0	193 652 ± 0	175 697 ± 0	453 9502 ± 151	459 9920 ± 253
554	x-laboratory-000	520020	197310	360 1524	437 2056 ± 0	349 808 ± 7	345 897 ± 113	325 907 ± 103	294 886 ± 103	165 673 ± 39	122 725 ± 19	124 749 ± 34
555	x-laboratory-001	625140	398792	402 1844	442 2056 ± 0	229 586 ± 2	210 596 ± 5	191 603 ± 6	177 620 ± 7	216 793 ± 14	135 813 ± 28	141 872 ± 32
556	xforwardai-001	340100	51163	440 2176	203 2048 ± 0	485 1180 ± 2	452 1182 ± 1	443 1194 ± 1	405 1186 ± 2	349 1203 ± 1	131 779 ± 17	132 797 ± 13
557	xforwardai-002	707715	51163	422 2003	480 4096 ± 0	409 944 ± 1	368 942 ± 1	342 943 ± 4	310 935 ± 1	276 967 ± 1	205 1406 ± 8	205 1405 ± 13
558	xm-000	578041	148920	163 684	404 2052 ± 0	387 878 ± 2	340 882 ± 1	366 988 ± 2	427 1258 ± 3	481 2434 ± 7	228 1634 ± 17	225 1632 ± 20
559	yisheng-004	486351	38653	316 1279	468 3704 ± 0	118 378 ± 12	-	-	-	-	113 693 ± 137	56 526 ± 34
560	yitu-003	1525719	138919	516 3737	454 2082 ± 0	378 860 ± 0	-	-	-	-	501 18305 ± 71	500 18286 ± 62
561	yoonik-003	346691	265415	438 2161	365 2048 ± 0	430 991 ± 3	384 980 ± 1	363 984 ± 4	327 982 ± 1	282 983 ± 1	109 684 ± 45	108 678 ± 41
562	yoonik-004	469597	88673	199 792	342 2048 ± 0	496 1219 ± 1	478 1284 ± 1	459 1255 ± 1	429 1266 ± 0	362 1251 ± 1	158 1039 ± 42	159 1030 ± 40
563	yoti-001	267246	470114	285 1125	126 2048 ± 0	502 1238 ± 4	489 1316 ± 17	534 4099 ± 13	530 4160 ± 45	508 4774 ± 95	464 10352 ± 247	463 10364 ± 246
564	ytu-000	1477360	44032	460 2484	129 2048 ± 0	195 530 ± 0	173 533 ± 0	217 640 ± 0	283 861 ± 2	469 1949 ± 8	527 31797 ± 131	526 31794 ± 133
565	yuan-005	258312	145564	216 843	313 2048 ± 0	121 381 ± 0	97 386 ± 0	79 387 ± 2	71 390 ± 4	64 421 ± 3	183 1156 ± 8	185 1196 ± 26
566	yuan-008	620369	167833	371 1626	504 4096 ± 0	480 1169 ± 0	292 752 ± 0	268 752 ± 3	250 775 ± 4	215 782 ± 0	198 1362 ± 16	200 1377 ± 19

Notes	
1	The configuration size does not capture static data included in libraries.
2	The library size is the combined total of all files provided in the submission lib folder. These libraries e.g. OpenCV may or may not be installed on any end user's platform natively and would not need to be installed with the algorithm. Some developers put neural network models in their libraries.
3	The memory usage is the peak resident set size reported by the ps system call during template generation.
4	The median template creation times are measured on Intel®Xeon®CPU E5-2630 v4 @ 2.20GHz processors.
5	The comparison durations, in nanoseconds, are estimated using std::chrono::high_resolution_clock which on the machine in (2) counts 1ns clock ticks. Precision is somewhat worse than that however. The ± value is the median absolute deviation times 1.48 for Normal consistency.

Table 22: Summary of algorithms and properties included in this report. The red superscripts give ranking for the quantity in that column.

	Algorithm	FALSE NON-MATCH RATE (FNMR)																	
		CONSTRAINED, COOPERATIVE																LESS CONSTRAINED, NON-COOP.	
	Name	VISAMC		VISA		MUGSHOT		MUGSHOT12+YRS		VISABORDER		BORDER		BORDER		KIOSKBORDER			
	FMR	0.0001		1E-06		1E-05		1E-05		1E-06		1E-06		1E-05		1E-06			
1	20face-000	0.1268	486	0.1828	484	0.1748	501	0.2768	501	0.1765	478	0.1864	340	0.0927	379	0.5943	239		
2	20face-001	0.0521	460	0.0732	459	0.1414	499	0.2549	500	0.0769	452	0.1354	332	0.0419	335	0.8953	279		
3	3divi-006	0.0064	266	0.0094	264	0.0047	254	0.0066	259	0.0091	265	0.0191	187	0.0113	204	0.2854	196		
4	3divi-007	0.0024	100	0.0038	106	0.0028	120	0.0034	120	0.0046	165	0.0101	118	0.0082	142	0.2515	183		
5	accurascan-002	0.4209	516	0.5213	516	0.5826	529	0.6642	525	0.6295	514	0.6937	420	0.3116	430	0.9162	283		
6	accurascan-003	0.0017	58	0.0028	63	0.0024	45	0.0024	37	0.0029	81	0.0057	40	0.0048	56	0.0629	42		
7	acer-001	0.0294	435	0.0504	439	0.0240	442	0.0463	448	0.0436	425	0.0622	293	0.0360	326	-			
8	acer-002	0.0169	402	0.0262	405	0.0103	378	0.0167	387	0.0182	363	0.0281	228	0.0159	250	0.1555	146		
9	acisw-007	0.4276	518	0.5493	519	0.8425	548	0.9185	548	0.8424	528	0.9976	504	0.9930	525	0.9999	350		
10	acisw-008	0.0100	337	0.0147	334	0.0094	371	0.0126	339	0.1740	477	0.6651	417	0.4545	452	0.9302	286		
11	adera-004	0.0014	38	0.0022	37	0.0035	192	0.0050	200	0.0023	24	0.0212	198	0.0058	81	0.1469	142		
12	adera-005	0.0017	51	0.0026	53	0.0027	106	0.0030	85	0.0024	28	0.0134	146	0.0049	57	0.1246	126		
13	advance-004	0.0083	308	0.0101	278	0.0037	207	0.0054	215	0.0051	183	0.3555	381	0.1088	385	0.8285	263		
14	advance-005	0.0059	255	0.0084	249	0.0043	238	0.0060	239	0.0065	222	0.9998	523	0.9993	536	1.0000	380		
15	afisbiometrics-000	0.0051	219	0.0073	221	0.0030	144	0.0050	202	0.0044	158	0.0077	72	0.0057	78	0.0796	70		
16	afrengine-002	0.0052	223	0.0071	215	0.0032	162	0.0043	177	0.0194	371	0.2125	349	0.0450	342	0.2330	177		
17	afrengine-003	-		-		0.0028	127	0.0031	103	0.0116	308	0.0224	206	0.0208	288	0.0860	79		
18	aifirst-001	0.0119	366	0.0170	353	0.0084	350	0.0127	343	0.0131	321	0.0212	197	0.0138	227	-			
19	aigen-001	0.0124	371	0.0219	386	0.0143	413	0.0217	409	0.0236	388	0.8960	458	0.3255	433	-			
20	aigen-002	0.0192	414	0.0343	417	0.0256	443	0.0402	439	0.0389	416	0.9196	462	0.3876	443	0.9994	339		
21	ailabs-001	0.0158	397	0.0276	409	0.0192	429	0.0317	428	0.0352	409	0.0608	290	0.0434	338	-			
22	aimall-002	0.0119	364	0.0167	351	0.0224	438	0.0411	440	0.0233	386	0.0373	261	0.0235	300	-			
23	aimall-003	0.0033	143	0.0041	120	0.0033	184	0.0035	137	0.0056	202	0.0109	126	0.0087	158	-			
24	aiseemu-001	0.0021	80	0.0029	67	0.0027	104	0.0033	115	0.0038	133	0.0339	249	0.0057	79	0.4819	227		
25	aiseemu-002	0.0023	91	0.0032	81	0.0026	84	0.0027	59	0.0036	125	0.0439	266	0.0057	77	0.4259	221		
26	aiunionface-000	0.0104	343	0.0154	341	0.0082	346	0.0122	335	0.0141	328	0.0243	212	0.0169	256	-			
27	aize-002	0.0210	421	0.0327	414	0.0280	447	0.0489	452	0.0504	436	0.0692	301	0.0434	337	0.2657	191		
28	aize-003	0.0086	313	0.0125	312	0.0072	328	0.0126	341	0.0516	439	0.6137	409	0.1038	384	0.9911	314		
29	ajou-001	0.0093	326	0.0147	332	0.0071	327	0.0126	340	0.0173	359	0.0274	223	0.0186	270	-			
30	alchera-006	0.0028	121	0.0039	110	0.0026	85	0.0031	96	0.0025	44	0.0090	94	0.0042	33	0.0867	80		
31	alchera-007	0.0034	160	0.0049	164	0.0026	83	0.0031	97	0.0026	55	0.0096	110	0.0044	40	0.0834	77		
32	alfabeta-001	0.4867	526	0.5831	523	0.6855	535	0.8156	537	0.8253	527	0.7765	435	0.6416	471	0.9627	291		
33	alice-000	0.0119	367	0.0192	372	0.0106	383	0.0170	388	0.0167	349	0.0265	220	0.0150	243	0.1824	161		
34	alice-001	0.0034	159	0.0046	150	0.0032	160	0.0037	153	0.0030	92	0.3164	374	0.1088	386	0.8336	264		
35	alleyes-000	0.0058	246	0.0090	258	0.0055	286	0.0087	306	0.0068	227	0.0105	123	0.0076	128	-			
36	allgovision-000	0.0346	448	0.0527	445	0.0232	439	0.0339	429	0.0372	413	0.0620	292	0.0443	341	-			
37	alphaface-001	0.0065	267	0.0097	273	0.0039	218	0.0063	251	0.0083	252	-		-		-			
38	alphaface-002	0.0052	224	0.0075	229	0.0030	137	0.0044	183	1.0000	556	0.0115	131	0.0084	152	-			
39	amplifiedgroup-001	0.5034	528	0.5848	524	0.6973	538	0.8316	538	0.7807	521	0.7724	432	0.6354	467	-			
40	androvideo-000	0.0243	427	0.0438	431	0.0239	441	0.0365	436	0.0483	432	0.1870	341	0.0635	362	-			
41	anke-004	0.0080	297	0.0154	342	0.0073	330	0.0112	327	0.0102	291	0.0178	179	0.0118	210	-			
42	anke-005	0.0070	274	0.0109	292	0.0059	295	0.0094	310	0.0105	293	0.0142	149	0.0102	185	-			
43	antheus-000	0.2564	503	0.3776	504	0.7240	539	0.8699	543	0.8899	536	0.9872	489	0.9483	510	-			
44	antheus-001	0.1311	487	0.2306	490	0.5113	524	0.6797	526	0.8748	535	0.9908	494	0.9649	518	-			

Table 23: FNMR is the proportion of mated comparisons below a threshold set to achieve the FMR given in the header on the fourth row. FMR is the proportion of impostor comparisons at or above that threshold. The light grey values give rank over all algorithms in that column. The pink columns use only same-sex impostors; others are selected regardless of demographics. The exception, in the green column, uses "matched-covariates" i.e. impostors of the same sex, age group, and country of birth. The second pink column includes effects of extended ageing. Missing entries for border, visa, mugshot and wild images generally mean the algorithm did not run to completion. The VISA *columns compare images described in section 2.1. The* MUGSHOT *columns compare images described in section 2.5. The* VISA-BORDER *column compare images described in section 2.2 with those of section 2.4. The* BORDER *column compares images described in section 2.4. The* KIOSK-BORDER *columns compare images described in section 2.6 with those of section 2.4.*

	Algorithm	FALSE NON-MATCH RATE (FNMR)																	
		CONSTRAINED, COOPERATIVE																LESS CONSTRAINED, NON-COOP.	
	Name	VISAMC		VISA		MUGSHOT		MUGSHOT12+YRS		VISABORDER		BORDER		BORDER		KIOSKBORDER			
	FMR	0.0001		1E-06		1E-05		1E-05		1E-06		1E-06		1E-05		1E-06			
45	anyvision-004	0.0267	431	0.0385	425	0.0258	444	0.0487	451	0.0234	387	0.0301	232	0.0191	272	-			
46	anyvision-005	0.0023	94	0.0037	104	0.0027	118	0.0035	129	0.0049	177	0.0084	85	0.0069	110	-			
47	aratek-001	0.0033	154	0.0045	144	0.0028	125	0.0031	104	0.0043	153	0.0092	102	0.0069	112	0.0897	90		
48	armatura-001	0.0033	147	0.0042	123	0.0031	151	0.0037	150	0.0056	201	0.0110	127	0.0092	167	0.4625	225		
49	armatura-003	0.0020	75	0.0029	64	0.0026	93	0.0028	64	0.0025	50	0.0049	26	0.0043	36	0.0608	35		
50	asusaics-000	0.0125	374	0.0209	382	0.0085	352	0.0134	352	0.0143	331	0.7189	423	0.0285	313	-			
51	asusaics-001	0.0125	375	0.0210	383	0.0085	354	0.0134	353	0.0143	332	0.7437	426	0.0289	315	-			
52	autentika-001	0.0444	456	0.0688	455	0.0987	491	0.1531	490	0.1547	472	1.0000	533	0.9997	540	1.0000	370		
53	autentika-002	0.0536	464	0.0866	464	0.0657	483	0.1084	481	0.1548	473	0.9993	515	0.9939	526	1.0000	373		
54	authenmetric-003	0.0036	172	0.0053	178	0.0039	223	0.0051	204	0.0095	275	0.9930	498	0.5932	462	1.0000	359		
55	authenmetric-004	0.0027	116	0.0042	124	0.0033	178	0.0036	147	0.0083	255	0.9879	490	0.4058	446	1.0000	355		
56	authme-001	0.0036	171	0.0049	162	0.0037	209	0.0040	163	0.0030	91	0.3075	370	0.1310	392	0.7046	252		
57	aware-007	0.0101	340	0.0198	377	0.0060	301	0.0133	351	0.0224	383	0.5813	406	0.1673	406	0.8871	275		
58	aware-008	-		-		0.0062	304	0.0143	366	0.0135	324	0.0332	244	0.0133	223	0.3622	207		
59	awiros-001	0.4044	514	0.4622	510	0.5530	525	0.6518	523	0.2008	481	0.1994	344	0.1386	395	-			
60	awiros-002	0.1990	494	0.2561	492	0.3319	513	0.4411	512	0.3821	502	0.9938	499	0.2634	421	-			
61	aximetria-001	0.0111	354	0.0186	368	0.0110	389	0.0148	371	0.0170	354	0.3928	386	0.2090	412	0.7924	261		
62	ayftech-001	0.0946	479	0.1941	485	0.2438	506	0.3625	506	0.1558	474	0.1589	335	0.0936	380	-			
63	ayftech-003	0.0023	96	0.0037	103	0.0026	98	0.0030	91	0.0072	235	0.5411	402	0.2515	417	0.8902	276		
64	ayonix-000	0.4351	520	0.4872	512	0.6150	531	0.7510	531	0.6557	515	0.6361	412	0.4981	453	-			
65	beethedata-000	0.0127	377	0.0195	374	0.0092	363	0.0157	377	0.0171	356	0.0306	234	0.0204	284	0.1617	151		
66	beyneai-000	0.0071	279	0.0107	288	0.0104	381	0.0131	349	0.0170	355	0.9837	487	0.6171	464	1.0000	351		
67	biocube-001	0.5596	535	0.6834	533	0.7700	545	0.8712	544	0.8446	529	0.9661	480	0.7922	488	0.9846	308		
68	biocube-002	0.0612	467	0.0856	463	0.2330	504	0.2972	503	0.2365	489	0.9327	469	0.6947	474	0.9989	332		
69	bioidtechswiss-001	0.0054	231	0.0072	218	0.0069	320	0.0124	337	0.0060	209	0.0094	105	0.0065	99	-			
70	bioidtechswiss-002	0.0049	208	0.0067	204	0.0064	307	0.0116	330	0.0067	225	0.0117	132	0.0086	155	-			
71	biometric-vision-000	0.0023	92	0.0036	97	0.0028	126	0.0034	125	0.0028	80	0.3109	372	0.1504	399	0.6849	249		
72	bm-001	0.7431	544	0.9494	546	0.9586	554	0.9843	554	0.9049	538	0.9021	460	0.8395	494	-			
73	boetech-001	0.0662	470	0.0802	462	0.0493	473	0.0791	471	0.0682	449	0.1074	320	0.0758	369	0.9951	321		
74	boetech-002	0.0535	463	0.0565	448	0.0114	398	0.0136	355	0.0403	418	0.0650	295	0.0606	360	0.3470	205		
75	bresee-001	0.0085	310	0.0143	328	0.0086	355	0.0153	374	0.0108	298	0.0168	171	0.0115	208	-			
76	bresee-002	0.0079	295	0.0101	277	0.0065	313	0.0079	289	0.0129	317	0.0263	219	0.0224	296	0.2137	174		
77	camvi-002	0.0125	373	0.0221	388	0.0089	359	0.0145	369	0.0142	329	0.2650	362	0.0166	255	-			
78	camvi-004	0.0171	405	0.0316	413	0.0042	235	0.0049	198	0.0097	282	0.6636	416	0.0141	231	-			
79	candour-001	0.1048	483	0.3189	497	0.0130	408	0.0182	391	0.3879	504	0.9216	463	0.7071	479	0.9836	304		
80	canon-004	0.0052	225	0.0091	261	0.0033	183	0.0058	230	0.0037	129	0.0770	307	0.0494	348	0.3192	202		
81	canon-005	0.0024	101	0.0035	93	0.0025	70	0.0033	119	0.0052	187	0.0096	111	0.0090	162	0.0542	19		
82	cchonolulu-000	0.7910	546	0.8611	542	0.9824	555	0.9926	555	0.9940	548	0.9861	488	0.9534	511	1.0000	353		
83	cchonolulu-001	0.4202	515	0.4853	511	0.6298	532	0.7694	532	0.7402	518	0.9720	482	0.8870	502	0.9951	322		
84	ceiec-003	0.0071	281	0.0107	287	0.0061	302	0.0079	292	0.0160	340	0.0316	237	0.0260	308	-			
85	ceiec-004	0.0038	179	0.0051	172	0.0045	247	0.0053	210	0.0062	216	0.3939	387	0.0104	192	-			
86	chosun-001	0.0525	461	0.0936	467	0.0742	486	0.1263	488	0.0978	465	1.0000	542	0.9354	507	-			
87	chosun-002	0.0390	451	0.0646	453	0.0339	459	0.0576	461	0.0455	430	0.6904	419	0.1746	407	-			
88	chtface-005	0.0033	146	0.0049	158	0.0029	134	0.0041	168	0.0044	157	0.0317	238	0.0066	100	0.1952	167		

Table 24: FNMR is the proportion of mated comparisons below a threshold set to achieve the FMR given in the header on the fourth row. FMR is the proportion of impostor comparisons at or above that threshold. The light grey values give rank over all algorithms in that column. The pink columns use only same-sex impostors; others are selected regardless of demographics. The exception, in the green column, uses "matched-covariates" i.e. impostors of the same sex, age group, and country of birth. The second pink column includes effects of extended ageing. Missing entries for border, visa, mugshot and wild images generally mean the algorithm did not run to completion. The VISA *columns compare images described in section 2.1. The* MUGSHOT *columns compare images described in section 2.5. The* VISA-BORDER *column compare images described in section 2.2 with those of section 2.4. The* BORDER *column compares images described in section 2.4. The* KIOSK-BORDER *columns compare images described in section 2.6 with those of section 2.4.*

FNMR(T) "False non-match rate"
FMR(T) "False match rate"

	Algorithm	FALSE NON-MATCH RATE (FNMR)															
		CONSTRAINED, COOPERATIVE														LESS CONSTRAINED, NON-COOP.	
	Name	VISAMC		VISA		MUGSHOT		MUGSHOT12+YRS		VISABORDER		BORDER		BORDER		KIOSKBORDER	
	FMR	0.0001		1E-06		1E-05		1E-05		1E-06		1E-06		1E-05		1E-06	
89	chtface-006	0.0029	124	0.0043	131	0.0026	100	0.0034	126	0.0040	139	0.2701	363	0.0065	98	0.4464	223
90	cist-003	0.0065	268	0.0087	253	0.0046	250	0.0068	262	0.9993	551	0.9994	516	0.9993	537	0.9995	341
91	cist-004	0.0043	192	0.0062	193	0.0031	150	0.0041	171	0.0031	97	0.0363	257	0.0069	113	0.2732	193
92	clearviewai-000	0.0010	20	0.0019	30	0.0024	35	0.0028	67	0.0030	86	0.0058	42	0.0050	61	0.0604	33
93	clearviewai-001	0.0015	41	0.0021	35	0.0024	39	0.0030	87	0.0022	21	0.0745	305	0.0194	277	0.2740	194
94	closeli-001	0.0136	381	0.0163	345	0.0039	221	0.0054	214	0.0072	234	1.0000	534	0.0094	171	1.0000	375
95	cloudmatrix-001	0.0668	471	0.1141	473	0.0539	476	0.0905	474	0.3509	499	0.9819	486	0.9010	504	0.9999	343
96	cloudmatrix-002	0.0075	289	0.0113	299	0.0084	351	0.0120	332	0.9248	541	0.9997	520	0.9985	535	1.0000	381
97	cloudwalk-hr-003	0.0026	111	0.0041	118	0.0040	227	0.0058	229	0.0060	212	0.9992	513	0.0094	169	-	
98	cloudwalk-hr-004	0.0009	13	0.0018	27	0.0034	185	0.0028	73	0.0052	185	0.9992	514	0.0093	168	-	
99	cloudwalk-mt-006	0.0006	6	0.0006	2	0.0023	21	0.0019	1	0.0016	3	0.0032	2	0.0030	5	0.0427	2
100	cloudwalk-mt-007	0.0006	8	0.0007	3	0.0023	23	0.0019	2	0.0016	2	0.0032	1	0.0030	4	0.0419	1
101	cmcuni-001	0.0025	108	0.0038	109	0.0025	66	0.0025	44	0.0022	19	0.0052	33	0.0034	11	0.0660	54
102	codeline-000	0.0057	239	0.0079	239	0.0037	202	0.0053	213	0.2721	492	1.0000	535	0.9763	519	1.0000	383
103	cogent-007	0.0022	90	0.0038	108	0.0028	129	0.0031	92	0.0040	140	0.0082	79	0.0067	102	0.1395	134
104	cogent-008	0.0015	42	0.0027	57	0.0023	24	0.0025	42	0.0033	113	0.0063	53	0.0055	72	0.0884	85
105	cognitec-004	0.0036	168	0.0053	177	0.0053	278	0.0056	221	0.0098	283	0.0202	195	0.0154	245	0.3436	204
106	cognitec-005	0.0022	85	0.0030	74	0.0035	190	0.0041	165	0.0079	245	0.0480	276	0.0233	298	0.2134	173
107	cor-001	0.0075	290	0.0113	297	0.0055	288	0.0084	298	0.0091	267	0.0148	154	0.0092	166	-	
108	coretech-001	0.0052	222	0.0067	206	0.0083	349	0.0092	308	0.0346	408	0.1363	333	0.0252	304	0.6210	242
109	coretech-002	0.0020	73	0.0036	95	0.0064	311	0.0064	254	0.0118	309	0.0157	163	0.0110	199	0.3091	199
110	corsight-002	0.0053	227	0.0068	212	0.0030	142	0.0041	170	0.0039	135	0.0079	75	0.0054	70	0.0747	65
111	corsight-003	0.0026	113	0.0040	116	0.0028	122	0.0045	186	0.0035	123	0.0059	47	0.0046	46	0.0637	49
112	csc-002	0.0099	334	0.0132	316	0.0077	335	0.0142	365	0.0126	315	0.0195	189	0.0146	238	-	
113	csc-003	0.0053	226	0.0065	198	0.0037	204	0.0047	190	0.0074	240	0.0124	139	0.0112	203	0.0928	100
114	ctbcbank-000	0.0168	401	0.0250	399	0.0146	416	0.0224	410	0.0211	380	0.8964	459	0.3779	442	-	
115	ctbcbank-001	0.0155	394	0.0235	393	0.0148	421	0.0243	416	0.0207	375	0.9279	466	0.3469	437	-	
116	cu-face-003	0.0036	170	0.0049	161	0.0031	157	0.0037	152	0.0030	88	0.3075	369	0.1310	393	0.7046	253
117	cu-face-004	-		-		0.0032	165	0.0035	132	0.0026	62	0.4284	391	0.2115	413	0.7861	260
118	cubox-002	0.0034	158	0.0041	119	0.0025	61	0.0025	45	0.0033	112	0.0064	54	0.0058	82	0.0519	15
119	cubox-003	0.0021	78	0.0028	62	0.0024	58	0.0026	50	0.0025	48	0.0046	16	0.0037	20	0.0495	12
120	cudocommunication-001	0.4777	522	1.0000	564	0.4373	520	0.5360	517	1.0000	567	1.0000	564	1.0000	560	1.0000	490
121	cuhkee-001	0.0036	174	0.0045	140	0.0031	158	0.0046	187	0.0051	184	0.0095	107	0.0079	132	-	
122	cybercore-002	0.0092	324	0.0119	302	0.0049	261	0.0072	270	0.9105	540	1.0000	541	1.0000	546	1.0000	379
123	cybercore-003	0.0155	395	0.0164	347	0.0032	168	0.0033	118	0.0024	30	0.9719	481	0.8213	492	0.9993	336
124	cyberextruder-003	0.0109	350	0.0169	352	0.0071	325	0.0112	328	0.0165	346	0.0410	265	0.0272	311	0.2308	176
125	cyberextruder-004	0.0118	363	0.0181	366	0.0081	343	0.0133	350	0.0191	369	0.0329	241	0.0268	309	0.1904	164
126	cyberlink-012	0.0010	22	0.0016	20	0.0036	196	0.0035	135	0.0047	170	0.0099	113	0.0074	125	0.1350	132
127	cyberlink-013	0.0011	27	0.0017	24	0.0037	200	0.0036	141	0.0045	160	0.0090	96	0.0080	136	0.0924	98
128	dahua-006	0.0027	114	0.0039	113	0.0031	155	0.0039	162	0.0039	134	0.0067	62	0.0058	80	-	
129	dahua-007	0.0017	55	0.0023	40	0.0026	91	0.0032	106	0.0033	108	0.0060	49	0.0054	69	0.0678	56
130	daon-000	0.0095	328	0.0117	301	0.0068	317	0.0077	285	0.0092	270	0.0174	177	0.0137	226	0.1430	139
131	datech-000	0.0020	74	0.0031	79	0.0031	153	0.0041	169	0.0033	111	0.1646	336	0.0667	364	0.4898	228
132	datech-001	-		-		0.0028	123	0.0034	124	0.0026	67	0.2308	355	0.0818	373	0.5505	232

Table 25: FNMR is the proportion of mated comparisons below a threshold set to achieve the FMR given in the header on the fourth row. FMR is the proportion of impostor comparisons at or above that threshold. The light grey values give rank over all algorithms in that column. The pink columns use only same-sex impostors; others are selected regardless of demographics. The exception, in the green column, uses "matched-covariates" i.e. impostors of the same sex, age group, and country of birth. The second pink column includes effects of extended ageing. Missing entries for border, visa, mugshot and wild images generally mean the algorithm did not run to completion. The VISA *columns compare images described in section 2.1. The* MUGSHOT *columns compare images described in section 2.5. The* VISA-BORDER *column compare images described in section 2.2 with those of section 2.4. The* BORDER *column compares images described in section 2.4. The* KIOSK-BORDER *columns compare images described in section 2.6 with those of section 2.4.*

	Algorithm	FALSE NON-MATCH RATE (FNMR)															
		CONSTRAINED, COOPERATIVE														LESS CONSTRAINED, NON-COOP.	
	Name	VISAMC		VISA		MUGSHOT		MUGSHOT12+YRS		VISABORDER		BORDER		BORDER		KIOSKBORDER	
	FMR	0.0001		1E-06		1E-05		1E-05		1E-06		1E-06		1E-05		1E-06	
133	decatur-000	0.0714	472	0.1115	471	0.0608	481	0.1106	484	0.0866	457	1.0000	539	0.0714	367	-	
134	decatur-001	0.0424	454	0.0711	457	0.0237	440	0.0458	444	0.0447	428	1.0000	531	0.9969	533	1.0000	389
135	decloakface-001	0.0795	475	0.1131	472	0.3127	510	0.4259	510	0.2118	485	0.7926	439	0.6088	463	0.9589	290
136	deepglint-004	0.0025	106	0.0034	87	0.0039	222	0.0061	246	0.0050	180	0.0091	99	0.0082	141	0.1003	107
137	deepglint-005	0.0052	221	0.0059	190	0.0030	138	0.0031	93	0.0033	116	0.7620	431	0.1535	400	0.9912	315
138	deepsea-001	0.0136	382	0.0215	385	0.0142	412	0.0214	408	0.0163	344	0.0250	215	0.0192	274	-	
139	deepsense-002	0.0010	21	0.0016	21	0.0024	30	0.0023	22	0.0026	54	0.0052	34	0.0043	37	0.0781	69
140	deepsense-003	0.0009	17	0.0015	18	0.0025	71	0.0024	26	0.0023	26	0.0457	271	0.0097	175	0.2547	186
141	dermalog-011	0.0045	199	0.0062	195	0.0035	191	0.0059	235	0.0057	206	0.2242	351	0.0407	331	0.6329	243
142	dermalog-012	0.0080	299	0.0101	279	0.0037	206	0.0057	226	0.0055	196	0.0095	108	0.0068	108	0.0834	78
143	dicio-001	0.5486	533	0.6442	527	0.7516	540	0.8607	539	0.8678	534	0.8268	447	0.7034	477	0.9752	298
144	didiglobalface-001	0.0055	236	0.0092	263	0.0030	141	0.0045	185	0.0088	260	0.0119	135	0.0085	153	-	
145	didiglobalface-002	0.0033	152	0.0051	170	0.0026	92	0.0034	128	0.0033	110	0.0085	86	0.0047	51	0.1135	118
146	digidata-000	0.0967	480	0.1410	477	0.2596	507	0.3462	505	0.0293	401	0.0363	256	0.0212	290	0.1849	163
147	digidata-001	0.0224	424	0.0352	419	0.0330	456	0.0570	460	0.0109	300	0.0481	277	0.0123	218	0.3055	198
148	digitalbarriers-002	0.3360	510	0.3690	502	0.0877	489	0.1557	491	0.0971	464	0.0951	314	0.0497	349	-	
149	dps-000	0.0115	359	0.0176	362	0.0149	422	0.0185	396	0.0173	358	0.0275	225	0.0180	265	0.1757	157
150	dsk-000	0.1526	491	0.2169	488	0.3787	515	0.5426	519	0.3115	495	0.3089	371	0.1994	410	-	
151	einetworks-000	0.0099	332	0.0180	365	0.0088	358	0.0140	361	0.0130	319	0.0225	208	0.0147	240	-	
152	einetworksindia-000	0.0058	249	0.0074	226	0.0051	273	0.0061	247	0.0074	238	0.0193	188	0.0102	186	0.1819	160
153	einetworksindia-001	0.0042	189	0.0062	194	0.0048	255	0.0064	252	0.0057	204	0.0473	274	0.0092	165	0.3984	217
154	ekin-002	0.1168	485	0.2042	486	0.1530	500	0.2524	499	0.1777	479	0.2773	365	0.1347	394	0.8954	280
155	element-000	0.0023	95	0.0035	94	0.0024	51	0.0026	46	0.0029	82	0.0060	50	0.0048	53	0.0631	46
156	enface-001	0.0072	285	0.0107	286	0.0071	322	0.0138	357	0.0068	228	0.0515	280	0.0094	172	0.9942	319
157	enface-002	0.0033	151	0.0052	174	0.0038	216	0.0073	273	0.0026	66	0.9998	524	0.9995	539	1.0000	377
158	eocortex-000	0.3485	511	0.6943	534	0.1122	492	0.1574	492	0.2155	486	0.2257	354	0.1606	404	-	
159	ercacat-001	0.0036	173	0.0044	134	0.0033	177	0.0047	191	0.0106	294	0.0202	194	0.0184	268	-	
160	euronovate-003	0.0061	260	0.0088	255	0.0040	229	0.0060	240	0.0065	223	0.7815	437	0.5034	455	0.9823	302
161	euronovate-004	0.0082	303	0.0110	293	0.0050	269	0.0077	284	0.0074	239	0.6949	421	0.3354	435	0.9791	301
162	expasoft-001	0.0328	444	0.0488	436	0.0211	435	0.0342	431	0.0629	447	0.6483	414	0.2816	425	-	
163	expasoft-002	0.0170	403	0.0274	407	0.0787	488	0.0768	470	0.1629	475	0.9996	519	0.9631	517	1.0000	365
164	f8-001	0.0249	428	0.0336	415	0.0178	427	0.0232	412	0.0303	403	0.0615	291	0.0408	332	-	
165	f8-002	0.0340	446	0.0591	451	0.0213	436	0.0374	437	0.0452	429	0.0760	306	0.0502	350	0.2708	192
166	facehawk-000	1.0000	559	1.0000	551	1.0000	568	1.0000	563	1.0000	559	1.0000	550	1.0000	564	1.0000	449
167	facelocate-001	-		-		0.0664	484	0.1171	486	0.0950	463	0.9219	464	0.7041	478	0.9985	330
168	faceonlive-001	0.0269	433	0.0359	422	0.0387	464	0.0721	468	0.0246	393	0.0349	252	0.0220	293	0.2408	179
169	faceonlive-002	0.0121	368	0.0135	319	0.0033	180	0.0041	167	0.0037	131	0.9427	471	0.7927	489	0.9993	335
170	facephi-000	0.0044	193	0.0059	187	0.0047	251	0.0057	227	0.0088	261	1.0000	545	1.0000	548	1.0000	385
171	facesoft-000	0.0085	311	0.0112	295	0.0064	308	0.0107	323	0.0091	266	0.0171	173	0.0107	195	-	
172	facetag-000	0.2836	505	0.4081	507	0.2933	509	0.4303	511	0.3448	497	0.6312	411	0.3530	438	0.9753	299
173	facetag-002	0.0098	331	0.0147	333	0.0064	312	0.0110	325	0.0116	307	0.0190	186	0.0119	215	0.1334	130
174	facex-001	1.0000	557	1.0000	568	1.0000	561	1.0000	561	1.0000	568	1.0000	566	1.0000	552	-	
175	facex-002	0.0803	476	0.1404	476	0.1283	496	0.1979	497	0.1440	470	0.1952	343	0.1299	391	0.7427	254
176	facia-001	0.0083	307	0.0124	306	0.0064	310	0.0097	315	0.0098	284	0.9983	508	0.9849	520	1.0000	374

Table 26: FNMR is the proportion of mated comparisons below a threshold set to achieve the FMR given in the header on the fourth row. FMR is the proportion of impostor comparisons at or above that threshold. The light grey values give rank over all algorithms in that column. The pink columns use only same-sex impostors; others are selected regardless of demographics. The exception, in the green column, uses "matched-covariates" i.e. impostors of the same sex, age group, and country of birth. The second pink column includes effects of extended ageing. Missing entries for border, visa, mugshot and wild images generally mean the algorithm did not run to completion. The VISA *columns compare images described in section 2.1. The* MUGSHOT *columns compare images described in section 2.5. The* VISA-BORDER *column compare images described in section 2.2 with those of section 2.4. The* BORDER *column compares images described in section 2.4. The* KIOSK-BORDER *columns compare images described in section 2.6 with those of section 2.4.*

	Algorithm	FALSE NON-MATCH RATE (FNMR)															
		CONSTRAINED, COOPERATIVE														LESS CONSTRAINED, NON-COOP.	
	Name	VISAMC		VISA		MUGSHOT		MUGSHOT12+YRS		VISABORDER		BORDER		BORDER		KIOSKBORDER	
	FMR	0.0001		1E-06		1E-05		1E-05		1E-06		1E-06		1E-05		1E-06	
177	farfaces-001	0.4890	527	0.5860	525	0.5650	526	0.7268	529	0.8015	523	0.7511	427	0.5892	461	0.9536	289
178	fastenterprises-000	0.0093	325	0.0151	338	0.0098	373	0.0140	362	0.0209	377	0.2991	366	0.1608	405	0.6727	247
179	fedu-001	-		-		0.0033	172	0.0047	189	0.0128	316	0.9816	485	0.9216	506	0.9999	346
180	fiberhome-nanjing-003	0.0090	316	0.0139	324	0.0082	345	0.0144	367	0.0110	301	0.0174	175	0.0107	196	-	
181	fiberhome-nanjing-004	0.0037	177	0.0056	184	0.0031	152	0.0043	175	0.0043	155	0.0083	83	0.0061	93	-	
182	fincore-000	0.0309	441	0.0502	438	0.0281	448	0.0510	454	0.0521	440	0.0815	309	0.0522	351	0.3100	200
183	firstcreditkz-002	0.0018	61	0.0026	49	0.0024	46	0.0024	31	0.0029	85	0.0056	39	0.0049	58	0.0624	40
184	firstcreditkz-003	-		-		0.0023	26	0.0024	33	0.0026	59	0.0104	120	0.0047	49	0.0910	95
185	foomobi-001	0.4827	524	0.5795	520	0.6823	534	0.8132	534	0.8217	524	1.0000	558	1.0000	555	1.0000	537
186	foomobi-002	0.4827	525	0.5795	521	0.6823	533	0.8132	535	0.8217	525	1.0000	567	1.0000	561	1.0000	510
187	fpt-000	-		-		0.0213	437	0.0375	438	0.0364	411	0.9528	473	0.8729	499	0.9993	337
188	fraudcom-000	0.0110	353	0.0173	355	0.0083	347	0.0139	359	0.0166	347	0.0258	218	0.0177	261	0.1488	144
189	frpkauai-001	0.0023	93	0.0035	92	0.0026	79	0.0030	89	0.0040	142	0.0080	76	0.0072	119	0.0706	58
190	frpkauai-002	0.0024	103	0.0035	91	0.0024	53	0.0024	35	0.0033	115	0.0065	57	0.0058	83	0.0599	31
191	fujitsulab-002	0.0091	320	0.0124	309	0.0105	382	0.0156	375	0.0169	353	0.0345	251	0.0146	239	-	
192	fujitsulab-003	0.0045	198	0.0065	199	0.0057	292	0.0083	295	0.0080	247	0.0154	158	0.0101	183	0.5564	233
193	g42-intellibrain-001	0.0006	7	0.0009	8	0.0037	201	0.0044	178	0.0030	93	0.0059	45	0.0053	67	0.0750	66
194	g42-intellibrain-002	0.0006	9	0.0011	9	0.0029	133	0.0037	154	0.0028	73	0.0212	199	0.0091	163	0.1398	135
195	geo-002	0.0171	406	0.0187	370	0.0035	189	0.0051	206	0.0064	217	0.0117	133	0.0083	149	0.0938	101
196	geo-004	0.0030	127	0.0041	117	0.0025	72	0.0030	81	0.0035	122	0.0065	56	0.0053	66	0.0648	51
197	gistouch-000	0.0296	437	0.0518	442	0.0342	460	0.0609	463	0.0493	435	1.0000	546	1.0000	551	1.0000	390
198	gistouch-001	0.0176	409	0.0312	411	0.8931	550	0.9735	550	0.8625	530	1.0000	551	1.0000	566	1.0000	459
199	glory-006	0.0050	210	0.0068	208	0.0051	275	0.0070	267	0.0069	229	0.7869	438	0.5076	456	0.9719	294
200	glory-007	0.0050	212	0.0068	211	0.0050	268	0.0069	265	0.0068	226	0.0126	143	0.0083	148	0.1066	113
201	gorilla-008	0.0058	248	0.0091	260	0.0049	260	0.0079	291	0.0079	246	0.0126	142	0.0091	164	0.1217	124
202	gorilla-009	0.0049	207	0.0072	217	0.0038	213	0.0056	222	0.0065	221	0.0104	119	0.0070	114	0.1103	115
203	gpstechvn-000	0.0202	418	0.0355	421	0.0142	411	0.0248	417	0.0208	376	0.0495	279	0.0207	286	0.5098	230
204	graymatics-001	0.1039	481	0.1620	482	0.1344	498	0.1917	496	0.1648	476	0.5160	398	0.2689	422	0.9194	284
205	griaule-001	0.0057	240	0.0078	236	0.0045	246	0.0065	257	0.0070	230	0.7515	428	0.5106	457	0.9747	296
206	griaule-002	0.0021	83	0.0032	82	0.0025	76	0.0027	61	0.0034	119	0.0996	318	0.0201	282	0.3978	215
207	hertasecurity-002	0.0206	419	0.0315	412	0.0060	296	0.0078	287	0.0253	395	0.0696	303	0.0457	343	0.4565	224
208	hertasecurity-003	0.0079	296	0.0104	282	0.0060	297	0.0078	286	0.0255	396	0.0732	304	0.0460	344	0.4731	226
209	hik-001	0.0096	330	0.0125	311	0.0093	369	0.0164	385	0.0108	299	0.0937	312	0.0127	219	-	
210	hisign-002	0.0029	123	0.0044	136	0.0027	115	0.0032	112	0.0028	79	0.0409	264	0.0132	222	0.2016	169
211	hisign-003	-		-		0.0030	139	0.0036	140	0.0036	126	0.0582	285	0.0201	283	0.2584	187
212	hyperverge-003	0.0019	68	0.0030	70	0.0025	63	0.0029	78	0.0027	68	0.0049	30	0.0042	34	0.0576	25
213	hyperverge-005	0.0026	112	0.0039	115	0.0027	102	0.0031	102	0.0036	128	0.0066	59	0.0055	71	0.0658	53
214	hzailu-005	0.0172	407	0.0197	376	0.0028	128	0.0036	144	0.0032	106	0.0058	43	0.0048	54	0.0751	67
215	hzailu-006	0.0161	399	0.0174	358	0.0024	48	0.0027	52	0.0026	60	0.0049	29	0.0044	43	0.0654	52
216	i2v-001	-		-		0.0946	490	0.1369	489	0.3989	506	0.9998	522	0.9966	531	1.0000	366
217	icm-004	0.0079	294	0.0120	303	0.0074	332	0.0107	322	0.0091	268	0.0281	229	0.0128	220	0.2778	195
218	icm-005	0.0100	336	0.0140	325	0.0091	360	0.0108	324	0.0169	352	0.0319	239	0.0290	316	0.1775	159
219	icomm-000	0.0019	66	0.0033	84	0.0033	179	0.0044	179	0.0031	101	0.1350	331	0.0552	356	0.4196	220
220	icthtc-000	0.0260	430	0.0396	427	0.0207	434	0.0339	430	0.0291	400	0.0474	275	0.0346	323	-	

Table 27: FNMR is the proportion of mated comparisons below a threshold set to achieve the FMR given in the header on the fourth row. FMR is the proportion of impostor comparisons at or above that threshold. The light grey values give rank over all algorithms in that column. The pink columns use only same-sex impostors; others are selected regardless of demographics. The exception, in the green column, uses "matched-covariates" i.e. impostors of the same sex, age group, and country of birth. The second pink column includes effects of extended ageing. Missing entries for border, visa, mugshot and wild images generally mean the algorithm did not run to completion. The VISA *columns compare images described in section 2.1. The* MUGSHOT *columns compare images described in section 2.5. The* VISA-BORDER *column compare images described in section 2.2 with those of section 2.4. The* BORDER *column compares images described in section 2.4. The* KIOSK-BORDER *columns compare images described in section 2.6 with those of section 2.4.*

	Algorithm	FALSE NON-MATCH RATE (FNMR)																	
		CONSTRAINED, COOPERATIVE																LESS CONSTRAINED, NON-COOP.	
	Name	VISAMC		VISA		MUGSHOT		MUGSHOT12+YRS		VISABORDER		BORDER		BORDER		KIOSKBORDER			
	FMR	0.0001		1E-06		1E-05		1E-05		1E-06		1E-06		1E-05		1E-06			
221	id3-006	0.0072	283	0.0103	281	0.0049	262	0.0074	276	0.0095	274	0.0165	169	0.0119	214	-			
222	id3-008	0.0039	182	0.0055	182	0.0032	166	0.0042	173	0.0081	249	0.0155	160	0.0134	224	0.1186	119		
223	idemia-009	0.0022	89	0.0030	75	0.0022	13	0.0023	24	0.0023	23	0.0046	17	0.0039	24	0.0533	16		
224	idemia-010	0.0015	43	0.0026	46	0.0022	14	0.0020	5	0.0020	13	0.0040	10	0.0033	9	0.0465	6		
225	identy-000	0.0073	286	0.0095	268	0.0050	265	0.0067	260	0.0071	233	0.8257	446	0.4310	448	0.9839	305		
226	igearx-face-000	0.0091	319	0.0146	331	0.0163	425	0.0362	435	0.0399	417	0.6436	413	0.3305	434	0.7832	259		
227	iit-002	0.0111	356	0.0177	364	0.0085	353	0.0140	360	0.0193	370	0.0332	246	0.0260	306	-			
228	iit-003	0.0082	306	0.0151	339	0.0053	280	0.0084	299	0.0122	312	0.0199	192	0.0137	225	-			
229	imds-software-002	0.0048	205	0.0072	220	0.0036	197	0.0052	209	0.0047	168	0.9981	506	0.0078	130	1.0000	367		
230	imds-software-003	0.0032	138	0.0047	153	0.0028	119	0.0036	146	0.0036	127	0.9987	509	0.0063	95	1.0000	364		
231	imperial-000	0.0067	271	0.0108	290	0.0080	341	0.0134	354	0.0087	258	0.0581	284	0.0102	187	-			
232	imperial-002	0.0058	250	0.0081	243	0.0055	287	0.0085	302	0.0083	253	0.0157	161	0.0103	188	-			
233	incode-009	0.0044	194	0.0067	207	0.0034	187	0.0051	203	0.0049	178	0.0091	98	0.0067	103	0.0892	88		
234	incode-013	0.0035	164	0.0049	160	0.0032	161	0.0039	161	0.0051	182	0.0094	104	0.0081	140	0.0768	68		
235	infocert-001	0.0105	345	0.0172	354	0.0078	337	0.0125	338	0.0159	338	0.1573	334	0.0565	357	0.5716	236		
236	innefulabs-000	0.0122	369	0.0199	378	0.0112	396	0.0197	402	0.0222	382	0.0372	260	0.0271	310	-			
237	innominds-001	0.5569	534	0.6541	529	0.7642	544	0.8665	542	0.7629	519	0.8200	443	0.6359	468	0.9841	307		
238	innovativetechnologyltd-001	0.0578	466	0.0938	468	0.0501	474	0.0981	476	0.0592	445	0.0779	308	0.0422	336	-			
239	innovativetechnologyltd-002	0.0451	457	0.0716	458	0.0541	477	0.1009	479	0.0506	437	0.0682	299	0.0371	327	-			
240	innovatrics-010	0.0017	57	0.0031	80	0.0027	112	0.0028	65	0.0041	146	0.0078	73	0.0066	101	0.0744	63		
241	innovatrics-011	-		-		0.0026	97	0.0027	55	0.0032	104	0.0060	48	0.0044	41	0.0615	38		
242	insightface-003	0.0015	46	0.0021	33	0.0045	245	0.0034	127	0.1298	466	1.0000	556	0.9407	508	1.0000	423		
243	insightface-004	0.0015	44	0.0023	39	0.0052	277	0.0036	145	0.1403	469	0.9923	497	0.9128	505	0.9989	331		
244	inspur-001	0.0035	163	0.0049	159	0.0025	67	0.0030	86	0.0029	84	0.9951	500	0.9592	514	1.0000	357		
245	inspur-002	0.0025	105	0.0039	112	0.0024	32	0.0027	54	0.0031	96	0.0062	52	0.0047	50	0.1112	117		
246	intellicloudai-001	0.0142	387	0.0234	392	0.0092	365	0.0145	368	0.0162	342	0.0371	259	0.0171	258	-			
247	intellicloudai-002	0.0059	254	0.0085	251	0.0060	298	0.0069	266	0.0108	297	0.2477	361	0.0171	257	-			
248	intellifusion-001	0.0072	282	0.0094	265	0.0056	291	0.0085	303	0.0111	303	0.0212	200	0.0143	233	-			
249	intellifusion-002	0.0059	251	0.0077	235	0.0040	226	0.0074	275	0.0085	256	0.5352	401	0.0104	193	-			
250	intellivision-006	0.0111	357	0.0174	357	0.0110	390	0.0162	382	0.0181	361	0.0313	235	0.0191	273	0.2416	180		
251	intellivision-007	0.0086	312	0.0128	315	0.0098	374	0.0159	380	0.0133	322	0.0218	204	0.0154	246	0.1751	156		
252	intellivix-004	0.0032	140	0.0045	143	0.0025	74	0.0031	101	0.0040	138	0.0074	68	0.0063	96	0.0662	55		
253	intellivix-005	0.0034	161	0.0048	155	0.0024	36	0.0027	60	0.0035	121	0.0067	61	0.0059	91	0.0609	36		
254	intelresearch-007	0.0009	19	0.0013	11	0.0025	65	0.0025	38	0.0035	120	0.0069	63	0.0057	76	0.0746	64		
255	intelresearch-008	0.0009	18	0.0013	12	0.0025	64	0.0025	39	0.0028	77	0.0304	233	0.0048	55	0.2375	178		
256	intema-000	0.0012	31	0.0017	22	0.0023	15	0.0022	16	0.0022	20	0.0172	174	0.0061	92	0.0996	106		
257	intema-001	0.0010	23	0.0014	17	0.0021	5	0.0020	8	0.0019	11	0.0037	7	0.0030	6	0.0457	5		
258	intozi-001	0.9982	549	0.9998	549	0.9998	559	1.0000	562	1.0000	554	1.0000	543	1.0000	550	1.0000	522		
259	intsysmsu-001	0.9543	548	0.9888	548	0.9923	556	0.9948	556	0.9977	549	0.9955	501	0.9892	523	-			
260	intsysmsu-002	0.0130	378	0.0254	401	0.0137	409	0.0267	423	0.0160	339	0.0267	222	0.0145	237	-			
261	ionetworks-001	0.0254	429	0.0388	426	0.0435	470	0.0662	465	0.0426	422	0.8936	457	0.7391	485	0.9964	326		
262	ionetworks-002	0.0045	195	0.0066	202	0.0033	176	0.0047	192	0.0544	441	0.9648	478	0.8765	501	0.9994	338		
263	iqface-000	0.0091	321	0.0143	327	0.0075	334	0.0110	326	0.0171	357	0.2234	350	0.0359	325	-			
264	iqface-003	0.0058	247	0.0079	237	0.0051	274	0.0058	232	0.0104	292	0.0200	193	0.0193	275	-			

Table 28: FNMR is the proportion of mated comparisons below a threshold set to achieve the FMR given in the header on the fourth row. FMR is the proportion of impostor comparisons at or above that threshold. The light grey values give rank over all algorithms in that column. The pink columns use only same-sex impostors; others are selected regardless of demographics. The exception, in the green column, uses "matched-covariates" i.e. impostors of the same sex, age group, and country of birth. The second pink column includes effects of extended ageing. Missing entries for border, visa, mugshot and wild images generally mean the algorithm did not run to completion. The VISA *columns compare images described in section 2.1. The* MUGSHOT *columns compare images described in section 2.5. The* VISA-BORDER *column compare images described in section 2.2 with those of section 2.4. The* BORDER *column compares images described in section 2.4. The* KIOSK-BORDER *columns compare images described in section 2.6 with those of section 2.4.*

FNMR(T) "False non-match rate"
FMR(T) "False match rate"

	Algorithm	FALSE NON-MATCH RATE (FNMR)															
		CONSTRAINED, COOPERATIVE														LESS CONSTRAINED, NON-COOP.	
	Name	VISAMC		VISA		MUGSHOT		MUGSHOT12+YRS		VISABORDER		BORDER		BORDER		KIOSKBORDER	
	FMR	0.0001		1E-06		1E-05		1E-05		1E-06		1E-06		1E-05		1E-06	
265	irex-000	0.0052	220	0.0099	274	0.0056	290	0.0083	296	0.0137	326	0.0163	167	0.0078	129	-	
266	isap-001	0.5092	529	0.6588	530	0.6899	537	0.7978	533	0.7200	516	0.7253	424	0.5373	459	-	
267	isap-002	0.0114	358	0.0186	369	0.0087	356	0.0151	373	0.0156	337	0.5134	397	0.0333	319	-	
268	isityou-000	0.5682	536	0.7033	536	1.0000	567	0.9999	559	1.0000	557	1.0000	547	1.0000	562	-	
269	isystems-001	0.0149	391	0.0245	397	0.0138	410	0.0210	406	0.0209	379	0.0332	245	0.0223	295	-	
270	isystems-002	0.0118	362	0.0182	367	0.0111	393	0.0162	383	0.0166	348	0.0284	230	0.0195	278	-	
271	itmo-007	0.0080	298	0.0125	310	0.0107	384	0.0185	394	0.0167	350	0.0222	205	0.0144	236	-	
272	itmo-008	0.0090	317	0.0150	337	0.0058	293	0.0059	237	0.0187	365	0.0355	253	0.0339	320	0.1758	158
273	ivacognitive-001	0.0189	412	0.0351	418	0.0123	404	0.0235	413	0.0198	373	0.0274	224	0.0155	247	-	
274	iws-000	0.4824	523	0.5801	522	0.6859	536	0.8155	536	0.8251	526	0.7756	434	0.6400	470	-	
275	jaakit-001	0.5830	537	0.7146	537	0.8173	547	0.8893	546	0.8950	537	0.8387	450	0.7091	480	0.9733	295
276	kakao-008	0.0011	25	0.0018	28	0.0023	17	0.0023	20	0.0021	18	0.0041	11	0.0035	13	0.0475	8
277	kakao-009	0.0009	15	0.0013	13	0.0023	19	0.0023	21	0.0020	14	0.0039	9	0.0034	10	0.0468	7
278	kakaobank-000	0.0041	188	0.0058	185	0.0041	231	0.0058	234	0.0060	211	0.9988	511	0.3243	432	1.0000	363
279	kakaobank-001	0.0030	129	0.0046	147	0.0032	169	0.0039	158	0.0049	176	0.9998	525	0.9994	538	1.0000	388
280	kakaopay-001	0.0152	393	0.0252	400	0.0145	415	0.0270	424	0.0232	385	0.0344	250	0.0194	276	0.2005	168
281	kasikornlabs-002	0.0069	273	0.0091	259	0.0048	256	0.0063	250	0.0076	242	0.0144	152	0.0110	200	0.1249	127
282	kasikornlabs-003	0.0057	237	0.0076	230	0.0042	236	0.0056	223	0.0059	208	0.0123	137	0.0098	176	0.1212	123
283	kedacom-000	0.0055	233	0.0081	244	0.0111	395	0.0120	333	0.0415	420	0.0966	316	0.0686	365	-	
284	kiwitech-000	0.0076	291	0.0105	284	0.0081	344	0.0128	345	0.0096	276	0.0163	166	0.0101	184	-	
285	kneron-003	0.0542	465	0.0902	465	0.0346	461	0.0562	458	0.0919	461	0.1251	327	0.0973	381	-	
286	kneron-005	0.0157	396	0.0259	403	0.0126	407	0.0212	407	0.0406	419	0.0693	302	0.0542	355	-	
287	knowutech-000	0.0039	183	0.0055	180	0.0028	132	0.0042	172	0.0042	149	0.0077	71	0.0059	87	0.0820	75
288	kogniza-001	-		-		0.0028	131	0.0031	105	0.0025	46	0.0048	23	0.0042	31	0.0557	21
289	kookmin-002	0.0054	230	0.0077	234	0.0043	239	0.0065	256	0.0123	313	0.7591	430	0.0198	281	-	
290	koreaid-001	0.0031	134	0.0045	141	0.0026	90	0.0032	108	0.0043	154	0.0083	80	0.0068	109	0.0743	62
291	krungthai-002	0.0105	346	0.0161	343	0.0091	362	0.0141	363	0.7350	517	0.9889	491	0.9605	515	0.9999	345
292	kuke3d-001	0.0058	245	0.0104	283	0.0083	348	0.0093	309	0.0270	398	0.9901	493	0.8341	493	1.0000	358
293	kuke3d-002	0.0077	292	0.0135	320	0.0069	319	0.0098	316	0.0111	302	1.0000	544	1.0000	549	1.0000	369
294	lebentech-000	0.5940	538	0.7032	535	0.8854	549	0.9511	549	0.9089	539	0.9970	503	0.9861	522	0.9999	348
295	lebentech-001	0.0304	440	0.9032	544	0.9998	560	1.0000	560	1.0000	555	1.0000	538	0.9999	545	1.0000	387
296	lemalabs-001	0.0111	355	0.0175	360	0.0088	357	0.0142	364	0.0143	330	0.0228	209	0.0140	229	0.1646	153
297	lineclova-002	0.0021	79	0.0035	88	0.0025	60	0.0027	57	0.0041	144	0.0086	89	0.0072	118	0.1595	148
298	lineclova-003	0.0018	62	0.0030	71	0.0028	130	0.0031	94	0.0041	145	0.0083	82	0.0075	127	0.1014	108
299	lookman-002	0.0297	438	0.0547	447	0.0339	458	0.0562	457	0.0614	446	0.0960	315	0.0790	370	-	
300	lookman-004	0.0074	288	0.0099	275	0.0124	406	0.0149	372	0.0430	424	0.0866	310	0.0694	366	-	
301	luxand-000	0.2056	495	0.2814	494	0.4053	517	0.5365	518	0.3497	498	0.3743	385	0.2605	419	-	
302	luxand-001	0.0116	360	0.0925	466	0.0144	414	0.0267	422	1.0000	560	1.0000	552	1.0000	567	1.0000	464
303	mantra-000	0.0037	175	0.0052	175	0.0054	284	0.0056	224	0.0097	281	0.0181	180	0.0151	244	-	
304	maxvision-005	0.0014	37	0.0026	48	0.0024	41	0.0024	27	0.0025	40	0.1216	325	0.0332	318	0.3922	214
305	maxvision-006	0.0016	50	0.0026	54	0.0024	44	0.0024	30	0.0024	38	0.4012	389	0.1799	408	0.7634	255
306	megvii-008	0.0003	3	0.0008	7	0.0023	27	0.0021	11	0.0024	39	0.0049	27	0.0047	52	0.0541	18
307	megvii-009	0.0003	1	0.0008	6	0.0023	28	0.0021	10	0.0018	6	0.0149	155	0.0036	15	0.1096	114
308	meituan-003	0.0017	52	0.0021	34	0.0024	38	0.0023	25	0.0024	34	0.0084	84	0.0046	45	0.0883	84

Table 29: FNMR is the proportion of mated comparisons below a threshold set to achieve the FMR given in the header on the fourth row. FMR is the proportion of impostor comparisons at or above that threshold. The light grey values give rank over all algorithms in that column. The pink columns use only same-sex impostors; others are selected regardless of demographics. The exception, in the green column, uses "matched-covariates" i.e. impostors of the same sex, age group, and country of birth. The second pink column includes effects of extended ageing. Missing entries for border, visa, mugshot and wild images generally mean the algorithm did not run to completion. The VISA *columns compare images described in section 2.1. The* MUGSHOT *columns compare images described in section 2.5. The* VISA-BORDER *column compare images described in section 2.2 with those of section 2.4. The* BORDER *column compares images described in section 2.4. The* KIOSK-BORDER *columns compare images described in section 2.6 with those of section 2.4.*

FNMR(T) "False non-match rate"
FMR(T) "False match rate"

	Algorithm	FALSE NON-MATCH RATE (FNMR)															
		CONSTRAINED, COOPERATIVE														LESS CONSTRAINED, NON-COOP.	
	Name	VISAMC		VISA		MUGSHOT		MUGSHOT12+YRS		VISABORDER		BORDER		BORDER		KIOSKBORDER	
	FMR	0.0001		1E-06		1E-05		1E-05		1E-06		1E-06		1E-05		1E-06	
309	meituan-004	0.0014	35	0.0021	32	0.0024	40	0.0024	34	0.0023	27	0.0070	64	0.0044	42	0.0813	74
310	meiya-001	0.0171	404	0.0275	408	0.0159	424	0.0261	421	0.0311	404	0.2250	353	0.0245	302	-	
311	mendaxiatech-000	0.0027	115	0.0036	96	0.0029	135	0.0036	148	0.0031	98	0.0057	41	0.0051	62	-	
312	metsakuurcompany-002	0.0048	204	0.0071	216	0.0030	143	0.0043	176	0.0032	105	0.2059	347	0.0665	363	0.5374	231
313	metsakuurcompany-003	0.0034	157	0.0051	171	0.0026	88	0.0036	139	0.0028	74	0.2418	359	0.1001	383	0.5866	238
314	miaxis-002	0.0745	473	0.0774	461	0.3215	511	0.4000	509	0.1485	471	0.2087	348	0.2058	411	0.3846	212
315	miaxis-003	0.0045	196	0.0067	203	0.0037	208	0.0050	201	0.0061	214	0.0139	148	0.0088	159	0.1322	128
316	microfocus-002	0.3605	512	0.5057	515	0.5783	528	0.7223	528	0.5909	512	0.5963	407	0.4160	447	-	
317	microfocus-003	0.0416	452	0.0607	452	0.0652	482	0.1025	480	0.0793	453	0.2248	352	0.0923	378	0.6153	241
318	minivision-000	0.0033	145	0.0048	157	0.0038	215	0.0049	195	0.0055	193	0.0094	106	0.0079	134	-	
319	mitek-000	0.6882	542	0.8192	541	0.9568	553	0.9788	553	0.9545	546	0.9437	472	0.8494	496	0.9931	317
320	mobai-000	0.0360	449	0.0439	432	0.0372	462	0.0700	466	0.0367	412	0.0939	313	0.0795	372	-	
321	mobai-001	0.0199	416	0.0219	387	0.0047	252	0.0061	243	0.0093	272	0.0174	176	0.0138	228	-	
322	mobbl-001	0.3208	506	0.4375	508	0.5680	527	0.7193	527	0.6282	513	0.5783	404	0.3984	444	0.8864	274
323	mobbl-003	0.0087	314	0.0134	318	0.0062	303	0.0087	305	0.0099	285	0.0197	190	0.0122	217	0.1618	152
324	mobipintech-000	0.0090	318	0.0149	335	0.0039	225	0.0057	225	0.0115	306	0.0465	272	0.0182	267	0.6443	244
325	momovn-001	0.1044	482	0.1694	483	0.3253	512	0.5244	515	0.3861	503	0.9995	518	0.9985	534	1.0000	378
326	moredian-000	0.3874	513	0.4912	513	0.9988	557	0.9999	558	0.9990	550	0.9999	528	0.9998	542	-	
327	mukh-003	0.0077	293	0.0113	298	0.0111	394	0.0224	411	0.0061	213	0.7813	436	0.4504	451	0.9899	312
328	mukh-004	0.0050	214	0.0069	214	0.0051	272	0.0099	317	0.0045	159	0.0083	81	0.0059	89	0.1030	110
329	multimodality-000	0.0034	155	0.0047	151	0.0036	198	0.0044	182	0.0077	243	0.9976	505	0.4456	450	1.0000	368
330	multimodality-001	0.0029	125	0.0042	122	0.0031	148	0.0035	131	0.0038	132	0.0071	66	0.0059	86	0.0732	60
331	mvision-001	0.0191	413	0.0233	390	0.0204	432	0.0356	433	0.0198	374	0.0337	248	0.0242	301	-	
332	nazhiai-000	0.0040	185	0.0059	188	0.0036	193	0.0048	194	0.0057	205	0.0125	140	0.0083	147	-	
333	ncssg-001	0.0207	420	0.1540	479	0.0045	244	0.0067	261	0.0056	203	0.1180	324	0.0301	317	0.3908	213
334	neosystems-004	0.0279	434	0.0495	437	0.0289	452	0.0585	462	0.0439	427	0.9621	476	0.1296	390	0.9996	342
335	netbridgetech-001	0.4749	521	0.6599	531	0.4438	521	0.5676	520	0.4491	509	1.0000	532	0.9541	512	-	
336	netbridgetech-002	0.0101	339	0.0166	350	0.0077	336	0.0127	342	0.0133	323	0.8215	444	0.0523	352	-	
337	neurotechnology-017	0.0017	56	0.0031	78	0.0023	16	0.0025	43	0.0025	49	0.0047	22	0.0038	23	0.0612	37
338	neurotechnology-018	0.0020	71	0.0029	66	0.0022	11	0.0024	32	0.0024	36	0.0046	18	0.0037	19	0.0586	27
339	nhn-004	0.0030	126	0.0044	138	0.0025	73	0.0029	80	0.0030	94	0.0331	242	0.0113	205	0.1598	149
340	nhn-005	0.0028	117	0.0043	128	0.0023	25	0.0027	53	0.0025	41	0.0047	19	0.0038	22	0.0554	20
341	nodeflux-002	0.0186	411	0.0340	416	0.0261	445	0.0451	442	0.0548	442	1.0000	540	1.0000	547	-	
342	nominder-002	0.0025	109	0.0037	102	0.0033	174	0.0037	151	0.0026	65	0.5785	405	0.1435	397	0.8381	265
343	nominder-003	-		-		0.0031	147	0.0034	123	0.0026	53	0.7010	422	0.2159	414	0.8909	277
344	notiontag-001	0.6846	541	0.8006	540	0.3955	516	0.5247	516	0.8669	532	0.8313	449	0.6362	469	-	
345	notiontag-002	0.0066	270	0.0089	256	0.0045	243	0.0061	244	0.0077	244	0.0137	147	0.0104	191	0.1106	116
346	nsensecorp-004	0.1370	488	0.1397	475	0.0066	315	0.0094	311	1.0000	564	1.0000	557	1.0000	553	1.0000	528
347	nsensecorp-005	0.0055	235	0.0080	241	0.0039	220	0.0058	233	0.2723	493	0.9999	527	0.9949	527	1.0000	382
348	ntechlab-011	0.0012	28	0.0019	29	0.0024	49	0.0028	74	0.0029	83	0.0055	38	0.0047	48	0.0630	44
349	ntechlab-012	0.0011	26	0.0016	19	0.0023	29	0.0030	84	0.0026	56	0.0050	32	0.0043	35	0.0587	29
350	omface-000	0.2573	504	0.3835	505	0.3590	514	0.4903	513	0.3956	505	0.5003	395	0.2595	418	0.9137	282
351	omface-001	0.0137	384	0.0212	384	0.0114	399	0.0187	397	0.0174	360	1.0000	555	0.0214	292	1.0000	397
352	omnigarde-002	0.0033	153	0.0046	148	0.0027	117	0.0039	159	0.0041	147	0.0076	70	0.0059	90	0.0806	72

Table 30: FNMR is the proportion of mated comparisons below a threshold set to achieve the FMR given in the header on the fourth row. FMR is the proportion of impostor comparisons at or above that threshold. The light grey values give rank over all algorithms in that column. The pink columns use only same-sex impostors; others are selected regardless of demographics. The exception, in the green column, uses "matched-covariates" i.e. impostors of the same sex, age group, and country of birth. The second pink column includes effects of extended ageing. Missing entries for border, visa, mugshot and wild images generally mean the algorithm did not run to completion. The VISA *columns compare images described in section 2.1. The* MUGSHOT *columns compare images described in section 2.5. The* VISA-BORDER *column compare images described in section 2.2 with those of section 2.4. The* BORDER *column compares images described in section 2.4. The* KIOSK-BORDER *columns compare images described in section 2.6 with those of section 2.4.*

FNMR(T) "False non-match rate"
FMR(T) "False match rate"

	Algorithm	FALSE NON-MATCH RATE (FNMR)																	
		CONSTRAINED, COOPERATIVE																LESS CONSTRAINED, NON-COOP.	
	Name	VISAMC		VISA		MUGSHOT		MUGSHOT12+YRS		VISABORDER		BORDER		BORDER		KIOSKBORDER			
	FMR	0.0001		1E-06		1E-05		1E-05		1E-06		1E-06		1E-05		1E-06			
353	omnigarde-003	0.0024	98	0.0038	105	0.0024	59	0.0029	77	0.0032	107	0.0059	46	0.0049	60	0.0706	59		
354	onfido-000	0.1472	490	0.2881	495	0.0335	457	0.0731	469	0.0515	438	0.9915	496	0.9579	513	1.0000	352		
355	openedge-000	0.0045	197	0.0062	196	0.0049	259	0.0069	264	0.0049	175	0.9889	492	0.7991	490	0.9999	347		
356	openface-001	0.1804	492	0.2921	496	0.2878	508	0.3906	508	0.2054	483	0.2338	357	0.1549	401	0.6531	245		
357	oz-003	0.0095	329	0.0143	326	0.0054	285	0.0077	283	0.0096	279	0.0175	178	0.0118	211	0.1404	136		
358	oz-004	0.0033	150	0.0049	165	0.0038	217	0.0055	217	0.0081	250	0.0163	168	0.0142	232	-			
359	palit-000	0.0062	261	0.0084	250	0.0039	219	0.0055	216	0.0055	195	0.4610	394	0.2468	416	0.8695	269		
360	palit-001	0.0050	211	0.0068	209	0.0032	170	0.0047	193	0.0045	162	0.0110	128	0.0058	85	0.1446	140		
361	pangiam-001	0.0031	136	0.0044	137	0.0029	136	0.0040	164	0.0028	78	0.0362	255	0.0056	75	0.1711	155		
362	pangiam-002	0.0030	130	0.0042	125	0.0026	99	0.0031	98	0.0030	90	0.1772	338	0.0385	329	0.6076	240		
363	papago-001	0.0067	272	0.0096	272	0.0051	276	0.0077	282	0.0071	231	0.0126	141	0.0086	156	0.1033	111		
364	papil11-000	0.0021	84	0.0030	72	0.0024	31	0.0024	36	0.0025	51	0.0047	21	0.0040	29	0.0536	17		
365	papsav1923-002	0.0021	82	0.0034	85	0.0026	81	0.0030	90	0.0048	172	0.0093	103	0.0086	154	0.0630	43		
366	papsav1923-003	0.0025	110	0.0035	90	0.0024	56	0.0025	40	0.0034	117	0.0066	58	0.0058	84	0.0603	32		
367	paravision-011	0.0008	10	0.0020	31	0.0021	8	0.0020	7	0.0026	57	0.0053	35	0.0049	59	0.0498	13		
368	paravision-013	0.0010	24	0.0018	26	0.0021	6	0.0019	3	0.0019	12	0.0041	12	0.0036	17	0.0442	4		
369	pensees-001	0.0087	315	0.0133	317	0.0071	324	0.0122	336	0.0145	333	0.0252	216	0.0195	279	-			
370	pixelall-009	0.0018	60	0.0025	45	0.0024	52	0.0026	48	0.0031	100	0.3475	378	0.0053	65	0.9006	281		
371	pixelall-010	0.0020	72	0.0030	73	0.0025	69	0.0028	76	0.0031	99	0.3512	379	0.0054	68	0.8813	273		
372	privid-001	0.3350	509	0.5013	514	0.4327	519	0.5880	521	0.9790	547	1.0000	537	0.9998	541	1.0000	386		
373	privid-002	0.0460	458	0.0652	454	0.0524	475	0.0882	473	0.0671	448	0.9769	483	0.8960	503	0.9999	344		
374	psl-011	0.0013	34	0.0026	51	0.0021	1	0.0021	9	0.0024	31	0.0047	20	0.0035	14	0.0565	24		
375	psl-012	0.0017	53	0.0027	58	0.0021	9	0.0023	18	0.0021	15	0.0039	8	0.0032	7	0.0494	11		
376	ptakuratsatu-000	0.0060	256	0.0089	257	0.0070	321	0.0104	320	0.0096	280	0.0152	156	0.0100	181	-			
377	pxl-001	0.0488	459	0.0752	460	0.0586	480	0.1087	482	0.0946	462	0.1065	319	0.0625	361	-			
378	pyramid-000	0.0136	380	0.0233	391	0.0117	401	0.0192	400	0.0185	364	0.0322	240	0.0206	285	-			
379	qazbs-000	0.0058	244	0.0083	248	0.0046	249	0.0072	269	0.0130	320	0.0244	213	0.0196	280	0.7784	258		
380	qazsmartvisionai-000	0.0008	12	0.0011	10	0.0021	2	0.0022	12	0.0018	8	0.0035	5	0.0030	3	0.0441	3		
381	qluevision-001	0.0223	423	0.0419	429	0.0205	433	0.0343	432	0.0327	407	0.8762	452	0.7413	486	0.9908	313		
382	qnap-004	0.0046	201	0.0061	192	0.0038	212	0.0059	238	0.0042	151	0.9960	502	0.9442	509	1.0000	356		
383	qnap-005	0.0033	149	0.0047	154	0.0068	318	0.0071	268	0.0096	278	0.0184	183	0.0163	252	0.0948	103		
384	quantasoft-003	0.0081	302	0.0113	296	0.0056	289	0.0076	280	0.0091	269	0.0161	165	0.0107	197	0.1193	120		
385	rankone-015	0.0009	16	0.0014	16	0.0024	37	0.0026	47	0.0024	37	0.0044	15	0.0037	18	0.0635	48		
386	realnetworks-007	0.0031	137	0.0051	169	0.0028	124	0.0035	133	0.0048	173	0.0091	97	0.0074	124	0.0945	102		
387	realnetworks-008	0.0022	88	0.0039	114	0.0038	211	0.0045	184	0.0055	191	0.0100	117	0.0080	139	0.0889	86		
388	rebs-000	0.0030	128	0.0043	133	0.0024	43	0.0032	107	0.0024	29	0.3069	368	0.1170	388	0.7667	256		
389	rebs-001	0.0037	176	0.0049	163	0.0024	55	0.0033	114	0.0025	42	0.0257	217	0.0096	174	0.1487	143		
390	recognito-000	0.0004	4	0.0006	1	0.0021	7	0.0022	17	0.0016	4	0.0555	282	0.0207	287	0.1943	165		
391	recognito-001	0.0003	2	0.0007	4	0.0021	4	0.0022	14	0.0016	1	0.0663	296	0.0257	305	0.1825	162		
392	regula-000	0.0184	410	0.0376	424	0.0103	379	0.0185	393	0.0120	310	0.9983	507	0.0231	297	1.0000	371		
393	regula-001	0.0072	284	0.0107	289	0.0102	377	0.0179	390	0.0123	314	0.0333	247	0.0174	259	0.3711	210		
394	remarkai-001	0.0144	388	0.0256	402	0.0102	376	0.0159	381	0.0162	343	0.0582	286	0.0185	269	-			
395	remarkai-003	0.0047	203	0.0063	197	0.0033	182	0.0049	196	0.0054	188	0.0100	116	0.0072	120	0.0908	93		
396	rendip-000	0.0055	234	0.0077	233	0.0048	258	0.0060	242	0.0080	248	0.0142	151	0.0110	201	0.1027	109		

Table 31: FNMR is the proportion of mated comparisons below a threshold set to achieve the FMR given in the header on the fourth row. FMR is the proportion of impostor comparisons at or above that threshold. The light grey values give rank over all algorithms in that column. The pink columns use only same-sex impostors; others are selected regardless of demographics. The exception, in the green column, uses "matched-covariates" i.e. impostors of the same sex, age group, and country of birth. The second pink column includes effects of extended ageing. Missing entries for border, visa, mugshot and wild images generally mean the algorithm did not run to completion. The VISA *columns compare images described in section 2.1. The* MUGSHOT *columns compare images described in section 2.5. The* VISA-BORDER *column compare images described in section 2.2 with those of section 2.4. The* BORDER *column compares images described in section 2.4. The* KIOSK-BORDER *columns compare images described in section 2.6 with those of section 2.4.*

FNMR(T) "False non-match rate"
FMR(T) "False match rate"

	Algorithm	FALSE NON-MATCH RATE (FNMR)															
		CONSTRAINED, COOPERATIVE														LESS CONSTRAINED, NON-COOP.	
	Name	VISAMC		VISA		MUGSHOT		MUGSHOT12+YRS		VISABORDER		BORDER		BORDER		KIOSKBORDER	
	FMR	0.0001		1E-06		1E-05		1E-05		1E-06		1E-06		1E-05		1E-06	
397	revealmedia-005	0.0050	215	0.0074	225	0.0050	266	0.0068	263	0.0075	241	0.0124	138	0.0104	194	0.0895	89
398	revealmedia-006	0.0040	184	0.0067	205	0.0041	233	0.0056	220	0.0056	198	0.0085	88	0.0068	106	0.0872	82
399	roc-016	0.0009	14	0.0014	15	0.0023	20	0.0024	28	0.0024	32	0.0042	13	0.0035	12	0.0558	22
400	rokid-000	0.0093	327	0.0145	329	0.0073	331	0.0102	319	0.0164	345	0.0280	227	0.0214	291	-	
401	rokid-001	0.0105	347	0.0162	344	0.0094	372	0.0163	384	0.0181	362	0.0276	226	0.0165	253	-	
402	s1-005	0.0024	102	0.0036	100	0.0025	75	0.0029	79	0.0026	63	0.0048	25	0.0038	21	0.0638	50
403	s1-007	0.0023	97	0.0056	183	0.0024	33	0.0028	62	0.0025	47	0.0048	24	0.0039	25	0.0608	34
404	saffe-001	0.4339	519	0.5261	517	0.7539	542	0.8736	545	0.7977	522	0.9810	484	0.7435	487	-	
405	saffe-002	0.0119	365	0.0206	379	0.0107	387	0.0177	389	0.0244	392	0.9998	521	0.2785	424	-	
406	samsungsds-001	0.0015	40	0.0026	52	0.0023	22	0.0023	23	0.0024	33	0.1660	337	0.0536	353	0.4995	229
407	samsungsds-002	0.0017	59	0.0027	56	0.0023	18	0.0022	13	0.0021	17	0.0043	14	0.0036	16	0.0586	28
408	samtech-001	0.0197	415	0.0365	423	0.0146	419	0.0241	415	0.0238	391	0.0394	262	0.0251	303	-	
409	samtech-002	0.0084	309	0.0127	314	0.0093	367	0.0158	378	0.0113	305	0.0442	268	0.0132	221	0.4110	219
410	scanovate-002	0.0175	408	0.0355	420	0.0146	417	0.0286	425	0.0269	397	0.0301	231	0.0178	263	-	
411	scanovate-003	0.0054	229	0.0080	240	0.0054	281	0.0072	272	0.0312	405	0.0599	287	0.0568	358	-	
412	sdc-000	0.0303	439	0.0526	444	0.0572	479	0.1094	483	0.0867	458	0.6230	410	0.3682	441	0.8797	272
413	seamfix-001	-		-		0.1973	502	0.2878	502	0.2613	491	0.3156	373	0.1976	409	0.8176	262
414	securifai-007	0.0124	372	0.0175	361	0.0064	309	0.0105	321	0.0108	296	0.9999	526	0.9966	532	1.0000	376
415	securifai-008	-		-		0.0060	300	0.0102	318	0.2096	484	0.9649	479	0.8757	500	0.9990	333
416	sensetime-007	0.0012	33	0.0022	36	0.0021	10	0.0020	6	0.0018	7	0.0034	4	0.0029	2	0.0479	10
417	sensetime-008	0.0008	11	0.0014	14	0.0021	3	0.0020	4	0.0018	9	0.0036	6	0.0033	8	0.0504	14
418	serendipity-000	0.0046	200	0.0069	213	0.0042	237	0.0056	219	0.0073	237	0.9129	461	0.7189	483	0.9952	323
419	sertis-002	0.0049	206	0.0061	191	0.0039	224	0.0061	248	0.0055	192	0.0099	114	0.0070	115	0.0921	97
420	sertis-003	0.0049	209	0.0059	189	0.0037	203	0.0058	231	0.0055	197	0.0100	115	0.0072	121	0.0881	83
421	seventhsense-003	0.0035	165	0.0046	146	0.0026	96	0.0033	113	0.0062	215	0.0448	269	0.0175	260	0.2594	188
422	seventhsense-005	0.0031	135	0.0045	142	0.0028	121	0.0030	82	0.0028	76	0.0466	273	0.0165	254	0.1949	166
423	shaman-000	0.9297	547	0.9774	547	0.9990	558	0.9997	557	0.9999	552	1.0000	536	0.9999	544	-	
424	shaman-001	0.3346	508	0.4616	509	0.2368	505	0.3723	507	0.3574	500	0.3527	380	0.2304	415	-	
425	shu-002	-		0.0079	238	0.0146	418	0.0308	426	1.0000	553	0.0183	181	0.0115	207	-	
426	shu-003	0.0028	118	0.0041	121	0.0050	264	0.0088	307	0.0081	251	0.0133	145	0.0094	170	-	
427	siat-002	0.0091	322	0.0126	313	0.0109	388	0.0190	399	0.0276	399	0.0516	281	0.0464	346	-	
428	siat-005	0.0021	81	0.0038	107	0.0059	294	0.0049	197	0.0742	450	0.9623	477	0.6801	472	0.9833	303
429	sjtu-004	0.0014	36	0.0025	44	0.0027	105	0.0028	75	0.0046	163	0.0086	91	0.0073	122	0.0906	92
430	sjtu-005	0.0029	122	0.0036	99	0.0025	77	0.0027	58	0.0044	156	0.0120	136	0.0072	117	0.1325	129
431	sktelecom-000	0.0038	181	0.0054	179	0.0031	146	0.0051	205	0.0042	148	0.3418	376	0.0061	94	0.9499	288
432	smartbiometrik-001	0.5485	532	0.6442	526	0.7550	543	0.8611	541	0.8677	533	0.8270	448	0.7030	476	0.9752	297
433	smartengines-000	0.6240	539	0.7562	538	0.9552	552	0.9784	552	0.9515	545	0.9288	468	0.8200	491	0.9930	316
434	smartengines-001	0.6434	540	0.7666	539	0.9446	551	0.9750	551	0.9387	543	0.9556	474	0.8647	498	0.9972	328
435	smartvist-000	0.0912	477	0.1587	480	0.1163	494	0.1841	494	0.1397	468	0.9372	470	0.7107	481	0.9990	334
436	smartvist-001	0.0137	383	0.0244	395	0.0099	375	0.0158	379	0.0151	334	0.1349	330	0.0419	334	0.5589	235
437	smilart-002	0.2440	500	0.3532	501	-		-		0.3785	501	0.4145	390	0.2611	420	-	
438	smilart-003	0.6944	543	0.8836	543	0.0695	485	0.1193	487	0.0894	460	0.1221	326	0.0737	368	-	
439	sodec-000	0.0033	148	0.0044	139	0.0040	228	0.0053	211	0.0054	189	0.0096	109	0.0080	135	0.0915	96
440	sparsh-001	0.0018	64	0.0029	68	0.0026	87	0.0028	71	0.0027	69	0.8806	453	0.6313	466	0.9963	324

Table 32: FNMR is the proportion of mated comparisons below a threshold set to achieve the FMR given in the header on the fourth row. FMR is the proportion of impostor comparisons at or above that threshold. The light grey values give rank over all algorithms in that column. The pink columns use only same-sex impostors; others are selected regardless of demographics. The exception, in the green column, uses "matched-covariates" i.e. impostors of the same sex, age group, and country of birth. The second pink column includes effects of extended ageing. Missing entries for border, visa, mugshot and wild images generally mean the algorithm did not run to completion. The VISA *columns compare images described in section 2.1. The* MUGSHOT *columns compare images described in section 2.5. The* VISA-BORDER *column compare images described in section 2.2 with those of section 2.4. The* BORDER *column compares images described in section 2.4. The* KIOSK-BORDER *columns compare images described in section 2.6 with those of section 2.4.*

		FALSE NON-MATCH RATE (FNMR)															
	Algorithm	CONSTRAINED, COOPERATIVE														LESS CONSTRAINED, NON-COOP.	
	Name	VISAMC		VISA		MUGSHOT		MUGSHOT12+YRS		VISABORDER		BORDER		BORDER		KIOSKBORDER	
	FMR	0.0001		1E-06		1E-05		1E-05		1E-06		1E-06		1E-05		1E-06	
441	sqisoft-002	0.0082	305	0.0124	307	0.0051	271	0.0086	304	0.0102	290	0.0183	182	0.0122	216	0.1498	145
442	sqisoft-003	0.0041	186	0.0055	181	0.0026	80	0.0032	111	0.0039	136	1.0000	565	1.0000	559	1.0000	495
443	staqu-000	0.0139	386	0.0208	381	0.0104	380	0.0145	370	0.0156	336	0.8063	442	0.1408	396	-	
444	starhybrid-001	0.0108	348	0.0138	322	0.0081	342	0.0113	329	0.0152	335	0.0265	221	0.0189	271	-	
445	stcon-002	0.0031	132	0.0043	130	0.0025	62	0.0034	122	0.0030	89	0.9988	510	0.9855	521	1.0000	360
446	stcon-003	0.0038	180	0.0050	167	0.0024	34	0.0032	110	0.0023	25	0.1082	321	0.0350	324	0.3982	216
447	stengg-000	0.0059	253	0.0082	246	0.0037	205	0.0060	241	0.0050	179	0.5065	396	0.0792	371	0.9348	287
448	sukshi-000	0.5409	530	0.6612	532	0.4556	522	0.6567	524	0.9296	542	0.8898	456	0.7384	484	0.9899	311
449	suprema-004	0.0024	99	0.0035	89	0.0032	164	0.0036	142	0.0028	71	0.0053	36	0.0045	44	0.0625	41
450	suprema-005	0.0022	86	0.0036	98	0.0034	188	0.0031	100	0.0026	64	0.0050	31	0.0044	39	0.0588	30
451	supremaid-001	0.0053	228	0.0073	224	0.0045	242	0.0066	258	0.0099	287	0.0186	184	0.0148	241	0.1040	112
452	supremaid-002	0.0063	265	0.0094	266	0.0044	240	0.0062	249	0.0072	236	0.0229	210	0.0095	173	0.2986	197
453	surrey-cvssp-002	0.0019	65	0.0028	60	0.0027	113	0.0028	66	0.0024	35	0.5978	408	0.1206	389	0.8488	267
454	surrey-cvssp-003	0.0016	49	0.0028	61	0.0022	12	0.0024	29	0.0022	22	0.3048	367	0.0539	354	0.5830	237
455	swsam-001	0.0268	432	0.0476	434	0.0271	446	0.0460	445	0.0584	444	0.7745	433	0.5013	454	0.9642	292
456	synesis-006	0.0070	276	0.0096	270	0.0107	385	0.0166	386	-		0.0128	144	0.0089	160	-	
457	synesis-007	0.0050	216	0.0073	222	0.0062	306	0.0076	279	-		0.0105	121	0.0080	137	-	
458	synology-000	0.0149	390	0.0238	394	0.0148	420	0.0261	419	0.0221	381	0.0331	243	0.0209	289	-	
459	synology-002	0.0104	344	0.0153	340	0.0107	386	0.0184	392	0.0189	367	0.2032	345	0.0180	264	-	
460	sztu-000	0.0092	323	0.0139	323	0.0091	361	0.0201	404	0.0136	325	0.0685	300	0.0118	213	-	
461	sztu-001	0.0031	133	0.0043	132	0.0025	68	0.0028	72	0.0051	181	0.0113	129	0.0089	161	0.9963	325
462	t4isb-000	0.0058	243	0.0087	252	0.0041	234	0.0064	255	0.0083	254	0.0157	162	0.0103	189	0.1196	121
463	tech5-007	0.0020	70	0.0029	65	0.0024	42	0.0028	63	0.0034	118	0.8622	451	0.5335	458	0.9867	309
464	tech5-008	0.0020	69	0.0031	77	0.0026	86	0.0028	69	0.0026	58	0.9238	465	0.7170	482	0.9984	329
465	techainer-001	0.0061	258	0.0092	262	0.0046	248	0.0073	274	0.0060	210	0.9575	475	0.8567	497	0.9995	340
466	techsign-000	0.0325	443	0.0511	440	0.0435	471	0.0710	467	0.0746	451	0.1104	322	0.0841	374	0.4288	222
467	techsign-001	0.0110	351	0.0196	375	0.0067	316	0.0120	334	0.0087	259	0.2475	360	0.0883	377	0.6767	248
468	tevian-007	0.0019	67	0.0027	55	0.0032	167	0.0041	166	0.0045	161	0.0086	90	0.0078	131	0.0925	99
469	tevian-008	0.0012	32	0.0017	23	0.0033	171	0.0042	174	0.0042	150	0.0081	77	0.0068	107	0.0909	94
470	tiger-005	0.0624	468	0.2450	491	0.0292	454	0.0556	456	0.0430	423	1.0000	530	0.9964	530	1.0000	361
471	tiger-006	0.0066	269	0.0101	280	0.0050	270	0.0075	278	0.0089	263	0.0158	164	0.0117	209	0.1466	141
472	tinkoff-001	0.0145	389	0.0244	396	0.0318	455	0.0636	464	0.0236	389	1.0000	568	0.0339	321	1.0000	516
473	tnitech-000	0.0025	107	0.0037	101	0.0033	175	0.0035	134	0.0025	45	0.8893	455	0.6283	465	0.9883	310
474	tongyi-005	0.0073	287	0.0146	330	0.0187	428	0.0421	441	0.0161	341	0.0215	201	0.0149	242	-	
475	toppanidgate-000	0.0021	77	0.0033	83	0.0026	82	0.0028	68	0.0039	137	0.0075	69	0.0068	104	0.0631	45
476	toshiba-007	0.0016	47	0.0023	42	0.0024	57	0.0023	19	0.0021	16	0.0629	294	0.0056	73	0.2301	175
477	toshiba-008	0.0012	30	0.0017	25	0.0024	47	0.0022	15	0.0019	10	0.0108	125	0.0039	27	0.0899	91
478	touchlessid-002	0.0070	277	0.0096	271	0.0407	466	0.0469	449	0.4234	508	0.9991	512	0.9953	529	1.0000	362
479	touchlessid-003	0.0061	259	0.0081	242	0.0040	230	0.0053	212	0.0056	200	0.0155	159	0.0082	143	0.1370	133
480	trueface-002	0.0060	257	0.0096	269	0.0048	257	0.0061	245	0.0112	304	0.0198	191	0.0155	248	-	
481	trueface-003	0.0070	275	0.0094	267	0.0053	279	0.0081	293	0.0122	311	0.0217	203	0.0159	251	0.1204	122
482	trueidvng-001	0.0063	263	0.0077	232	0.0033	181	0.0044	180	0.0046	164	0.0086	92	0.0069	111	0.0809	73
483	truststamp-001	0.0242	426	0.0484	435	0.0194	431	0.0359	434	0.0381	415	0.8808	454	0.6898	473	0.9948	320
484	tuputech-000	0.3218	507	0.3696	503	-		-		0.3237	496	0.4304	392	0.2973	429	-	

Table 33: FNMR is the proportion of mated comparisons below a threshold set to achieve the FMR given in the header on the fourth row. FMR is the proportion of impostor comparisons at or above that threshold. The light grey values give rank over all algorithms in that column. The pink columns use only same-sex impostors; others are selected regardless of demographics. The exception, in the green column, uses "matched-covariates" i.e. impostors of the same sex, age group, and country of birth. The second pink column includes effects of extended ageing. Missing entries for border, visa, mugshot and wild images generally mean the algorithm did not run to completion. The VISA *columns compare images described in section 2.1. The* MUGSHOT *columns compare images described in section 2.5. The* VISA-BORDER *column compare images described in section 2.2 with those of section 2.4. The* BORDER *column compares images described in section 2.4. The* KIOSK-BORDER *columns compare images described in section 2.6 with those of section 2.4.*

FNMR(T) "False non-match rate"
FMR(T) "False match rate"

	Algorithm	FALSE NON-MATCH RATE (FNMR)															
		CONSTRAINED, COOPERATIVE														LESS CONSTRAINED, NON-COOP.	
	Name	VISAMC		VISA		MUGSHOT		MUGSHOT12+YRS		VISABORDER		BORDER		BORDER		KIOSKBORDER	
	FMR	0.0001		1E-06		1E-05		1E-05		1E-06		1E-06		1E-05		1E-06	
485	turingtechvip-001	0.0330	445	0.0540	446	0.0458	472	0.1007	477	0.4715	510	0.9286	467	0.8448	495	0.9964	327
486	turingtechvip-002	0.0126	376	0.0163	346	0.0092	366	0.0118	331	0.2264	488	1.0000	553	0.9925	524	0.9999	349
487	turkcell-000	0.1134	484	0.1288	474	0.0770	487	0.1112	485	0.2570	490	1.0000	529	0.9999	543	1.0000	372
488	turkcell-001	0.0043	191	0.0066	200	0.0037	210	0.0055	218	0.0043	152	0.0440	267	0.0082	144	0.3148	201
489	twface-000	0.0051	217	0.0072	219	0.0041	232	0.0058	228	0.0071	232	0.0153	157	0.0100	178	0.1595	147
490	twface-001	0.0036	169	0.0051	168	0.0031	156	0.0038	156	0.0049	174	0.0091	100	0.0075	126	0.0831	76
491	ulsee-001	0.0151	392	0.0246	398	0.0113	397	0.0185	395	0.0187	366	0.6766	418	0.0181	266	-	
492	ultinous-000	0.2343	498	0.3484	500	-		-		-		-		-		-	
493	ultinous-001	0.2485	501	0.4003	506	-		-		-		-		-		-	
494	uluface-002	0.0081	301	0.0123	305	0.0071	323	0.0095	314	0.0107	295	1.0000	563	0.0140	230	-	
495	uluface-003	0.0100	335	0.0150	336	0.0079	338	0.0128	344	-		-		-		-	
496	unicc-002	0.2153	497	0.2190	489	0.0417	468	0.0526	455	0.0891	459	0.1321	329	0.1125	387	0.3813	211
497	unicc-003	0.0217	422	0.0260	404	0.0093	370	0.0136	356	0.0129	318	0.0216	202	0.0143	234	0.2091	170
498	unissey-003	0.0057	238	0.0082	245	0.0047	253	0.0082	294	0.0067	224	0.5179	399	0.2863	427	0.8684	268
499	unissey-004	0.0043	190	0.0066	201	0.0037	199	0.0052	207	0.0048	171	0.5272	400	0.2903	428	0.8777	271
500	upc-001	0.0234	425	0.0519	443	0.0291	453	0.0490	453	0.0294	402	0.2316	356	0.0389	330	-	
501	useb-001	0.0035	166	0.0053	176	0.0027	110	0.0033	117	0.0027	70	0.0085	87	0.0044	38	0.0806	71
502	useb-002	0.0028	120	0.0039	111	0.0027	109	0.0031	99	0.0025	43	0.0090	95	0.0042	32	0.0867	81
503	uxlabs-001	0.0534	462	0.0570	449	0.0118	402	0.0131	348	0.0237	390	0.0399	263	0.0288	314	0.2097	172
504	uxlabs-003	0.2133	496	0.2143	487	0.0386	463	0.0457	443	0.0374	414	0.3343	375	0.1554	402	0.6941	251
505	vcog-002	0.7522	545	0.9033	545	-		-		-		-		-		-	
506	vcortex-001	0.0131	379	0.0207	380	0.0192	430	0.0315	427	0.2238	487	0.3586	382	0.3536	439	0.3569	206
507	vd-002	0.0429	455	0.0704	456	0.0569	478	0.0844	472	0.0801	454	0.0937	311	0.0577	359	-	
508	vd-003	0.0199	417	0.0222	389	0.0115	400	0.0130	347	0.0138	327	0.0239	211	0.0177	262	0.1647	154
509	veridas-008	0.0032	139	0.0045	145	0.0030	140	0.0033	116	0.0085	257	0.0206	196	0.0143	235	0.1228	125
510	veridas-009	0.0031	131	0.0043	129	0.0030	145	0.0035	130	0.0055	190	0.0106	124	0.0100	179	0.0959	104
511	veridium-002	0.0343	447	0.0427	430	0.0283	450	0.0460	446	0.0489	433	0.0673	297	0.0464	345	0.3658	208
512	veridium-003	-		-		0.0286	451	0.0462	447	0.0492	434	0.0679	298	0.0470	347	0.3672	209
513	verigram-001	0.0032	142	0.0044	135	0.0027	107	0.0032	109	0.0030	87	0.9995	517	0.9953	528	1.0000	384
514	verigram-003	0.0101	338	0.0109	291	0.0034	186	0.0039	160	0.0037	130	0.0070	65	0.0063	97	0.0559	23
515	verihubs-inteligensia-001	0.0071	278	0.0114	300	0.0050	267	0.0076	281	0.0096	277	0.0165	170	0.0114	206	0.1409	138
516	verihubs-inteligensia-002	0.0028	119	0.0043	127	0.0025	78	0.0030	83	0.0047	167	0.0092	101	0.0083	150	0.0983	105
517	verijelas-000	0.2488	502	0.3431	499	0.4861	523	0.6004	522	0.0811	455	0.1148	323	0.0440	339	0.4077	218
518	via-004	0.0099	333	0.0135	321	0.0031	159	0.0044	181	0.0055	194	0.4009	388	0.0080	138	0.9840	306
519	via-005	0.0063	264	0.0082	247	0.0031	149	0.0037	155	0.0032	102	0.3659	384	0.0068	105	0.8709	270
520	viante-000	0.0004	5	0.0007	5	0.0026	95	0.0026	51	0.0017	5	0.0033	3	0.0029	1	0.0475	9
521	videmo-001	0.0295	436	0.0417	428	0.0164	426	0.0261	420	0.0355	410	0.0603	289	0.0442	340	0.2428	181
522	videmo-002	0.0158	398	0.0288	410	0.0149	423	0.0249	418	0.0230	384	0.3429	377	0.1468	398	0.8393	266
523	videonetics-001	0.5483	531	0.6446	528	0.7517	541	0.8607	540	0.8664	531	0.8255	445	0.6956	475	-	
524	videonetics-002	0.4274	517	0.5329	518	0.6081	530	0.7438	530	0.7775	520	0.7297	425	0.5756	460	-	
525	viettelhightech-000	0.0117	361	0.0166	349	0.0110	391	0.0198	403	0.0167	351	0.0249	214	0.0158	249	0.1604	150
526	vigilantsolutions-010	0.0109	349	0.0164	348	0.0074	333	0.0095	313	0.0209	378	0.0365	258	0.0233	299	0.2465	182
527	vigilantsolutions-011	0.0124	370	0.0176	363	0.0073	329	0.0095	312	0.0196	372	0.0360	254	0.0221	294	0.2633	190
528	vinai-000	0.0081	300	0.0124	308	0.0045	241	0.0072	271	0.0089	262	0.1814	339	0.0112	202	-	

Table 34: FNMR is the proportion of mated comparisons below a threshold set to achieve the FMR given in the header on the fourth row. FMR is the proportion of impostor comparisons at or above that threshold. The light grey values give rank over all algorithms in that column. The pink columns use only same-sex impostors; others are selected regardless of demographics. The exception, in the green column, uses "matched-covariates" i.e. impostors of the same sex, age group, and country of birth. The second pink column includes effects of extended ageing. Missing entries for border, visa, mugshot and wild images generally mean the algorithm did not run to completion. The VISA *columns compare images described in section 2.1. The* MUGSHOT *columns compare images described in section 2.5. The* VISA-BORDER *column compare images described in section 2.2 with those of section 2.4. The* BORDER *column compares images described in section 2.4. The* KIOSK-BORDER *columns compare images described in section 2.6 with those of section 2.4.*

		FALSE NON-MATCH RATE (FNMR)															
	Algorithm	CONSTRAINED, COOPERATIVE														LESS CONSTRAINED, NON-COOP.	
	Name	VISAMC		VISA		MUGSHOT		MUGSHOT12+YRS		VISABORDER		BORDER		BORDER		KIOSKBORDER	
	FMR	0.0001		1E-06		1E-05		1E-05		1E-06		1E-06		1E-05		1E-06	
529	vinbigdata-002	0.0102	341	0.0175	359	0.0071	326	0.0084	300	0.0090	264	0.8017	441	0.3134	431	0.9936	318
530	vinbigdata-003	0.0771	474	0.0992	470	0.1202	495	0.1756	493	0.2762	494	0.2369	358	0.0100	180	0.8914	278
531	vion-000	0.0419	453	0.0590	450	0.0422	469	0.0478	450	0.0581	443	0.0968	317	0.0847	375	-	
532	visage-000	0.0933	478	0.1441	478	0.1316	497	0.2416	498	0.1395	467	0.1920	342	0.1001	382	-	
533	visionbox-003	0.0057	242	0.0075	227	0.0062	305	0.0083	297	0.0100	288	0.9915	495	0.9625	516	1.0000	354
534	visionbox-004	0.0046	202	0.0075	228	0.0060	299	0.0075	277	0.0056	199	0.0316	236	0.0070	116	0.2528	184
535	visionlabs-010	0.0017	54	0.0024	43	0.0026	94	0.0030	88	0.0033	114	0.0061	51	0.0052	64	-	
536	visionlabs-011	0.0012	29	0.0022	38	0.0024	54	0.0026	49	0.0028	72	0.0053	37	0.0046	47	0.0635	47
537	visteam-007	0.0312	442	0.0448	433	0.0416	467	0.1008	478	0.0466	431	0.0602	288	0.0281	312	0.2601	189
538	visteam-008	0.0378	450	0.0515	441	0.0391	465	0.0937	475	0.0437	426	0.0567	283	0.0260	307	0.2533	185
539	vixvizion-006	0.0082	304	0.0122	304	0.0093	368	0.0194	401	0.0099	286	0.0169	172	0.0108	198	0.1338	131
540	vixvizion-007	0.0110	352	0.0191	371	0.0080	340	0.0157	376	0.0101	289	0.0190	185	0.0118	212	0.1407	137
541	vnis-000	0.1397	489	0.1608	481	0.2184	503	0.2976	504	0.5277	511	0.3603	383	0.2714	423	0.6929	250
542	vnpay-000	0.2380	499	0.2614	493	0.4054	518	0.4968	514	0.3993	507	0.4389	393	0.4006	445	0.7693	257
543	vnpt-005	0.0036	167	0.0052	173	0.0027	108	0.0031	95	0.0036	124	0.0066	60	0.0056	74	0.0621	39
544	vnpt-006	0.0034	162	0.0050	166	0.0027	103	0.0035	138	0.0026	61	0.0049	28	0.0040	30	0.0585	26
545	vocord-009	0.0022	87	0.0029	69	0.0036	194	0.0046	188	0.0052	186	0.0098	112	0.0086	157	-	
546	vocord-010	0.0024	104	0.0031	76	0.0036	195	0.0049	199	0.0025	52	0.0065	55	0.0040	28	0.0679	57
547	vtcc-000	0.0051	218	0.0068	210	0.0054	282	0.0064	253	0.9451	544	1.0000	560	1.0000	554	1.0000	552
548	vtcc-001	0.0054	232	0.0076	231	0.0049	263	0.0079	290	0.0064	219	0.0225	207	0.0083	146	1.0000	460
549	vts-000	0.0103	342	0.0174	356	0.0080	339	0.0129	346	0.0250	394	0.0450	270	0.0372	328	-	
550	vts-001	0.0033	144	0.0048	156	0.0027	111	0.0036	143	0.0032	103	0.6519	415	0.3563	440	0.9218	285
551	wicket-000	0.0018	63	0.0028	59	0.0024	50	0.0027	56	0.0031	95	0.7968	440	0.4340	449	0.9788	300
552	winsense-001	0.0062	262	0.0099	276	0.0092	364	0.0210	405	0.0093	271	0.0144	153	0.0098	177	-	
553	winsense-002	0.0050	213	0.0073	223	0.0038	214	0.0059	236	0.0064	218	0.0118	134	0.0084	151	-	
554	wiseai-001	0.0658	469	0.0964	469	0.7743	546	0.8956	547	0.1967	480	0.7526	429	0.3419	436	0.9695	293
555	wuhantianyu-001	0.0163	400	0.0262	406	0.0281	449	0.0569	459	0.0316	406	0.0486	278	0.0344	322	0.2097	171
556	x-laboratory-000	0.0071	280	0.0106	285	0.0123	405	0.0138	358	0.0419	421	0.5629	403	0.2852	426	-	
557	x-laboratory-001	0.0059	252	0.0110	294	0.0054	283	0.0078	288	0.0094	273	0.0142	150	0.0100	182	-	
558	xforwardai-001	0.0021	76	0.0034	86	0.0027	114	0.0028	70	0.0046	166	0.0088	93	0.0079	133	-	
559	xforwardai-002	0.0016	48	0.0023	41	0.0026	101	0.0025	41	0.0040	141	0.0081	78	0.0074	123	-	
560	xm-000	0.0015	39	0.0026	50	0.0031	154	0.0038	157	0.0058	207	0.0105	122	0.0082	145	-	
561	yisheng-004	0.1988	493	0.3329	498	0.1147	493	0.1849	495	0.2044	482	-		-		-	
562	yitu-003	0.0015	45	0.0026	47	0.0066	314	0.0085	301	0.0064	220	0.0114	130	0.0103	190	-	
563	yoonik-003	0.0034	156	0.0047	152	0.0032	163	0.0037	149	0.0816	456	0.2033	346	0.1601	403	0.3210	203
564	yoonik-004	0.0041	187	0.0059	186	0.0033	173	0.0052	208	0.0040	143	0.0071	67	0.0051	63	0.0732	61
565	yoti-001	0.0139	385	0.0195	373	0.0110	392	0.0187	398	0.0191	368	0.1255	328	0.0415	333	0.5578	234
566	ytu-000	0.0057	241	0.0087	254	0.0121	403	0.0238	414	0.0047	169	0.0078	74	0.0059	88	-	
567	yuan-005	0.0037	178	0.0046	149	0.0027	116	0.0035	136	0.0033	109	0.2706	364	0.0876	376	0.6695	246
568	yuan-008	0.0032	141	0.0043	126	0.0026	89	0.0034	121	0.0028	75	0.0059	44	0.0039	26	0.0891	87

Table 35: FNMR is the proportion of mated comparisons below a threshold set to achieve the FMR given in the header on the fourth row. FMR is the proportion of impostor comparisons at or above that threshold. The light grey values give rank over all algorithms in that column. The pink columns use only same-sex impostors; others are selected regardless of demographics. The exception, in the green column, uses "matched-covariates" i.e. impostors of the same sex, age group, and country of birth. The second pink column includes effects of extended ageing. Missing entries for border, visa, mugshot and wild images generally mean the algorithm did not run to completion. The VISA *columns compare images described in section 2.1. The* MUGSHOT *columns compare images described in section 2.5. The* VISA-BORDER *column compare images described in section 2.2 with those of section 2.4. The* BORDER *column compares images described in section 2.4. The* KIOSK-BORDER *columns compare images described in section 2.6 with those of section 2.4.*

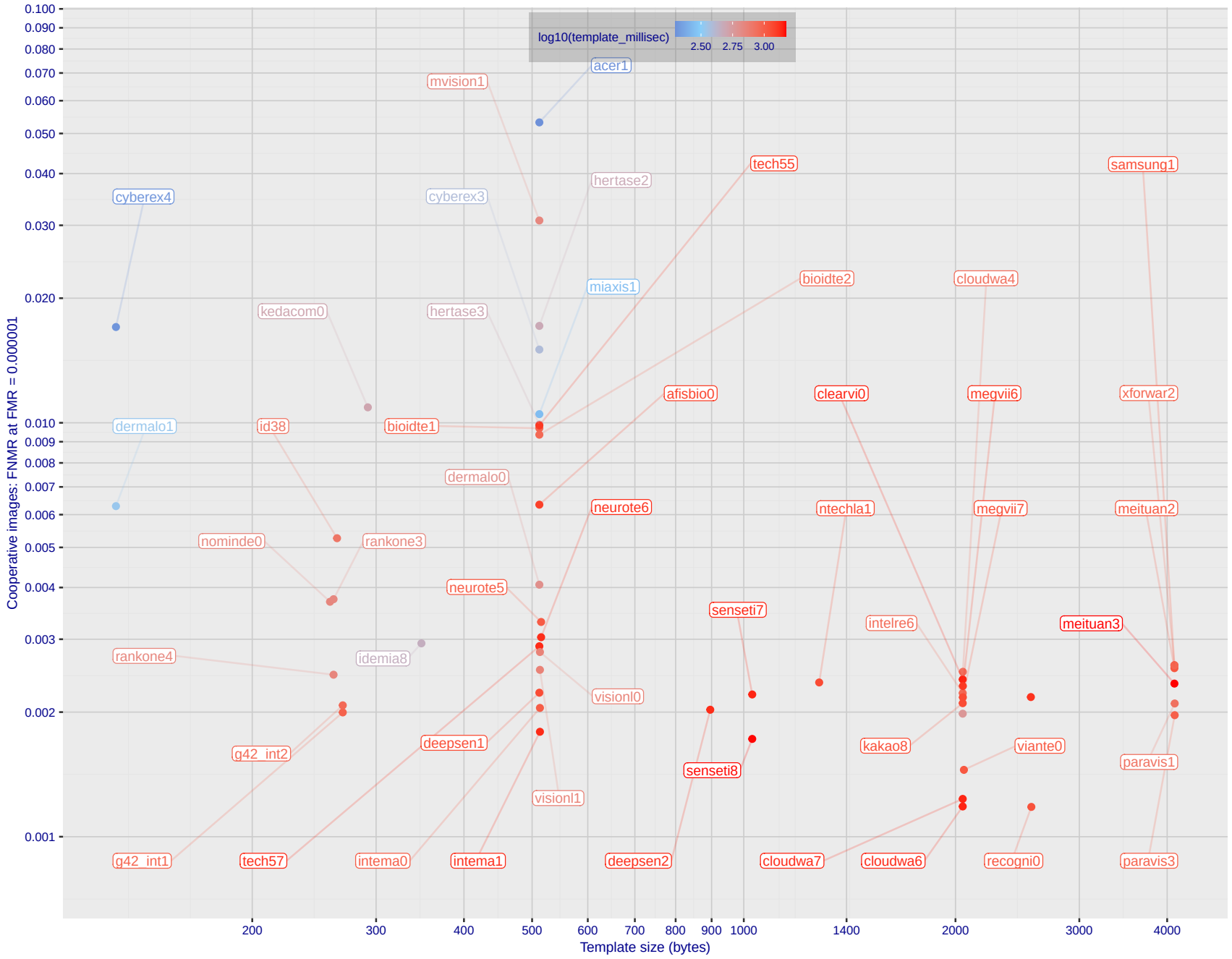

Figure 1: The points show false non-match rates (FNMR) versus the size of the encoded template. FNMR is the geometric mean of FNMR values for visa and mugshot images (from Figs. 106 and 135) at the false match rate (FMR) given in the y-axis label. The color of the points encodes template generation time - which spans at least one order of magnitude. Durations are measured on a single core of a c. 2016 Intel Xeon CPU E5-2630 v4 running at 2.20GHz. Algorithms with poor FNMR are omitted.

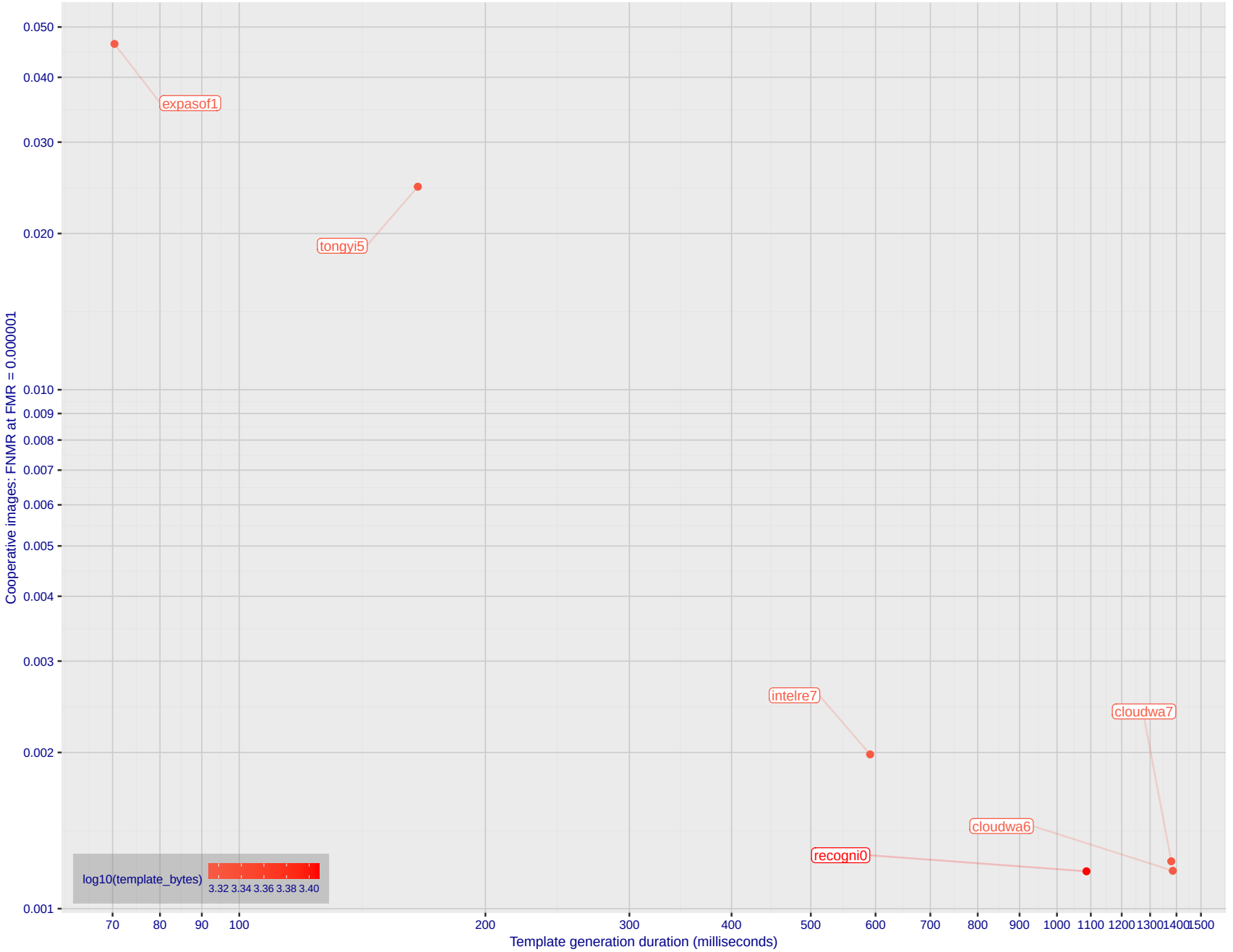

Figure 2: The points show false non-match rates (FNMR) versus the duration of the template generation operation. FNMR is the geometric mean of FNMR values for visa and mugshot images (from Figs. 106 and 135) at a false match rate (FMR) given in the y-axis label. Template generation time is a median estimated over 640 x 480 pixel portraits. It is measured on a single core of a c. 2016 Intel Xeon CPU E5-2630 v4 running at 2.20GHz. The color of the points encodes template size - which span two orders of magnitude. Algorithms with poor FNMR are omitted.

1 Metrics

1.1 Core accuracy

Given a vector of N genuine scores, u, the false non-match rate (FNMR) is computed as the proportion below some threshold, T:

$$\text{FNMR}(T) = 1 - \frac{1}{N}\sum_{i=1}^{N} H(u_i - T) \tag{1}$$

where $H(x)$ is the unit step function, and $H(0)$ taken to be 1.

Similarly, given a vector of N impostor scores, v, the false match rate (FMR) is computed as the proportion above T:

$$\text{FMR}(T) = \frac{1}{N}\sum_{i=1}^{N} H(v_i - T) \tag{2}$$

The threshold, T, can take on any value. We typically generate a set of thresholds from quantiles of the observed impostor scores, v, as follows. Given some interesting false match rate range, $[\text{FMR}_L, \text{FMR}_U]$, we form a vector of K thresholds corresponding to FMR measurements evenly spaced on a logarithmic scale

$$T_k = Q_v(1 - \text{FMR}_k) \tag{3}$$

where Q is the quantile function, and FMR_k comes from

$$\log_{10}\text{FMR}_k = \log_{10}\text{FMR}_L + \frac{k}{K}\ [\log_{10}\text{FMR}_U - \log_{10}\text{FMR}_L] \tag{4}$$

Error tradeoff characteristics are plots of FNMR(T) vs. FMR(T). These are plotted with $\text{FMR}_U \to 1$ and FMR_L as low as is sustained by the number of impostor comparisons, N. This is somewhat higher than the "rule of three" limit $3/N$ because samples are not independent, due to re-use of images.

1.2 Multi-template scoring methodology

There are some scenarios when one or more people exist and are detected in an image, and some of the proposed test images include K $>$ 1 persons for some images and situations where the subject of interest may or may not be the foreground face (largest face in the image). The NIST FRTE 1:1 API supports this by allowing generation of multiple templates representing each person detected in an image. When this occurs, NIST will match all templates generated from the enrollment image with all templates generated from the verification image and use the **maximum** similarity score across all template comparisons. This scoring approach will be used in our calculation of FMR and FNMR (this applies to both genuine and imposter comparisons).

FNMR(T) "False non-match rate"
FMR(T) "False match rate"

2 Datasets

2.1 Visa images

- The number of images is on the order of 10^5.
- The number of subjects is on the order of 10^5.
- The number of subjects with two images is on the order of 10^4.
- The images have geometry in reasonable conformance with the ISO/IEC 19794-5 Full Frontal image type. Pose is generally excellent.
- The images are of size 252x300 pixels. The mean interocular distance (IOD) is 69 pixels.
- The images are of subjects from greater than 100 countries, with significant imbalance due to visa issuance patterns.
- The images are of subjects of all ages, including children, again with imbalance due to visa issuance demand.
- Many of the images are live capture. A substantial number of the images are photographs of paper photographs.
- When these images are input to the algorithm, they are labelled as being of type "ISO" - see Table 4 of the FRTE API.

2.2 Application images

- The number of images is on the order of 10^6.
- The number of subjects is on the order of 10^6.
- The number of subjects with two images is on the order of 10^6.
- The images have geometry in good conformance with the ISO/IEC 19794-5 Full Frontal image type. Pose is generally excellent.
- The images are of size 300x300 pixels. The mean interocular distance (IOD) is 61 pixels.
- The images are of subjects from greater than 100 countries, with significant imbalance due to population and immigration patterns.
- The images are of subjects of adults.
- All of the images are live capture.
- When these images are input to the algorithm, they are labelled as being of type "ISO" - see Table 4 of the FRTE API.

2.3 Application images with head yaw

- The number of images is on the order of 10^5.
- The number of subjects is on the order of 10^5.
- The number of subjects with two images is on the order of 10^5.
- The images have geometry in good conformance with the ISO/IEC 19794-5 Full Frontal image type *except* the yaw angle is between 25 and 85 degrees. Our pose estimates are approximate, with an angular error that increases with yaw. The angular estimates will be improved over time.
- The images are of size 300x300 pixels. The mean interocular distance (IOD), if frontal, would be about pixels, but reduces with cosine of yaw.
- The images are of subjects from greater than 100 countries, with significant imbalance due to population and immigration patterns.

FNMR(T) "False non-match rate"
FMR(T) "False match rate"

- ▷ The images are of subjects of adults.
- ▷ All of the images are live capture.
- ▷ When these images are input to the algorithm, they are labelled as being of type ”WILD” - see Table 4 of the FRTE API.

2.4 Border crossing images

- ▷ The number of images is on the order of 10^6.
- ▷ The number of subjects is on the order of 10^6.
- ▷ The number of subjects with two images is on the order of 10^6.
- ▷ The images are taken with at camera oriented by an attendant toward a cooperating subject. This is done under time constraints so there are role, pitch and yaw angle variations. Also background illumination is sometimes strong, so the face is under-exposed. There is some perspective distortion due to close range images. Some faces are partially cropped.
- ▷ The images have mean IOD of 38 pixels.
- ▷ The images are of subjects of adults and childen aged 12 or above.
- ▷ The images are of subjects from greater than 100 countries, with significant imbalance due to population and immigration patterns.
- ▷ The images are all live capture.
- ▷ When these images are input to the algorithm, they are labelled as being of type ”WILD” - see Table 4 of the FRTE API.

2.5 Mugshot images

- ▷ The number of images is on the order of 10^6.
- ▷ The number of subjects is on the order of 10^6.
- ▷ The number of subjects with two images is on the order of 10^6.
- ▷ The images have geometry in reasonable conformance with the ISO/IEC 19794-5 Full Frontal image type.
- ▷ The images are of variable sizes. The median IOD is 105 pixels. The mean IOD is 113 pixels. The 1-st, 5-th, 10-th, 25-th, 75-th, 90-th and 99-th percentiles are 34, 58, 70, 87, 121, 161 and 297 pixels.
- ▷ The images are of subjects from the United States.
- ▷ The images are of adults.
- ▷ The images are all live capture.
- ▷ When these images are input to the algorithm, they are labelled as being of type ”mugshot” - see Table 4 of the FRTE API.

2.6 Kiosk images

- ▷ The number of images is on the order of 10^6.
- ▷ The number of subjects is on the order of 10^5.
- ▷ The number of subjects with multiple images is the order of 10^5.

FNMR(T) “False non-match rate”
FMR(T) “False match rate”

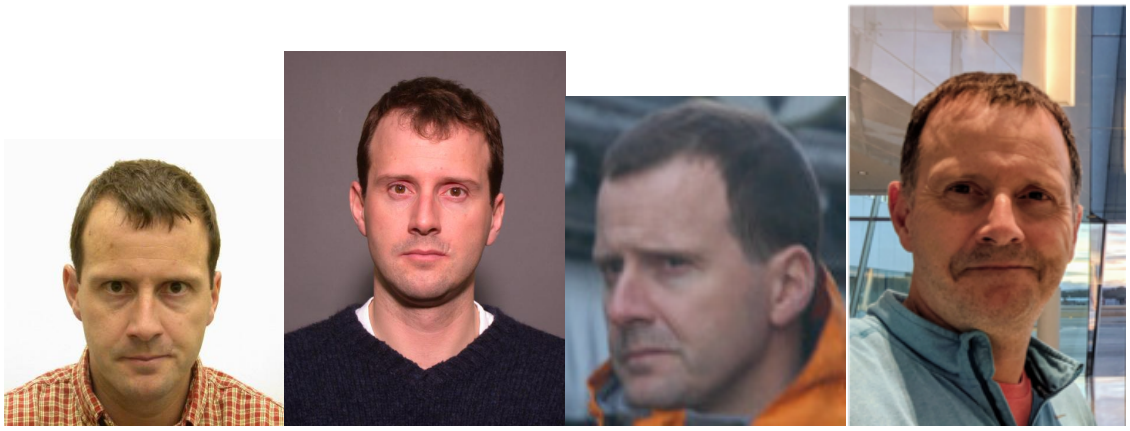

(a) Visa (b) Mugshot (c) Wild (d) Border

Figure 3: The figure gives simulated samples of image types used in this report.

- The images are taken at kiosk equipped with a camera intended to capture a centered face. However the images have specific quality defects arising from the camera triggering before the subject looks at it. These are downward pitch of the face relative to the optical axis; cropping of the forehead; and cropping of left or right part of the face. Partial cropping affects perhaps 10% of the images. Resolution does not vary widely.
- The images are of adults.
- The images have mean IOD of 44 pixels, with maximum below 75, and minimum when both eyes are present above 25 pixels.
- All of the images are live capture, none are scanned.
- When these images are input to the algorithm, they are labelled as being of type ”WILD” - see Table 4 of the FRTE API.

2.7 Wild images

- The number of images is on the order of 10^5.
- The number of subjects is on the order of 10^4.
- The number of subjects with two images on the order of 10^4.
- The images include many photojournalism-style images. Images are given to the algorithm using a variable but generally tight crop of the head. Resolution varies very widely. The images are very unconstrained, with wide yaw and pitch pose variation. Faces can be occluded, including hair and hands.
- The images are of adults.
- All of the images are live capture, none are scanned.
- When these images are input to the algorithm, they are labelled as being of type ”WILD” - see Table 4 of the FRTE API.

3 Results

3.1 Test goals

- To state absolute accuracy for different kinds of images, including those with and without subject cooperation.

FNMR(T) “False non-match rate”
FMR(T) “False match rate”

▷ To state comparative accuracy, across algorithms.

3.2 Test design

Method: For visa images:

▷ The comparisons are of visa photos against visa photos.
▷ The number of genuine comparisons is on the order of 10^4.
▷ The number of impostor comparisons is on the order of 10^{10}.
▷ The comparisons are fully zero-effort, meaning impostors are paired without attention to sex, age or other covariates. However, later analysis is conducted on subsets.
▷ The number of persons is on the order of 10^5.
▷ The number of images used to make a template is one.
▷ The number of templates used to make each comparison score is two corresponding to simple one-to-one verification.

Method: For mugshot images:

▷ The comparisons are of mugshot photos against mugshot photos.
▷ The number of genuine comparisons is on the order of 10^6.
▷ The number of impostor comparisons is on the order of 10^8.
▷ The impostors are paired by sex, but not by age or other covariates.
▷ The number of persons is on the order of 10^6.
▷ The number of images used to make a template is one.
▷ The number of templates used to make each comparison score is two, corresponding to simple one-to-one verification.

Method: For visa-border comparisons:

▷ The comparisons are of visa-like frontals against border crossing webcam photos.
▷ The number of genuine comparisons is on the order of 10^6.
▷ The number of impostor comparisons is on the order of 10^8.
▷ The impostors are paired by sex, but not by age or other covariates.
▷ The number of persons is on the order of 10^6.
▷ The number of images used to make a template is one.
▷ The number of templates used to make each comparison score is two, corresponding to simple one-to-one verification.

Method: For visa-border non-frontal yaw comparisons:

▷ The comparisons are of visa-like images with yaw 25 to 85 degrees against border crossing webcam photos.
▷ The number of genuine comparisons is on the order of 10^5.
▷ The number of impostor comparisons is on the order of 10^8.
▷ The impostors are paired by sex, but not by age or other covariates.

FNMR(T) "False non-match rate"
FMR(T) "False match rate"

- ▷ The number of persons is on the order of 10^5.
- ▷ The number of images used to make a template is one.
- ▷ The number of templates used to make each comparison score is two, corresponding to simple one-to-one verification.

Method: For kiosk-border comparisons:

- ▷ The comparisons are of visa-like frontals against kiosk-style photos.
- ▷ The number of genuine comparisons is on the order of 10^6.
- ▷ The number of impostor comparisons is on the order of 10^8.
- ▷ The impostors are paired by sex, but not by age or other covariates.
- ▷ The number of persons is on the order of 10^5.
- ▷ The number of images used to make a template is one.
- ▷ The number of templates used to make each comparison score is two, corresponding to simple one-to-one verification.

Method: For border-border comparisons:

- ▷ The comparisons are of border crossing webcam photos.
- ▷ The number of genuine comparisons is on the order of 10^6.
- ▷ The number of impostor comparisons is on the order of 10^8.
- ▷ The impostors are paired by sex, but not by age or other covariates.
- ▷ The number of persons is on the order of 10^6.
- ▷ The number of images used to make a template is one.
- ▷ The number of templates used to make each comparison score is two corresponding to simple one-to-one verification.

Method: For wild images:

- ▷ The comparisons are of wild photos against wild photos.
- ▷ The number of genuine comparisons is on the order of 10^6.
- ▷ The number of impostor comparisons is on the order of 10^8.
- ▷ The comparisons are fully zero-effort, meaning impostors are paired without attention to sex, age or other covariates.
- ▷ The number of persons is on the order of 10^4.
- ▷ The number of images used to make a template is one.
- ▷ The number of templates used to make each comparison score is two corresponding to simple one-to-one verification.

Method: For child exploitation images:

- ▷ The comparisons are of unconstrained child exploitation photos against others of the same type.
- ▷ The number of genuine comparisons is on the order of 10^4.
- ▷ The number of impostor comparisons is on the order of 10^7.

FNMR(T) "False non-match rate"
FMR(T) "False match rate"

- ▷ The comparisons are fully zero-effort, meaning impostors are paired without attention to sex, age or other covariates.
- ▷ The number of persons is on the order of 10^3.
- ▷ The number of images used to make 1 template is 1.
- ▷ The number of templates used to make each comparison score is two corresponding to simple one-to-one verification.
- ▷ We produce two performance statements. First, is a DET as used for visa and mugshot images. The second is a cumulative match characteristic (CMC) summarizing a simulated one-to-many search process. This is done as follows.
  - We regard M enrollment templates as items in a gallery.
  - These M templates come from $M > N$ individuals, because multiple images of a subject are present in the gallery under separate identifiers.
  - We regard the verification templates as search templates.
  - For each search we compute the rank of the highest scoring mate.
  - This process should properly be conducted with a 1:N algorithm, such as those tested in NIST IR 8009. We use the 1:1 algorithms in a simulated 1:N mode here to a) better reflect what a child exploitation analyst does, and b) to show algorithm efficacy is better than that revealed in the verification DETs.

FNMR(T) "False non-match rate"
FMR(T) "False match rate"

3.3 Failure to enroll

FNMR(T) "False non-match rate"
FMR(T) "False match rate"

	Algorithm	Failure to Enrol Rate[1]									
	Name	APPLICATION		BORDER		KIOSK		MUGSHOT		VISA	
	Name	SEC. 2.2		SEC. 2.4		SEC. 2.6		SEC. 2.5		SEC. 2.1	
1	20face-000	0.0000	328	0.0008	287	0.0217	240	0.0000	161	0.0004	315
2	20face-001	0.0000	336	0.0008	288	0.0000	51	0.0000	160	0.0004	317
3	3divi-006	0.0000	371	0.0007	249	0.0214	238	0.0001	298	0.0002	148
4	3divi-007	0.0000	346	0.0007	250	0.0214	237	0.0001	297	0.0002	147
5	accurascan-002	0.0001	503	0.0060	507	0.0838	386	0.0006	473	0.0022	528
6	accurascan-003	0.0000	241	0.0009	324	0.0226	247	0.0000	195	0.0003	208
7	acer-001	0.0000	373	0.0011	355	-	567	0.0001	259	0.0004	334
8	acer-002	0.0000	462	0.0008	278	0.0191	208	0.0003	409	0.0004	335
9	acisw-007	0.0000	180	0.0000	51	0.0000	55	0.0000	116	0.0000	5
10	acisw-008	0.0000	263	0.0009	315	0.0173	189	0.0004	434	0.0004	226
11	adera-004	0.0000	353	0.0008	274	0.0202	218	0.0003	424	0.0004	286
12	adera-005	0.0000	276	0.0008	275	0.0202	217	0.0003	423	0.0004	291
13	advance-004	0.0001	507	0.0010	344	0.0157	172	0.0008	492	0.0006	464
14	advance-005	0.0000	250	0.0003	151	0.0074	104	0.0002	367	0.0003	151
15	afisbiometrics-000	0.0000	311	0.0008	266	0.0213	235	0.0000	158	0.0004	338
16	afrengine-002	0.0000	363	0.0007	259	0.0183	197	0.0005	450	0.0004	391
17	afrengine-003	0.0000	251	0.0099	521	0.0384	330	0.0005	449	-	567
18	aifirst-001	0.0000	151	0.0000	6	-	507	0.0000	96	0.0000	53
19	aigen-001	0.0000	43	0.0000	68	-	438	0.0000	33	0.0000	117
20	aigen-002	0.0000	162	0.0000	15	0.0000	45	0.0000	92	0.0000	61
21	ailabs-001	0.0000	239	0.0090	519	-	421	0.0007	484	0.0005	416
22	aimall-002	0.0000	442	0.0043	488	-	439	0.0012	508	0.0005	438
23	aimall-003	0.0000	417	0.0012	373	-	504	0.0004	428	0.0005	410
24	aiseemu-001	0.0000	193	0.0000	57	0.0000	58	0.0000	105	0.0000	18
25	aiseemu-002	0.0000	65	0.0000	77	0.0000	17	0.0000	22	0.0000	128
26	aiunionface-000	0.0000	133	0.0000	30	-	495	0.0000	77	0.0000	45
27	aize-002	0.0000	30	0.0014	394	0.0230	254	0.0005	466	0.0004	320
28	aize-003	0.0000	24	0.0000	130	0.0001	75	0.0000	2	0.0000	135
29	ajou-001	0.0000	370	0.0020	425	-	558	0.0001	304	0.0004	393
30	alchera-006	0.0000	283	0.0009	313	0.0228	249	0.0001	332	0.0004	268
31	alchera-007	0.0000	323	0.0009	310	0.0228	250	0.0001	335	0.0004	264
32	alfabeta-001	0.0005	534	0.0650	557	0.2142	401	0.0024	533	0.0018	522
33	alice-000	0.0000	33	0.0006	214	0.0133	151	0.0000	183	0.0004	257
34	alice-001	0.0000	228	0.0006	213	0.0133	152	0.0000	187	0.0004	246
35	alleyes-000	0.0000	247	0.0010	334	-	425	0.0002	348	0.0004	371
36	allgovision-000	0.0007	541	0.0062	508	-	431	0.0026	536	0.0052	539
37	alphaface-001	0.0000	292	0.0012	363	-	483	0.0000	245	0.0004	367
38	alphaface-002	0.0000	321	0.0012	359	-	508	0.0000	248	0.0004	364
39	amplifiedgroup-001	0.0114	559	0.1023	562	-	559	0.0189	560	0.0279	547
40	androvideo-000	0.0000	96	0.0000	101	-	472	0.0000	66	0.0000	83
41	anke-004	0.0000	327	0.0011	352	-	514	0.0001	313	0.0004	378
42	anke-005	0.0000	333	0.0012	364	-	516	0.0001	325	0.0004	389
43	antheus-000	0.0000	126	0.0000	18	-	491	0.0000	80	0.0000	41
44	antheus-001	0.0000	155	0.0000	2	-	511	0.0000	94	0.0000	57
45	anyvision-004	0.0000	428	0.0017	410	-	566	0.0001	326	0.0004	324
46	anyvision-005	0.0000	318	0.0013	378	-	500	0.0000	204	0.0004	249
47	aratek-001	0.0000	73	0.0000	112	0.0000	18	0.0000	55	0.0000	69
48	armatura-001	0.0000	452	0.0021	433	0.0257	275	0.0005	459	0.0005	417
49	armatura-003	0.0000	299	0.0012	366	0.0333	309	0.0004	431	0.0004	302
50	asusaics-000	0.0000	161	0.0000	16	-	517	0.0000	90	0.0000	59
51	asusaics-001	0.0000	150	0.0000	7	-	506	0.0000	97	0.0000	54
52	autentika-001	0.0000	222	0.0000	43	0.0000	67	0.0000	125	0.0000	31
53	autentika-002	0.0000	51	0.0000	70	0.0000	13	0.0000	32	0.0000	115
54	authenmetric-003	0.0000	159	0.0000	12	0.0000	48	0.0000	93	0.0000	62
55	authenmetric-004	0.0000	191	0.0000	59	0.0000	59	0.0000	107	0.0000	17
56	authme-001	0.0000	468	0.0009	321	0.0245	263	0.0003	421	0.0005	409
57	aware-007	0.0000	351	0.0012	367	0.0325	301	0.0000	219	0.0004	344
58	aware-008	0.0000	259	0.0012	370	0.0327	303	0.0000	215	-	559

Table 36: FTE is the proportion of failed template generation attempts. Failures can occur because the software throws an exception, or because the software electively refuses to process the input image. This would typically occur if a face is not detected. FTE is measured as the number of function calls that give EITHER a non-zero error code OR that give a "small" template. This is defined as one whose size is less than 0.3 times the median template size for that algorithm. This second rule is needed because some algorithms incorrectly fail to return a non-zero error code when template generation fails.
A hyphen "-" indicates the dataset was not produced. [1]*The effects of FTE are included in the accuracy results of this report by regarding any template comparison involving a failed template to produce a low similarity score. Thus higher FTE results in higher FNMR and lower FMR.*

FNMR(T) "False non-match rate"
FMR(T) "False match rate"

	Algorithm	Failure to Enrol Rate[1]									
	Name	APPLICATION		BORDER		KIOSK		MUGSHOT		VISA	
	Name	SEC. 2.2		SEC. 2.4		SEC. 2.6		SEC. 2.5		SEC. 2.1	
59	awiros-001	0.0039	547	0.0369	548	-	502	0.0386	562	0.0872	551
60	awiros-002	0.0000	466	0.0038	477	-	482	0.0007	482	0.0012	512
61	aximetria-001	0.0000	403	0.0010	346	0.0217	241	0.0001	347	0.0004	313
62	ayftech-001	0.0002	525	0.0046	493	-	497	0.0043	550	0.0011	491
63	ayftech-003	0.0000	81	0.0006	234	0.0123	145	0.0000	49	0.0000	72
64	ayonix-000	0.0053	550	0.0341	544	-	447	0.0113	558	0.0137	544
65	beethedata-000	0.0005	532	0.0042	486	0.0366	322	0.0002	363	0.0010	486
66	beyneai-000	0.0000	200	0.0000	38	0.0000	61	0.0000	134	0.0000	21
67	biocube-001	0.0006	536	0.0391	549	0.1207	390	0.0015	515	0.0020	525
68	biocube-002	0.0000	343	0.0046	496	0.0721	380	0.0008	490	0.0012	507
69	bioidtechswiss-001	0.0000	342	0.0007	245	-	530	0.0000	192	0.0004	352
70	bioidtechswiss-002	0.0000	273	0.0007	248	-	458	0.0000	193	0.0004	349
71	biometric-vision-000	0.0000	243	0.0005	189	0.0107	133	0.0002	394	0.0004	284
72	bm-001	0.0000	205	0.0000	39	-	550	0.0000	141	0.0000	20
73	boetech-001	0.0087	556	0.0272	538	0.2117	399	0.0032	543	0.0160	545
74	boetech-002	0.0087	555	0.0272	539	0.2117	398	0.0032	542	0.0160	546
75	bresee-001	0.0000	309	0.0010	341	-	493	0.0002	362	0.0003	185
76	bresee-002	0.0000	430	0.0020	428	0.0219	243	0.0008	485	0.0004	298
77	camvi-002	0.0000	71	0.0000	114	-	449	0.0000	53	0.0000	68
78	camvi-004	0.0000	179	0.0000	127	-	534	0.0000	115	0.0000	4
79	candour-001	0.0000	204	0.0000	40	0.0000	60	0.0000	133	0.0000	19
80	canon-004	0.0000	249	0.0008	267	0.0234	257	0.0000	236	0.0004	343
81	canon-005	0.0000	137	0.0044	490	0.0269	283	0.0000	189	0.0004	279
82	cchonolulu-000	0.0054	551	0.0395	551	0.2802	406	0.0036	545	0.0012	505
83	cchonolulu-001	0.0056	552	0.0414	552	0.2894	407	0.0038	548	0.0012	509
84	ceiec-003	0.0000	41	0.0013	389	-	423	0.0001	269	0.0004	360
85	ceiec-004	0.0000	120	0.0008	286	-	485	0.0000	198	0.0004	263
86	chosun-001	0.0000	186	0.0000	63	-	543	0.0000	109	0.0000	10
87	chosun-002	0.0000	53	0.0000	82	-	445	0.0000	28	0.0000	122
88	chtface-005	0.0000	135	0.0017	406	0.0320	297	0.0000	221	0.0004	362
89	chtface-006	0.0000	45	0.0017	407	0.0320	296	0.0000	220	0.0004	372
90	cist-003	0.0000	115	0.0011	350	0.0343	315	0.0000	85	0.0000	37
91	cist-004	0.0000	13	0.0005	191	0.0108	134	0.0000	13	0.0000	102
92	clearviewai-000	0.0000	297	0.0003	155	0.0081	112	0.0000	225	0.0003	164
93	clearviewai-001	0.0000	258	0.0006	225	0.0174	190	0.0001	251	0.0004	239
94	closeli-001	0.0000	169	0.0000	9	0.0000	49	0.0000	88	0.0000	65
95	cloudmatrix-001	0.0000	396	0.0028	450	0.0225	245	0.0001	267	0.0004	232
96	cloudmatrix-002	0.0000	391	0.0028	449	0.0225	244	0.0001	265	0.0004	236
97	cloudwalk-hr-003	0.0000	286	0.0008	289	-	475	0.0001	276	0.0004	255
98	cloudwalk-hr-004	0.0000	238	0.0011	358	-	420	0.0004	429	0.0003	217
99	cloudwalk-mt-006	0.0000	358	0.0006	219	0.0158	174	0.0002	377	0.0004	374
100	cloudwalk-mt-007	0.0000	314	0.0006	217	0.0158	173	0.0002	376	0.0004	376
101	cmcuni-001	0.0000	166	0.0005	198	0.0119	142	0.0000	86	0.0000	63
102	codeline-000	0.0000	3	0.0000	90	0.0000	3	0.0000	18	0.0000	100
103	cogent-007	0.0000	435	0.0000	125	0.0000	72	0.0000	205	0.0000	136
104	cogent-008	0.0000	91	0.0010	347	0.0304	291	0.0000	230	0.0004	227
105	cognitec-004	0.0001	496	0.0037	476	0.0580	354	0.0003	420	0.0005	419
106	cognitec-005	0.0000	455	0.0026	445	0.0550	352	0.0002	356	0.0005	415
107	cor-001	0.0000	305	0.0006	223	-	489	0.0002	396	0.0004	326
108	coretech-001	0.0000	488	0.0033	467	0.0677	368	0.0005	463	0.0011	500
109	coretech-002	0.0000	127	0.0013	390	0.0301	290	0.0000	159	0.0004	337
110	corsight-002	0.0000	284	0.0005	210	0.0152	165	0.0001	316	0.0004	308
111	corsight-003	0.0000	244	0.0006	232	0.0175	191	0.0001	305	0.0004	321
112	csc-002	0.0015	546	0.0033	463	-	522	0.0006	476	0.0006	467
113	csc-003	0.0015	545	0.0033	464	0.0445	344	0.0006	475	0.0006	468
114	ctbcbank-000	0.0001	499	0.0051	500	-	478	0.0011	505	0.0019	523
115	ctbcbank-001	0.0000	465	0.0036	475	-	470	0.0005	460	0.0010	485
116	cu-face-003	0.0000	429	0.0009	322	0.0245	262	0.0003	411	0.0004	379

Table 37: FTE is the proportion of failed template generation attempts. Failures can occur because the software throws an exception, or because the software electively refuses to process the input image. This would typically occur if a face is not detected. FTE is measured as the number of function calls that give EITHER a non-zero error code OR that give a "small" template. This is defined as one whose size is less than 0.3 times the median template size for that algorithm. This second rule is needed because some algorithms incorrectly fail to return a non-zero error code when template generation fails.
A hyphen "-" indicates the dataset was not produced. [1]*The effects of FTE are included in the accuracy results of this report by regarding any template comparison involving a failed template to produce a low similarity score. Thus higher FTE results in higher FNMR and lower FMR.*

FNMR(T) "False non-match rate"
FMR(T) "False match rate"

	Algorithm	Failure to Enrol Rate[1]									
	Name	APPLICATION		BORDER		KIOSK		MUGSHOT		VISA	
	Name	SEC. 2.2		SEC. 2.4		SEC. 2.6		SEC. 2.5		SEC. 2.1	
117	cu-face-004	0.0000	398	0.0007	260	0.0179	193	0.0001	324	-	555
118	cubox-002	0.0000	382	0.0006	228	0.0159	177	0.0002	395	0.0005	441
119	cubox-003	0.0000	111	0.0010	343	0.0210	231	0.0002	357	0.0004	358
120	cudocommunication-001	0.0000	89	0.0000	102	0.0000	26	0.0000	69	0.0000	82
121	cuhkee-001	0.0000	312	0.0011	357	-	492	0.0000	157	0.0004	303
122	cybercore-002	0.0000	443	0.0001	134	0.0014	78	0.0002	354	0.0002	143
123	cybercore-003	0.0000	300	0.0003	156	0.0060	92	0.0005	464	0.0003	168
124	cyberextruder-003	0.0000	444	0.0077	512	0.0887	387	0.0001	340	0.0006	462
125	cyberextruder-004	0.0000	439	0.0097	520	0.1025	388	0.0001	329	0.0007	469
126	cyberlink-012	0.0000	36	0.0004	183	0.0106	130	0.0000	146	0.0003	188
127	cyberlink-013	0.0000	218	0.0004	182	0.0106	131	0.0000	152	0.0003	184
128	dahua-006	0.0000	213	0.0000	123	-	555	0.0000	235	0.0003	212
129	dahua-007	0.0000	195	0.0000	124	0.0000	74	0.0000	233	0.0003	211
130	daon-000	0.0000	472	0.0028	453	0.0577	353	0.0014	512	0.0015	517
131	datech-000	0.0000	279	0.0004	167	0.0089	121	0.0000	203	0.0003	154
132	datech-001	0.0000	295	0.0004	168	0.0089	122	0.0000	202	-	561
133	decatur-000	0.0000	397	0.0020	423	-	526	0.0004	441	0.0005	406
134	decatur-001	0.0000	360	0.0009	317	0.0194	212	0.0001	281	0.0004	287
135	decloakface-001	0.0000	256	0.0016	403	0.0392	333	0.0001	308	0.0005	447
136	deepglint-004	0.0000	288	0.0005	186	0.0130	149	0.0002	391	0.0004	269
137	deepglint-005	0.0000	409	0.0019	417	0.0438	343	0.0006	471	0.0006	465
138	deepsea-001	0.0000	14	0.0000	84	-	416	0.0000	12	0.0000	103
139	deepsense-002	0.0000	2	0.0006	233	0.0191	207	0.0000	181	0.0004	229
140	deepsense-003	0.0000	187	0.0004	179	0.0110	136	0.0000	163	0.0003	166
141	dermalog-011	0.0000	483	0.0005	187	0.0116	139	0.0001	258	0.0003	162
142	dermalog-012	0.0000	362	0.0003	161	0.0068	100	0.0003	412	0.0005	448
143	dicio-001	0.0005	535	0.0649	555	0.2136	400	0.0024	531	0.0012	506
144	didiglobalface-001	0.0000	234	0.0012	361	-	412	0.0000	244	0.0004	369
145	didiglobalface-002	0.0000	316	0.0012	360	0.0247	264	0.0000	246	0.0004	363
146	digidata-000	0.0000	277	0.0023	439	0.0375	328	0.0004	446	0.0006	457
147	digidata-001	0.0000	294	0.0023	440	0.0375	329	0.0004	445	0.0006	458
148	digitalbarriers-002	0.0001	513	0.0045	491	-	424	0.0028	539	0.0027	532
149	dps-000	0.0000	84	0.0000	118	0.0000	24	0.0000	43	0.0000	77
150	dsk-000	0.0000	177	0.0000	52	-	533	0.0000	117	0.0000	6
151	einetworks-000	0.0000	464	0.0017	408	-	448	0.0002	380	0.0005	431
152	einetworksindia-000	0.0000	449	0.0018	412	0.0516	347	0.0002	403	0.0005	436
153	einetworksindia-001	0.0000	450	0.0018	414	0.0516	348	0.0002	404	0.0005	434
154	ekin-002	0.0000	44	0.0000	128	0.0004	76	0.0000	144	0.0000	134
155	element-000	0.0000	240	0.0008	294	0.0192	209	0.0000	196	0.0003	192
156	enface-001	0.0000	172	0.0012	371	0.0304	292	0.0000	191	0.0004	300
157	enface-002	0.0000	246	0.0004	172	0.0084	119	0.0000	170	0.0004	230
158	eocortex-000	0.0095	557	0.0602	554	-	460	0.0094	556	0.0059	540
159	ercacat-001	0.0000	140	0.0005	200	-	503	0.0000	217	0.0003	190
160	euronovate-003	0.0000	293	0.0006	222	0.0159	176	0.0002	378	0.0004	368
161	euronovate-004	0.0000	454	0.0016	402	0.0236	258	0.0015	516	0.0006	461
162	expasoft-001	0.0000	196	0.0000	60	-	545	0.0000	101	0.0000	13
163	expasoft-002	0.0000	211	0.0000	34	0.0000	62	0.0000	129	0.0000	24
164	f8-001	0.0003	527	0.0059	505	-	510	0.0035	544	0.0030	538
165	f8-002	0.0000	491	0.0150	530	0.0685	372	0.0005	448	0.0013	514
166	facehawk-000	0.0000	437	0.0357	545	0.0720	379	0.0021	527	0.0009	482
167	facelocate-001	0.0000	183	0.0019	419	0.0329	304	0.0000	226	-	554
168	faceonlive-001	0.0000	479	0.0029	458	0.0481	345	0.0013	510	0.0011	492
169	faceonlive-002	0.0002	523	0.0009	320	0.0075	107	0.0008	488	0.0008	481
170	facephi-000	0.0000	108	0.0004	169	0.0090	123	0.0001	315	0.0004	242
171	facesoft-000	0.0000	32	0.0000	73	-	433	0.0000	37	0.0000	112
172	facetag-000	0.0000	113	0.0000	107	0.0000	29	0.0000	57	0.0000	89
173	facetag-002	0.0000	164	0.0000	8	0.0000	50	0.0000	89	0.0000	66
174	facex-001	0.0001	520	0.0360	546	-	486	0.0047	553	0.0027	533

Table 38: FTE is the proportion of failed template generation attempts. Failures can occur because the software throws an exception, or because the software electively refuses to process the input image. This would typically occur if a face is not detected. FTE is measured as the number of function calls that give EITHER a non-zero error code OR that give a "small" template. This is defined as one whose size is less than 0.3 times the median template size for that algorithm. This second rule is needed because some algorithms incorrectly fail to return a non-zero error code when template generation fails.
A hyphen "-" indicates the dataset was not produced. [1]*The effects of FTE are included in the accuracy results of this report by regarding any template comparison involving a failed template to produce a low similarity score. Thus higher FTE results in higher FNMR and lower FMR.*

FNMR(T) "False non-match rate"
FMR(T) "False match rate"

	Algorithm	Failure to Enrol Rate[1]									
	Name	APPLICATION		BORDER		KIOSK		MUGSHOT		VISA	
	Name	SEC. 2.2		SEC. 2.4		SEC. 2.6		SEC. 2.5		SEC. 2.1	
175	facex-002	0.0001	519	0.0360	547	0.2663	404	0.0047	552	0.0027	534
176	facia-001	0.0000	152	0.0005	185	0.0122	144	0.0001	253	0.0004	251
177	farfaces-001	0.0000	461	0.0007	247	0.0061	94	0.0003	418	0.0003	174
178	fastenterprises-000	0.0000	320	0.0082	516	0.0169	186	0.0001	339	0.0003	186
179	fedu-001	0.0000	170	0.0000	55	0.0000	53	0.0000	119	-	553
180	fiberhome-nanjing-003	0.0000	37	0.0004	174	-	430	0.0000	38	0.0003	159
181	fiberhome-nanjing-004	0.0000	29	0.0004	175	-	419	0.0000	1	0.0003	158
182	fincore-000	0.0000	310	0.0008	291	0.0185	199	0.0001	255	0.0004	355
183	firstcreditkz-002	0.0000	290	0.0010	348	0.0232	256	0.0000	216	0.0004	271
184	firstcreditkz-003	0.0000	467	0.0010	345	0.0219	242	0.0000	208	-	565
185	foomobi-001	0.0007	539	0.0000	31	0.0000	64	0.0020	526	0.0011	493
186	foomobi-002	0.0007	537	0.0000	86	0.0000	6	0.0020	524	0.0011	495
187	fpt-000	0.0001	501	0.0007	251	0.0076	108	0.0006	477	-	564
188	fraudcom-000	0.0000	406	0.0055	504	0.0308	294	0.0002	384	0.0004	354
189	frpkauai-001	0.0000	411	0.0024	443	0.0360	321	0.0001	261	0.0004	386
190	frpkauai-002	0.0000	410	0.0019	422	0.0321	298	0.0000	241	0.0004	309
191	fujitsulab-002	0.0000	98	0.0009	303	-	471	0.0001	322	0.0003	157
192	fujitsulab-003	0.0000	26	0.0008	272	0.0166	181	0.0001	312	0.0001	139
193	g42-intellibrain-001	0.0000	105	0.0000	105	0.0000	31	0.0000	61	0.0000	92
194	g42-intellibrain-002	0.0000	148	0.0000	3	0.0000	42	0.0000	98	0.0000	56
195	geo-002	0.0000	301	0.0015	397	0.0332	307	0.0001	252	0.0004	388
196	geo-004	0.0000	267	0.0005	209	0.0138	155	0.0001	295	0.0004	280
197	gistouch-000	0.0000	489	0.0188	533	0.1345	393	0.0018	521	0.0007	470
198	gistouch-001	0.0000	223	0.0002	136	0.0027	80	0.0001	293	0.0003	163
199	glory-006	0.0000	405	0.0020	427	0.0345	316	0.0001	318	0.0004	383
200	glory-007	0.0000	419	0.0020	431	0.0403	338	0.0002	386	0.0005	408
201	gorilla-008	0.0000	356	0.0009	325	0.0259	276	0.0001	280	0.0004	353
202	gorilla-009	0.0000	304	0.0010	337	0.0276	284	0.0001	264	0.0004	336
203	gpstechvn-000	0.0000	5	0.0000	93	0.0000	2	0.0000	15	0.0000	94
204	graymatics-001	0.0000	100	0.0010	327	0.0210	228	0.0001	338	0.0004	290
205	griaule-001	0.0000	209	0.0012	372	0.0366	324	0.0000	179	0.0004	345
206	griaule-002	0.0000	15	0.0007	252	0.0209	222	0.0000	238	0.0004	299
207	hertasecurity-002	0.0000	158	0.0000	11	0.0000	47	0.0000	169	0.0000	131
208	hertasecurity-003	0.0000	185	0.0000	62	0.0000	56	0.0000	150	0.0000	130
209	hik-001	0.0000	60	0.0000	131	-	440	0.0000	24	0.0000	120
210	hisign-002	0.0000	395	0.0006	229	0.0150	161	0.0001	320	0.0003	201
211	hisign-003	0.0000	381	0.0008	292	0.0237	259	0.0001	319	-	560
212	hyperverge-003	0.0000	75	0.0008	270	0.0210	230	0.0002	400	0.0004	289
213	hyperverge-005	0.0000	68	0.0008	269	0.0210	229	0.0002	399	0.0004	294
214	hzailu-005	0.0000	270	0.0004	171	0.0081	113	0.0002	353	0.0003	198
215	hzailu-006	0.0000	317	0.0004	170	0.0081	114	0.0002	355	0.0003	196
216	i2v-001	0.0000	448	0.0018	416	0.0341	314	0.0001	291	-	566
217	icm-004	0.0000	473	0.0033	469	0.0698	374	0.0006	474	0.0010	490
218	icm-005	0.0002	522	0.0117	526	0.1223	391	0.0018	523	0.0014	516
219	icomm-000	0.0000	265	0.0004	177	0.0098	127	0.0000	223	0.0003	175
220	icthtc-000	0.0001	517	0.0047	497	-	467	0.0028	540	0.0029	535
221	id3-006	0.0000	420	0.0009	323	-	553	0.0004	435	0.0005	427
222	id3-008	0.0000	165	0.0006	231	0.0184	198	0.0001	336	0.0004	225
223	idemia-009	0.0000	48	0.0004	181	0.0077	109	0.0000	166	0.0003	200
224	idemia-010	0.0000	35	0.0004	166	0.0074	105	0.0000	39	0.0003	176
225	identy-000	0.0000	490	0.0020	429	0.0152	164	0.0012	507	0.0004	385
226	igearx-face-000	0.0000	233	0.0006	215	0.0153	167	0.0004	433	0.0004	351
227	iit-002	0.0000	471	0.0021	432	-	434	0.0009	497	0.0005	444
228	iit-003	0.0000	340	0.0008	290	-	521	0.0000	200	0.0004	238
229	imds-software-002	0.0000	90	0.0000	103	0.0000	25	0.0000	67	0.0000	80
230	imds-software-003	0.0000	8	0.0000	92	0.0000	1	0.0000	17	0.0000	97
231	imperial-000	0.0000	167	0.0000	10	-	524	0.0000	87	0.0000	64
232	imperial-002	0.0000	143	0.0000	29	-	499	0.0000	72	0.0000	46

Table 39: FTE is the proportion of failed template generation attempts. Failures can occur because the software throws an exception, or because the software electively refuses to process the input image. This would typically occur if a face is not detected. FTE is measured as the number of function calls that give EITHER a non-zero error code OR that give a "small" template. This is defined as one whose size is less than 0.3 times the median template size for that algorithm. This second rule is needed because some algorithms incorrectly fail to return a non-zero error code when template generation fails.
A hyphen "-" indicates the dataset was not produced. [1]*The effects of FTE are included in the accuracy results of this report by regarding any template comparison involving a failed template to produce a low similarity score. Thus higher FTE results in higher FNMR and lower FMR.*

FNMR(T) "False non-match rate"
FMR(T) "False match rate"

	Algorithm	Failure to Enrol Rate[1]									
	Name	APPLICATION		BORDER		KIOSK		MUGSHOT		VISA	
	Name	SEC. 2.2		SEC. 2.4		SEC. 2.6		SEC. 2.5		SEC. 2.1	
233	incode-009	0.0000	386	0.0009	309	0.0255	274	0.0002	364	0.0004	282
234	incode-013	0.0001	521	0.0012	368	0.0254	273	0.0005	458	0.0004	398
235	infocert-001	0.0000	426	0.0059	506	0.0424	340	0.0001	287	0.0006	449
236	innefulabs-000	0.0000	260	0.0024	442	-	454	0.0003	417	0.0005	424
237	innominds-001	0.0000	441	0.0030	461	0.0637	362	0.0010	503	0.0008	479
238	innovativetechnologyltd-001	0.0001	516	0.0050	499	-	494	0.0024	535	0.0025	531
239	innovativetechnologyltd-002	0.0000	413	0.0046	492	-	459	0.0057	555	0.0005	426
240	innovatrics-010	0.0000	339	0.0019	418	0.0393	334	0.0001	279	0.0004	224
241	innovatrics-011	0.0000	302	0.0001	133	0.0017	79	0.0000	149	-	557
242	insightface-003	0.0000	226	0.0000	41	0.0000	70	0.0000	121	0.0000	35
243	insightface-004	0.0000	80	0.0000	122	0.0000	21	0.0000	46	0.0000	71
244	inspur-001	0.0000	97	0.0000	100	0.0000	27	0.0000	65	0.0000	84
245	inspur-002	0.0000	125	0.0000	19	0.0000	36	0.0000	81	0.0000	42
246	intellicloudai-001	0.0000	212	0.0000	35	-	556	0.0000	130	0.0000	25
247	intellicloudai-002	0.0000	102	0.0008	281	-	476	0.0000	197	0.0004	228
248	intellifusion-001	0.0000	361	0.0005	204	-	554	0.0001	275	0.0003	202
249	intellifusion-002	0.0000	110	0.0000	129	-	481	0.0000	137	0.0000	93
250	intellivision-006	0.0001	512	0.0041	482	0.0528	351	0.0005	456	0.0007	473
251	intellivision-007	0.0001	510	0.0041	483	0.0528	350	0.0005	454	0.0007	475
252	intellivix-004	0.0000	85	0.0022	436	0.0333	311	0.0000	45	0.0000	79
253	intellivix-005	0.0000	50	0.0022	435	0.0333	310	0.0000	30	0.0000	114
254	intelresearch-007	0.0000	42	0.0007	239	0.0168	184	0.0000	145	0.0004	274
255	intelresearch-008	0.0000	136	0.0006	235	0.0169	187	0.0000	148	0.0004	278
256	intema-000	0.0000	131	0.0005	192	0.0126	147	0.0000	231	0.0004	233
257	intema-001	0.0000	315	0.0004	180	0.0106	132	0.0000	147	0.0003	215
258	intozi-001	0.0000	296	0.0005	208	0.0126	146	0.0001	346	0.0004	219
259	intsysmsu-001	0.0000	160	0.0010	339	-	519	0.0001	303	0.0004	327
260	intsysmsu-002	0.0000	95	0.0010	340	-	474	0.0001	301	0.0004	328
261	ionetworks-001	0.0000	138	0.0081	514	0.0666	363	0.0000	76	0.0000	44
262	ionetworks-002	0.0000	76	0.0003	147	0.0048	85	0.0000	51	0.0000	75
263	iqface-000	0.0000	201	0.0000	37	-	552	0.0000	135	0.0000	22
264	iqface-003	0.0000	469	0.0076	511	-	484	0.0006	468	0.0005	446
265	irex-000	0.0000	422	0.0009	319	-	452	0.0000	224	0.0005	411
266	isap-001	0.0000	18	0.0000	97	-	417	0.0000	6	0.0000	106
267	isap-002	0.0000	20	0.0000	96	-	418	0.0000	5	0.0000	105
268	isityou-000	0.0068	554	0.0316	542	-	427	0.0023	530	0.0010	488
269	isystems-001	0.0000	477	0.0035	473	-	450	0.0010	500	0.0007	471
270	isystems-002	0.0000	478	0.0035	472	-	480	0.0010	501	0.0007	472
271	itmo-007	0.0000	142	0.0009	301	-	501	0.0003	425	0.0000	52
272	itmo-008	0.0000	57	0.0135	527	0.1239	392	0.0024	534	0.0000	126
273	ivacognitive-001	0.0000	407	0.0011	354	-	564	0.0001	268	0.0004	387
274	iws-000	0.0005	533	0.0650	558	-	429	0.0024	532	0.0012	508
275	jaakit-001	0.0008	543	0.0858	561	0.2713	405	0.0042	549	0.0021	527
276	kakao-008	0.0000	214	0.0009	305	0.0209	226	0.0001	294	0.0004	262
277	kakao-009	0.0000	178	0.0009	306	0.0209	225	0.0001	292	0.0004	260
278	kakaobank-000	0.0000	34	0.0000	71	0.0000	12	0.0000	40	0.0000	113
279	kakaobank-001	0.0000	21	0.0006	221	0.0176	192	0.0000	165	0.0004	243
280	kakaopay-001	0.0000	388	0.0013	387	0.0322	300	0.0001	271	0.0004	392
281	kasikornlabs-002	0.0000	482	0.0033	465	0.0698	375	0.0004	438	0.0012	503
282	kasikornlabs-003	0.0000	484	0.0033	466	0.0698	376	0.0004	440	0.0012	502
283	kedacom-000	0.0000	31	0.0000	72	-	432	0.0000	36	0.0000	111
284	kiwitech-000	0.0000	281	0.0009	299	-	473	0.0004	436	0.0005	414
285	kneron-003	0.0239	561	0.0306	540	-	518	0.0044	551	0.0016	520
286	kneron-005	0.0000	481	0.0226	534	-	513	0.0006	467	0.0005	421
287	knowutech-000	0.0000	257	0.0008	268	0.0215	239	0.0000	209	0.0004	339
288	kogniza-001	0.0000	354	0.0012	375	0.0337	313	0.0003	422	-	556
289	kookmin-002	0.0000	153	0.0000	1	-	515	0.0000	95	0.0000	58
290	koreaid-001	0.0000	199	0.0023	441	0.0371	326	0.0000	237	0.0005	407

Table 40: FTE is the proportion of failed template generation attempts. Failures can occur because the software throws an exception, or because the software electively refuses to process the input image. This would typically occur if a face is not detected. FTE is measured as the number of function calls that give EITHER a non-zero error code OR that give a "small" template. This is defined as one whose size is less than 0.3 times the median template size for that algorithm. This second rule is needed because some algorithms incorrectly fail to return a non-zero error code when template generation fails.
A hyphen "-" indicates the dataset was not produced. [1]*The effects of FTE are included in the accuracy results of this report by regarding any template comparison involving a failed template to produce a low similarity score. Thus higher FTE results in higher FNMR and lower FMR.*

FNMR(T) "False non-match rate"
FMR(T) "False match rate"

	Algorithm	Failure to Enrol Rate[1]									
	Name	APPLICATION		BORDER		KIOSK		MUGSHOT		VISA	
	Name	SEC. 2.2		SEC. 2.4		SEC. 2.6		SEC. 2.5		SEC. 2.1	
291	krungthai-002	0.0000	282	0.0005	197	0.0111	138	0.0002	382	0.0003	216
292	kuke3d-001	0.0000	11	0.0000	87	0.0000	8	0.0000	11	0.0000	101
293	kuke3d-002	0.0000	208	0.0000	32	0.0000	65	0.0000	131	0.0000	26
294	lebentech-000	0.0042	548	0.0029	460	0.0252	271	0.0051	554	0.0066	541
295	lebentech-001	0.0000	493	0.0012	374	0.0317	295	0.0004	442	0.0005	429
296	lemalabs-001	0.0000	72	0.0005	207	0.0141	156	0.0002	375	0.0004	240
297	lineclova-002	0.0000	220	0.0007	238	0.0181	195	0.0000	126	0.0000	32
298	lineclova-003	0.0000	457	0.0023	437	0.0700	377	0.0002	401	0.0005	412
299	lookman-002	0.0000	146	0.0000	26	-	496	0.0000	73	0.0000	49
300	lookman-004	0.0000	55	0.0000	81	-	444	0.0000	26	0.0000	123
301	luxand-000	0.0000	128	0.0000	17	-	488	0.0000	82	0.0000	43
302	luxand-001	0.0000	425	0.0016	405	0.0366	323	0.0006	470	0.0005	430
303	mantra-000	0.0001	497	0.0041	485	0.0680	371	0.0003	416	0.0004	399
304	maxvision-005	0.0000	266	0.0009	297	0.0229	253	0.0002	351	0.0004	307
305	maxvision-006	0.0000	313	0.0007	262	0.0226	246	0.0002	360	0.0004	304
306	megvii-008	0.0000	237	0.0010	331	0.0206	220	0.0002	389	0.0004	370
307	megvii-009	0.0000	330	0.0010	329	0.0206	221	0.0002	390	0.0004	365
308	meituan-003	0.0000	275	0.0013	384	0.0251	268	0.0001	306	0.0004	341
309	meituan-004	0.0000	359	0.0013	383	0.0251	269	0.0001	307	0.0004	333
310	meiya-001	0.0000	475	0.0028	454	-	528	0.0004	443	0.0010	489
311	mendaxiatech-000	0.0000	280	0.0010	332	0.0206	219	0.0002	392	0.0004	366
312	metsakuurcompany-002	0.0000	116	0.0000	22	0.0000	34	0.0000	84	0.0000	38
313	metsakuurcompany-003	0.0000	163	0.0000	14	0.0000	46	0.0000	91	0.0000	60
314	miaxis-002	0.0448	565	0.1162	563	0.2565	403	0.2128	563	0.0347	549
315	miaxis-003	0.0000	236	0.0013	380	0.0262	279	0.0001	337	0.0003	169
316	microfocus-002	0.0001	515	0.0053	502	-	461	0.0008	489	0.0016	519
317	microfocus-003	0.0001	509	0.0049	498	0.0819	385	0.0007	483	0.0015	518
318	minivision-000	0.0000	83	0.0000	117	-	464	0.0000	42	0.0000	78
319	mitek-000	0.0000	427	0.0029	457	0.0521	349	0.0002	379	0.0003	181
320	mobai-000	0.0000	438	0.0114	524	-	562	0.0003	419	0.0012	511
321	mobai-001	0.0000	376	0.0040	479	-	435	0.0001	314	0.0012	510
322	mobbl-001	0.0000	470	0.0052	501	0.0678	369	0.0002	359	0.0005	432
323	mobbl-003	0.0000	480	0.0029	459	0.0633	361	0.0002	385	0.0009	483
324	mobipintech-000	0.0000	182	0.0000	49	0.0000	54	0.0000	113	0.0000	7
325	momovn-001	0.0015	544	0.0010	326	0.0103	128	0.0011	506	0.0008	477
326	moredian-000	0.0000	274	0.0009	300	-	469	0.0004	437	0.0005	413
327	mukh-003	0.0000	235	0.0003	144	0.0060	93	0.0001	345	0.0003	206
328	mukh-004	0.0000	308	0.0013	386	0.0327	302	0.0000	232	0.0004	218
329	multimodality-000	0.0000	147	0.0000	4	0.0000	43	0.0000	99	0.0000	55
330	multimodality-001	0.0000	194	0.0009	296	0.0259	277	0.0000	100	0.0000	12
331	mvision-001	0.0000	132	0.0000	20	-	487	0.0000	79	0.0000	40
332	nazhiai-000	0.0000	25	0.0000	95	-	422	0.0000	3	0.0000	108
333	ncssg-001	0.0000	227	0.0000	42	0.0000	69	0.0000	120	0.0000	34
334	neosystems-004	0.0000	58	0.0000	79	0.0000	15	0.0000	29	0.0000	125
335	netbridgetech-001	0.0000	175	0.0000	53	-	535	0.0000	111	0.0000	2
336	netbridgetech-002	0.0000	82	0.0000	121	-	455	0.0000	48	0.0000	73
337	neurotechnology-017	0.0000	78	0.0003	163	0.0065	98	0.0000	47	0.0000	132
338	neurotechnology-018	0.0000	368	0.0003	165	0.0074	106	0.0000	188	0.0004	222
339	nhn-004	0.0000	416	0.0000	5	0.0000	41	0.0001	344	0.0004	347
340	nhn-005	0.0000	335	0.0000	13	0.0000	44	0.0000	213	0.0004	252
341	nodeflux-002	0.0000	349	0.0261	537	-	532	0.0008	487	0.0005	425
342	nominder-002	0.0000	298	0.0006	220	0.0119	140	0.0002	383	0.0003	205
343	nominder-003	0.0000	253	0.0005	199	0.0095	125	0.0002	361	-	568
344	notiontag-001	0.0000	46	0.0000	67	-	437	0.0027	538	0.0000	118
345	notiontag-002	0.0000	224	0.0000	47	0.0000	66	0.0000	122	0.0000	28
346	nsensecorp-004	0.0406	564	0.0035	471	0.0181	194	0.0016	518	0.0760	550
347	nsensecorp-005	0.0000	174	0.0000	56	0.0000	52	0.0000	118	0.0000	1
348	ntechlab-011	0.0000	49	0.0003	141	0.0057	89	0.0000	228	0.0004	221

Table 41: FTE is the proportion of failed template generation attempts. Failures can occur because the software throws an exception, or because the software electively refuses to process the input image. This would typically occur if a face is not detected. FTE is measured as the number of function calls that give EITHER a non-zero error code OR that give a "small" template. This is defined as one whose size is less than 0.3 times the median template size for that algorithm. This second rule is needed because some algorithms incorrectly fail to return a non-zero error code when template generation fails.
A hyphen "-" indicates the dataset was not produced. [1]*The effects of FTE are included in the accuracy results of this report by regarding any template comparison involving a failed template to produce a low similarity score. Thus higher FTE results in higher FNMR and lower FMR.*

FNMR(T) "False non-match rate"
FMR(T) "False match rate"

	Algorithm	Failure to Enrol Rate[1]									
	Name	APPLICATION		BORDER		KIOSK		MUGSHOT		VISA	
	Name	SEC. 2.2		SEC. 2.4		SEC. 2.6		SEC. 2.5		SEC. 2.1	
349	ntechlab-012	0.0000	27	0.0003	142	0.0057	88	0.0000	227	0.0004	220
350	omface-000	0.0000	87	0.0000	119	0.0000	22	0.0000	41	0.0000	76
351	omface-001	0.0000	74	0.0000	126	0.0000	73	0.0000	52	0.0000	70
352	omnigarde-002	0.0000	350	0.0008	264	0.0213	234	0.0000	190	0.0004	323
353	omnigarde-003	0.0000	28	0.0007	261	0.0212	233	0.0000	142	0.0004	273
354	onfido-000	0.0000	476	0.0040	478	0.0804	384	0.0004	427	0.0012	504
355	openedge-000	0.0000	322	0.0014	391	0.0212	232	0.0003	415	0.0004	356
356	openface-001	0.0000	440	0.0104	523	0.0668	364	0.0004	432	0.0006	466
357	oz-003	0.0000	225	0.0002	137	0.0042	83	0.0000	151	0.0003	150
358	oz-004	0.0000	453	0.0003	150	0.0041	82	0.0000	154	0.0002	140
359	palit-000	0.0000	248	0.0005	201	0.0134	154	0.0002	368	0.0004	275
360	palit-001	0.0000	369	0.0007	263	0.0201	215	0.0002	369	0.0004	261
361	pangiam-001	0.0000	189	0.0005	205	0.0128	148	0.0002	406	0.0003	210
362	pangiam-002	0.0000	59	0.0003	160	0.0072	102	0.0000	182	0.0003	183
363	papago-001	0.0000	389	0.0008	271	0.0159	178	0.0002	405	0.0004	295
364	papil11-000	0.0000	347	0.0008	293	0.0192	210	0.0000	206	0.0003	209
365	papsav1923-002	0.0000	357	0.0018	415	0.0268	282	0.0000	218	0.0004	332
366	papsav1923-003	0.0000	418	0.0019	421	0.0321	299	0.0000	243	0.0004	306
367	paravision-011	0.0000	121	0.0010	333	0.0201	214	0.0001	284	0.0004	223
368	paravision-013	0.0000	64	0.0010	335	0.0201	213	0.0001	283	0.0004	231
369	pensees-001	0.0000	231	0.0000	89	-	415	0.0000	19	0.0000	99
370	pixelall-009	0.0000	215	0.0000	46	0.0000	68	0.0000	124	0.0000	29
371	pixelall-010	0.0000	141	0.0000	24	0.0000	39	0.0000	75	0.0000	51
372	privid-001	0.0001	518	0.0176	532	0.0598	358	0.0021	528	0.0021	526
373	privid-002	0.0198	560	0.0040	480	0.0386	332	0.0014	513	0.0011	496
374	psl-011	0.0000	306	0.0003	143	0.0063	96	0.0000	139	0.0003	195
375	psl-012	0.0000	289	0.0003	148	0.0067	99	0.0000	138	0.0003	199
376	ptakuratsatu-000	0.0000	252	0.0007	258	-	442	0.0001	250	0.0003	177
377	pxl-001	0.0000	495	0.0044	489	-	411	0.0005	457	0.0022	529
378	pyramid-000	0.0001	511	0.0041	484	-	453	0.0005	455	0.0007	474
379	qazbs-000	0.0000	109	0.0009	307	0.0265	281	0.0000	175	0.0004	292
380	qazsmartvisionai-000	0.0000	364	0.0003	164	0.0083	117	0.0000	153	0.0003	180
381	qluevision-001	0.0000	423	0.0008	277	0.0153	166	0.0008	486	0.0004	403
382	qnap-004	0.0000	206	0.0016	401	0.0402	337	0.0000	240	0.0001	137
383	qnap-005	0.0001	502	0.0078	513	0.0581	355	0.0010	502	0.0005	445
384	quantasoft-003	0.0000	434	0.0015	399	0.0355	319	0.0005	453	0.0006	460
385	rankone-015	0.0000	39	0.0000	75	0.0000	11	0.0000	35	0.0000	109
386	realnetworks-007	0.0000	255	0.0013	388	0.0425	341	0.0000	143	0.0004	311
387	realnetworks-008	0.0000	264	0.0002	139	0.0045	84	0.0000	136	0.0002	149
388	rebs-000	0.0000	10	0.0005	188	0.0130	150	0.0000	180	0.0004	256
389	rebs-001	0.0000	156	0.0005	196	0.0144	159	0.0000	201	0.0004	297
390	recognito-000	0.0000	374	0.0003	145	0.0056	87	0.0000	212	0.0003	194
391	recognito-001	0.0000	345	0.0003	146	0.0056	86	0.0000	211	0.0003	193
392	regula-000	0.0000	1	0.0000	91	0.0000	4	0.0000	20	0.0000	98
393	regula-001	0.0000	22	0.0000	99	0.0000	9	0.0000	4	0.0000	104
394	remarkai-001	0.0000	192	0.0000	58	-	547	0.0000	106	0.0000	16
395	remarkai-003	0.0000	324	0.0007	246	0.0187	200	0.0000	222	0.0004	250
396	rendip-000	0.0000	414	0.0016	404	0.0293	287	0.0002	365	0.0004	400
397	revealmedia-005	0.0000	421	0.0007	253	0.0189	203	0.0009	496	0.0004	404
398	revealmedia-006	0.0000	61	0.0009	316	0.0238	260	0.0001	309	0.0004	361
399	roc-016	0.0000	16	0.0000	132	0.0006	77	0.0000	9	0.0000	133
400	rokid-000	0.0000	9	0.0072	509	-	409	0.0001	290	0.0005	423
401	rokid-001	0.0000	190	0.0013	382	-	548	0.0000	104	0.0000	15
402	s1-005	0.0000	79	0.0004	176	0.0120	143	0.0001	262	0.0002	142
403	s1-007	0.0000	171	0.0006	218	0.0110	137	0.0001	266	0.0002	141
404	saffe-001	0.0000	176	0.0000	54	-	536	0.0000	112	0.0000	3
405	saffe-002	0.0000	77	0.0000	120	-	456	0.0000	50	0.0000	74
406	samsungsds-001	0.0000	4	0.0005	203	0.0146	160	0.0001	282	0.0003	207

Table 42: FTE is the proportion of failed template generation attempts. Failures can occur because the software throws an exception, or because the software electively refuses to process the input image. This would typically occur if a face is not detected. FTE is measured as the number of function calls that give EITHER a non-zero error code OR that give a "small" template. This is defined as one whose size is less than 0.3 times the median template size for that algorithm. This second rule is needed because some algorithms incorrectly fail to return a non-zero error code when template generation fails.
A hyphen "-" indicates the dataset was not produced. [1]*The effects of FTE are included in the accuracy results of this report by regarding any template comparison involving a failed template to produce a low similarity score. Thus higher FTE results in higher FNMR and lower FMR.*

FNMR(T) "False non-match rate"
FMR(T) "False match rate"

	Algorithm	Failure to Enrol Rate[1]									
	Name	APPLICATION		BORDER		KIOSK		MUGSHOT		VISA	
	Name	SEC. 2.2		SEC. 2.4		SEC. 2.6		SEC. 2.5		SEC. 2.1	
407	samsungsds-002	0.0000	173	0.0004	178	0.0119	141	0.0001	288	0.0003	189
408	samtech-001	0.0001	508	0.0032	462	-	565	0.0004	439	0.0008	476
409	samtech-002	0.0000	447	0.0018	413	0.0516	346	0.0002	402	0.0005	435
410	scanovate-002	0.0000	394	0.0018	411	-	525	0.0000	247	0.0004	395
411	scanovate-003	0.0000	385	0.0233	535	0.3371	408	0.0006	469	0.0004	402
412	sdc-000	0.0000	487	0.0035	470	0.0678	370	0.0005	462	0.0011	499
413	seamfix-001	0.0000	12	0.0000	85	0.0000	7	0.0000	10	-	563
414	securifai-007	0.0000	112	0.0000	108	0.0000	30	0.0000	58	0.0000	88
415	securifai-008	0.0000	17	0.0000	88	0.0000	5	0.0000	8	-	562
416	sensetime-007	0.0000	217	0.0004	173	0.0106	129	0.0000	194	0.0003	173
417	sensetime-008	0.0000	117	0.0007	257	0.0250	266	0.0000	140	0.0003	214
418	serendipity-000	0.0000	271	0.0008	273	0.0202	216	0.0001	343	0.0004	318
419	sertis-002	0.0000	106	0.0007	243	0.0152	163	0.0000	242	0.0004	283
420	sertis-003	0.0000	367	0.0008	283	0.0183	196	0.0000	207	0.0004	314
421	seventhsense-003	0.0000	344	0.0003	158	0.0083	118	0.0000	174	0.0002	146
422	seventhsense-005	0.0000	341	0.0002	140	0.0065	97	0.0000	177	0.0003	160
423	shaman-000	0.0000	52	0.0000	69	-	436	0.0000	31	0.0000	116
424	shaman-001	0.0000	67	0.0000	76	-	446	0.0000	23	0.0000	129
425	shu-002	0.0000	384	0.0010	342	-	468	0.0005	447	0.0004	384
426	shu-003	0.0000	219	0.0007	241	-	560	0.0001	257	0.0003	170
427	siat-002	0.0000	365	0.0012	369	-	549	0.0000	214	0.0004	301
428	siat-005	0.0000	103	0.0000	111	0.0000	71	0.0000	63	0.0000	85
429	sjtu-004	0.0000	86	0.0000	116	0.0000	23	0.0000	44	0.0003	161
430	sjtu-005	0.0000	492	0.0000	113	0.0000	19	0.0000	56	0.0006	456
431	sktelecom-000	0.0000	348	0.0008	284	0.0190	205	0.0000	234	0.0004	331
432	smartbiometrik-001	0.0005	531	0.0649	556	0.2147	402	0.0017	520	0.0008	480
433	smartengines-000	0.0066	553	0.0150	529	0.1656	396	0.0022	529	0.0013	513
434	smartengines-001	0.0003	528	0.0073	510	0.0714	378	0.0007	480	0.0005	428
435	smartvist-000	0.0000	118	0.0026	448	0.0357	320	0.0002	349	0.0011	498
436	smartvist-001	0.0000	332	0.0005	190	0.0069	101	0.0001	330	0.0003	187
437	smilart-002	0.0000	485	0.0036	474	-	451	-	565	0.0011	497
438	smilart-003	0.0003	526	0.0100	522	-	465	0.0014	511	0.0013	515
439	sodec-000	0.0000	19	0.0000	98	0.0000	10	0.0000	7	0.0000	107
440	sparsh-001	0.0000	66	0.0007	237	0.0168	182	0.0000	155	0.0004	259
441	sqisoft-002	0.0000	123	0.0003	154	0.0078	110	0.0000	172	0.0003	213
442	sqisoft-003	0.0000	154	0.0003	159	0.0078	111	0.0000	173	0.0003	182
443	staqu-000	0.0000	207	0.0000	33	-	557	0.0000	132	0.0000	27
444	starhybrid-001	0.0001	514	0.0033	468	-	462	0.0009	495	0.0023	530
445	stcon-002	0.0000	325	0.0011	351	0.0226	248	0.0000	186	0.0003	165
446	stcon-003	0.0000	124	0.0005	193	0.0142	158	0.0000	184	0.0004	248
447	stengg-000	0.0000	168	0.0013	385	0.0350	317	0.0000	199	0.0004	316
448	sukshi-000	0.0000	198	0.0000	61	0.0000	57	0.0000	103	0.0000	14
449	suprema-004	0.0000	303	0.0014	392	0.0299	289	0.0000	168	0.0004	276
450	suprema-005	0.0000	387	0.0014	393	0.0299	288	0.0005	452	0.0004	350
451	supremaid-001	0.0000	307	0.0020	424	0.0330	306	0.0001	302	0.0004	394
452	supremaid-002	0.0000	261	0.0020	426	0.0330	305	0.0001	300	0.0004	396
453	surrey-cvssp-002	0.0000	459	0.0006	224	0.0156	170	0.0001	278	0.0004	296
454	surrey-cvssp-003	0.0000	197	0.0009	302	0.0165	180	0.0000	102	0.0001	138
455	swsam-001	0.0000	88	0.0012	376	0.0263	280	0.0000	68	0.0000	81
456	synesis-006	0.0000	92	0.0003	162	-	466	0.0000	229	0.0003	156
457	synesis-007	0.0000	329	0.0013	381	-	512	0.0002	388	0.0004	305
458	synology-000	0.0000	184	0.0000	64	-	542	0.0000	110	0.0000	11
459	synology-002	0.0000	221	0.0000	44	-	561	0.0000	127	0.0000	33
460	sztu-000	0.0000	54	0.0000	80	-	443	0.0000	27	0.0000	124
461	sztu-001	0.0000	139	0.0000	25	0.0000	40	0.0000	74	0.0000	50
462	t4isb-000	0.0000	122	0.0000	23	0.0000	33	0.0000	83	0.0000	36
463	tech5-007	0.0000	287	0.0014	395	0.0305	293	0.0000	176	0.0004	270
464	tech5-008	0.0000	203	0.0007	236	0.0168	183	0.0000	164	0.0004	245

Table 43: FTE is the proportion of failed template generation attempts. Failures can occur because the software throws an exception, or because the software electively refuses to process the input image. This would typically occur if a face is not detected. FTE is measured as the number of function calls that give EITHER a non-zero error code OR that give a "small" template. This is defined as one whose size is less than 0.3 times the median template size for that algorithm. This second rule is needed because some algorithms incorrectly fail to return a non-zero error code when template generation fails.
A hyphen "-" indicates the dataset was not produced. [1]*The effects of FTE are included in the accuracy results of this report by regarding any template comparison involving a failed template to produce a low similarity score. Thus higher FTE results in higher FNMR and lower FMR.*

FNMR(T) "False non-match rate"
FMR(T) "False match rate"

	Algorithm	Failure to Enrol Rate[1]									
	Name	APPLICATION		BORDER		KIOSK		MUGSHOT		VISA	
	Name	SEC. 2.2		SEC. 2.4		SEC. 2.6		SEC. 2.5		SEC. 2.1	
465	techainer-001	0.0000	474	0.0004	184	0.0085	120	0.0005	451	0.0004	348
466	techsign-000	0.0007	538	0.0334	543	0.2093	397	0.0020	525	0.0011	494
467	techsign-001	0.0000	278	0.0008	295	0.0253	272	0.0002	370	0.0004	319
468	tevian-007	0.0000	291	0.0015	400	0.0429	342	0.0002	381	0.0004	342
469	tevian-008	0.0000	331	0.0006	216	0.0109	135	0.0000	185	0.0003	172
470	tiger-005	0.0000	245	0.0009	318	0.0194	211	0.0001	277	0.0004	293
471	tiger-006	0.0000	378	0.0011	356	0.0396	335	0.0001	331	0.0004	405
472	tinkoff-001	0.0000	399	0.0008	282	0.0171	188	0.0001	323	0.0004	285
473	tnitech-000	0.0000	366	0.0003	157	0.0060	91	0.0005	465	0.0003	167
474	tongyi-005	0.0000	188	0.0000	65	-	540	0.0000	108	0.0000	9
475	toppanidgate-000	0.0000	242	0.0008	276	0.0232	255	0.0004	426	0.0004	329
476	toshiba-007	0.0000	400	0.0005	194	0.0082	116	0.0002	398	0.0004	312
477	toshiba-008	0.0000	377	0.0005	195	0.0082	115	0.0002	397	0.0004	322
478	touchlessid-002	0.0000	7	0.0043	487	0.1087	389	0.0000	14	0.0000	96
479	touchlessid-003	0.0000	232	0.0010	338	0.0287	285	0.0002	350	0.0004	390
480	trueface-002	0.0000	401	0.0046	495	-	541	0.0003	408	0.0005	439
481	trueface-003	0.0000	390	0.0046	494	0.0397	336	0.0003	407	0.0005	440
482	trueidvng-001	0.0000	380	0.0020	430	0.0385	331	0.0002	374	0.0005	422
483	truststamp-001	0.0000	268	0.0010	336	0.0189	204	0.0000	171	0.0003	191
484	tuputech-000	0.0003	529	0.0116	525	-	520	-	566	0.0081	543
485	turingtechvip-001	0.0001	504	0.0007	256	0.0061	95	0.0007	478	0.0006	453
486	turingtechvip-002	0.0001	505	0.0017	409	0.0097	126	0.0007	479	0.0006	452
487	turkcell-000	0.0110	558	0.0234	536	0.0350	318	0.0103	557	0.0306	548
488	turkcell-001	0.0000	38	0.0002	138	0.0034	81	0.0001	289	0.0003	152
489	twface-000	0.0000	69	0.0000	78	0.0000	16	0.0000	21	0.0000	127
490	twface-001	0.0000	47	0.0000	66	0.0000	14	0.0000	34	0.0000	119
491	ulsee-001	0.0000	114	0.0000	106	-	479	0.0000	59	0.0000	90
492	ultinous-000	-	568	-	567	-	538	-	567	0.0003	179
493	ultinous-001	-	567	-	565	-	527	-	568	0.0003	178
494	uluface-002	0.0000	181	0.0000	50	-	531	0.0000	114	0.0000	8
495	uluface-003	0.0000	202	0.0001	135	-	551	0.0002	352	0.0002	144
496	unicc-002	0.0316	563	0.0082	515	0.0188	201	0.0226	561	0.0936	552
497	unicc-003	0.0007	540	0.0022	434	0.0094	124	0.0026	537	0.0029	536
498	unissey-003	0.0000	157	0.0008	265	0.0191	206	0.0001	285	0.0004	265
499	unissey-004	0.0000	63	0.0009	308	0.0240	261	0.0001	311	0.0004	310
500	upc-001	0.0000	451	0.0003	152	-	523	0.0003	410	0.0003	197
501	useb-001	0.0000	338	0.0009	311	0.0228	252	0.0001	333	0.0004	266
502	useb-002	0.0000	337	0.0009	312	0.0228	251	0.0001	334	0.0004	267
503	uxlabs-001	0.0000	210	0.0000	36	0.0000	63	0.0000	128	0.0000	23
504	uxlabs-003	0.0000	145	0.0000	27	0.0000	37	0.0000	71	0.0000	47
505	vcog-002	-	566	-	568	-	428	-	564	0.0019	524
506	vcortex-001	0.0000	463	0.2295	564	0.0802	383	0.0017	519	0.0006	451
507	vd-002	0.0000	216	0.0000	45	1.0000	563	0.0000	123	0.0000	30
508	vd-003	0.0001	506	0.0041	481	0.0676	367	0.0030	541	0.0029	537
509	veridas-008	0.0000	445	0.0026	446	0.0595	356	0.0001	317	0.0005	418
510	veridas-009	0.0000	446	0.0026	447	0.0597	357	0.0001	286	0.0005	420
511	veridium-002	0.0000	494	0.0083	517	0.1591	394	0.0010	499	0.0005	437
512	veridium-003	0.0001	500	0.0087	518	0.1615	395	0.0014	514	-	558
513	verigram-001	0.0000	393	0.0003	153	0.0060	90	0.0002	387	0.0003	203
514	verigram-003	0.0000	486	0.0025	444	0.0288	286	0.0009	498	0.0008	478
515	verihubs-inteligensia-001	0.0000	285	0.0029	456	0.0669	366	0.0001	263	0.0004	357
516	verihubs-inteligensia-002	0.0000	230	0.0029	455	0.0669	365	0.0001	260	0.0004	359
517	verijelas-000	0.0000	254	0.0023	438	0.0375	327	0.0004	444	0.0006	459
518	via-004	0.0000	129	0.0000	21	0.0000	35	0.0000	78	0.0000	39
519	via-005	0.0000	144	0.0000	28	0.0000	38	0.0000	70	0.0000	48
520	viante-000	0.0000	379	0.0008	285	0.0168	185	0.0001	310	0.0004	401
521	videmo-001	0.0000	431	0.0170	531	0.0332	308	0.0010	504	0.0011	501
522	videmo-002	0.0000	99	0.0006	230	0.0189	202	0.0001	296	0.0004	254

Table 44: FTE is the proportion of failed template generation attempts. Failures can occur because the software throws an exception, or because the software electively refuses to process the input image. This would typically occur if a face is not detected. FTE is measured as the number of function calls that give EITHER a non-zero error code OR that give a "small" template. This is defined as one whose size is less than 0.3 times the median template size for that algorithm. This second rule is needed because some algorithms incorrectly fail to return a non-zero error code when template generation fails.
A hyphen "-" indicates the dataset was not produced. [1]*The effects of FTE are included in the accuracy results of this report by regarding any template comparison involving a failed template to produce a low similarity score. Thus higher FTE results in higher FNMR and lower FMR.*

FNMR(T) "False non-match rate"
FMR(T) "False match rate"

	Algorithm	Failure to Enrol Rate[1]							
	Name	APPLICATION		BORDER		KIOSK		MUGSHOT		VISA	
	Name	SEC. 2.2		SEC. 2.4		SEC. 2.6		SEC. 2.5		SEC. 2.1	
523	videonetics-001	0.0004	530	0.0309	541	-	529	0.0015	517	0.0010	487
524	videonetics-002	0.0000	415	0.0459	553	-	505	0.0006	472	0.0005	443
525	viettelhightech-000	0.0000	458	0.0019	420	0.0368	325	0.0007	481	0.0005	442
526	vigilantsolutions-010	0.0000	433	0.0028	451	0.0609	360	0.0001	272	0.0004	235
527	vigilantsolutions-011	0.0000	432	0.0028	452	0.0609	359	0.0001	270	0.0004	234
528	vinai-000	0.0000	101	0.0000	109	-	477	0.0000	64	0.0000	87
529	vinbigdata-002	0.0000	130	0.0015	398	0.0250	267	0.0000	210	0.0004	375
530	vinbigdata-003	0.0000	372	0.0007	242	0.0151	162	0.0000	249	0.0004	247
531	vion-000	0.0050	549	0.0392	550	-	410	0.0130	559	0.0078	542
532	visage-000	0.0000	460	0.0054	503	-	568	0.0009	494	0.0006	454
533	visionbox-003	0.0000	412	0.0010	328	0.0209	227	0.0001	299	0.0004	340
534	visionbox-004	0.0000	404	0.0013	377	0.0248	265	0.0001	327	0.0004	382
535	visionlabs-010	0.0000	424	0.0009	304	-	490	0.0001	328	0.0004	325
536	visionlabs-011	0.0000	56	0.0006	227	0.0156	171	0.0001	273	0.0004	258
537	visteam-007	0.0000	269	0.0008	280	0.0209	223	0.0000	156	0.0004	241
538	visteam-008	0.0000	326	0.0008	279	0.0209	224	0.0000	162	0.0004	237
539	vixvizion-006	0.0000	107	0.0000	104	0.0000	32	0.0000	60	0.0000	91
540	vixvizion-007	0.0000	70	0.0000	115	0.0000	20	0.0000	54	0.0000	67
541	vnis-000	0.0007	542	0.0695	560	0.0756	381	0.0038	547	0.0009	484
542	vnpay-000	0.0000	436	0.0657	559	0.0693	373	0.0037	546	0.0006	450
543	vnpt-005	0.0000	94	0.0006	212	0.0154	168	0.0002	371	0.0004	281
544	vnpt-006	0.0000	119	0.0006	211	0.0154	169	0.0002	372	0.0004	277
545	vocord-009	0.0000	272	0.0006	226	-	457	0.0001	341	0.0003	155
546	vocord-010	0.0000	383	0.0005	206	0.0141	157	0.0002	373	0.0003	204
547	vtcc-000	0.0000	104	0.0000	110	0.0000	28	0.0000	62	0.0000	86
548	vtcc-001	0.0000	402	0.0010	330	0.0161	179	0.0000	239	0.0004	244
549	vts-000	0.0000	408	0.0011	353	-	413	0.0001	342	0.0004	397
550	vts-001	0.0000	134	0.0003	149	0.0073	103	0.0000	167	0.0003	153
551	wicket-000	0.0000	334	0.0009	298	0.0260	278	0.0000	178	0.0004	288
552	winsense-001	0.0000	6	0.0000	94	-	414	0.0000	16	0.0000	95
553	winsense-002	0.0000	62	0.0000	83	-	441	0.0000	25	0.0000	121
554	wiseai-001	0.0001	498	0.0137	528	0.0768	382	0.0018	522	0.0018	521
555	wuhantianyu-001	0.0000	23	0.0007	244	0.0159	175	0.0001	254	0.0004	330
556	x-laboratory-000	0.0247	562	0.0000	48	-	537	0.0005	461	0.0002	145
557	x-laboratory-001	0.0000	355	0.0012	365	-	539	0.0001	321	0.0004	381
558	xforwardai-001	0.0000	319	0.0007	254	-	498	0.0003	414	0.0004	377
559	xforwardai-002	0.0000	262	0.0007	255	-	463	0.0003	413	0.0004	380
560	xm-000	0.0000	149	0.0007	240	-	509	0.0001	256	0.0003	171
561	yisheng-004	0.0002	524	-	566	-	546	0.0013	509	0.0006	463
562	yitu-003	0.0000	40	0.0000	74	-	426	0.0009	493	0.0000	110
563	yoonik-003	0.0000	392	0.0009	314	0.0214	236	0.0002	358	0.0004	346
564	yoonik-004	0.0000	93	0.0012	362	0.0251	270	0.0001	274	0.0004	253
565	yoti-001	0.0000	375	0.0014	396	0.0418	339	0.0008	491	0.0006	455
566	ytu-000	0.0000	352	0.0010	349	-	544	0.0002	393	0.0004	373
567	yuan-005	0.0000	229	0.0005	202	0.0134	153	0.0002	366	0.0004	272
568	yuan-008	0.0000	456	0.0013	379	0.0336	312	0.0004	430	0.0005	433

Table 45: FTE is the proportion of failed template generation attempts. Failures can occur because the software throws an exception, or because the software electively refuses to process the input image. This would typically occur if a face is not detected. FTE is measured as the number of function calls that give EITHER a non-zero error code OR that give a "small" template. This is defined as one whose size is less than 0.3 times the median template size for that algorithm. This second rule is needed because some algorithms incorrectly fail to return a non-zero error code when template generation fails.
A hyphen "-" indicates the dataset was not produced. [1]*The effects of FTE are included in the accuracy results of this report by regarding any template comparison involving a failed template to produce a low similarity score. Thus higher FTE results in higher FNMR and lower FMR.*

FNMR(T) "False non-match rate"
FMR(T) "False match rate"

3.4 Recognition accuracy

Core algorithm accuracy is stated via:

- ▷ **Cooperative subjects**
  - The summary table of Figure 35;
  - The visa image DETs of Figure 106;
  - The mugshot DETs of Figure 135;
  - The mugshot ageing profiles of Figure 368;
  - The human-difficult pairs of Figure 50
- ▷ **Non-cooperative subjects**
  - The photojournalism DET of Figure 152

Figure 286 shows dependence of false match rate on algorithm score threshold. This allows a deployer to set a threshold to target a particular false match rate appropriate to the security objectives of the application.

Figure 285 likewise shows FMR(T) but for mugshots, and specially four subsets of the population.

Note that in both the mugshot and visa sets false match rates vary with the ethnicity, age, and sex, of the enrollee and impostor. For example figure 181 summarizes FMR for impostors paired from four groups black females, black males, white females, white males.

FNMR(T) "False non-match rate"
FMR(T) "False match rate"

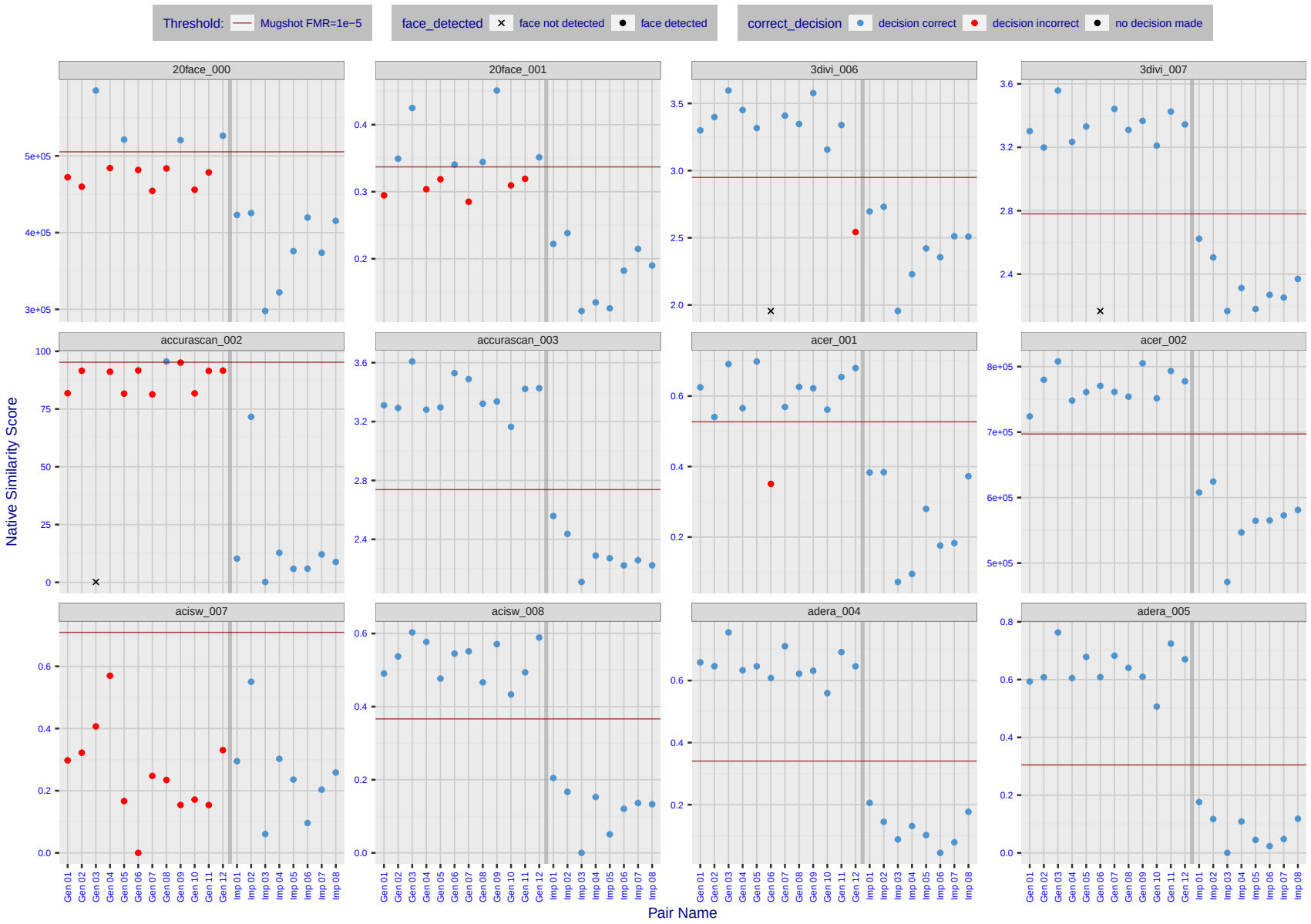

Figure 4: The figure shows algorithms' similarity scores for 12 genuine and 8 impostor image pairs used in a May 2018 paper by Phillips et al. ([1]). The threshold (red horizontal line) is a value calibrated to give FMR = 0.0001 on mugshot images. Points above the threshold correspond to pairs determined to be genuine, and points below the threshold correspond to pairs determined to be impostors. If the determined class (genuine or impostor) matches the real class, points will be blue; if not, red. An X represents face detection failure in either of the images in the pair. Note that the sample size (n=20) is small, and the figure may change substantially if larger or different sets are used. The images can be viewed on p. 13 of the Appendix, where Gen 01 corresponds to Same-Identity Pair 1, Gen 02 corresponds to Same-Identity Pair 2, and so on.

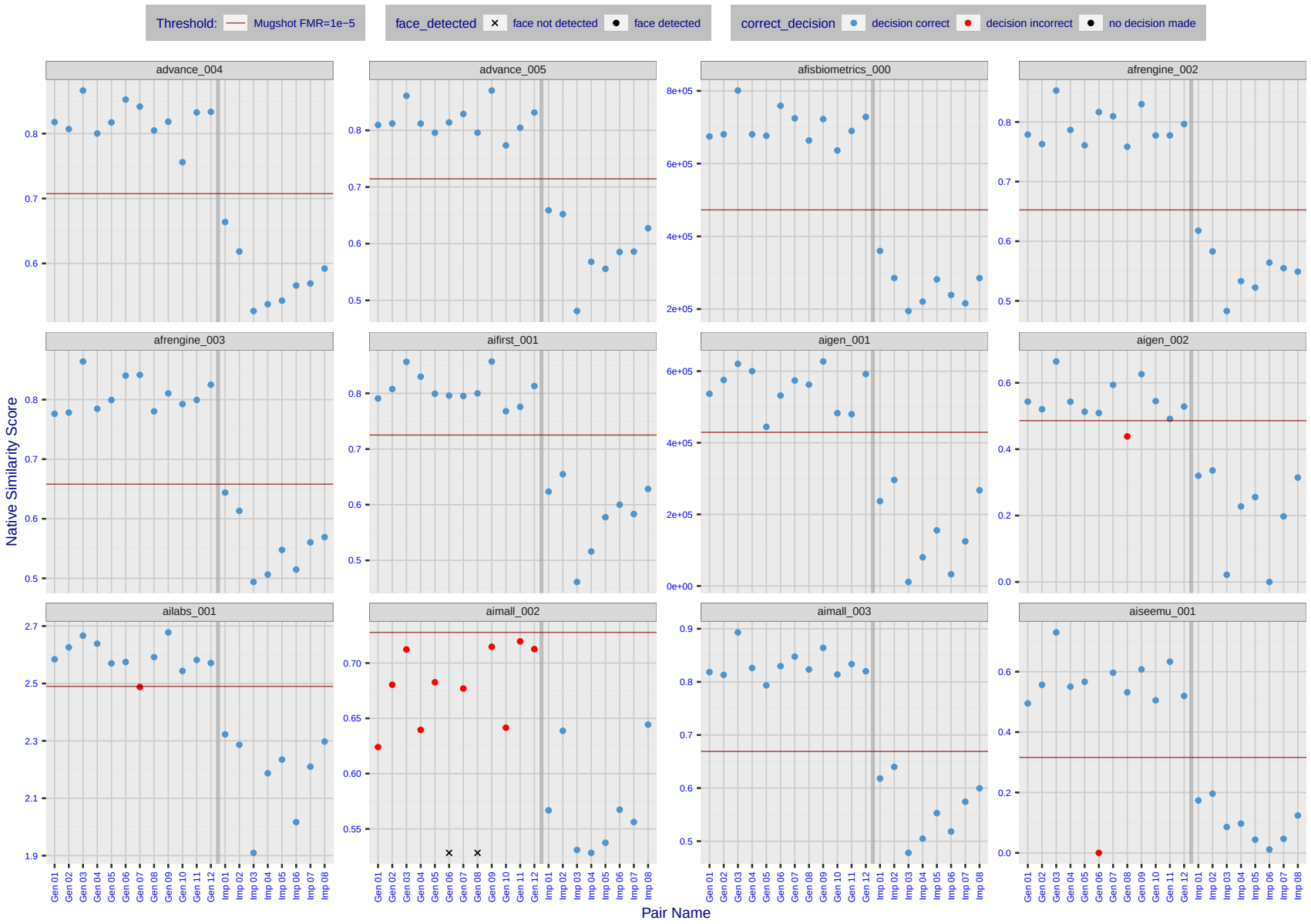

Figure 5: The figure shows algorithms' similarity scores for 12 genuine and 8 impostor image pairs used in a May 2018 paper by Phillips et al. ([1]). The threshold (red horizontal line) is a value calibrated to give FMR = 0.0001 on mugshot images. Points above the threshold correspond to pairs determined to be genuine, and points below the threshold correspond to pairs determined to be impostors. If the determined class (genuine or impostor) matches the real class, points will be blue; if not, red. An X represents face detection failure in either of the images in the pair. Note that the sample size (n=20) is small, and the figure may change substantially if larger or different sets are used. The images can be viewed on p. 13 of the Appendix, where Gen 01 corresponds to Same-Identity Pair 1, Gen 02 corresponds to Same-Identity Pair 2, and so on.

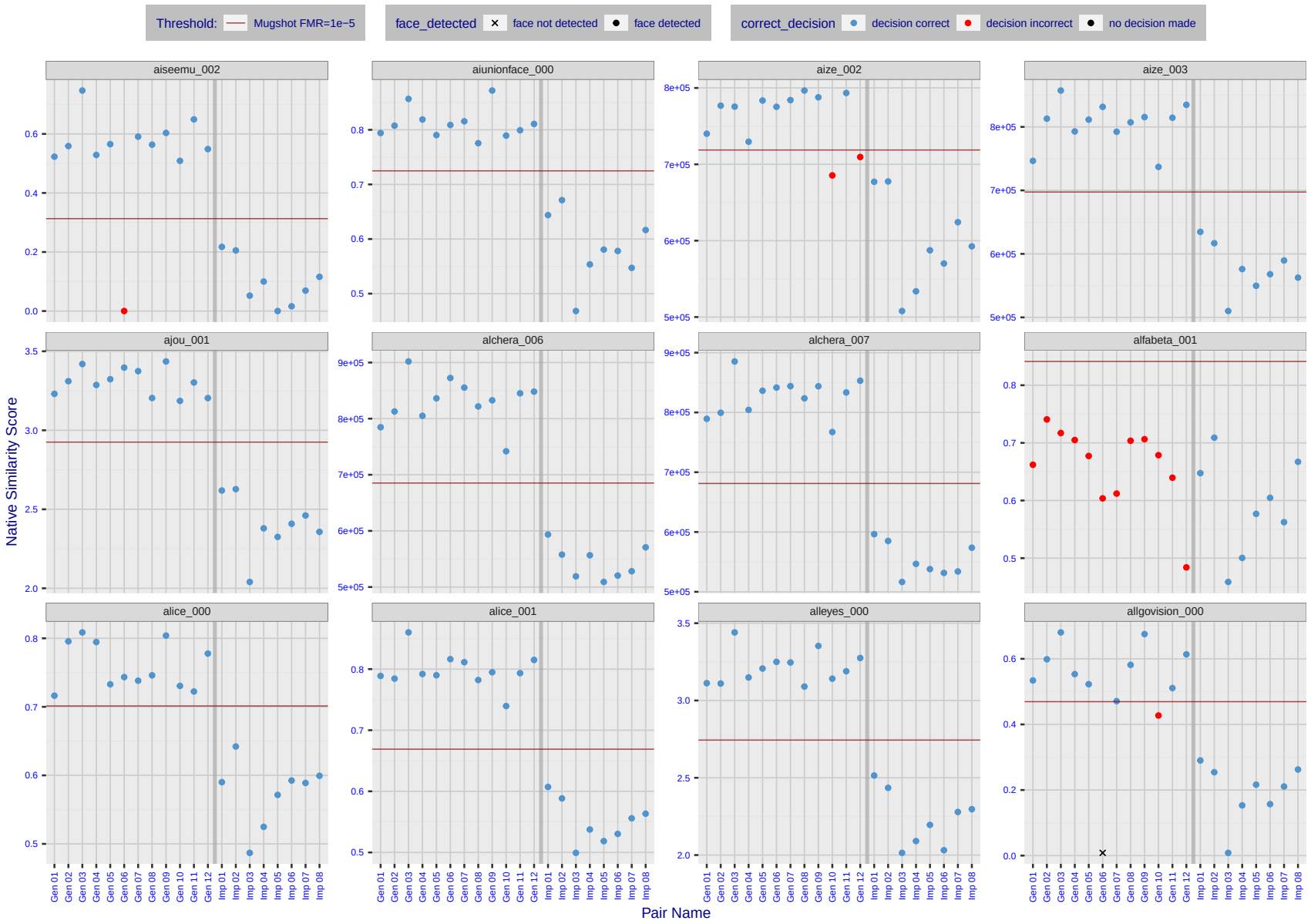

Figure 6: The figure shows algorithms' similarity scores for 12 genuine and 8 impostor image pairs used in a May 2018 paper by Phillips et al. ([1]). The threshold (red horizontal line) is a value calibrated to give FMR = 0.0001 on mugshot images. Points above the threshold correspond to pairs determined to be genuine, and points below the threshold correspond to pairs determined to be impostors. If the determined class (genuine or impostor) matches the real class, points will be blue; if not, red. An X represents face detection failure in either of the images in the pair. Note that the sample size (n=20) is small, and the figure may change substantially if larger or different sets are used. The images can be viewed on p. 13 of the Appendix, where Gen 01 corresponds to Same-Identity Pair 1, Gen 02 corresponds to Same-Identity Pair 2, and so on.

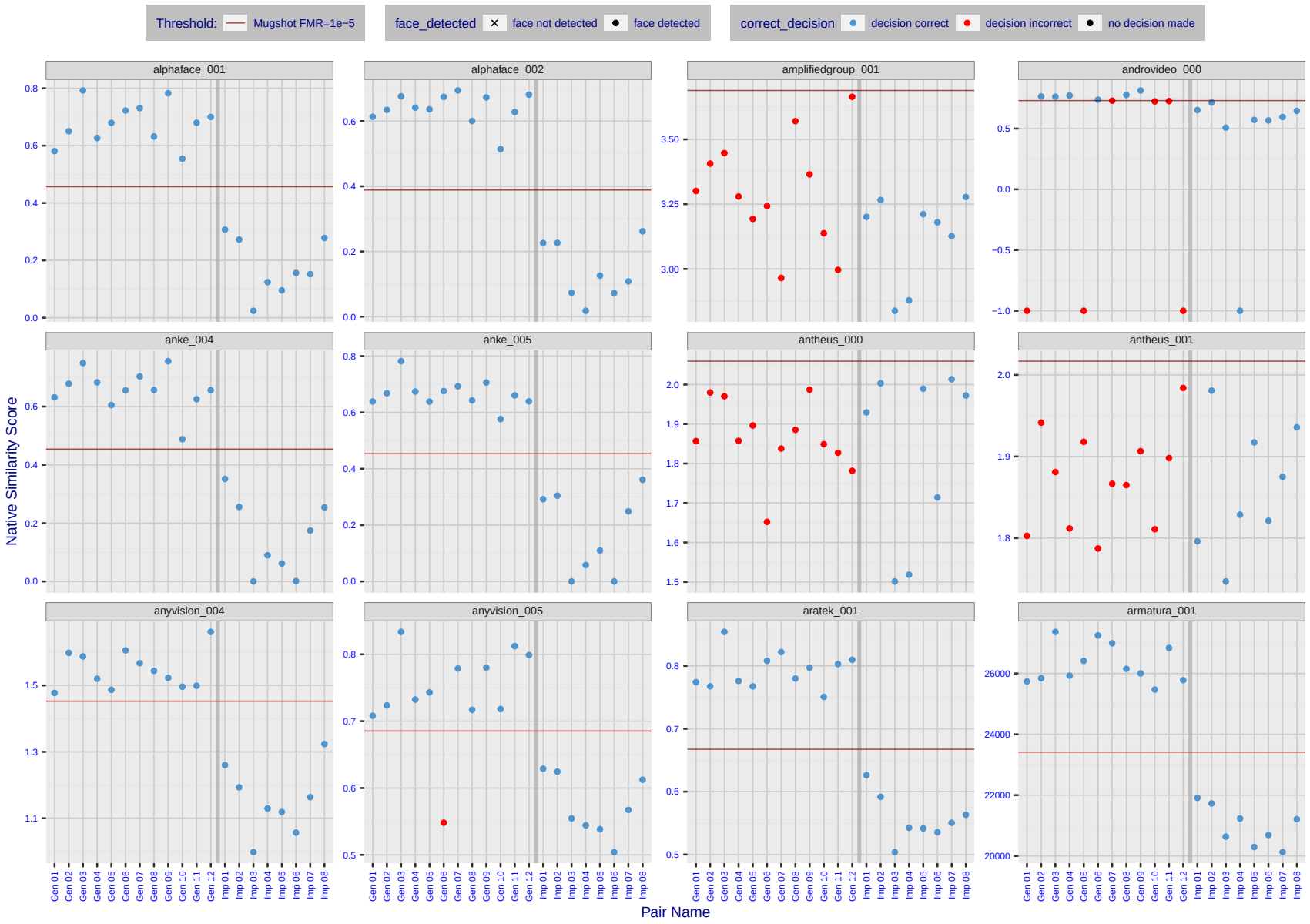

Figure 7: The figure shows algorithms' similarity scores for 12 genuine and 8 impostor image pairs used in a May 2018 paper by Phillips et al. ([1]). The threshold (red horizontal line) is a value calibrated to give FMR = 0.0001 on mugshot images. Points above the threshold correspond to pairs determined to be genuine, and points below the threshold correspond to pairs determined to be impostors. If the determined class (genuine or impostor) matches the real class, points will be blue; if not, red. An X represents face detection failure in either of the images in the pair. Note that the sample size (n=20) is small, and the figure may change substantially if larger or different sets are used. The images can be viewed on p. 13 of the Appendix, where Gen 01 corresponds to Same-Identity Pair 1, Gen 02 corresponds to Same-Identity Pair 2, and so on.

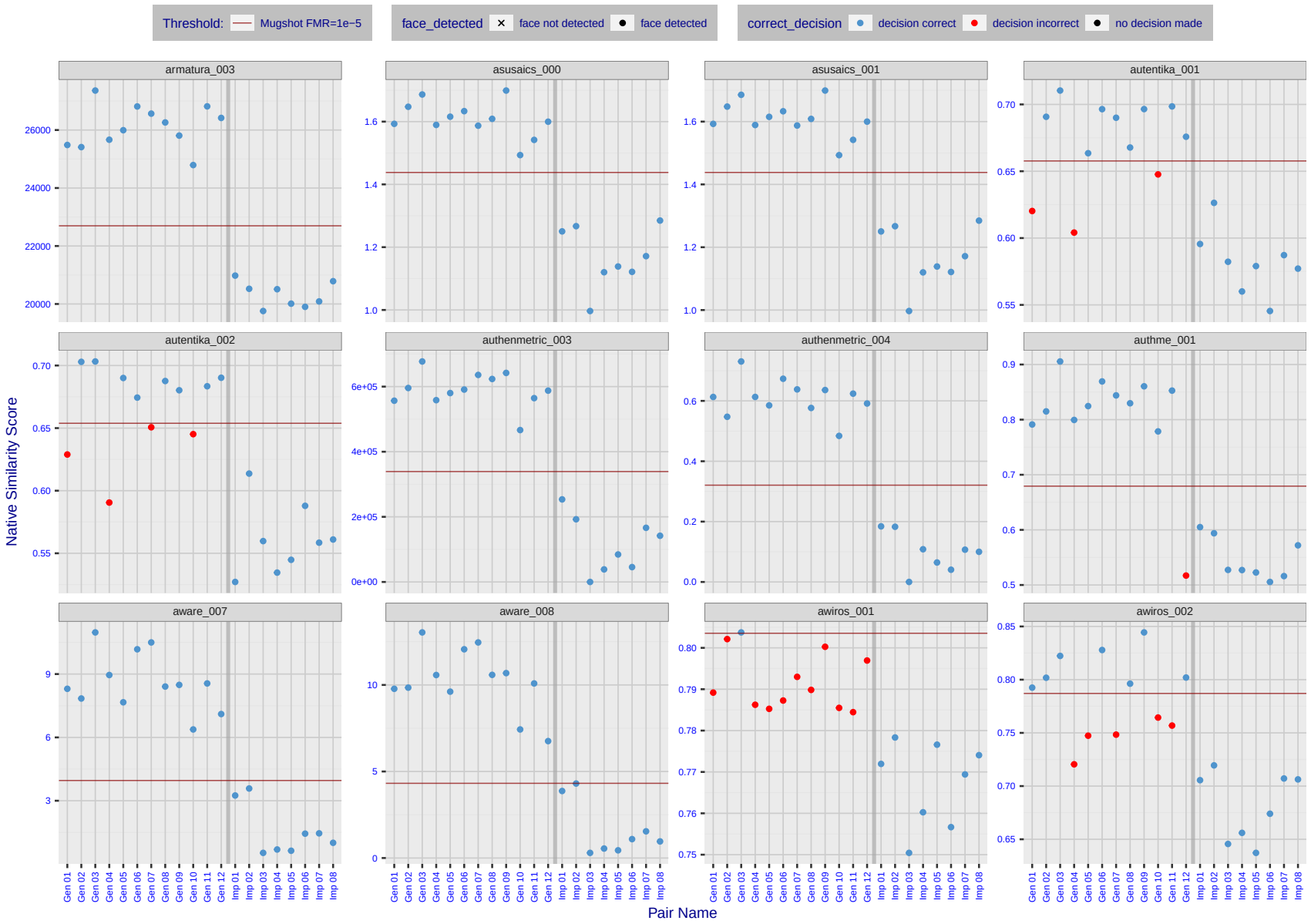

Figure 8: The figure shows algorithms' similarity scores for 12 genuine and 8 impostor image pairs used in a May 2018 paper by Phillips et al. ([1]). The threshold (red horizontal line) is a value calibrated to give FMR = 0.0001 on mugshot images. Points above the threshold correspond to pairs determined to be genuine, and points below the threshold correspond to pairs determined to be impostors. If the determined class (genuine or impostor) matches the real class, points will be blue; if not, red. An X represents face detection failure in either of the images in the pair. Note that the sample size (n=20) is small, and the figure may change substantially if larger or different sets are used. The images can be viewed on p. 13 of the Appendix, where Gen 01 corresponds to Same-Identity Pair 1, Gen 02 corresponds to Same-Identity Pair 2, and so on.

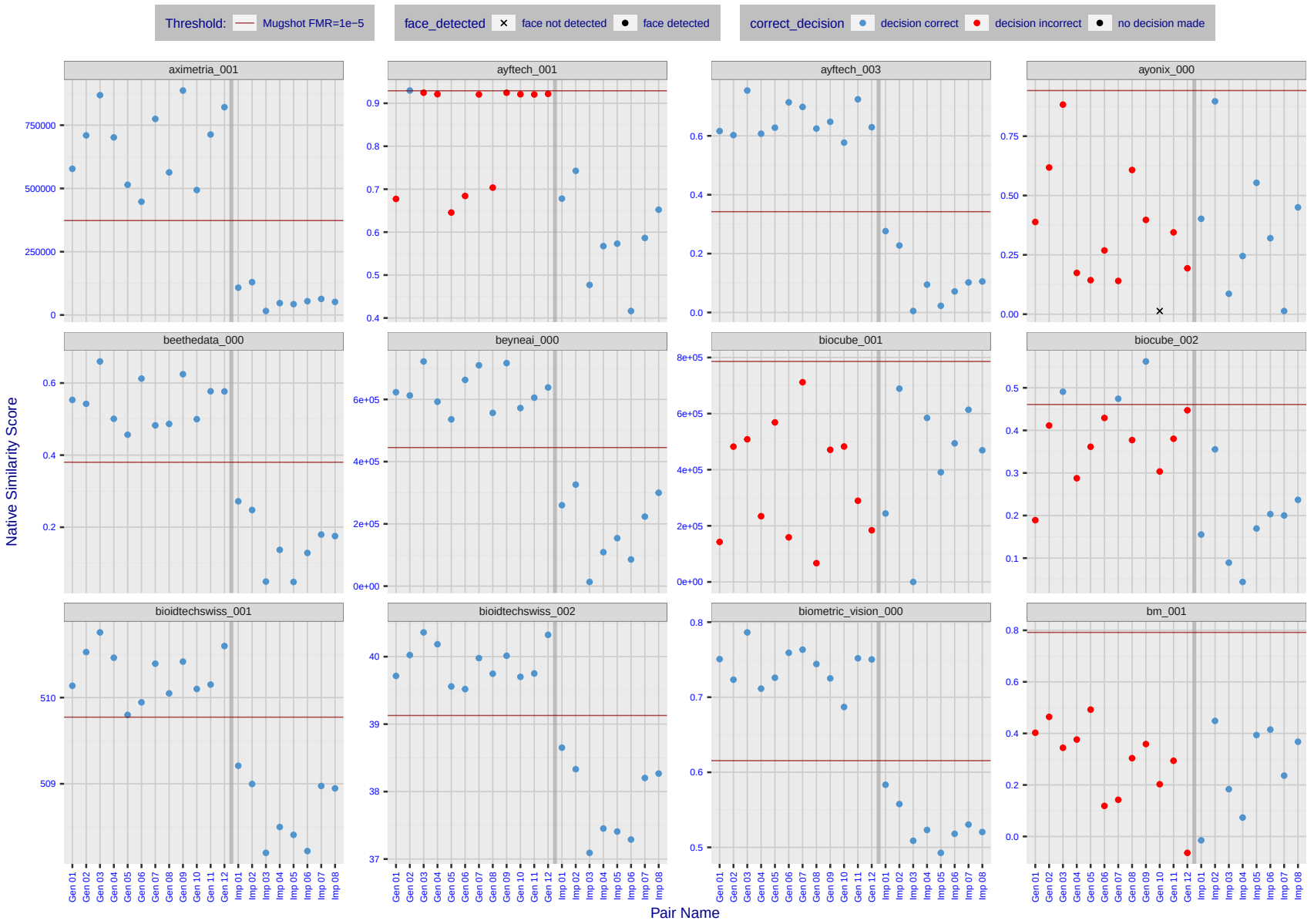

Figure 9: The figure shows algorithms' similarity scores for 12 genuine and 8 impostor image pairs used in a May 2018 paper by Phillips et al. ([1]). The threshold (red horizontal line) is a value calibrated to give FMR = 0.0001 on mugshot images. Points above the threshold correspond to pairs determined to be genuine, and points below the threshold correspond to pairs determined to be impostors. If the determined class (genuine or impostor) matches the real class, points will be blue; if not, red. An X represents face detection failure in either of the images in the pair. Note that the sample size (n=20) is small, and the figure may change substantially if larger or different sets are used. The images can be viewed on p. 13 of the Appendix, where Gen 01 corresponds to Same-Identity Pair 1, Gen 02 corresponds to Same-Identity Pair 2, and so on.

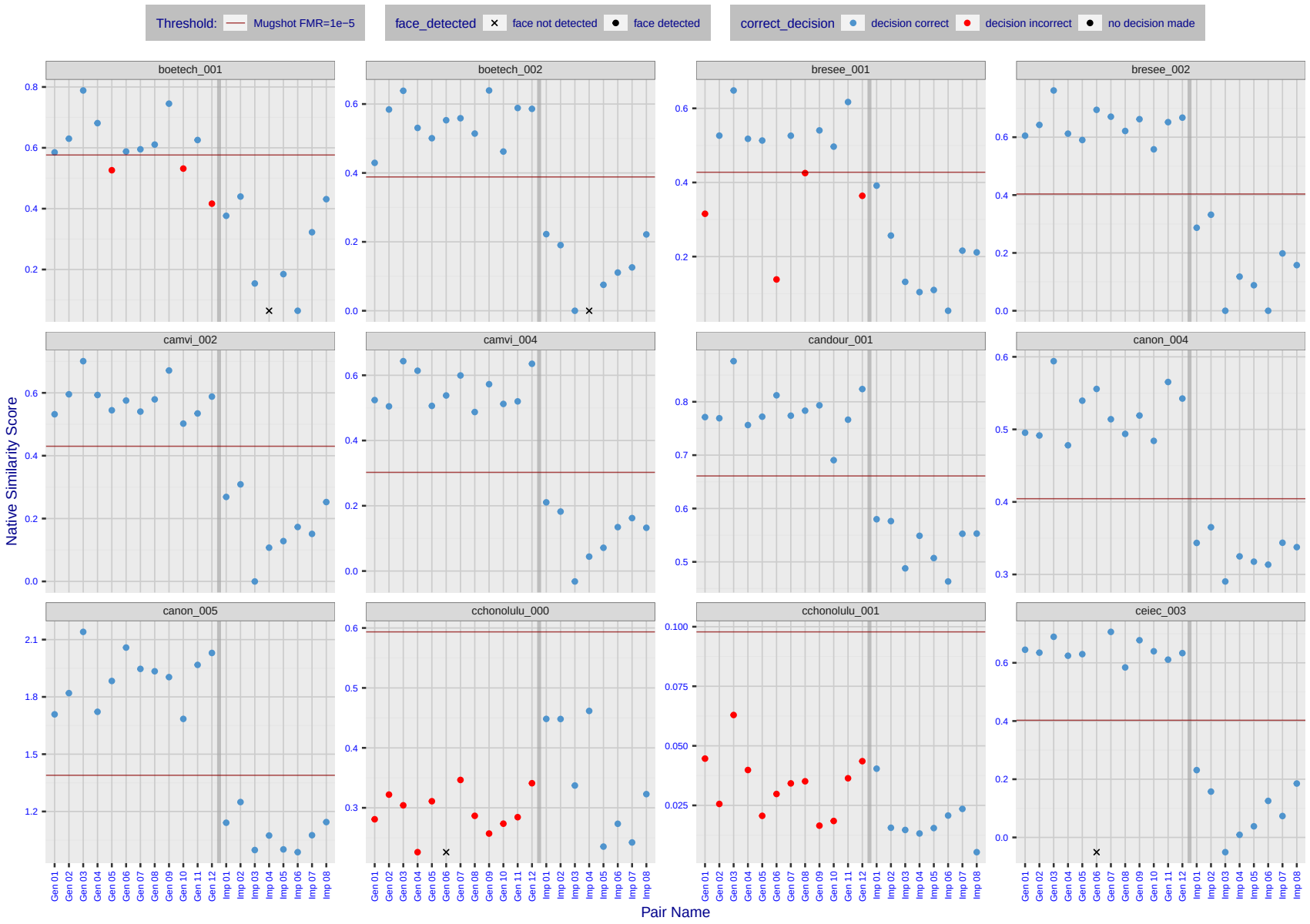

Figure 10: The figure shows algorithms' similarity scores for 12 genuine and 8 impostor image pairs used in a May 2018 paper by Phillips et al. ([1]). The threshold (red horizontal line) is a value calibrated to give FMR = 0.0001 on mugshot images. Points above the threshold correspond to pairs determined to be genuine, and points below the threshold correspond to pairs determined to be impostors. If the determined class (genuine or impostor) matches the real class, points will be blue; if not, red. An X represents face detection failure in either of the images in the pair. Note that the sample size (n=20) is small, and the figure may change substantially if larger or different sets are used. The images can be viewed on p. 13 of the Appendix, where Gen 01 corresponds to Same-Identity Pair 1, Gen 02 corresponds to Same-Identity Pair 2, and so on.

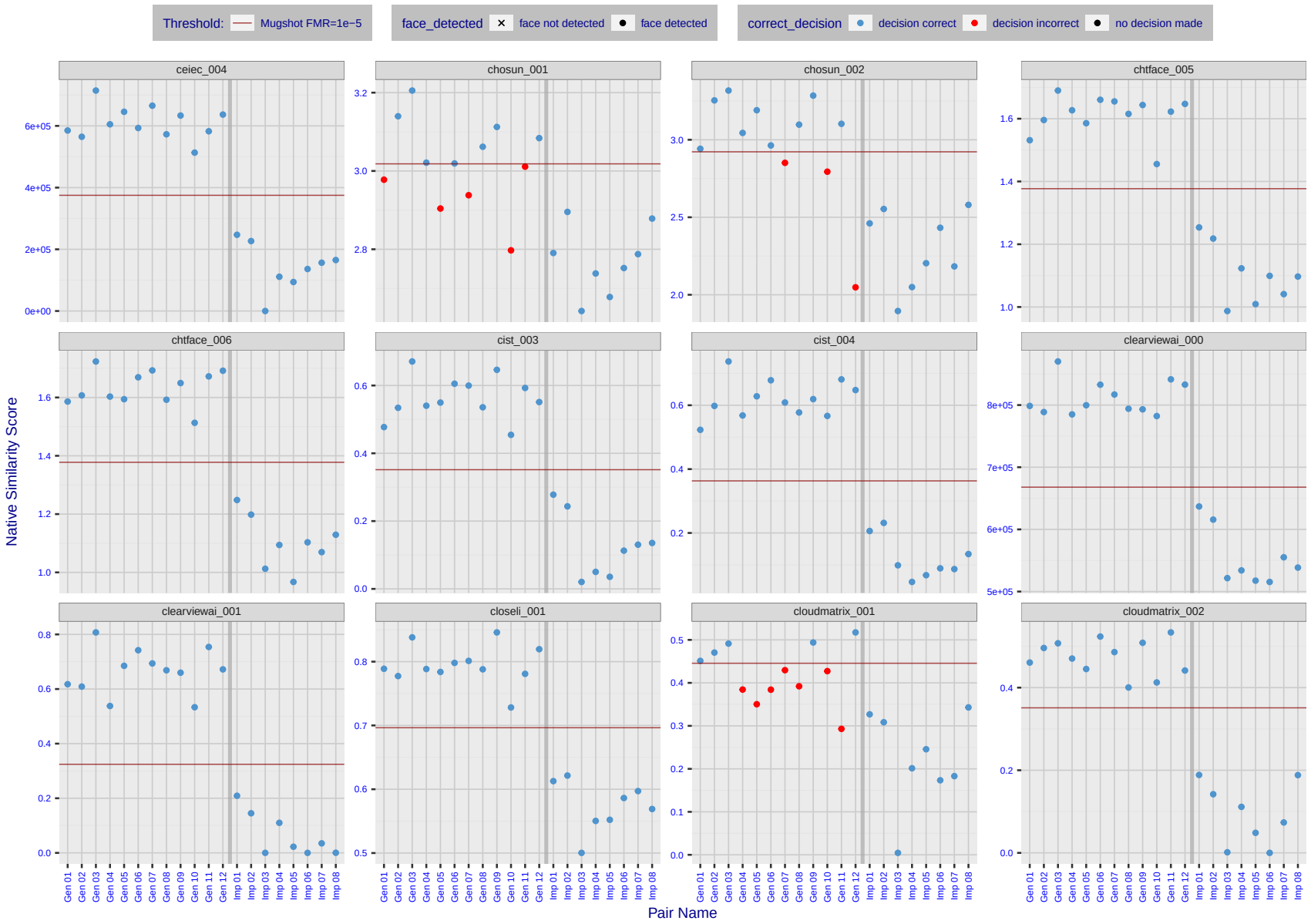

Figure 11: The figure shows algorithms' similarity scores for 12 genuine and 8 impostor image pairs used in a May 2018 paper by Phillips et al. ([1]). The threshold (red horizontal line) is a value calibrated to give FMR = 0.0001 on mugshot images. Points above the threshold correspond to pairs determined to be genuine, and points below the threshold correspond to pairs determined to be impostors. If the determined class (genuine or impostor) matches the real class, points will be blue; if not, red. An X represents face detection failure in either of the images in the pair. Note that the sample size (n=20) is small, and the figure may change substantially if larger or different sets are used. The images can be viewed on p. 13 of the Appendix, where Gen 01 corresponds to Same-Identity Pair 1, Gen 02 corresponds to Same-Identity Pair 2, and so on.

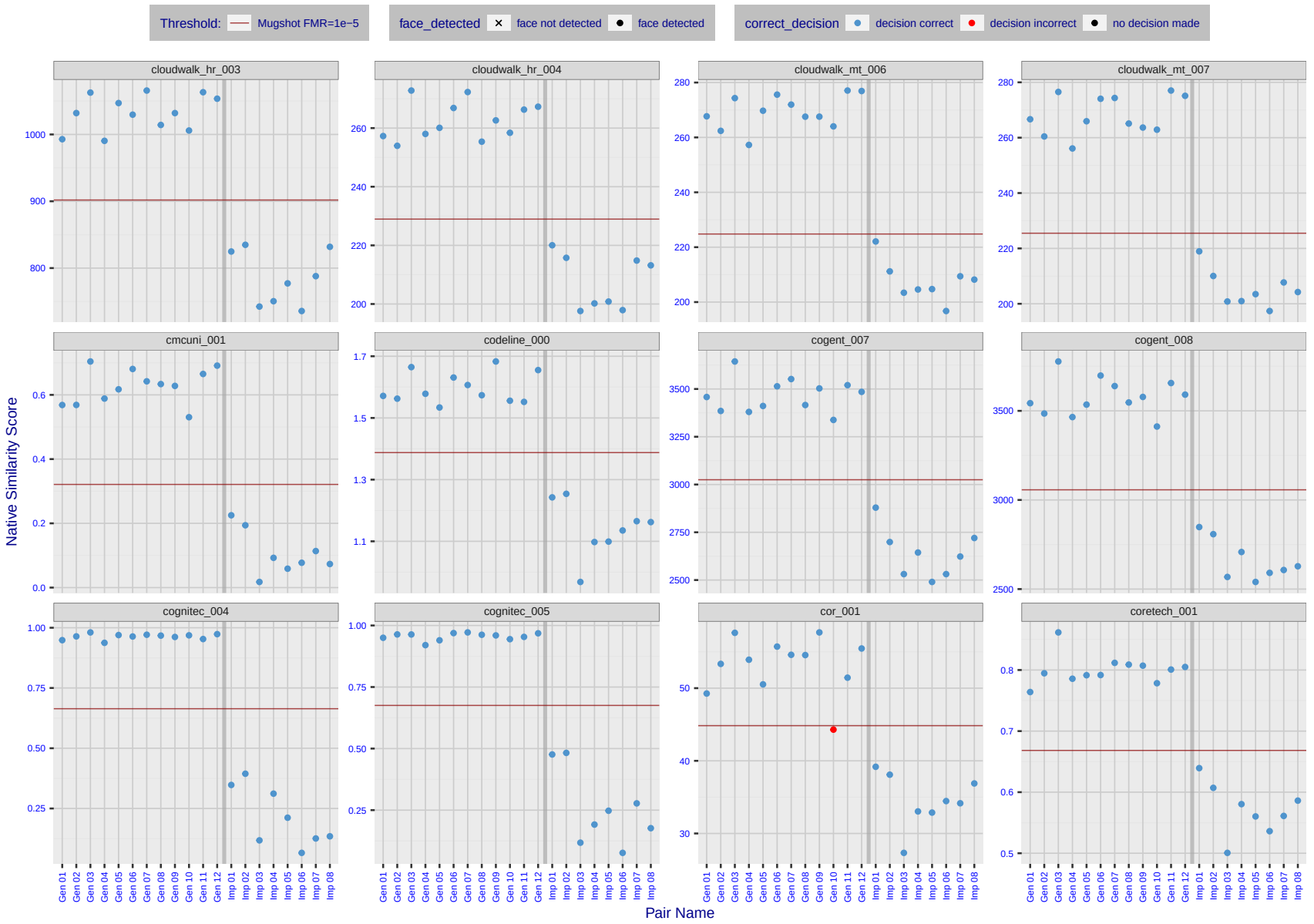

Figure 12: The figure shows algorithms' similarity scores for 12 genuine and 8 impostor image pairs used in a May 2018 paper by Phillips et al. ([1]). The threshold (red horizontal line) is a value calibrated to give FMR = 0.0001 on mugshot images. Points above the threshold correspond to pairs determined to be genuine, and points below the threshold correspond to pairs determined to be impostors. If the determined class (genuine or impostor) matches the real class, points will be blue; if not, red. An X represents face detection failure in either of the images in the pair. Note that the sample size (n=20) is small, and the figure may change substantially if larger or different sets are used. The images can be viewed on p. 13 of the Appendix, where Gen 01 corresponds to Same-Identity Pair 1, Gen 02 corresponds to Same-Identity Pair 2, and so on.

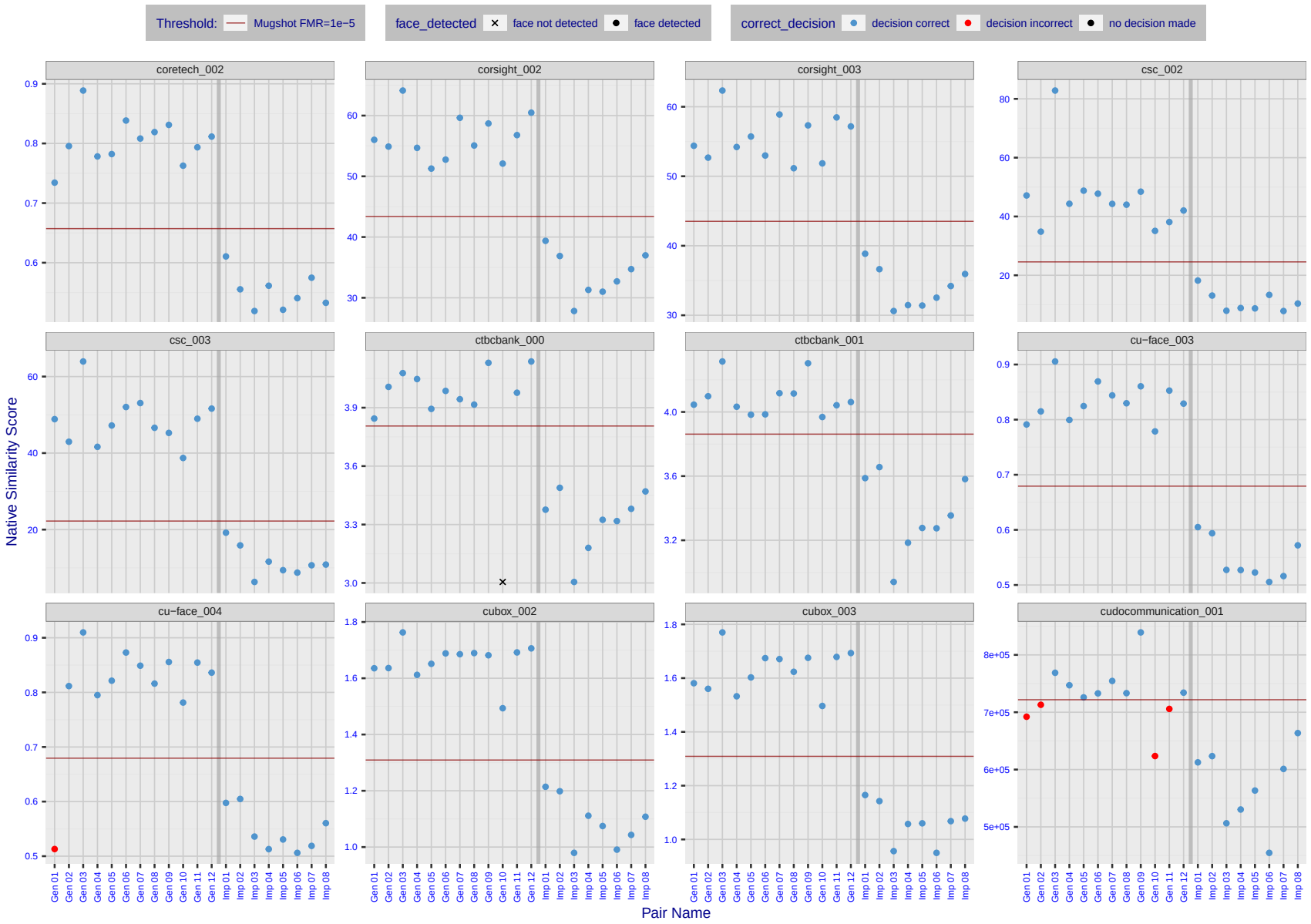

Figure 13: The figure shows algorithms' similarity scores for 12 genuine and 8 impostor image pairs used in a May 2018 paper by Phillips et al. ([1]). The threshold (red horizontal line) is a value calibrated to give FMR = 0.0001 on mugshot images. Points above the threshold correspond to pairs determined to be genuine, and points below the threshold correspond to pairs determined to be impostors. If the determined class (genuine or impostor) matches the real class, points will be blue; if not, red. An X represents face detection failure in either of the images in the pair. Note that the sample size (n=20) is small, and the figure may change substantially if larger or different sets are used. The images can be viewed on p. 13 of the Appendix, where Gen 01 corresponds to Same-Identity Pair 1, Gen 02 corresponds to Same-Identity Pair 2, and so on.

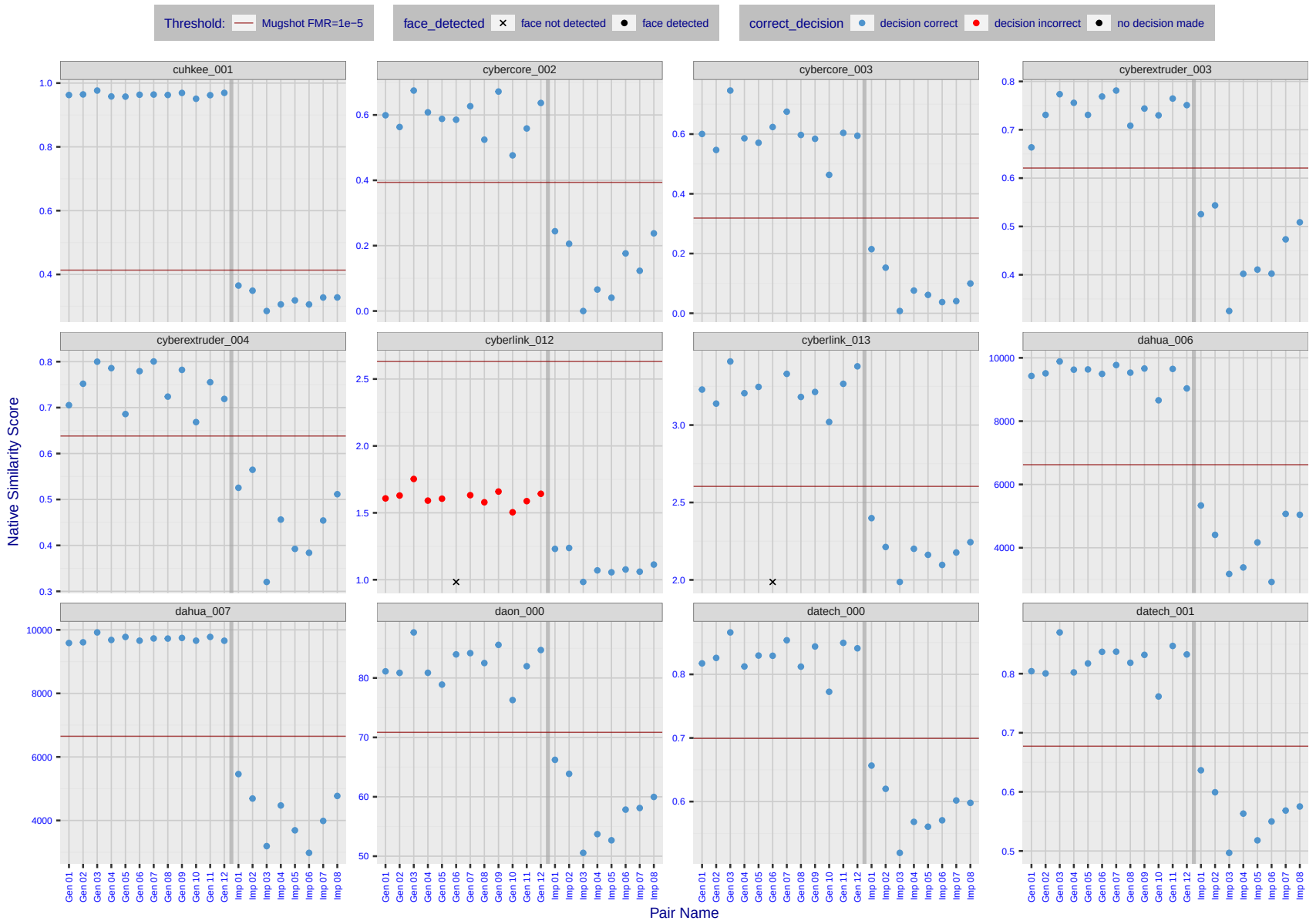

Figure 14: The figure shows algorithms' similarity scores for 12 genuine and 8 impostor image pairs used in a May 2018 paper by Phillips et al. ([1]). The threshold (red horizontal line) is a value calibrated to give FMR = 0.0001 on mugshot images. Points above the threshold correspond to pairs determined to be genuine, and points below the threshold correspond to pairs determined to be impostors. If the determined class (genuine or impostor) matches the real class, points will be blue; if not, red. An X represents face detection failure in either of the images in the pair. Note that the sample size (n=20) is small, and the figure may change substantially if larger or different sets are used. The images can be viewed on p. 13 of the Appendix, where Gen 01 corresponds to Same-Identity Pair 1, Gen 02 corresponds to Same-Identity Pair 2, and so on.

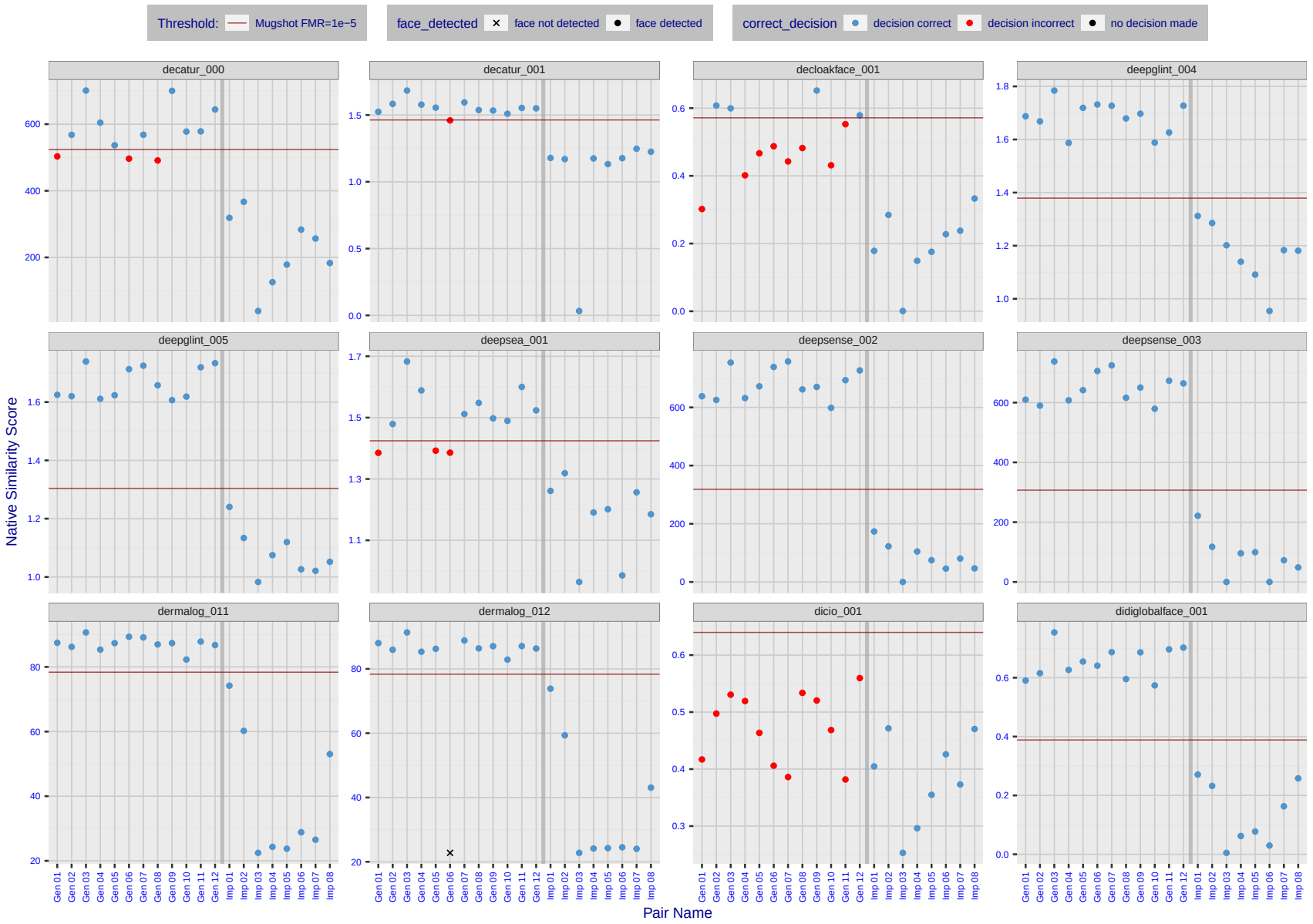

Figure 15: The figure shows algorithms' similarity scores for 12 genuine and 8 impostor image pairs used in a May 2018 paper by Phillips et al. ([1]). The threshold (red horizontal line) is a value calibrated to give FMR = 0.0001 on mugshot images. Points above the threshold correspond to pairs determined to be genuine, and points below the threshold correspond to pairs determined to be impostors. If the determined class (genuine or impostor) matches the real class, points will be blue; if not, red. An X represents face detection failure in either of the images in the pair. Note that the sample size (n=20) is small, and the figure may change substantially if larger or different sets are used. The images can be viewed on p. 13 of the Appendix, where Gen 01 corresponds to Same-Identity Pair 1, Gen 02 corresponds to Same-Identity Pair 2, and so on.

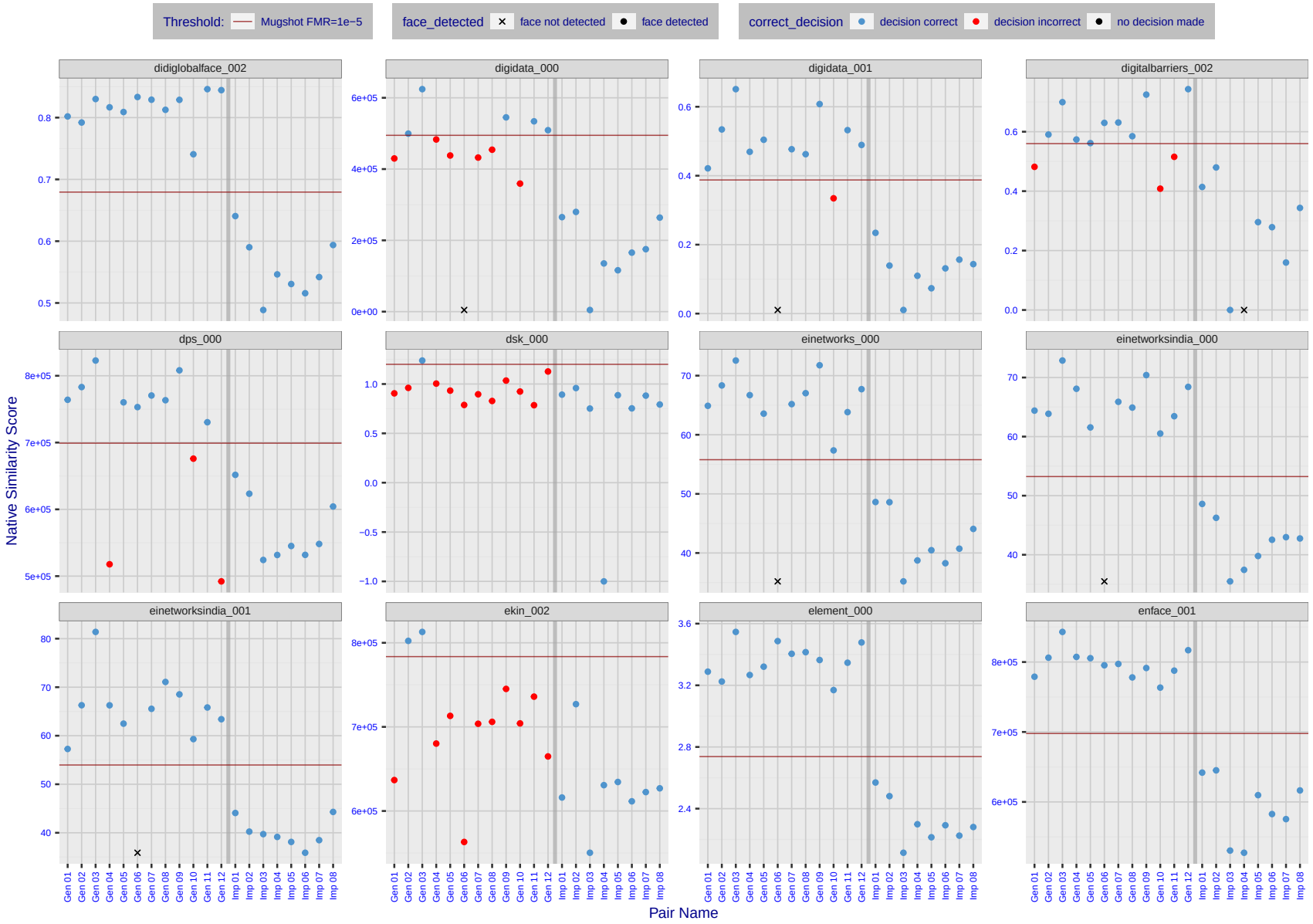

Figure 16: The figure shows algorithms' similarity scores for 12 genuine and 8 impostor image pairs used in a May 2018 paper by Phillips et al. ([1]). The threshold (red horizontal line) is a value calibrated to give FMR = 0.0001 on mugshot images. Points above the threshold correspond to pairs determined to be genuine, and points below the threshold correspond to pairs determined to be impostors. If the determined class (genuine or impostor) matches the real class, points will be blue; if not, red. An X represents face detection failure in either of the images in the pair. Note that the sample size (n=20) is small, and the figure may change substantially if larger or different sets are used. The images can be viewed on p. 13 of the Appendix, where Gen 01 corresponds to Same-Identity Pair 1, Gen 02 corresponds to Same-Identity Pair 2, and so on.

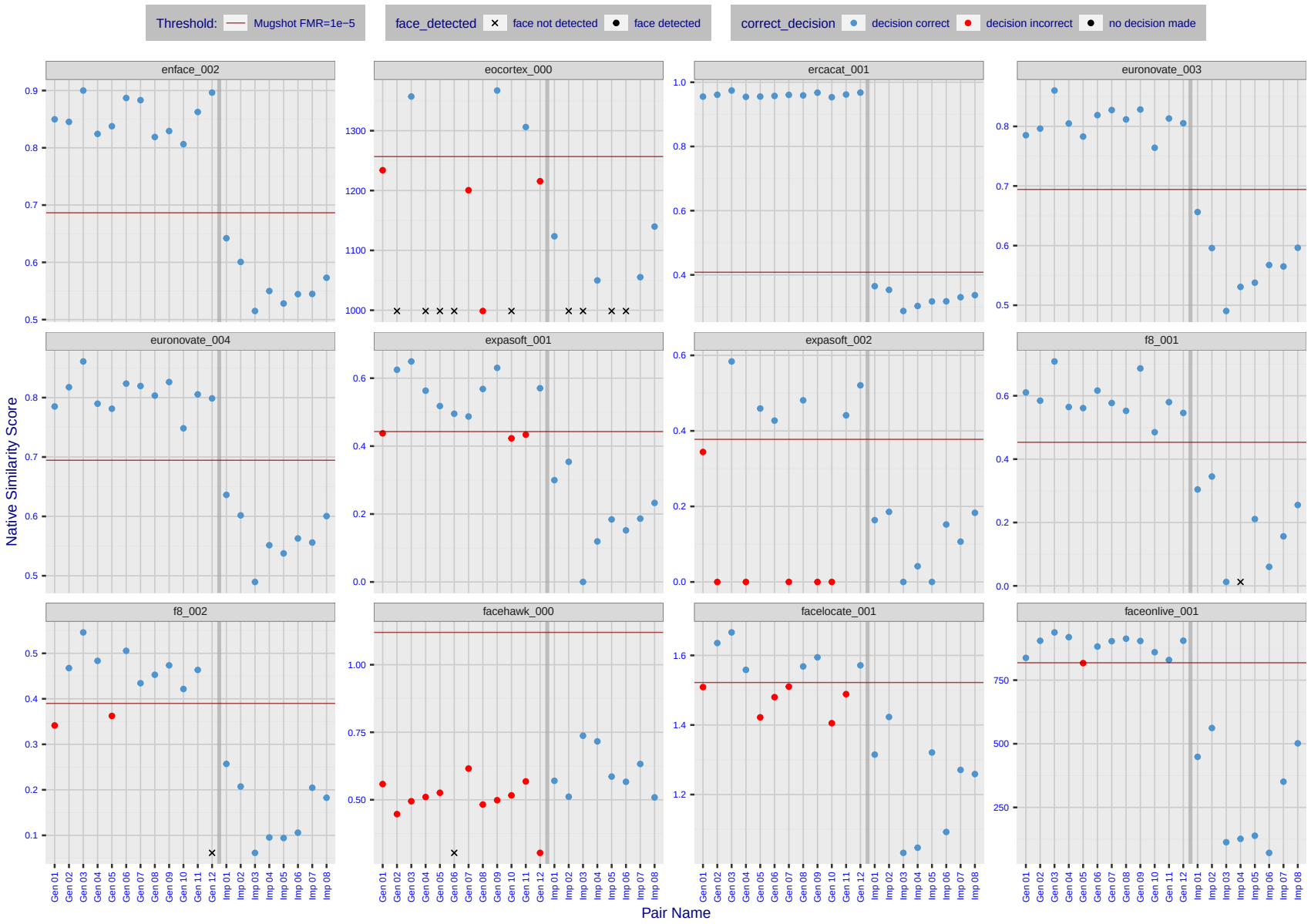

Figure 17: The figure shows algorithms' similarity scores for 12 genuine and 8 impostor image pairs used in a May 2018 paper by Phillips et al. ([1]). The threshold (red horizontal line) is a value calibrated to give FMR = 0.0001 on mugshot images. Points above the threshold correspond to pairs determined to be genuine, and points below the threshold correspond to pairs determined to be impostors. If the determined class (genuine or impostor) matches the real class, points will be blue; if not, red. An X represents face detection failure in either of the images in the pair. Note that the sample size (n=20) is small, and the figure may change substantially if larger or different sets are used. The images can be viewed on p. 13 of the Appendix, where Gen 01 corresponds to Same-Identity Pair 1, Gen 02 corresponds to Same-Identity Pair 2, and so on.

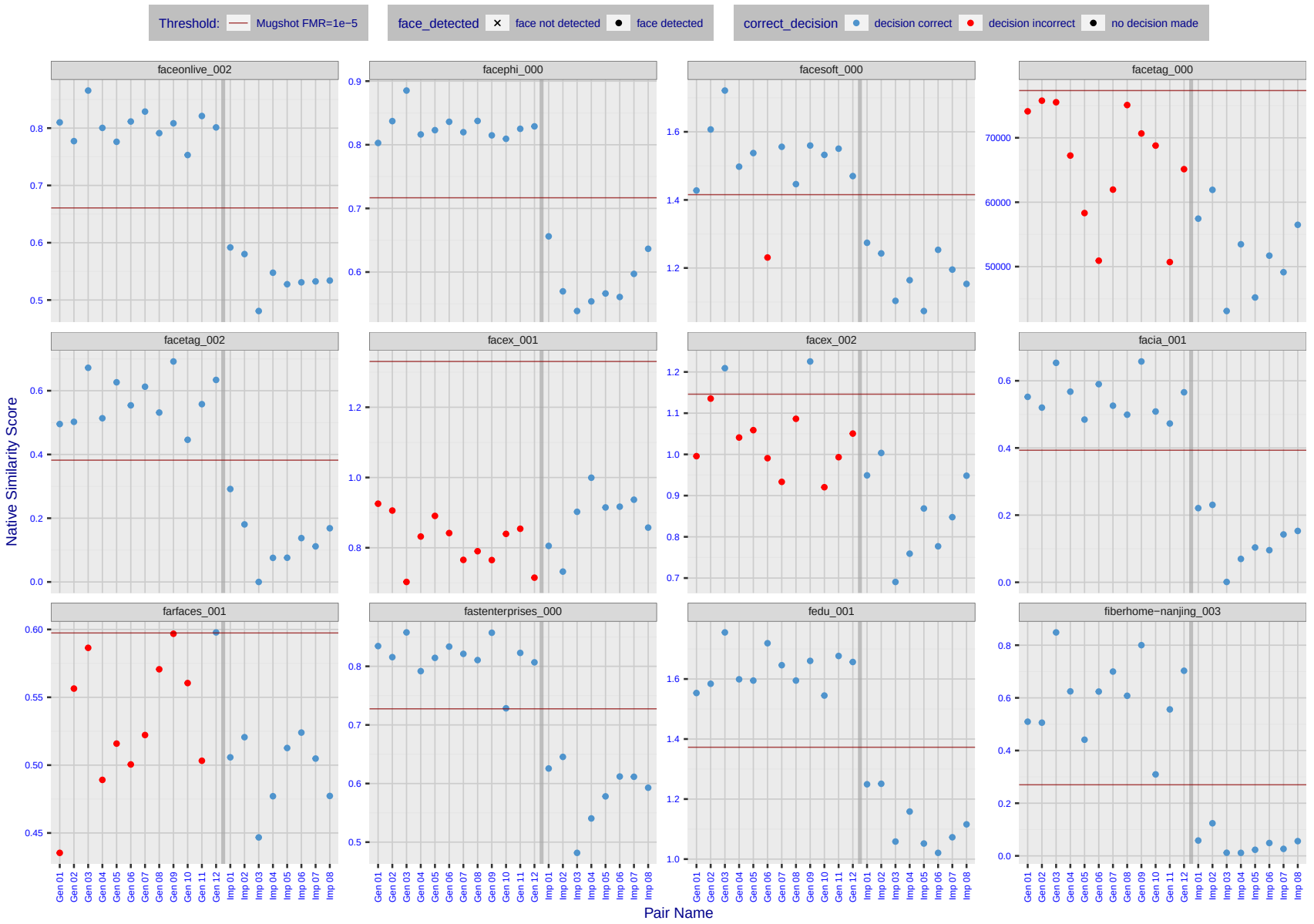

Figure 18: The figure shows algorithms' similarity scores for 12 genuine and 8 impostor image pairs used in a May 2018 paper by Phillips et al. ([1]). The threshold (red horizontal line) is a value calibrated to give FMR = 0.0001 on mugshot images. Points above the threshold correspond to pairs determined to be genuine, and points below the threshold correspond to pairs determined to be impostors. If the determined class (genuine or impostor) matches the real class, points will be blue; if not, red. An X represents face detection failure in either of the images in the pair. Note that the sample size (n=20) is small, and the figure may change substantially if larger or different sets are used. The images can be viewed on p. 13 of the Appendix, where Gen 01 corresponds to Same-Identity Pair 1, Gen 02 corresponds to Same-Identity Pair 2, and so on.

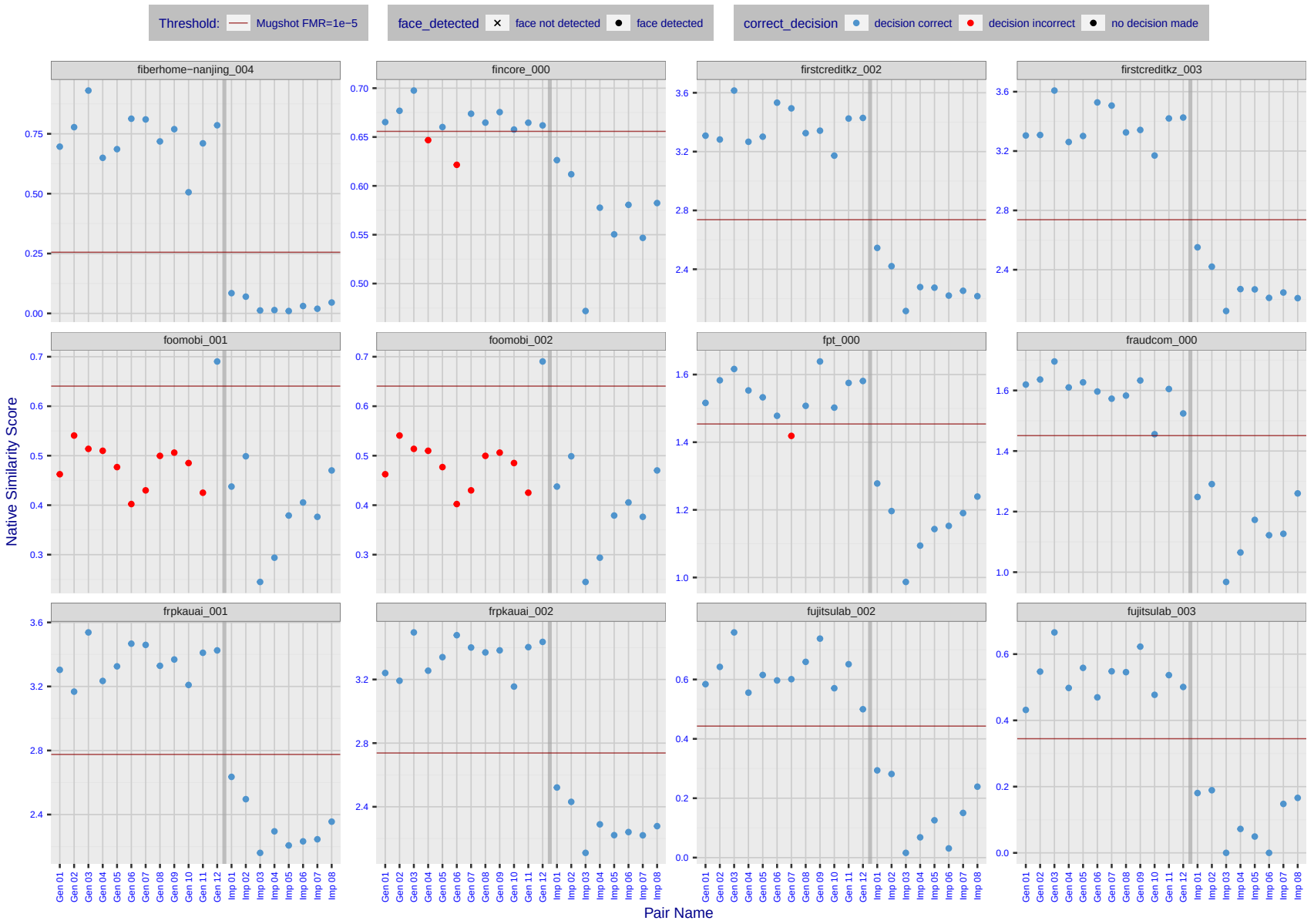

Figure 19: The figure shows algorithms' similarity scores for 12 genuine and 8 impostor image pairs used in a May 2018 paper by Phillips et al. ([1]). The threshold (red horizontal line) is a value calibrated to give FMR = 0.0001 on mugshot images. Points above the threshold correspond to pairs determined to be genuine, and points below the threshold correspond to pairs determined to be impostors. If the determined class (genuine or impostor) matches the real class, points will be blue; if not, red. An X represents face detection failure in either of the images in the pair. Note that the sample size (n=20) is small, and the figure may change substantially if larger or different sets are used. The images can be viewed on p. 13 of the Appendix, where Gen 01 corresponds to Same-Identity Pair 1, Gen 02 corresponds to Same-Identity Pair 2, and so on.

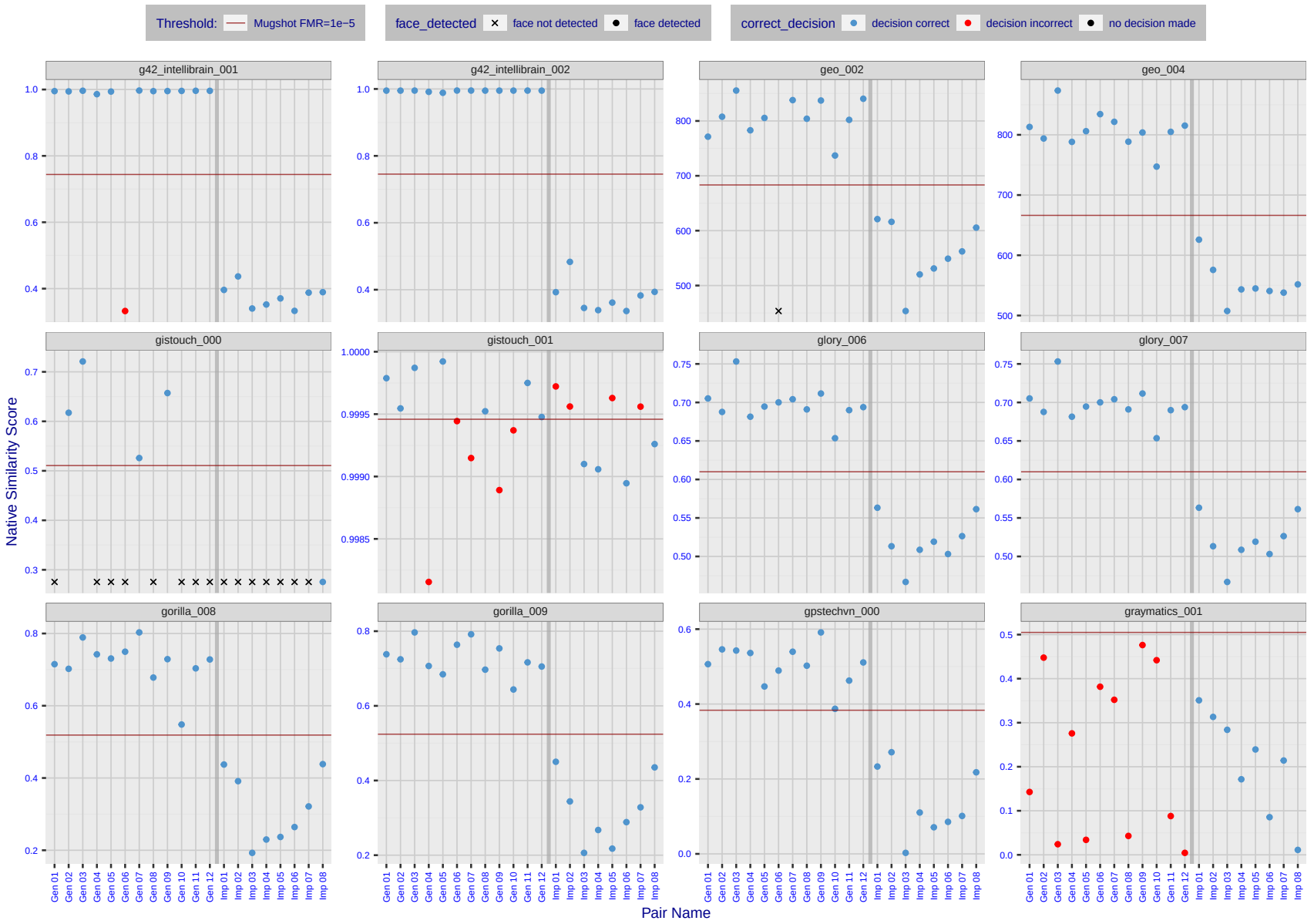

Figure 20: The figure shows algorithms' similarity scores for 12 genuine and 8 impostor image pairs used in a May 2018 paper by Phillips et al. ([1]). The threshold (red horizontal line) is a value calibrated to give FMR = 0.0001 on mugshot images. Points above the threshold correspond to pairs determined to be genuine, and points below the threshold correspond to pairs determined to be impostors. If the determined class (genuine or impostor) matches the real class, points will be blue; if not, red. An X represents face detection failure in either of the images in the pair. Note that the sample size (n=20) is small, and the figure may change substantially if larger or different sets are used. The images can be viewed on p. 13 of the Appendix, where Gen 01 corresponds to Same-Identity Pair 1, Gen 02 corresponds to Same-Identity Pair 2, and so on.

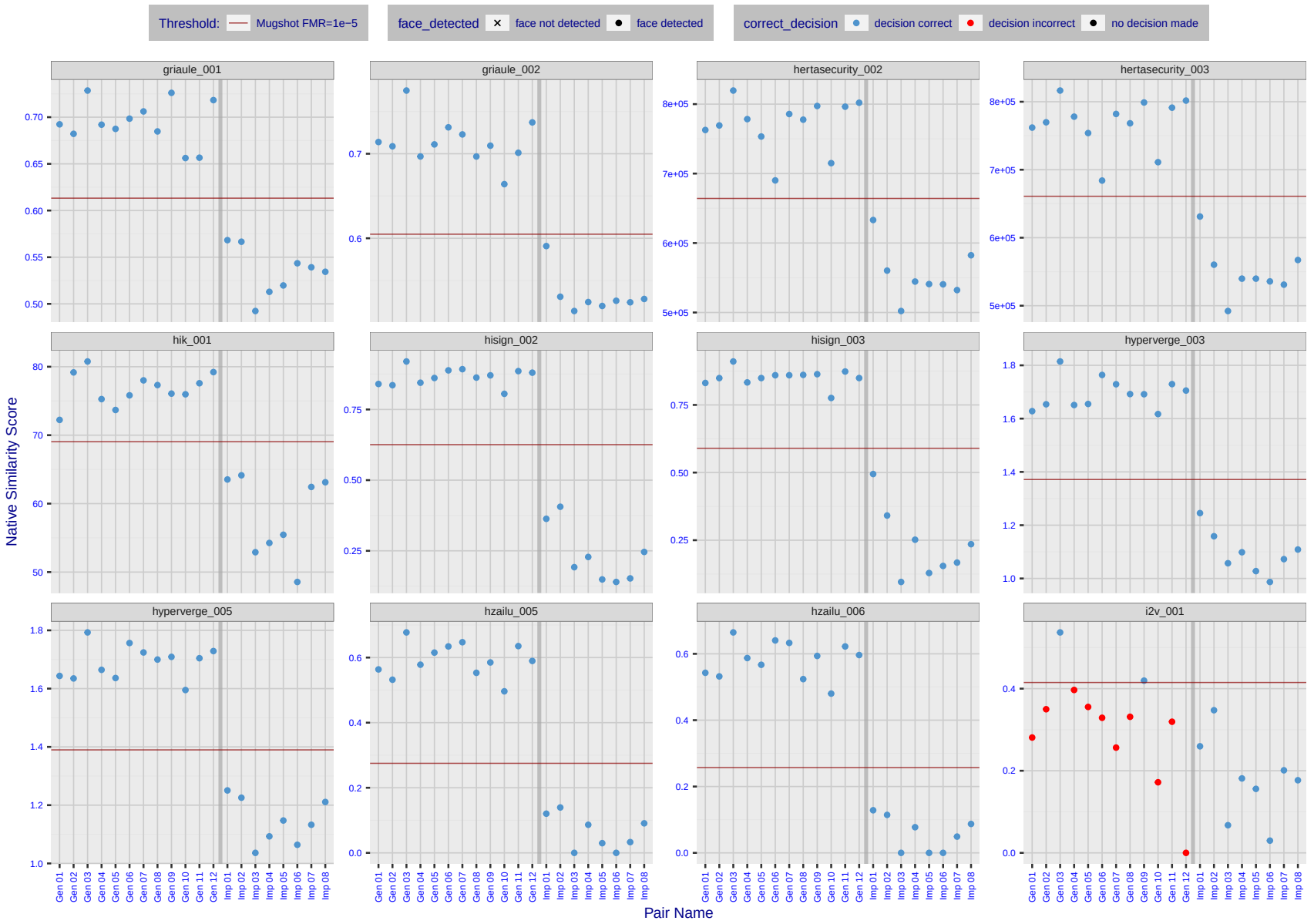

Figure 21: The figure shows algorithms' similarity scores for 12 genuine and 8 impostor image pairs used in a May 2018 paper by Phillips et al. ([1]). The threshold (red horizontal line) is a value calibrated to give FMR = 0.0001 on mugshot images. Points above the threshold correspond to pairs determined to be genuine, and points below the threshold correspond to pairs determined to be impostors. If the determined class (genuine or impostor) matches the real class, points will be blue; if not, red. An X represents face detection failure in either of the images in the pair. Note that the sample size (n=20) is small, and the figure may change substantially if larger or different sets are used. The images can be viewed on p. 13 of the Appendix, where Gen 01 corresponds to Same-Identity Pair 1, Gen 02 corresponds to Same-Identity Pair 2, and so on.

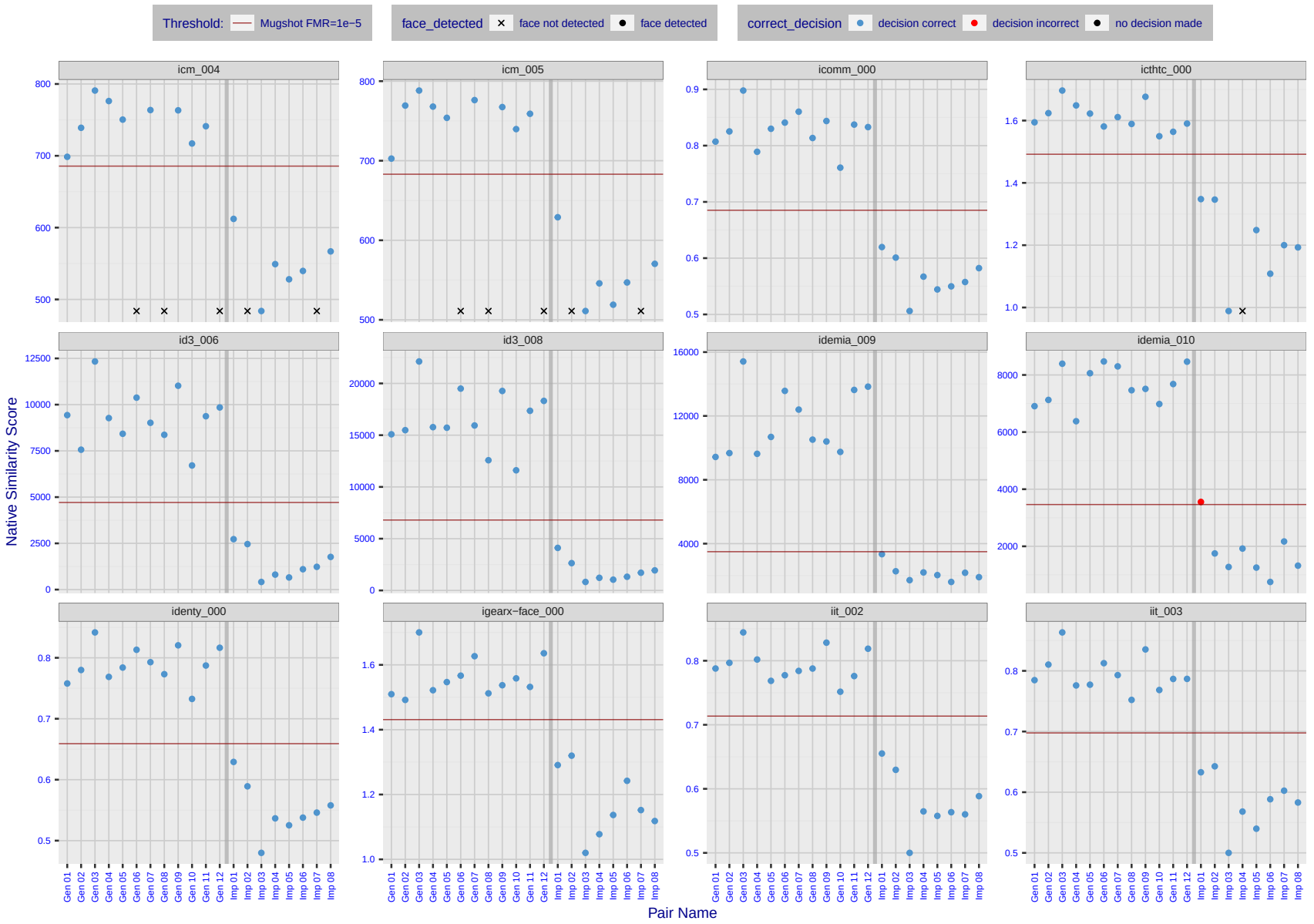

Figure 22: The figure shows algorithms' similarity scores for 12 genuine and 8 impostor image pairs used in a May 2018 paper by Phillips et al. ([1]). The threshold (red horizontal line) is a value calibrated to give FMR = 0.0001 on mugshot images. Points above the threshold correspond to pairs determined to be genuine, and points below the threshold correspond to pairs determined to be impostors. If the determined class (genuine or impostor) matches the real class, points will be blue; if not, red. An X represents face detection failure in either of the images in the pair. Note that the sample size (n=20) is small, and the figure may change substantially if larger or different sets are used. The images can be viewed on p. 13 of the Appendix, where Gen 01 corresponds to Same-Identity Pair 1, Gen 02 corresponds to Same-Identity Pair 2, and so on.

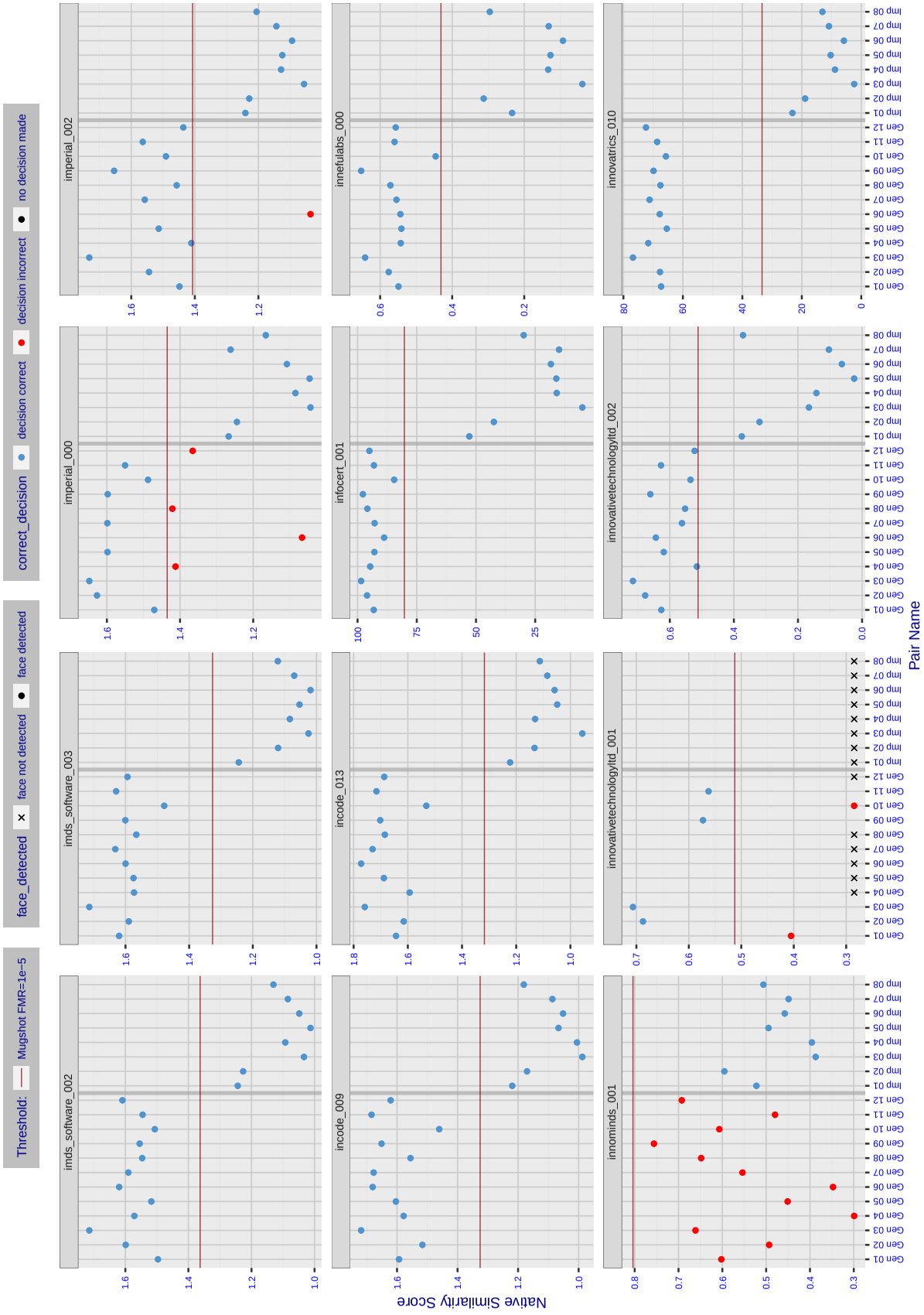

Figure 23: The figure shows algorithms' similarity scores for 12 genuine and 8 impostor image pairs used in a May 2018 paper by Phillips et al. ([1]). The threshold (red horizontal line) is a value calibrated to give FMR = 0.0001 on mugshot images. Points above the threshold correspond to pairs determined to be genuine, and points below the threshold correspond to pairs determined to be impostors. If the determined class (genuine or impostor) matches the real class, points will be blue; if not, red. An X represents face detection failure in either of the images in the pair. Note that the sample size (n=20) is small, and the figure may change substantially if larger or different sets are used. The images can be viewed on p. 13 of the Appendix, where Gen 01 corresponds to Same-Identity Pair 1, Gen 02 corresponds to Same-Identity Pair 2, and so on.

FNMR(T) "False non-match rate"
FMR(T) "False match rate"

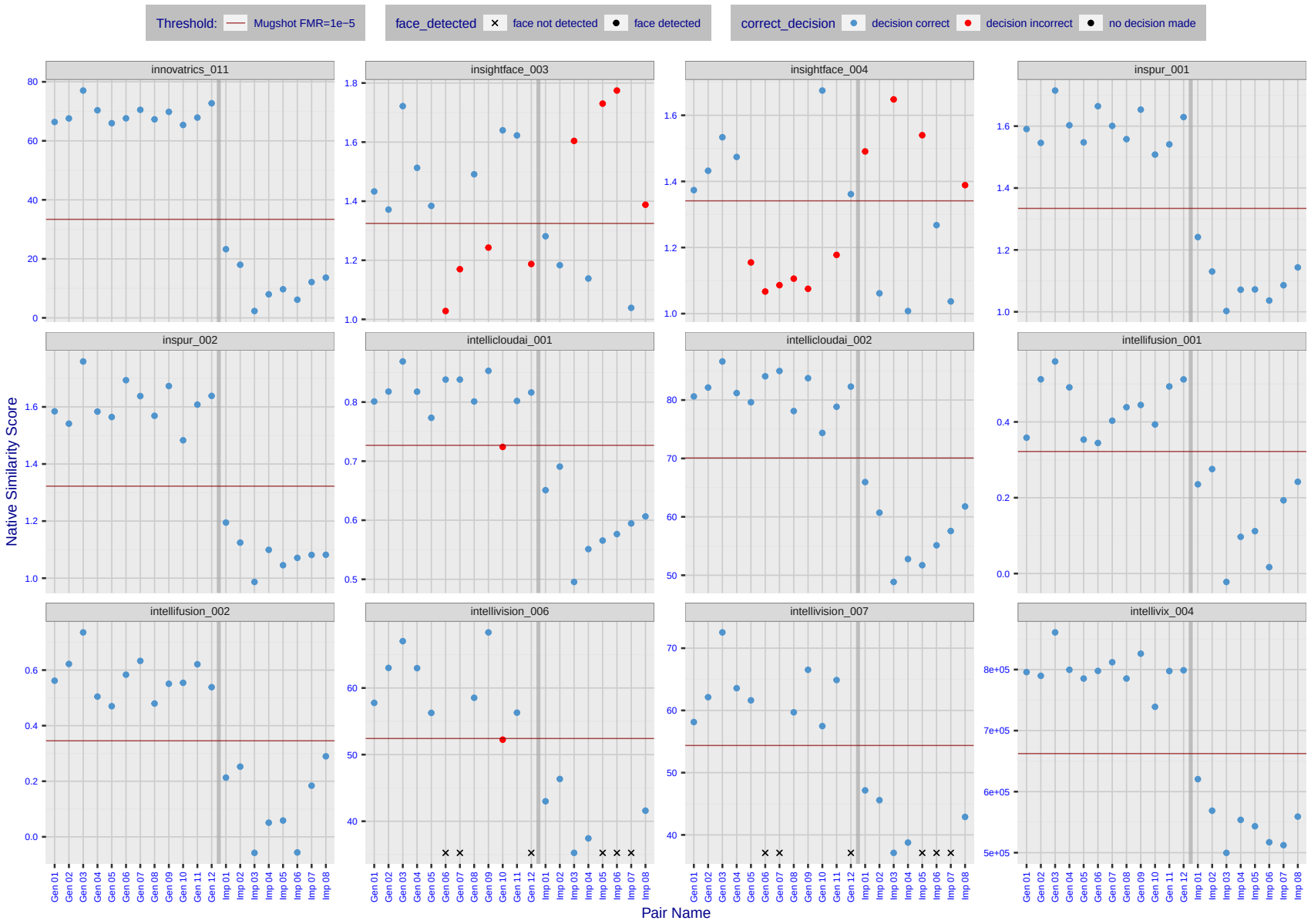

Figure 24: The figure shows algorithms' similarity scores for 12 genuine and 8 impostor image pairs used in a May 2018 paper by Phillips et al. ([1]). The threshold (red horizontal line) is a value calibrated to give FMR = 0.0001 on mugshot images. Points above the threshold correspond to pairs determined to be genuine, and points below the threshold correspond to pairs determined to be impostors. If the determined class (genuine or impostor) matches the real class, points will be blue; if not, red. An X represents face detection failure in either of the images in the pair. Note that the sample size (n=20) is small, and the figure may change substantially if larger or different sets are used. The images can be viewed on p. 13 of the Appendix, where Gen 01 corresponds to Same-Identity Pair 1, Gen 02 corresponds to Same-Identity Pair 2, and so on.

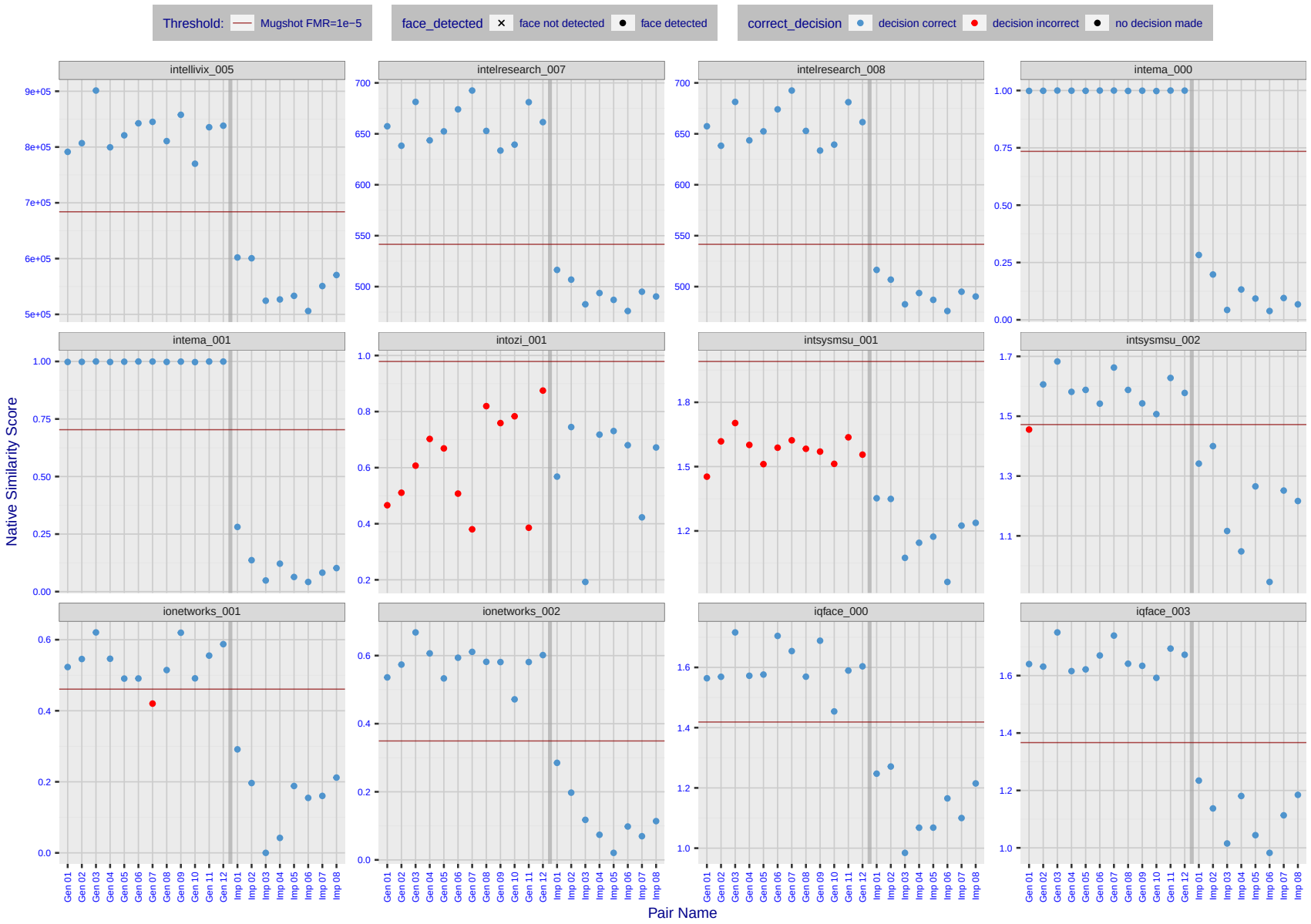

Figure 25: The figure shows algorithms' similarity scores for 12 genuine and 8 impostor image pairs used in a May 2018 paper by Phillips et al. ([1]). The threshold (red horizontal line) is a value calibrated to give FMR = 0.0001 on mugshot images. Points above the threshold correspond to pairs determined to be genuine, and points below the threshold correspond to pairs determined to be impostors. If the determined class (genuine or impostor) matches the real class, points will be blue; if not, red. An X represents face detection failure in either of the images in the pair. Note that the sample size (n=20) is small, and the figure may change substantially if larger or different sets are used. The images can be viewed on p. 13 of the Appendix, where Gen 01 corresponds to Same-Identity Pair 1, Gen 02 corresponds to Same-Identity Pair 2, and so on.

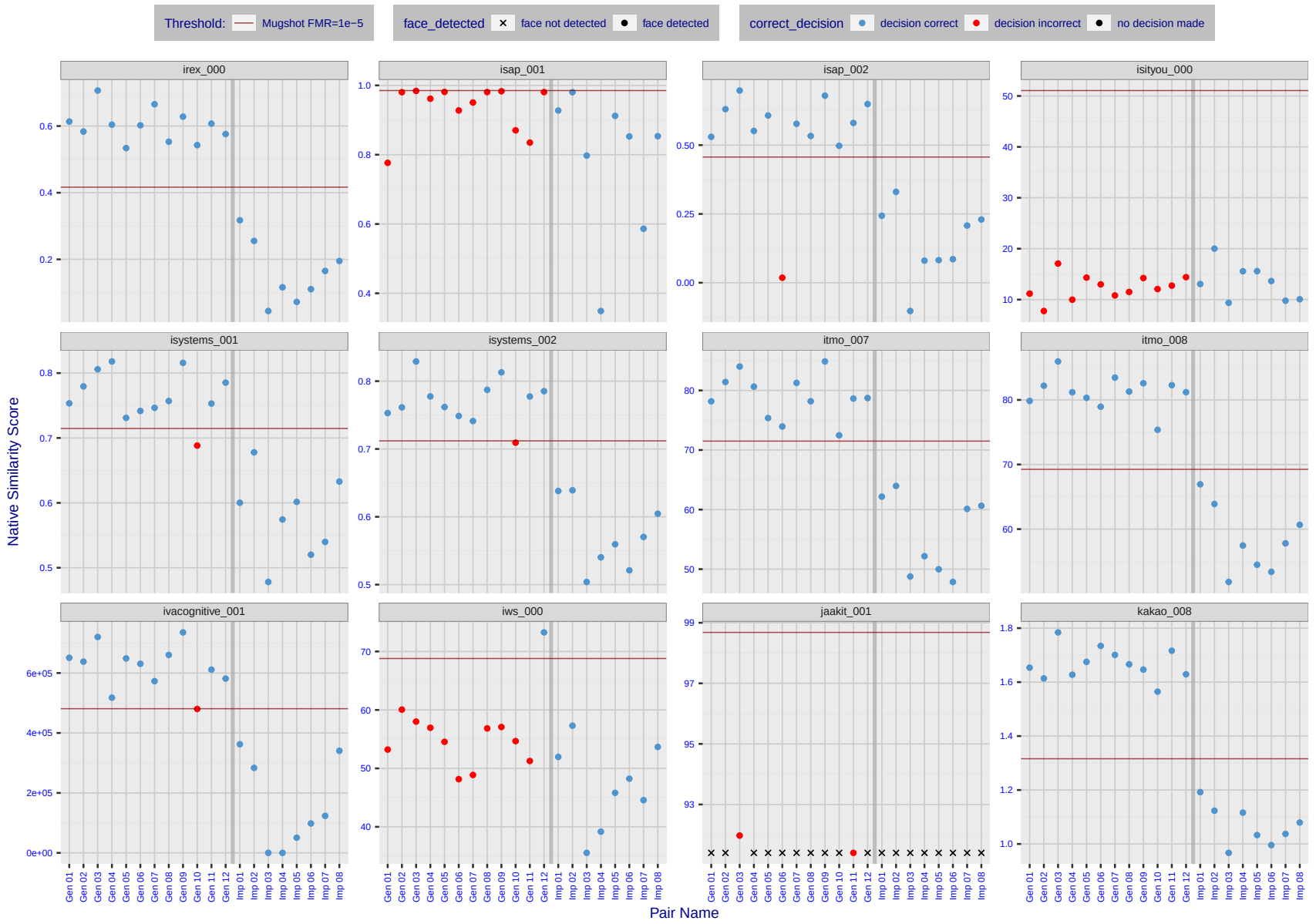

Figure 26: The figure shows algorithms' similarity scores for 12 genuine and 8 impostor image pairs used in a May 2018 paper by Phillips et al. ([1]). The threshold (red horizontal line) is a value calibrated to give FMR = 0.0001 on mugshot images. Points above the threshold correspond to pairs determined to be genuine, and points below the threshold correspond to pairs determined to be impostors. If the determined class (genuine or impostor) matches the real class, points will be blue; if not, red. An X represents face detection failure in either of the images in the pair. Note that the sample size (n=20) is small, and the figure may change substantially if larger or different sets are used. The images can be viewed on p. 13 of the Appendix, where Gen 01 corresponds to Same-Identity Pair 1, Gen 02 corresponds to Same-Identity Pair 2, and so on.

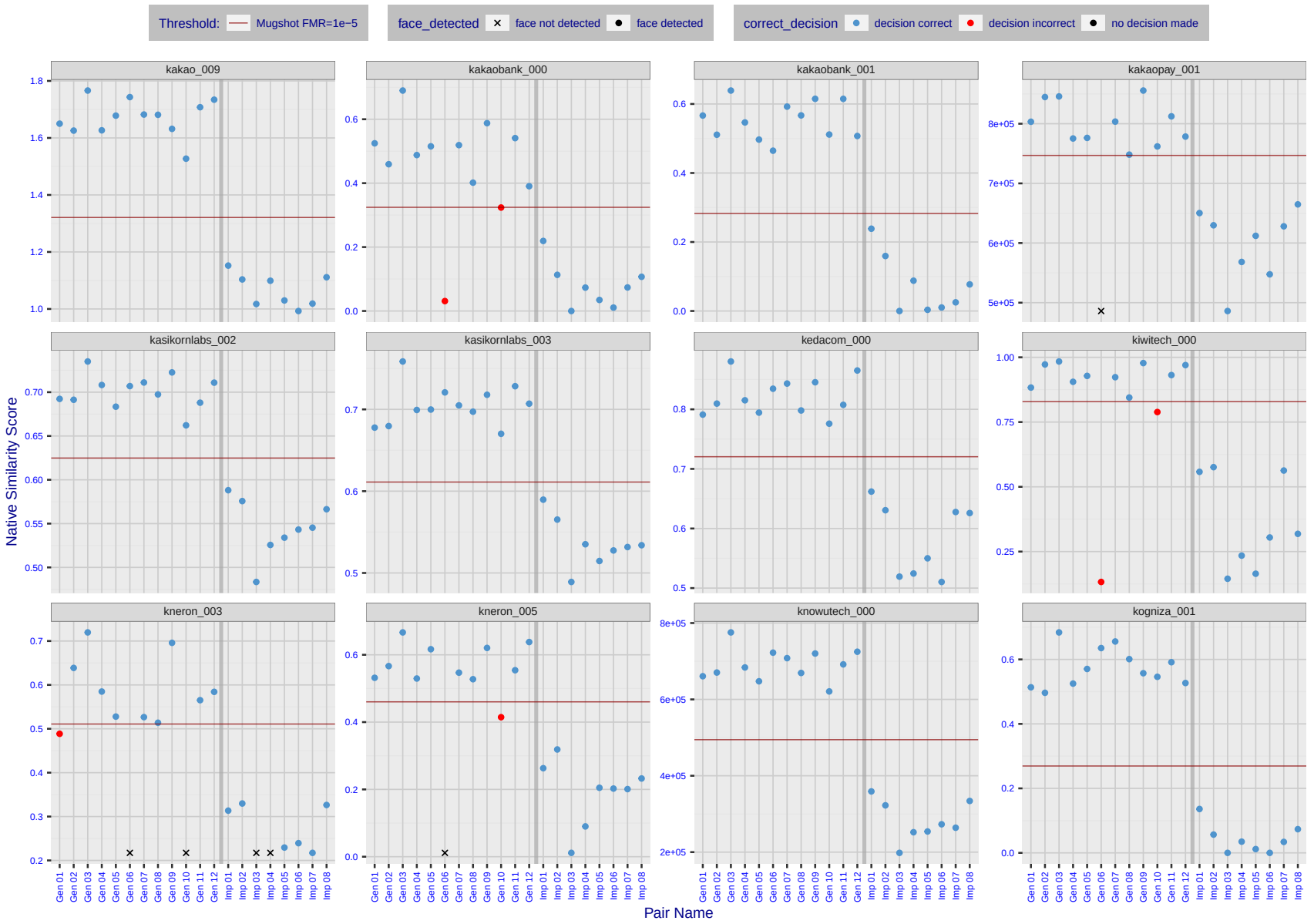

Figure 27: The figure shows algorithms' similarity scores for 12 genuine and 8 impostor image pairs used in a May 2018 paper by Phillips et al. ([1]). The threshold (red horizontal line) is a value calibrated to give FMR = 0.0001 on mugshot images. Points above the threshold correspond to pairs determined to be genuine, and points below the threshold correspond to pairs determined to be impostors. If the determined class (genuine or impostor) matches the real class, points will be blue; if not, red. An X represents face detection failure in either of the images in the pair. Note that the sample size (n=20) is small, and the figure may change substantially if larger or different sets are used. The images can be viewed on p. 13 of the Appendix, where Gen 01 corresponds to Same-Identity Pair 1, Gen 02 corresponds to Same-Identity Pair 2, and so on.

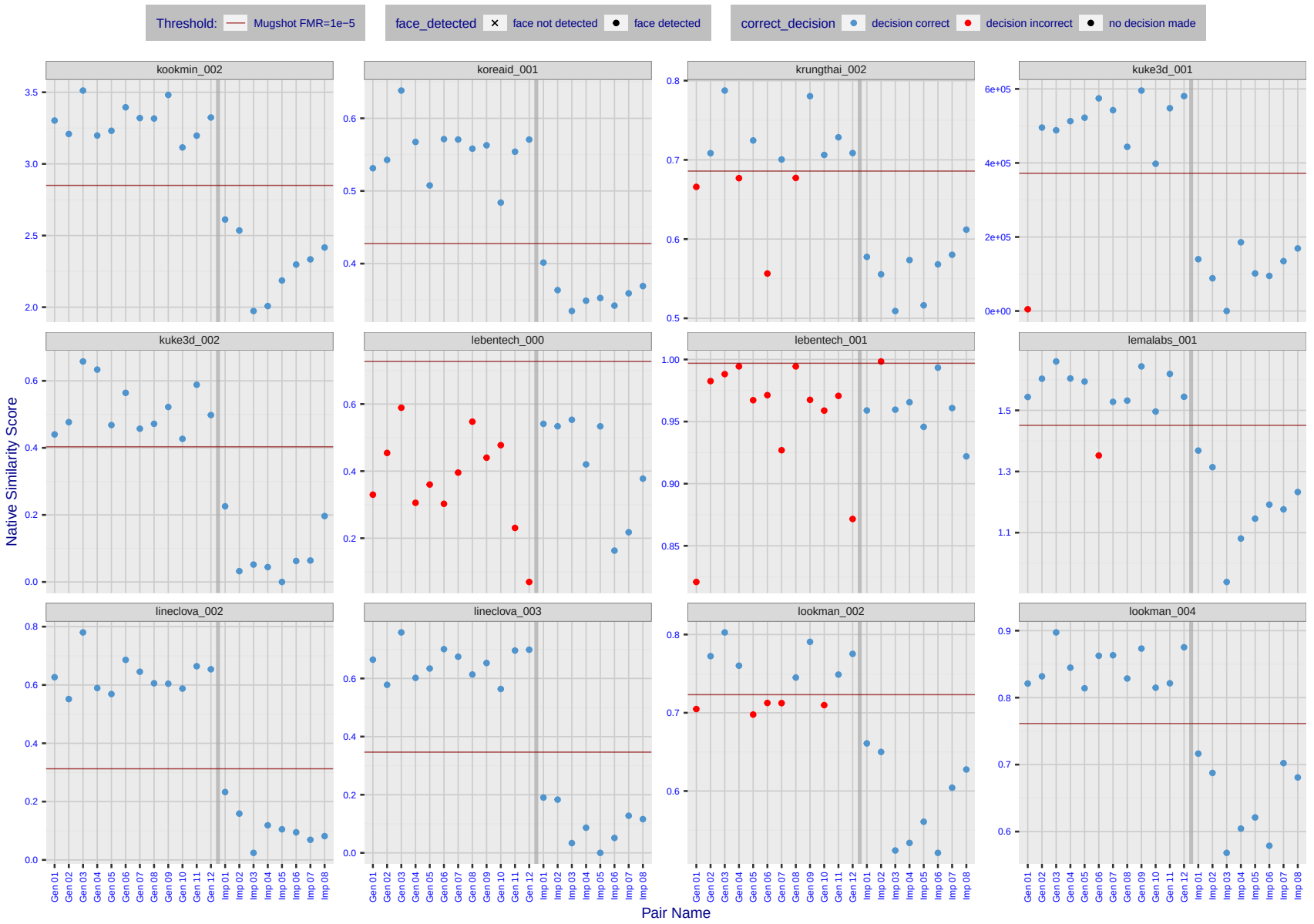

Figure 28: The figure shows algorithms' similarity scores for 12 genuine and 8 impostor image pairs used in a May 2018 paper by Phillips et al. ([1]). The threshold (red horizontal line) is a value calibrated to give FMR = 0.0001 on mugshot images. Points above the threshold correspond to pairs determined to be genuine, and points below the threshold correspond to pairs determined to be impostors. If the determined class (genuine or impostor) matches the real class, points will be blue; if not, red. An X represents face detection failure in either of the images in the pair. Note that the sample size (n=20) is small, and the figure may change substantially if larger or different sets are used. The images can be viewed on p. 13 of the Appendix, where Gen 01 corresponds to Same-Identity Pair 1, Gen 02 corresponds to Same-Identity Pair 2, and so on.

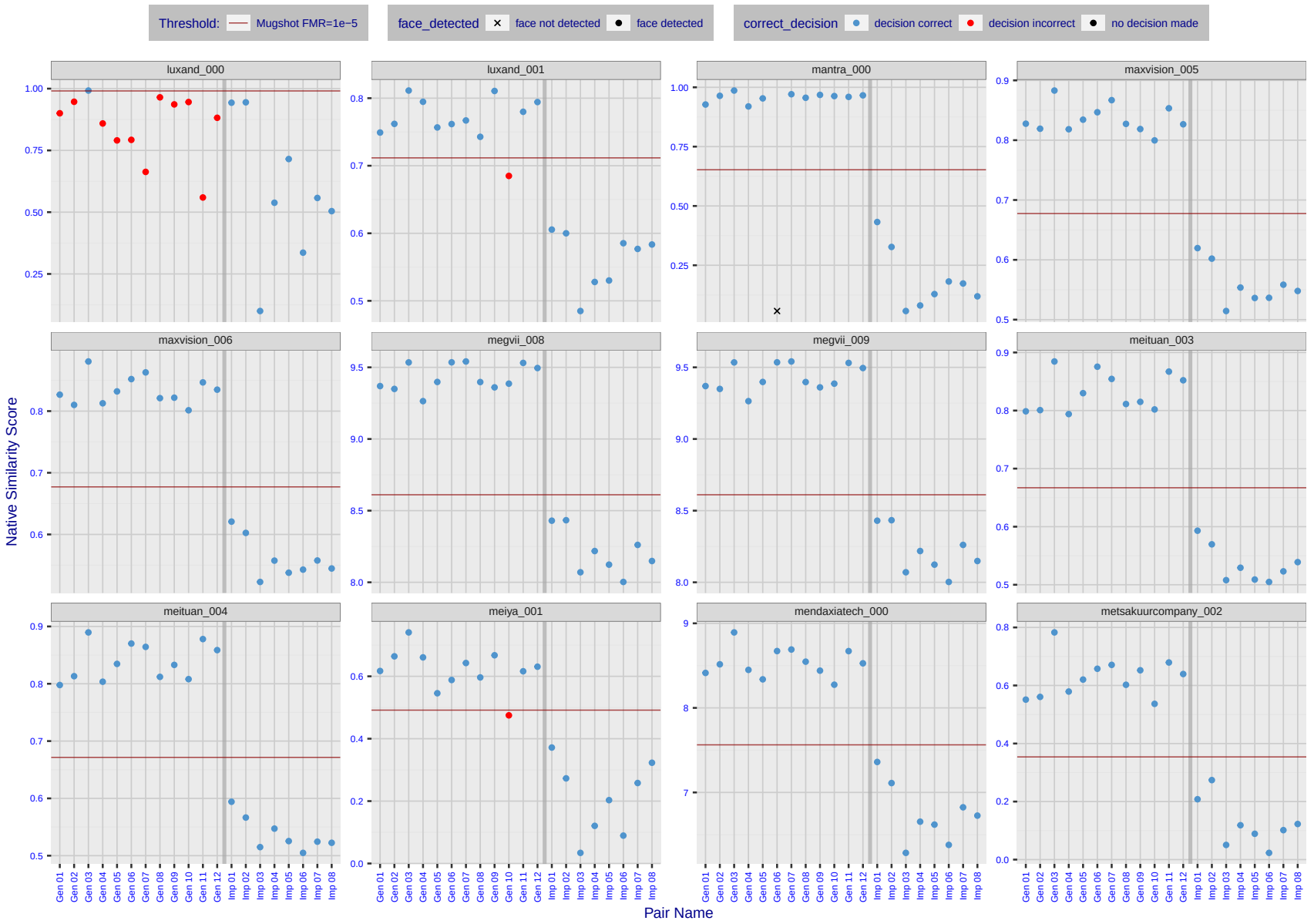

Figure 29: The figure shows algorithms' similarity scores for 12 genuine and 8 impostor image pairs used in a May 2018 paper by Phillips et al. ([1]). The threshold (red horizontal line) is a value calibrated to give FMR = 0.0001 on mugshot images. Points above the threshold correspond to pairs determined to be genuine, and points below the threshold correspond to pairs determined to be impostors. If the determined class (genuine or impostor) matches the real class, points will be blue; if not, red. An X represents face detection failure in either of the images in the pair. Note that the sample size (n=20) is small, and the figure may change substantially if larger or different sets are used. The images can be viewed on p. 13 of the Appendix, where Gen 01 corresponds to Same-Identity Pair 1, Gen 02 corresponds to Same-Identity Pair 2, and so on.

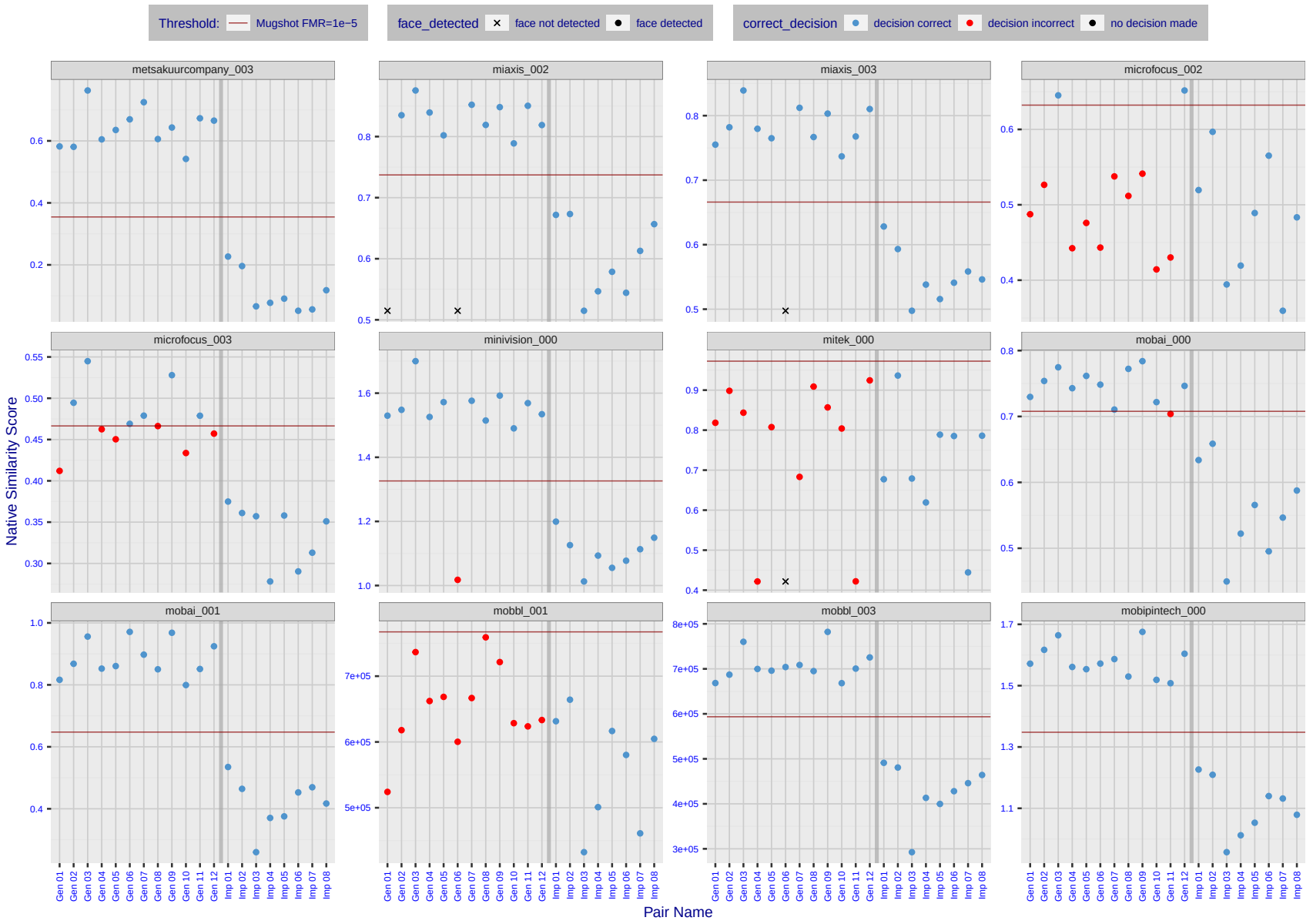

Figure 30: The figure shows algorithms' similarity scores for 12 genuine and 8 impostor image pairs used in a May 2018 paper by Phillips et al. ([1]). The threshold (red horizontal line) is a value calibrated to give FMR = 0.0001 on mugshot images. Points above the threshold correspond to pairs determined to be genuine, and points below the threshold correspond to pairs determined to be impostors. If the determined class (genuine or impostor) matches the real class, points will be blue; if not, red. An X represents face detection failure in either of the images in the pair. Note that the sample size (n=20) is small, and the figure may change substantially if larger or different sets are used. The images can be viewed on p. 13 of the Appendix, where Gen 01 corresponds to Same-Identity Pair 1, Gen 02 corresponds to Same-Identity Pair 2, and so on.

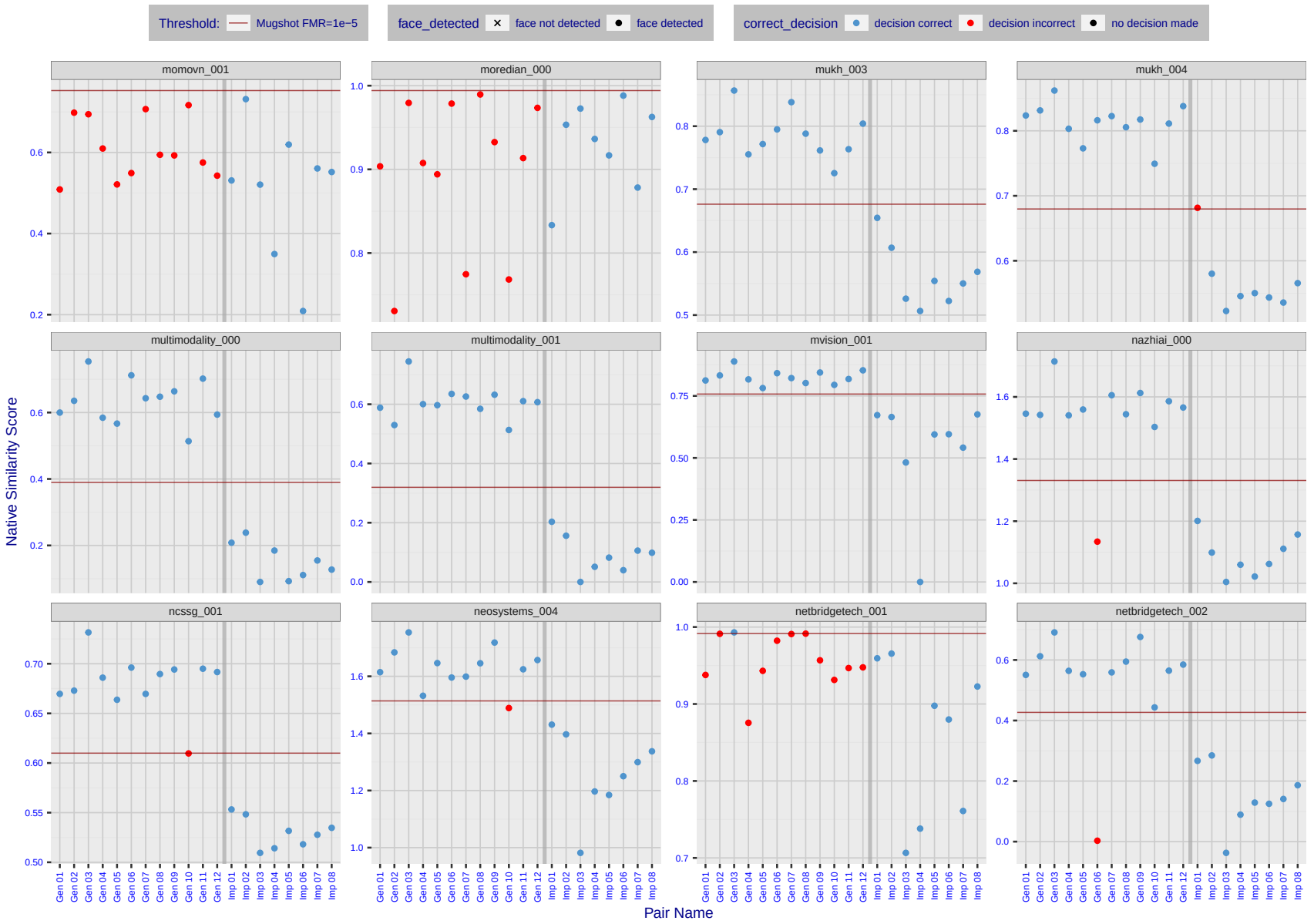

Figure 31: The figure shows algorithms' similarity scores for 12 genuine and 8 impostor image pairs used in a May 2018 paper by Phillips et al. ([1]). The threshold (red horizontal line) is a value calibrated to give FMR = 0.0001 on mugshot images. Points above the threshold correspond to pairs determined to be genuine, and points below the threshold correspond to pairs determined to be impostors. If the determined class (genuine or impostor) matches the real class, points will be blue; if not, red. An X represents face detection failure in either of the images in the pair. Note that the sample size (n=20) is small, and the figure may change substantially if larger or different sets are used. The images can be viewed on p. 13 of the Appendix, where Gen 01 corresponds to Same-Identity Pair 1, Gen 02 corresponds to Same-Identity Pair 2, and so on.

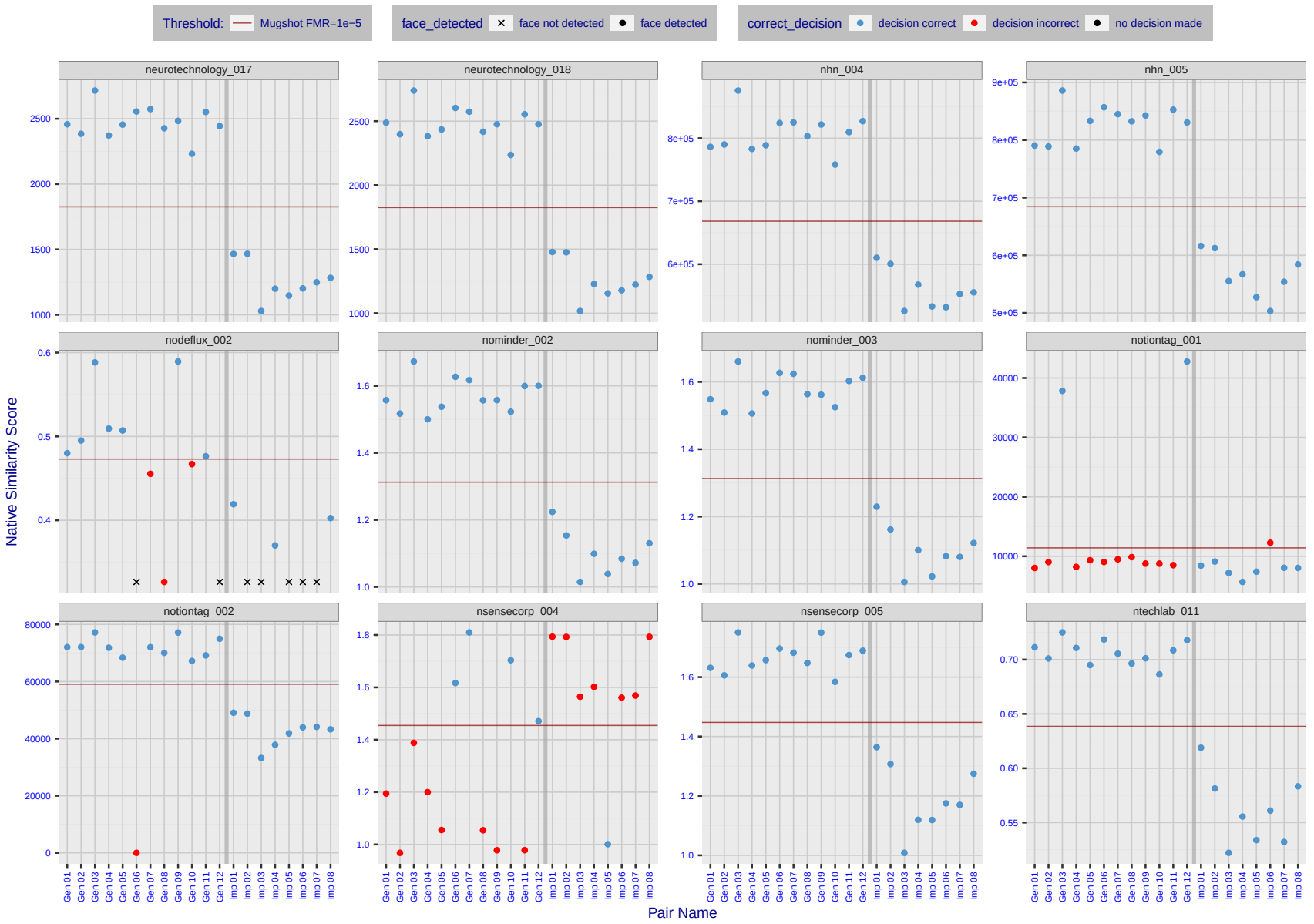

Figure 32: The figure shows algorithms' similarity scores for 12 genuine and 8 impostor image pairs used in a May 2018 paper by Phillips et al. ([1]). The threshold (red horizontal line) is a value calibrated to give FMR = 0.0001 on mugshot images. Points above the threshold correspond to pairs determined to be genuine, and points below the threshold correspond to pairs determined to be impostors. If the determined class (genuine or impostor) matches the real class, points will be blue; if not, red. An X represents face detection failure in either of the images in the pair. Note that the sample size (n=20) is small, and the figure may change substantially if larger or different sets are used. The images can be viewed on p. 13 of the Appendix, where Gen 01 corresponds to Same-Identity Pair 1, Gen 02 corresponds to Same-Identity Pair 2, and so on.

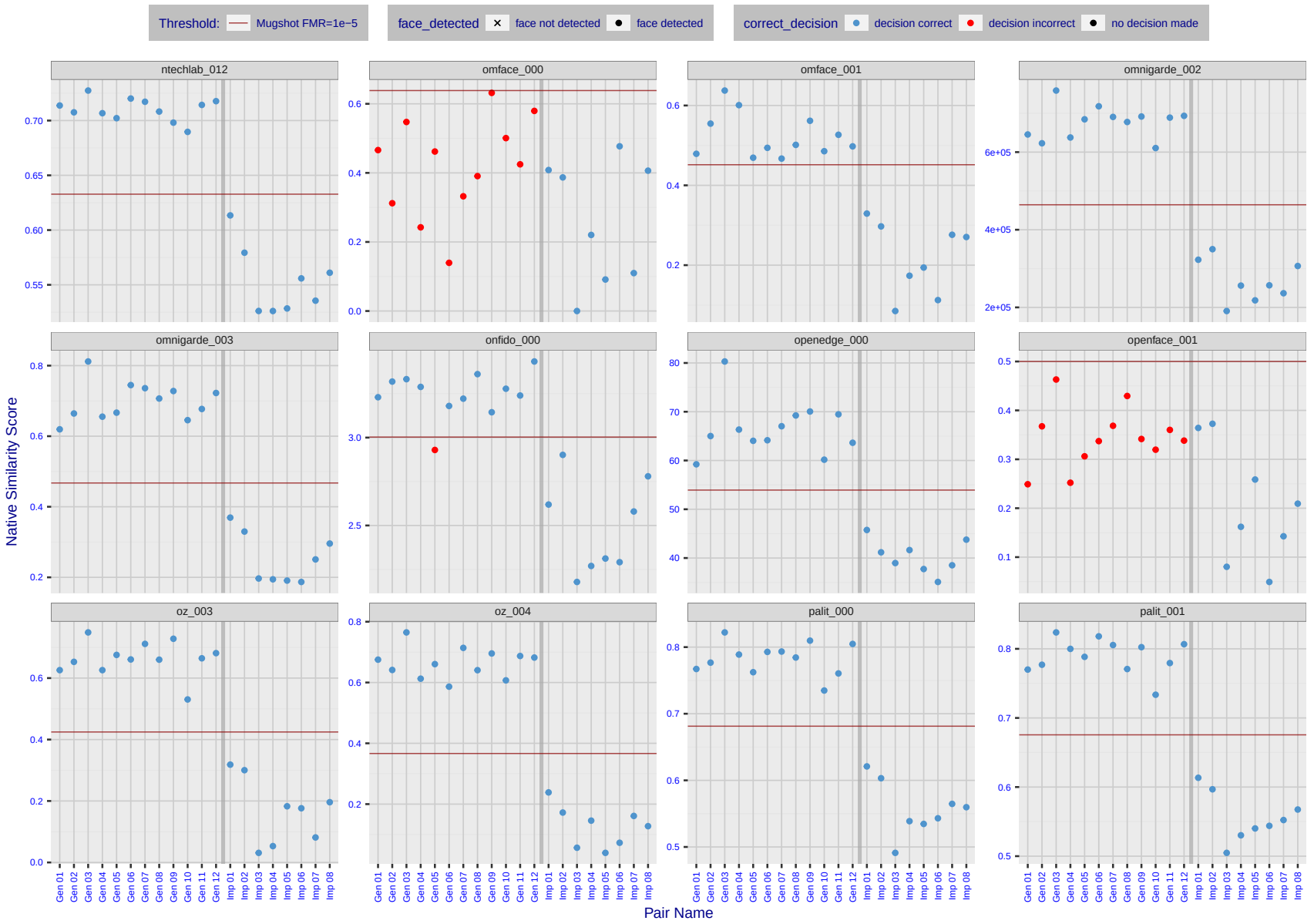

Figure 33: The figure shows algorithms' similarity scores for 12 genuine and 8 impostor image pairs used in a May 2018 paper by Phillips et al. ([1]). The threshold (red horizontal line) is a value calibrated to give FMR = 0.0001 on mugshot images. Points above the threshold correspond to pairs determined to be genuine, and points below the threshold correspond to pairs determined to be impostors. If the determined class (genuine or impostor) matches the real class, points will be blue; if not, red. An X represents face detection failure in either of the images in the pair. Note that the sample size (n=20) is small, and the figure may change substantially if larger or different sets are used. The images can be viewed on p. 13 of the Appendix, where Gen 01 corresponds to Same-Identity Pair 1, Gen 02 corresponds to Same-Identity Pair 2, and so on.

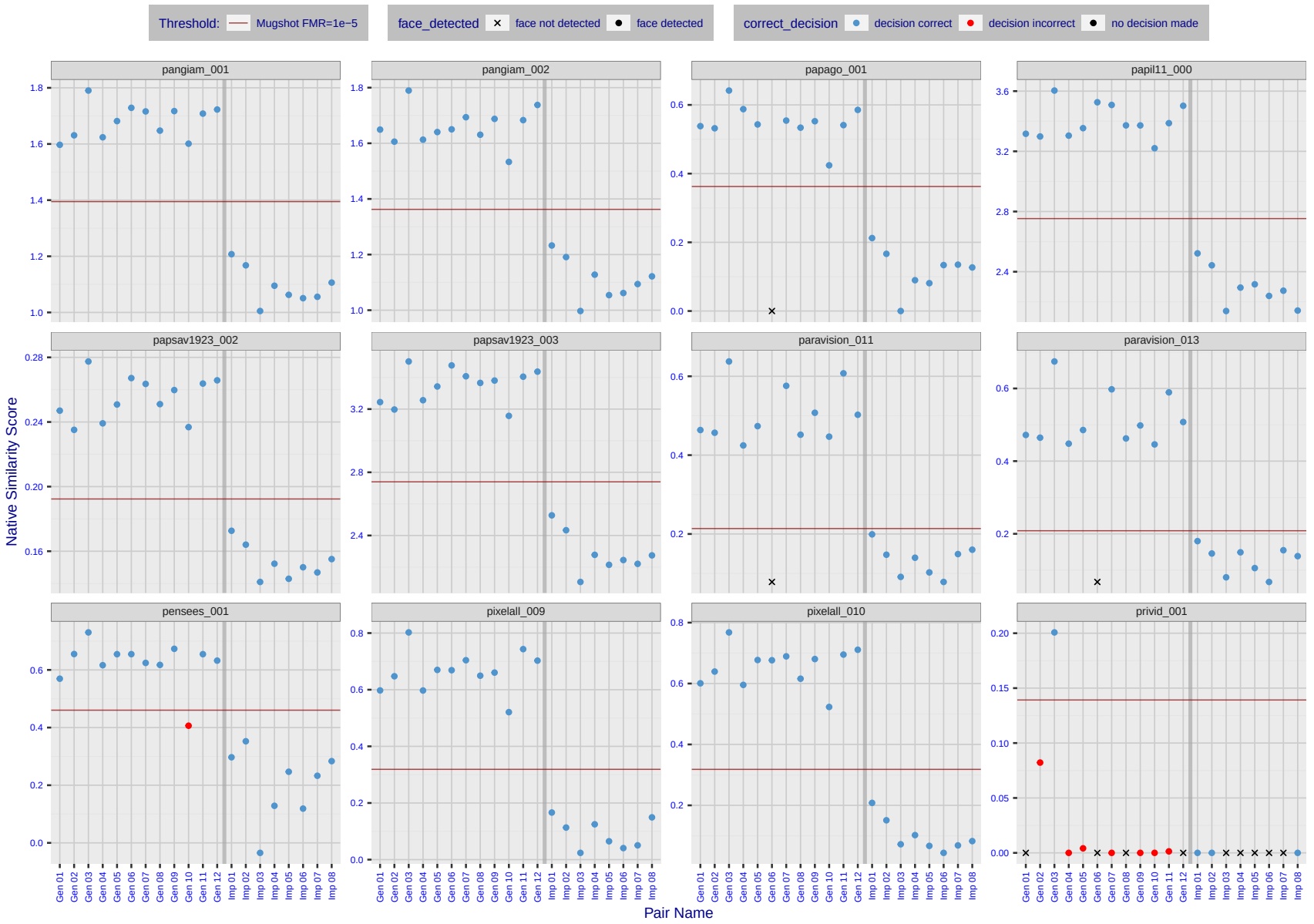

Figure 34: The figure shows algorithms' similarity scores for 12 genuine and 8 impostor image pairs used in a May 2018 paper by Phillips et al. ([1]). The threshold (red horizontal line) is a value calibrated to give FMR = 0.0001 on mugshot images. Points above the threshold correspond to pairs determined to be genuine, and points below the threshold correspond to pairs determined to be impostors. If the determined class (genuine or impostor) matches the real class, points will be blue; if not, red. An X represents face detection failure in either of the images in the pair. Note that the sample size (n=20) is small, and the figure may change substantially if larger or different sets are used. The images can be viewed on p. 13 of the Appendix, where Gen 01 corresponds to Same-Identity Pair 1, Gen 02 corresponds to Same-Identity Pair 2, and so on.

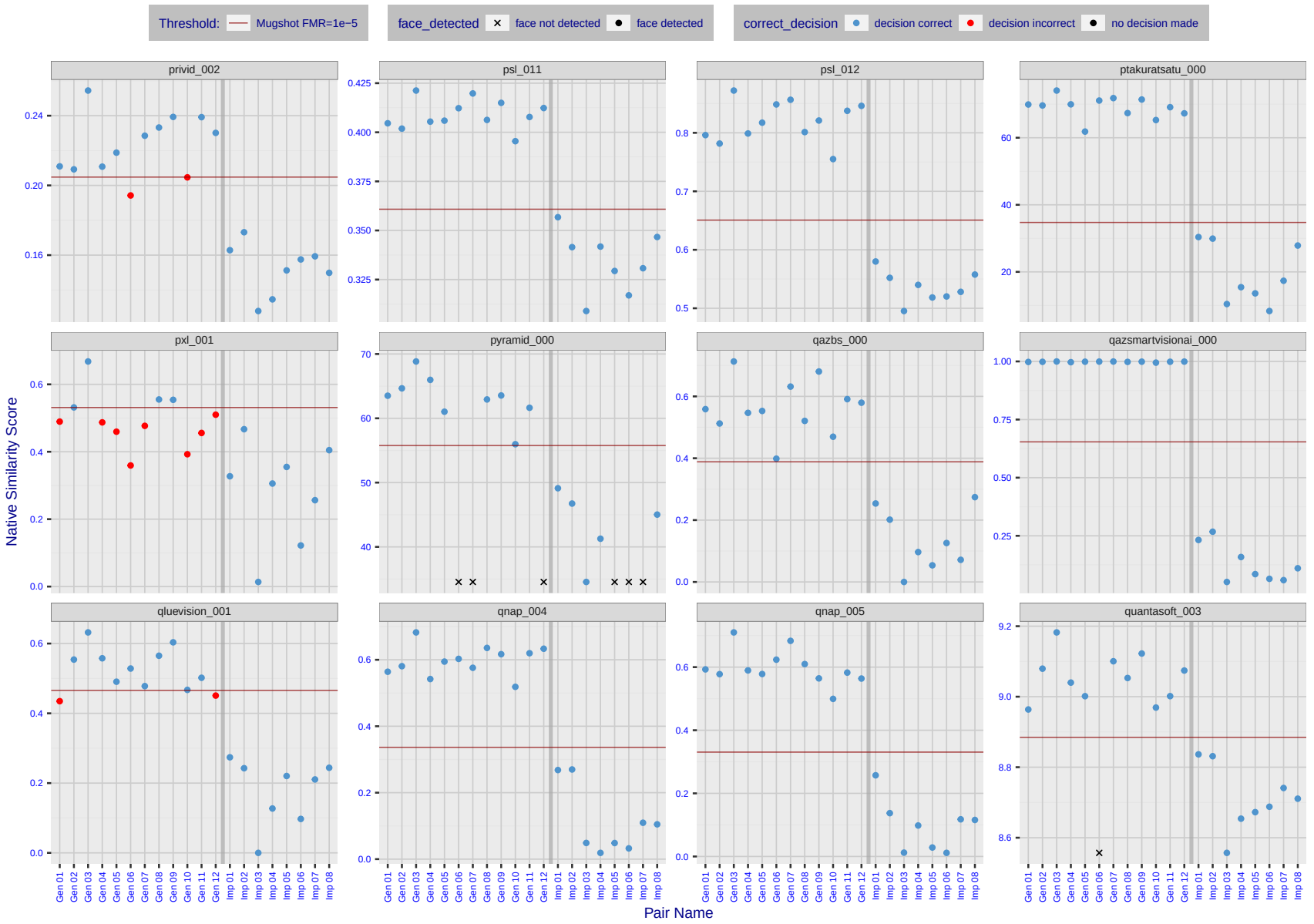

Figure 35: The figure shows algorithms' similarity scores for 12 genuine and 8 impostor image pairs used in a May 2018 paper by Phillips et al. ([1]). The threshold (red horizontal line) is a value calibrated to give FMR = 0.0001 on mugshot images. Points above the threshold correspond to pairs determined to be genuine, and points below the threshold correspond to pairs determined to be impostors. If the determined class (genuine or impostor) matches the real class, points will be blue; if not, red. An X represents face detection failure in either of the images in the pair. Note that the sample size (n=20) is small, and the figure may change substantially if larger or different sets are used. The images can be viewed on p. 13 of the Appendix, where Gen 01 corresponds to Same-Identity Pair 1, Gen 02 corresponds to Same-Identity Pair 2, and so on.

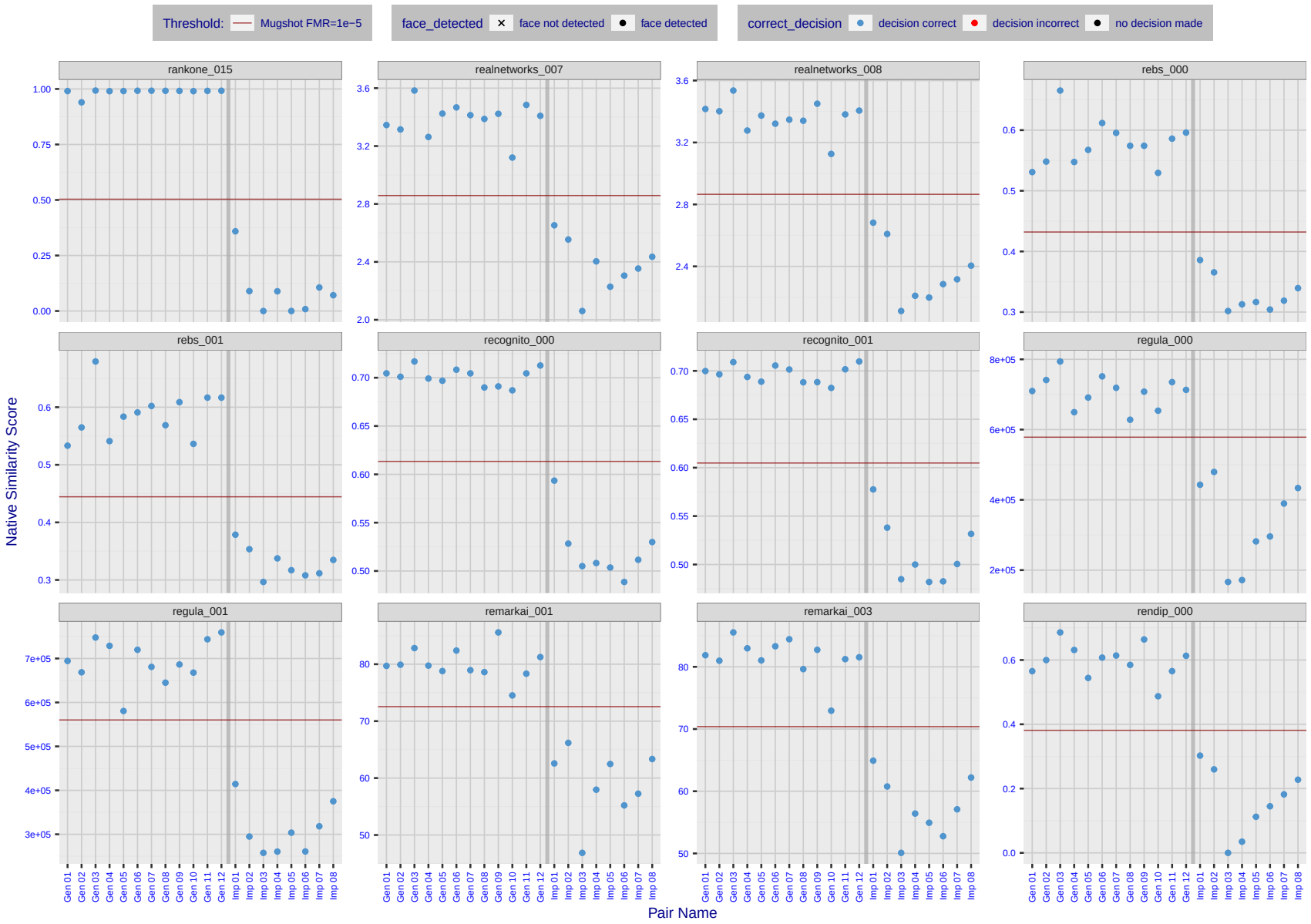

Figure 36: The figure shows algorithms' similarity scores for 12 genuine and 8 impostor image pairs used in a May 2018 paper by Phillips et al. ([1]). The threshold (red horizontal line) is a value calibrated to give FMR = 0.0001 on mugshot images. Points above the threshold correspond to pairs determined to be genuine, and points below the threshold correspond to pairs determined to be impostors. If the determined class (genuine or impostor) matches the real class, points will be blue; if not, red. An X represents face detection failure in either of the images in the pair. Note that the sample size (n=20) is small, and the figure may change substantially if larger or different sets are used. The images can be viewed on p. 13 of the Appendix, where Gen 01 corresponds to Same-Identity Pair 1, Gen 02 corresponds to Same-Identity Pair 2, and so on.

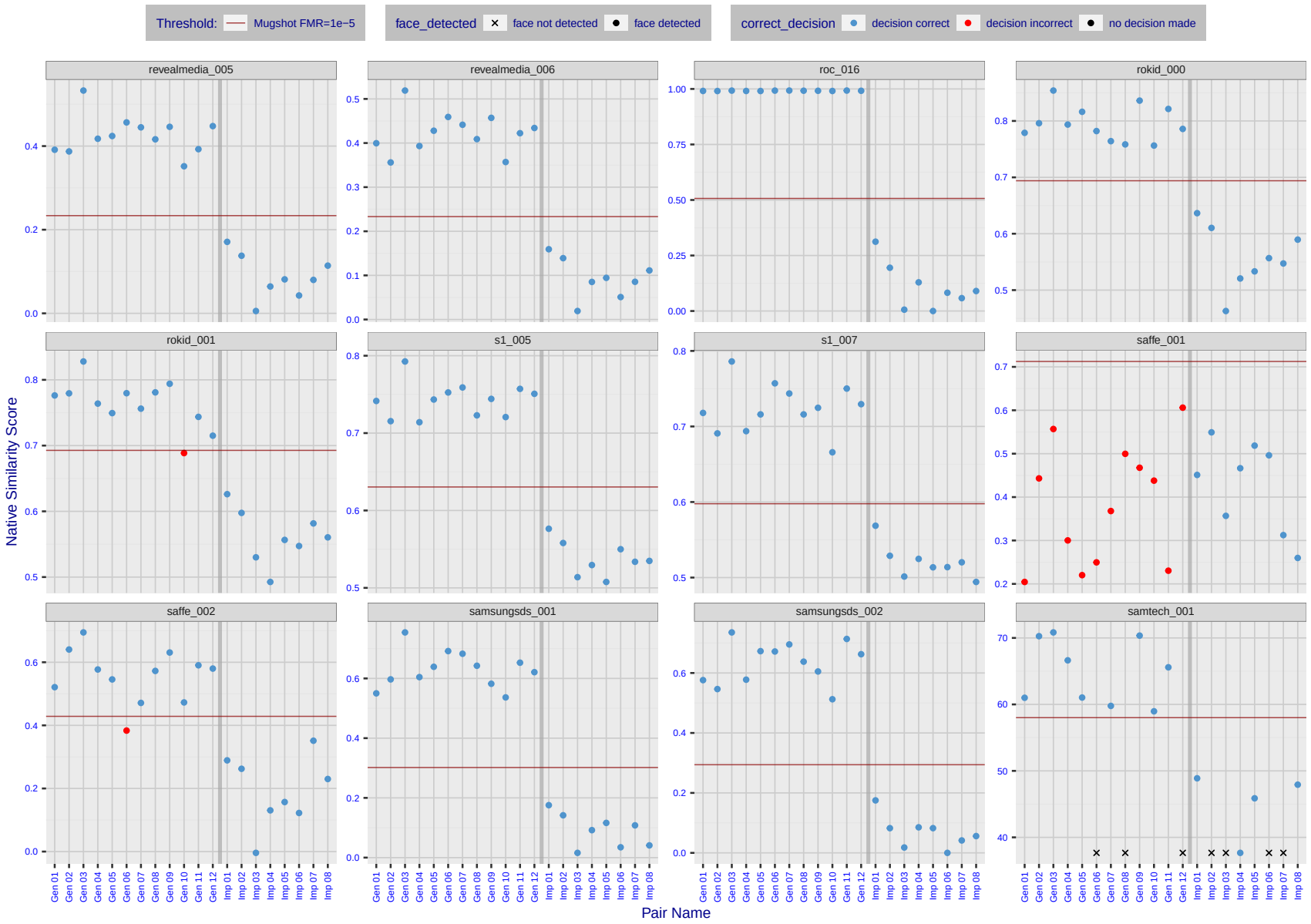

Figure 37: The figure shows algorithms' similarity scores for 12 genuine and 8 impostor image pairs used in a May 2018 paper by Phillips et al. ([1]). The threshold (red horizontal line) is a value calibrated to give FMR = 0.0001 on mugshot images. Points above the threshold correspond to pairs determined to be genuine, and points below the threshold correspond to pairs determined to be impostors. If the determined class (genuine or impostor) matches the real class, points will be blue; if not, red. An X represents face detection failure in either of the images in the pair. Note that the sample size (n=20) is small, and the figure may change substantially if larger or different sets are used. The images can be viewed on p. 13 of the Appendix, where Gen 01 corresponds to Same-Identity Pair 1, Gen 02 corresponds to Same-Identity Pair 2, and so on.

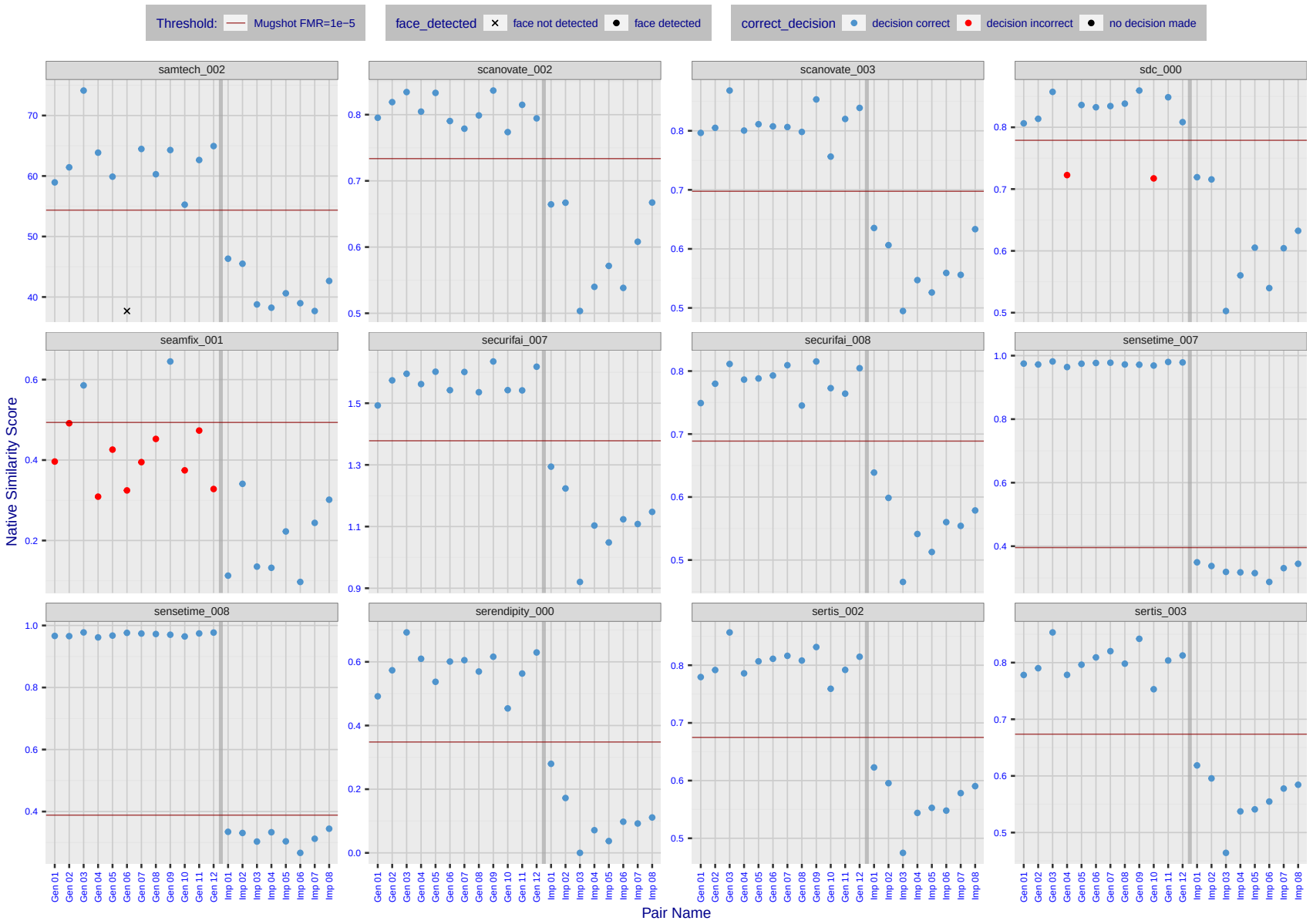

Figure 38: The figure shows algorithms' similarity scores for 12 genuine and 8 impostor image pairs used in a May 2018 paper by Phillips et al. ([1]). The threshold (red horizontal line) is a value calibrated to give FMR = 0.0001 on mugshot images. Points above the threshold correspond to pairs determined to be genuine, and points below the threshold correspond to pairs determined to be impostors. If the determined class (genuine or impostor) matches the real class, points will be blue; if not, red. An X represents face detection failure in either of the images in the pair. Note that the sample size (n=20) is small, and the figure may change substantially if larger or different sets are used. The images can be viewed on p. 13 of the Appendix, where Gen 01 corresponds to Same-Identity Pair 1, Gen 02 corresponds to Same-Identity Pair 2, and so on.

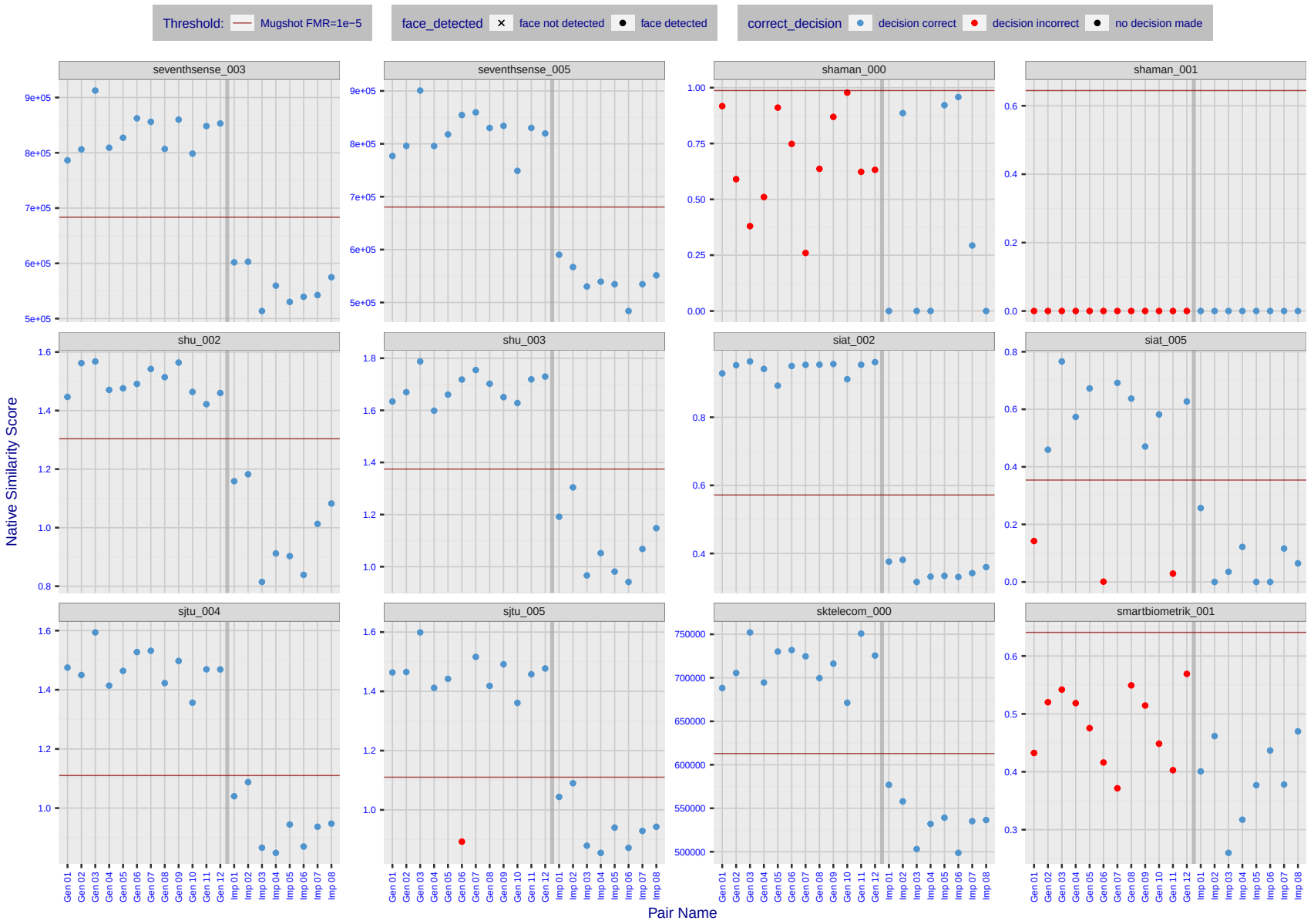

Figure 39: The figure shows algorithms' similarity scores for 12 genuine and 8 impostor image pairs used in a May 2018 paper by Phillips et al. ([1]). The threshold (red horizontal line) is a value calibrated to give FMR = 0.0001 on mugshot images. Points above the threshold correspond to pairs determined to be genuine, and points below the threshold correspond to pairs determined to be impostors. If the determined class (genuine or impostor) matches the real class, points will be blue; if not, red. An X represents face detection failure in either of the images in the pair. Note that the sample size (n=20) is small, and the figure may change substantially if larger or different sets are used. The images can be viewed on p. 13 of the Appendix, where Gen 01 corresponds to Same-Identity Pair 1, Gen 02 corresponds to Same-Identity Pair 2, and so on.

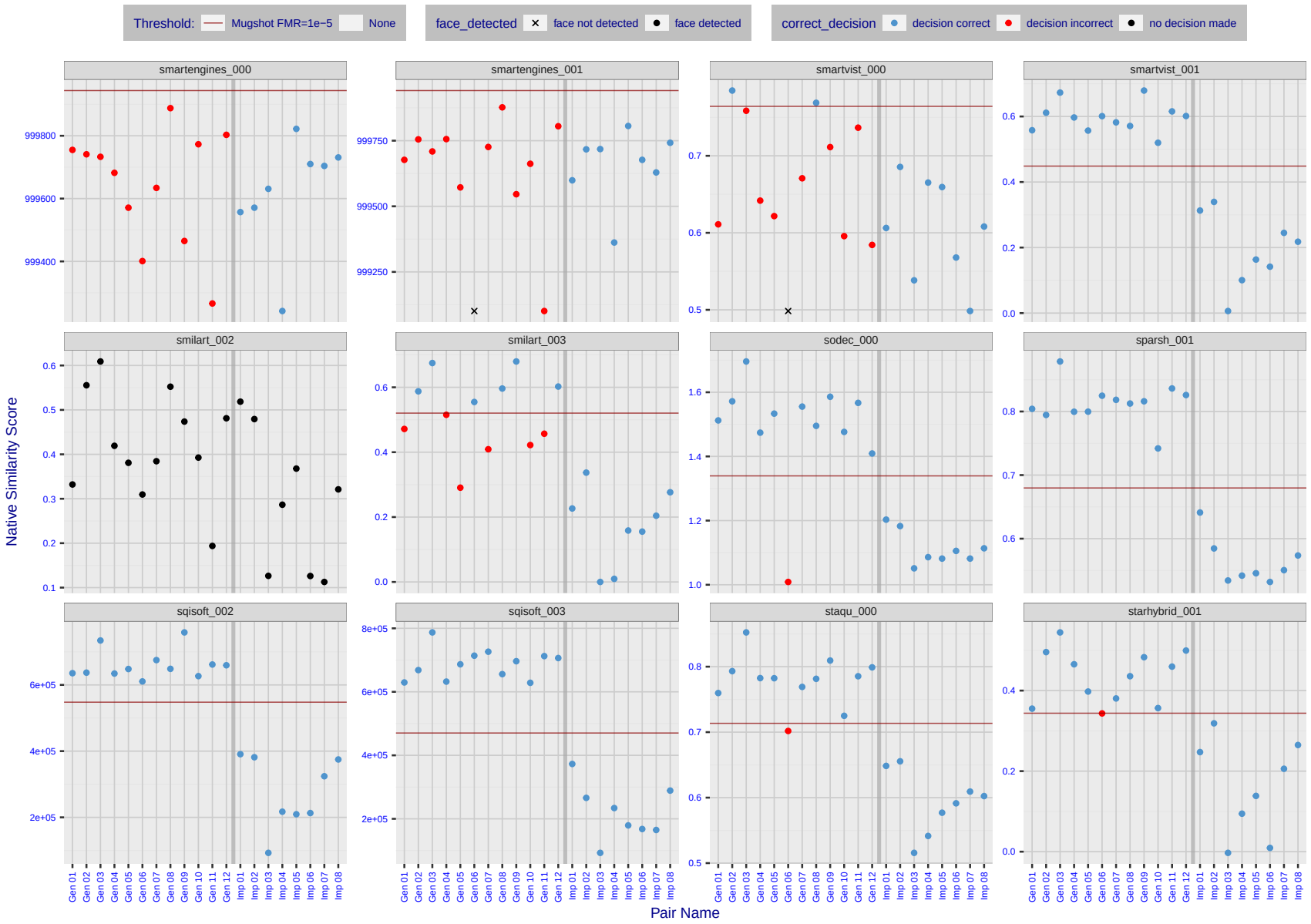

Figure 40: The figure shows algorithms' similarity scores for 12 genuine and 8 impostor image pairs used in a May 2018 paper by Phillips et al. ([1]). The threshold (red horizontal line) is a value calibrated to give FMR = 0.0001 on mugshot images. Points above the threshold correspond to pairs determined to be genuine, and points below the threshold correspond to pairs determined to be impostors. If the determined class (genuine or impostor) matches the real class, points will be blue; if not, red. An X represents face detection failure in either of the images in the pair. Note that the sample size (n=20) is small, and the figure may change substantially if larger or different sets are used. The images can be viewed on p. 13 of the Appendix, where Gen 01 corresponds to Same-Identity Pair 1, Gen 02 corresponds to Same-Identity Pair 2, and so on.

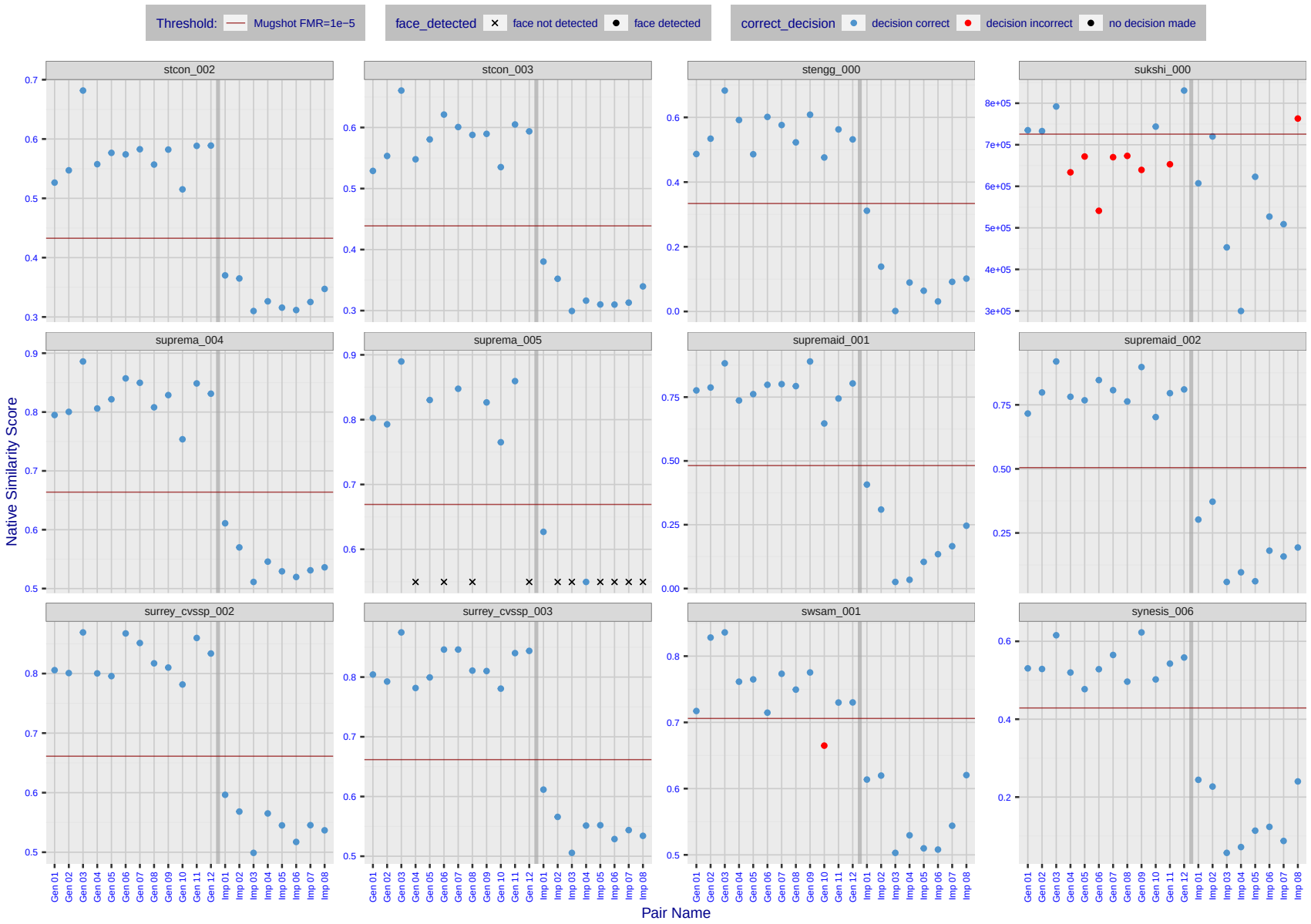

Figure 41: The figure shows algorithms' similarity scores for 12 genuine and 8 impostor image pairs used in a May 2018 paper by Phillips et al. ([1]). The threshold (red horizontal line) is a value calibrated to give FMR = 0.0001 on mugshot images. Points above the threshold correspond to pairs determined to be genuine, and points below the threshold correspond to pairs determined to be impostors. If the determined class (genuine or impostor) matches the real class, points will be blue; if not, red. An X represents face detection failure in either of the images in the pair. Note that the sample size (n=20) is small, and the figure may change substantially if larger or different sets are used. The images can be viewed on p. 13 of the Appendix, where Gen 01 corresponds to Same-Identity Pair 1, Gen 02 corresponds to Same-Identity Pair 2, and so on.

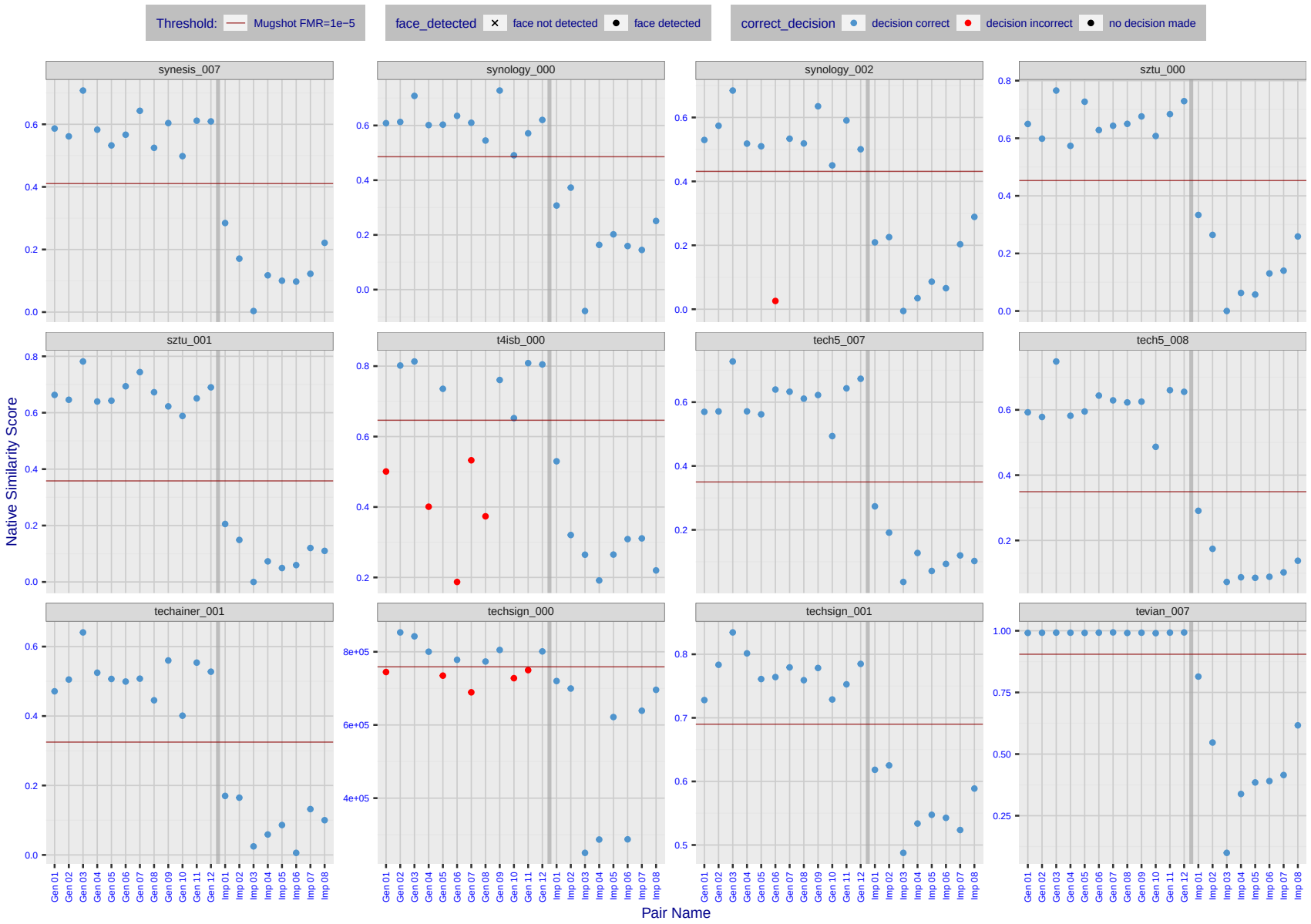

Figure 42: The figure shows algorithms' similarity scores for 12 genuine and 8 impostor image pairs used in a May 2018 paper by Phillips et al. ([1]). The threshold (red horizontal line) is a value calibrated to give FMR = 0.0001 on mugshot images. Points above the threshold correspond to pairs determined to be genuine, and points below the threshold correspond to pairs determined to be impostors. If the determined class (genuine or impostor) matches the real class, points will be blue; if not, red. An X represents face detection failure in either of the images in the pair. Note that the sample size (n=20) is small, and the figure may change substantially if larger or different sets are used. The images can be viewed on p. 13 of the Appendix, where Gen 01 corresponds to Same-Identity Pair 1, Gen 02 corresponds to Same-Identity Pair 2, and so on.

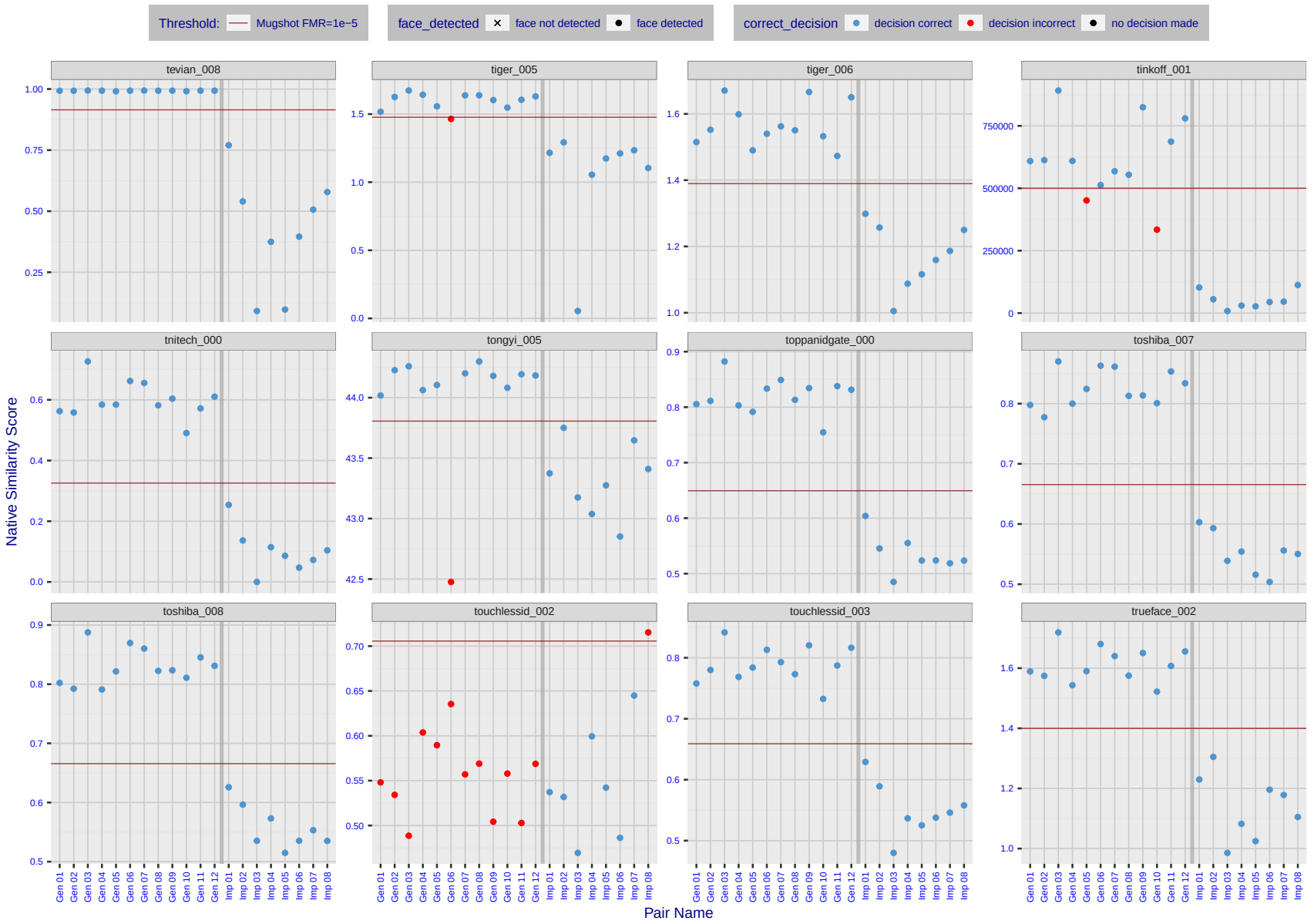

Figure 43: The figure shows algorithms' similarity scores for 12 genuine and 8 impostor image pairs used in a May 2018 paper by Phillips et al. ([1]). The threshold (red horizontal line) is a value calibrated to give FMR = 0.0001 on mugshot images. Points above the threshold correspond to pairs determined to be genuine, and points below the threshold correspond to pairs determined to be impostors. If the determined class (genuine or impostor) matches the real class, points will be blue; if not, red. An X represents face detection failure in either of the images in the pair. Note that the sample size (n=20) is small, and the figure may change substantially if larger or different sets are used. The images can be viewed on p. 13 of the Appendix, where Gen 01 corresponds to Same-Identity Pair 1, Gen 02 corresponds to Same-Identity Pair 2, and so on.

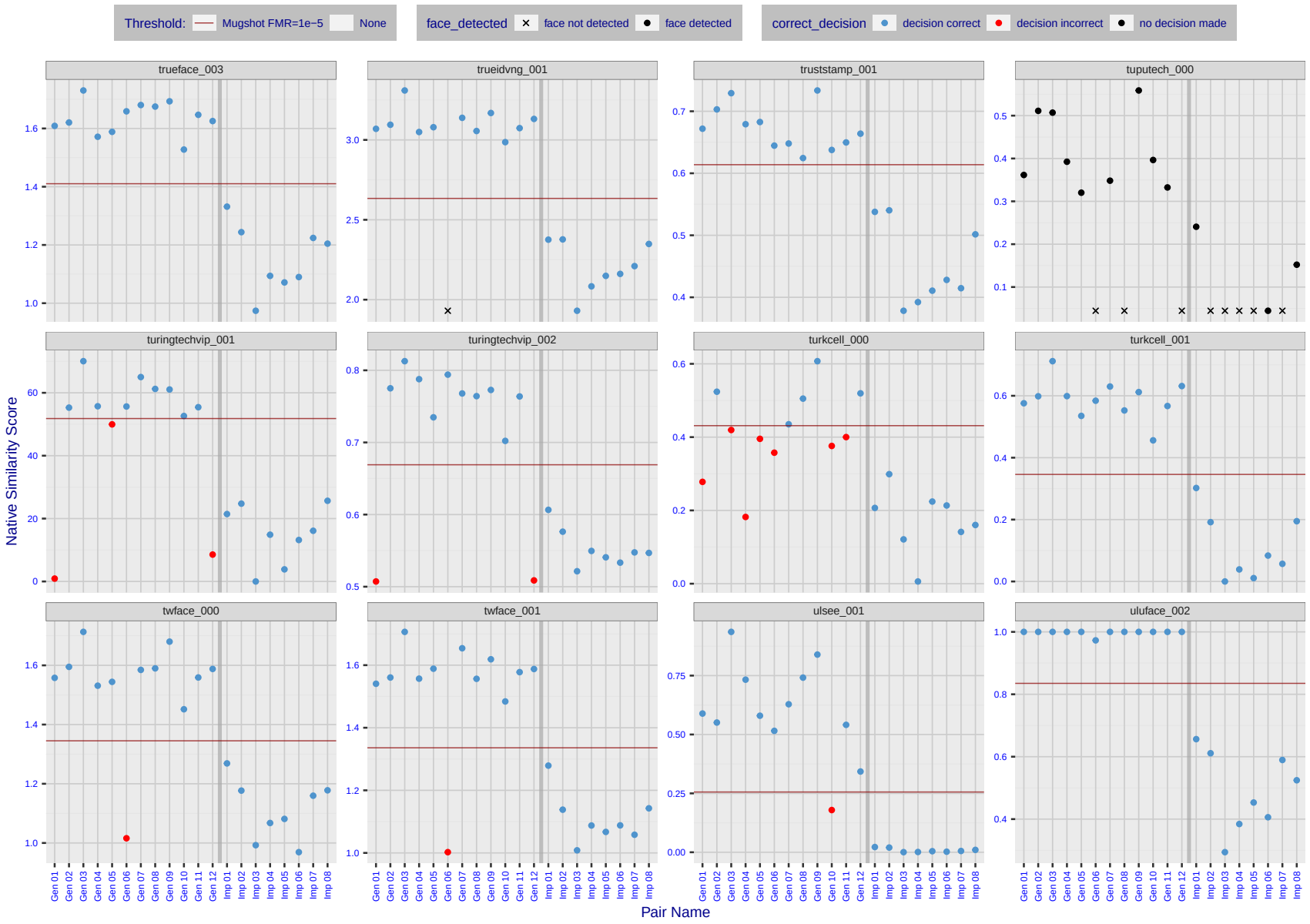

Figure 44: The figure shows algorithms' similarity scores for 12 genuine and 8 impostor image pairs used in a May 2018 paper by Phillips et al. ([1]). The threshold (red horizontal line) is a value calibrated to give FMR = 0.0001 on mugshot images. Points above the threshold correspond to pairs determined to be genuine, and points below the threshold correspond to pairs determined to be impostors. If the determined class (genuine or impostor) matches the real class, points will be blue; if not, red. An X represents face detection failure in either of the images in the pair. Note that the sample size (n=20) is small, and the figure may change substantially if larger or different sets are used. The images can be viewed on p. 13 of the Appendix, where Gen 01 corresponds to Same-Identity Pair 1, Gen 02 corresponds to Same-Identity Pair 2, and so on.

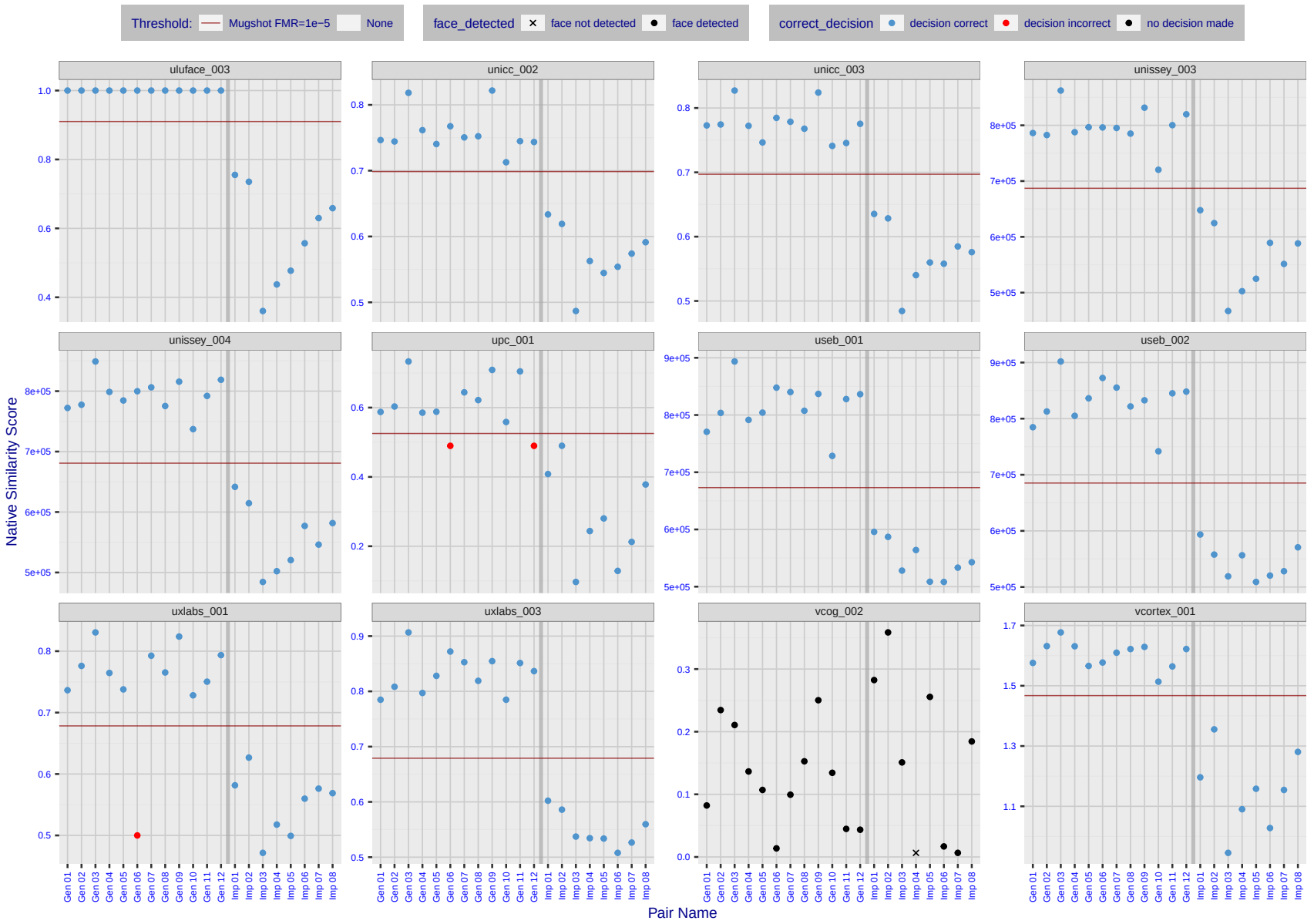

Figure 45: The figure shows algorithms' similarity scores for 12 genuine and 8 impostor image pairs used in a May 2018 paper by Phillips et al. ([1]). The threshold (red horizontal line) is a value calibrated to give FMR = 0.0001 on mugshot images. Points above the threshold correspond to pairs determined to be genuine, and points below the threshold correspond to pairs determined to be impostors. If the determined class (genuine or impostor) matches the real class, points will be blue; if not, red. An X represents face detection failure in either of the images in the pair. Note that the sample size (n=20) is small, and the figure may change substantially if larger or different sets are used. The images can be viewed on p. 13 of the Appendix, where Gen 01 corresponds to Same-Identity Pair 1, Gen 02 corresponds to Same-Identity Pair 2, and so on.

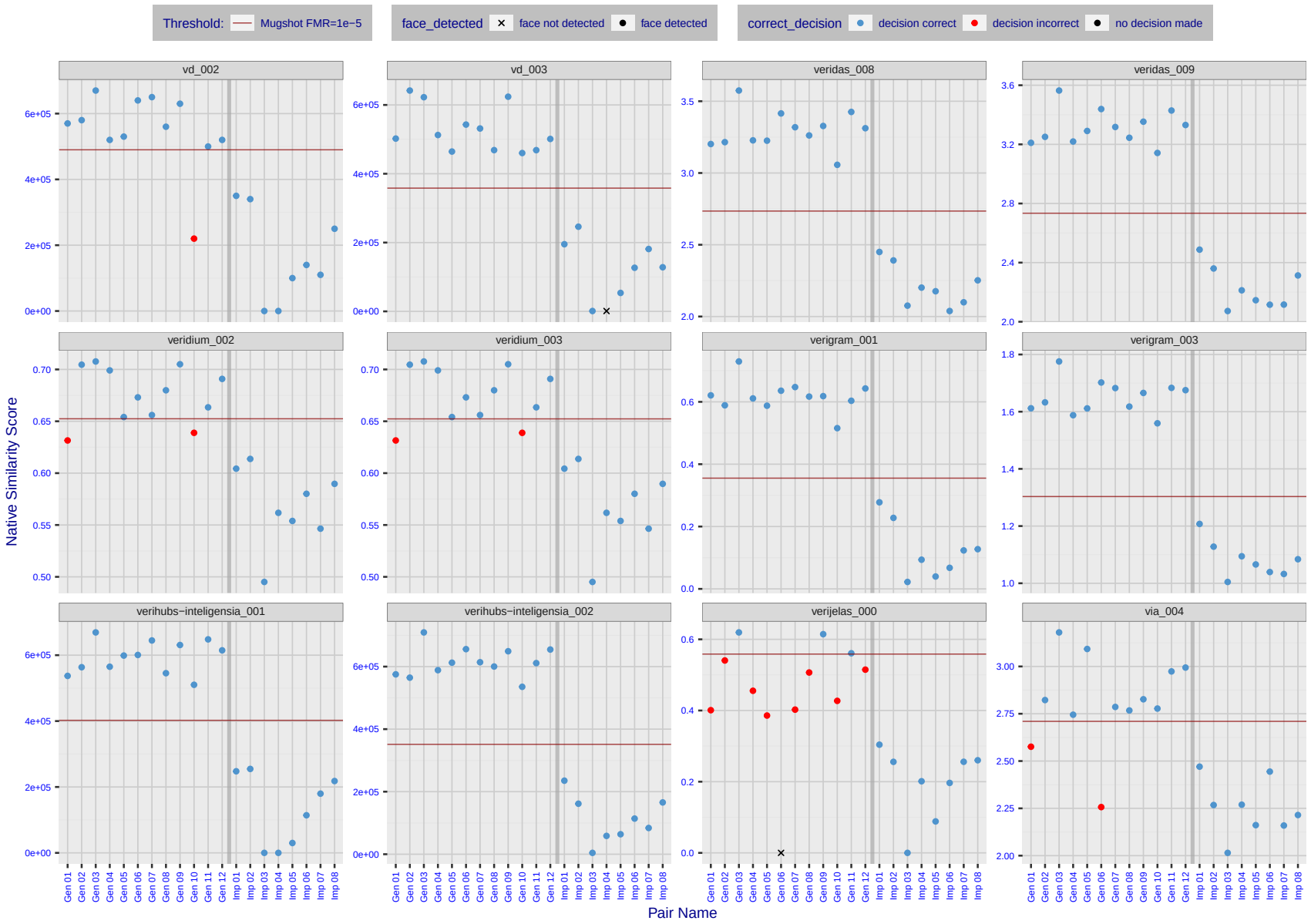

Figure 46: The figure shows algorithms' similarity scores for 12 genuine and 8 impostor image pairs used in a May 2018 paper by Phillips et al. ([1]). The threshold (red horizontal line) is a value calibrated to give FMR = 0.0001 on mugshot images. Points above the threshold correspond to pairs determined to be genuine, and points below the threshold correspond to pairs determined to be impostors. If the determined class (genuine or impostor) matches the real class, points will be blue; if not, red. An X represents face detection failure in either of the images in the pair. Note that the sample size (n=20) is small, and the figure may change substantially if larger or different sets are used. The images can be viewed on p. 13 of the Appendix, where Gen 01 corresponds to Same-Identity Pair 1, Gen 02 corresponds to Same-Identity Pair 2, and so on.

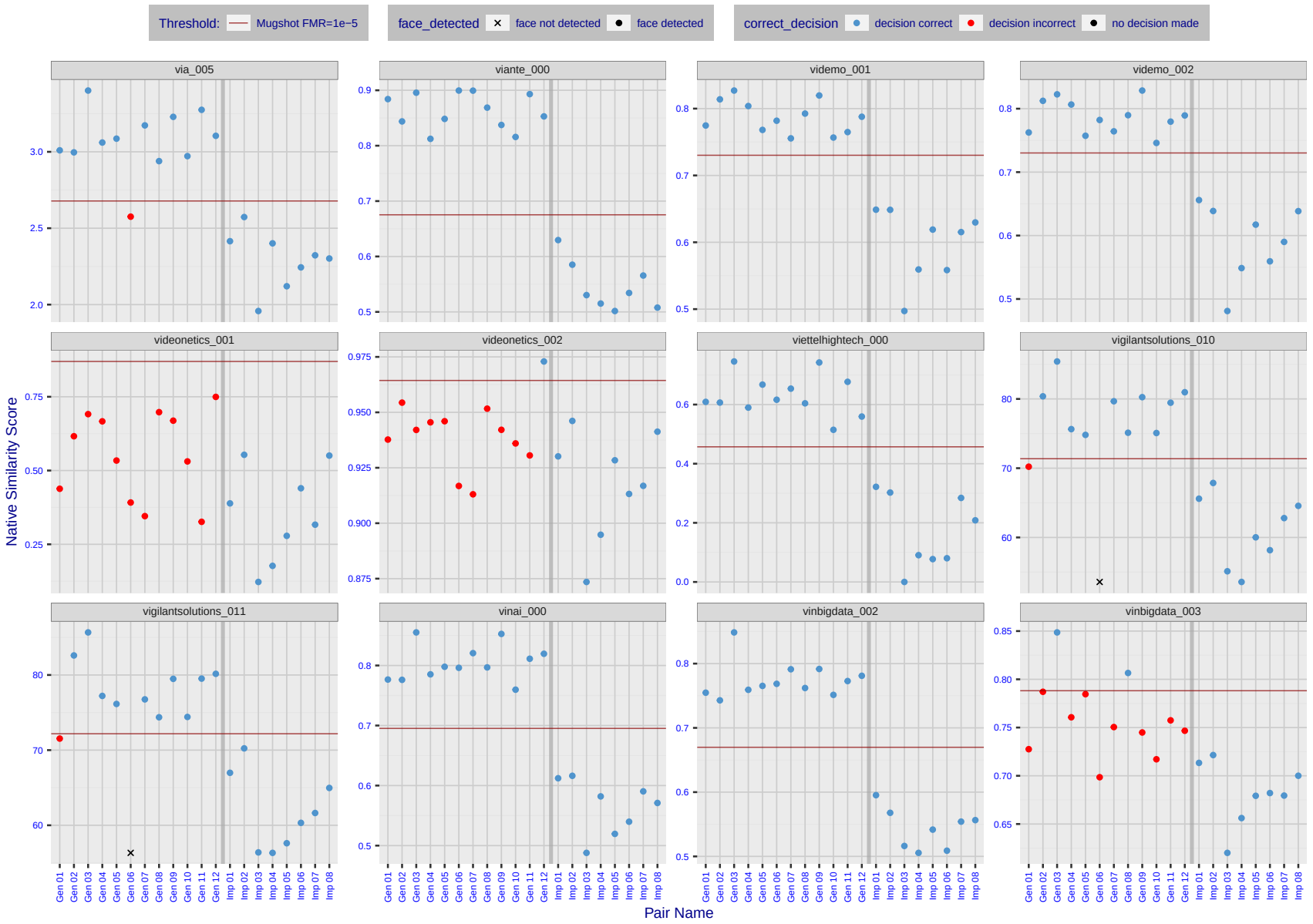

Figure 47: The figure shows algorithms' similarity scores for 12 genuine and 8 impostor image pairs used in a May 2018 paper by Phillips et al. ([1]). The threshold (red horizontal line) is a value calibrated to give FMR = 0.0001 on mugshot images. Points above the threshold correspond to pairs determined to be genuine, and points below the threshold correspond to pairs determined to be impostors. If the determined class (genuine or impostor) matches the real class, points will be blue; if not, red. An X represents face detection failure in either of the images in the pair. Note that the sample size (n=20) is small, and the figure may change substantially if larger or different sets are used. The images can be viewed on p. 13 of the Appendix, where Gen 01 corresponds to Same-Identity Pair 1, Gen 02 corresponds to Same-Identity Pair 2, and so on.

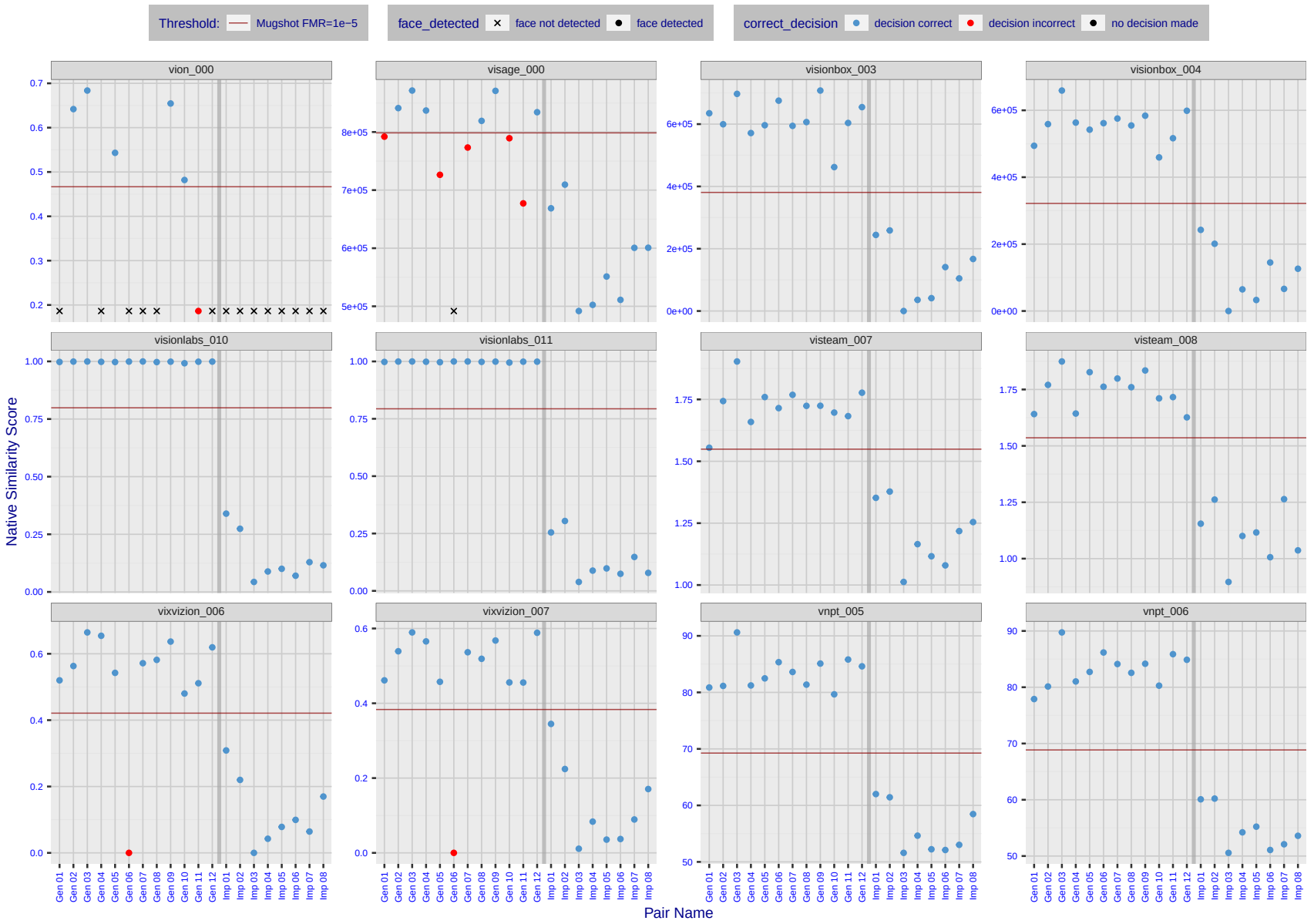

Figure 48: The figure shows algorithms' similarity scores for 12 genuine and 8 impostor image pairs used in a May 2018 paper by Phillips et al. ([1]). The threshold (red horizontal line) is a value calibrated to give FMR = 0.0001 on mugshot images. Points above the threshold correspond to pairs determined to be genuine, and points below the threshold correspond to pairs determined to be impostors. If the determined class (genuine or impostor) matches the real class, points will be blue; if not, red. An X represents face detection failure in either of the images in the pair. Note that the sample size (n=20) is small, and the figure may change substantially if larger or different sets are used. The images can be viewed on p. 13 of the Appendix, where Gen 01 corresponds to Same-Identity Pair 1, Gen 02 corresponds to Same-Identity Pair 2, and so on.

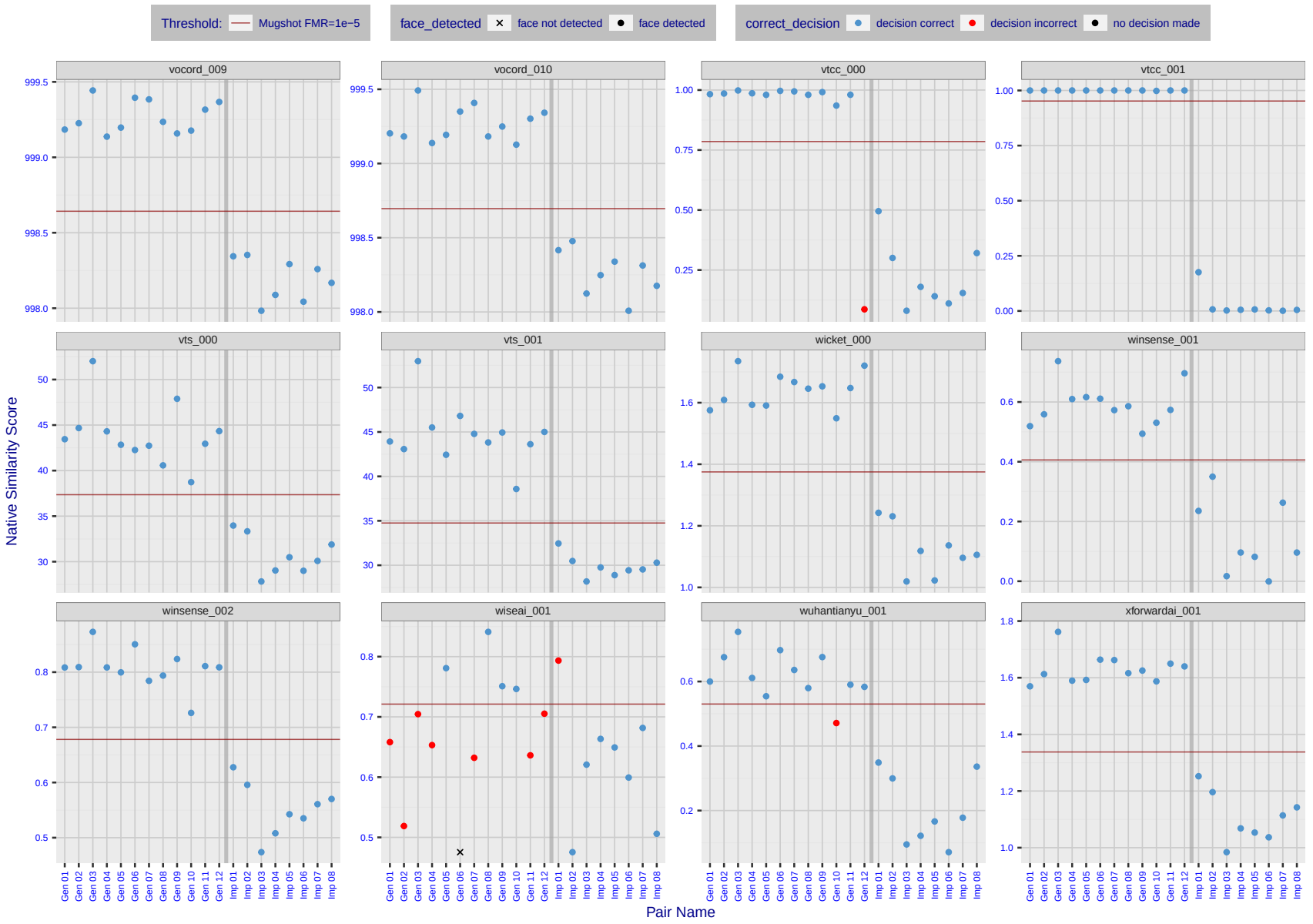

Figure 49: The figure shows algorithms' similarity scores for 12 genuine and 8 impostor image pairs used in a May 2018 paper by Phillips et al. ([1]). The threshold (red horizontal line) is a value calibrated to give FMR = 0.0001 on mugshot images. Points above the threshold correspond to pairs determined to be genuine, and points below the threshold correspond to pairs determined to be impostors. If the determined class (genuine or impostor) matches the real class, points will be blue; if not, red. An X represents face detection failure in either of the images in the pair. Note that the sample size (n=20) is small, and the figure may change substantially if larger or different sets are used. The images can be viewed on p. 13 of the Appendix, where Gen 01 corresponds to Same-Identity Pair 1, Gen 02 corresponds to Same-Identity Pair 2, and so on.

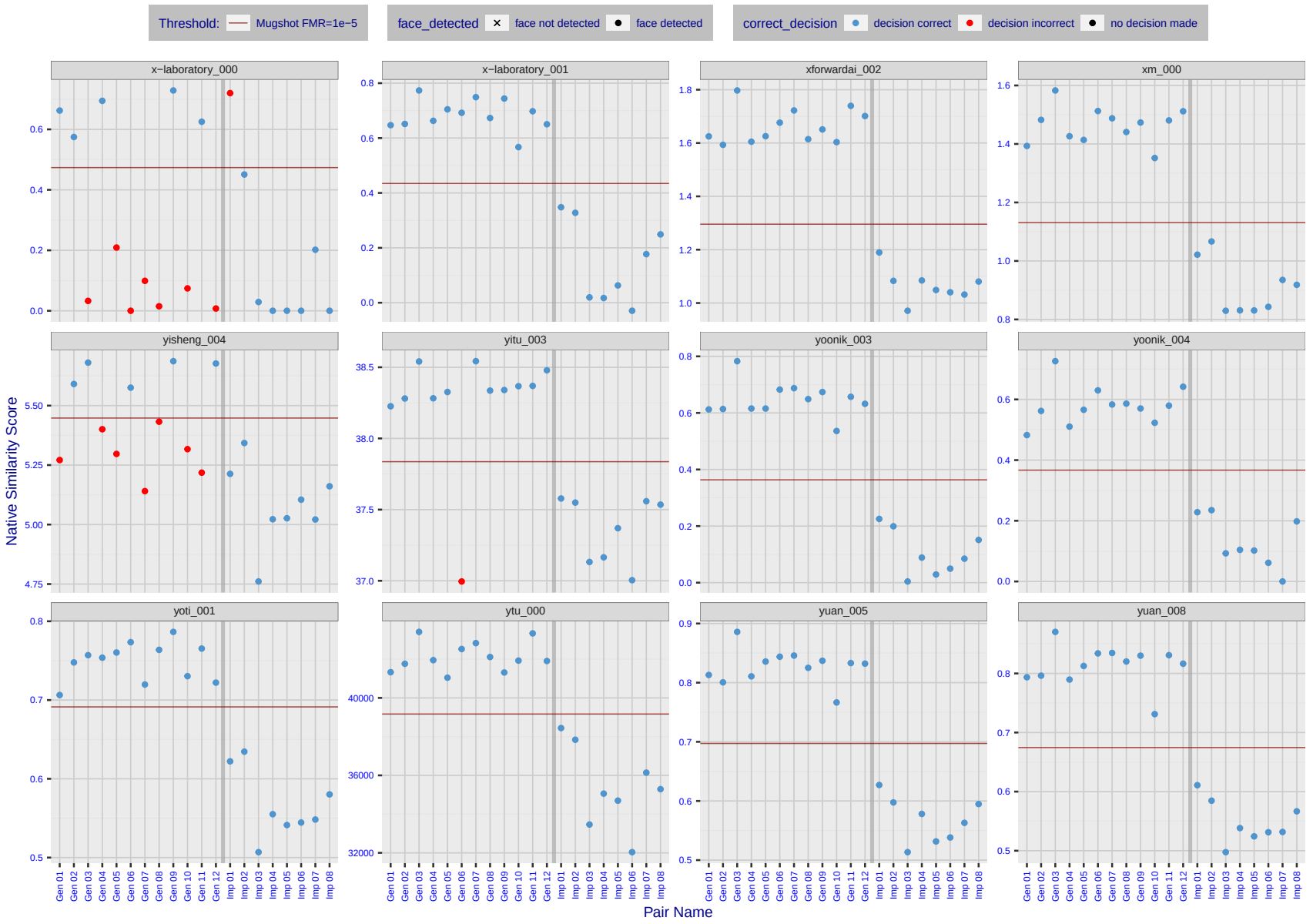

Figure 50: The figure shows algorithms' similarity scores for 12 genuine and 8 impostor image pairs used in a May 2018 paper by Phillips et al. ([1]). The threshold (red horizontal line) is a value calibrated to give FMR = 0.0001 on mugshot images. Points above the threshold correspond to pairs determined to be genuine, and points below the threshold correspond to pairs determined to be impostors. If the determined class (genuine or impostor) matches the real class, points will be blue; if not, red. An X represents face detection failure in either of the images in the pair. Note that the sample size (n=20) is small, and the figure may change substantially if larger or different sets are used. The images can be viewed on p. 13 of the Appendix, where Gen 01 corresponds to Same-Identity Pair 1, Gen 02 corresponds to Same-Identity Pair 2, and so on.

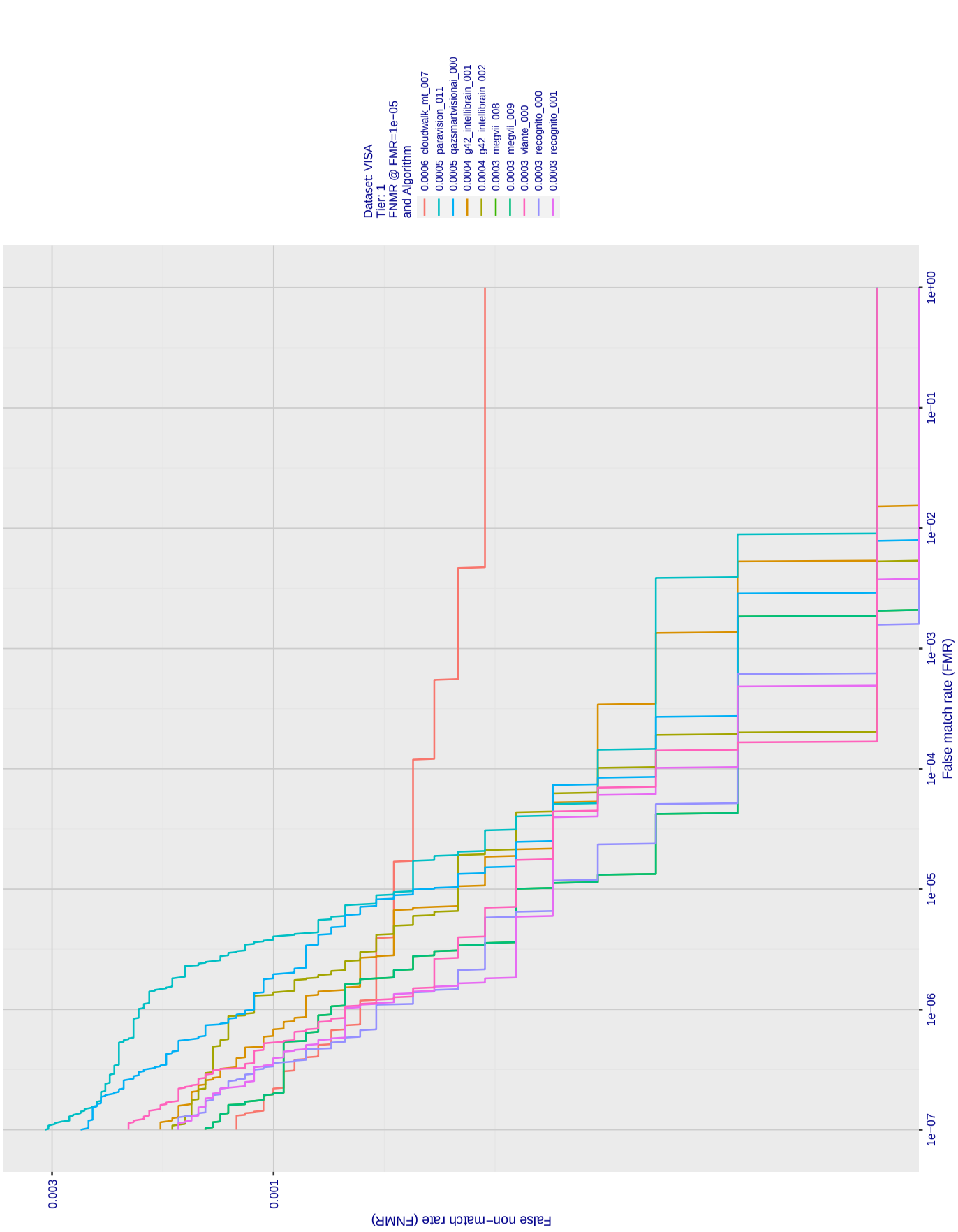

Figure 51: For the visa images, detection error tradeoff (DET) characteristics showing false non-match rate vs. false match rate plotted parametrically on threshold, T. The scales are logarithmic in order to show many decades of FMR.

FNMR(T) "False non-match rate"
FMR(T) "False match rate"

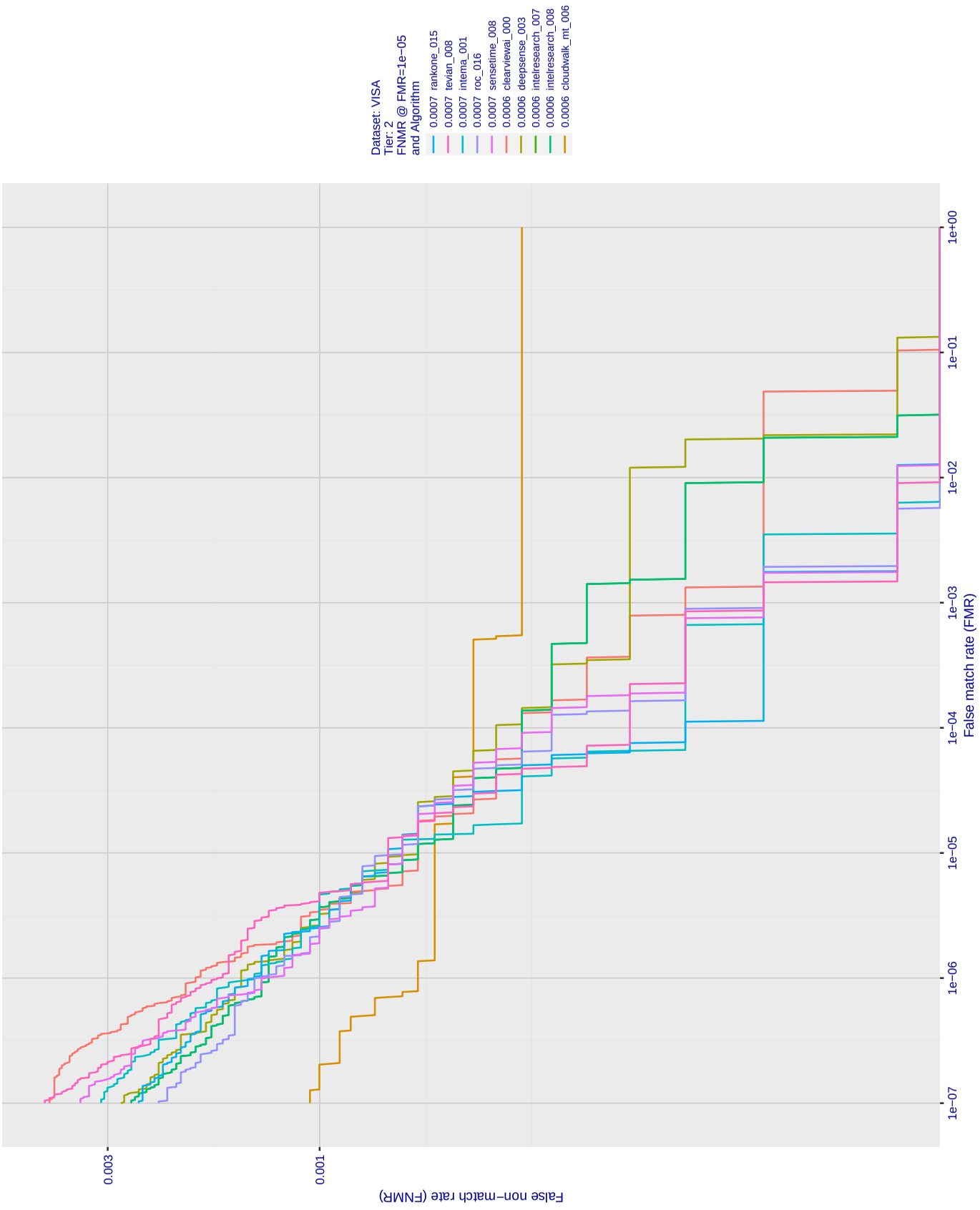

Figure 52: For the visa images, detection error tradeoff (DET) characteristics showing false non-match rate vs. false match rate plotted parametrically on threshold, T. The scales are logarithmic in order to show many decades of FMR.

FNMR(T) "False non-match rate"
FMR(T) "False match rate"

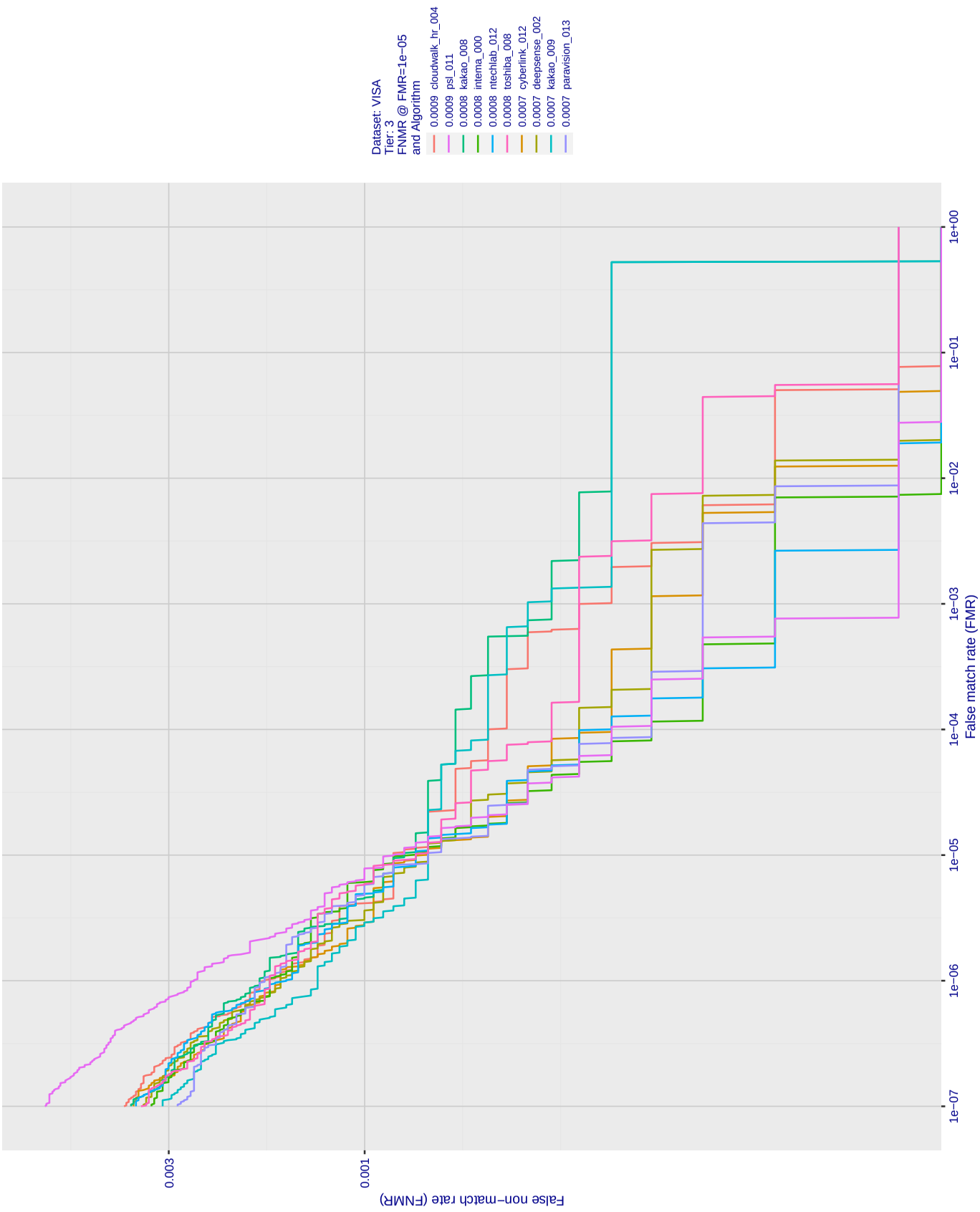

Figure 53: For the visa images, detection error tradeoff (DET) characteristics showing false non-match rate vs. false match rate plotted parametrically on threshold, T. The scales are logarithmic in order to show many decades of FMR.

FNMR(T) "False non-match rate"
FMR(T) "False match rate"

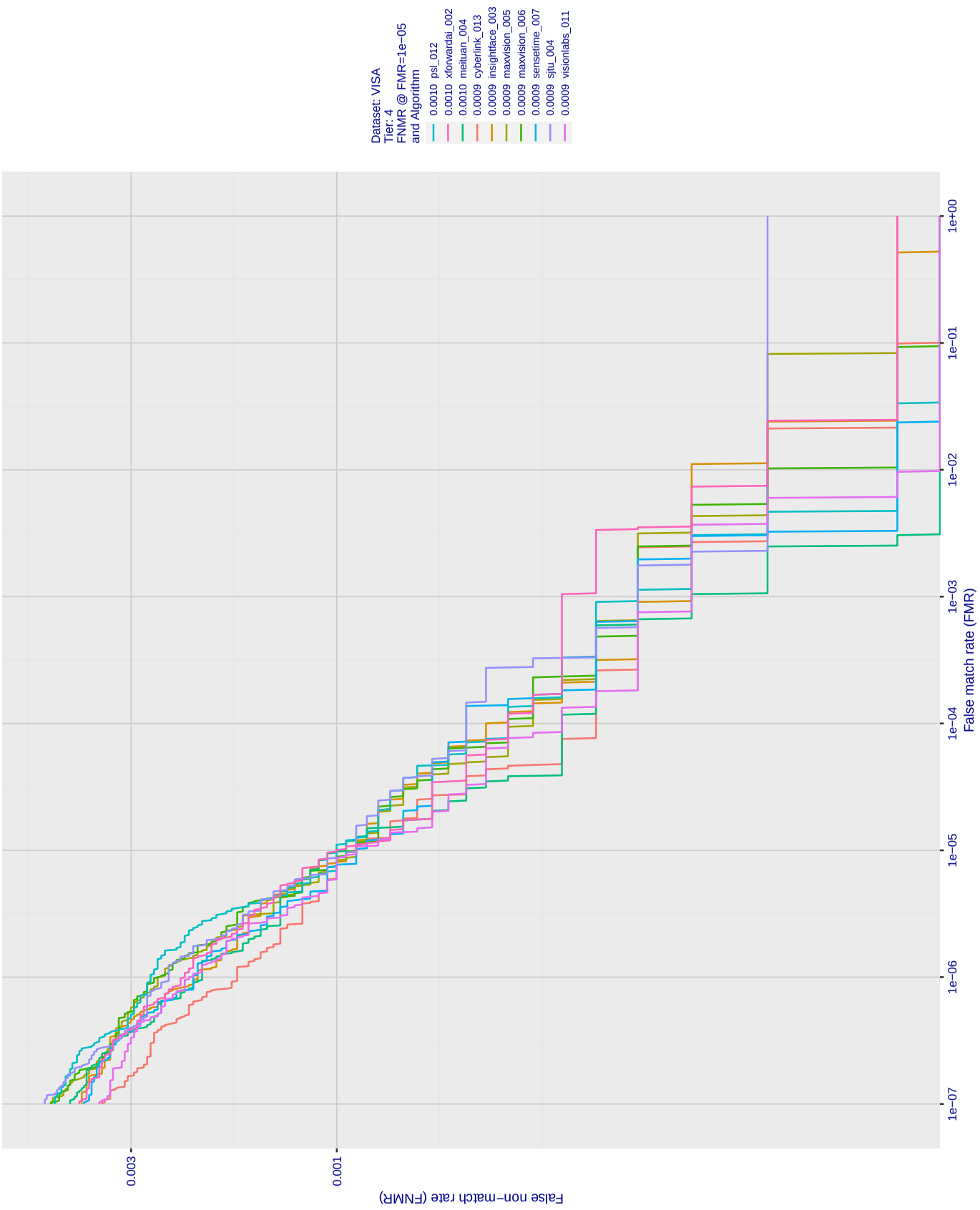

Figure 54: For the visa images, detection error tradeoff (DET) characteristics showing false non-match rate vs. false match rate plotted parametrically on threshold, T. The scales are logarithmic in order to show many decades of FMR.

FNMR(T) "False non-match rate"
FMR(T) "False match rate"

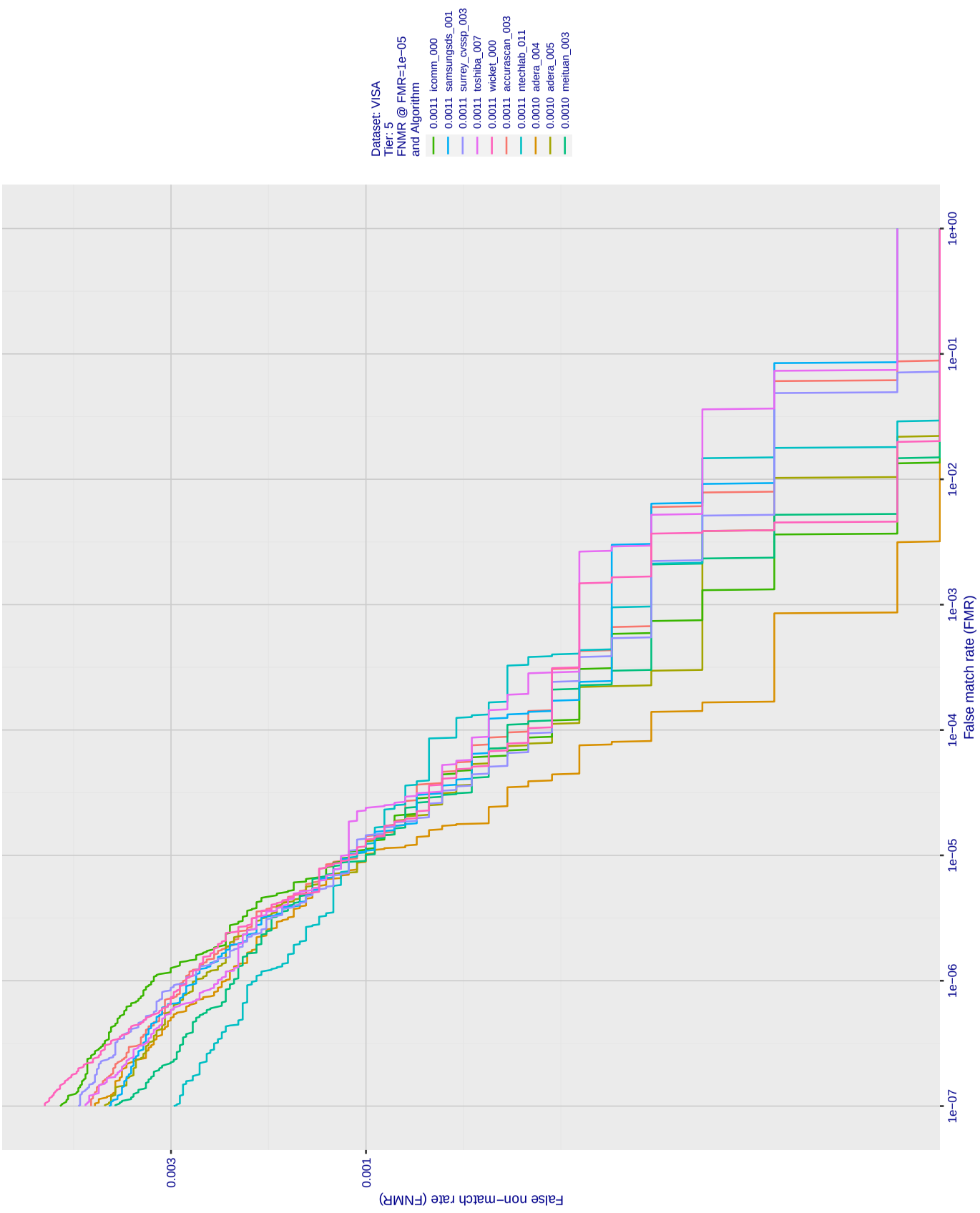

Figure 55: For the visa images, detection error tradeoff (DET) characteristics showing false non-match rate vs. false match rate plotted parametrically on threshold, T. The scales are logarithmic in order to show many decades of FMR.

FNMR(T) "False non-match rate"
FMR(T) "False match rate"

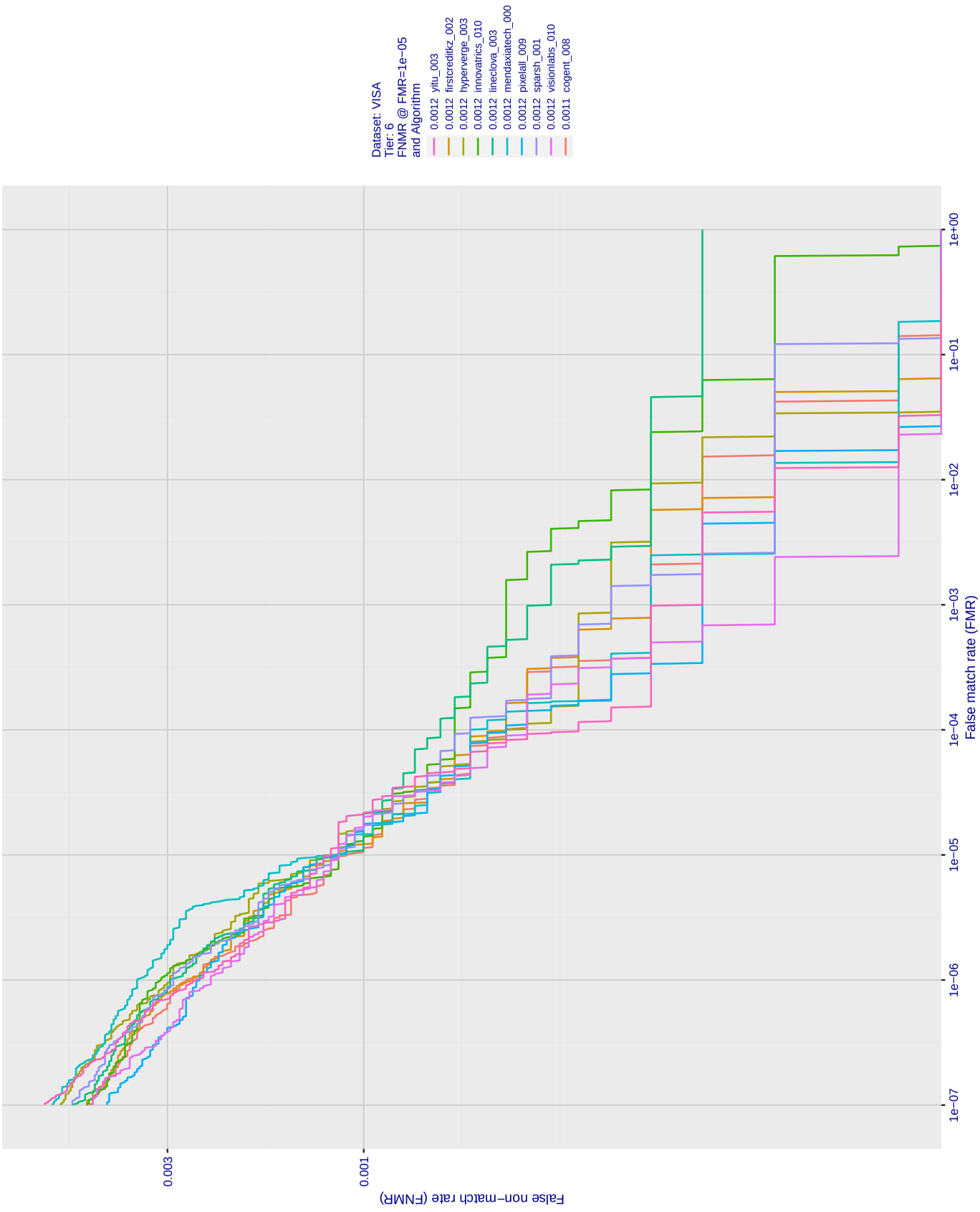

Figure 56: For the visa images, detection error tradeoff (DET) characteristics showing false non-match rate vs. false match rate plotted parametrically on threshold, T. The scales are logarithmic in order to show many decades of FMR.

FNMR(T) "False non-match rate"
FMR(T) "False match rate"

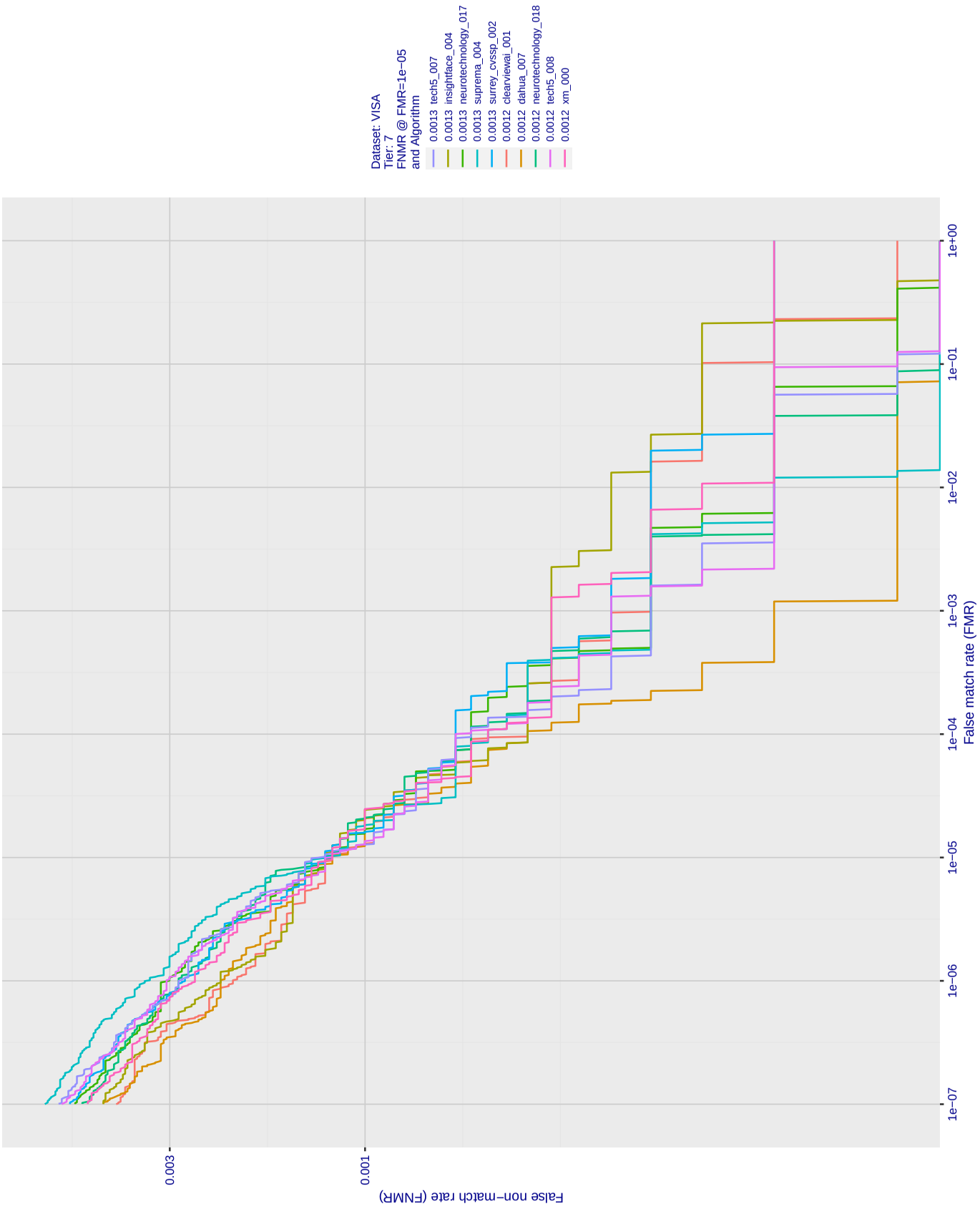

Figure 57: For the visa images, detection error tradeoff (DET) characteristics showing false non-match rate vs. false match rate plotted parametrically on threshold, T. The scales are logarithmic in order to show many decades of FMR.

FNMR(T) "False non-match rate"
FMR(T) "False match rate"

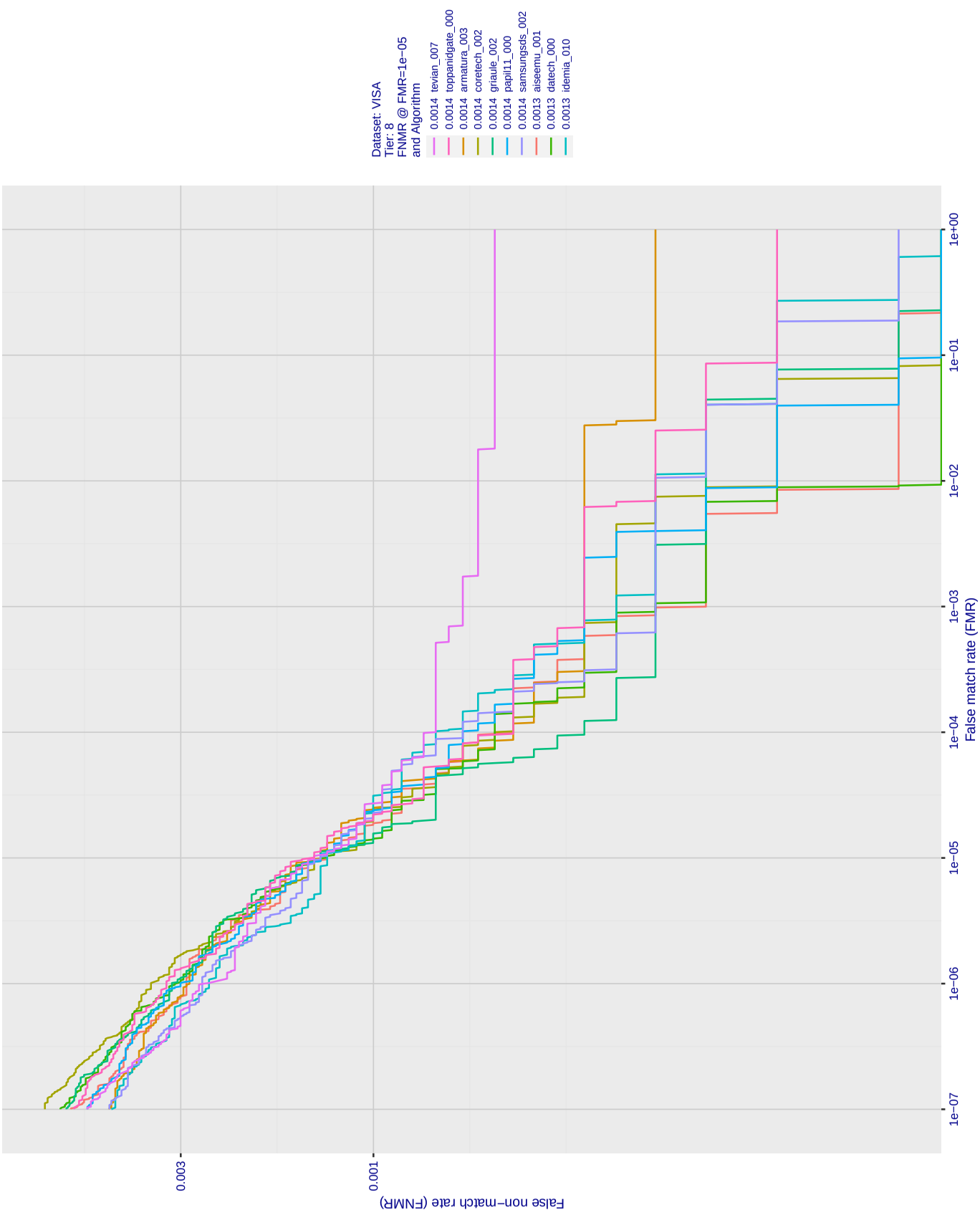

Figure 58: For the visa images, detection error tradeoff (DET) characteristics showing false non-match rate vs. false match rate plotted parametrically on threshold, T. The scales are logarithmic in order to show many decades of FMR.

FNMR(T) "False non-match rate"
FMR(T) "False match rate"

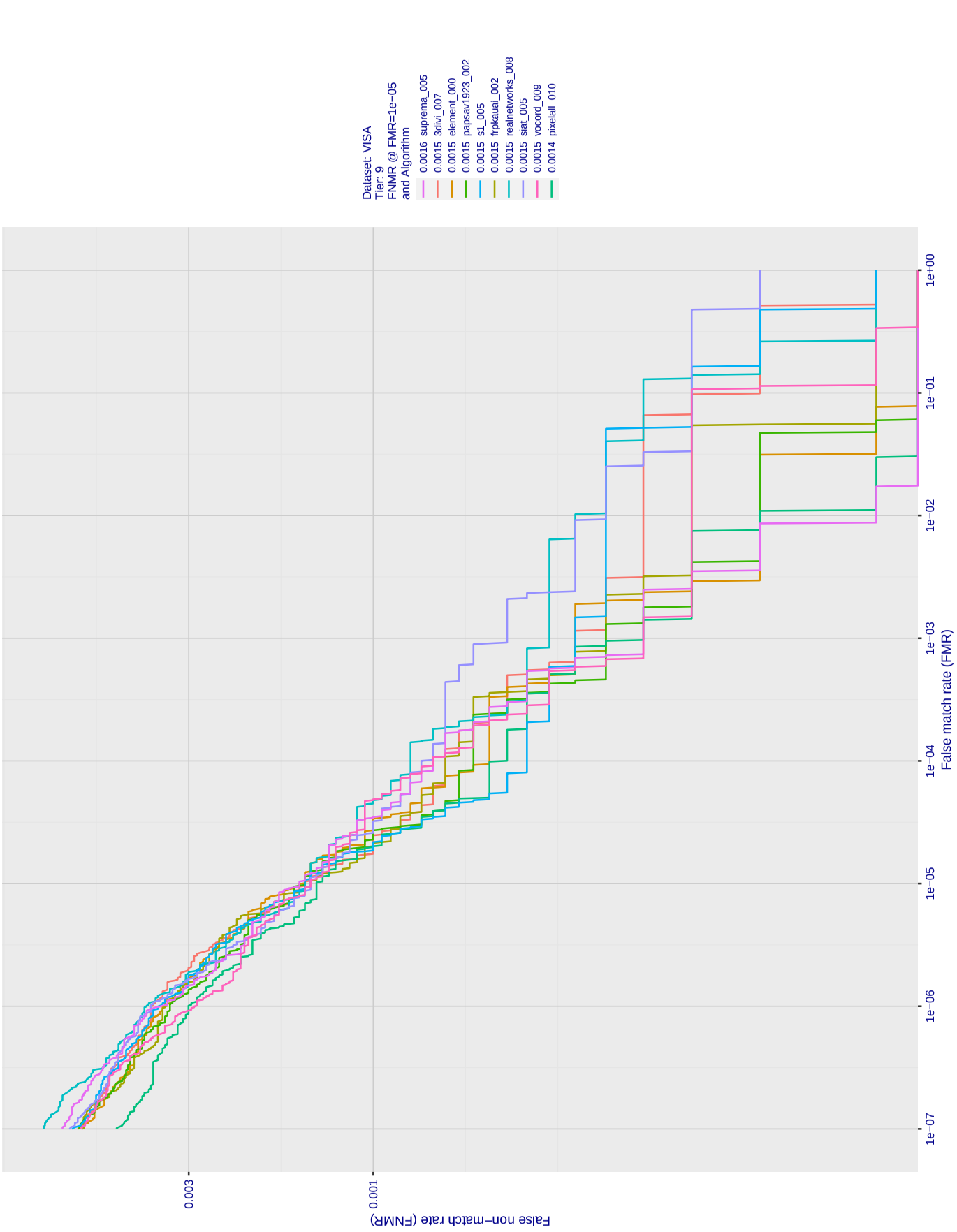

Figure 59: For the visa images, detection error tradeoff (DET) characteristics showing false non-match rate vs. false match rate plotted parametrically on threshold, T. The scales are logarithmic in order to show many decades of FMR.

FNMR(T) "False non-match rate"
FMR(T) "False match rate"

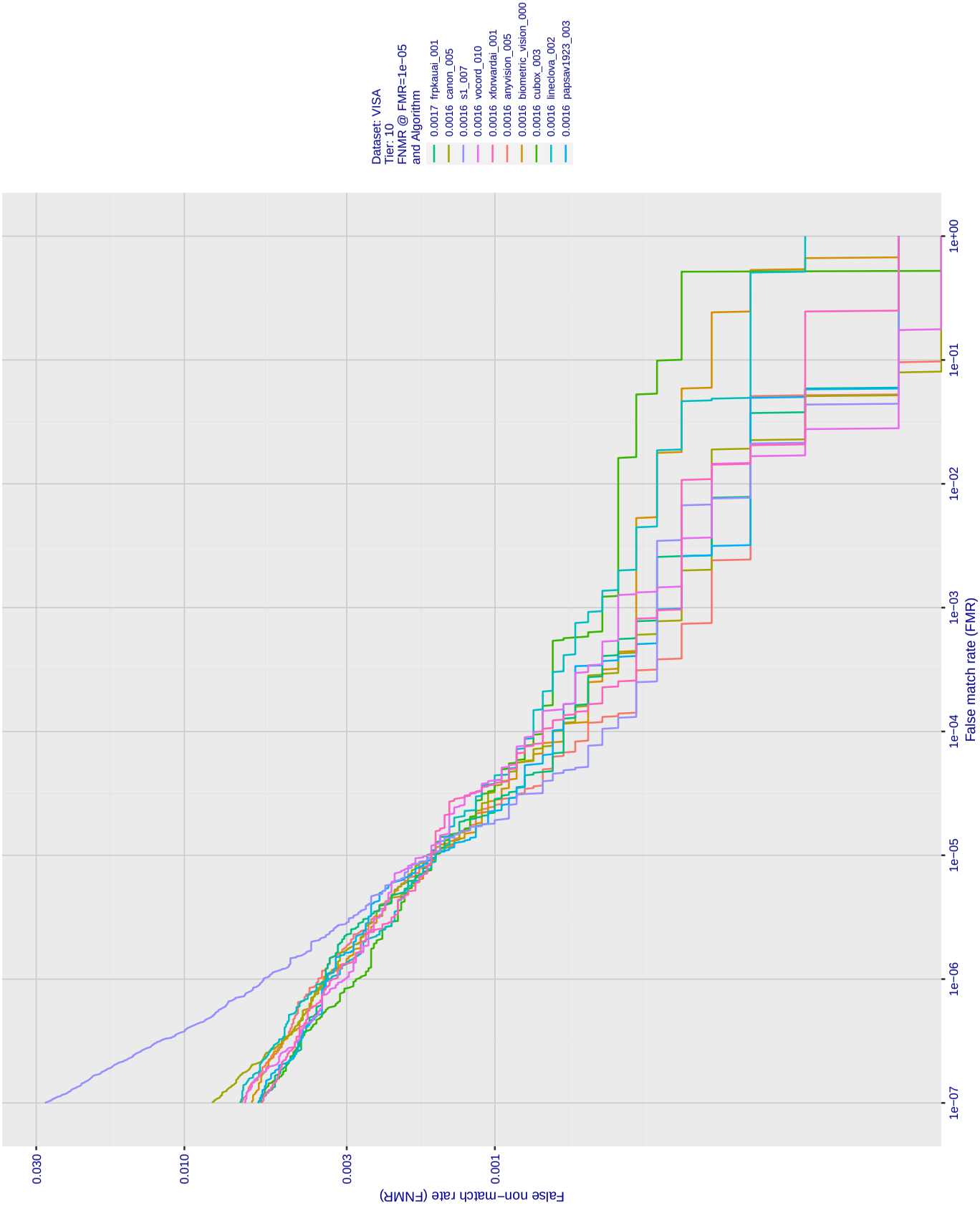

Figure 60: For the visa images, detection error tradeoff (DET) *characteristics showing false non-match rate vs. false match rate plotted parametrically on threshold, T. The scales are logarithmic in order to show many decades of* FMR.

FNMR(T) "False non-match rate"
FMR(T) "False match rate"

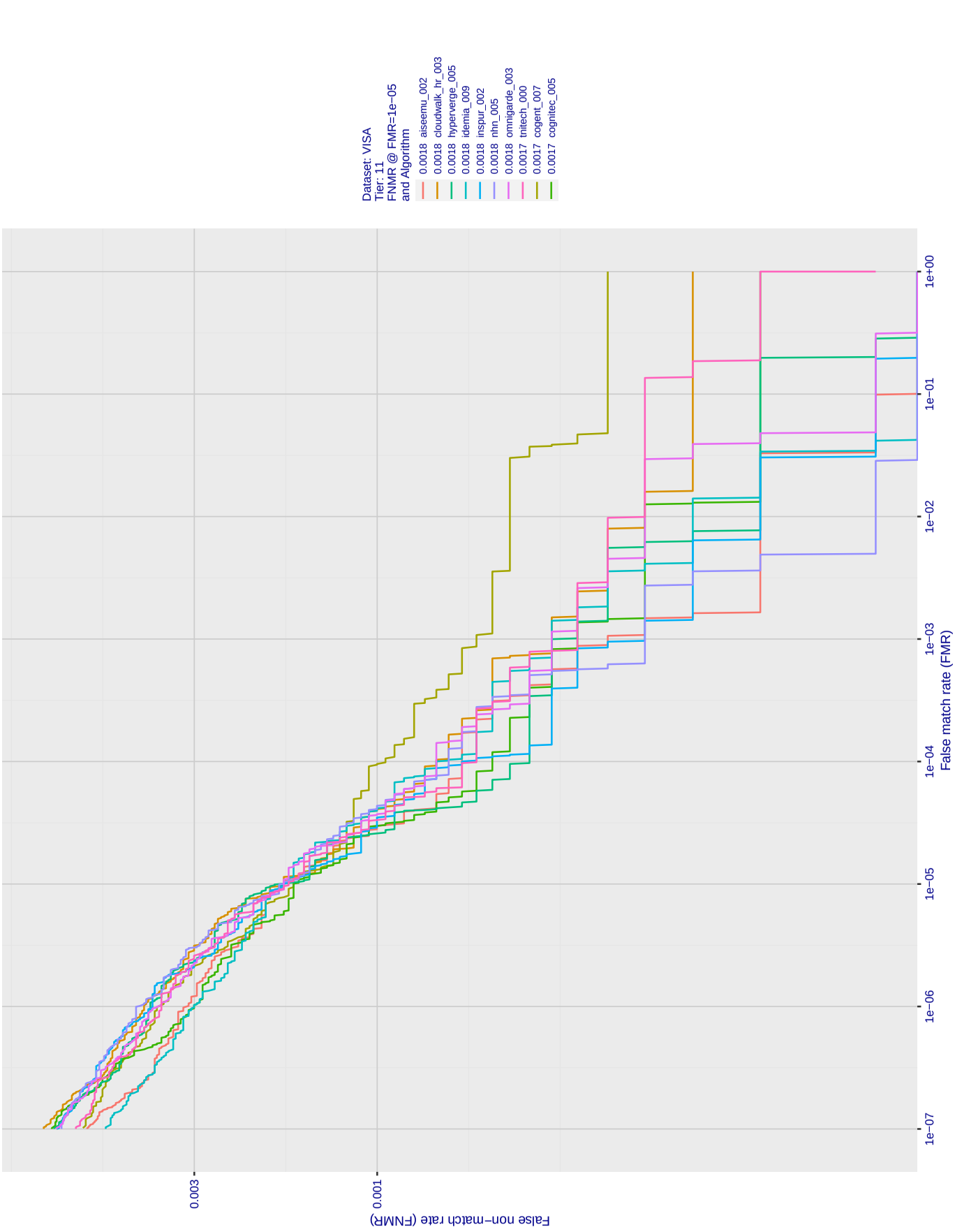

Figure 61: For the visa images, detection error tradeoff (DET) characteristics showing false non-match rate vs. false match rate plotted parametrically on threshold, T. The scales are logarithmic in order to show many decades of FMR.

FNMR(T) "False non-match rate"
FMR(T) "False match rate"

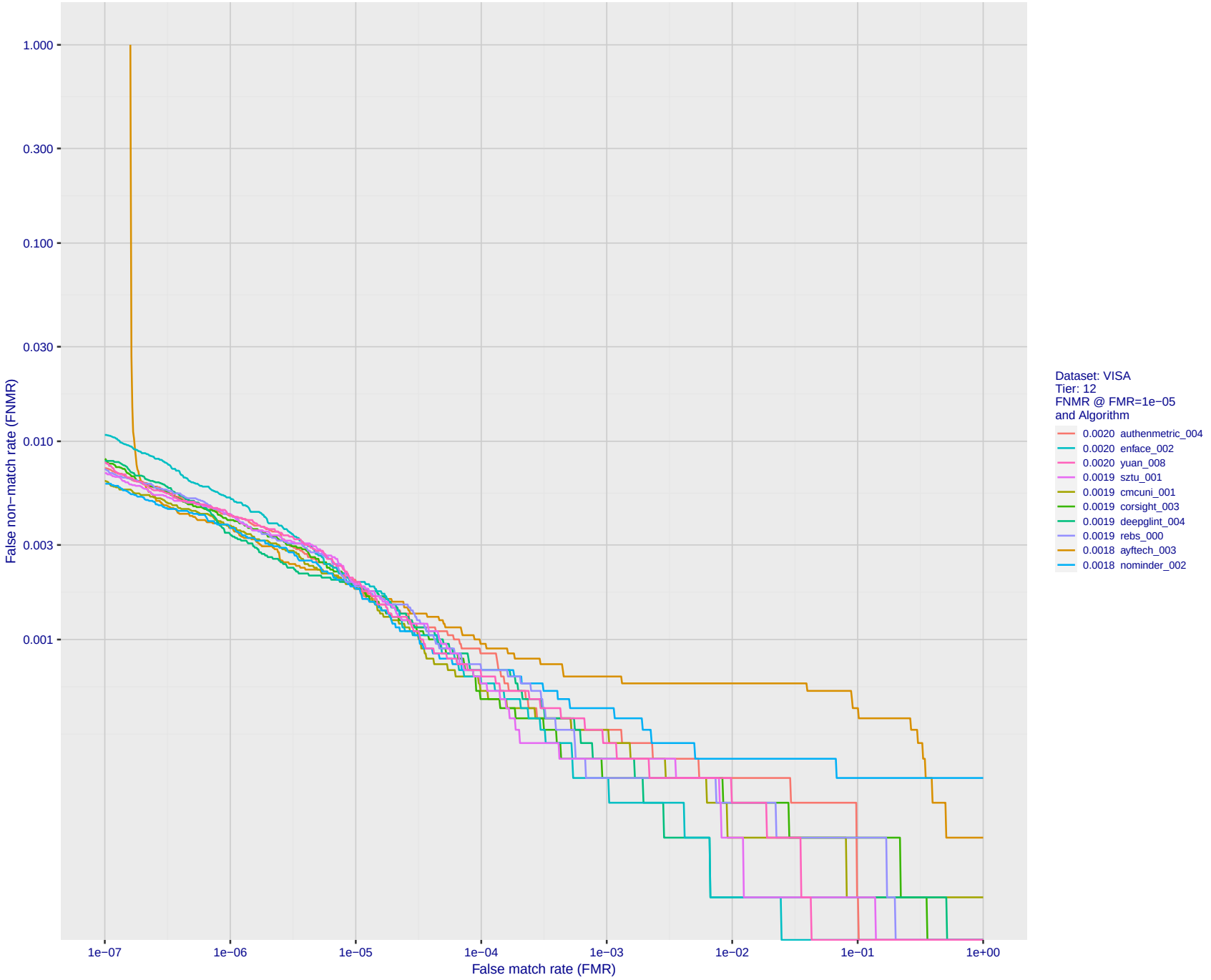

*Figure 62: For the visa images, detection error tradeoff (*DET*) characteristics showing false non-match rate vs. false match rate plotted parametrically on threshold, T. The scales are logarithmic in order to show many decades of* FMR*.*

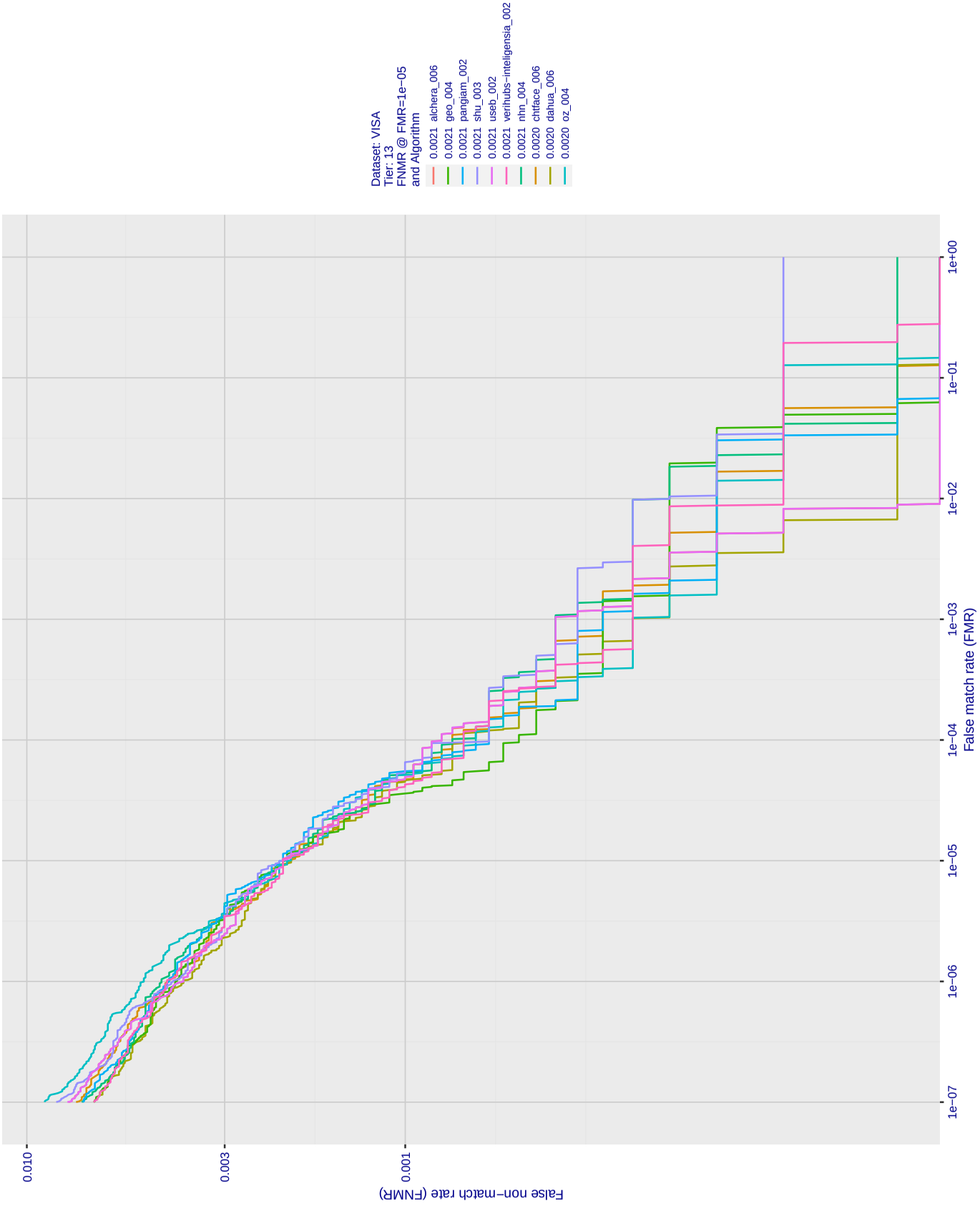

Figure 63: For the visa images, detection error tradeoff (DET) characteristics showing false non-match rate vs. false match rate plotted parametrically on threshold, T. The scales are logarithmic in order to show many decades of FMR.

FNMR(T) "False non-match rate"
FMR(T) "False match rate"

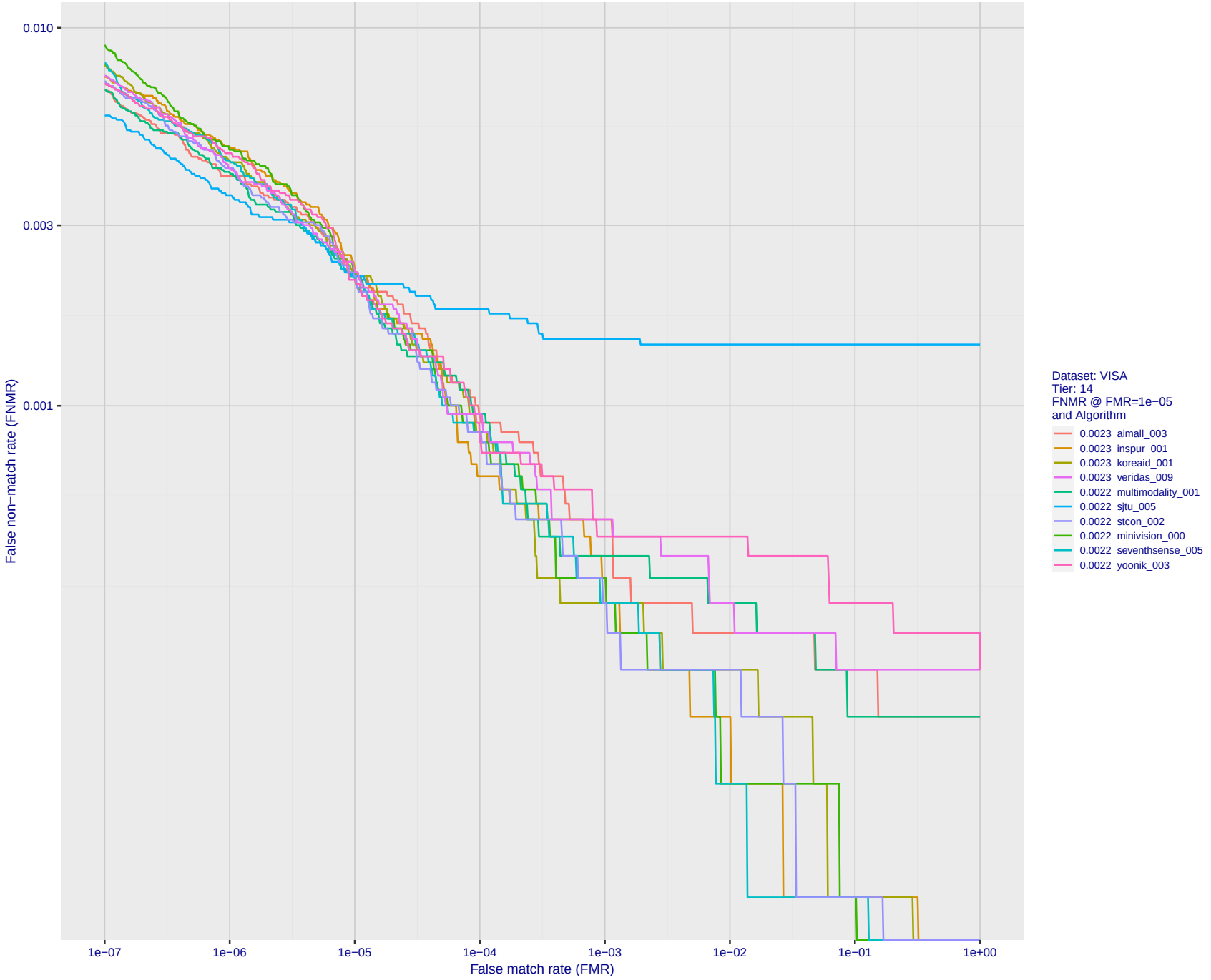

Figure 64: For the visa images, detection error tradeoff (DET) characteristics showing false non-match rate vs. false match rate plotted parametrically on threshold, T. The scales are logarithmic in order to show many decades of FMR.

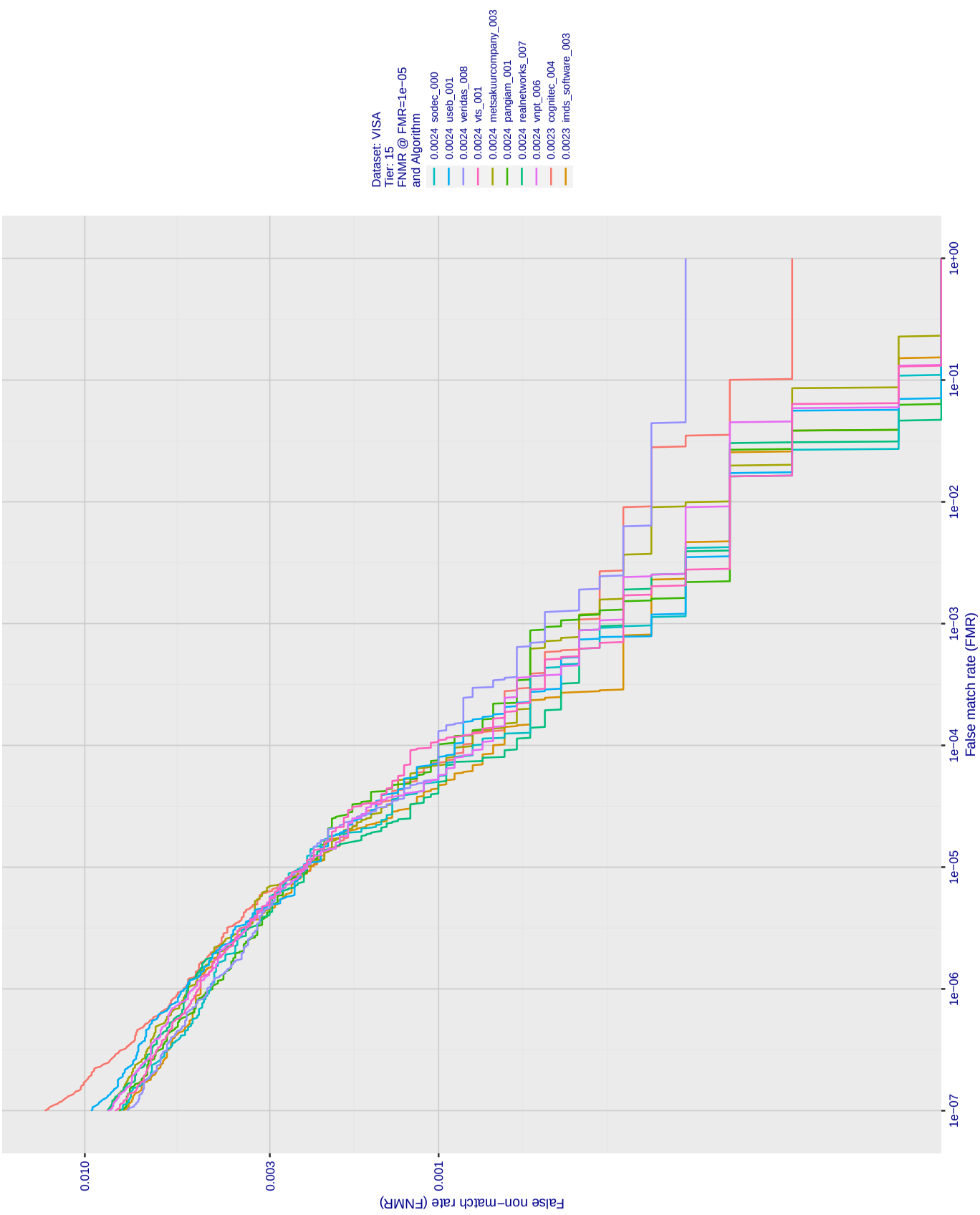

Figure 65: For the visa images, detection error tradeoff (DET) characteristics showing false non-match rate vs. false match rate plotted parametrically on threshold, T. The scales are logarithmic in order to show many decades of FMR.

FNMR(T) "False non-match rate"
FMR(T) "False match rate"

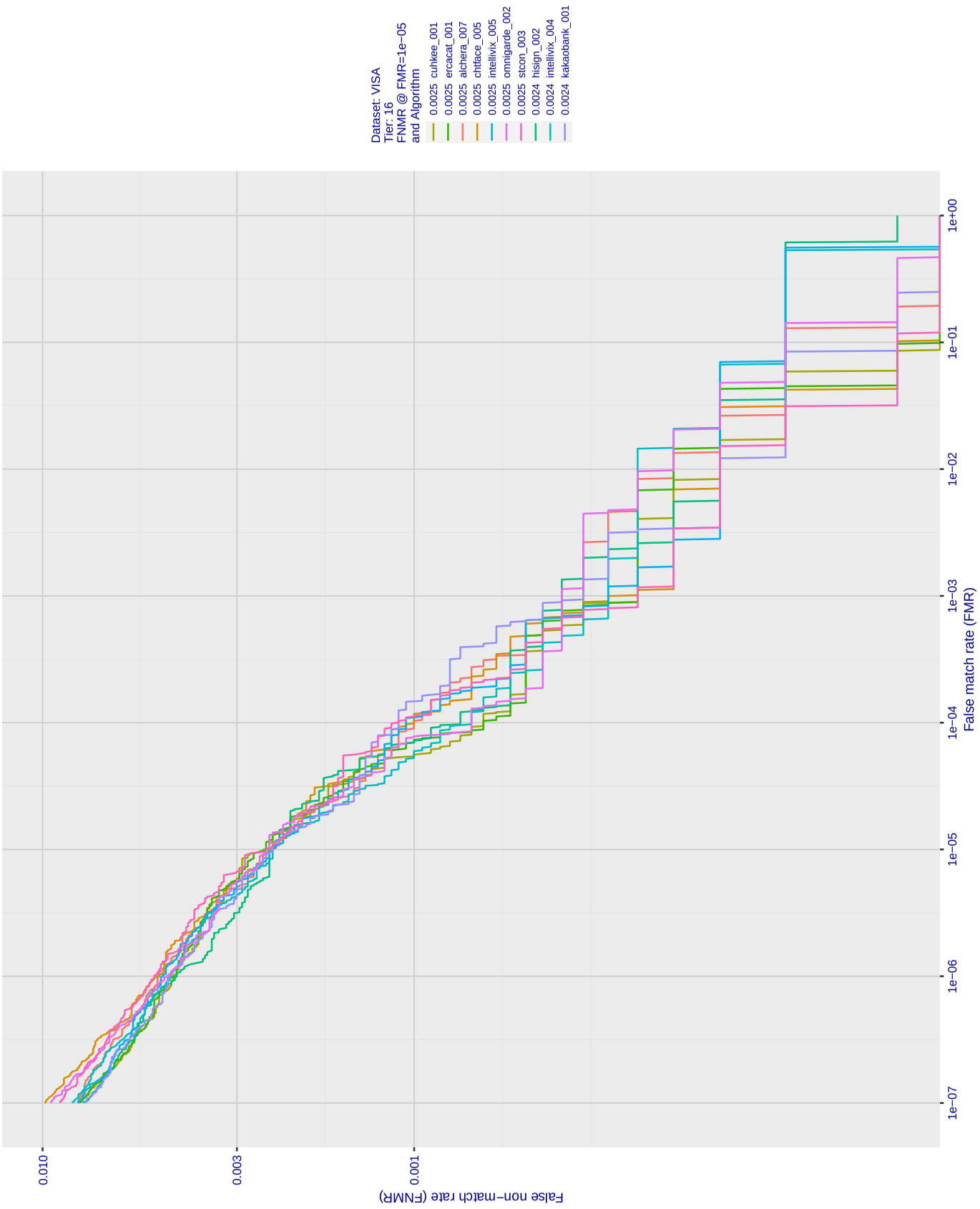

Figure 66: For the visa images, detection error tradeoff (DET) characteristics showing false non-match rate vs. false match rate plotted parametrically on threshold, T. The scales are logarithmic in order to show many decades of FMR.

FNMR(T) "False non-match rate"
FMR(T) "False match rate"

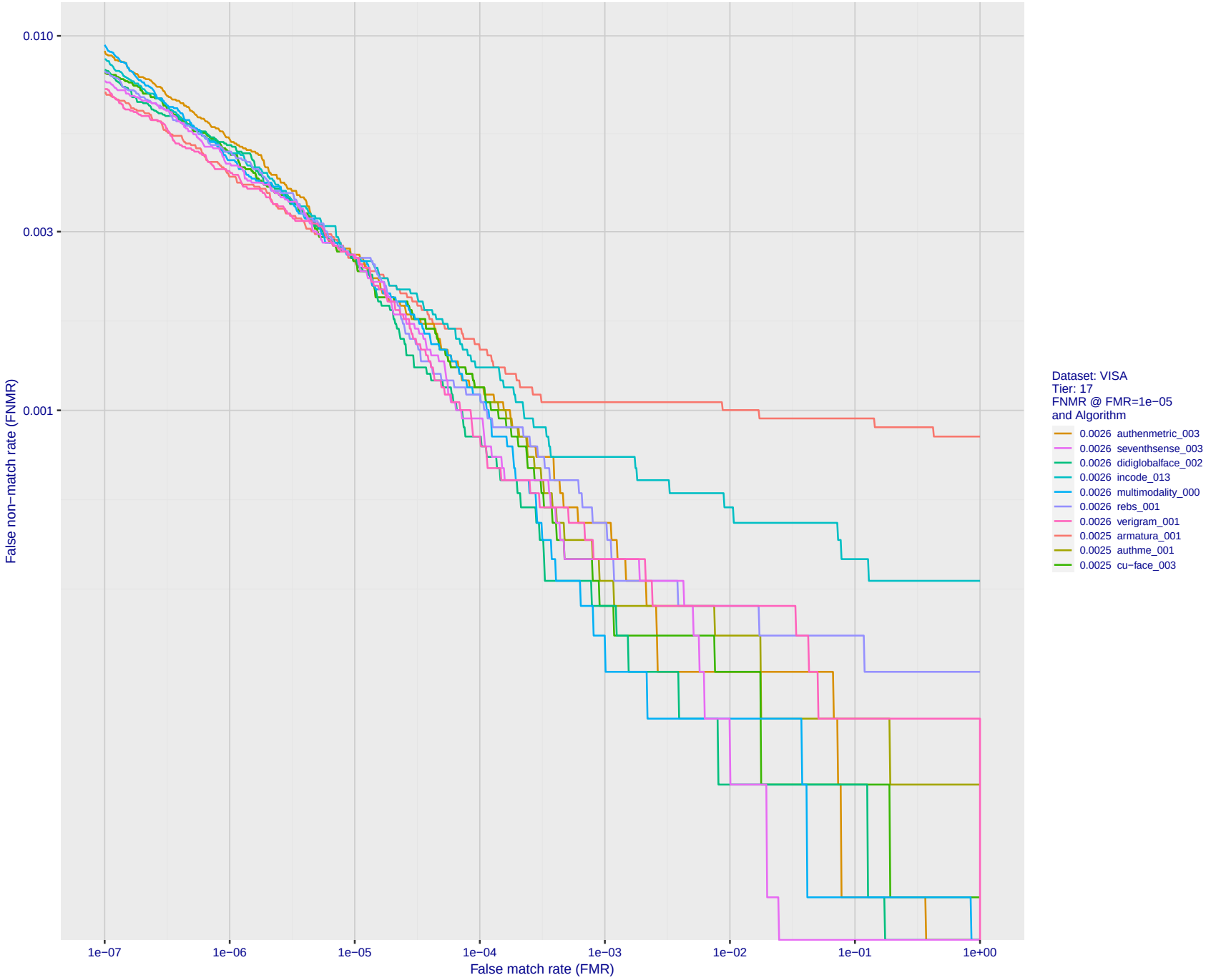

Figure 67: For the visa images, detection error tradeoff (DET) characteristics showing false non-match rate vs. false match rate plotted parametrically on threshold, T. The scales are logarithmic in order to show many decades of FMR.

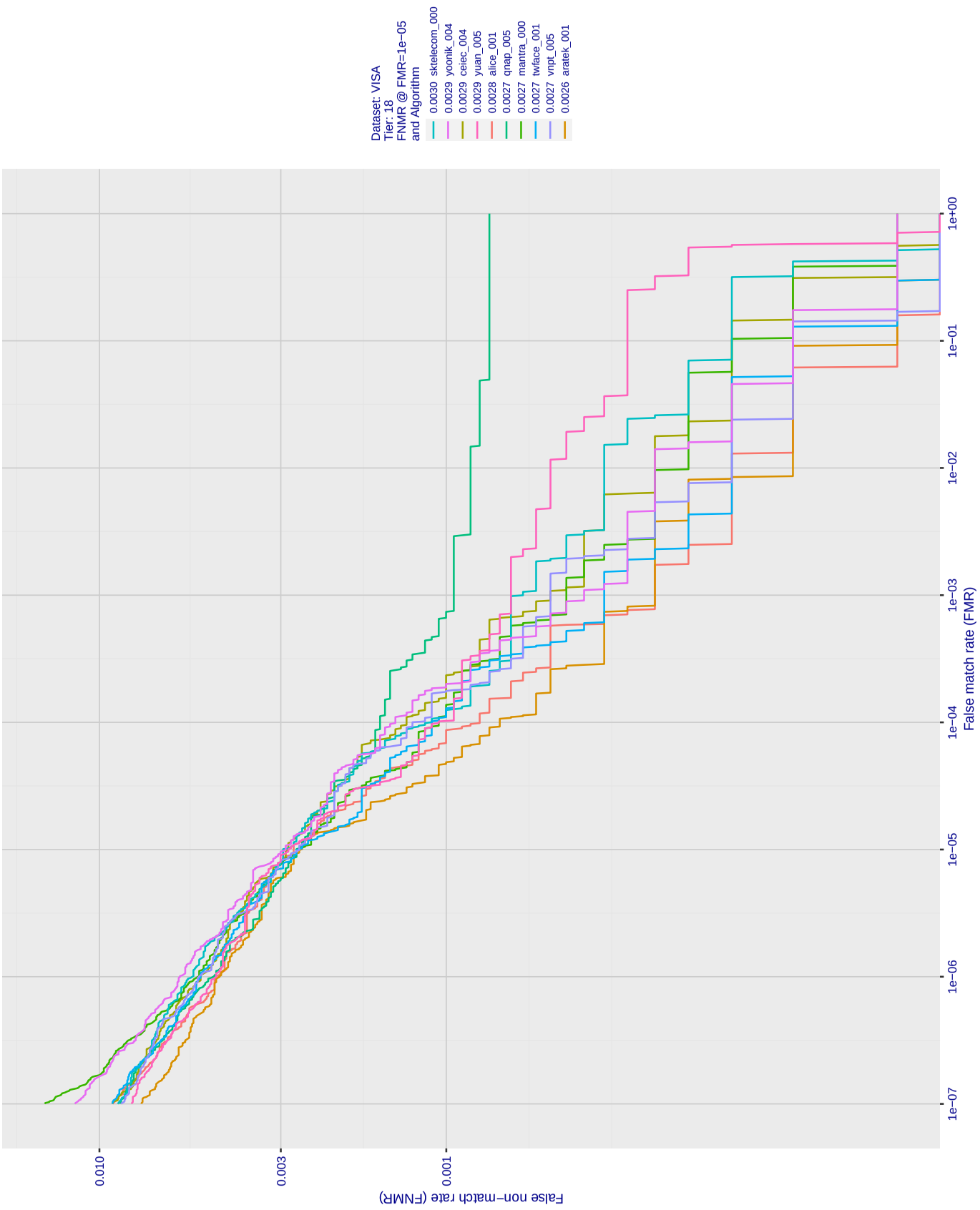

Figure 68: For the visa images, detection error tradeoff (DET) characteristics showing false non-match rate vs. false match rate plotted parametrically on threshold, T. The scales are logarithmic in order to show many decades of FMR.

FNMR(T) "False non-match rate"
FMR(T) "False match rate"

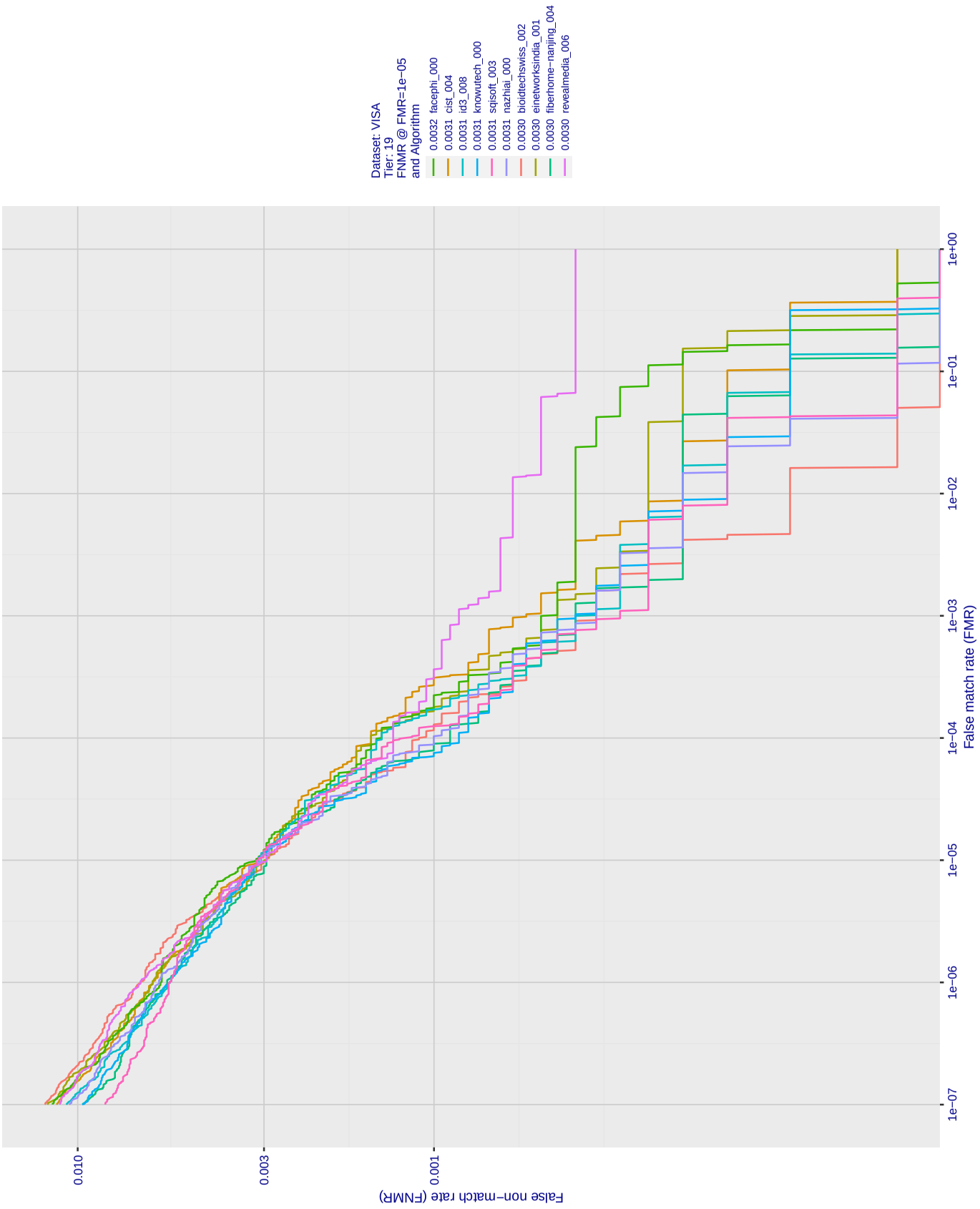

Figure 69: For the visa images, detection error tradeoff (DET) characteristics showing false non-match rate vs. false match rate plotted parametrically on threshold, T. The scales are logarithmic in order to show many decades of FMR.

FNMR(T) "False non-match rate"
FMR(T) "False match rate"

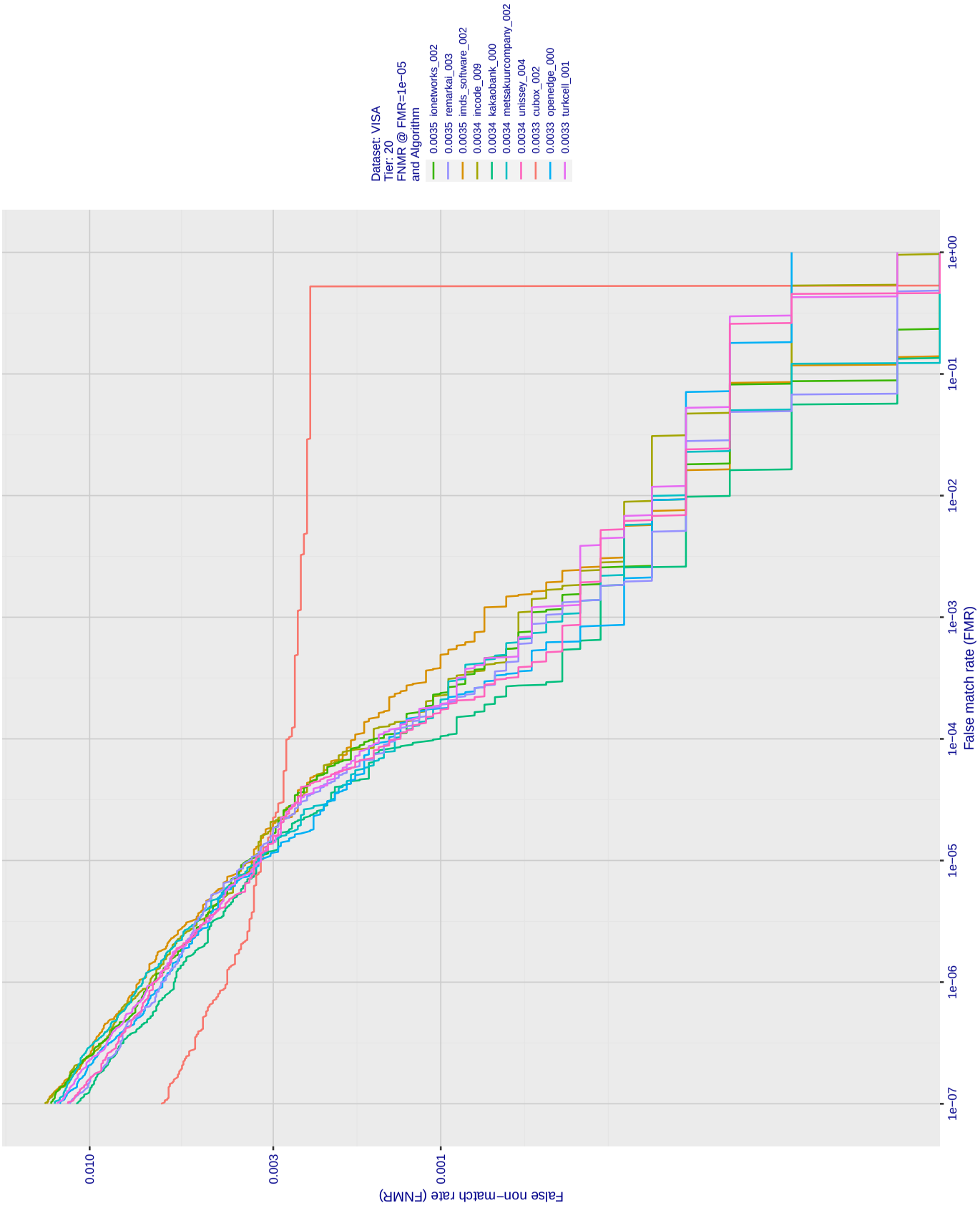

Figure 70: For the visa images, detection error tradeoff (DET) characteristics showing false non-match rate vs. false match rate plotted parametrically on threshold, T. The scales are logarithmic in order to show many decades of FMR.

FNMR(T) "False non-match rate"
FMR(T) "False match rate"

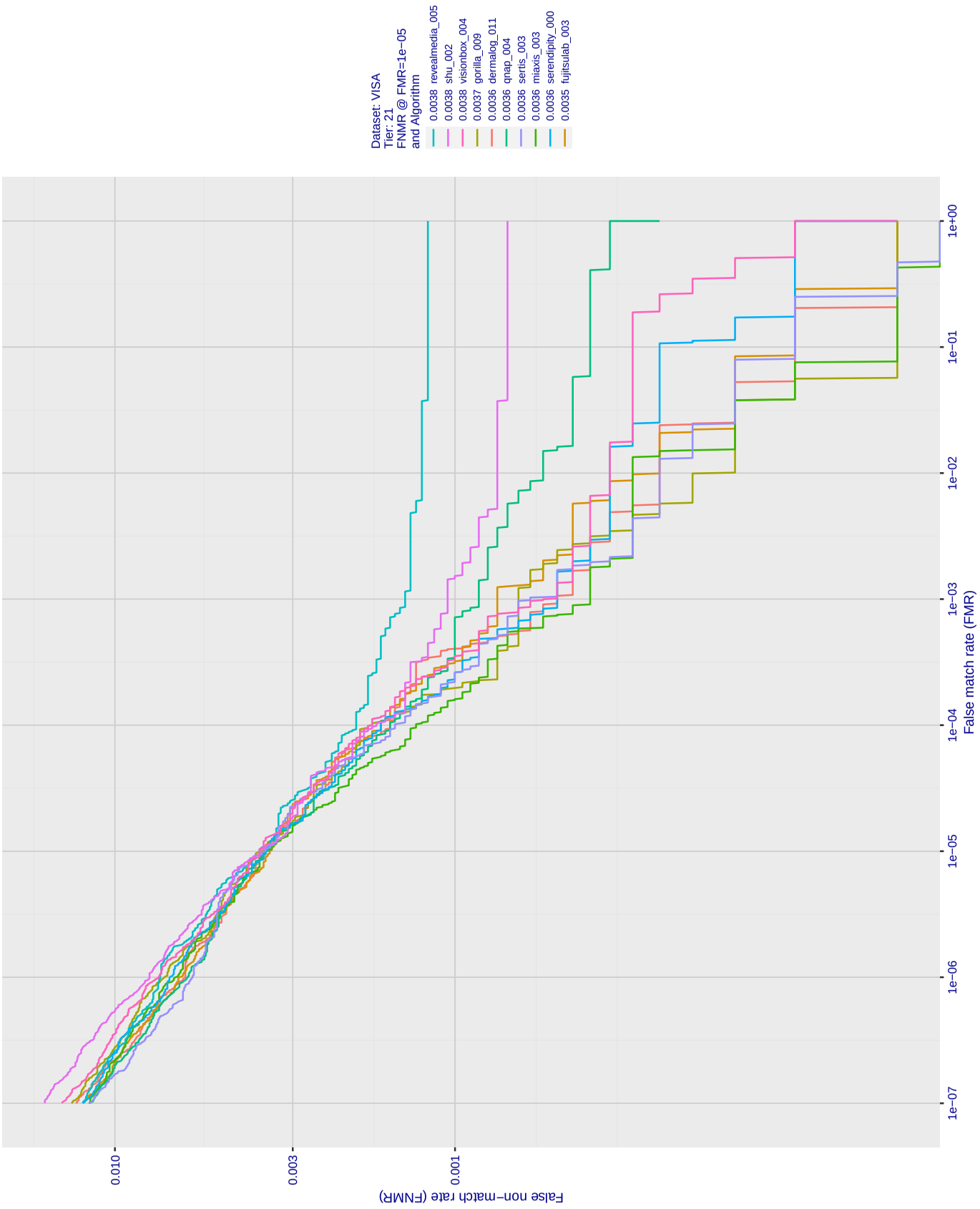

Figure 71: For the visa images, detection error tradeoff (DET) characteristics showing false non-match rate vs. false match rate plotted parametrically on threshold, T. The scales are logarithmic in order to show many decades of FMR.

FNMR(T) "False non-match rate"
FMR(T) "False match rate"

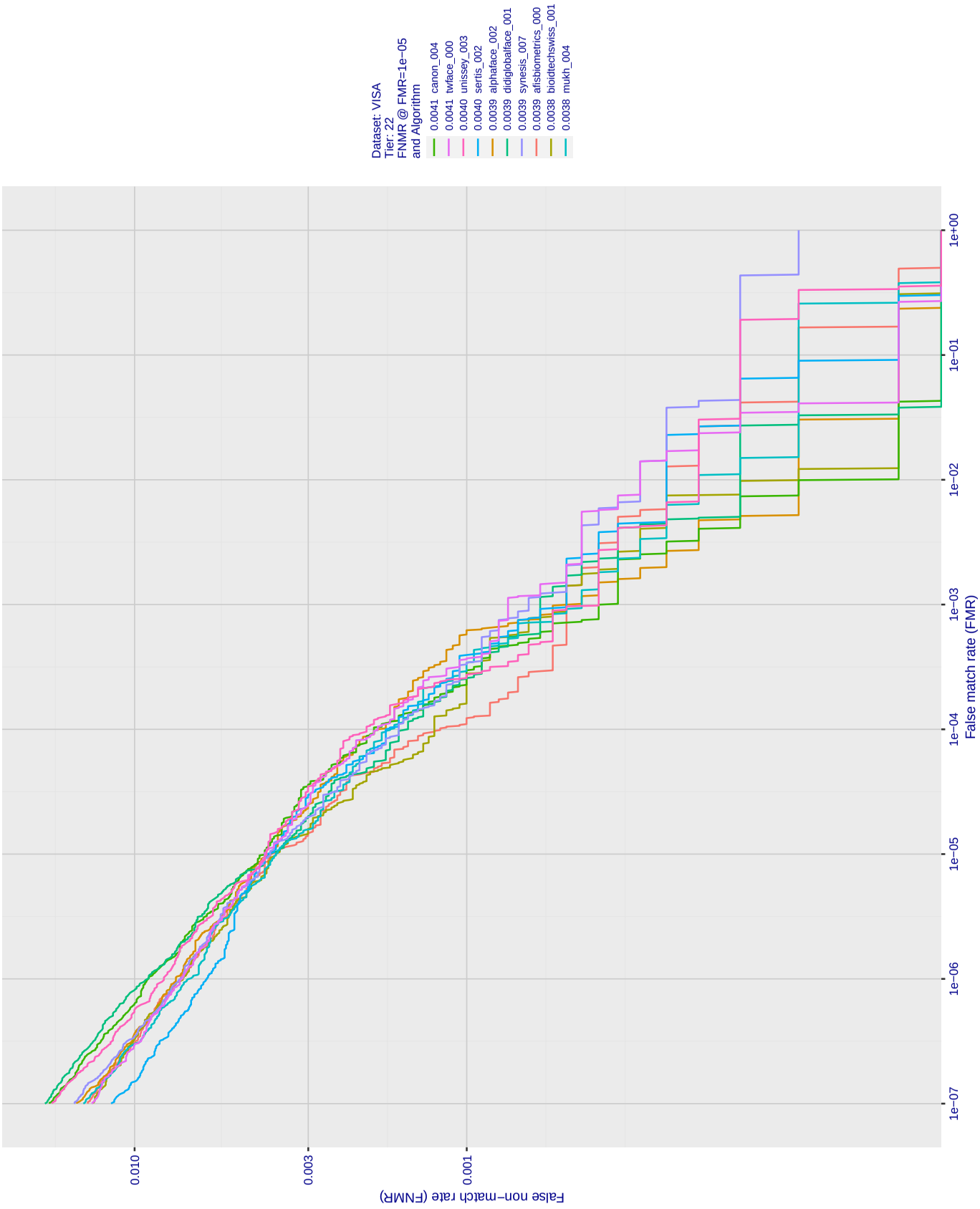

Figure 72: For the visa images, detection error tradeoff (DET) characteristics showing false non-match rate vs. false match rate plotted parametrically on threshold, T. The scales are logarithmic in order to show many decades of FMR.

FNMR(T) "False non-match rate"
FMR(T) "False match rate"

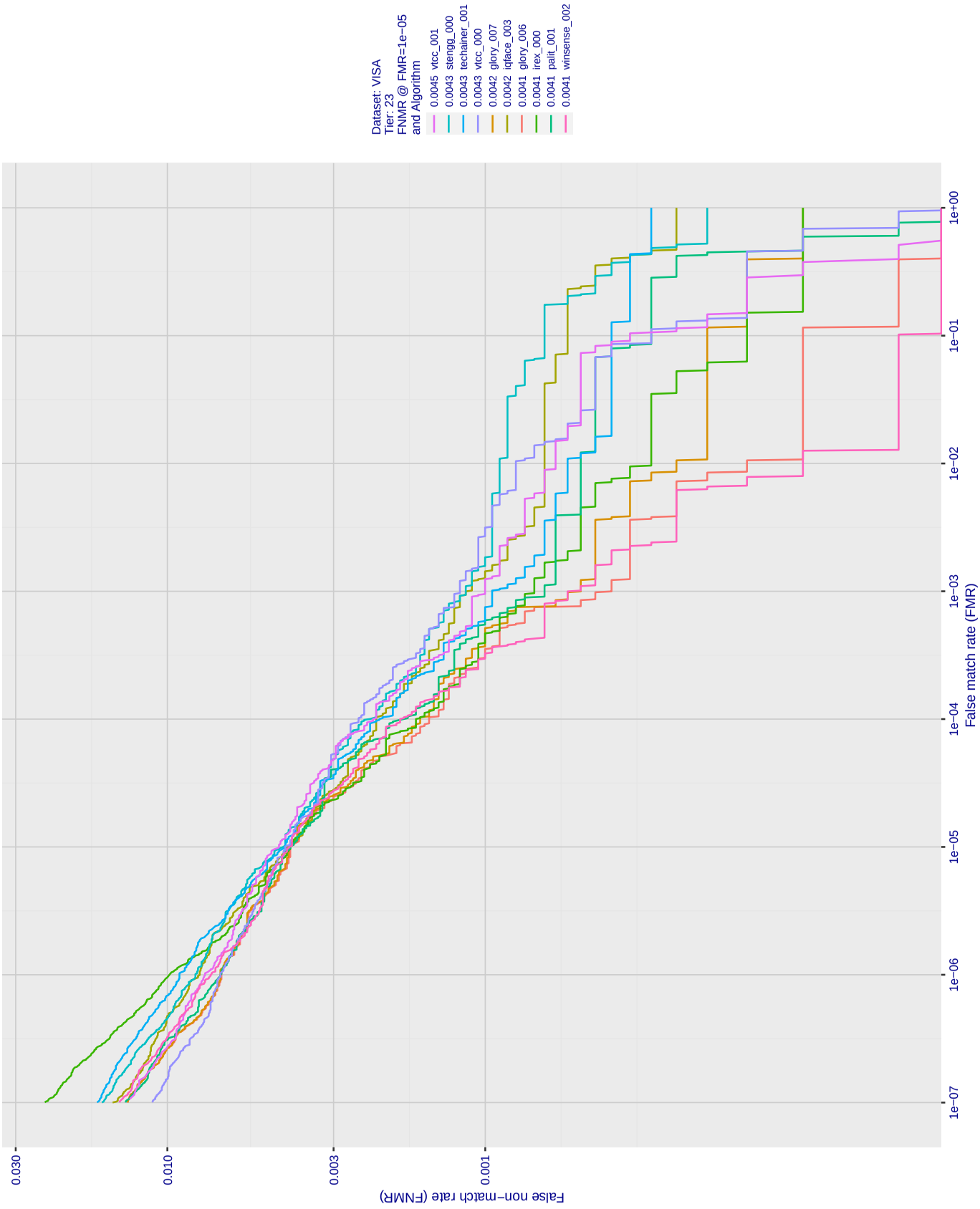

Figure 73: For the visa images, detection error tradeoff (DET) characteristics showing false non-match rate vs. false match rate plotted parametrically on threshold, T. The scales are logarithmic in order to show many decades of FMR.

FNMR(T) "False non-match rate"
FMR(T) "False match rate"

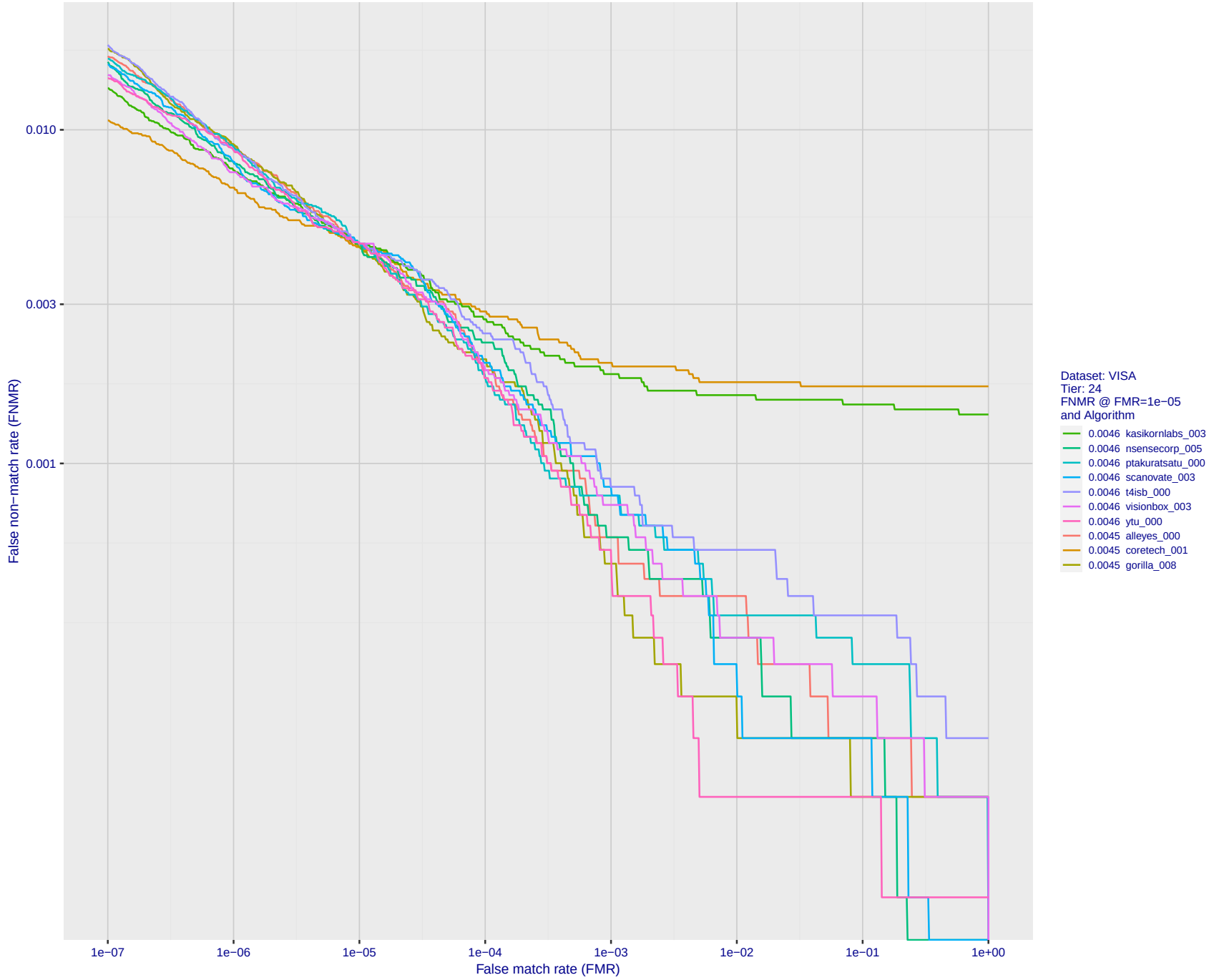

Figure 74: For the visa images, detection error tradeoff (DET) characteristics showing false non-match rate vs. false match rate plotted parametrically on threshold, T. The scales are logarithmic in order to show many decades of FMR.

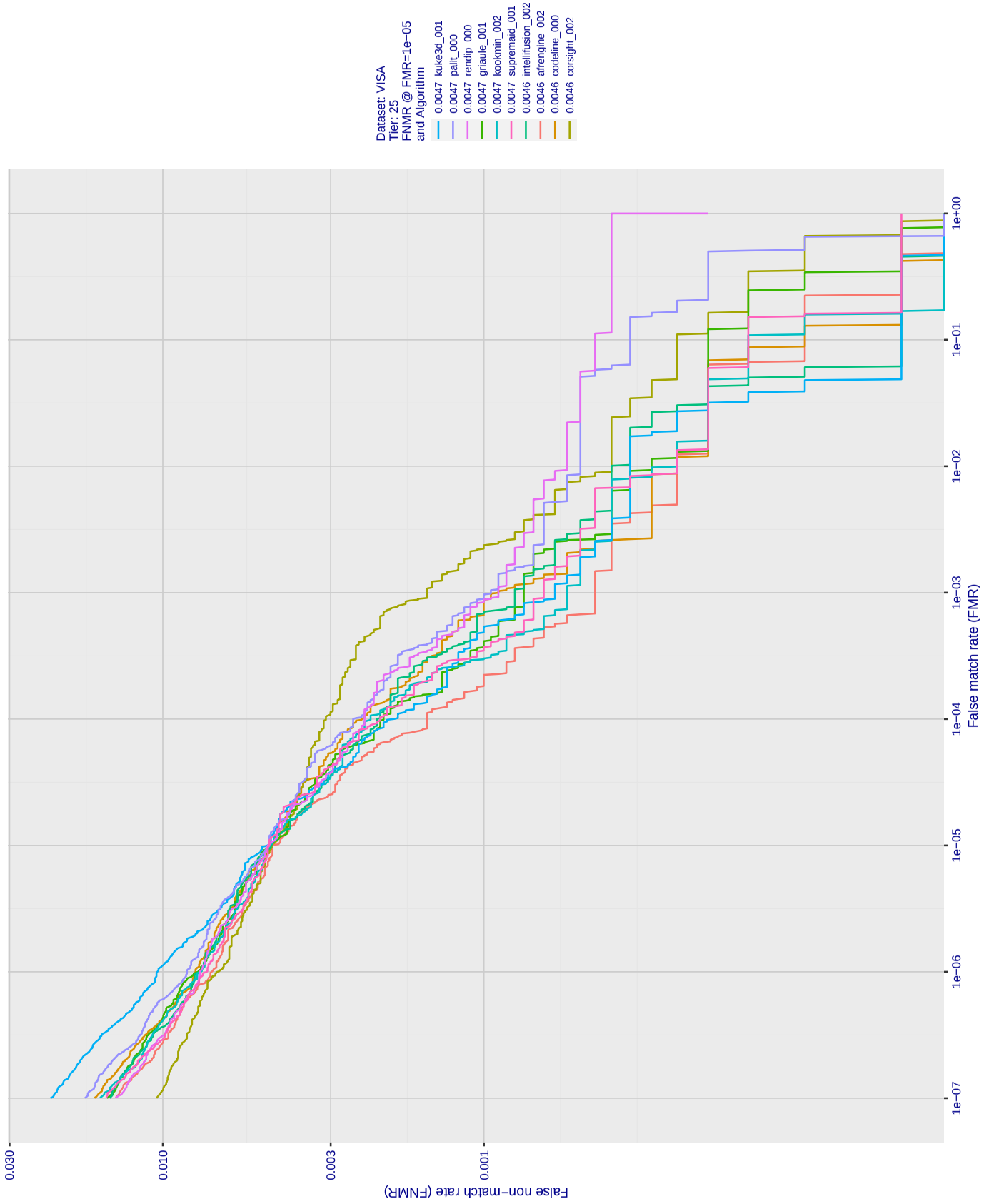

Figure 75: For the visa images, detection error tradeoff (DET) characteristics showing false non-match rate vs. false match rate plotted parametrically on threshold, T. The scales are logarithmic in order to show many decades of FMR.

FNMR(T) "False non-match rate"
FMR(T) "False match rate"

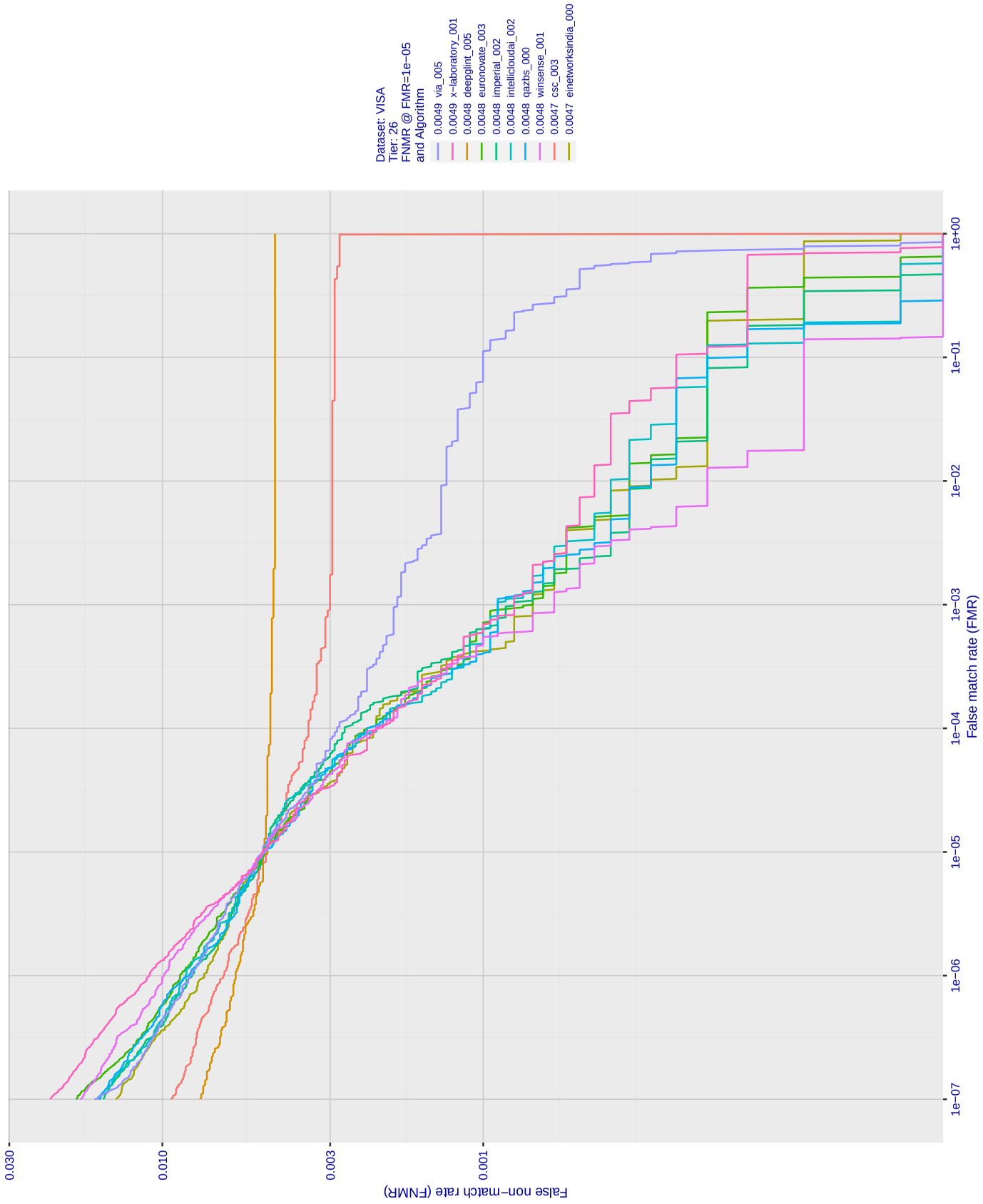

Figure 76: For the visa images, detection error tradeoff (DET) *characteristics showing false non-match rate vs. false match rate plotted parametrically on threshold, T. The scales are logarithmic in order to show many decades of* FMR.

FNMR(T) "False non-match rate"
FMR(T) "False match rate"

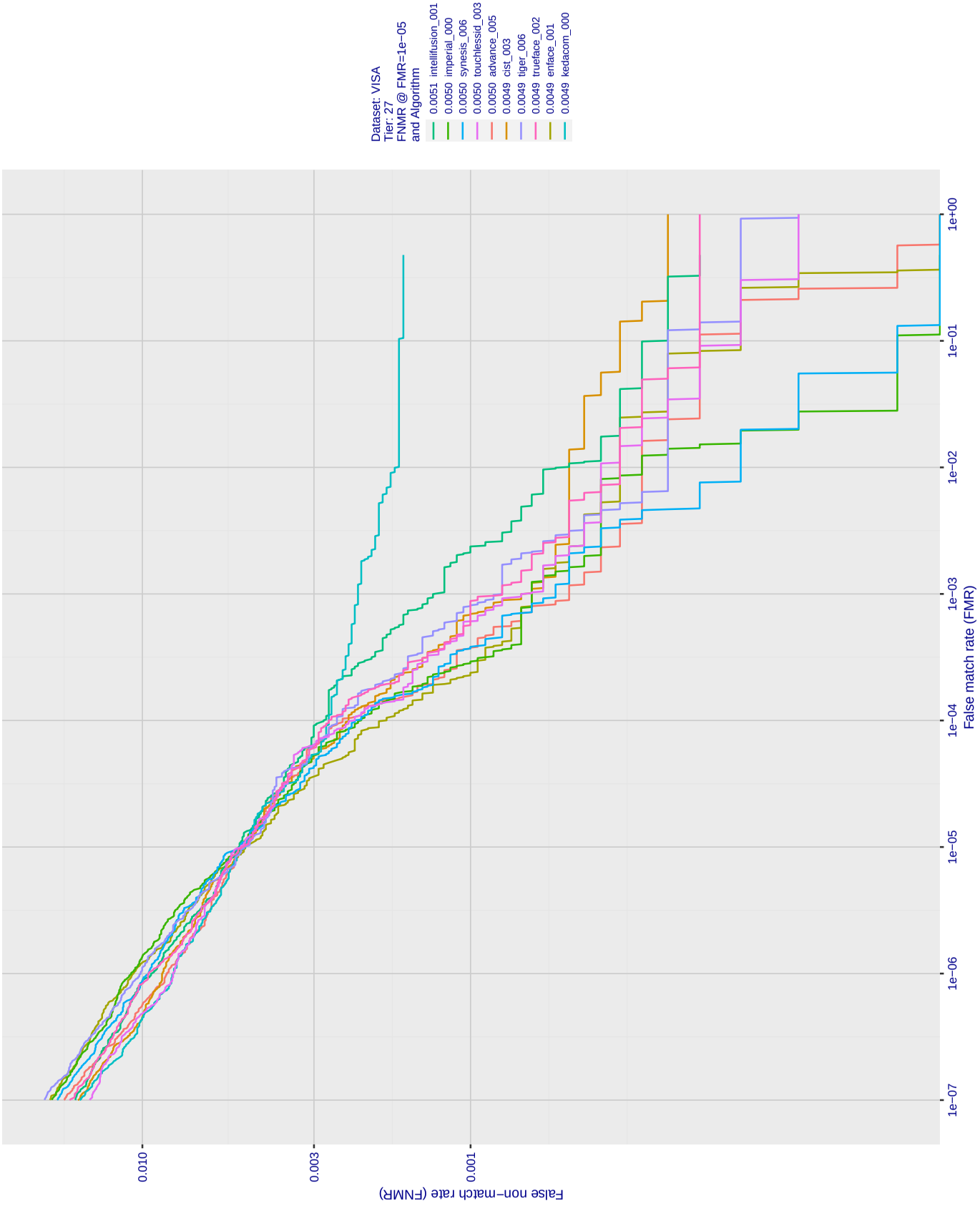

Figure 77: For the visa images, detection error tradeoff (DET) characteristics showing false non-match rate vs. false match rate plotted parametrically on threshold, T. The scales are logarithmic in order to show many decades of FMR.

FNMR(T) "False non-match rate"
FMR(T) "False match rate"

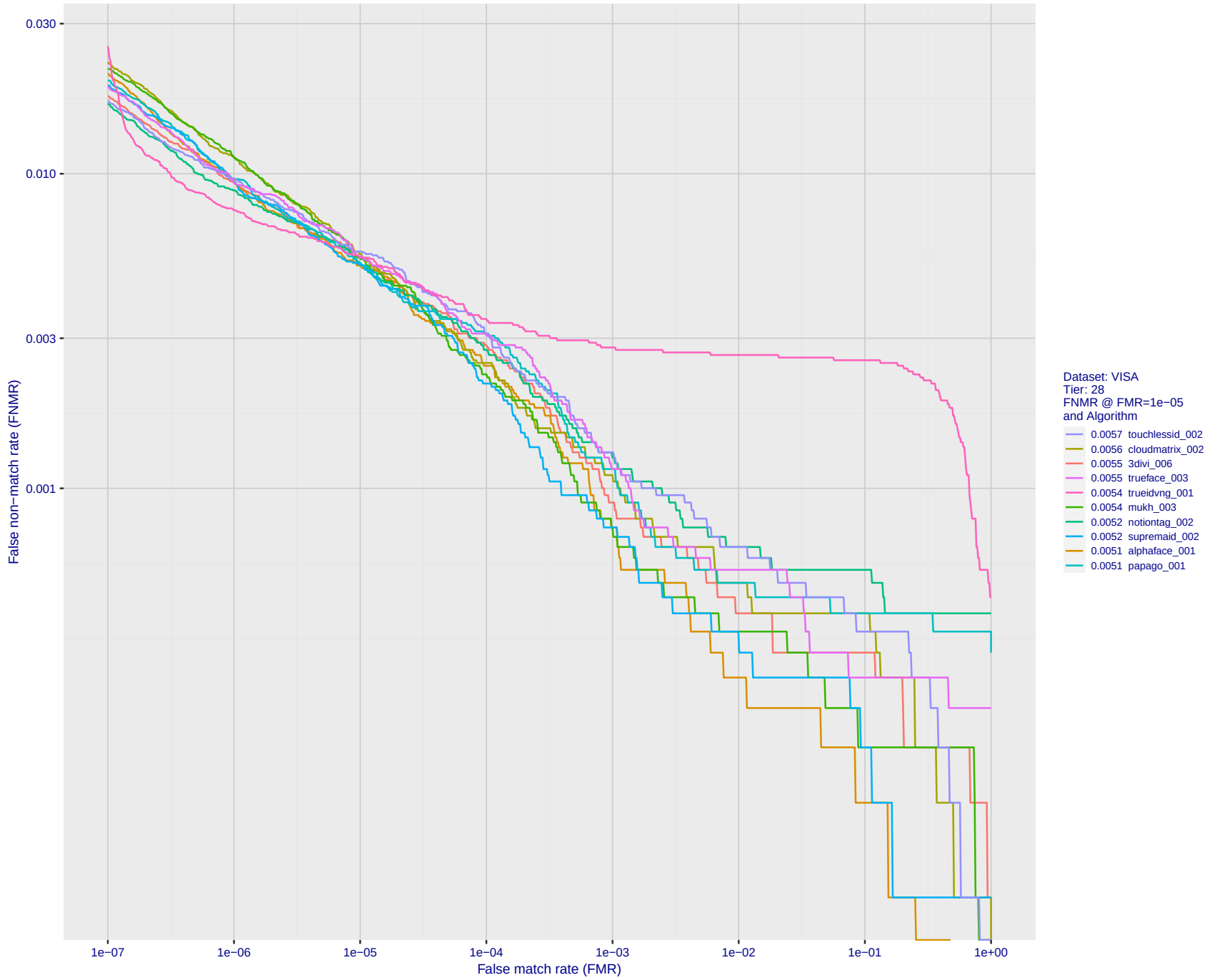

Figure 78: For the visa images, detection error tradeoff (DET) characteristics showing false non-match rate vs. false match rate plotted parametrically on threshold, T. The scales are logarithmic in order to show many decades of FMR.

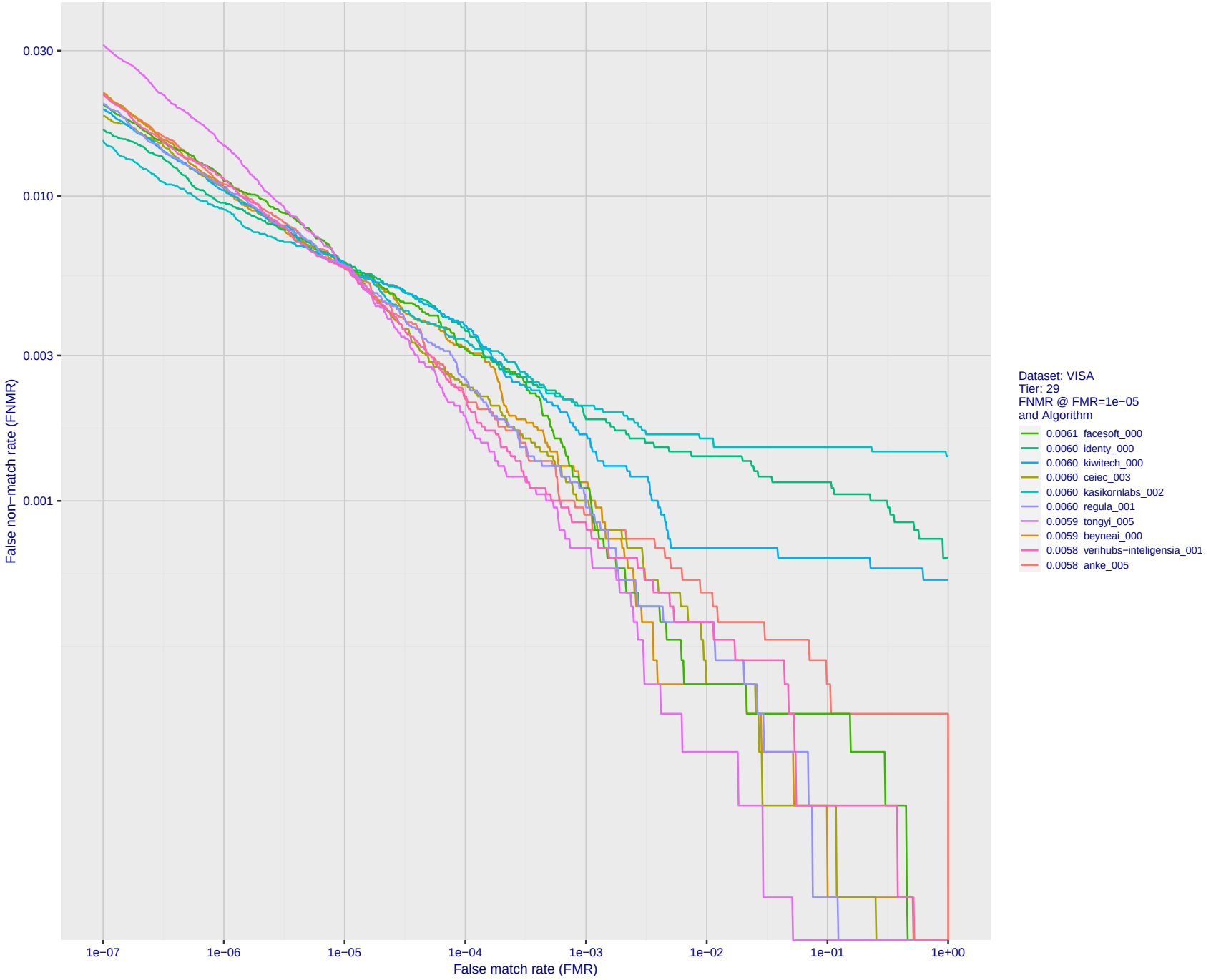

Figure 79: For the visa images, detection error tradeoff (DET) characteristics showing false non-match rate vs. false match rate plotted parametrically on threshold, T. The scales are logarithmic in order to show many decades of FMR.

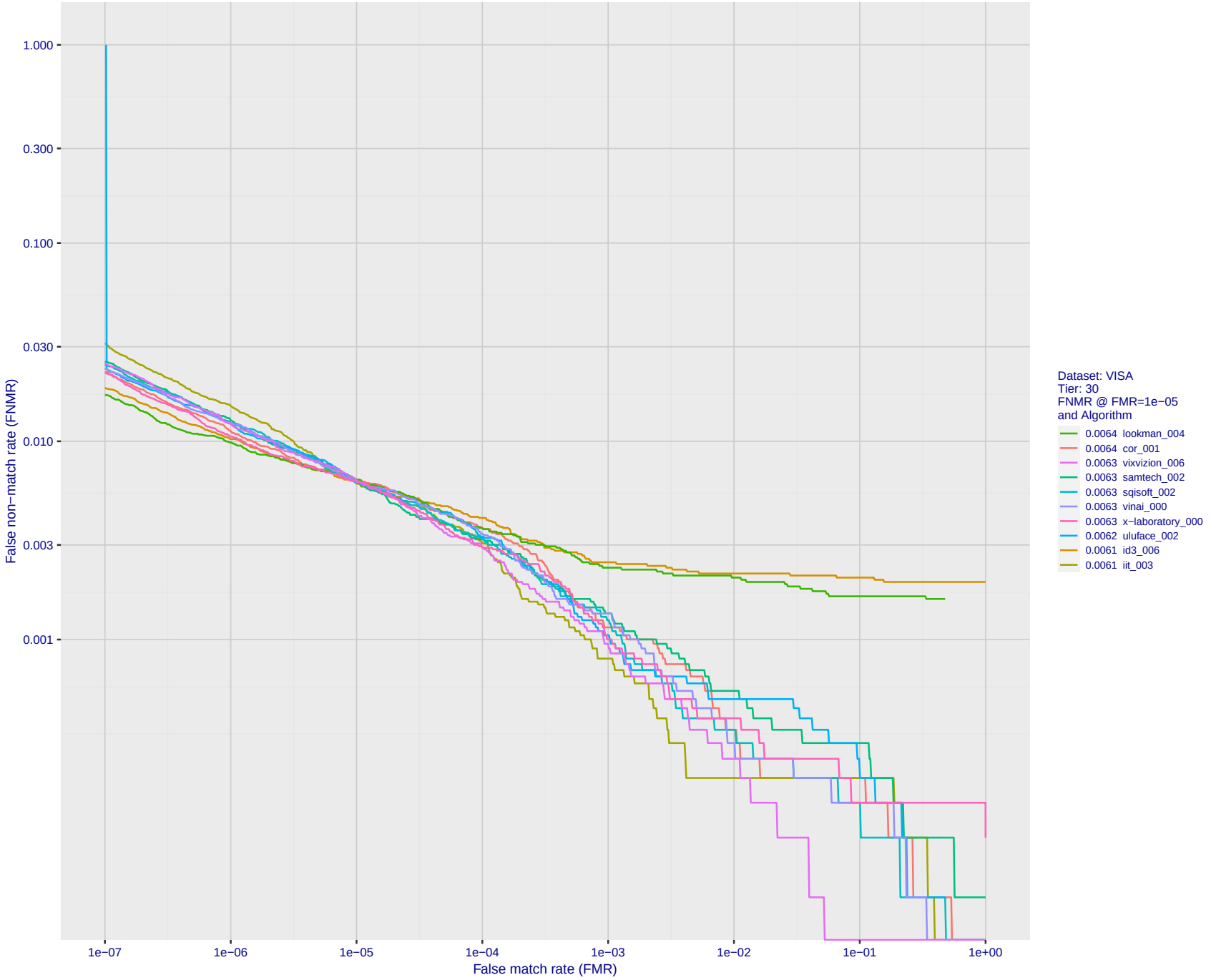

Figure 80: For the visa images, detection error tradeoff (DET) characteristics showing false non-match rate vs. false match rate plotted parametrically on threshold, T. The scales are logarithmic in order to show many decades of FMR.

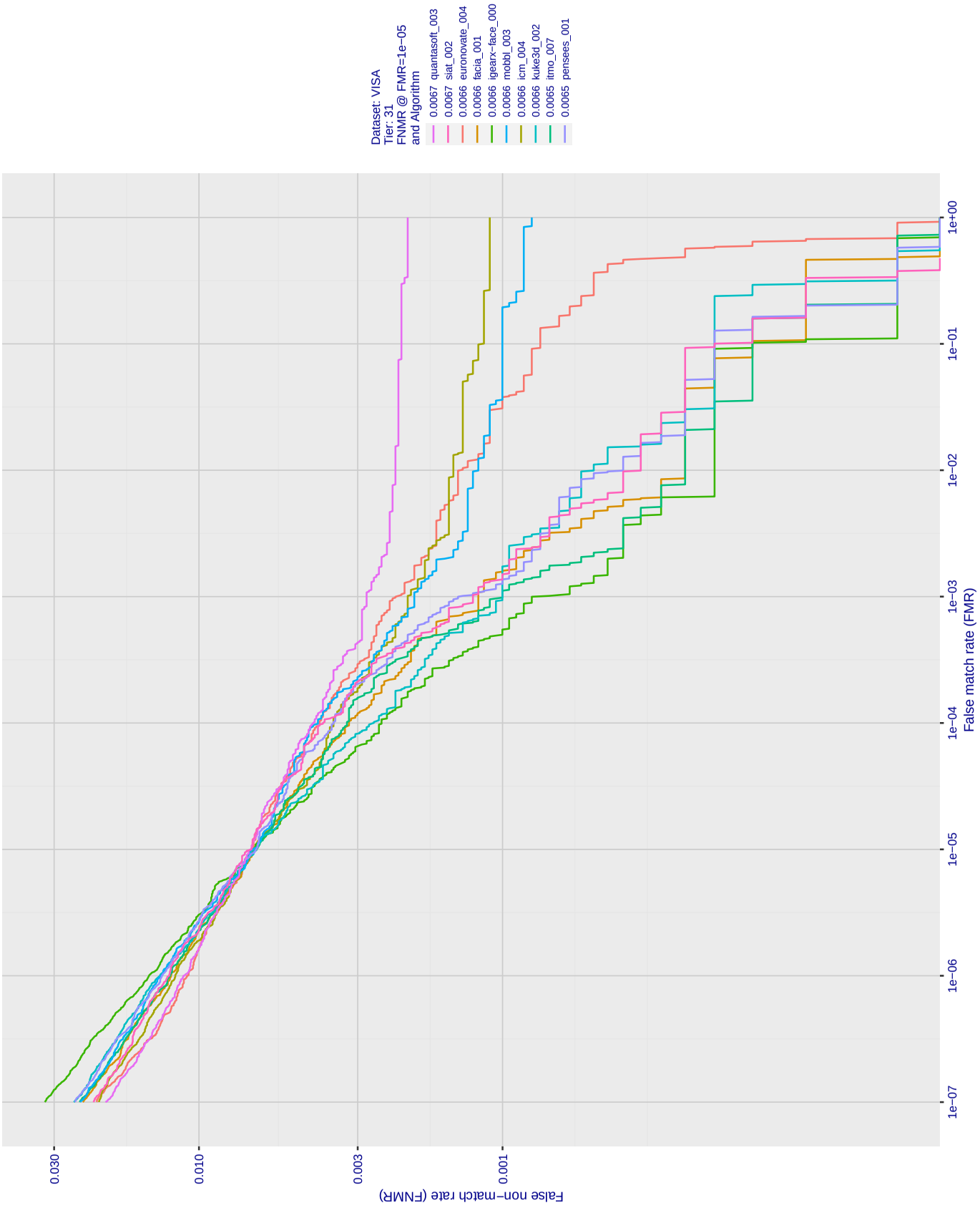

Figure 81: For the visa images, detection error tradeoff (DET) characteristics showing false non-match rate vs. false match rate plotted parametrically on threshold, T. The scales are logarithmic in order to show many decades of FMR.

FNMR(T) "False non-match rate"
FMR(T) "False match rate"

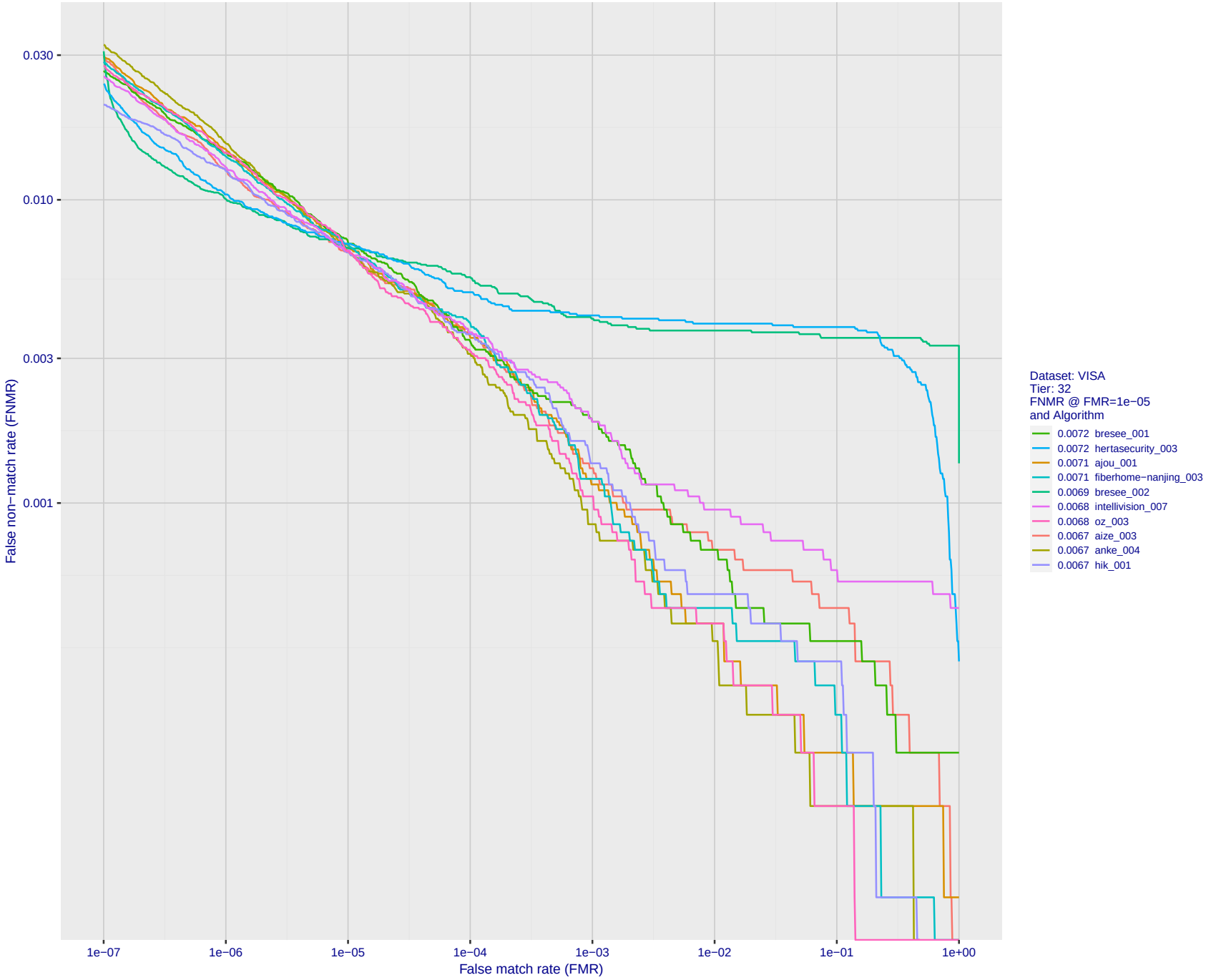

*Figure 82: For the visa images, detection error tradeoff (*DET*) characteristics showing false non-match rate vs. false match rate plotted parametrically on threshold, T. The scales are logarithmic in order to show many decades of* FMR*.*

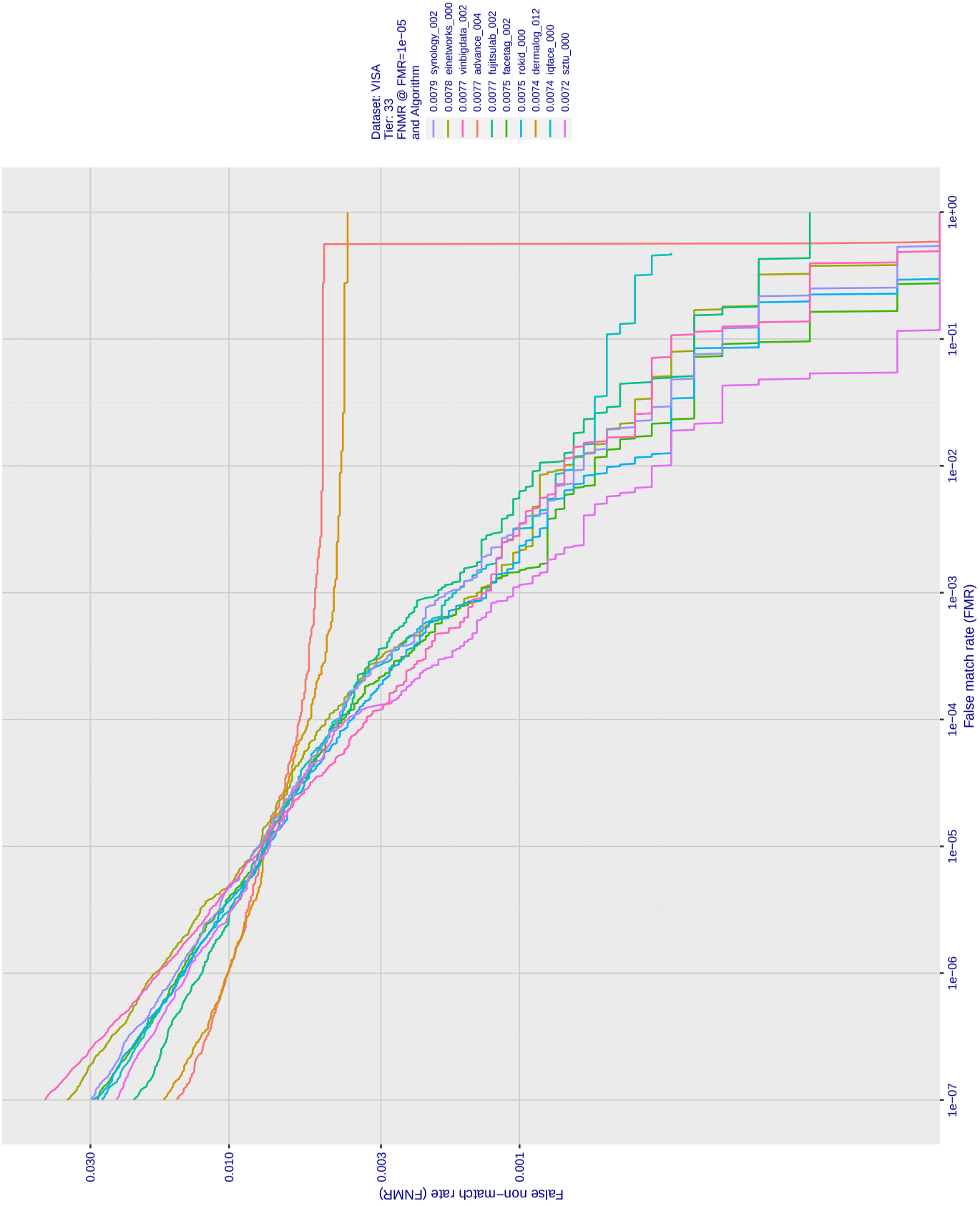

Figure 83: For the visa images, detection error tradeoff (DET) characteristics showing false non-match rate vs. false match rate plotted parametrically on threshold, T. The scales are logarithmic in order to show many decades of FMR.

FNMR(T) "False non-match rate"
FMR(T) "False match rate"

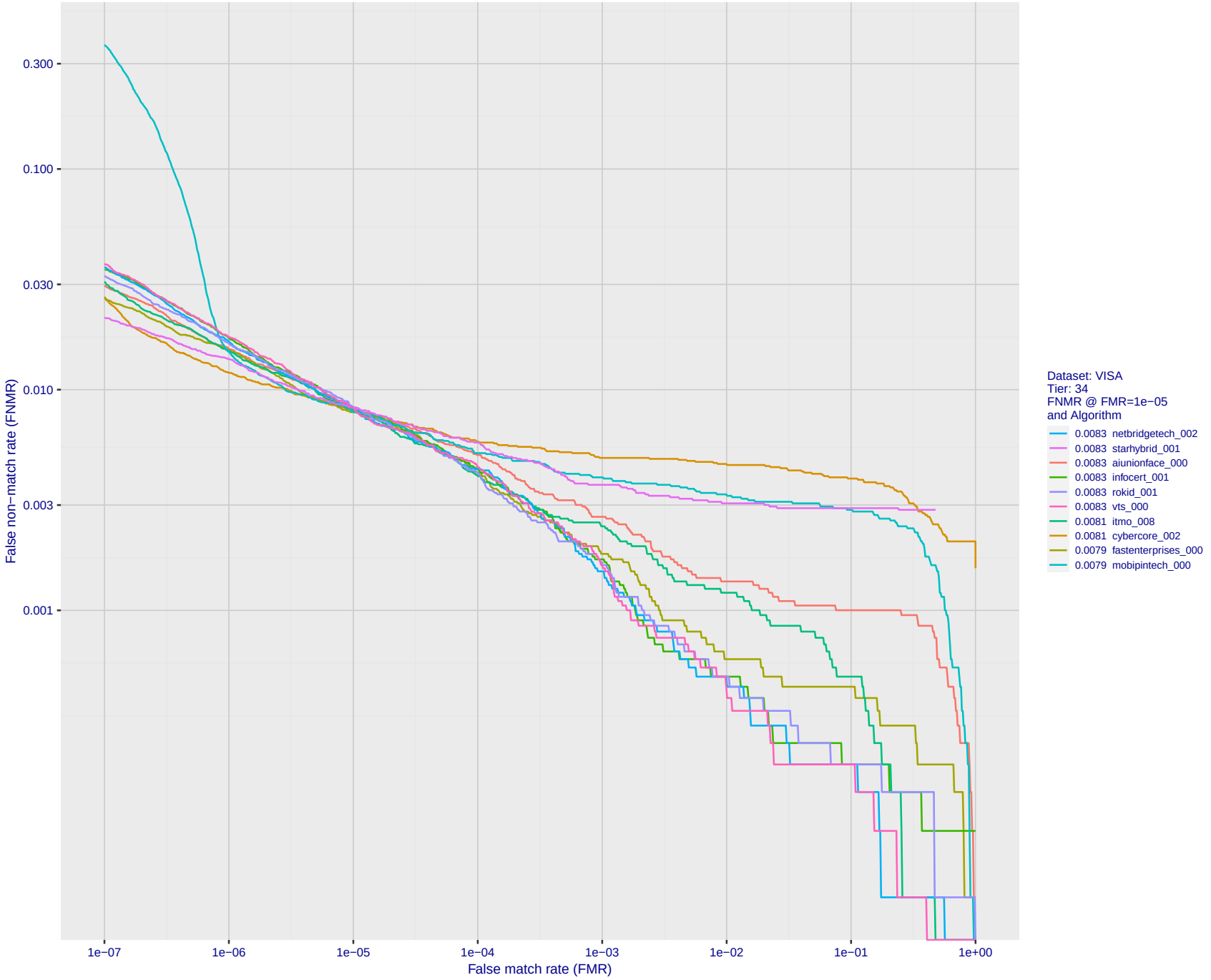

Figure 84: For the visa images, detection error tradeoff (DET) characteristics showing false non-match rate vs. false match rate plotted parametrically on threshold, T. The scales are logarithmic in order to show many decades of FMR.

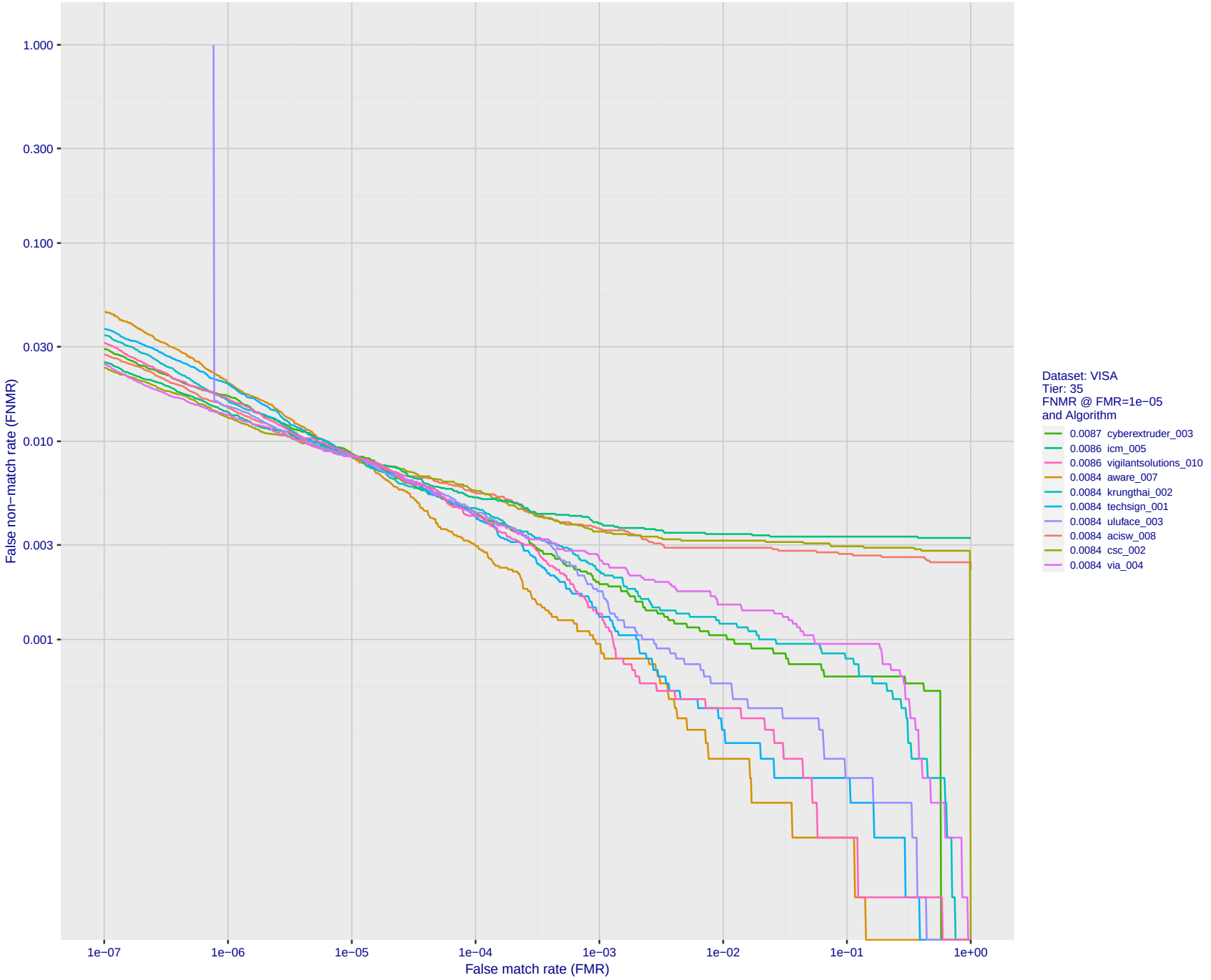

Figure 85: For the visa images, detection error tradeoff (DET) characteristics showing false non-match rate vs. false match rate plotted parametrically on threshold, T. The scales are logarithmic in order to show many decades of FMR.

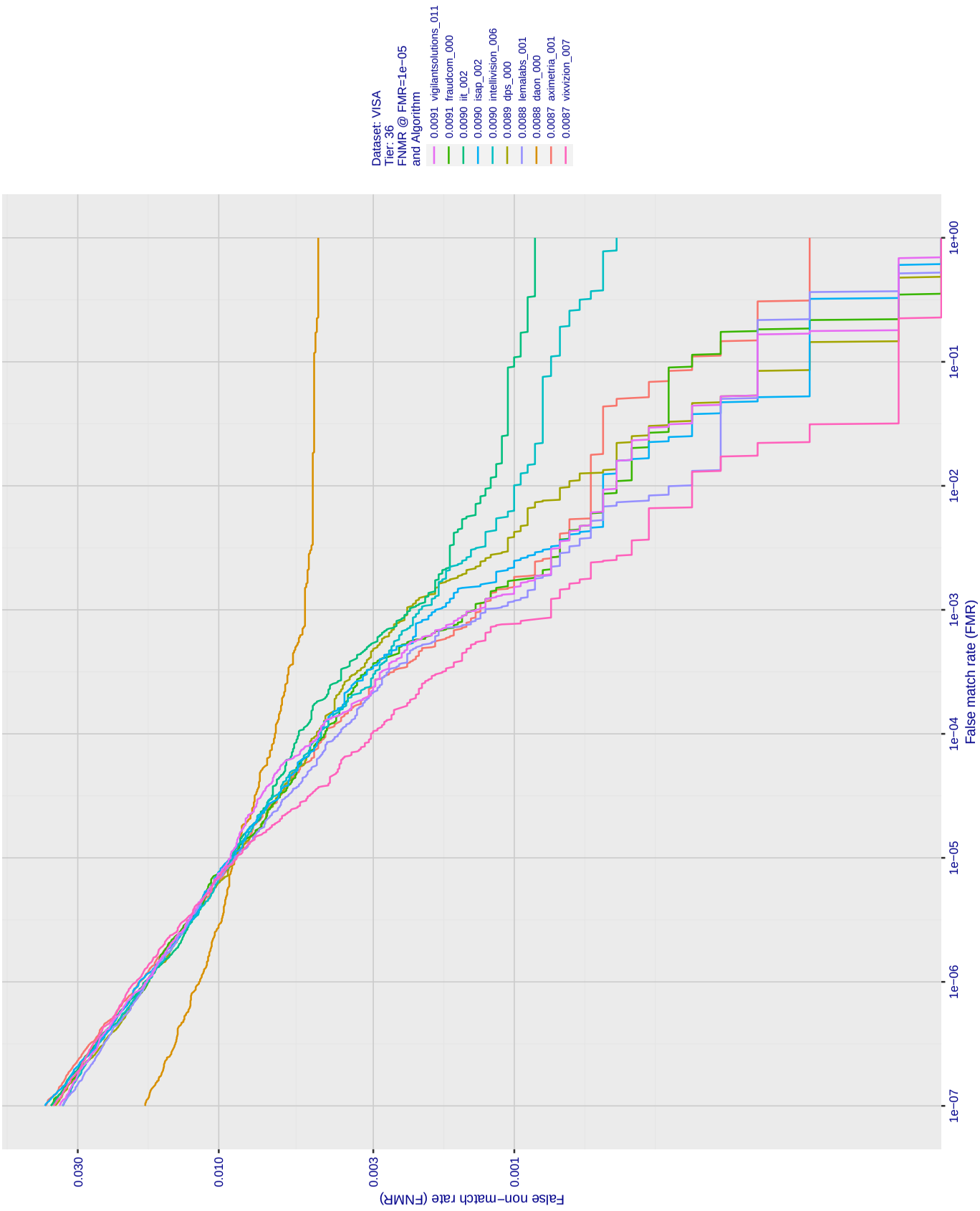

Figure 86: For the visa images, detection error tradeoff (DET) characteristics showing false non-match rate vs. false match rate plotted parametrically on threshold, T. The scales are logarithmic in order to show many decades of FMR.

FNMR(T) "False non-match rate"
FMR(T) "False match rate"

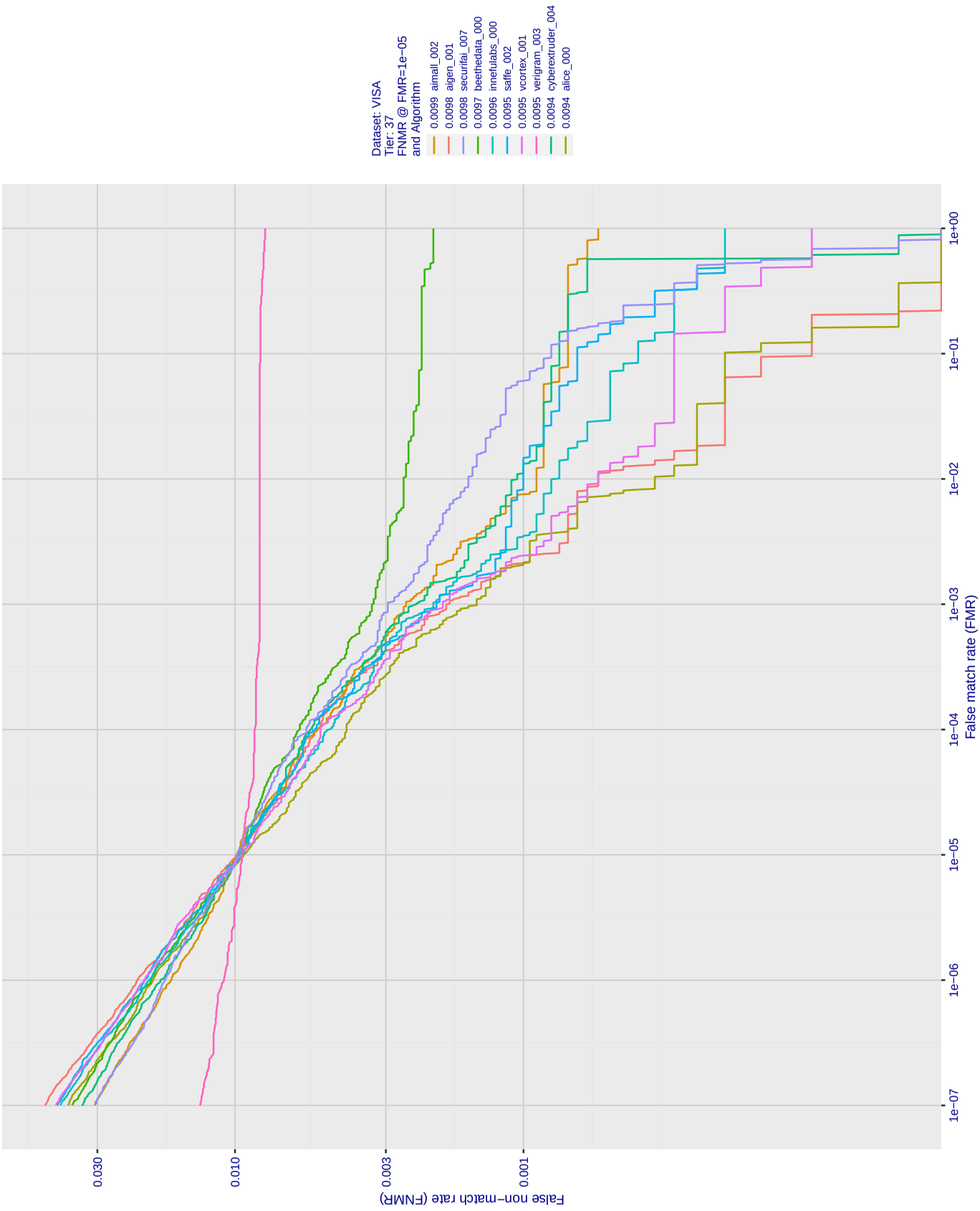

Figure 87: For the visa images, detection error tradeoff (DET) characteristics showing false non-match rate vs. false match rate plotted parametrically on threshold, T. The scales are logarithmic in order to show many decades of FMR.

FNMR(T) "False non-match rate"
FMR(T) "False match rate"

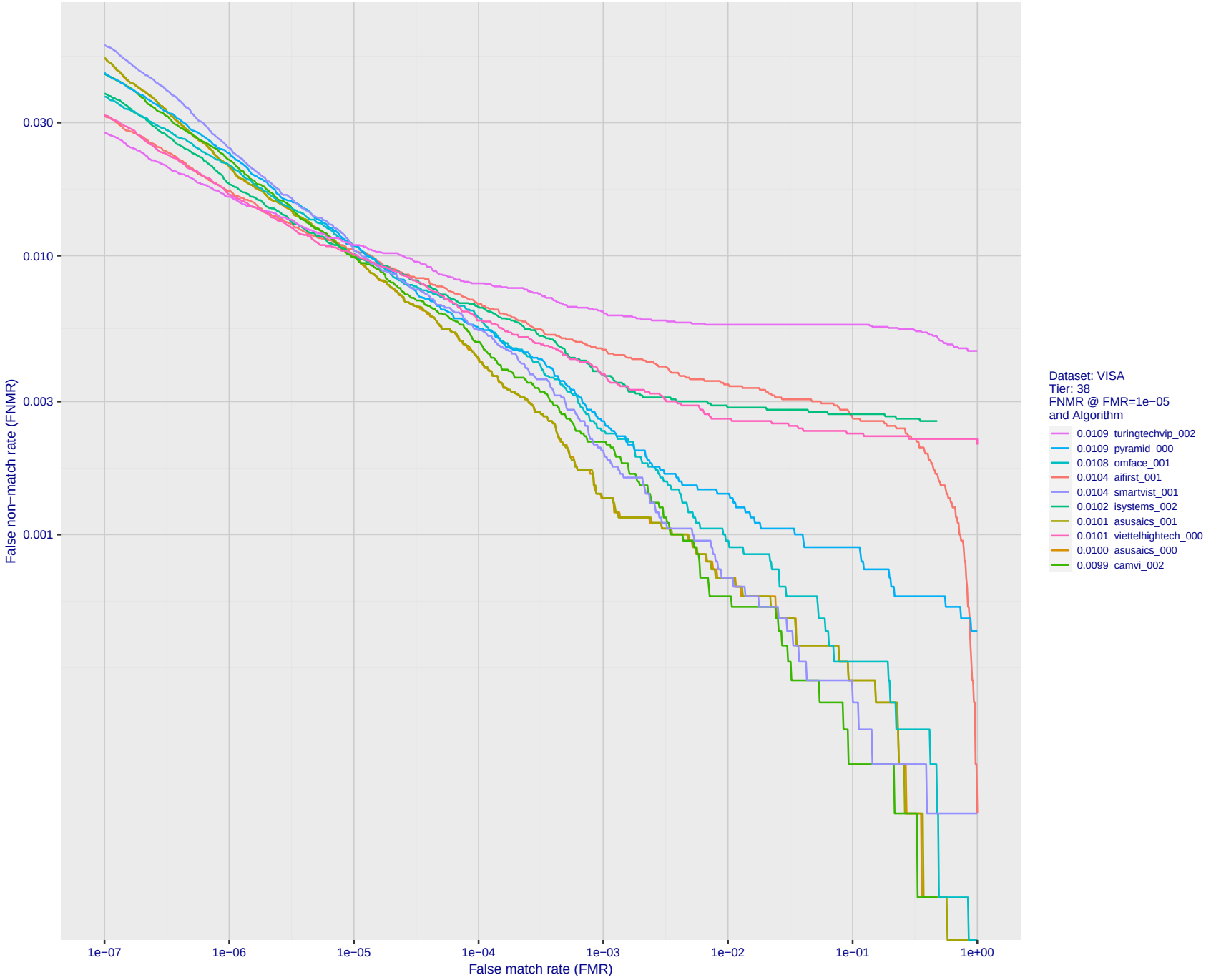

Figure 88: For the visa images, detection error tradeoff (DET) characteristics showing false non-match rate vs. false match rate plotted parametrically on threshold, T. The scales are logarithmic in order to show many decades of FMR.

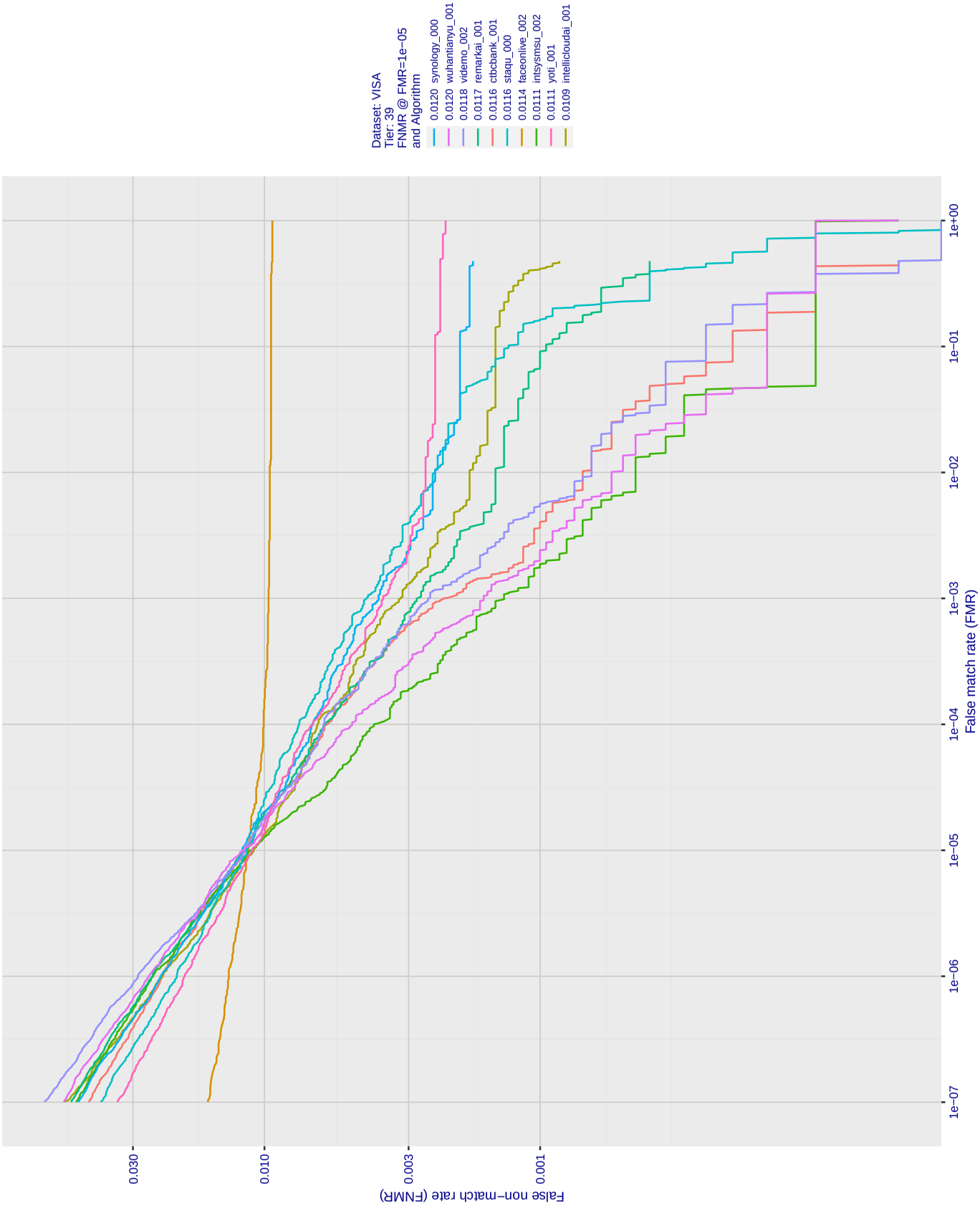

Figure 89: For the visa images, detection error tradeoff (DET) characteristics showing false non-match rate vs. false match rate plotted parametrically on threshold, T. The scales are logarithmic in order to show many decades of FMR.

FNMR(T) "False non-match rate"
FMR(T) "False match rate"

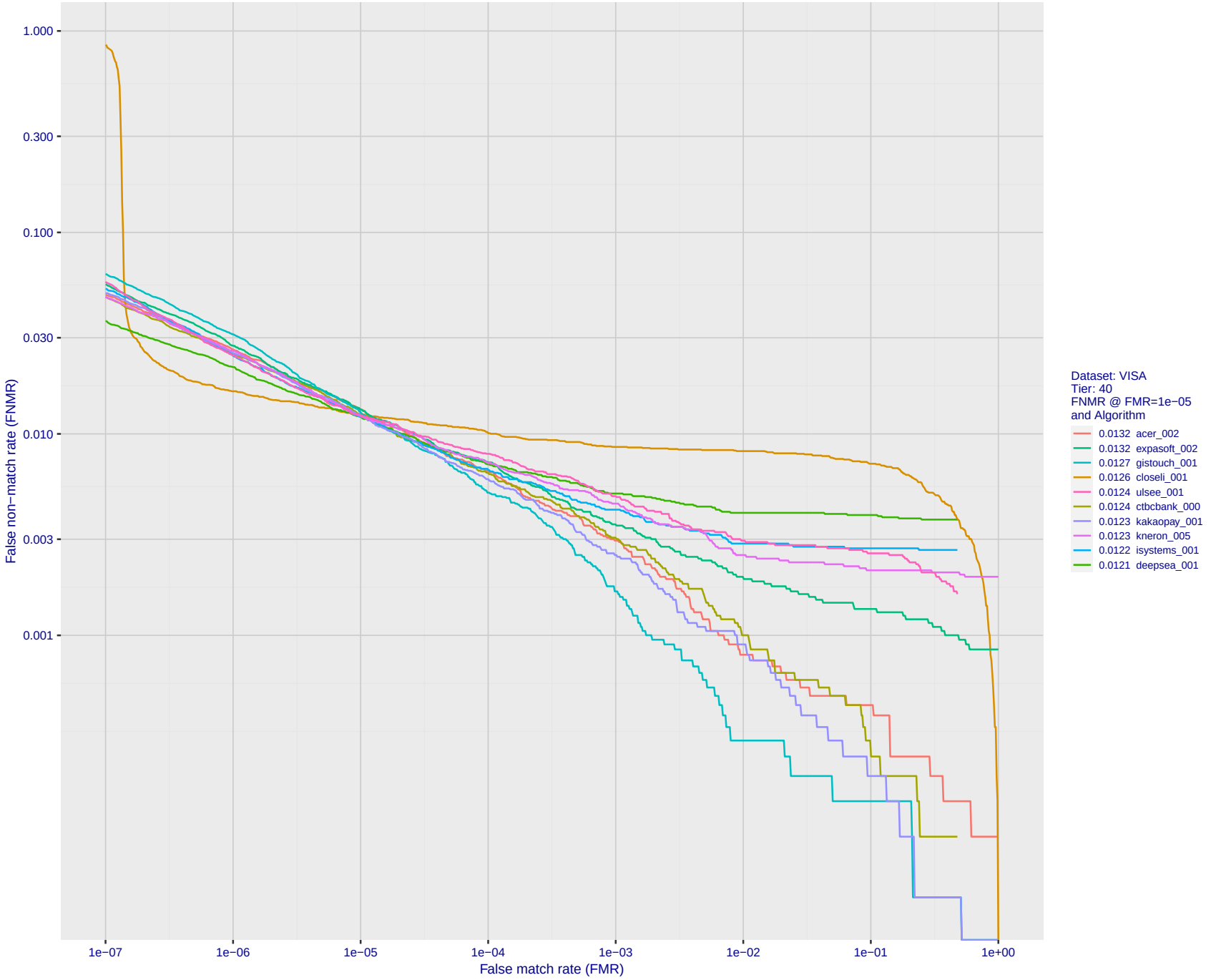

*Figure 90: For the visa images, detection error tradeoff (*DET*) characteristics showing false non-match rate vs. false match rate plotted parametrically on threshold, T. The scales are logarithmic in order to show many decades of* FMR*.*

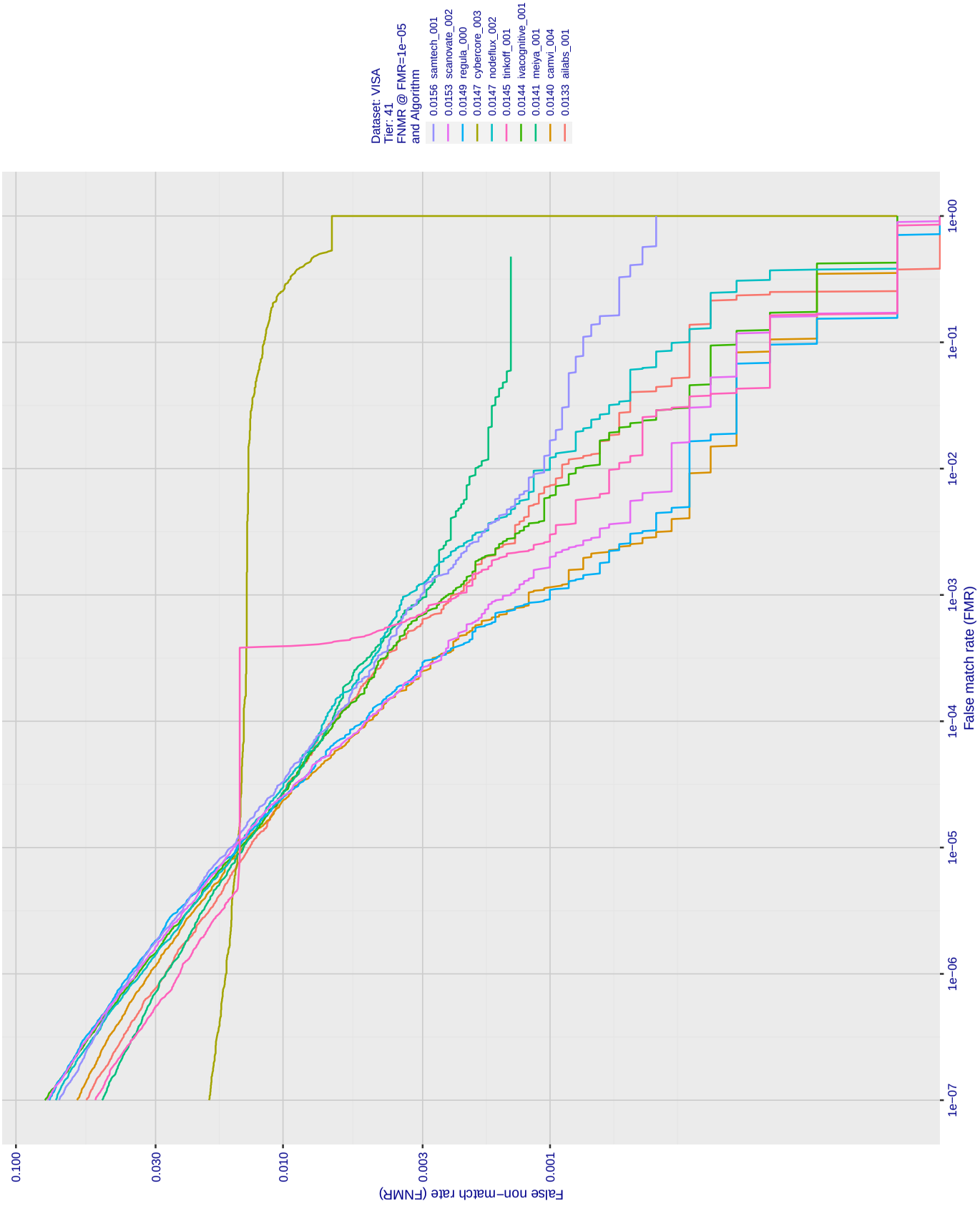

Figure 91: For the visa images, detection error tradeoff (DET) characteristics showing false non-match rate vs. false match rate plotted parametrically on threshold, T. The scales are logarithmic in order to show many decades of FMR.

FNMR(T) "False non-match rate"
FMR(T) "False match rate"

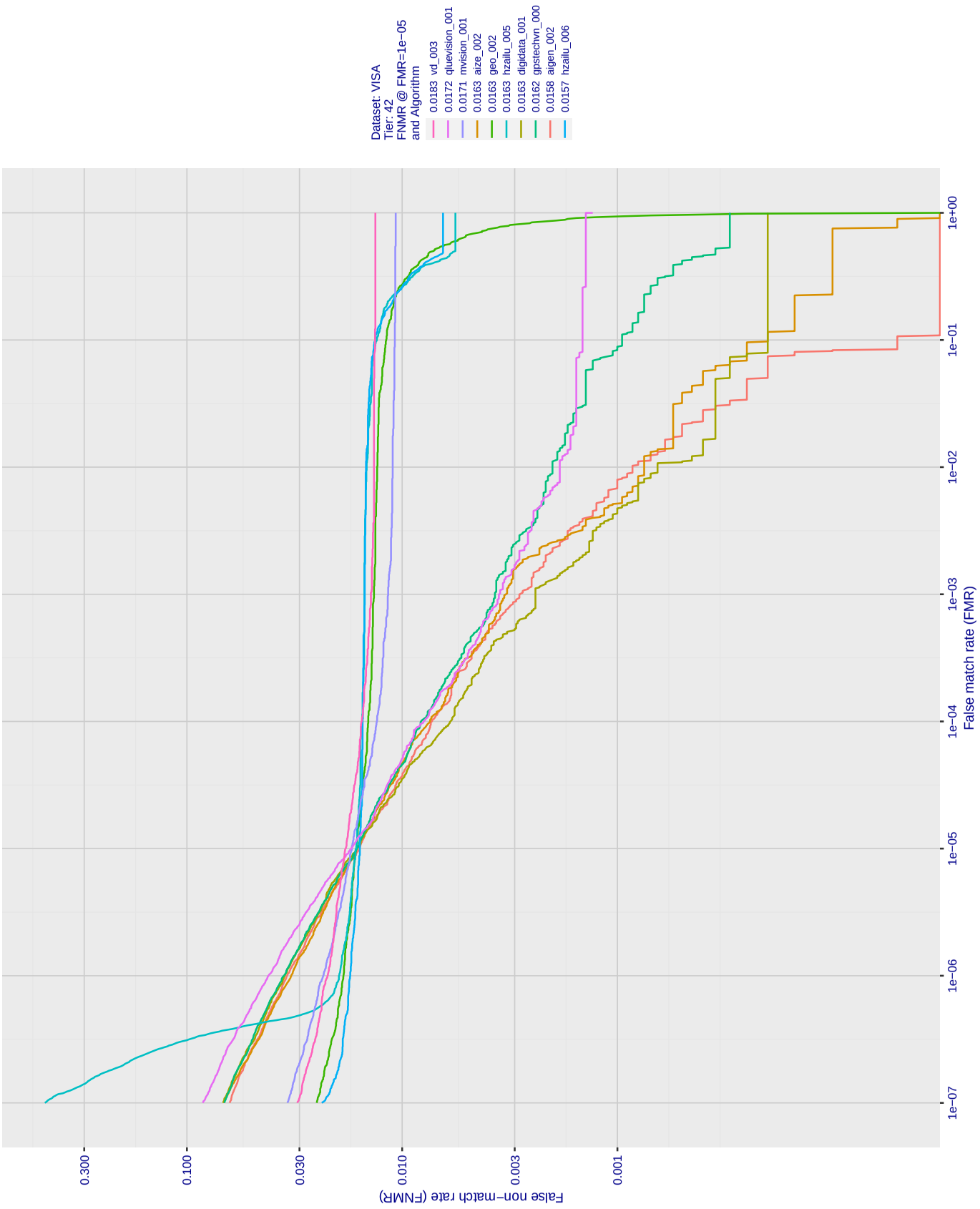

Figure 92: For the visa images, detection error tradeoff (DET) characteristics showing false non-match rate vs. false match rate plotted parametrically on threshold, T. The scales are logarithmic in order to show many decades of FMR.

FNMR(T) "False non-match rate"
FMR(T) "False match rate"

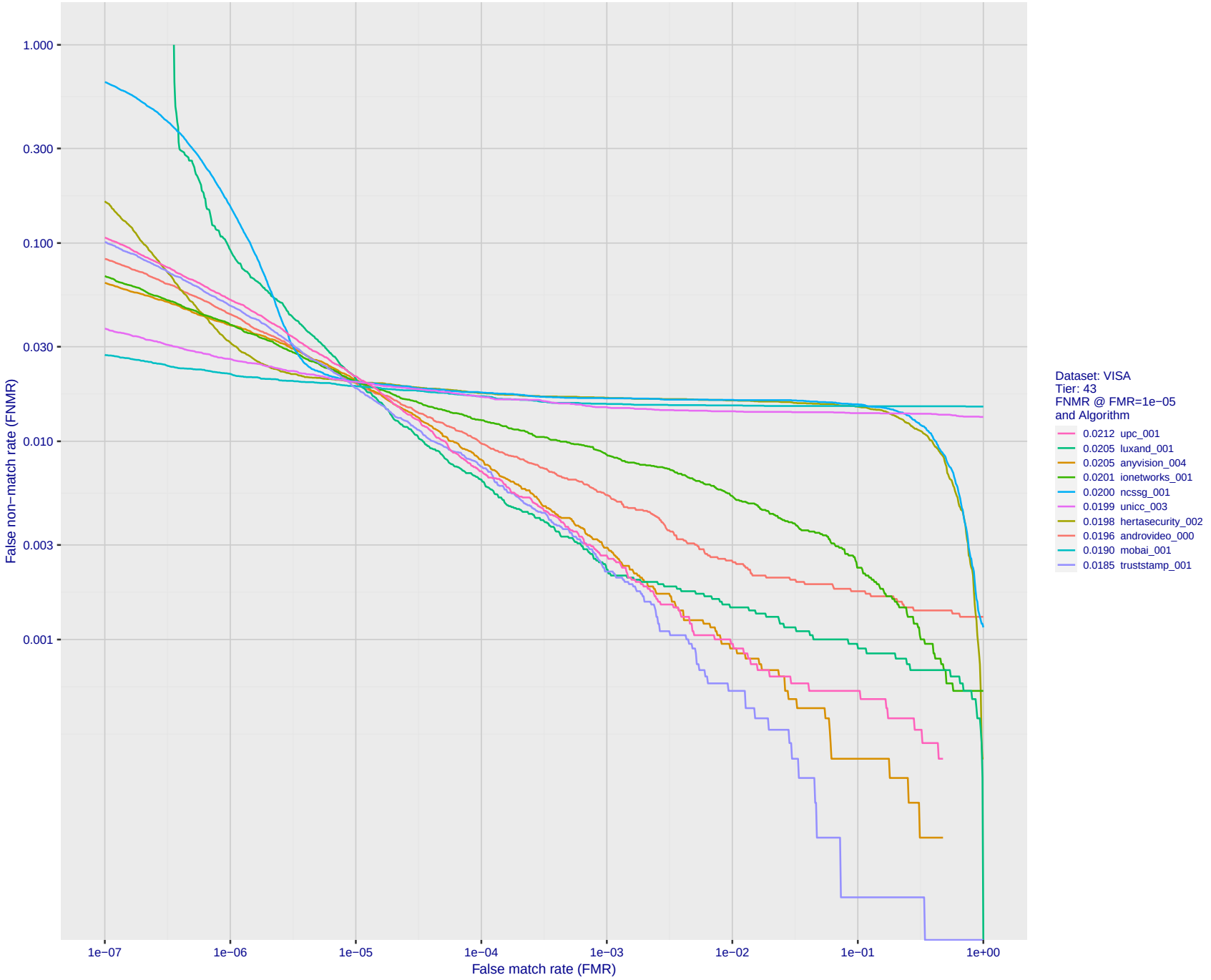

*Figure 93: For the visa images, detection error tradeoff (*DET*) characteristics showing false non-match rate vs. false match rate plotted parametrically on threshold, T. The scales are logarithmic in order to show many decades of* FMR*.*

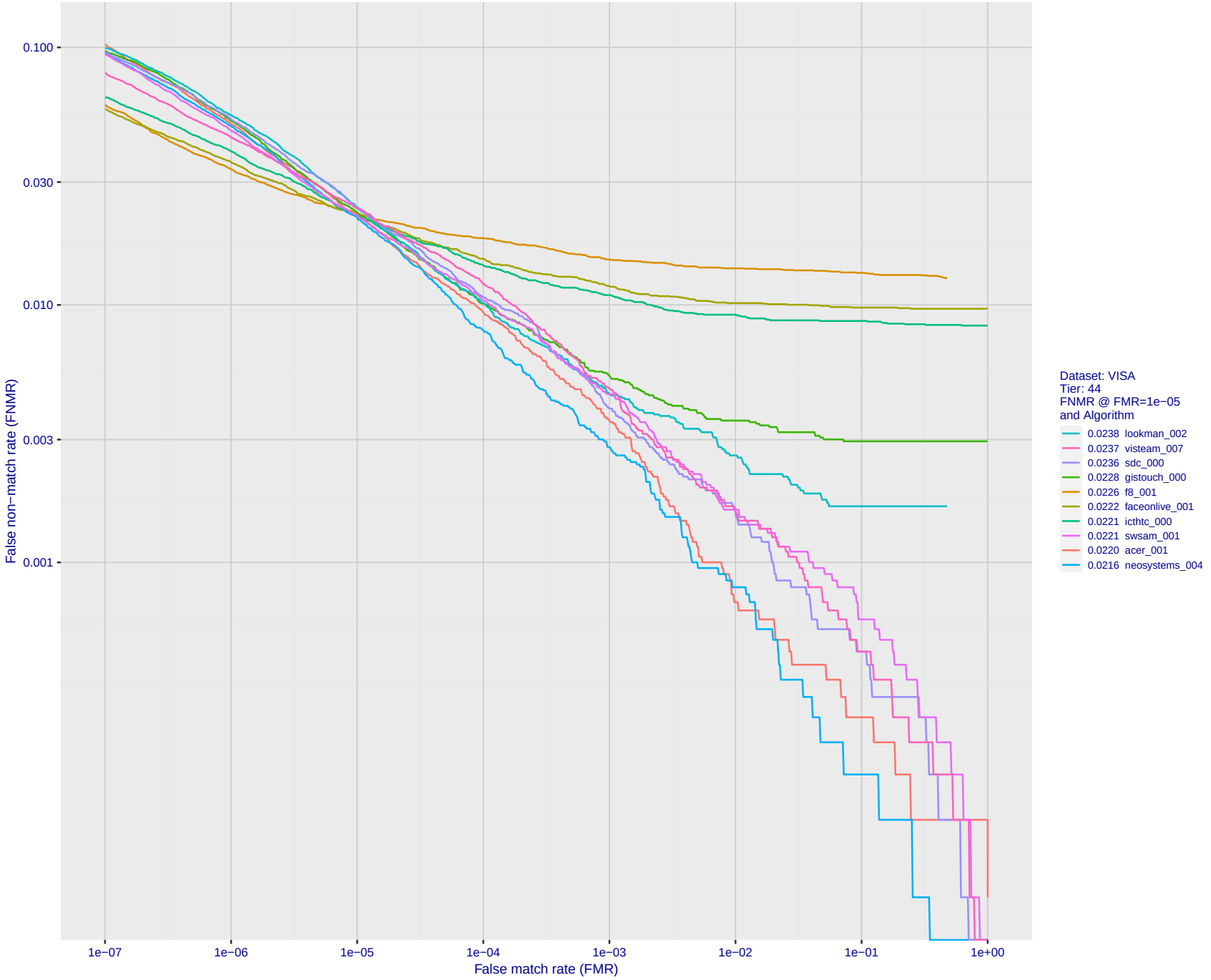

Figure 94: For the visa images, detection error tradeoff (DET) characteristics showing false non-match rate vs. false match rate plotted parametrically on threshold, T. The scales are logarithmic in order to show many decades of FMR.

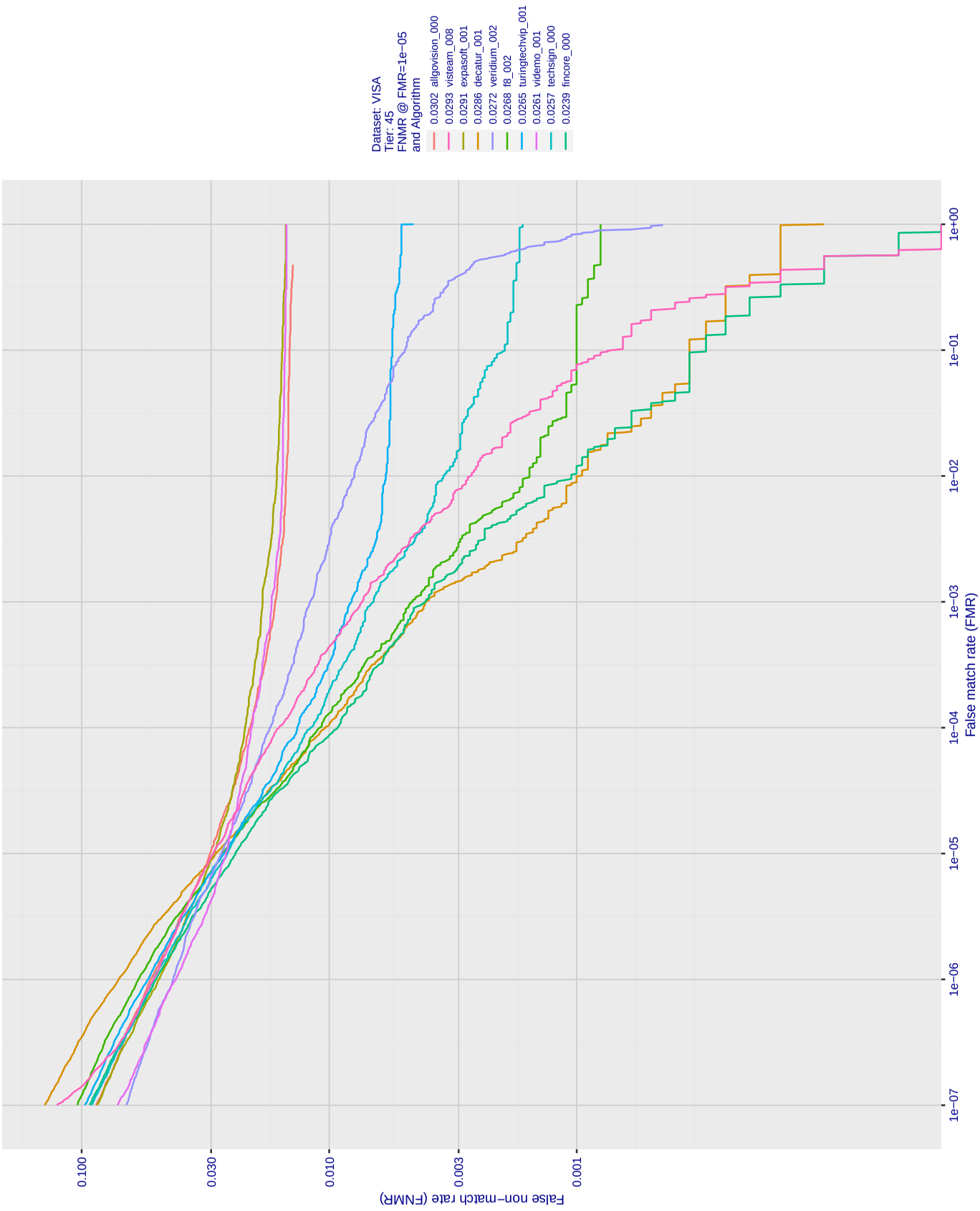

Figure 95: For the visa images, detection error tradeoff (DET) characteristics showing false non-match rate vs. false match rate plotted parametrically on threshold, T. The scales are logarithmic in order to show many decades of FMR.

FNMR(T) "False non-match rate"
FMR(T) "False match rate"

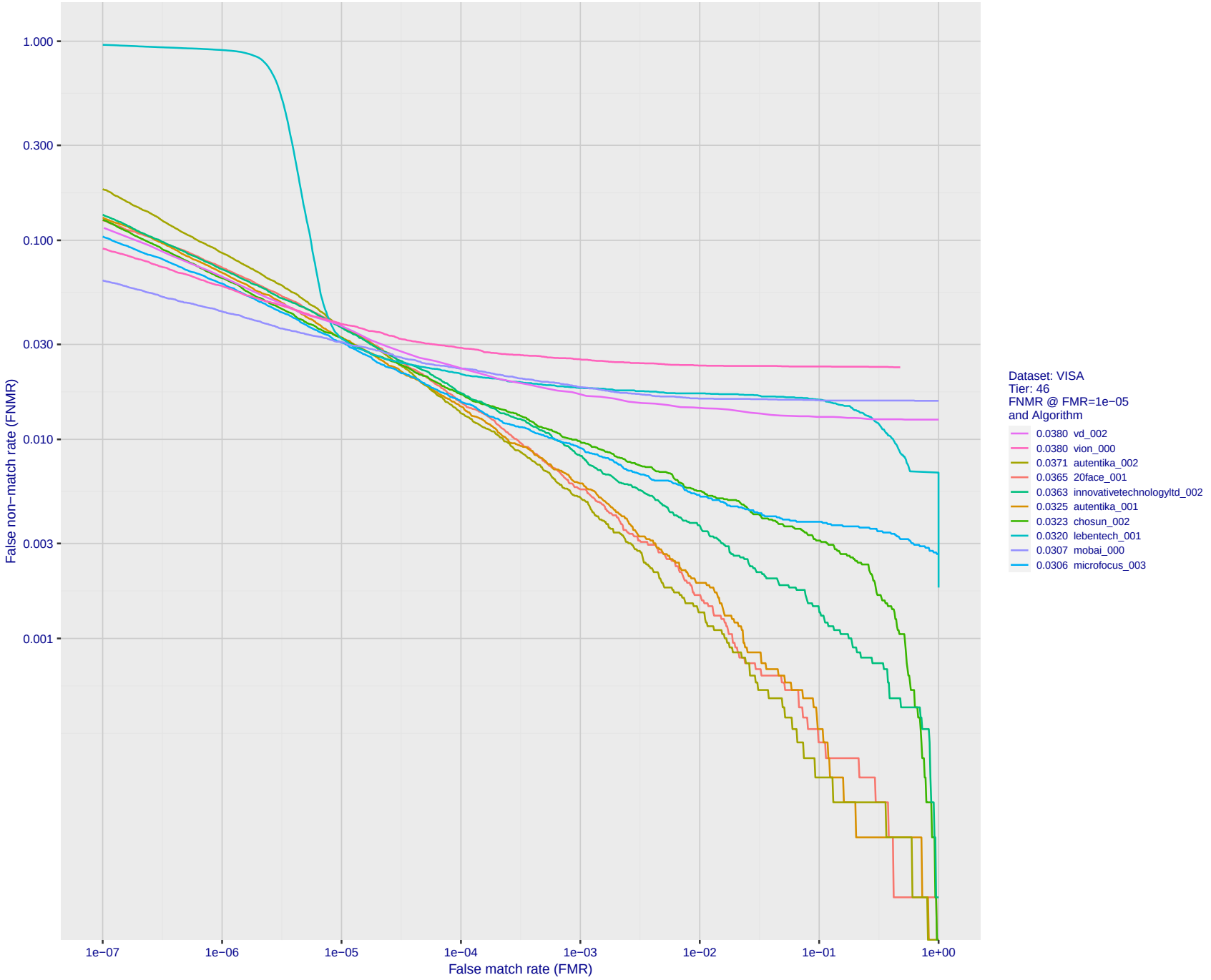

Figure 96: For the visa images, detection error tradeoff (DET) characteristics showing false non-match rate vs. false match rate plotted parametrically on threshold, T. The scales are logarithmic in order to show many decades of FMR.

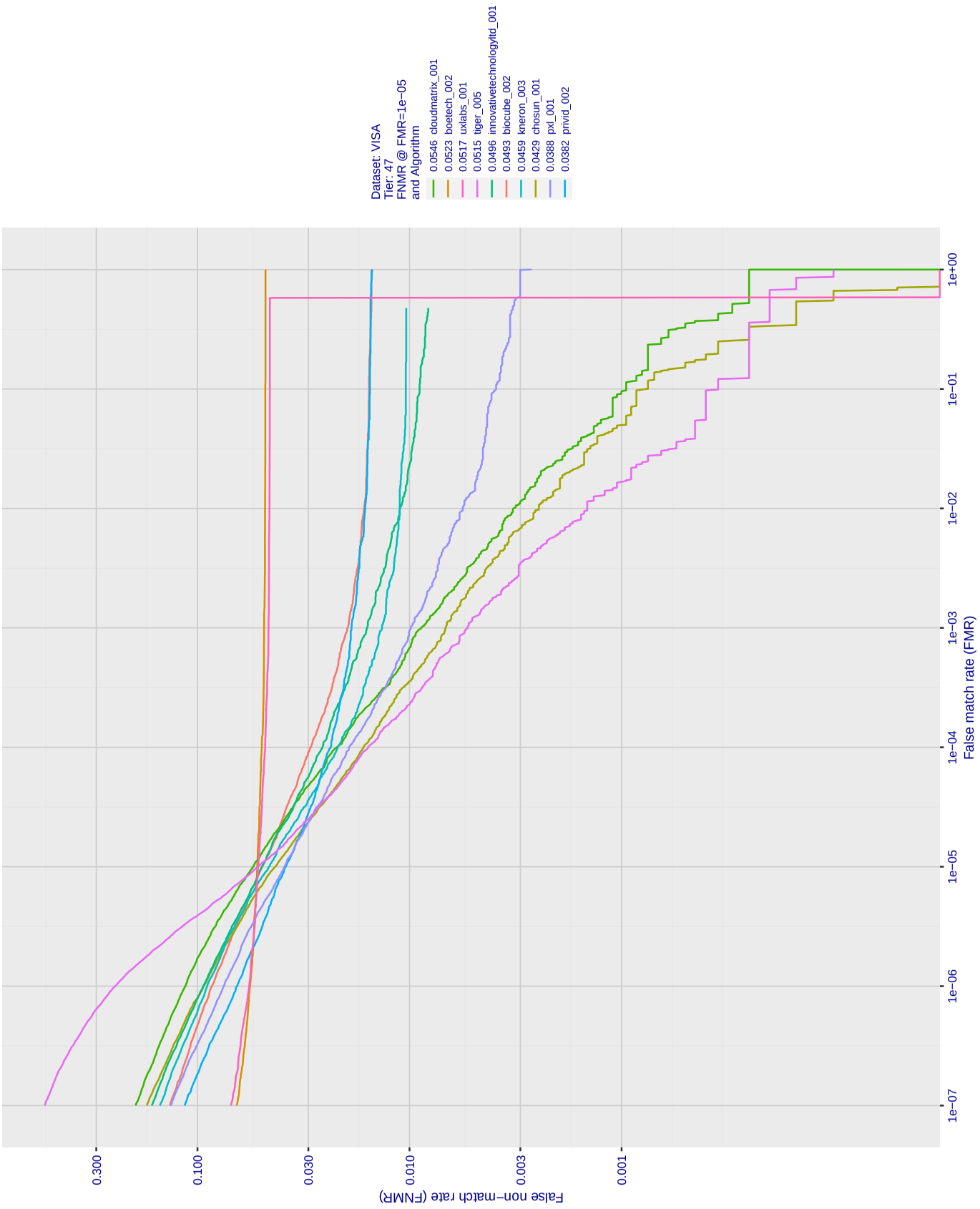

Figure 97: For the visa images, detection error tradeoff (DET) characteristics showing false non-match rate vs. false match rate plotted parametrically on threshold, T. The scales are logarithmic in order to show many decades of FMR.

FNMR(T) "False non-match rate"
FMR(T) "False match rate"

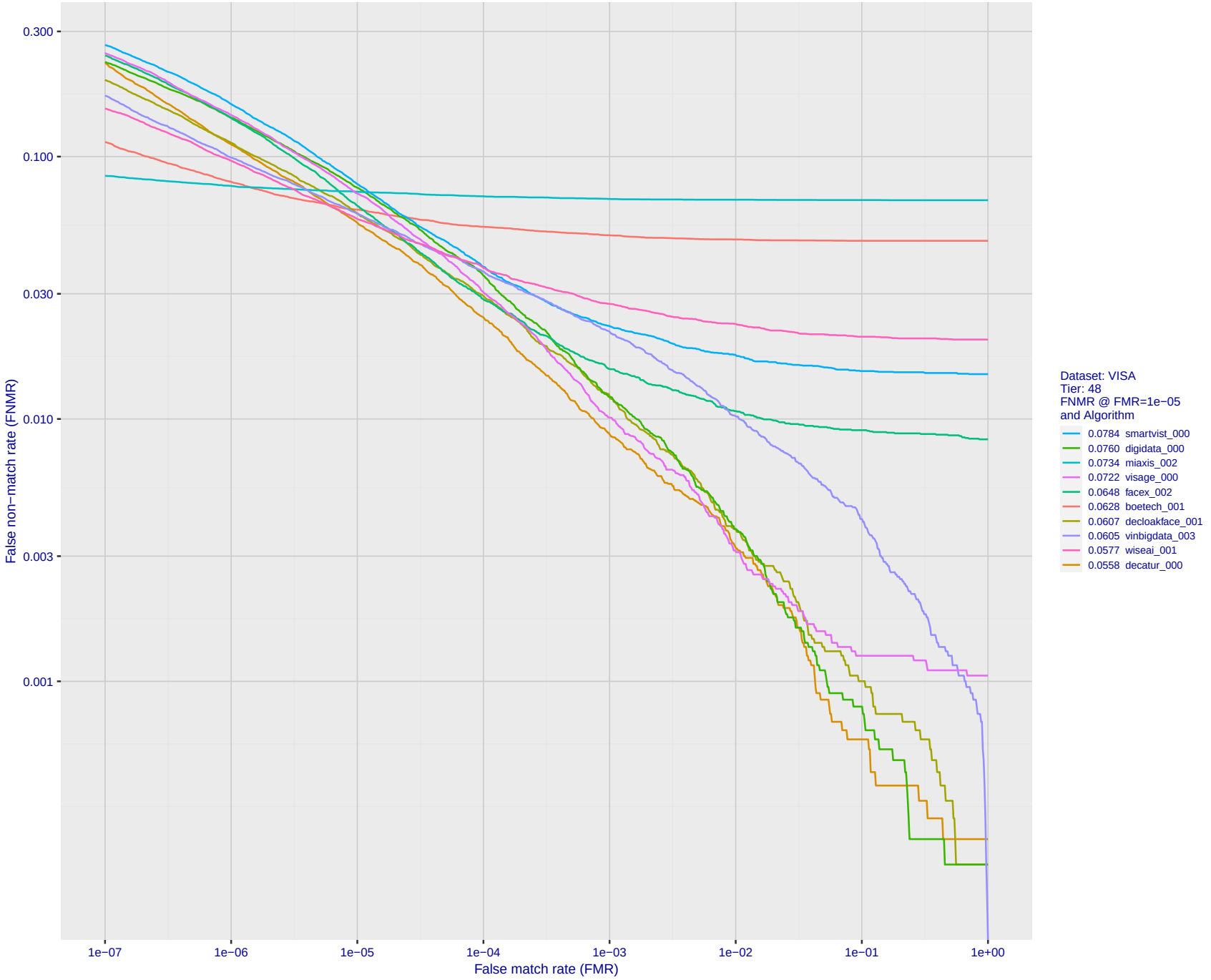

Figure 98: For the visa images, detection error tradeoff (DET) characteristics showing false non-match rate vs. false match rate plotted parametrically on threshold, T. The scales are logarithmic in order to show many decades of FMR.

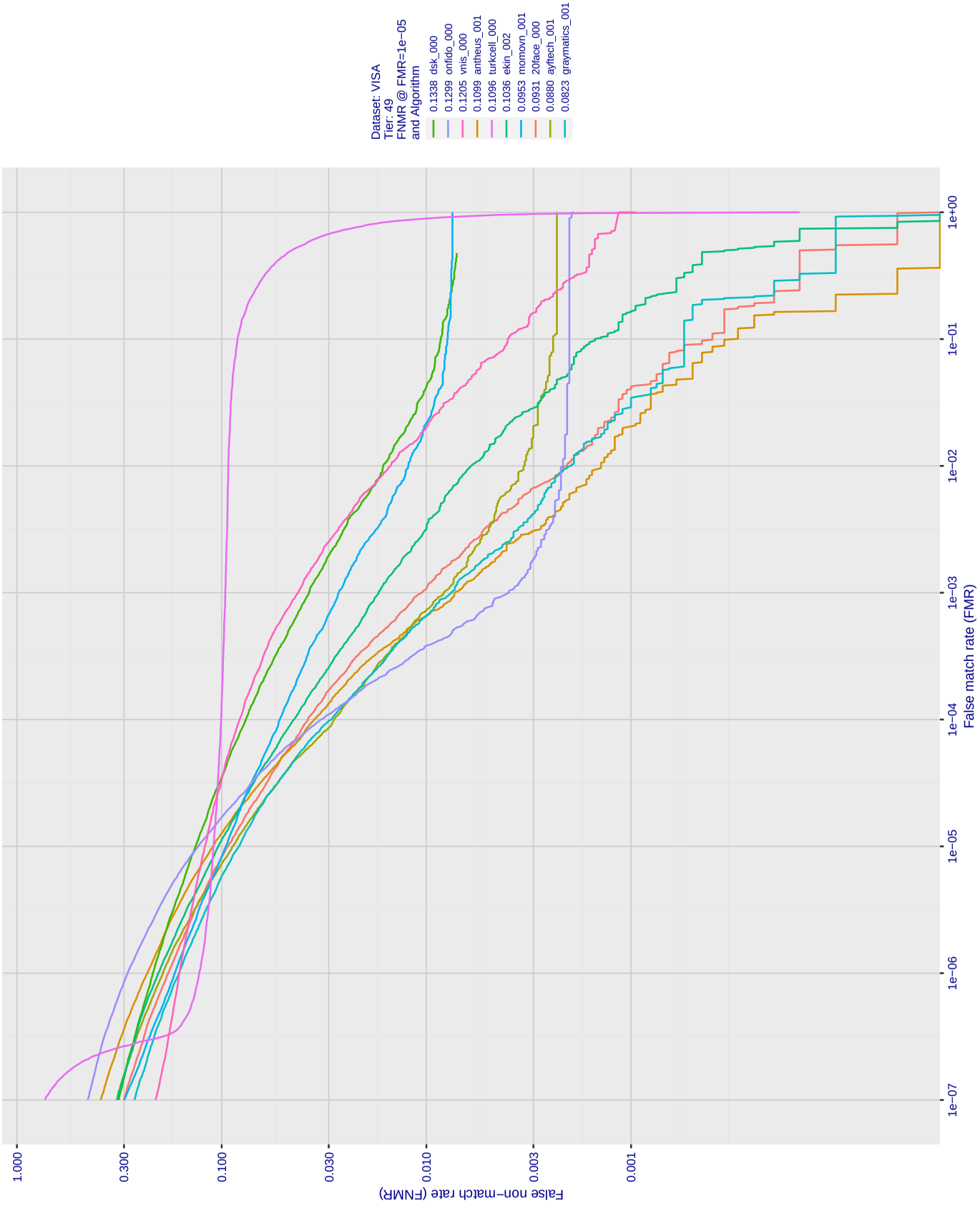

Figure 99: For the visa images, detection error tradeoff (DET) characteristics showing false non-match rate vs. false match rate plotted parametrically on threshold, T. The scales are logarithmic in order to show many decades of FMR.

FNMR(T) "False non-match rate"
FMR(T) "False match rate"

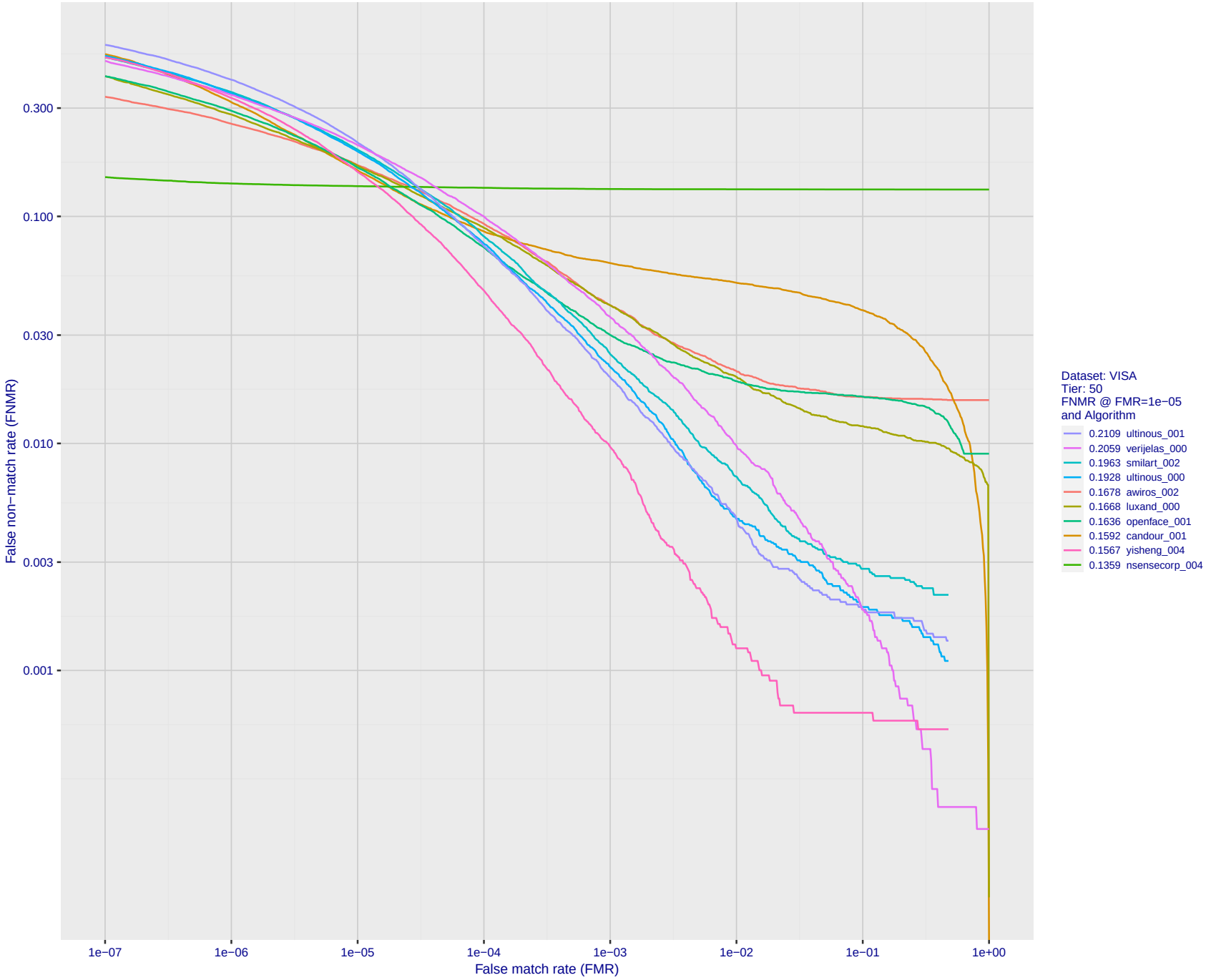

Figure 100: For the visa images, detection error tradeoff (DET) characteristics showing false non-match rate vs. false match rate plotted parametrically on threshold, T. The scales are logarithmic in order to show many decades of FMR.

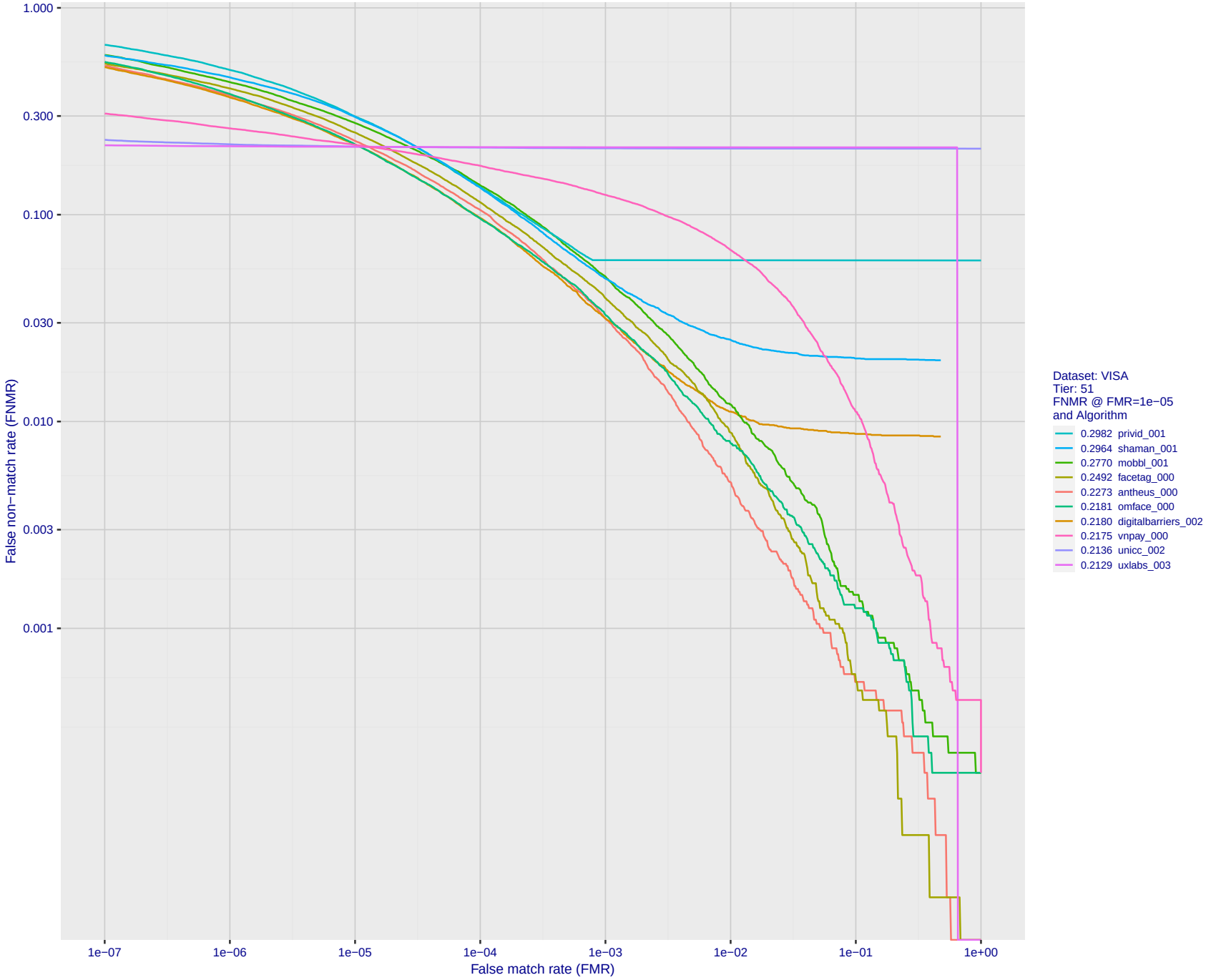

Figure 101: For the visa images, detection error tradeoff (DET) characteristics showing false non-match rate vs. false match rate plotted parametrically on threshold, T. The scales are logarithmic in order to show many decades of FMR.

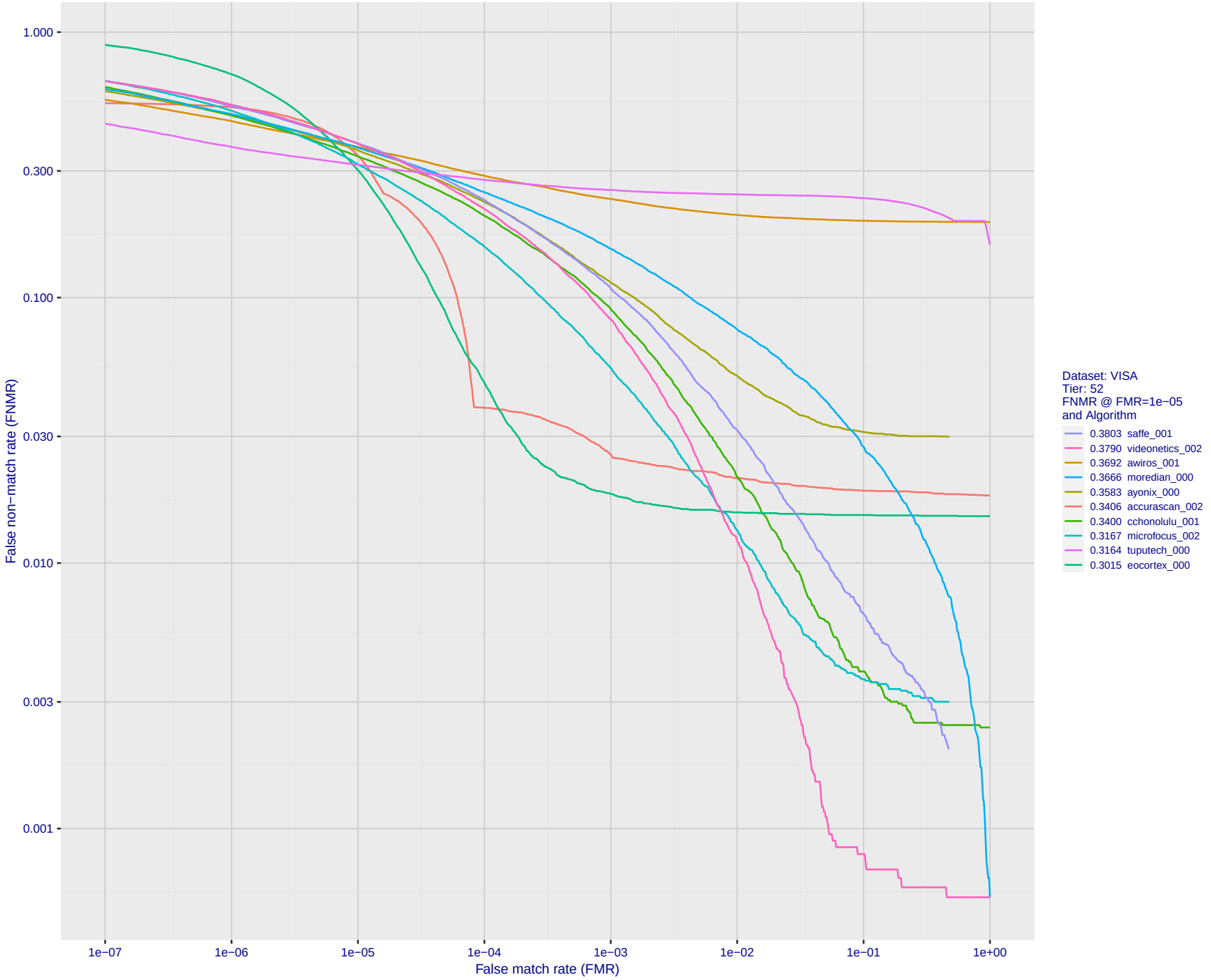

Figure 102: For the visa images, detection error tradeoff (DET) characteristics showing false non-match rate vs. false match rate plotted parametrically on threshold, T. The scales are logarithmic in order to show many decades of FMR.

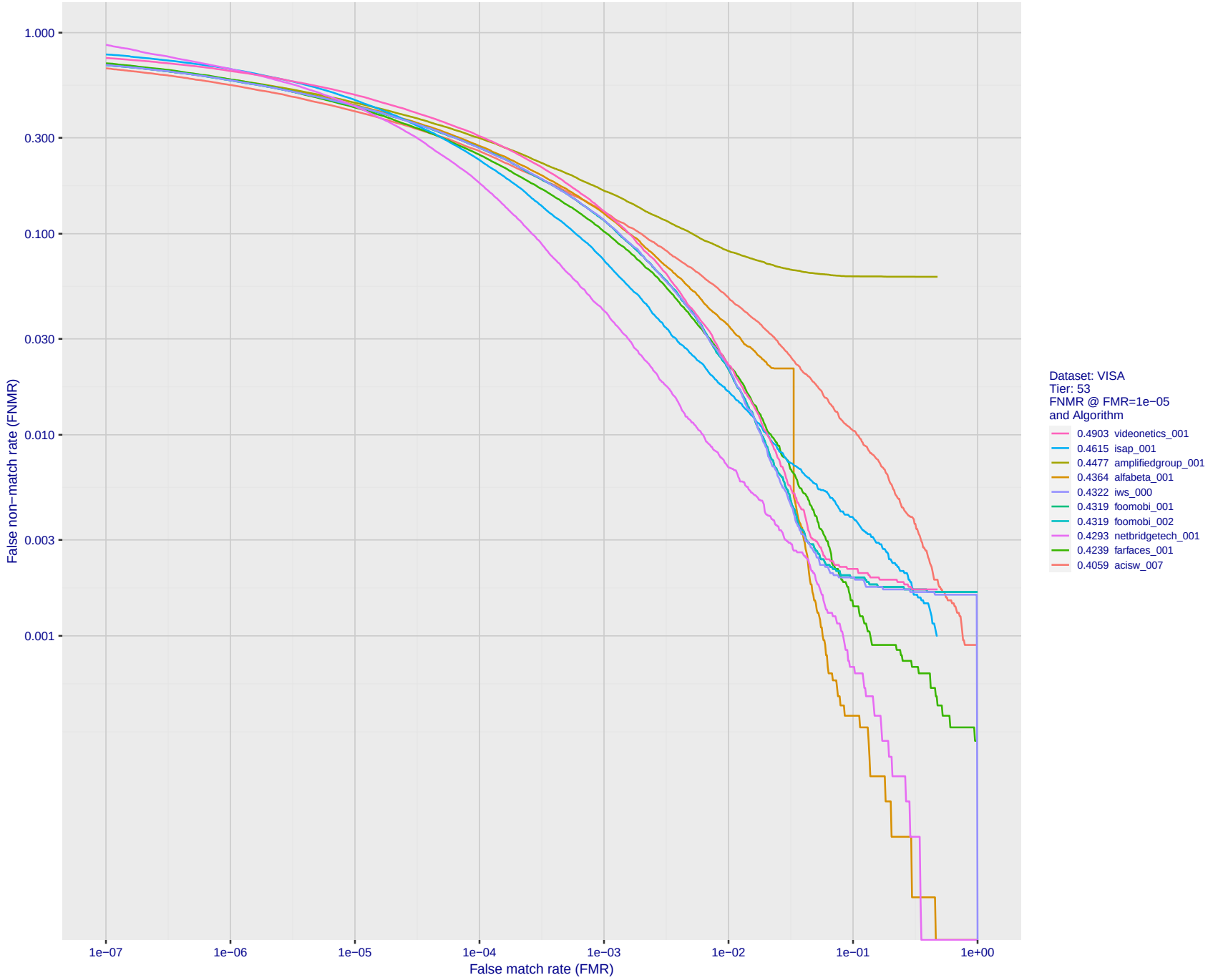

Figure 103: For the visa images, detection error tradeoff (DET) characteristics showing false non-match rate vs. false match rate plotted parametrically on threshold, T. The scales are logarithmic in order to show many decades of FMR.

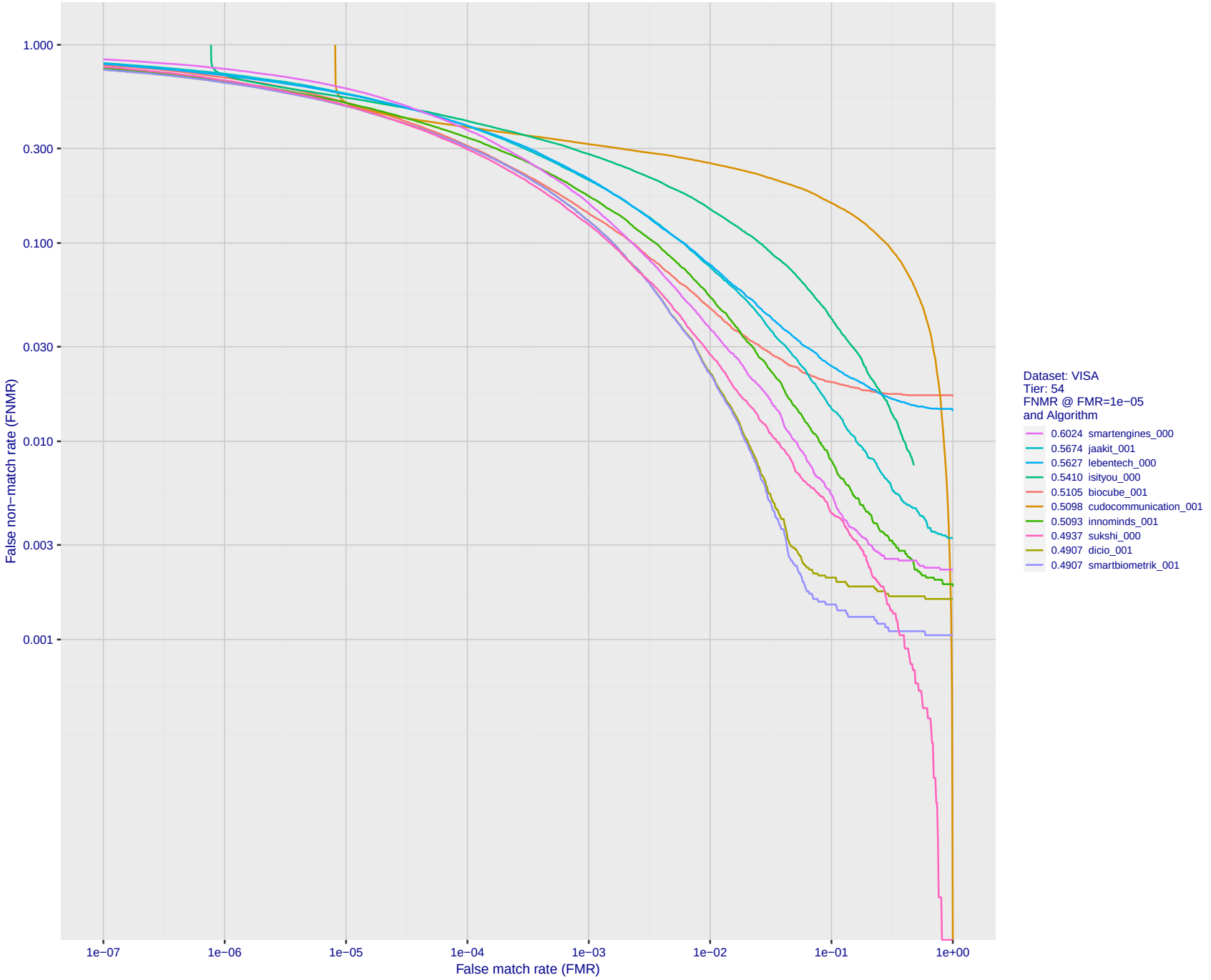

Figure 104: For the visa images, detection error tradeoff (DET) characteristics showing false non-match rate vs. false match rate plotted parametrically on threshold, T. The scales are logarithmic in order to show many decades of FMR.

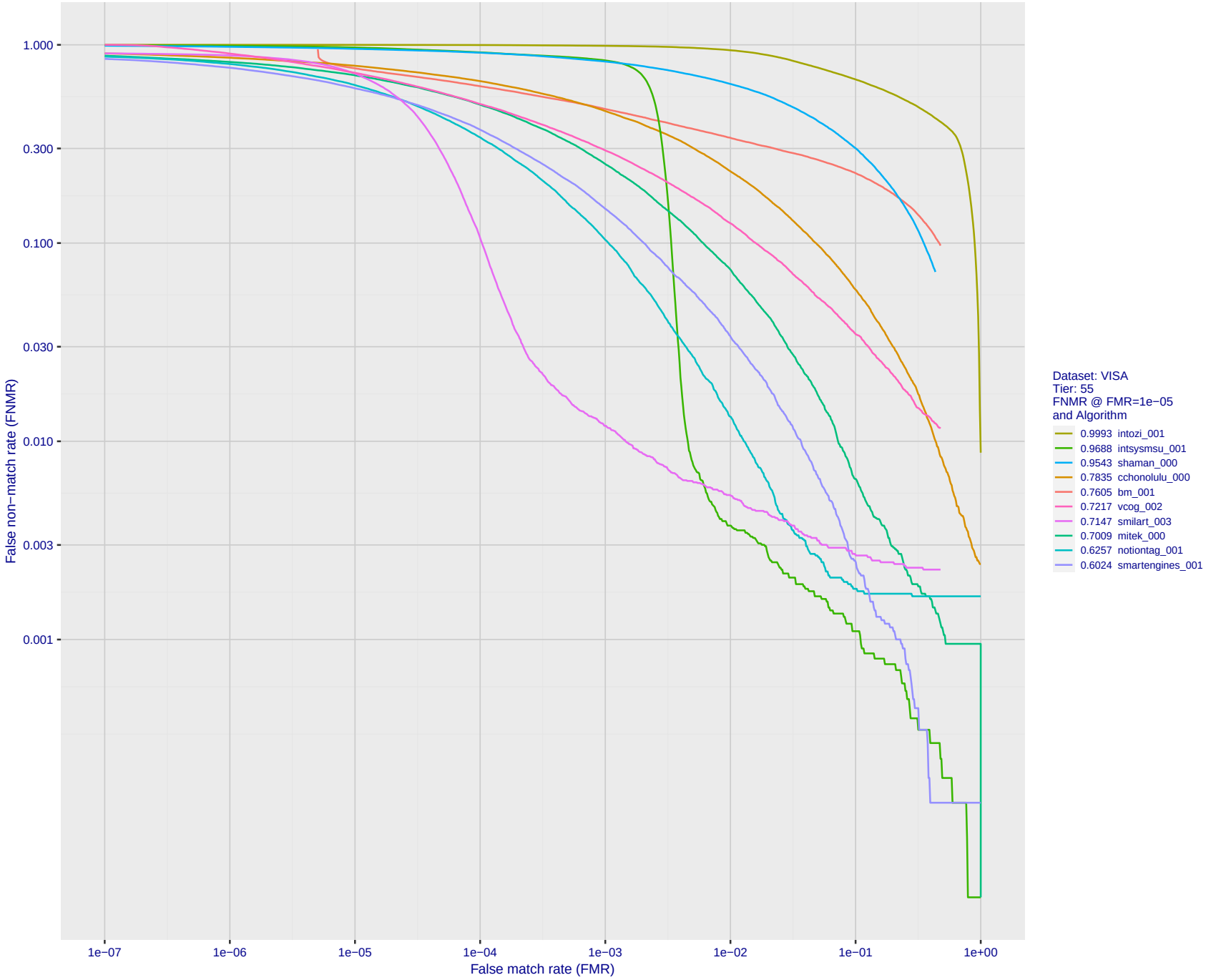

Figure 105: For the visa images, detection error tradeoff (DET) characteristics showing false non-match rate vs. false match rate plotted parametrically on threshold, T. The scales are logarithmic in order to show many decades of FMR.

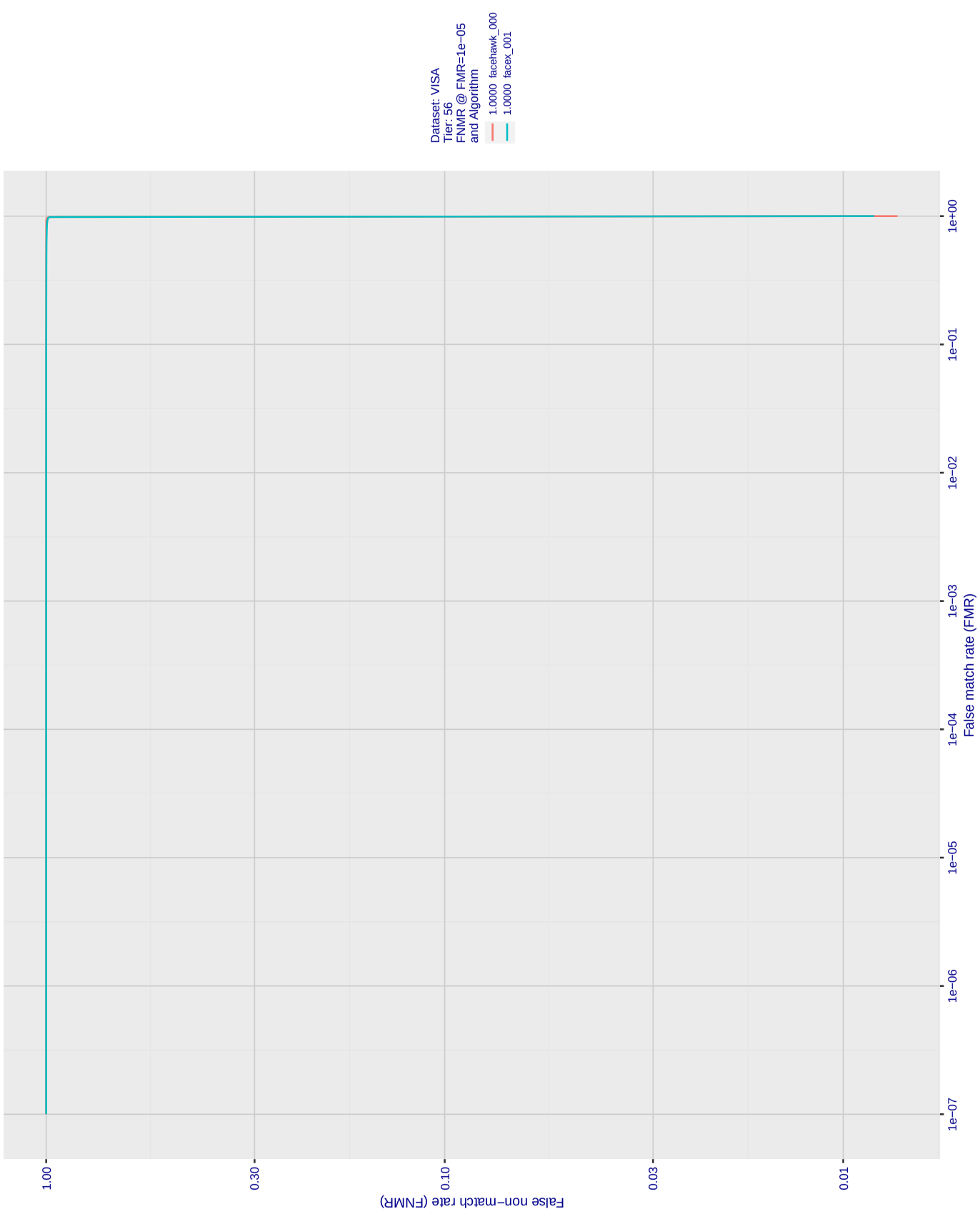

Figure 106: For the visa images, detection error tradeoff (DET) characteristics showing false non-match rate vs. false match rate plotted parametrically on threshold, T. The scales are logarithmic in order to show many decades of FMR.

FNMR(T) "False non-match rate"
FMR(T) "False match rate"

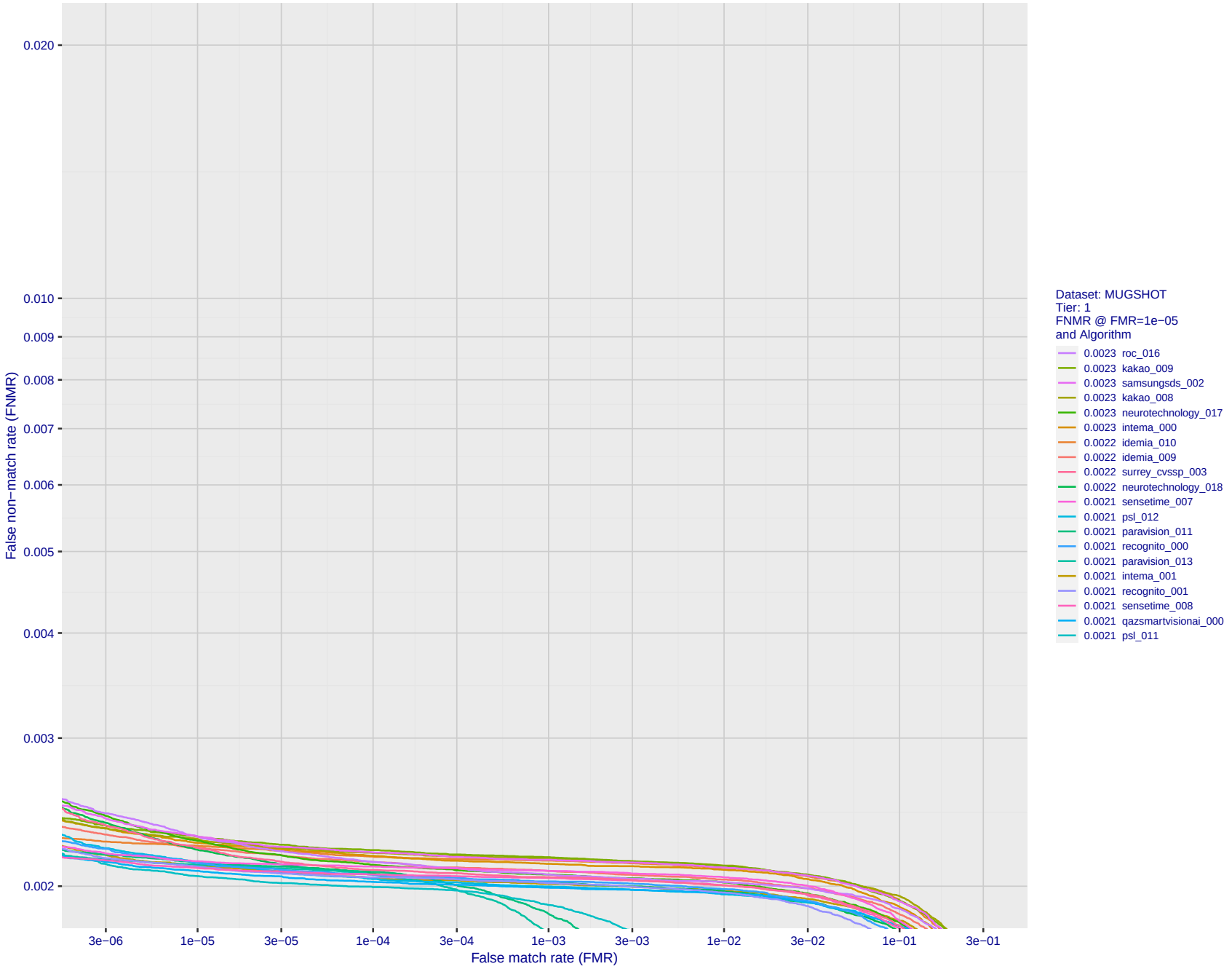

*Figure 107: For the mugshot images, detection error tradeoff (*DET*) characteristics showing false non-match rate vs. false match rate plotted parametrically on threshold, T. The scales are logarithmic in order to show decades of* FMR*.*

FNMR(T) "False non-match rate"
FMR(T) "False match rate"

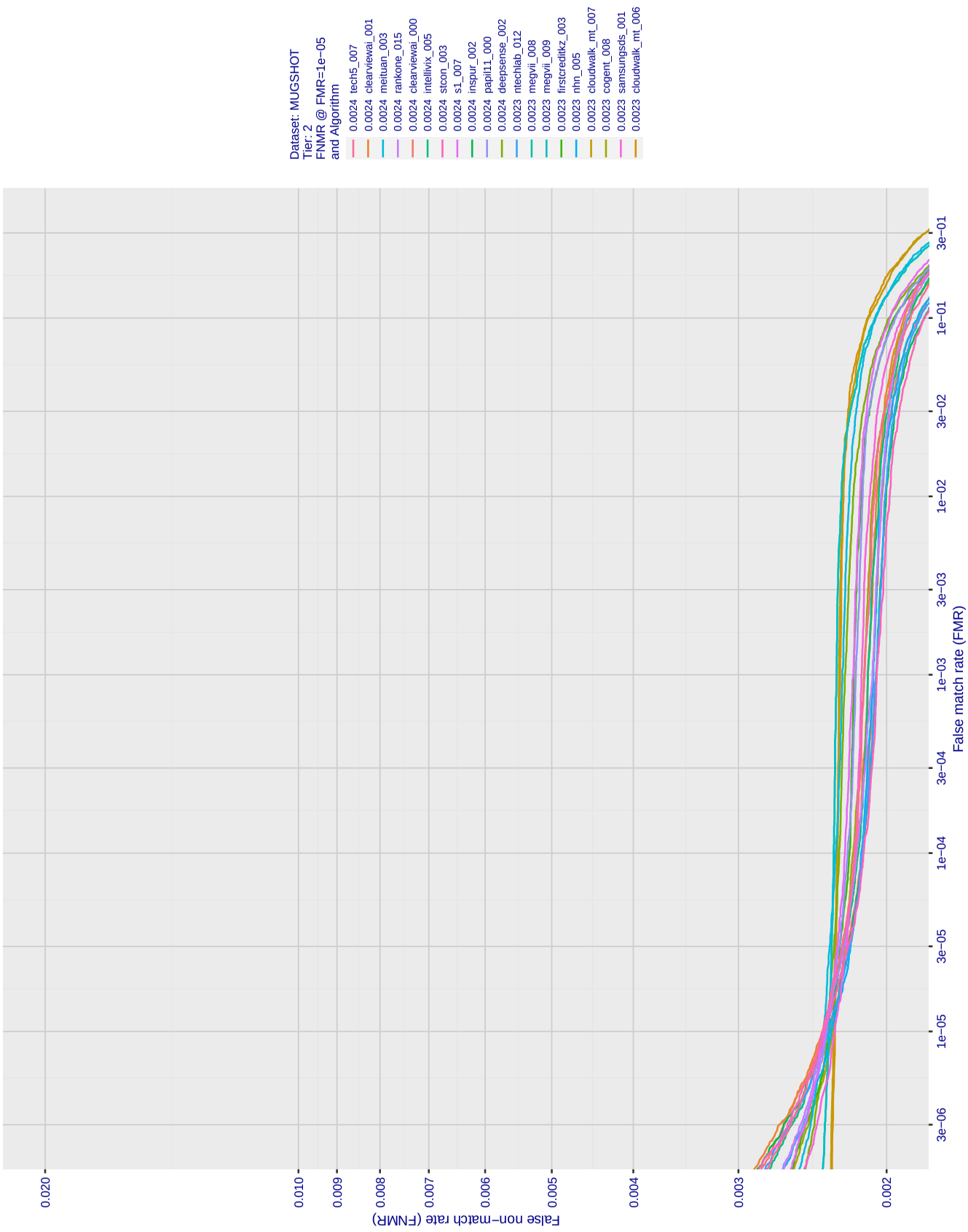

Figure 108: For the mugshot images, detection error tradeoff (DET) characteristics showing false non-match rate vs. false match rate plotted parametrically on threshold, T. The scales are logarithmic in order to show decades of FMR.

FNMR(T) "False non-match rate"
FMR(T) "False match rate"

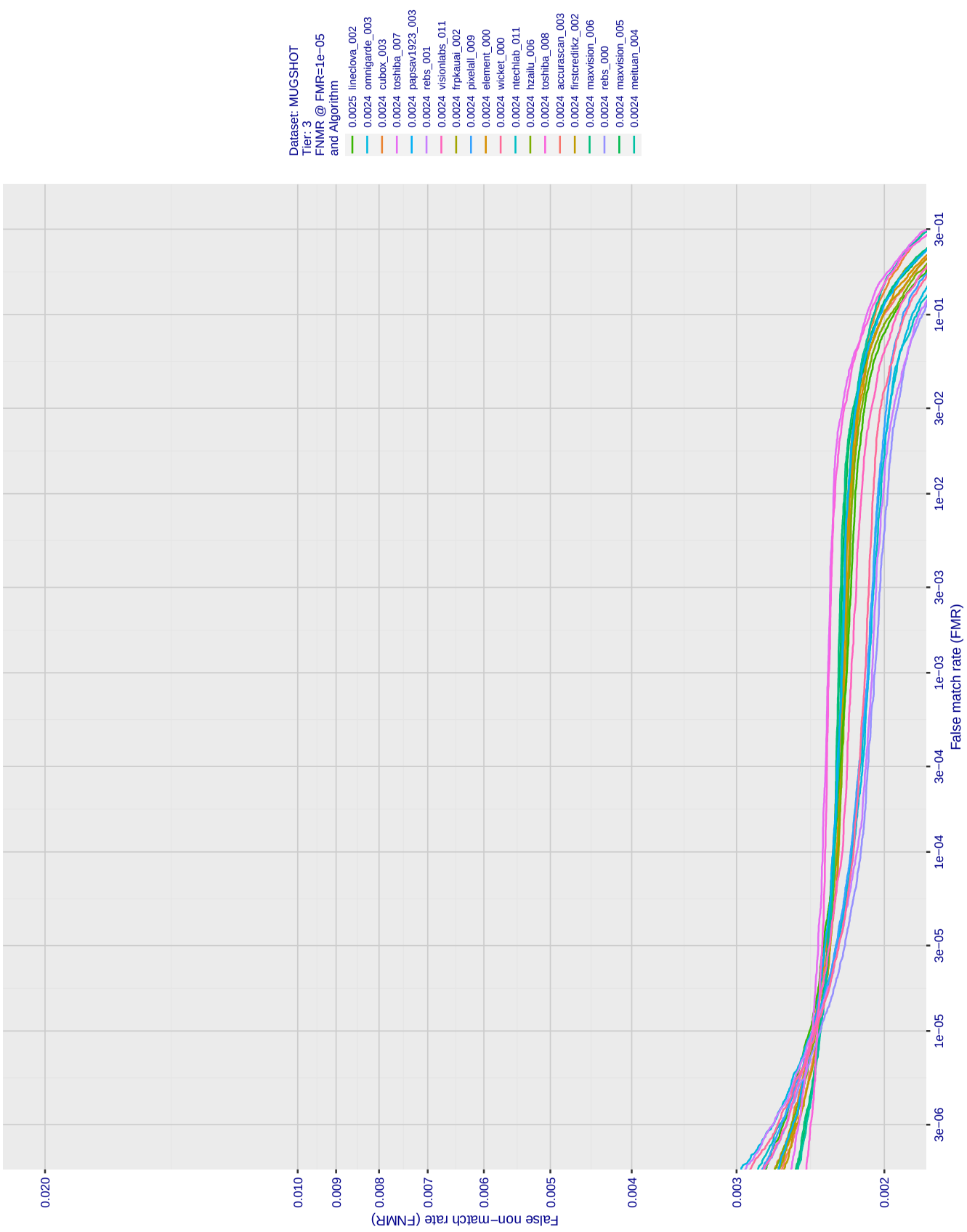

Figure 109: For the mugshot images, detection error tradeoff (DET) characteristics showing false non-match rate vs. false match rate plotted parametrically on threshold, T. The scales are logarithmic in order to show decades of FMR.

FNMR(T) "False non-match rate"
FMR(T) "False match rate"

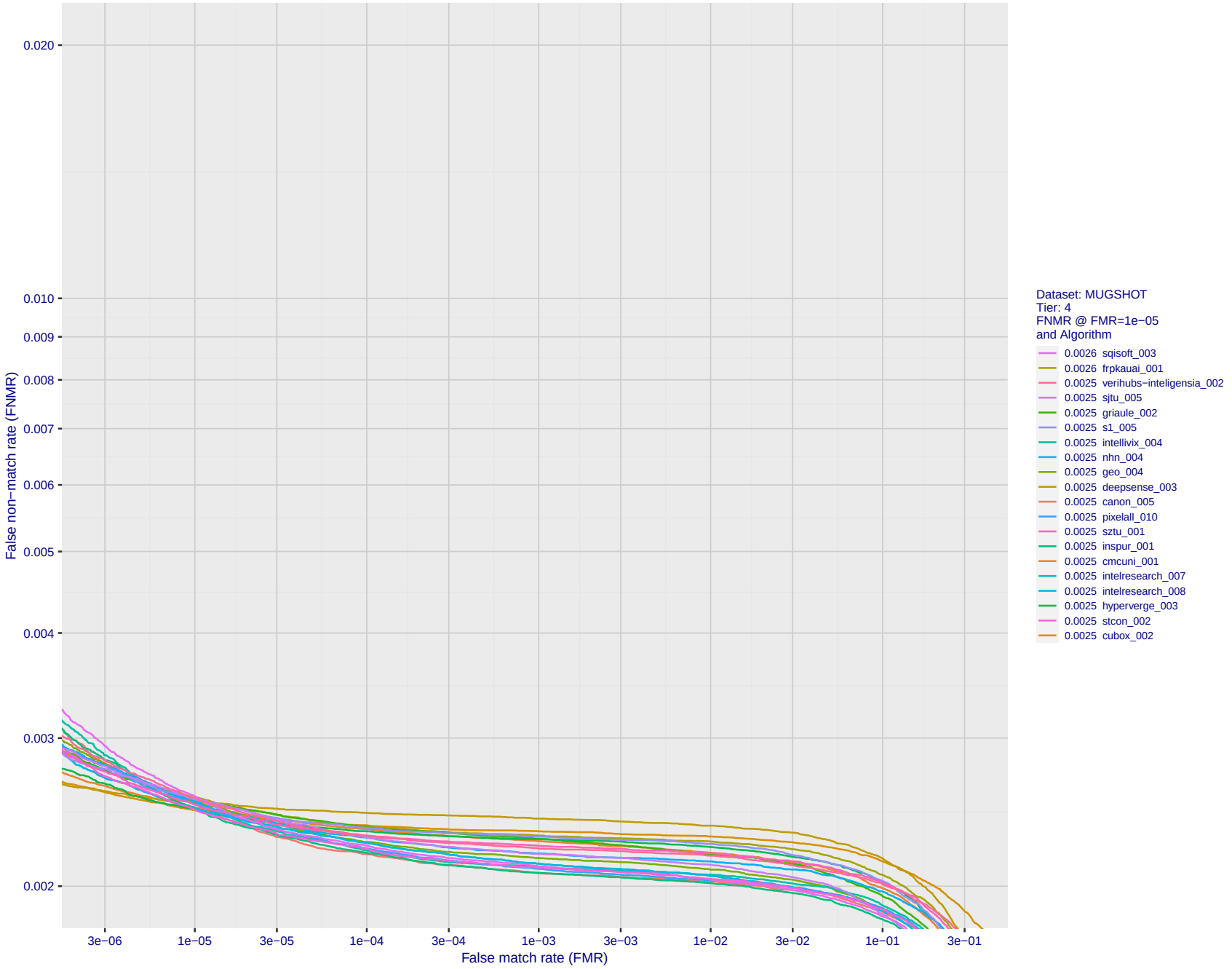

*Figure 110: For the mugshot images, detection error tradeoff (*DET*) characteristics showing false non-match rate vs. false match rate plotted parametrically on threshold, T. The scales are logarithmic in order to show decades of* FMR.

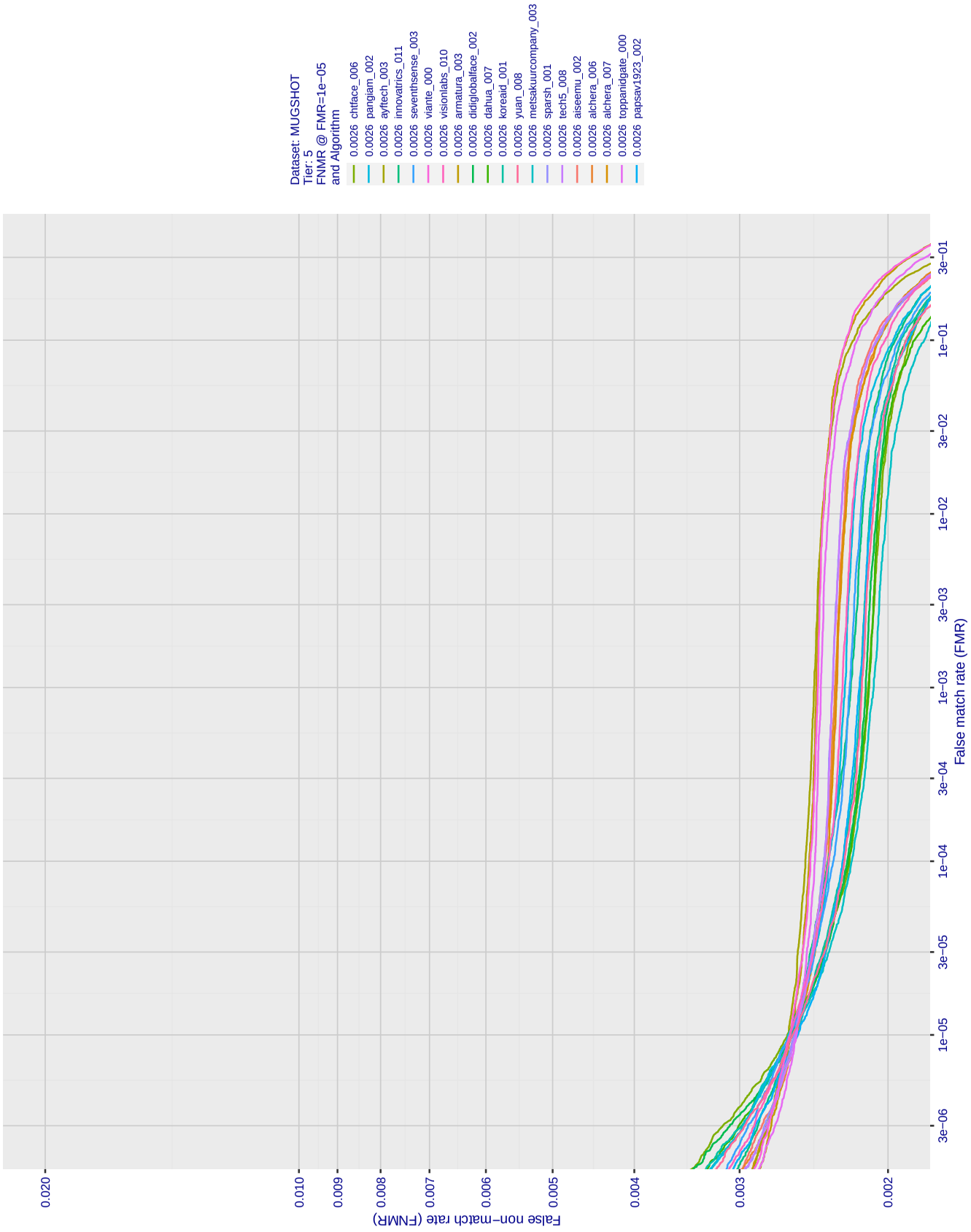

Figure 111: For the mugshot images, detection error tradeoff (DET) characteristics showing false non-match rate vs. false match rate plotted parametrically on threshold, T. The scales are logarithmic in order to show decades of FMR.

FNMR(T) "False non-match rate"
FMR(T) "False match rate"

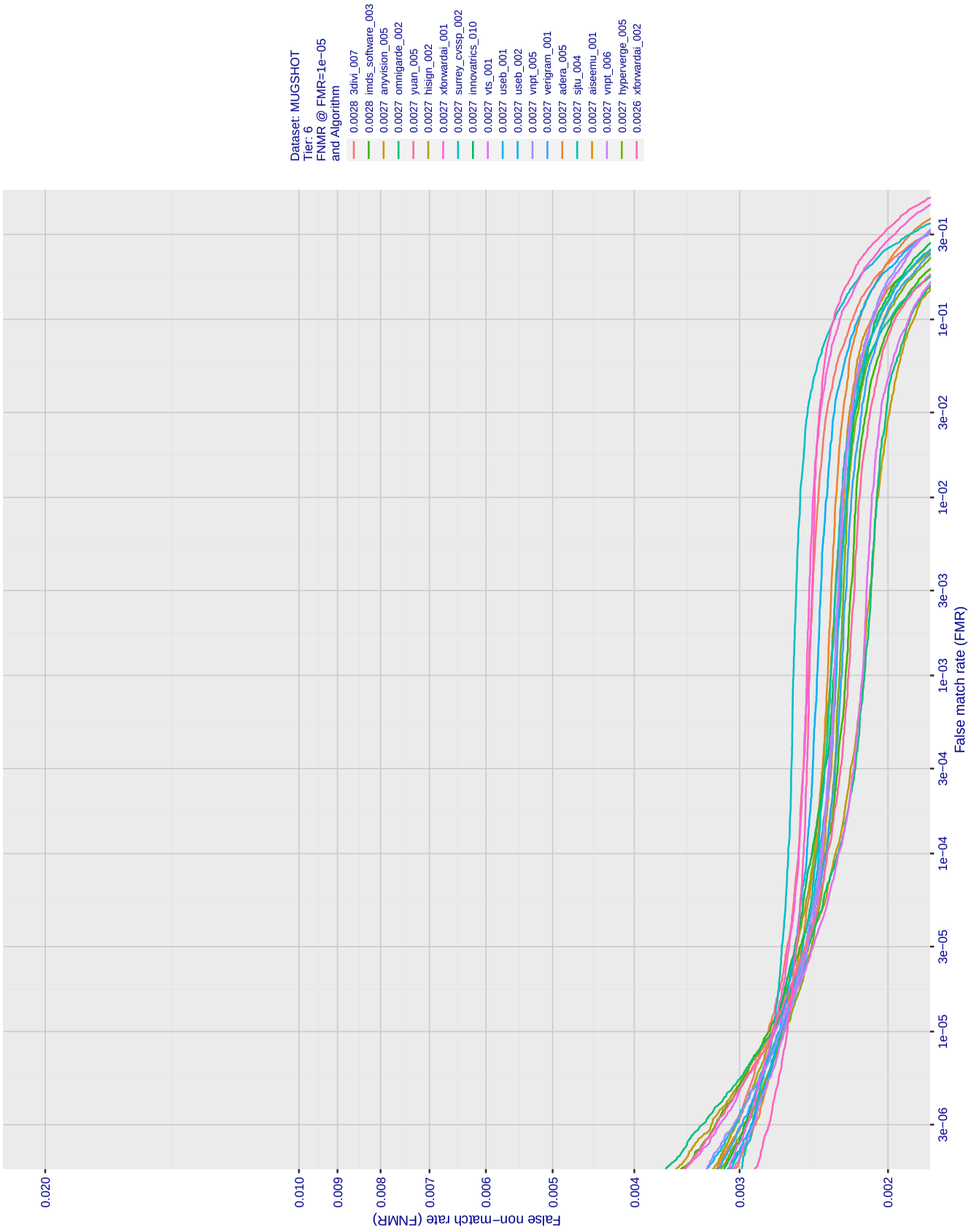

Figure 112: For the mugshot images, detection error tradeoff (DET) characteristics showing false non-match rate vs. false match rate plotted parametrically on threshold, T. The scales are logarithmic in order to show decades of FMR.

FNMR(T) "False non-match rate"
FMR(T) "False match rate"

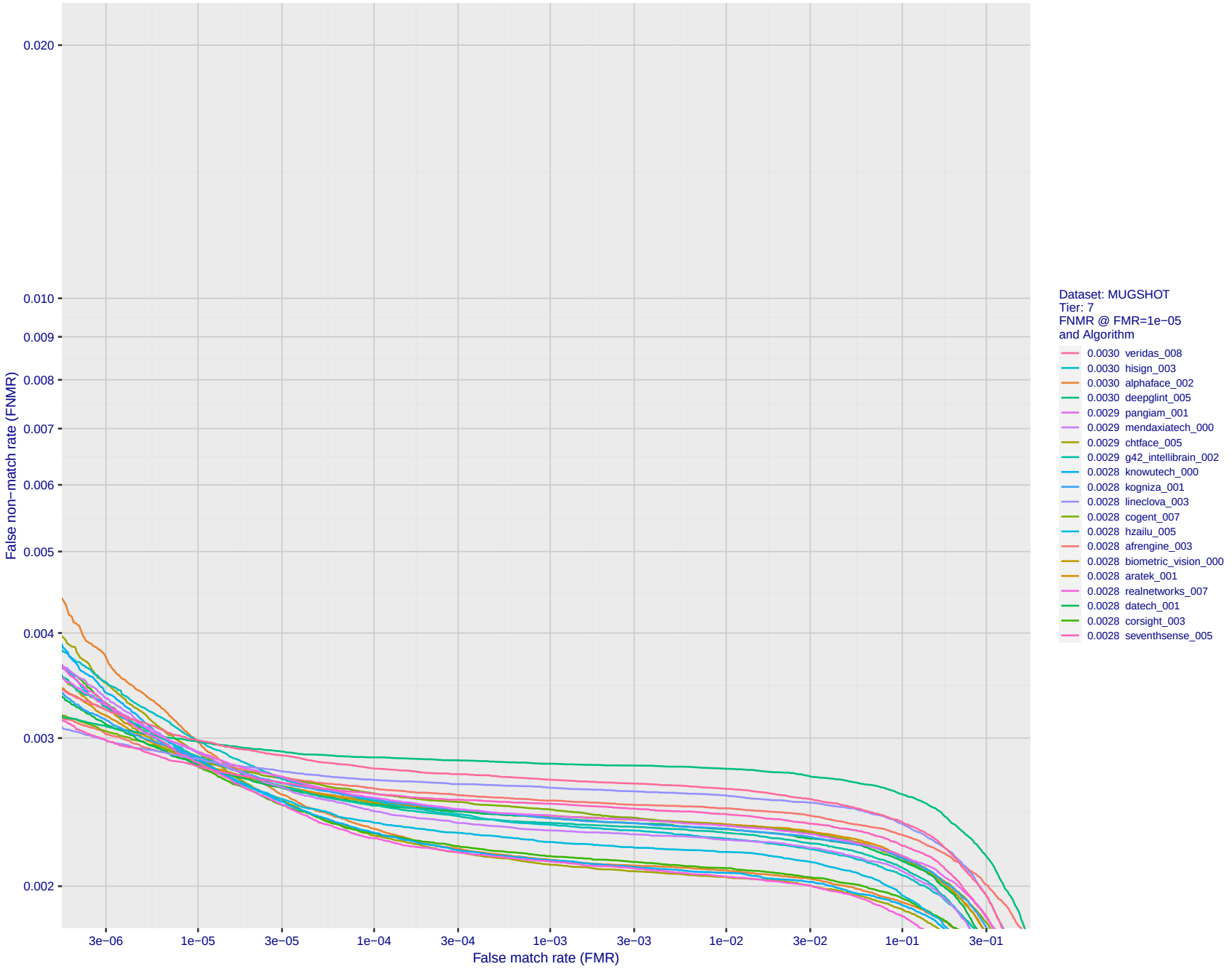

Figure 113: For the mugshot images, detection error tradeoff (DET) characteristics showing false non-match rate vs. false match rate plotted parametrically on threshold, T. The scales are logarithmic in order to show decades of FMR.

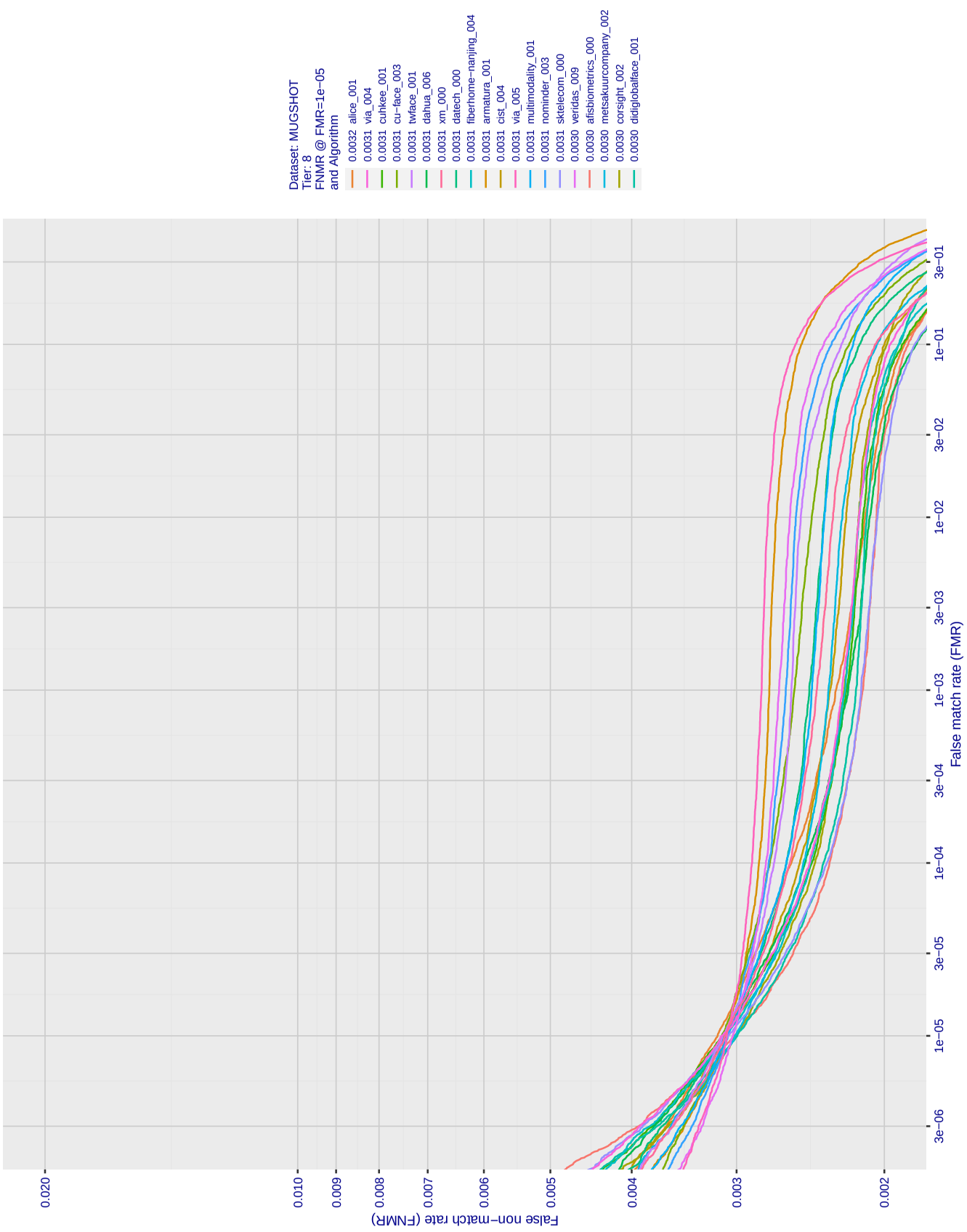

Figure 114: For the mugshot images, detection error tradeoff (DET) characteristics showing false non-match rate vs. false match rate plotted parametrically on threshold, T. The scales are logarithmic in order to show decades of FMR.

FNMR(T) "False non-match rate"
FMR(T) "False match rate"

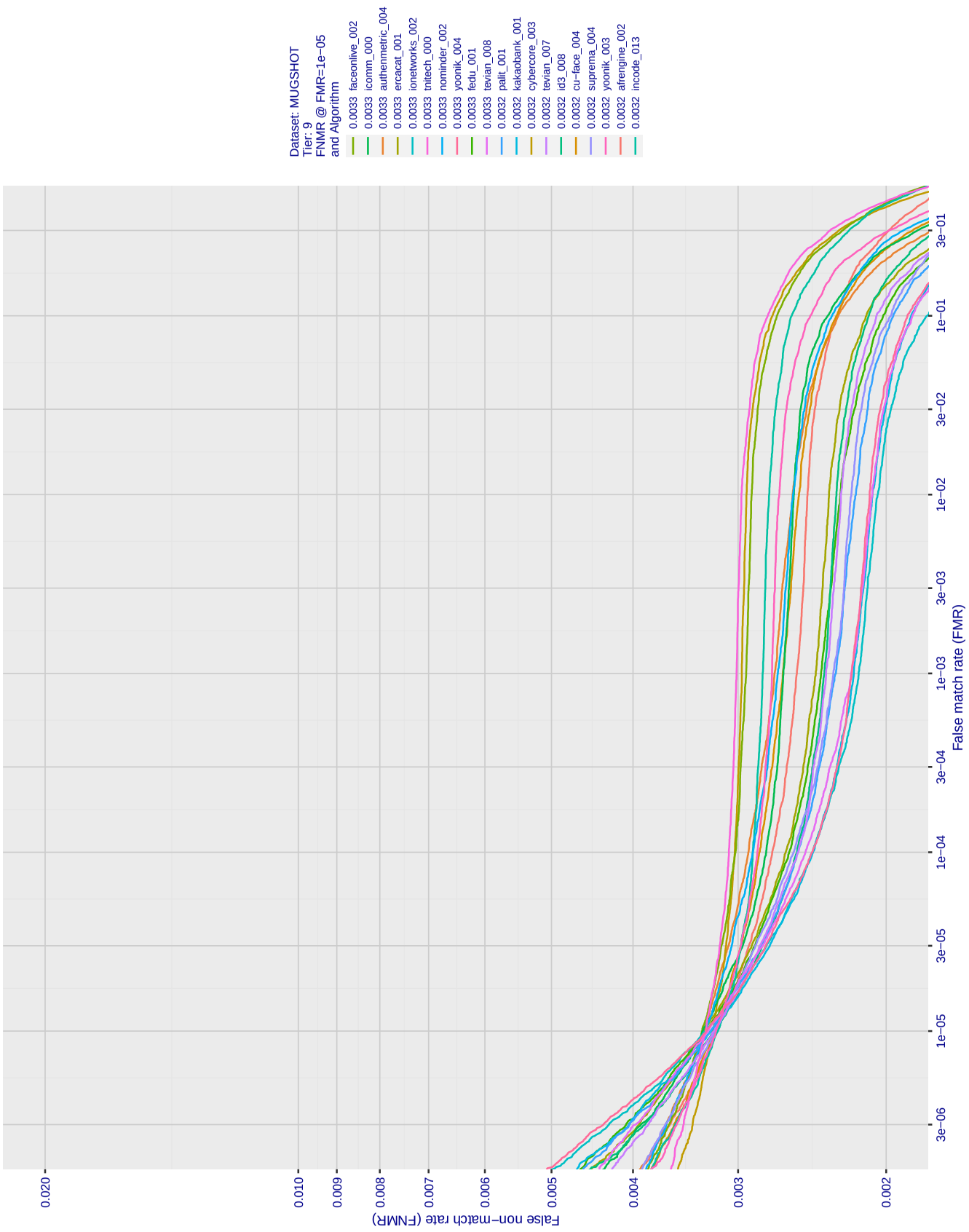

Figure 115: For the mugshot images, detection error tradeoff (DET) characteristics showing false non-match rate vs. false match rate plotted parametrically on threshold, T. The scales are logarithmic in order to show decades of FMR.

FNMR(T) "False non-match rate"
FMR(T) "False match rate"

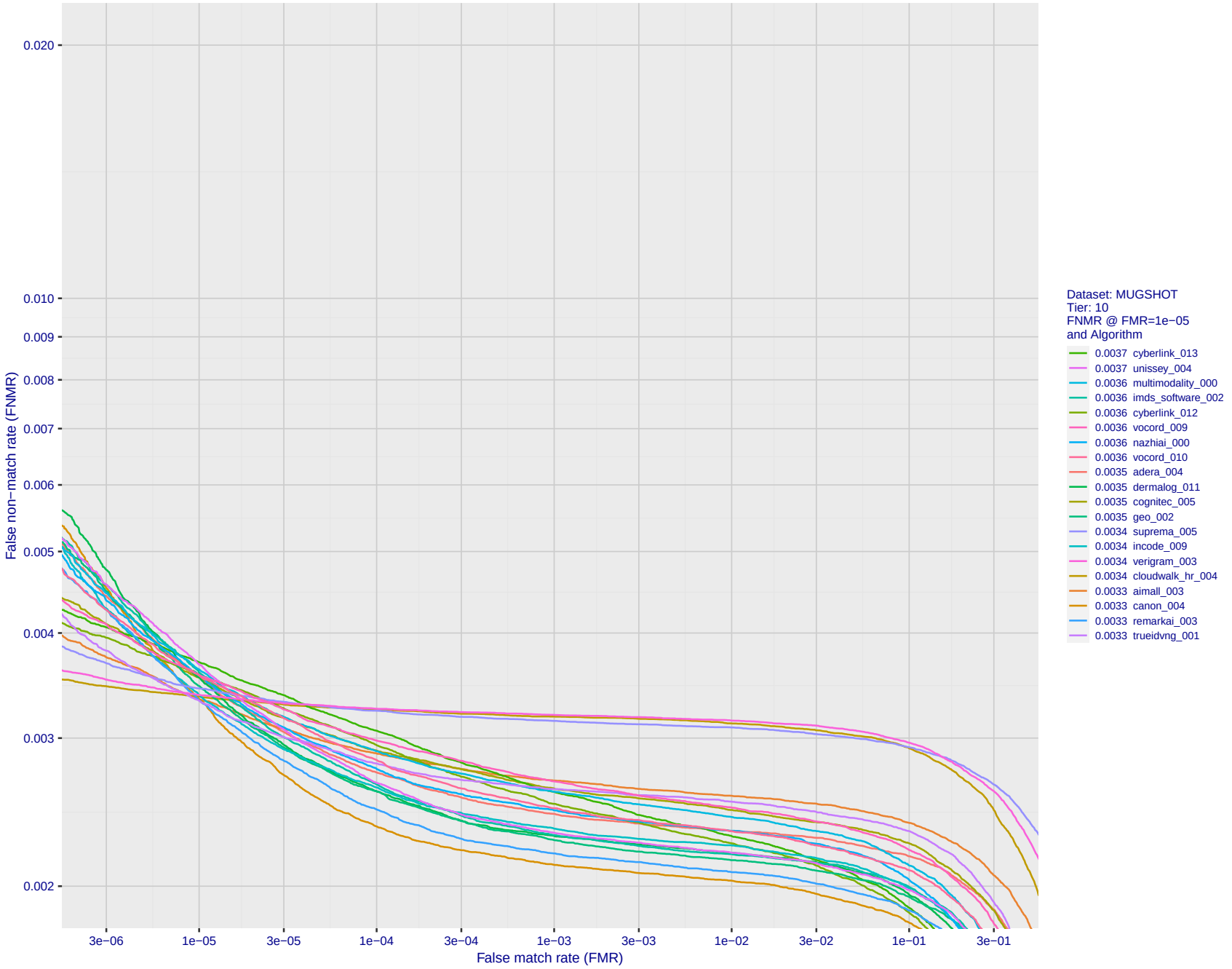

*Figure 116: For the mugshot images, detection error tradeoff (*DET*) characteristics showing false non-match rate vs. false match rate plotted parametrically on threshold, T. The scales are logarithmic in order to show decades of* FMR*.*

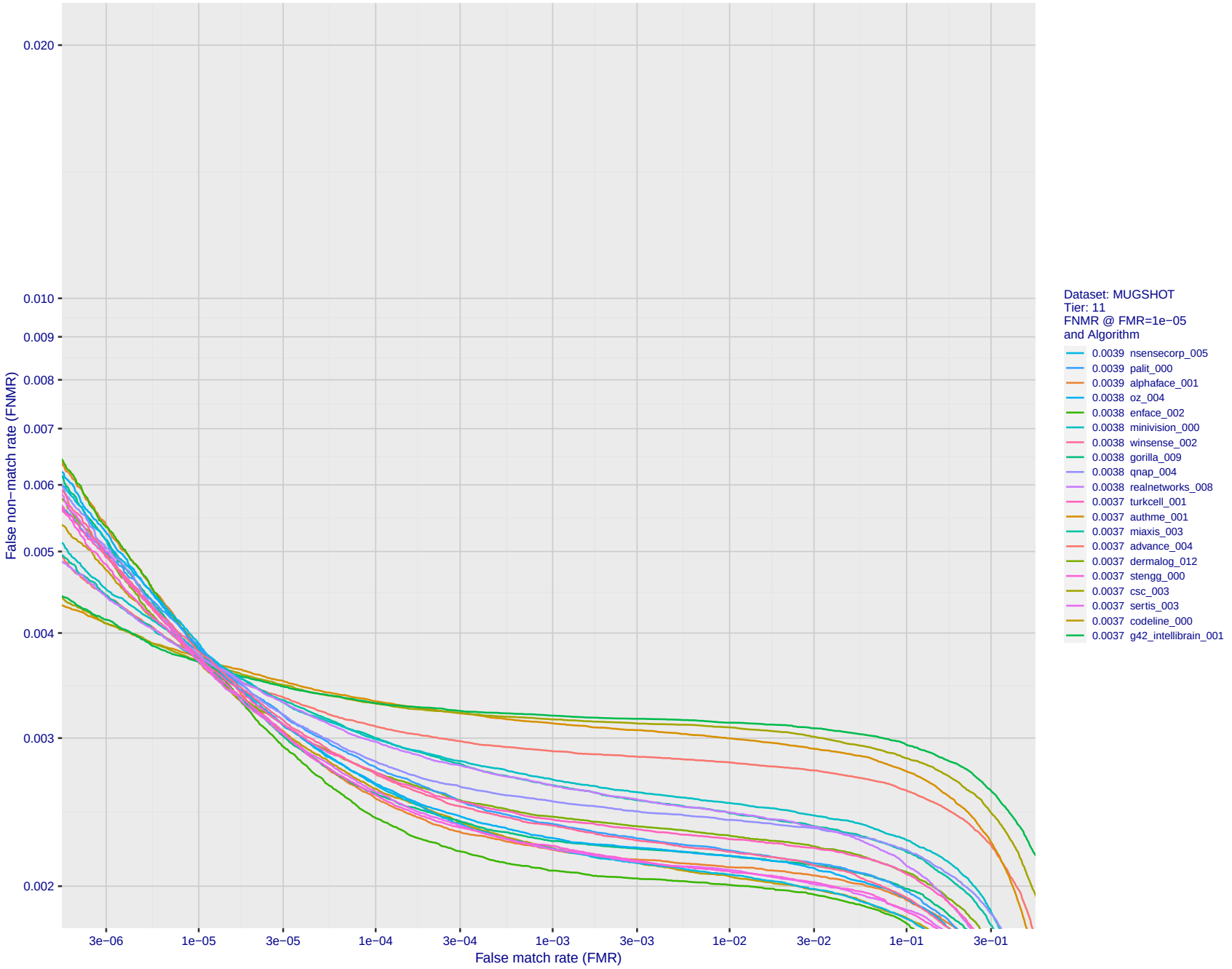

*Figure 117: For the mugshot images, detection error tradeoff (*DET*) characteristics showing false non-match rate vs. false match rate plotted parametrically on threshold, T. The scales are logarithmic in order to show decades of* FMR.

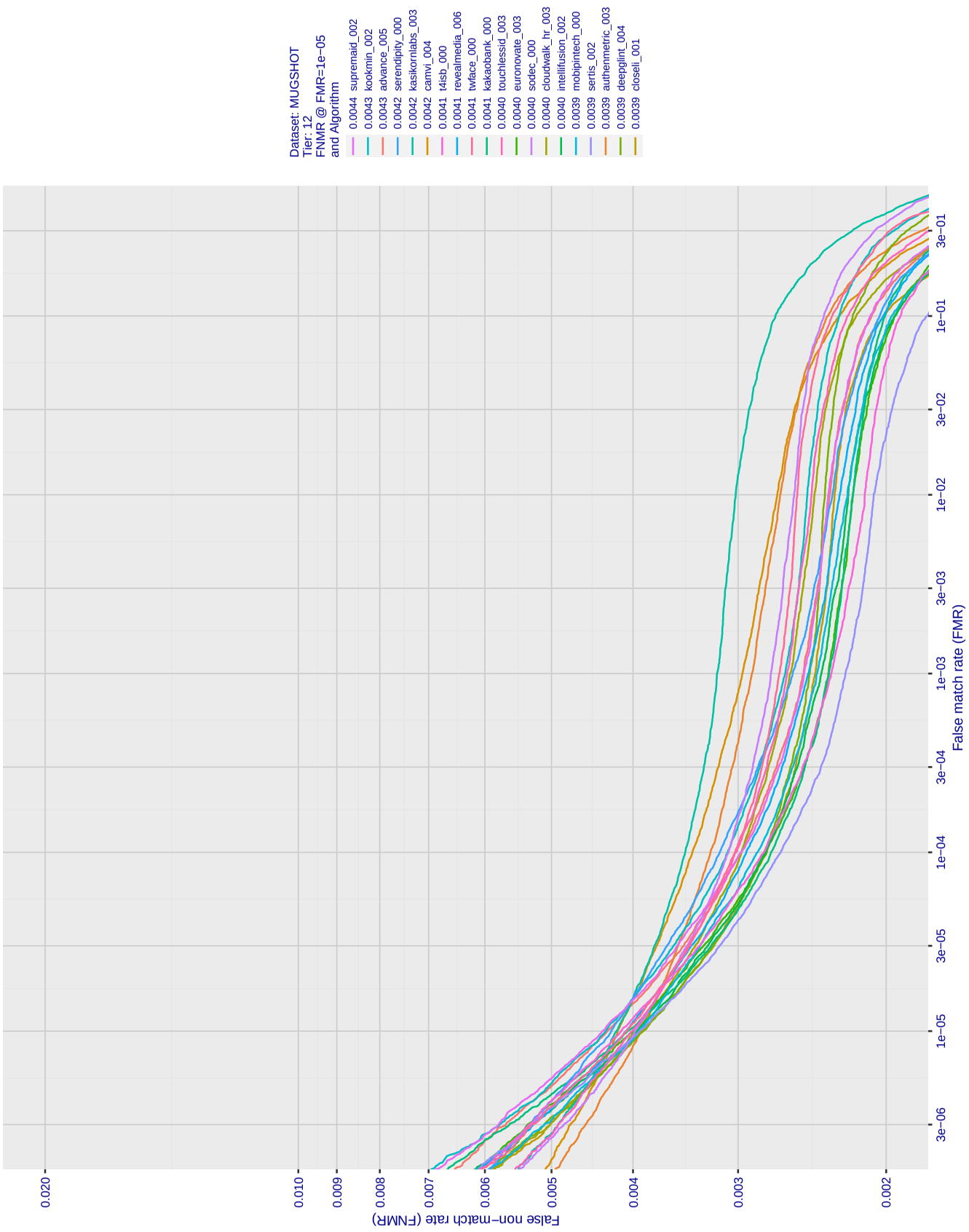

Figure 118: For the mugshot images, detection error tradeoff (DET) characteristics showing false non-match rate vs. false match rate plotted parametrically on threshold, T. The scales are logarithmic in order to show decades of FMR.

FNMR(T) "False non-match rate"
FMR(T) "False match rate"

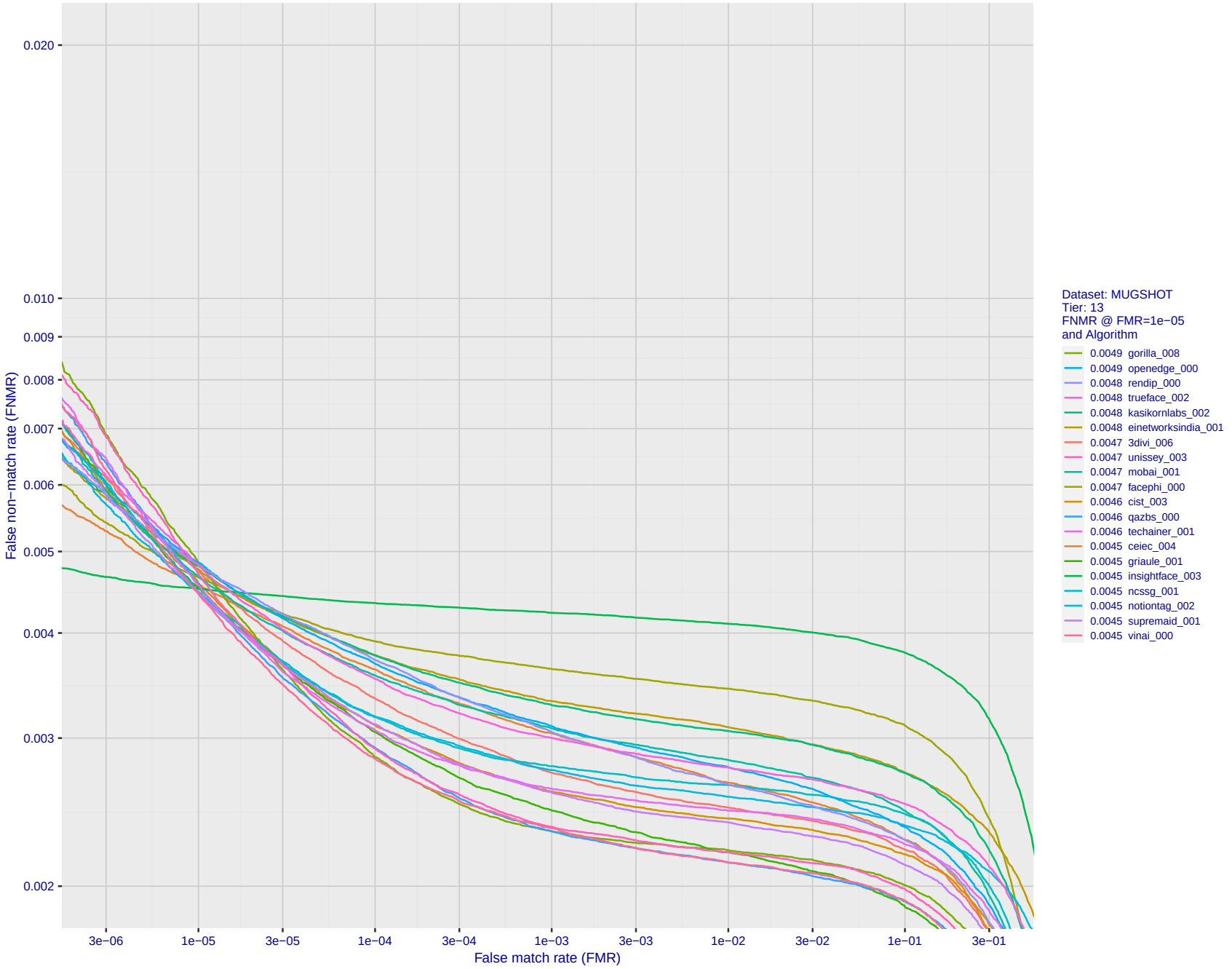

*Figure 119: For the mugshot images, detection error tradeoff (*DET*) characteristics showing false non-match rate vs. false match rate plotted parametrically on threshold, T. The scales are logarithmic in order to show decades of* FMR.

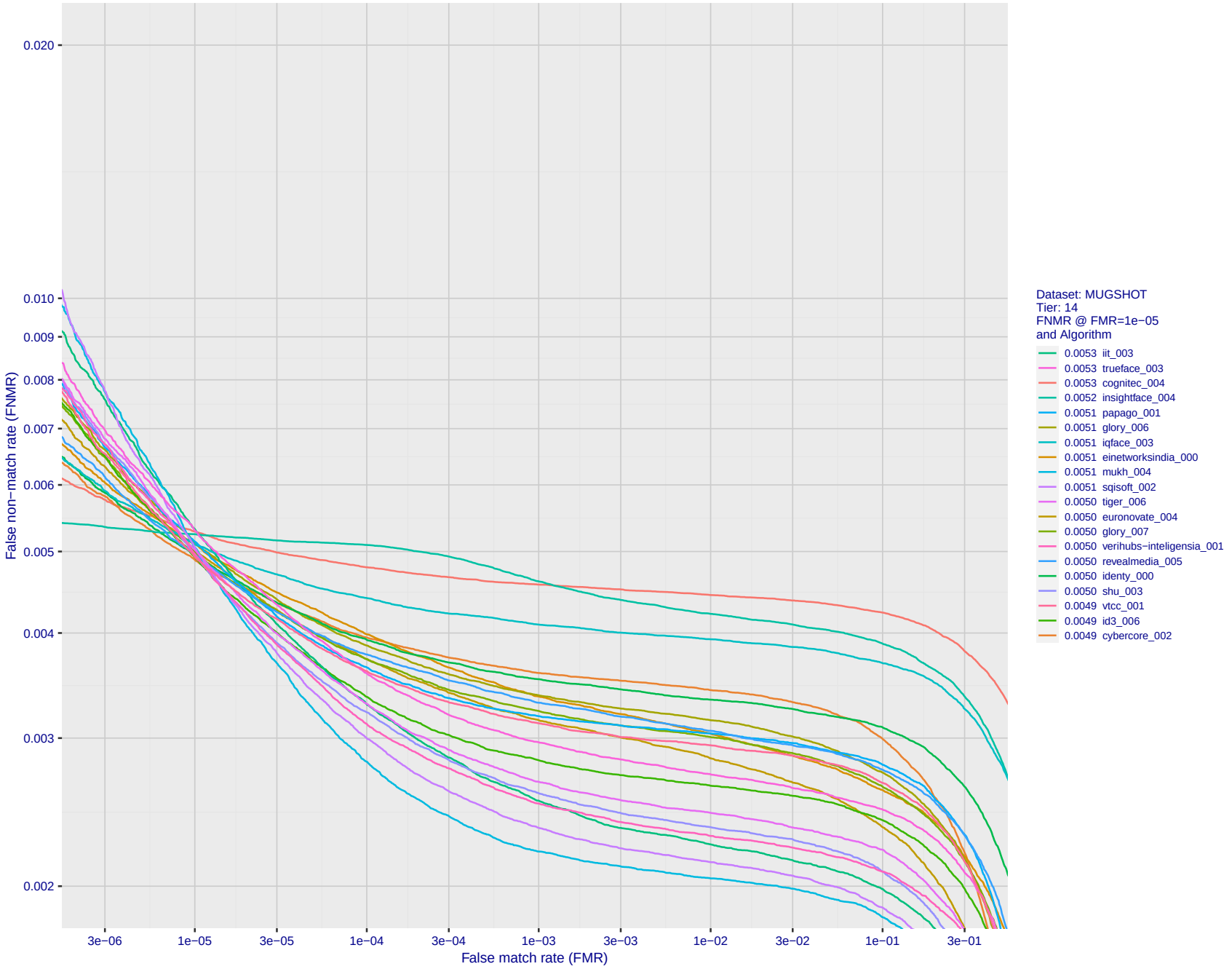

Figure 120: For the mugshot images, detection error tradeoff (DET) characteristics showing false non-match rate vs. false match rate plotted parametrically on threshold, T. The scales are logarithmic in order to show decades of FMR.

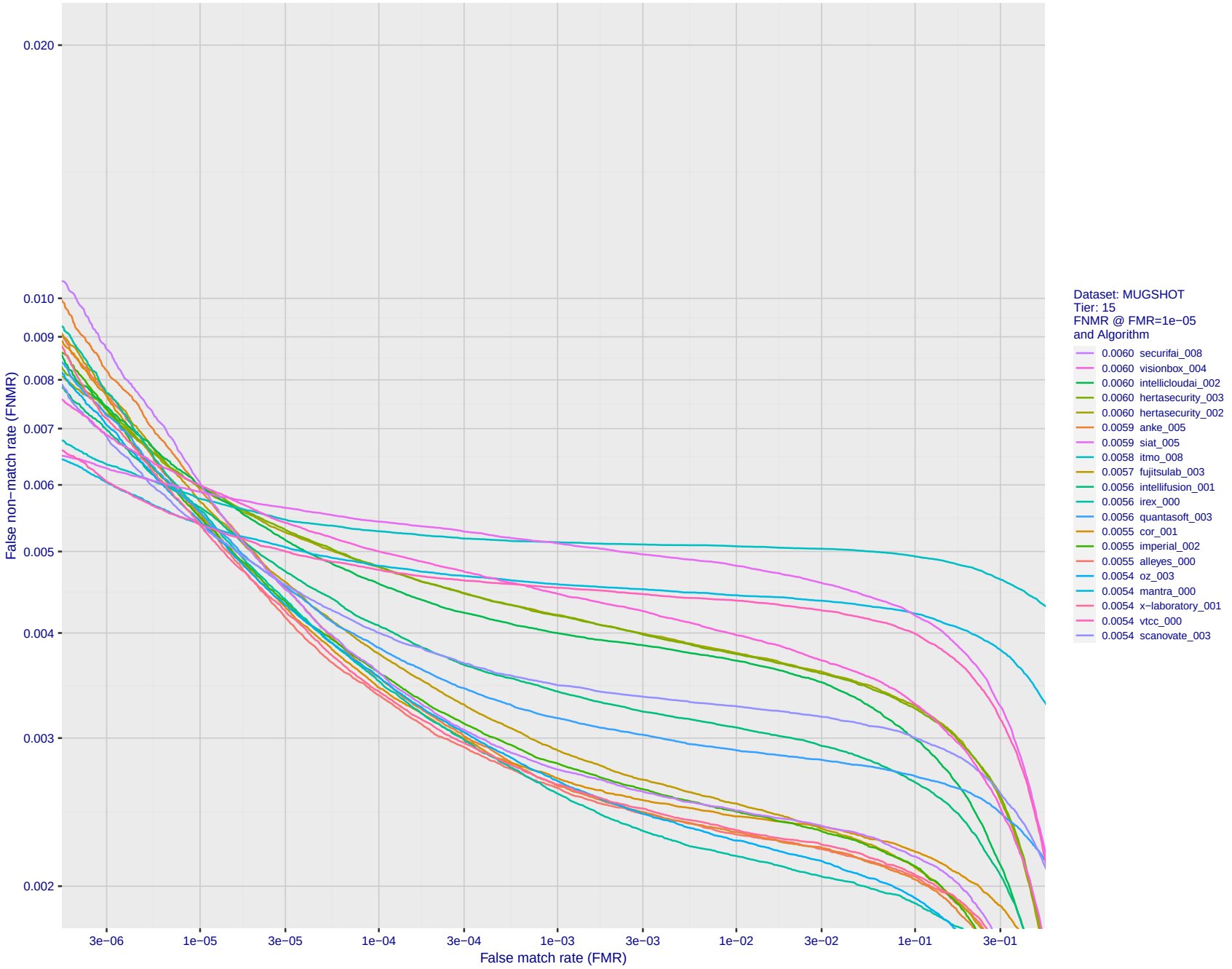

*Figure 121: For the mugshot images, detection error tradeoff (*DET*) characteristics showing false non-match rate vs. false match rate plotted parametrically on threshold, T. The scales are logarithmic in order to show decades of* FMR*.*

FNMR(T) "False non-match rate"
FMR(T) "False match rate"

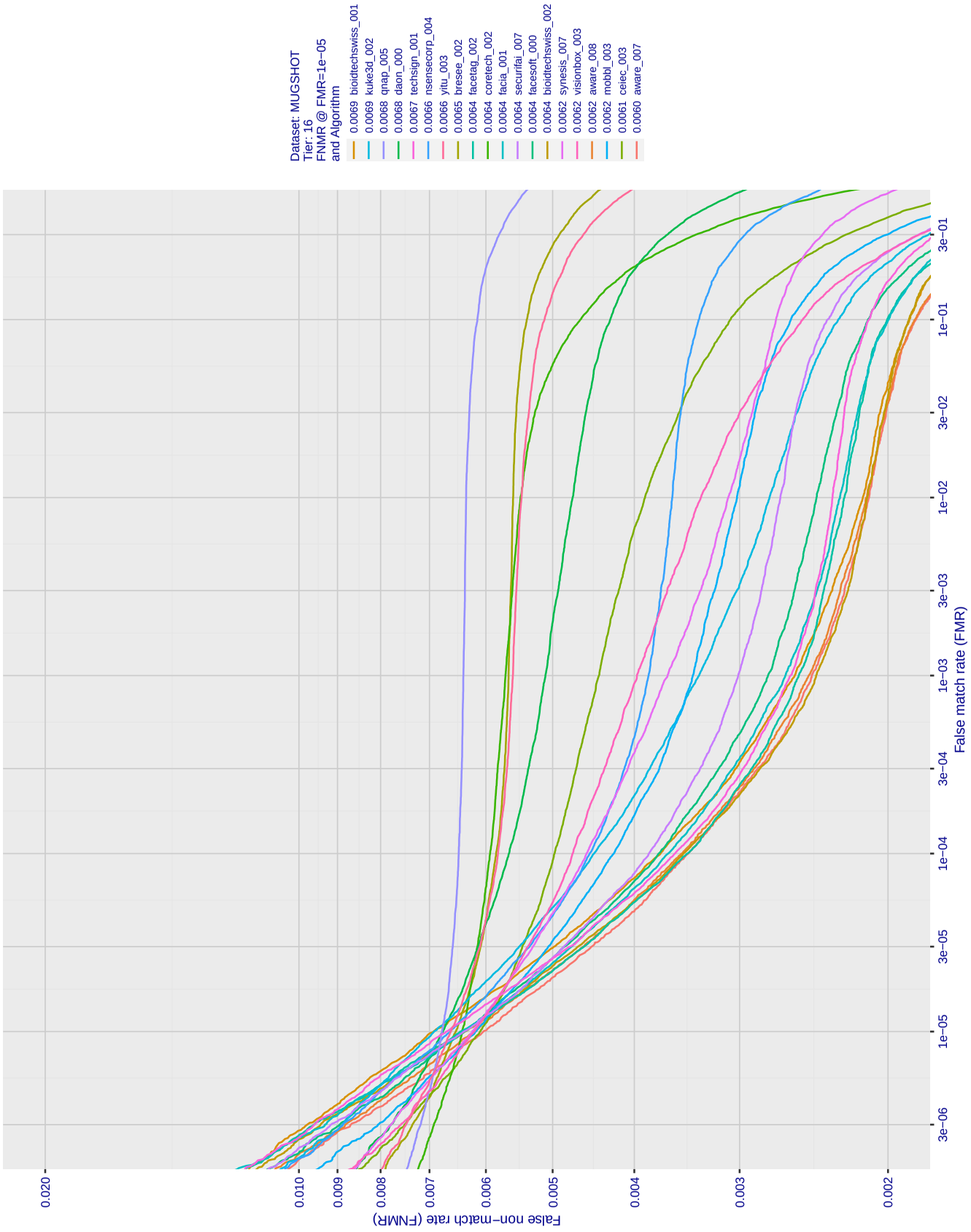

Figure 122: For the mugshot images, detection error tradeoff (DET) characteristics showing false non-match rate vs. false match rate plotted parametrically on threshold, T. The scales are logarithmic in order to show decades of FMR.

FNMR(T) "False non-match rate"
FMR(T) "False match rate"

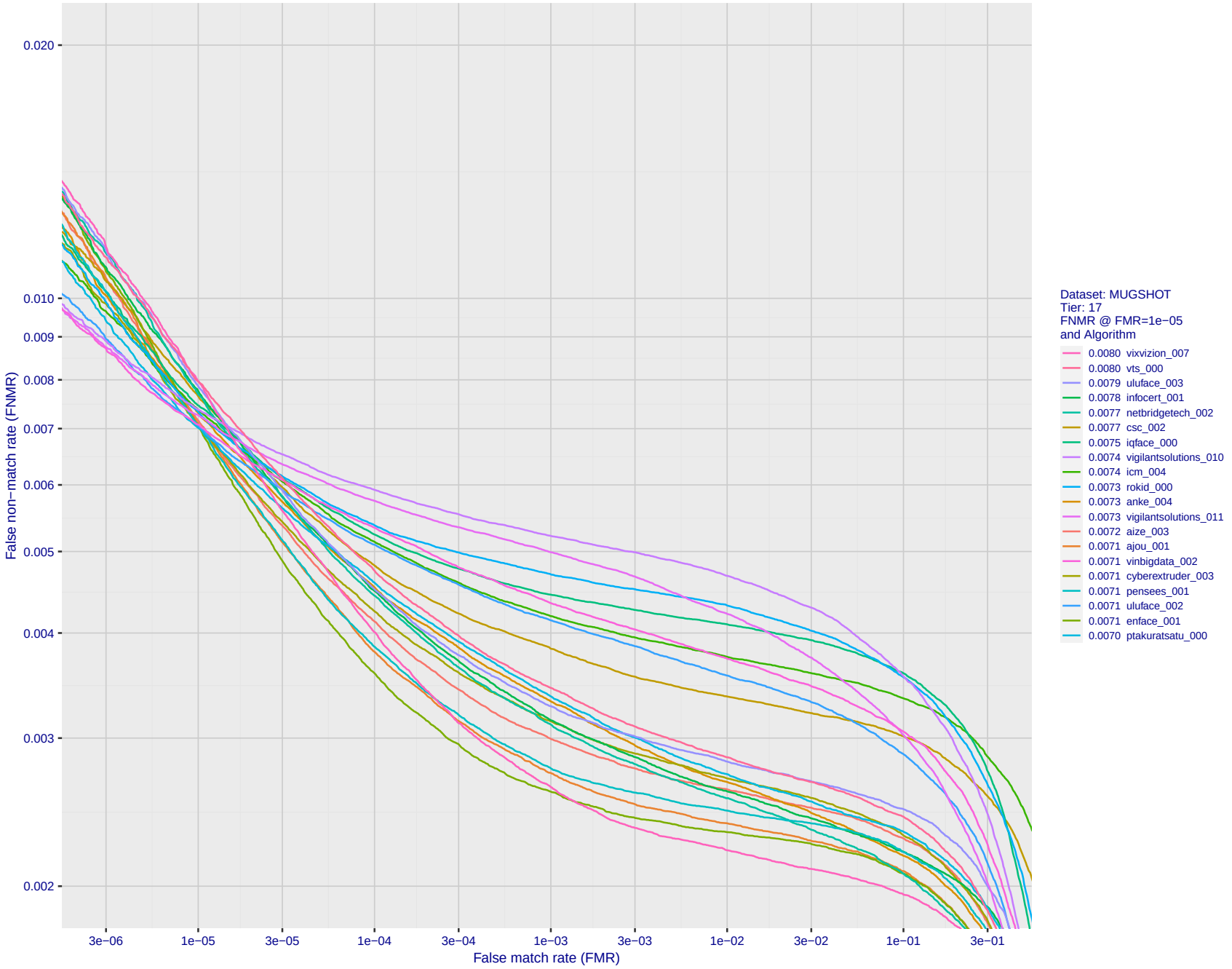

Figure 123: For the mugshot images, detection error tradeoff (DET) characteristics showing false non-match rate vs. false match rate plotted parametrically on threshold, T. The scales are logarithmic in order to show decades of FMR.

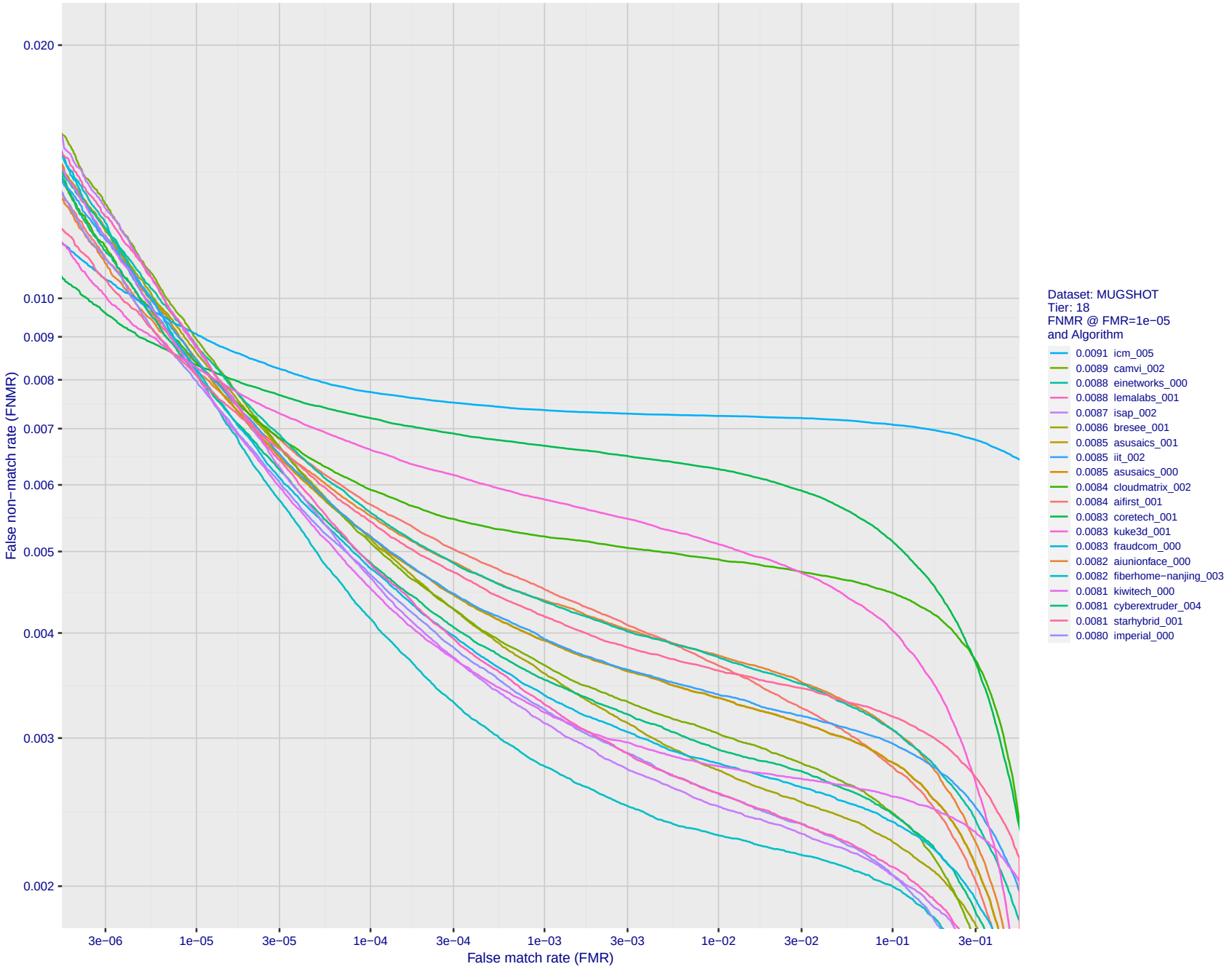

Figure 124: For the mugshot images, detection error tradeoff (DET) characteristics showing false non-match rate vs. false match rate plotted parametrically on threshold, T. The scales are logarithmic in order to show decades of FMR.

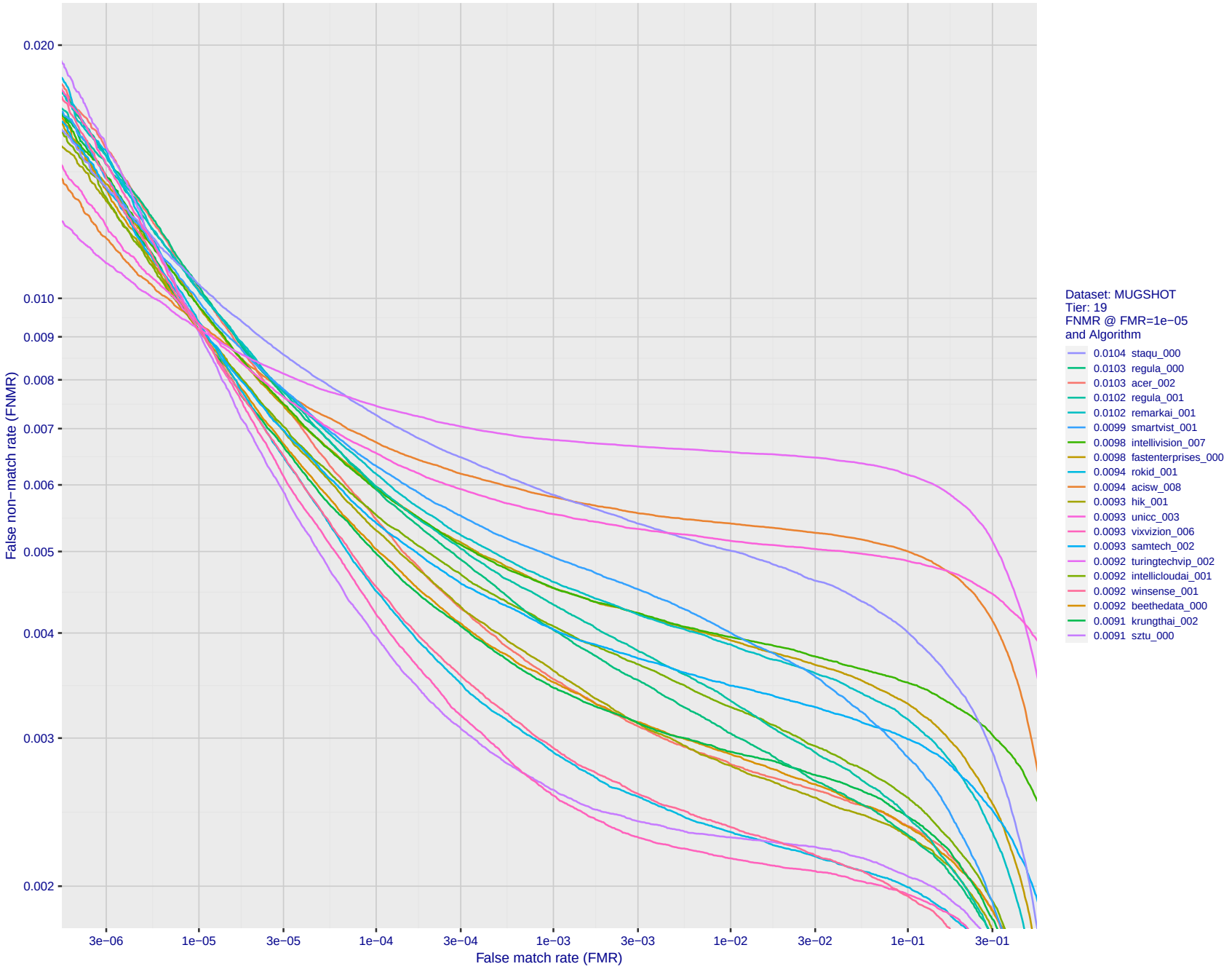

Figure 125: For the mugshot images, detection error tradeoff (DET) characteristics showing false non-match rate vs. false match rate plotted parametrically on threshold, T. The scales are logarithmic in order to show decades of FMR.

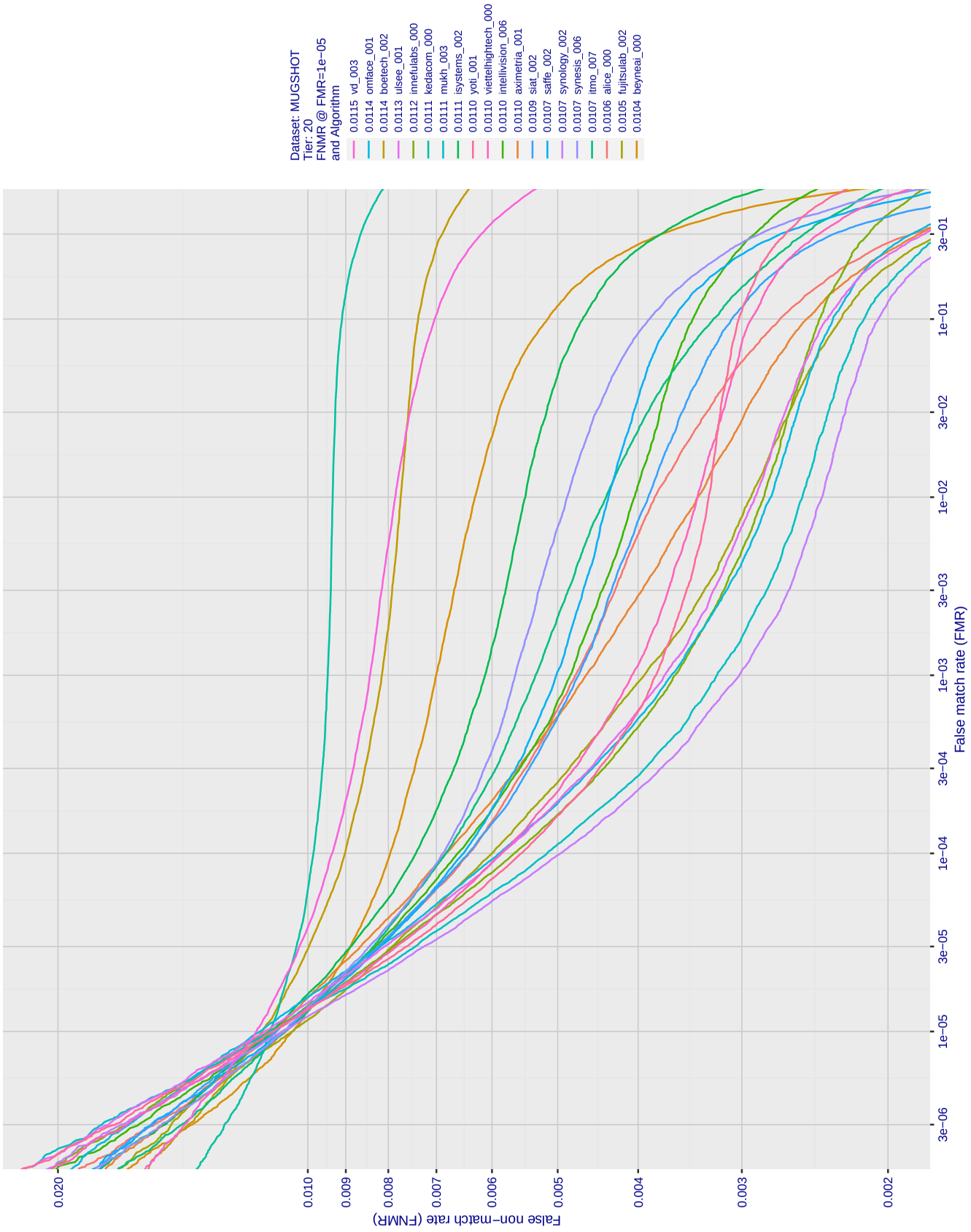

Figure 126: For the mugshot images, detection error tradeoff (DET) characteristics showing false non-match rate vs. false match rate plotted parametrically on threshold, T. The scales are logarithmic in order to show decades of FMR.

FNMR(T) "False non-match rate"
FMR(T) "False match rate"

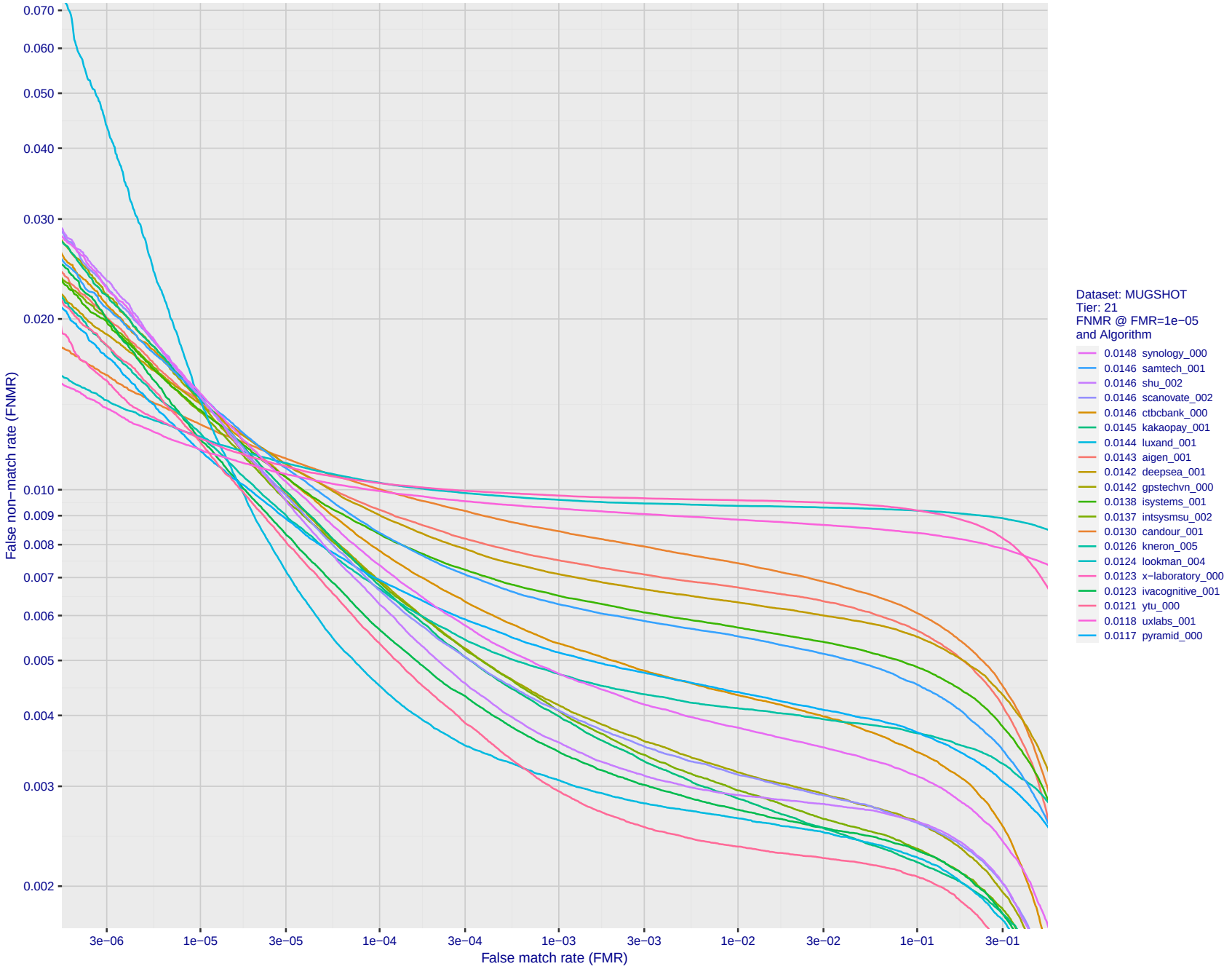

Figure 127: For the mugshot images, detection error tradeoff (DET) characteristics showing false non-match rate vs. false match rate plotted parametrically on threshold, T. The scales are logarithmic in order to show decades of FMR.

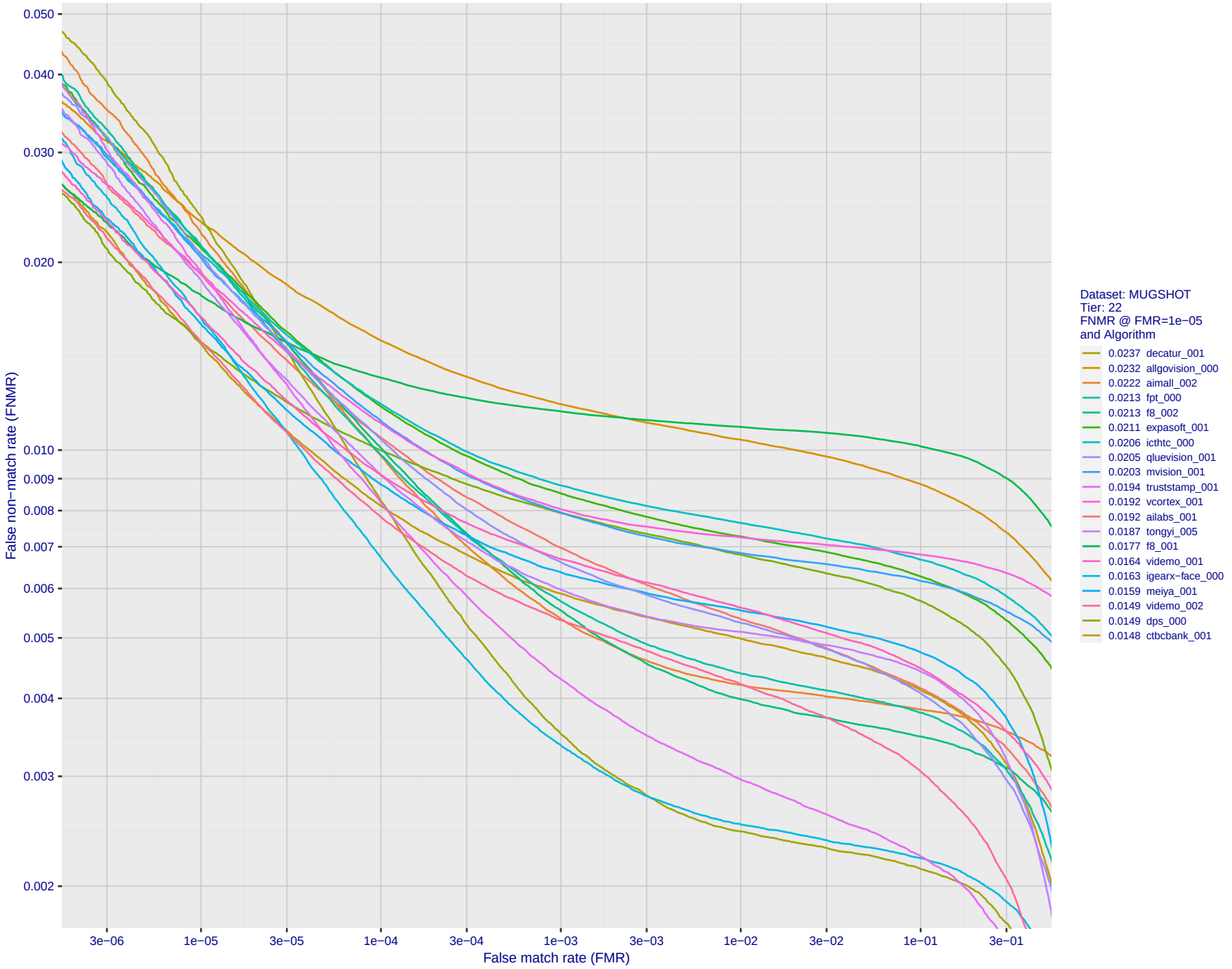

Figure 128: For the mugshot images, detection error tradeoff (DET) characteristics showing false non-match rate vs. false match rate plotted parametrically on threshold, T. The scales are logarithmic in order to show decades of FMR.

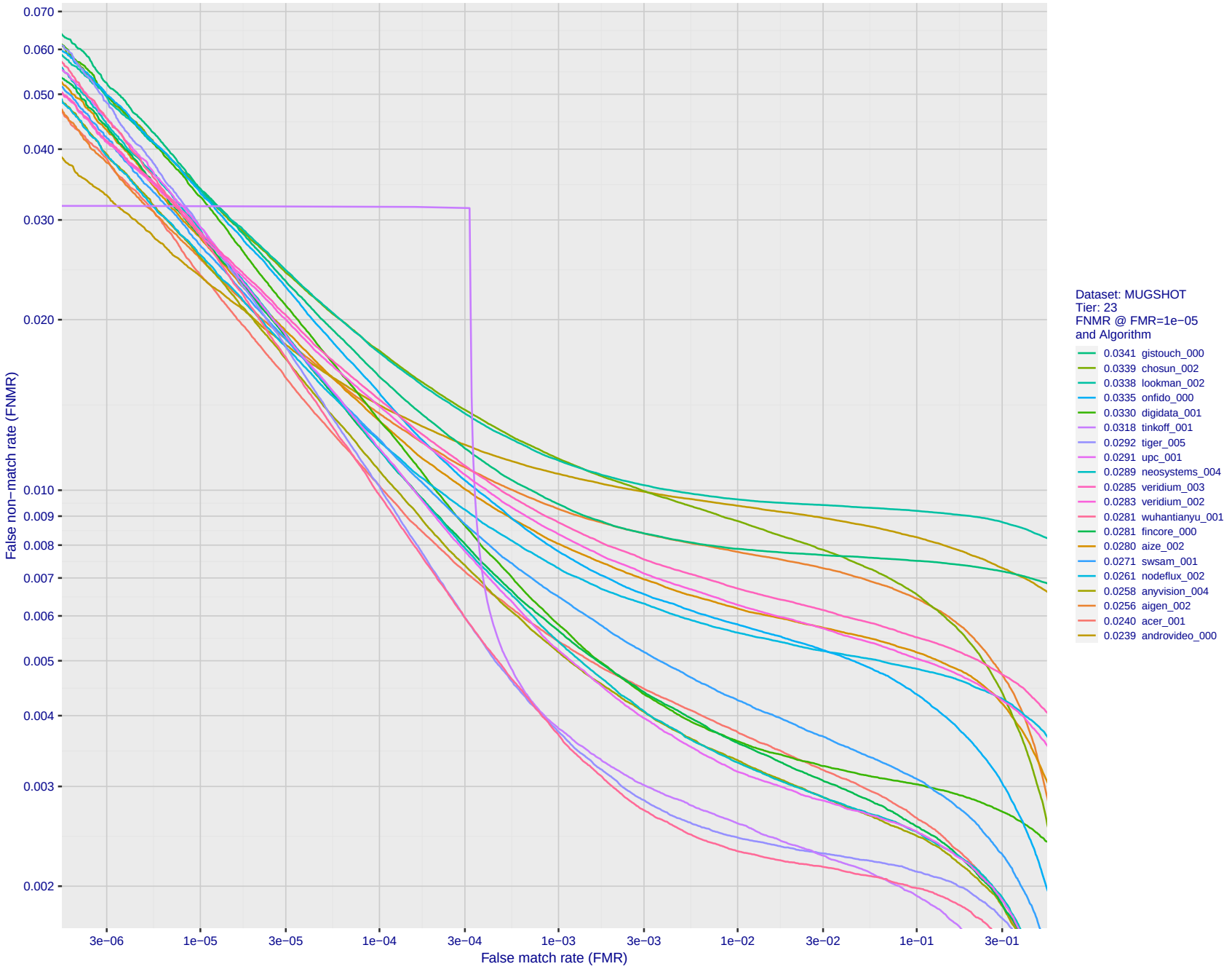

Figure 129: For the mugshot images, detection error tradeoff (DET) characteristics showing false non-match rate vs. false match rate plotted parametrically on threshold, T. The scales are logarithmic in order to show decades of FMR.

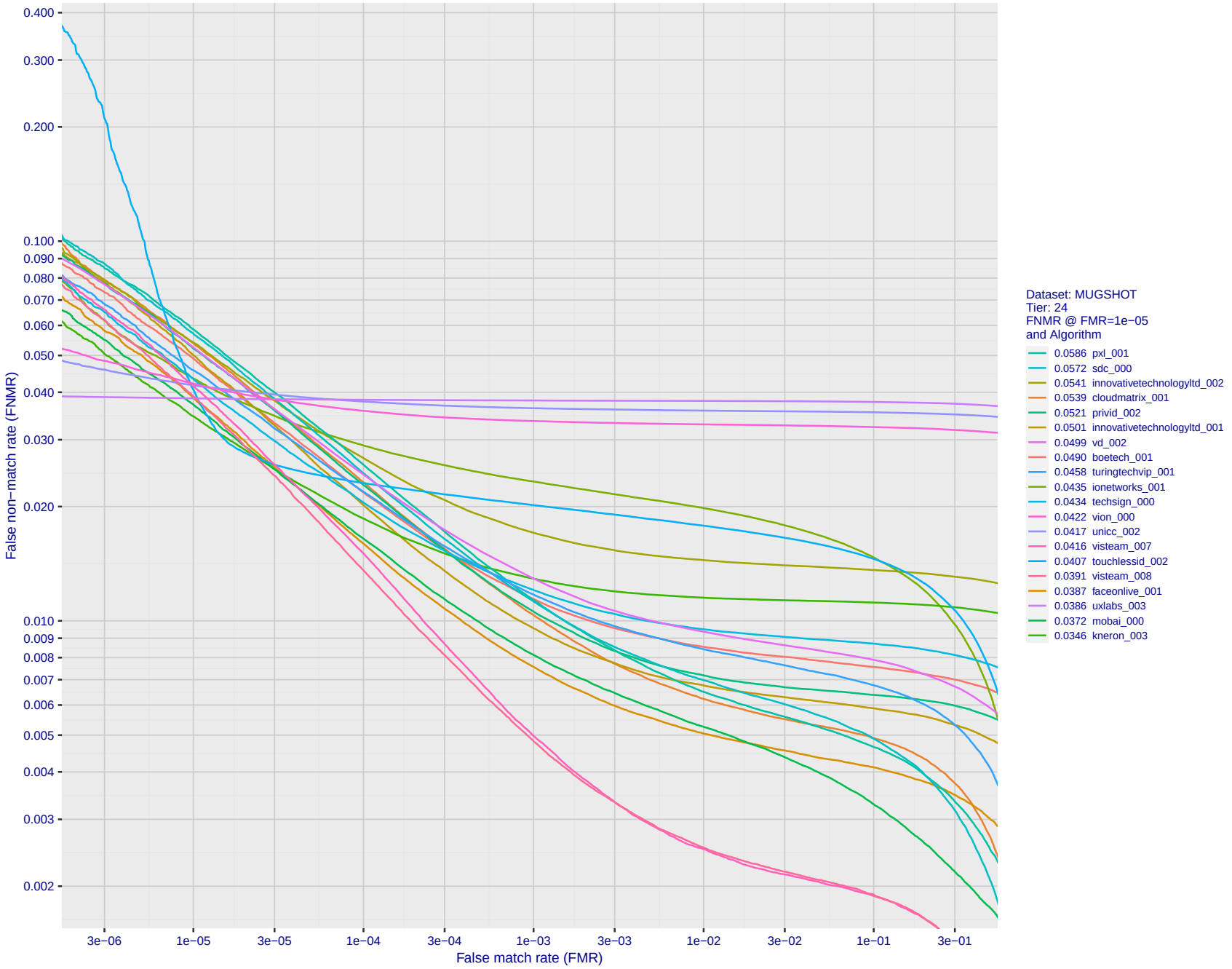

Figure 130: For the mugshot images, detection error tradeoff (DET) characteristics showing false non-match rate vs. false match rate plotted parametrically on threshold, T. The scales are logarithmic in order to show decades of FMR.

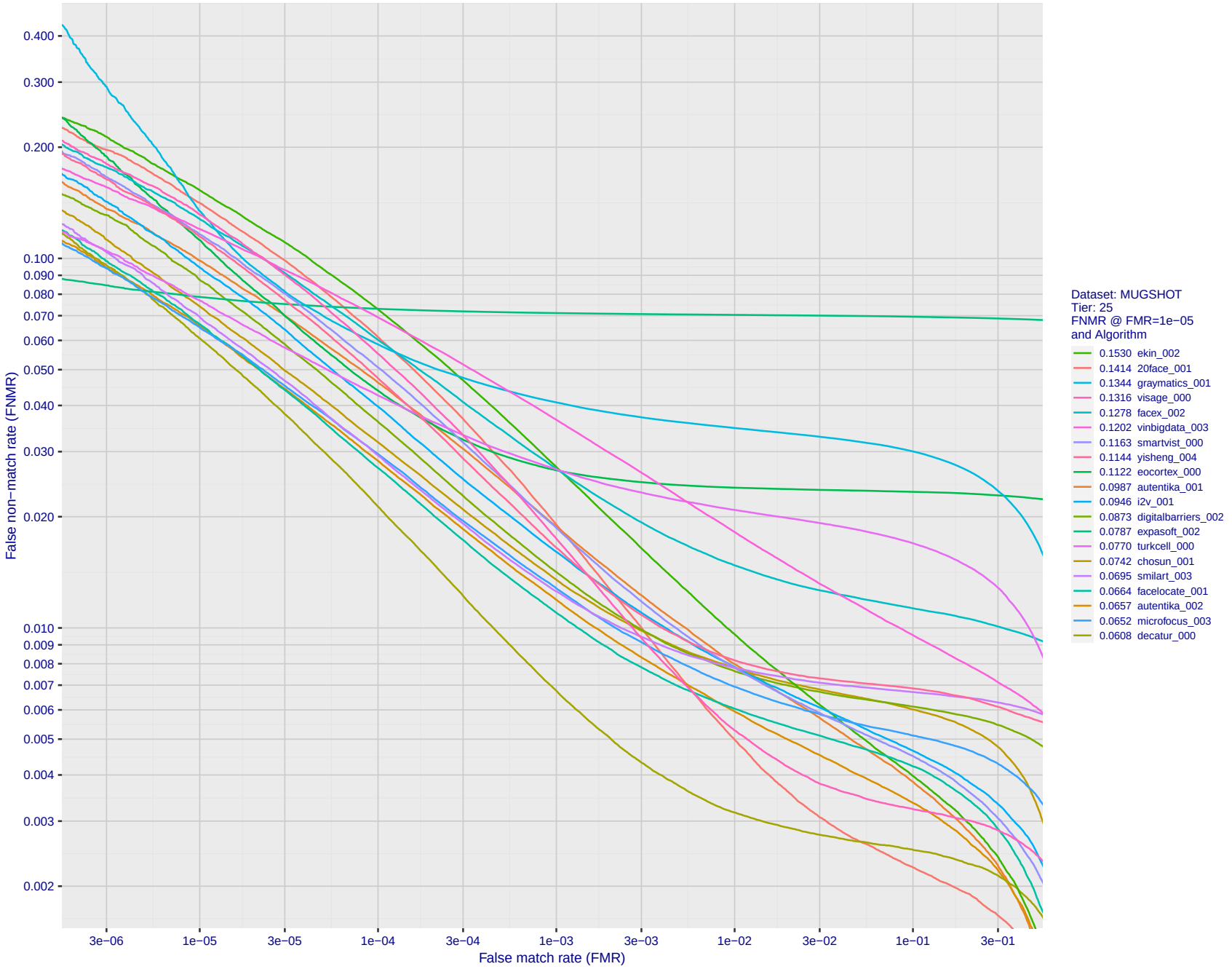

Figure 131: For the mugshot images, detection error tradeoff (DET) characteristics showing false non-match rate vs. false match rate plotted parametrically on threshold, T. The scales are logarithmic in order to show decades of FMR.

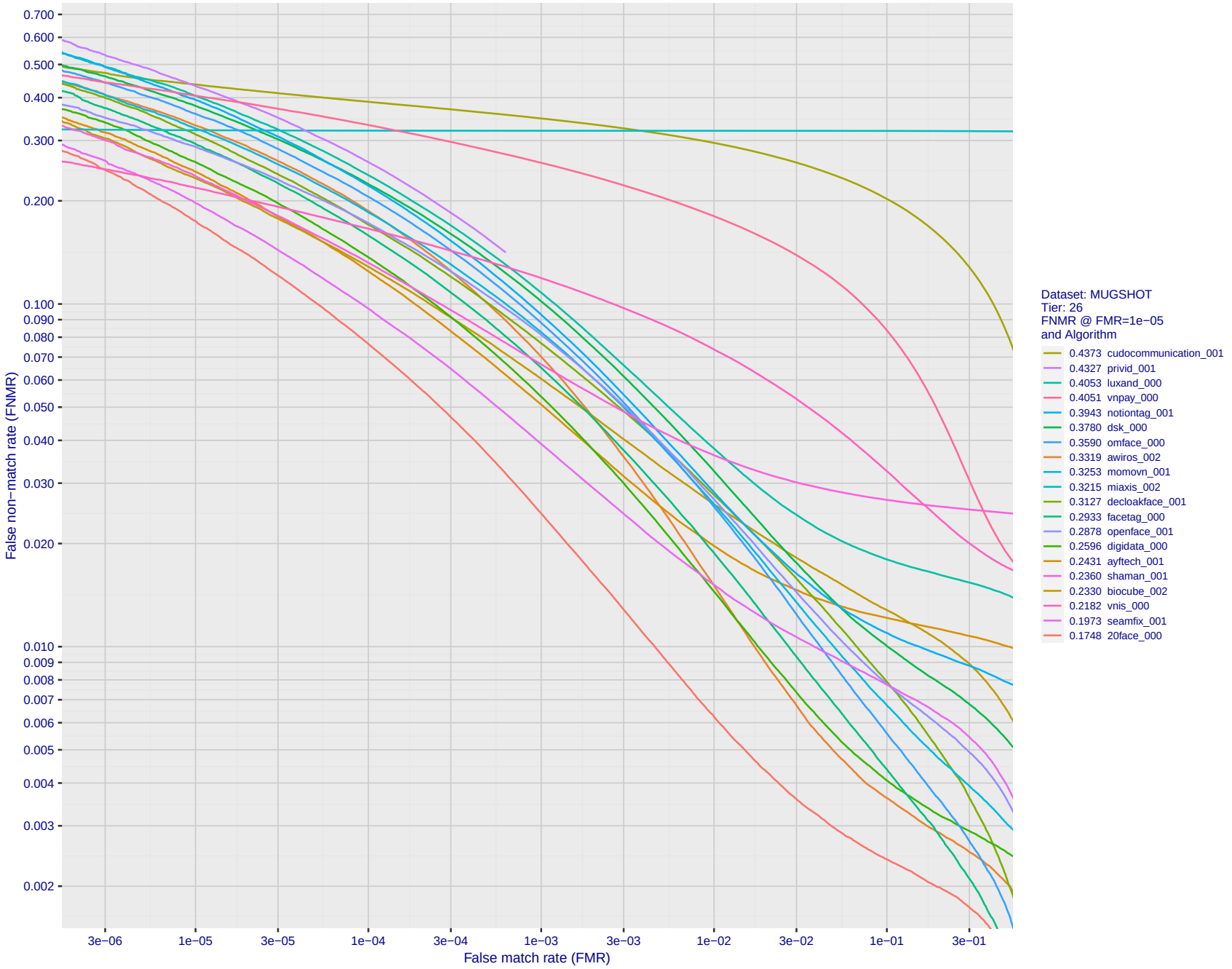

*Figure 132: For the mugshot images, detection error tradeoff (*DET*) characteristics showing false non-match rate vs. false match rate plotted parametrically on threshold, T. The scales are logarithmic in order to show decades of* FMR*.*

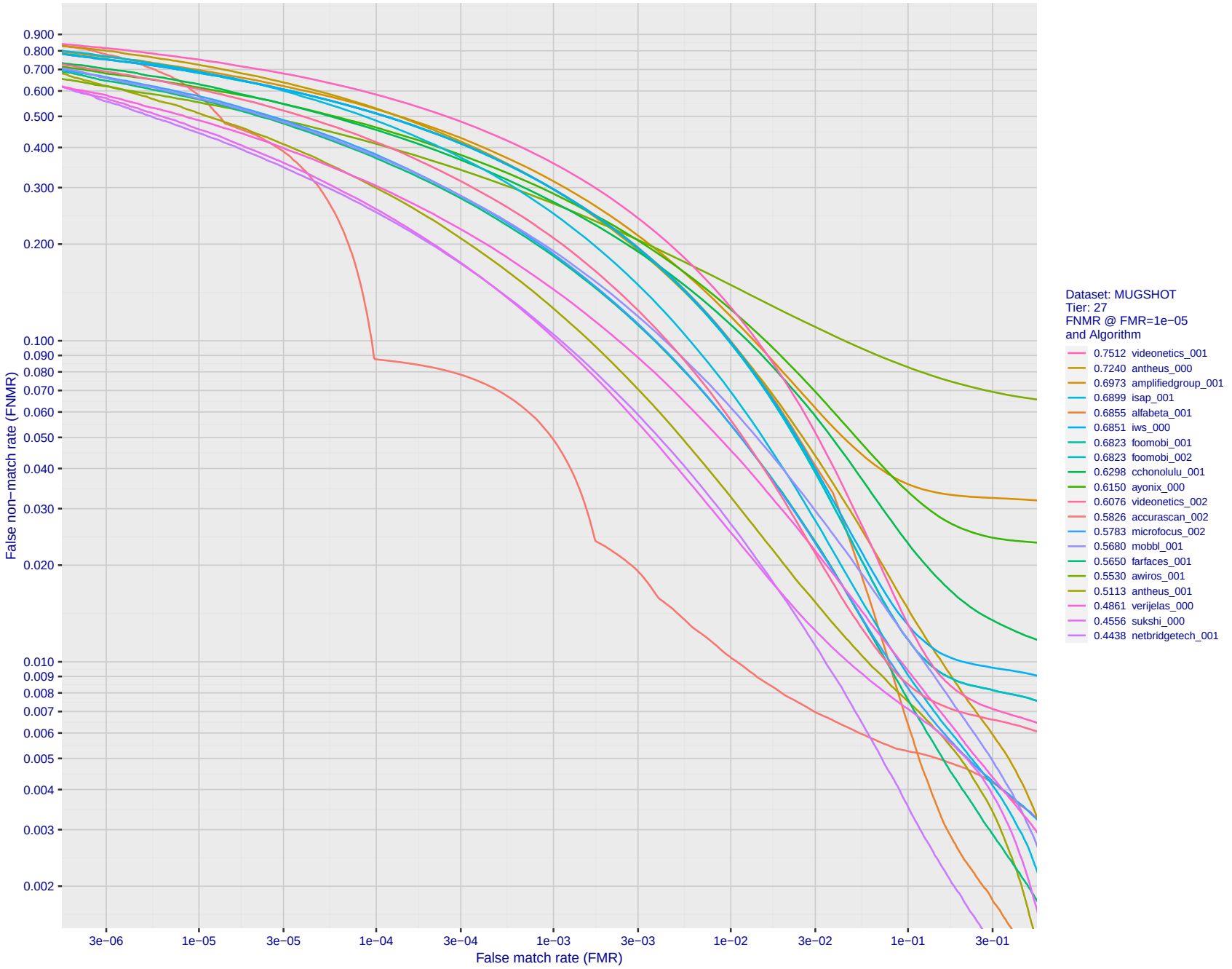

Figure 133: For the mugshot images, detection error tradeoff (DET) characteristics showing false non-match rate vs. false match rate plotted parametrically on threshold, T. The scales are logarithmic in order to show decades of FMR.

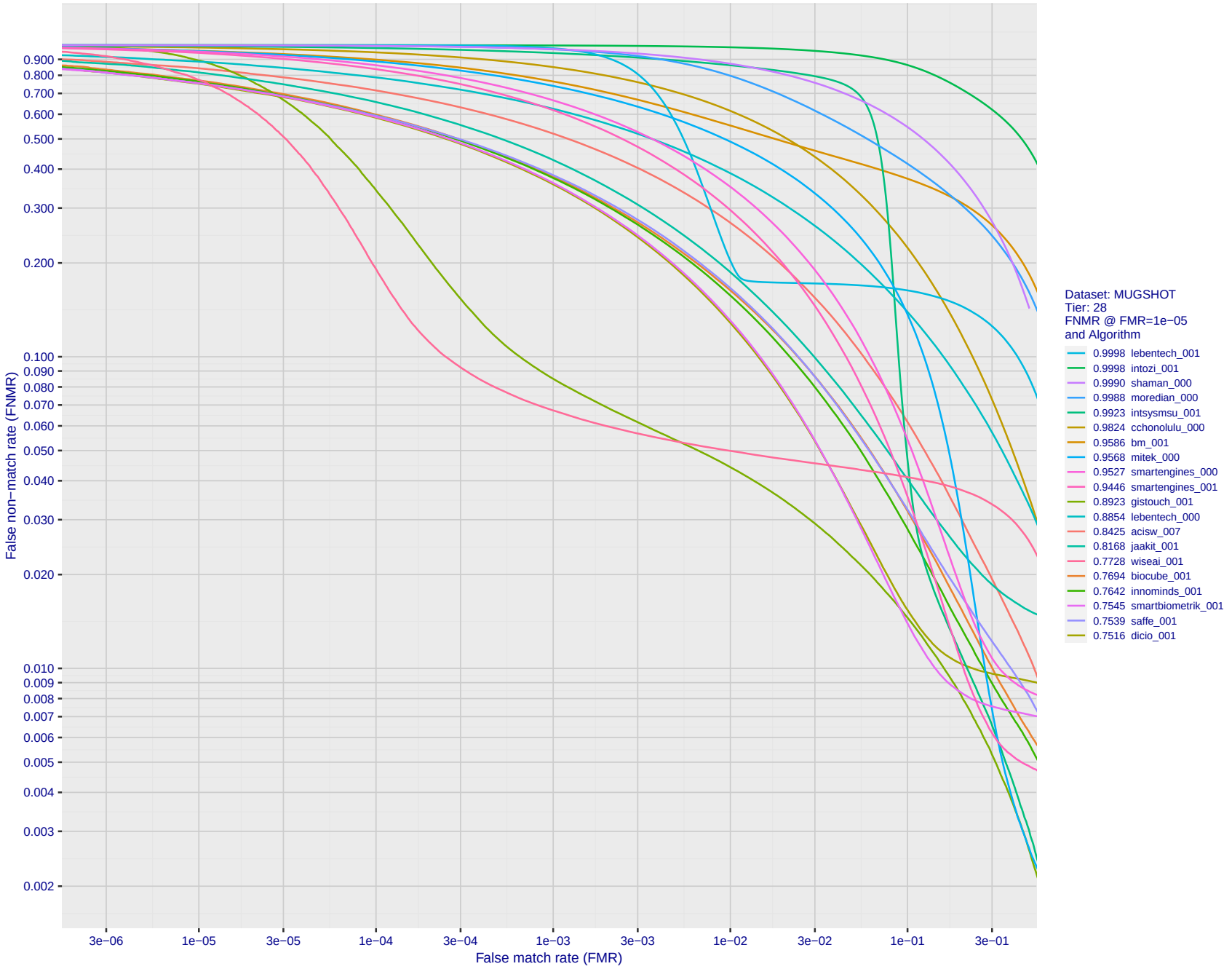

Figure 134: For the mugshot images, detection error tradeoff (DET) characteristics showing false non-match rate vs. false match rate plotted parametrically on threshold, T. The scales are logarithmic in order to show decades of FMR.

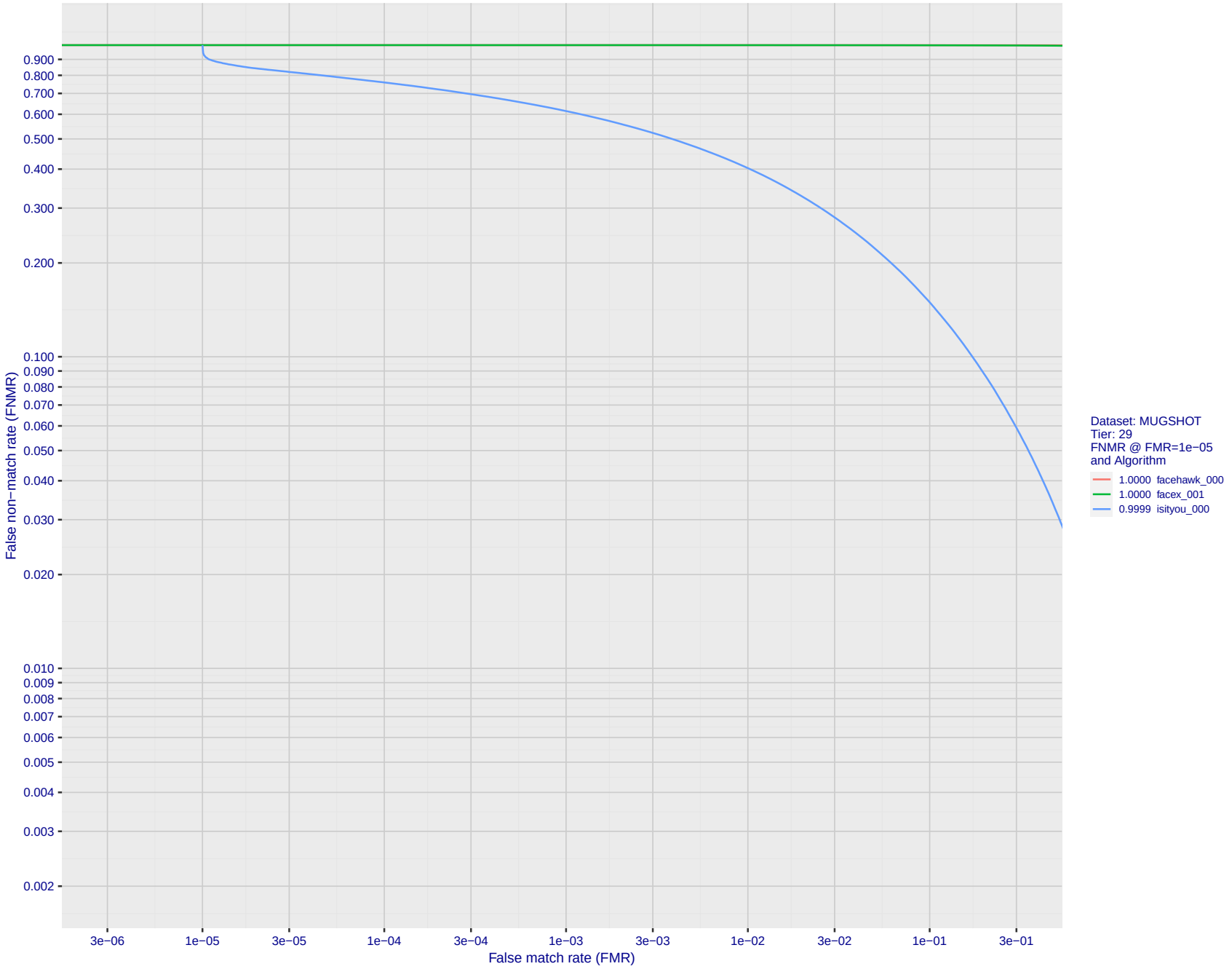

Figure 135: For the mugshot images, detection error tradeoff (DET) characteristics showing false non-match rate vs. false match rate plotted parametrically on threshold, T. The scales are logarithmic in order to show decades of FMR.

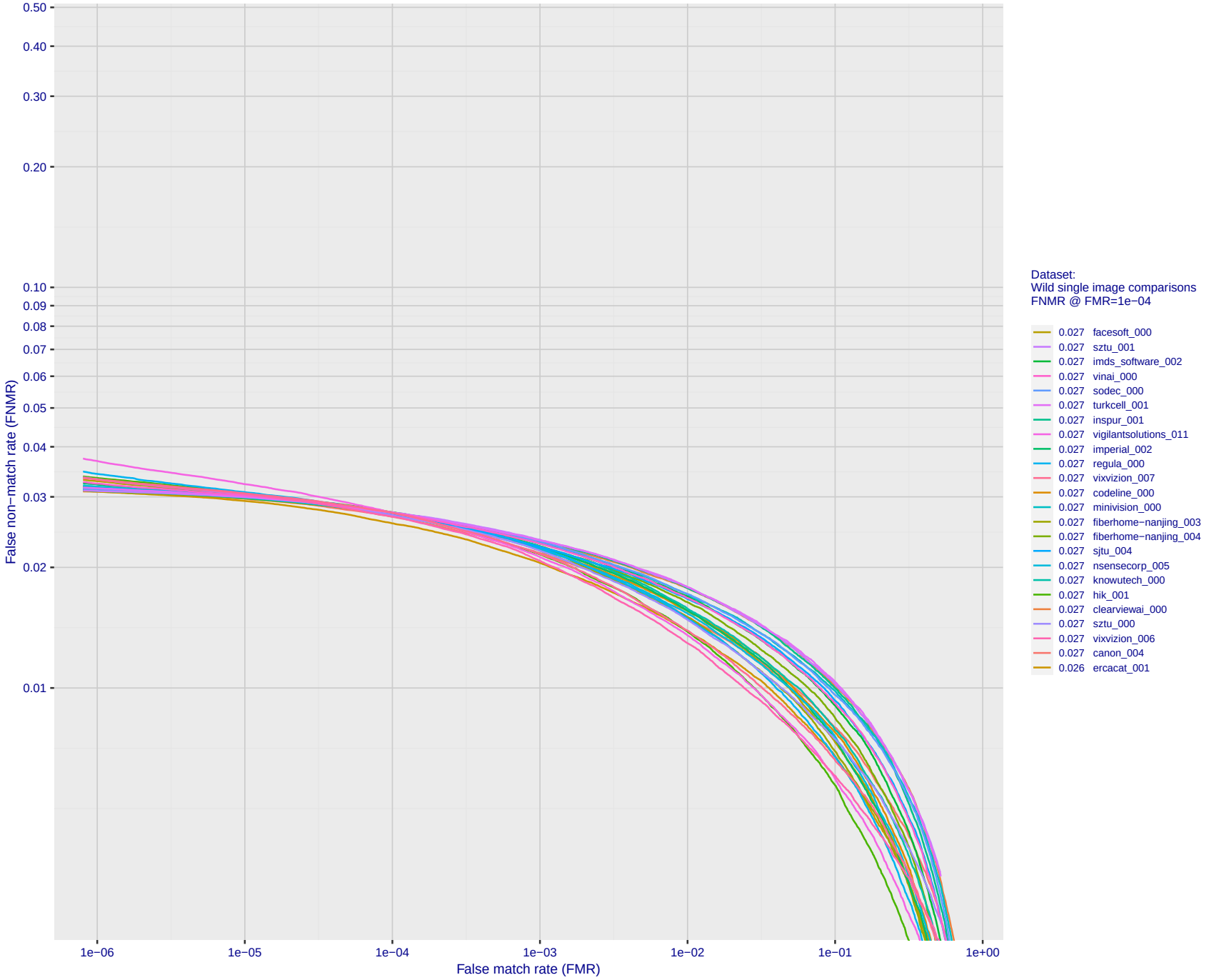

Figure 136: For the 2018 wild image comparisons, detection error tradeoff (DET) characteristics showing false non-match rate vs. false match rate plotted parametrically on threshold, T. The scales are logarithmic in order to show several decades of FMR.

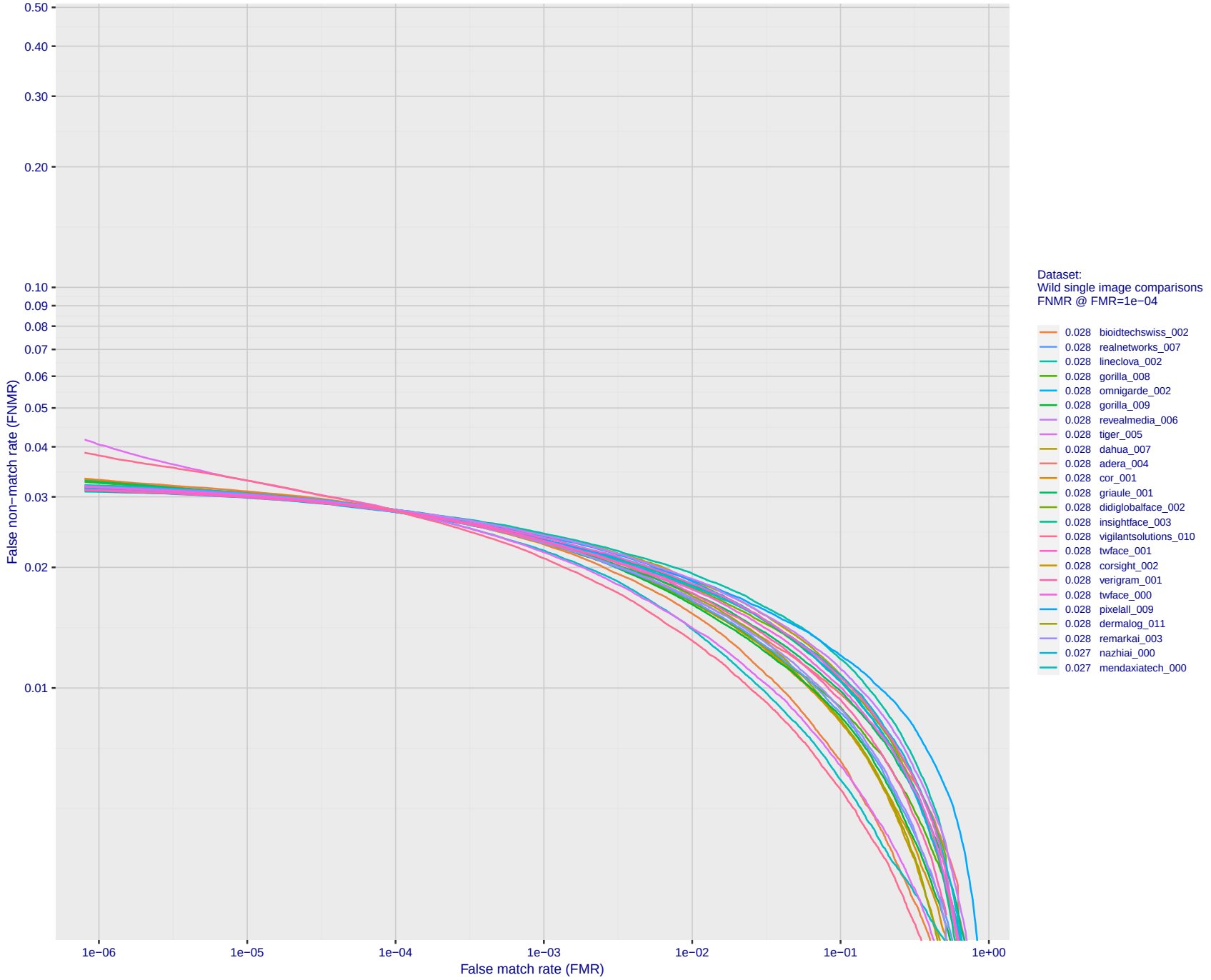

Figure 137: For the 2018 wild image comparisons, detection error tradeoff (DET) characteristics showing false non-match rate vs. false match rate plotted parametrically on threshold, T. The scales are logarithmic in order to show several decades of FMR.

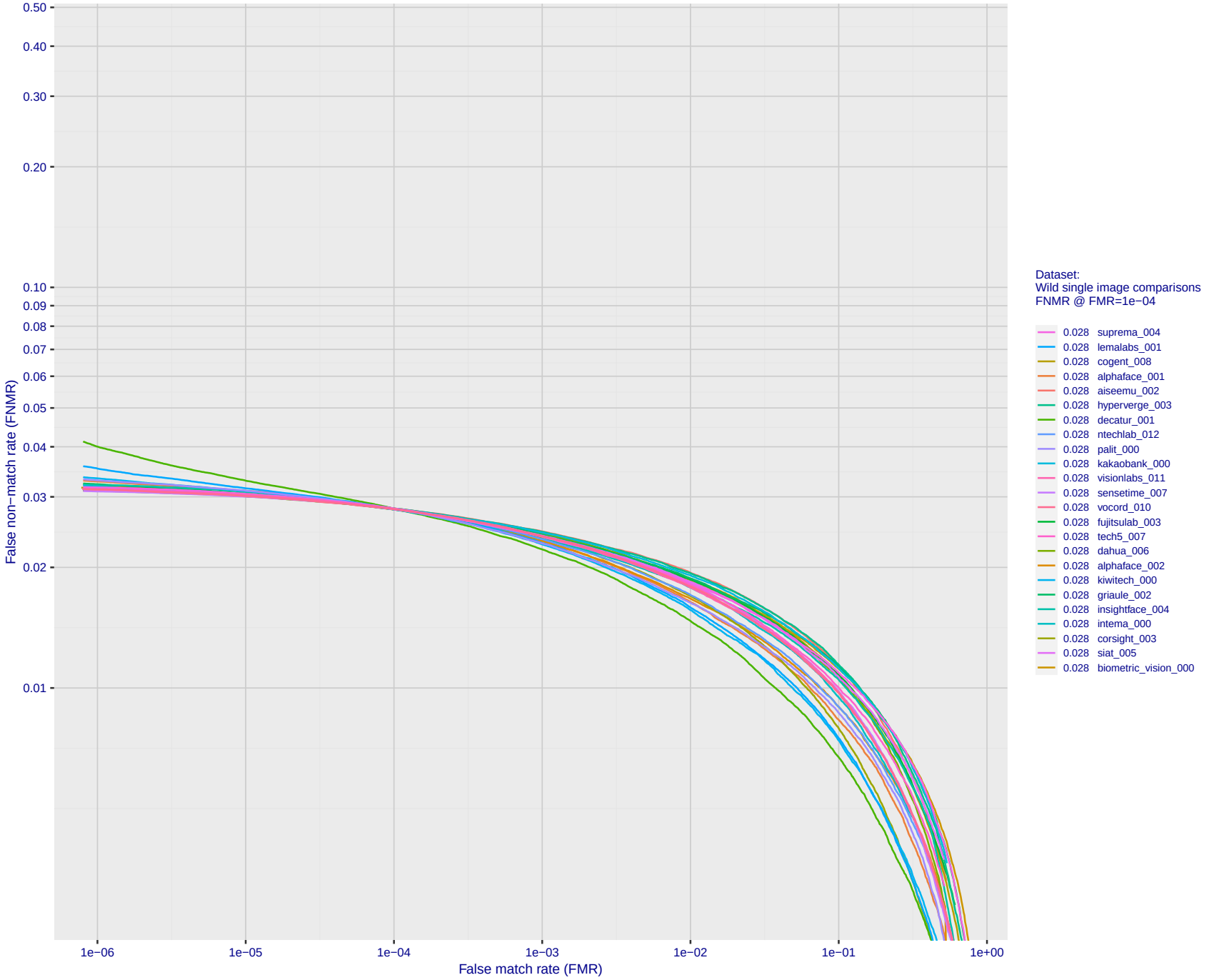

Figure 138: For the 2018 wild image comparisons, detection error tradeoff (DET) characteristics showing false non-match rate vs. false match rate plotted parametrically on threshold, T. The scales are logarithmic in order to show several decades of FMR.

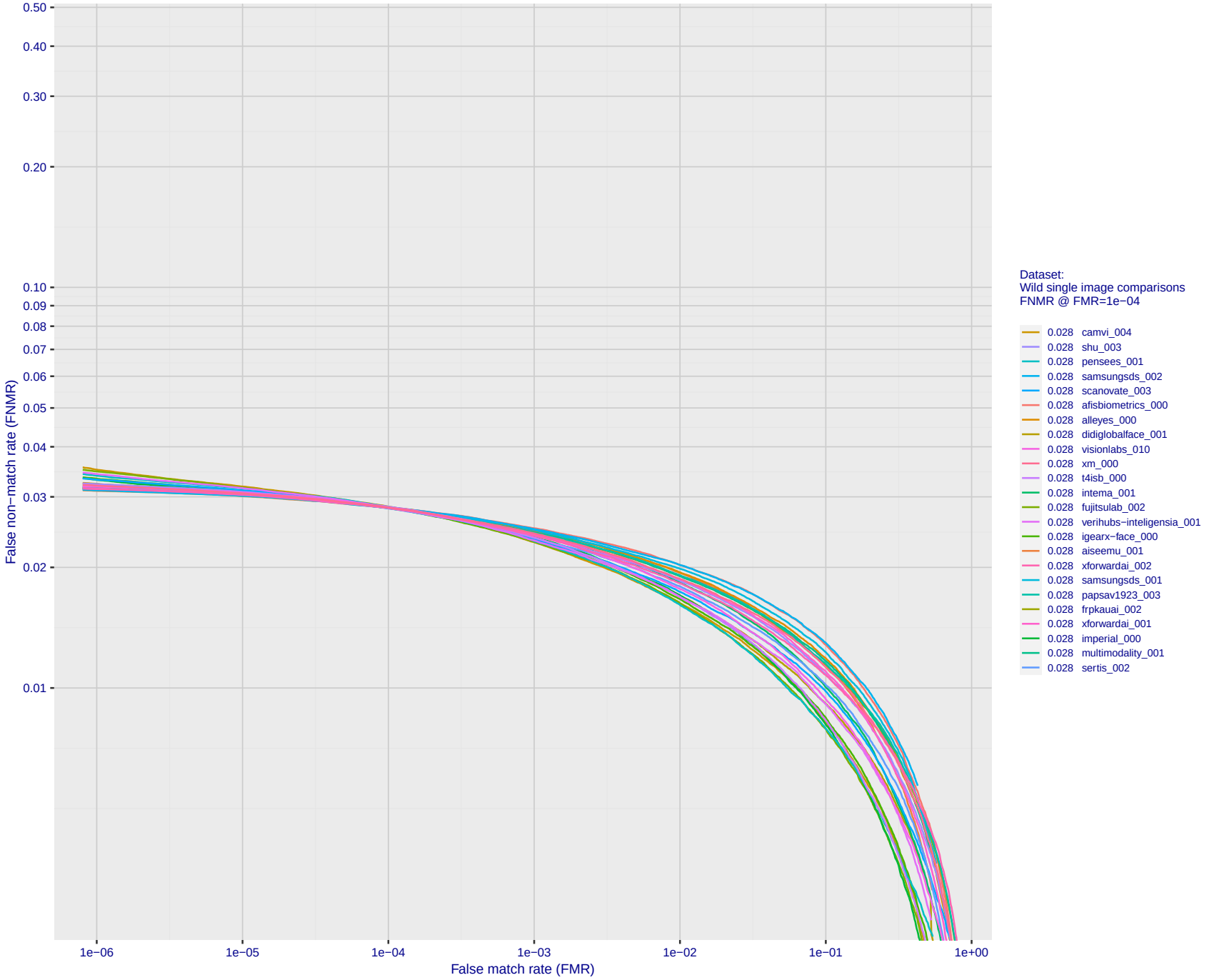

Figure 139: For the 2018 wild image comparisons, detection error tradeoff (DET) characteristics showing false non-match rate vs. false match rate plotted parametrically on threshold, T. The scales are logarithmic in order to show several decades of FMR.

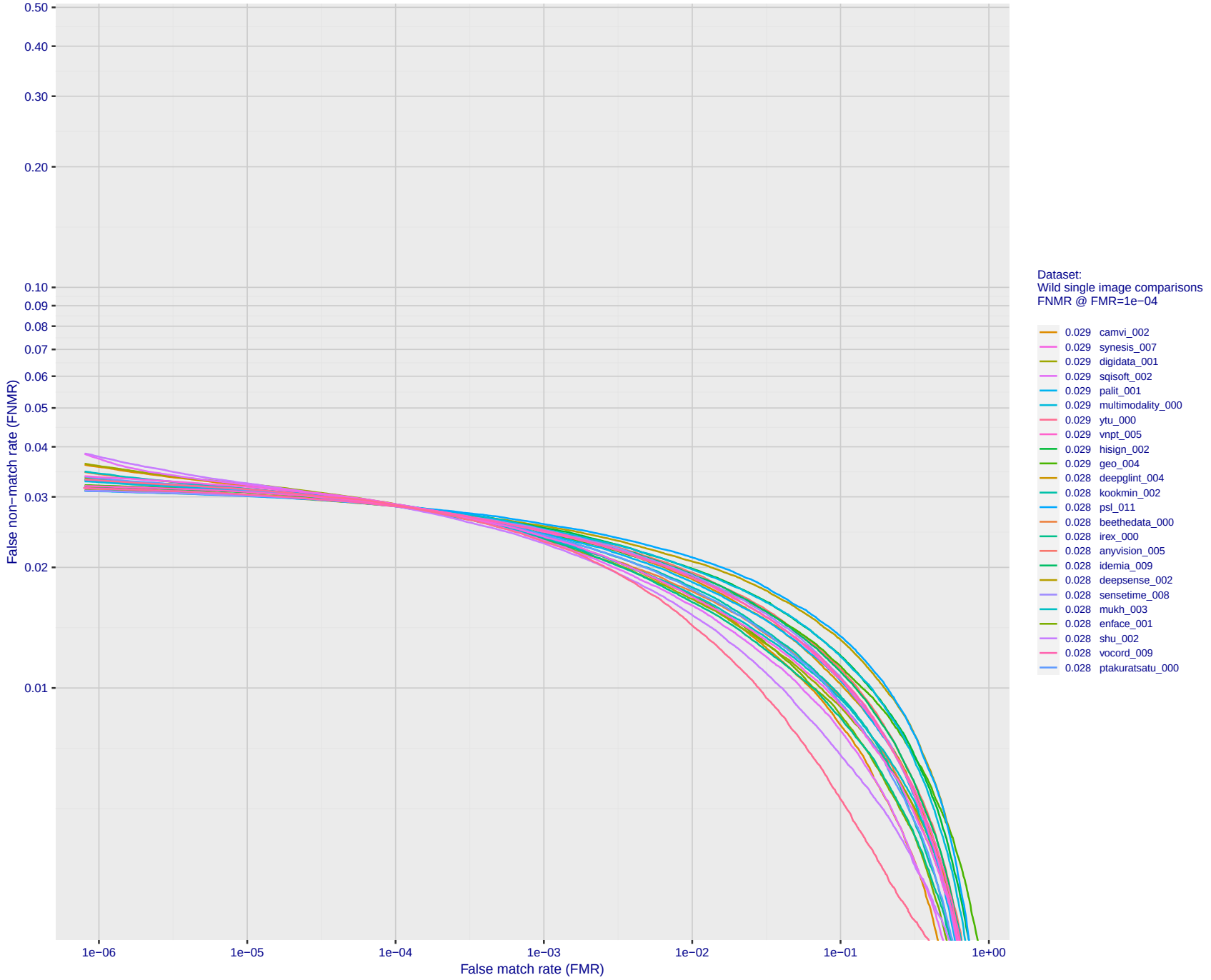

Figure 140: For the 2018 wild image comparisons, detection error tradeoff (DET) characteristics showing false non-match rate vs. false match rate plotted parametrically on threshold, T. The scales are logarithmic in order to show several decades of FMR.

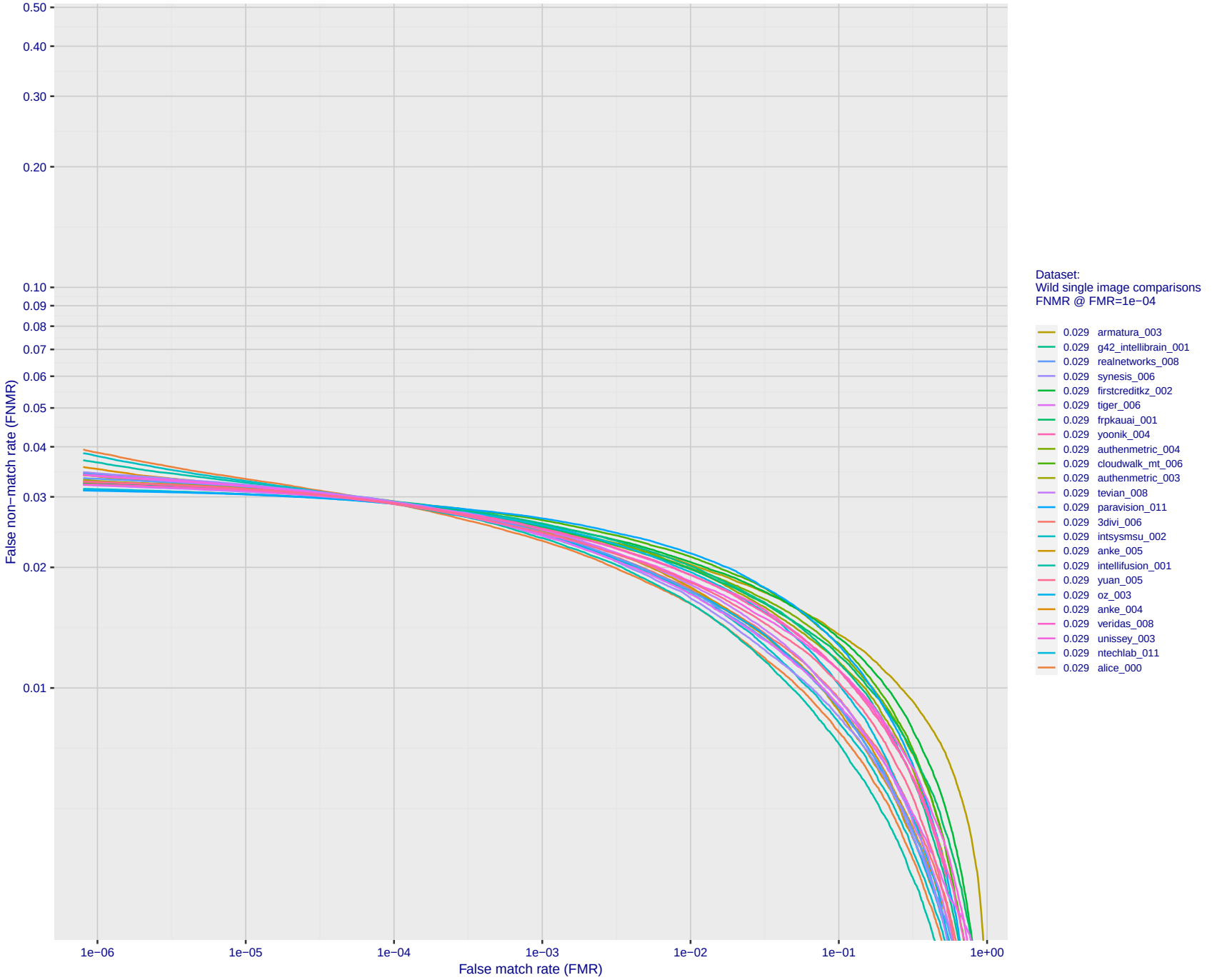

Figure 141: For the 2018 wild image comparisons, detection error tradeoff (DET) characteristics showing false non-match rate vs. false match rate plotted parametrically on threshold, T. The scales are logarithmic in order to show several decades of FMR.

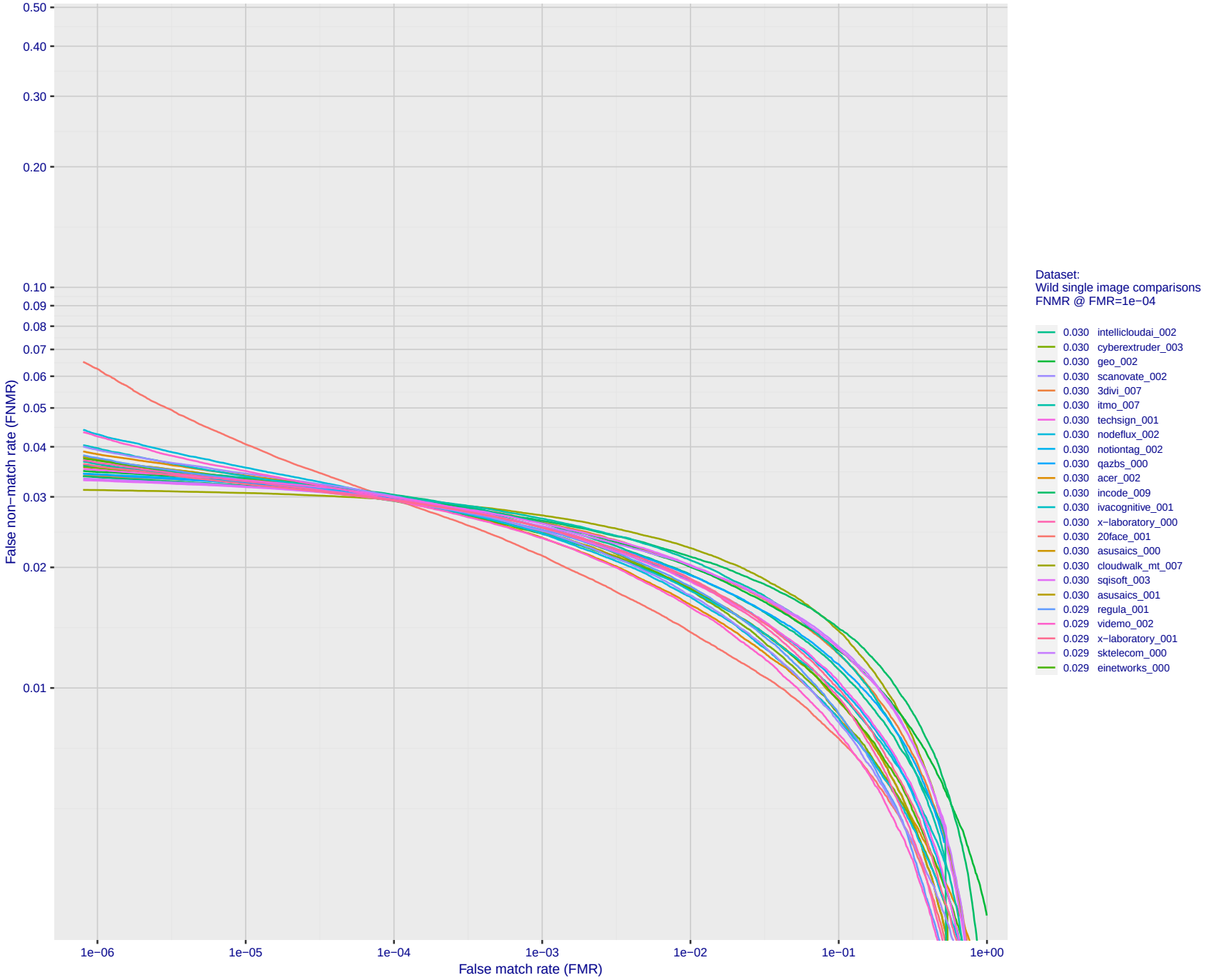

Figure 142: For the 2018 wild image comparisons, detection error tradeoff (DET) characteristics showing false non-match rate vs. false match rate plotted parametrically on threshold, T. The scales are logarithmic in order to show several decades of FMR.

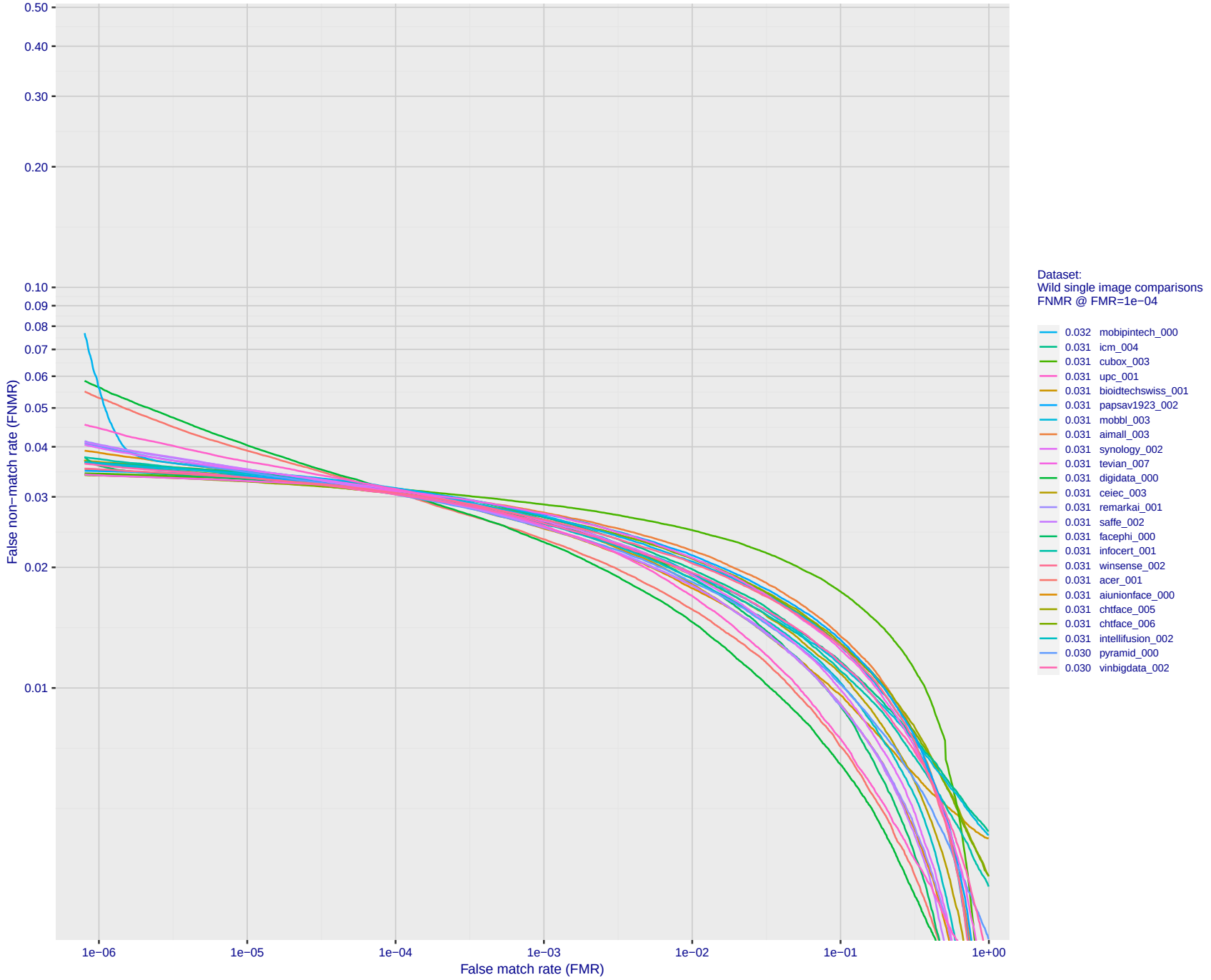

Figure 143: For the 2018 wild image comparisons, detection error tradeoff (DET) characteristics showing false non-match rate vs. false match rate plotted parametrically on threshold, T. The scales are logarithmic in order to show several decades of FMR.

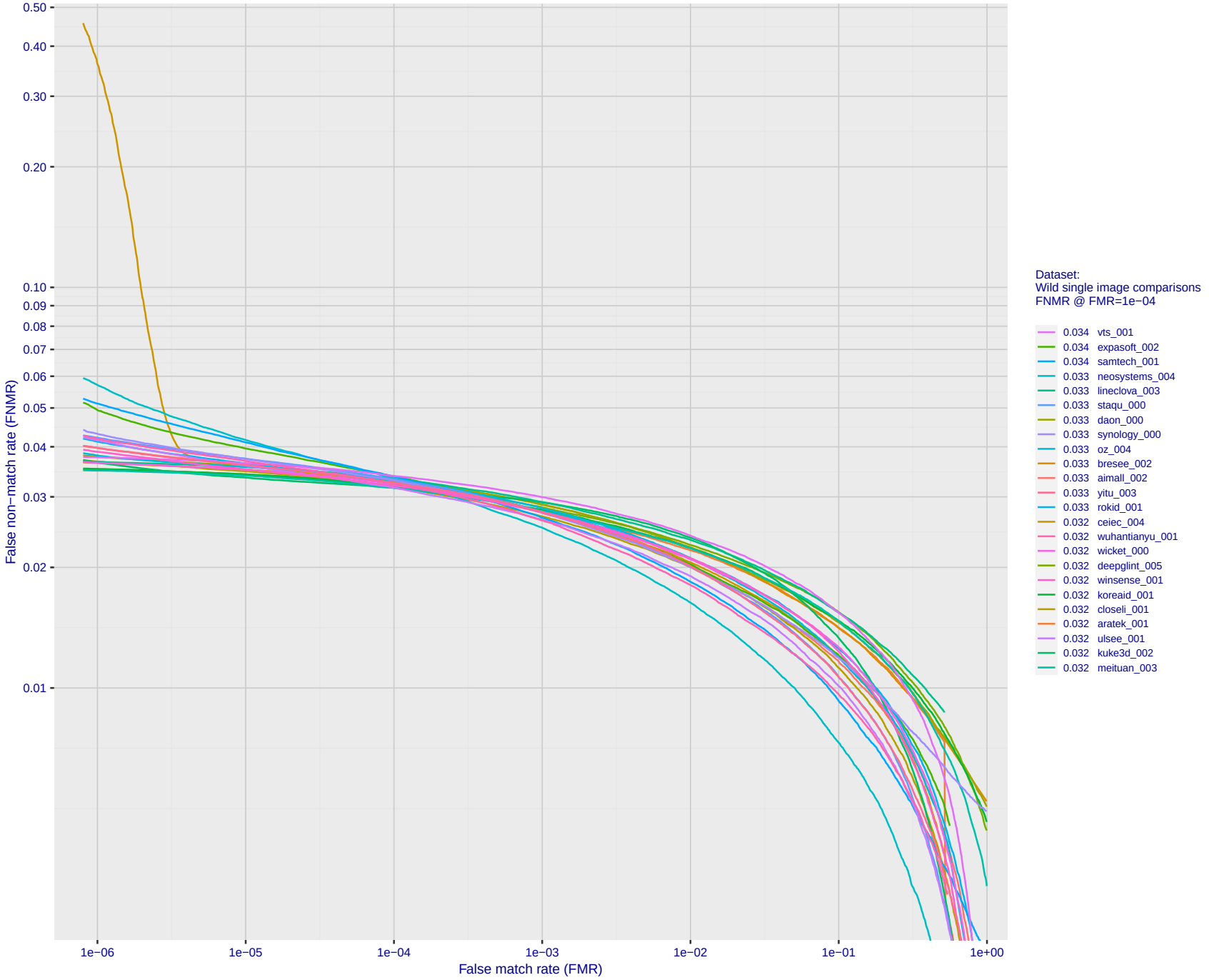

Figure 144: For the 2018 wild image comparisons, detection error tradeoff (DET) characteristics showing false non-match rate vs. false match rate plotted parametrically on threshold, T. The scales are logarithmic in order to show several decades of FMR.

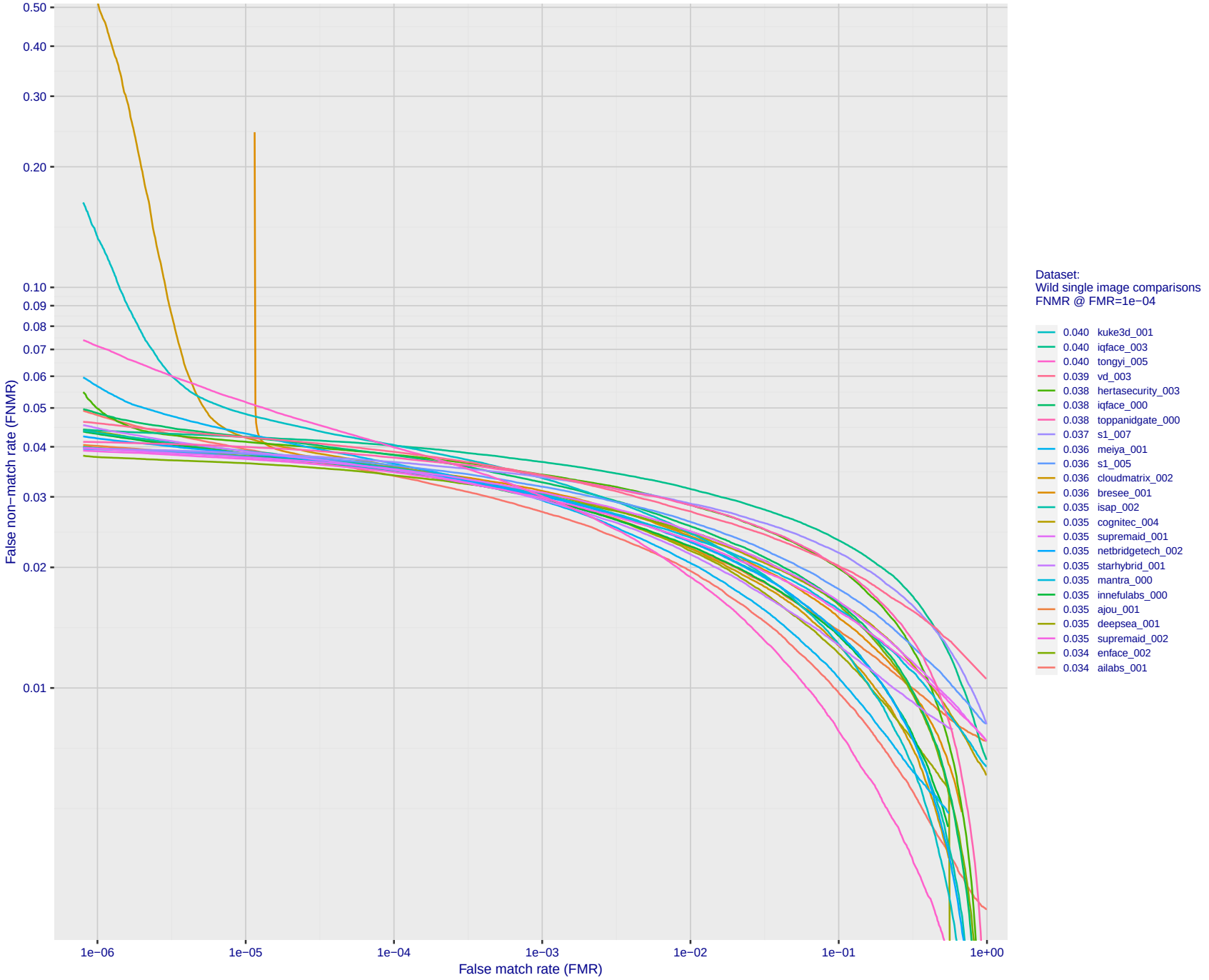

Figure 145: For the 2018 wild image comparisons, detection error tradeoff (DET) characteristics showing false non-match rate vs. false match rate plotted parametrically on threshold, T. The scales are logarithmic in order to show several decades of FMR.

FNMR(T) "False non-match rate"
FMR(T) "False match rate"

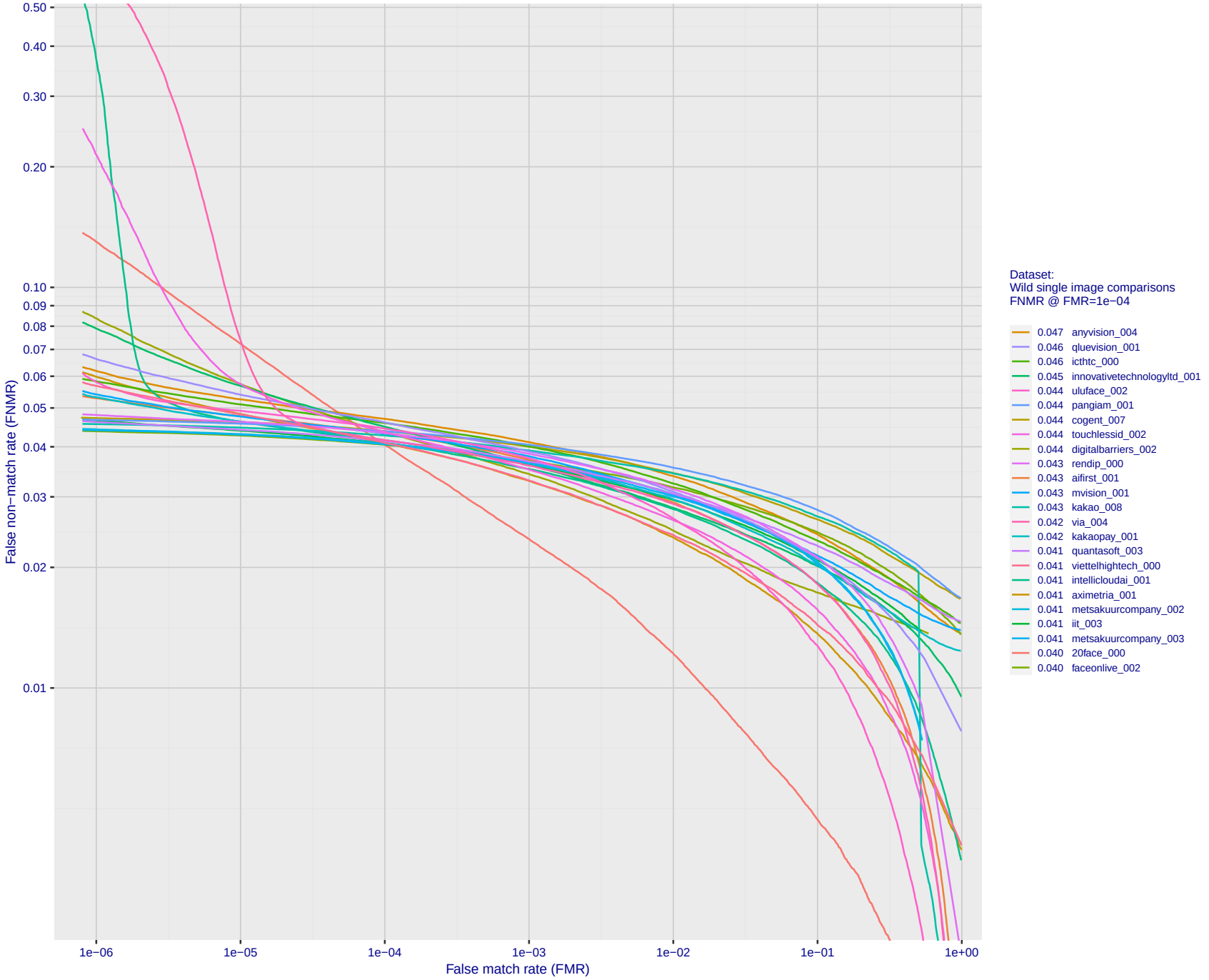

Figure 146: For the 2018 wild image comparisons, detection error tradeoff (DET) characteristics showing false non-match rate vs. false match rate plotted parametrically on threshold, T. The scales are logarithmic in order to show several decades of FMR.

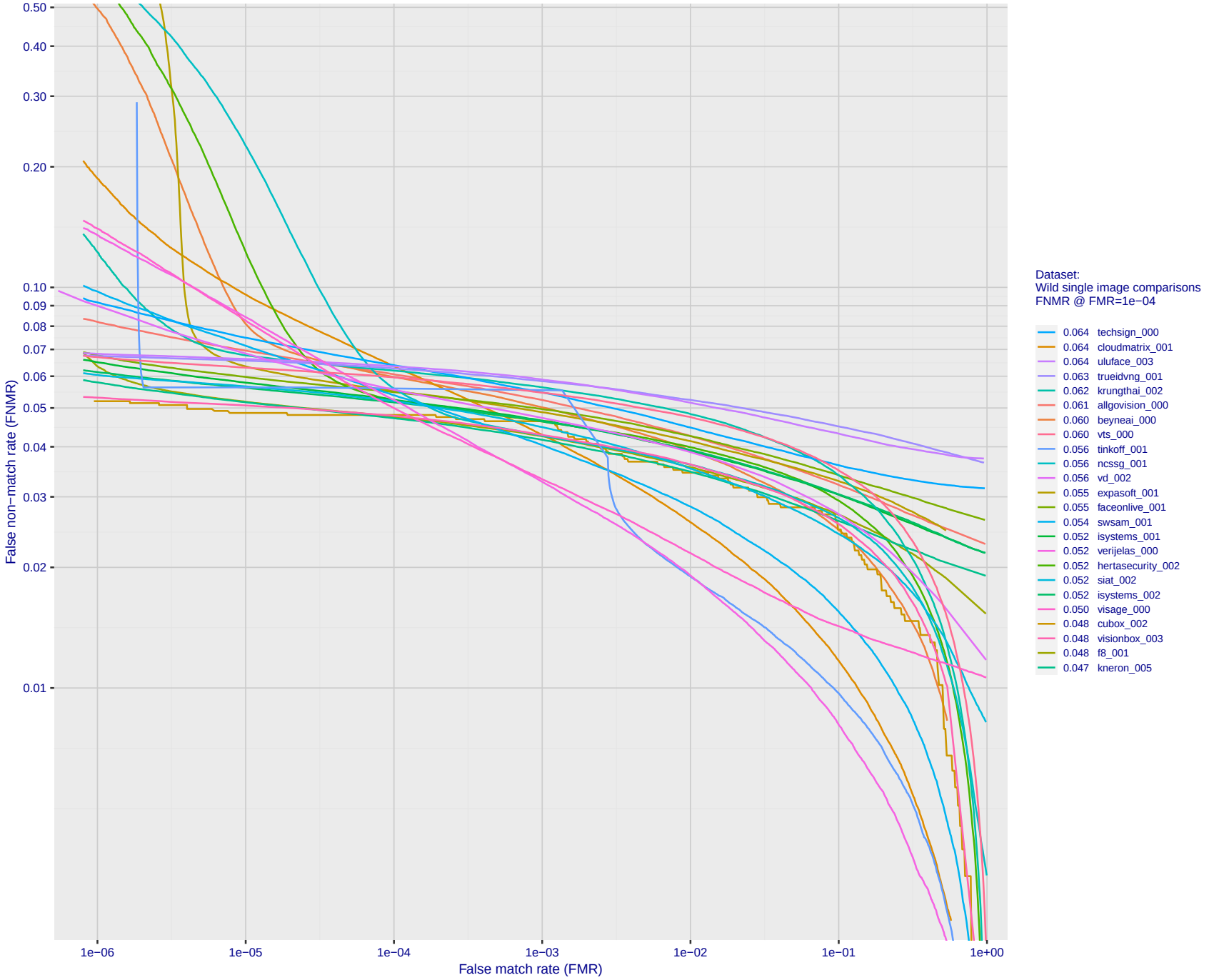

Figure 147: For the 2018 wild image comparisons, detection error tradeoff (DET) characteristics showing false non-match rate vs. false match rate plotted parametrically on threshold, T. The scales are logarithmic in order to show several decades of FMR.

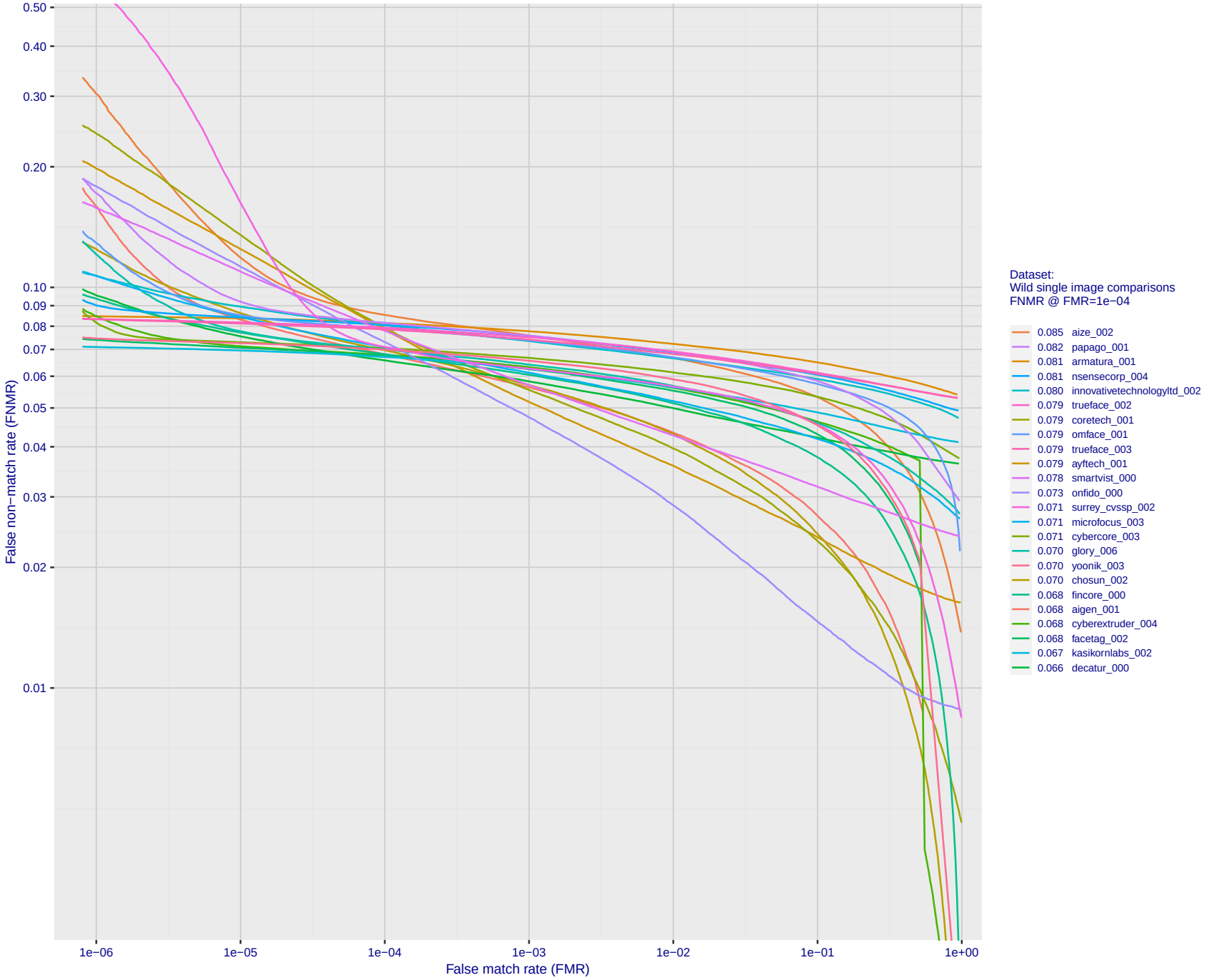

Figure 148: For the 2018 wild image comparisons, detection error tradeoff (DET) characteristics showing false non-match rate vs. false match rate plotted parametrically on threshold, T. The scales are logarithmic in order to show several decades of FMR.

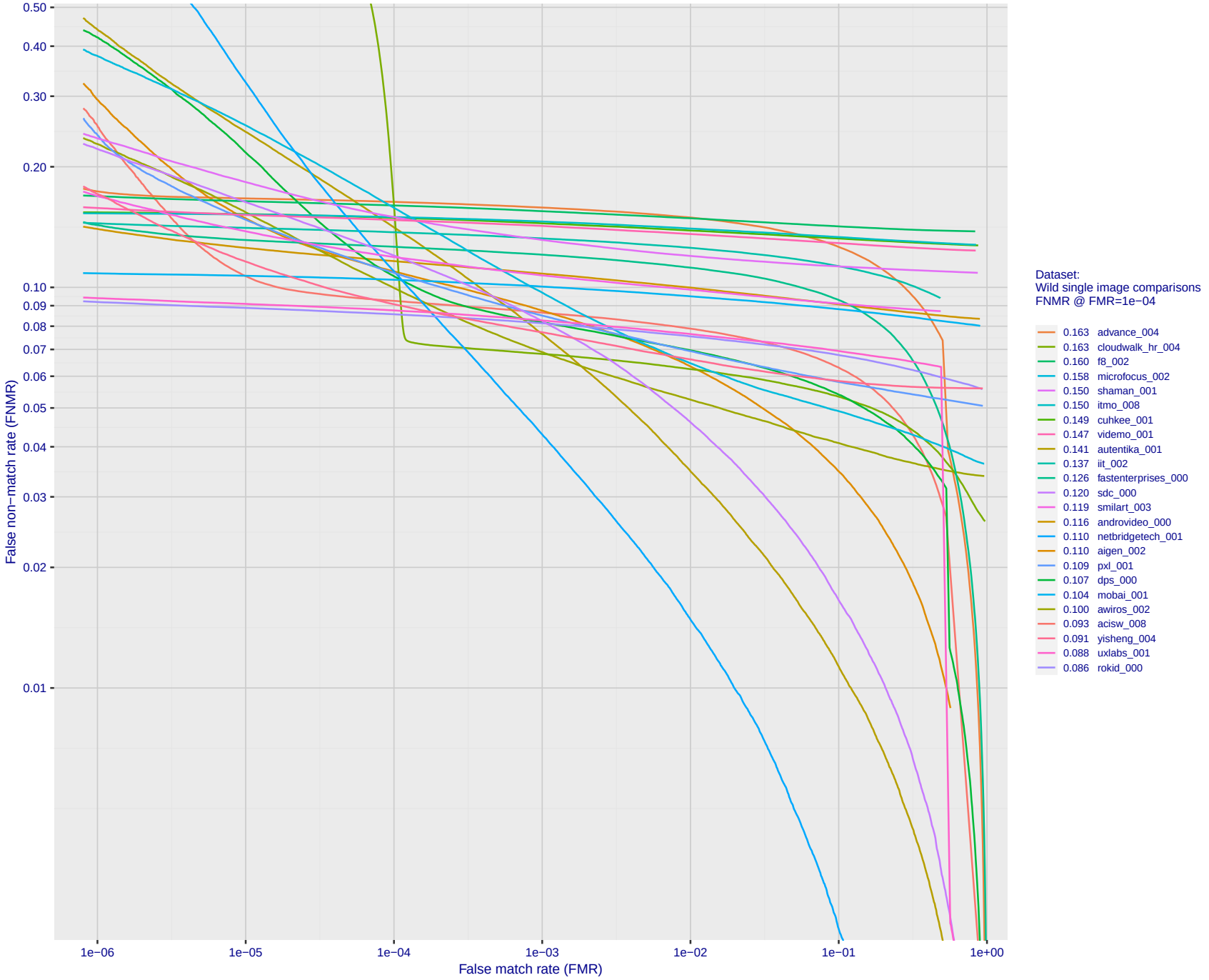

Figure 149: For the 2018 wild image comparisons, detection error tradeoff (DET) characteristics showing false non-match rate vs. false match rate plotted parametrically on threshold, T. The scales are logarithmic in order to show several decades of FMR.

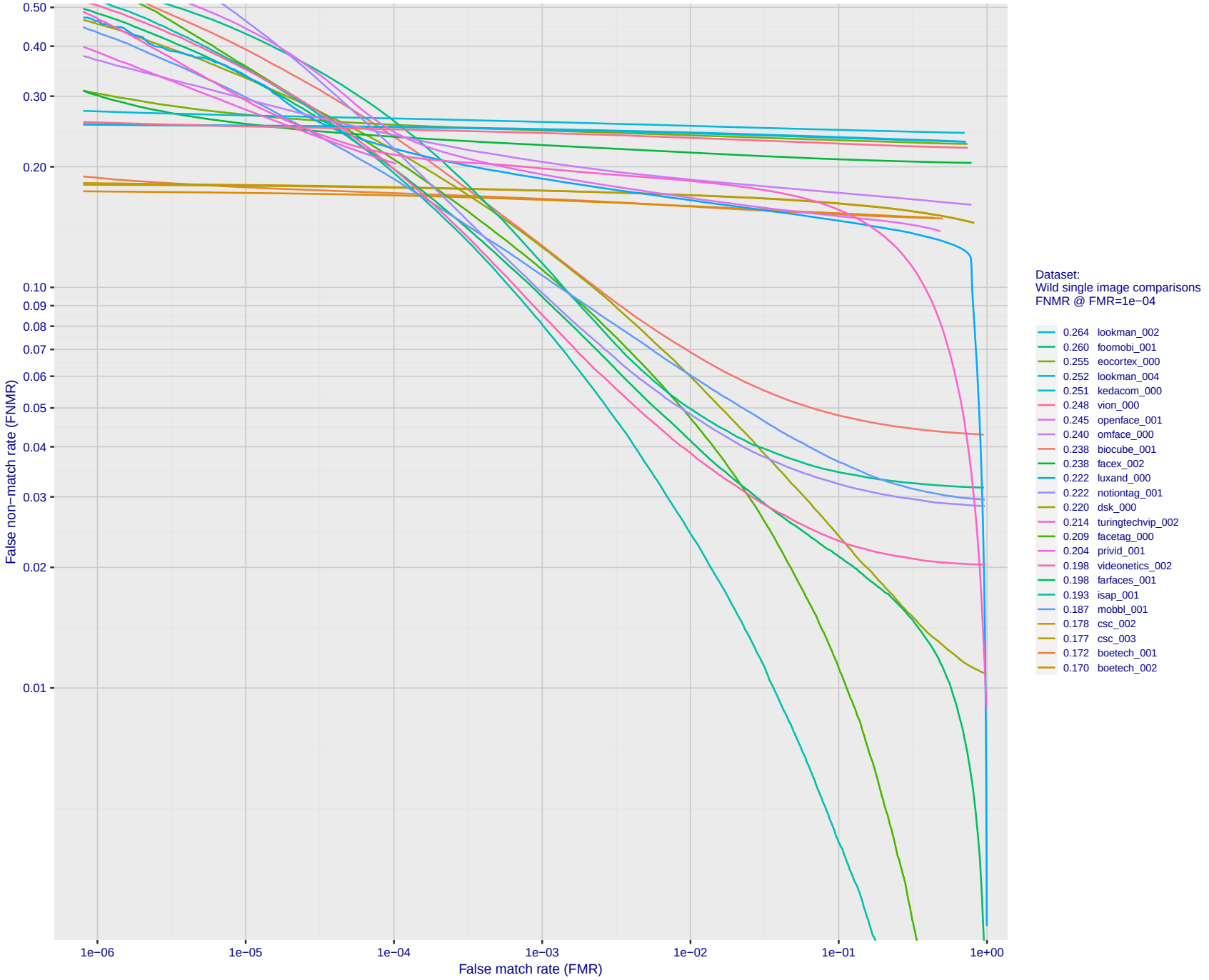

Figure 150: For the 2018 wild image comparisons, detection error tradeoff (DET) characteristics showing false non-match rate vs. false match rate plotted parametrically on threshold, T. The scales are logarithmic in order to show several decades of FMR.

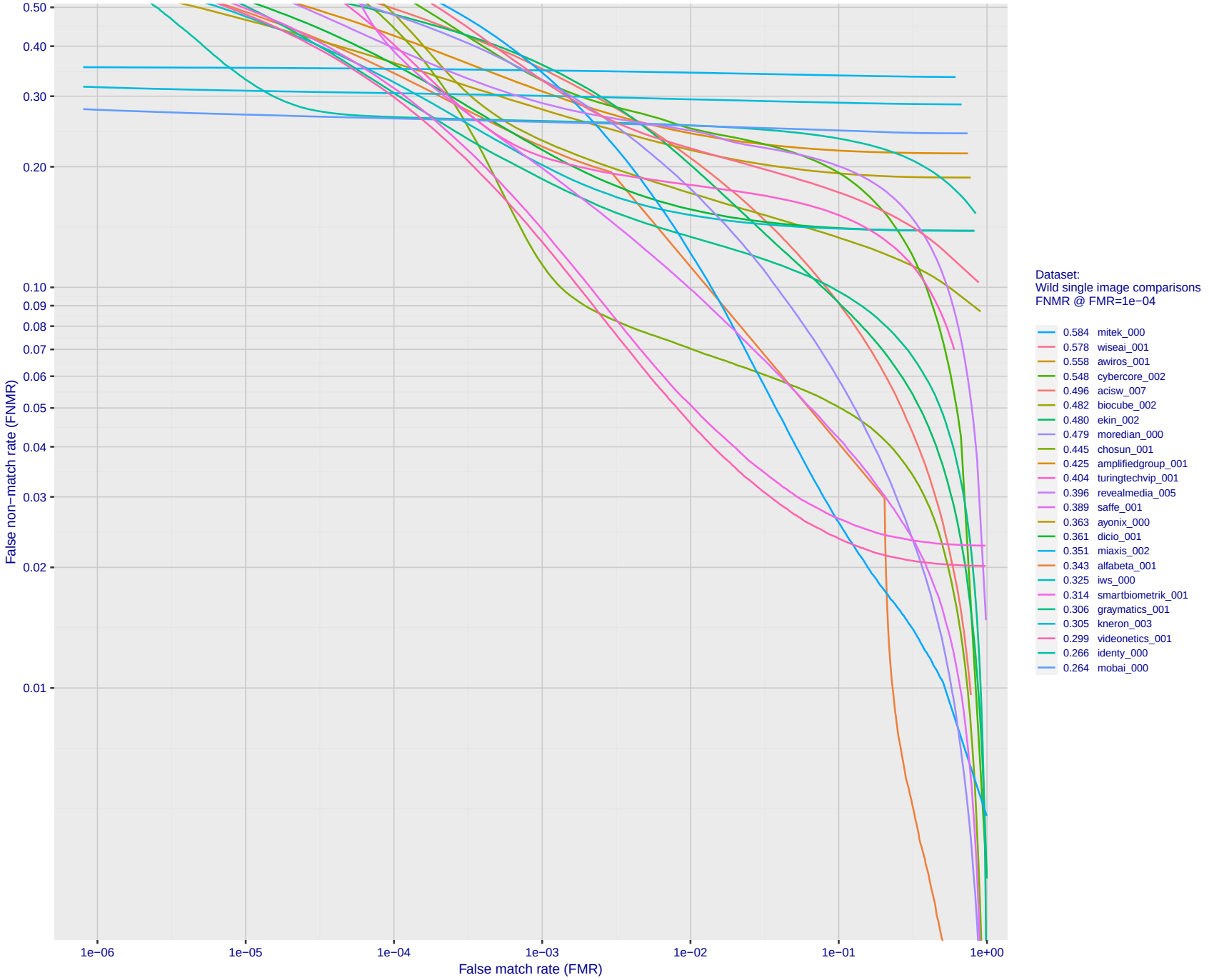

Figure 151: For the 2018 wild image comparisons, detection error tradeoff (DET) characteristics showing false non-match rate vs. false match rate plotted parametrically on threshold, T. The scales are logarithmic in order to show several decades of FMR.

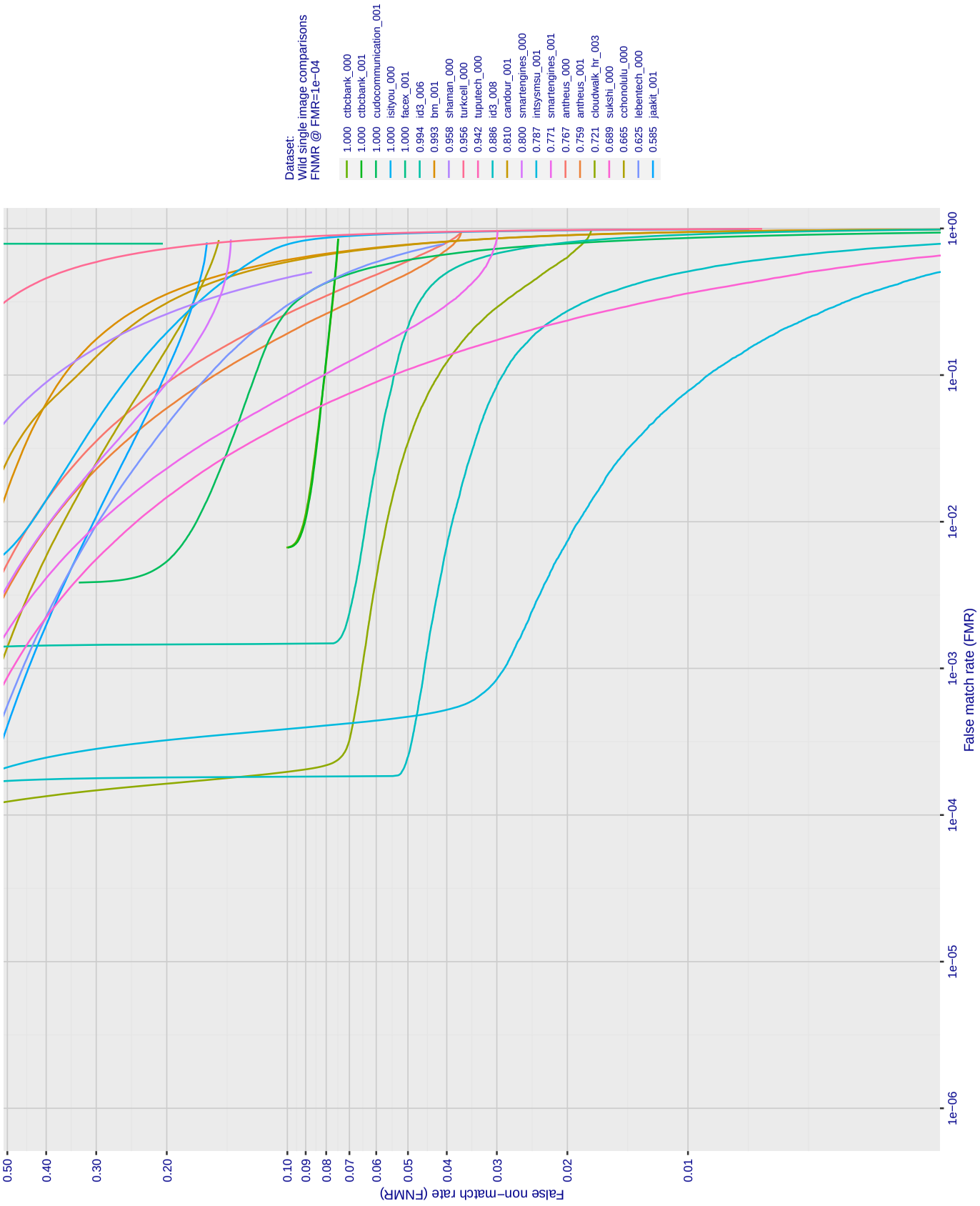

Figure 152: For the 2018 wild image comparisons, detection error tradeoff (DET) characteristics showing false non-match rate vs. false match rate plotted parametrically on threshold, T. The scales are logarithmic in order to show several decades of FMR.

FNMR(T) "False non-match rate"
FMR(T) "False match rate"

Figure 153: For the mugshot images, FMR *for same-sex impostor pairs of images annotated with codes for black female, black male, white female, white male. The threshold is set for each algorithm to give* FMR *= 0.001 for white males which is the demographic that usually gives the lowest* FMR*. This means the top right box is the same color in all panels. The panels are sorted over multiple pages in order of* FMR *on black females, which is the demographc that usually gives the highest* FMR*.*

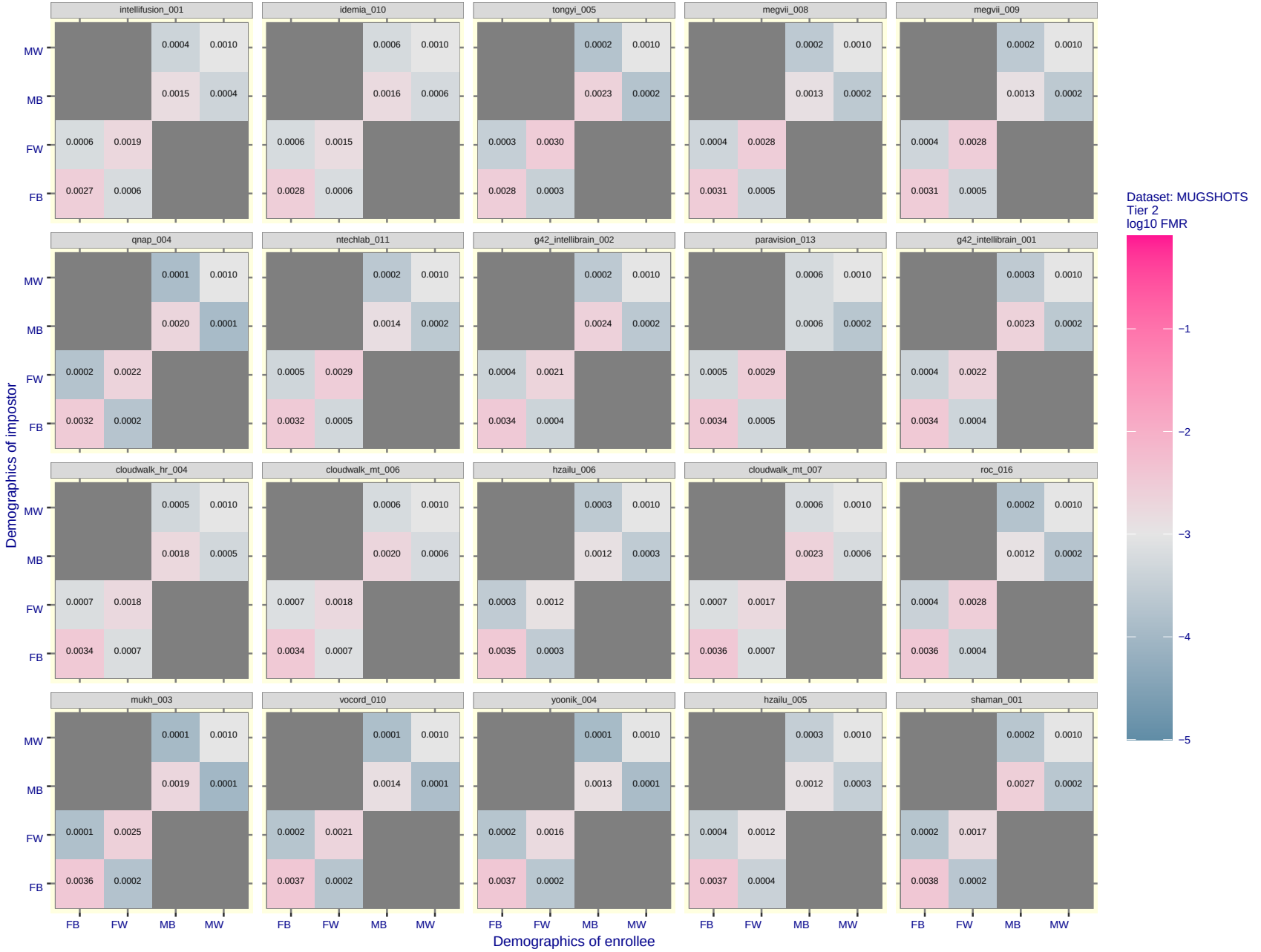

Figure 154: For the mugshot images, FMR *for same-sex impostor pairs of images annotated with codes for black female, black male, white female, white male. The threshold is set for each algorithm to give* FMR *= 0.001 for white males which is the demographic that usually gives the lowest* FMR*. This means the top right box is the same color in all panels. The panels are sorted over multiple pages in order of* FMR *on black females, which is the demographc that usually gives the highest* FMR*.*

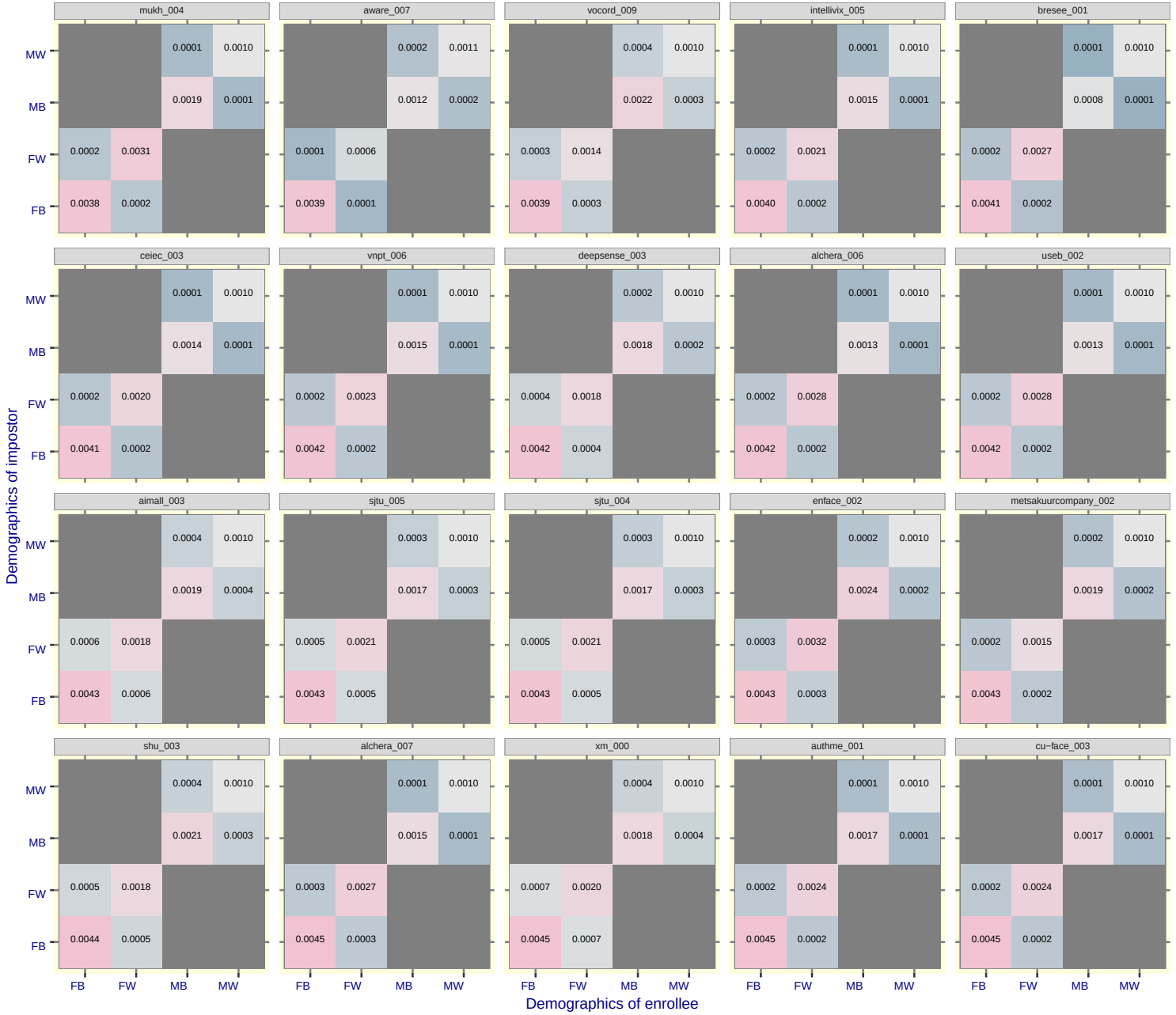

Figure 155: For the mugshot images, FMR *for same-sex impostor pairs of images annotated with codes for black female, black male, white female, white male. The threshold is set for each algorithm to give* FMR *= 0.001 for white males which is the demographic that usually gives the lowest* FMR*. This means the top right box is the same color in all panels. The panels are sorted over multiple pages in order of* FMR *on black females, which is the demographc that usually gives the highest* FMR*.*

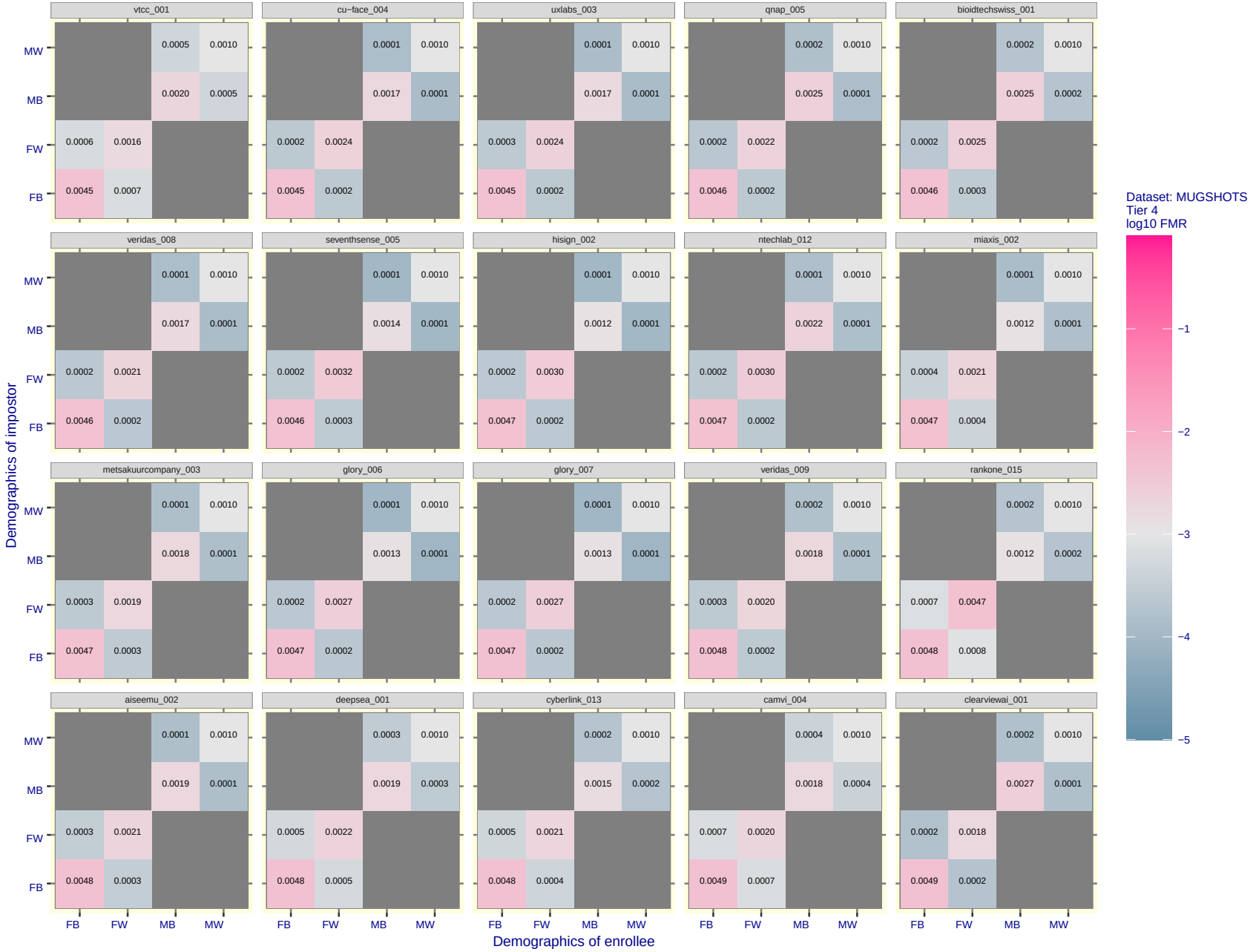

Figure 156: For the mugshot images, FMR *for same-sex impostor pairs of images annotated with codes for black female, black male, white female, white male. The threshold is set for each algorithm to give* FMR *= 0.001 for white males which is the demographic that usually gives the lowest* FMR*. This means the top right box is the same color in all panels. The panels are sorted over multiple pages in order of* FMR *on black females, which is the demographc that usually gives the highest* FMR*.*

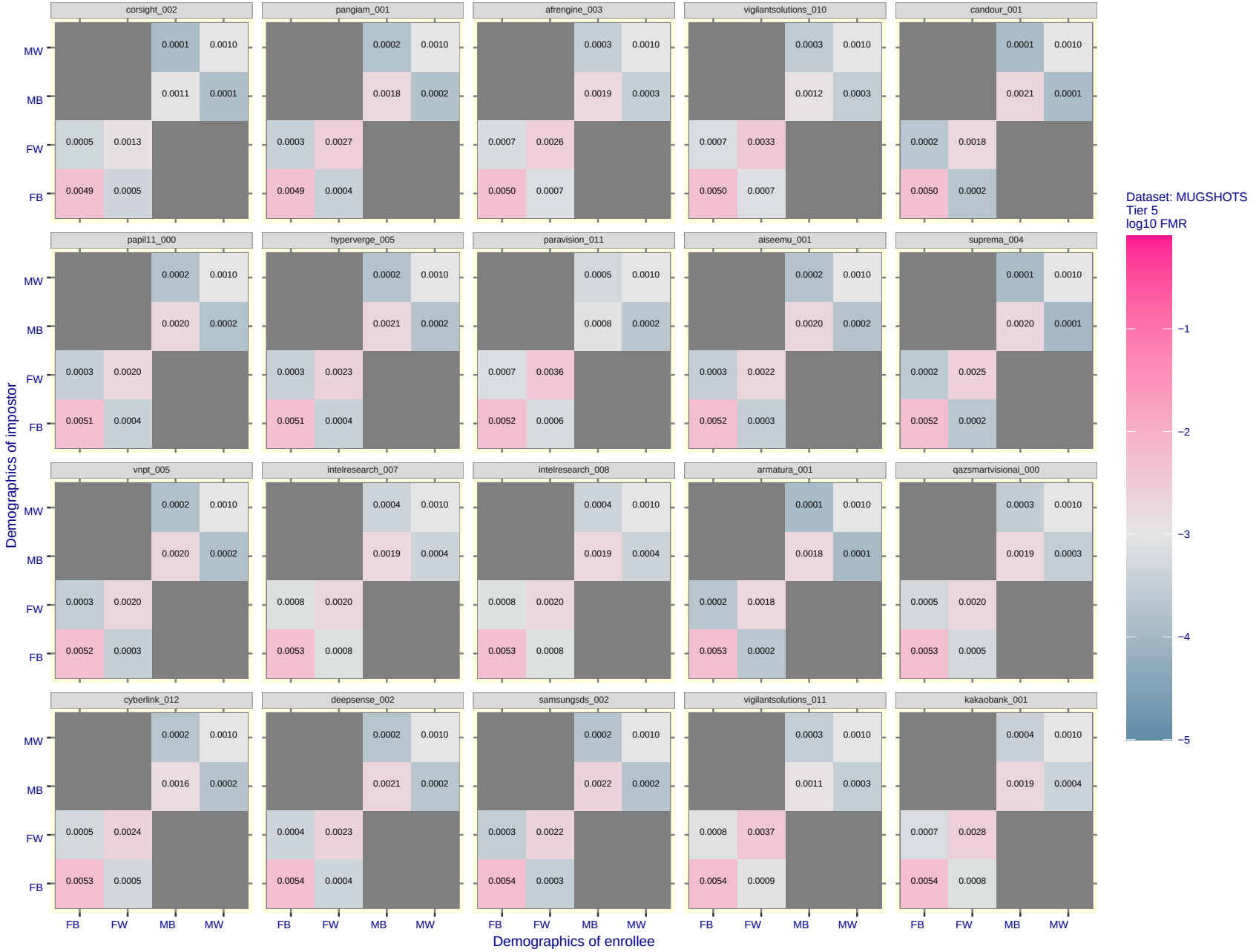

Figure 157: For the mugshot images, FMR *for same-sex impostor pairs of images annotated with codes for black female, black male, white female, white male. The threshold is set for each algorithm to give* FMR *= 0.001 for white males which is the demographic that usually gives the lowest* FMR*. This means the top right box is the same color in all panels. The panels are sorted over multiple pages in order of* FMR *on black females, which is the demographc that usually gives the highest* FMR*.*

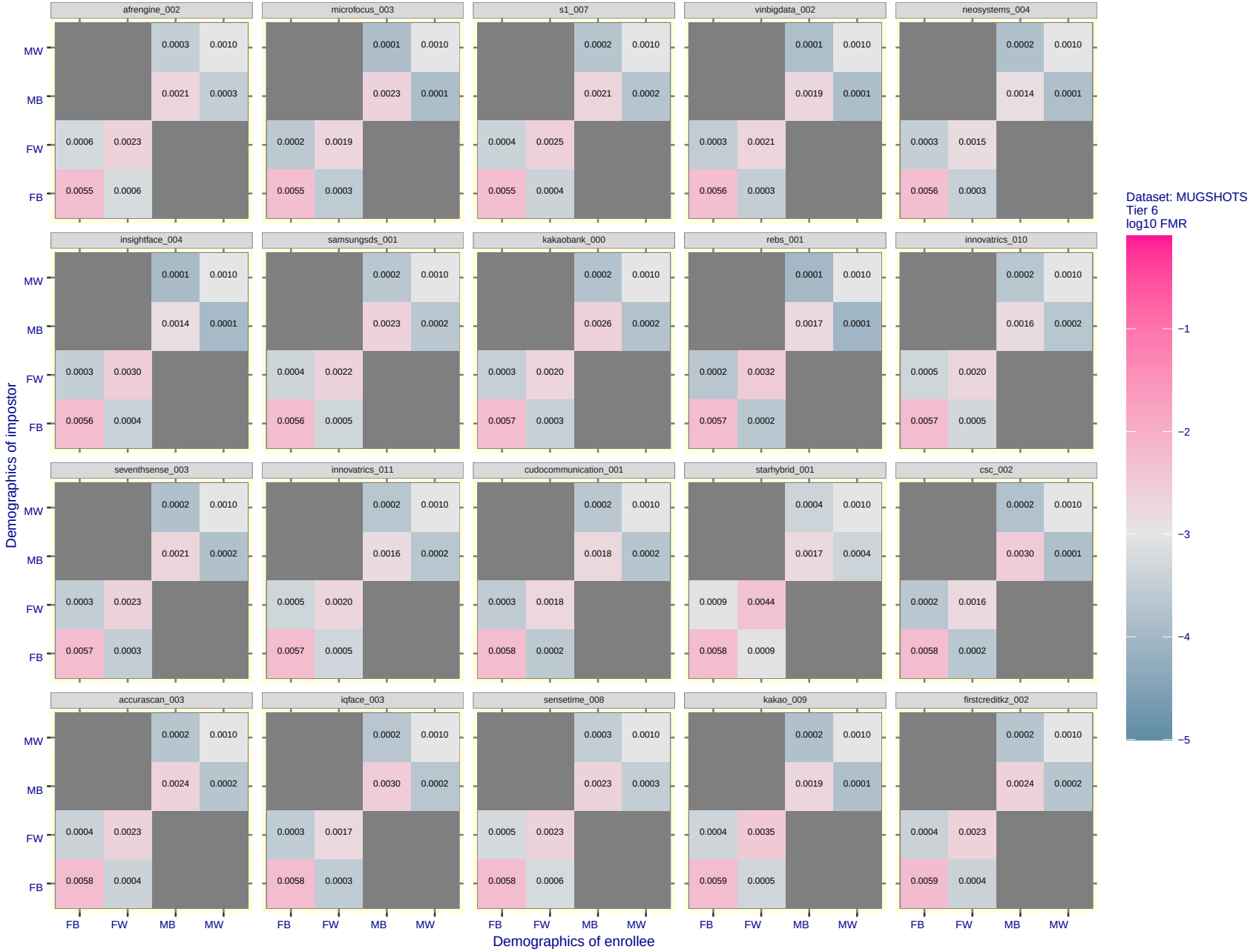

Figure 158: For the mugshot images, FMR *for same-sex impostor pairs of images annotated with codes for black female, black male, white female, white male. The threshold is set for each algorithm to give* FMR *= 0.001 for white males which is the demographic that usually gives the lowest* FMR*. This means the top right box is the same color in all panels. The panels are sorted over multiple pages in order of* FMR *on black females, which is the demographc that usually gives the highest* FMR*.*

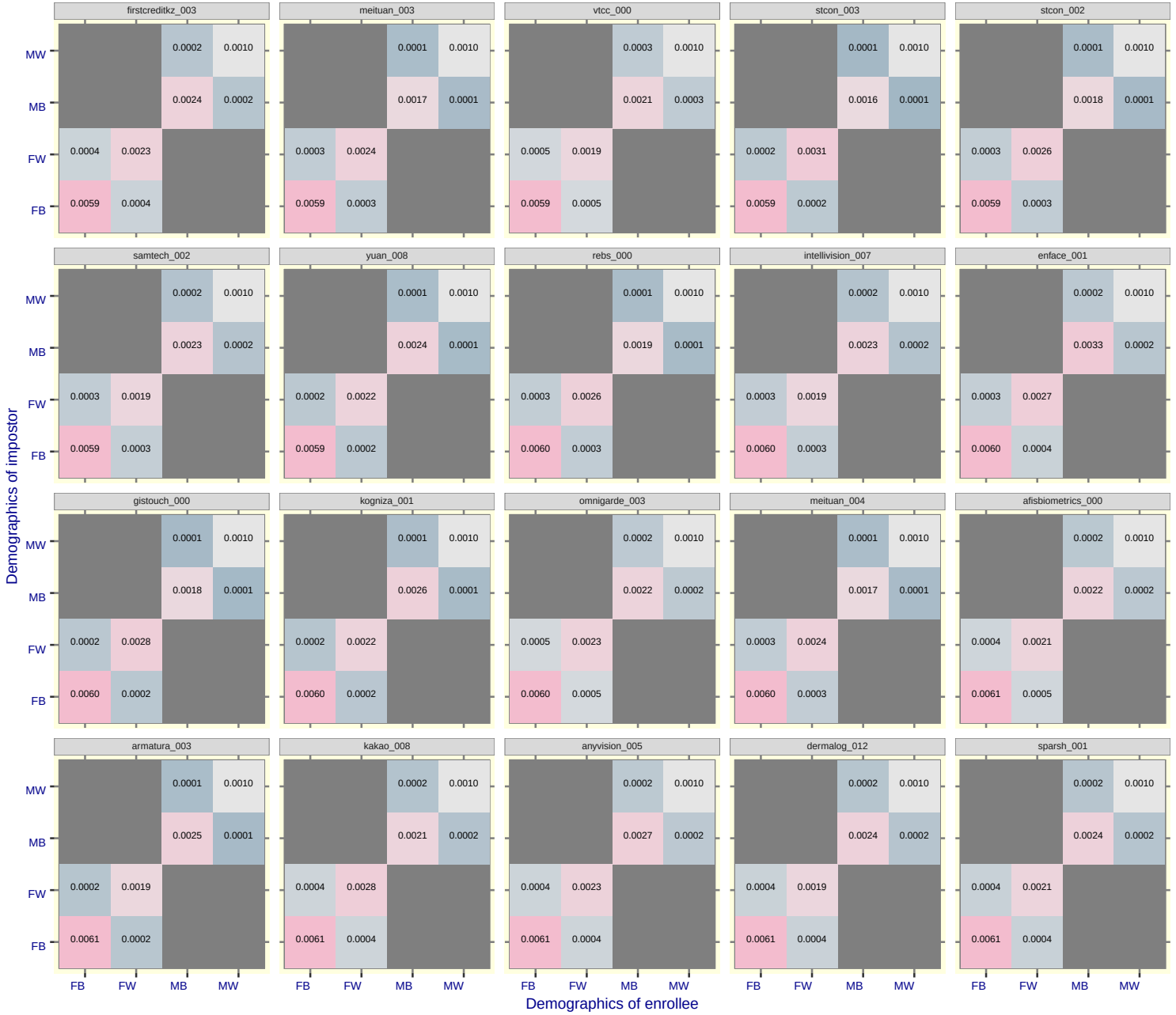

Figure 159: For the mugshot images, FMR *for same-sex impostor pairs of images annotated with codes for black female, black male, white female, white male. The threshold is set for each algorithm to give* FMR *= 0.001 for white males which is the demographic that usually gives the lowest* FMR*. This means the top right box is the same color in all panels. The panels are sorted over multiple pages in order of* FMR *on black females, which is the demographc that usually gives the highest* FMR*.*

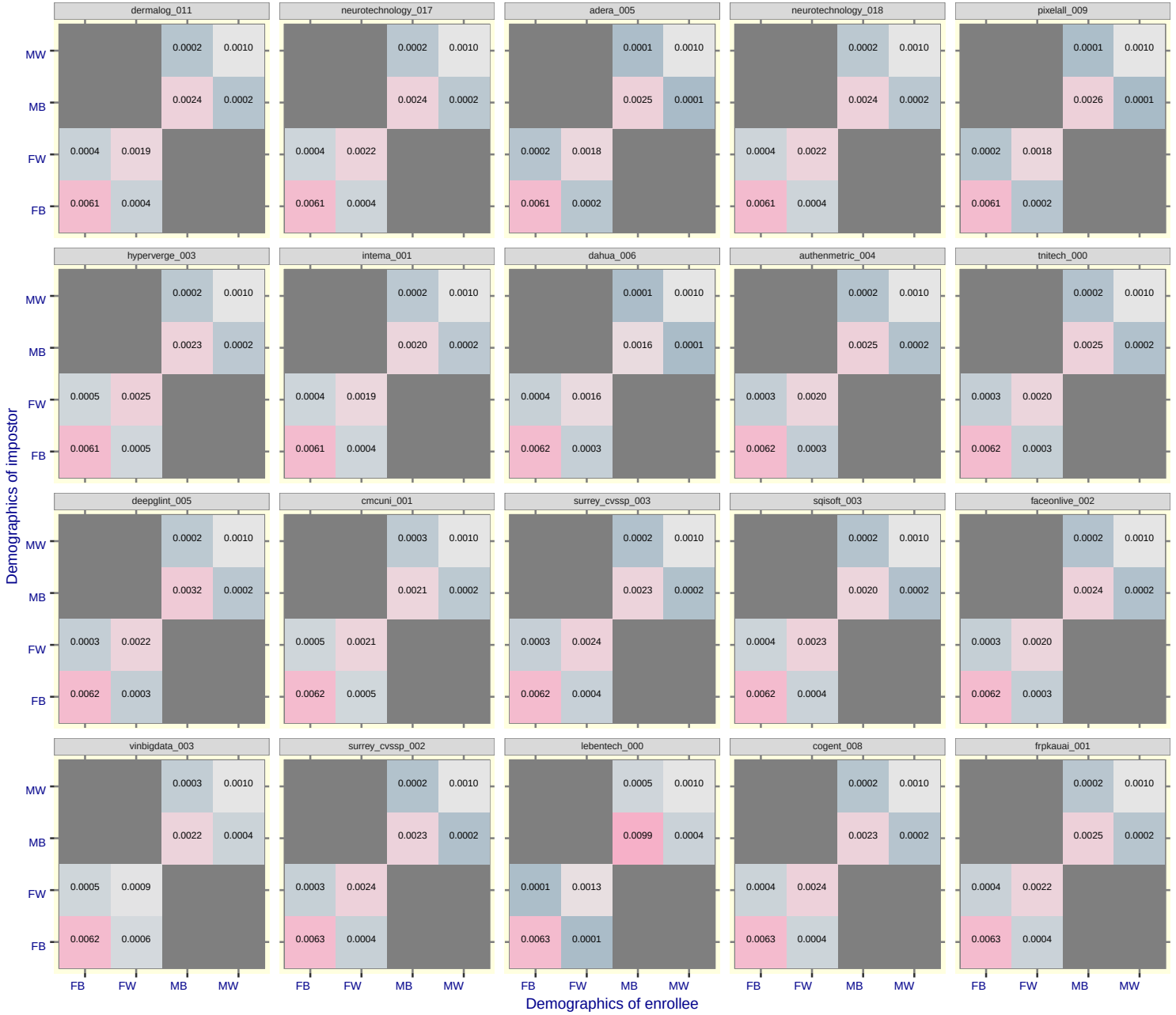

Figure 160: For the mugshot images, FMR *for same-sex impostor pairs of images annotated with codes for black female, black male, white female, white male. The threshold is set for each algorithm to give* FMR *= 0.001 for white males which is the demographic that usually gives the lowest* FMR*. This means the top right box is the same color in all panels. The panels are sorted over multiple pages in order of* FMR *on black females, which is the demographc that usually gives the highest* FMR*.*

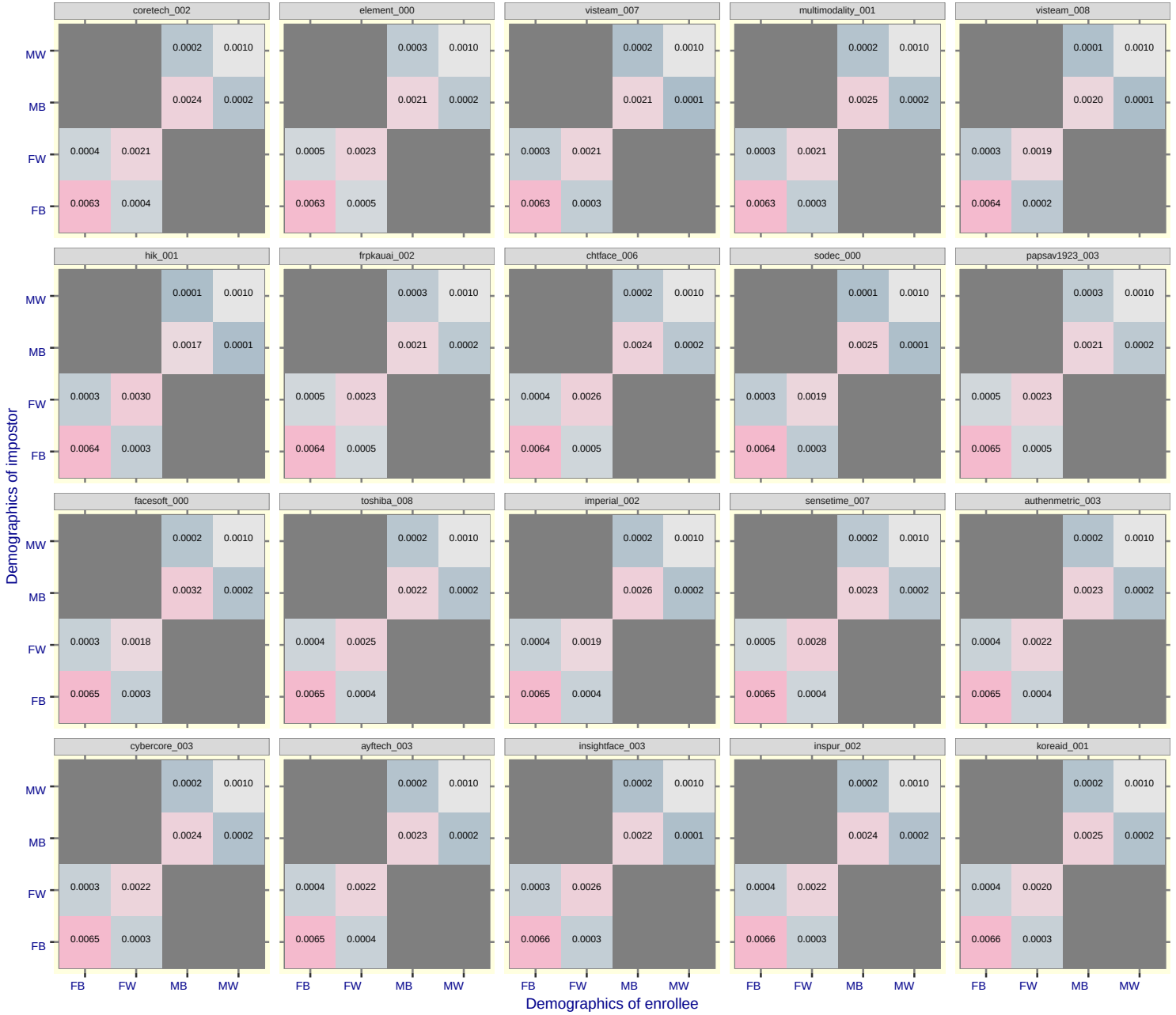

Figure 161: For the mugshot images, FMR *for same-sex impostor pairs of images annotated with codes for black female, black male, white female, white male. The threshold is set for each algorithm to give* FMR *= 0.001 for white males which is the demographic that usually gives the lowest* FMR*. This means the top right box is the same color in all panels. The panels are sorted over multiple pages in order of* FMR *on black females, which is the demographc that usually gives the highest* FMR*.*

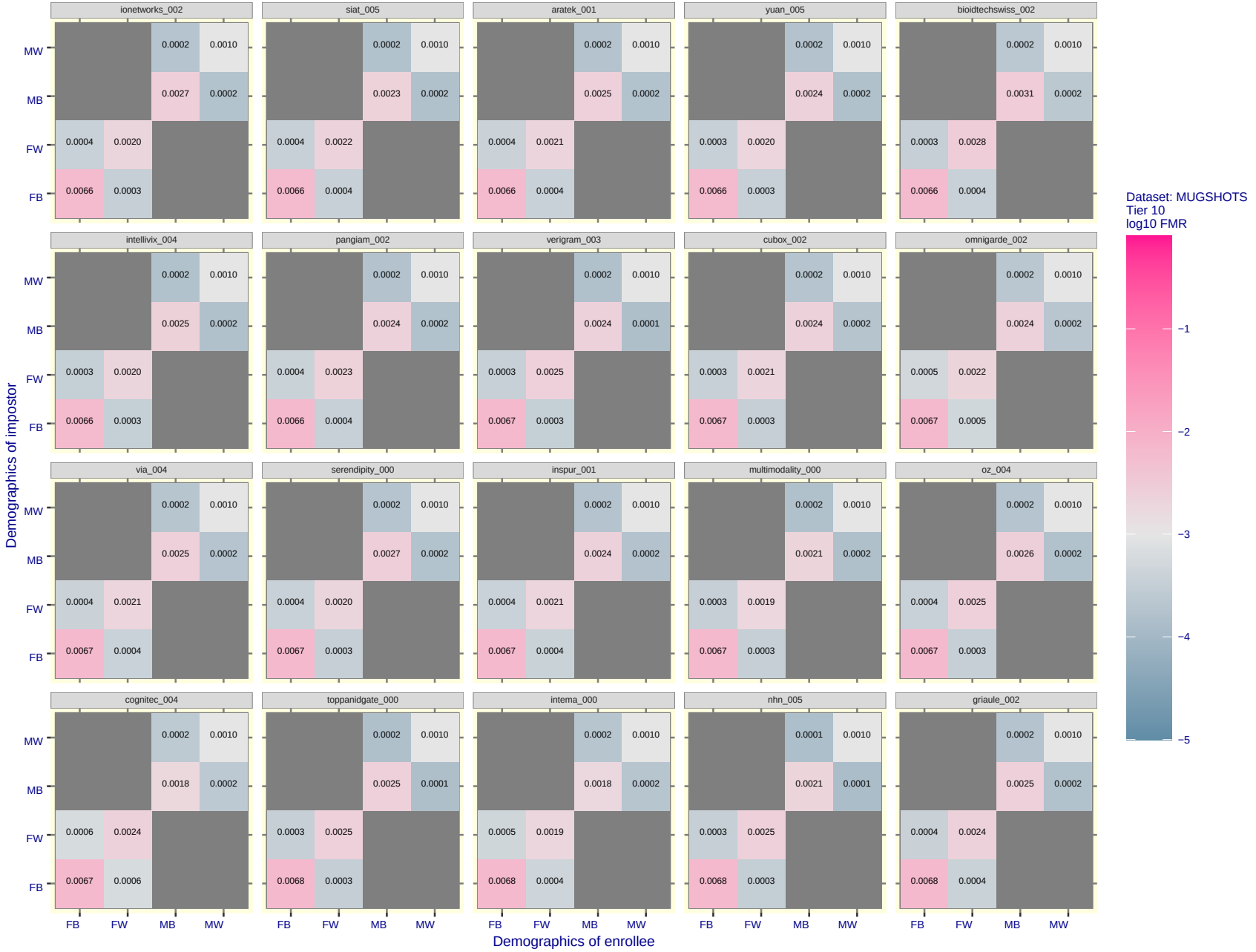

Figure 162: For the mugshot images, FMR *for same-sex impostor pairs of images annotated with codes for black female, black male, white female, white male. The threshold is set for each algorithm to give* FMR *= 0.001 for white males which is the demographic that usually gives the lowest* FMR*. This means the top right box is the same color in all panels. The panels are sorted over multiple pages in order of* FMR *on black females, which is the demographc that usually gives the highest* FMR*.*

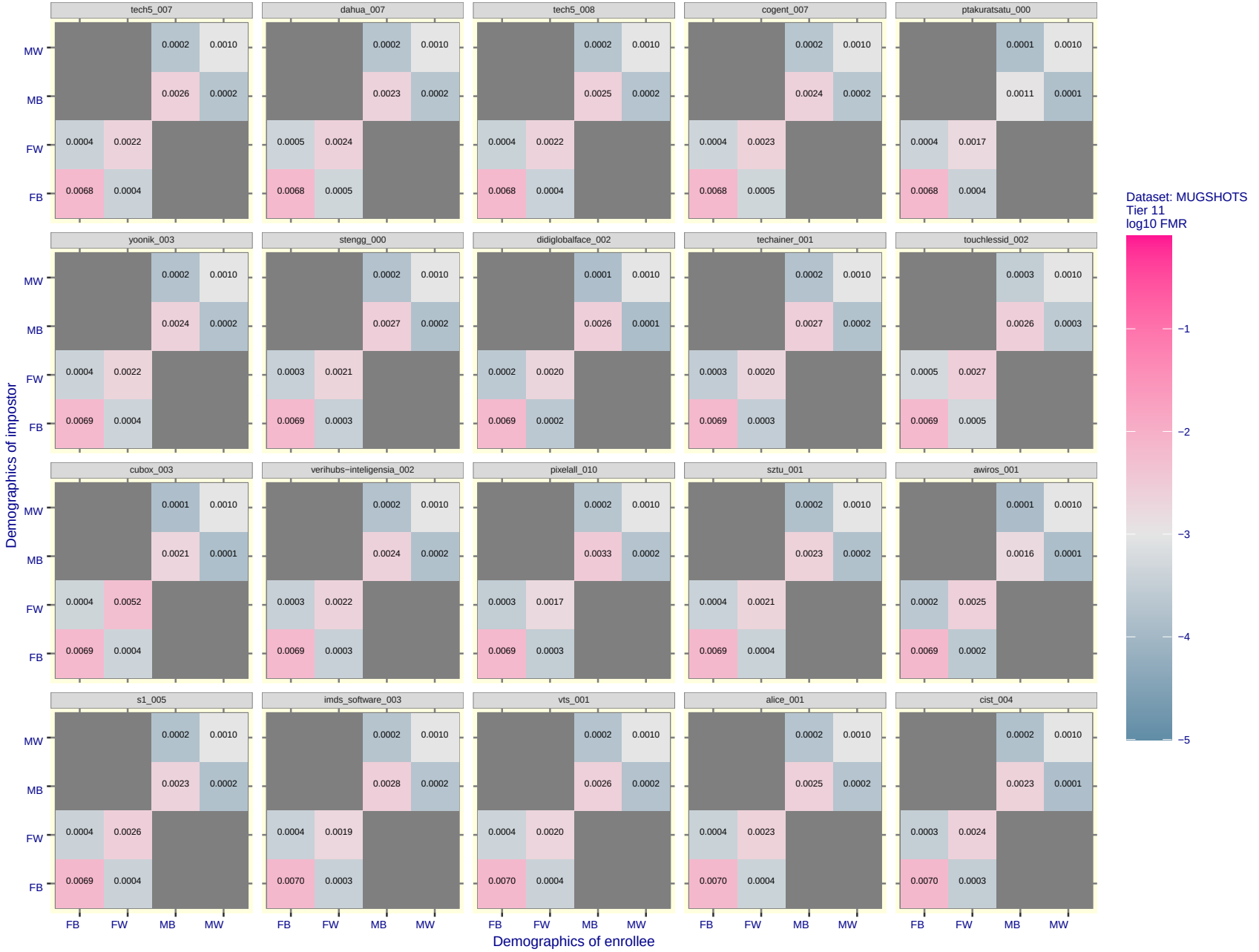

Figure 163: For the mugshot images, FMR *for same-sex impostor pairs of images annotated with codes for black female, black male, white female, white male. The threshold is set for each algorithm to give* FMR *= 0.001 for white males which is the demographic that usually gives the lowest* FMR*. This means the top right box is the same color in all panels. The panels are sorted over multiple pages in order of* FMR *on black females, which is the demographc that usually gives the highest* FMR*.*

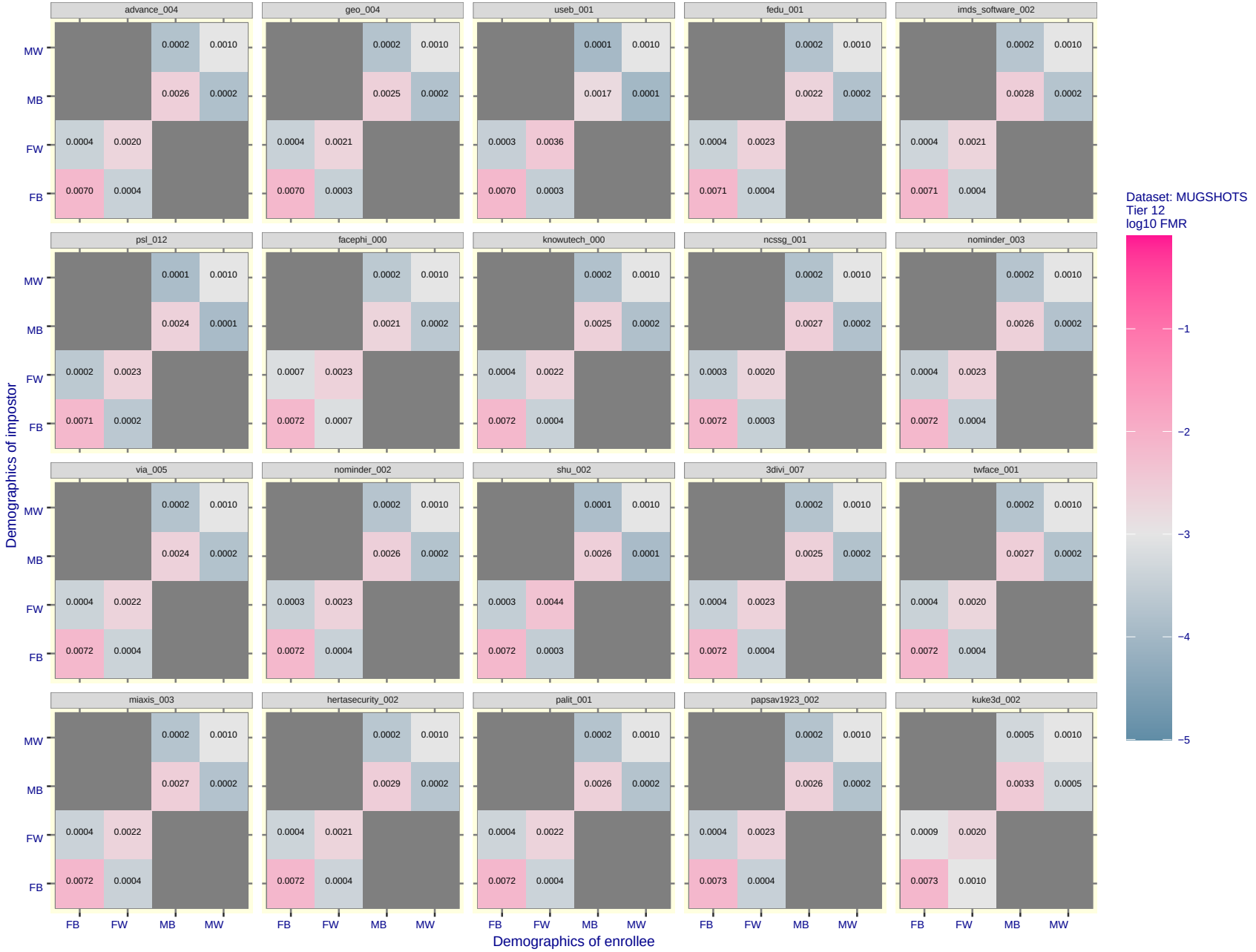

Figure 164: For the mugshot images, FMR *for same-sex impostor pairs of images annotated with codes for black female, black male, white female, white male. The threshold is set for each algorithm to give* FMR *= 0.001 for white males which is the demographic that usually gives the lowest* FMR*. This means the top right box is the same color in all panels. The panels are sorted over multiple pages in order of* FMR *on black females, which is the demographc that usually gives the highest* FMR*.*

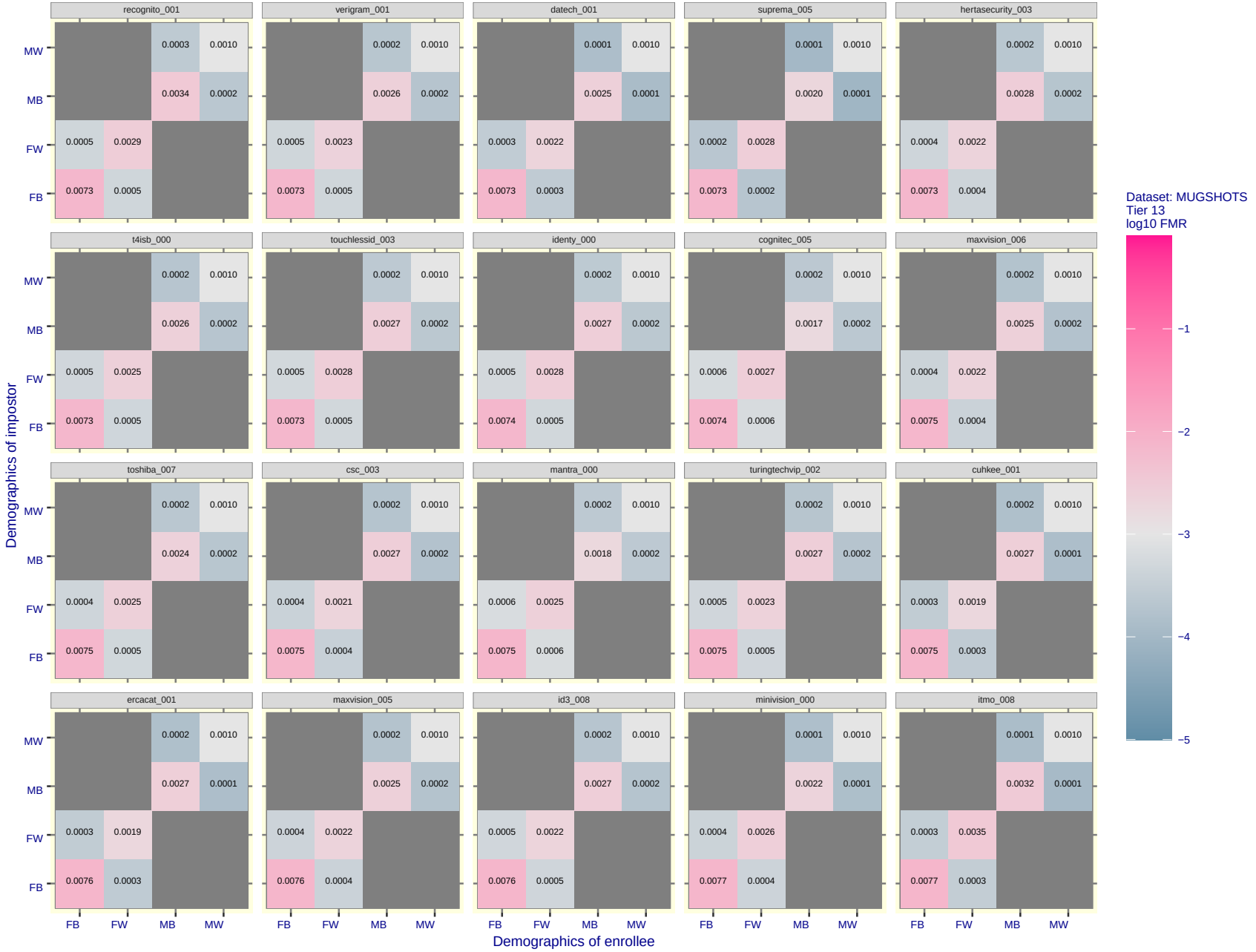

Figure 165: For the mugshot images, FMR *for same-sex impostor pairs of images annotated with codes for black female, black male, white female, white male. The threshold is set for each algorithm to give* FMR *= 0.001 for white males which is the demographic that usually gives the lowest* FMR*. This means the top right box is the same color in all panels. The panels are sorted over multiple pages in order of* FMR *on black females, which is the demographc that usually gives the highest* FMR*.*

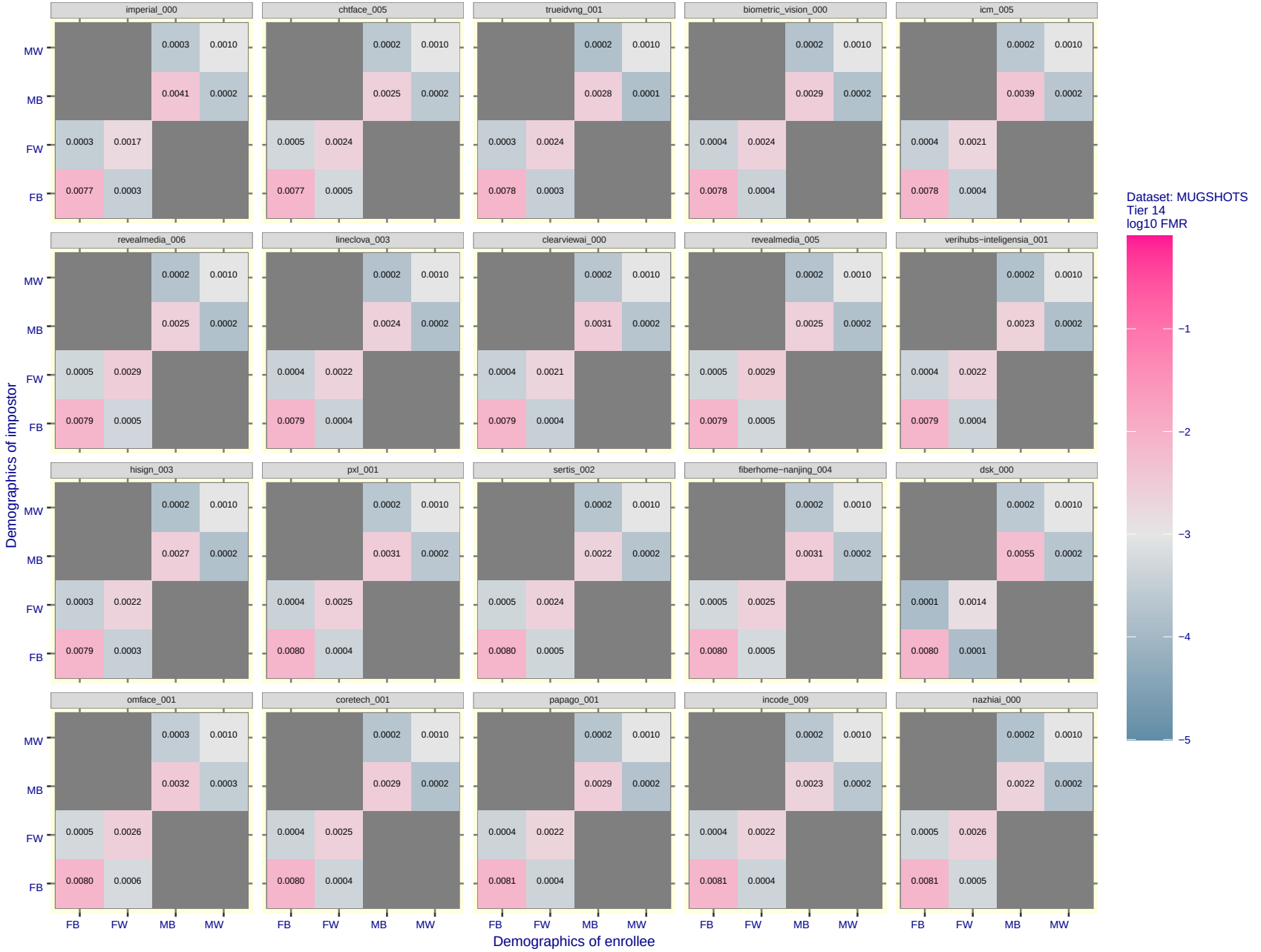

Figure 166: For the mugshot images, FMR *for same-sex impostor pairs of images annotated with codes for black female, black male, white female, white male. The threshold is set for each algorithm to give* FMR *= 0.001 for white males which is the demographic that usually gives the lowest* FMR*. This means the top right box is the same color in all panels. The panels are sorted over multiple pages in order of* FMR *on black females, which is the demographc that usually gives the highest* FMR*.*

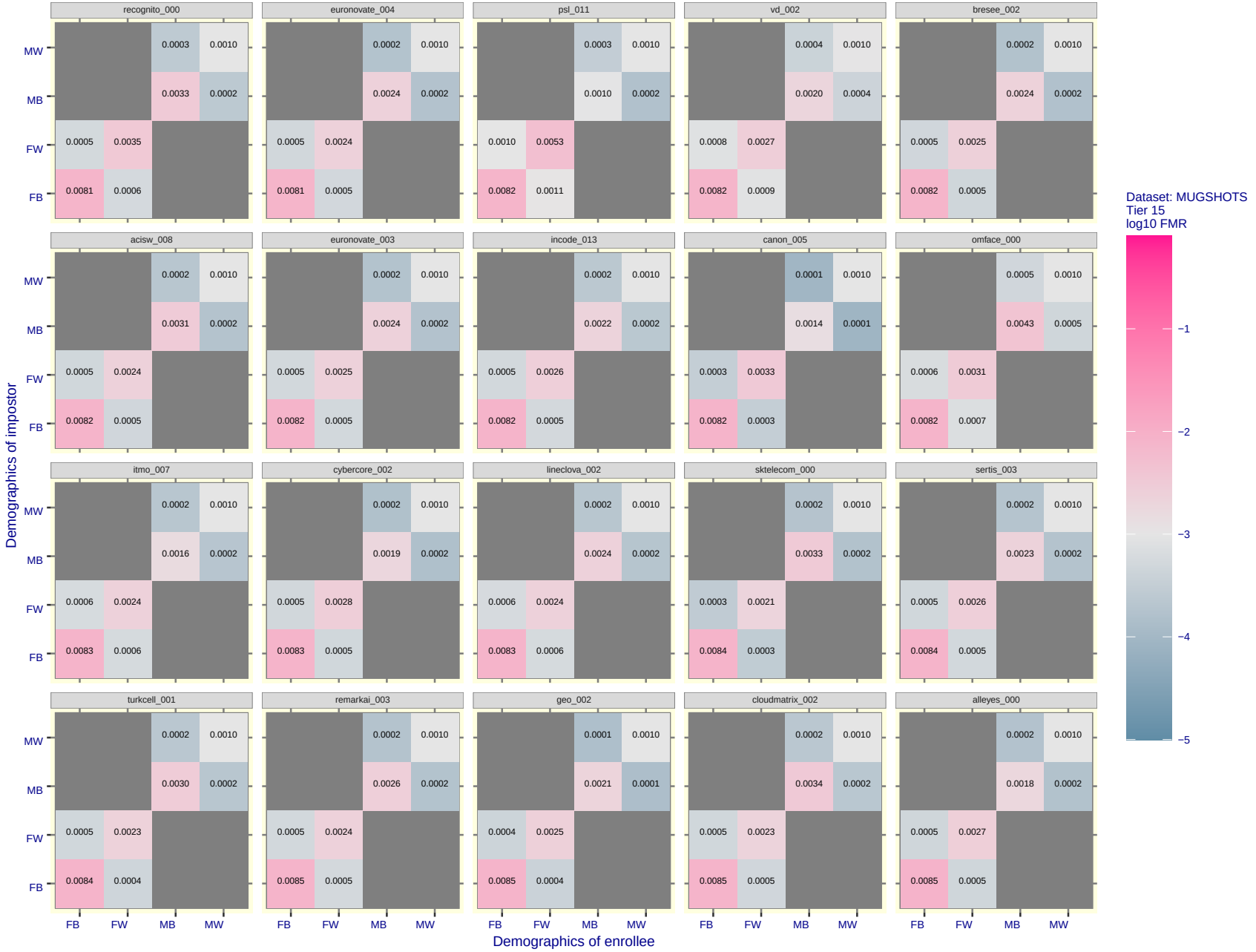

Figure 167: For the mugshot images, FMR *for same-sex impostor pairs of images annotated with codes for black female, black male, white female, white male. The threshold is set for each algorithm to give* FMR *= 0.001 for white males which is the demographic that usually gives the lowest* FMR*. This means the top right box is the same color in all panels. The panels are sorted over multiple pages in order of* FMR *on black females, which is the demographc that usually gives the highest* FMR*.*

2024/03/27 10:44:08
FNMR(T) "False non-match rate"
FMR(T) "False match rate"

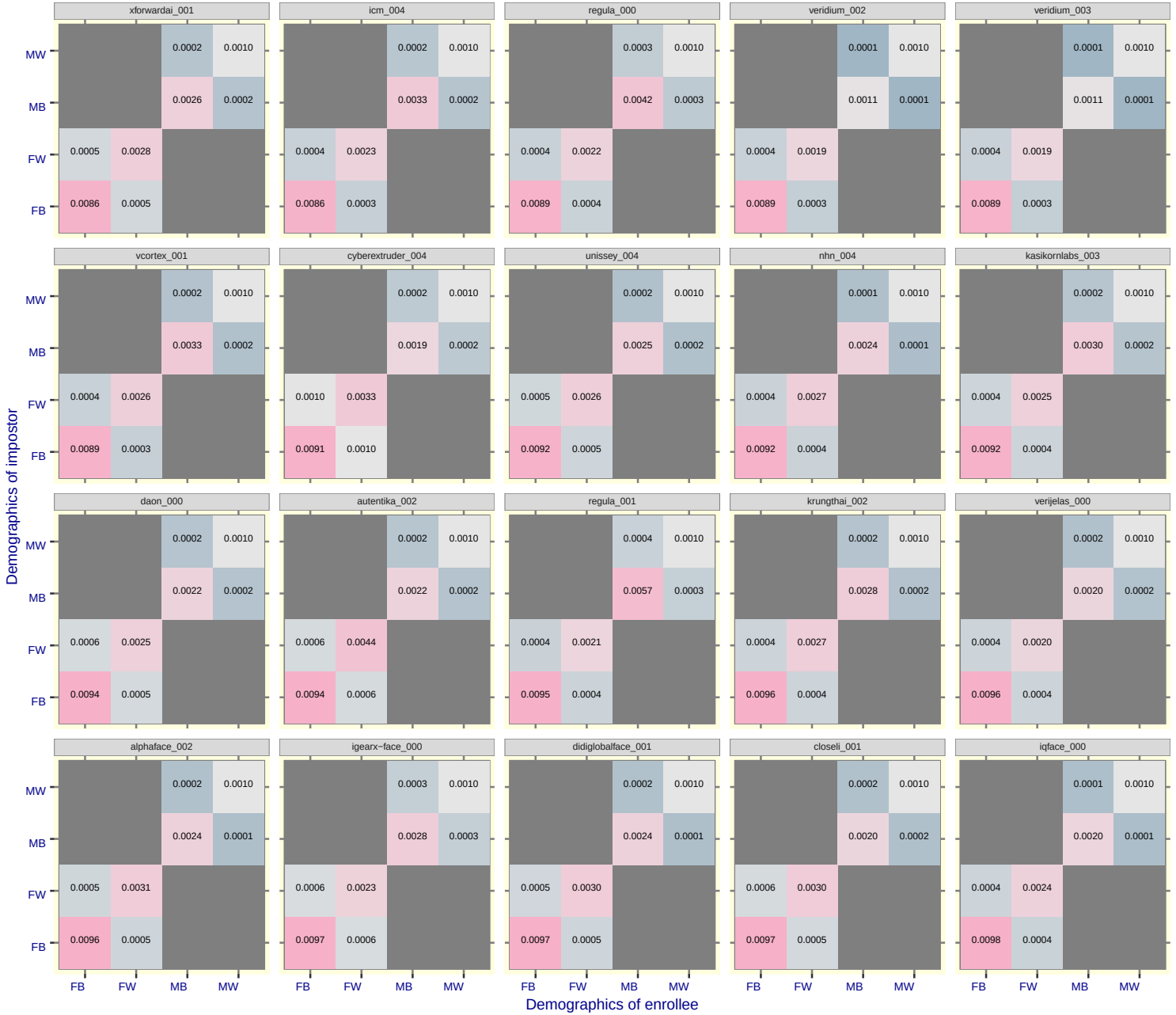

Figure 168: For the mugshot images, FMR *for same-sex impostor pairs of images annotated with codes for black female, black male, white female, white male. The threshold is set for each algorithm to give* FMR *= 0.001 for white males which is the demographic that usually gives the lowest* FMR*. This means the top right box is the same color in all panels. The panels are sorted over multiple pages in order of* FMR *on black females, which is the demographc that usually gives the highest* FMR*.*

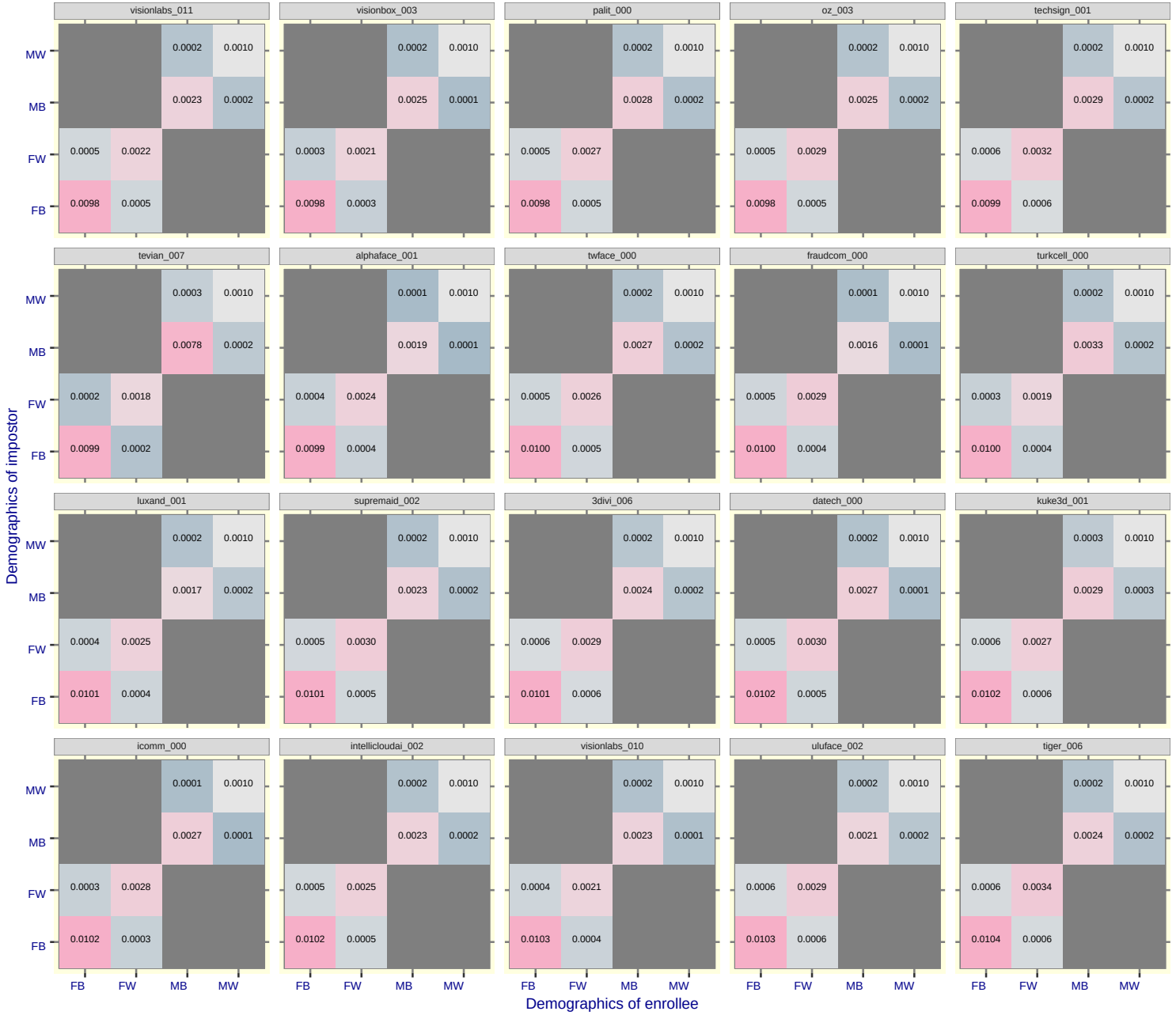

Figure 169: For the mugshot images, FMR *for same-sex impostor pairs of images annotated with codes for black female, black male, white female, white male. The threshold is set for each algorithm to give* FMR *= 0.001 for white males which is the demographic that usually gives the lowest* FMR*. This means the top right box is the same color in all panels. The panels are sorted over multiple pages in order of* FMR *on black females, which is the demographc that usually gives the highest* FMR*.*

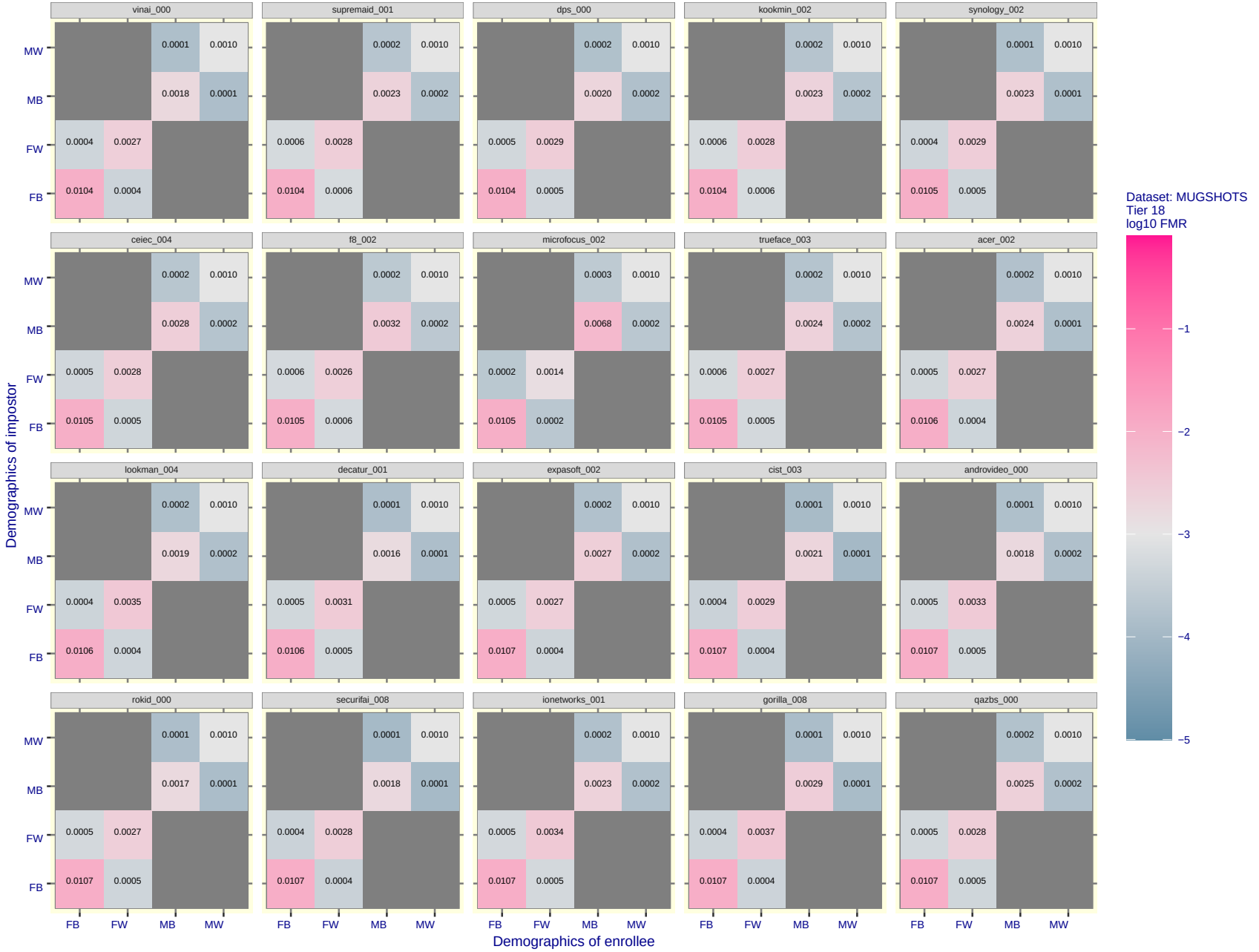

Figure 170: For the mugshot images, FMR *for same-sex impostor pairs of images annotated with codes for black female, black male, white female, white male. The threshold is set for each algorithm to give* FMR *= 0.001 for white males which is the demographic that usually gives the lowest* FMR*. This means the top right box is the same color in all panels. The panels are sorted over multiple pages in order of* FMR *on black females, which is the demographc that usually gives the highest* FMR*.*

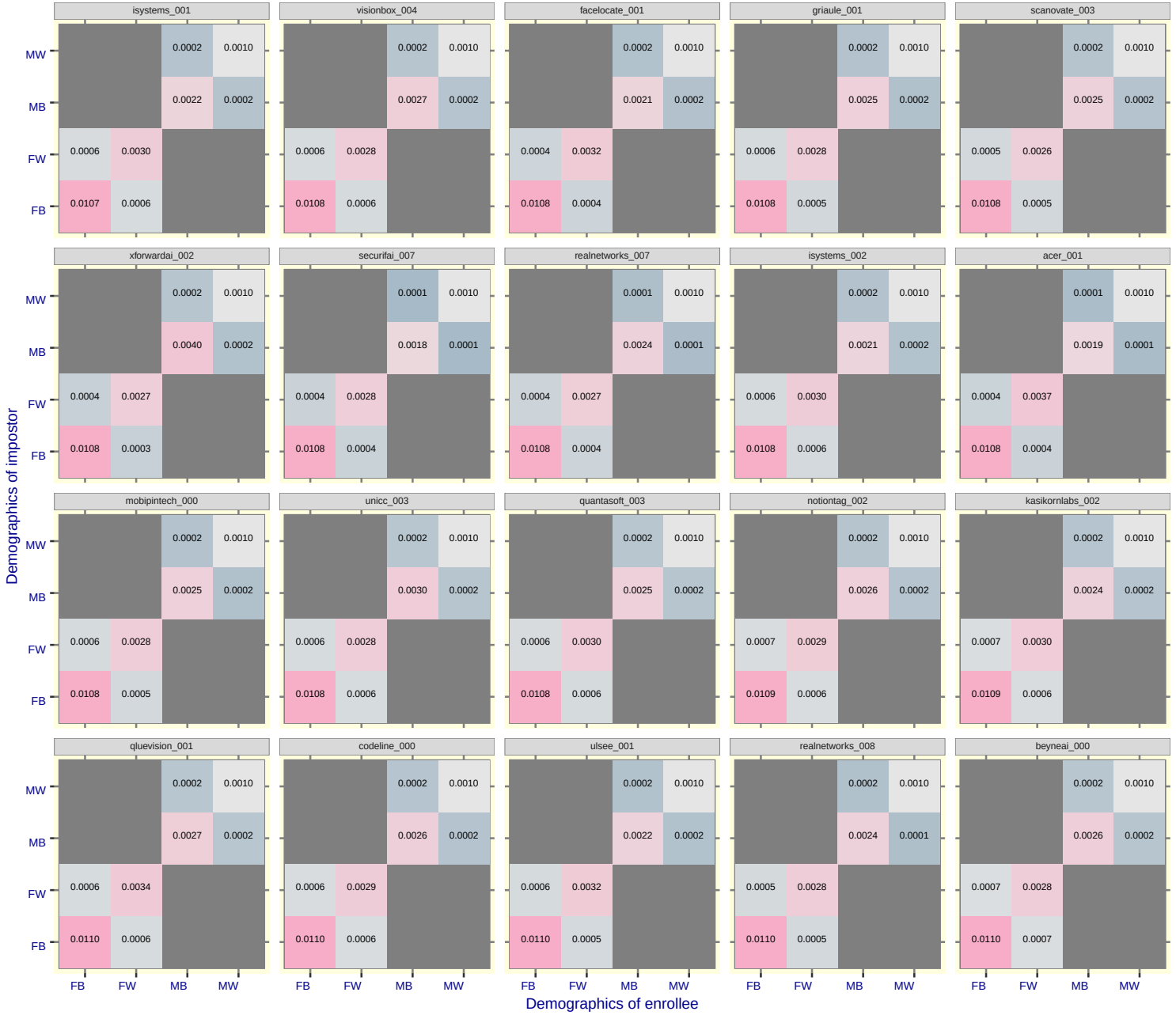

Figure 171: For the mugshot images, FMR *for same-sex impostor pairs of images annotated with codes for black female, black male, white female, white male. The threshold is set for each algorithm to give* FMR *= 0.001 for white males which is the demographic that usually gives the lowest* FMR*. This means the top right box is the same color in all panels. The panels are sorted over multiple pages in order of* FMR *on black females, which is the demographc that usually gives the highest* FMR*.*

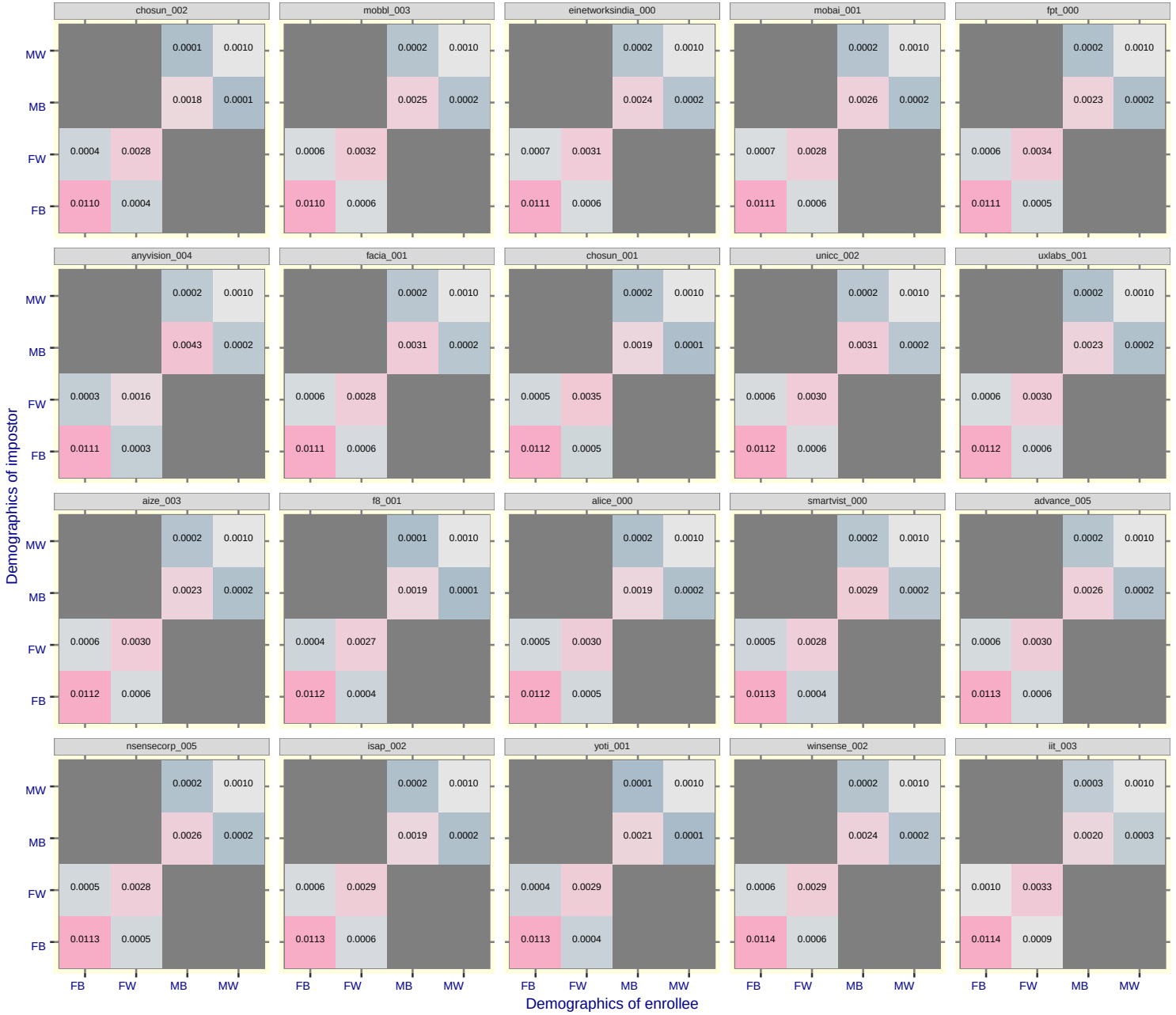

Figure 172: For the mugshot images, FMR *for same-sex impostor pairs of images annotated with codes for black female, black male, white female, white male. The threshold is set for each algorithm to give* FMR *= 0.001 for white males which is the demographic that usually gives the lowest* FMR*. This means the top right box is the same color in all panels. The panels are sorted over multiple pages in order of* FMR *on black females, which is the demographc that usually gives the highest* FMR*.*

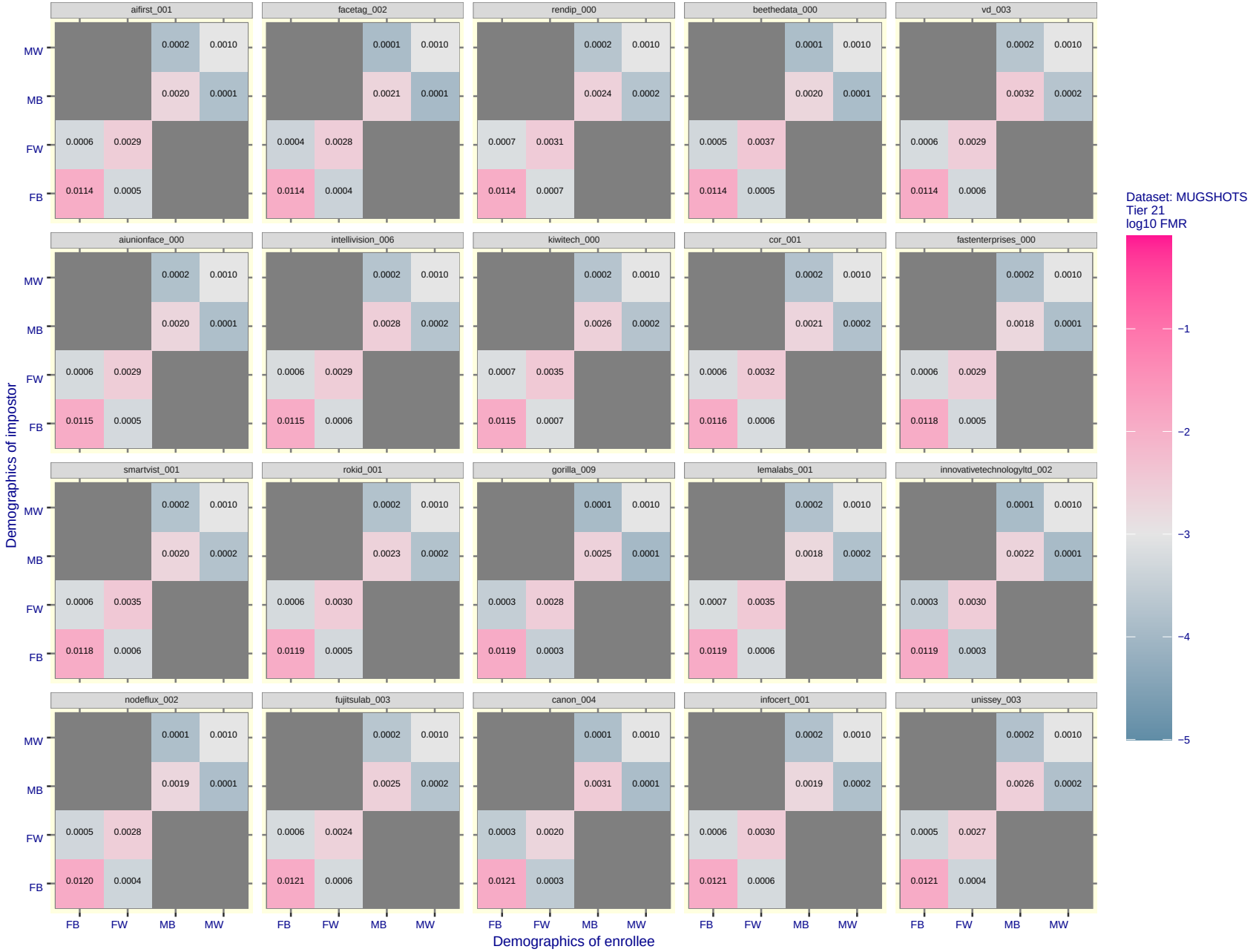

Figure 173: For the mugshot images, FMR *for same-sex impostor pairs of images annotated with codes for black female, black male, white female, white male. The threshold is set for each algorithm to give* FMR *= 0.001 for white males which is the demographic that usually gives the lowest* FMR*. This means the top right box is the same color in all panels. The panels are sorted over multiple pages in order of* FMR *on black females, which is the demographc that usually gives the highest* FMR*.*

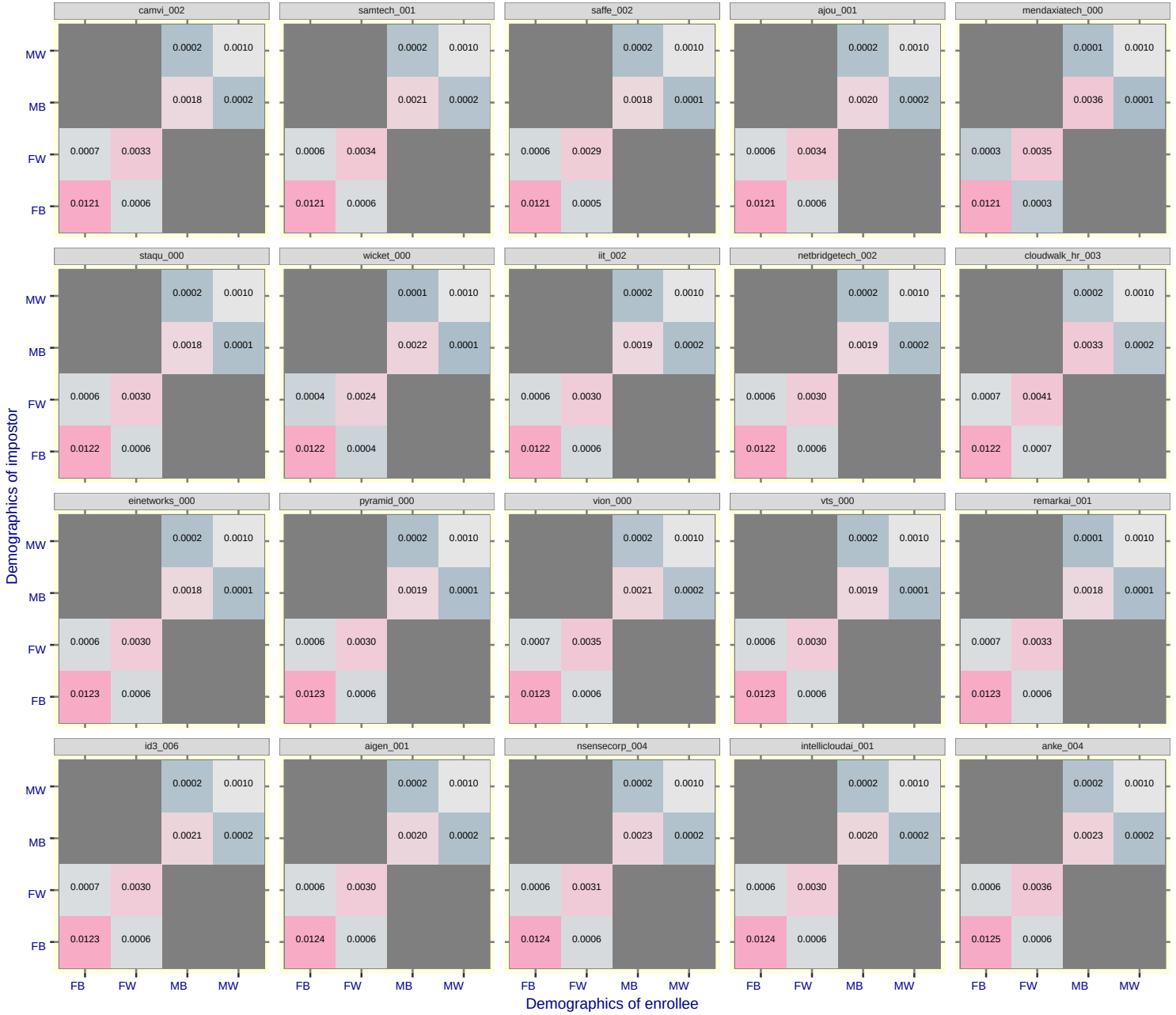

Figure 174: For the mugshot images, FMR *for same-sex impostor pairs of images annotated with codes for black female, black male, white female, white male. The threshold is set for each algorithm to give* FMR *= 0.001 for white males which is the demographic that usually gives the lowest* FMR*. This means the top right box is the same color in all panels. The panels are sorted over multiple pages in order of* FMR *on black females, which is the demographc that usually gives the highest* FMR*.*

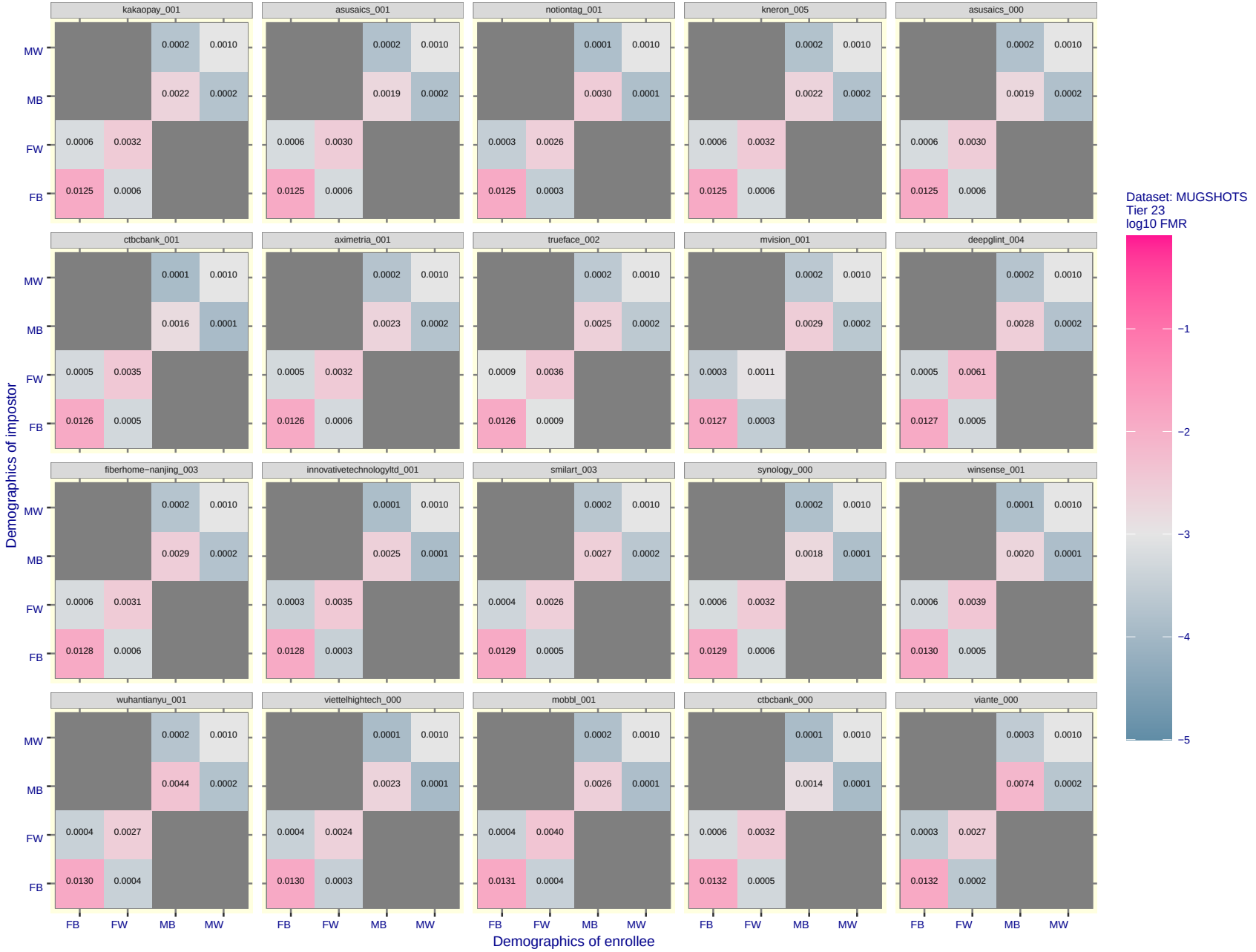

Figure 175: For the mugshot images, FMR *for same-sex impostor pairs of images annotated with codes for black female, black male, white female, white male. The threshold is set for each algorithm to give* FMR *= 0.001 for white males which is the demographic that usually gives the lowest* FMR*. This means the top right box is the same color in all panels. The panels are sorted over multiple pages in order of* FMR *on black females, which is the demographc that usually gives the highest* FMR*.*

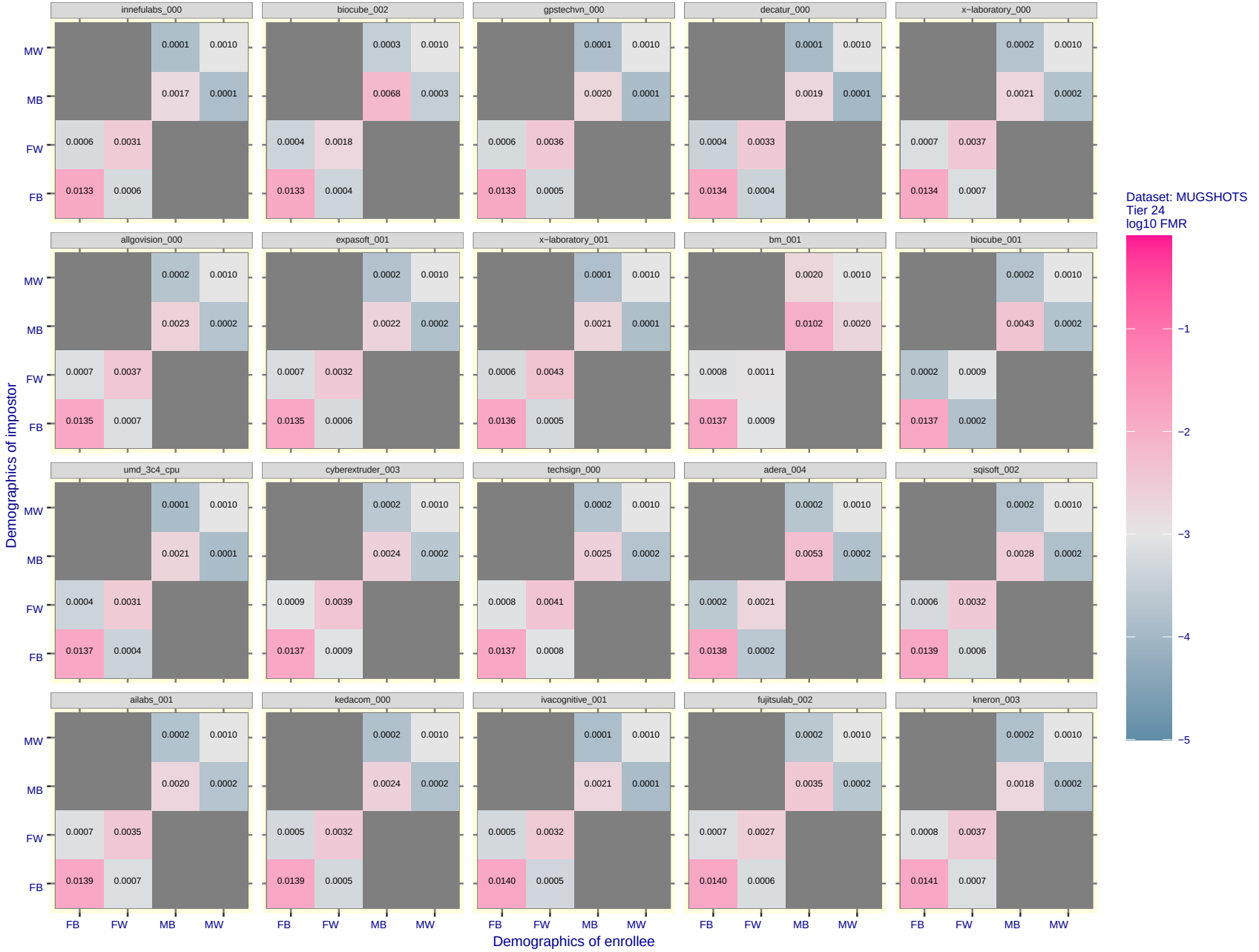

Figure 176: For the mugshot images, FMR *for same-sex impostor pairs of images annotated with codes for black female, black male, white female, white male. The threshold is set for each algorithm to give* FMR *= 0.001 for white males which is the demographic that usually gives the lowest* FMR*. This means the top right box is the same color in all panels. The panels are sorted over multiple pages in order of* FMR *on black females, which is the demographc that usually gives the highest* FMR*.*

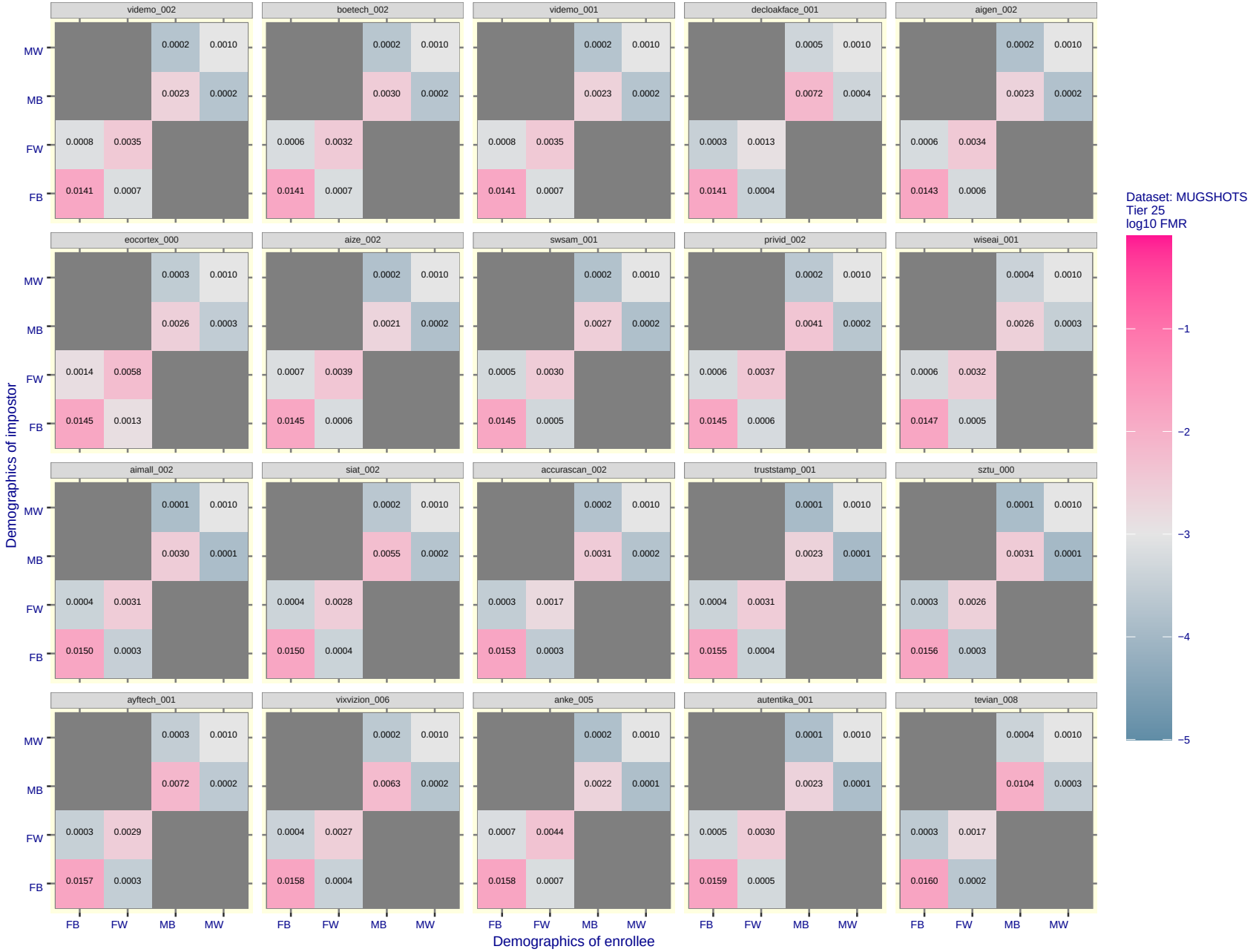

Figure 177: For the mugshot images, FMR *for same-sex impostor pairs of images annotated with codes for black female, black male, white female, white male. The threshold is set for each algorithm to give* FMR *= 0.001 for white males which is the demographic that usually gives the lowest* FMR*. This means the top right box is the same color in all panels. The panels are sorted over multiple pages in order of* FMR *on black females, which is the demographc that usually gives the highest* FMR*.*

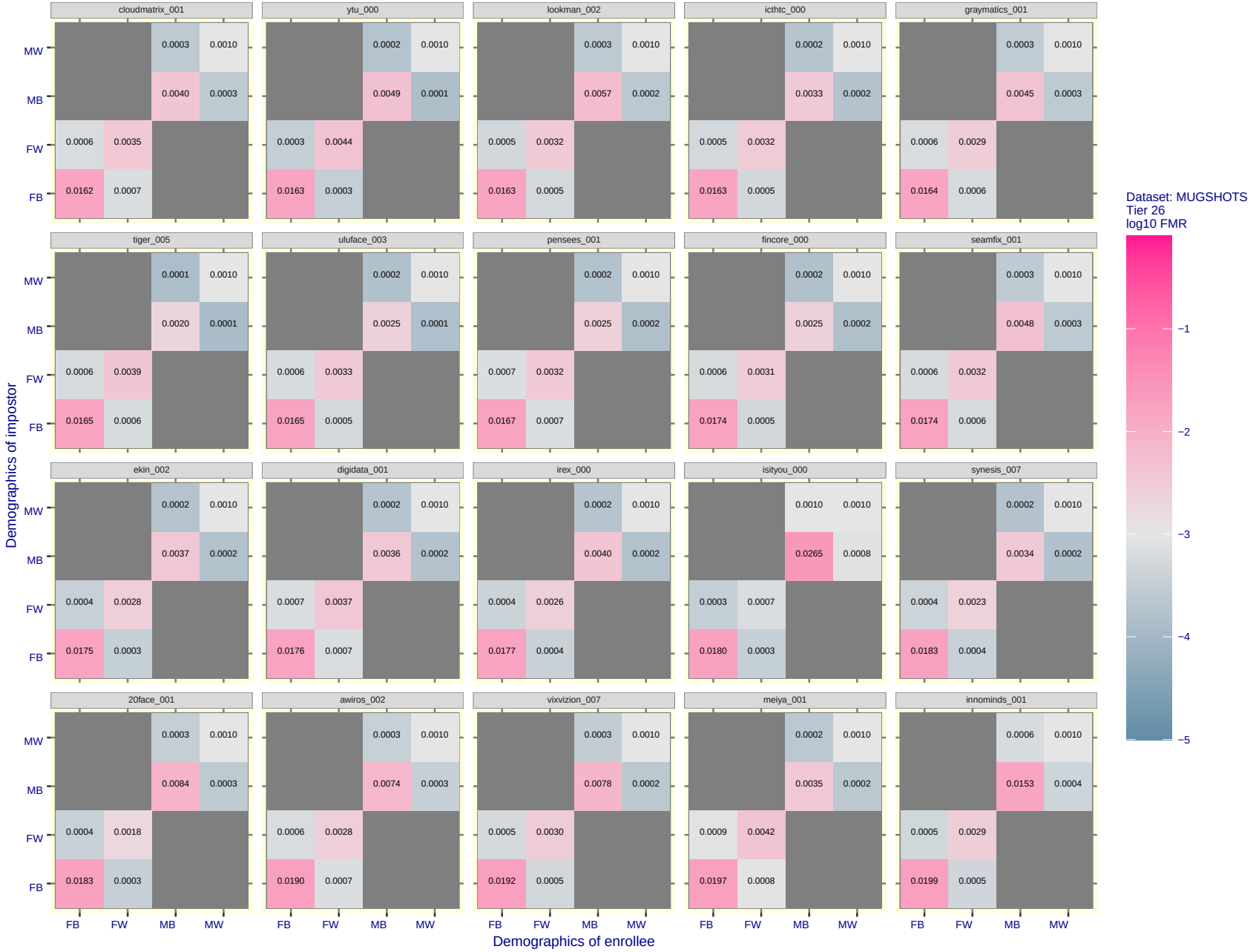

Figure 178: For the mugshot images, FMR *for same-sex impostor pairs of images annotated with codes for black female, black male, white female, white male. The threshold is set for each algorithm to give* FMR *= 0.001 for white males which is the demographic that usually gives the lowest* FMR*. This means the top right box is the same color in all panels. The panels are sorted over multiple pages in order of* FMR *on black females, which is the demographc that usually gives the highest* FMR*.*

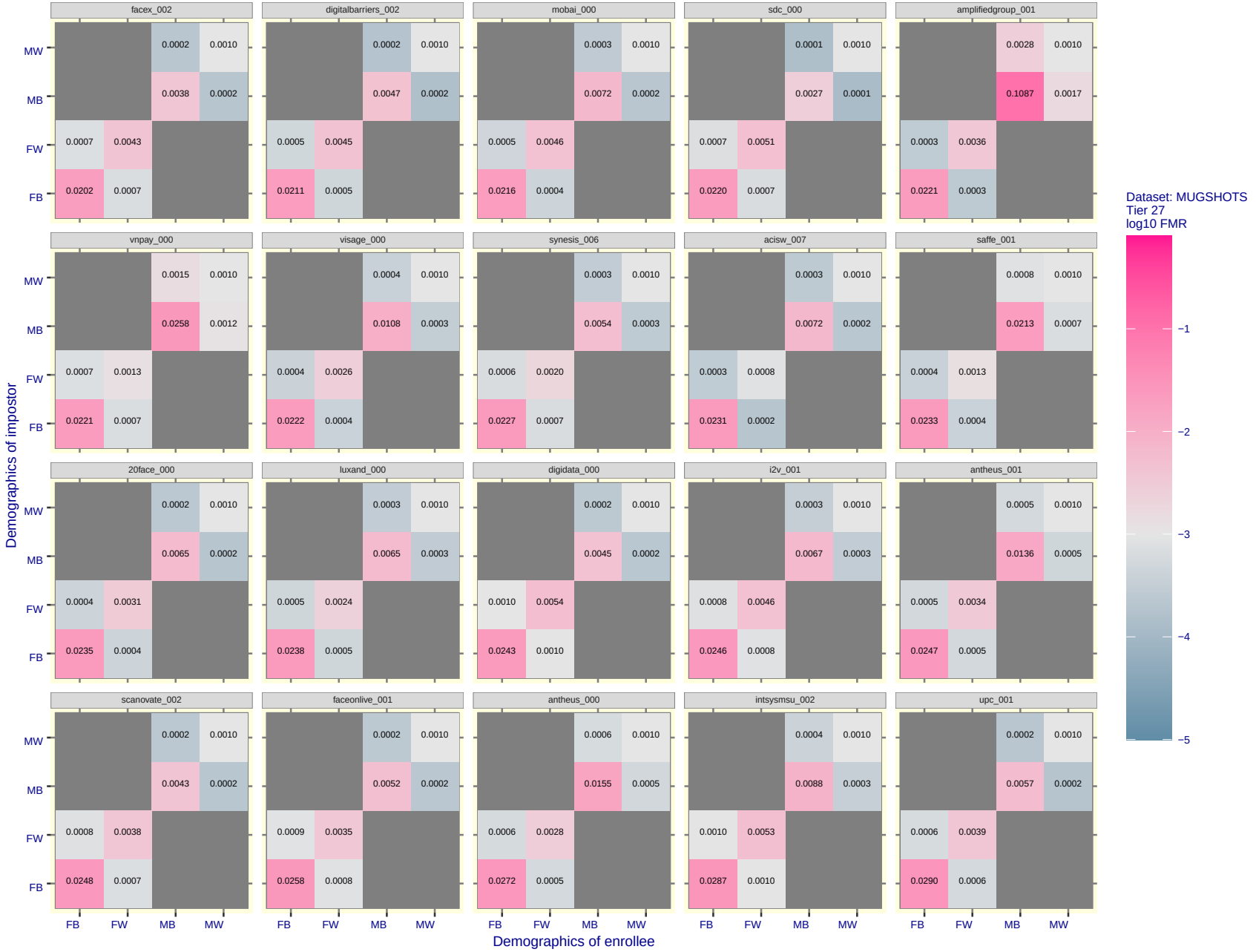

Figure 179: For the mugshot images, FMR *for same-sex impostor pairs of images annotated with codes for black female, black male, white female, white male. The threshold is set for each algorithm to give* FMR *= 0.001 for white males which is the demographic that usually gives the lowest* FMR*. This means the top right box is the same color in all panels. The panels are sorted over multiple pages in order of* FMR *on black females, which is the demographc that usually gives the highest* FMR*.*

Figure 180: For the mugshot images, FMR *for same-sex impostor pairs of images annotated with codes for black female, black male, white female, white male. The threshold is set for each algorithm to give* FMR *= 0.001 for white males which is the demographic that usually gives the lowest* FMR*. This means the top right box is the same color in all panels. The panels are sorted over multiple pages in order of* FMR *on black females, which is the demographc that usually gives the highest* FMR*.*

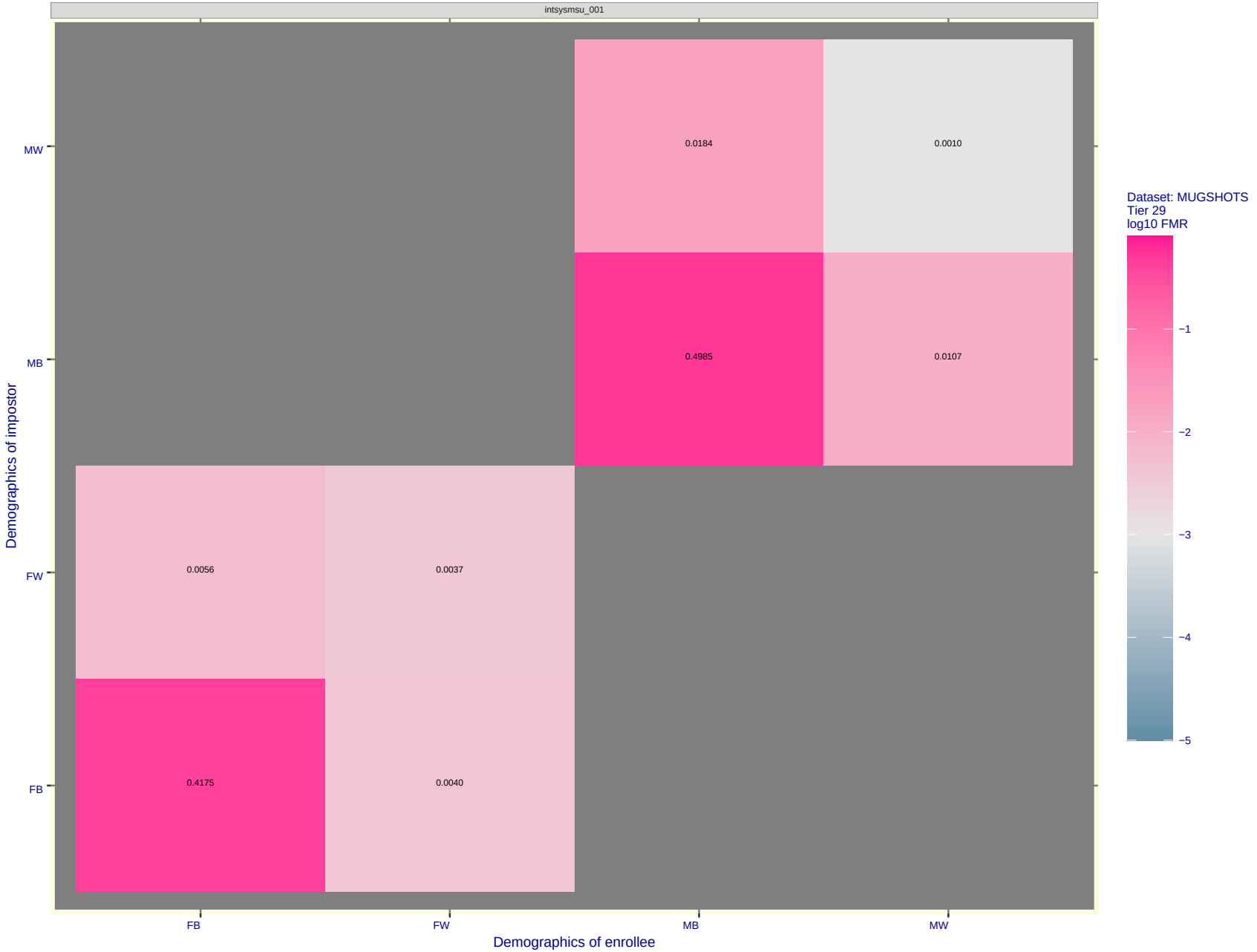

Figure 181: For the mugshot images, FMR *for same-sex impostor pairs of images annotated with codes for black female, black male, white female, white male. The threshold is set for each algorithm to give* FMR *= 0.001 for white males which is the demographic that usually gives the lowest* FMR*. This means the top right box is the same color in all panels. The panels are sorted over multiple pages in order of* FMR *on black females, which is the demographc that usually gives the highest* FMR*.*

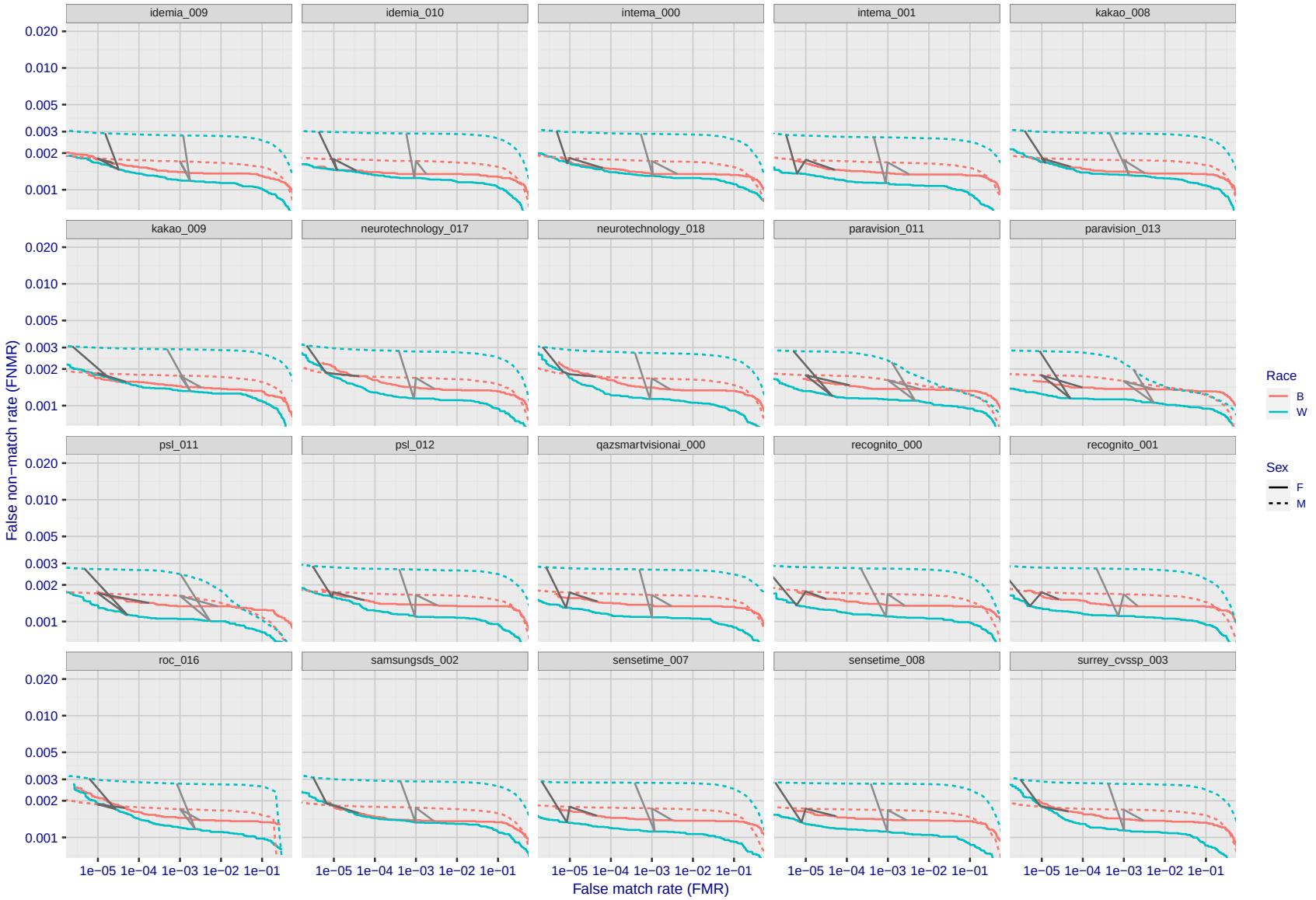

Figure 182: For the mugshot images, error tradeoff characteristics for white females, black females, black males and white males. The Z-shaped grey lines correspond to fixed thresholds, showing both *FNMR and FMR vary at one T value. Note: Many of the plots will naively be read as saying women gives worse error rates than men because the solid traces lie above the dotted ones. However, this is misleading and incomplete: The grey lines show the traces reveal horizontal shifts. Thus for the cogent-003 algorithm FNMR for men is* higher *than for women* at a fixed threshold *but, at the same time, FMR is higher for women - see Figure 285. As access control systems almost always operate at a fixed threshold, the naive interpretation is incorrect.*

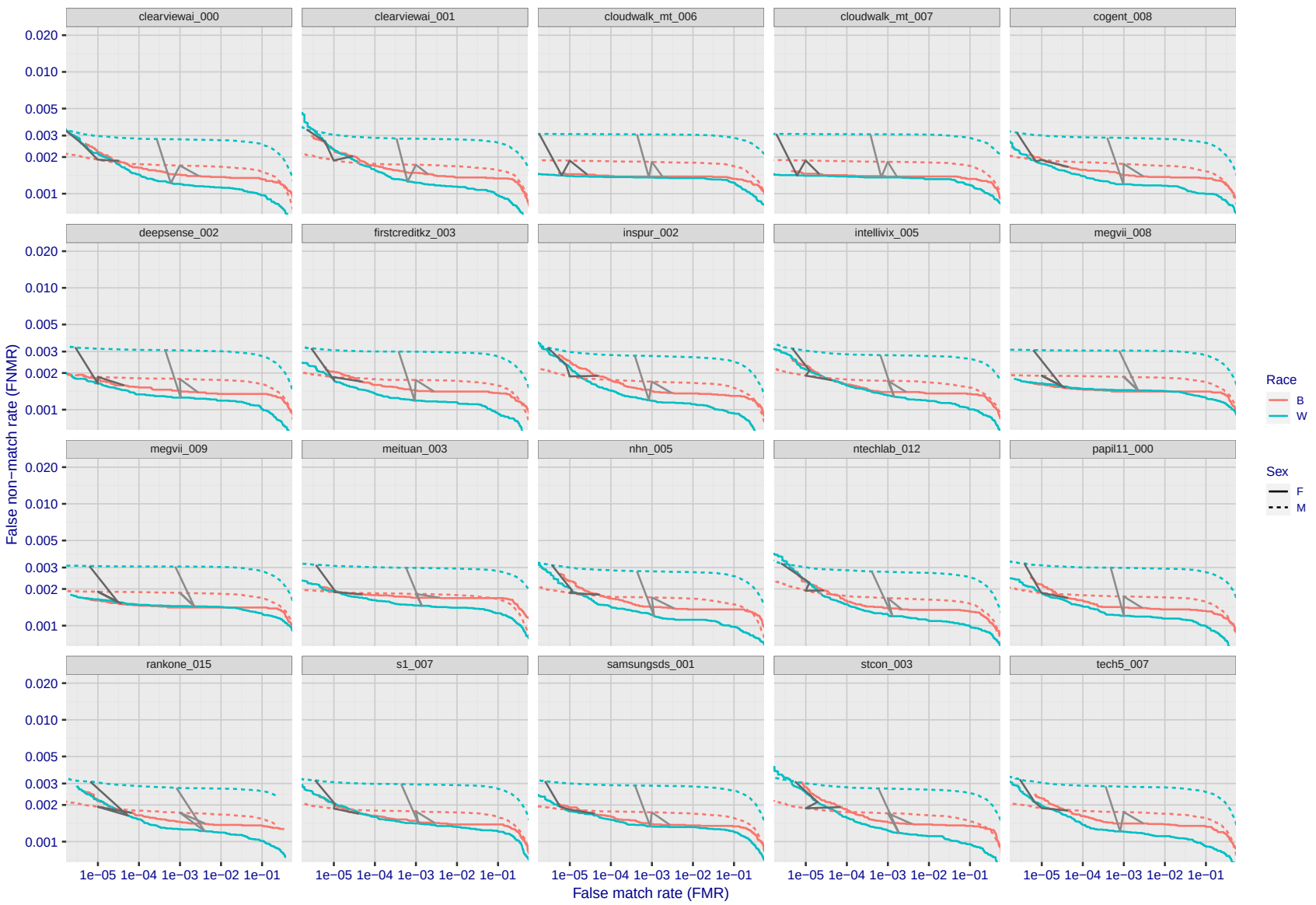

Figure 183: For the mugshot images, error tradeoff characteristics for white females, black females, black males and white males. The Z-shaped grey lines correspond to fixed thresholds, showing both *FNMR and FMR vary at one T value. Note: Many of the plots will naively be read as saying women gives worse error rates than men because the solid traces lie above the dotted ones. However, this is misleading and incomplete: The grey lines show the traces reveal horizontal shifts. Thus for the cogent-003 algorithm FNMR for men is* higher *than for women* at a fixed threshold *but, at the same time, FMR is higher for women - see Figure 285. As access control systems almost always operate at a fixed threshold, the naive interpretation is incorrect.*

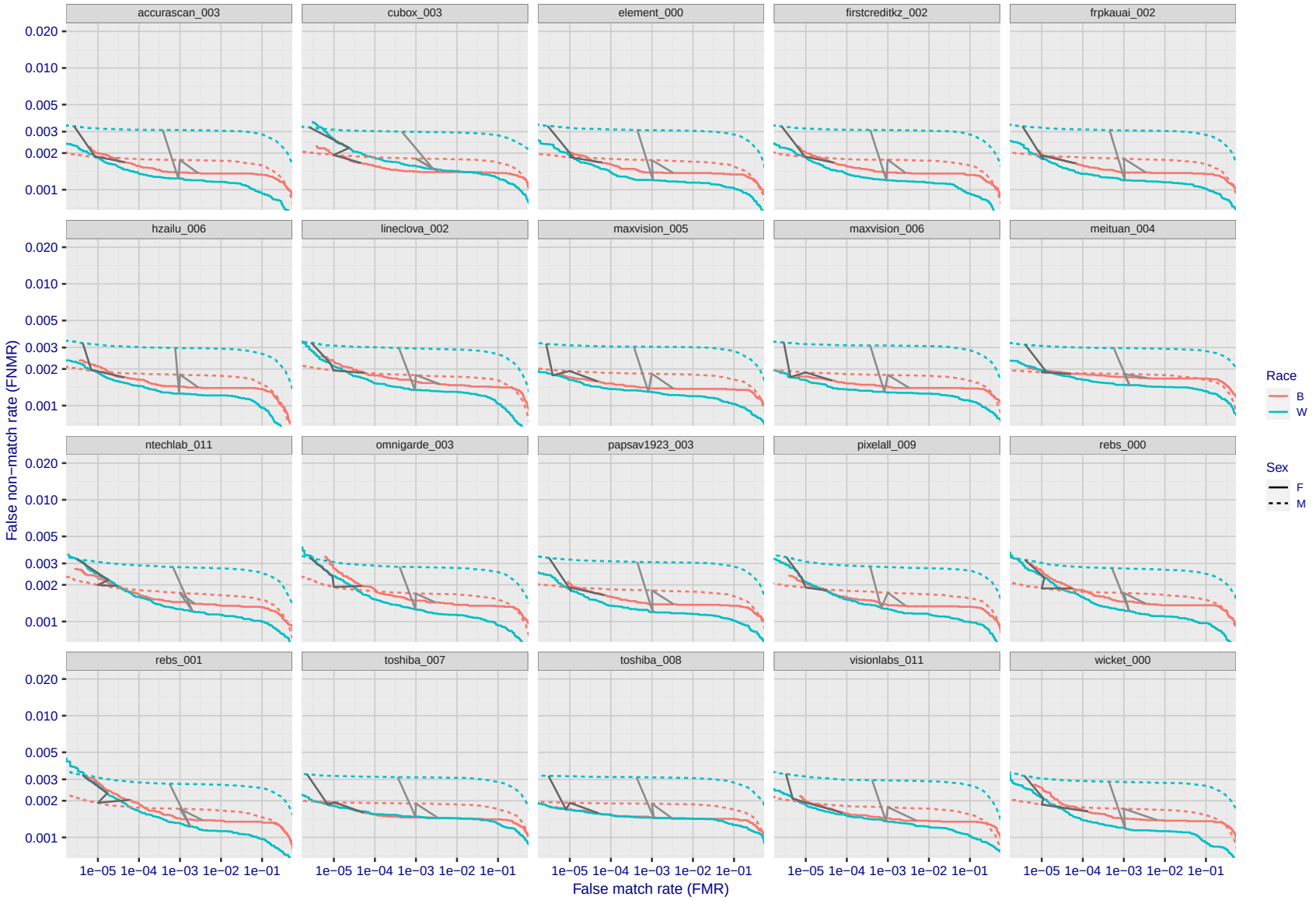

Figure 184: For the mugshot images, error tradeoff characteristics for white females, black females, black males and white males. The Z-shaped grey lines correspond to fixed thresholds, showing both *FNMR and FMR vary at one T value. Note: Many of the plots will naively be read as saying women gives worse error rates than men because the solid traces lie above the dotted ones. However, this is misleading and incomplete: The grey lines show the traces reveal horizontal shifts. Thus for the cogent-003 algorithm FNMR for men is* higher *than for women* at a fixed threshold *but, at the same time, FMR is higher for women - see Figure 285. As access control systems almost always operate at a fixed threshold, the naive interpretation is incorrect.*

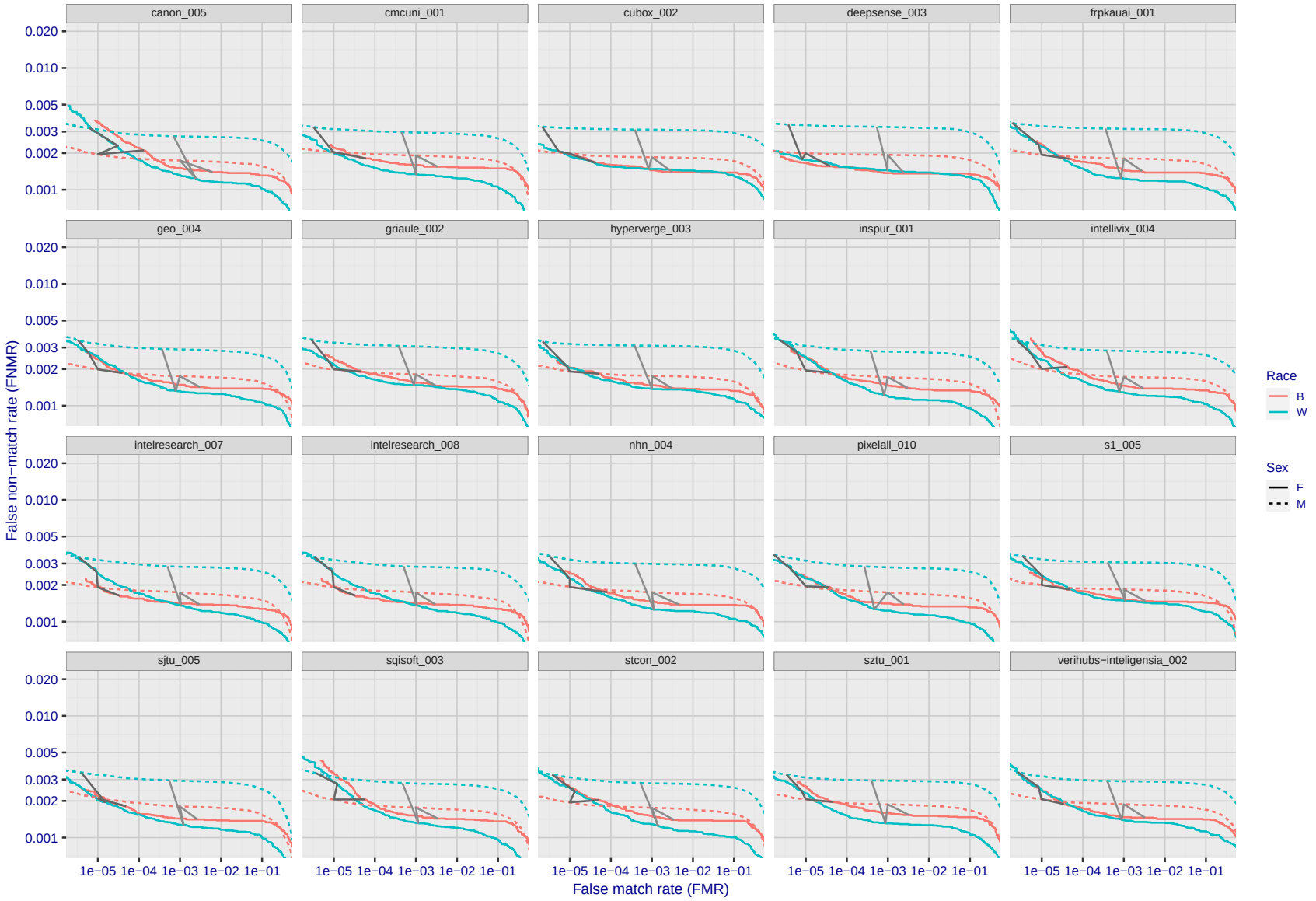

Figure 185: For the mugshot images, error tradeoff characteristics for white females, black females, black males and white males. The Z-shaped grey lines correspond to fixed thresholds, showing both *FNMR and FMR vary at one T value. Note: Many of the plots will naively be read as saying women gives worse error rates than men because the solid traces lie above the dotted ones. However, this is misleading and incomplete: The grey lines show the traces reveal horizontal shifts. Thus for the cogent-003 algorithm FNMR for men is* higher *than for women* at a fixed threshold *but, at the same time, FMR is higher for women - see Figure 285. As access control systems almost always operate at a fixed threshold, the naive interpretation is incorrect.*

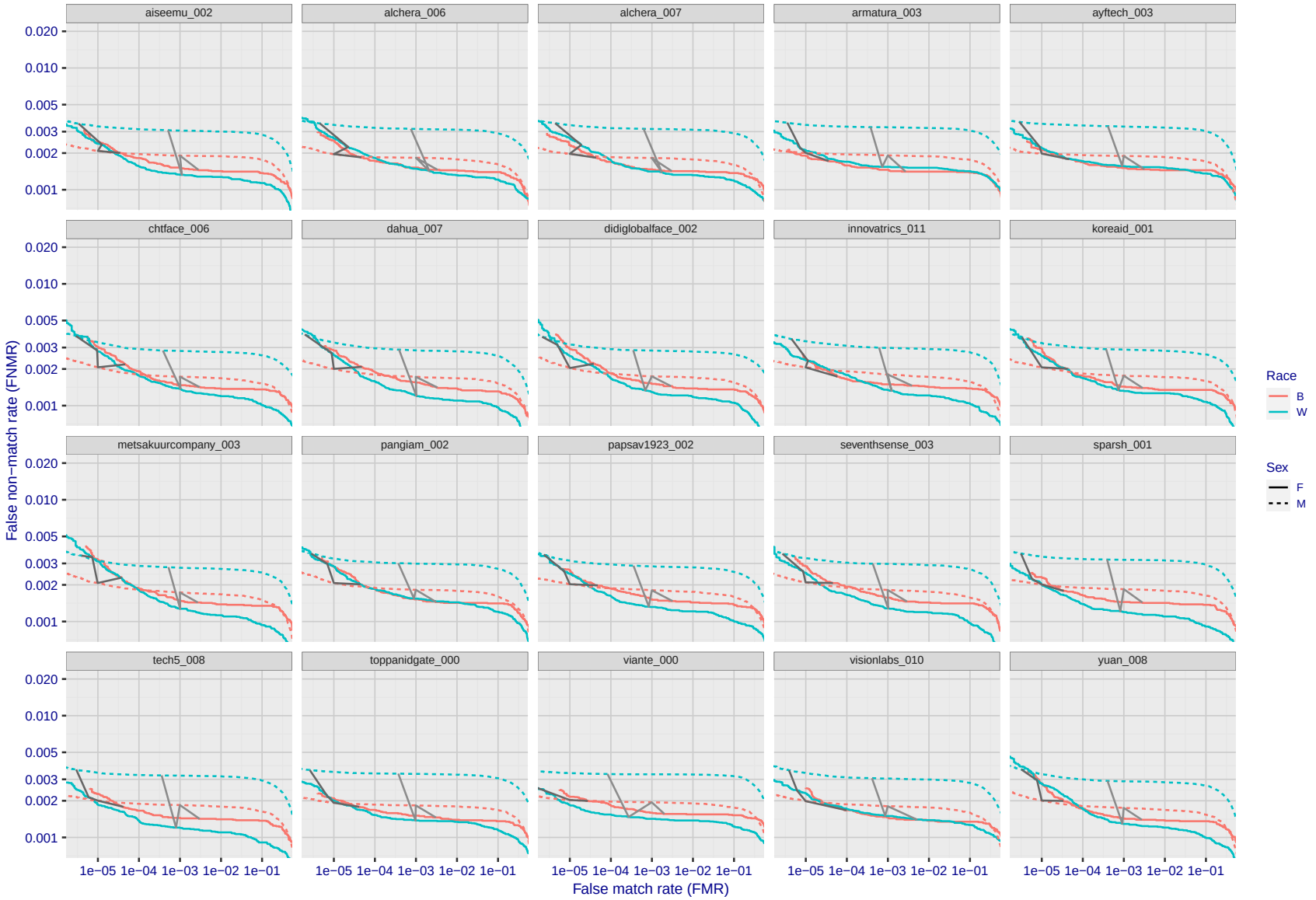

Figure 186: For the mugshot images, error tradeoff characteristics for white females, black females, black males and white males. The Z-shaped grey lines correspond to fixed thresholds, showing both *FNMR and FMR vary at one T value. Note: Many of the plots will naively be read as saying women gives worse error rates than men because the solid traces lie above the dotted ones. However, this is misleading and incomplete: The grey lines show the traces reveal horizontal shifts. Thus for the cogent-003 algorithm FNMR for men is* higher *than for women* at a fixed threshold *but, at the same time, FMR is higher for women - see Figure 285. As access control systems almost always operate at a fixed threshold, the naive interpretation is incorrect.*

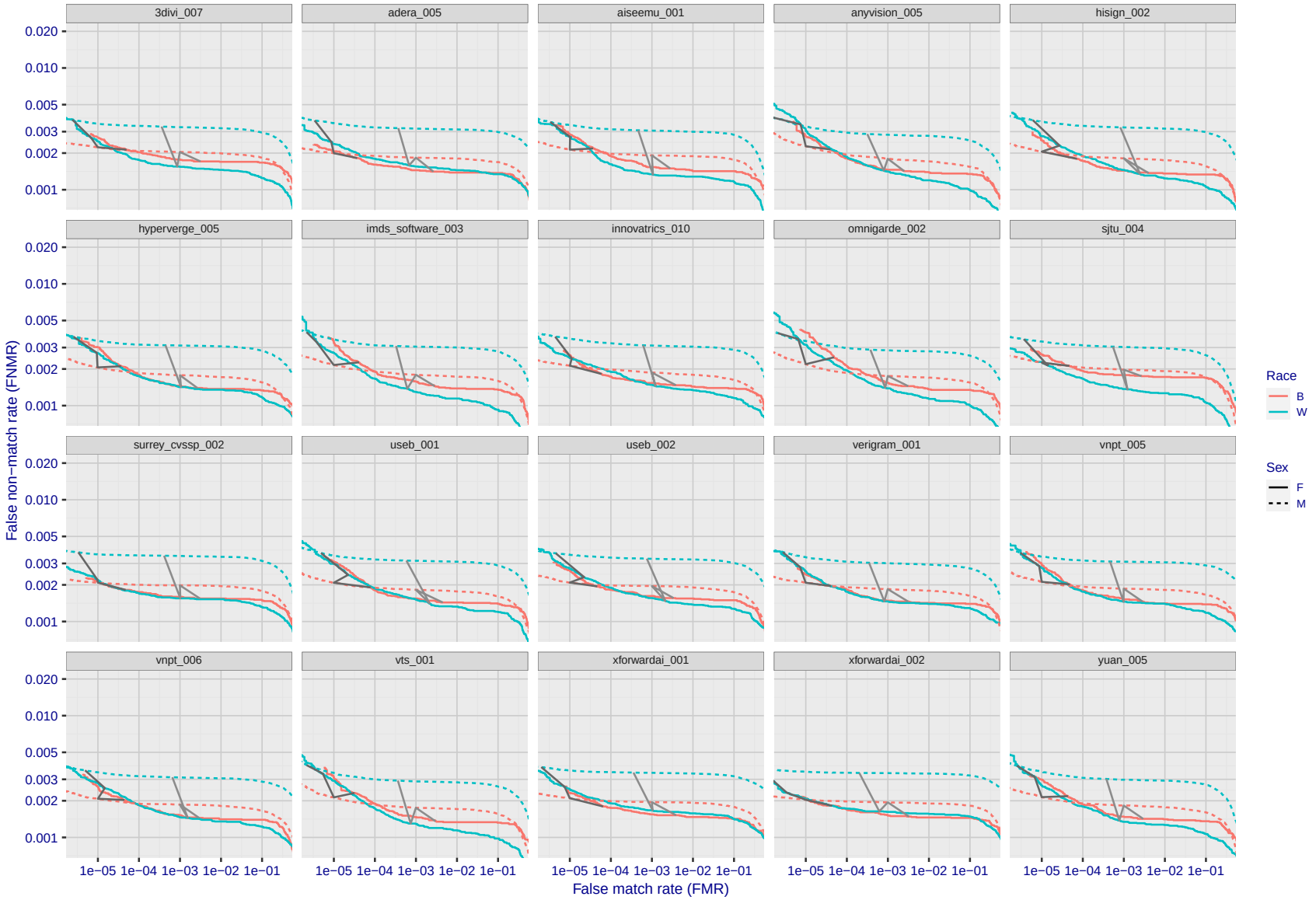

Figure 187: For the mugshot images, error tradeoff characteristics for white females, black females, black males and white males. The Z-shaped grey lines correspond to fixed thresholds, showing both *FNMR and FMR vary at one T value. Note: Many of the plots will naively be read as saying women gives worse error rates than men because the solid traces lie above the dotted ones. However, this is misleading and incomplete: The grey lines show the traces reveal horizontal shifts. Thus for the cogent-003 algorithm FNMR for men is* higher *than for women* at a fixed threshold *but, at the same time, FMR is higher for women - see Figure 285. As access control systems almost always operate at a fixed threshold, the naive interpretation is incorrect.*

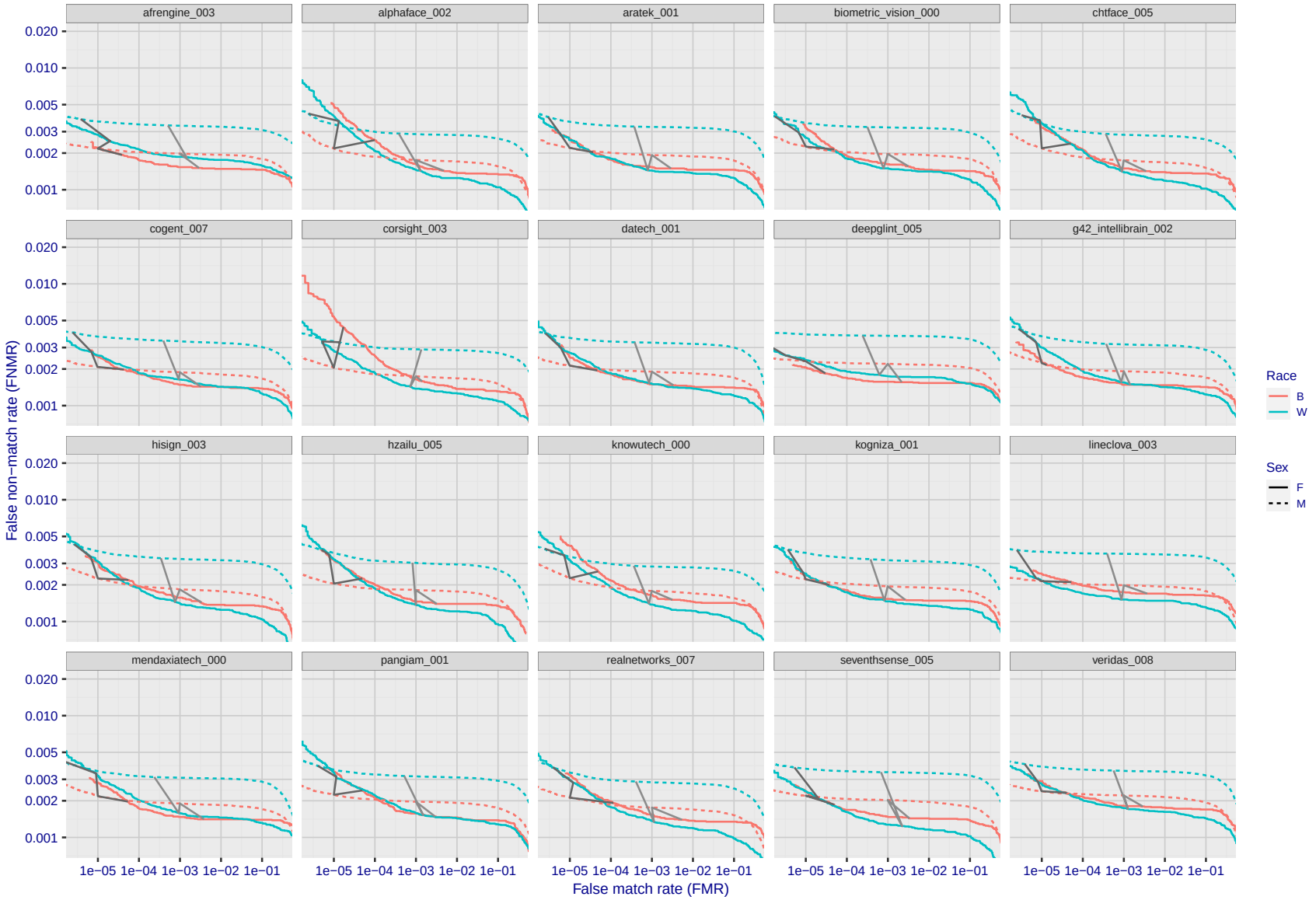

Figure 188: For the mugshot images, error tradeoff characteristics for white females, black females, black males and white males. The Z-shaped grey lines correspond to fixed thresholds, showing both *FNMR and FMR vary at one T value. Note: Many of the plots will naively be read as saying women gives worse error rates than men because the solid traces lie above the dotted ones. However, this is misleading and incomplete: The grey lines show the traces reveal horizontal shifts. Thus for the cogent-003 algorithm FNMR for men is* higher *than for women* at a fixed threshold *but, at the same time, FMR is higher for women - see Figure 285. As access control systems almost always operate at a fixed threshold, the naive interpretation is incorrect.*

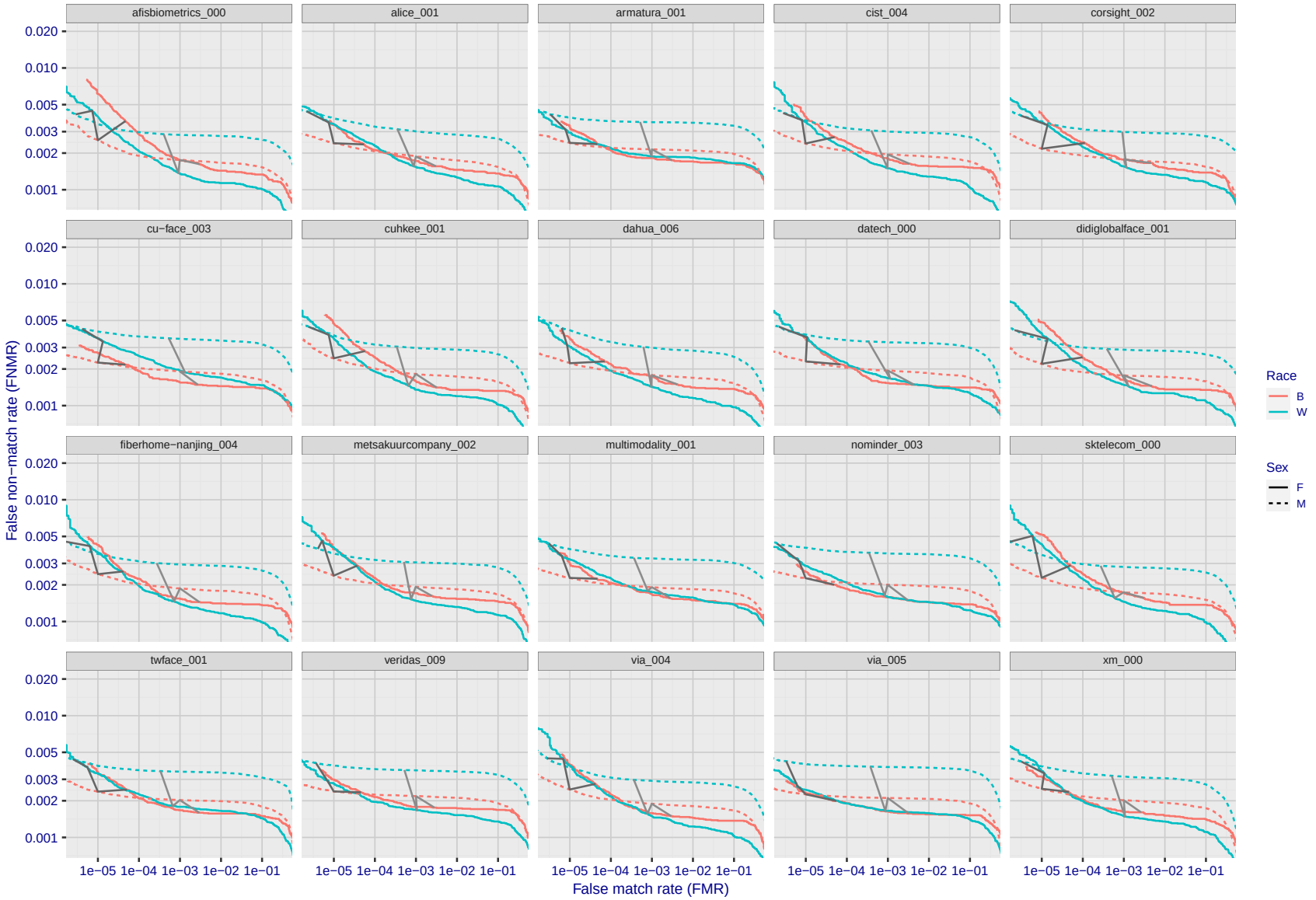

Figure 189: For the mugshot images, error tradeoff characteristics for white females, black females, black males and white males. The Z-shaped grey lines correspond to fixed thresholds, showing both *FNMR and FMR vary at one T value. Note: Many of the plots will naively be read as saying women gives worse error rates than men because the solid traces lie above the dotted ones. However, this is misleading and incomplete: The grey lines show the traces reveal horizontal shifts. Thus for the cogent-003 algorithm FNMR for men is* higher *than for women* at a fixed threshold *but, at the same time, FMR is higher for women - see Figure 285. As access control systems almost always operate at a fixed threshold, the naive interpretation is incorrect.*

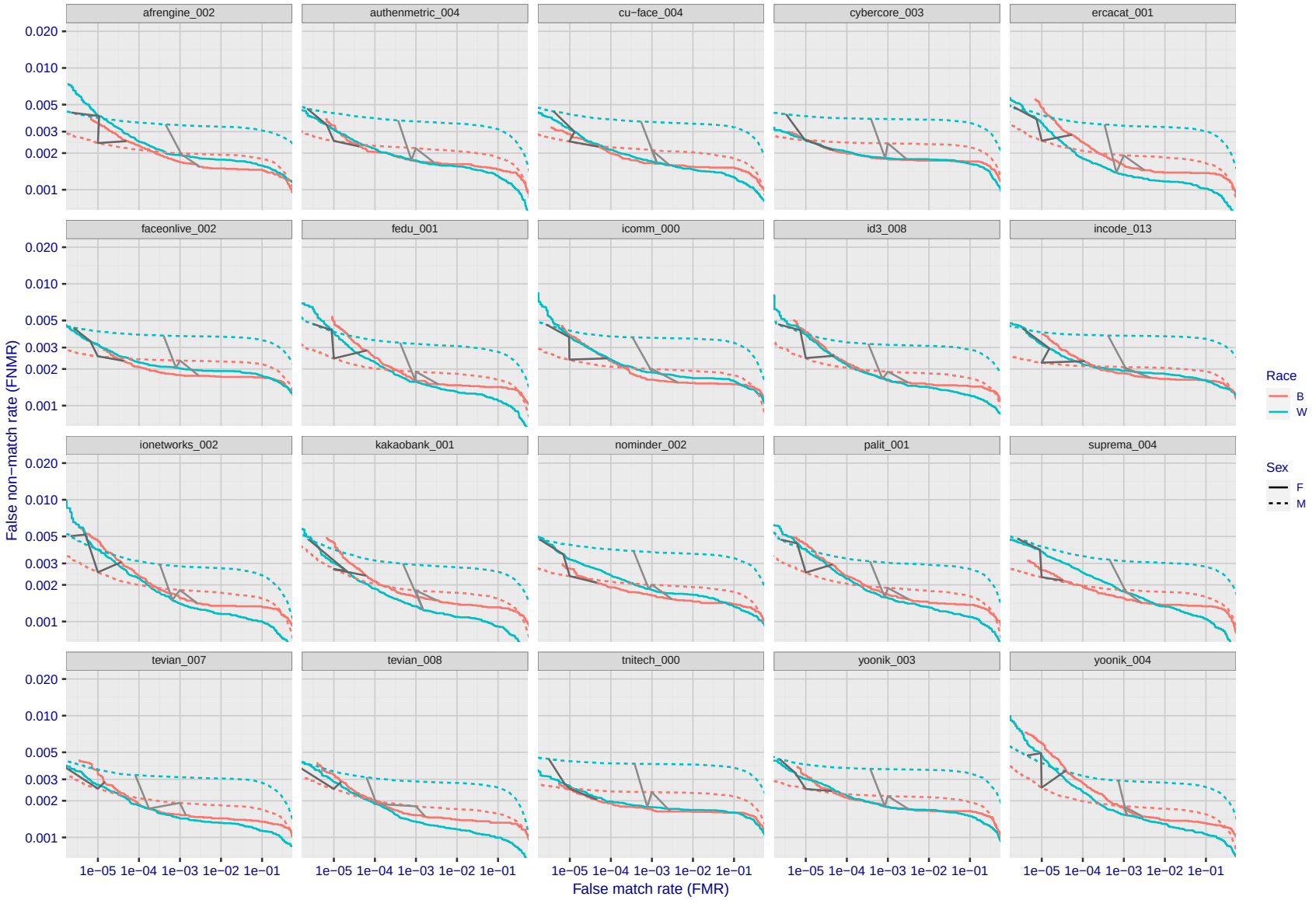

Figure 190: For the mugshot images, error tradeoff characteristics for white females, black females, black males and white males. The Z-shaped grey lines correspond to fixed thresholds, showing both *FNMR and FMR vary at one T value. Note: Many of the plots will naively be read as saying women gives worse error rates than men because the solid traces lie above the dotted ones. However, this is misleading and incomplete: The grey lines show the traces reveal horizontal shifts. Thus for the cogent-003 algorithm FNMR for men is* higher *than for women* at a fixed threshold *but, at the same time, FMR is higher for women - see Figure 285. As access control systems almost always operate at a fixed threshold, the naive interpretation is incorrect.*

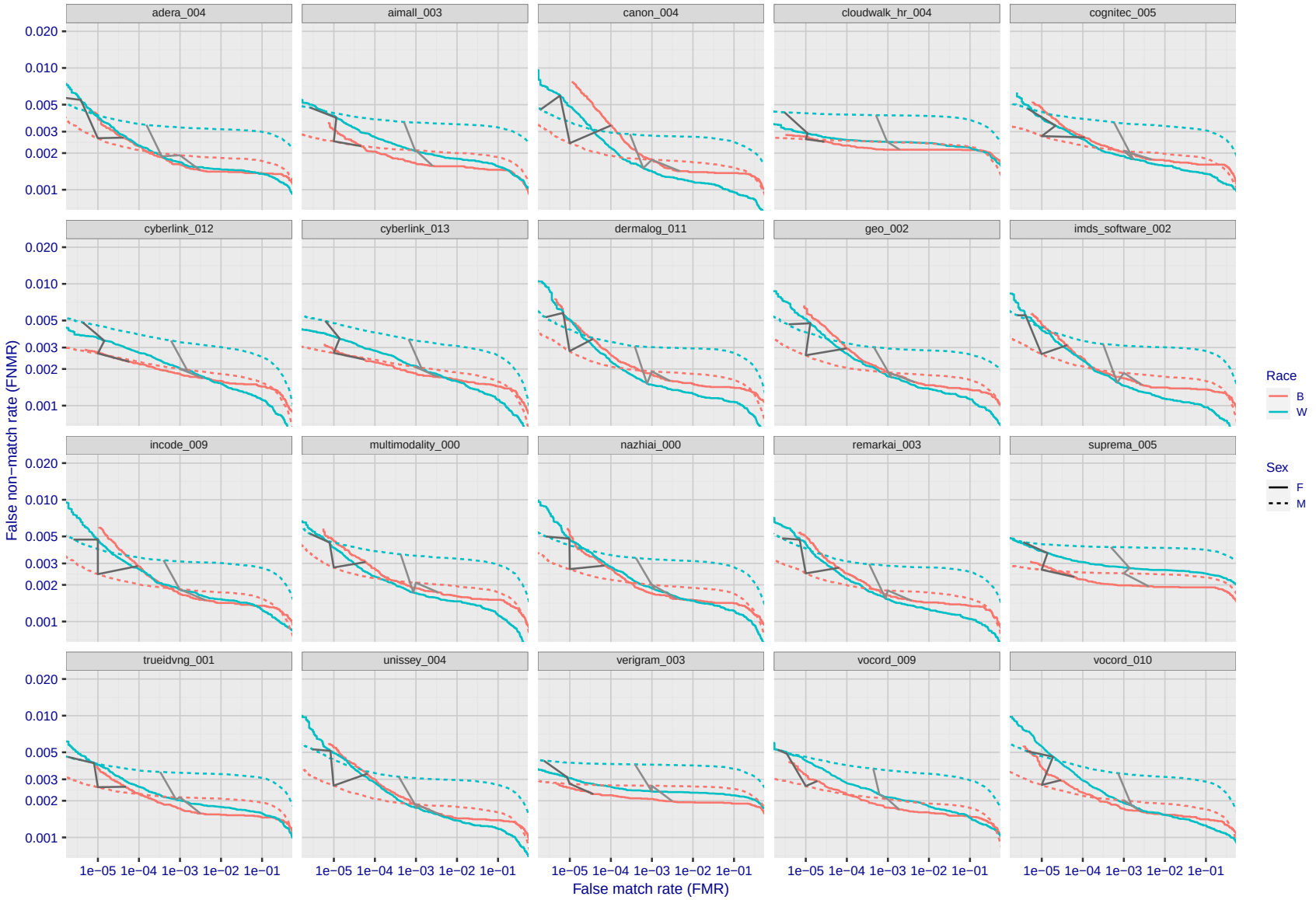

Figure 191: For the mugshot images, error tradeoff characteristics for white females, black females, black males and white males. The Z-shaped grey lines correspond to fixed thresholds, showing both *FNMR and FMR vary at one T value. Note: Many of the plots will naively be read as saying women gives worse error rates than men because the solid traces lie above the dotted ones. However, this is misleading and incomplete: The grey lines show the traces reveal horizontal shifts. Thus for the cogent-003 algorithm FNMR for men is* higher *than for women* at a fixed threshold *but, at the same time, FMR is higher for women - see Figure 285. As access control systems almost always operate at a fixed threshold, the naive interpretation is incorrect.*

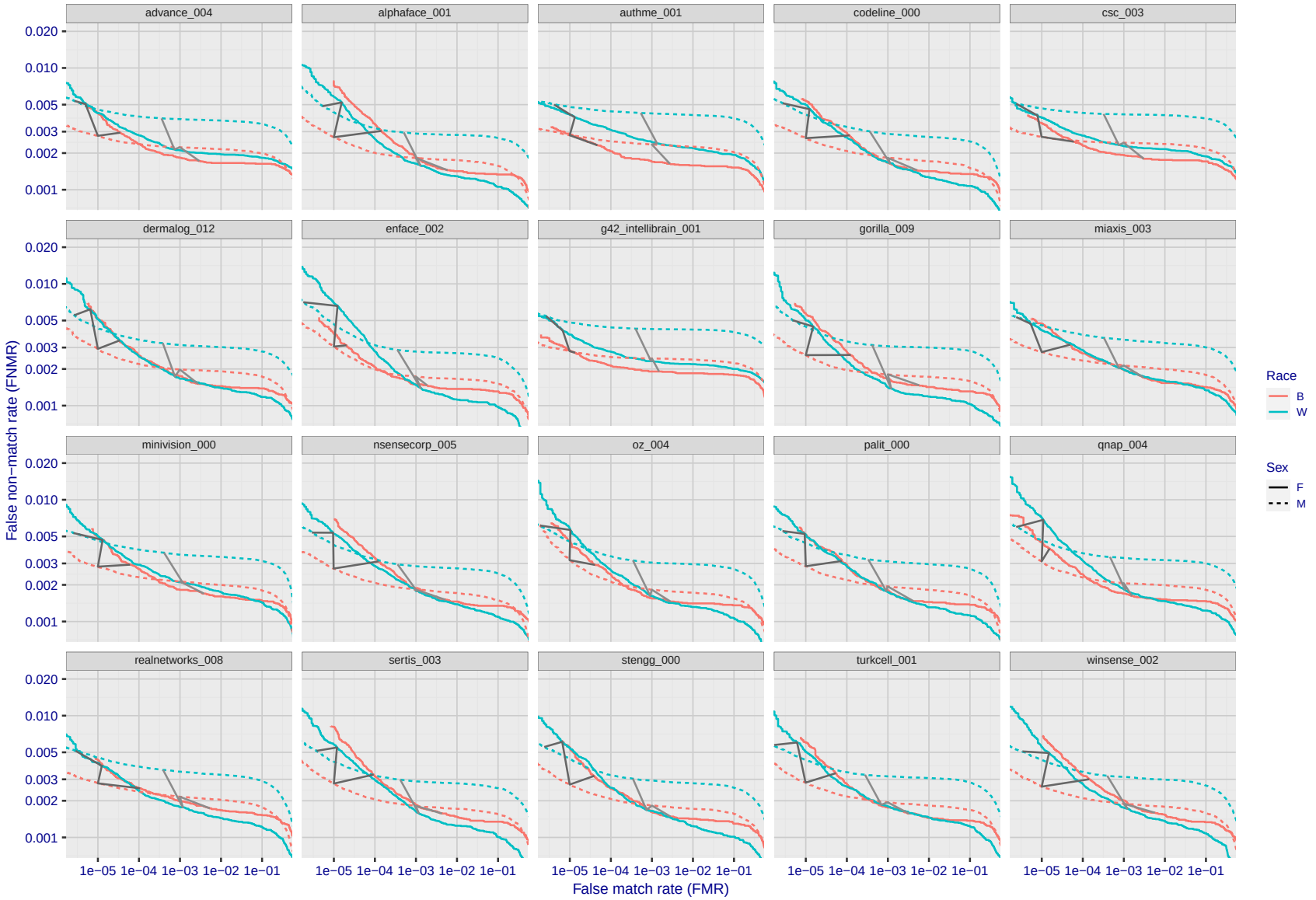

Figure 192: For the mugshot images, error tradeoff characteristics for white females, black females, black males and white males. The Z-shaped grey lines correspond to fixed thresholds, showing both *FNMR and FMR vary at one T value. Note: Many of the plots will naively be read as saying women gives worse error rates than men because the solid traces lie above the dotted ones. However, this is misleading and incomplete: The grey lines show the traces reveal horizontal shifts. Thus for the cogent-003 algorithm FNMR for men is* higher *than for women* at a fixed threshold *but, at the same time, FMR is higher for women - see Figure 285. As access control systems almost always operate at a fixed threshold, the naive interpretation is incorrect.*

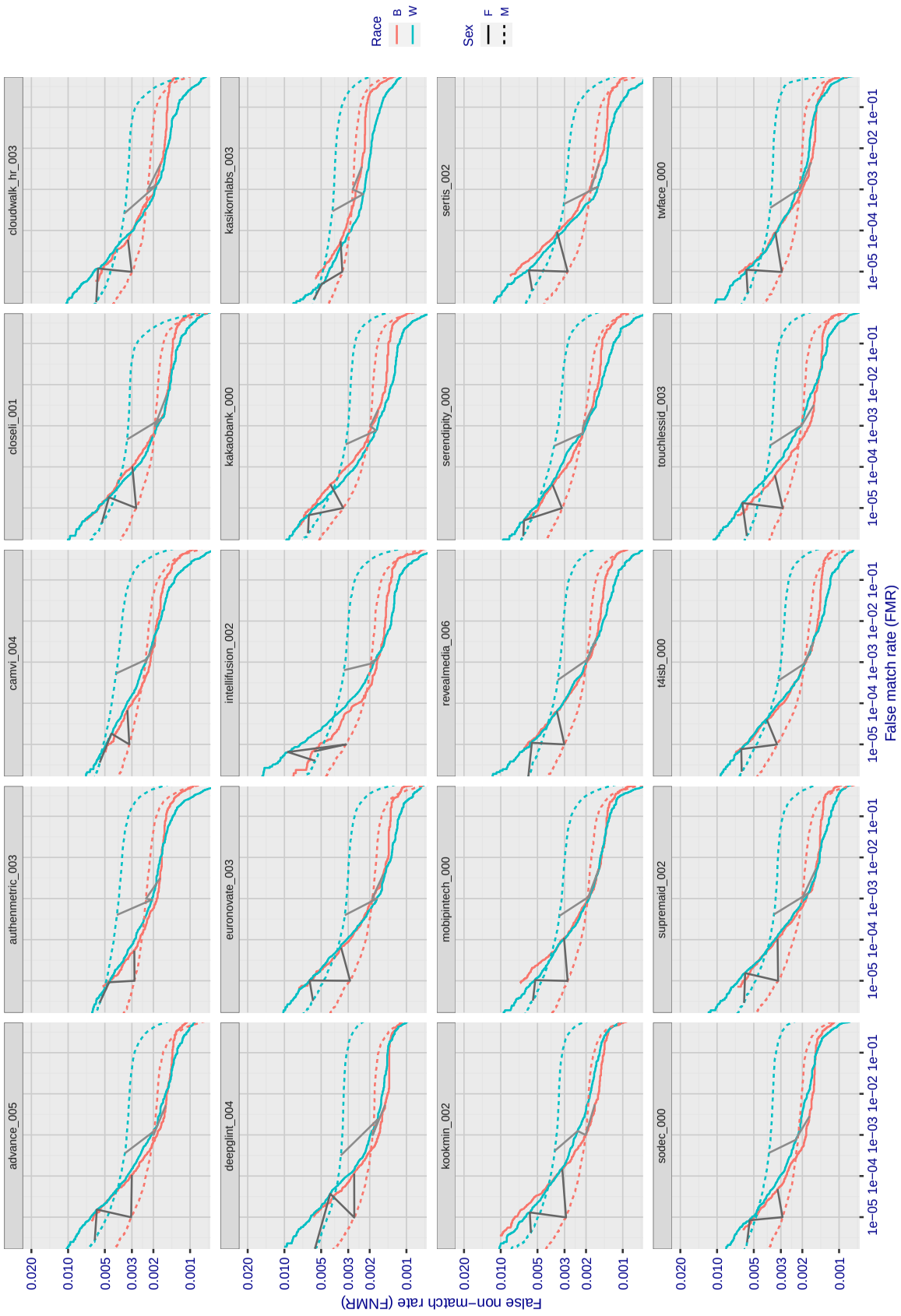

Figure 193: For the mugshot images, error tradeoff characteristics for white females, black females, black males and white males. The Z-shaped grey lines correspond to fixed thresholds, showing both *FNMR and FMR vary at one T value. Note: Many of the plots will naively be read as saying women gives worse error rates than men because the solid traces lie above the dotted ones. However, this is misleading and incomplete: The grey lines show the traces reveal horizontal shifts. Thus for the cogent-003 algorithm FNMR for men is* higher *than for women at a fixed threshold but, at the same time, FMR is higher for women - see Figure 285. As access control systems almost always operate at a fixed threshold, the naive interpretation is incorrect.*

FNMR(T) "False non-match rate"
FMR(T) "False match rate"

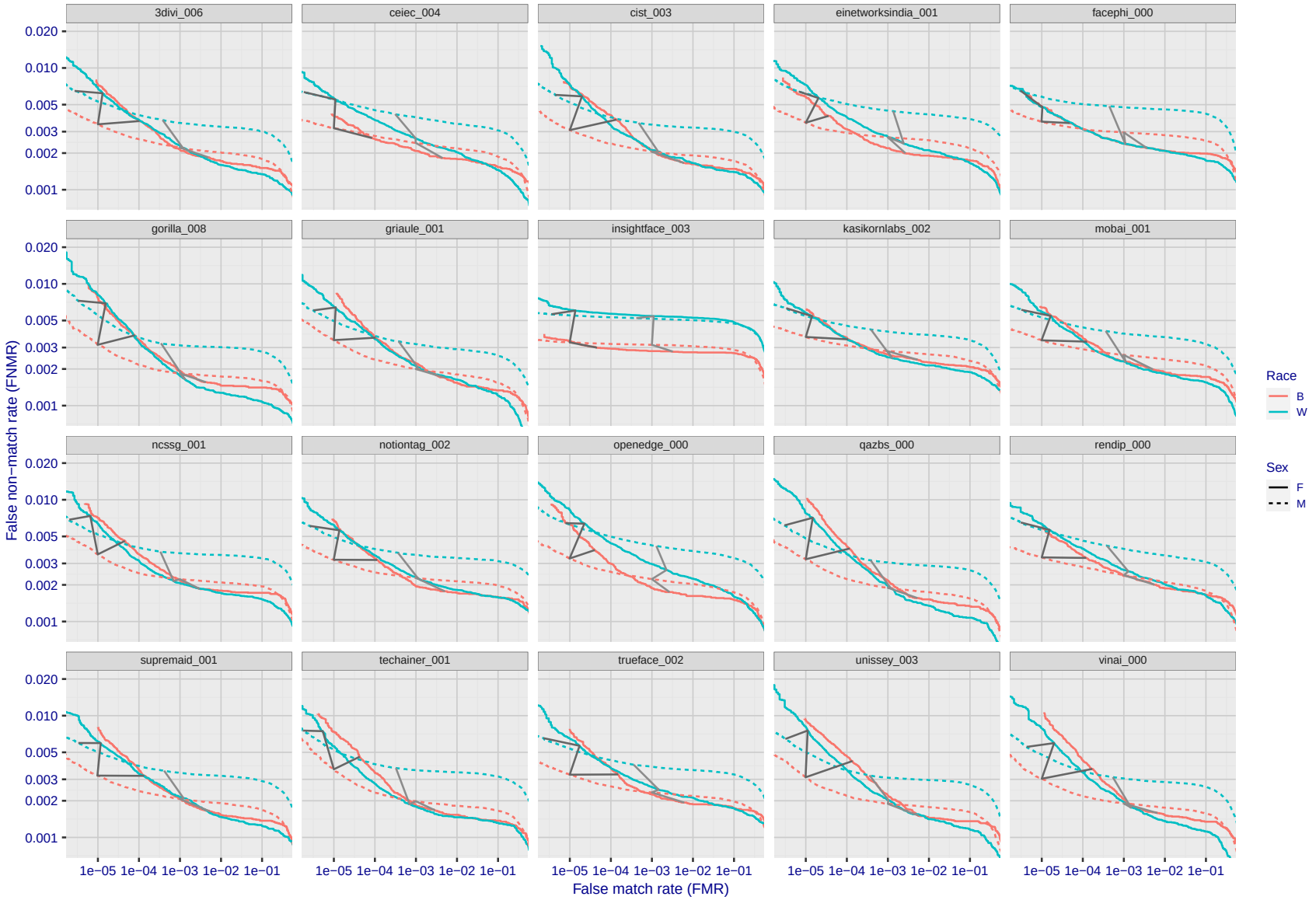

Figure 194: For the mugshot images, error tradeoff characteristics for white females, black females, black males and white males. The Z-shaped grey lines correspond to fixed thresholds, showing both *FNMR and FMR vary at one T value. Note: Many of the plots will naively be read as saying women gives worse error rates than men because the solid traces lie above the dotted ones. However, this is misleading and incomplete: The grey lines show the traces reveal horizontal shifts. Thus for the cogent-003 algorithm FNMR for men is* higher *than for women* at a fixed threshold *but, at the same time, FMR is higher for women - see Figure 285. As access control systems almost always operate at a fixed threshold, the naive interpretation is incorrect.*

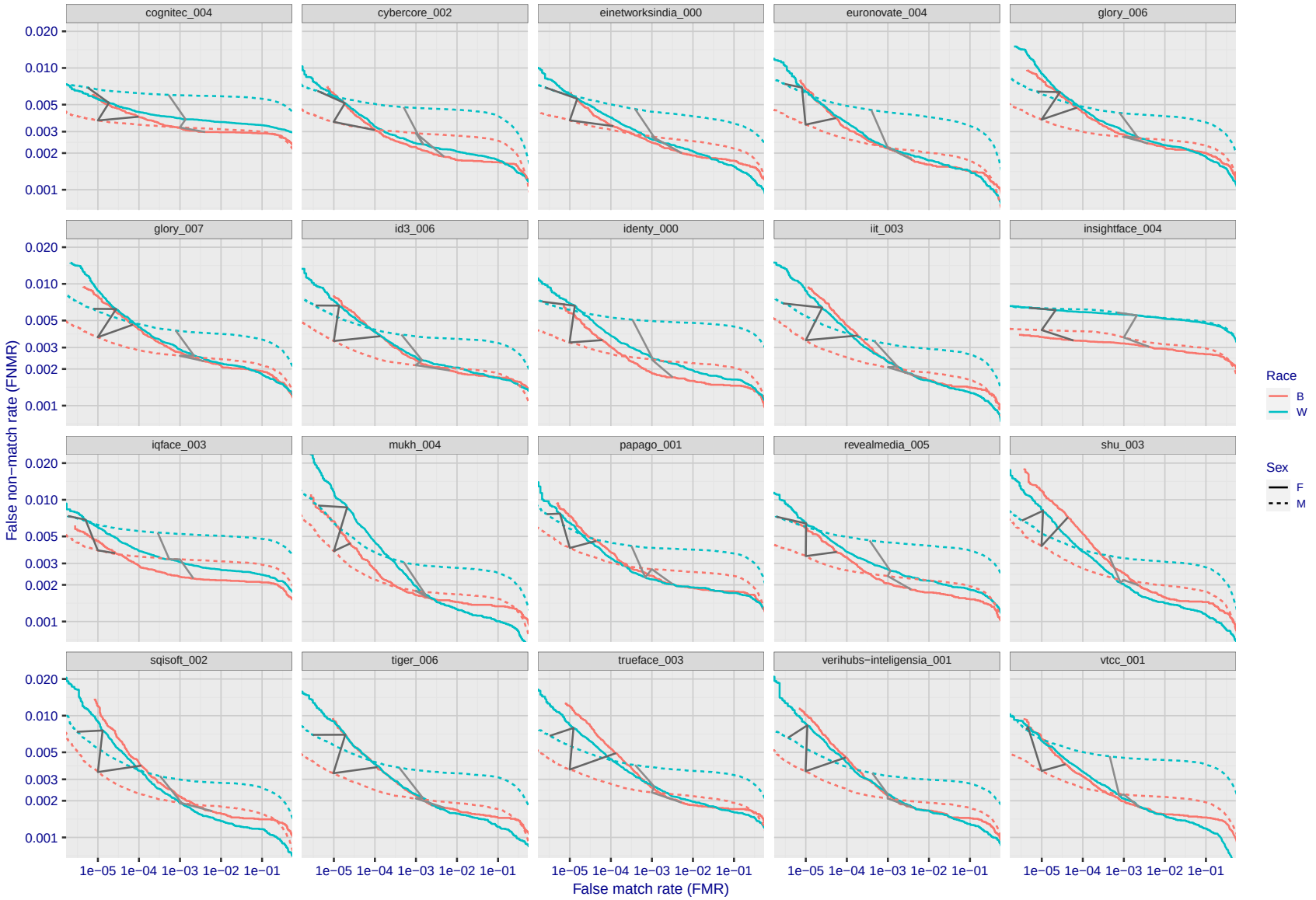

Figure 195: For the mugshot images, error tradeoff characteristics for white females, black females, black males and white males. The Z-shaped grey lines correspond to fixed thresholds, showing both *FNMR and FMR vary at one T value. Note: Many of the plots will naively be read as saying women gives worse error rates than men because the solid traces lie above the dotted ones. However, this is misleading and incomplete: The grey lines show the traces reveal horizontal shifts. Thus for the cogent-003 algorithm FNMR for men is* higher *than for women* at a fixed threshold *but, at the same time, FMR is higher for women - see Figure 285. As access control systems almost always operate at a fixed threshold, the naive interpretation is incorrect.*

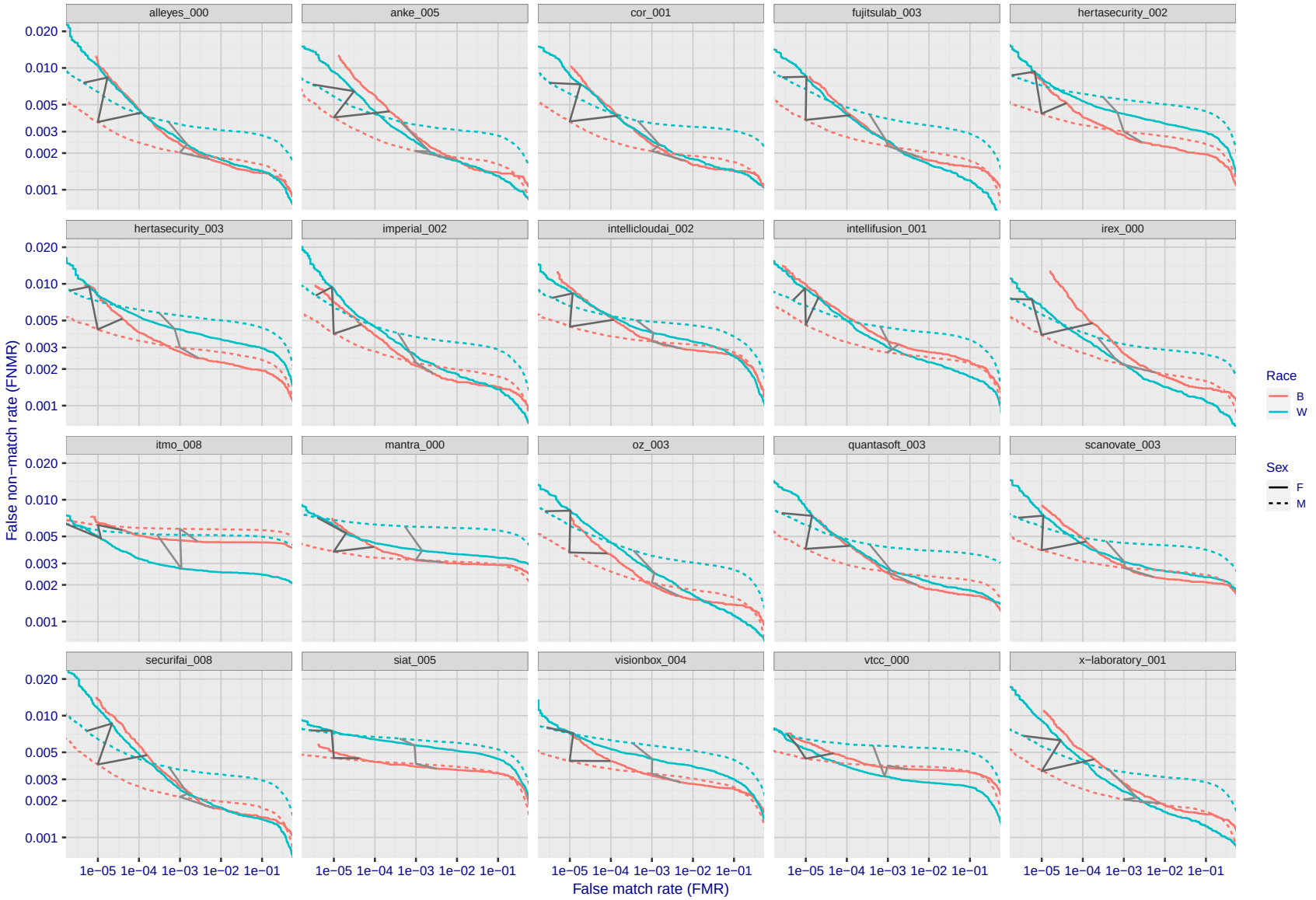

Figure 196: For the mugshot images, error tradeoff characteristics for white females, black females, black males and white males. The Z-shaped grey lines correspond to fixed thresholds, showing both *FNMR and FMR vary at one T value. Note: Many of the plots will naively be read as saying women gives worse error rates than men because the solid traces lie above the dotted ones. However, this is misleading and incomplete: The grey lines show the traces reveal horizontal shifts. Thus for the cogent-003 algorithm FNMR for men is* higher *than for women* at a fixed threshold *but, at the same time, FMR is higher for women - see Figure 285. As access control systems almost always operate at a fixed threshold, the naive interpretation is incorrect.*

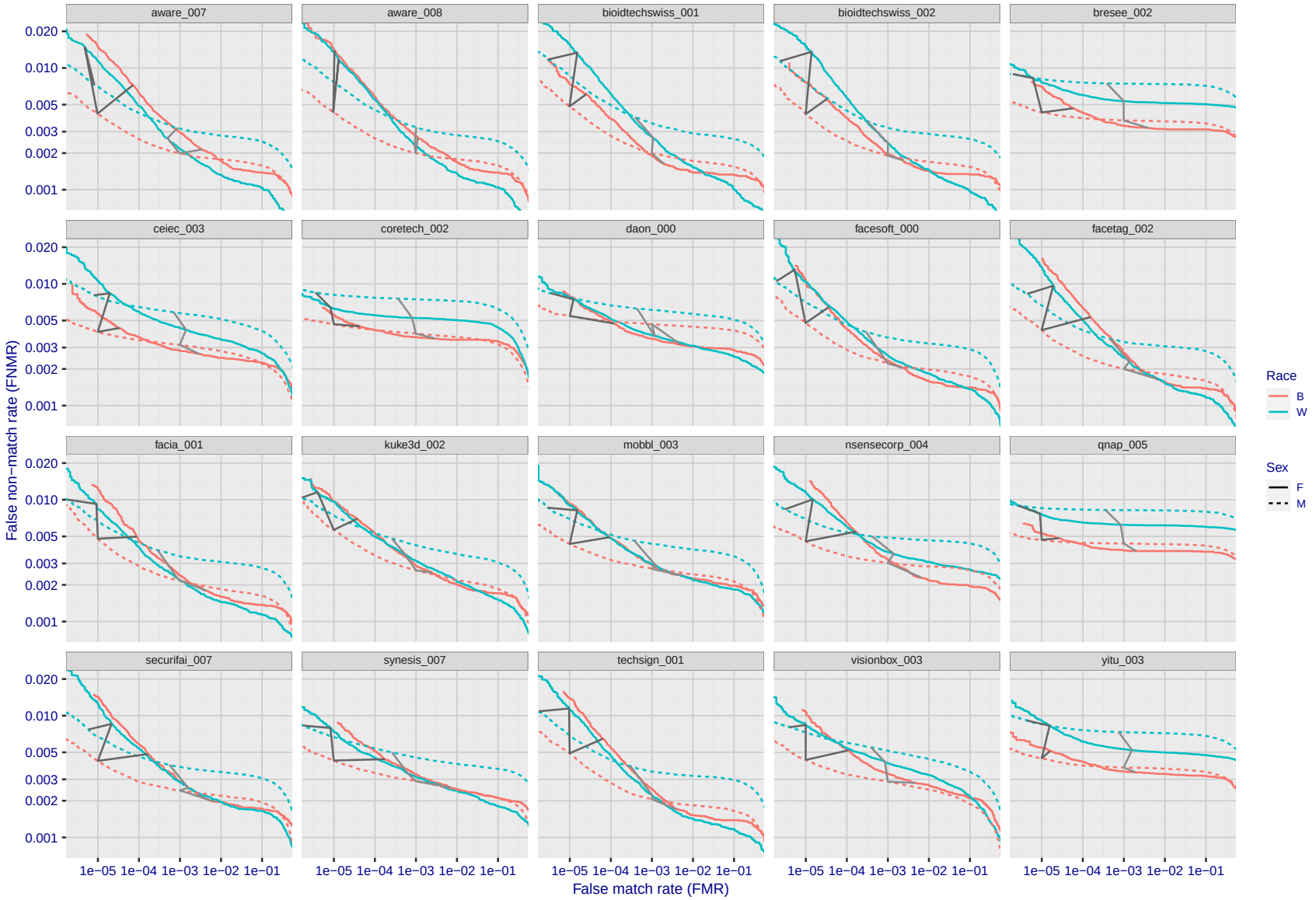

Figure 197: For the mugshot images, error tradeoff characteristics for white females, black females, black males and white males. The Z-shaped grey lines correspond to fixed thresholds, showing both *FNMR and FMR vary at one T value. Note: Many of the plots will naively be read as saying women gives worse error rates than men because the solid traces lie above the dotted ones. However, this is misleading and incomplete: The grey lines show the traces reveal horizontal shifts. Thus for the cogent-003 algorithm FNMR for men is* higher *than for women* at a fixed threshold *but, at the same time, FMR is higher for women - see Figure 285. As access control systems almost always operate at a fixed threshold, the naive interpretation is incorrect.*

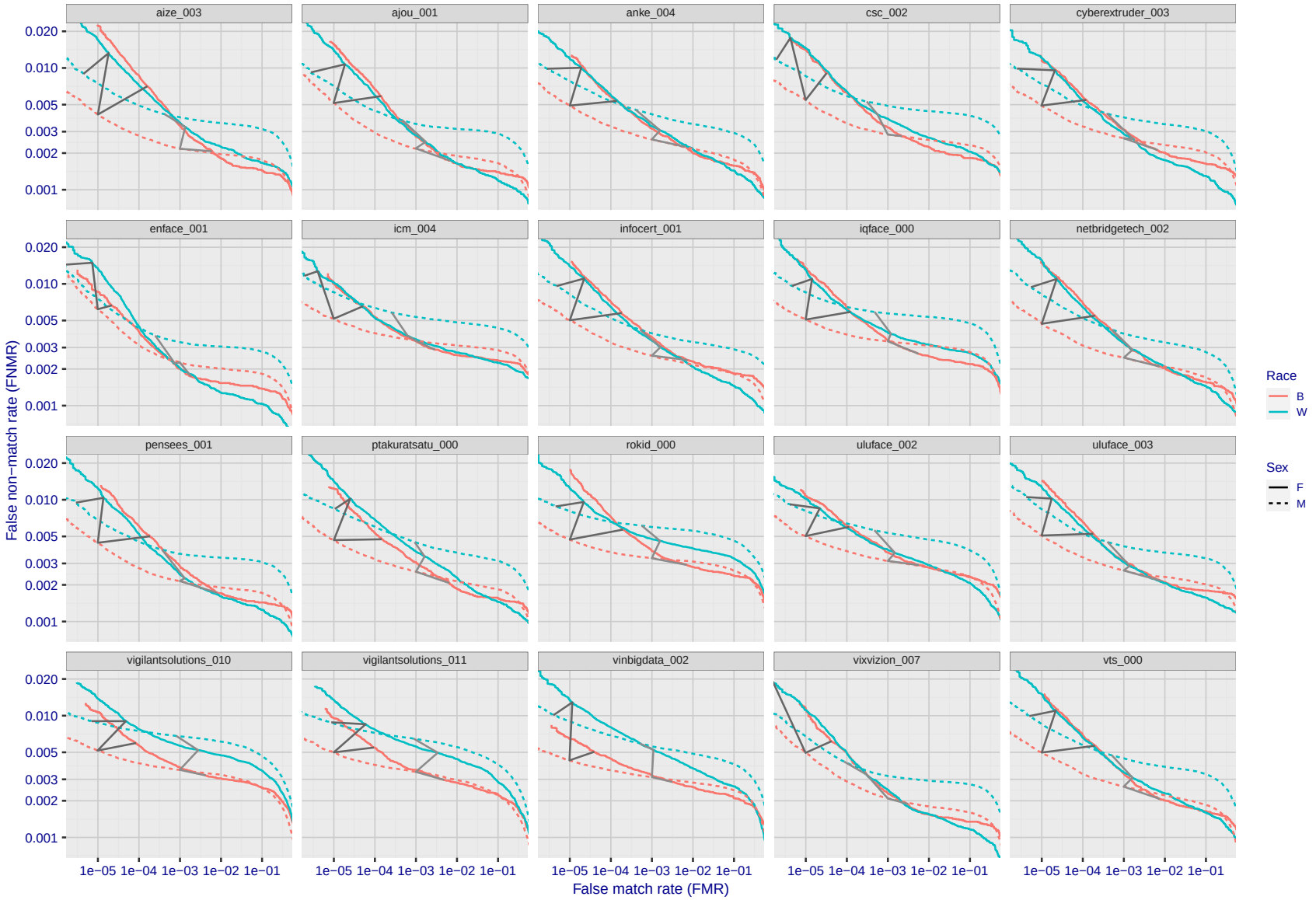

Figure 198: For the mugshot images, error tradeoff characteristics for white females, black females, black males and white males. The Z-shaped grey lines correspond to fixed thresholds, showing both *FNMR and FMR vary at one T value. Note: Many of the plots will naively be read as saying women gives worse error rates than men because the solid traces lie above the dotted ones. However, this is misleading and incomplete: The grey lines show the traces reveal horizontal shifts. Thus for the cogent-003 algorithm FNMR for men is* higher *than for women* at a fixed threshold *but, at the same time, FMR is higher for women - see Figure 285. As access control systems almost always operate at a fixed threshold, the naive interpretation is incorrect.*

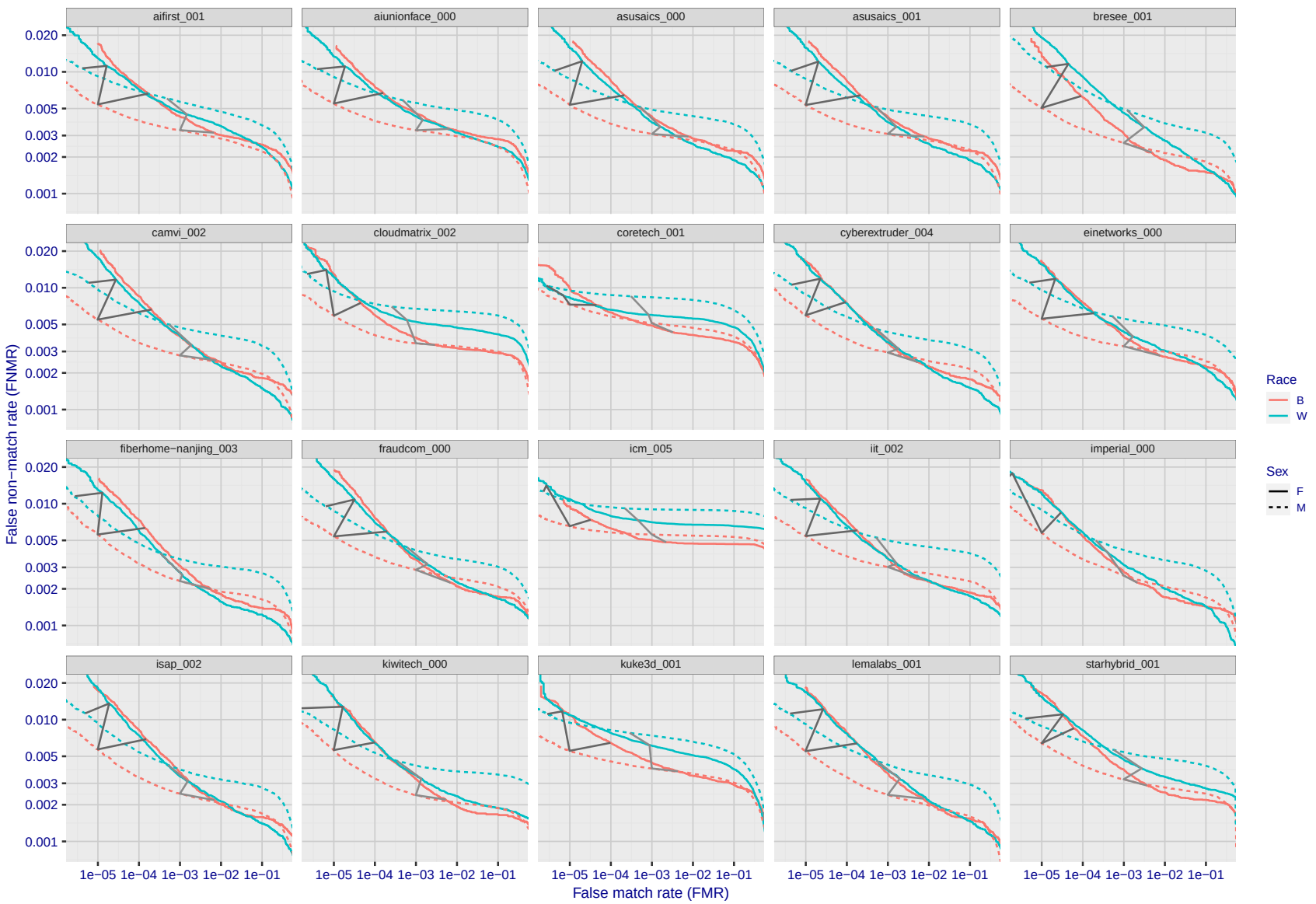

Figure 199: For the mugshot images, error tradeoff characteristics for white females, black females, black males and white males. The Z-shaped grey lines correspond to fixed thresholds, showing both *FNMR and FMR vary at one T value. Note: Many of the plots will naively be read as saying women gives worse error rates than men because the solid traces lie above the dotted ones. However, this is misleading and incomplete: The grey lines show the traces reveal horizontal shifts. Thus for the cogent-003 algorithm FNMR for men is* higher *than for women* at a fixed threshold *but, at the same time, FMR is higher for women - see Figure 285. As access control systems almost always operate at a fixed threshold, the naive interpretation is incorrect.*

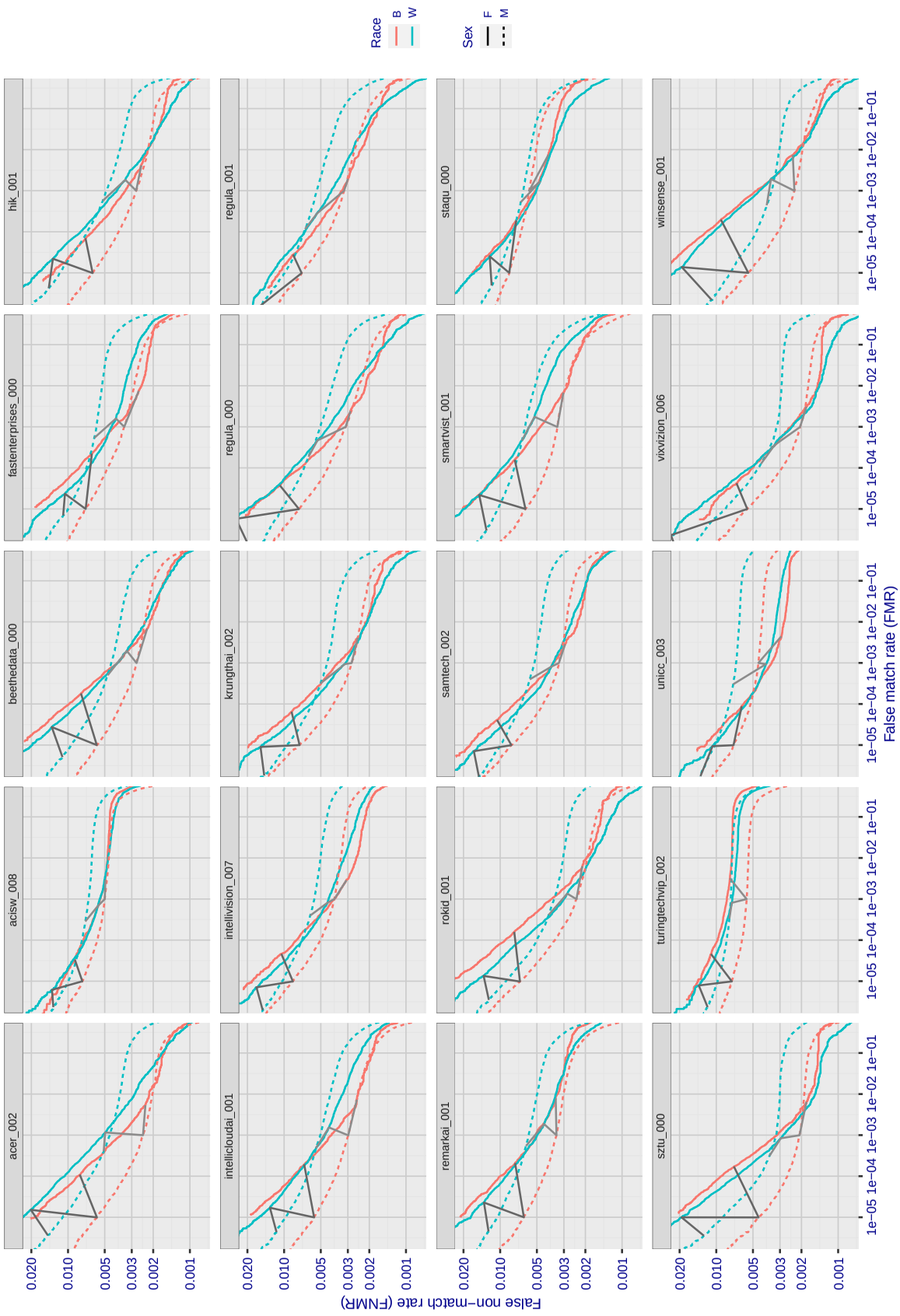

Figure 200: For the mugshot images, error tradeoff characteristics for white females, black females, black males and white males. The Z-shaped grey lines correspond to fixed thresholds, showing both FNMR and FMR vary at one T value. Note: Many of the plots will naively be read as saying women gives worse error rates than men because the solid traces lie above the dotted ones. However, this is misleading and incomplete: The grey lines show the traces reveal horizontal shifts. Thus for the cogent-003 algorithm FNMR for men is higher than for women at a fixed threshold but, at the same time, FMR is higher for women - see Figure 285. As access control systems almost always operate at a fixed threshold, the naive interpretation is incorrect.

FNMR(T) "False non-match rate"
FMR(T) "False match rate"

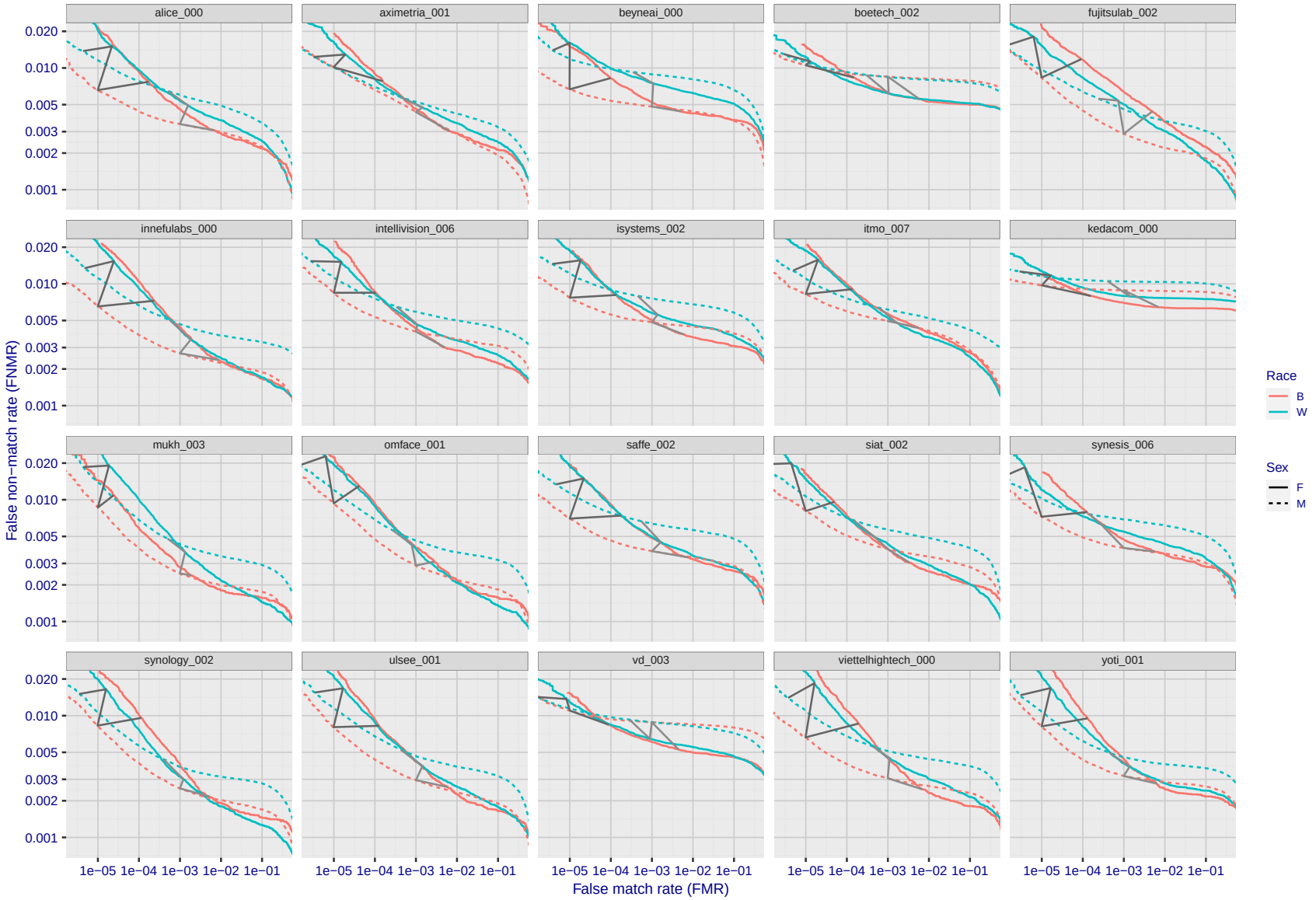

Figure 201: For the mugshot images, error tradeoff characteristics for white females, black females, black males and white males. The Z-shaped grey lines correspond to fixed thresholds, showing both *FNMR and FMR vary at one T value. Note: Many of the plots will naively be read as saying women gives worse error rates than men because the solid traces lie above the dotted ones. However, this is misleading and incomplete: The grey lines show the traces reveal horizontal shifts. Thus for the cogent-003 algorithm FNMR for men is* higher *than for women* at a fixed threshold *but, at the same time, FMR is higher for women - see Figure 285. As access control systems almost always operate at a fixed threshold, the naive interpretation is incorrect.*

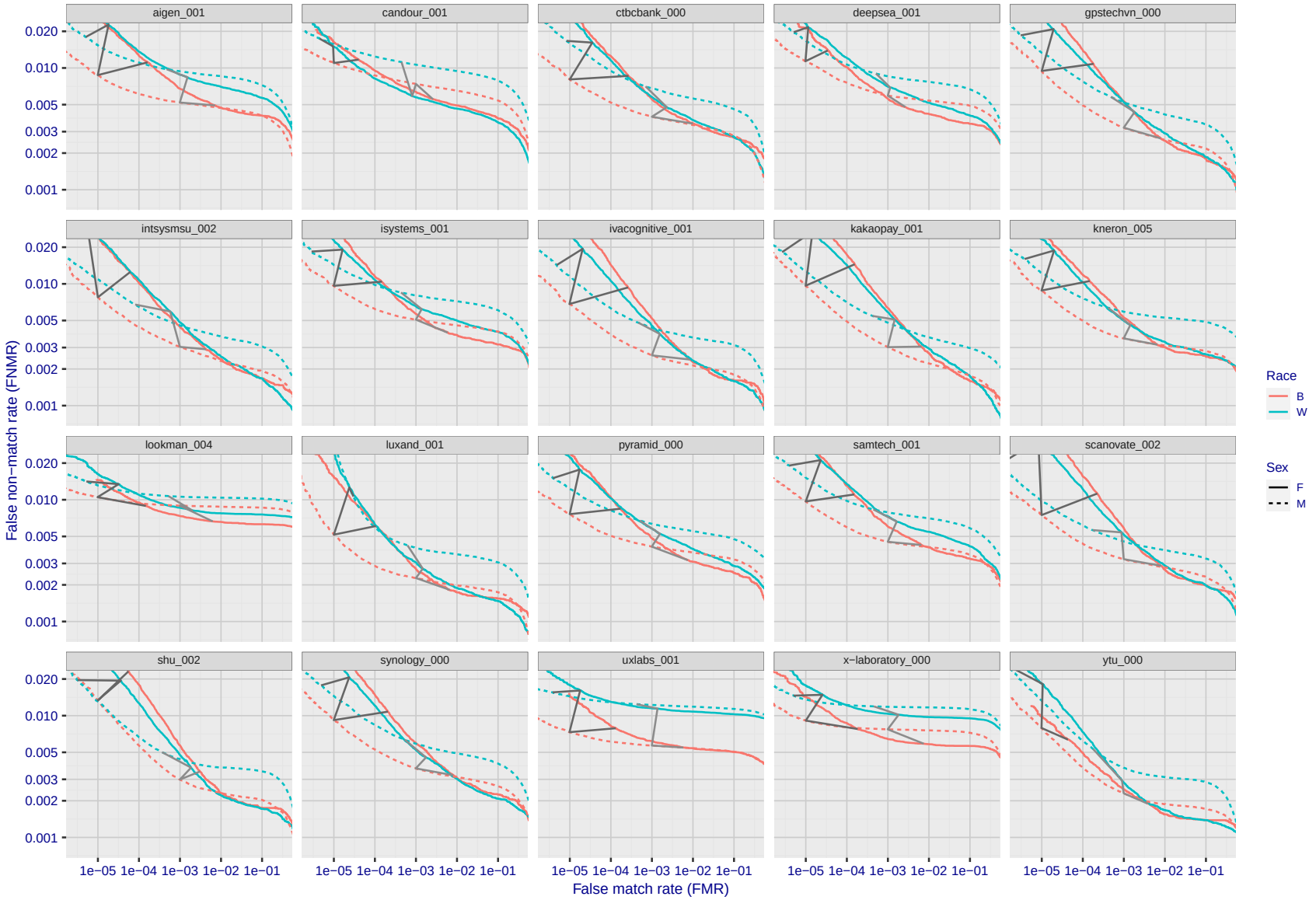

Figure 202: For the mugshot images, error tradeoff characteristics for white females, black females, black males and white males. The Z-shaped grey lines correspond to fixed thresholds, showing both *FNMR and FMR vary at one T value. Note: Many of the plots will naively be read as saying women gives worse error rates than men because the solid traces lie above the dotted ones. However, this is misleading and incomplete: The grey lines show the traces reveal horizontal shifts. Thus for the cogent-003 algorithm FNMR for men is* higher *than for women* at a fixed threshold *but, at the same time, FMR is higher for women - see Figure 285. As access control systems almost always operate at a fixed threshold, the naive interpretation is incorrect.*

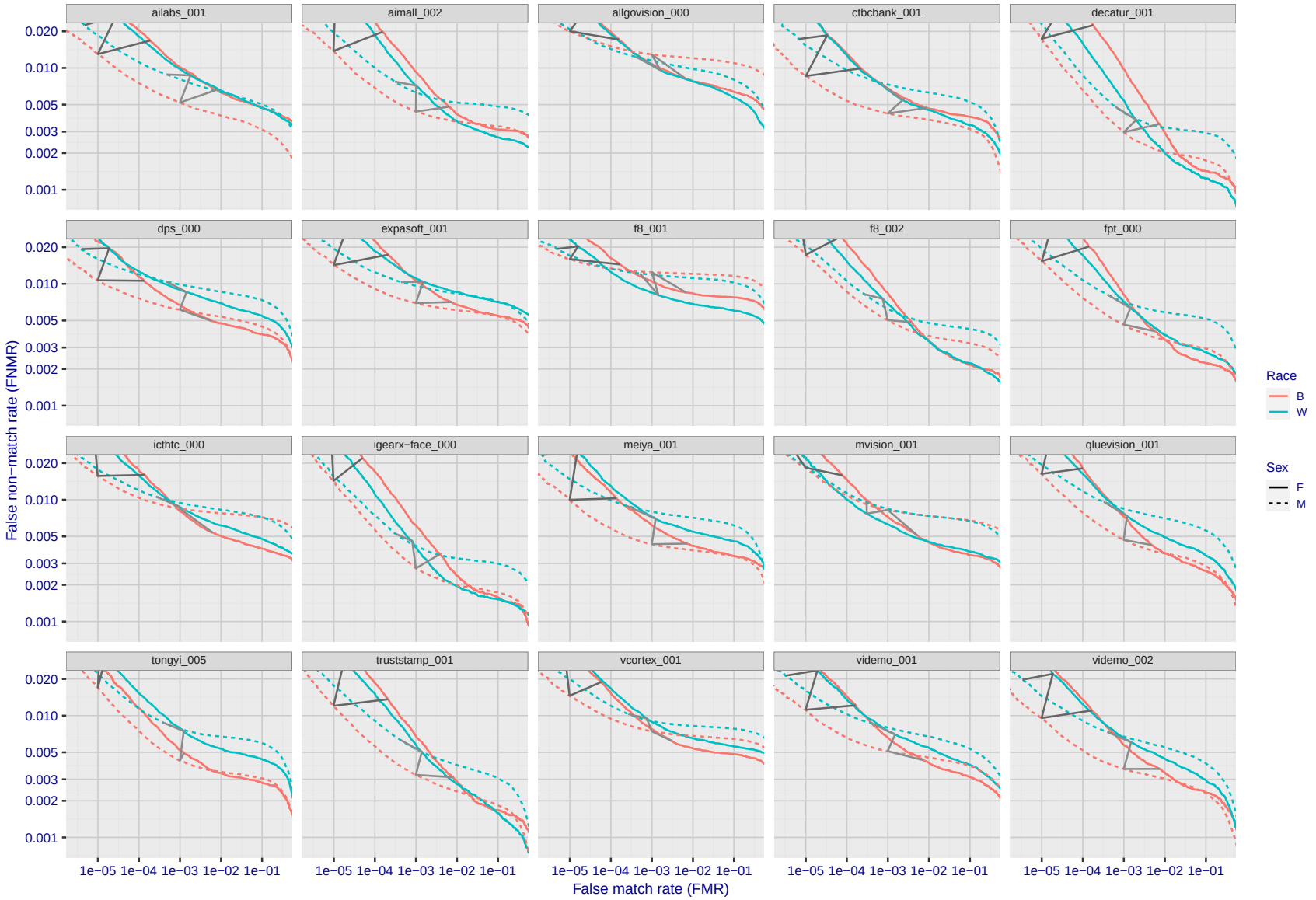

Figure 203: For the mugshot images, error tradeoff characteristics for white females, black females, black males and white males. The Z-shaped grey lines correspond to fixed thresholds, showing both *FNMR and FMR vary at one T value. Note: Many of the plots will naively be read as saying women gives worse error rates than men because the solid traces lie above the dotted ones. However, this is misleading and incomplete: The grey lines show the traces reveal horizontal shifts. Thus for the cogent-003 algorithm FNMR for men is* higher *than for women* at a fixed threshold *but, at the same time, FMR is higher for women - see Figure 285. As access control systems almost always operate at a fixed threshold, the naive interpretation is incorrect.*

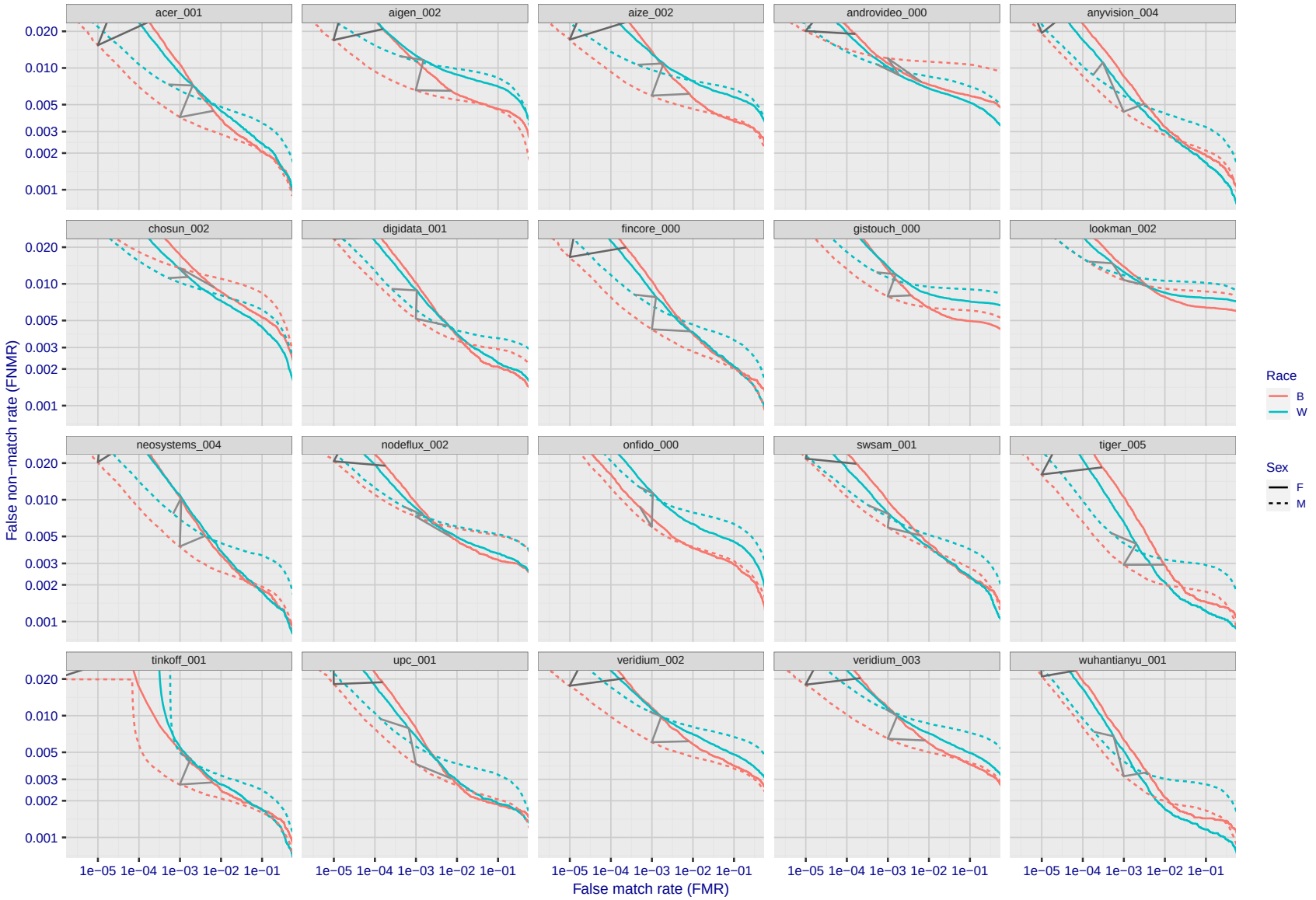

Figure 204: For the mugshot images, error tradeoff characteristics for white females, black females, black males and white males. The Z-shaped grey lines correspond to fixed thresholds, showing both *FNMR and FMR vary at one T value. Note: Many of the plots will naively be read as saying women gives worse error rates than men because the solid traces lie above the dotted ones. However, this is misleading and incomplete: The grey lines show the traces reveal horizontal shifts. Thus for the cogent-003 algorithm FNMR for men is* higher *than for women* at a fixed threshold *but, at the same time, FMR is higher for women - see Figure 285. As access control systems almost always operate at a fixed threshold, the naive interpretation is incorrect.*

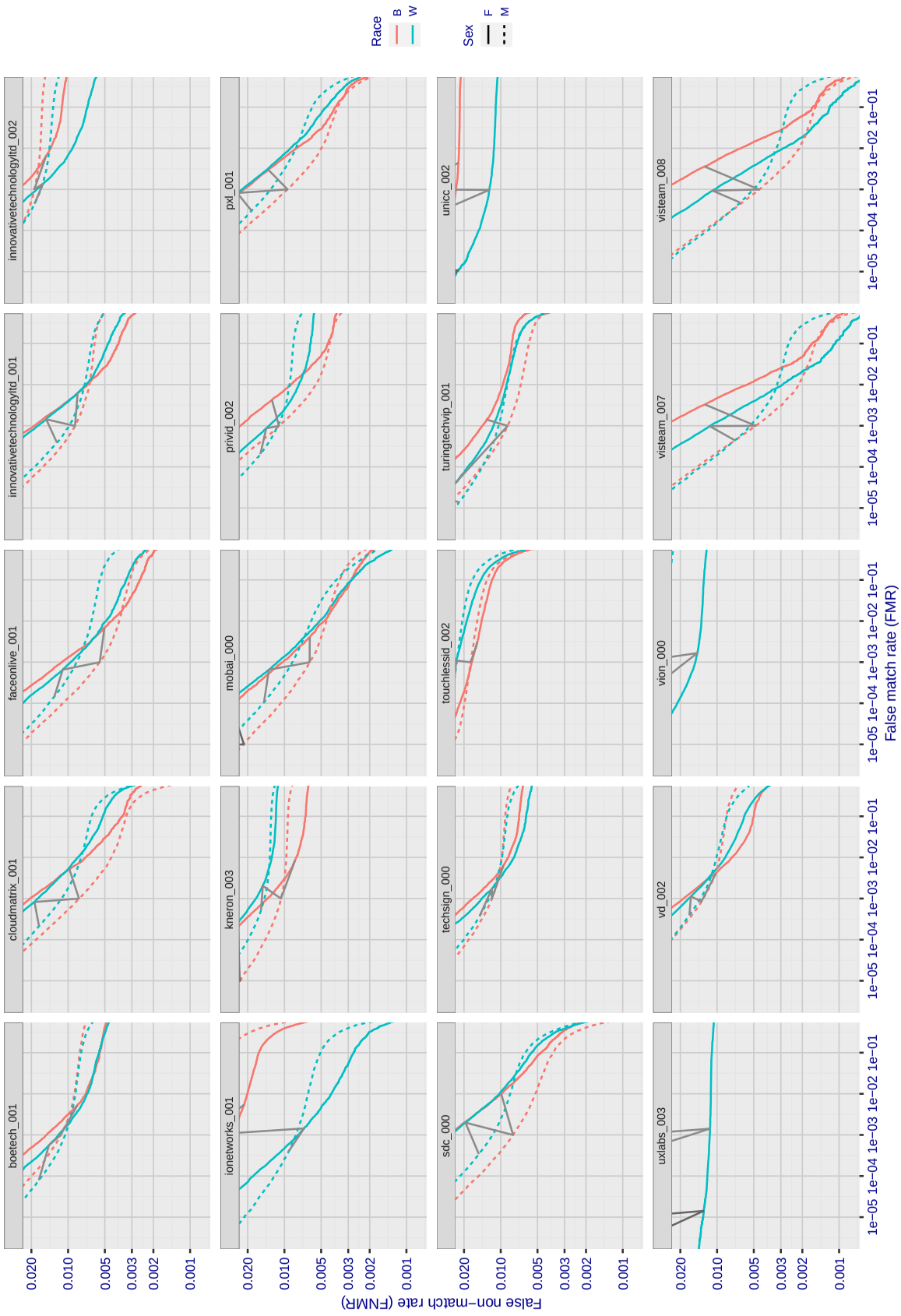

Figure 205: For the mugshot images, error tradeoff characteristics for white females, black females, black males and white males. The Z-shaped grey lines correspond to fixed thresholds, showing both FNMR and FMR vary at one T value. Note: Many of the plots will naively be read as saying women gives worse error rates than men because the solid traces lie above the dotted ones. However, this is misleading and incomplete: The grey lines show the traces reveal horizontal shifts. Thus for the cogent-003 algorithm FNMR for men is higher than for women at a fixed threshold but, at the same time, FMR is higher for women - see Figure 285. As access control systems almost always operate at a fixed threshold, the naive interpretation is incorrect.

FNMR(T) "False non-match rate"
FMR(T) "False match rate"

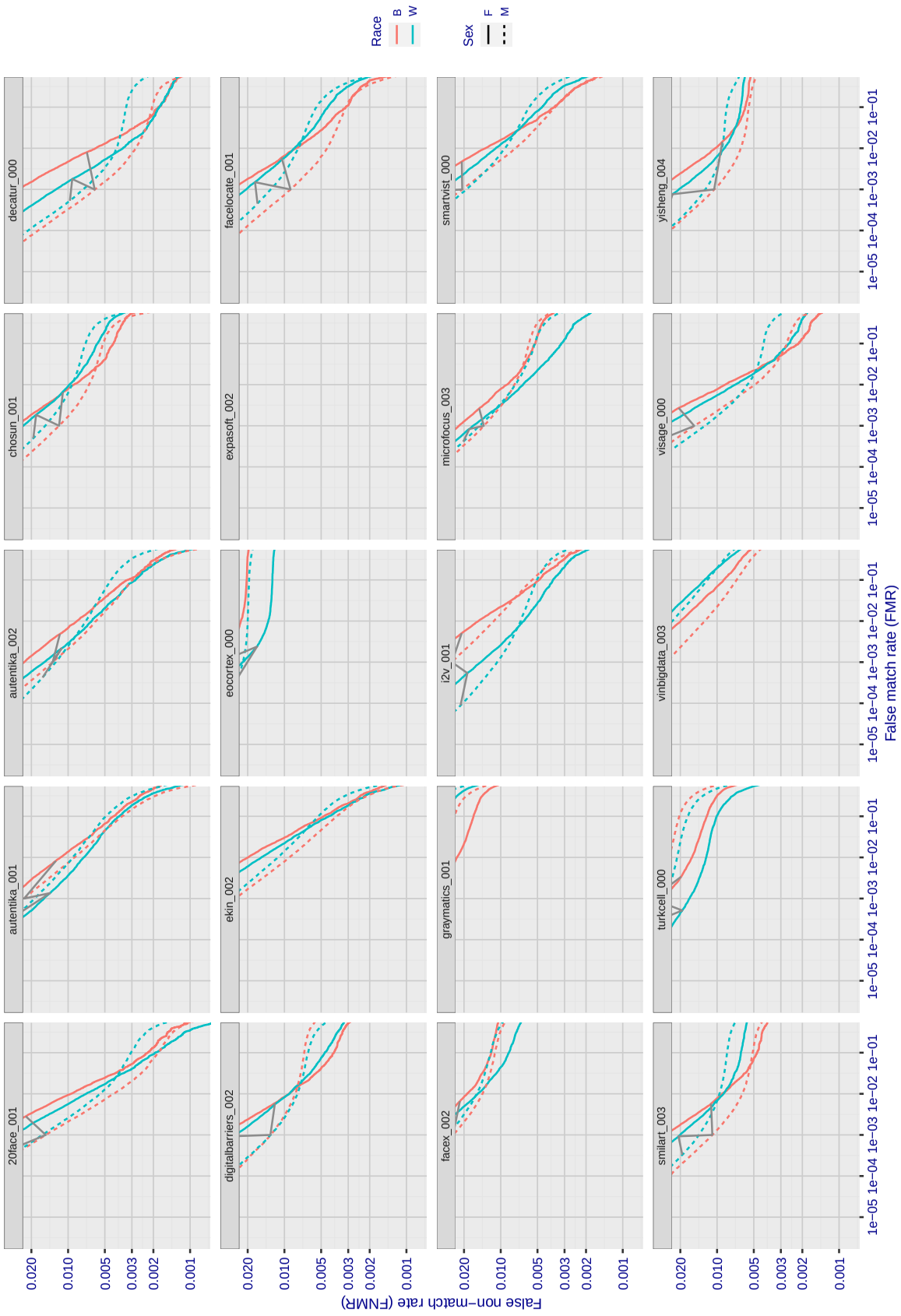

Figure 206: For the mugshot images, error tradeoff characteristics for white females, black females, black males and white males. The Z-shaped grey lines correspond to fixed thresholds, showing both FNMR and FMR vary at one T value. Note: Many of the plots will naively be read as saying women gives worse error rates than men because the solid traces lie above the dotted ones. However, this is misleading and incomplete: The grey lines show the traces reveal horizontal shifts. Thus for the cogent-003 algorithm FNMR for men is higher than for women at a fixed threshold but, at the same time, FMR is higher for women - see Figure 285. As access control systems almost always operate at a fixed threshold, the naive interpretation is incorrect.

FNMR(T) "False non-match rate"
FMR(T) "False match rate"

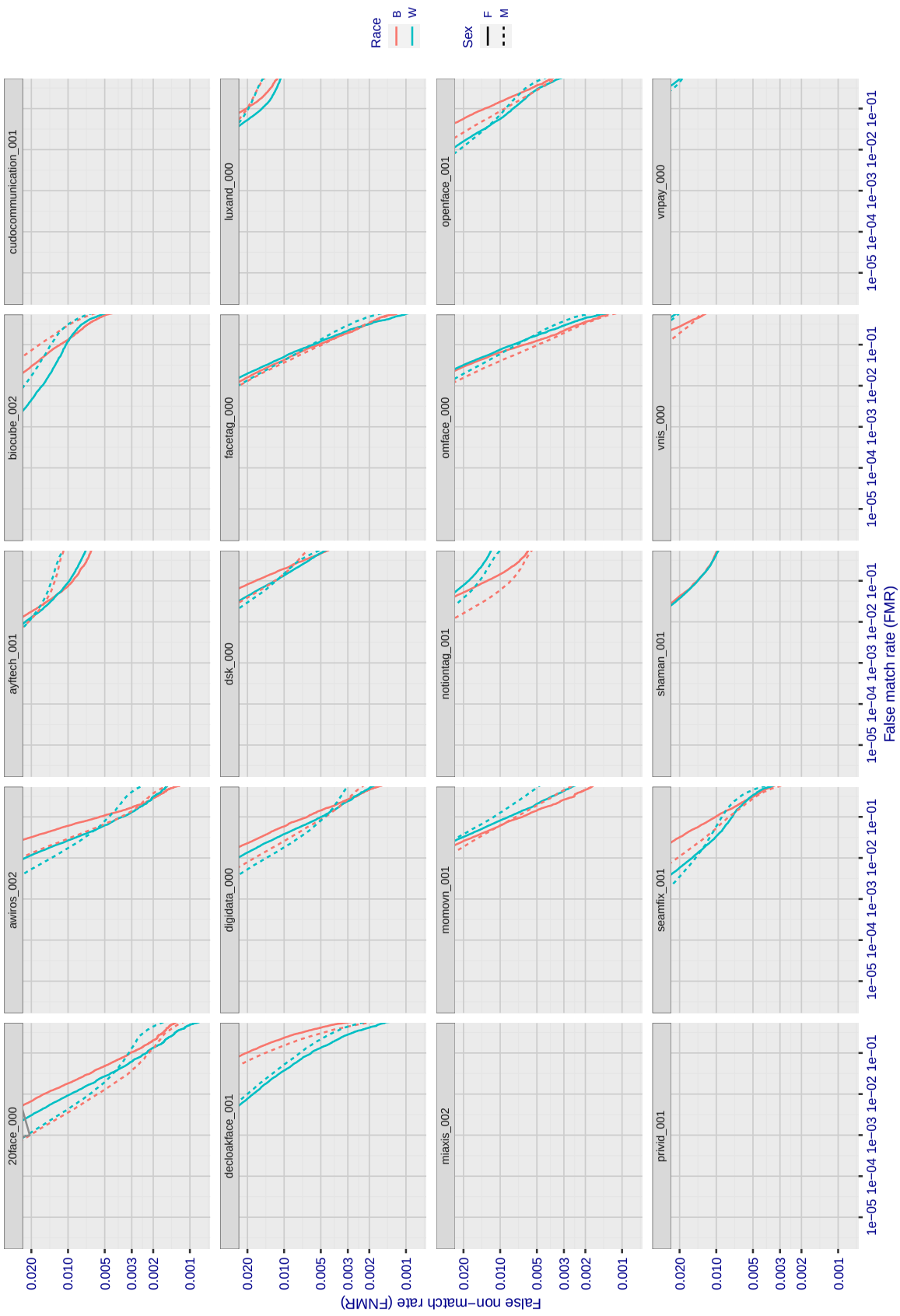

Figure 207: For the mugshot images, error tradeoff characteristics for white females, black females, black males and white males. The Z-shaped grey lines correspond to fixed thresholds, showing both FNMR and FMR vary at one T value. Note: Many of the plots will naively be read as saying women gives worse error rates than men because the solid traces lie above the dotted ones. However, this is misleading and incomplete: The grey lines show the traces reveal horizontal shifts. Thus for the cogent-003 algorithm FNMR for men is higher than for women at a fixed threshold but, at the same time, FMR is higher for women - see Figure 285. As access control systems almost always operate at a fixed threshold, the naive interpretation is incorrect.

FNMR(T) "False non-match rate"
FMR(T) "False match rate"

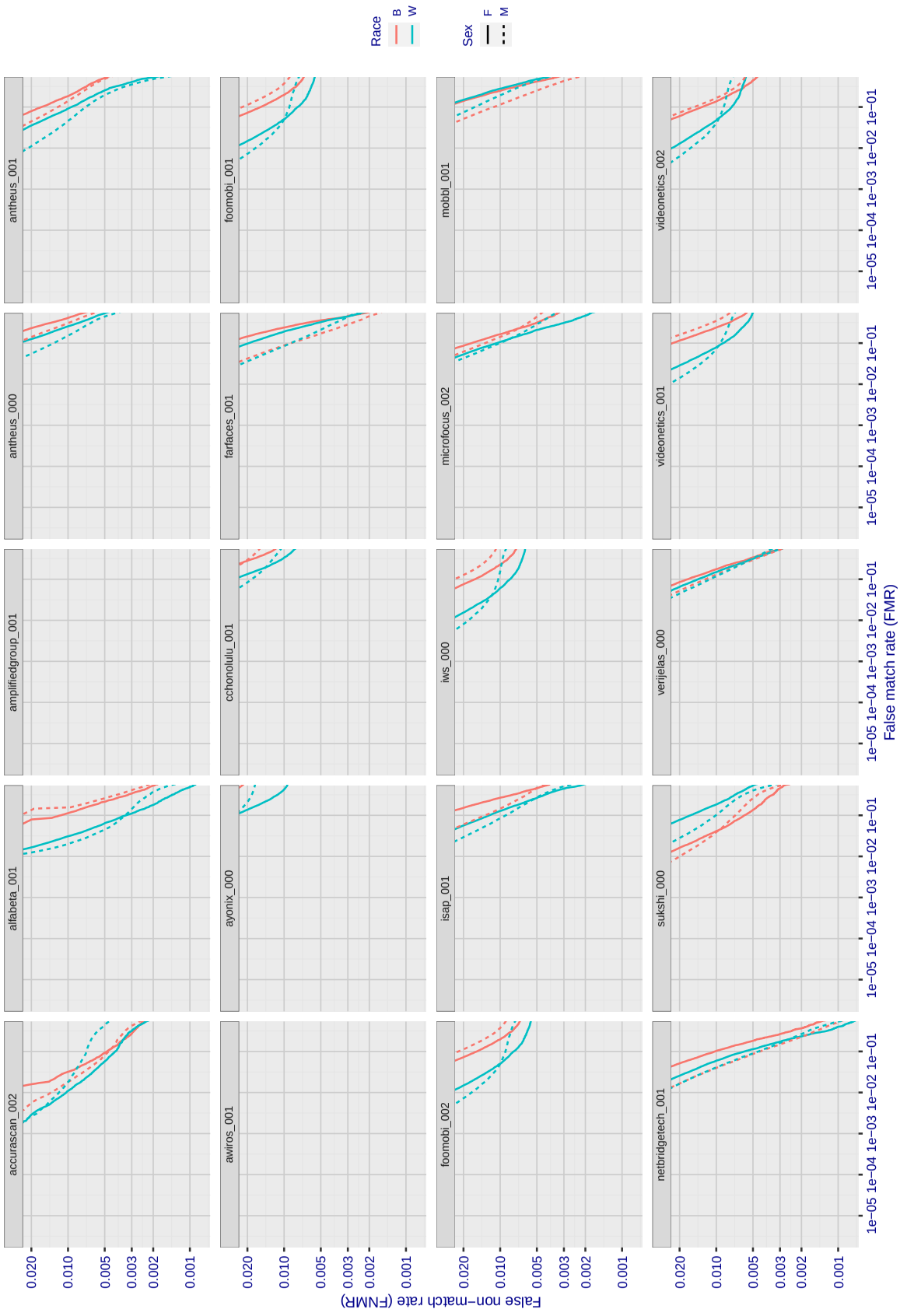

Figure 208: For the mugshot images, error tradeoff characteristics for white females, black females, black males and white males. The Z-shaped grey lines correspond to fixed thresholds, showing both *FNMR and FMR vary at one T value. Note: Many of the plots will naively be read as saying women gives worse error rates than men because the solid traces lie above the dotted ones. However, this is misleading and incomplete: The grey lines show the traces reveal horizontal shifts. Thus for the cogent-003 algorithm FNMR for men is* higher *than for women at a fixed threshold but, at the same time, FMR is higher for women - see Figure 285. As access control systems almost always operate at a fixed threshold, the naive interpretation is incorrect.*

FNMR(T) "False non-match rate"
FMR(T) "False match rate"

Figure 209: For the mugshot images, error tradeoff characteristics for white females, black females, black males and white males. The Z-shaped grey lines correspond to fixed thresholds, showing both *FNMR and FMR vary at one T value. Note: Many of the plots will naively be read as saying women gives worse error rates than men because the solid traces lie above the dotted ones. However, this is misleading and incomplete: The grey lines show the traces reveal horizontal shifts. Thus for the cogent-003 algorithm FNMR for men is* higher *than for women* at a fixed threshold *but, at the same time, FMR is higher for women - see Figure 285. As access control systems almost always operate at a fixed threshold, the naive interpretation is incorrect.*

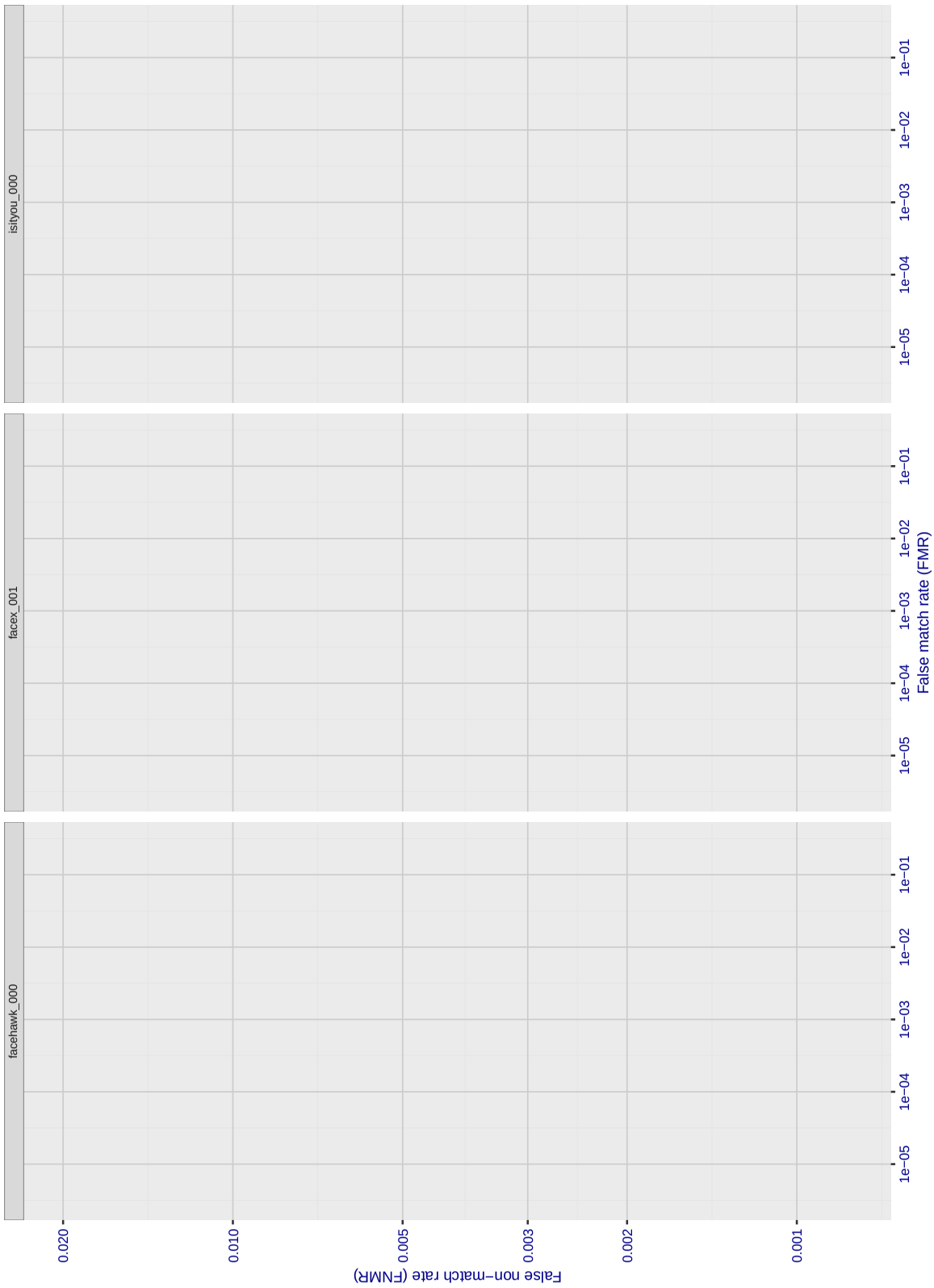

Figure 210: For the mugshot images, error tradeoff characteristics for white females, black females, black males and white males. The Z-shaped grey lines correspond to fixed thresholds, showing both *FNMR and FMR vary at one T value. Note: Many of the plots will naively be read as saying women gives worse error rates than men because the solid traces lie above the dotted ones. However, this is misleading and incomplete: The grey lines show the traces reveal horizontal shifts. Thus for the cogent-003 algorithm FNMR for men is* higher *than for women at a fixed threshold but, at the same time, FMR is higher for women - see Figure 285. As access control systems almost always operate at a fixed threshold, the naive interpretation is incorrect.*

FNMR(T) "False non-match rate"
FMR(T) "False match rate"

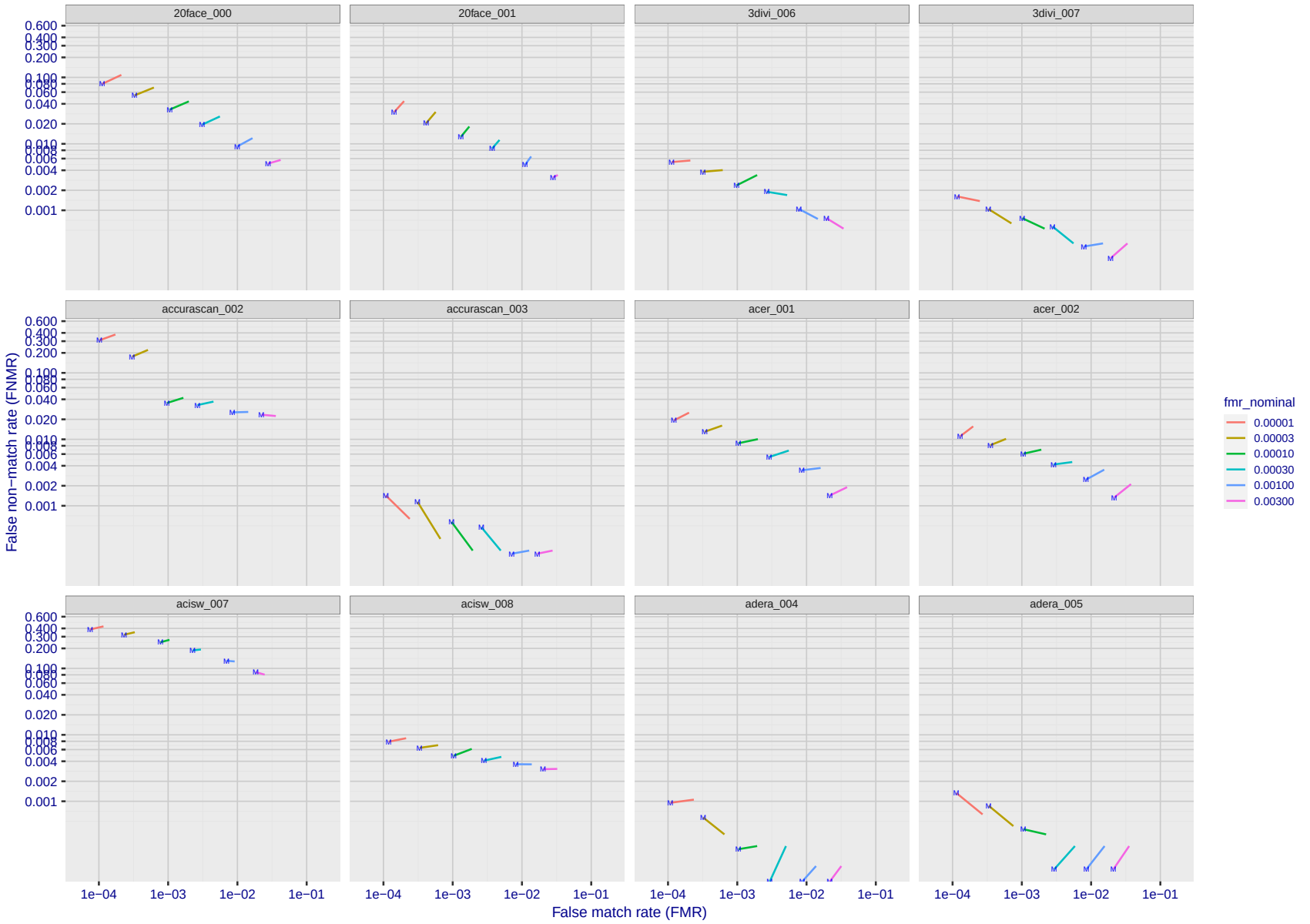

Figure 211: For the visa images, FNMR and FMR at six operating points along the DET characteristic. At each point a line is drawn between (FMR,FNMR)$_{\text{MALE}}$ and (FMR,FNMR)$_{\text{FEMALE}}$ showing how which sex has lower FMR and/or FNMR. The "M" label denotes male, the other end of the line corresponds to female. The six operating thresholds are selected to give the nominal false match rates given in the legend, and are computed over all impostor pairs regardless of age, sex, and place of birth. The plotted FMR values are broadly an order of magnitude larger than the nominal rates because FMR is computed over demographically-matched impostor pairs i.e individuals of the same sex, from the same geographic region (see section 3.6.1), and the same age group (see section 3.6.2).

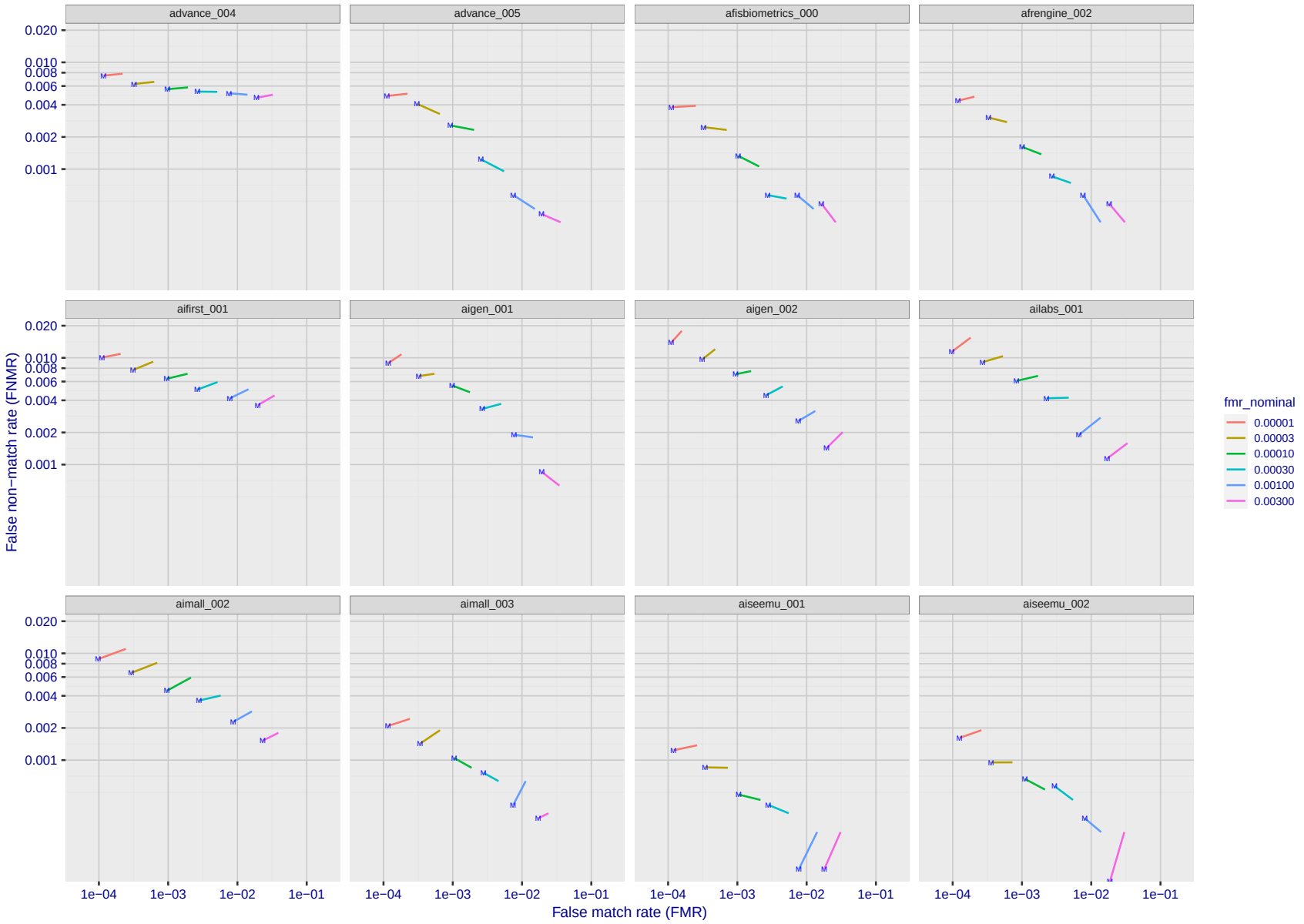

Figure 212: For the visa images, FNMR and FMR at six operating points along the DET characteristic. At each point a line is drawn between (FMR,FNMR)$_{\text{MALE}}$ and (FMR,FNMR)$_{\text{FEMALE}}$ showing how which sex has lower FMR and/or FNMR. The "M" label denotes male, the other end of the line corresponds to female. The six operating thresholds are selected to give the nominal false match rates given in the legend, and are computed over all impostor pairs regardless of age, sex, and place of birth. The plotted FMR values are broadly an order of magnitude larger than the nominal rates because FMR is computed over demographically-matched impostor pairs i.e individuals of the same sex, from the same geographic region (see section 3.6.1), and the same age group (see section 3.6.2).

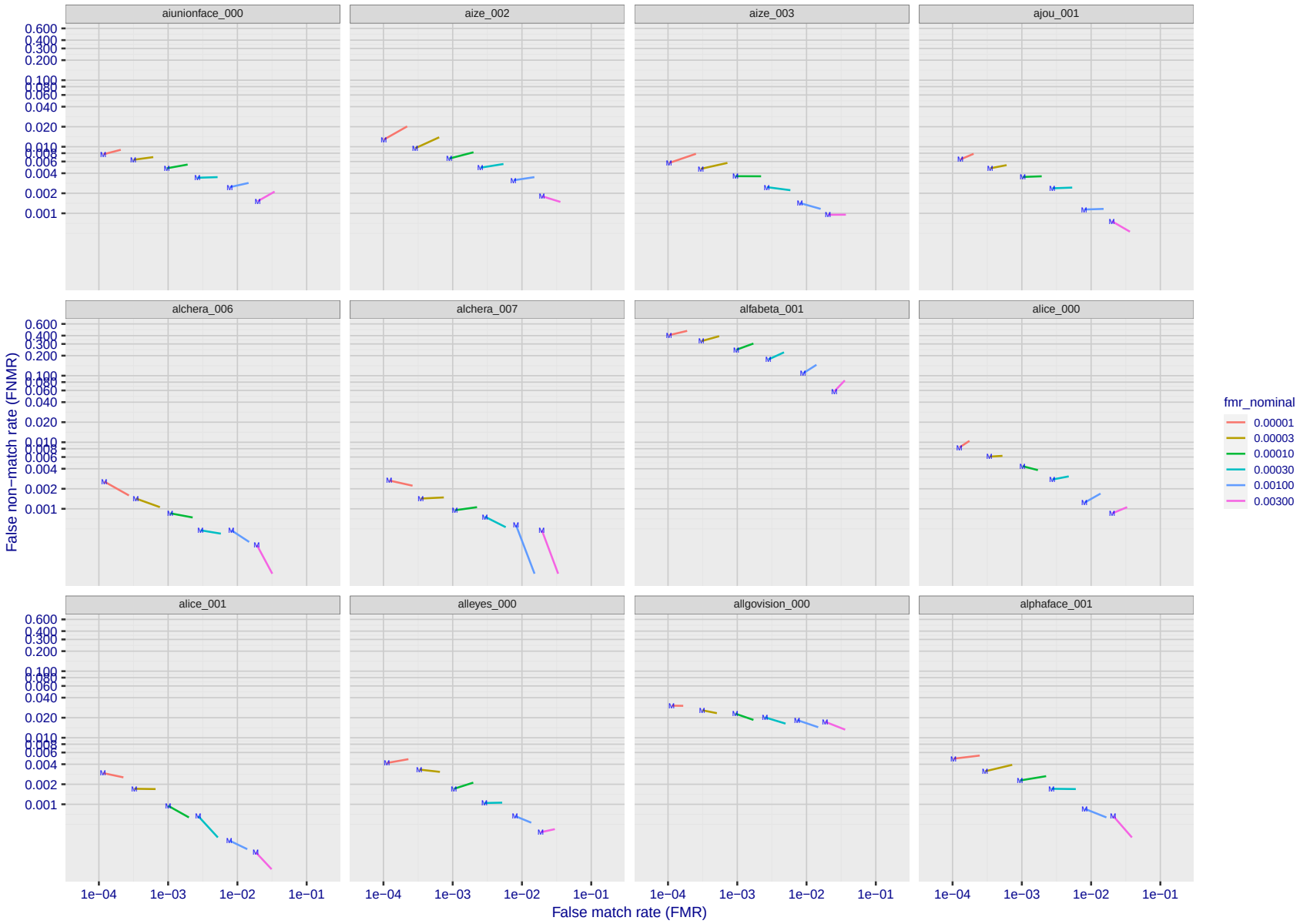

Figure 213: For the visa images, FNMR and FMR at six operating points along the DET characteristic. At each point a line is drawn between (FMR,FNMR)$_{\text{MALE}}$ and (FMR,FNMR)$_{\text{FEMALE}}$ showing how which sex has lower FMR and/or FNMR. The "M" label denotes male, the other end of the line corresponds to female. The six operating thresholds are selected to give the nominal false match rates given in the legend, and are computed over all impostor pairs regardless of age, sex, and place of birth. The plotted FMR values are broadly an order of magnitude larger than the nominal rates because FMR is computed over demographically-matched impostor pairs i.e individuals of the same sex, from the same geographic region (see section 3.6.1), and the same age group (see section 3.6.2).

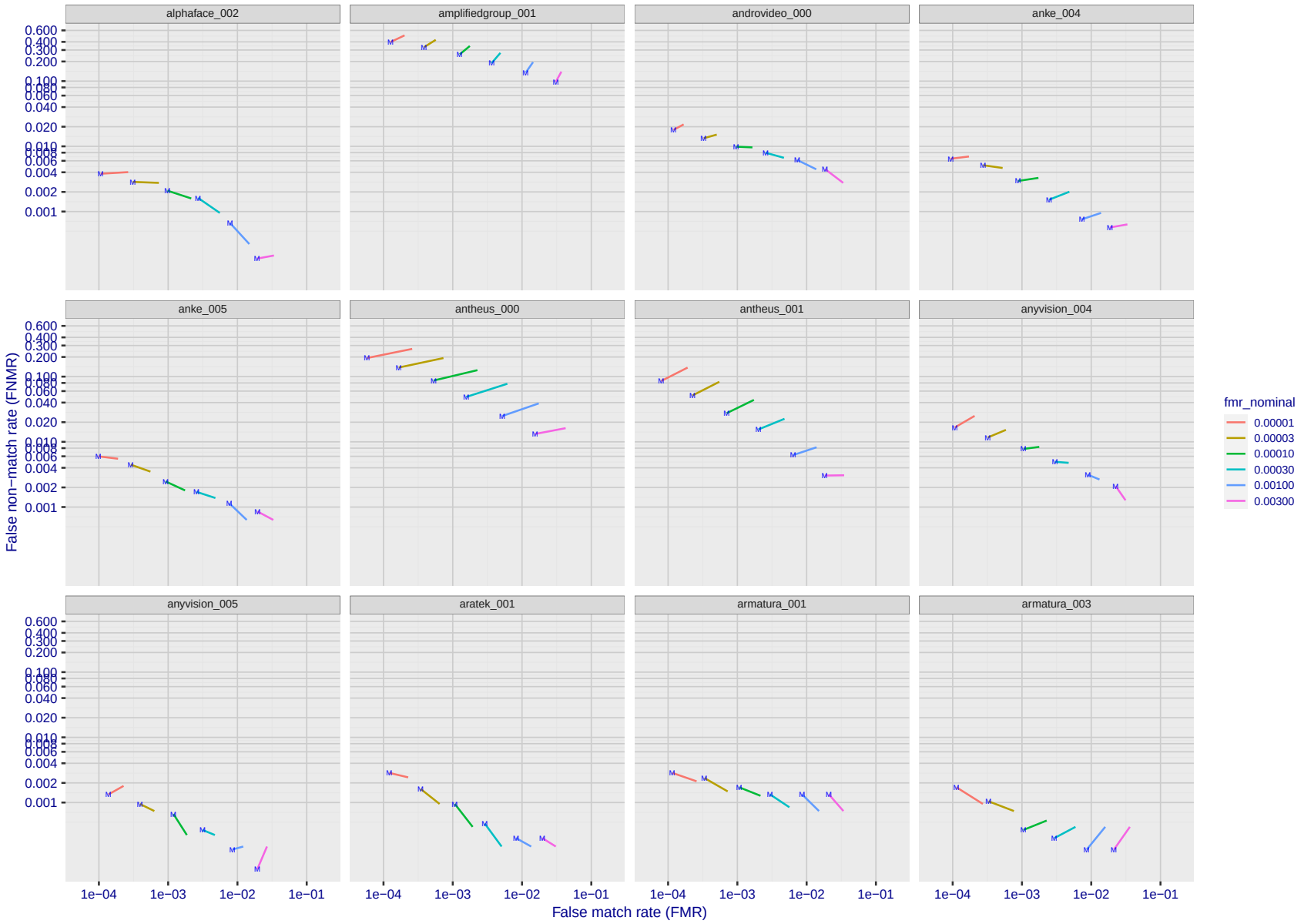

Figure 214: For the visa images, FNMR and FMR at six operating points along the DET characteristic. At each point a line is drawn between (FMR,FNMR)$_{\text{MALE}}$ and (FMR,FNMR)$_{\text{FEMALE}}$ showing how which sex has lower FMR and/or FNMR. The "M" label denotes male, the other end of the line corresponds to female. The six operating thresholds are selected to give the nominal false match rates given in the legend, and are computed over all impostor pairs regardless of age, sex, and place of birth. The plotted FMR values are broadly an order of magnitude larger than the nominal rates because FMR is computed over demographically-matched impostor pairs i.e individuals of the same sex, from the same geographic region (see section 3.6.1), and the same age group (see section 3.6.2).

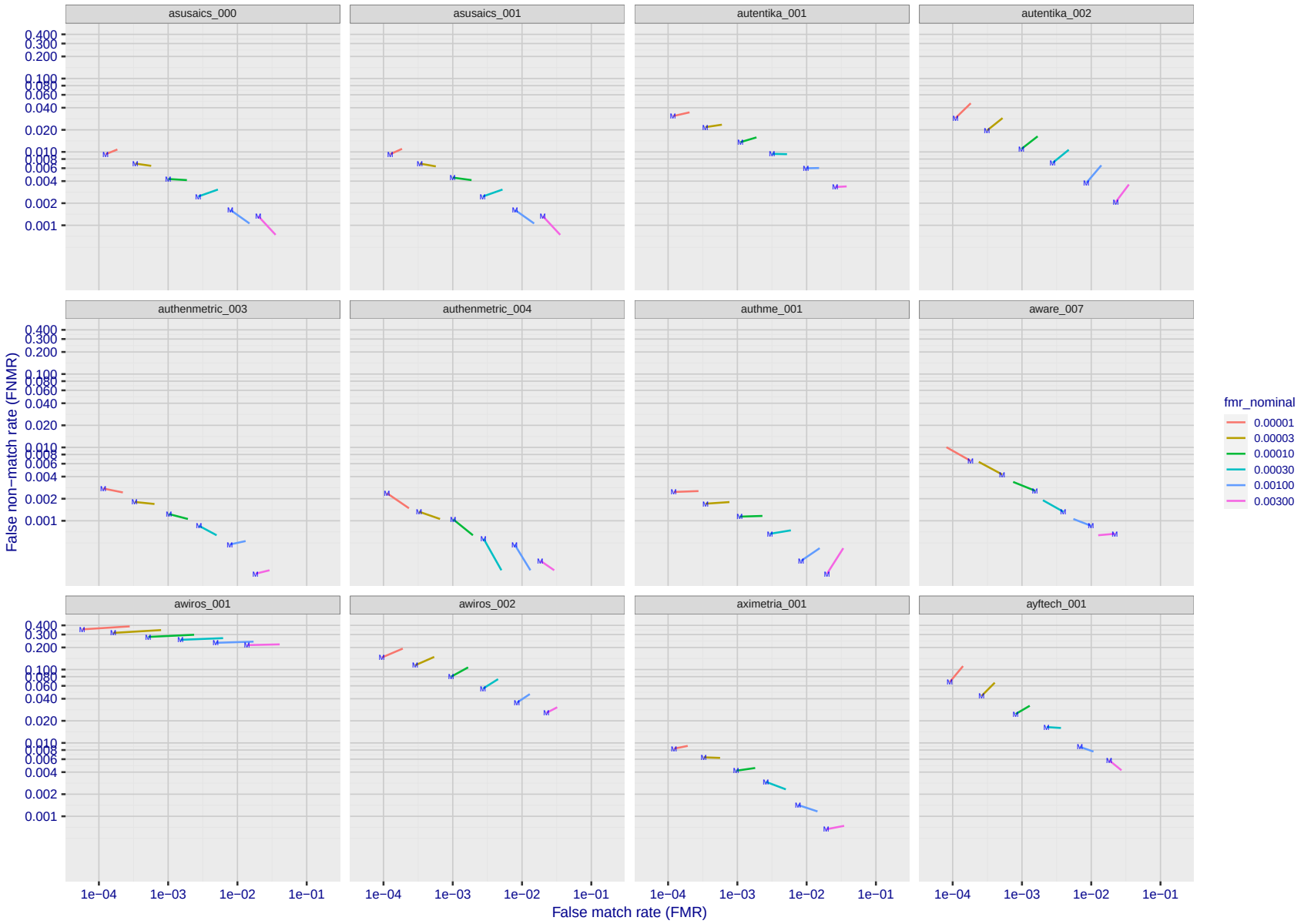

Figure 215: For the visa images, FNMR and FMR at six operating points along the DET characteristic. At each point a line is drawn between (FMR,FNMR)$_{\text{MALE}}$ and (FMR,FNMR)$_{\text{FEMALE}}$ showing how which sex has lower FMR and/or FNMR. The "M" label denotes male, the other end of the line corresponds to female. The six operating thresholds are selected to give the nominal false match rates given in the legend, and are computed over all impostor pairs regardless of age, sex, and place of birth. The plotted FMR values are broadly an order of magnitude larger than the nominal rates because FMR is computed over demographically-matched impostor pairs i.e individuals of the same sex, from the same geographic region (see section 3.6.1), and the same age group (see section 3.6.2).

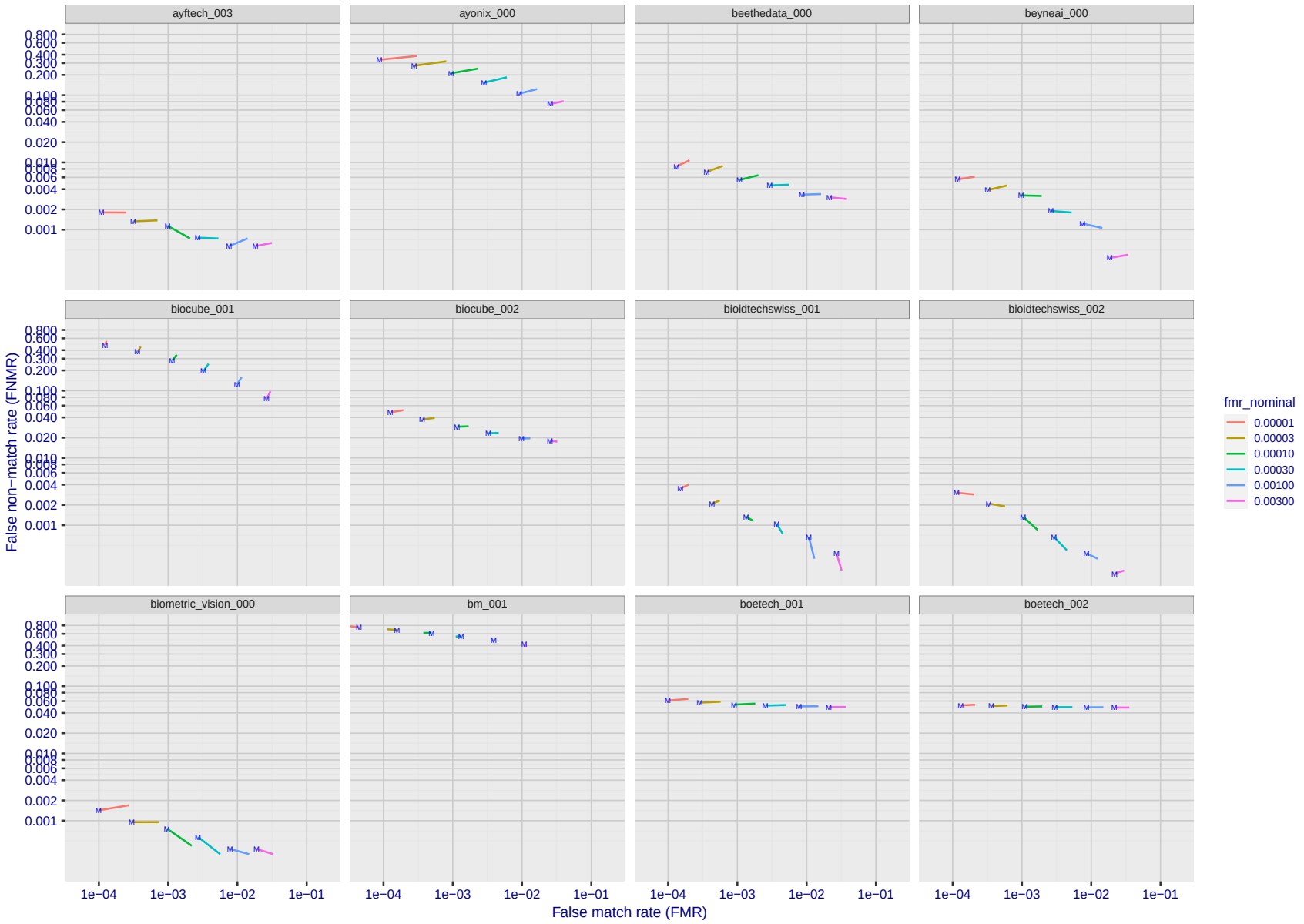

Figure 216: For the visa images, FNMR and FMR at six operating points along the DET characteristic. At each point a line is drawn between (FMR,FNMR)$_{\text{MALE}}$ and (FMR,FNMR)$_{\text{FEMALE}}$ showing how which sex has lower FMR and/or FNMR. The "M" label denotes male, the other end of the line corresponds to female. The six operating thresholds are selected to give the nominal false match rates given in the legend, and are computed over all impostor pairs regardless of age, sex, and place of birth. The plotted FMR values are broadly an order of magnitude larger than the nominal rates because FMR is computed over demographically-matched impostor pairs i.e individuals of the same sex, from the same geographic region (see section 3.6.1), and the same age group (see section 3.6.2).

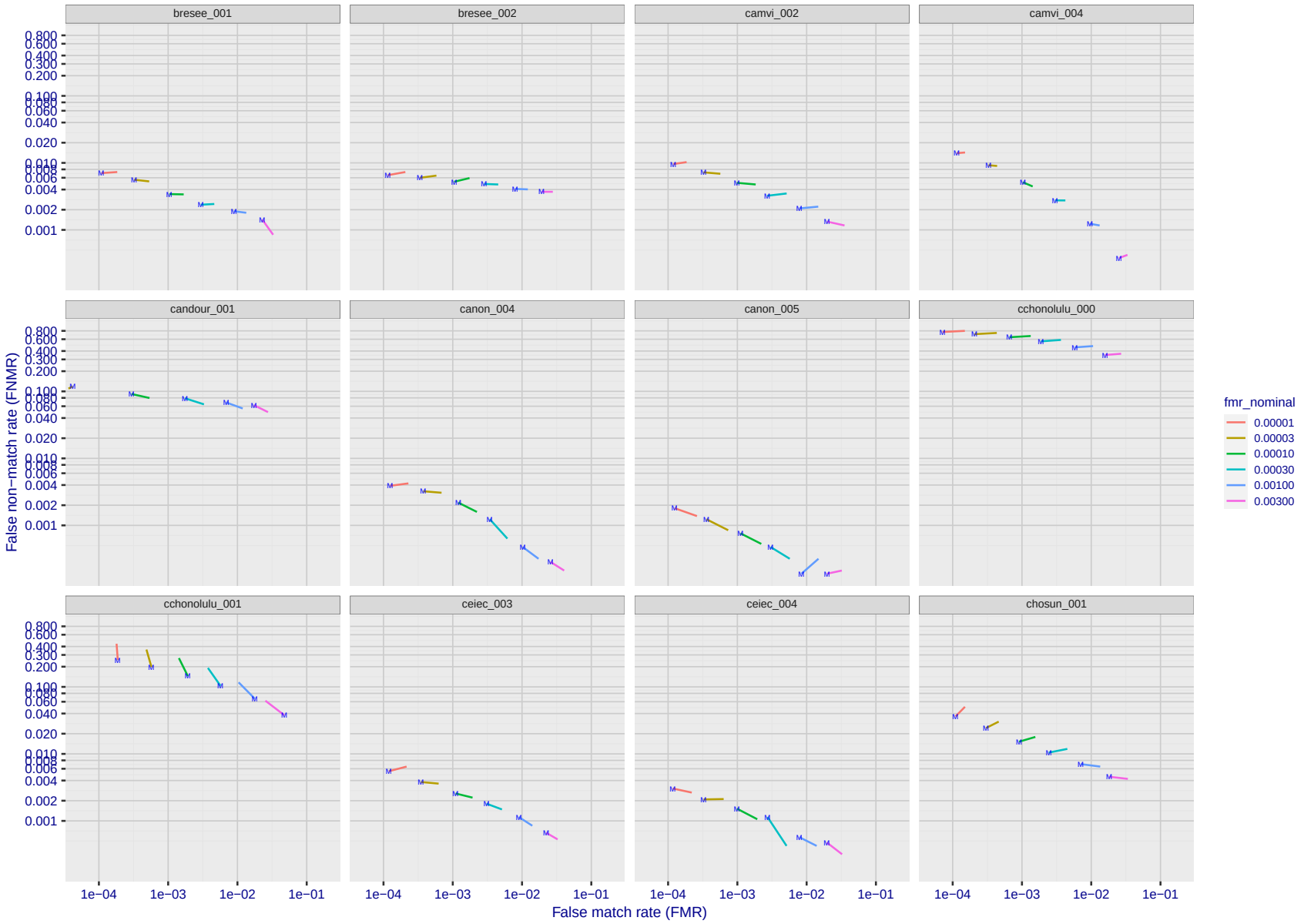

Figure 217: For the visa images, FNMR and FMR at six operating points along the DET characteristic. At each point a line is drawn between (FMR,FNMR)$_{\text{MALE}}$ and (FMR,FNMR)$_{\text{FEMALE}}$ showing how which sex has lower FMR and/or FNMR. The "M" label denotes male, the other end of the line corresponds to female. The six operating thresholds are selected to give the nominal false match rates given in the legend, and are computed over all impostor pairs regardless of age, sex, and place of birth. The plotted FMR values are broadly an order of magnitude larger than the nominal rates because FMR is computed over demographically-matched impostor pairs i.e individuals of the same sex, from the same geographic region (see section 3.6.1), and the same age group (see section 3.6.2).

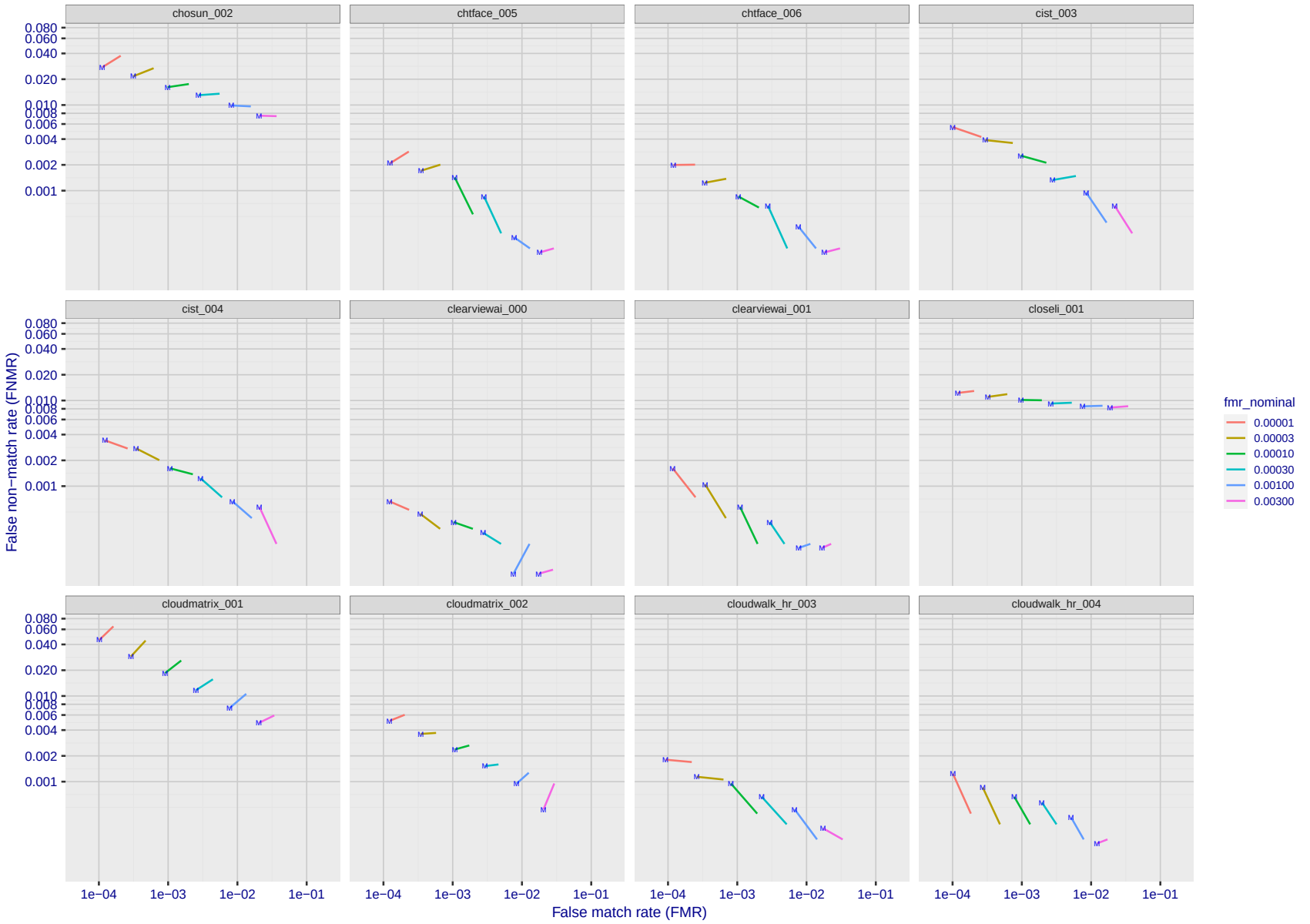

Figure 218: For the visa images, FNMR and FMR at six operating points along the DET characteristic. At each point a line is drawn between (FMR,FNMR)$_{\text{MALE}}$ and (FMR,FNMR)$_{\text{FEMALE}}$ showing how which sex has lower FMR and/or FNMR. The "M" label denotes male, the other end of the line corresponds to female. The six operating thresholds are selected to give the nominal false match rates given in the legend, and are computed over all impostor pairs regardless of age, sex, and place of birth. The plotted FMR values are broadly an order of magnitude larger than the nominal rates because FMR is computed over demographically-matched impostor pairs i.e individuals of the same sex, from the same geographic region (see section 3.6.1), and the same age group (see section 3.6.2).

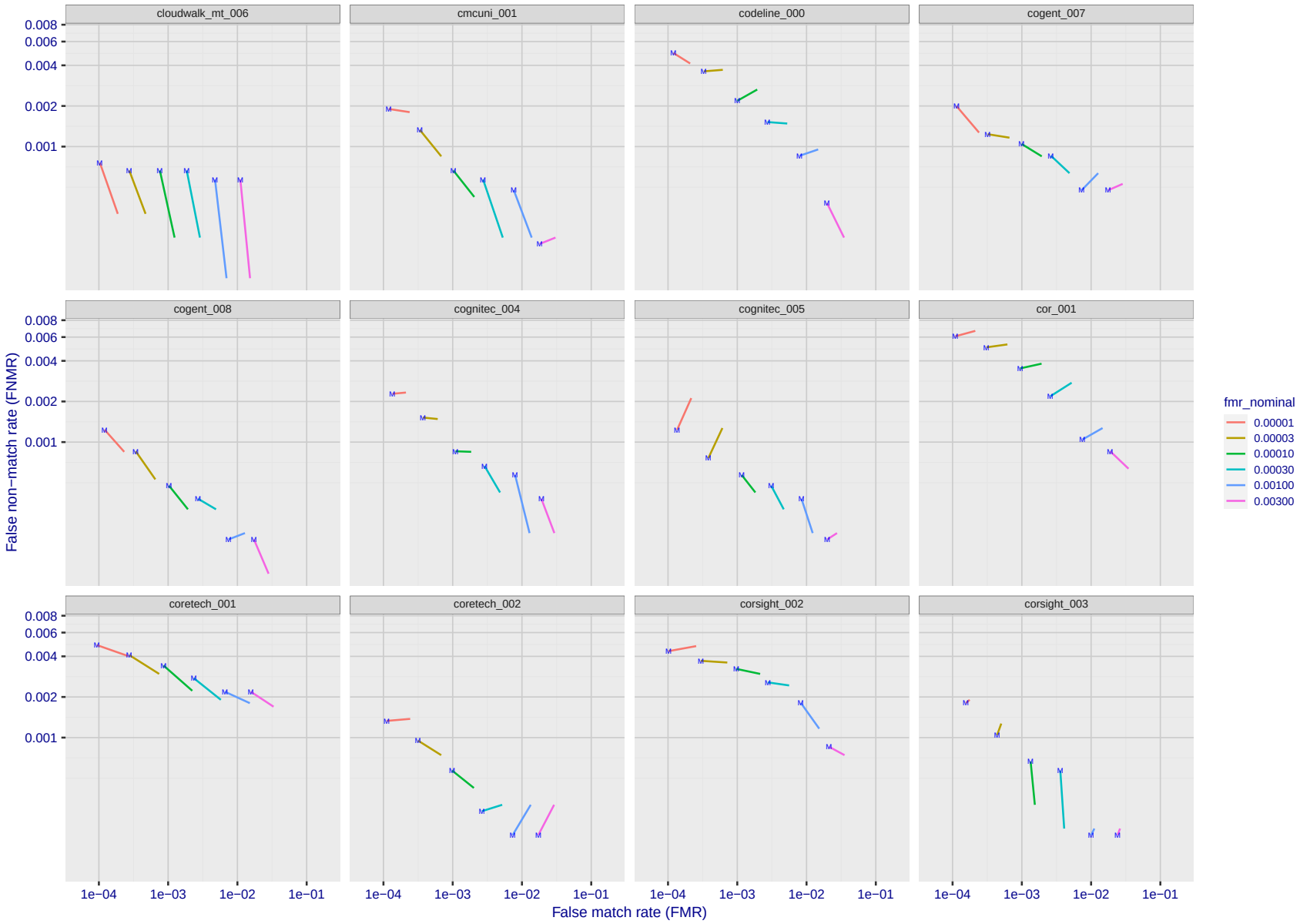

Figure 219: For the visa images, FNMR and FMR at six operating points along the DET characteristic. At each point a line is drawn between (FMR,FNMR)$_{\text{MALE}}$ and (FMR,FNMR)$_{\text{FEMALE}}$ showing how which sex has lower FMR and/or FNMR. The "M" label denotes male, the other end of the line corresponds to female. The six operating thresholds are selected to give the nominal false match rates given in the legend, and are computed over all impostor pairs regardless of age, sex, and place of birth. The plotted FMR values are broadly an order of magnitude larger than the nominal rates because FMR is computed over demographically-matched impostor pairs i.e individuals of the same sex, from the same geographic region (see section 3.6.1), and the same age group (see section 3.6.2).

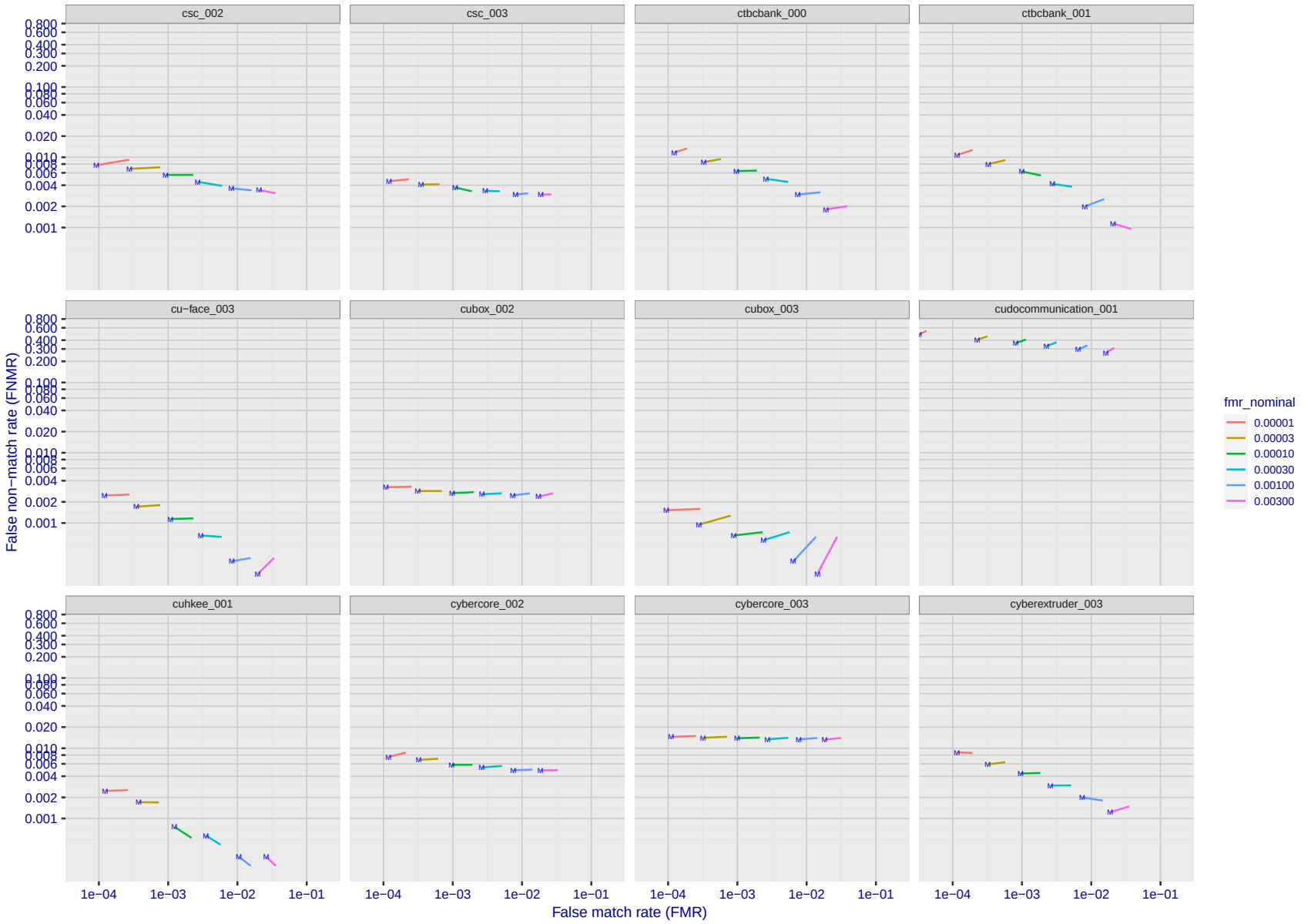

Figure 220: For the visa images, FNMR and FMR at six operating points along the DET characteristic. At each point a line is drawn between (FMR,FNMR)$_{\text{MALE}}$ and (FMR,FNMR)$_{\text{FEMALE}}$ showing how which sex has lower FMR and/or FNMR. The "M" label denotes male, the other end of the line corresponds to female. The six operating thresholds are selected to give the nominal false match rates given in the legend, and are computed over all impostor pairs regardless of age, sex, and place of birth. The plotted FMR values are broadly an order of magnitude larger than the nominal rates because FMR is computed over demographically-matched impostor pairs i.e individuals of the same sex, from the same geographic region (see section 3.6.1), and the same age group (see section 3.6.2).

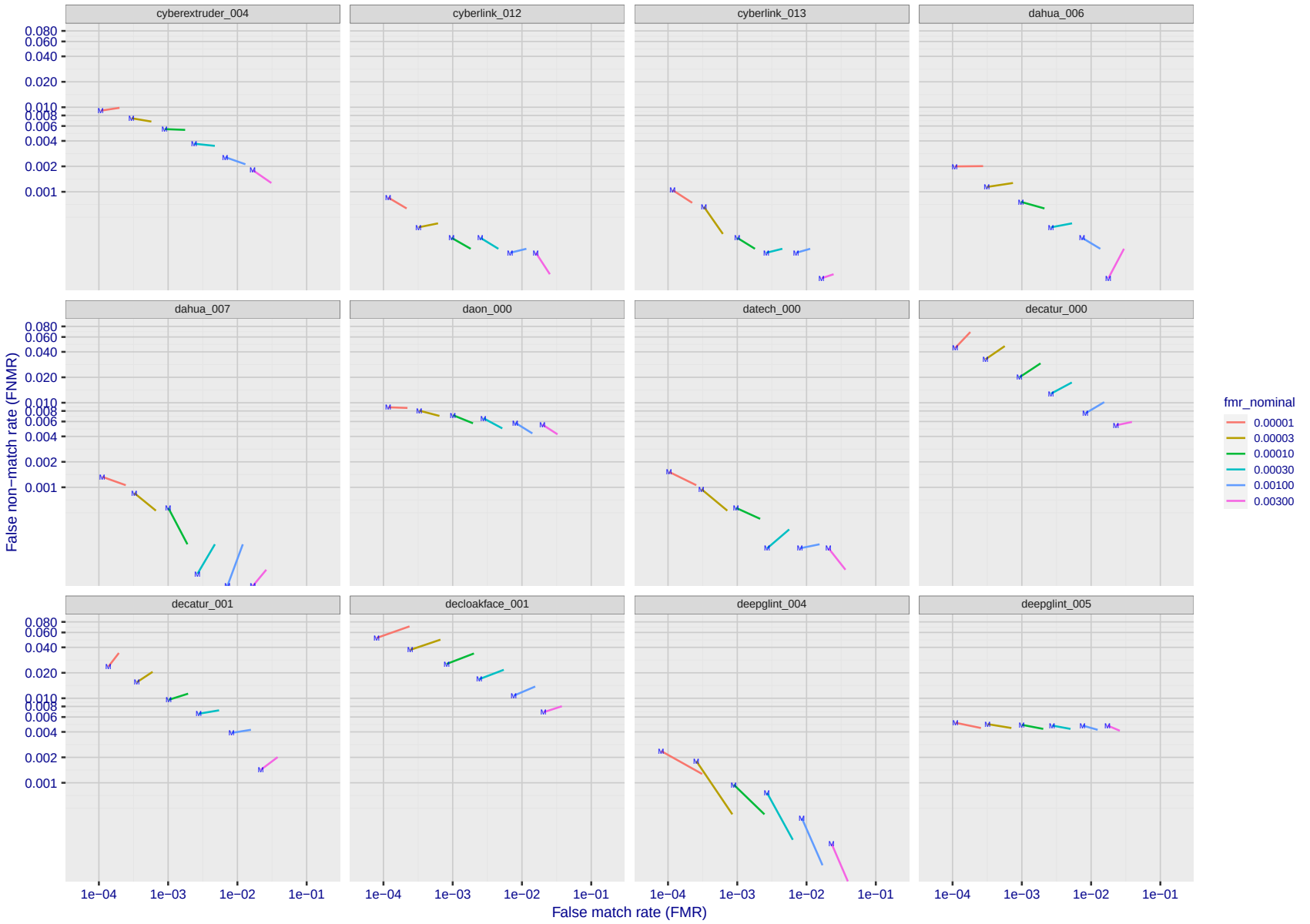

Figure 221: For the visa images, FNMR and FMR at six operating points along the DET characteristic. At each point a line is drawn between (FMR,FNMR)$_{\text{MALE}}$ and (FMR,FNMR)$_{\text{FEMALE}}$ showing how which sex has lower FMR and/or FNMR. The "M" label denotes male, the other end of the line corresponds to female. The six operating thresholds are selected to give the nominal false match rates given in the legend, and are computed over all impostor pairs regardless of age, sex, and place of birth. The plotted FMR values are broadly an order of magnitude larger than the nominal rates because FMR is computed over demographically-matched impostor pairs i.e individuals of the same sex, from the same geographic region (see section 3.6.1), and the same age group (see section 3.6.2).

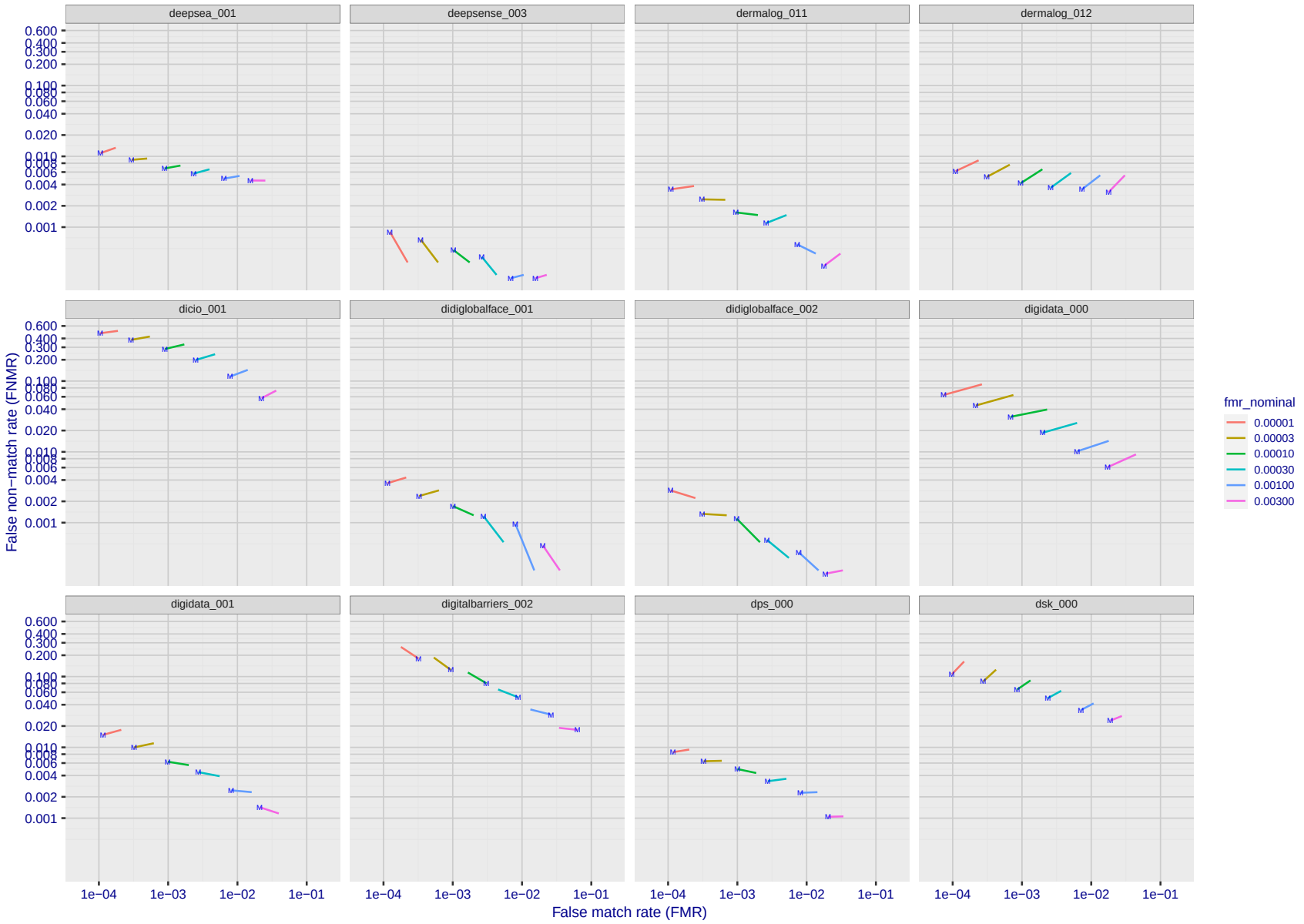

Figure 222: For the visa images, FNMR and FMR at six operating points along the DET characteristic. At each point a line is drawn between (FMR,FNMR)$_{\text{MALE}}$ and (FMR,FNMR)$_{\text{FEMALE}}$ showing how which sex has lower FMR and/or FNMR. The "M" label denotes male, the other end of the line corresponds to female. The six operating thresholds are selected to give the nominal false match rates given in the legend, and are computed over all impostor pairs regardless of age, sex, and place of birth. The plotted FMR values are broadly an order of magnitude larger than the nominal rates because FMR is computed over demographically-matched impostor pairs i.e individuals of the same sex, from the same geographic region (see section 3.6.1), and the same age group (see section 3.6.2).

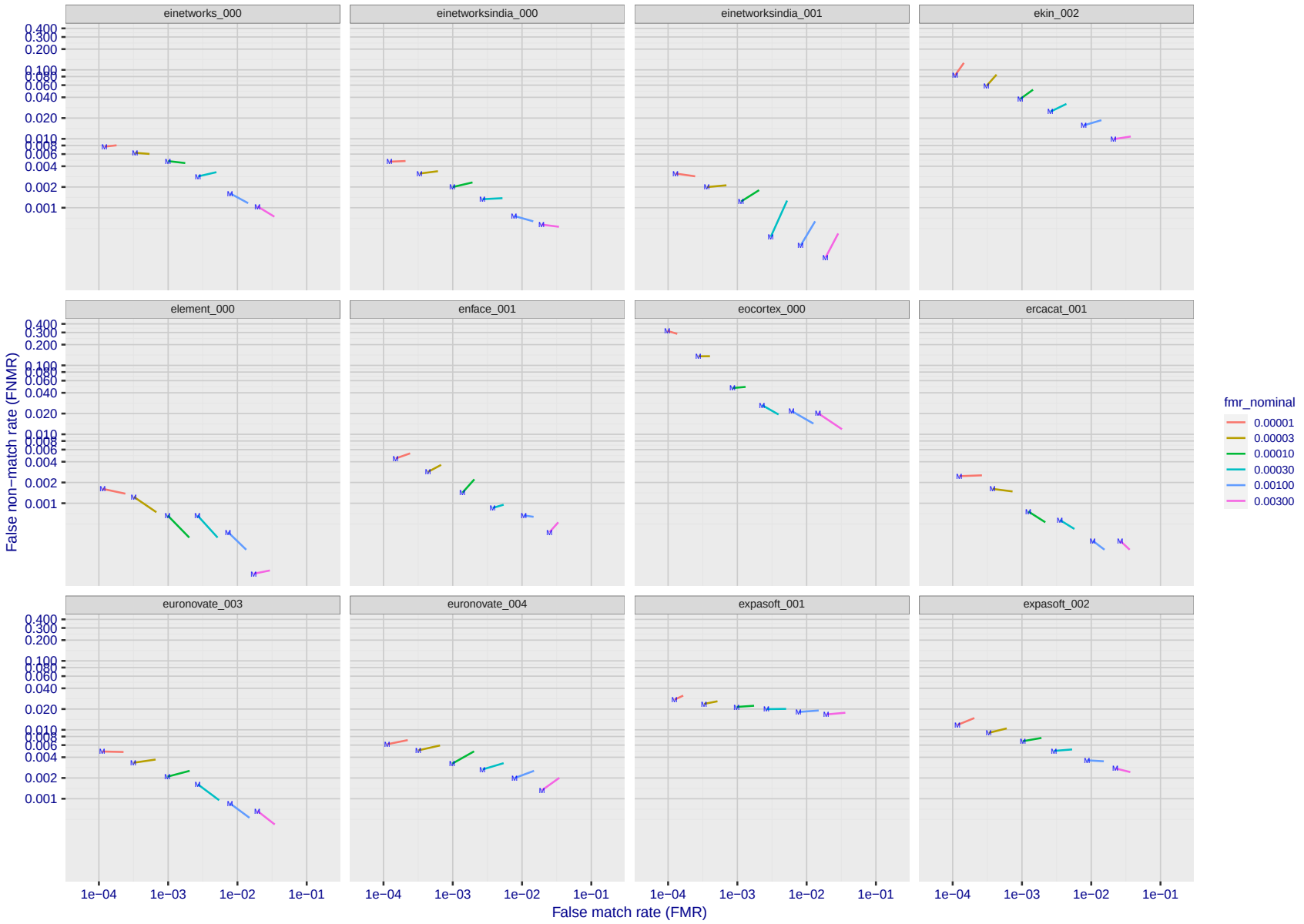

Figure 223: For the visa images, FNMR and FMR at six operating points along the DET characteristic. At each point a line is drawn between (FMR,FNMR)$_{\text{MALE}}$ and (FMR,FNMR)$_{\text{FEMALE}}$ showing how which sex has lower FMR and/or FNMR. The "M" label denotes male, the other end of the line corresponds to female. The six operating thresholds are selected to give the nominal false match rates given in the legend, and are computed over all impostor pairs regardless of age, sex, and place of birth. The plotted FMR values are broadly an order of magnitude larger than the nominal rates because FMR is computed over demographically-matched impostor pairs i.e individuals of the same sex, from the same geographic region (see section 3.6.1), and the same age group (see section 3.6.2).

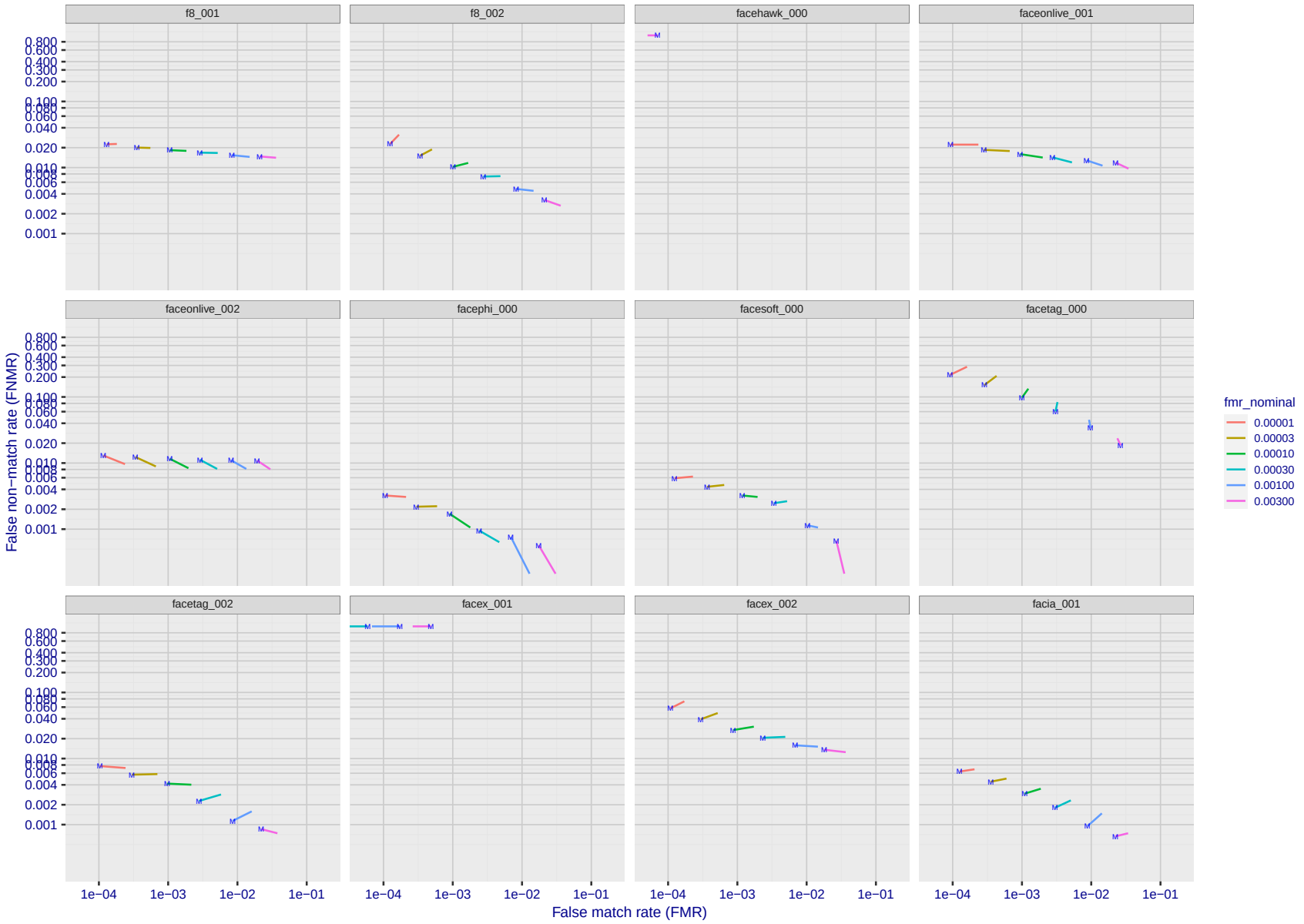

Figure 224: For the visa images, FNMR and FMR at six operating points along the DET characteristic. At each point a line is drawn between (FMR,FNMR)$_{\text{MALE}}$ and (FMR,FNMR)$_{\text{FEMALE}}$ showing how which sex has lower FMR and/or FNMR. The "M" label denotes male, the other end of the line corresponds to female. The six operating thresholds are selected to give the nominal false match rates given in the legend, and are computed over all impostor pairs regardless of age, sex, and place of birth. The plotted FMR values are broadly an order of magnitude larger than the nominal rates because FMR is computed over demographically-matched impostor pairs i.e individuals of the same sex, from the same geographic region (see section 3.6.1), and the same age group (see section 3.6.2).

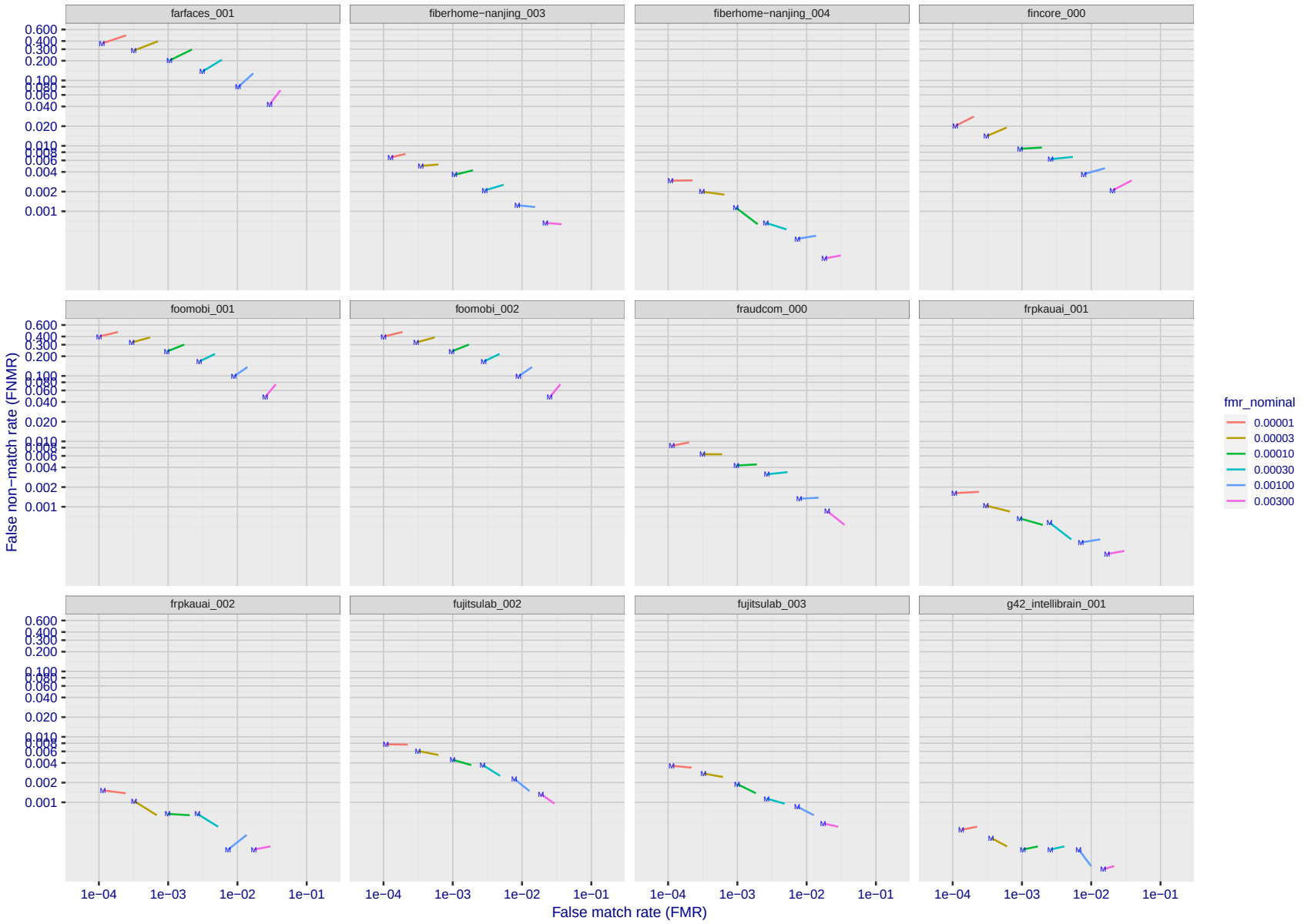

Figure 225: For the visa images, FNMR and FMR at six operating points along the DET characteristic. At each point a line is drawn between (FMR,FNMR)$_{\text{MALE}}$ and (FMR,FNMR)$_{\text{FEMALE}}$ showing how which sex has lower FMR and/or FNMR. The "M" label denotes male, the other end of the line corresponds to female. The six operating thresholds are selected to give the nominal false match rates given in the legend, and are computed over all impostor pairs regardless of age, sex, and place of birth. The plotted FMR values are broadly an order of magnitude larger than the nominal rates because FMR is computed over demographically-matched impostor pairs i.e individuals of the same sex, from the same geographic region (see section 3.6.1), and the same age group (see section 3.6.2).

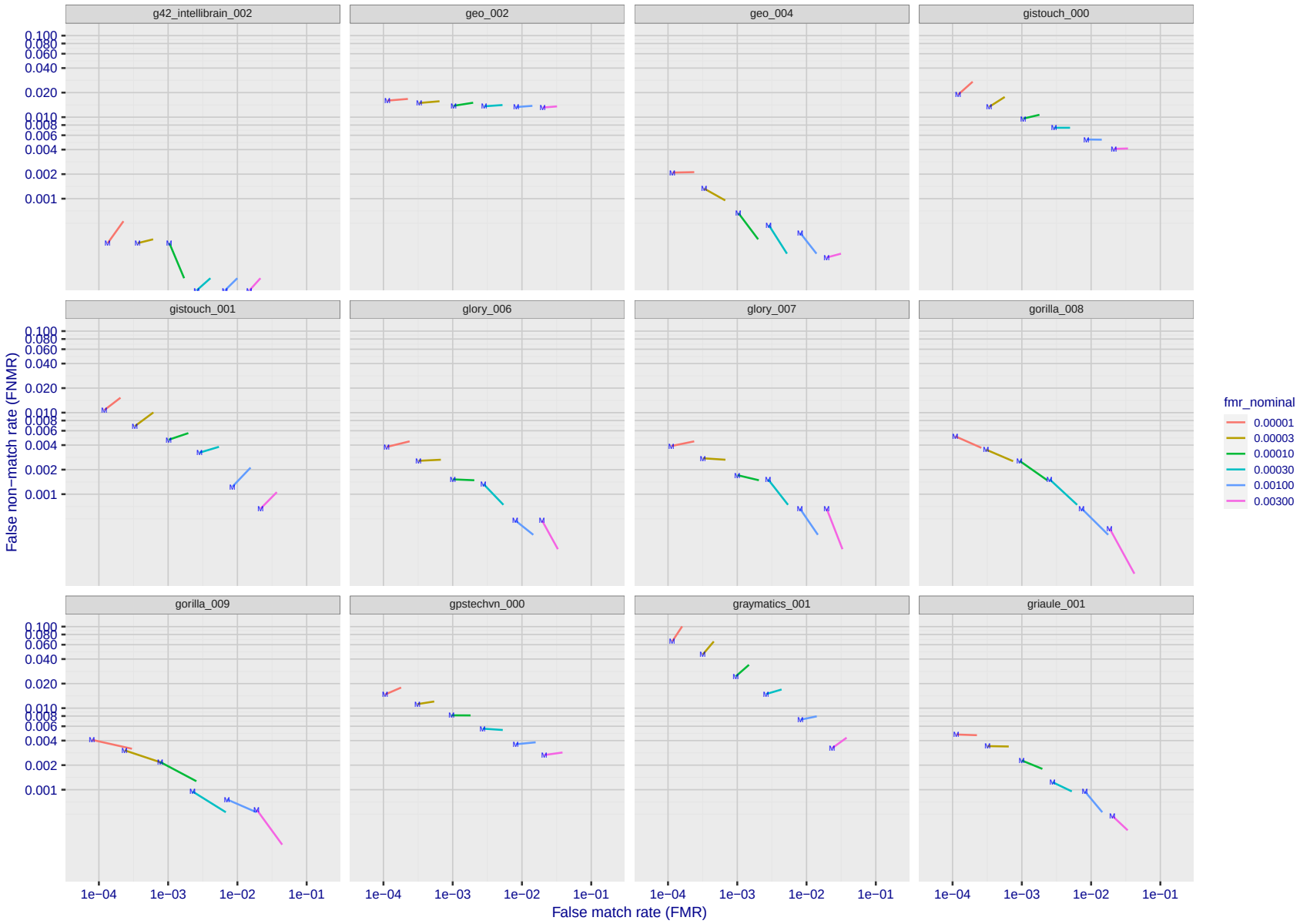

Figure 226: For the visa images, FNMR and FMR at six operating points along the DET characteristic. At each point a line is drawn between (FMR,FNMR)$_{\text{MALE}}$ and (FMR,FNMR)$_{\text{FEMALE}}$ showing how which sex has lower FMR and/or FNMR. The "M" label denotes male, the other end of the line corresponds to female. The six operating thresholds are selected to give the nominal false match rates given in the legend, and are computed over all impostor pairs regardless of age, sex, and place of birth. The plotted FMR values are broadly an order of magnitude larger than the nominal rates because FMR is computed over demographically-matched impostor pairs i.e individuals of the same sex, from the same geographic region (see section 3.6.1), and the same age group (see section 3.6.2).

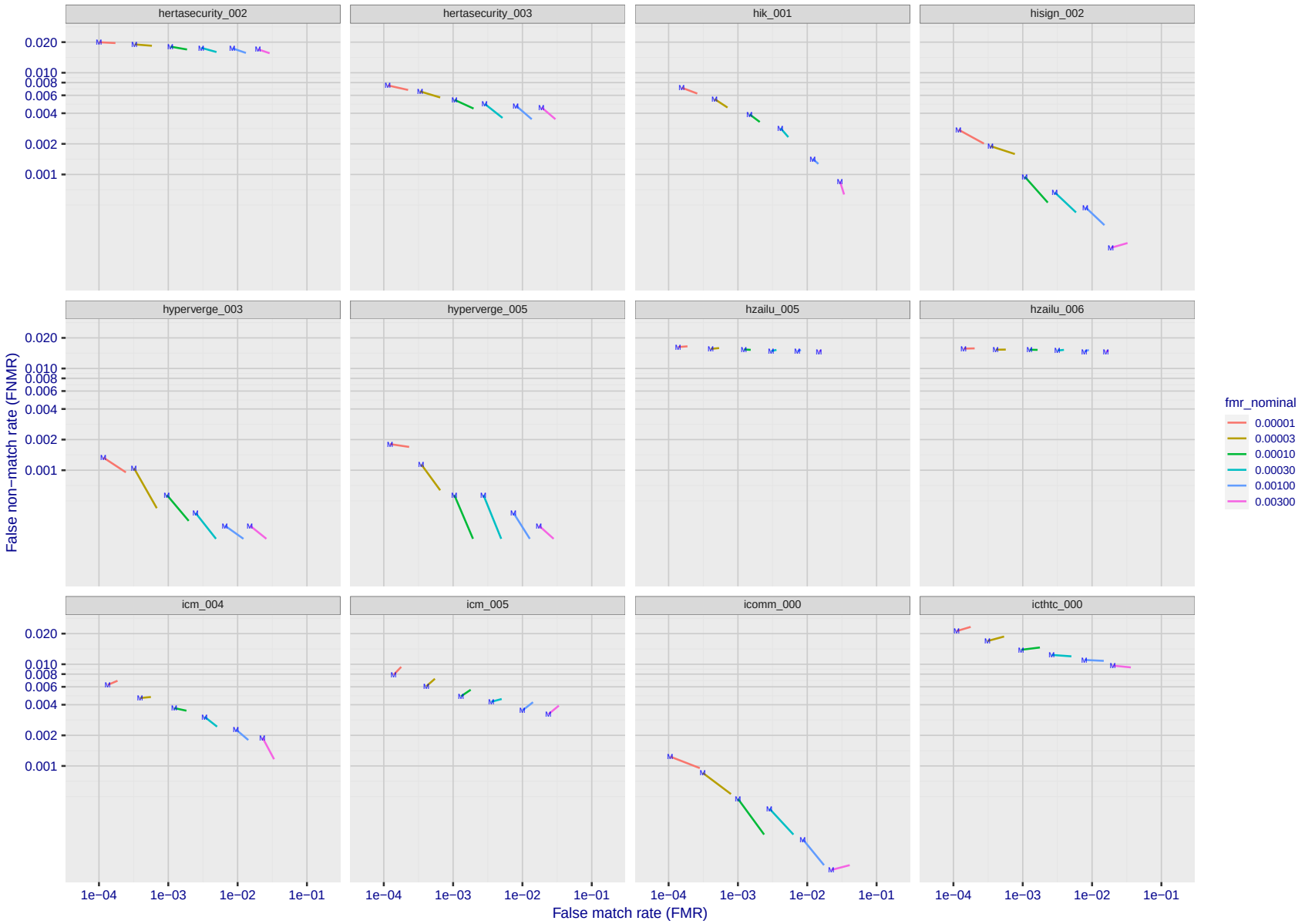

Figure 227: For the visa images, FNMR and FMR at six operating points along the DET characteristic. At each point a line is drawn between (FMR,FNMR)$_{\text{MALE}}$ and (FMR,FNMR)$_{\text{FEMALE}}$ showing how which sex has lower FMR and/or FNMR. The "M" label denotes male, the other end of the line corresponds to female. The six operating thresholds are selected to give the nominal false match rates given in the legend, and are computed over all impostor pairs regardless of age, sex, and place of birth. The plotted FMR values are broadly an order of magnitude larger than the nominal rates because FMR is computed over demographically-matched impostor pairs i.e individuals of the same sex, from the same geographic region (see section 3.6.1), and the same age group (see section 3.6.2).

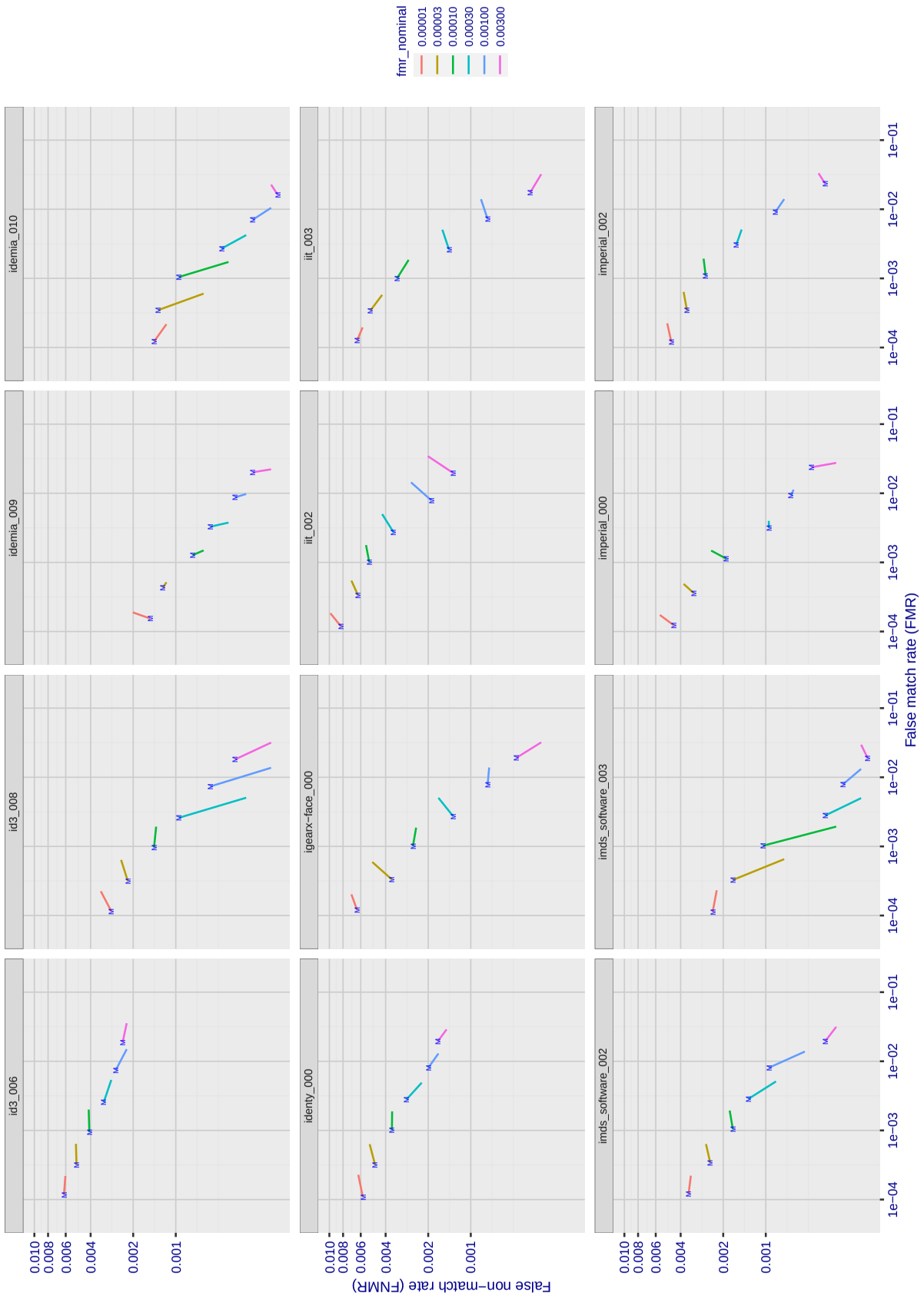

Figure 228: For the visa images, FNMR and FMR at six operating points along the DET characteristic. At each point a line is drawn between (FMR,FNMR)$_{\text{MALE}}$ and (FMR,FNMR)$_{\text{FEMALE}}$ showing how which sex has lower FMR and/or FNMR. The "M" label denotes male, the other end of the line corresponds to female. The six operating thresholds are selected to give the nominal false match rates given in the legend, and are computed over all impostor pairs regardless of age, sex, and place of birth. The plotted FMR values are broadly an order of magnitude larger than the nominal rates because FMR is computed over demographically-matched impostor pairs i.e individuals of the same sex, from the same geographic region (see section 3.6.1), and the same age group (see section 3.6.2).

FNMR(T) "False non-match rate"
FMR(T) "False match rate"

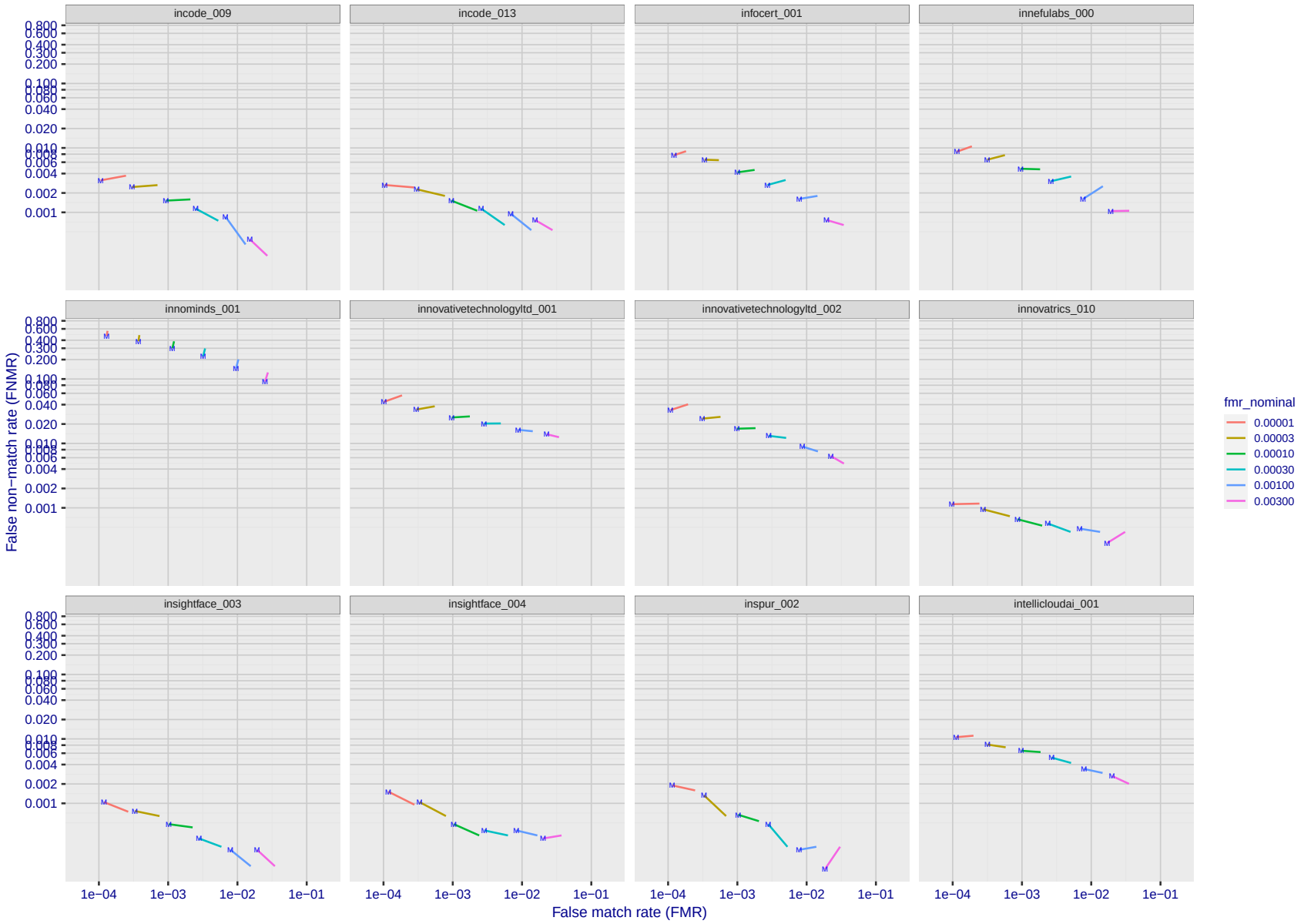

Figure 229: For the visa images, FNMR and FMR at six operating points along the DET characteristic. At each point a line is drawn between (FMR,FNMR)$_{\text{MALE}}$ and (FMR,FNMR)$_{\text{FEMALE}}$ showing how which sex has lower FMR and/or FNMR. The "M" label denotes male, the other end of the line corresponds to female. The six operating thresholds are selected to give the nominal false match rates given in the legend, and are computed over all impostor pairs regardless of age, sex, and place of birth. The plotted FMR values are broadly an order of magnitude larger than the nominal rates because FMR is computed over demographically-matched impostor pairs i.e individuals of the same sex, from the same geographic region (see section 3.6.1), and the same age group (see section 3.6.2).

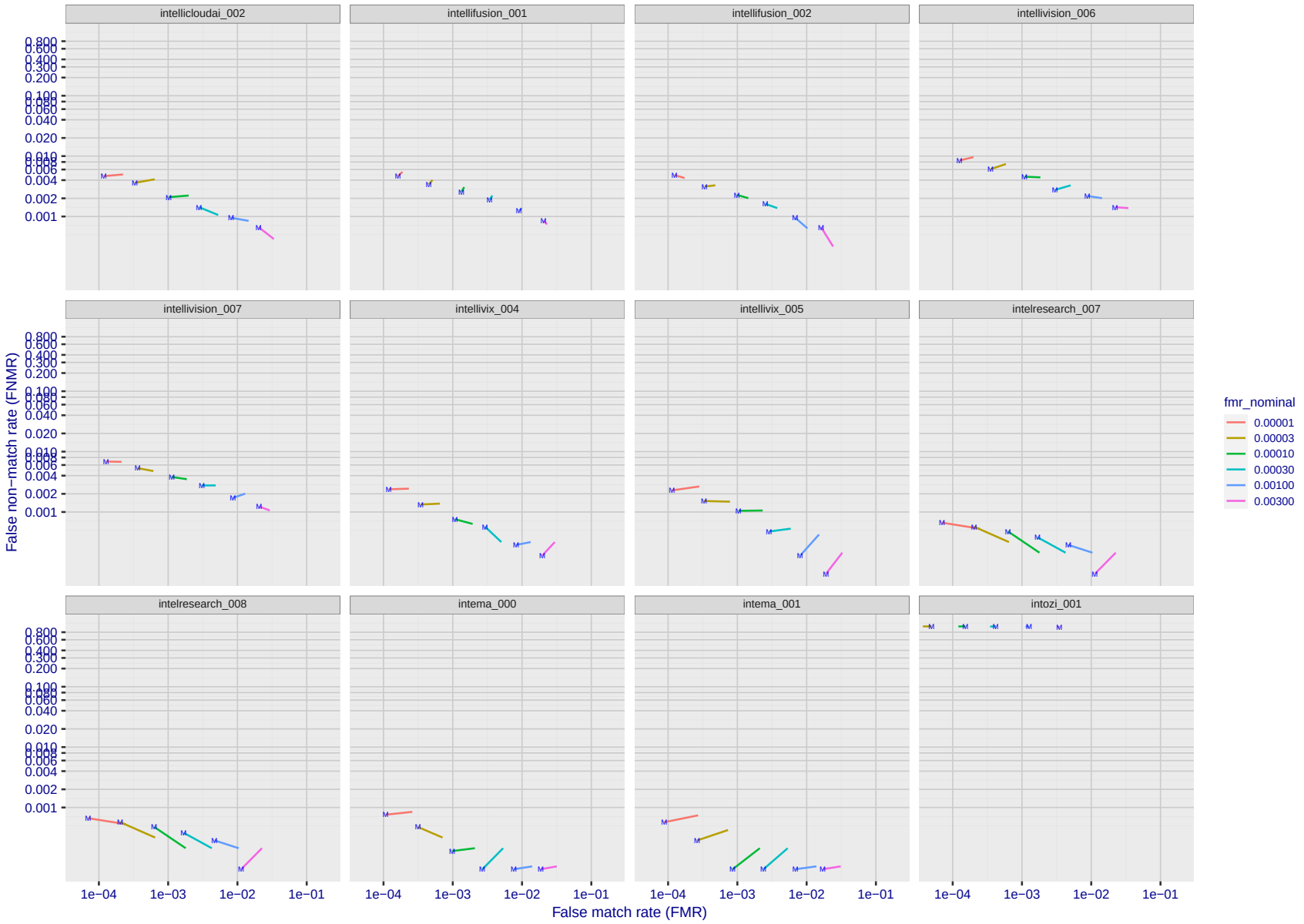

Figure 230: For the visa images, FNMR and FMR at six operating points along the DET characteristic. At each point a line is drawn between (FMR,FNMR)$_{\text{MALE}}$ and (FMR,FNMR)$_{\text{FEMALE}}$ showing how which sex has lower FMR and/or FNMR. The "M" label denotes male, the other end of the line corresponds to female. The six operating thresholds are selected to give the nominal false match rates given in the legend, and are computed over all impostor pairs regardless of age, sex, and place of birth. The plotted FMR values are broadly an order of magnitude larger than the nominal rates because FMR is computed over demographically-matched impostor pairs i.e individuals of the same sex, from the same geographic region (see section 3.6.1), and the same age group (see section 3.6.2).

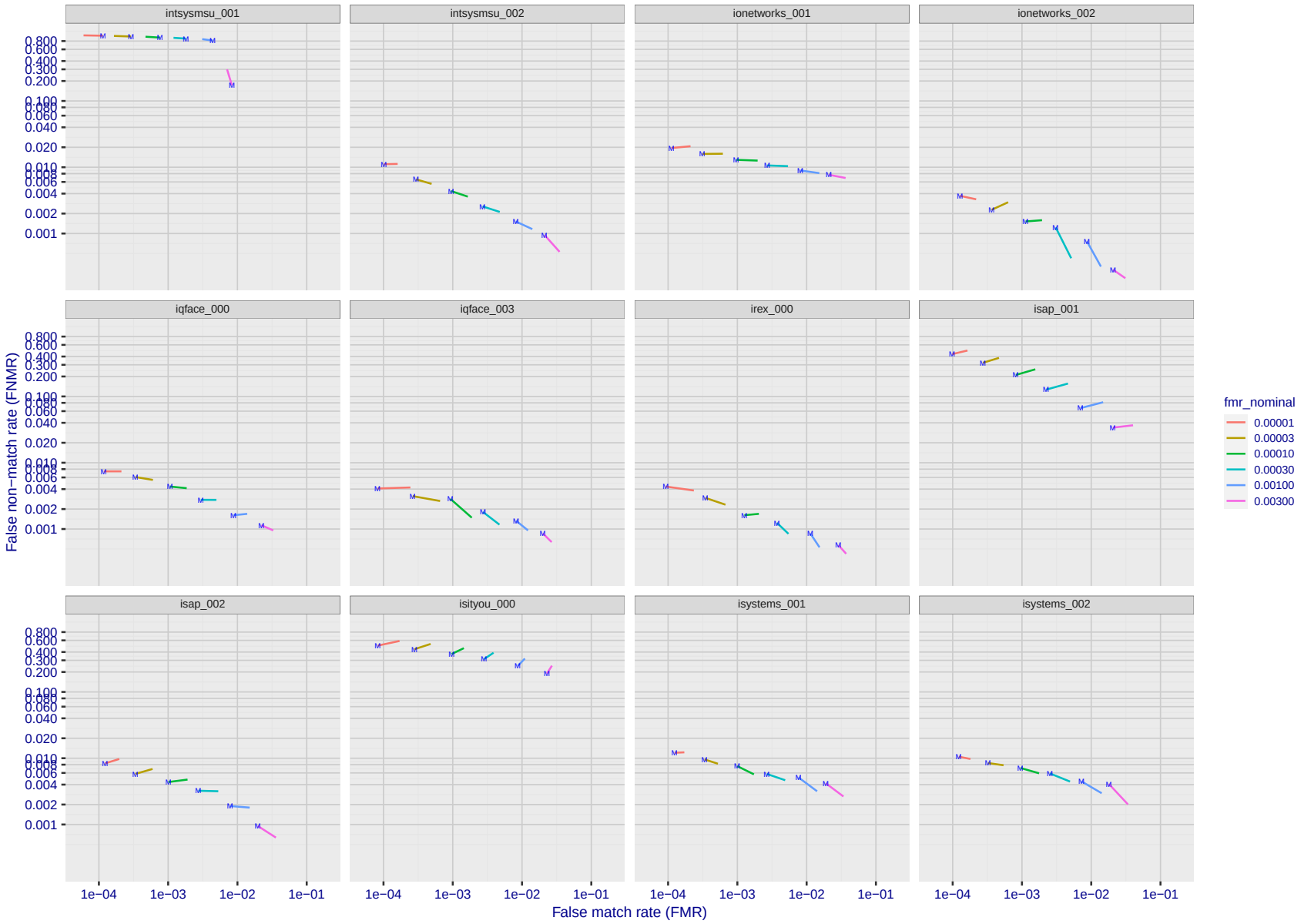

Figure 231: For the visa images, FNMR and FMR at six operating points along the DET characteristic. At each point a line is drawn between (FMR,FNMR)$_{\text{MALE}}$ and (FMR,FNMR)$_{\text{FEMALE}}$ showing how which sex has lower FMR and/or FNMR. The "M" label denotes male, the other end of the line corresponds to female. The six operating thresholds are selected to give the nominal false match rates given in the legend, and are computed over all impostor pairs regardless of age, sex, and place of birth. The plotted FMR values are broadly an order of magnitude larger than the nominal rates because FMR is computed over demographically-matched impostor pairs i.e individuals of the same sex, from the same geographic region (see section 3.6.1), and the same age group (see section 3.6.2).

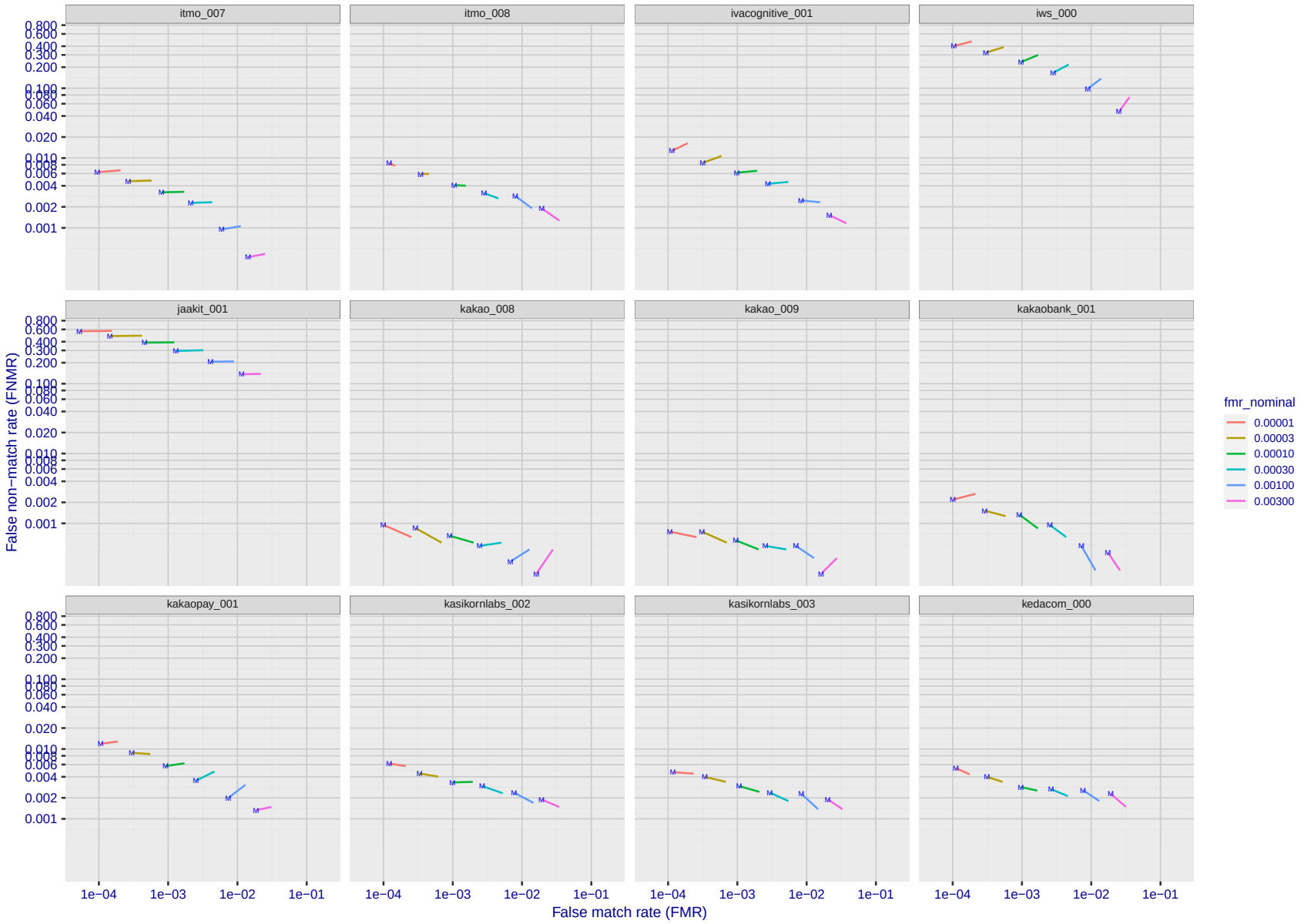

Figure 232: For the visa images, FNMR and FMR at six operating points along the DET characteristic. At each point a line is drawn between (FMR,FNMR)$_{\text{MALE}}$ and (FMR,FNMR)$_{\text{FEMALE}}$ showing how which sex has lower FMR and/or FNMR. The "M" label denotes male, the other end of the line corresponds to female. The six operating thresholds are selected to give the nominal false match rates given in the legend, and are computed over all impostor pairs regardless of age, sex, and place of birth. The plotted FMR values are broadly an order of magnitude larger than the nominal rates because FMR is computed over demographically-matched impostor pairs i.e individuals of the same sex, from the same geographic region (see section 3.6.1), and the same age group (see section 3.6.2).

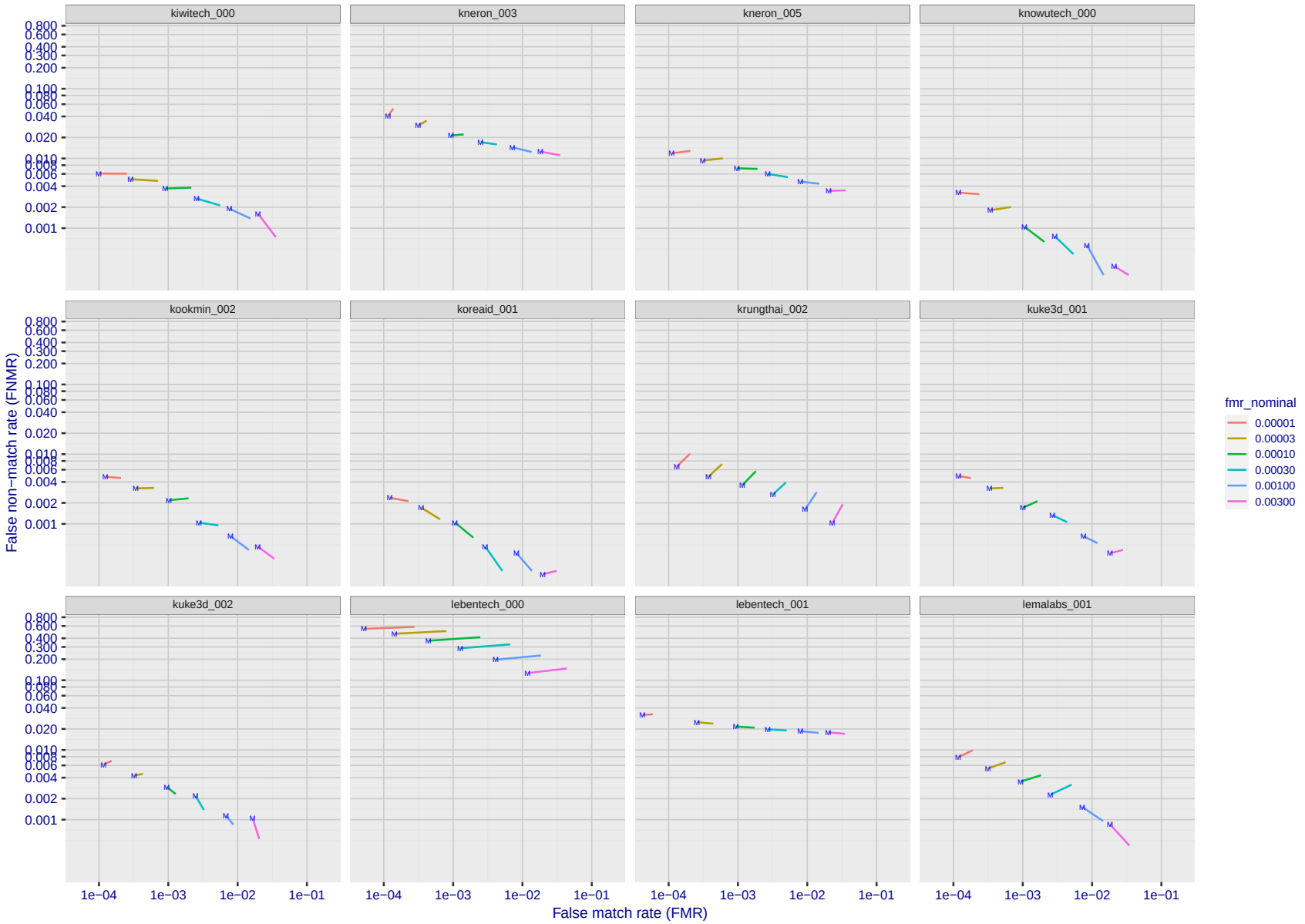

Figure 233: For the visa images, FNMR and FMR at six operating points along the DET characteristic. At each point a line is drawn between (FMR,FNMR)$_{\text{MALE}}$ and (FMR,FNMR)$_{\text{FEMALE}}$ showing how which sex has lower FMR and/or FNMR. The "M" label denotes male, the other end of the line corresponds to female. The six operating thresholds are selected to give the nominal false match rates given in the legend, and are computed over all impostor pairs regardless of age, sex, and place of birth. The plotted FMR values are broadly an order of magnitude larger than the nominal rates because FMR is computed over demographically-matched impostor pairs i.e individuals of the same sex, from the same geographic region (see section 3.6.1), and the same age group (see section 3.6.2).

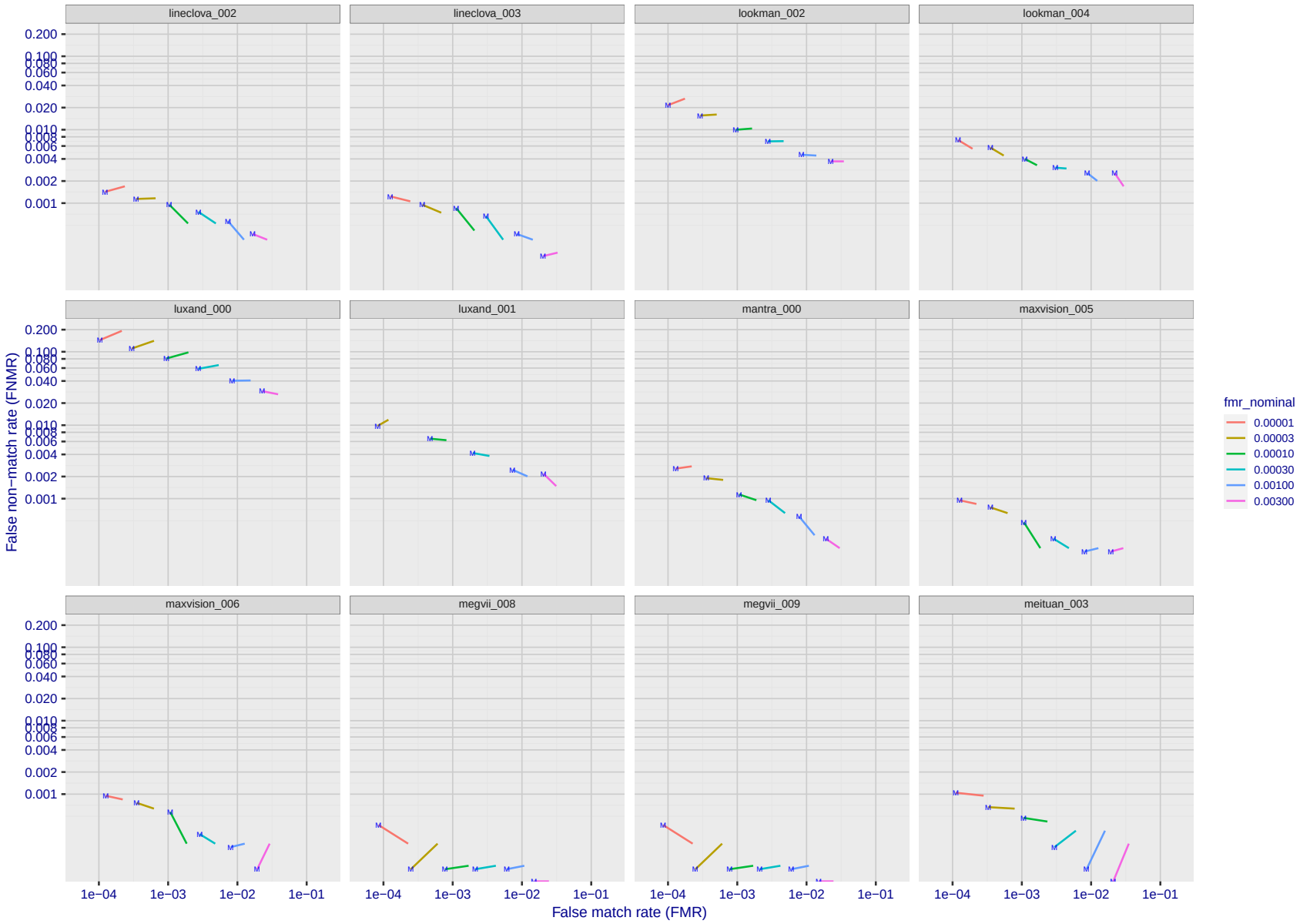

Figure 234: For the visa images, FNMR and FMR at six operating points along the DET characteristic. At each point a line is drawn between (FMR,FNMR)$_{\text{MALE}}$ and (FMR,FNMR)$_{\text{FEMALE}}$ showing how which sex has lower FMR and/or FNMR. The "M" label denotes male, the other end of the line corresponds to female. The six operating thresholds are selected to give the nominal false match rates given in the legend, and are computed over all impostor pairs regardless of age, sex, and place of birth. The plotted FMR values are broadly an order of magnitude larger than the nominal rates because FMR is computed over demographically-matched impostor pairs i.e individuals of the same sex, from the same geographic region (see section 3.6.1), and the same age group (see section 3.6.2).

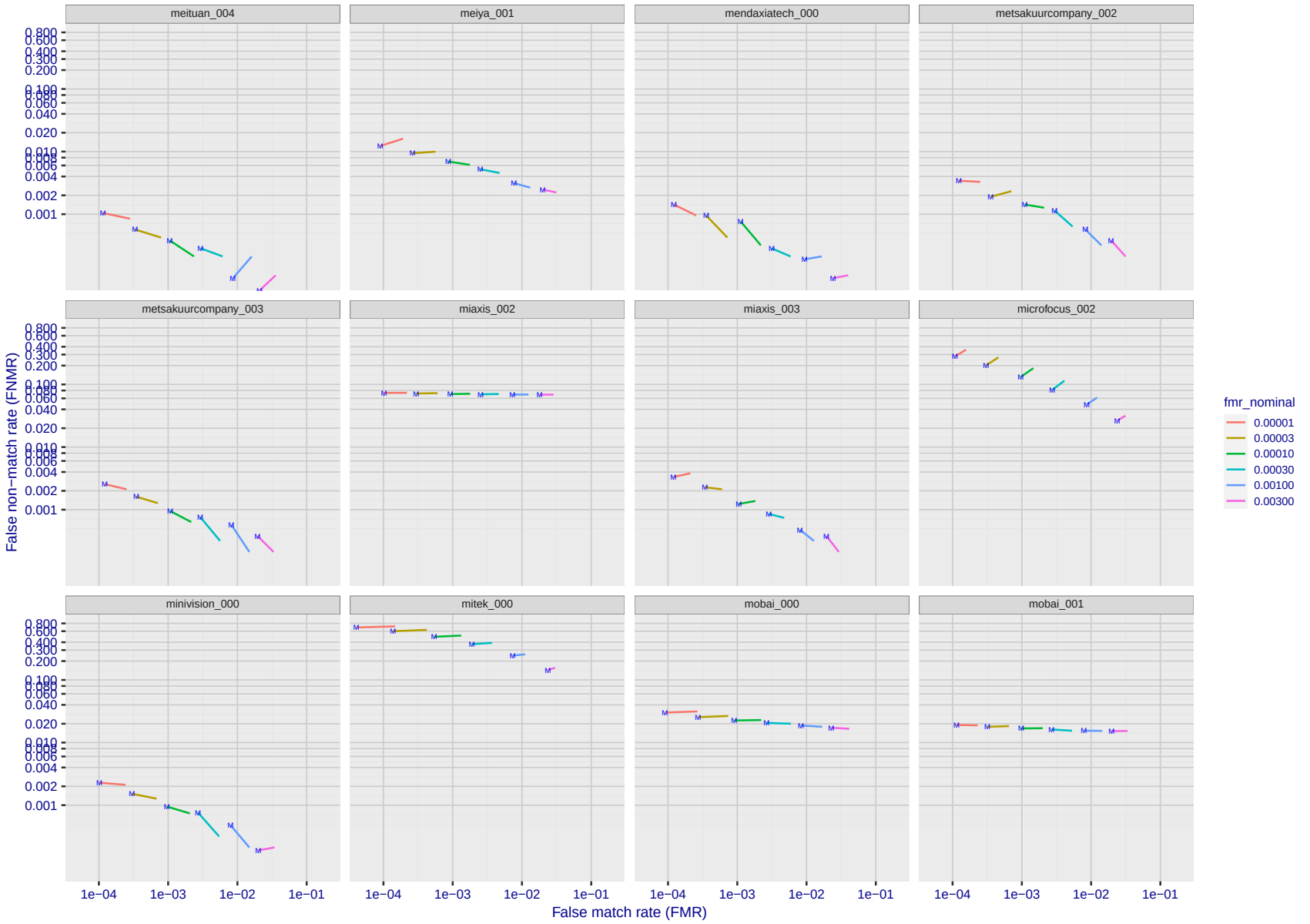

Figure 235: For the visa images, FNMR and FMR at six operating points along the DET characteristic. At each point a line is drawn between (FMR,FNMR)$_{\text{MALE}}$ and (FMR,FNMR)$_{\text{FEMALE}}$ showing how which sex has lower FMR and/or FNMR. The "M" label denotes male, the other end of the line corresponds to female. The six operating thresholds are selected to give the nominal false match rates given in the legend, and are computed over all impostor pairs regardless of age, sex, and place of birth. The plotted FMR values are broadly an order of magnitude larger than the nominal rates because FMR is computed over demographically-matched impostor pairs i.e individuals of the same sex, from the same geographic region (see section 3.6.1), and the same age group (see section 3.6.2).

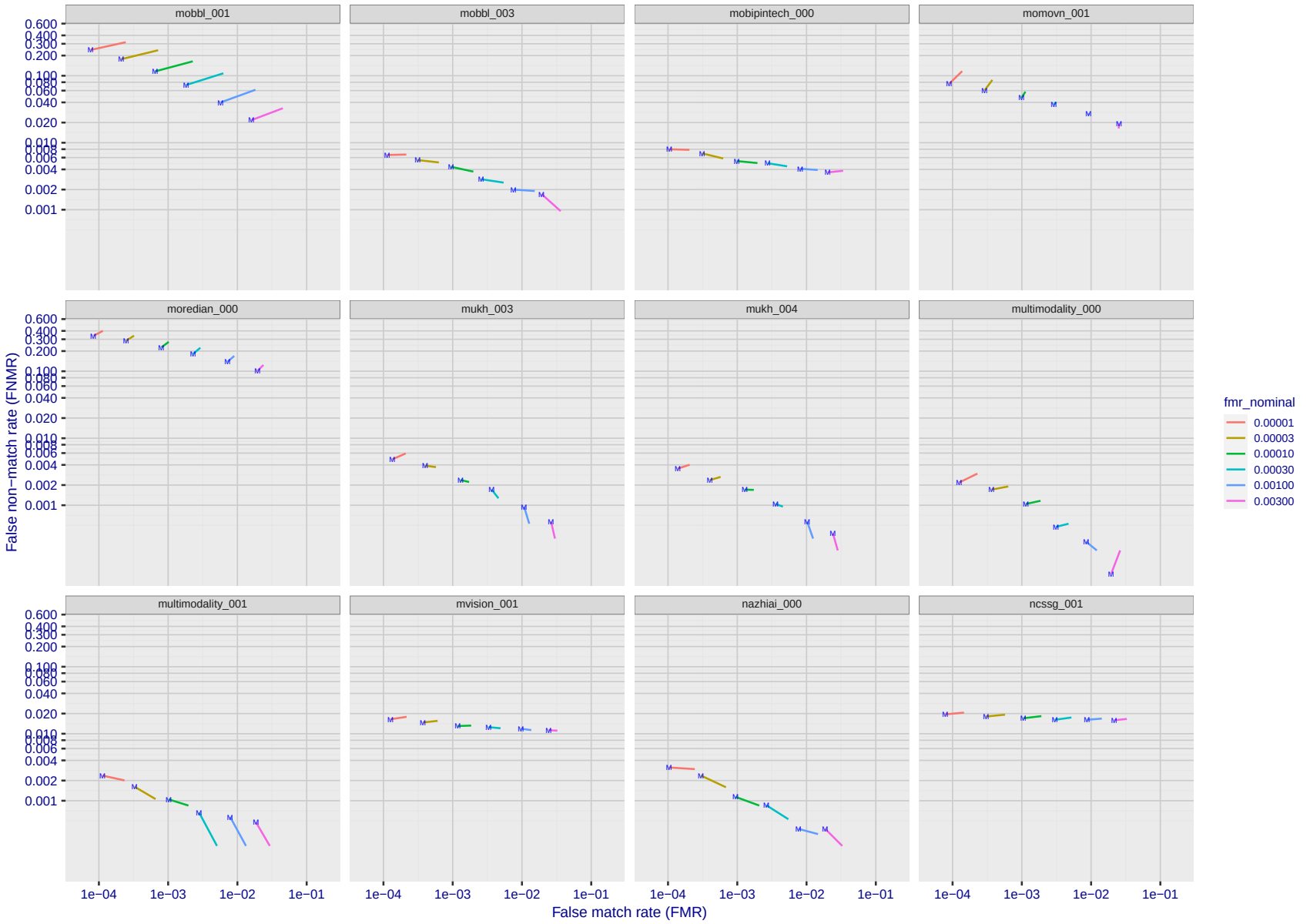

Figure 236: For the visa images, FNMR and FMR at six operating points along the DET characteristic. At each point a line is drawn between (FMR,FNMR)$_{\text{MALE}}$ and (FMR,FNMR)$_{\text{FEMALE}}$ showing how which sex has lower FMR and/or FNMR. The "M" label denotes male, the other end of the line corresponds to female. The six operating thresholds are selected to give the nominal false match rates given in the legend, and are computed over all impostor pairs regardless of age, sex, and place of birth. The plotted FMR values are broadly an order of magnitude larger than the nominal rates because FMR is computed over demographically-matched impostor pairs i.e individuals of the same sex, from the same geographic region (see section 3.6.1), and the same age group (see section 3.6.2).

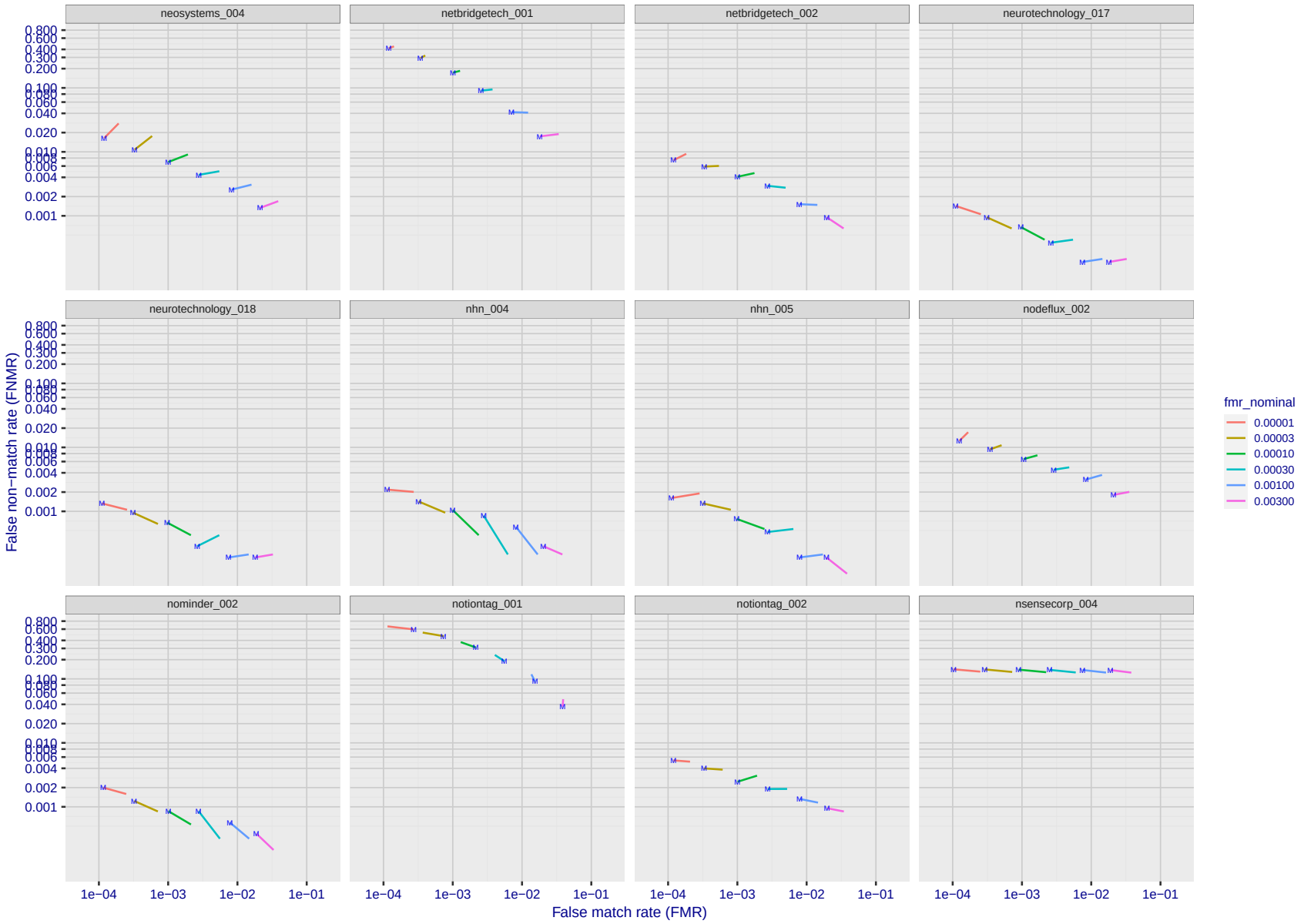

Figure 237: For the visa images, FNMR and FMR at six operating points along the DET characteristic. At each point a line is drawn between (FMR,FNMR)$_{\text{MALE}}$ and (FMR,FNMR)$_{\text{FEMALE}}$ showing how which sex has lower FMR and/or FNMR. The "M" label denotes male, the other end of the line corresponds to female. The six operating thresholds are selected to give the nominal false match rates given in the legend, and are computed over all impostor pairs regardless of age, sex, and place of birth. The plotted FMR values are broadly an order of magnitude larger than the nominal rates because FMR is computed over demographically-matched impostor pairs i.e individuals of the same sex, from the same geographic region (see section 3.6.1), and the same age group (see section 3.6.2).

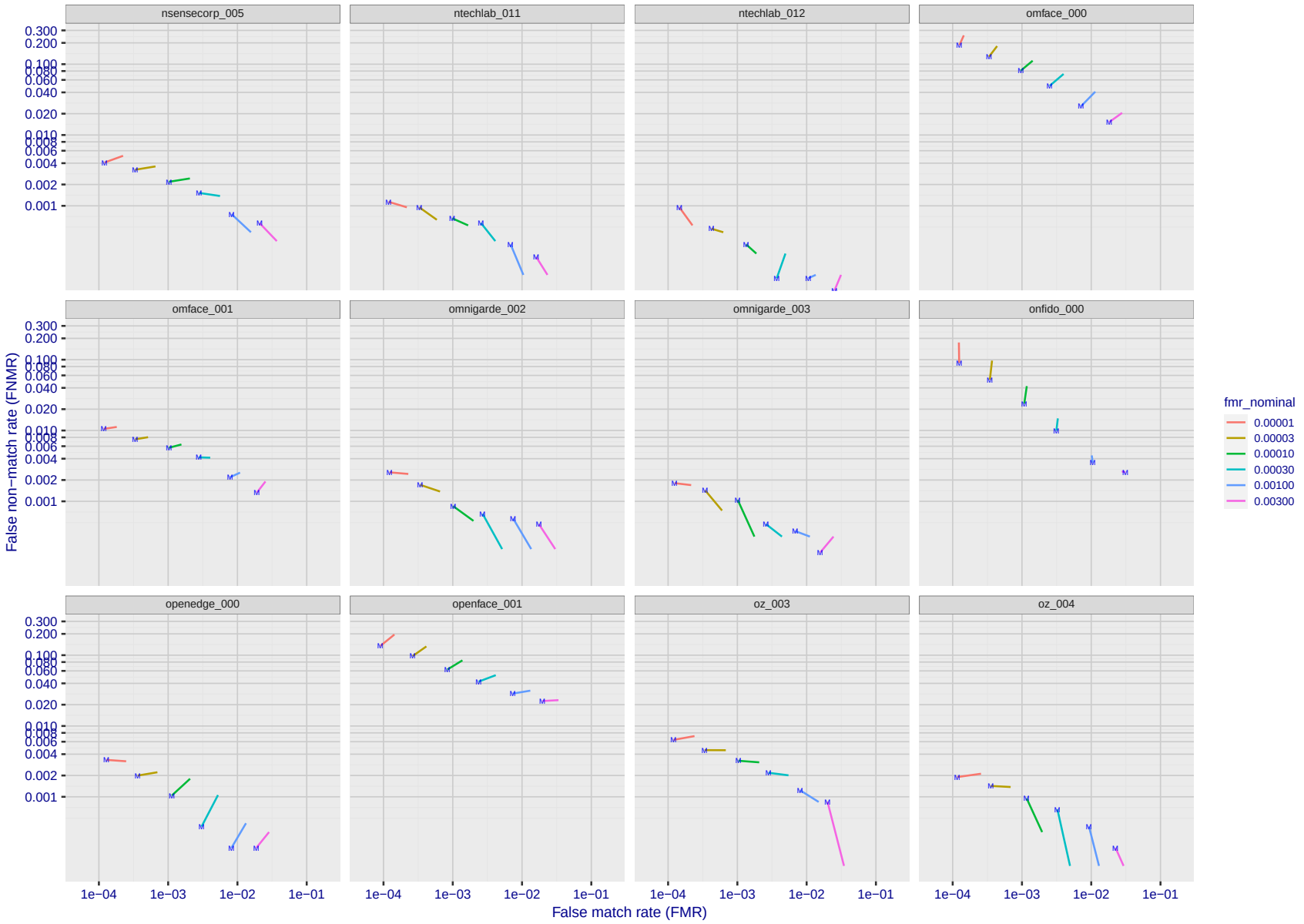

Figure 238: For the visa images, FNMR and FMR at six operating points along the DET characteristic. At each point a line is drawn between (FMR,FNMR)$_{\text{MALE}}$ and (FMR,FNMR)$_{\text{FEMALE}}$ showing how which sex has lower FMR and/or FNMR. The "M" label denotes male, the other end of the line corresponds to female. The six operating thresholds are selected to give the nominal false match rates given in the legend, and are computed over all impostor pairs regardless of age, sex, and place of birth. The plotted FMR values are broadly an order of magnitude larger than the nominal rates because FMR is computed over demographically-matched impostor pairs i.e individuals of the same sex, from the same geographic region (see section 3.6.1), and the same age group (see section 3.6.2).

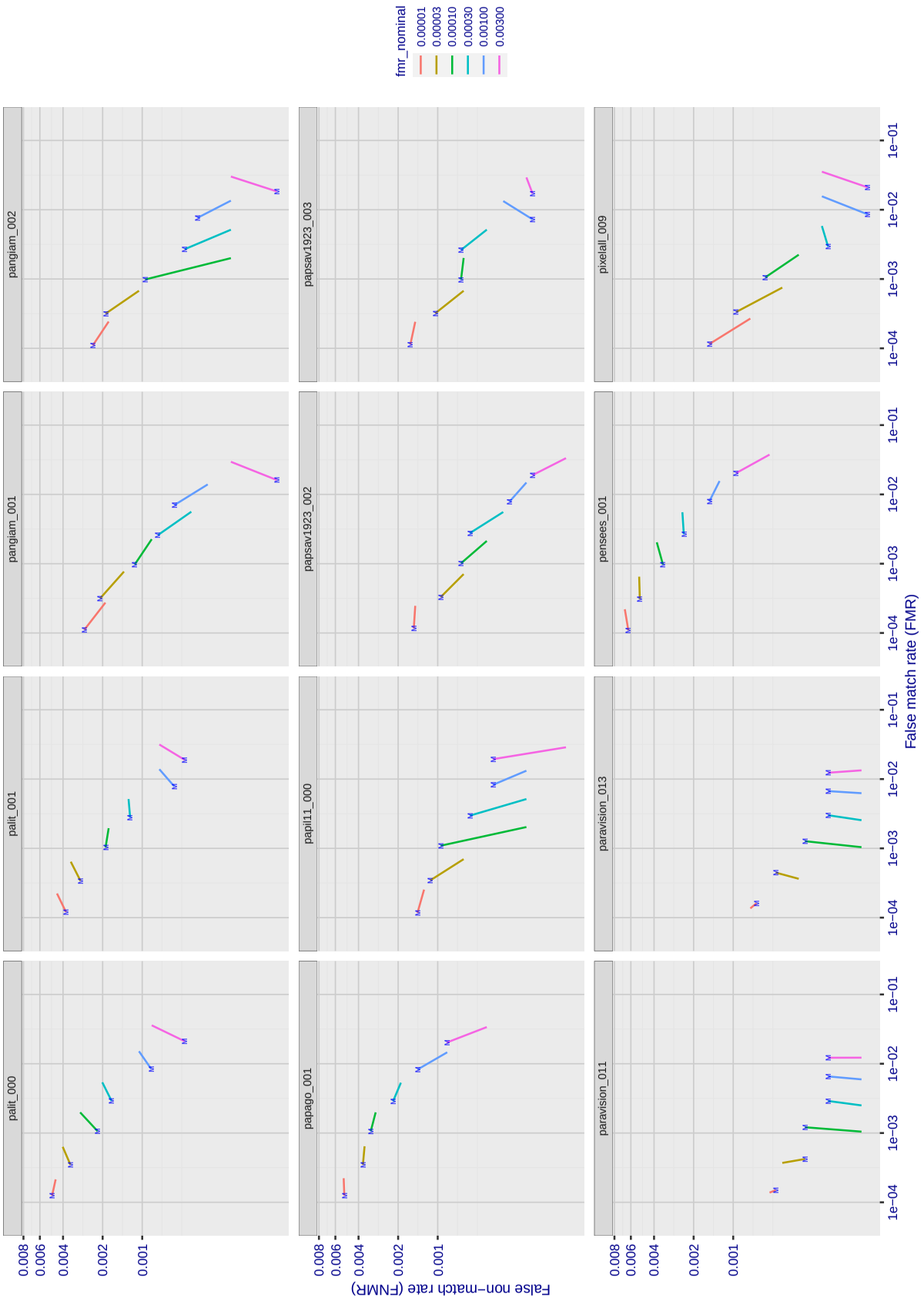

Figure 239: For the visa images, FNMR and FMR at six operating points along the DET characteristic. At each point a line is drawn between (FMR,FNMR)$_{\text{MALE}}$ and (FMR,FNMR)$_{\text{FEMALE}}$ showing how which sex has lower FMR and/or FNMR. The "M" label denotes male, the other end of the line corresponds to female. The six operating thresholds are selected to give the nominal false match rates given in the legend, and are computed over all impostor pairs regardless of age, sex, and place of birth. The plotted FMR values are broadly an order of magnitude larger than the nominal rates because FMR is computed over demographically-matched impostor pairs i.e individuals of the same sex, from the same geographic region (see section 3.6.1), and the same age group (see section 3.6.2).

FNMR(T) "False non-match rate"
FMR(T) "False match rate"

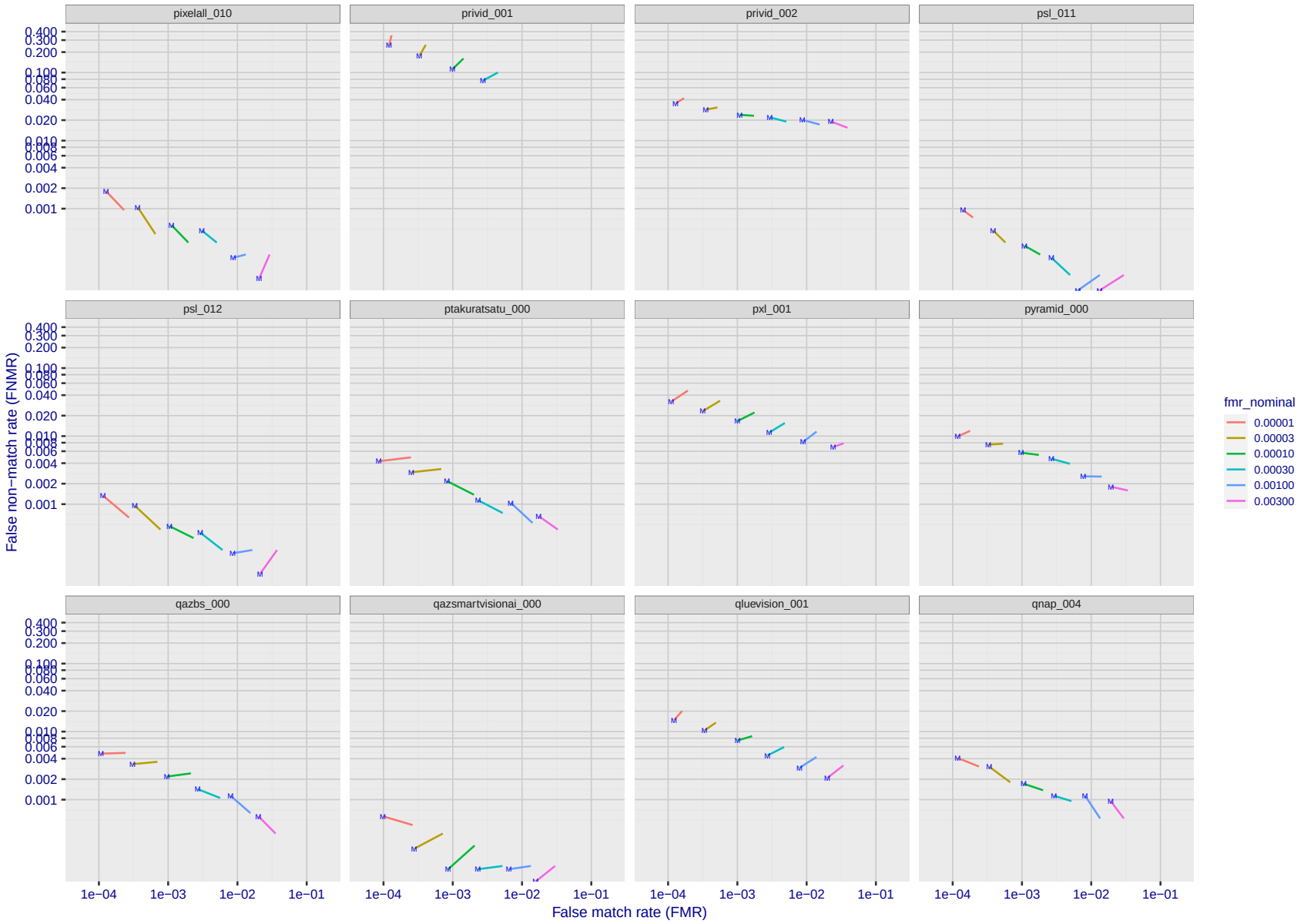

Figure 240: For the visa images, FNMR and FMR at six operating points along the DET characteristic. At each point a line is drawn between (FMR,FNMR)$_{\text{MALE}}$ and (FMR,FNMR)$_{\text{FEMALE}}$ showing how which sex has lower FMR and/or FNMR. The "M" label denotes male, the other end of the line corresponds to female. The six operating thresholds are selected to give the nominal false match rates given in the legend, and are computed over all impostor pairs regardless of age, sex, and place of birth. The plotted FMR values are broadly an order of magnitude larger than the nominal rates because FMR is computed over demographically-matched impostor pairs i.e individuals of the same sex, from the same geographic region (see section 3.6.1), and the same age group (see section 3.6.2).

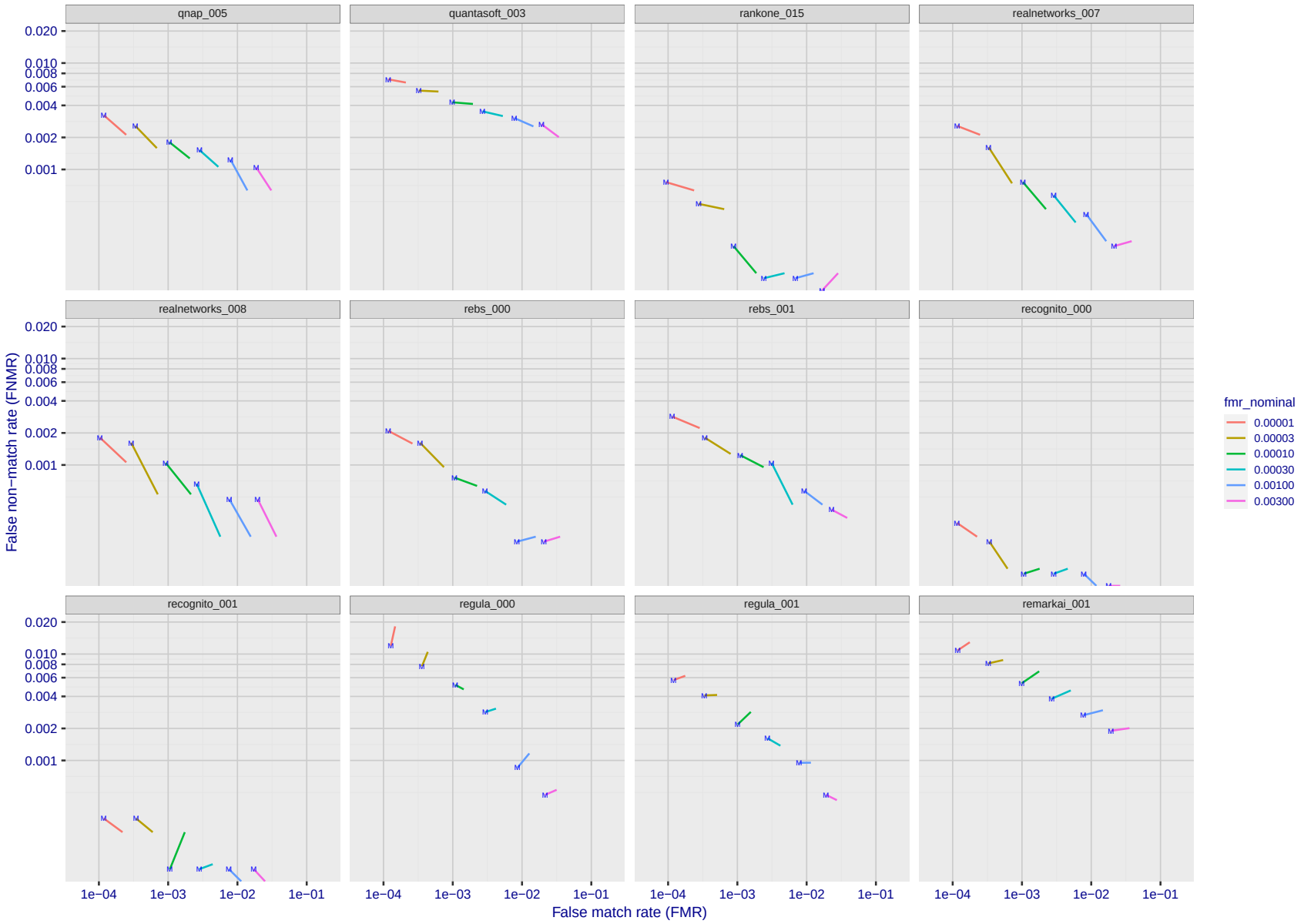

Figure 241: For the visa images, FNMR and FMR at six operating points along the DET characteristic. At each point a line is drawn between (FMR,FNMR)$_{\text{MALE}}$ and (FMR,FNMR)$_{\text{FEMALE}}$ showing how which sex has lower FMR and/or FNMR. The "M" label denotes male, the other end of the line corresponds to female. The six operating thresholds are selected to give the nominal false match rates given in the legend, and are computed over all impostor pairs regardless of age, sex, and place of birth. The plotted FMR values are broadly an order of magnitude larger than the nominal rates because FMR is computed over demographically-matched impostor pairs i.e individuals of the same sex, from the same geographic region (see section 3.6.1), and the same age group (see section 3.6.2).

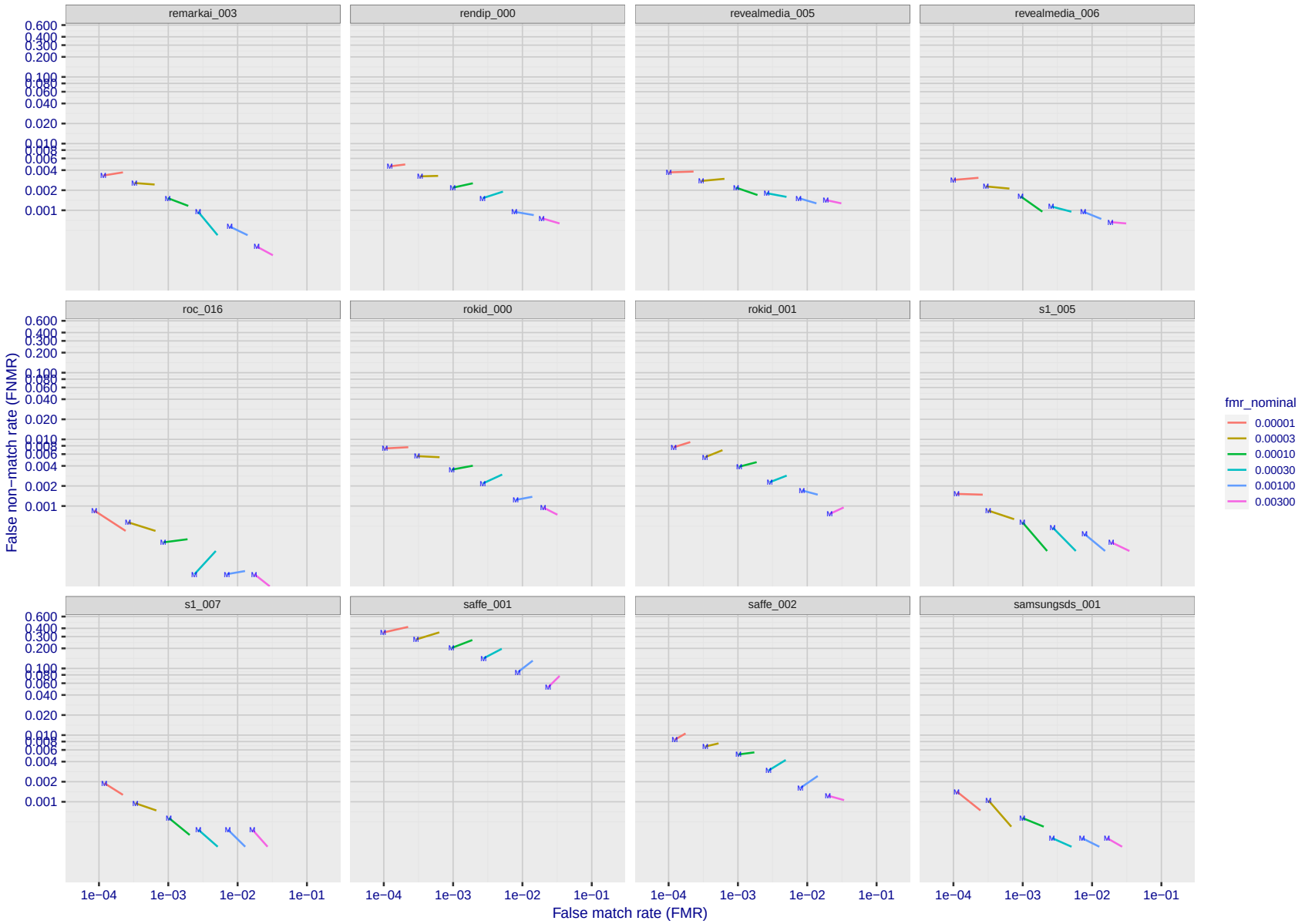

Figure 242: For the visa images, FNMR and FMR at six operating points along the DET characteristic. At each point a line is drawn between (FMR,FNMR)$_{\text{MALE}}$ and (FMR,FNMR)$_{\text{FEMALE}}$ showing how which sex has lower FMR and/or FNMR. The "M" label denotes male, the other end of the line corresponds to female. The six operating thresholds are selected to give the nominal false match rates given in the legend, and are computed over all impostor pairs regardless of age, sex, and place of birth. The plotted FMR values are broadly an order of magnitude larger than the nominal rates because FMR is computed over demographically-matched impostor pairs i.e individuals of the same sex, from the same geographic region (see section 3.6.1), and the same age group (see section 3.6.2).

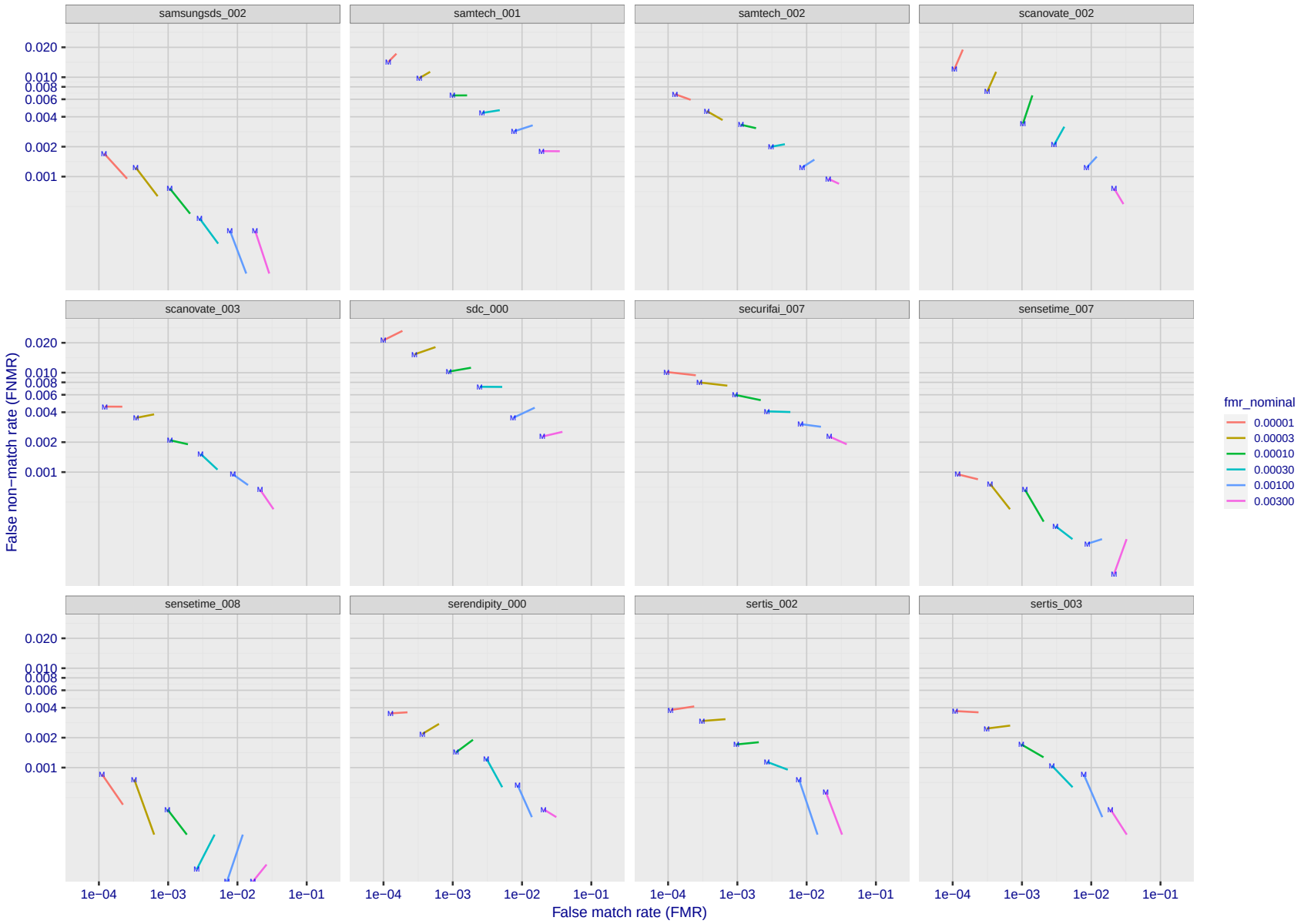

Figure 243: For the visa images, FNMR and FMR at six operating points along the DET characteristic. At each point a line is drawn between (FMR,FNMR)$_{\text{MALE}}$ and (FMR,FNMR)$_{\text{FEMALE}}$ showing how which sex has lower FMR and/or FNMR. The "M" label denotes male, the other end of the line corresponds to female. The six operating thresholds are selected to give the nominal false match rates given in the legend, and are computed over all impostor pairs regardless of age, sex, and place of birth. The plotted FMR values are broadly an order of magnitude larger than the nominal rates because FMR is computed over demographically-matched impostor pairs i.e individuals of the same sex, from the same geographic region (see section 3.6.1), and the same age group (see section 3.6.2).

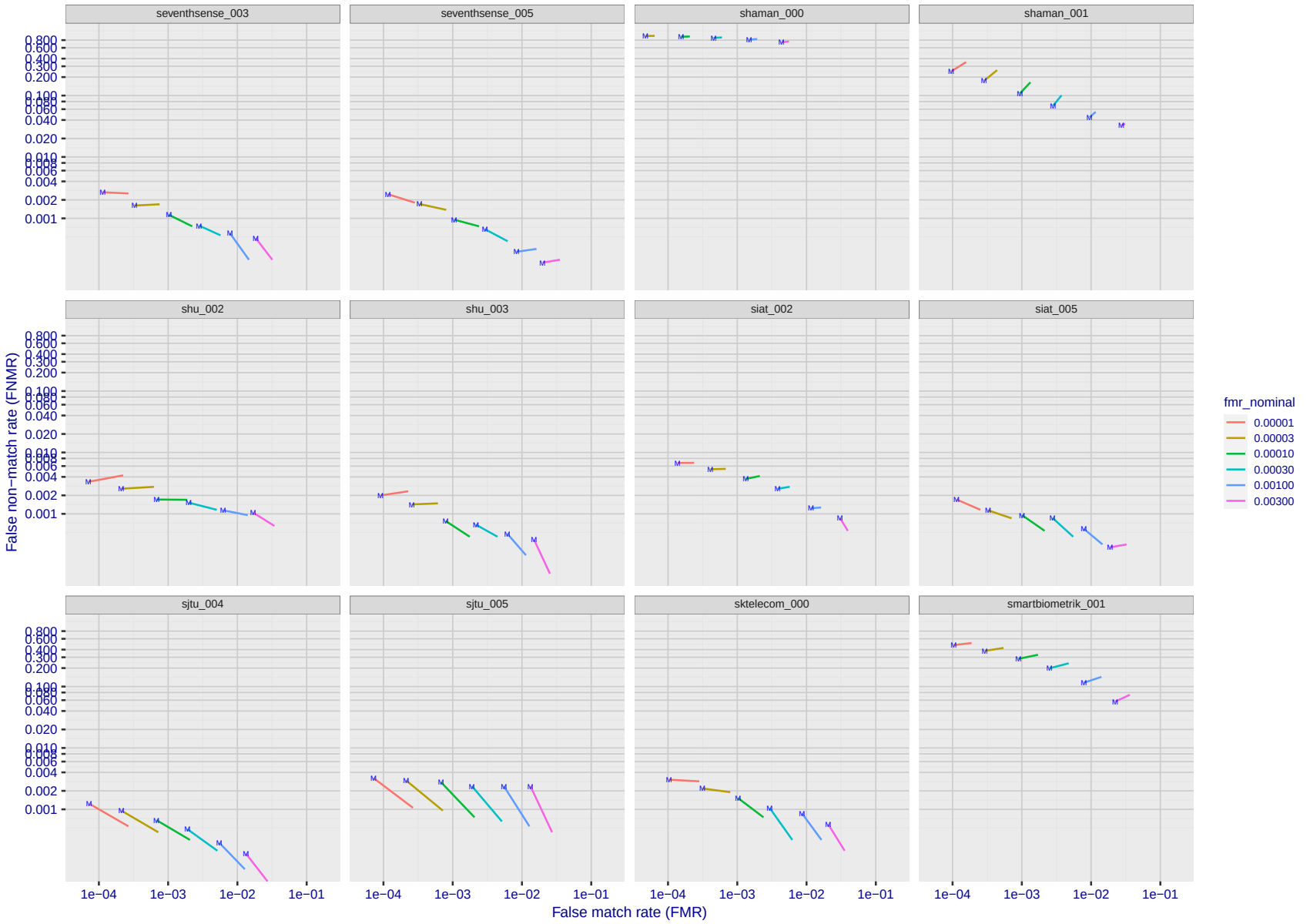

Figure 244: For the visa images, FNMR and FMR at six operating points along the DET characteristic. At each point a line is drawn between (FMR,FNMR)$_{\text{MALE}}$ and (FMR,FNMR)$_{\text{FEMALE}}$ showing how which sex has lower FMR and/or FNMR. The "M" label denotes male, the other end of the line corresponds to female. The six operating thresholds are selected to give the nominal false match rates given in the legend, and are computed over all impostor pairs regardless of age, sex, and place of birth. The plotted FMR values are broadly an order of magnitude larger than the nominal rates because FMR is computed over demographically-matched impostor pairs i.e individuals of the same sex, from the same geographic region (see section 3.6.1), and the same age group (see section 3.6.2).

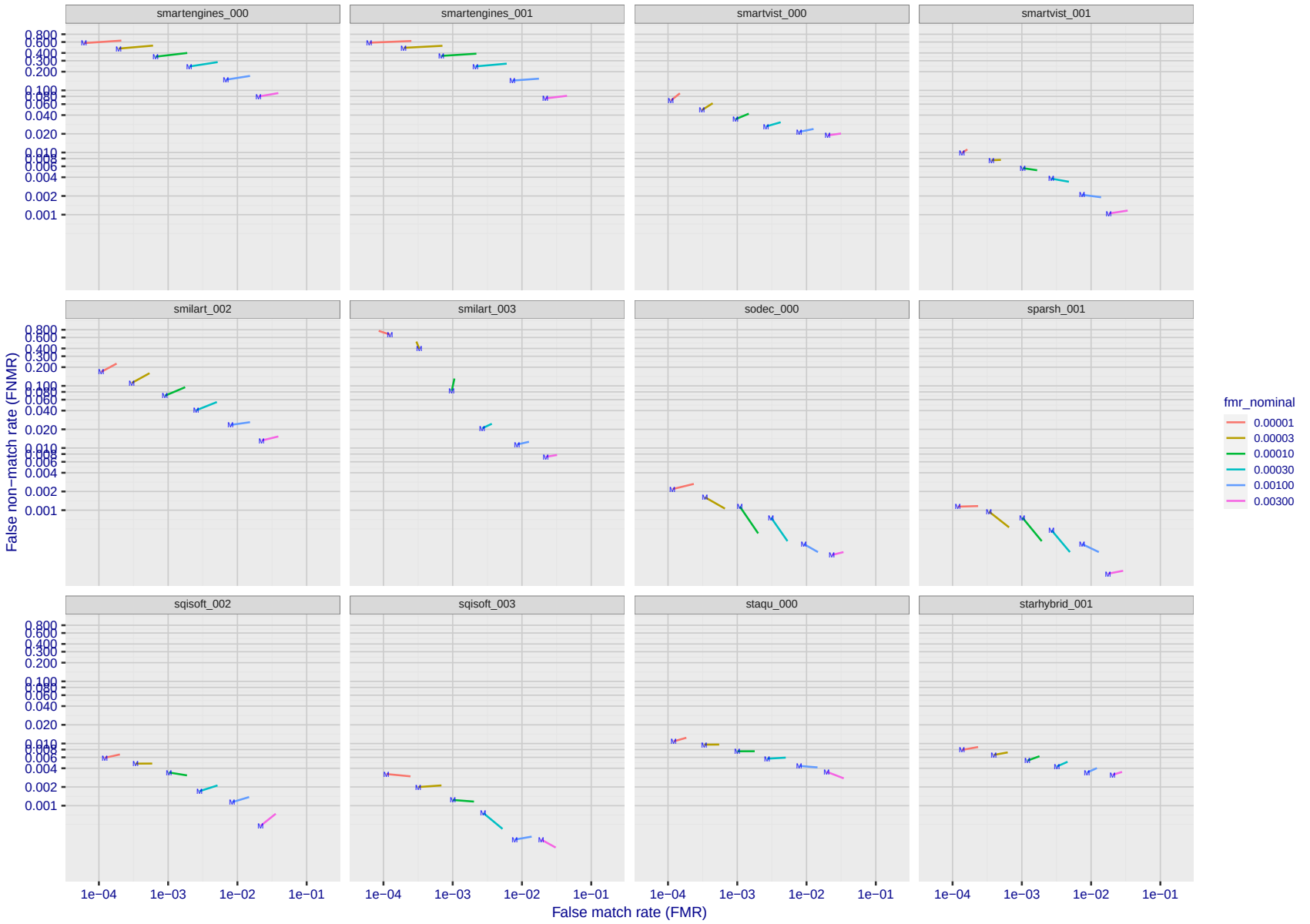

Figure 245: For the visa images, FNMR and FMR at six operating points along the DET characteristic. At each point a line is drawn between (FMR,FNMR)$_{\text{MALE}}$ and (FMR,FNMR)$_{\text{FEMALE}}$ showing how which sex has lower FMR and/or FNMR. The "M" label denotes male, the other end of the line corresponds to female. The six operating thresholds are selected to give the nominal false match rates given in the legend, and are computed over all impostor pairs regardless of age, sex, and place of birth. The plotted FMR values are broadly an order of magnitude larger than the nominal rates because FMR is computed over demographically-matched impostor pairs i.e individuals of the same sex, from the same geographic region (see section 3.6.1), and the same age group (see section 3.6.2).

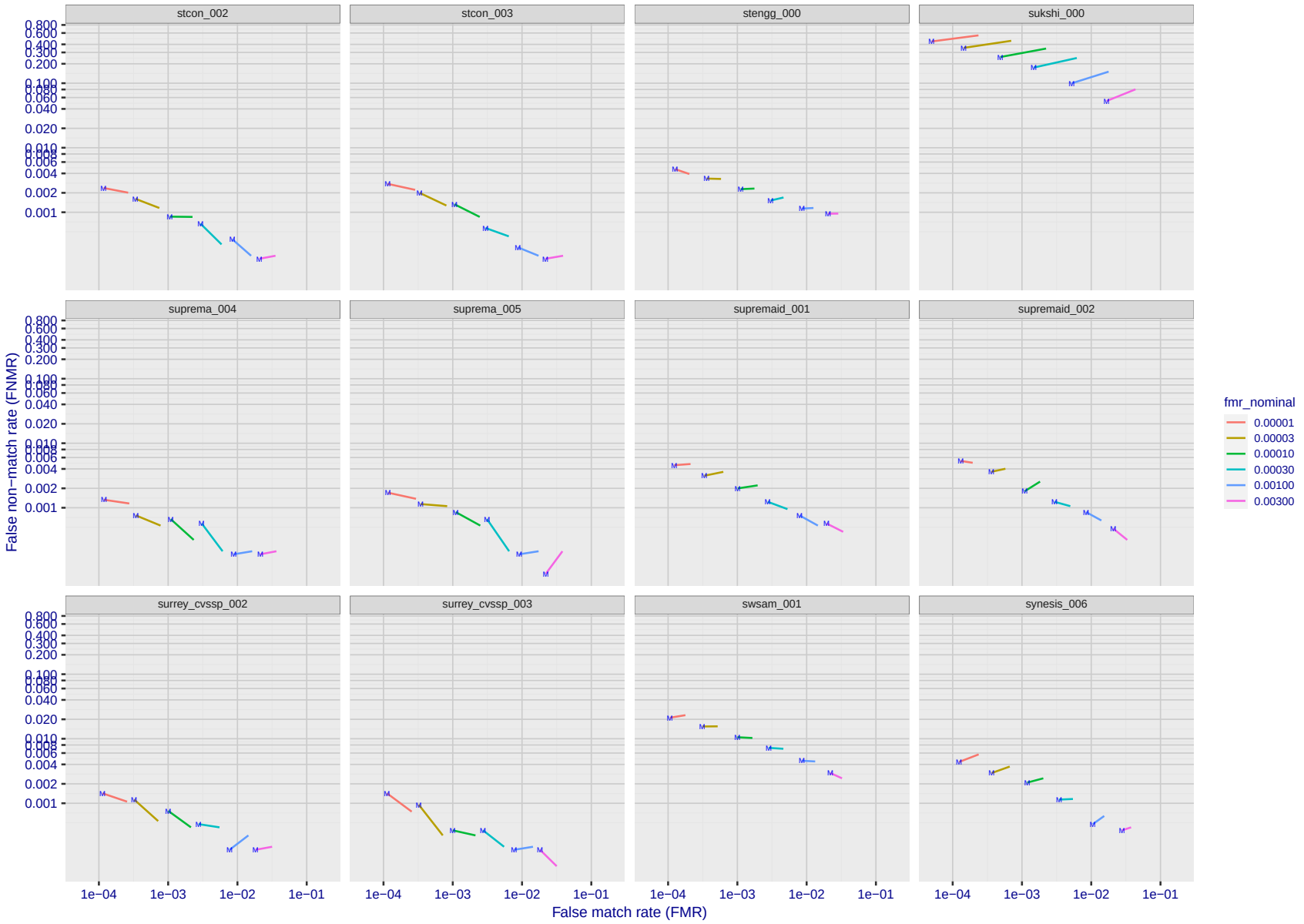

Figure 246: For the visa images, FNMR and FMR at six operating points along the DET characteristic. At each point a line is drawn between (FMR,FNMR)$_{\text{MALE}}$ and (FMR,FNMR)$_{\text{FEMALE}}$ showing how which sex has lower FMR and/or FNMR. The "M" label denotes male, the other end of the line corresponds to female. The six operating thresholds are selected to give the nominal false match rates given in the legend, and are computed over all impostor pairs regardless of age, sex, and place of birth. The plotted FMR values are broadly an order of magnitude larger than the nominal rates because FMR is computed over demographically-matched impostor pairs i.e individuals of the same sex, from the same geographic region (see section 3.6.1), and the same age group (see section 3.6.2).

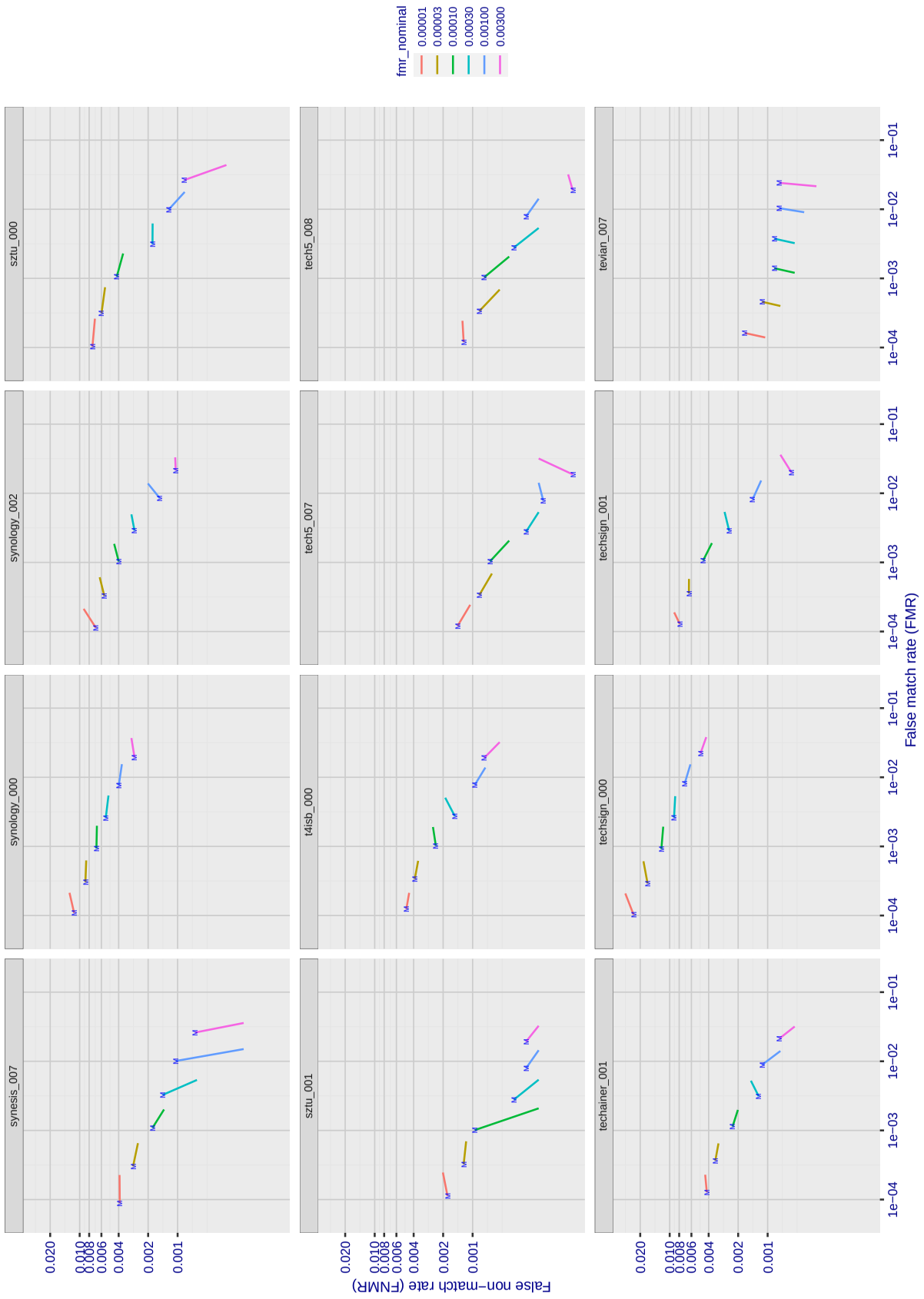

Figure 247: For the visa images, FNMR and FMR at six operating points along the DET characteristic. At each point a line is drawn between (FMR,FNMR)$_{\text{MALE}}$ and (FMR,FNMR)$_{\text{FEMALE}}$ showing how which sex has lower FMR and/or FNMR. The "M" label denotes male, the other end of the line corresponds to female. The six operating thresholds are selected to give the nominal false match rates given in the legend, and are computed over all impostor pairs regardless of age, sex, and place of birth. The plotted FMR values are broadly an order of magnitude larger than the nominal rates because FMR is computed over demographically-matched impostor pairs i.e individuals of the same sex, from the same geographic region (see section 3.6.1), and the same age group (see section 3.6.2).

FNMR(T) "False non-match rate"
FMR(T) "False match rate"

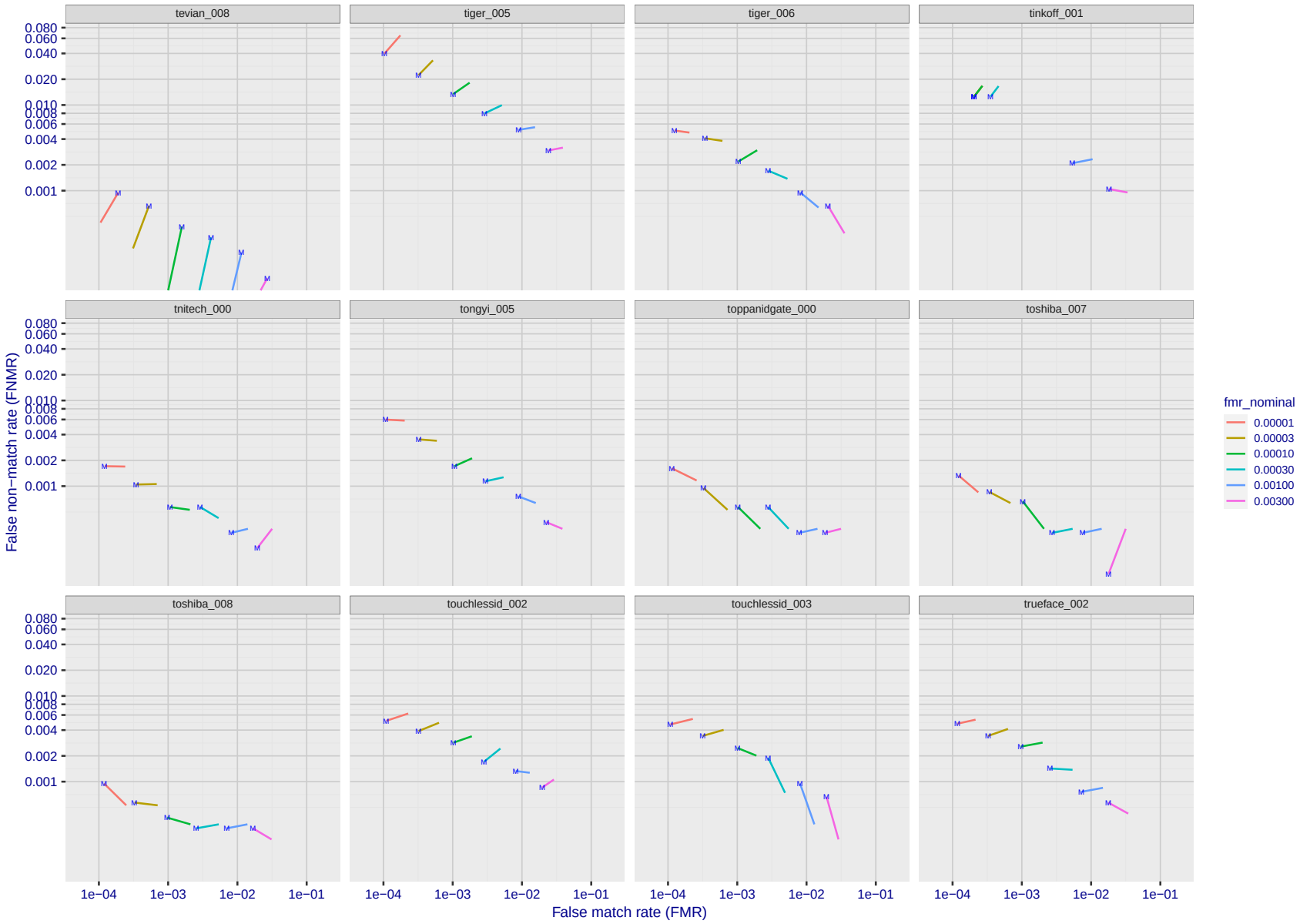

Figure 248: For the visa images, FNMR and FMR at six operating points along the DET characteristic. At each point a line is drawn between (FMR,FNMR)$_{\text{MALE}}$ and (FMR,FNMR)$_{\text{FEMALE}}$ showing how which sex has lower FMR and/or FNMR. The "M" label denotes male, the other end of the line corresponds to female. The six operating thresholds are selected to give the nominal false match rates given in the legend, and are computed over all impostor pairs regardless of age, sex, and place of birth. The plotted FMR values are broadly an order of magnitude larger than the nominal rates because FMR is computed over demographically-matched impostor pairs i.e individuals of the same sex, from the same geographic region (see section 3.6.1), and the same age group (see section 3.6.2).

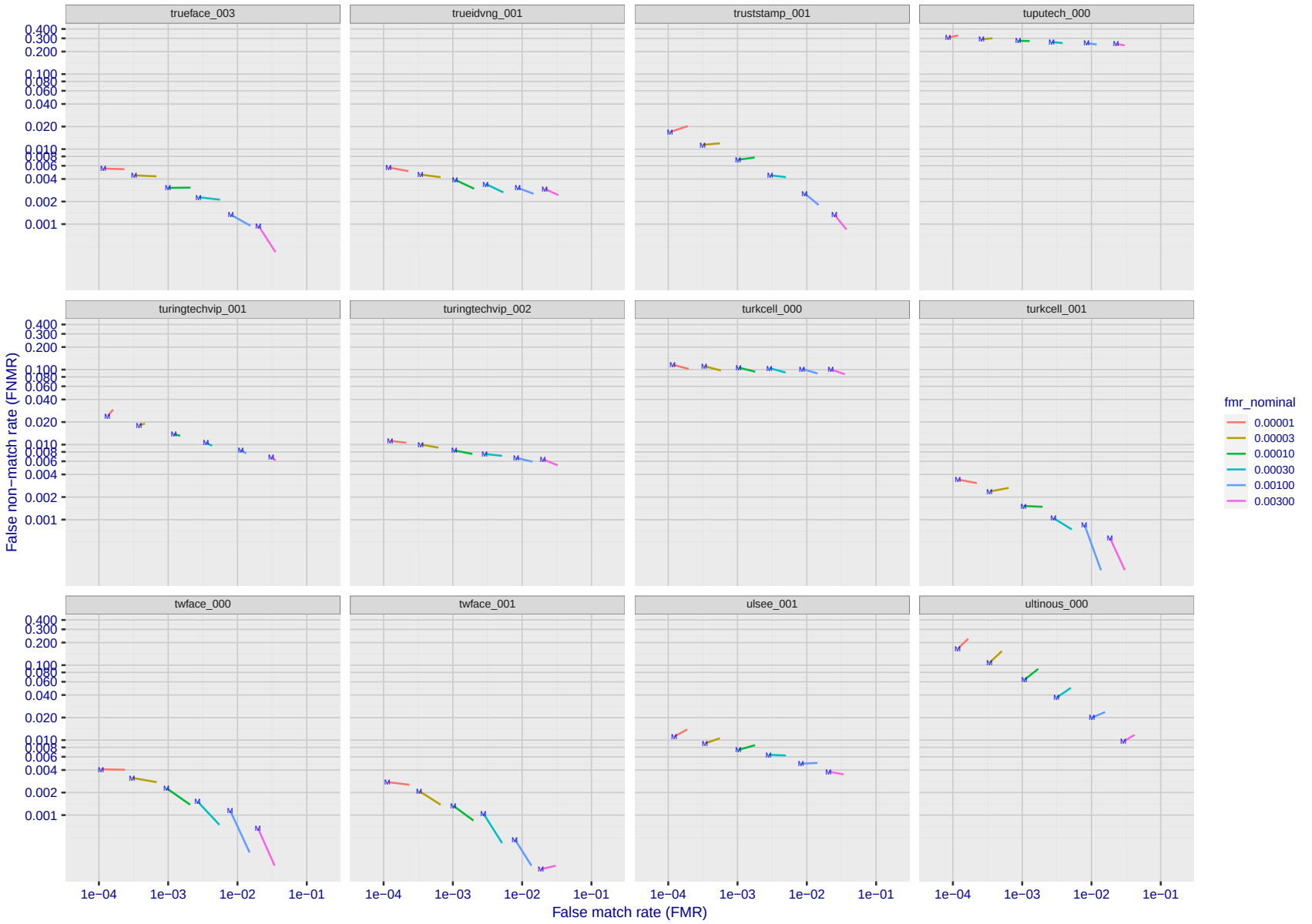

Figure 249: For the visa images, FNMR and FMR at six operating points along the DET characteristic. At each point a line is drawn between (FMR,FNMR)$_{\text{MALE}}$ and (FMR,FNMR)$_{\text{FEMALE}}$ showing how which sex has lower FMR and/or FNMR. The "M" label denotes male, the other end of the line corresponds to female. The six operating thresholds are selected to give the nominal false match rates given in the legend, and are computed over all impostor pairs regardless of age, sex, and place of birth. The plotted FMR values are broadly an order of magnitude larger than the nominal rates because FMR is computed over demographically-matched impostor pairs i.e individuals of the same sex, from the same geographic region (see section 3.6.1), and the same age group (see section 3.6.2).

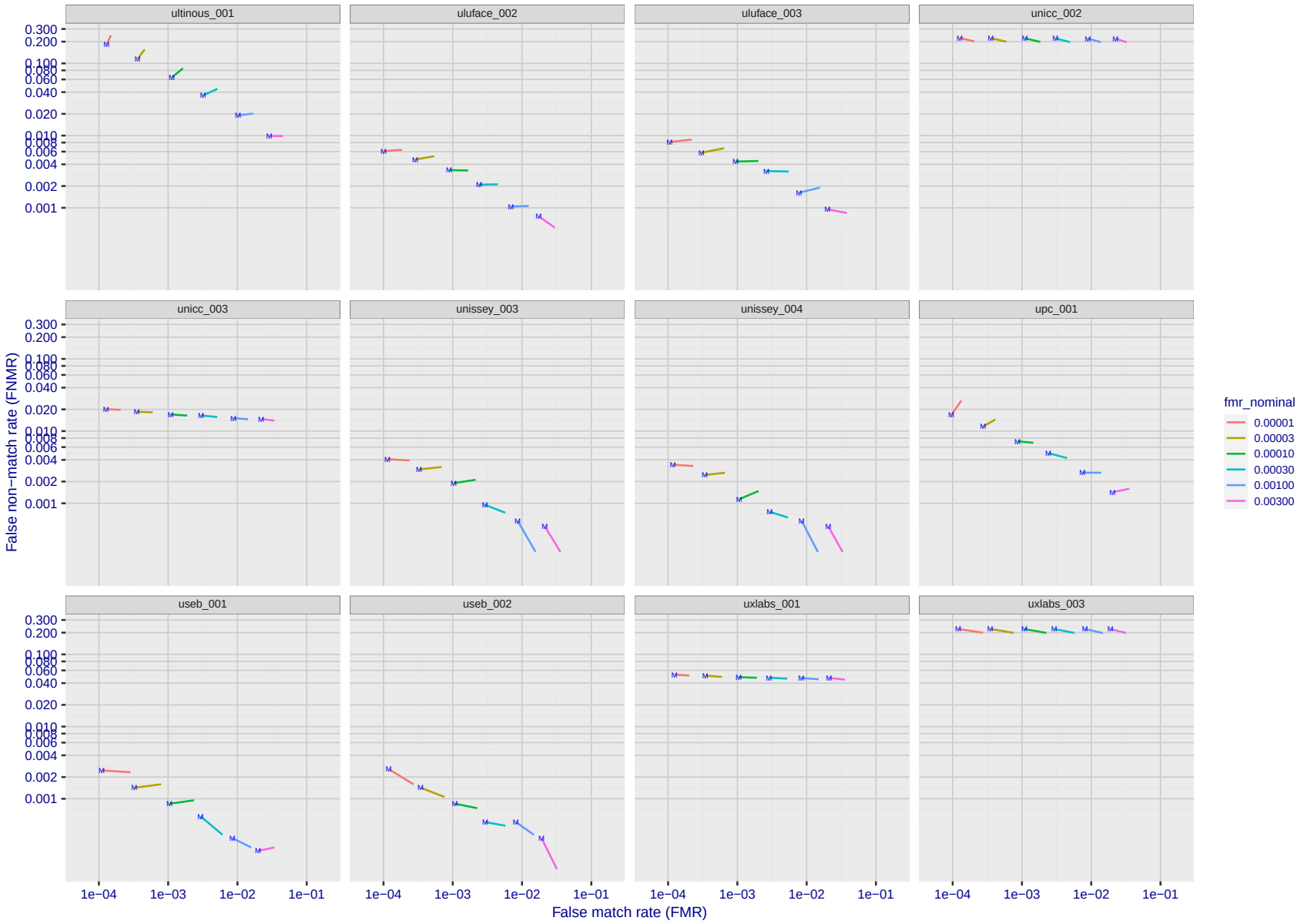

Figure 250: For the visa images, FNMR and FMR at six operating points along the DET characteristic. At each point a line is drawn between (FMR,FNMR)$_{\text{MALE}}$ and (FMR,FNMR)$_{\text{FEMALE}}$ showing how which sex has lower FMR and/or FNMR. The "M" label denotes male, the other end of the line corresponds to female. The six operating thresholds are selected to give the nominal false match rates given in the legend, and are computed over all impostor pairs regardless of age, sex, and place of birth. The plotted FMR values are broadly an order of magnitude larger than the nominal rates because FMR is computed over demographically-matched impostor pairs i.e individuals of the same sex, from the same geographic region (see section 3.6.1), and the same age group (see section 3.6.2).

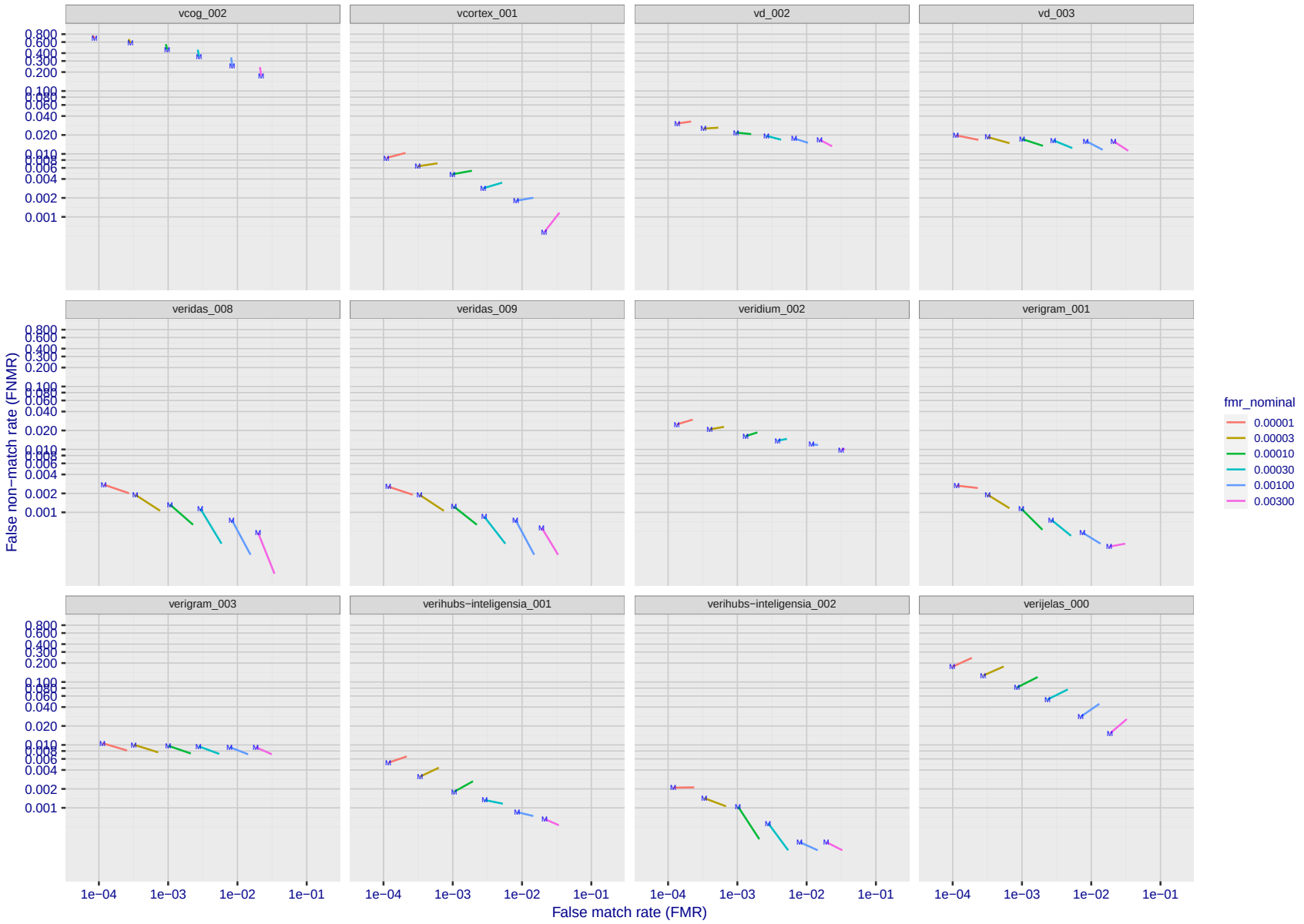

Figure 251: For the visa images, FNMR and FMR at six operating points along the DET characteristic. At each point a line is drawn between (FMR,FNMR)$_{\text{MALE}}$ and (FMR,FNMR)$_{\text{FEMALE}}$ showing how which sex has lower FMR and/or FNMR. The "M" label denotes male, the other end of the line corresponds to female. The six operating thresholds are selected to give the nominal false match rates given in the legend, and are computed over all impostor pairs regardless of age, sex, and place of birth. The plotted FMR values are broadly an order of magnitude larger than the nominal rates because FMR is computed over demographically-matched impostor pairs i.e individuals of the same sex, from the same geographic region (see section 3.6.1), and the same age group (see section 3.6.2).

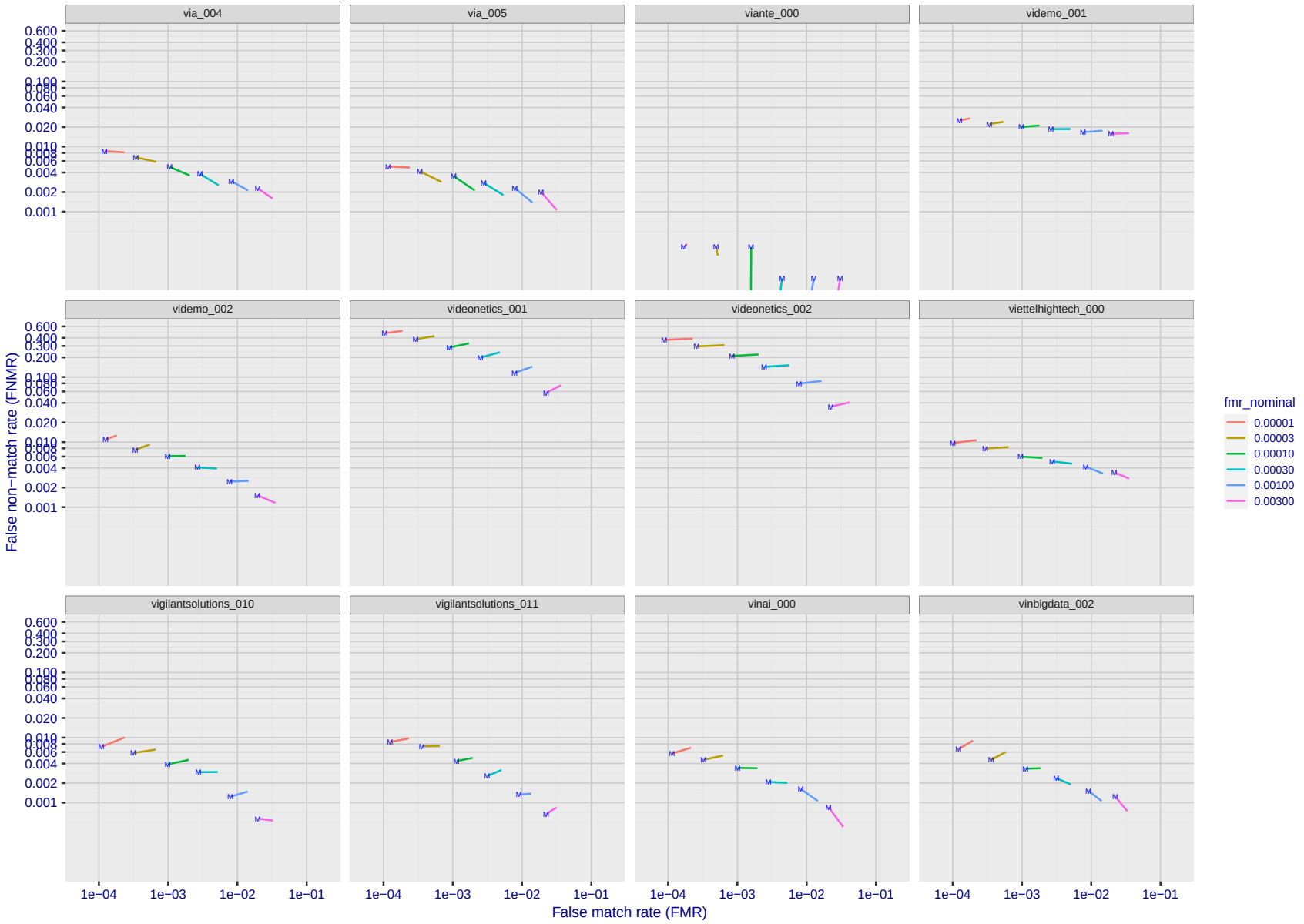

Figure 252: For the visa images, FNMR and FMR at six operating points along the DET characteristic. At each point a line is drawn between (FMR,FNMR)$_{\text{MALE}}$ and (FMR,FNMR)$_{\text{FEMALE}}$ showing how which sex has lower FMR and/or FNMR. The "M" label denotes male, the other end of the line corresponds to female. The six operating thresholds are selected to give the nominal false match rates given in the legend, and are computed over all impostor pairs regardless of age, sex, and place of birth. The plotted FMR values are broadly an order of magnitude larger than the nominal rates because FMR is computed over demographically-matched impostor pairs i.e individuals of the same sex, from the same geographic region (see section 3.6.1), and the same age group (see section 3.6.2).

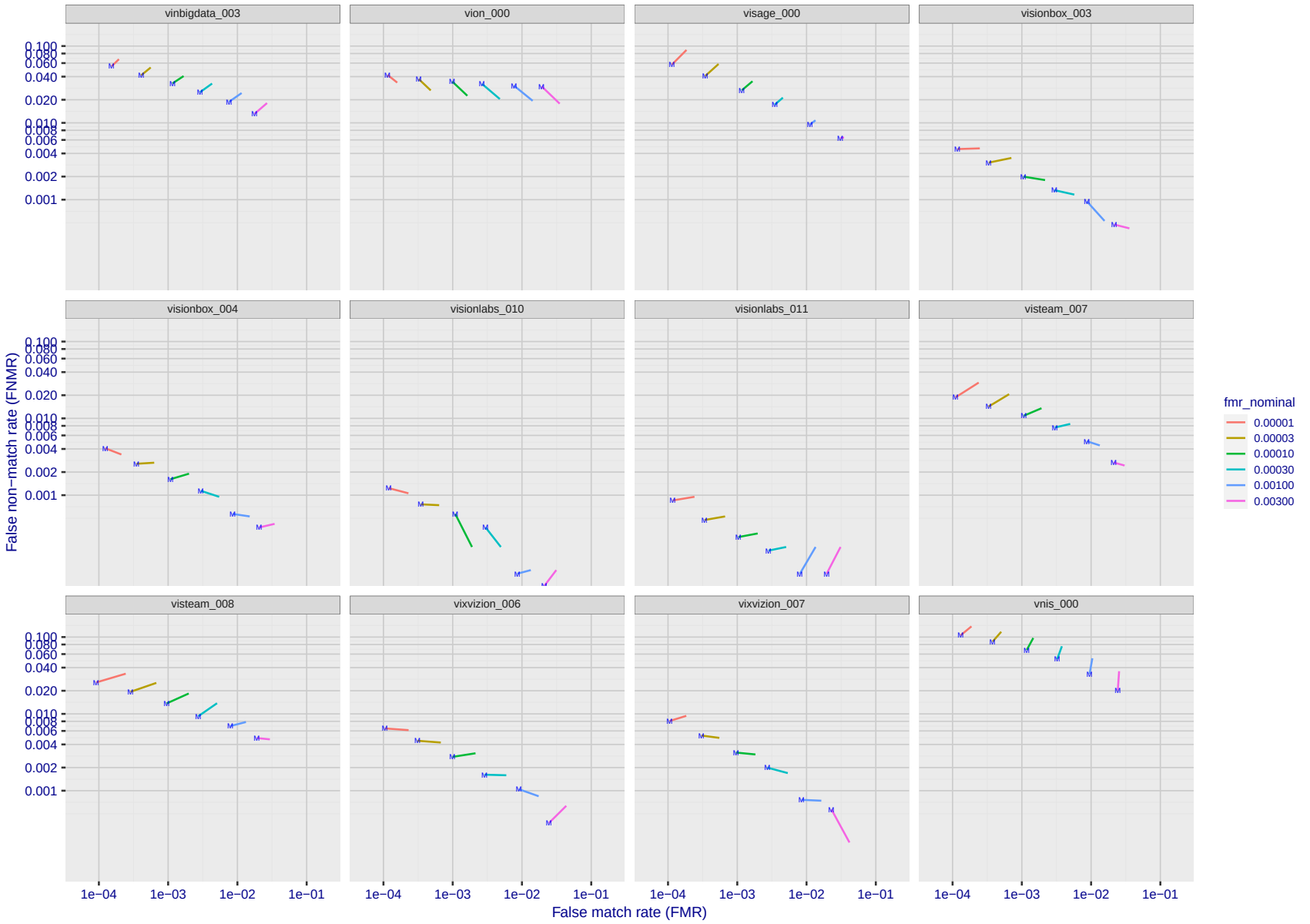

Figure 253: For the visa images, FNMR and FMR at six operating points along the DET characteristic. At each point a line is drawn between (FMR,FNMR)$_{\text{MALE}}$ and (FMR,FNMR)$_{\text{FEMALE}}$ showing how which sex has lower FMR and/or FNMR. The "M" label denotes male, the other end of the line corresponds to female. The six operating thresholds are selected to give the nominal false match rates given in the legend, and are computed over all impostor pairs regardless of age, sex, and place of birth. The plotted FMR values are broadly an order of magnitude larger than the nominal rates because FMR is computed over demographically-matched impostor pairs i.e individuals of the same sex, from the same geographic region (see section 3.6.1), and the same age group (see section 3.6.2).

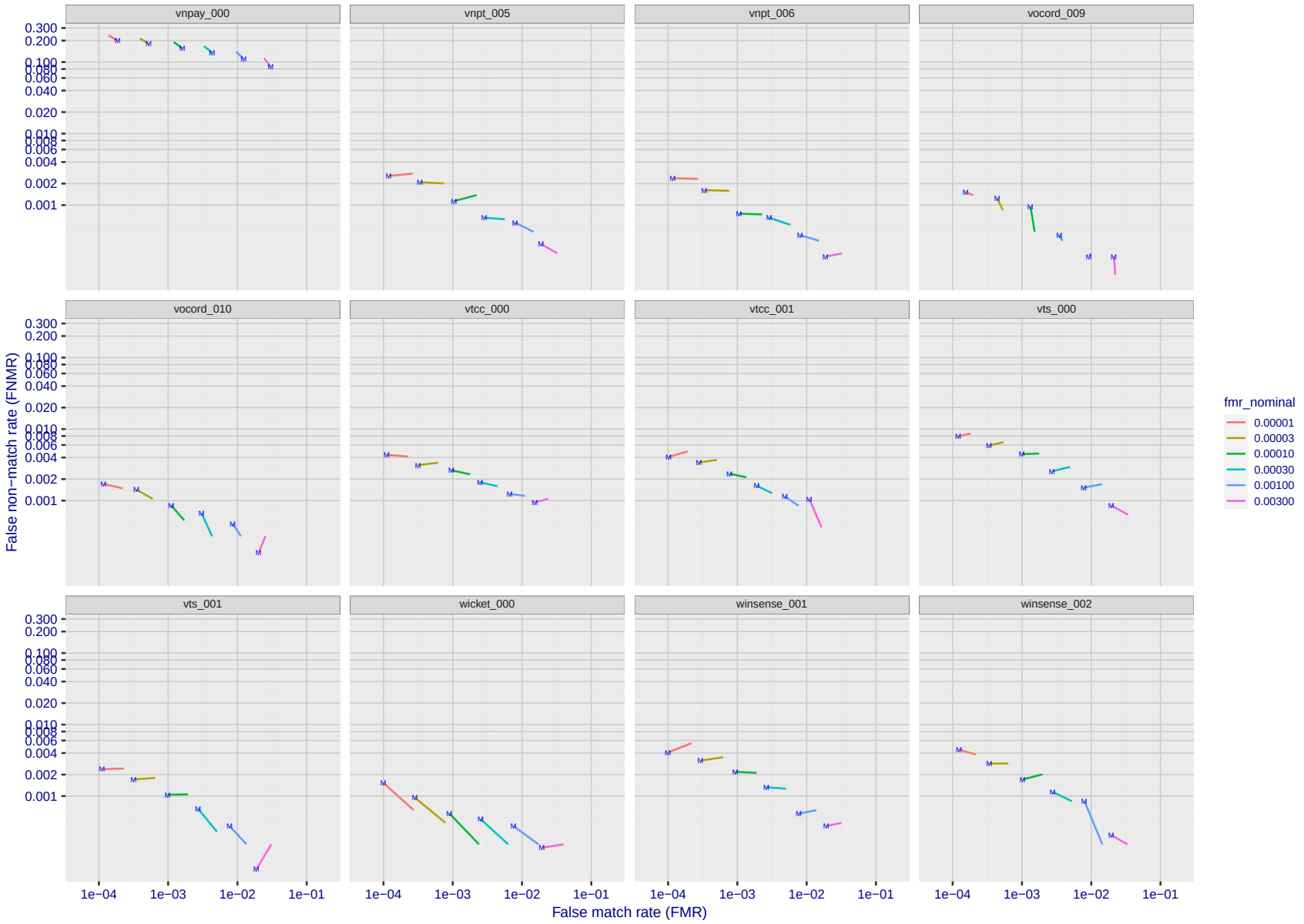

Figure 254: For the visa images, FNMR and FMR at six operating points along the DET characteristic. At each point a line is drawn between (FMR,FNMR)$_{\text{MALE}}$ and (FMR,FNMR)$_{\text{FEMALE}}$ showing how which sex has lower FMR and/or FNMR. The "M" label denotes male, the other end of the line corresponds to female. The six operating thresholds are selected to give the nominal false match rates given in the legend, and are computed over all impostor pairs regardless of age, sex, and place of birth. The plotted FMR values are broadly an order of magnitude larger than the nominal rates because FMR is computed over demographically-matched impostor pairs i.e individuals of the same sex, from the same geographic region (see section 3.6.1), and the same age group (see section 3.6.2).

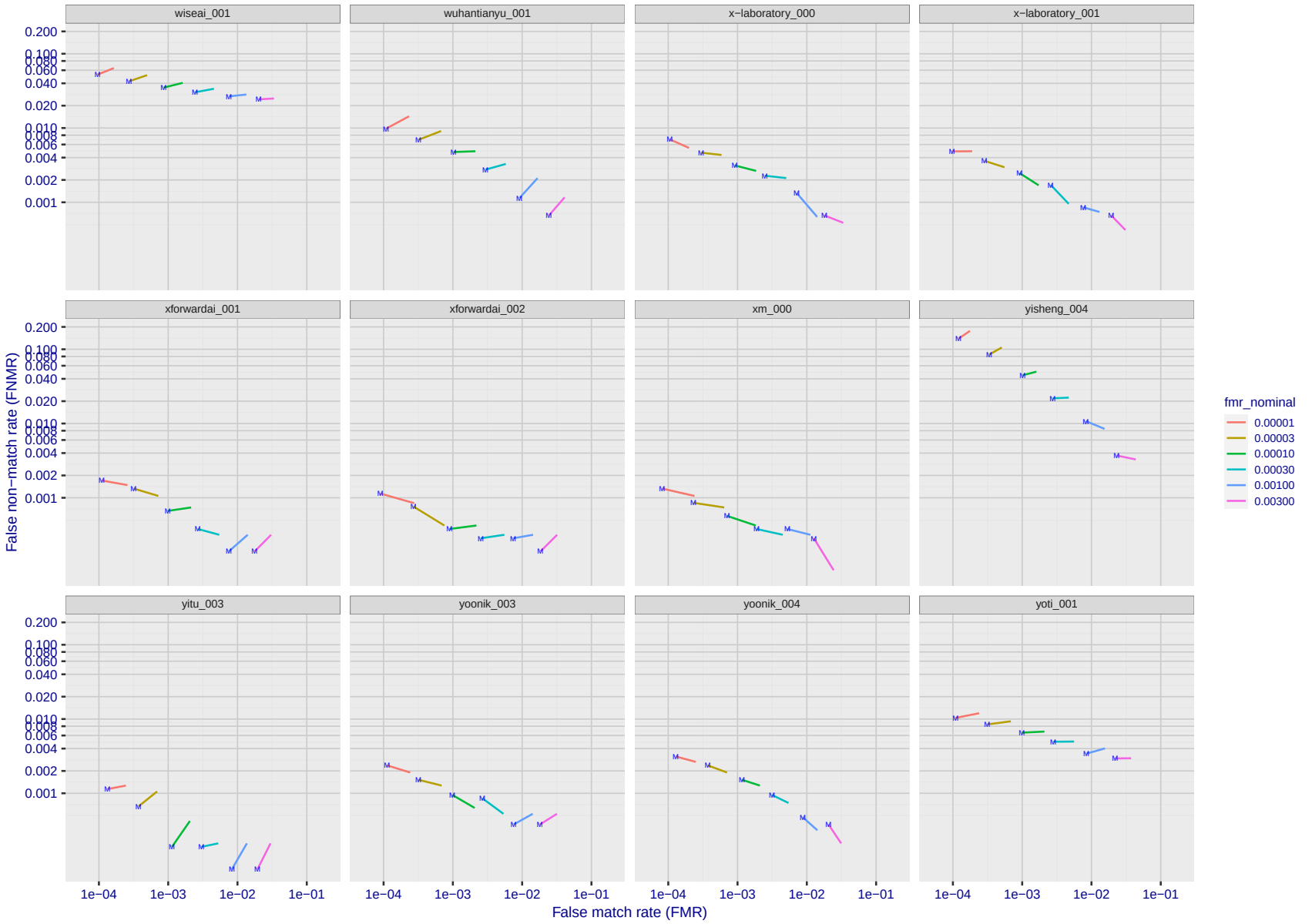

Figure 255: For the visa images, FNMR and FMR at six operating points along the DET characteristic. At each point a line is drawn between (FMR,FNMR)$_{\text{MALE}}$ and (FMR,FNMR)$_{\text{FEMALE}}$ showing how which sex has lower FMR and/or FNMR. The "M" label denotes male, the other end of the line corresponds to female. The six operating thresholds are selected to give the nominal false match rates given in the legend, and are computed over all impostor pairs regardless of age, sex, and place of birth. The plotted FMR values are broadly an order of magnitude larger than the nominal rates because FMR is computed over demographically-matched impostor pairs i.e individuals of the same sex, from the same geographic region (see section 3.6.1), and the same age group (see section 3.6.2).

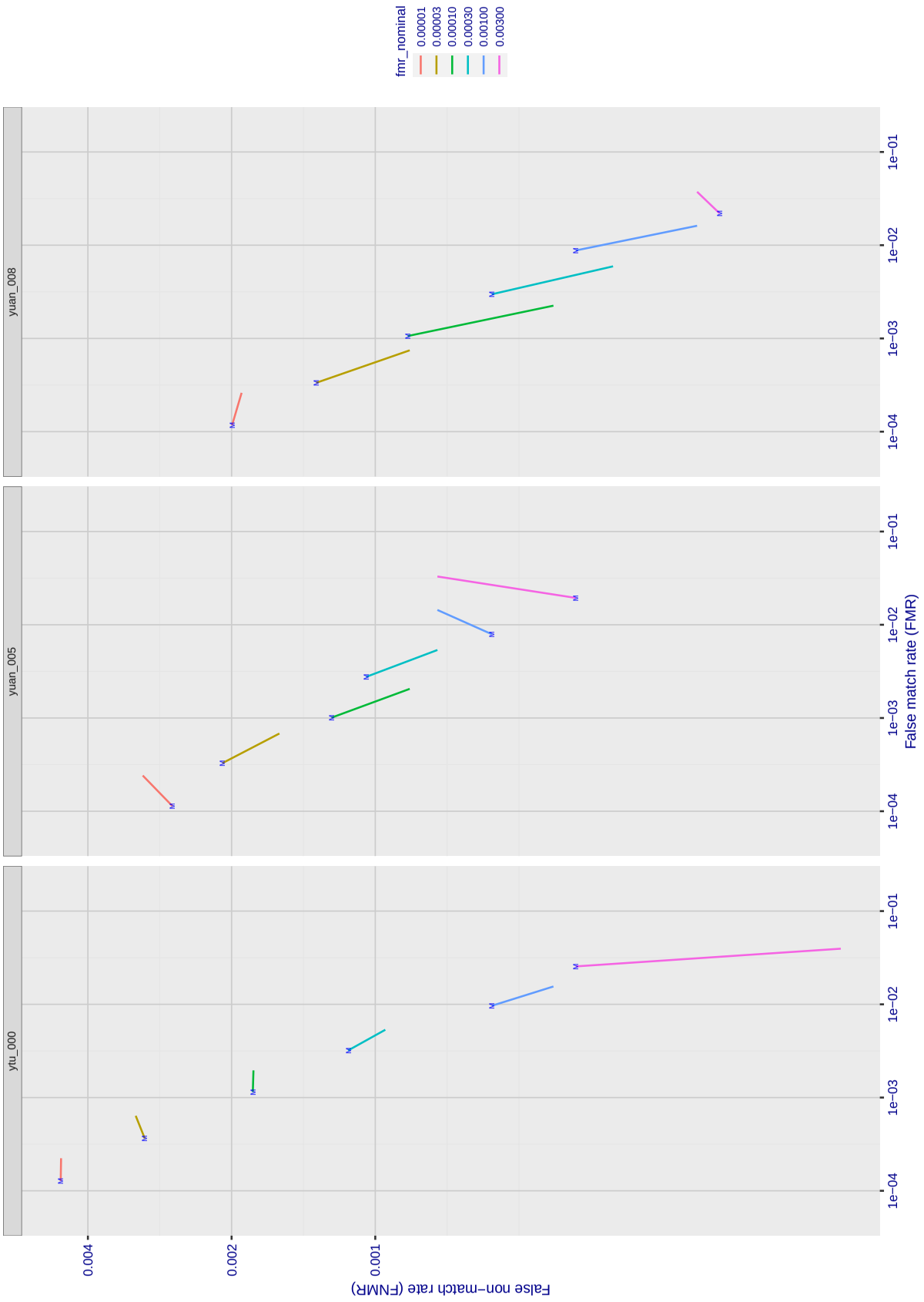

Figure 256: For the visa images, FNMR and FMR at six operating points along the DET characteristic. At each point a line is drawn between (FMR,FNMR)$_{\text{MALE}}$ and (FMR,FNMR)$_{\text{FEMALE}}$ showing how which sex has lower FMR and/or FNMR. The "M" label denotes male, the other end of the line corresponds to female. The six operating thresholds are selected to give the nominal false match rates given in the legend, and are computed over all impostor pairs regardless of age, sex, and place of birth. The plotted FMR values are broadly an order of magnitude larger than the nominal rates because FMR is computed over demographically-matched impostor pairs i.e individuals of the same sex, from the same geographic region (see section 3.6.1), and the same age group (see section 3.6.2).

FNMR(T) "False non-match rate"
FMR(T) "False match rate"

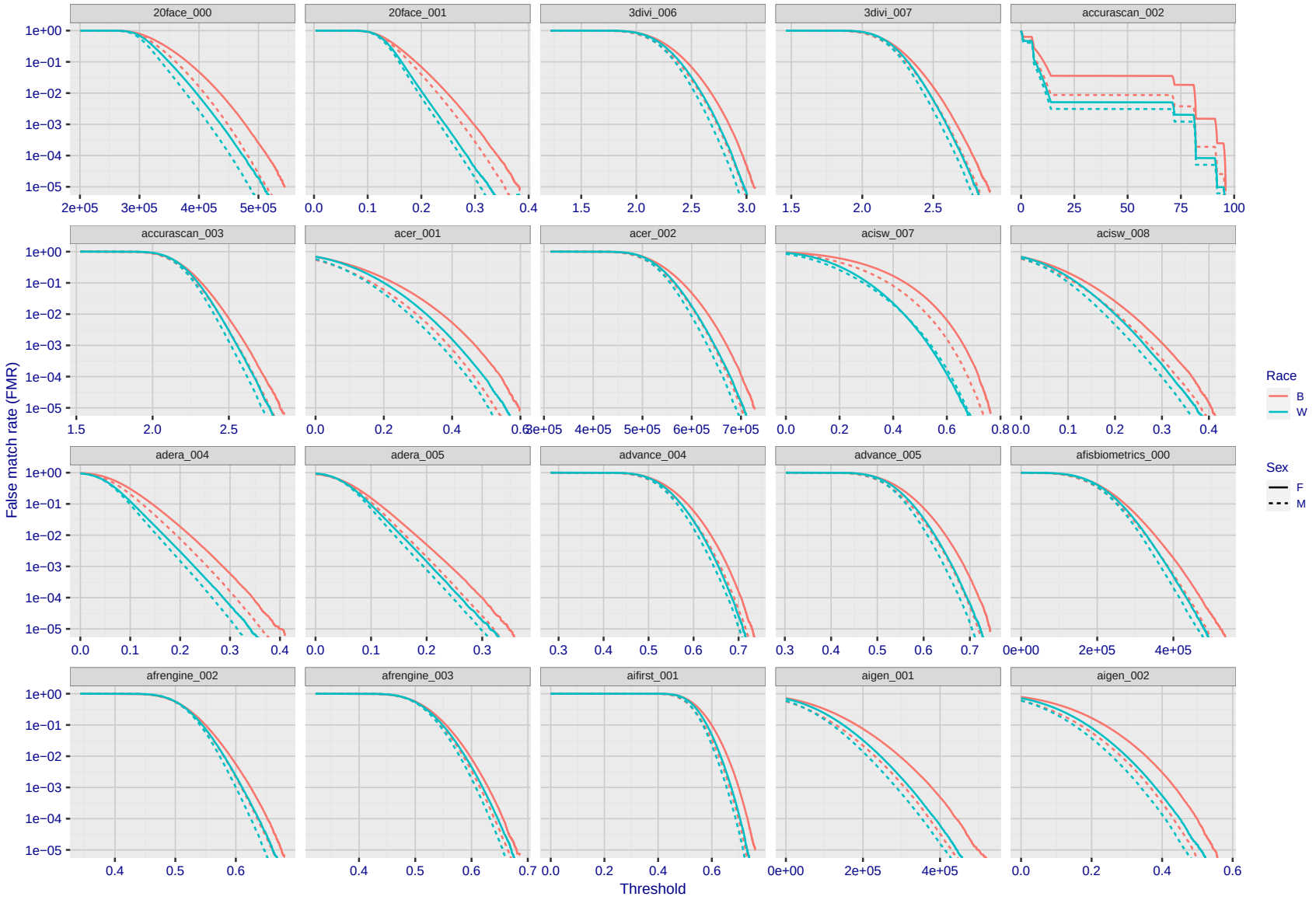

Figure 257: For the mugshot images, the false match calibration curves show false match rate vs. threshold. Separate curves appear for white females, black females, black males and white males.

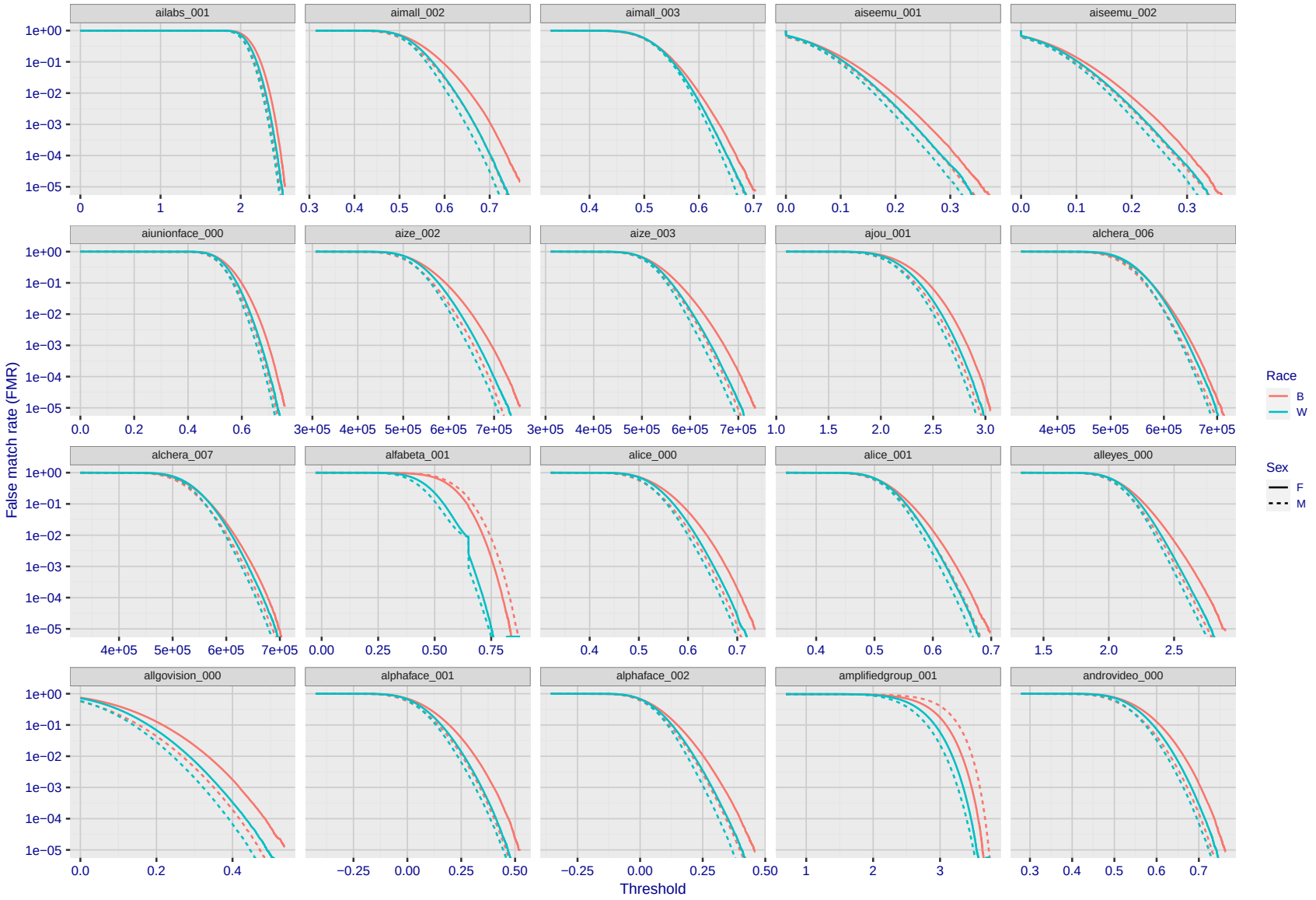

Figure 258: For the mugshot images, the false match calibration curves show false match rate vs. threshold. Separate curves appear for white females, black females, black males and white males.

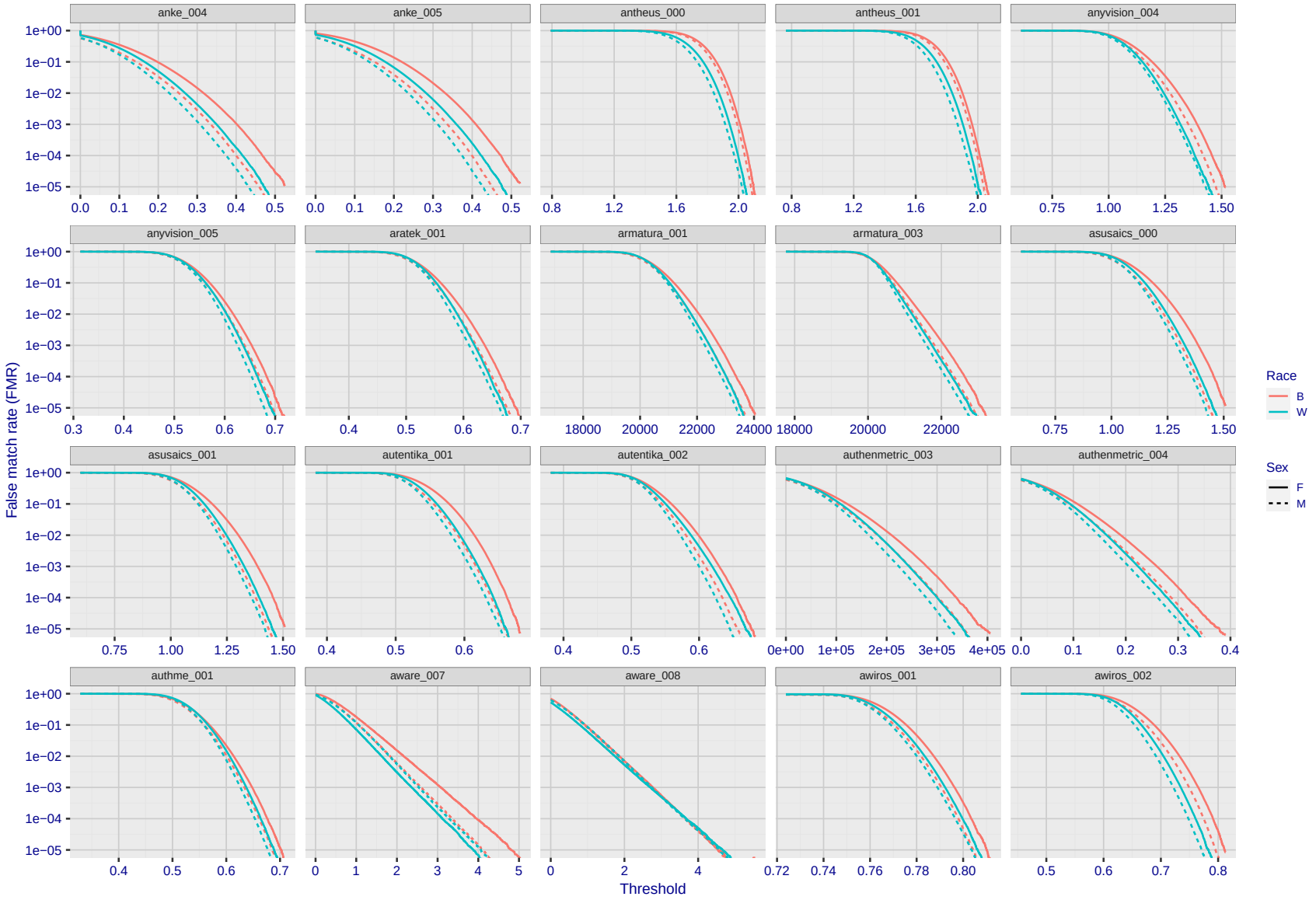

Figure 259: For the mugshot images, the false match calibration curves show false match rate vs. threshold. Separate curves appear for white females, black females, black males and white males.

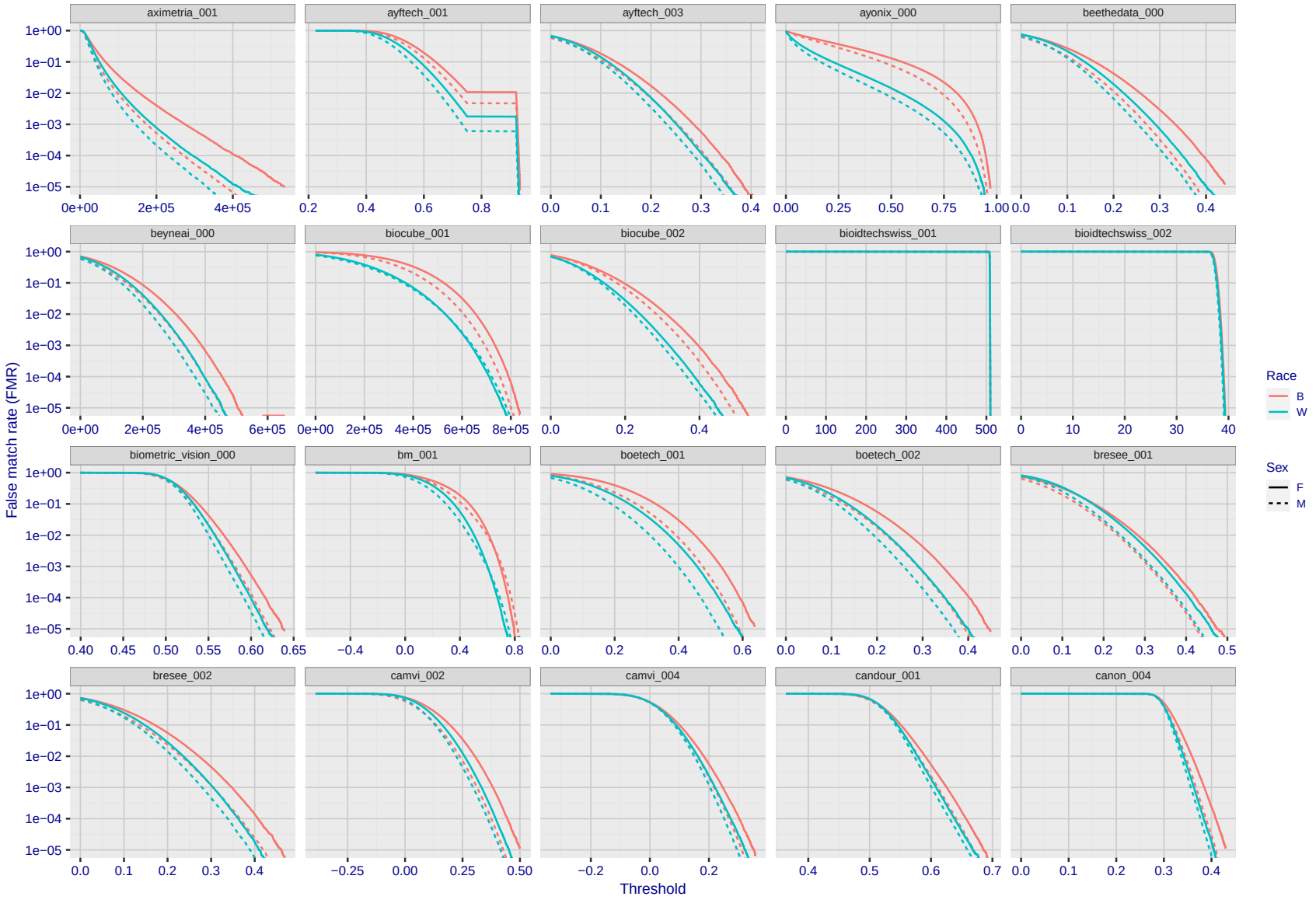

Figure 260: For the mugshot images, the false match calibration curves show false match rate vs. threshold. Separate curves appear for white females, black females, black males and white males.

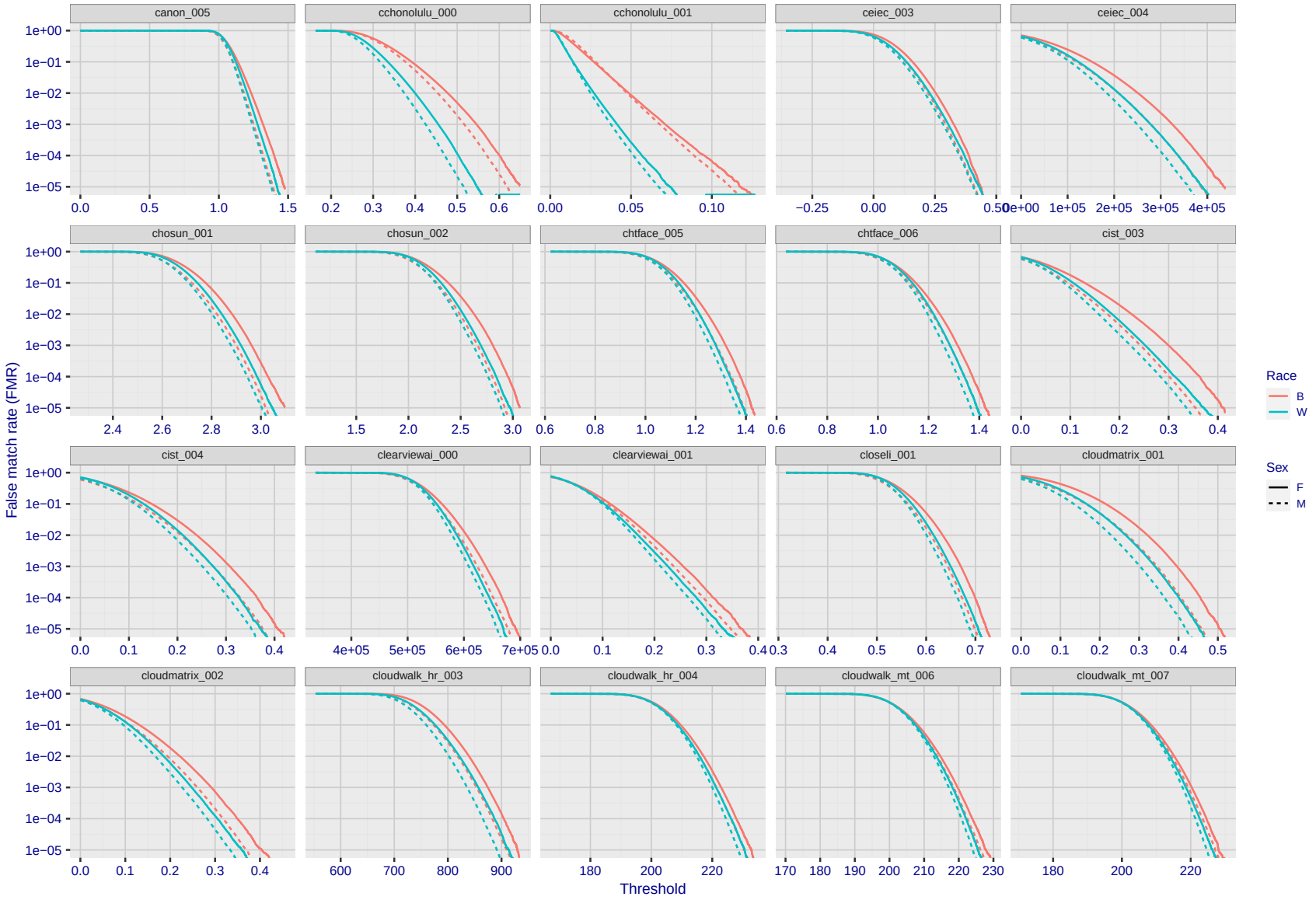

Figure 261: For the mugshot images, the false match calibration curves show false match rate vs. threshold. Separate curves appear for white females, black females, black males and white males.

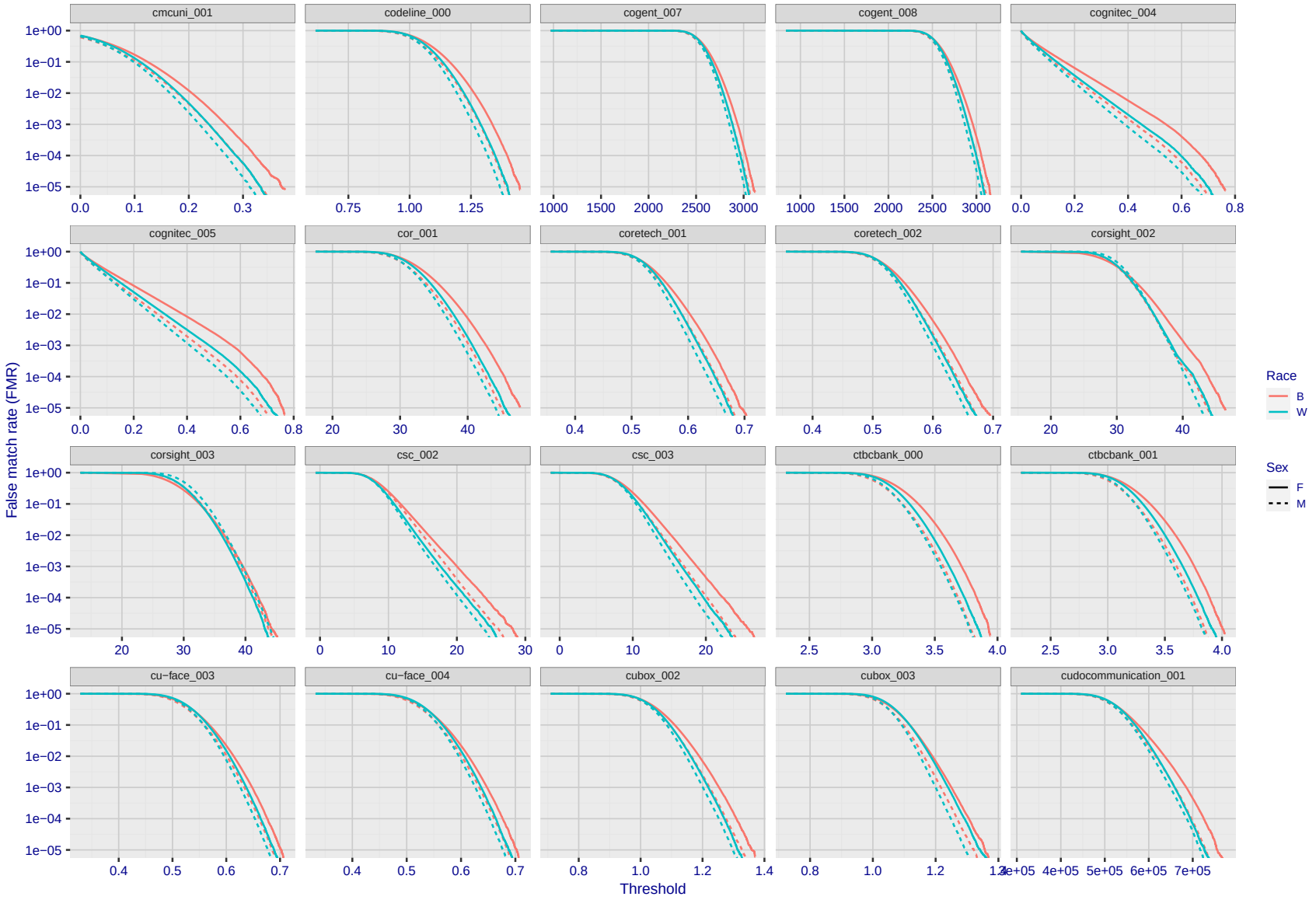

Figure 262: For the mugshot images, the false match calibration curves show false match rate vs. threshold. Separate curves appear for white females, black females, black males and white males.

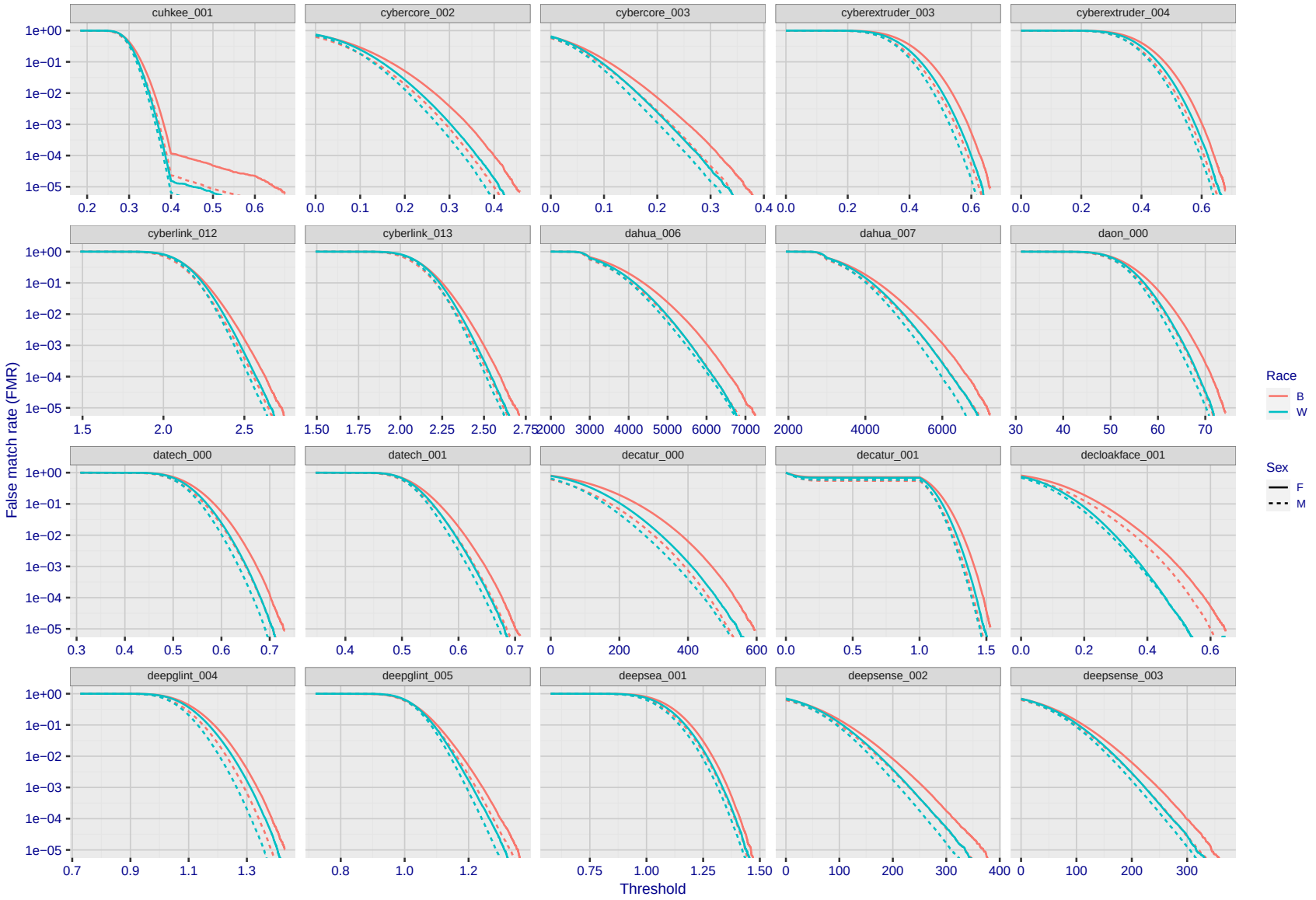

Figure 263: For the mugshot images, the false match calibration curves show false match rate vs. threshold. Separate curves appear for white females, black females, black males and white males.

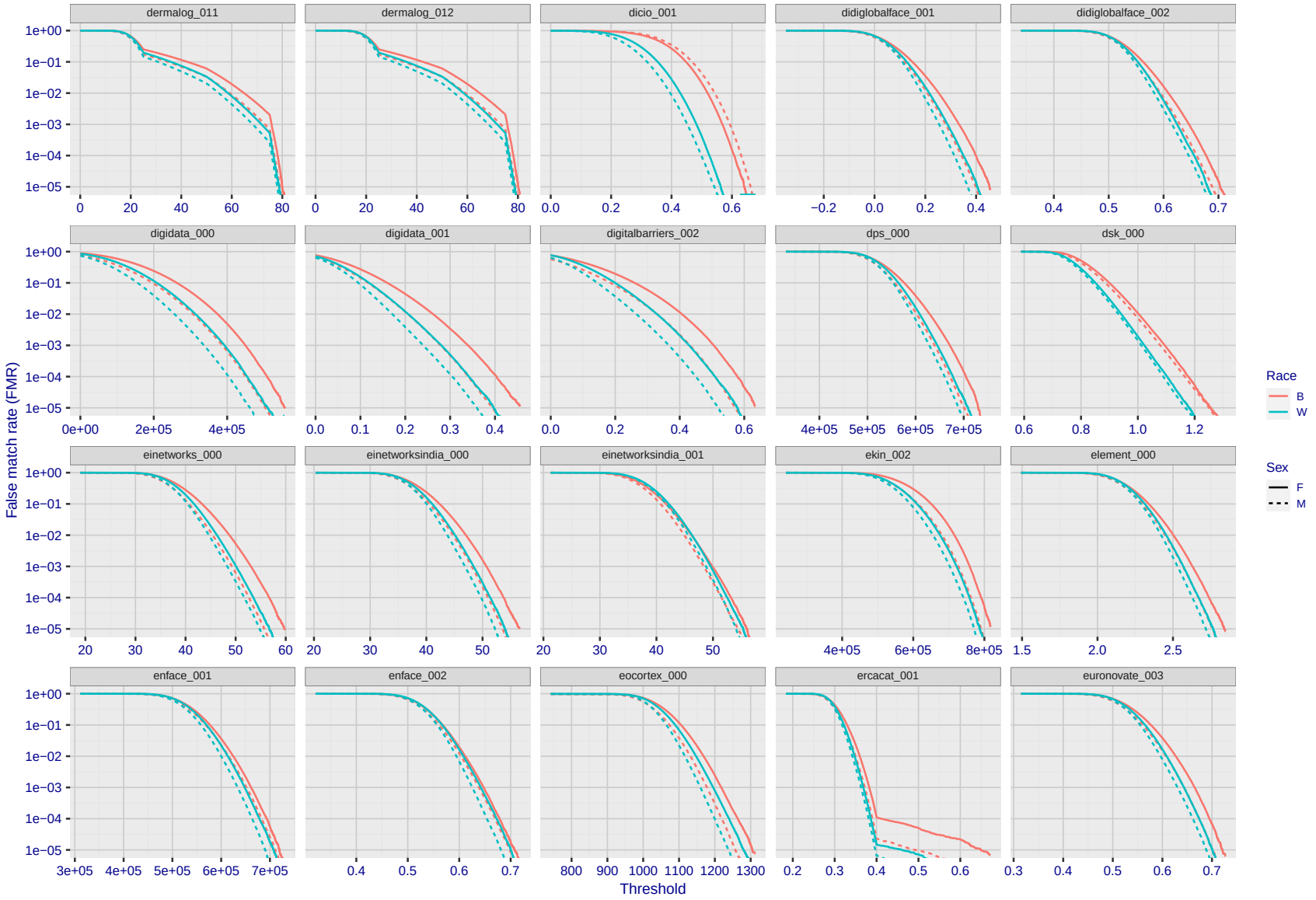

Figure 264: For the mugshot images, the false match calibration curves show false match rate vs. threshold. Separate curves appear for white females, black females, black males and white males.

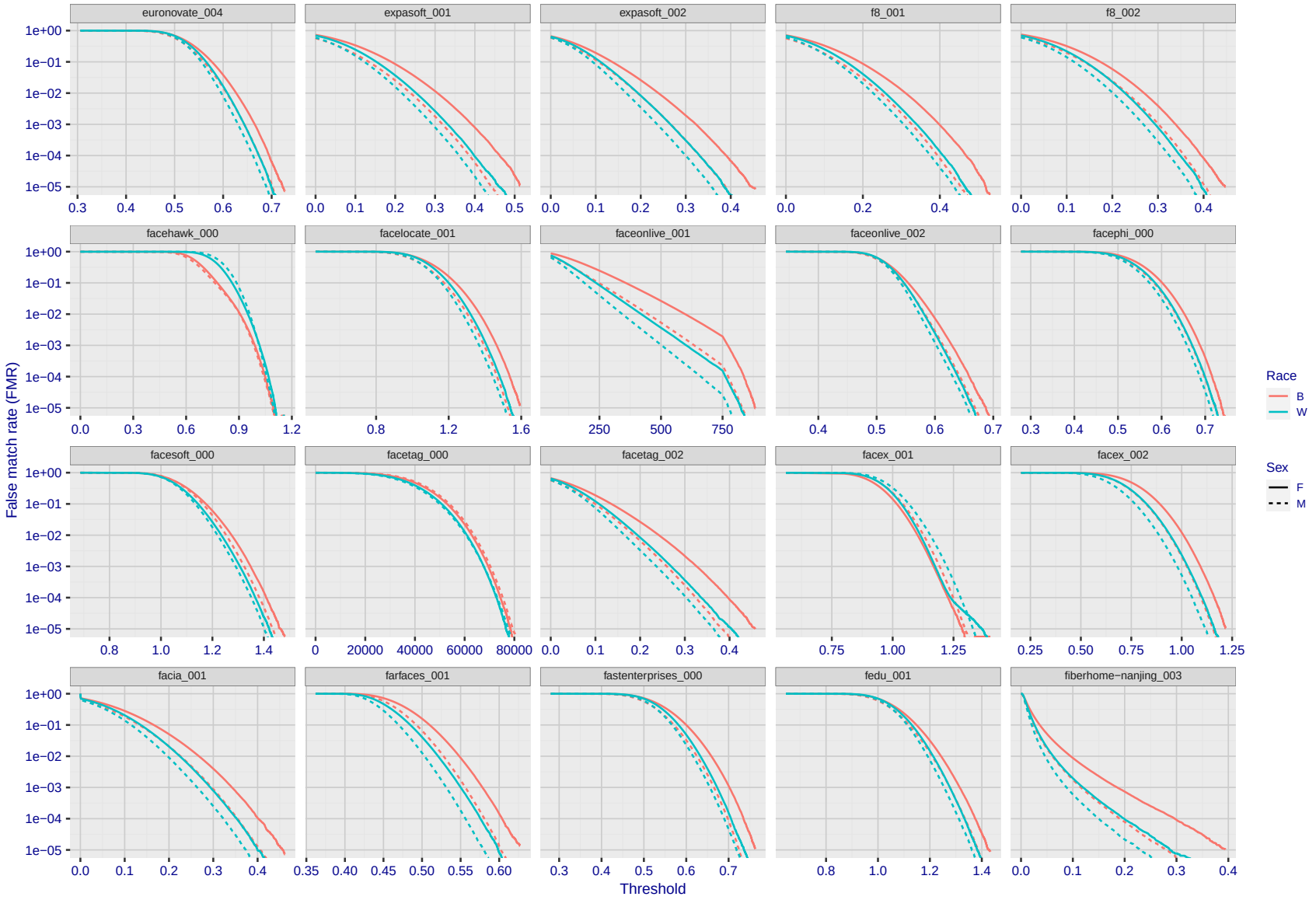

Figure 265: For the mugshot images, the false match calibration curves show false match rate vs. threshold. Separate curves appear for white females, black females, black males and white males.

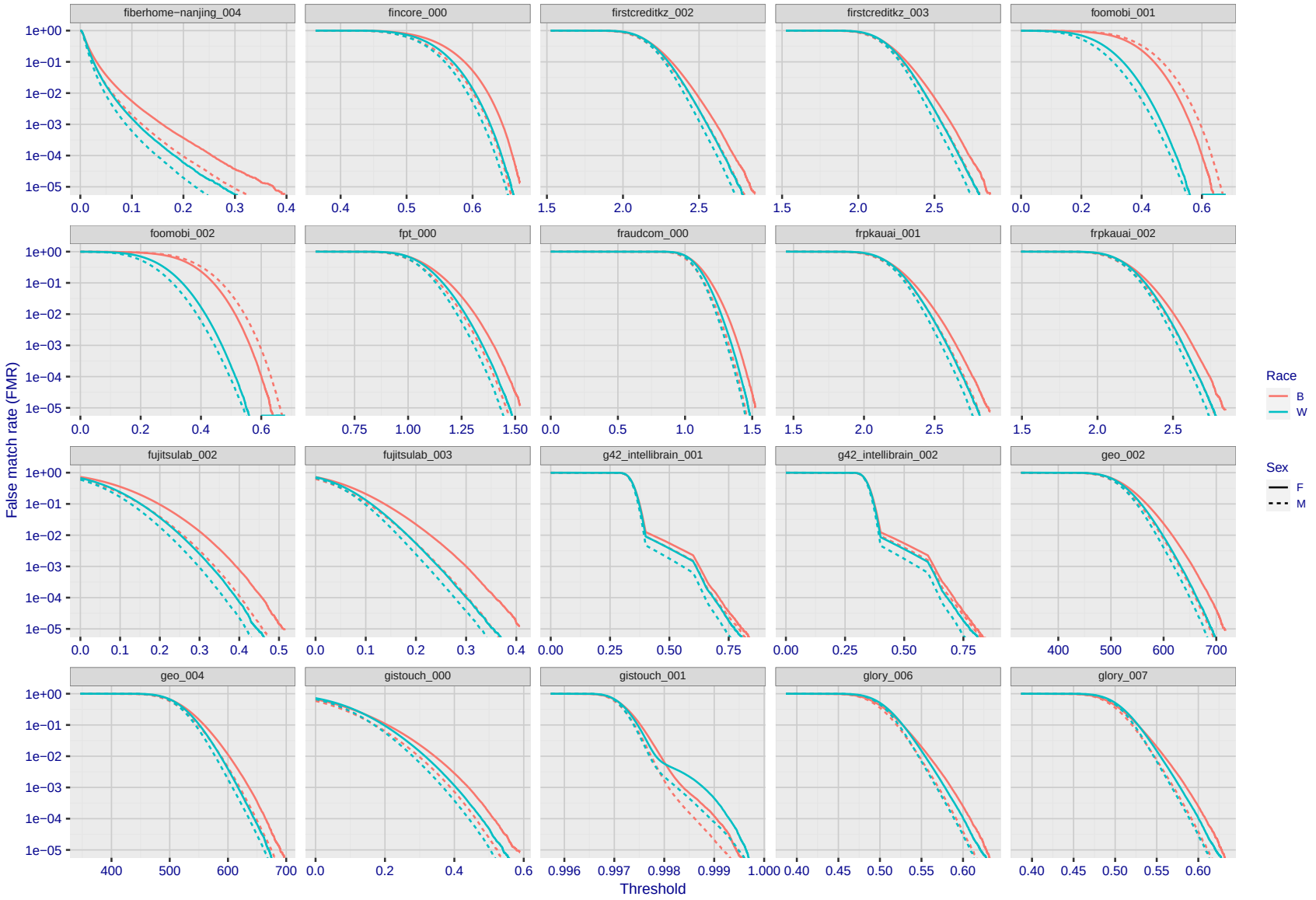

Figure 266: For the mugshot images, the false match calibration curves show false match rate vs. threshold. Separate curves appear for white females, black females, black males and white males.

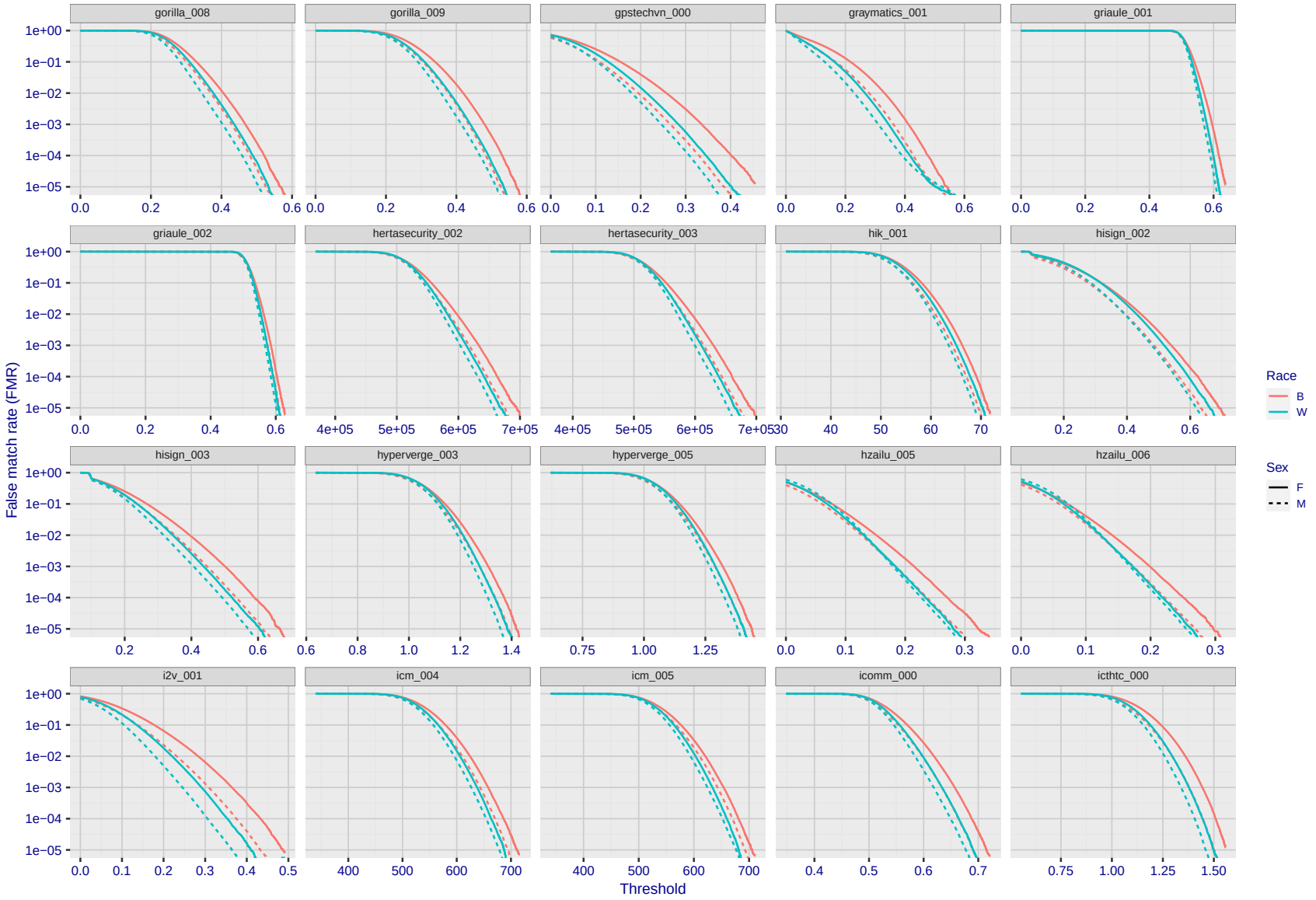

Figure 267: For the mugshot images, the false match calibration curves show false match rate vs. threshold. Separate curves appear for white females, black females, black males and white males.

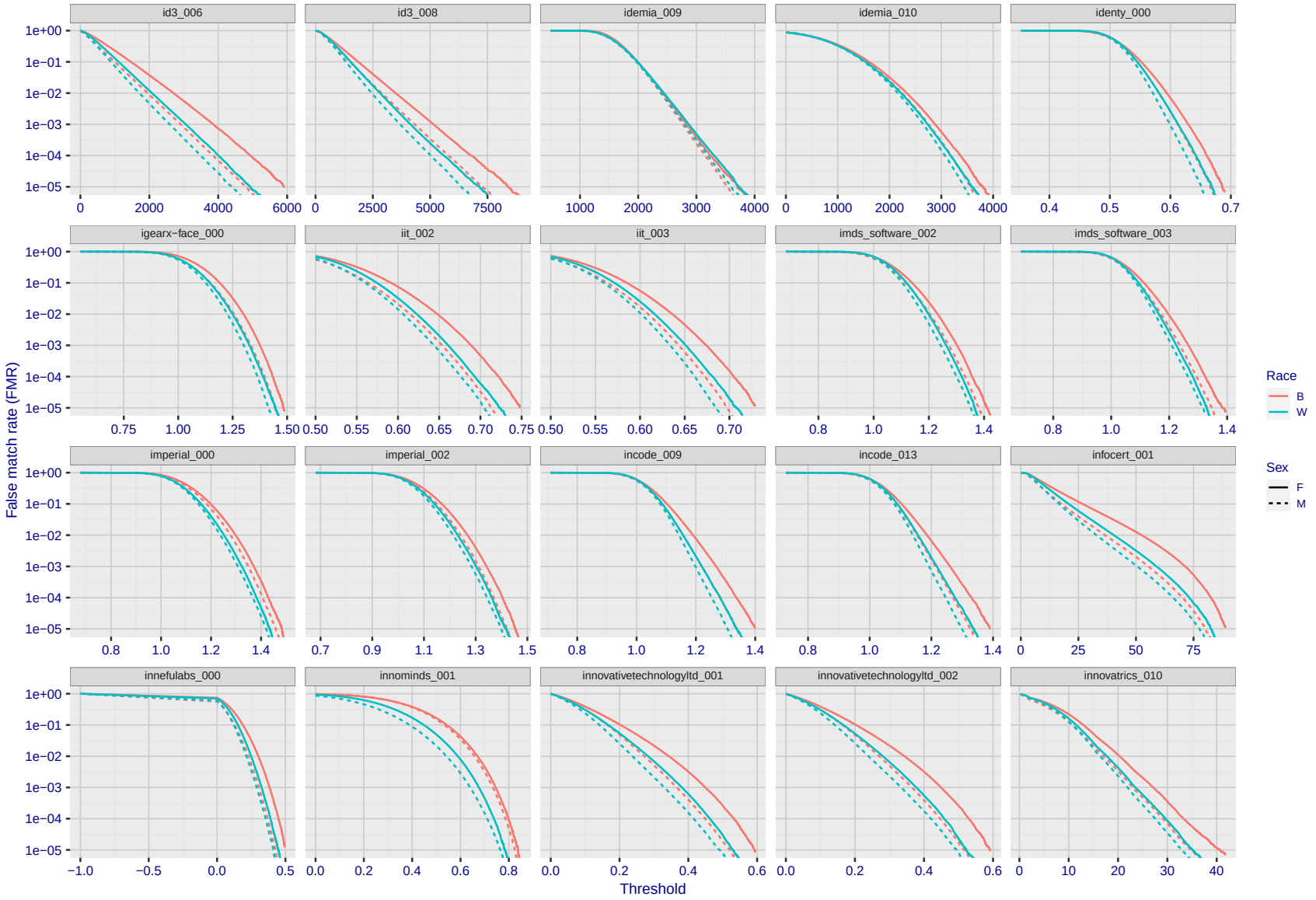

Figure 268: For the mugshot images, the false match calibration curves show false match rate vs. threshold. Separate curves appear for white females, black females, black males and white males.

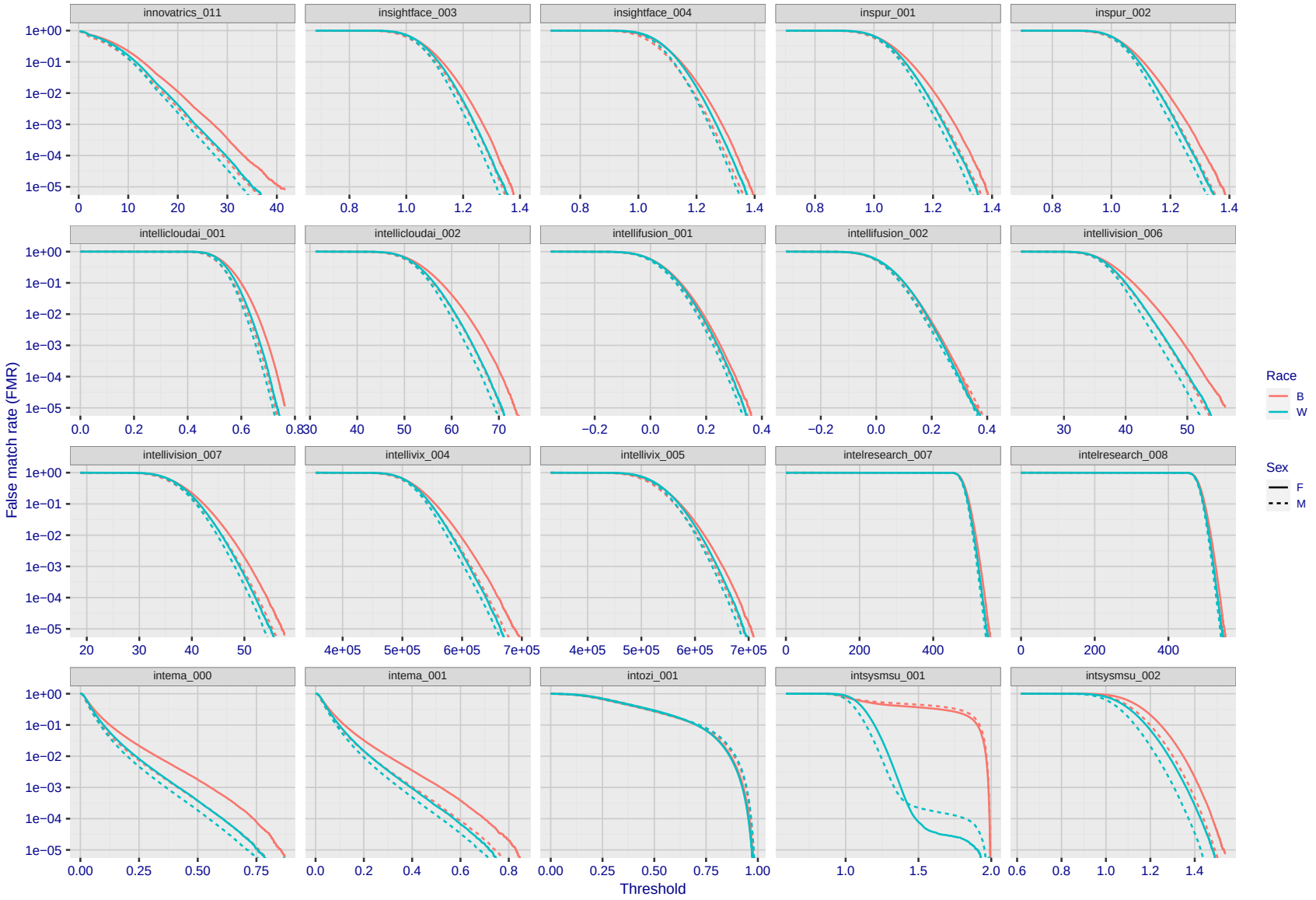

Figure 269: For the mugshot images, the false match calibration curves show false match rate vs. threshold. Separate curves appear for white females, black females, black males and white males.

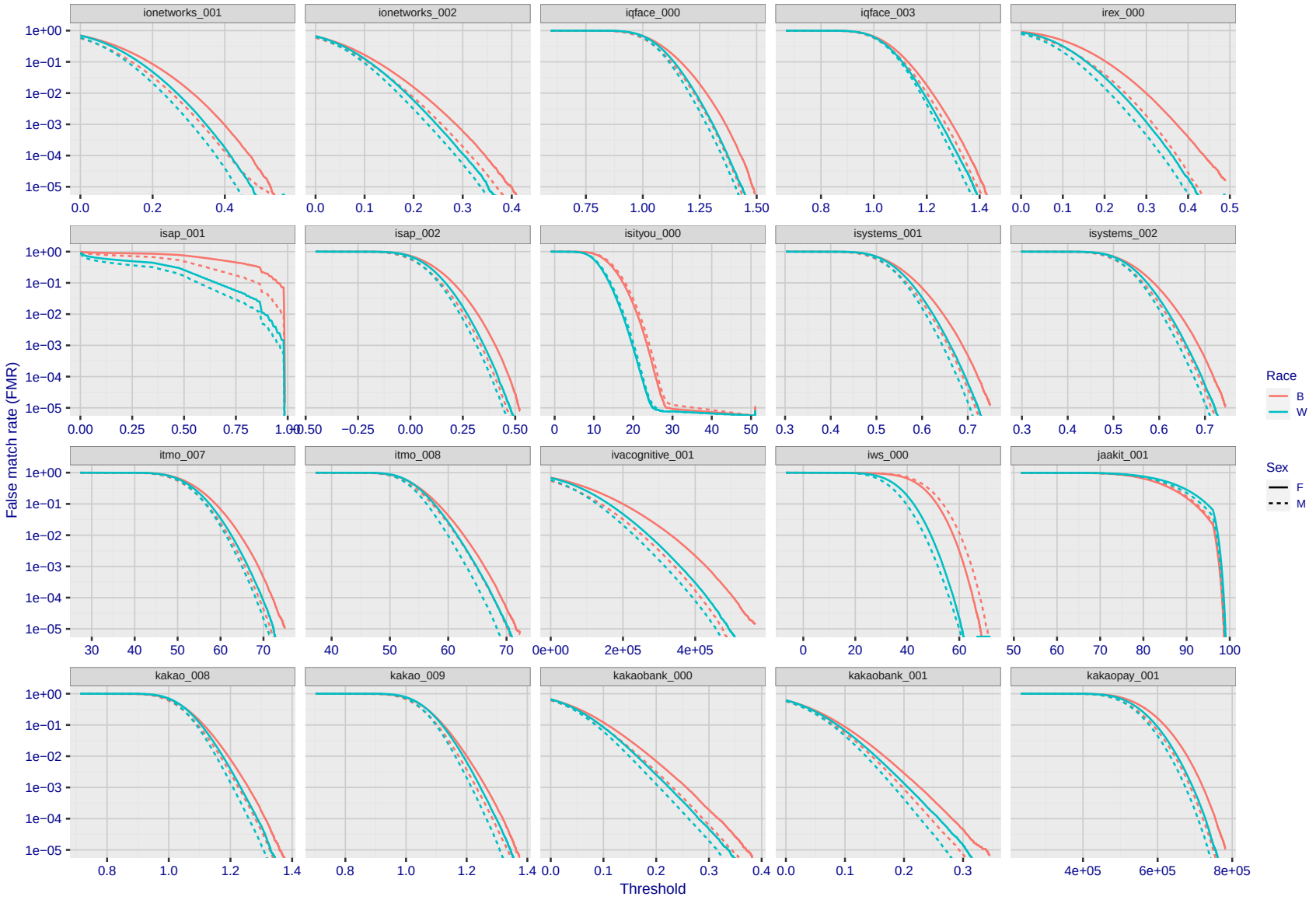

Figure 270: For the mugshot images, the false match calibration curves show false match rate vs. threshold. Separate curves appear for white females, black females, black males and white males.

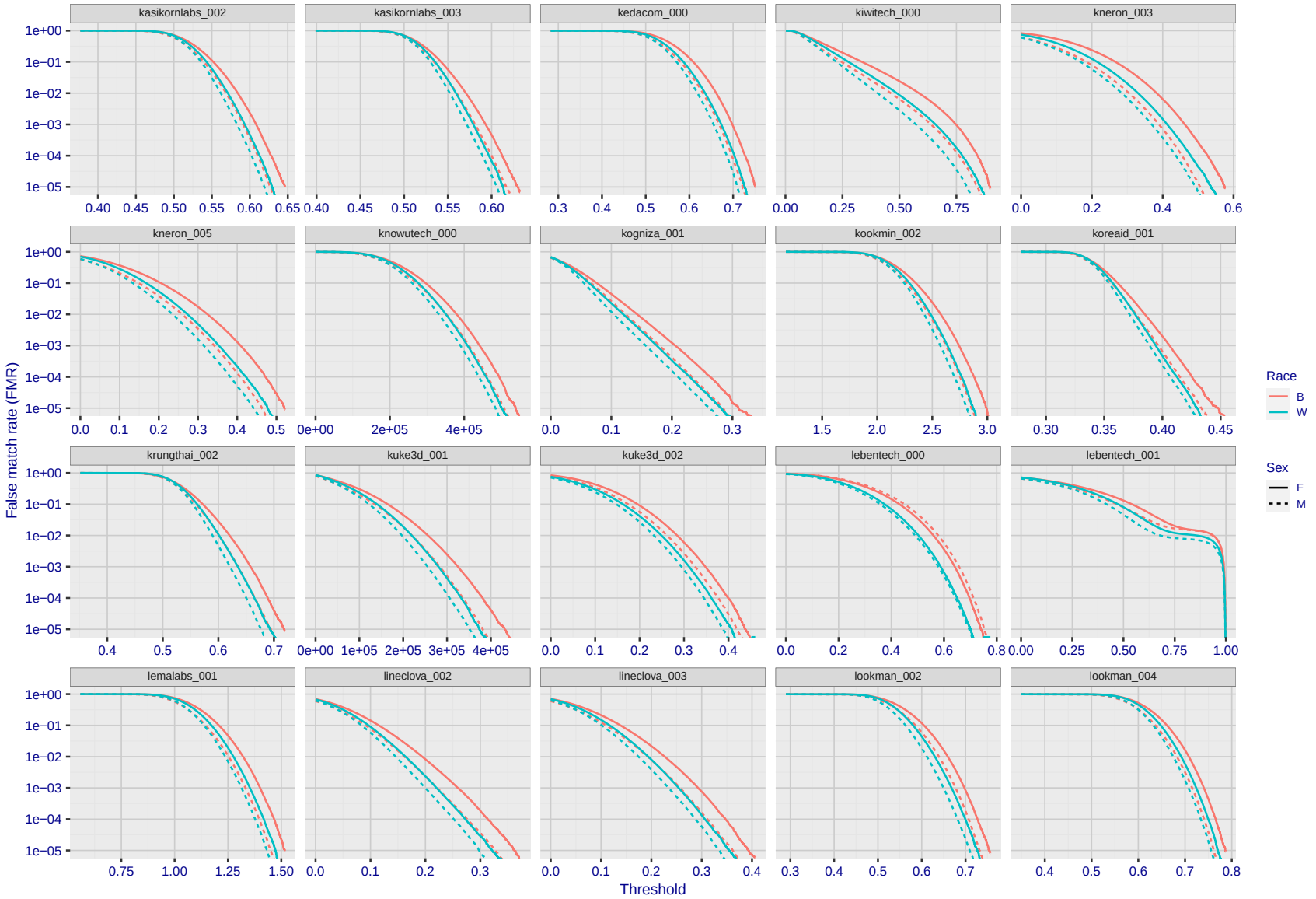

Figure 271: For the mugshot images, the false match calibration curves show false match rate vs. threshold. Separate curves appear for white females, black females, black males and white males.

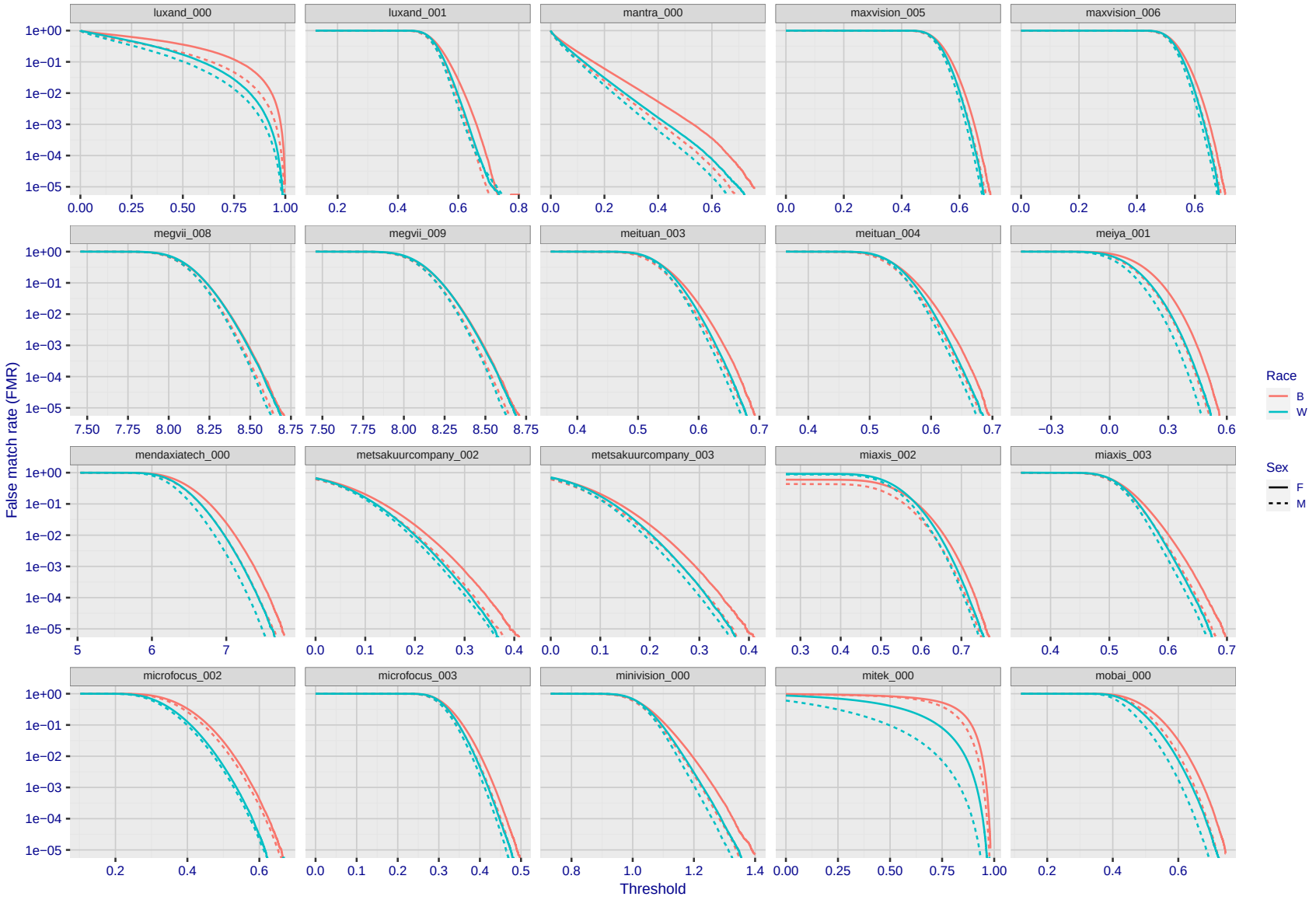

Figure 272: For the mugshot images, the false match calibration curves show false match rate vs. threshold. Separate curves appear for white females, black females, black males and white males.

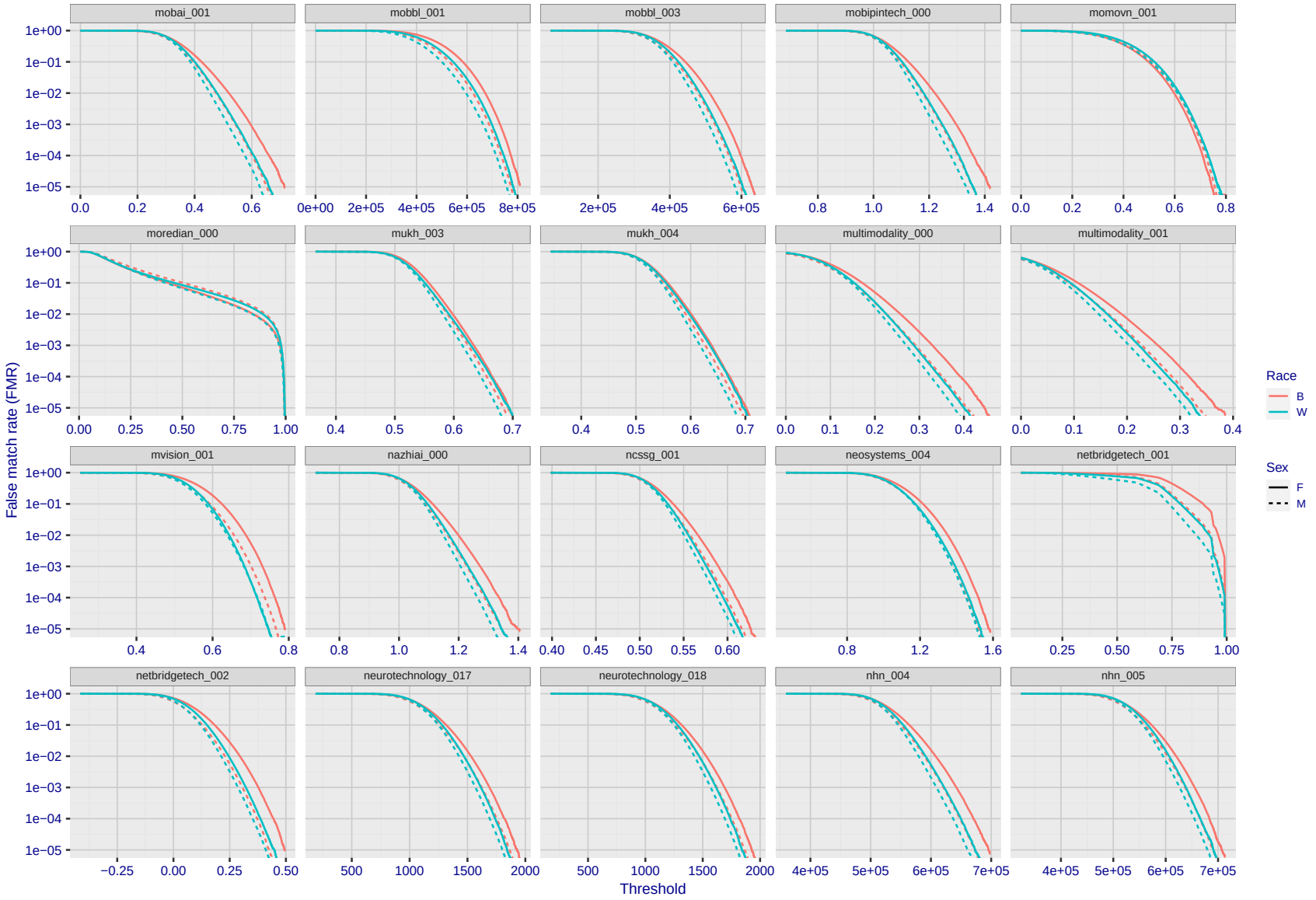

Figure 273: For the mugshot images, the false match calibration curves show false match rate vs. threshold. Separate curves appear for white females, black females, black males and white males.

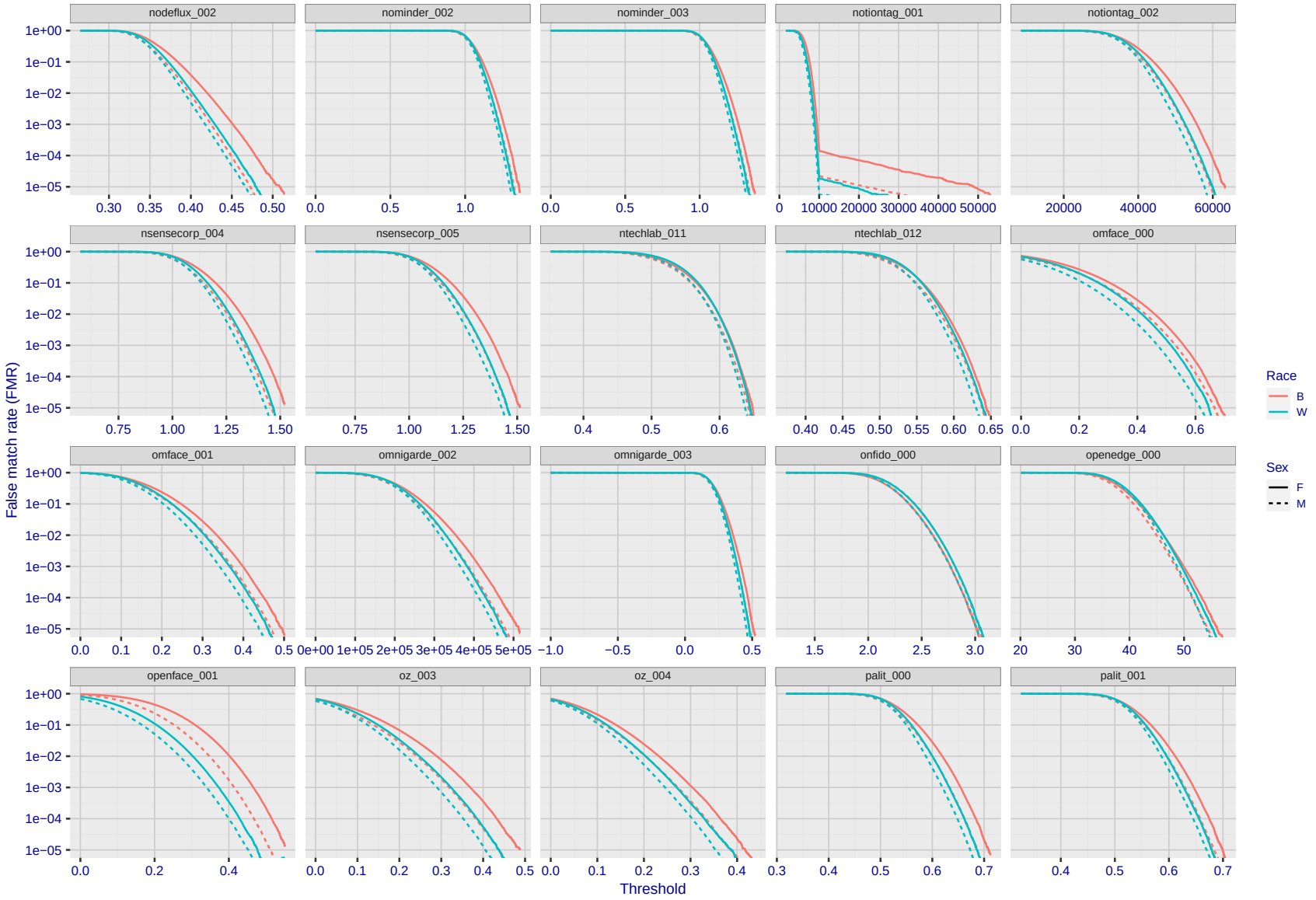

Figure 274: For the mugshot images, the false match calibration curves show false match rate vs. threshold. Separate curves appear for white females, black females, black males and white males.

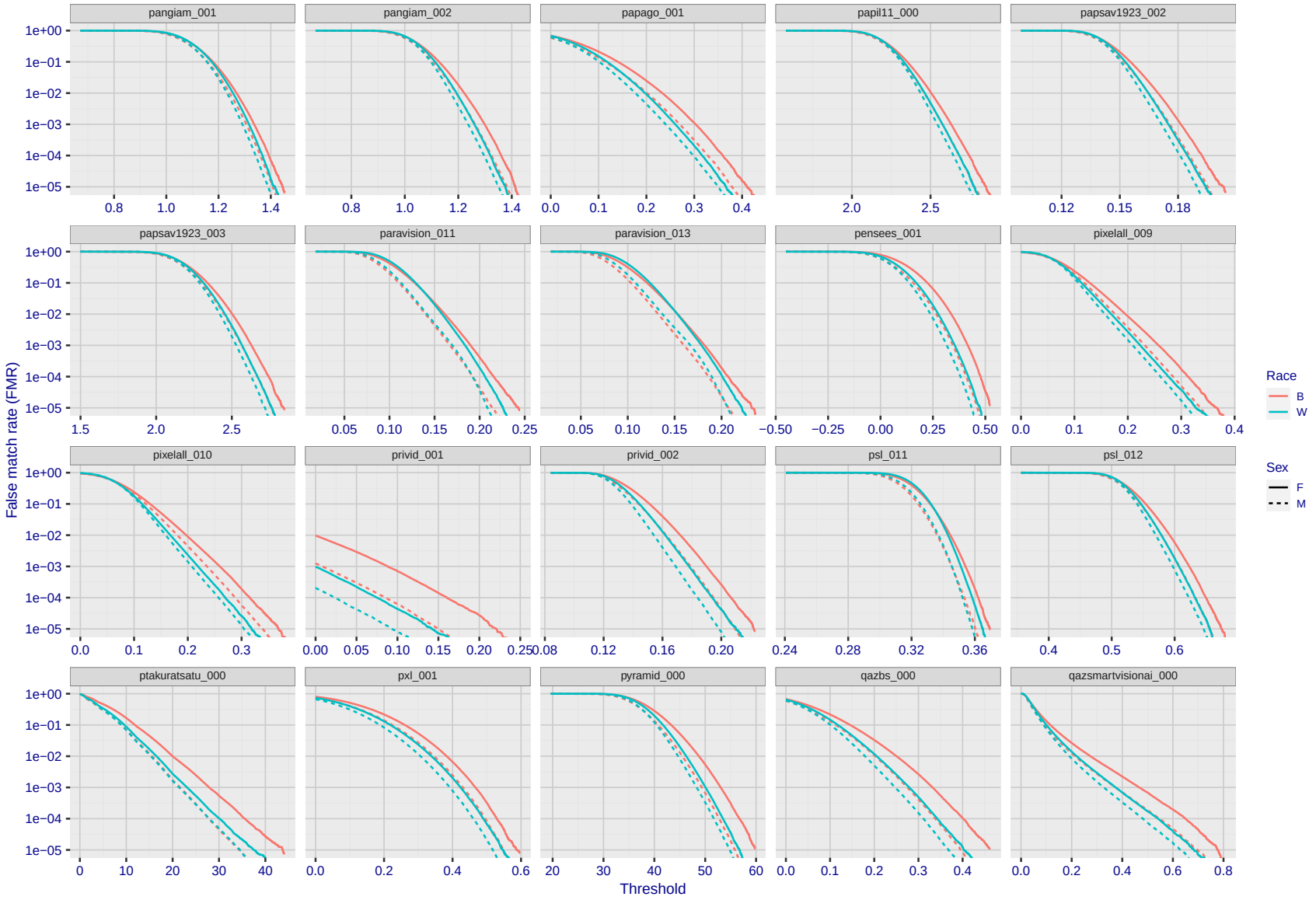

Figure 275: For the mugshot images, the false match calibration curves show false match rate vs. threshold. Separate curves appear for white females, black females, black males and white males.

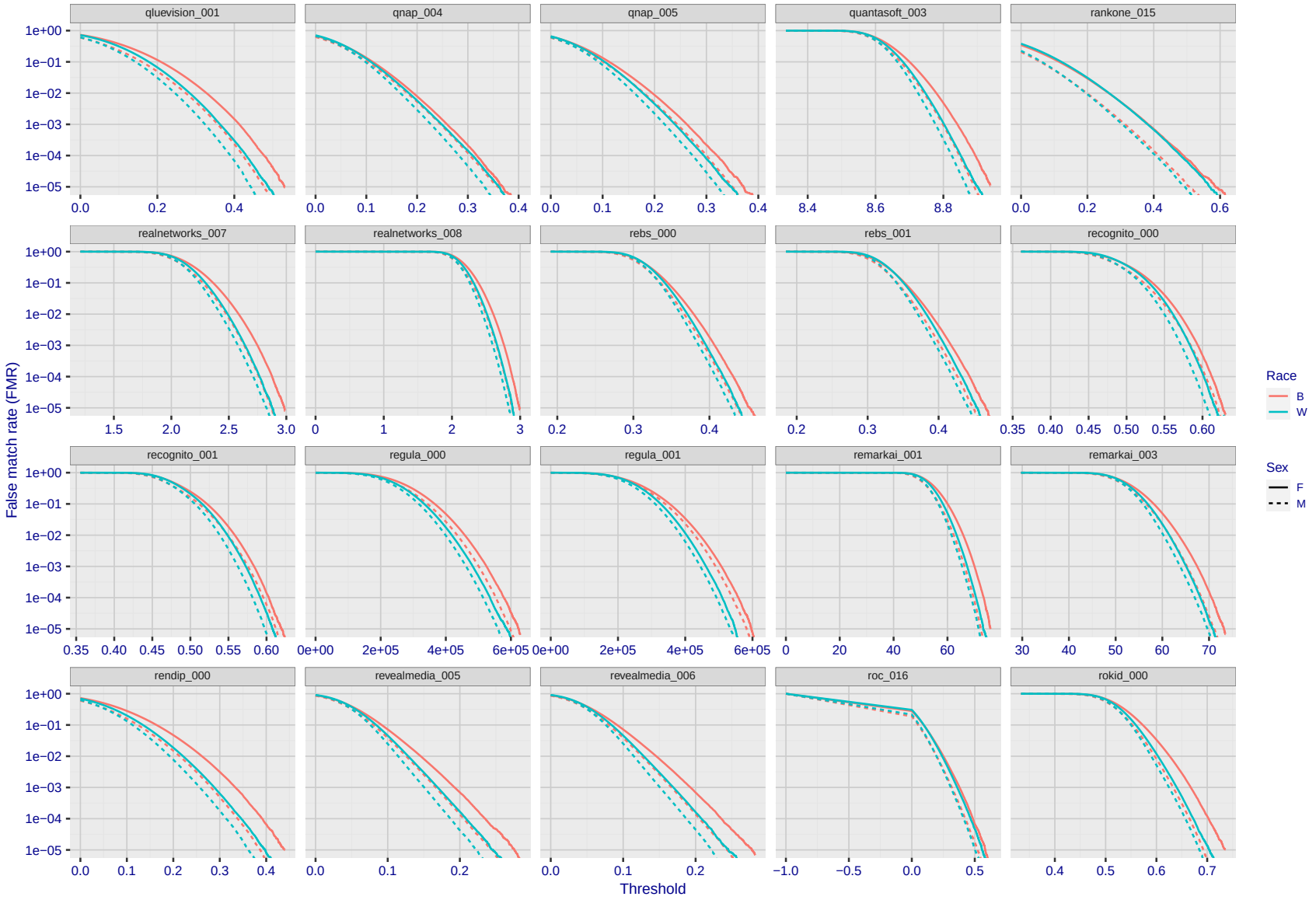

Figure 276: For the mugshot images, the false match calibration curves show false match rate vs. threshold. Separate curves appear for white females, black females, black males and white males.

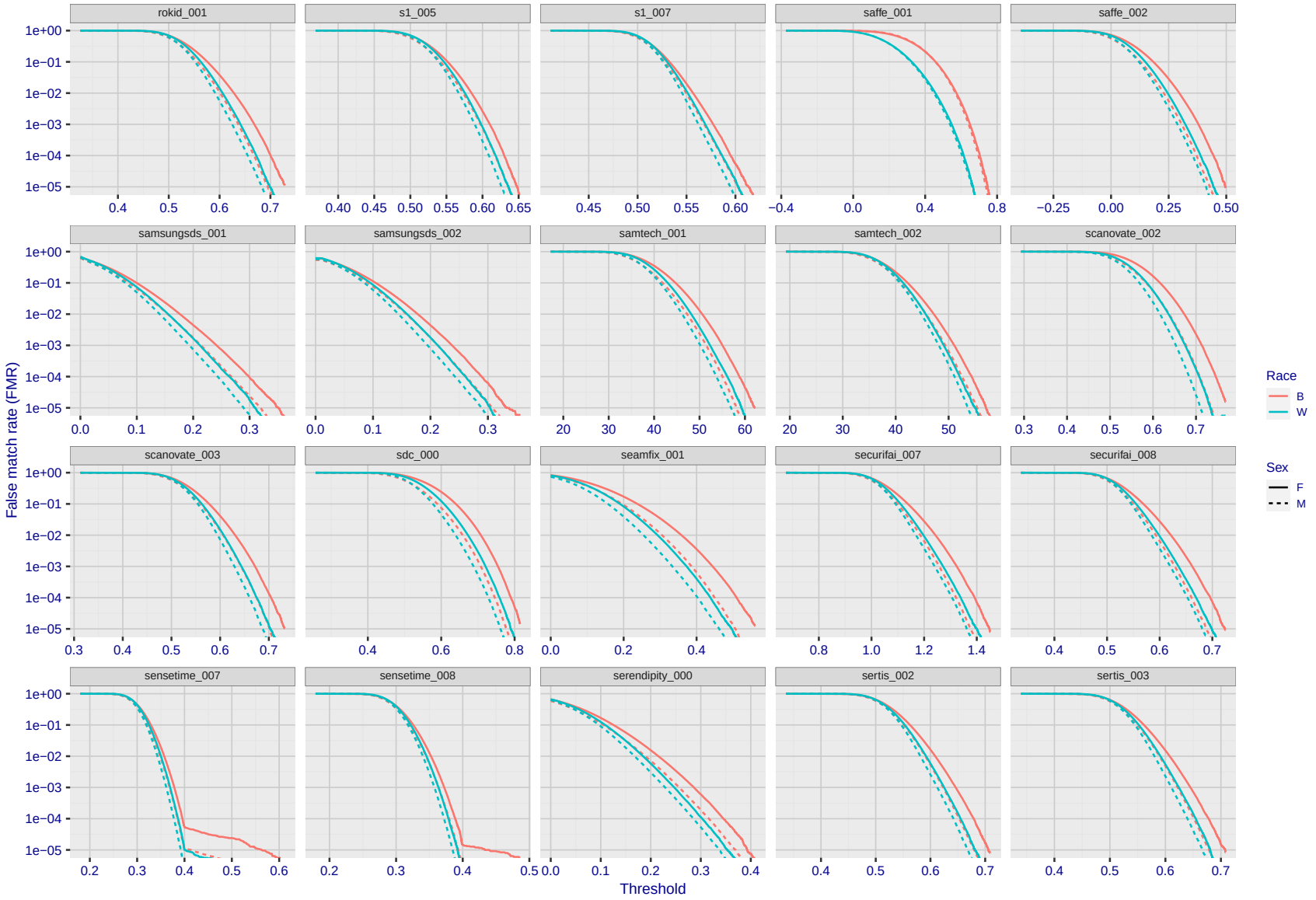

Figure 277: For the mugshot images, the false match calibration curves show false match rate vs. threshold. Separate curves appear for white females, black females, black males and white males.

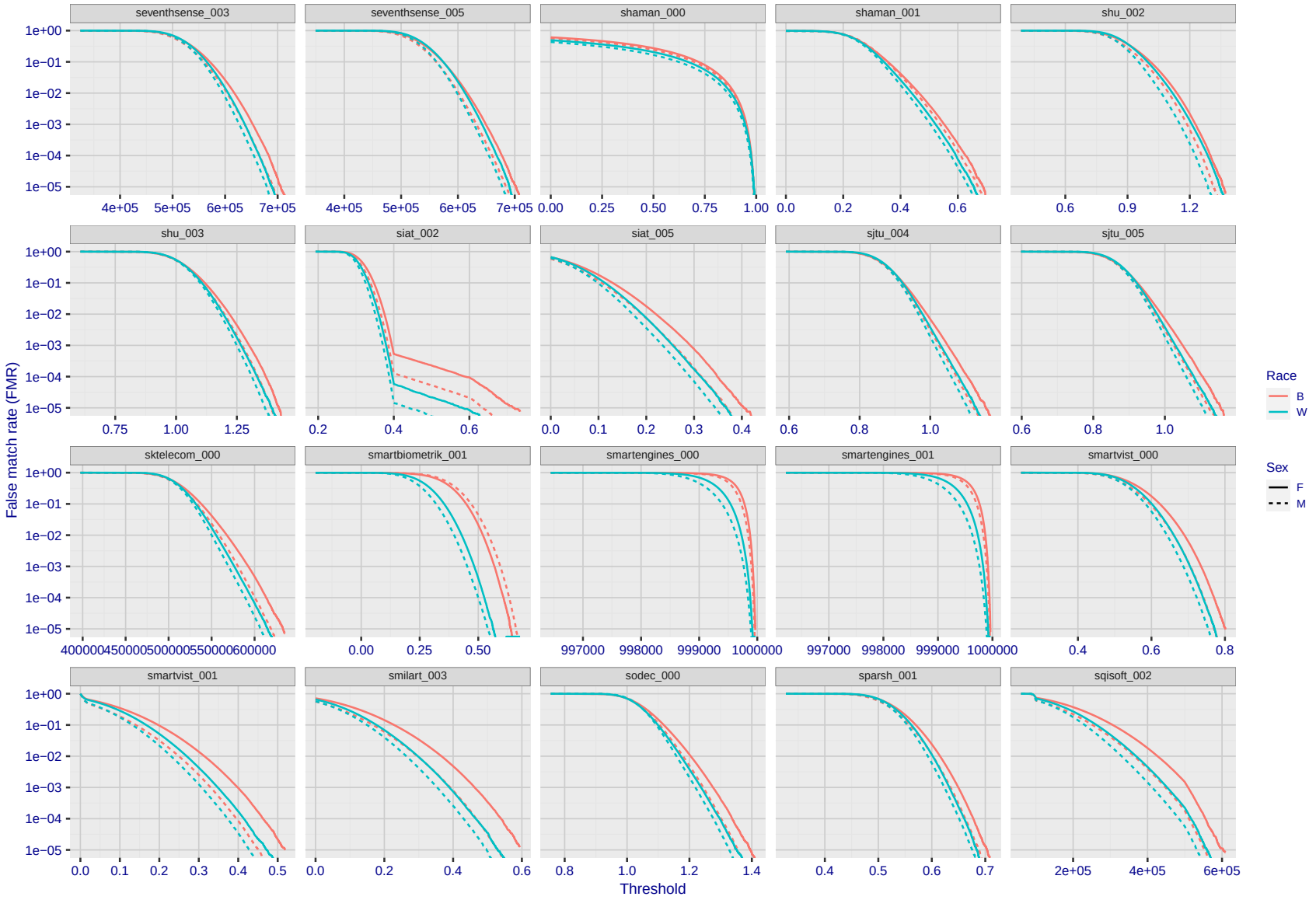

Figure 278: For the mugshot images, the false match calibration curves show false match rate vs. threshold. Separate curves appear for white females, black females, black males and white males.

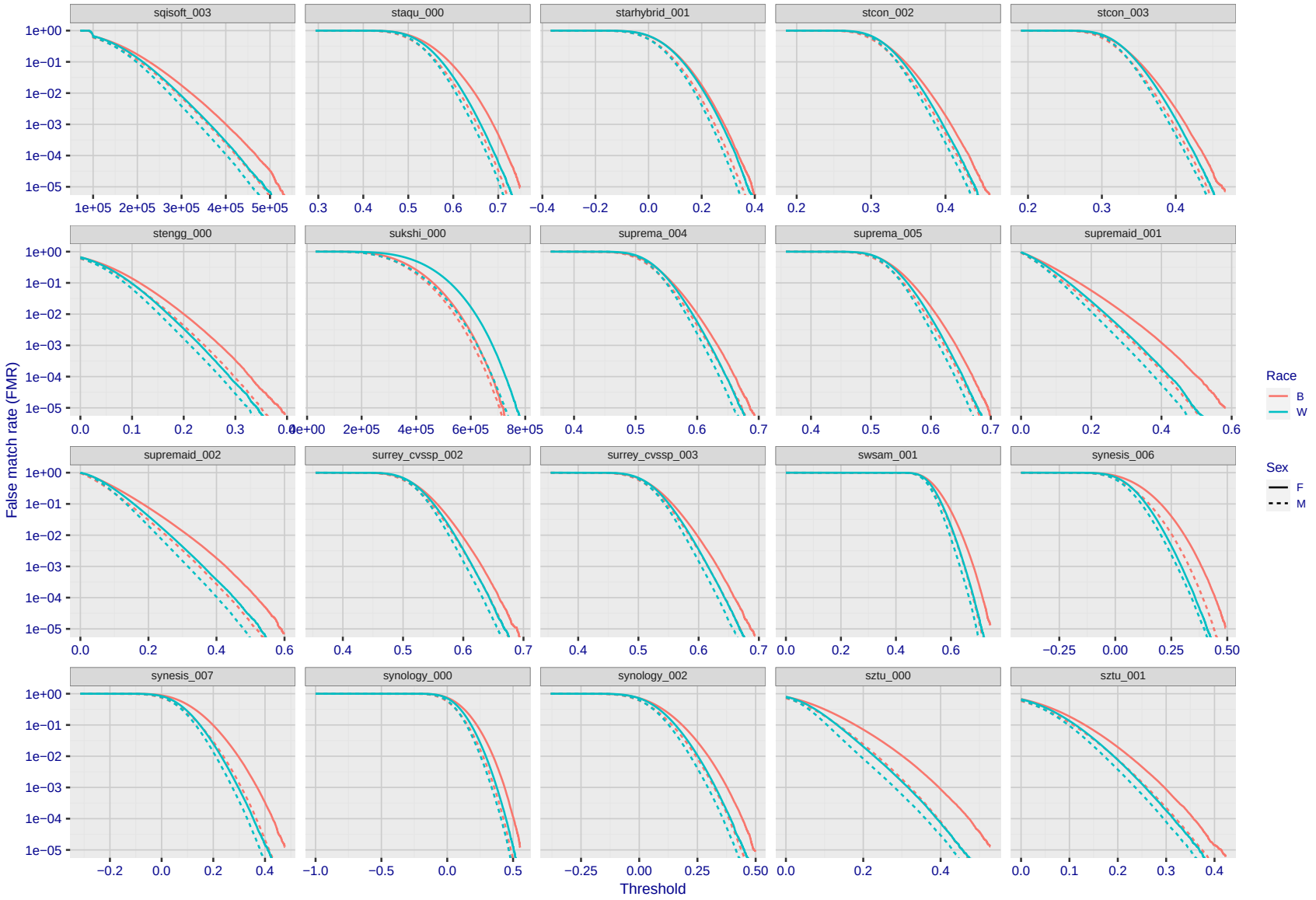

Figure 279: For the mugshot images, the false match calibration curves show false match rate vs. threshold. Separate curves appear for white females, black females, black males and white males.

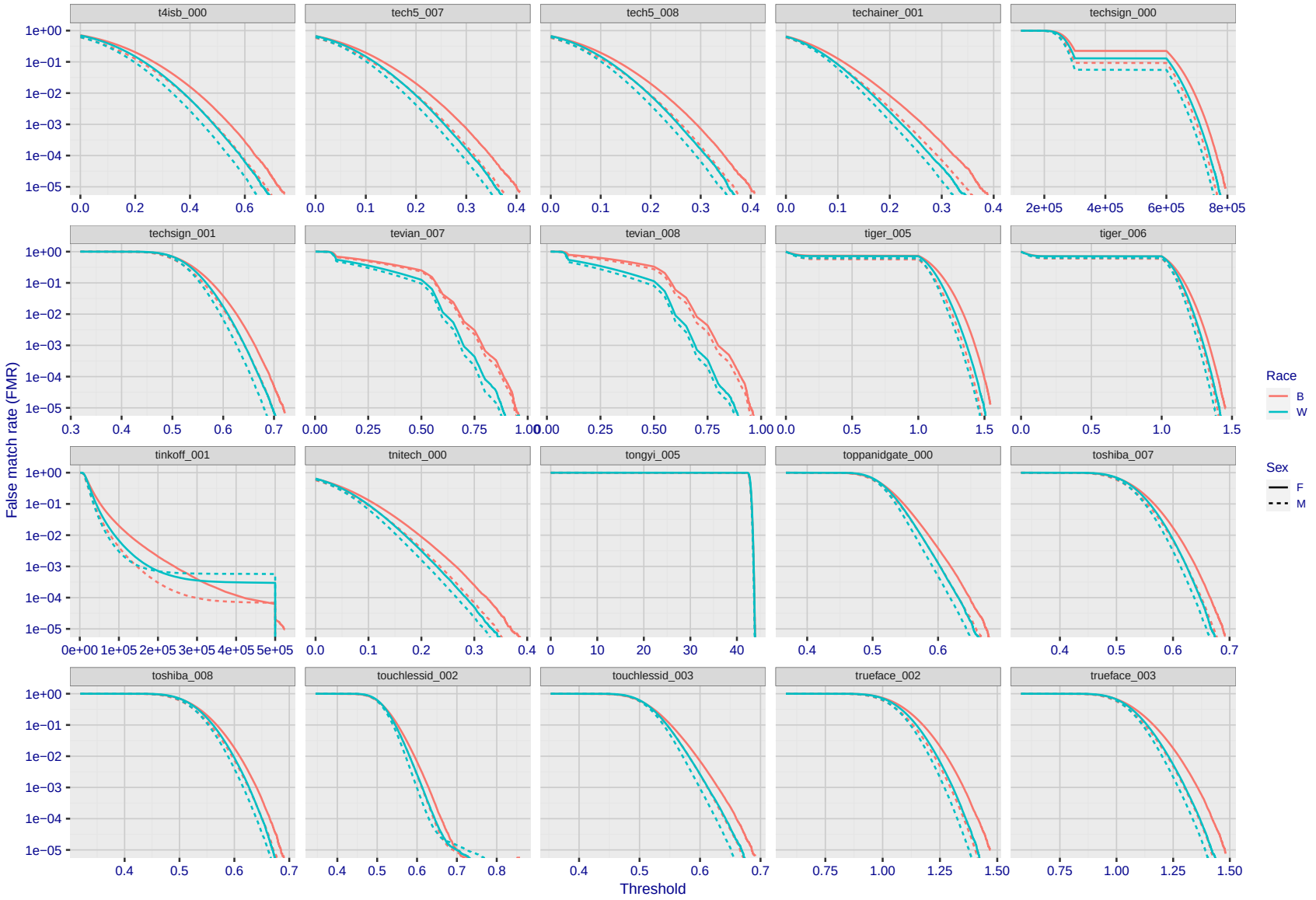

Figure 280: For the mugshot images, the false match calibration curves show false match rate vs. threshold. Separate curves appear for white females, black females, black males and white males.

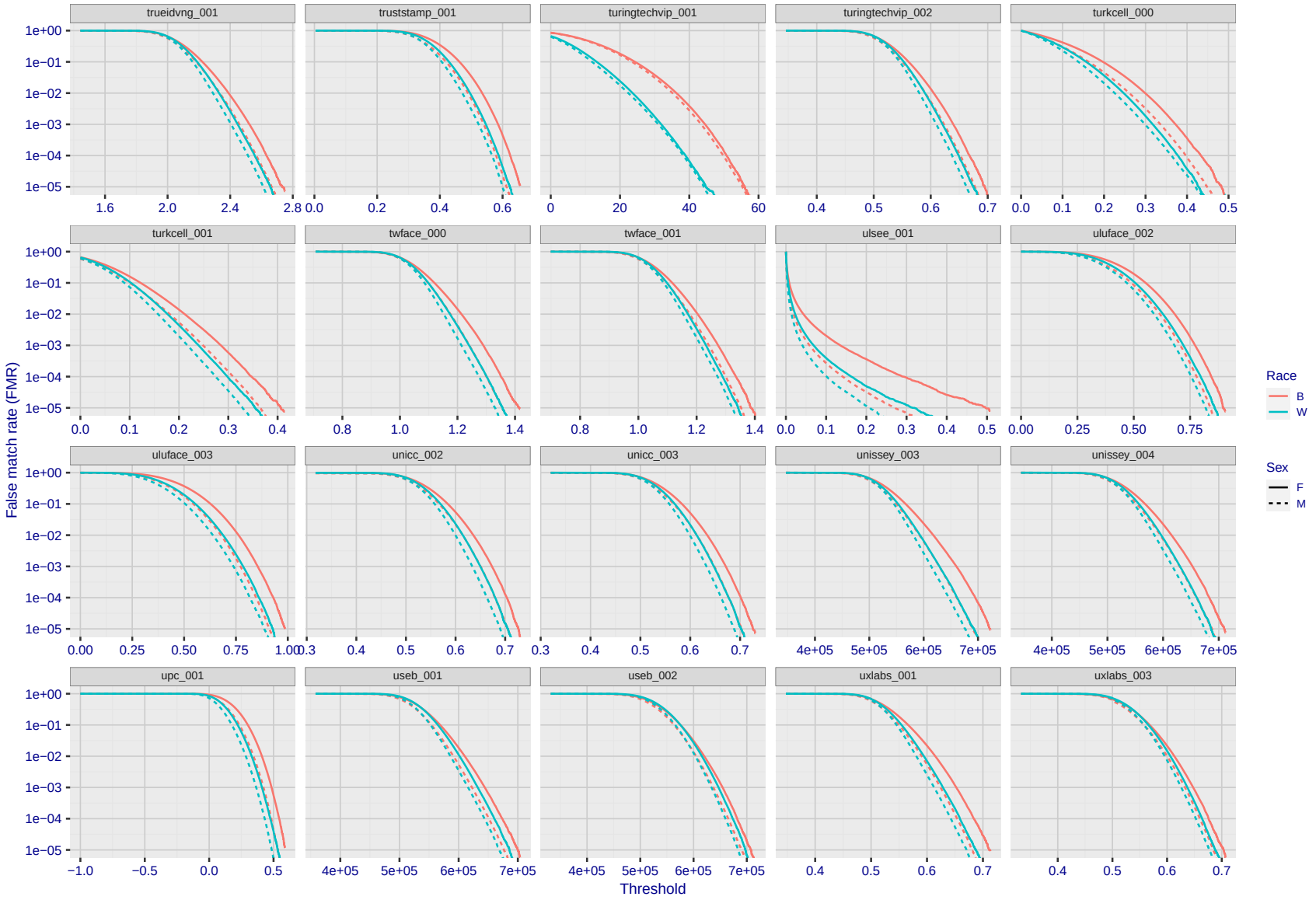

Figure 281: For the mugshot images, the false match calibration curves show false match rate vs. threshold. Separate curves appear for white females, black females, black males and white males.

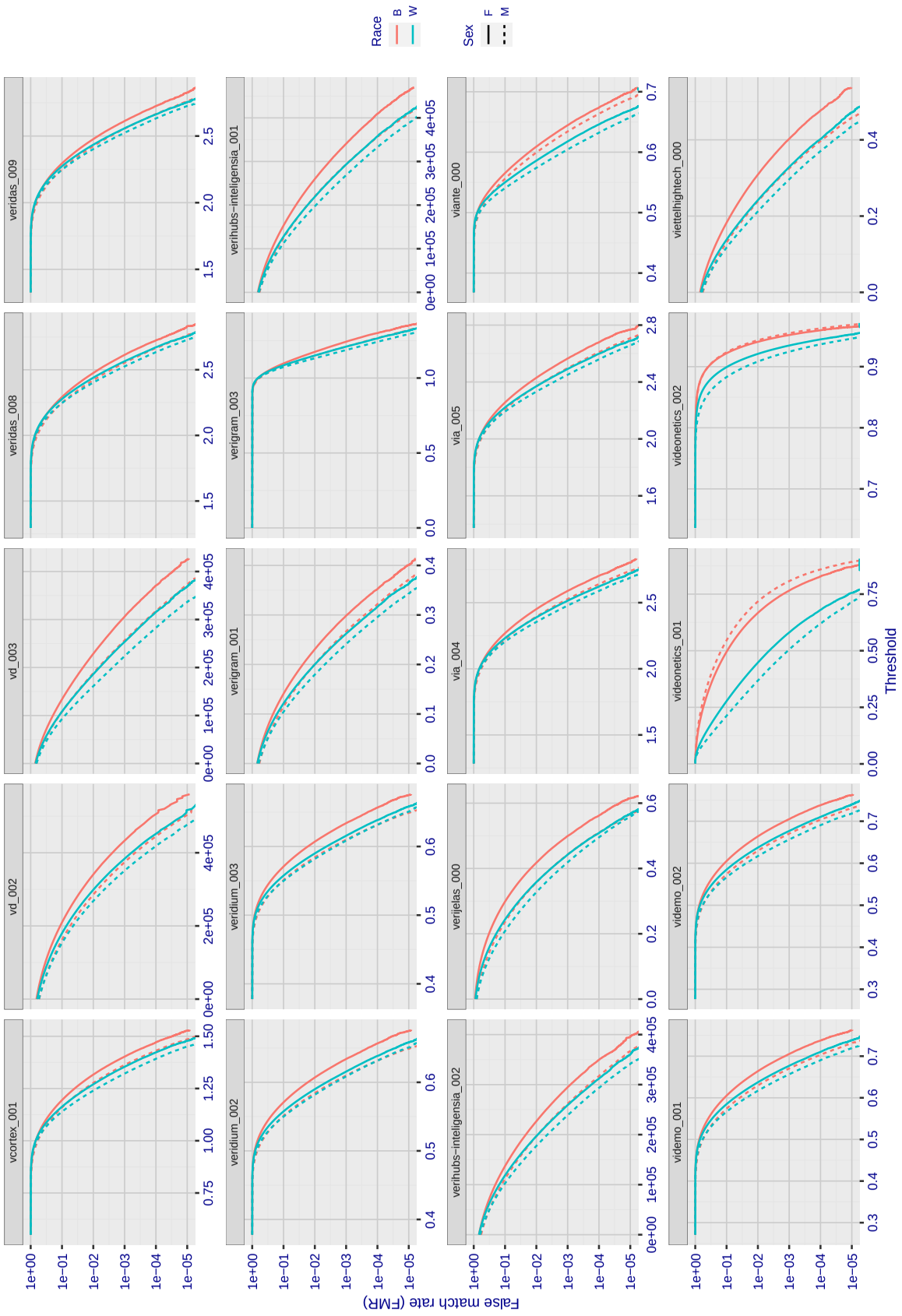

Figure 282: For the mugshot images, the false match calibration curves show false match rate vs. threshold. Separate curves appear for white females, black females, black males and white males.

FNMR(T) "False non-match rate"
FMR(T) "False match rate"

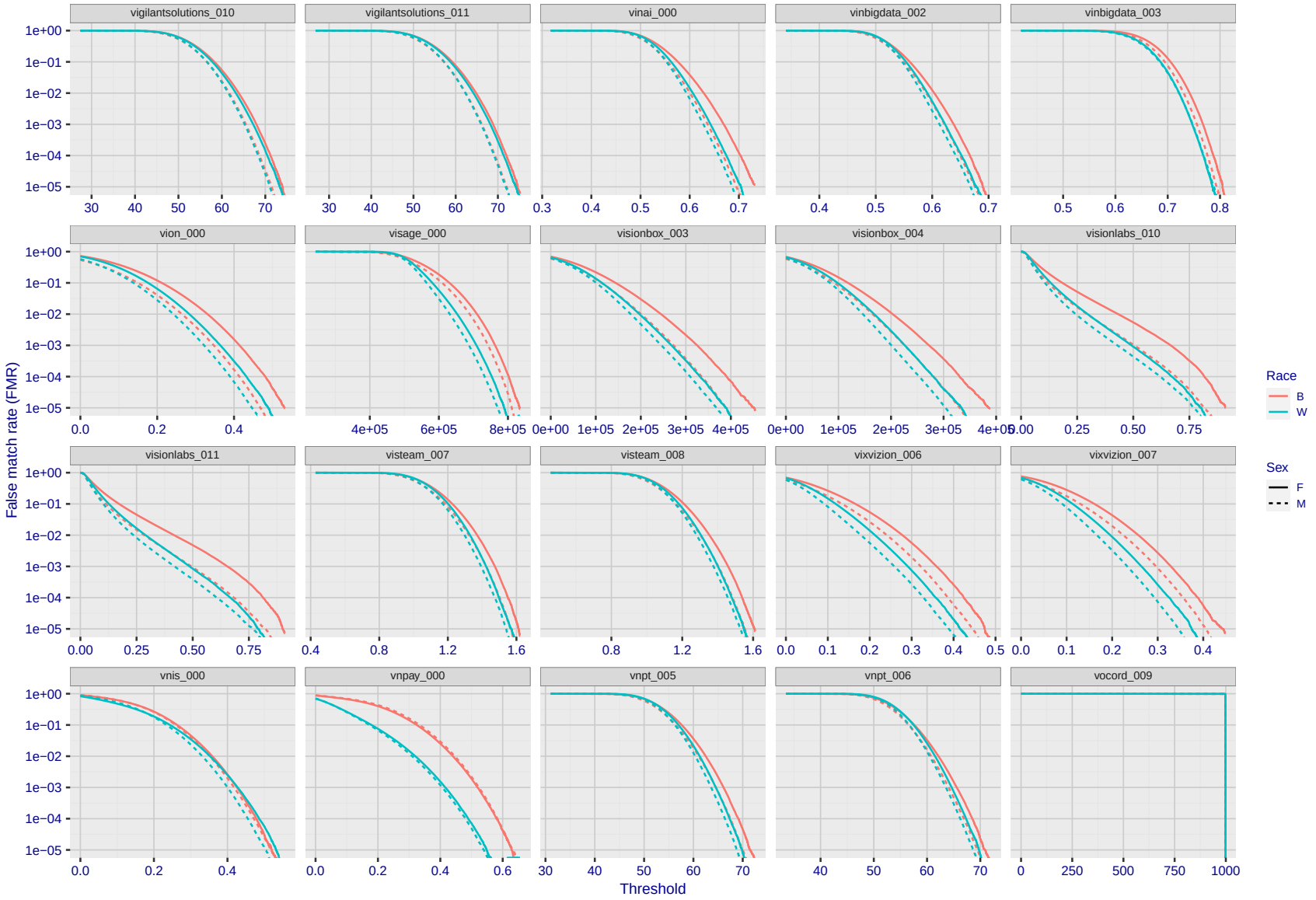

Figure 283: For the mugshot images, the false match calibration curves show false match rate vs. threshold. Separate curves appear for white females, black females, black males and white males.

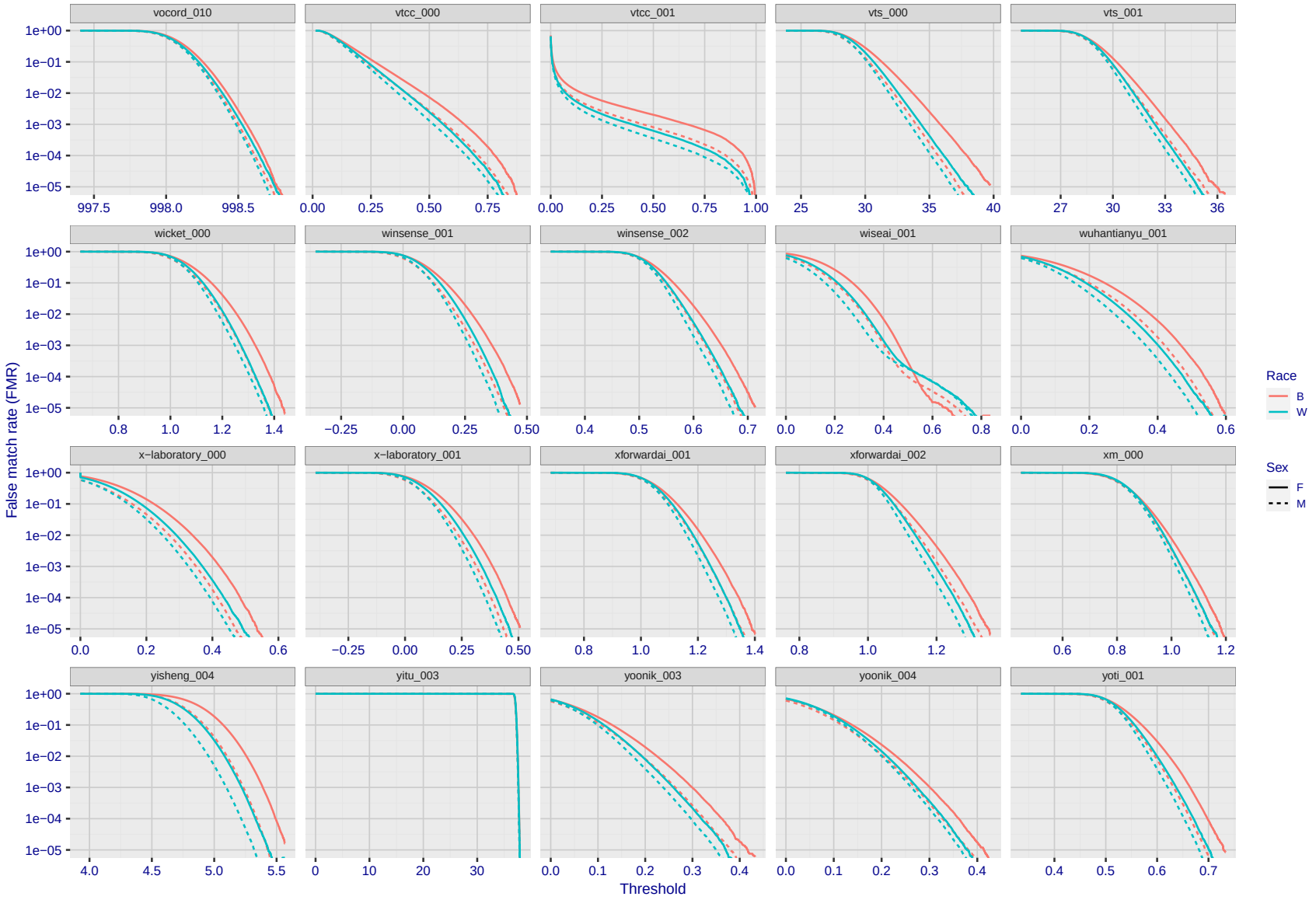

Figure 284: For the mugshot images, the false match calibration curves show false match rate vs. threshold. Separate curves appear for white females, black females, black males and white males.

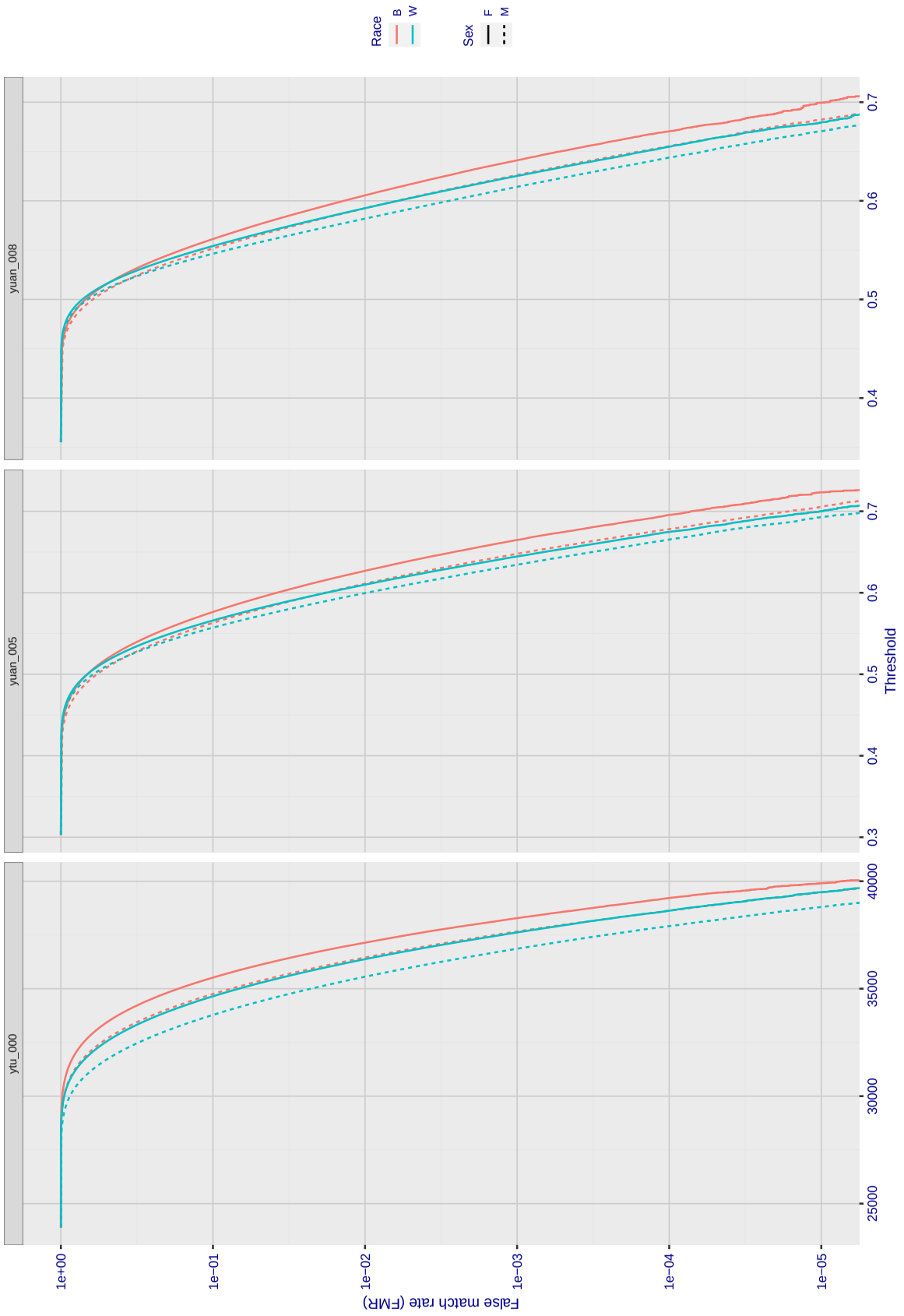

Figure 285: For the mugshot images, the false match calibration curves show false match rate vs. threshold. Separate curves appear for white females, black females, black males and white males.

FNMR(T) "False non-match rate"
FMR(T) "False match rate"

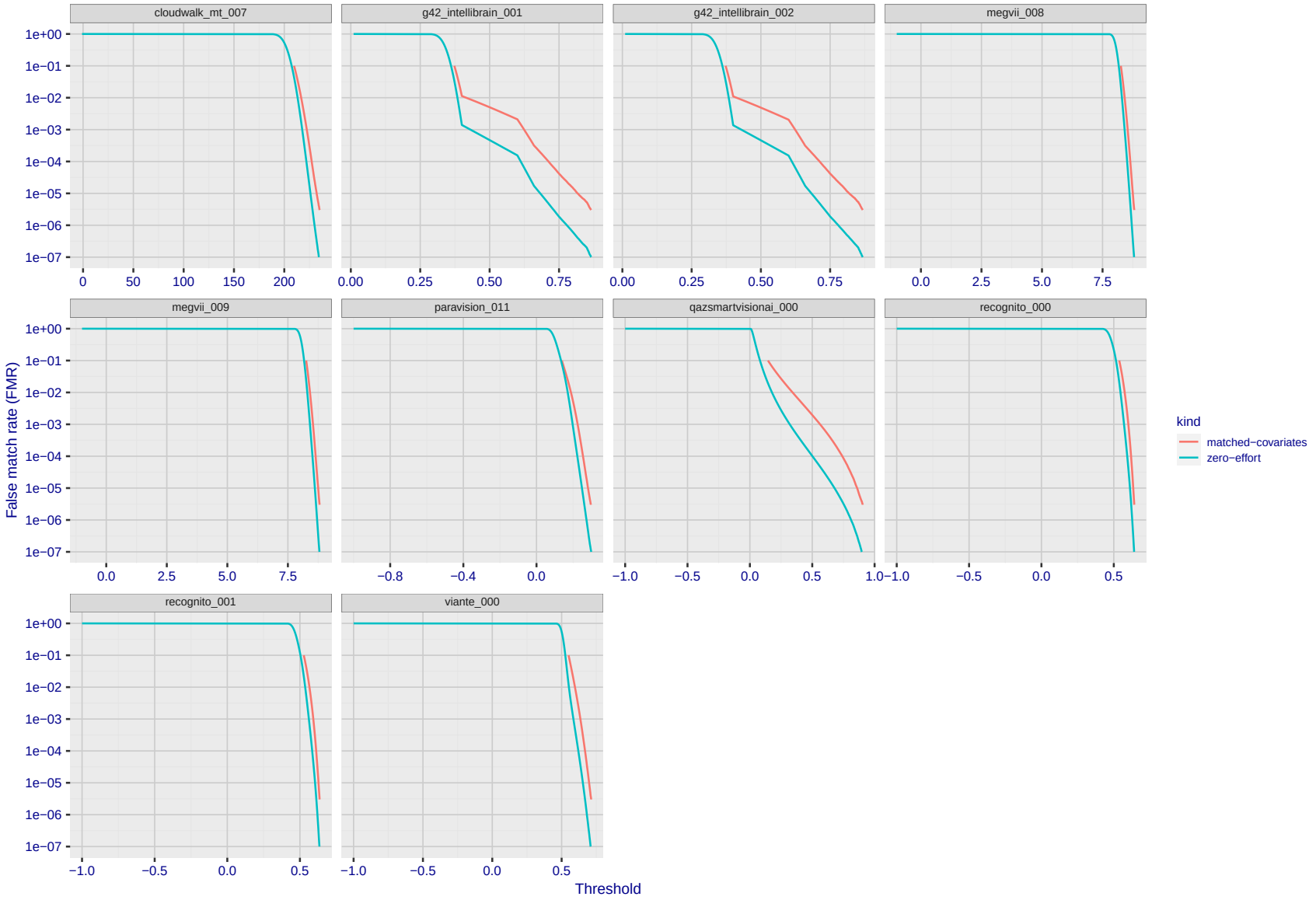

Figure 286: For the visa images, the false match calibration curves show FMR vs. threshold, T. The blue (lower) curves are for zero-effort impostors (i.e. comparing all images against all). The red (upper) curves are for persons of the same-sex, same-age, and same national-origin. This shows that FMR is underestimated (by a factor of 10 or more) by using a zero-effort impostor calculation to calibrate T. As shown later (sec. 3.6), FMR is higher for demographic-matched impostors.

3.5 Genuine distribution stability

3.5.1 Effect of birth place on the genuine distribution

Background: Both skin tone and bone structure vary geographically. Prior studies have reported variations in FNMR and FMR.

Goal: To measure false non-match rate (FNMR) variation with country of birth.

Methods: Thresholds are determined that give FMR = $\{0.001, 0.0001\}$ over the entire impostor set. Then FNMR is measured over 1000 bootstrap replications of the genuine scores. Only those countries with at least 140 individuals are included in the analysis.

Results: Figure 332 shows FNMR by country of birth for the two thresholds.

FNMR(T) "False non-match rate"
FMR(T) "False match rate"

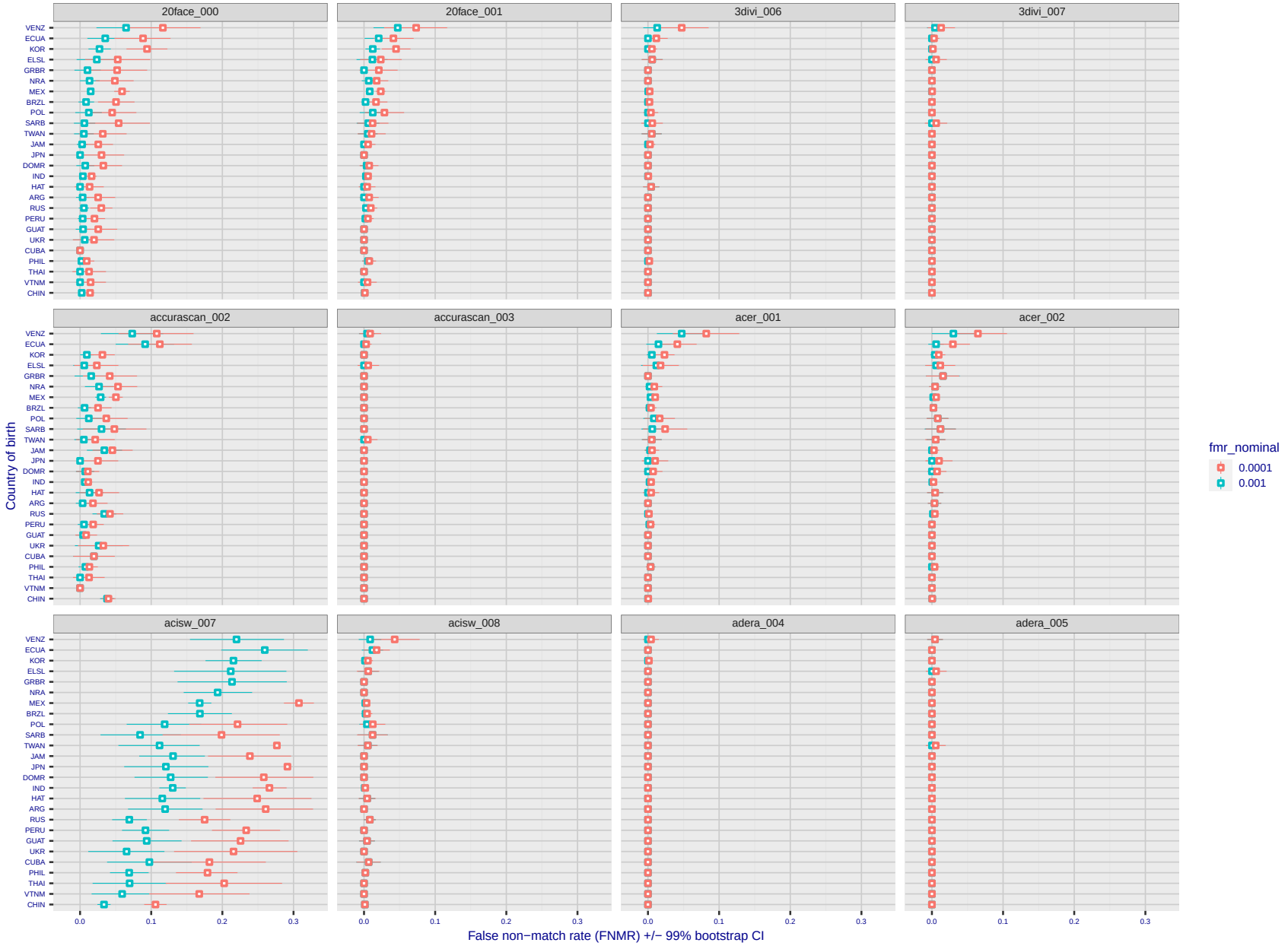

Figure 287: For the visa images, the dots show FNMR by country of birth for two globally set operating thresholds corresponding to FMR = $\{0.001, 0.0001\}$ computed over all on the order of 10^{10} impostor scores. The FMR in each bin will vary also - see subsequent impostor heatmaps in sec. 3.6.1. The figures shows an order of magnitude variation in FNMR across country of birth; these effects are likely due quality variations, then demographics like age and race. The error rates in some cases are zero, and in others the DET is flat so the error rates at the two thresholds are identical. The lines span 1% and 99% of boostrap replicated FNMR estimates.

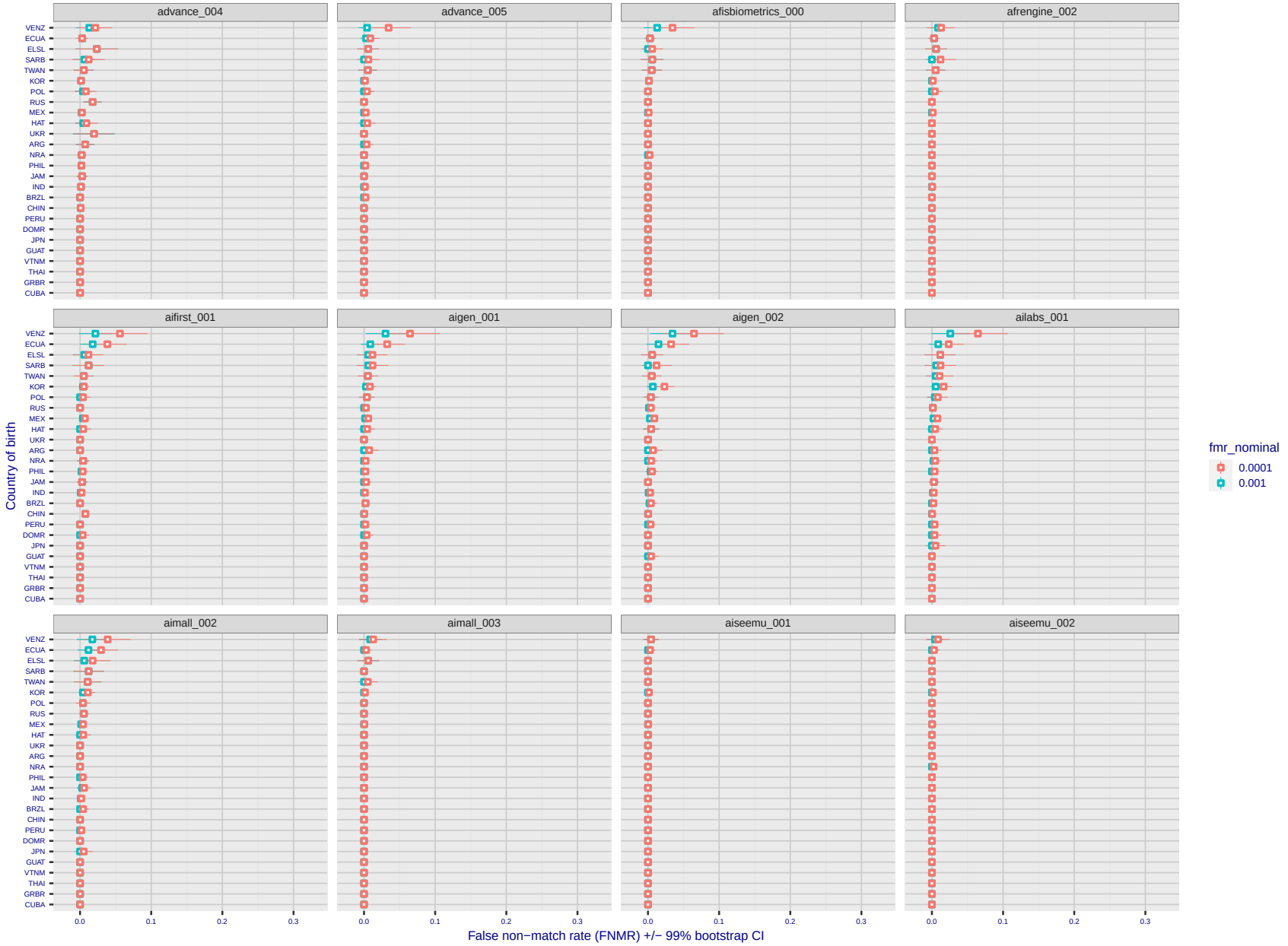

Figure 288: For the visa images, the dots show FNMR by country of birth for two globally set operating thresholds corresponding to FMR = $\{0.001, 0.0001\}$ computed over all on the order of 10^{10} impostor scores. The FMR in each bin will vary also - see subsequent impostor heatmaps in sec. 3.6.1. The figures shows an order of magnitude variation in FNMR across country of birth; these effects are likely due quality variations, then demographics like age and race. The error rates in some cases are zero, and in others the DET is flat so the error rates at the two thresholds are identical. The lines span 1% and 99% of boostrap replicated FNMR estimates.

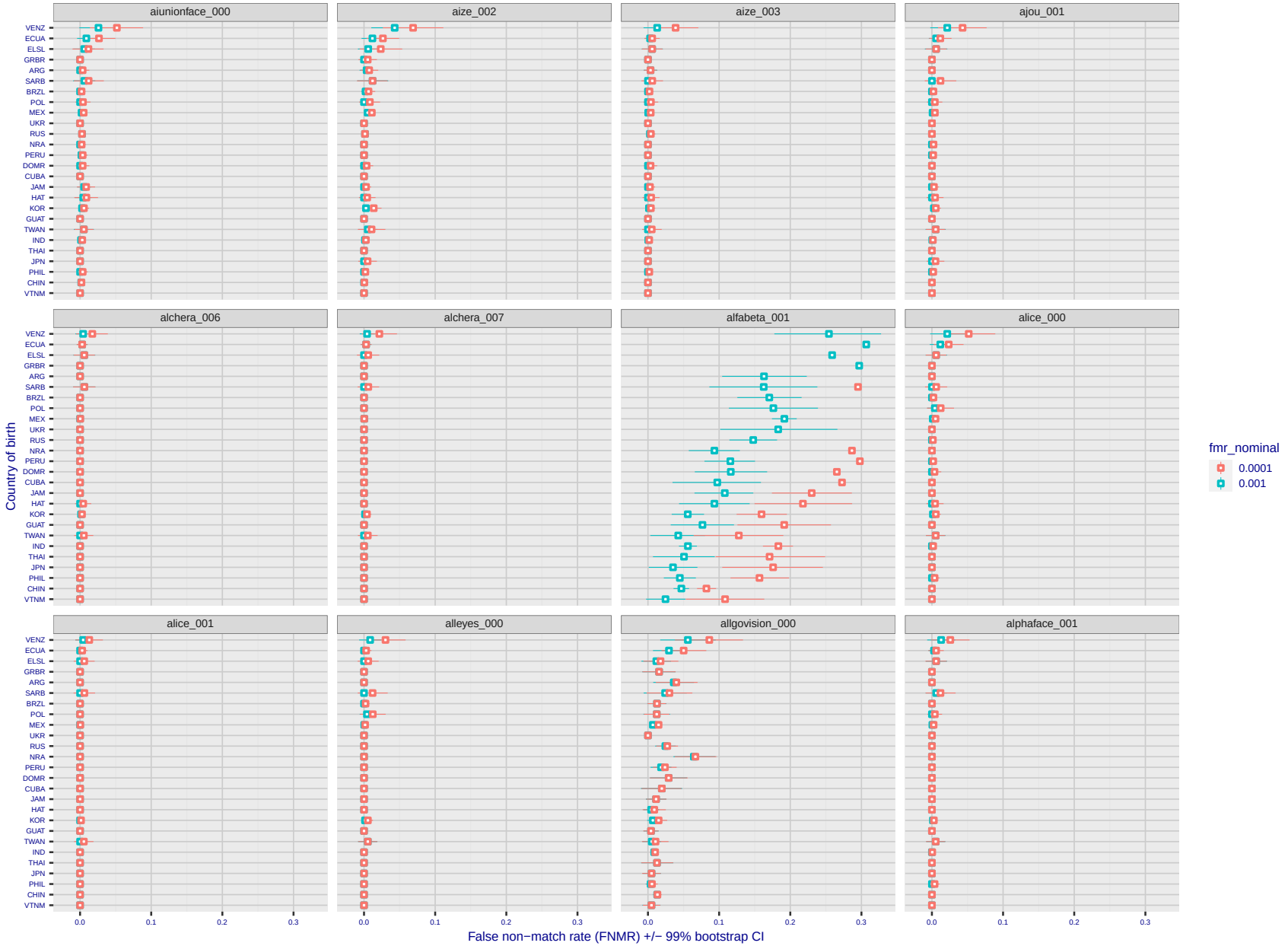

Figure 289: For the visa images, the dots show FNMR by country of birth for two globally set operating thresholds corresponding to FMR = $\{0.001, 0.0001\}$ computed over all on the order of 10^{10} impostor scores. The FMR in each bin will vary also - see subsequent impostor heatmaps in sec. 3.6.1. The figures shows an order of magnitude variation in FNMR across country of birth; these effects are likely due quality variations, then demographics like age and race. The error rates in some cases are zero, and in others the DET is flat so the error rates at the two thresholds are identical. The lines span 1% and 99% of boostrap replicated FNMR estimates.

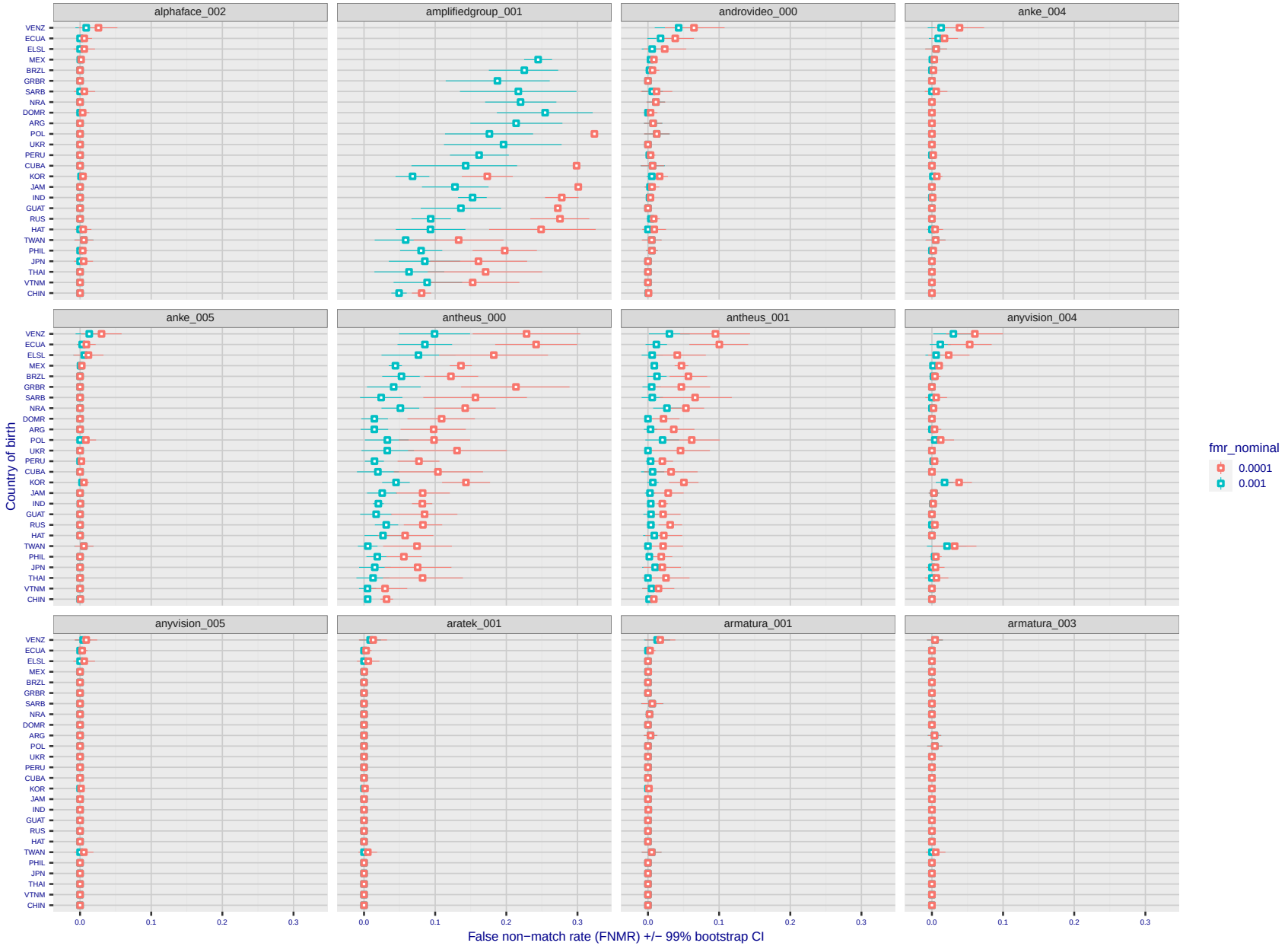

Figure 290: For the visa images, the dots show FNMR by country of birth for two globally set operating thresholds corresponding to FMR = $\{0.001, 0.0001\}$ computed over all on the order of 10^{10} impostor scores. The FMR in each bin will vary also - see subsequent impostor heatmaps in sec. 3.6.1. The figures shows an order of magnitude variation in FNMR across country of birth; these effects are likely due quality variations, then demographics like age and race. The error rates in some cases are zero, and in others the DET is flat so the error rates at the two thresholds are identical. The lines span 1% and 99% of boostrap replicated FNMR estimates.

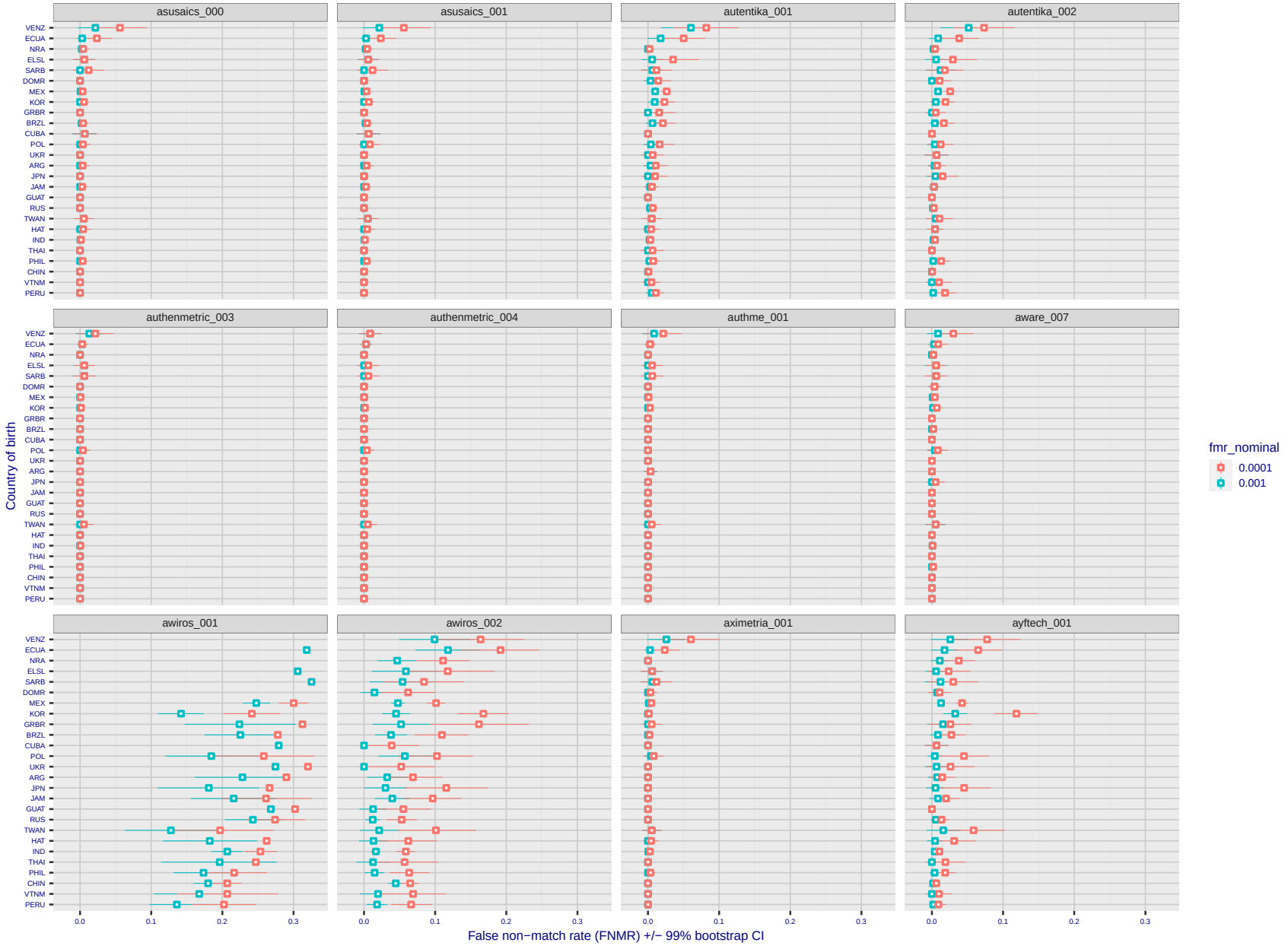

Figure 291: For the visa images, the dots show FNMR by country of birth for two globally set operating thresholds corresponding to FMR = $\{0.001, 0.0001\}$ computed over all on the order of 10^{10} impostor scores. The FMR in each bin will vary also - see subsequent impostor heatmaps in sec. 3.6.1. The figures shows an order of magnitude variation in FNMR across country of birth; these effects are likely due quality variations, then demographics like age and race. The error rates in some cases are zero, and in others the DET is flat so the error rates at the two thresholds are identical. The lines span 1% and 99% of boostrap replicated FNMR estimates.

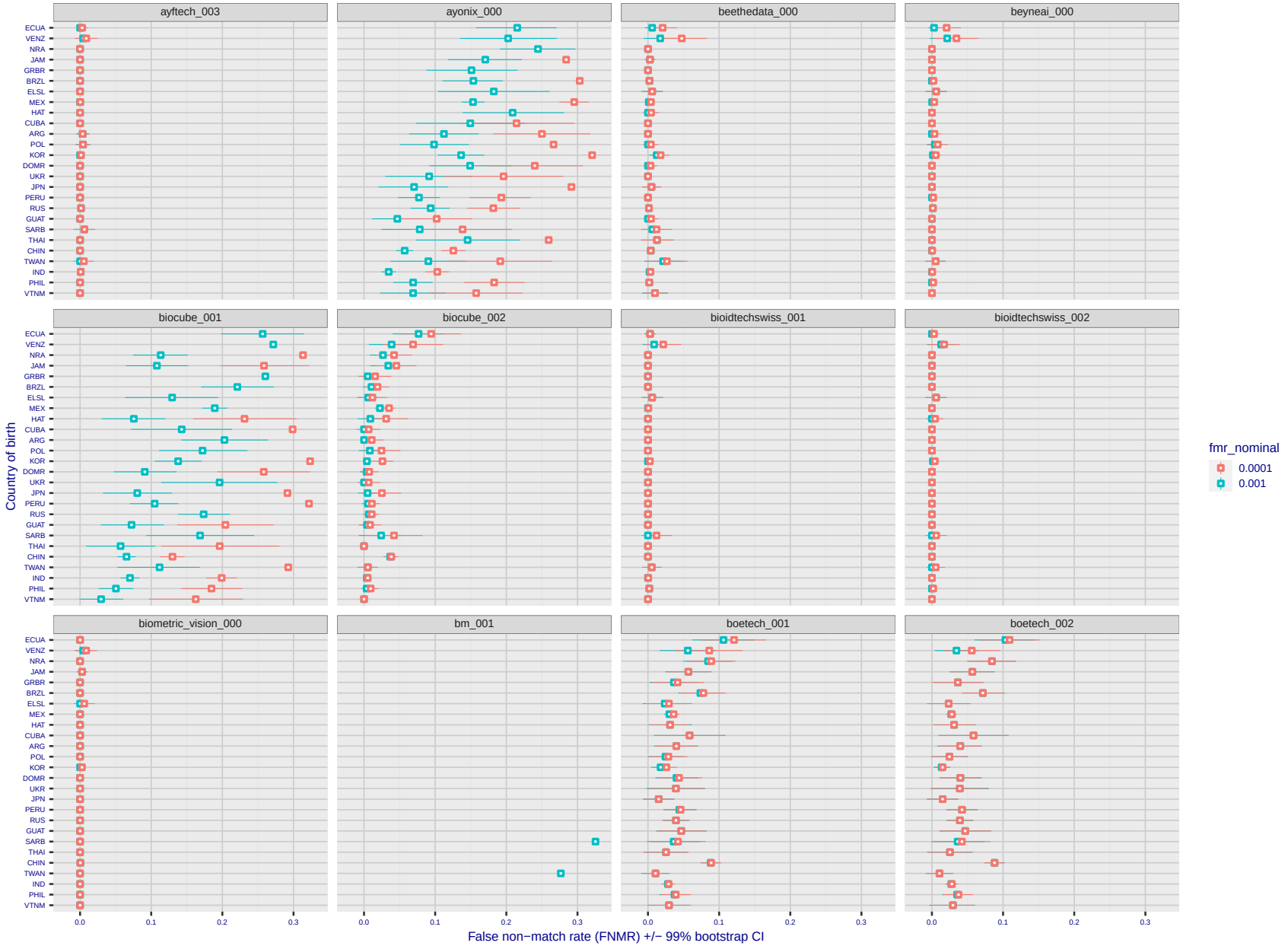

Figure 292: For the visa images, the dots show FNMR by country of birth for two globally set operating thresholds corresponding to FMR = $\{0.001, 0.0001\}$ computed over all on the order of 10^{10} impostor scores. The FMR in each bin will vary also - see subsequent impostor heatmaps in sec. 3.6.1. The figures shows an order of magnitude variation in FNMR across country of birth; these effects are likely due quality variations, then demographics like age and race. The error rates in some cases are zero, and in others the DET is flat so the error rates at the two thresholds are identical. The lines span 1% and 99% of boostrap replicated FNMR estimates.

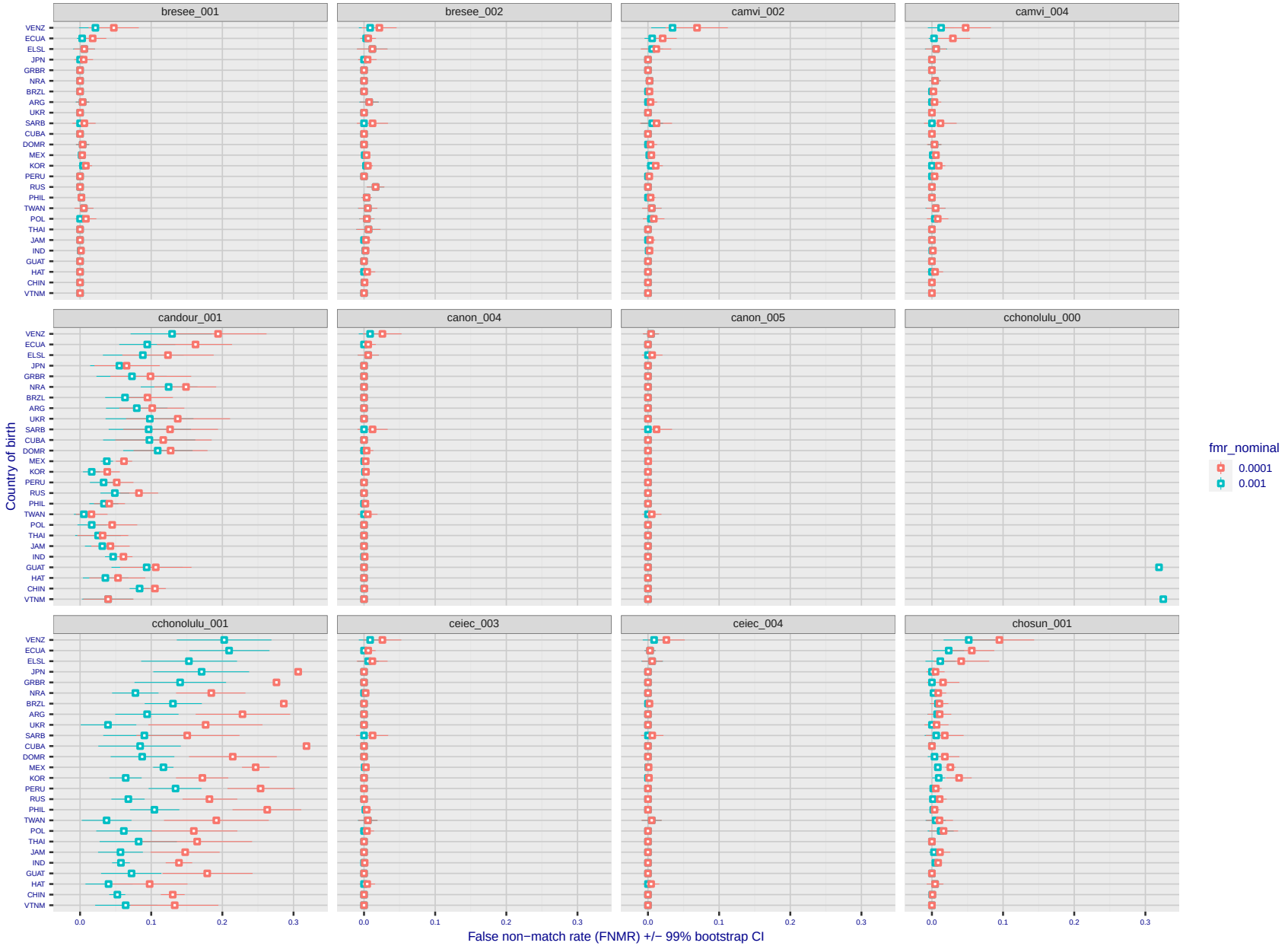

Figure 293: For the visa images, the dots show FNMR by country of birth for two globally set operating thresholds corresponding to FMR = $\{0.001, 0.0001\}$ computed over all on the order of 10^{10} impostor scores. The FMR in each bin will vary also - see subsequent impostor heatmaps in sec. 3.6.1. The figures shows an order of magnitude variation in FNMR across country of birth; these effects are likely due quality variations, then demographics like age and race. The error rates in some cases are zero, and in others the DET is flat so the error rates at the two thresholds are identical. The lines span 1% and 99% of boostrap replicated FNMR estimates.

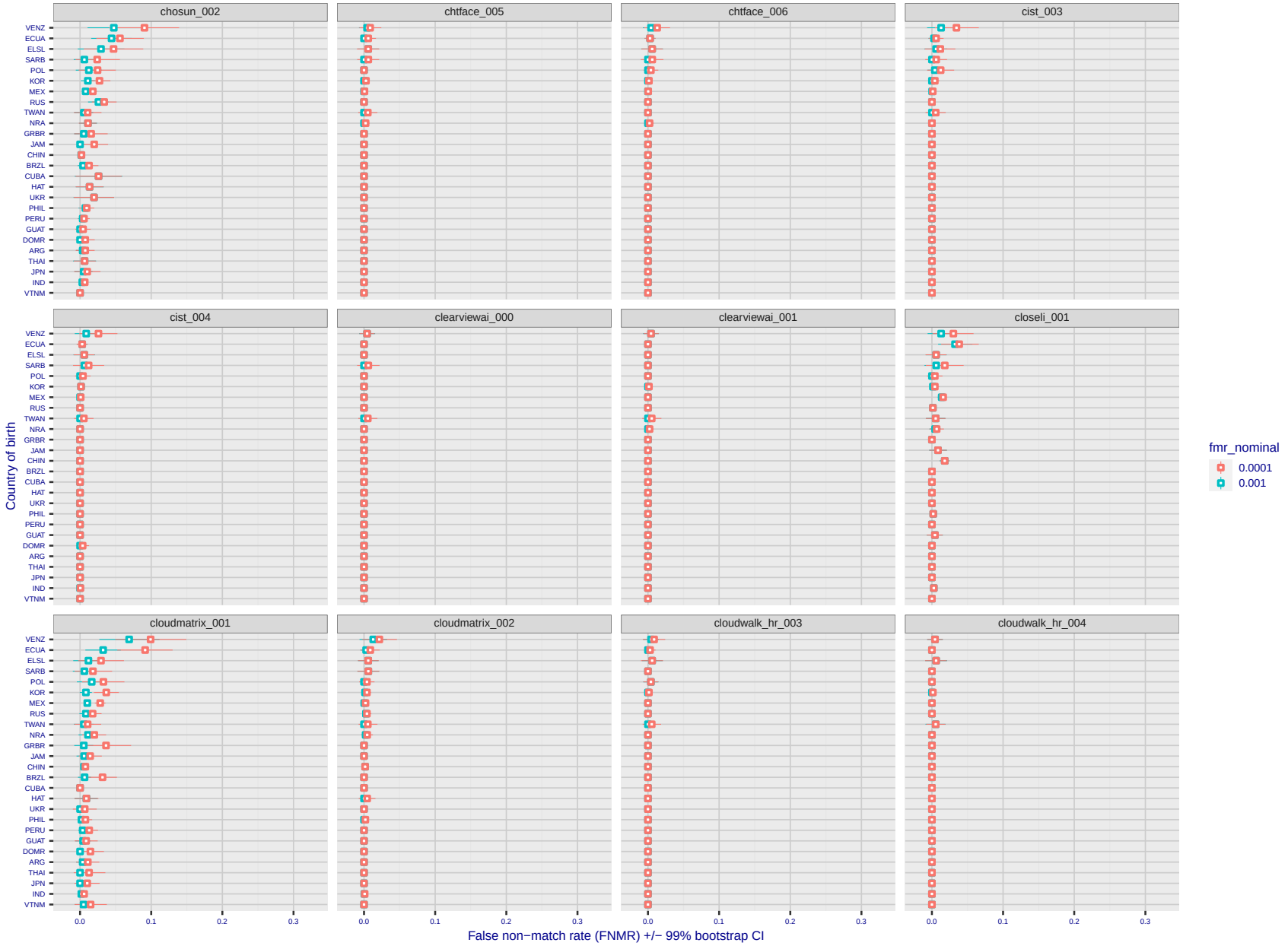

Figure 294: For the visa images, the dots show FNMR by country of birth for two globally set operating thresholds corresponding to FMR = $\{0.001, 0.0001\}$ computed over all on the order of 10^{10} impostor scores. The FMR in each bin will vary also - see subsequent impostor heatmaps in sec. 3.6.1. The figures shows an order of magnitude variation in FNMR across country of birth; these effects are likely due quality variations, then demographics like age and race. The error rates in some cases are zero, and in others the DET is flat so the error rates at the two thresholds are identical. The lines span 1% and 99% of boostrap replicated FNMR estimates.

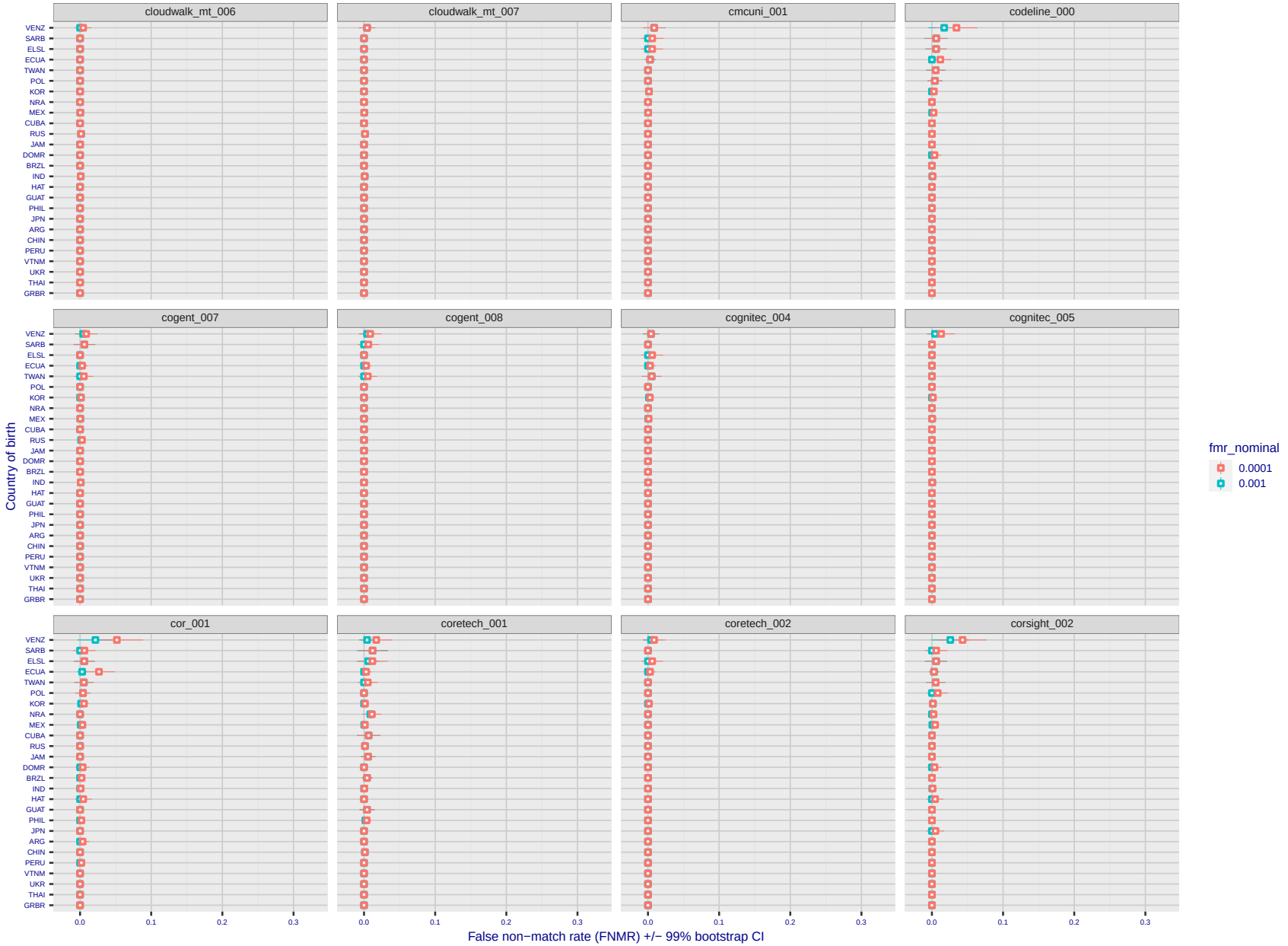

Figure 295: For the visa images, the dots show FNMR by country of birth for two globally set operating thresholds corresponding to FMR = $\{0.001, 0.0001\}$ computed over all on the order of 10^{10} impostor scores. The FMR in each bin will vary also - see subsequent impostor heatmaps in sec. 3.6.1. The figures shows an order of magnitude variation in FNMR across country of birth; these effects are likely due quality variations, then demographics like age and race. The error rates in some cases are zero, and in others the DET is flat so the error rates at the two thresholds are identical. The lines span 1% and 99% of boostrap replicated FNMR estimates.

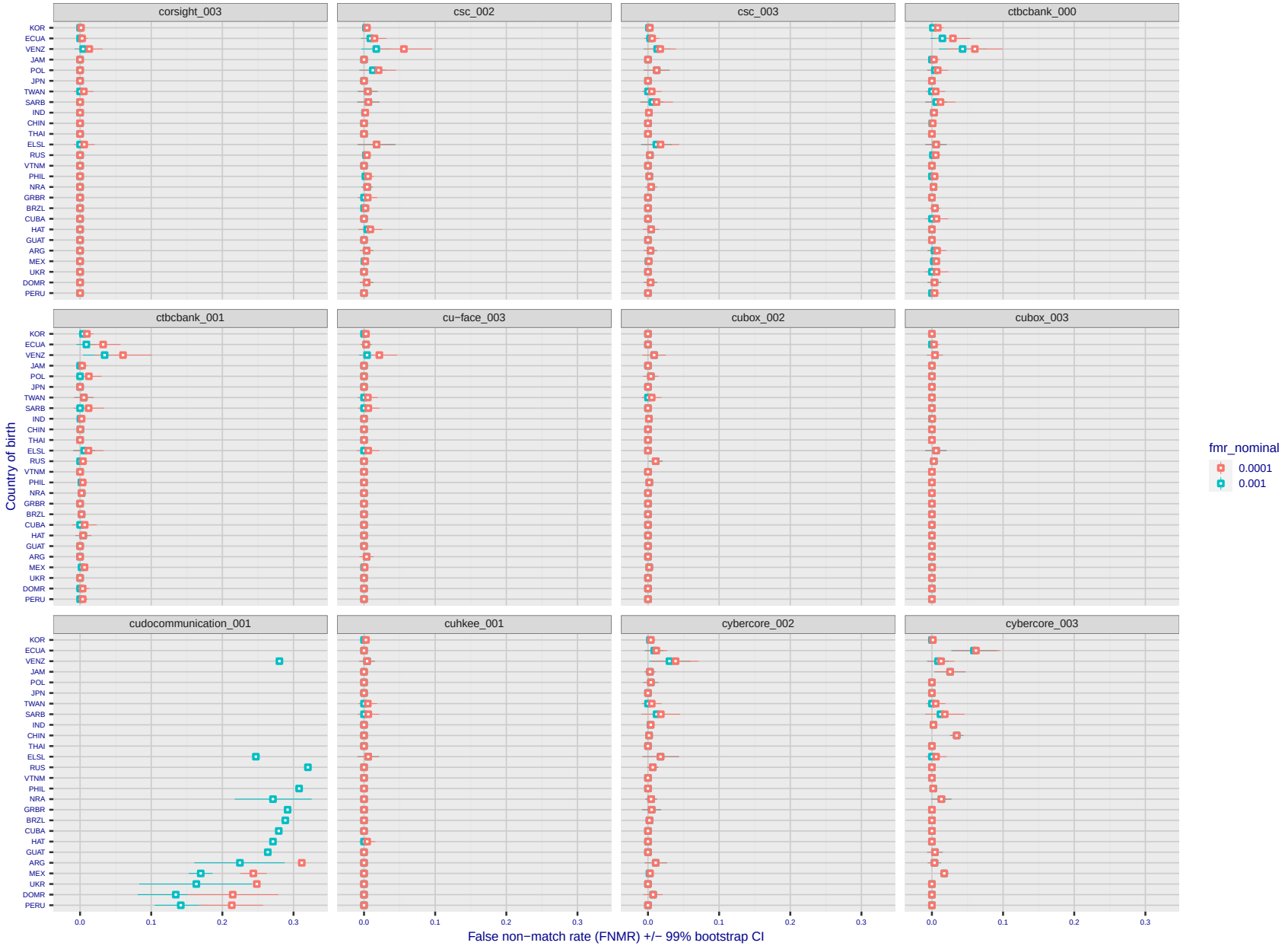

Figure 296: For the visa images, the dots show FNMR by country of birth for two globally set operating thresholds corresponding to FMR = $\{0.001, 0.0001\}$ computed over all on the order of 10^{10} impostor scores. The FMR in each bin will vary also - see subsequent impostor heatmaps in sec. 3.6.1. The figures shows an order of magnitude variation in FNMR across country of birth; these effects are likely due quality variations, then demographics like age and race. The error rates in some cases are zero, and in others the DET is flat so the error rates at the two thresholds are identical. The lines span 1% and 99% of boostrap replicated FNMR estimates.

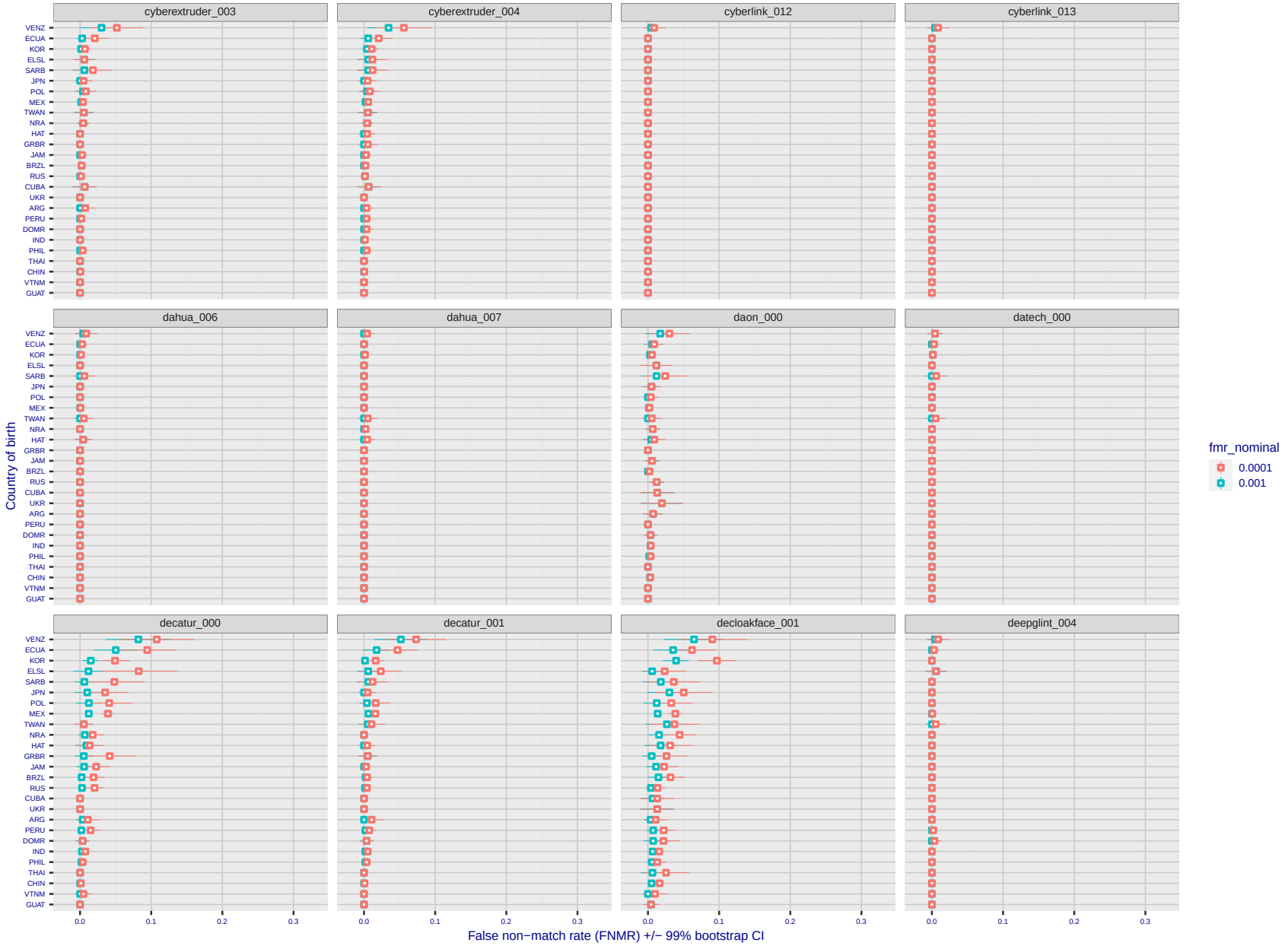

Figure 297: For the visa images, the dots show FNMR by country of birth for two globally set operating thresholds corresponding to FMR = $\{0.001, 0.0001\}$ computed over all on the order of 10^{10} impostor scores. The FMR in each bin will vary also - see subsequent impostor heatmaps in sec. 3.6.1. The figures shows an order of magnitude variation in FNMR across country of birth; these effects are likely due quality variations, then demographics like age and race. The error rates in some cases are zero, and in others the DET is flat so the error rates at the two thresholds are identical. The lines span 1% and 99% of boostrap replicated FNMR estimates.

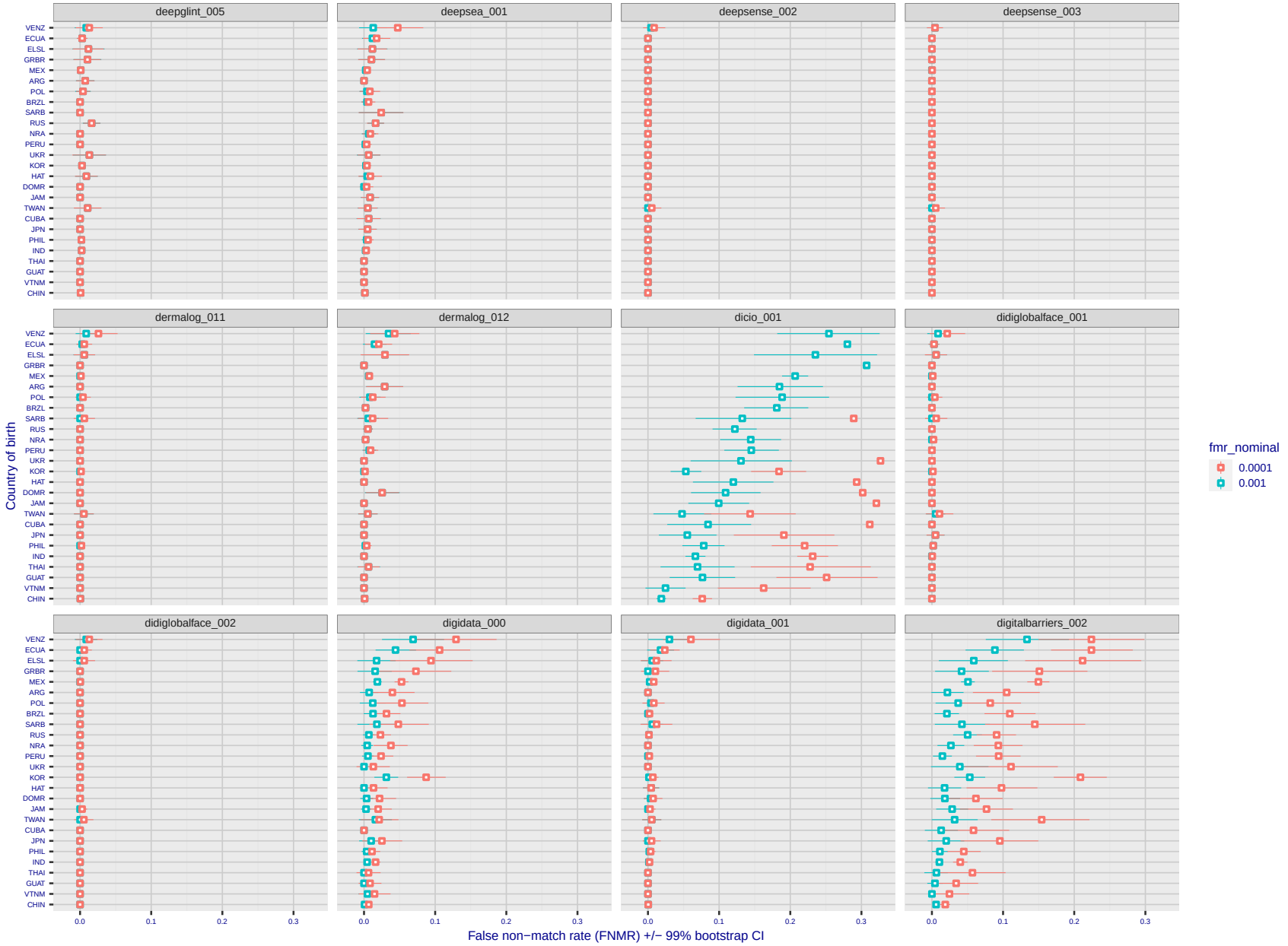

Figure 298: For the visa images, the dots show FNMR by country of birth for two globally set operating thresholds corresponding to FMR = $\{0.001, 0.0001\}$ computed over all on the order of 10^{10} impostor scores. The FMR in each bin will vary also - see subsequent impostor heatmaps in sec. 3.6.1. The figures shows an order of magnitude variation in FNMR across country of birth; these effects are likely due quality variations, then demographics like age and race. The error rates in some cases are zero, and in others the DET is flat so the error rates at the two thresholds are identical. The lines span 1% and 99% of boostrap replicated FNMR estimates.

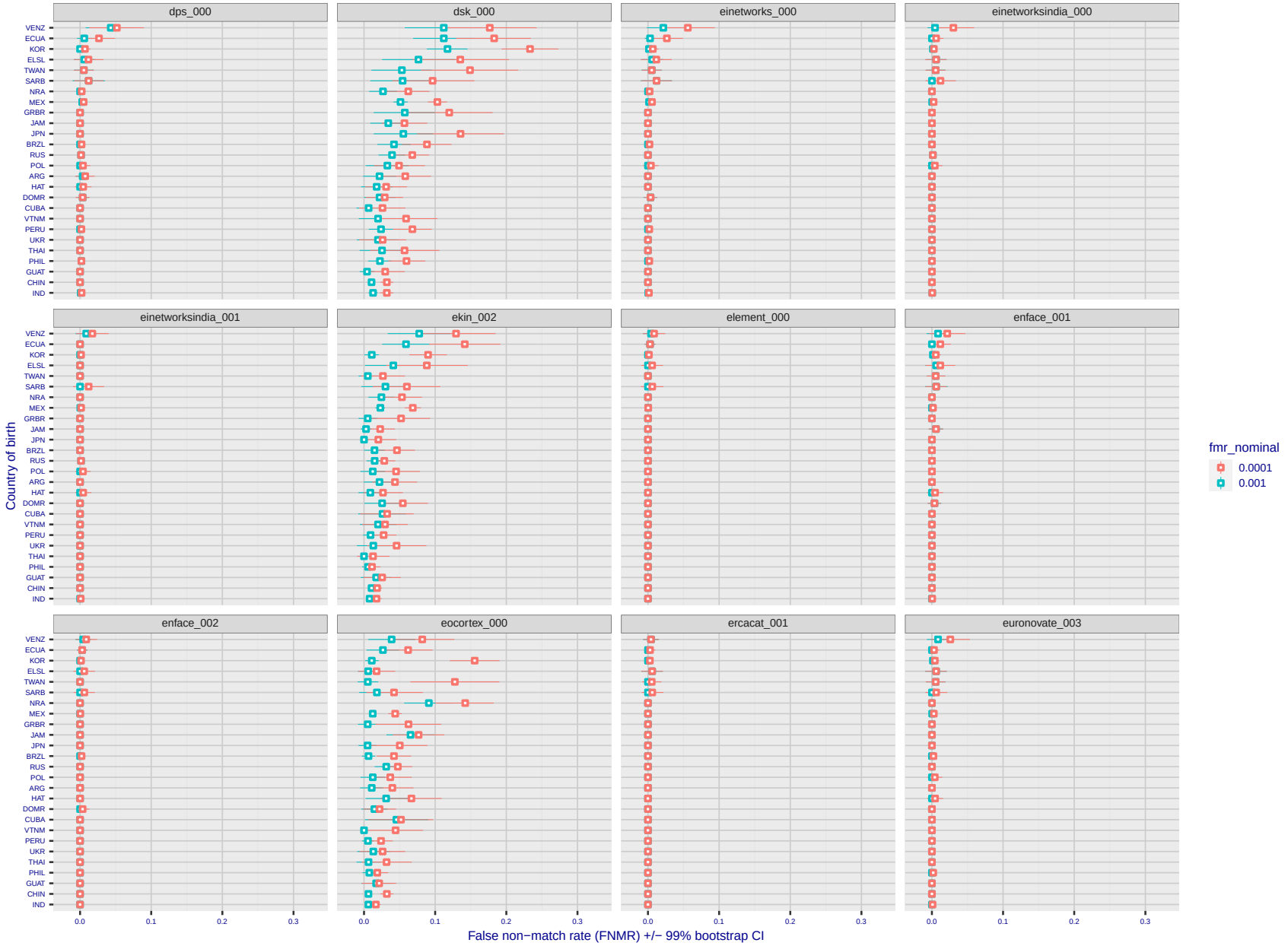

Figure 299: For the visa images, the dots show FNMR by country of birth for two globally set operating thresholds corresponding to FMR = $\{0.001, 0.0001\}$ computed over all on the order of 10^{10} impostor scores. The FMR in each bin will vary also - see subsequent impostor heatmaps in sec. 3.6.1. The figures shows an order of magnitude variation in FNMR across country of birth; these effects are likely due quality variations, then demographics like age and race. The error rates in some cases are zero, and in others the DET is flat so the error rates at the two thresholds are identical. The lines span 1% and 99% of boostrap replicated FNMR estimates.

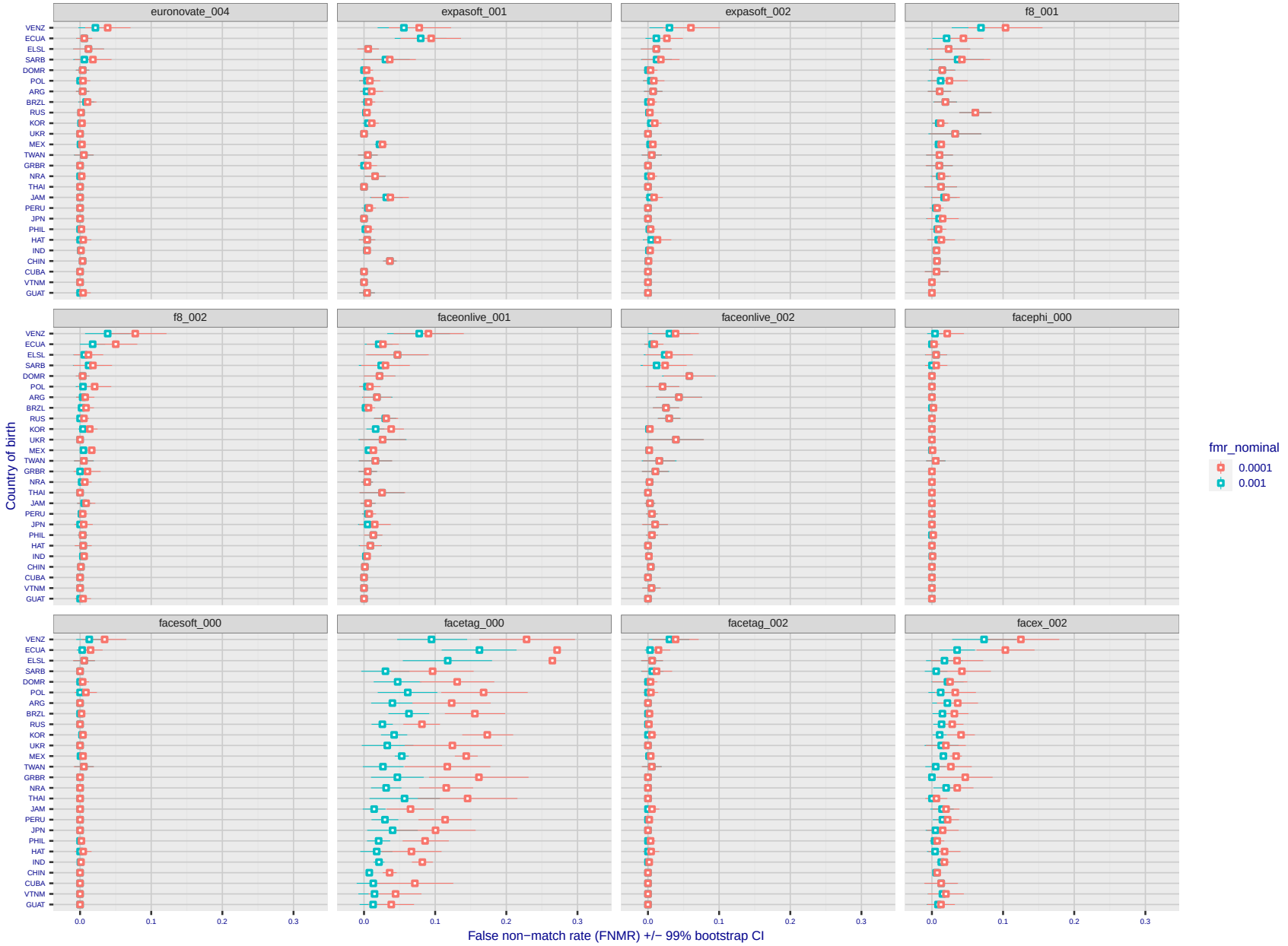

Figure 300: For the visa images, the dots show FNMR by country of birth for two globally set operating thresholds corresponding to FMR = $\{0.001, 0.0001\}$ computed over all on the order of 10^{10} impostor scores. The FMR in each bin will vary also - see subsequent impostor heatmaps in sec. 3.6.1. The figures shows an order of magnitude variation in FNMR across country of birth; these effects are likely due quality variations, then demographics like age and race. The error rates in some cases are zero, and in others the DET is flat so the error rates at the two thresholds are identical. The lines span 1% and 99% of boostrap replicated FNMR estimates.

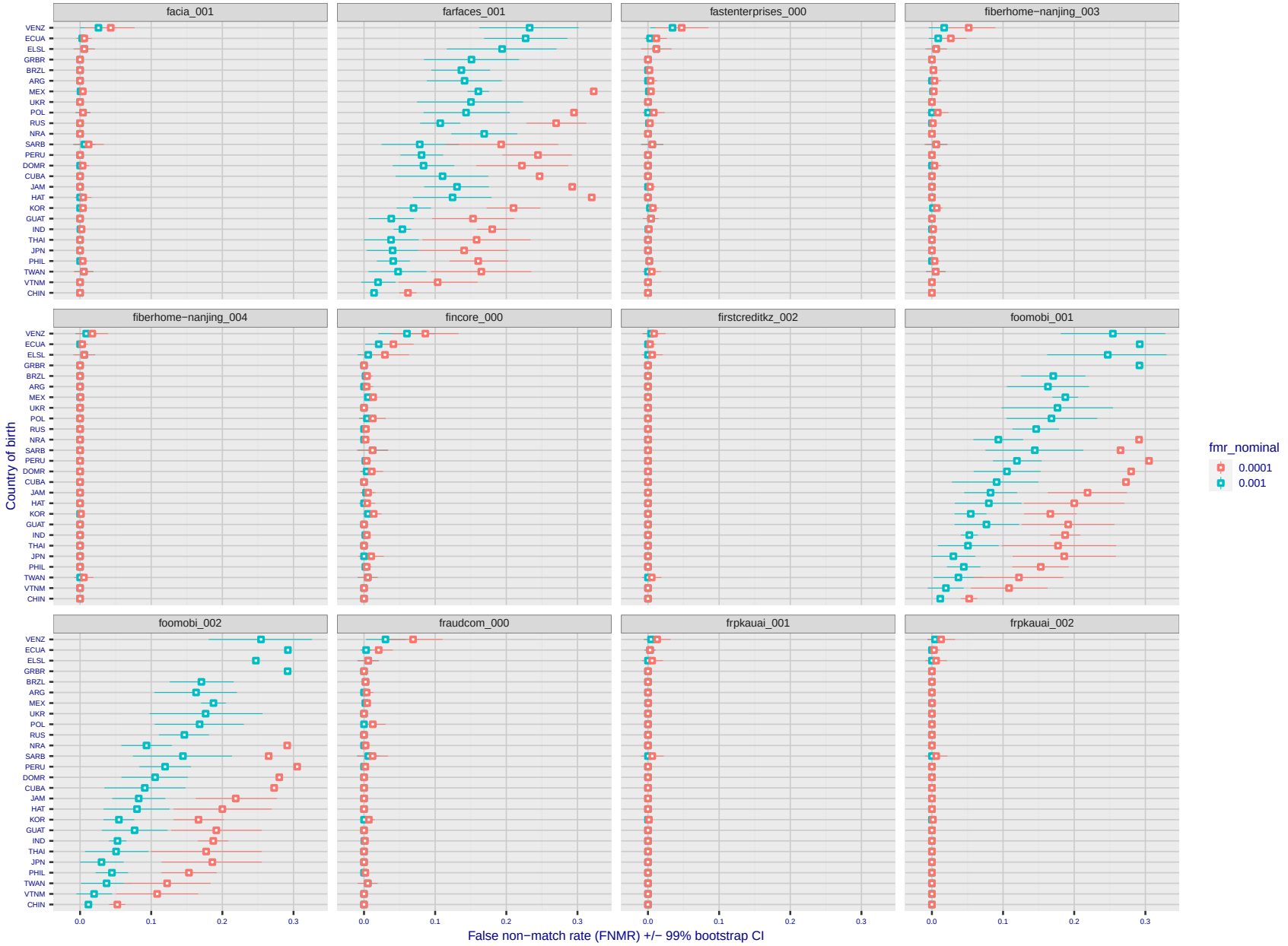

Figure 301: For the visa images, the dots show FNMR by country of birth for two globally set operating thresholds corresponding to FMR = $\{0.001, 0.0001\}$ computed over all on the order of 10^{10} impostor scores. The FMR in each bin will vary also - see subsequent impostor heatmaps in sec. 3.6.1. The figures shows an order of magnitude variation in FNMR across country of birth; these effects are likely due quality variations, then demographics like age and race. The error rates in some cases are zero, and in others the DET is flat so the error rates at the two thresholds are identical. The lines span 1% and 99% of boostrap replicated FNMR estimates.

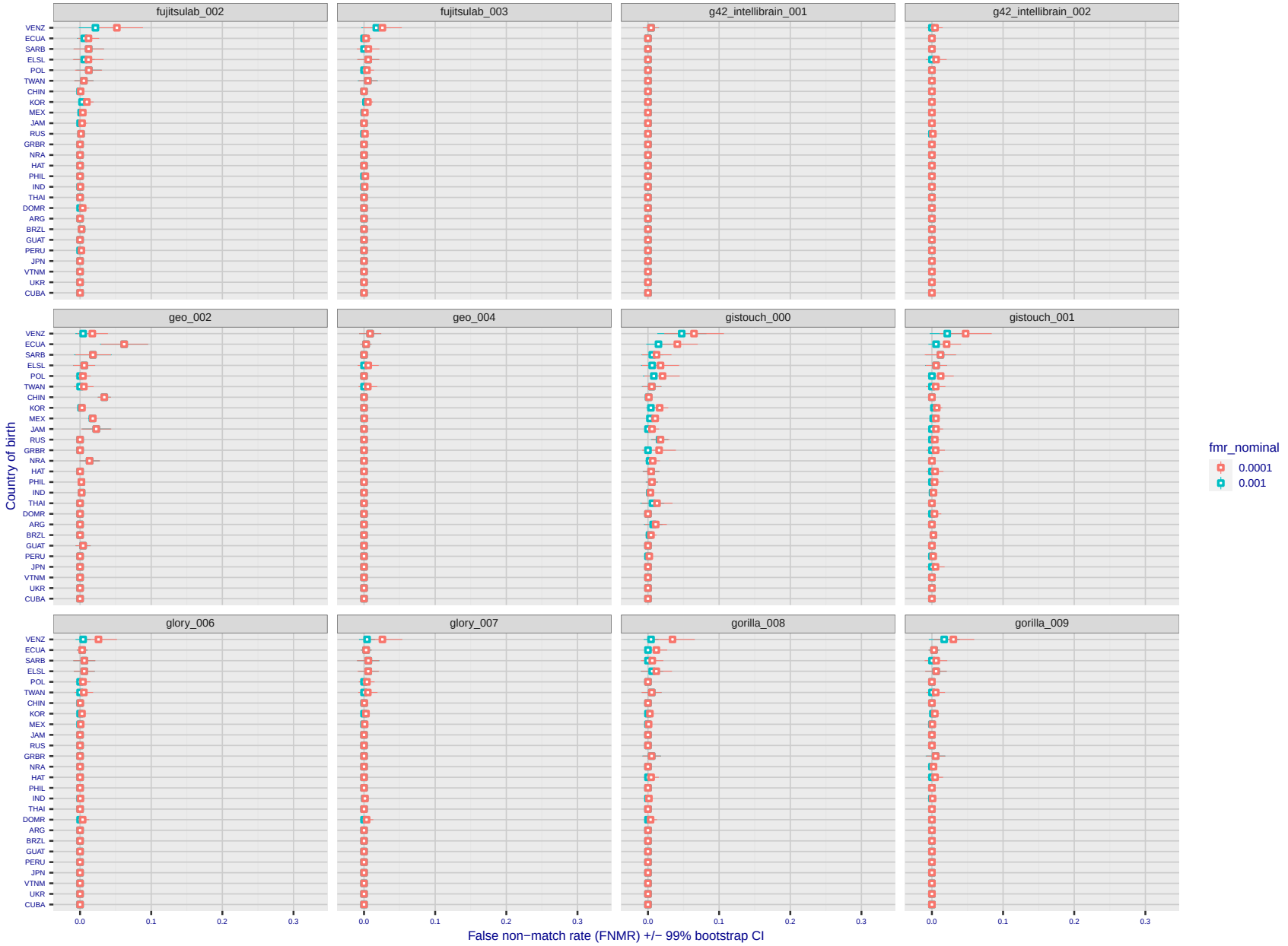

Figure 302: For the visa images, the dots show FNMR by country of birth for two globally set operating thresholds corresponding to FMR = $\{0.001, 0.0001\}$ computed over all on the order of 10^{10} impostor scores. The FMR in each bin will vary also - see subsequent impostor heatmaps in sec. 3.6.1. The figures shows an order of magnitude variation in FNMR across country of birth; these effects are likely due quality variations, then demographics like age and race. The error rates in some cases are zero, and in others the DET is flat so the error rates at the two thresholds are identical. The lines span 1% and 99% of boostrap replicated FNMR estimates.

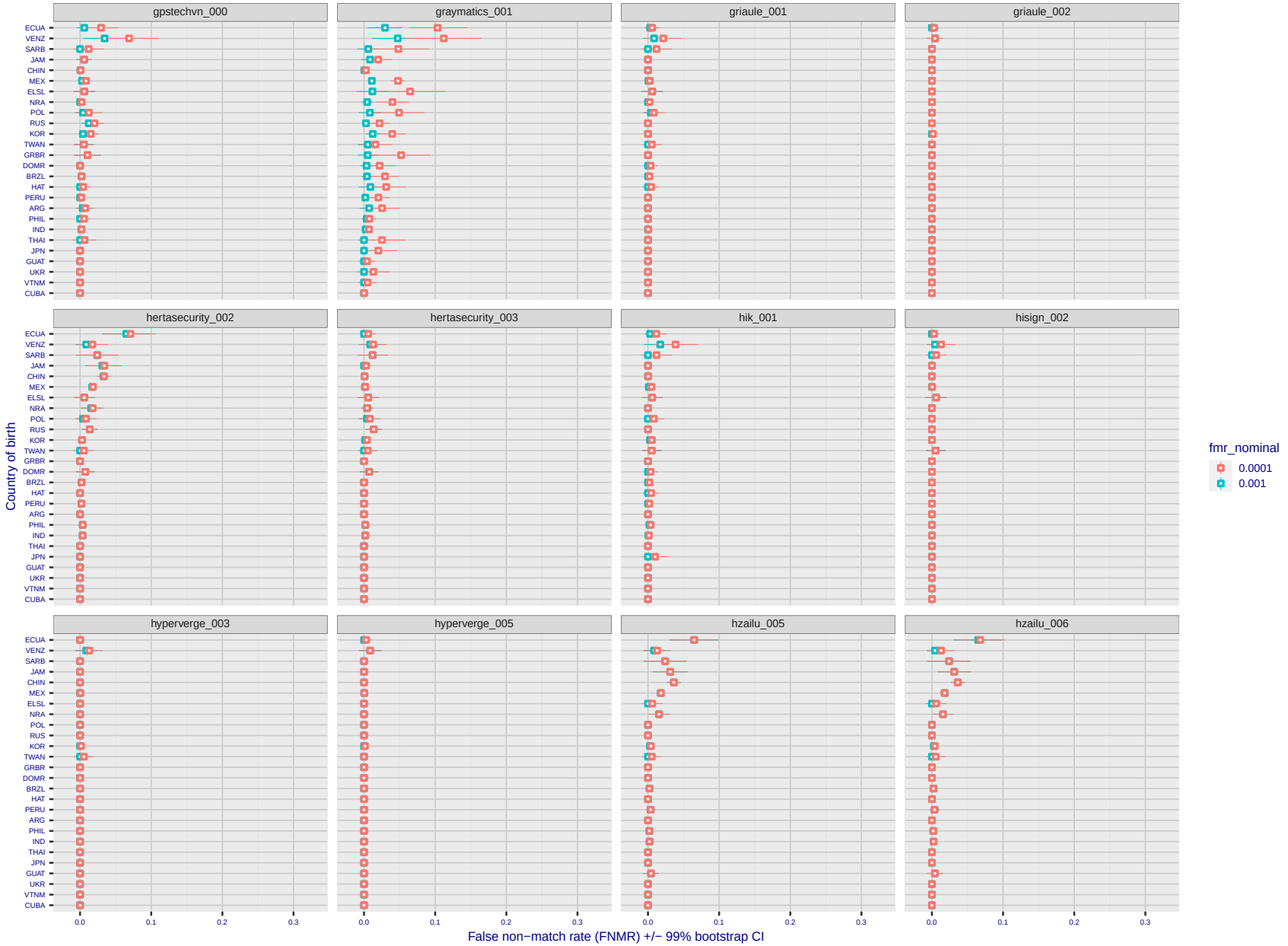

Figure 303: For the visa images, the dots show FNMR by country of birth for two globally set operating thresholds corresponding to FMR = $\{0.001, 0.0001\}$ computed over all on the order of 10^{10} impostor scores. The FMR in each bin will vary also - see subsequent impostor heatmaps in sec. 3.6.1. The figures shows an order of magnitude variation in FNMR across country of birth; these effects are likely due quality variations, then demographics like age and race. The error rates in some cases are zero, and in others the DET is flat so the error rates at the two thresholds are identical. The lines span 1% and 99% of boostrap replicated FNMR estimates.

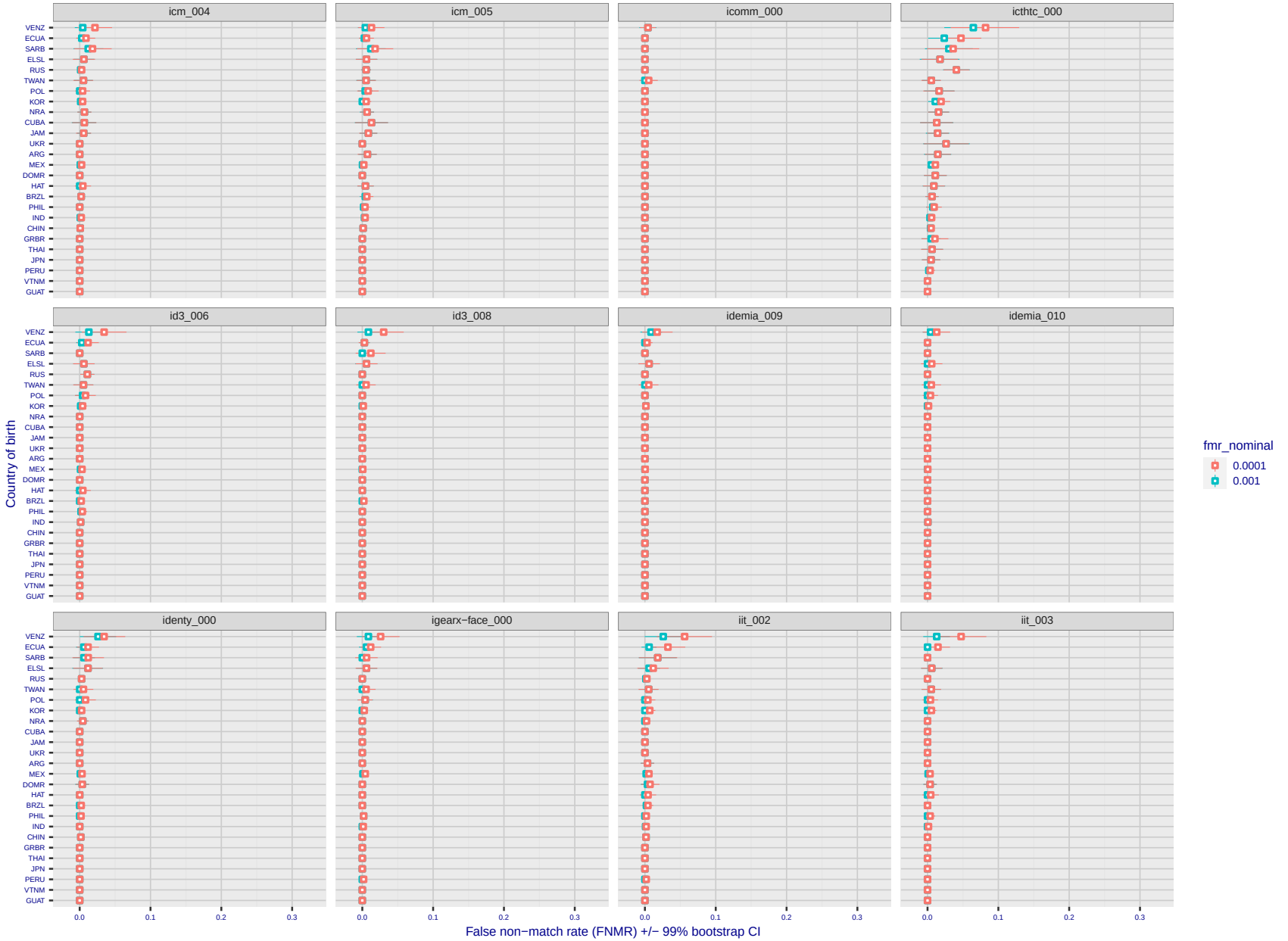

Figure 304: For the visa images, the dots show FNMR by country of birth for two globally set operating thresholds corresponding to FMR = $\{0.001, 0.0001\}$ computed over all on the order of 10^{10} impostor scores. The FMR in each bin will vary also - see subsequent impostor heatmaps in sec. 3.6.1. The figures shows an order of magnitude variation in FNMR across country of birth; these effects are likely due quality variations, then demographics like age and race. The error rates in some cases are zero, and in others the DET is flat so the error rates at the two thresholds are identical. The lines span 1% and 99% of boostrap replicated FNMR estimates.

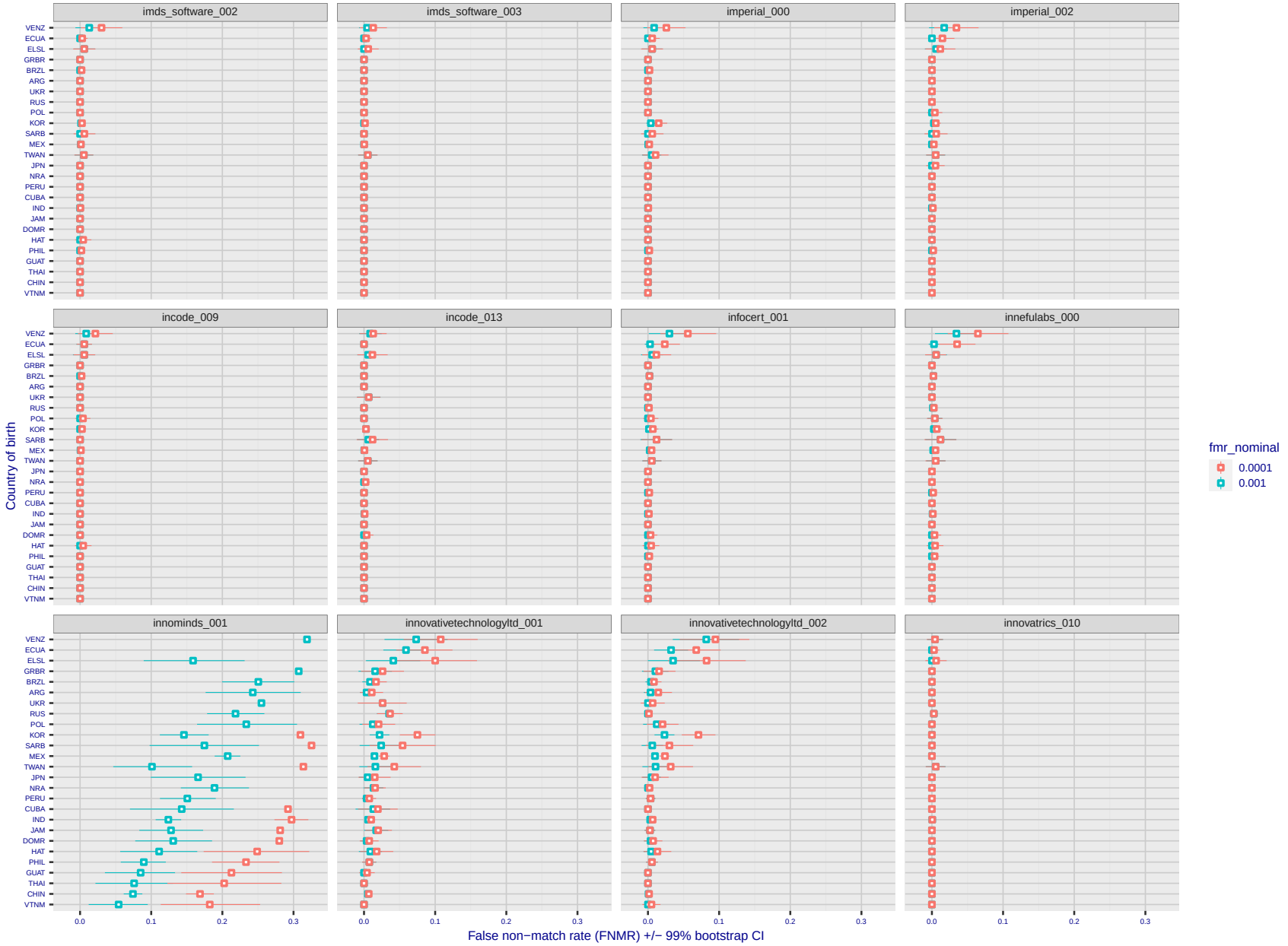

Figure 305: For the visa images, the dots show FNMR by country of birth for two globally set operating thresholds corresponding to FMR = $\{0.001, 0.0001\}$ computed over all on the order of 10^{10} impostor scores. The FMR in each bin will vary also - see subsequent impostor heatmaps in sec. 3.6.1. The figures shows an order of magnitude variation in FNMR across country of birth; these effects are likely due quality variations, then demographics like age and race. The error rates in some cases are zero, and in others the DET is flat so the error rates at the two thresholds are identical. The lines span 1% and 99% of boostrap replicated FNMR estimates.

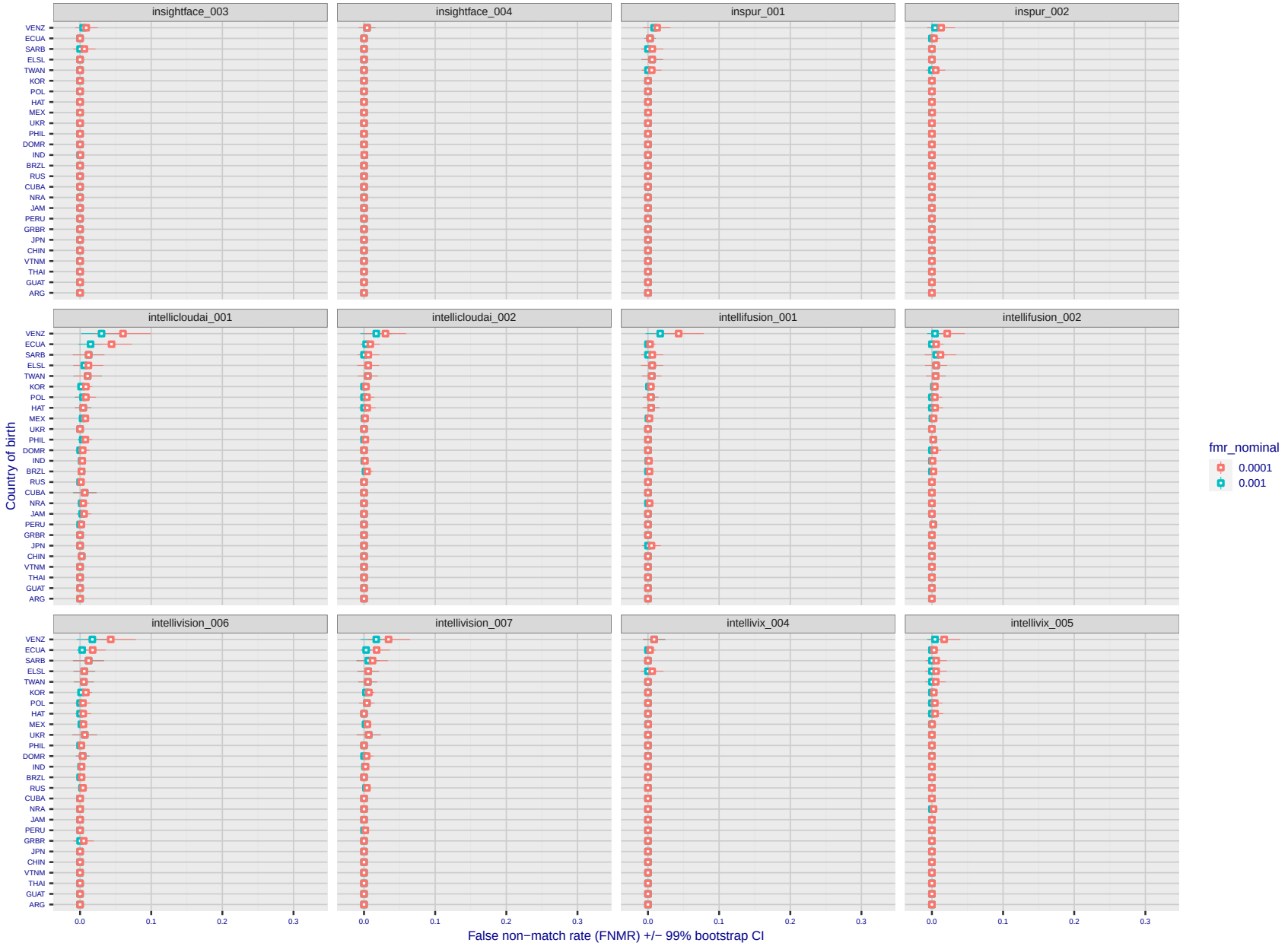

Figure 306: For the visa images, the dots show FNMR by country of birth for two globally set operating thresholds corresponding to FMR = $\{0.001, 0.0001\}$ computed over all on the order of 10^{10} impostor scores. The FMR in each bin will vary also - see subsequent impostor heatmaps in sec. 3.6.1. The figures shows an order of magnitude variation in FNMR across country of birth; these effects are likely due quality variations, then demographics like age and race. The error rates in some cases are zero, and in others the DET is flat so the error rates at the two thresholds are identical. The lines span 1% and 99% of boostrap replicated FNMR estimates.

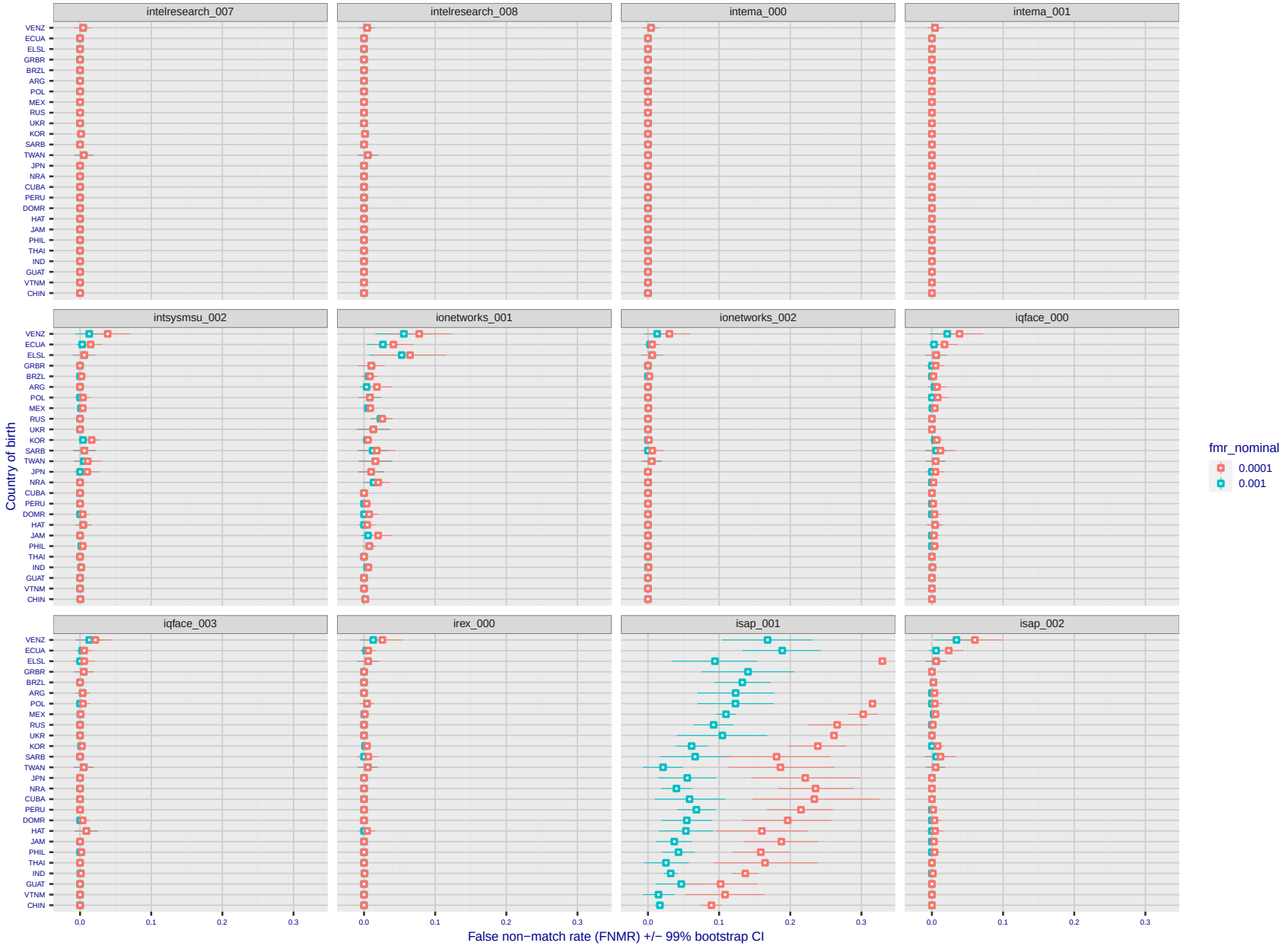

Figure 307: For the visa images, the dots show FNMR by country of birth for two globally set operating thresholds corresponding to FMR = $\{0.001, 0.0001\}$ computed over all on the order of 10^{10} impostor scores. The FMR in each bin will vary also - see subsequent impostor heatmaps in sec. 3.6.1. The figures shows an order of magnitude variation in FNMR across country of birth; these effects are likely due quality variations, then demographics like age and race. The error rates in some cases are zero, and in others the DET is flat so the error rates at the two thresholds are identical. The lines span 1% and 99% of boostrap replicated FNMR estimates.

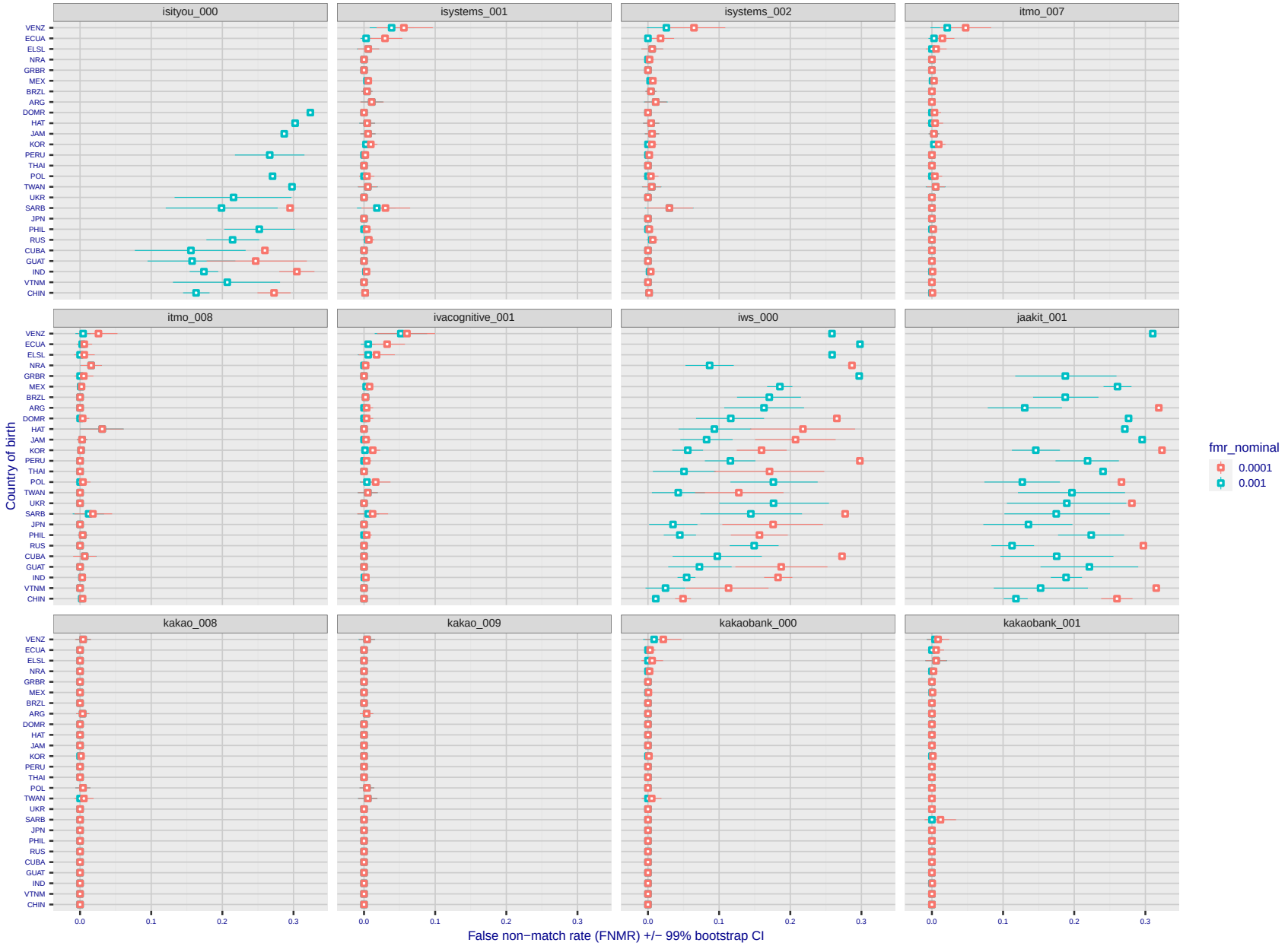

Figure 308: For the visa images, the dots show FNMR by country of birth for two globally set operating thresholds corresponding to FMR = $\{0.001, 0.0001\}$ computed over all on the order of 10^{10} impostor scores. The FMR in each bin will vary also - see subsequent impostor heatmaps in sec. 3.6.1. The figures shows an order of magnitude variation in FNMR across country of birth; these effects are likely due quality variations, then demographics like age and race. The error rates in some cases are zero, and in others the DET is flat so the error rates at the two thresholds are identical. The lines span 1% and 99% of boostrap replicated FNMR estimates.

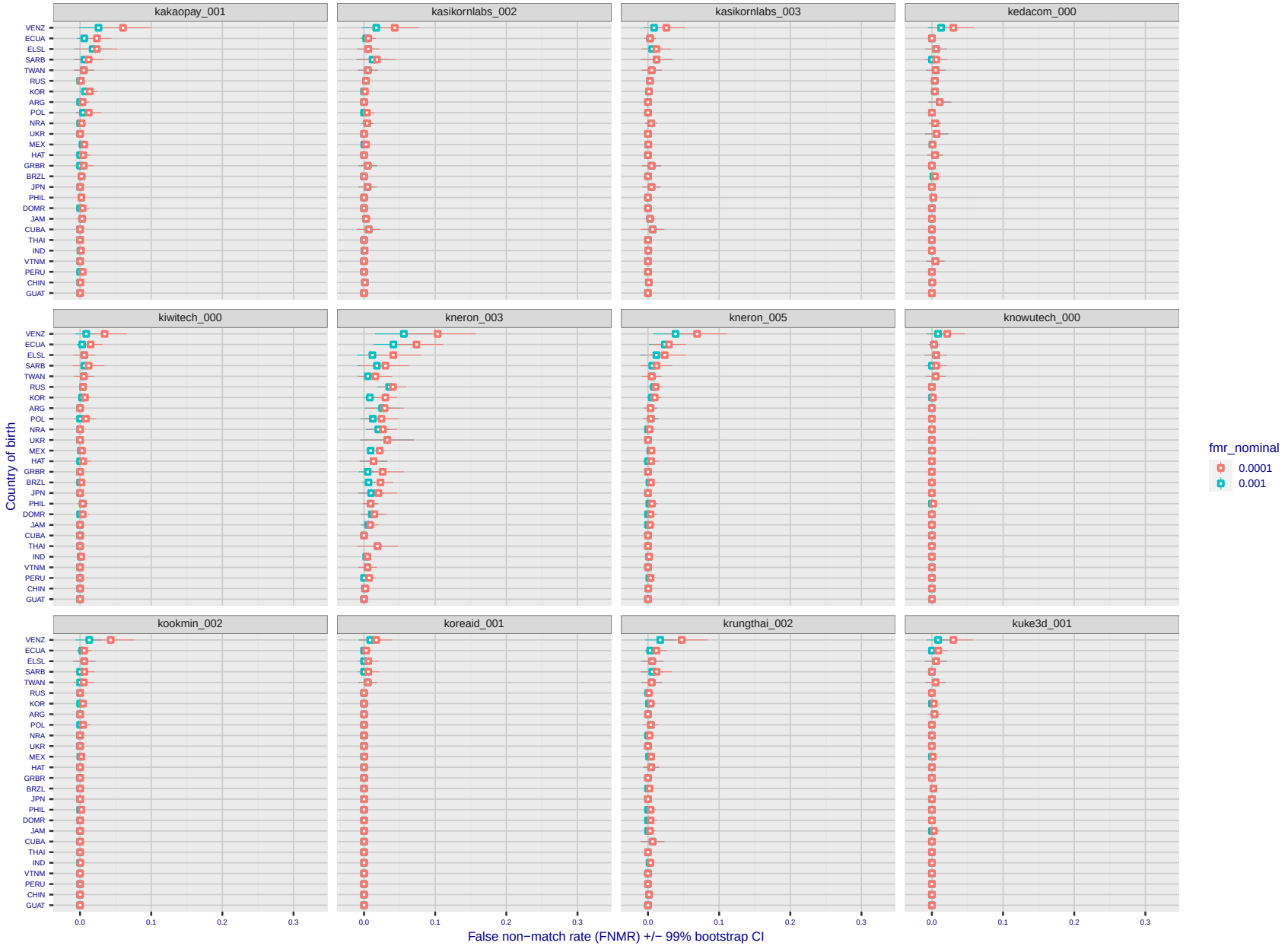

Figure 309: For the visa images, the dots show FNMR by country of birth for two globally set operating thresholds corresponding to FMR = $\{0.001, 0.0001\}$ computed over all on the order of 10^{10} impostor scores. The FMR in each bin will vary also - see subsequent impostor heatmaps in sec. 3.6.1. The figures shows an order of magnitude variation in FNMR across country of birth; these effects are likely due quality variations, then demographics like age and race. The error rates in some cases are zero, and in others the DET is flat so the error rates at the two thresholds are identical. The lines span 1% and 99% of boostrap replicated FNMR estimates.

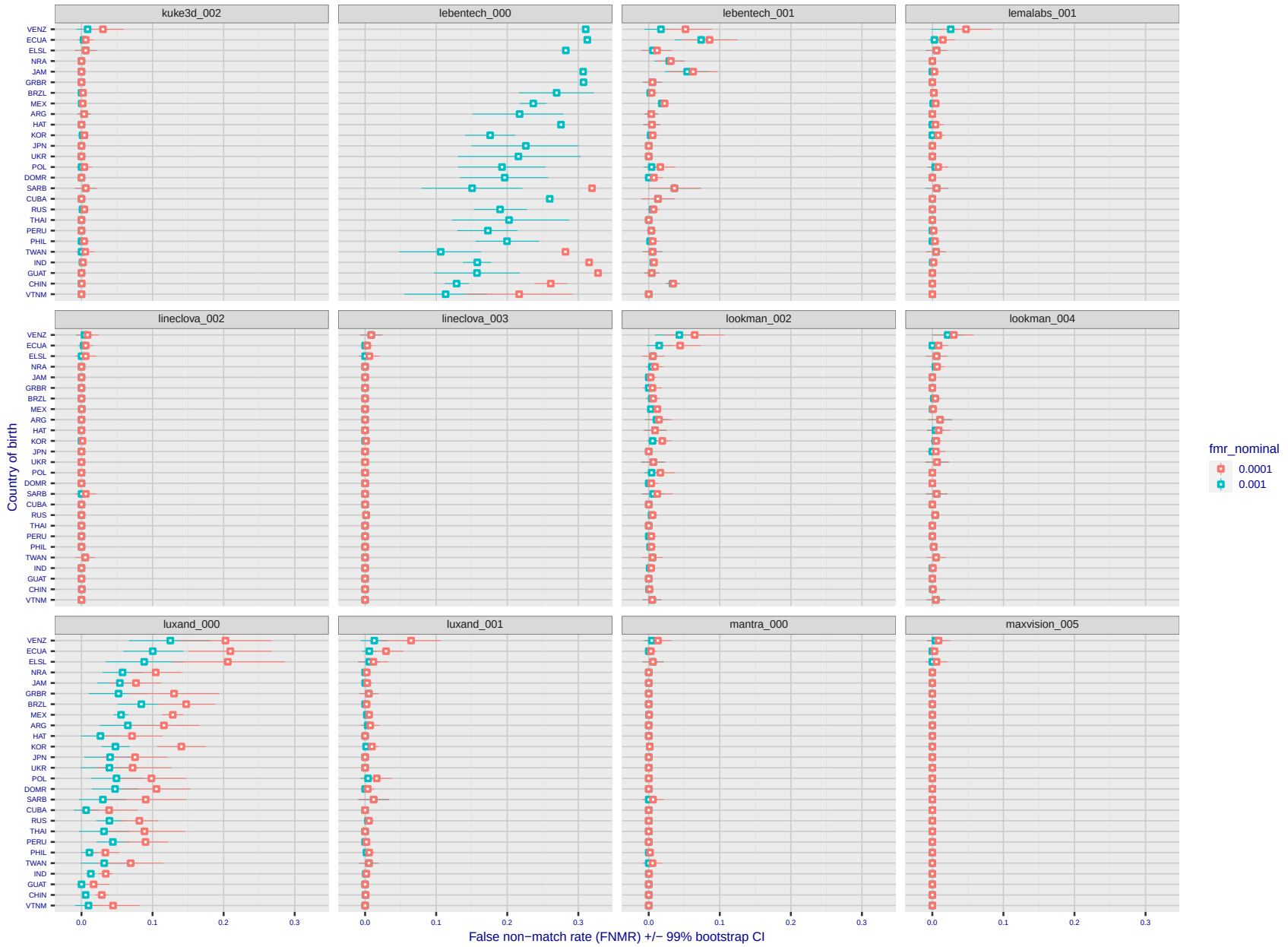

Figure 310: For the visa images, the dots show FNMR by country of birth for two globally set operating thresholds corresponding to FMR = $\{0.001, 0.0001\}$ computed over all on the order of 10^{10} impostor scores. The FMR in each bin will vary also - see subsequent impostor heatmaps in sec. 3.6.1. The figures shows an order of magnitude variation in FNMR across country of birth; these effects are likely due quality variations, then demographics like age and race. The error rates in some cases are zero, and in others the DET is flat so the error rates at the two thresholds are identical. The lines span 1% and 99% of boostrap replicated FNMR estimates.

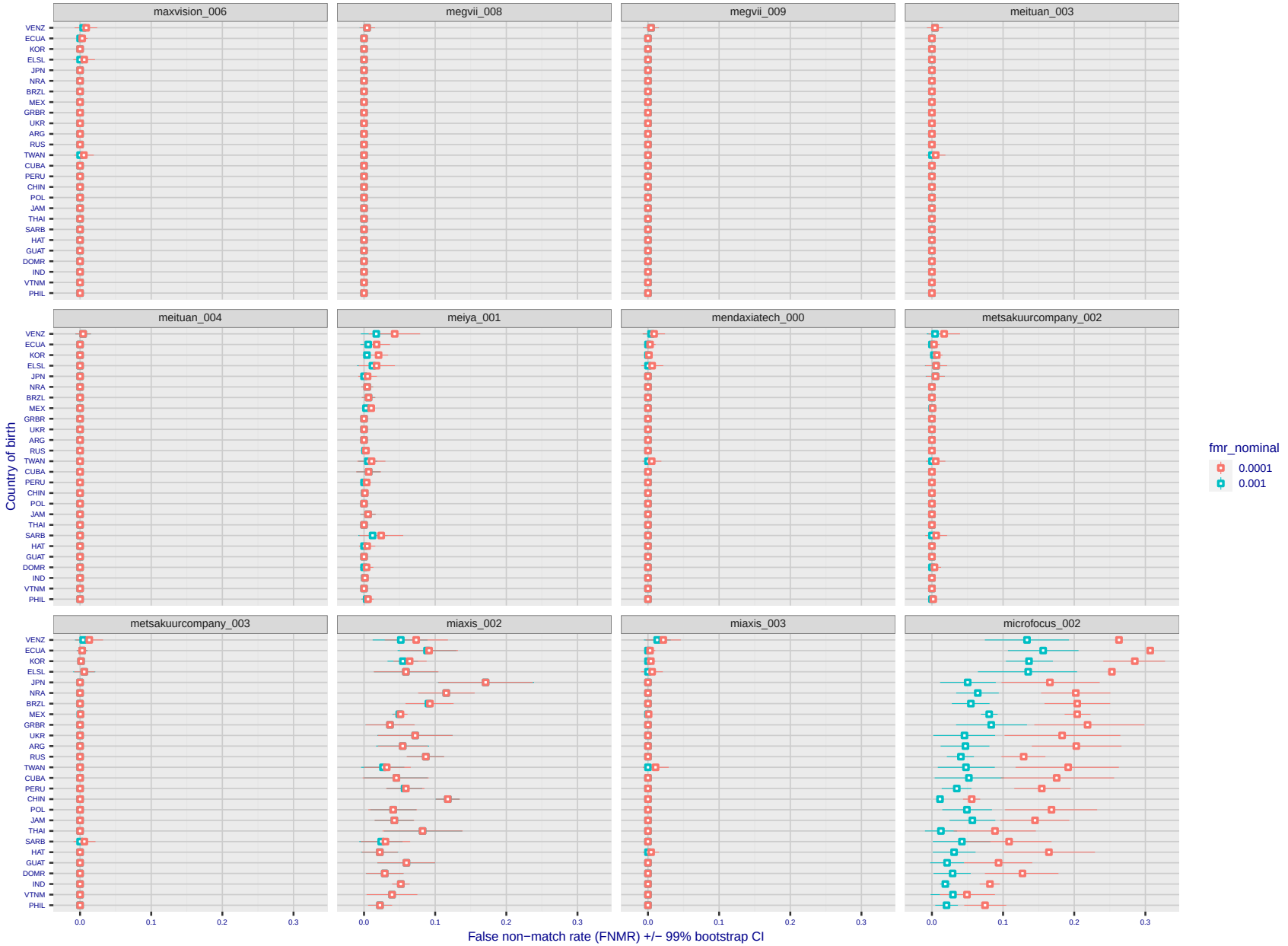

Figure 311: For the visa images, the dots show FNMR by country of birth for two globally set operating thresholds corresponding to FMR = $\{0.001, 0.0001\}$ computed over all on the order of 10^{10} impostor scores. The FMR in each bin will vary also - see subsequent impostor heatmaps in sec. 3.6.1. The figures shows an order of magnitude variation in FNMR across country of birth; these effects are likely due quality variations, then demographics like age and race. The error rates in some cases are zero, and in others the DET is flat so the error rates at the two thresholds are identical. The lines span 1% and 99% of boostrap replicated FNMR estimates.

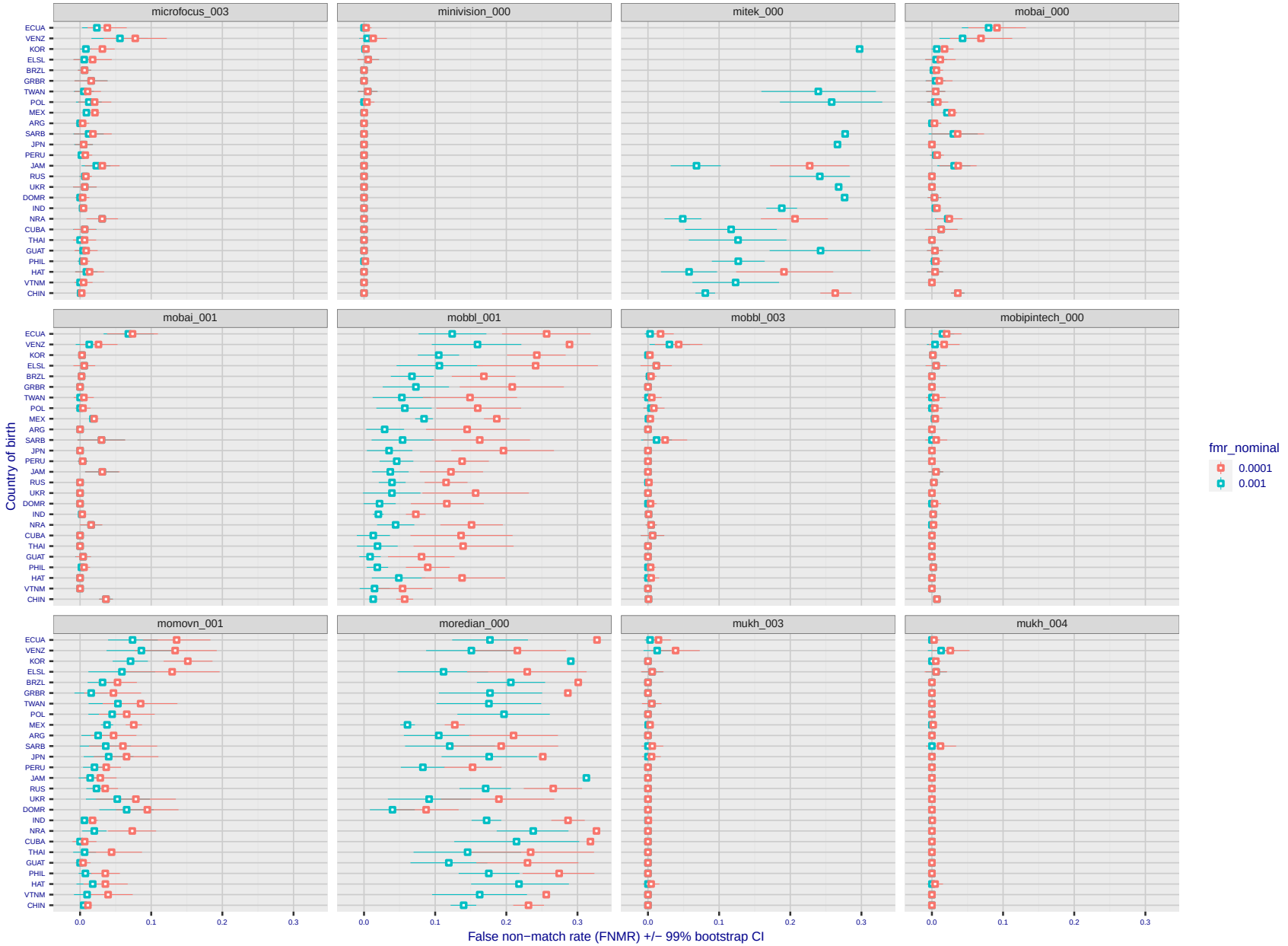

Figure 312: For the visa images, the dots show FNMR by country of birth for two globally set operating thresholds corresponding to FMR = $\{0.001, 0.0001\}$ computed over all on the order of 10^{10} impostor scores. The FMR in each bin will vary also - see subsequent impostor heatmaps in sec. 3.6.1. The figures shows an order of magnitude variation in FNMR across country of birth; these effects are likely due quality variations, then demographics like age and race. The error rates in some cases are zero, and in others the DET is flat so the error rates at the two thresholds are identical. The lines span 1% and 99% of boostrap replicated FNMR estimates.

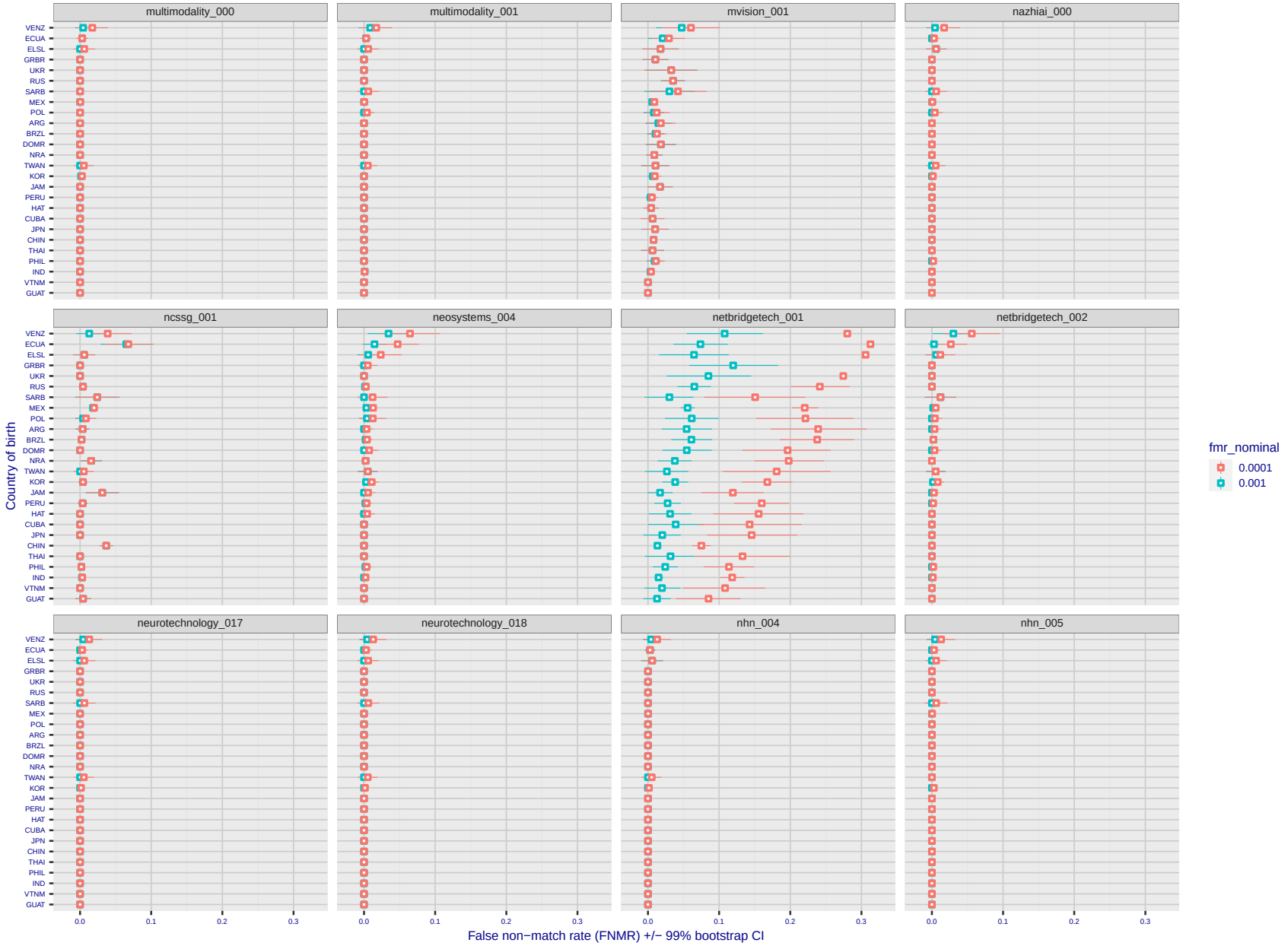

Figure 313: For the visa images, the dots show FNMR by country of birth for two globally set operating thresholds corresponding to FMR = $\{0.001, 0.0001\}$ computed over all on the order of 10^{10} impostor scores. The FMR in each bin will vary also - see subsequent impostor heatmaps in sec. 3.6.1. The figures shows an order of magnitude variation in FNMR across country of birth; these effects are likely due quality variations, then demographics like age and race. The error rates in some cases are zero, and in others the DET is flat so the error rates at the two thresholds are identical. The lines span 1% and 99% of boostrap replicated FNMR estimates.

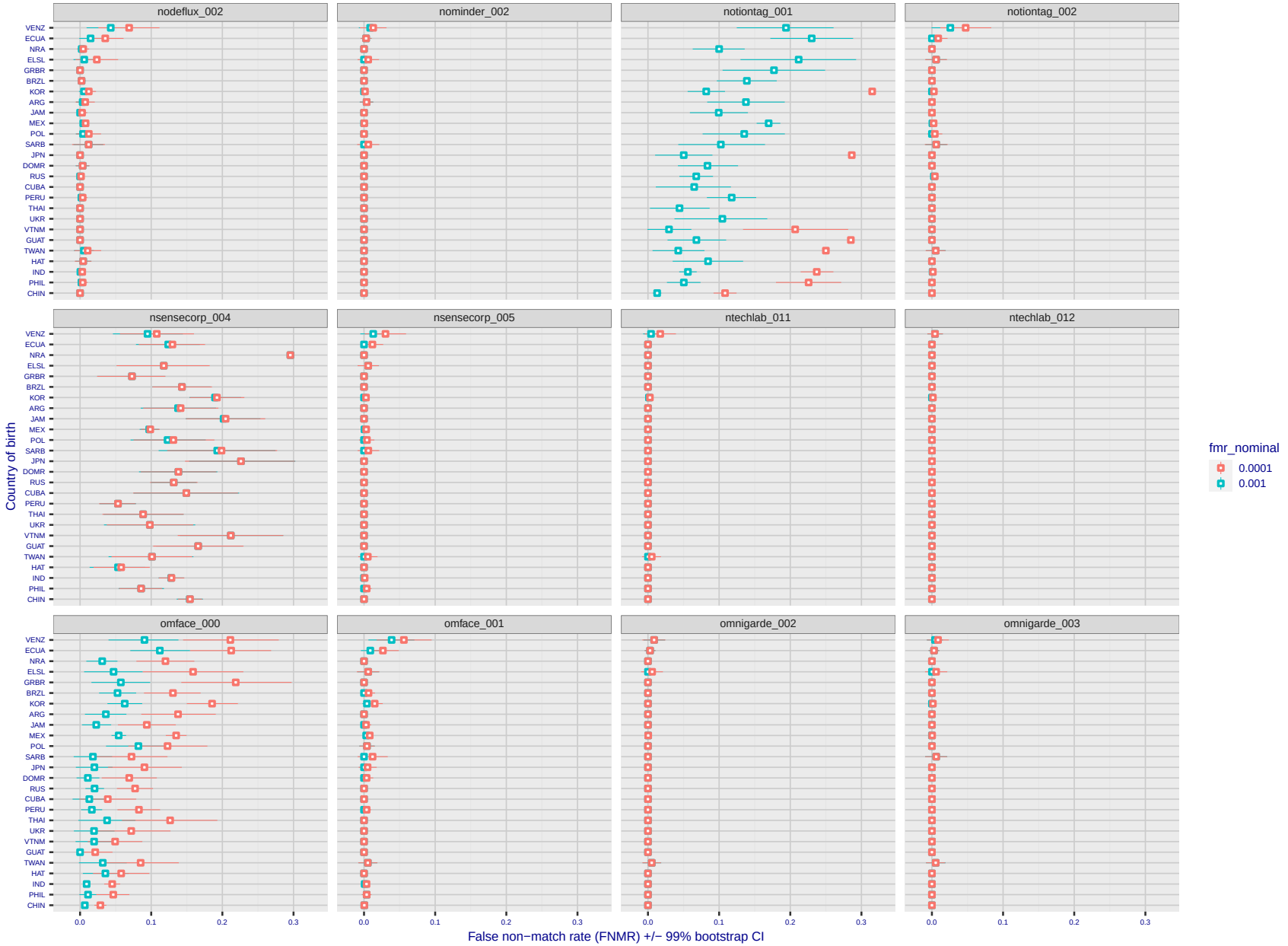

Figure 314: For the visa images, the dots show FNMR by country of birth for two globally set operating thresholds corresponding to FMR = $\{0.001, 0.0001\}$ computed over all on the order of 10^{10} impostor scores. The FMR in each bin will vary also - see subsequent impostor heatmaps in sec. 3.6.1. The figures shows an order of magnitude variation in FNMR across country of birth; these effects are likely due quality variations, then demographics like age and race. The error rates in some cases are zero, and in others the DET is flat so the error rates at the two thresholds are identical. The lines span 1% and 99% of boostrap replicated FNMR estimates.

Figure 315: For the visa images, the dots show FNMR by country of birth for two globally set operating thresholds corresponding to FMR = $\{0.001, 0.0001\}$ computed over all on the order of 10^{10} impostor scores. The FMR in each bin will vary also - see subsequent impostor heatmaps in sec. 3.6.1. The figures shows an order of magnitude variation in FNMR across country of birth; these effects are likely due quality variations, then demographics like age and race. The error rates in some cases are zero, and in others the DET is flat so the error rates at the two thresholds are identical. The lines span 1% and 99% of boostrap replicated FNMR estimates.

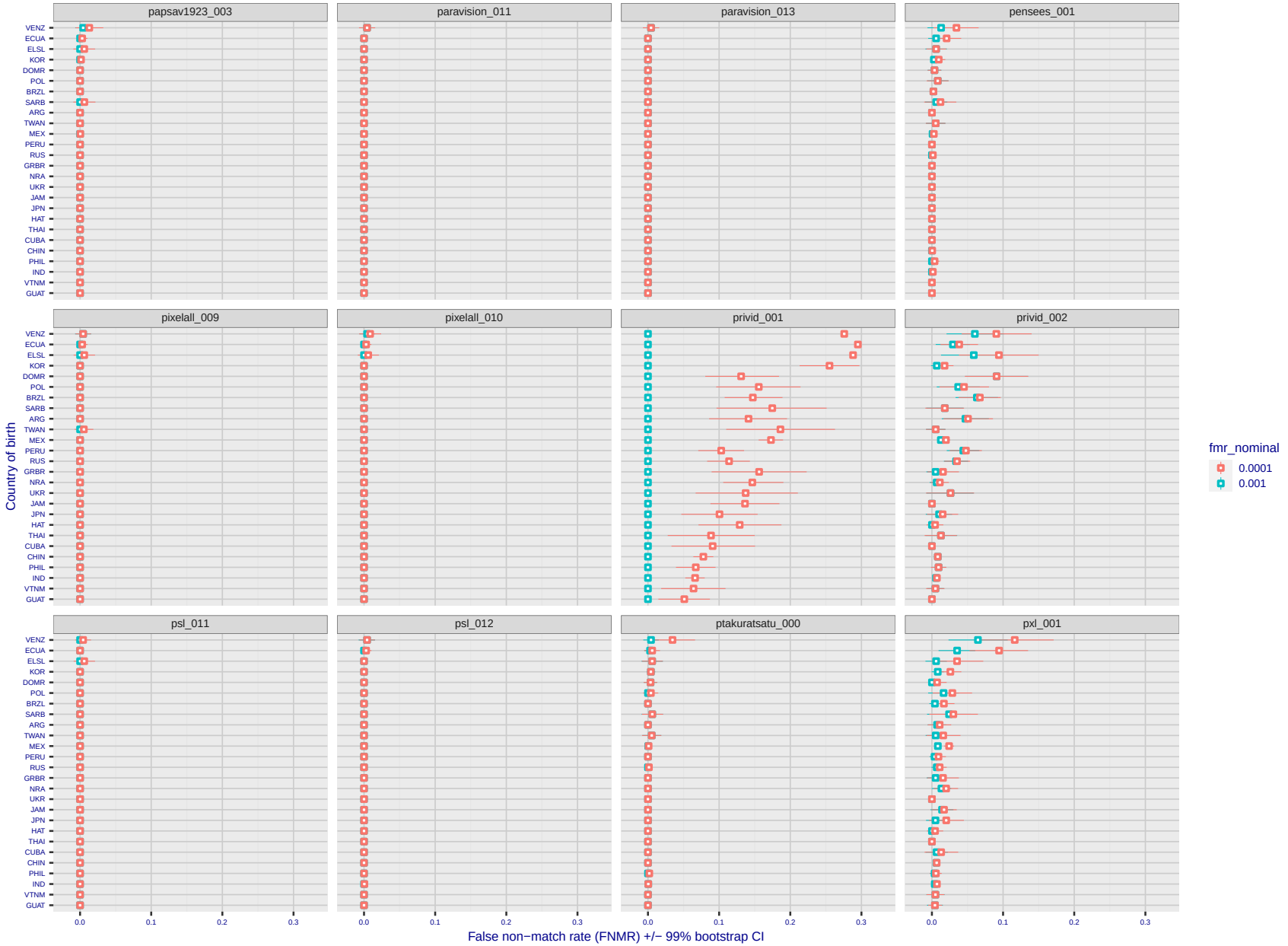

Figure 316: For the visa images, the dots show FNMR by country of birth for two globally set operating thresholds corresponding to FMR = $\{0.001, 0.0001\}$ computed over all on the order of 10^{10} impostor scores. The FMR in each bin will vary also - see subsequent impostor heatmaps in sec. 3.6.1. The figures shows an order of magnitude variation in FNMR across country of birth; these effects are likely due quality variations, then demographics like age and race. The error rates in some cases are zero, and in others the DET is flat so the error rates at the two thresholds are identical. The lines span 1% and 99% of boostrap replicated FNMR estimates.

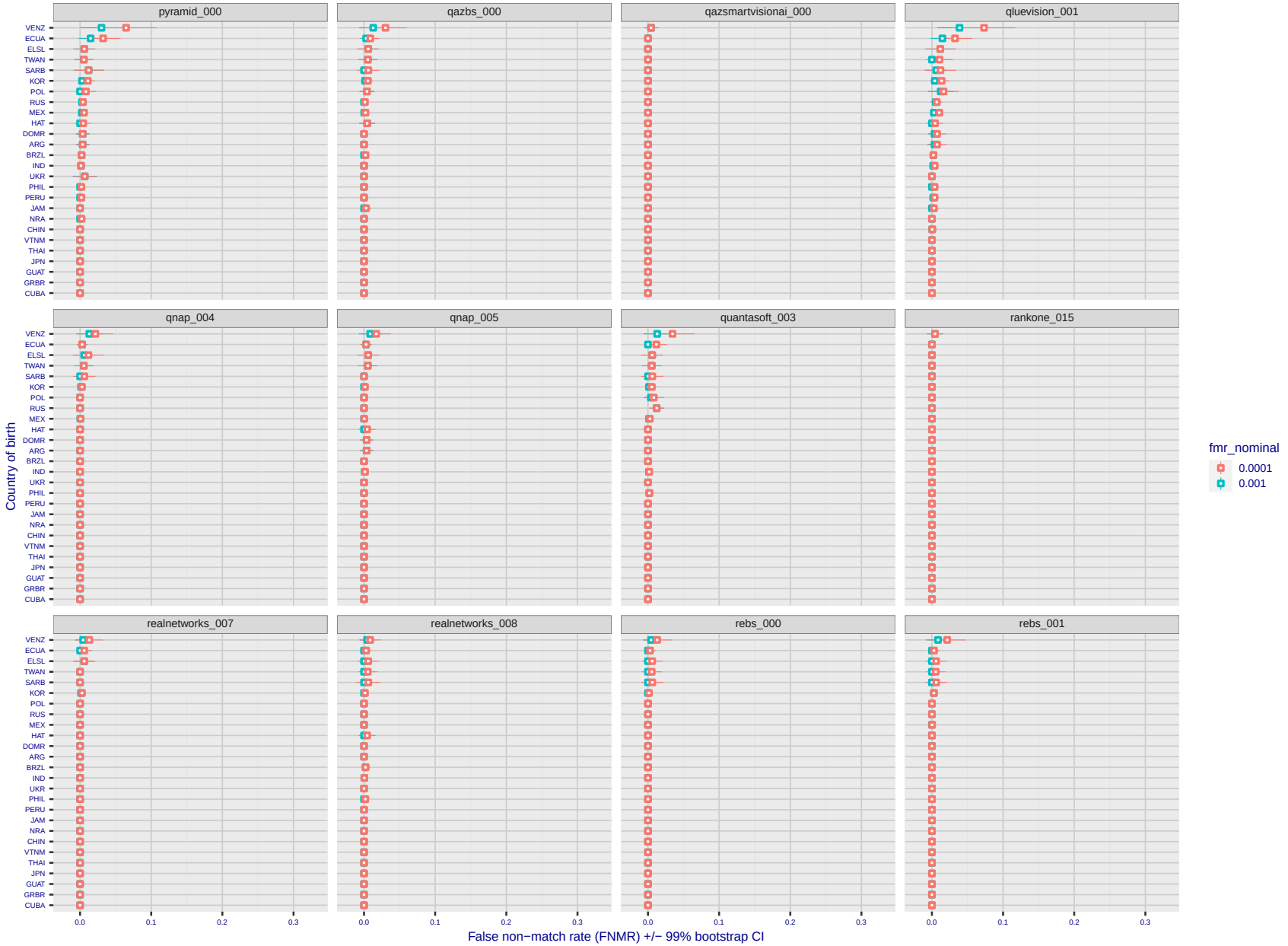

Figure 317: For the visa images, the dots show FNMR by country of birth for two globally set operating thresholds corresponding to FMR = $\{0.001, 0.0001\}$ computed over all on the order of 10^{10} impostor scores. The FMR in each bin will vary also - see subsequent impostor heatmaps in sec. 3.6.1. The figures shows an order of magnitude variation in FNMR across country of birth; these effects are likely due quality variations, then demographics like age and race. The error rates in some cases are zero, and in others the DET is flat so the error rates at the two thresholds are identical. The lines span 1% and 99% of boostrap replicated FNMR estimates.

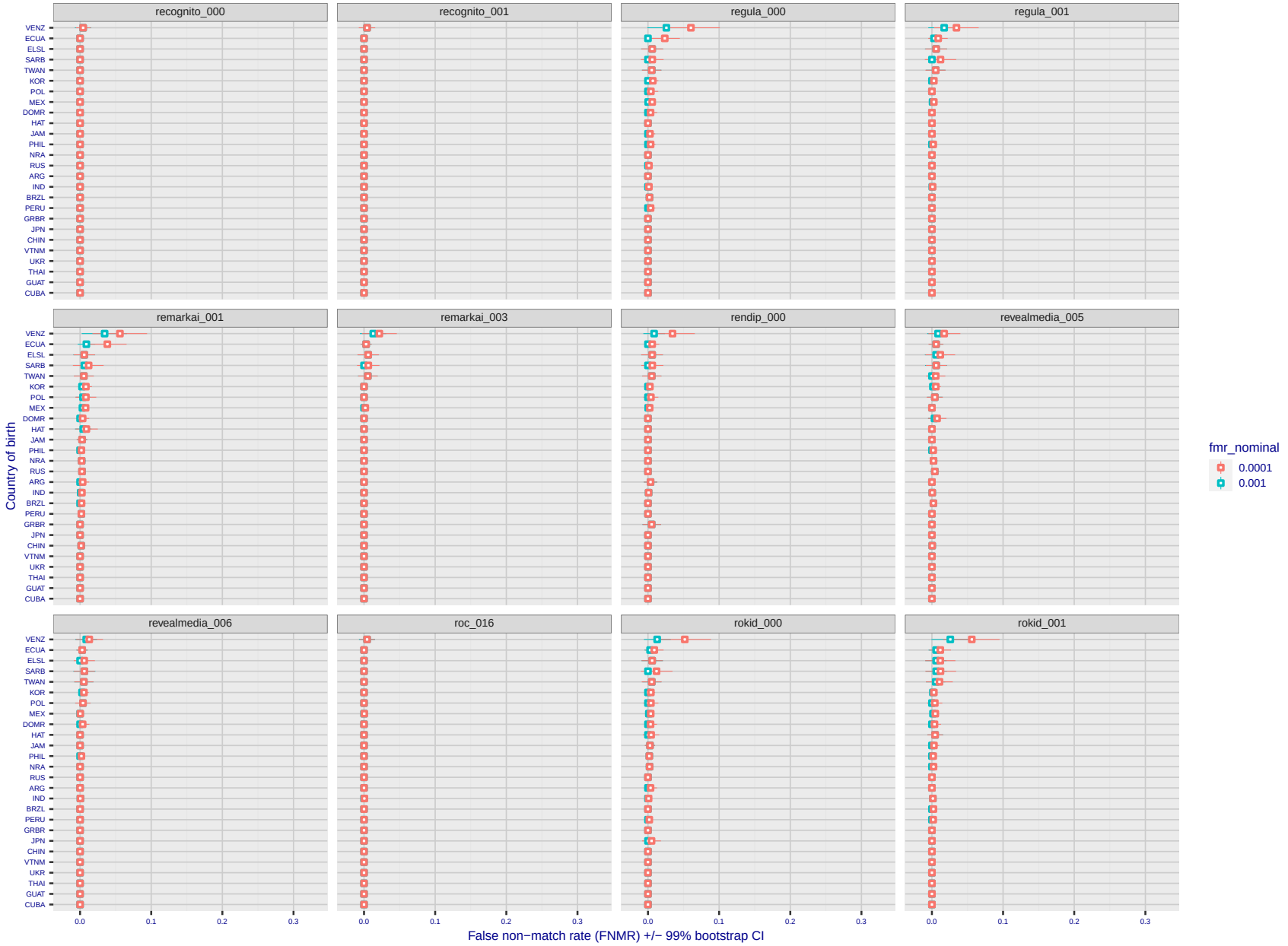

Figure 318: For the visa images, the dots show FNMR by country of birth for two globally set operating thresholds corresponding to FMR = $\{0.001, 0.0001\}$ computed over all on the order of 10^{10} impostor scores. The FMR in each bin will vary also - see subsequent impostor heatmaps in sec. 3.6.1. The figures shows an order of magnitude variation in FNMR across country of birth; these effects are likely due quality variations, then demographics like age and race. The error rates in some cases are zero, and in others the DET is flat so the error rates at the two thresholds are identical. The lines span 1% and 99% of boostrap replicated FNMR estimates.

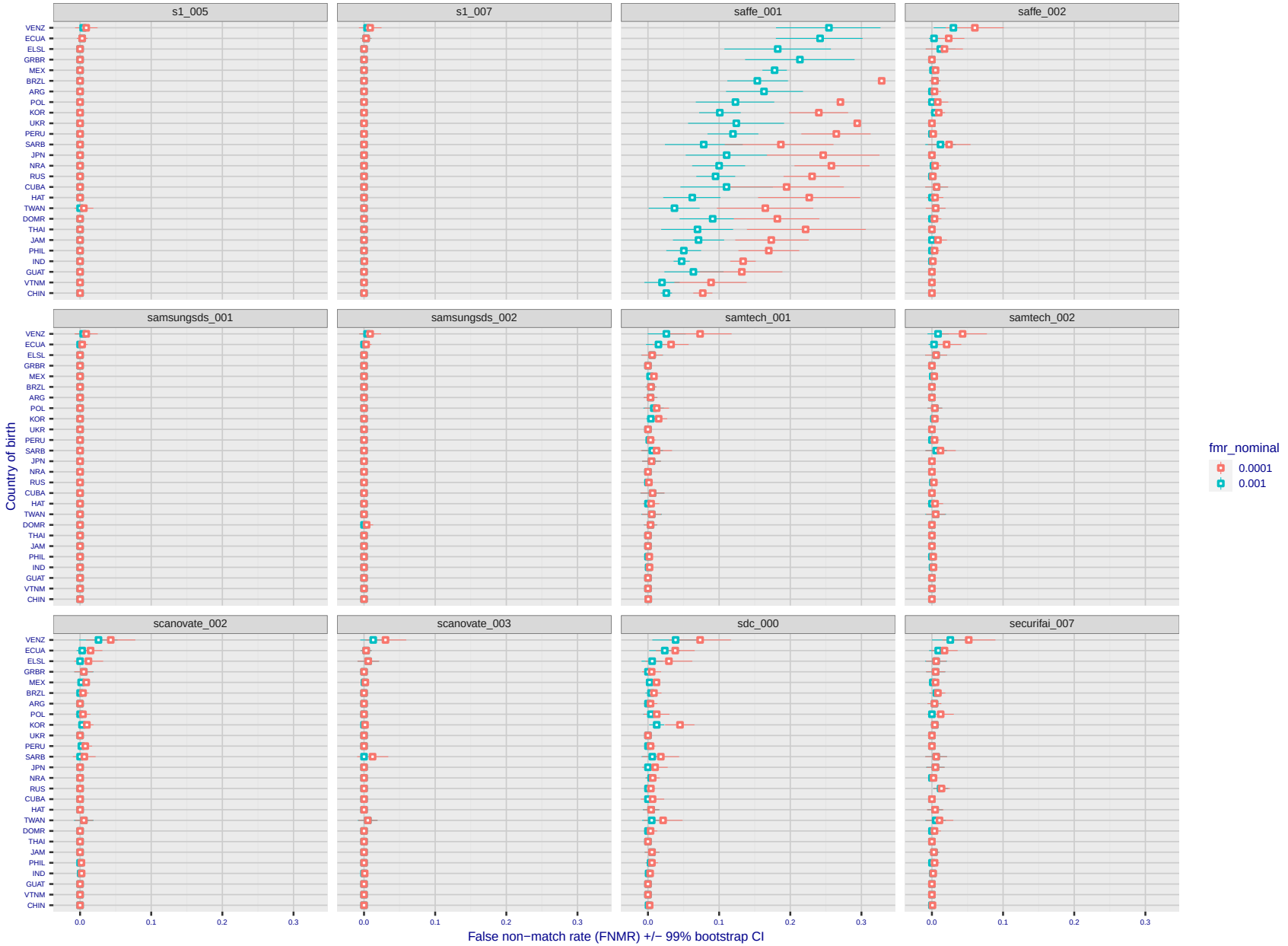

Figure 319: For the visa images, the dots show FNMR by country of birth for two globally set operating thresholds corresponding to FMR = $\{0.001, 0.0001\}$ computed over all on the order of 10^{10} impostor scores. The FMR in each bin will vary also - see subsequent impostor heatmaps in sec. 3.6.1. The figures shows an order of magnitude variation in FNMR across country of birth; these effects are likely due quality variations, then demographics like age and race. The error rates in some cases are zero, and in others the DET is flat so the error rates at the two thresholds are identical. The lines span 1% and 99% of boostrap replicated FNMR estimates.

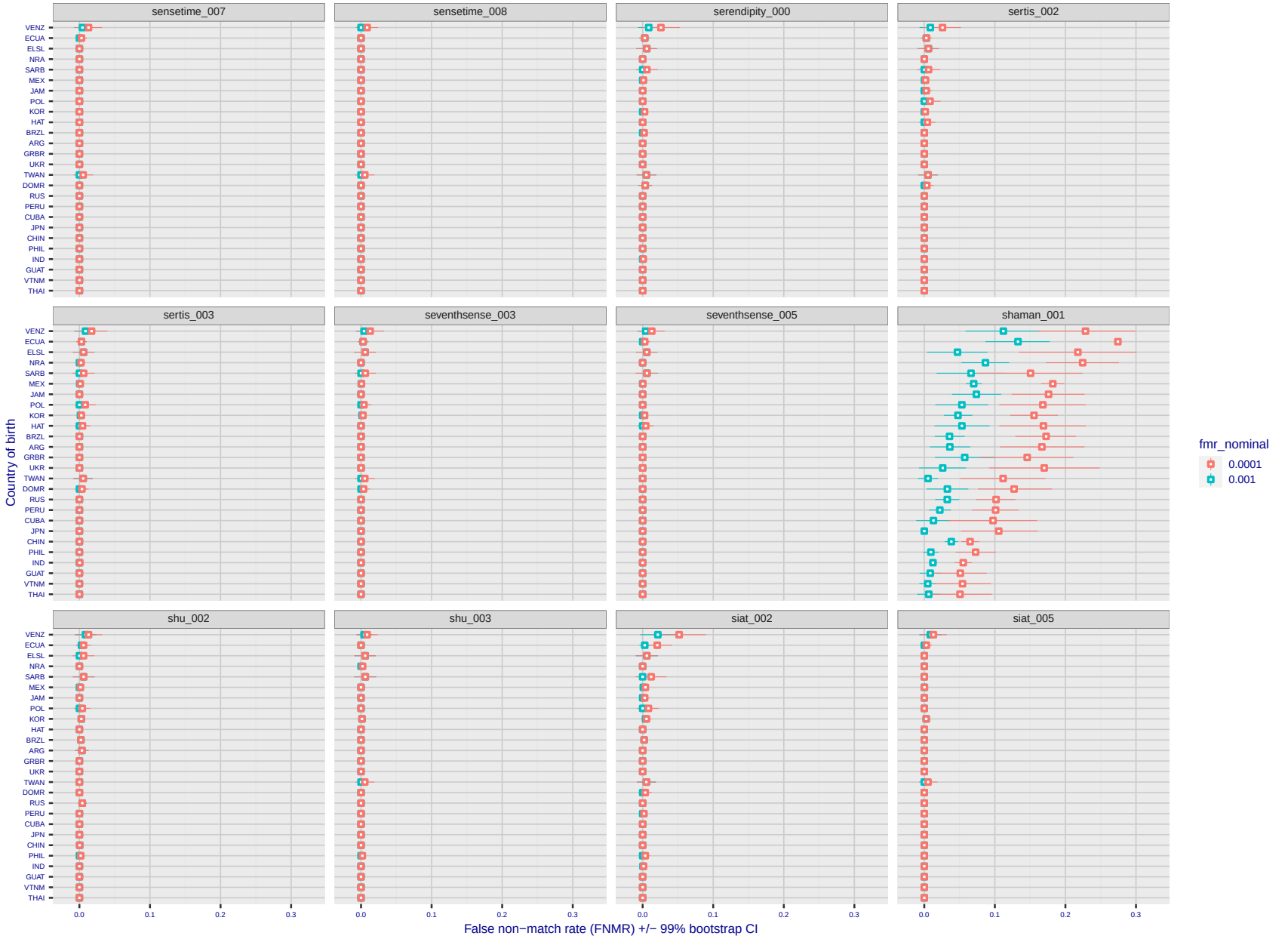

Figure 320: For the visa images, the dots show FNMR by country of birth for two globally set operating thresholds corresponding to FMR = $\{0.001, 0.0001\}$ computed over all on the order of 10^{10} impostor scores. The FMR in each bin will vary also - see subsequent impostor heatmaps in sec. 3.6.1. The figures shows an order of magnitude variation in FNMR across country of birth; these effects are likely due quality variations, then demographics like age and race. The error rates in some cases are zero, and in others the DET is flat so the error rates at the two thresholds are identical. The lines span 1% and 99% of boostrap replicated FNMR estimates.

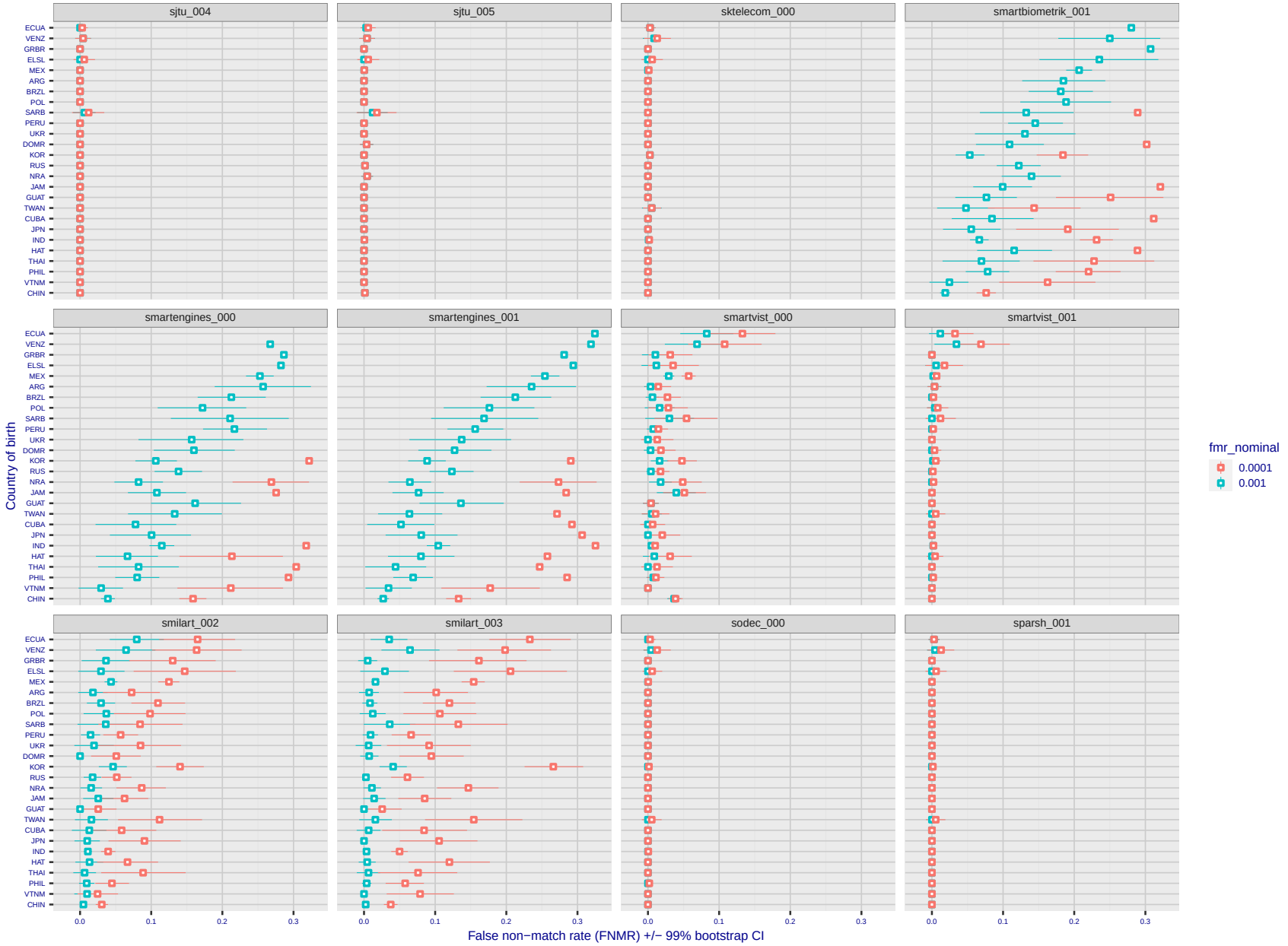

Figure 321: For the visa images, the dots show FNMR by country of birth for two globally set operating thresholds corresponding to FMR = $\{0.001, 0.0001\}$ computed over all on the order of 10^{10} impostor scores. The FMR in each bin will vary also - see subsequent impostor heatmaps in sec. 3.6.1. The figures shows an order of magnitude variation in FNMR across country of birth; these effects are likely due quality variations, then demographics like age and race. The error rates in some cases are zero, and in others the DET is flat so the error rates at the two thresholds are identical. The lines span 1% and 99% of boostrap replicated FNMR estimates.

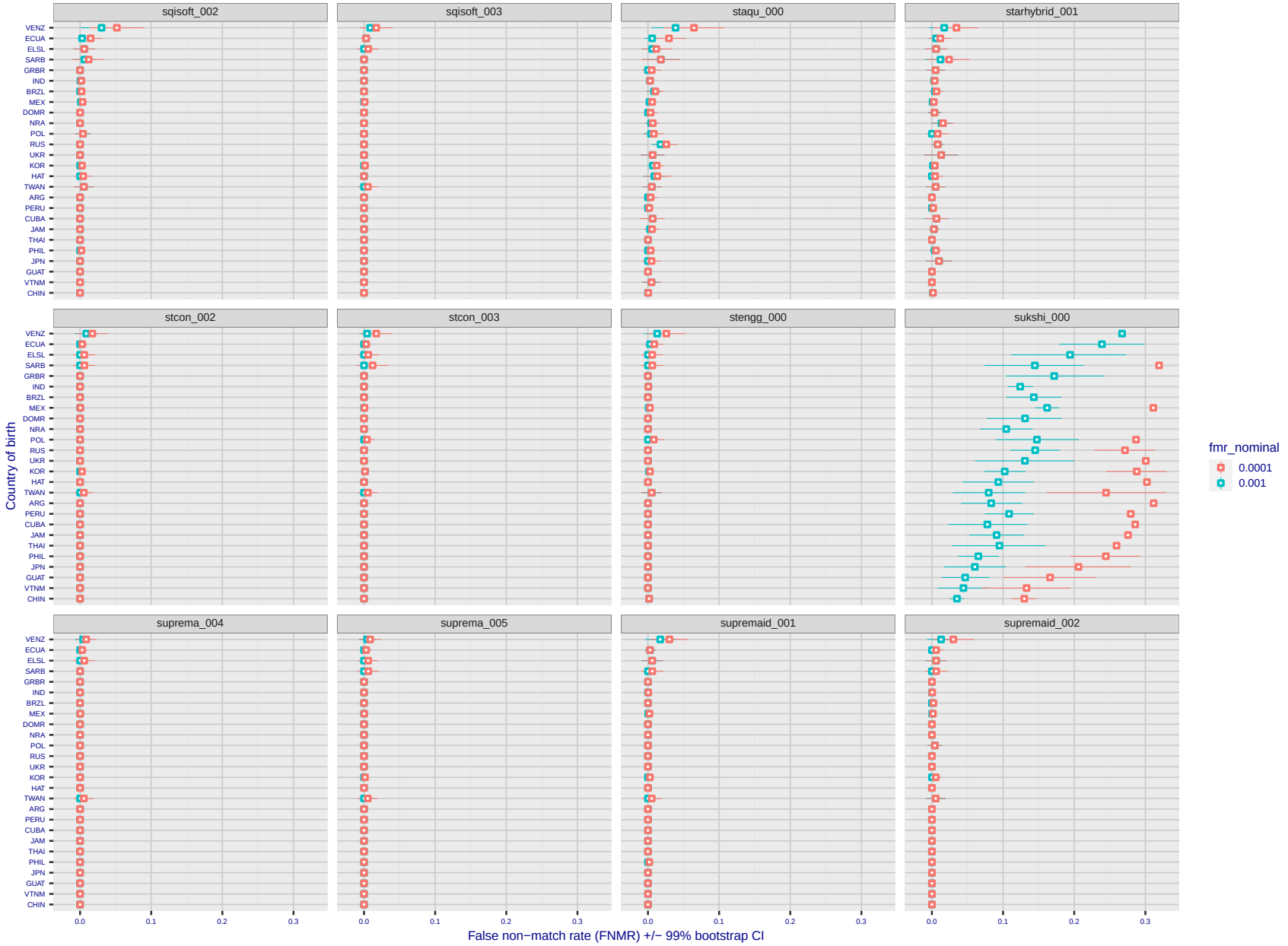

Figure 322: For the visa images, the dots show FNMR by country of birth for two globally set operating thresholds corresponding to FMR = $\{0.001, 0.0001\}$ computed over all on the order of 10^{10} impostor scores. The FMR in each bin will vary also - see subsequent impostor heatmaps in sec. 3.6.1. The figures shows an order of magnitude variation in FNMR across country of birth; these effects are likely due quality variations, then demographics like age and race. The error rates in some cases are zero, and in others the DET is flat so the error rates at the two thresholds are identical. The lines span 1% and 99% of boostrap replicated FNMR estimates.

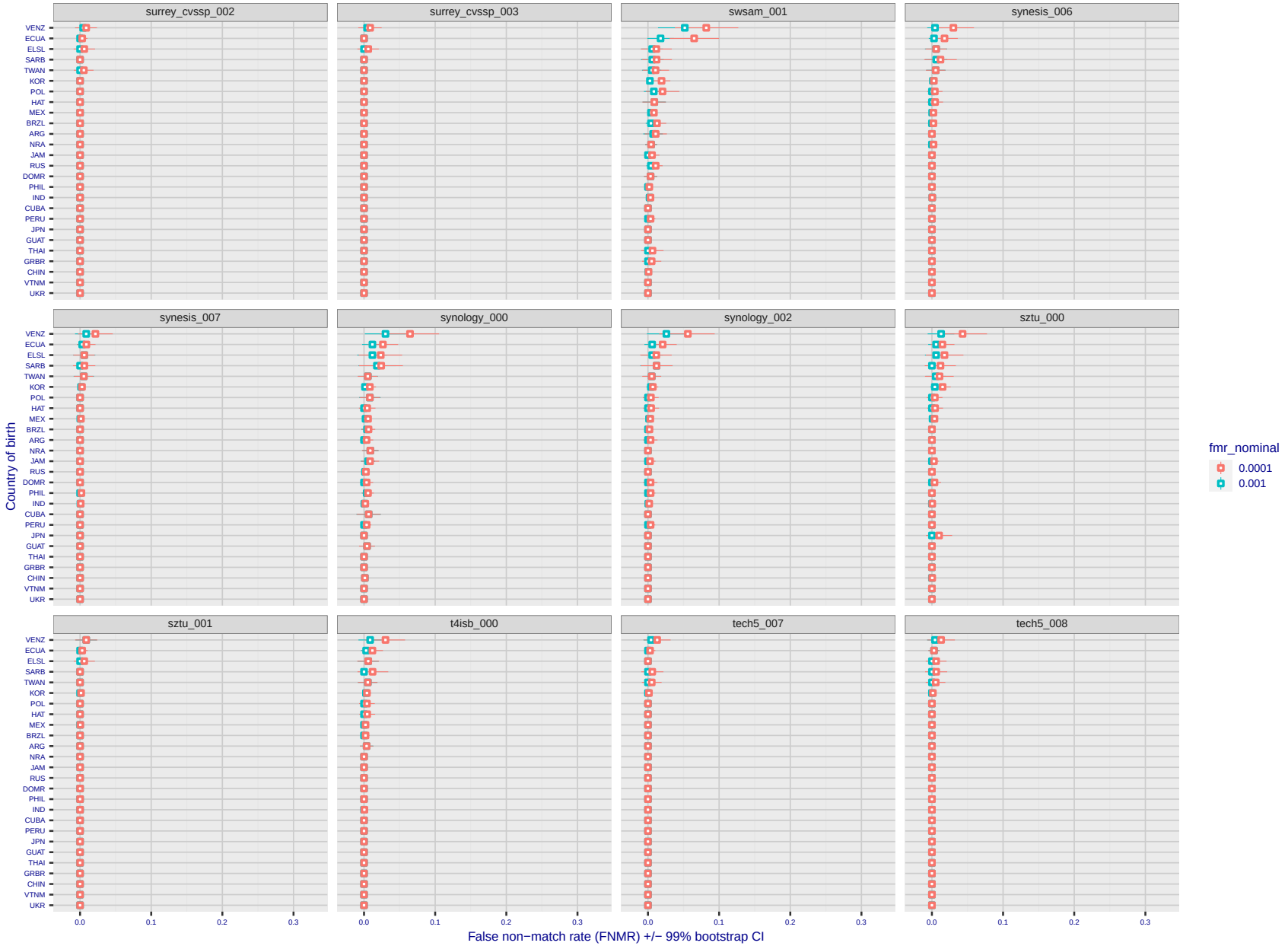

Figure 323: For the visa images, the dots show FNMR by country of birth for two globally set operating thresholds corresponding to FMR = $\{0.001, 0.0001\}$ computed over all on the order of 10^{10} impostor scores. The FMR in each bin will vary also - see subsequent impostor heatmaps in sec. 3.6.1. The figures shows an order of magnitude variation in FNMR across country of birth; these effects are likely due quality variations, then demographics like age and race. The error rates in some cases are zero, and in others the DET is flat so the error rates at the two thresholds are identical. The lines span 1% and 99% of boostrap replicated FNMR estimates.

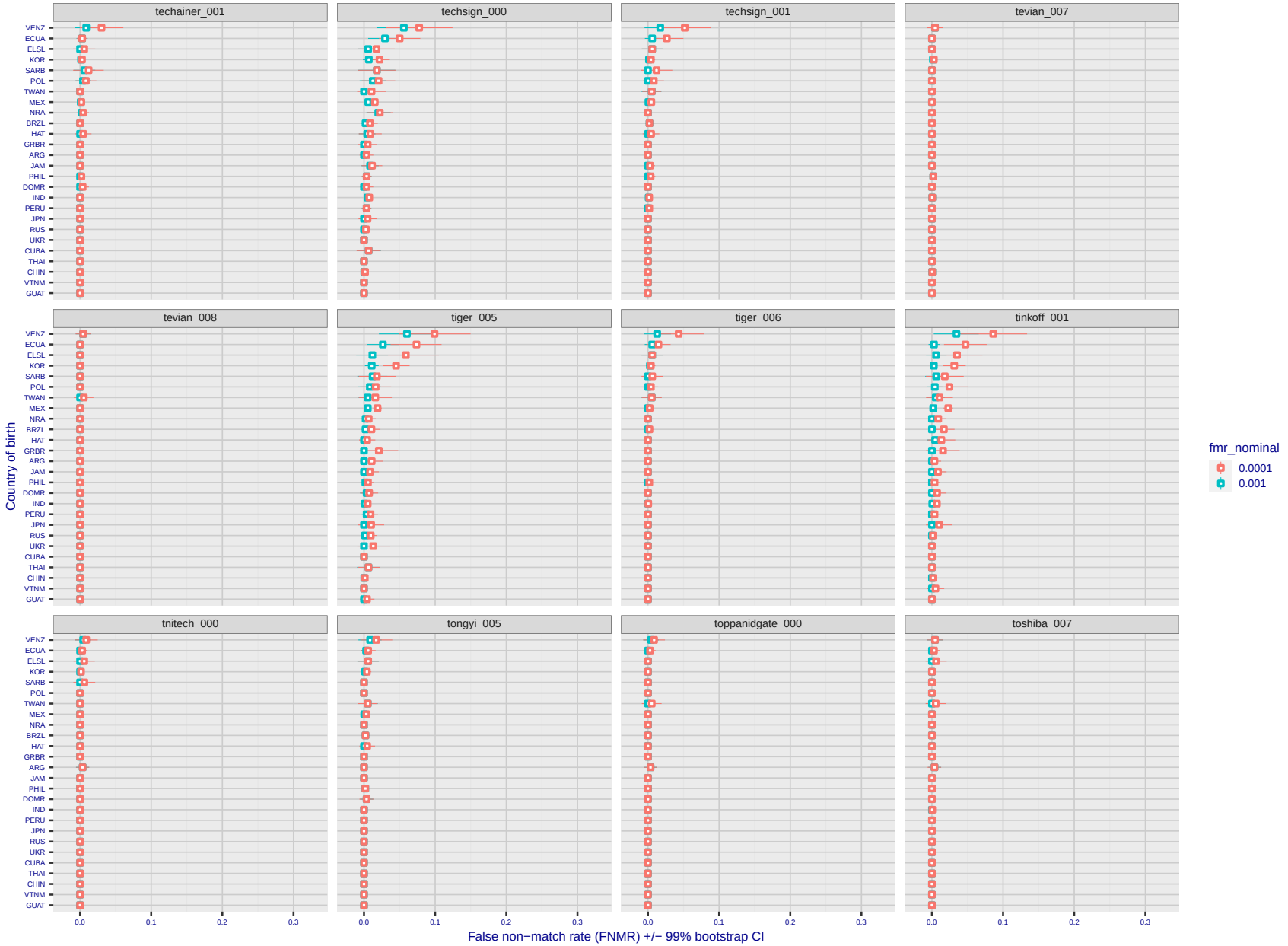

Figure 324: For the visa images, the dots show FNMR by country of birth for two globally set operating thresholds corresponding to FMR = $\{0.001, 0.0001\}$ computed over all on the order of 10^{10} impostor scores. The FMR in each bin will vary also - see subsequent impostor heatmaps in sec. 3.6.1. The figures shows an order of magnitude variation in FNMR across country of birth; these effects are likely due quality variations, then demographics like age and race. The error rates in some cases are zero, and in others the DET is flat so the error rates at the two thresholds are identical. The lines span 1% and 99% of boostrap replicated FNMR estimates.

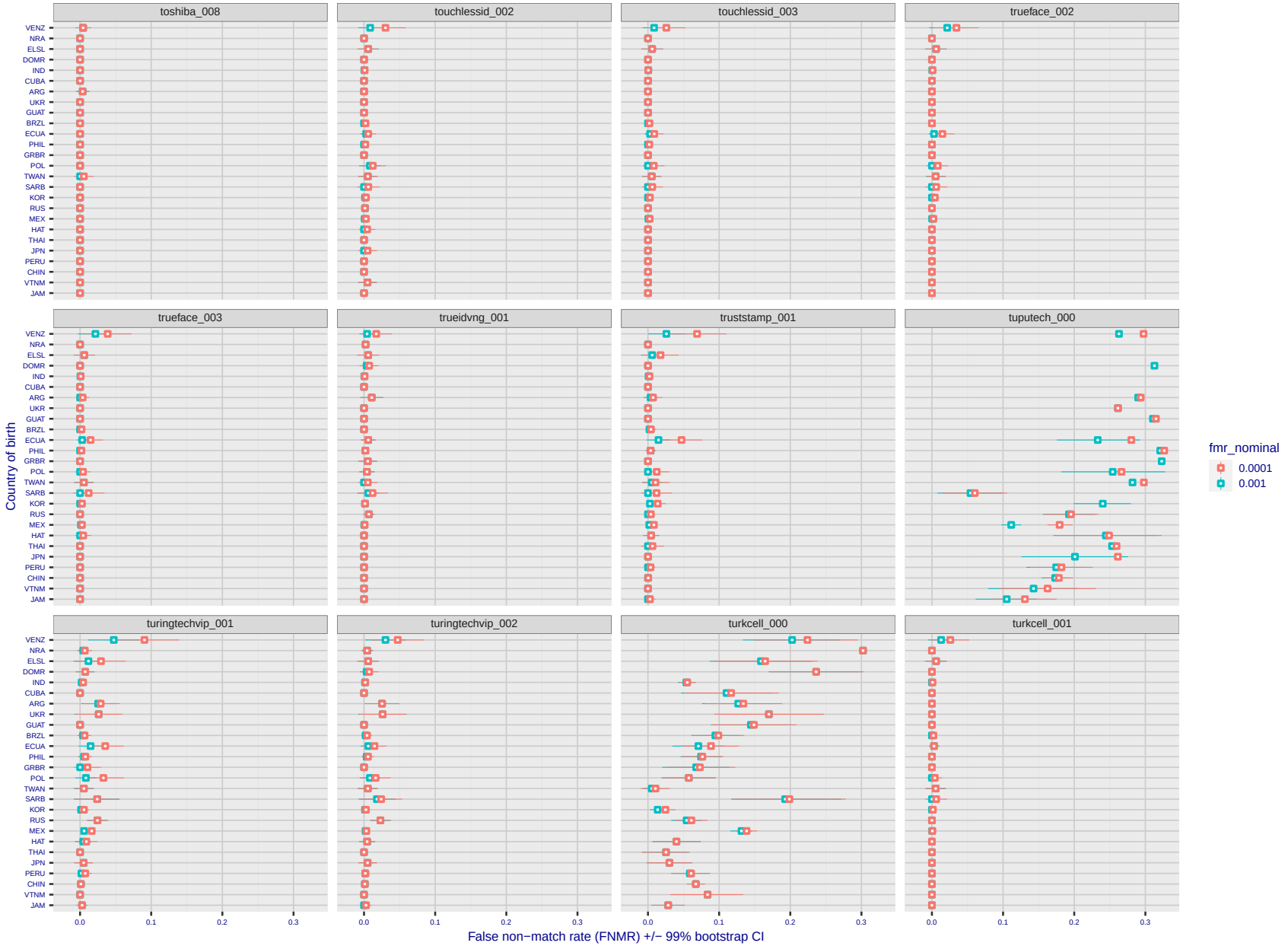

Figure 325: For the visa images, the dots show FNMR by country of birth for two globally set operating thresholds corresponding to FMR = $\{0.001, 0.0001\}$ computed over all on the order of 10^{10} impostor scores. The FMR in each bin will vary also - see subsequent impostor heatmaps in sec. 3.6.1. The figures shows an order of magnitude variation in FNMR across country of birth; these effects are likely due quality variations, then demographics like age and race. The error rates in some cases are zero, and in others the DET is flat so the error rates at the two thresholds are identical. The lines span 1% and 99% of boostrap replicated FNMR estimates.

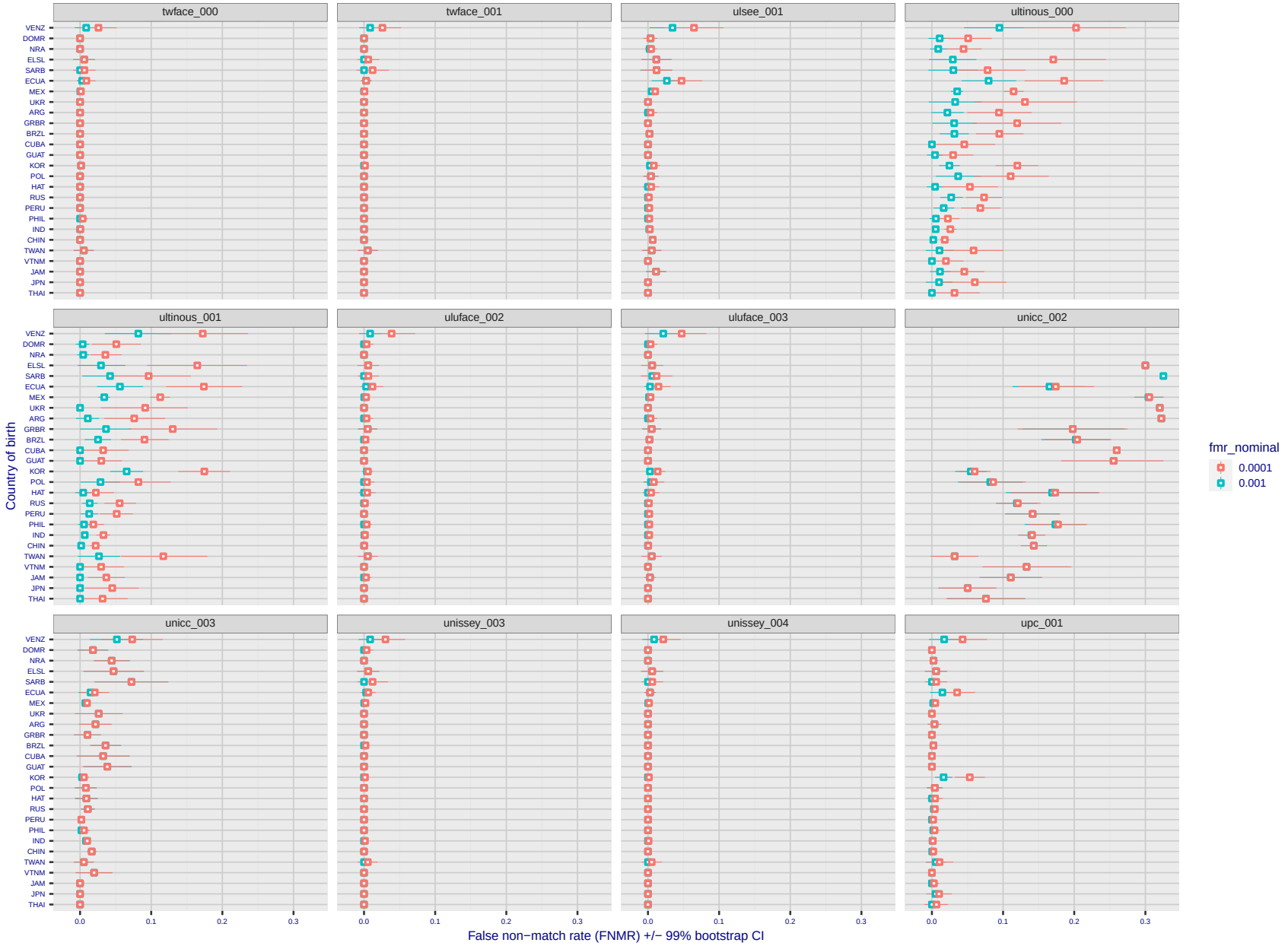

Figure 326: For the visa images, the dots show FNMR by country of birth for two globally set operating thresholds corresponding to FMR = $\{0.001, 0.0001\}$ computed over all on the order of 10^{10} impostor scores. The FMR in each bin will vary also - see subsequent impostor heatmaps in sec. 3.6.1. The figures shows an order of magnitude variation in FNMR across country of birth; these effects are likely due quality variations, then demographics like age and race. The error rates in some cases are zero, and in others the DET is flat so the error rates at the two thresholds are identical. The lines span 1% and 99% of boostrap replicated FNMR estimates.

Figure 327: For the visa images, the dots show FNMR by country of birth for two globally set operating thresholds corresponding to FMR = $\{0.001, 0.0001\}$ computed over all on the order of 10^{10} impostor scores. The FMR in each bin will vary also - see subsequent impostor heatmaps in sec. 3.6.1. The figures shows an order of magnitude variation in FNMR across country of birth; these effects are likely due quality variations, then demographics like age and race. The error rates in some cases are zero, and in others the DET is flat so the error rates at the two thresholds are identical. The lines span 1% and 99% of boostrap replicated FNMR estimates.

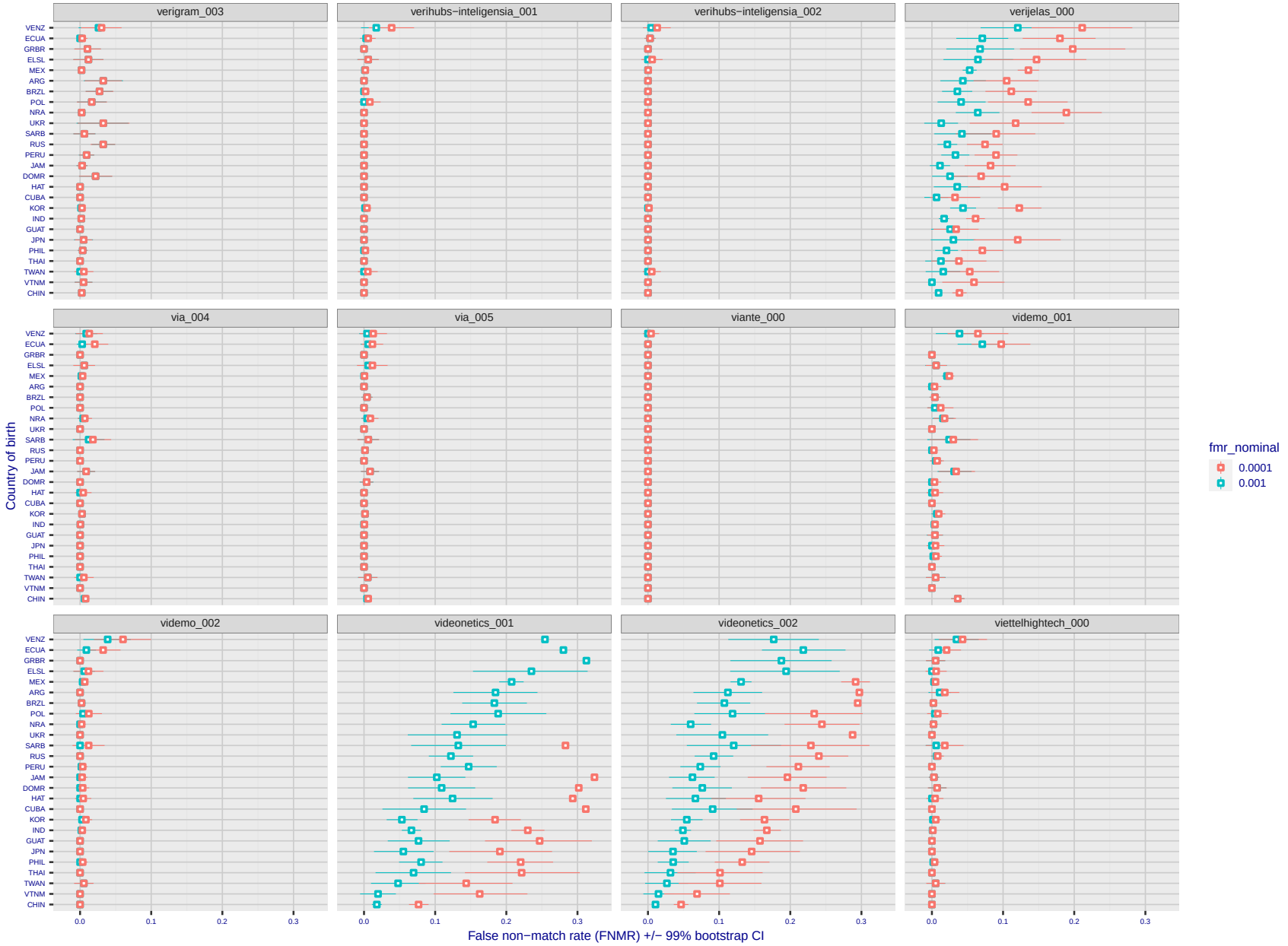

Figure 328: For the visa images, the dots show FNMR by country of birth for two globally set operating thresholds corresponding to FMR = $\{0.001, 0.0001\}$ computed over all on the order of 10^{10} impostor scores. The FMR in each bin will vary also - see subsequent impostor heatmaps in sec. 3.6.1. The figures shows an order of magnitude variation in FNMR across country of birth; these effects are likely due quality variations, then demographics like age and race. The error rates in some cases are zero, and in others the DET is flat so the error rates at the two thresholds are identical. The lines span 1% and 99% of boostrap replicated FNMR estimates.

Figure 329: For the visa images, the dots show FNMR by country of birth for two globally set operating thresholds corresponding to FMR = $\{0.001, 0.0001\}$ computed over all on the order of 10^{10} impostor scores. The FMR in each bin will vary also - see subsequent impostor heatmaps in sec. 3.6.1. The figures shows an order of magnitude variation in FNMR across country of birth; these effects are likely due quality variations, then demographics like age and race. The error rates in some cases are zero, and in others the DET is flat so the error rates at the two thresholds are identical. The lines span 1% and 99% of boostrap replicated FNMR estimates.

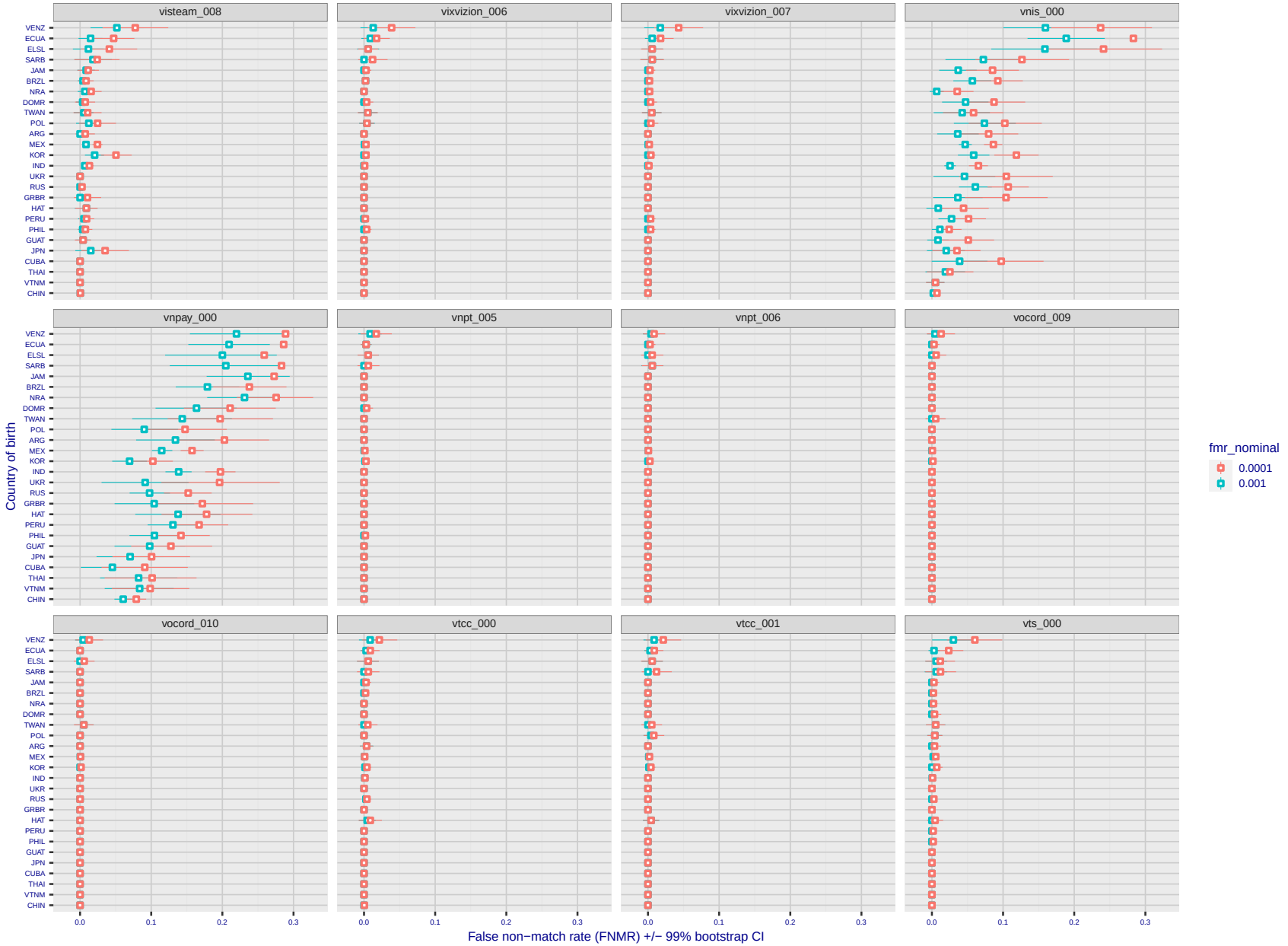

Figure 330: For the visa images, the dots show FNMR by country of birth for two globally set operating thresholds corresponding to FMR = $\{0.001, 0.0001\}$ computed over all on the order of 10^{10} impostor scores. The FMR in each bin will vary also - see subsequent impostor heatmaps in sec. 3.6.1. The figures shows an order of magnitude variation in FNMR across country of birth; these effects are likely due quality variations, then demographics like age and race. The error rates in some cases are zero, and in others the DET is flat so the error rates at the two thresholds are identical. The lines span 1% and 99% of boostrap replicated FNMR estimates.

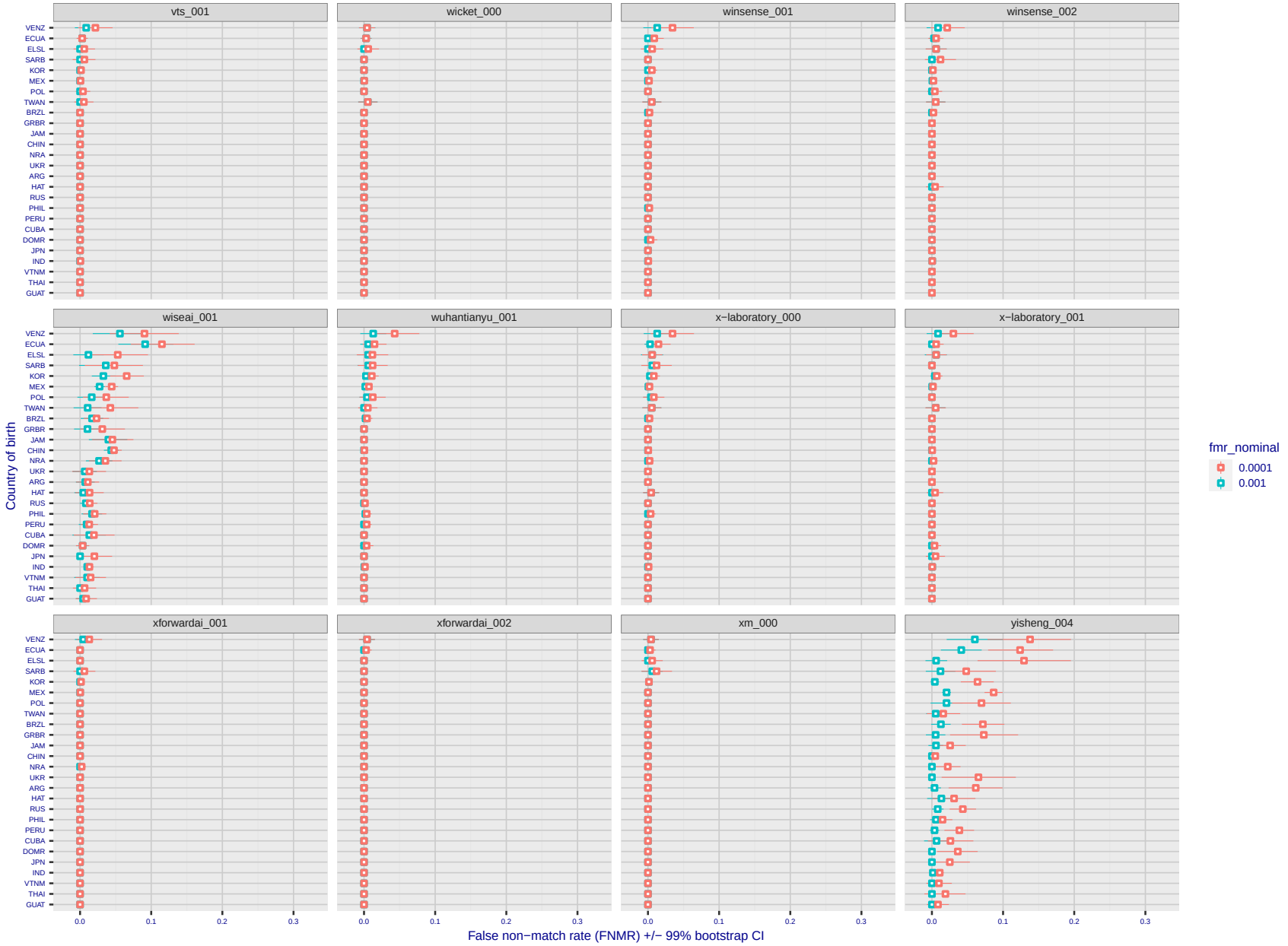

Figure 331: For the visa images, the dots show FNMR by country of birth for two globally set operating thresholds corresponding to FMR = $\{0.001, 0.0001\}$ computed over all on the order of 10^{10} impostor scores. The FMR in each bin will vary also - see subsequent impostor heatmaps in sec. 3.6.1. The figures shows an order of magnitude variation in FNMR across country of birth; these effects are likely due quality variations, then demographics like age and race. The error rates in some cases are zero, and in others the DET is flat so the error rates at the two thresholds are identical. The lines span 1% and 99% of boostrap replicated FNMR estimates.

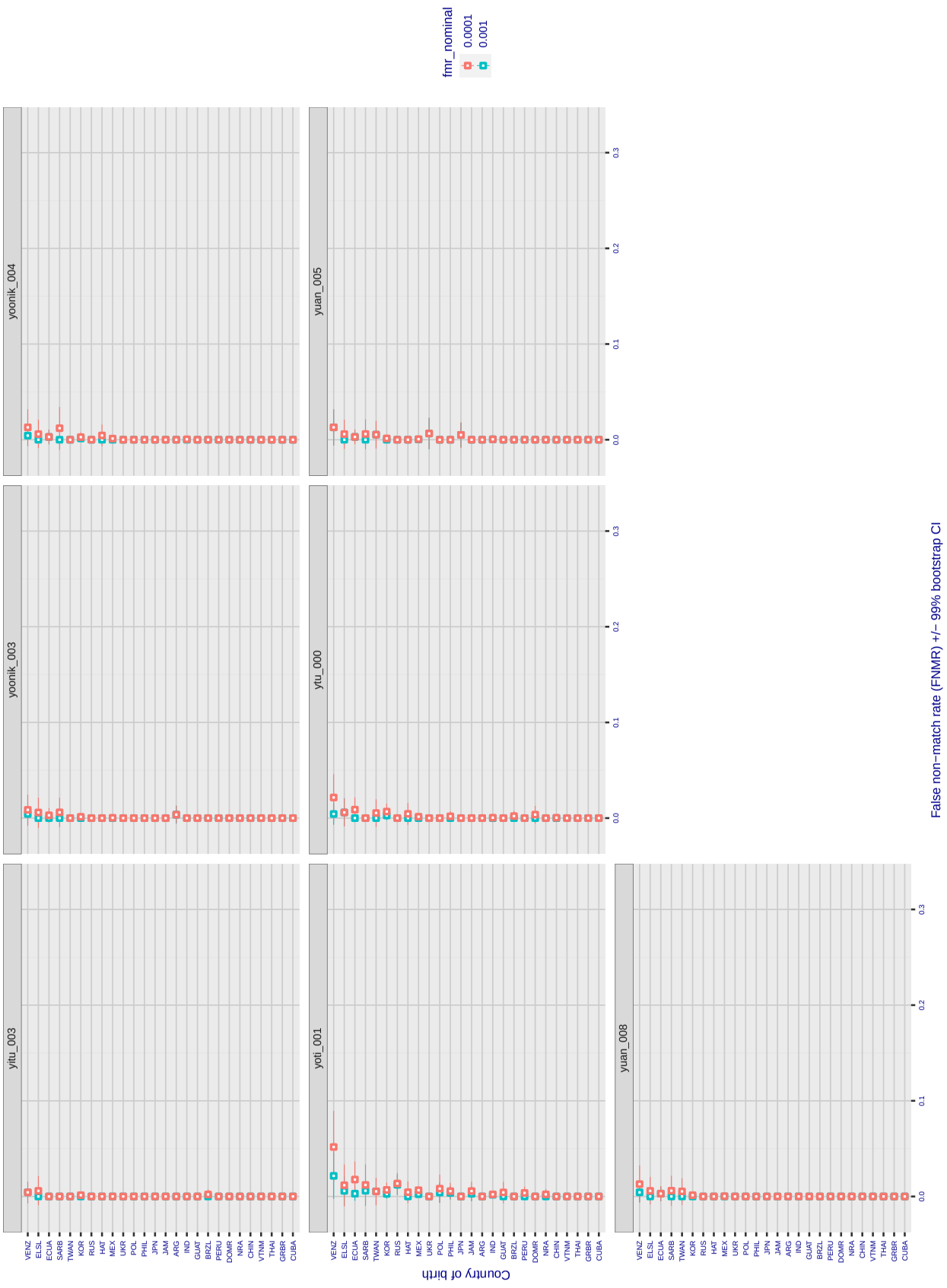

Figure 332: For the visa images, the dots show FNMR by country of birth for two globally set operating thresholds corresponding to FMR = {0.001, 0.0001} computed over all on the order of 10^{10} impostor scores. The FMR in each bin will vary also - see subsequent impostor heatmaps in sec. 3.6.1. The figures shows an order of magnitude variation in FNMR across country of birth; these effects are likely due quality variations, then demographics like age and race. The error rates in some cases are zero, and in others the DET is flat so the error rates at the two thresholds are identical. The lines span 1% and 99% of boostrap replicated FNMR estimates.

FNMR(T) "False non-match rate"
FMR(T) "False match rate"

Caveats: The results may not relate to subject-specific properties. Instead they could reflect image-specific quality differences, which could occur due to collection protocol or software processing variations.

3.5.2 Effect of ageing

Background: Faces change appearance throughout life. This change gradually reduces similarity of a new image to an earlier image. Face recognition algorithms give reduced similarity scores and more frequent false rejections.

Goal: To quantify false non-match rates (FNMR) as a function of elapsed time in an adult population.

Methods: Using the mugshot images, a threshold is set to give FMR = 0.00001 over the entire impostor set. Then FNMR is measured over 1000 bootstrap replications of the genuine scores.

Results: For the visa images, Figure 368 shows how false non-match rates for genuine users, as a function of age group.

FNMR(T) "False non-match rate"
FMR(T) "False match rate"

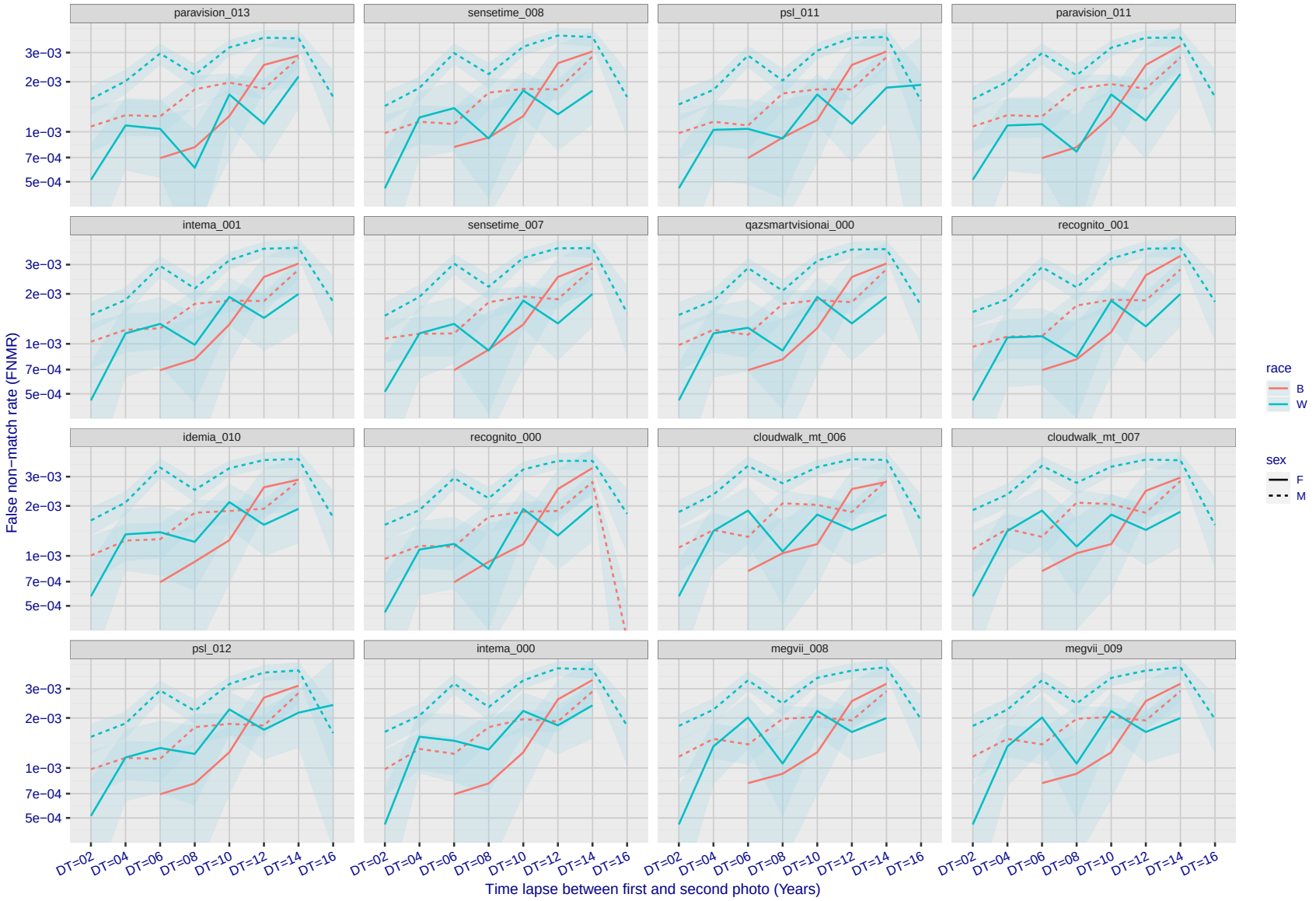

Figure 333: For the mugshot images, FNMR *as a function of elapsed time between initial enrollment and second verification images. The panels appear most accurate first, and vertical scale changes on each page. The four traces correspond to images annotated with codes for black female, black male, white female, white male. The threshold is fixed for each algorithm to give FMR = 0.00001 over all (10^8) impostor comparisons. For short time-lapses, the most accurate algorithms give very few errors (FNMR < 0.001) so that the uncertainty estimates are high.*

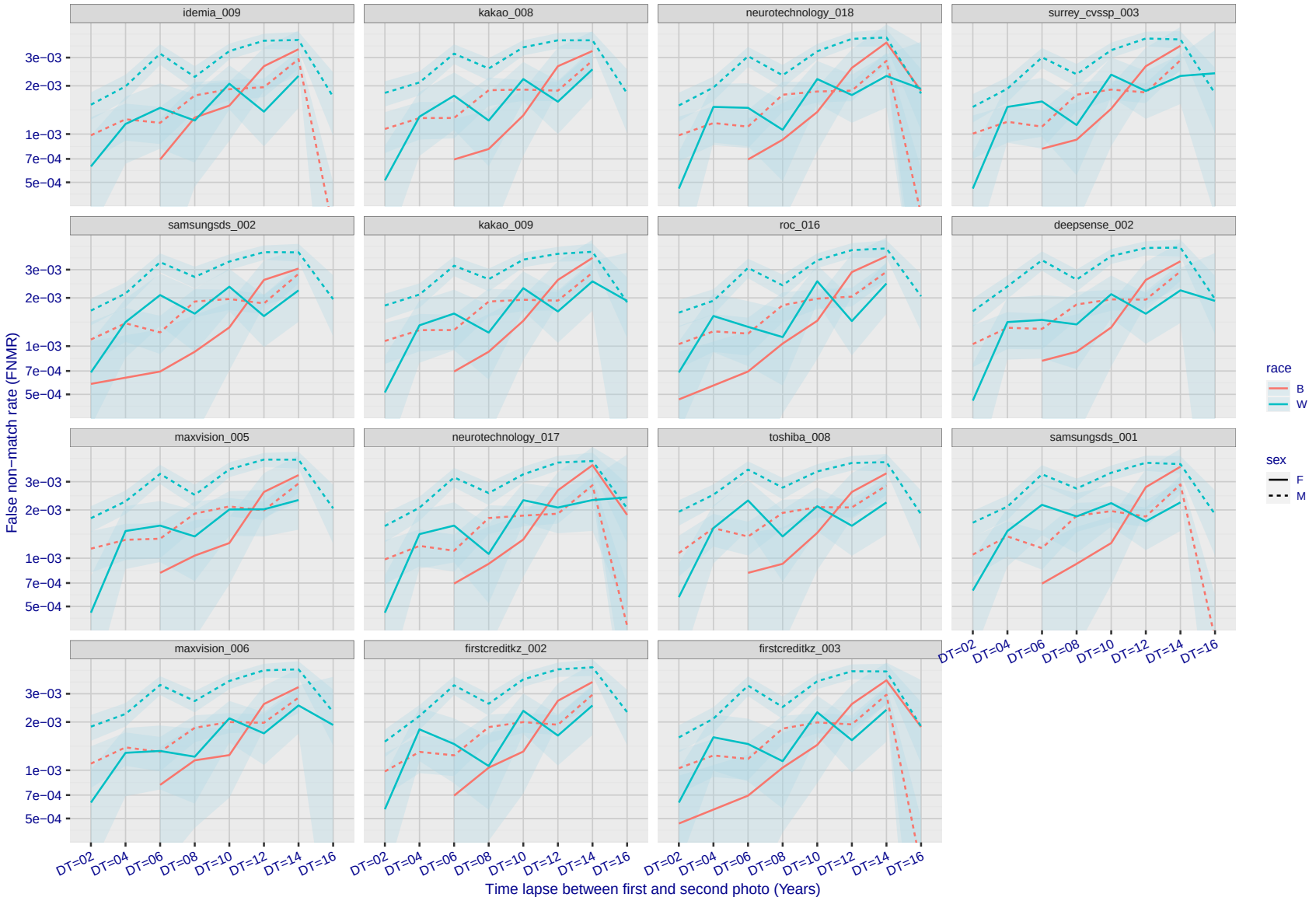

Figure 334: For the mugshot images, FNMR *as a function of elapsed time between initial enrollment and second verification images. The panels appear most accurate first, and vertical scale changes on each page. The four traces correspond to images annotated with codes for black female, black male, white female, white male. The threshold is fixed for each algorithm to give FMR = 0.00001 over all (10^8) impostor comparisons. For short time-lapses, the most accurate algorithms give very few errors (FNMR < 0.001) so that the uncertainty estimates are high.*

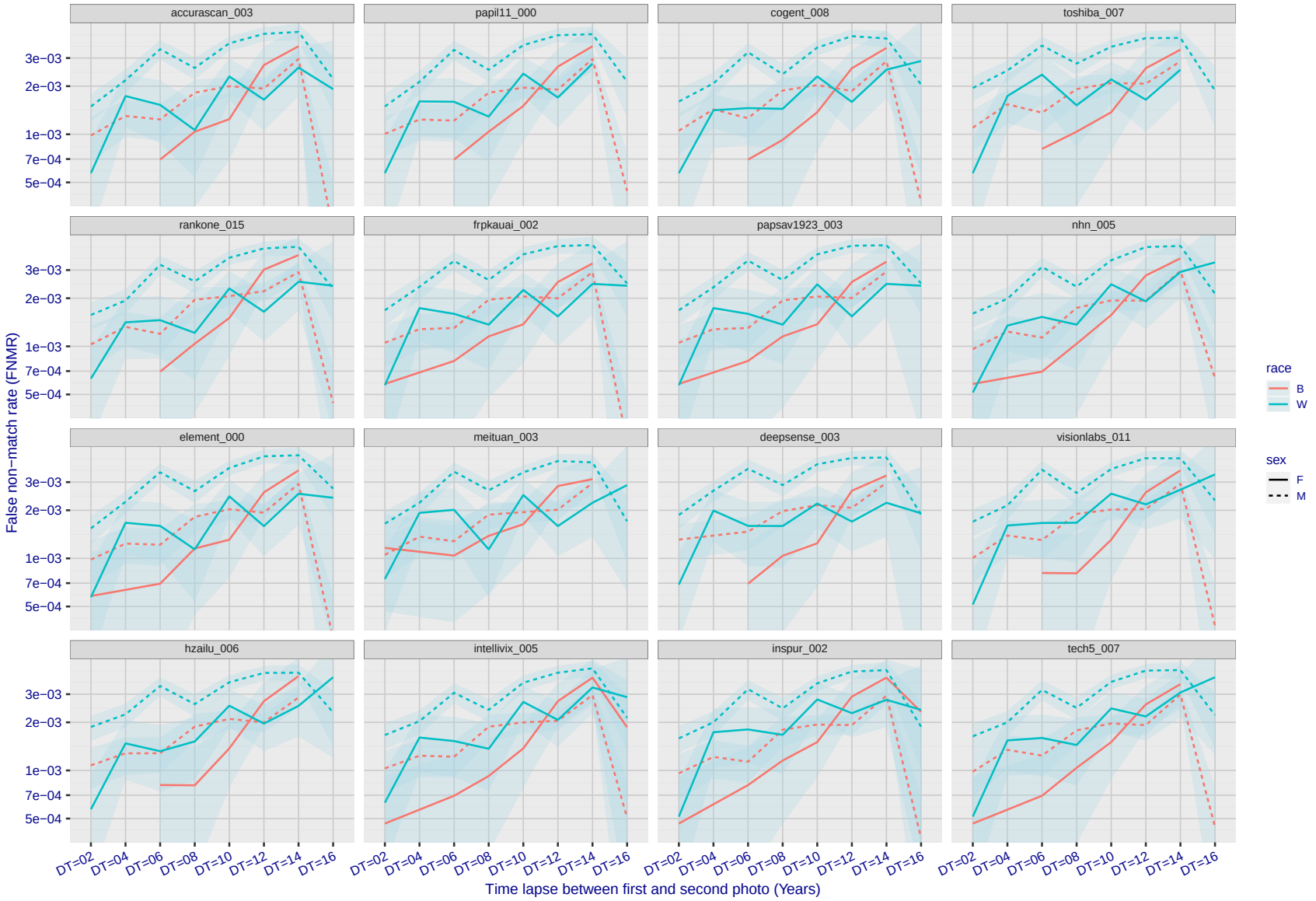

Figure 335: For the mugshot images, FNMR *as a function of elapsed time between initial enrollment and second verification images. The panels appear most accurate first, and vertical scale changes on each page. The four traces correspond to images annotated with codes for black female, black male, white female, white male. The threshold is fixed for each algorithm to give FMR = 0.00001 over all (10^8) impostor comparisons. For short time-lapses, the most accurate algorithms give very few errors (FNMR < 0.001) so that the uncertainty estimates are high.*

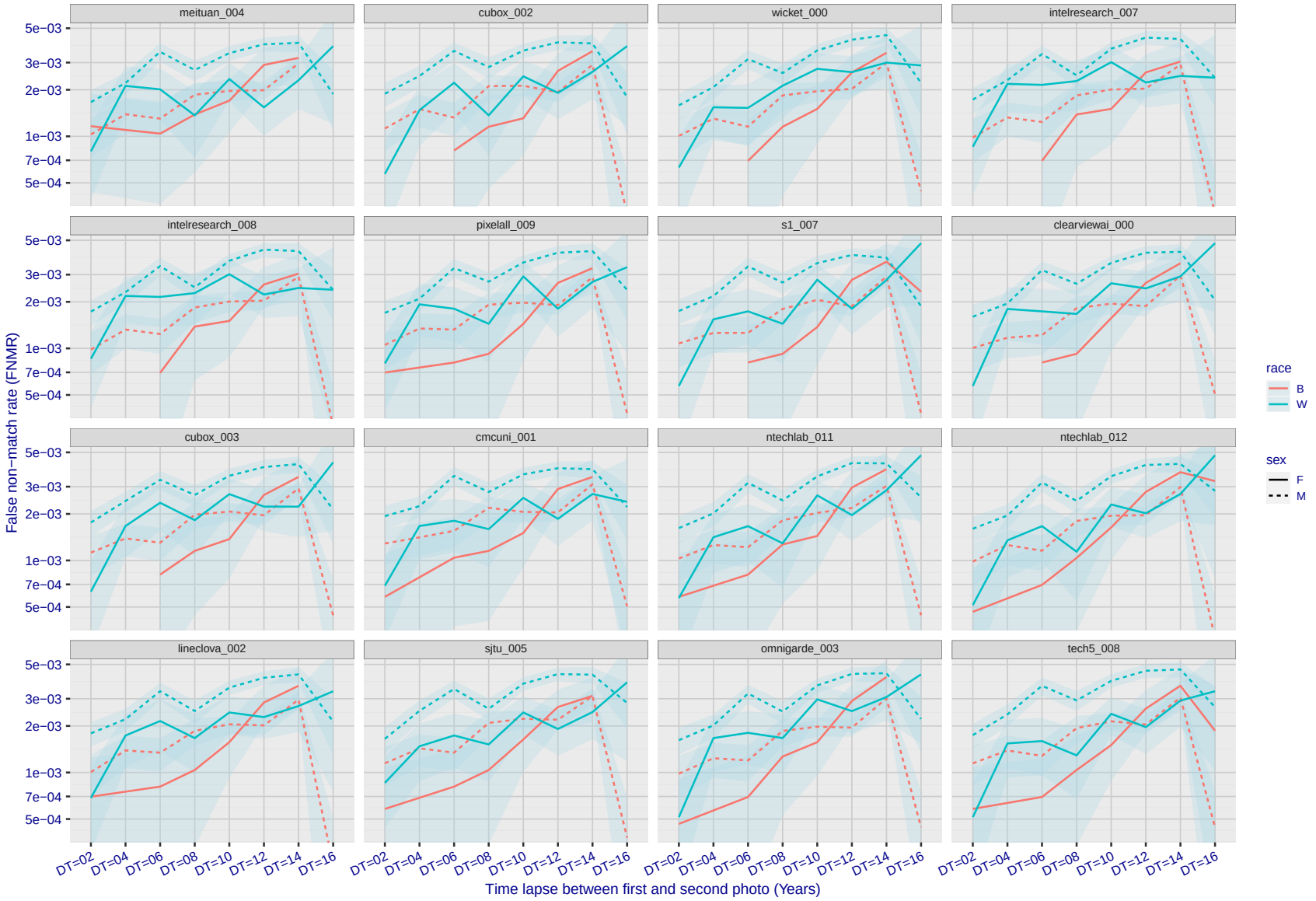

Figure 336: For the mugshot images, FNMR *as a function of elapsed time between initial enrollment and second verification images. The panels appear most accurate first, and vertical scale changes on each page. The four traces correspond to images annotated with codes for black female, black male, white female, white male. The threshold is fixed for each algorithm to give FMR = 0.00001 over all (10^8) impostor comparisons. For short time-lapses, the most accurate algorithms give very few errors (FNMR < 0.001) so that the uncertainty estimates are high.*

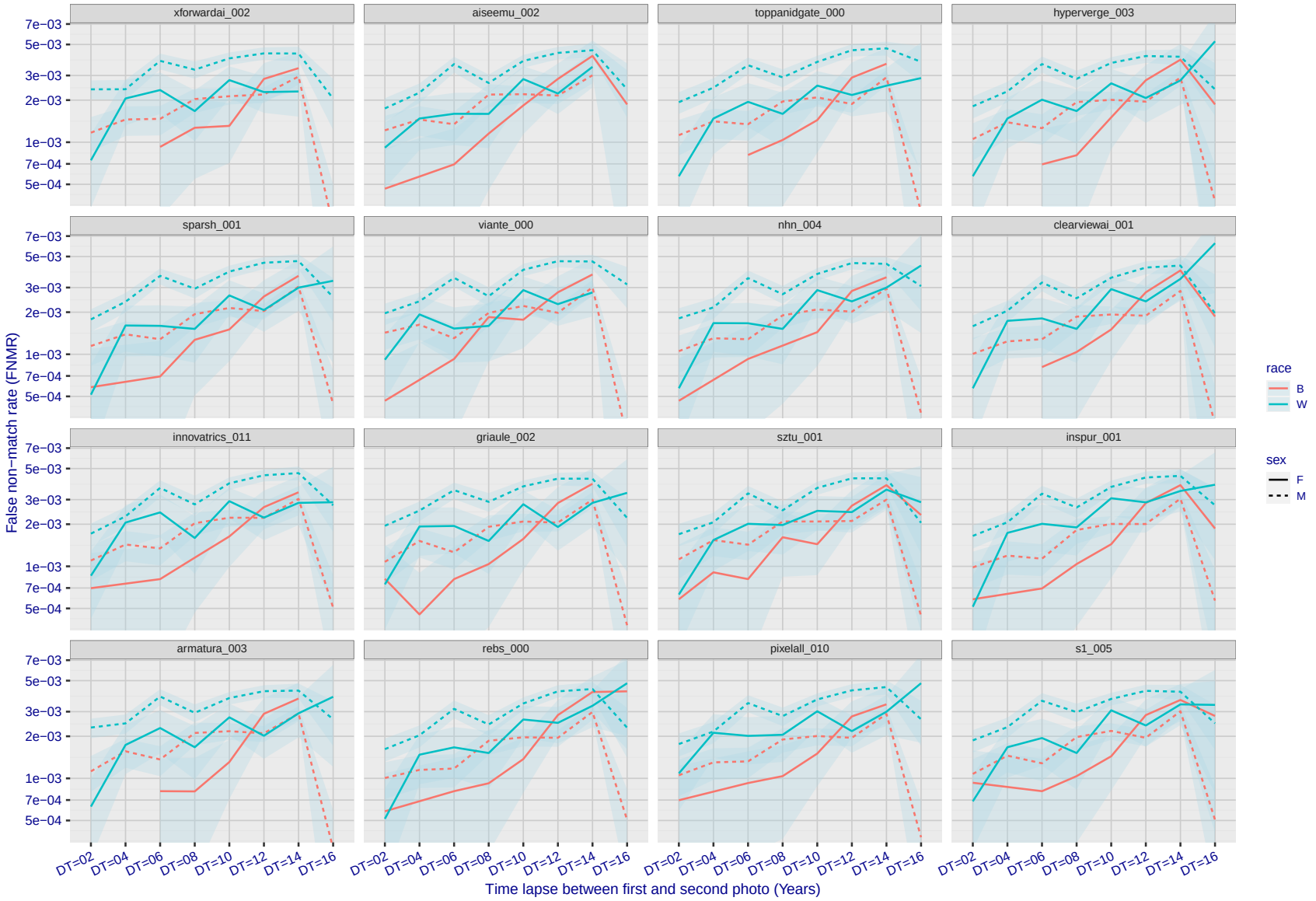

Figure 337: For the mugshot images, FNMR *as a function of elapsed time between initial enrollment and second verification images. The panels appear most accurate first, and vertical scale changes on each page. The four traces correspond to images annotated with codes for black female, black male, white female, white male. The threshold is fixed for each algorithm to give FMR = 0.00001 over all (10^8) impostor comparisons. For short time-lapses, the most accurate algorithms give very few errors (FNMR < 0.001) so that the uncertainty estimates are high.*

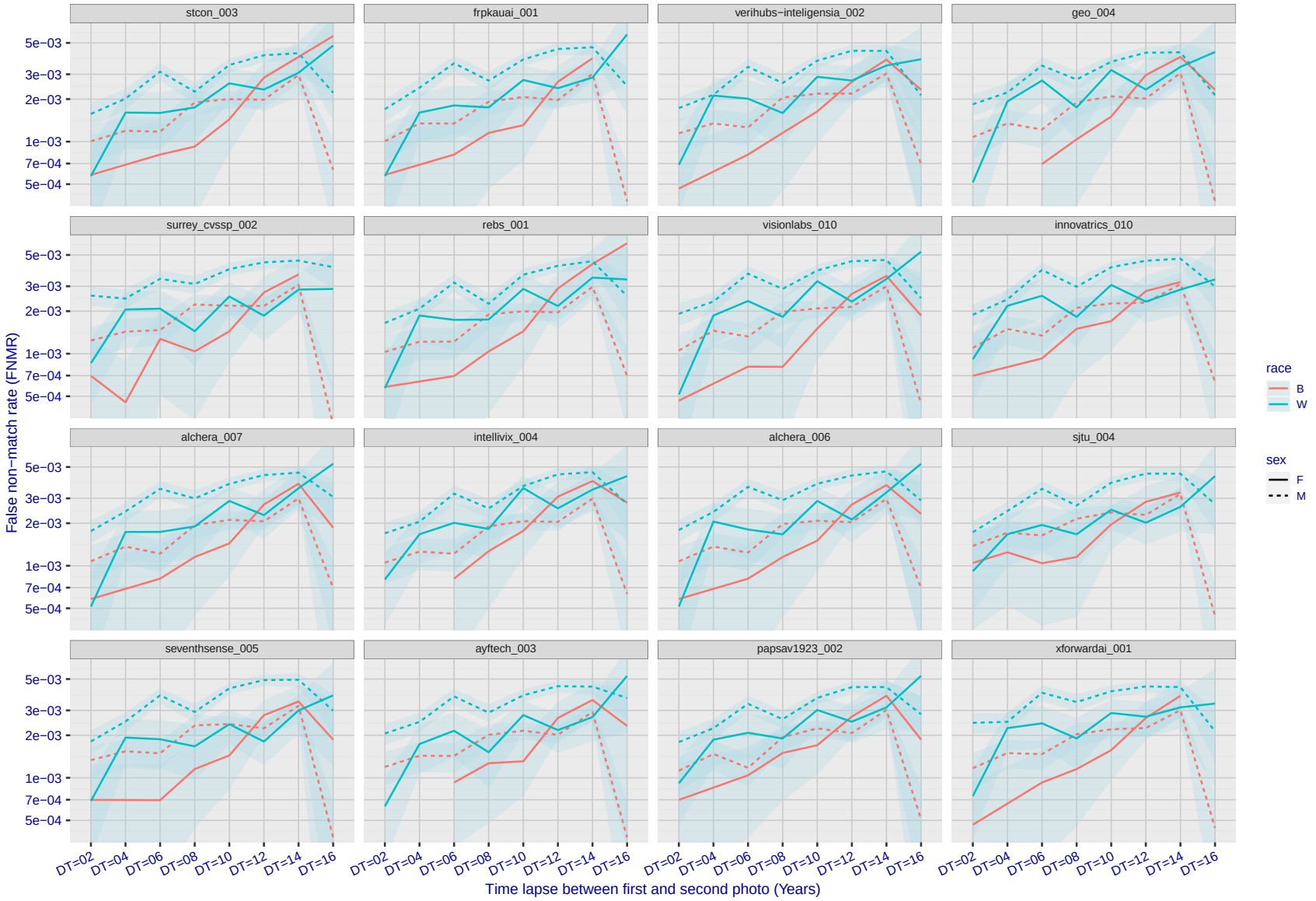

Figure 338: For the mugshot images, FNMR *as a function of elapsed time between initial enrollment and second verification images. The panels appear most accurate first, and vertical scale changes on each page. The four traces correspond to images annotated with codes for black female, black male, white female, white male. The threshold is fixed for each algorithm to give FMR = 0.00001 over all (10^8) impostor comparisons. For short time-lapses, the most accurate algorithms give very few errors (FNMR < 0.001) so that the uncertainty estimates are high.*

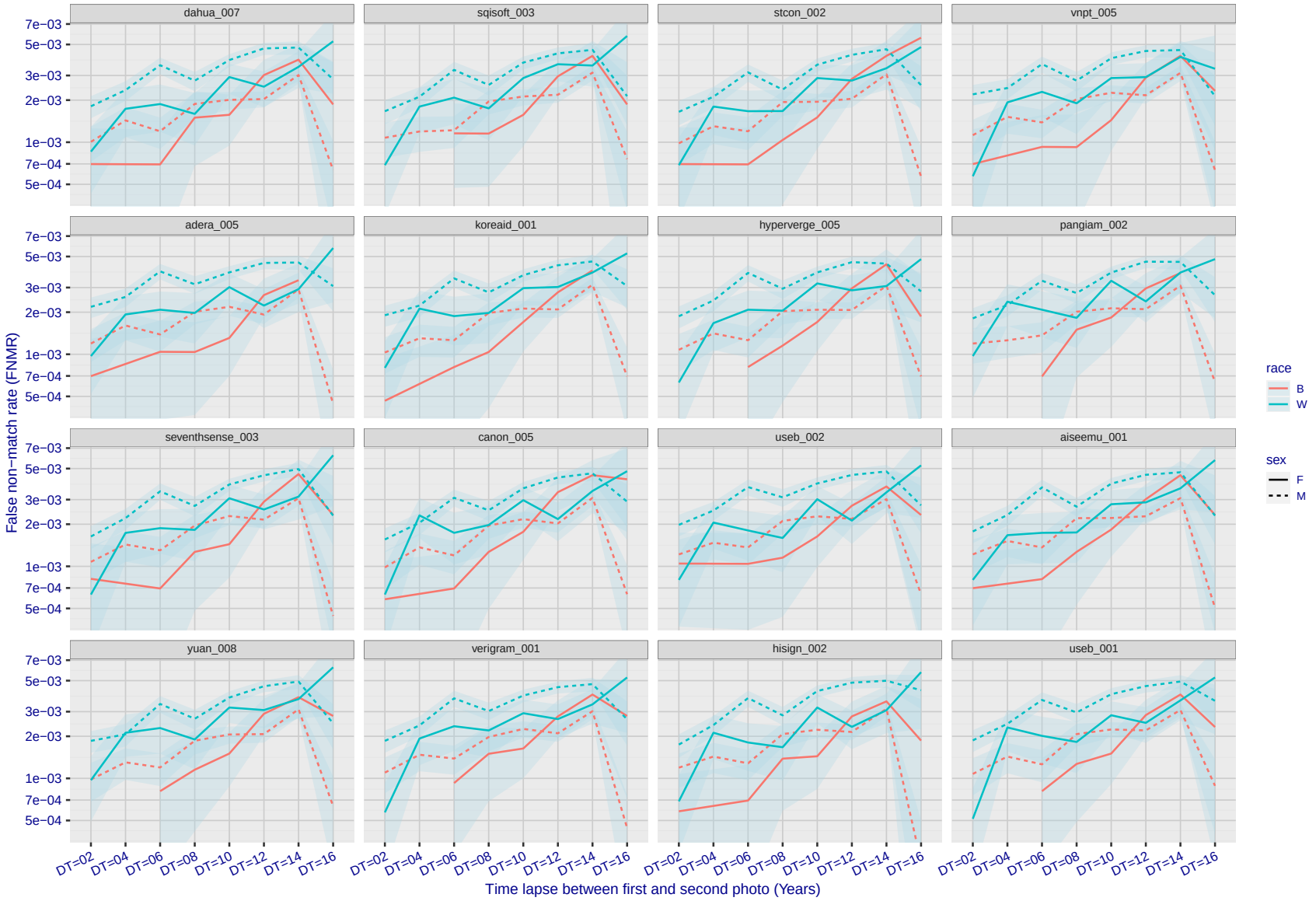

Figure 339: For the mugshot images, FNMR *as a function of elapsed time between initial enrollment and second verification images. The panels appear most accurate first, and vertical scale changes on each page. The four traces correspond to images annotated with codes for black female, black male, white female, white male. The threshold is fixed for each algorithm to give FMR = 0.00001 over all ($\bar{10}^8$) impostor comparisons. For short time-lapses, the most accurate algorithms give very few errors (FNMR < 0.001) so that the uncertainty estimates are high.*

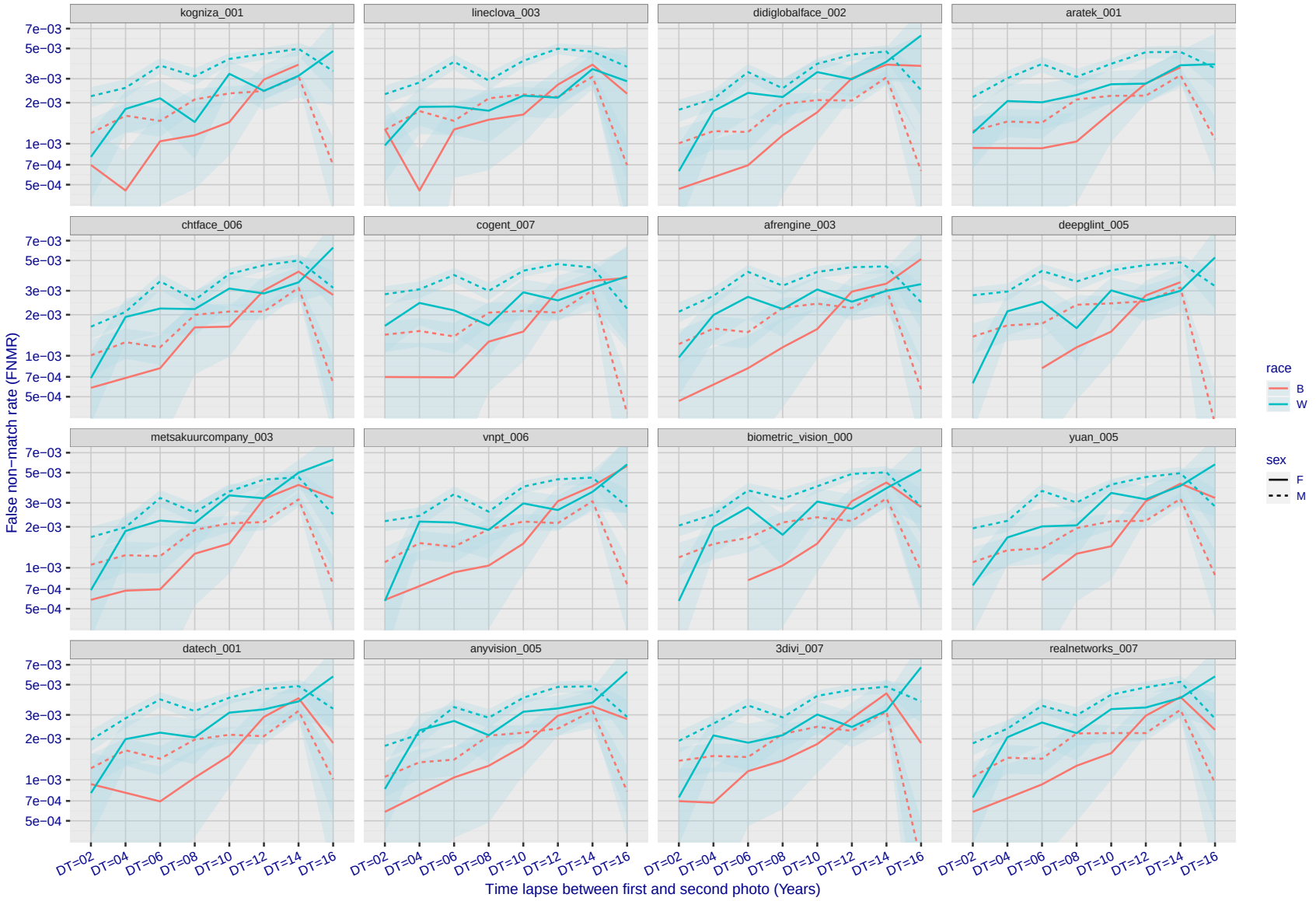

Figure 340: For the mugshot images, FNMR *as a function of elapsed time between initial enrollment and second verification images. The panels appear most accurate first, and vertical scale changes on each page. The four traces correspond to images annotated with codes for black female, black male, white female, white male. The threshold is fixed for each algorithm to give FMR = 0.00001 over all (10^8) impostor comparisons. For short time-lapses, the most accurate algorithms give very few errors (FNMR < 0.001) so that the uncertainty estimates are high.*

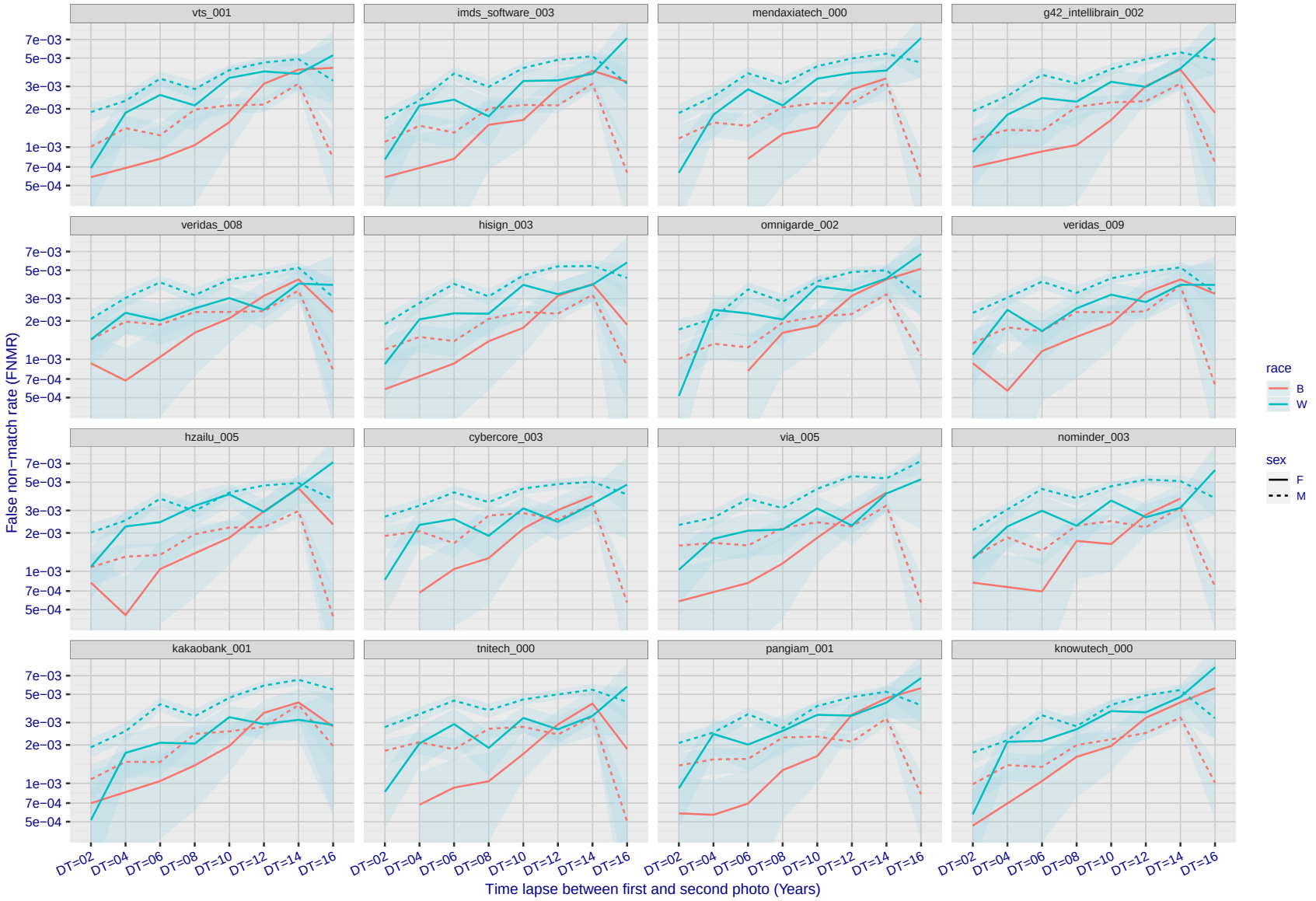

Figure 341: For the mugshot images, FNMR *as a function of elapsed time between initial enrollment and second verification images. The panels appear most accurate first, and vertical scale changes on each page. The four traces correspond to images annotated with codes for black female, black male, white female, white male. The threshold is fixed for each algorithm to give FMR = 0.00001 over all (10^8) impostor comparisons. For short time-lapses, the most accurate algorithms give very few errors (FNMR < 0.001) so that the uncertainty estimates are high.*

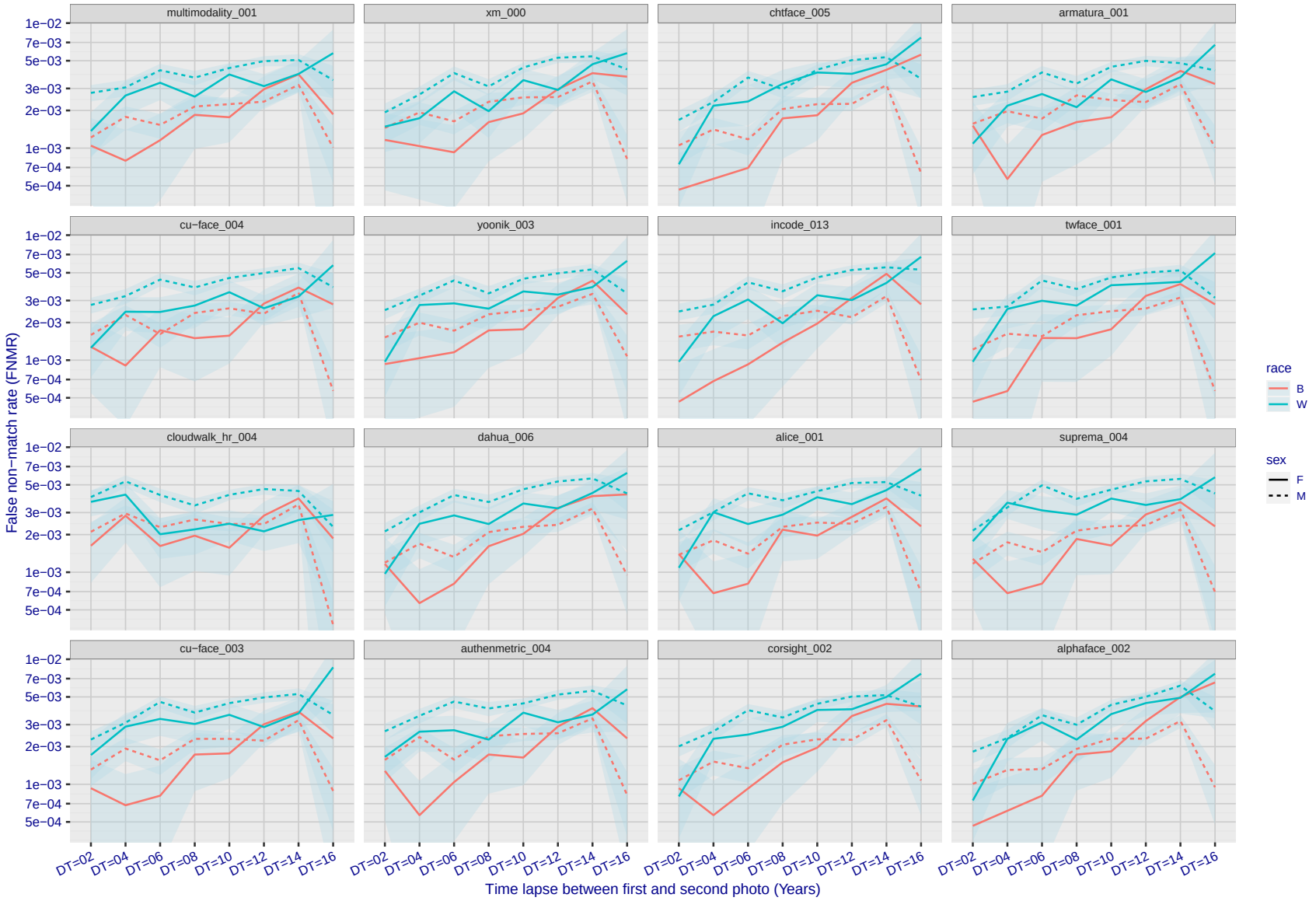

Figure 342: For the mugshot images, FNMR *as a function of elapsed time between initial enrollment and second verification images. The panels appear most accurate first, and vertical scale changes on each page. The four traces correspond to images annotated with codes for black female, black male, white female, white male. The threshold is fixed for each algorithm to give FMR = 0.00001 over all (10^8) impostor comparisons. For short time-lapses, the most accurate algorithms give very few errors (FNMR < 0.001) so that the uncertainty estimates are high.*

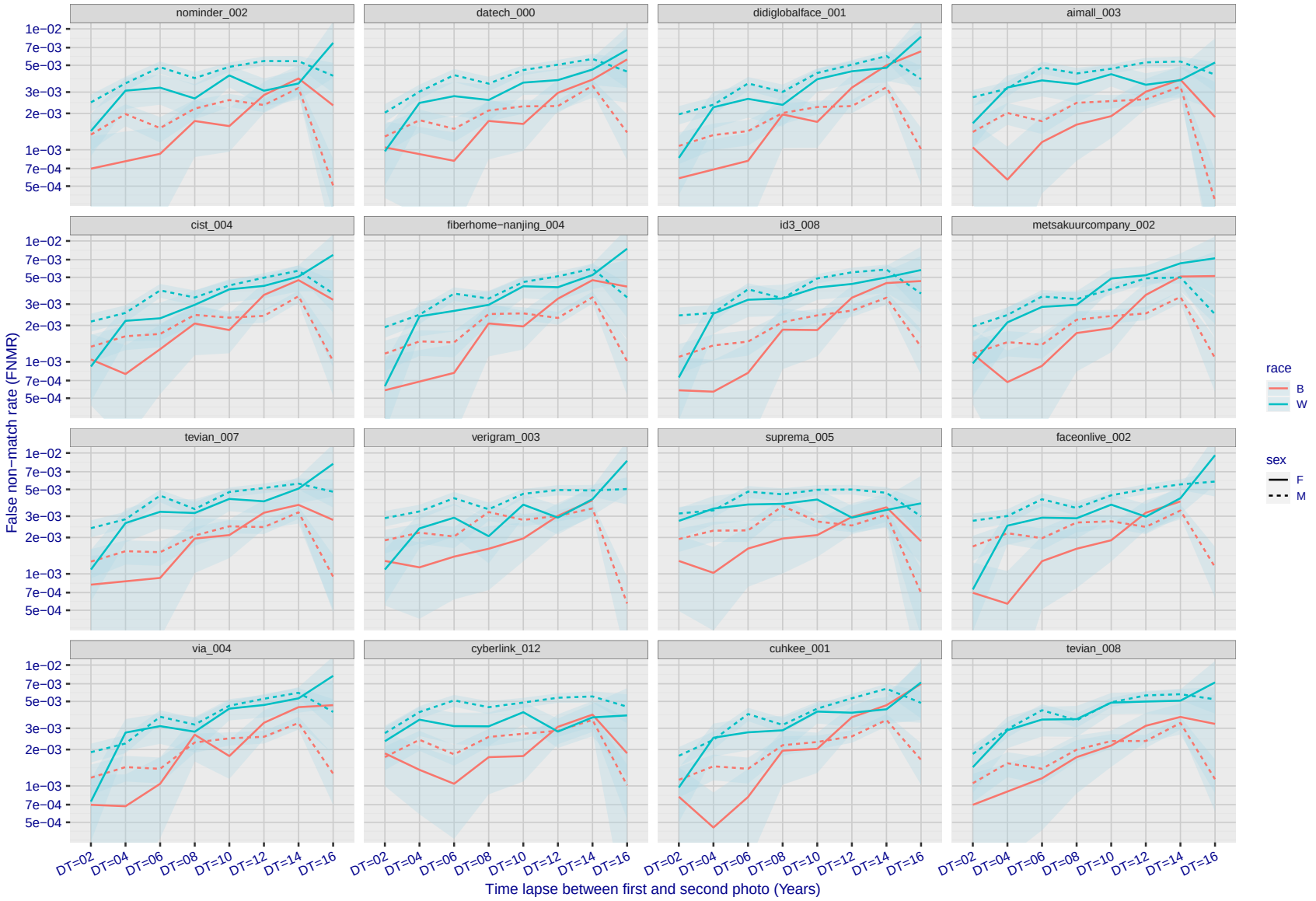

Figure 343: For the mugshot images, FNMR *as a function of elapsed time between initial enrollment and second verification images. The panels appear most accurate first, and vertical scale changes on each page. The four traces correspond to images annotated with codes for black female, black male, white female, white male. The threshold is fixed for each algorithm to give FMR = 0.00001 over all (10^8) impostor comparisons. For short time-lapses, the most accurate algorithms give very few errors (FNMR < 0.001) so that the uncertainty estimates are high.*

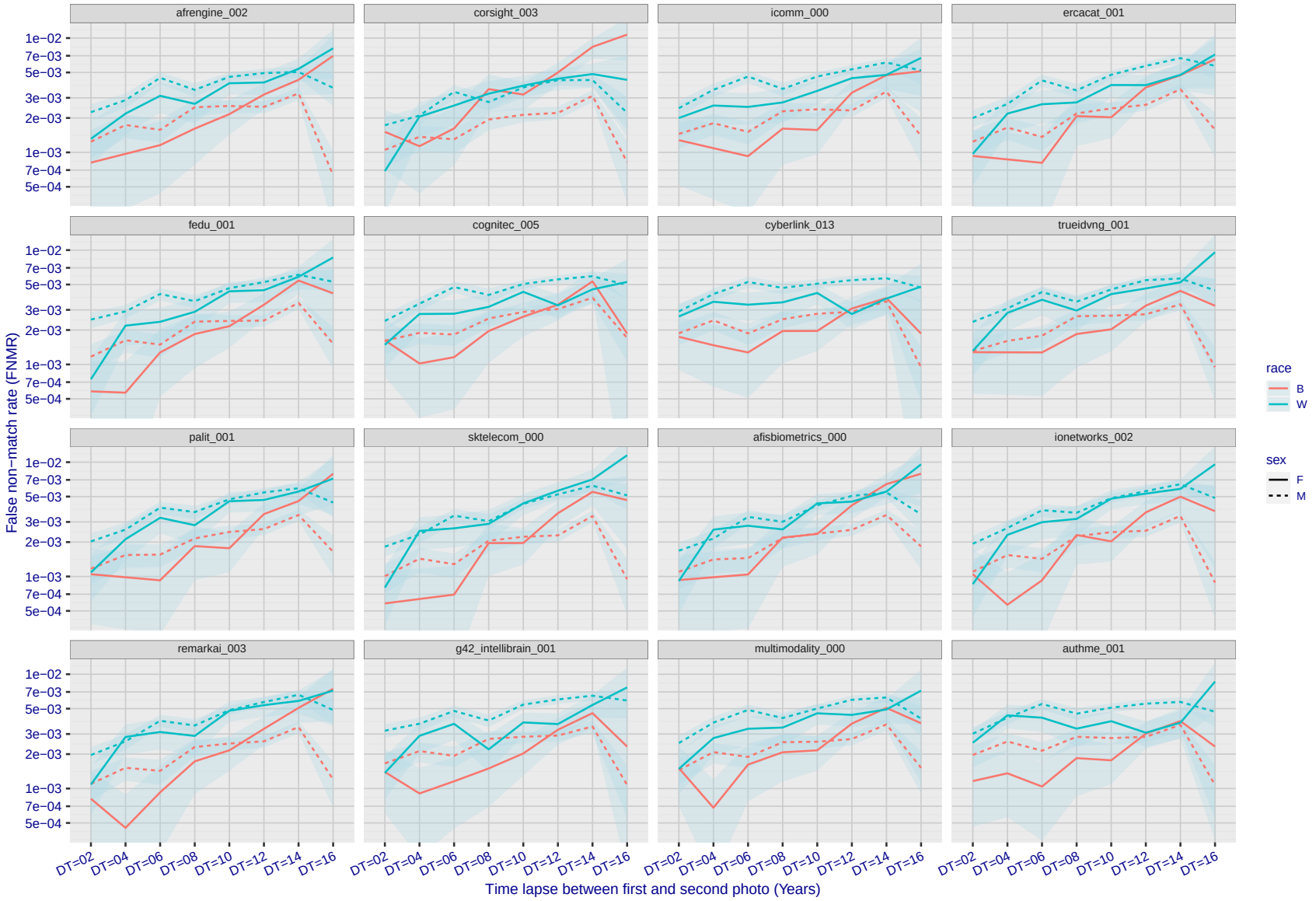

Figure 344: For the mugshot images, FNMR *as a function of elapsed time between initial enrollment and second verification images. The panels appear most accurate first, and vertical scale changes on each page. The four traces correspond to images annotated with codes for black female, black male, white female, white male. The threshold is fixed for each algorithm to give FMR = 0.00001 over all (10^8) impostor comparisons. For short time-lapses, the most accurate algorithms give very few errors (FNMR < 0.001) so that the uncertainty estimates are high.*

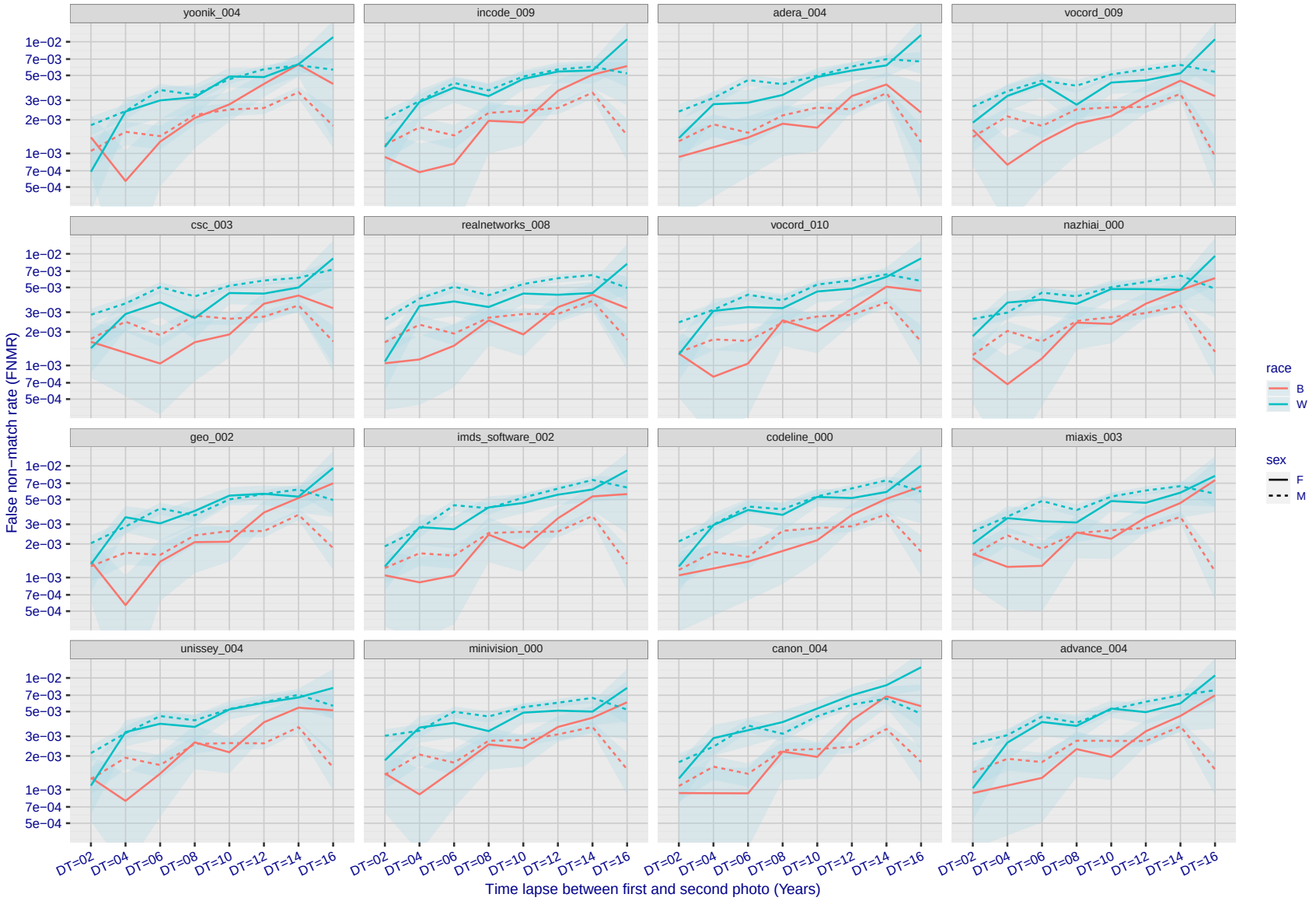

Figure 345: For the mugshot images, FNMR *as a function of elapsed time between initial enrollment and second verification images. The panels appear most accurate first, and vertical scale changes on each page. The four traces correspond to images annotated with codes for black female, black male, white female, white male. The threshold is fixed for each algorithm to give FMR = 0.00001 over all (10^8) impostor comparisons. For short time-lapses, the most accurate algorithms give very few errors (FNMR < 0.001) so that the uncertainty estimates are high.*

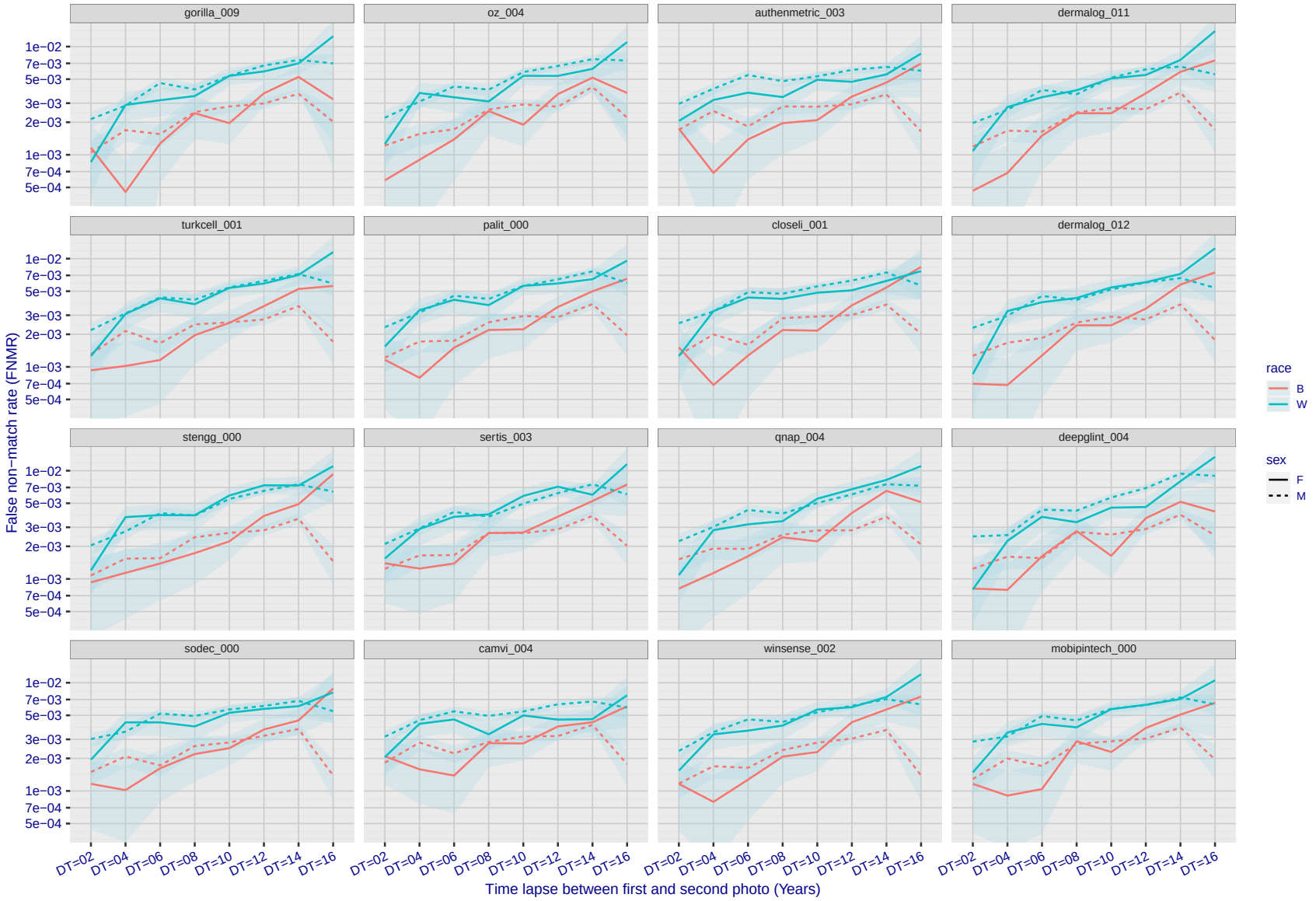

Figure 346: For the mugshot images, FNMR *as a function of elapsed time between initial enrollment and second verification images. The panels appear most accurate first, and vertical scale changes on each page. The four traces correspond to images annotated with codes for black female, black male, white female, white male. The threshold is fixed for each algorithm to give FMR = 0.00001 over all (10^8) impostor comparisons. For short time-lapses, the most accurate algorithms give very few errors (FNMR < 0.001) so that the uncertainty estimates are high.*

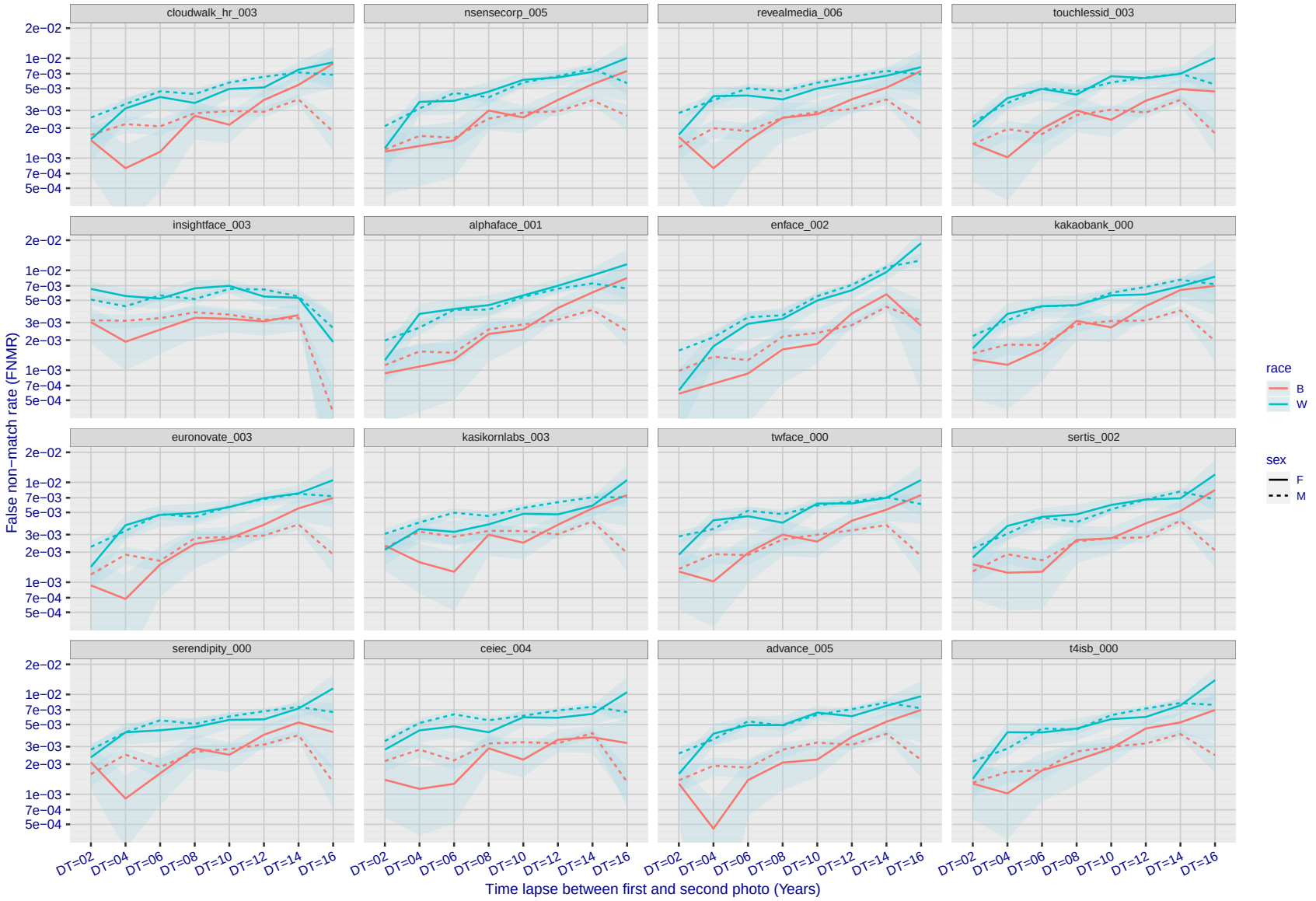

Figure 347: For the mugshot images, FNMR *as a function of elapsed time between initial enrollment and second verification images. The panels appear most accurate first, and vertical scale changes on each page. The four traces correspond to images annotated with codes for black female, black male, white female, white male. The threshold is fixed for each algorithm to give FMR = 0.00001 over all ($\tilde{10}^8$) impostor comparisons. For short time-lapses, the most accurate algorithms give very few errors (FNMR < 0.001) so that the uncertainty estimates are high.*

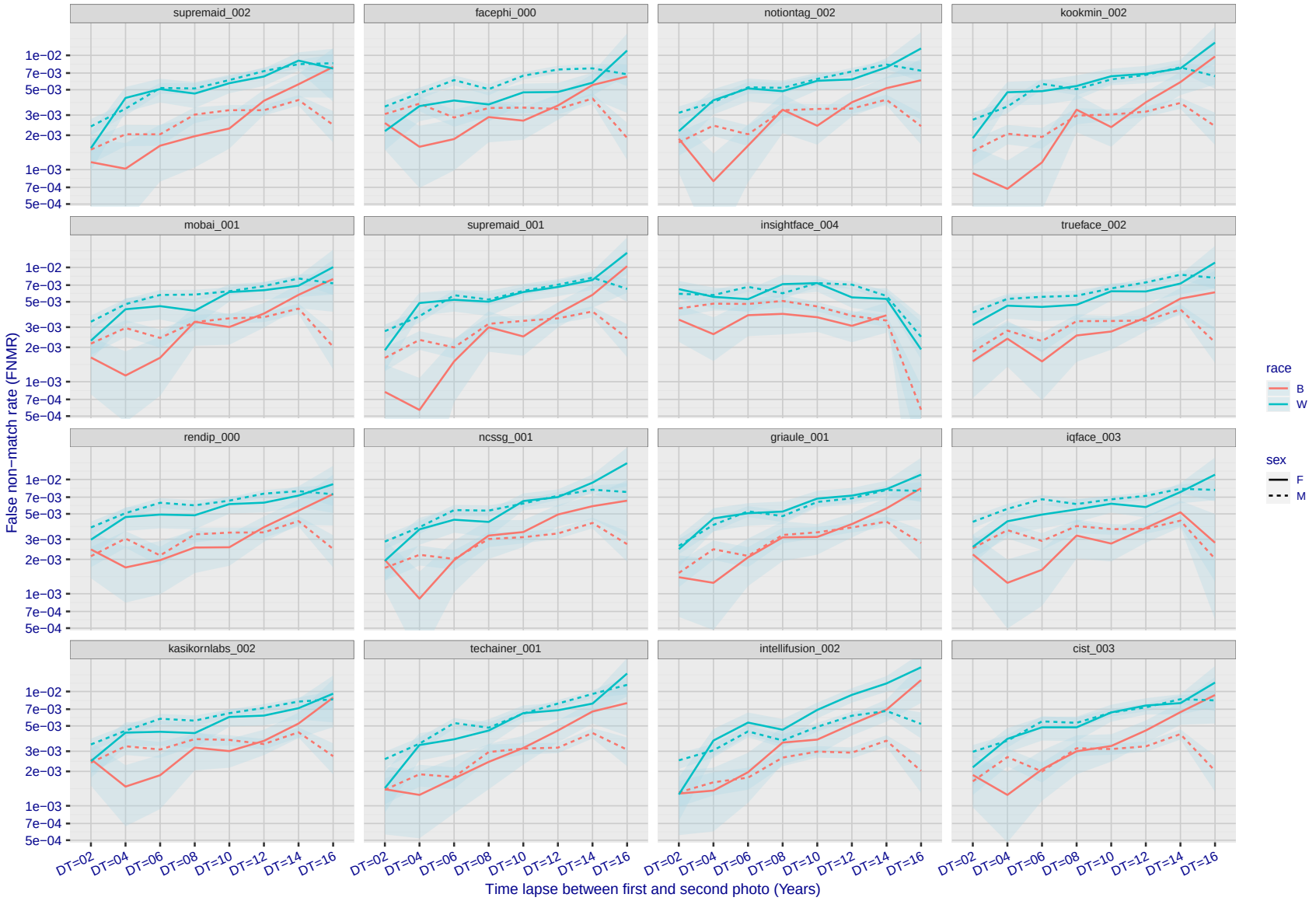

Figure 348: For the mugshot images, FNMR *as a function of elapsed time between initial enrollment and second verification images. The panels appear most accurate first, and vertical scale changes on each page. The four traces correspond to images annotated with codes for black female, black male, white female, white male. The threshold is fixed for each algorithm to give FMR = 0.00001 over all (10^8) impostor comparisons. For short time-lapses, the most accurate algorithms give very few errors (FNMR < 0.001) so that the uncertainty estimates are high.*

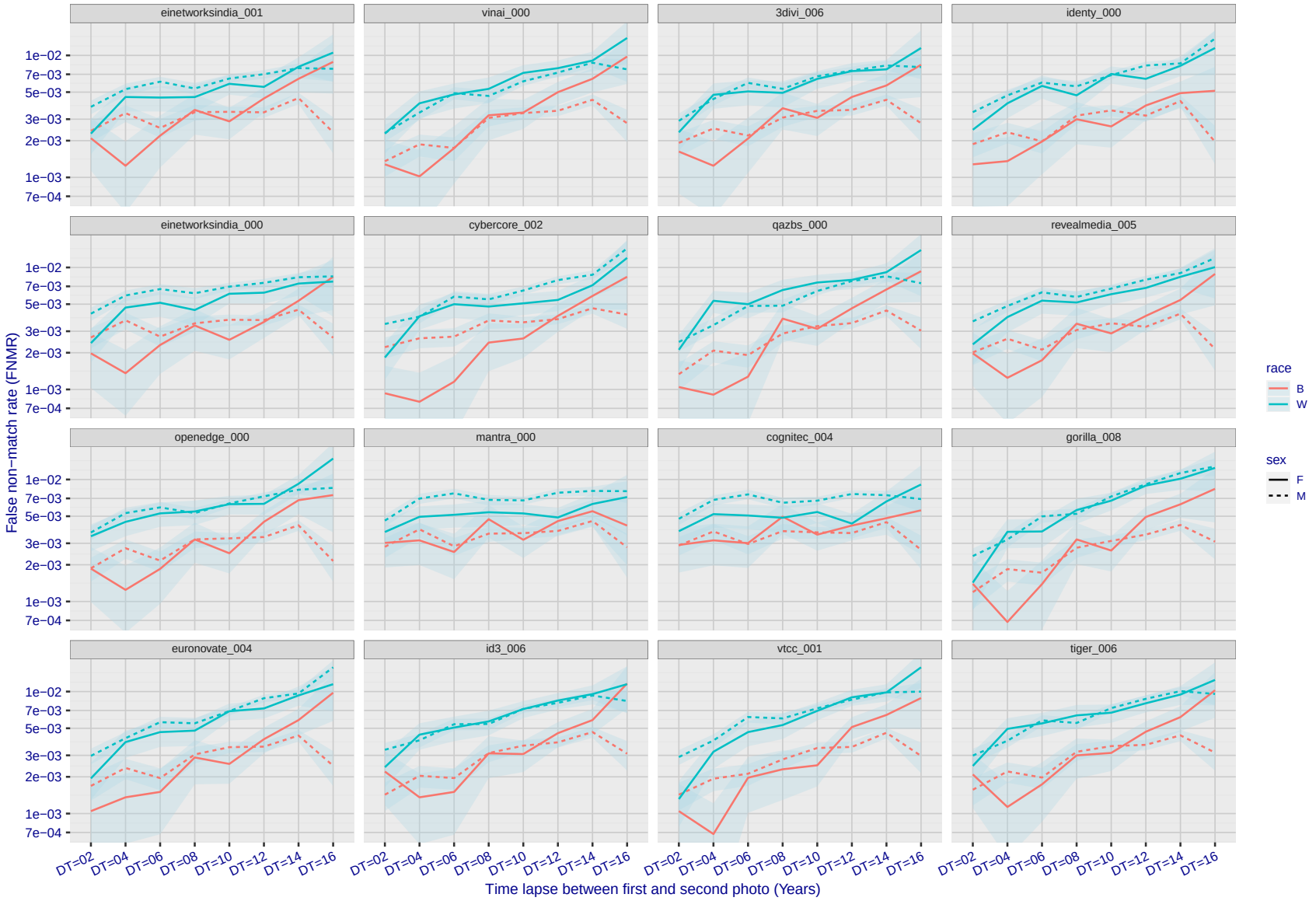

Figure 349: For the mugshot images, FNMR *as a function of elapsed time between initial enrollment and second verification images. The panels appear most accurate first, and vertical scale changes on each page. The four traces correspond to images annotated with codes for black female, black male, white female, white male. The threshold is fixed for each algorithm to give FMR = 0.00001 over all (10^8) impostor comparisons. For short time-lapses, the most accurate algorithms give very few errors (FNMR < 0.001) so that the uncertainty estimates are high.*

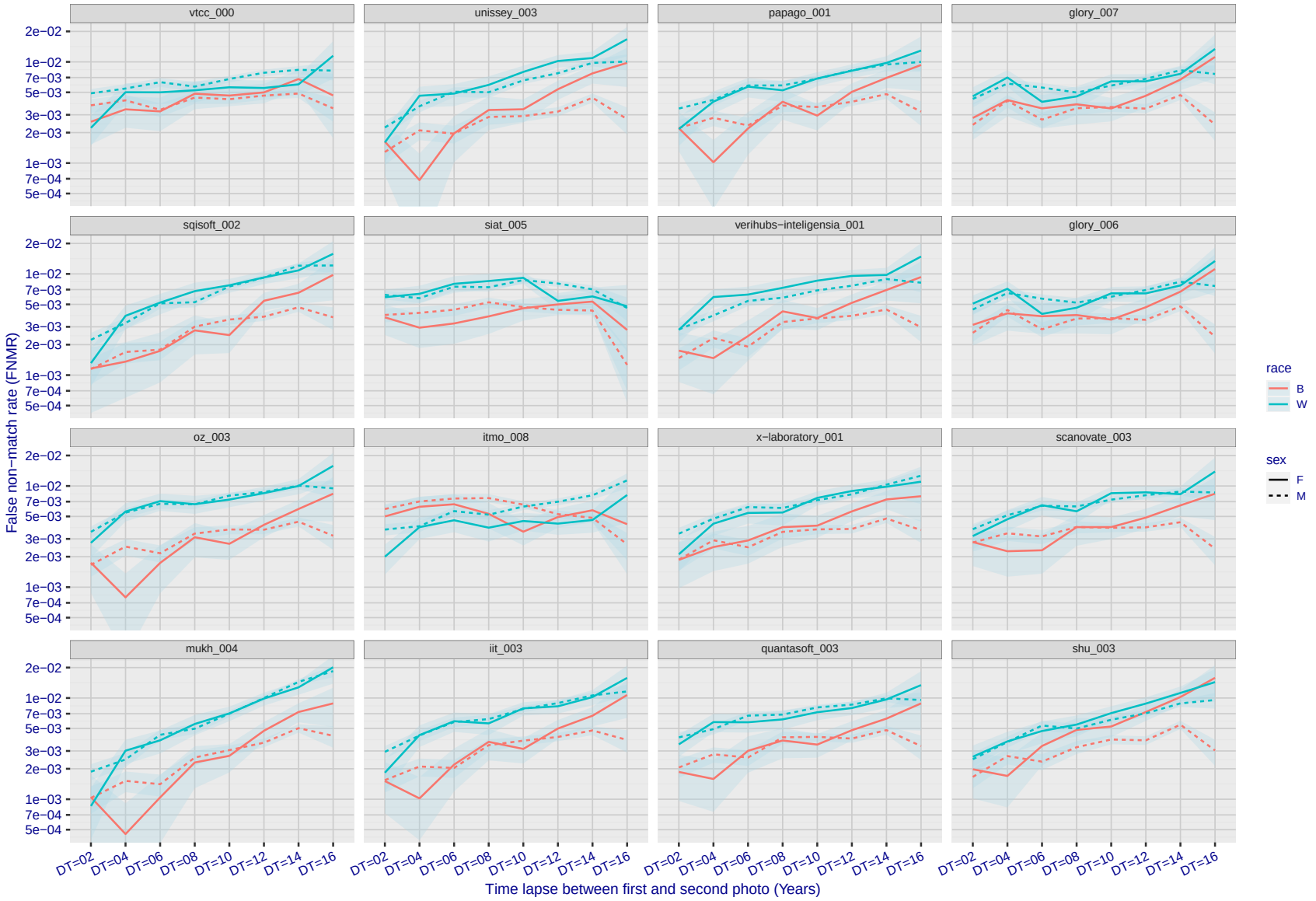

Figure 350: For the mugshot images, FNMR *as a function of elapsed time between initial enrollment and second verification images. The panels appear most accurate first, and vertical scale changes on each page. The four traces correspond to images annotated with codes for black female, black male, white female, white male. The threshold is fixed for each algorithm to give FMR = 0.00001 over all (10^8) impostor comparisons. For short time-lapses, the most accurate algorithms give very few errors (FNMR < 0.001) so that the uncertainty estimates are high.*

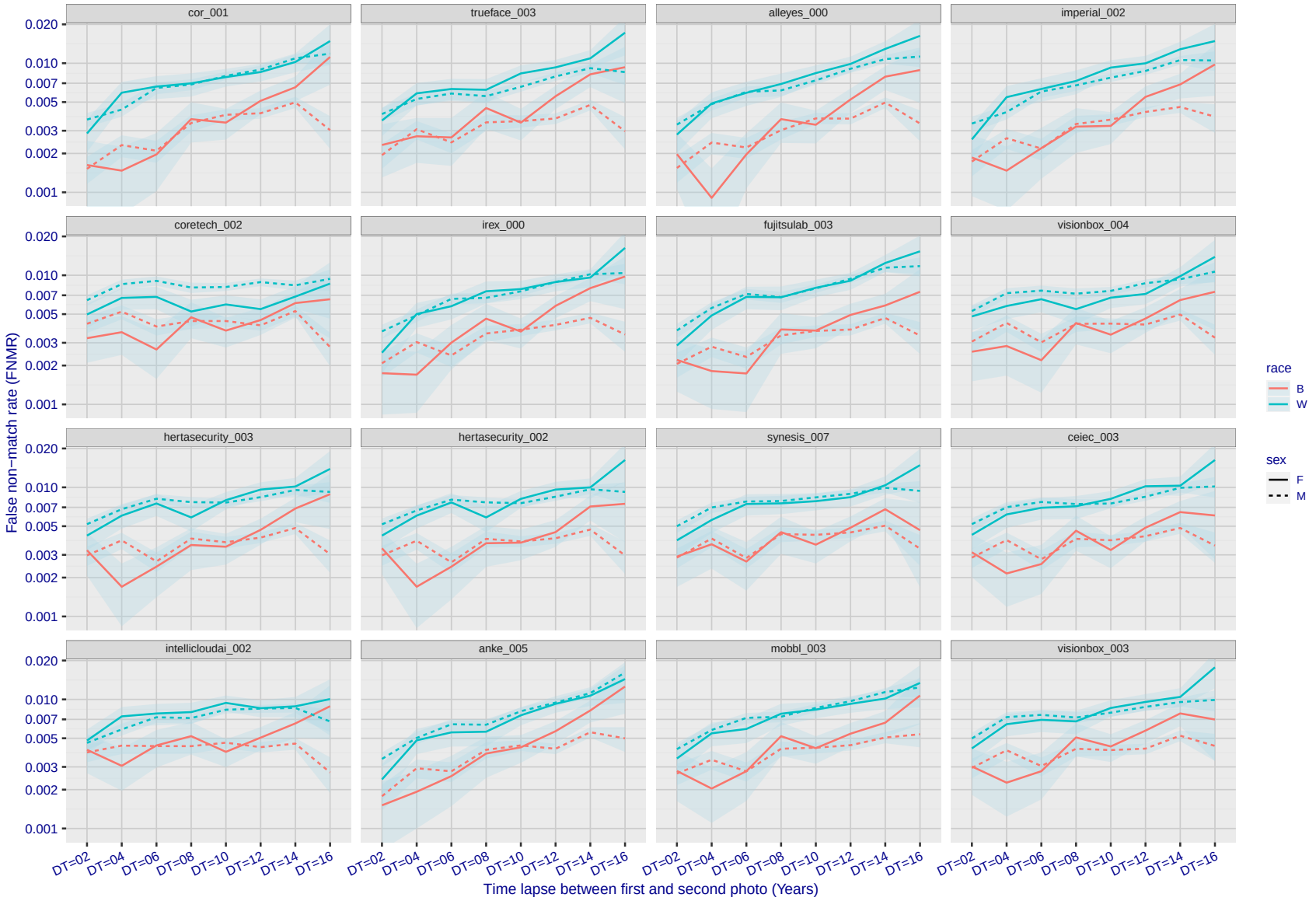

Figure 351: For the mugshot images, FNMR *as a function of elapsed time between initial enrollment and second verification images. The panels appear most accurate first, and vertical scale changes on each page. The four traces correspond to images annotated with codes for black female, black male, white female, white male. The threshold is fixed for each algorithm to give FMR = 0.00001 over all (10^8) impostor comparisons. For short time-lapses, the most accurate algorithms give very few errors (FNMR < 0.001) so that the uncertainty estimates are high.*

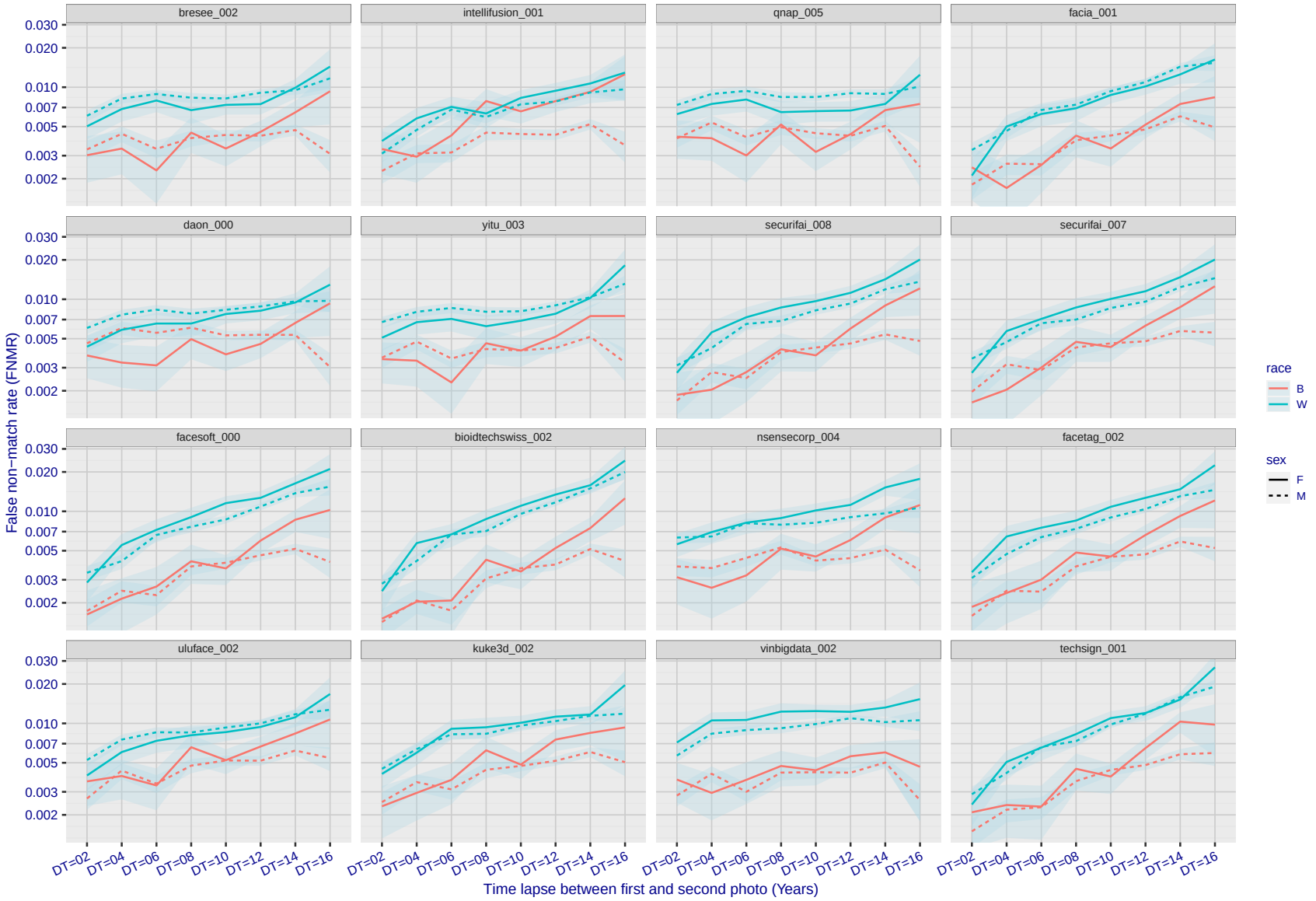

Figure 352: For the mugshot images, FNMR *as a function of elapsed time between initial enrollment and second verification images. The panels appear most accurate first, and vertical scale changes on each page. The four traces correspond to images annotated with codes for black female, black male, white female, white male. The threshold is fixed for each algorithm to give FMR = 0.00001 over all (10^8) impostor comparisons. For short time-lapses, the most accurate algorithms give very few errors (FNMR < 0.001) so that the uncertainty estimates are high.*

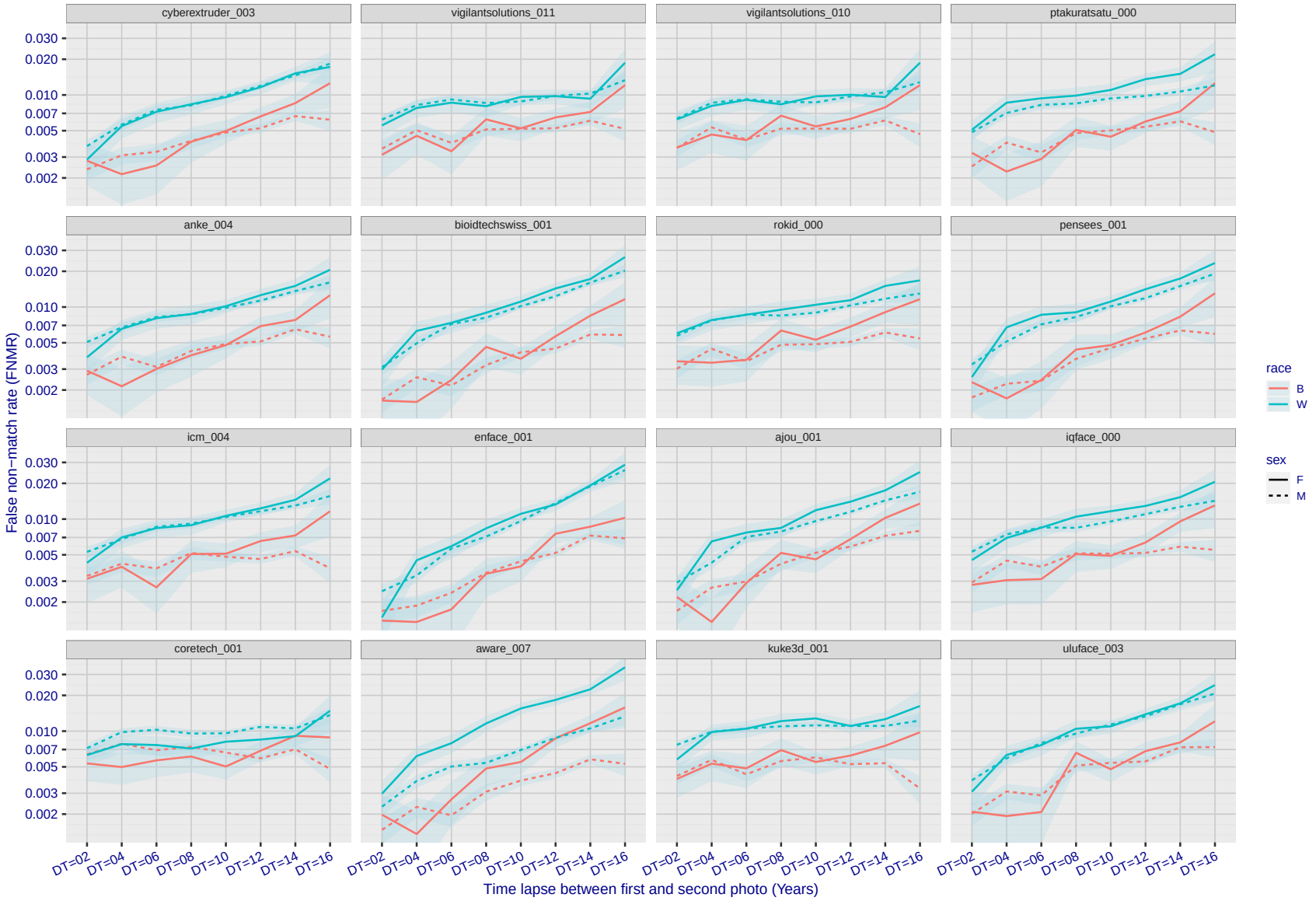

Figure 353: For the mugshot images, FNMR *as a function of elapsed time between initial enrollment and second verification images. The panels appear most accurate first, and vertical scale changes on each page. The four traces correspond to images annotated with codes for black female, black male, white female, white male. The threshold is fixed for each algorithm to give FMR = 0.00001 over all (10^8) impostor comparisons. For short time-lapses, the most accurate algorithms give very few errors (FNMR < 0.001) so that the uncertainty estimates are high.*

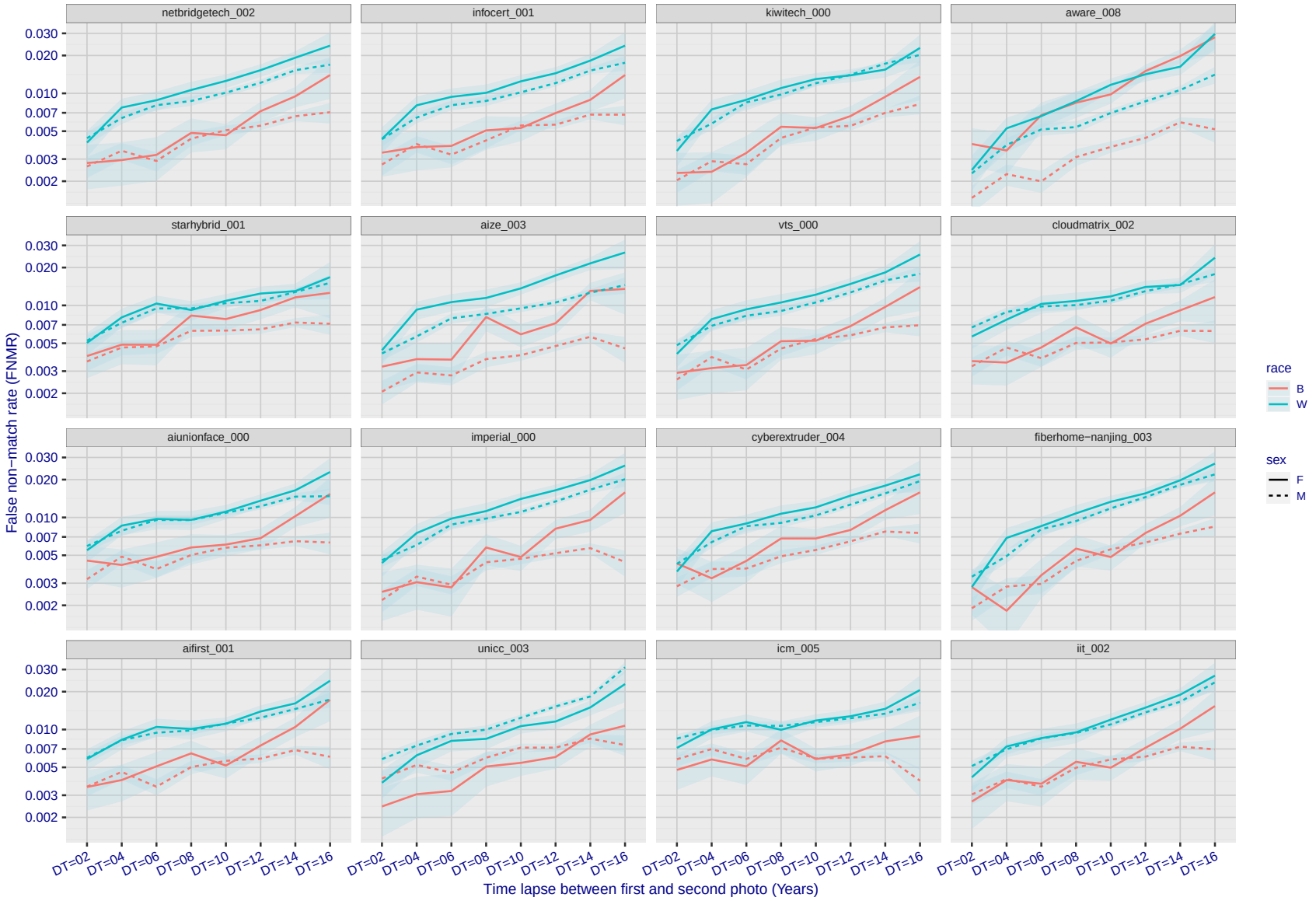

Figure 354: For the mugshot images, FNMR *as a function of elapsed time between initial enrollment and second verification images. The panels appear most accurate first, and vertical scale changes on each page. The four traces correspond to images annotated with codes for black female, black male, white female, white male. The threshold is fixed for each algorithm to give FMR = 0.00001 over all (10^8) impostor comparisons. For short time-lapses, the most accurate algorithms give very few errors (FNMR < 0.001) so that the uncertainty estimates are high.*

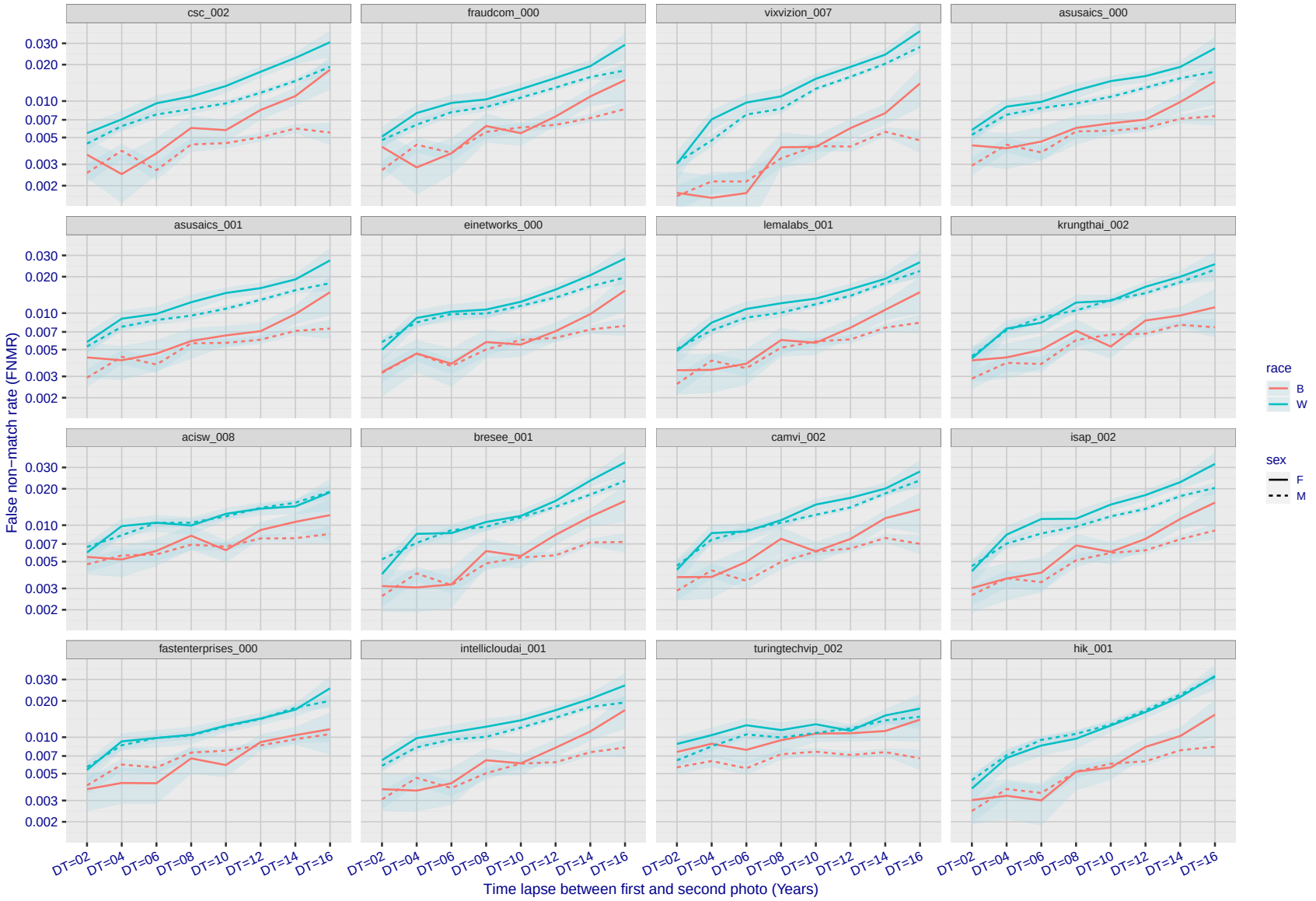

Figure 355: For the mugshot images, FNMR *as a function of elapsed time between initial enrollment and second verification images. The panels appear most accurate first, and vertical scale changes on each page. The four traces correspond to images annotated with codes for black female, black male, white female, white male. The threshold is fixed for each algorithm to give FMR = 0.00001 over all (10^8) impostor comparisons. For short time-lapses, the most accurate algorithms give very few errors (FNMR < 0.001) so that the uncertainty estimates are high.*

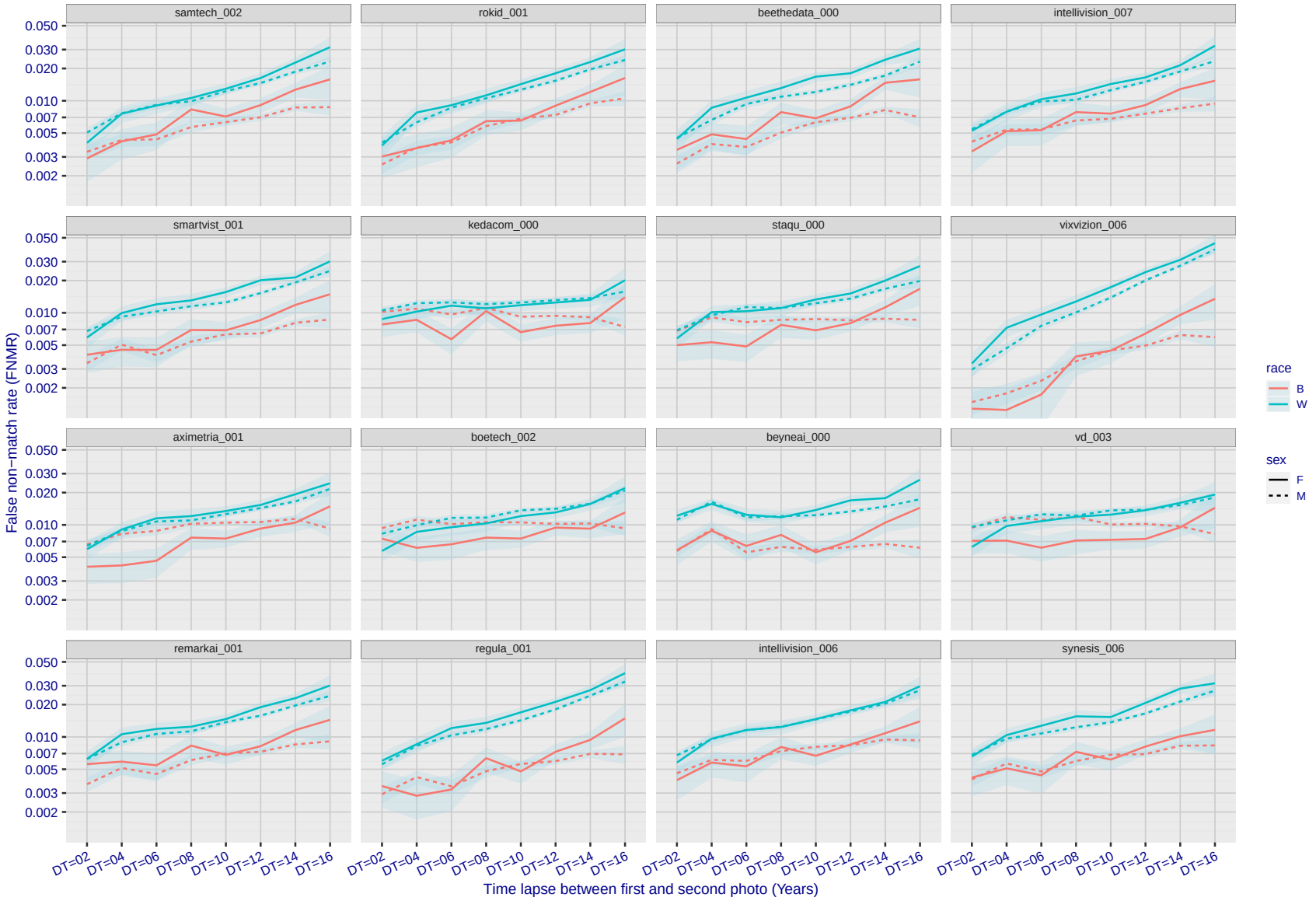

Figure 356: For the mugshot images, FNMR *as a function of elapsed time between initial enrollment and second verification images. The panels appear most accurate first, and vertical scale changes on each page. The four traces correspond to images annotated with codes for black female, black male, white female, white male. The threshold is fixed for each algorithm to give FMR = 0.00001 over all (10^8) impostor comparisons. For short time-lapses, the most accurate algorithms give very few errors (FNMR < 0.001) so that the uncertainty estimates are high.*

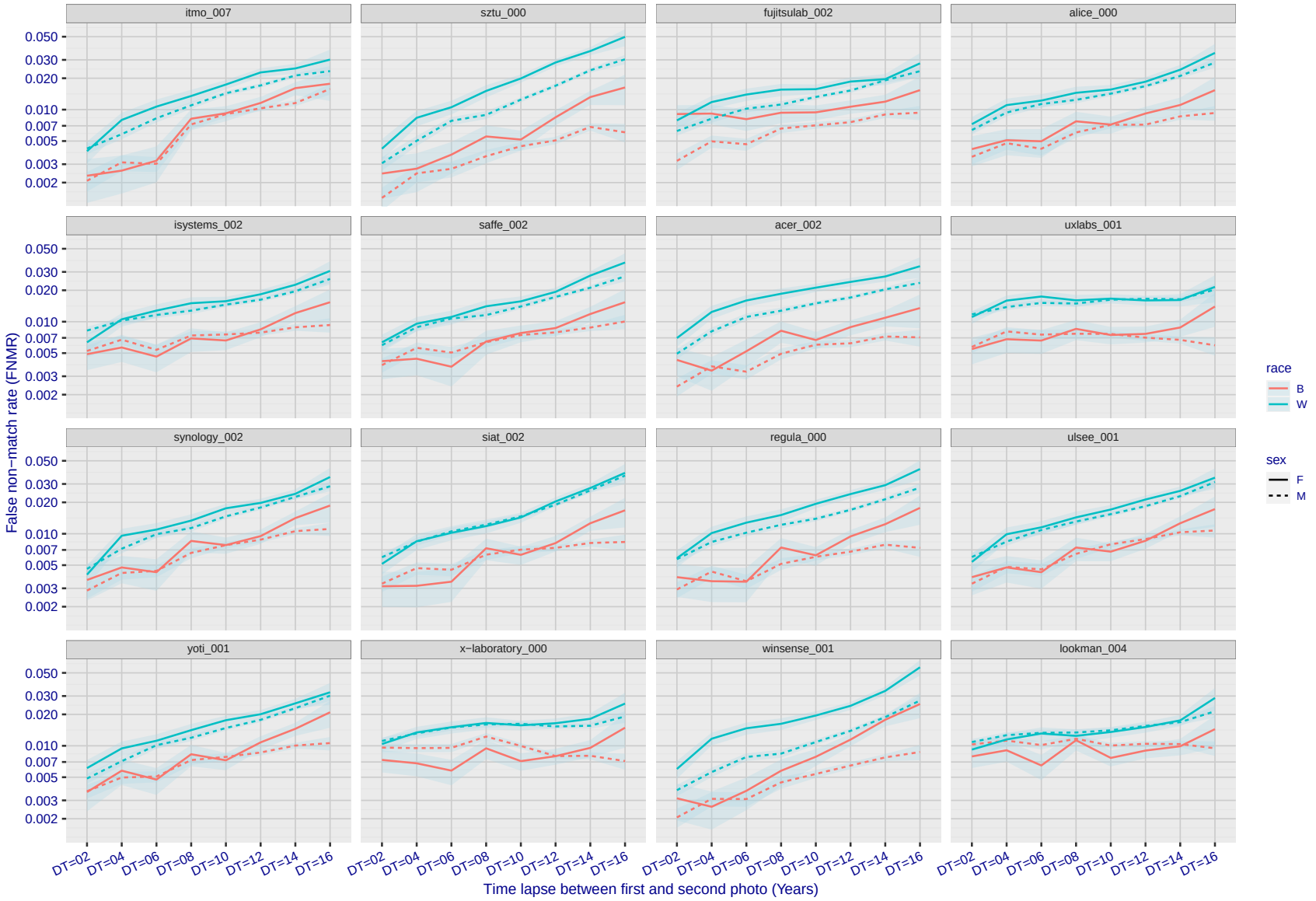

Figure 357: For the mugshot images, FNMR *as a function of elapsed time between initial enrollment and second verification images. The panels appear most accurate first, and vertical scale changes on each page. The four traces correspond to images annotated with codes for black female, black male, white female, white male. The threshold is fixed for each algorithm to give FMR = 0.00001 over all (10^8) impostor comparisons. For short time-lapses, the most accurate algorithms give very few errors (FNMR < 0.001) so that the uncertainty estimates are high.*

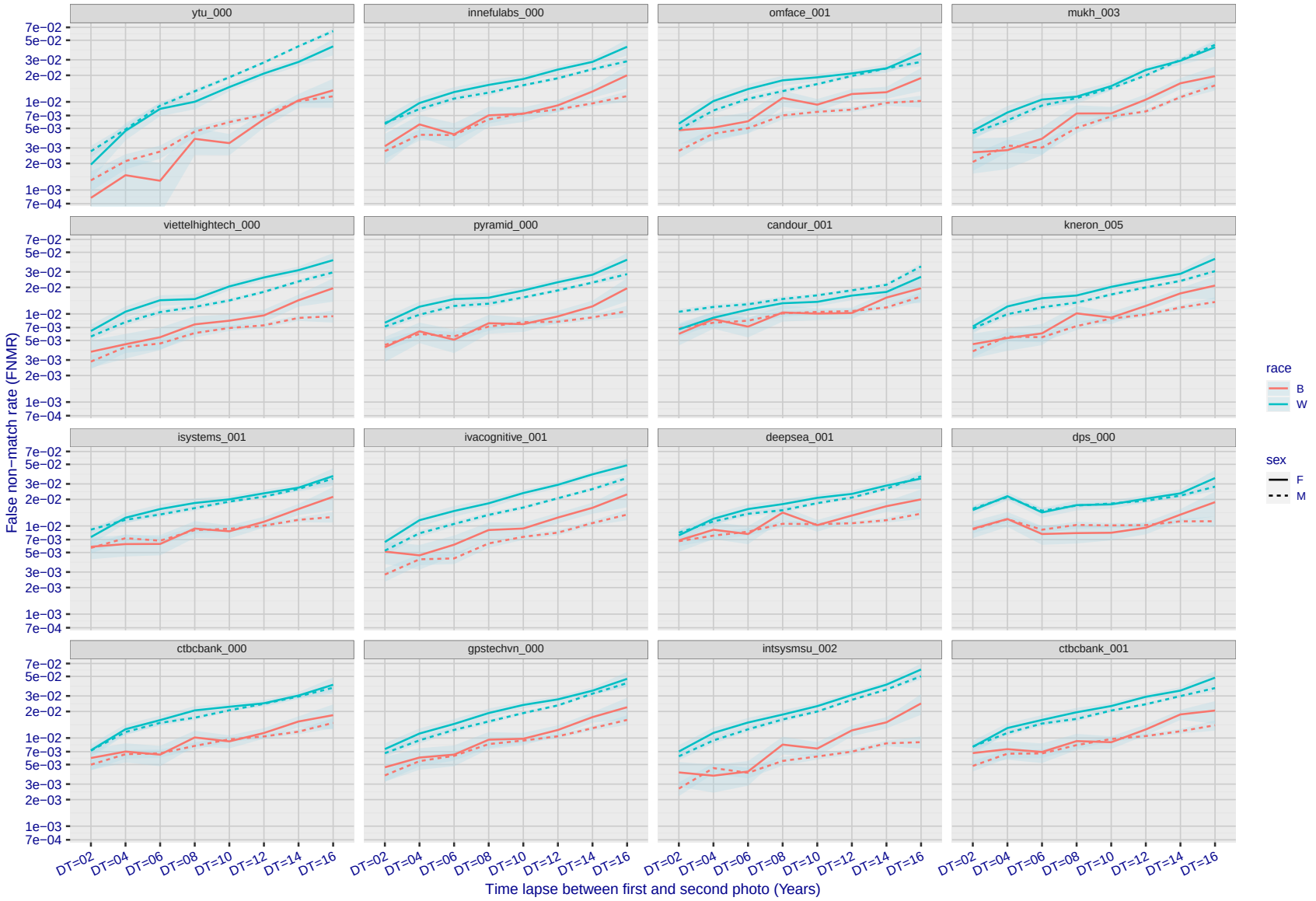

Figure 358: For the mugshot images, FNMR *as a function of elapsed time between initial enrollment and second verification images. The panels appear most accurate first, and vertical scale changes on each page. The four traces correspond to images annotated with codes for black female, black male, white female, white male. The threshold is fixed for each algorithm to give FMR = 0.00001 over all (10^8) impostor comparisons. For short time-lapses, the most accurate algorithms give very few errors (FNMR < 0.001) so that the uncertainty estimates are high.*

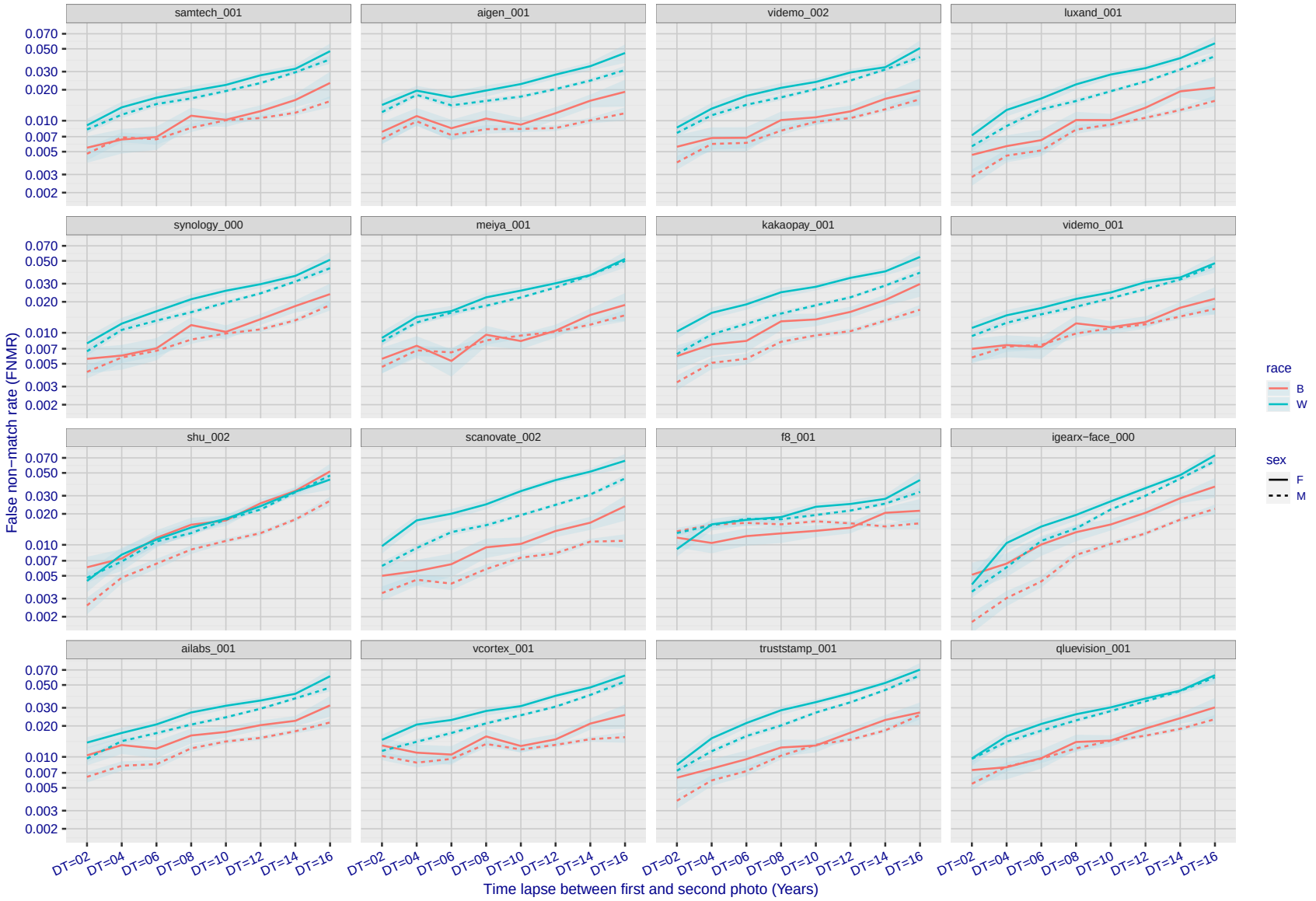

Figure 359: For the mugshot images, FNMR *as a function of elapsed time between initial enrollment and second verification images. The panels appear most accurate first, and vertical scale changes on each page. The four traces correspond to images annotated with codes for black female, black male, white female, white male. The threshold is fixed for each algorithm to give FMR = 0.00001 over all (10^8) impostor comparisons. For short time-lapses, the most accurate algorithms give very few errors (FNMR < 0.001) so that the uncertainty estimates are high.*

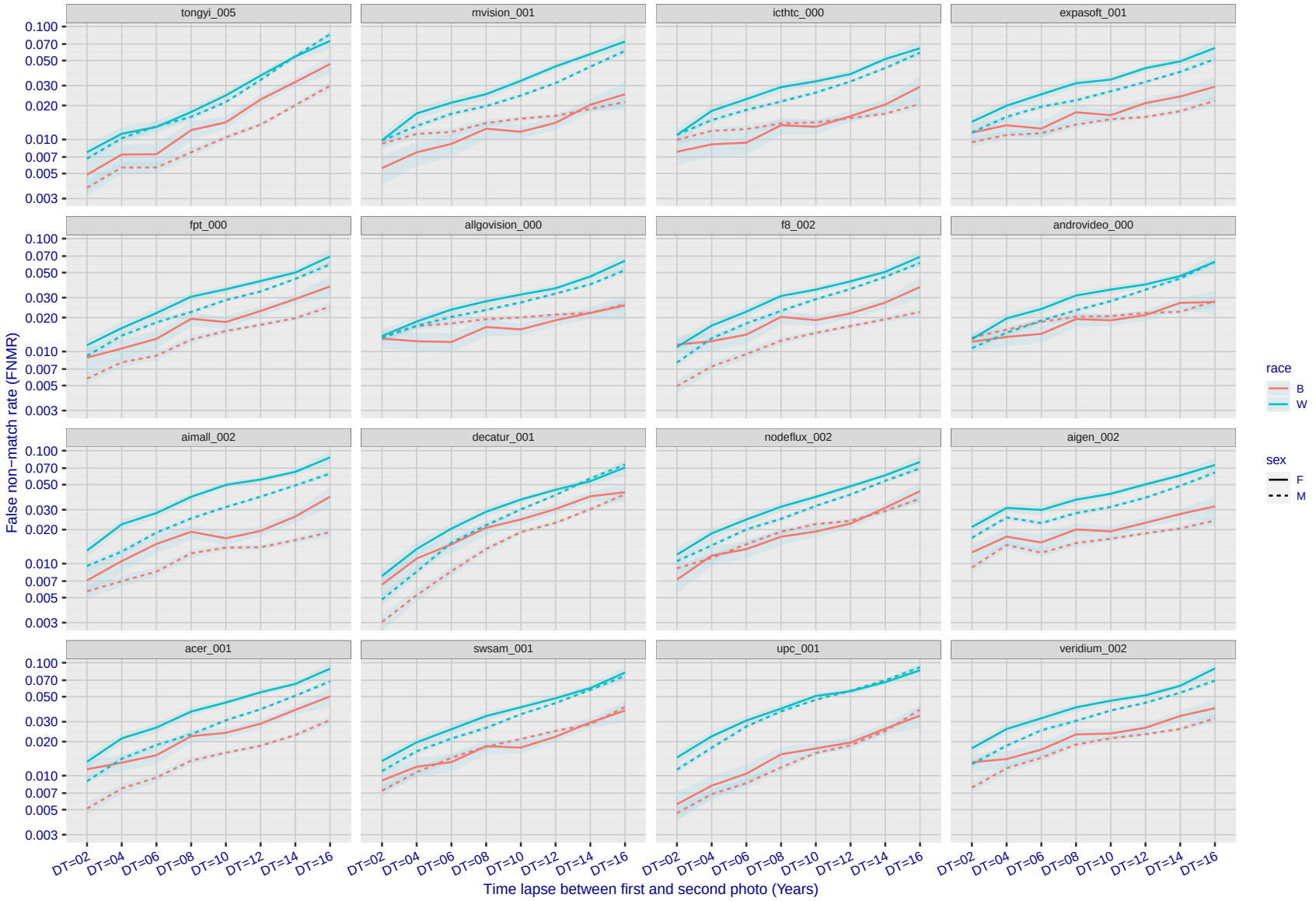

Figure 360: For the mugshot images, FNMR *as a function of elapsed time between initial enrollment and second verification images. The panels appear most accurate first, and vertical scale changes on each page. The four traces correspond to images annotated with codes for black female, black male, white female, white male. The threshold is fixed for each algorithm to give FMR = 0.00001 over all (10^8) impostor comparisons. For short time-lapses, the most accurate algorithms give very few errors (FNMR < 0.001) so that the uncertainty estimates are high.*

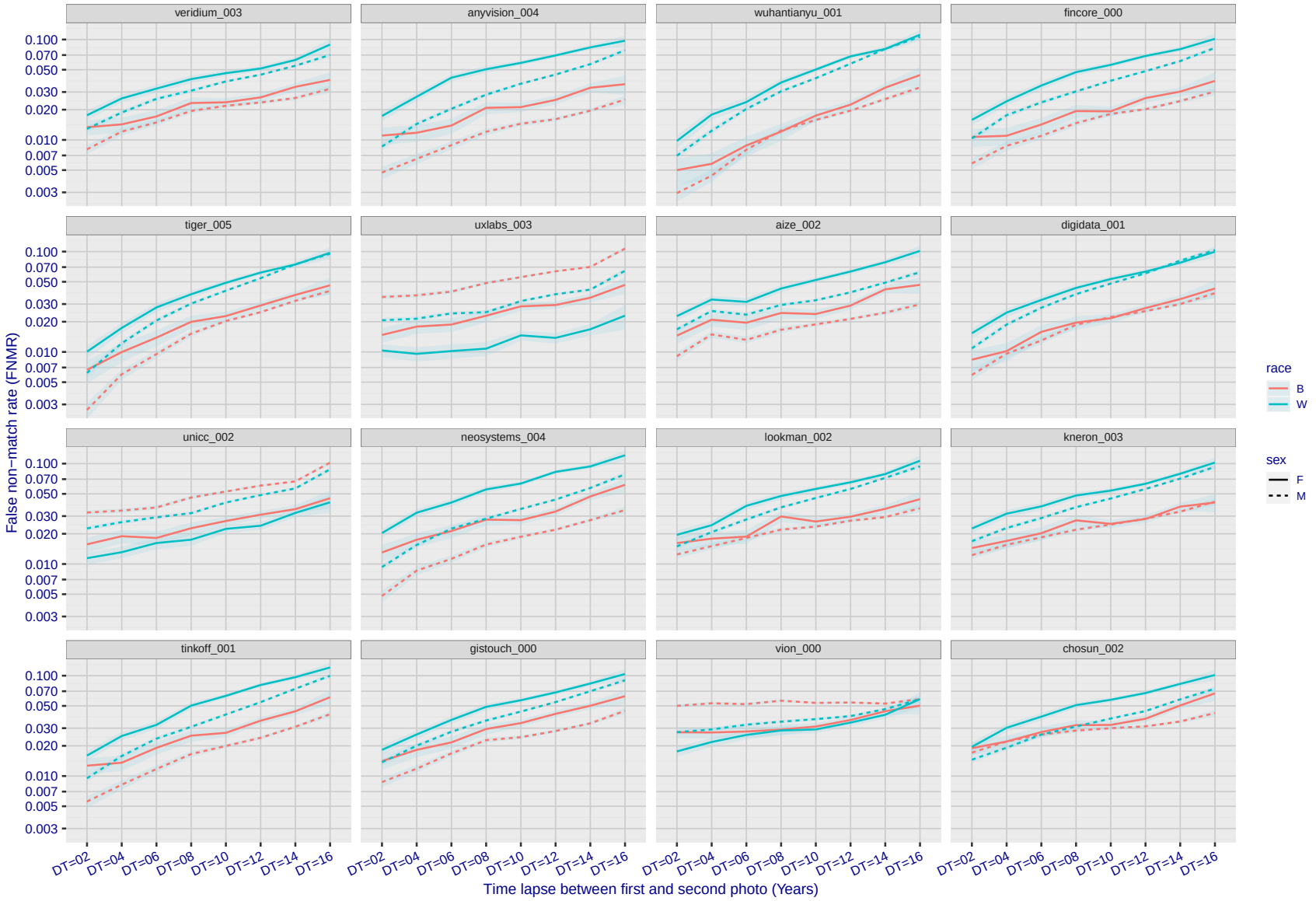

Figure 361: For the mugshot images, FNMR *as a function of elapsed time between initial enrollment and second verification images. The panels appear most accurate first, and vertical scale changes on each page. The four traces correspond to images annotated with codes for black female, black male, white female, white male. The threshold is fixed for each algorithm to give FMR = 0.00001 over all (10^8) impostor comparisons. For short time-lapses, the most accurate algorithms give very few errors (FNMR < 0.001) so that the uncertainty estimates are high.*

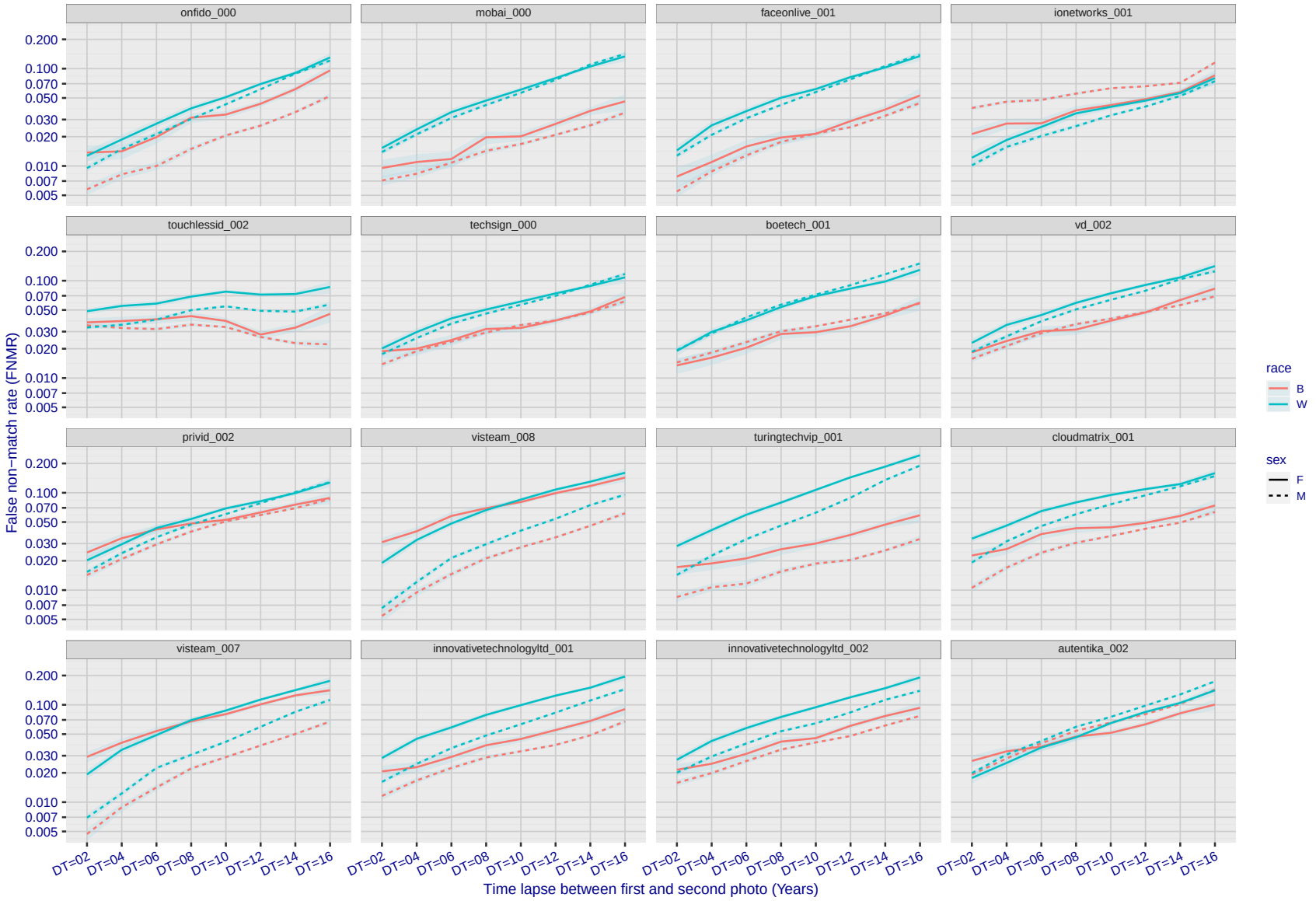

Figure 362: For the mugshot images, FNMR *as a function of elapsed time between initial enrollment and second verification images. The panels appear most accurate first, and vertical scale changes on each page. The four traces correspond to images annotated with codes for black female, black male, white female, white male. The threshold is fixed for each algorithm to give FMR = 0.00001 over all (10^8) impostor comparisons. For short time-lapses, the most accurate algorithms give very few errors (FNMR < 0.001) so that the uncertainty estimates are high.*

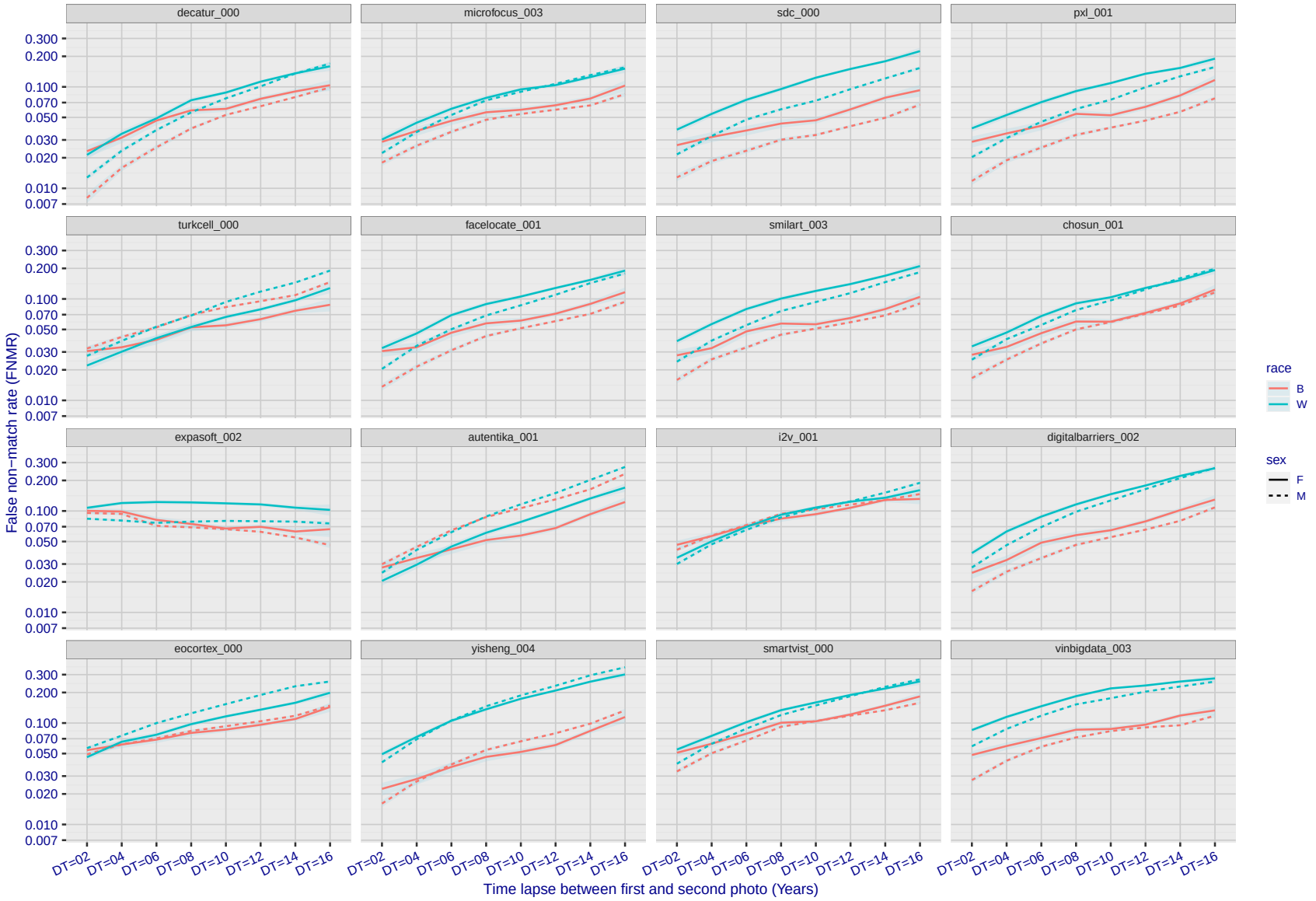

Figure 363: For the mugshot images, FNMR *as a function of elapsed time between initial enrollment and second verification images. The panels appear most accurate first, and vertical scale changes on each page. The four traces correspond to images annotated with codes for black female, black male, white female, white male. The threshold is fixed for each algorithm to give FMR = 0.00001 over all (10^8) impostor comparisons. For short time-lapses, the most accurate algorithms give very few errors (FNMR < 0.001) so that the uncertainty estimates are high.*

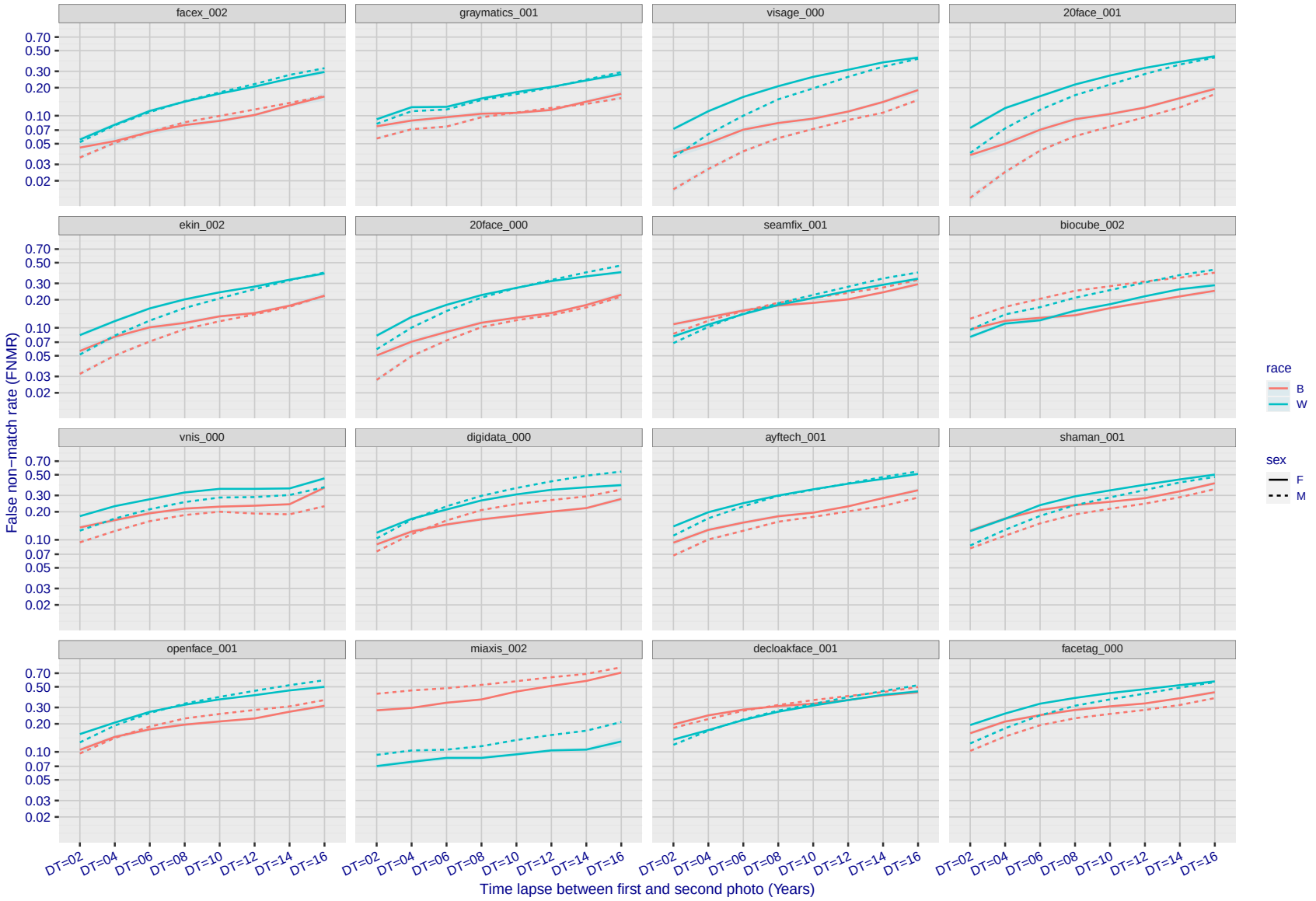

Figure 364: For the mugshot images, FNMR *as a function of elapsed time between initial enrollment and second verification images. The panels appear most accurate first, and vertical scale changes on each page. The four traces correspond to images annotated with codes for black female, black male, white female, white male. The threshold is fixed for each algorithm to give FMR = 0.00001 over all (10^8) impostor comparisons. For short time-lapses, the most accurate algorithms give very few errors (FNMR < 0.001) so that the uncertainty estimates are high.*

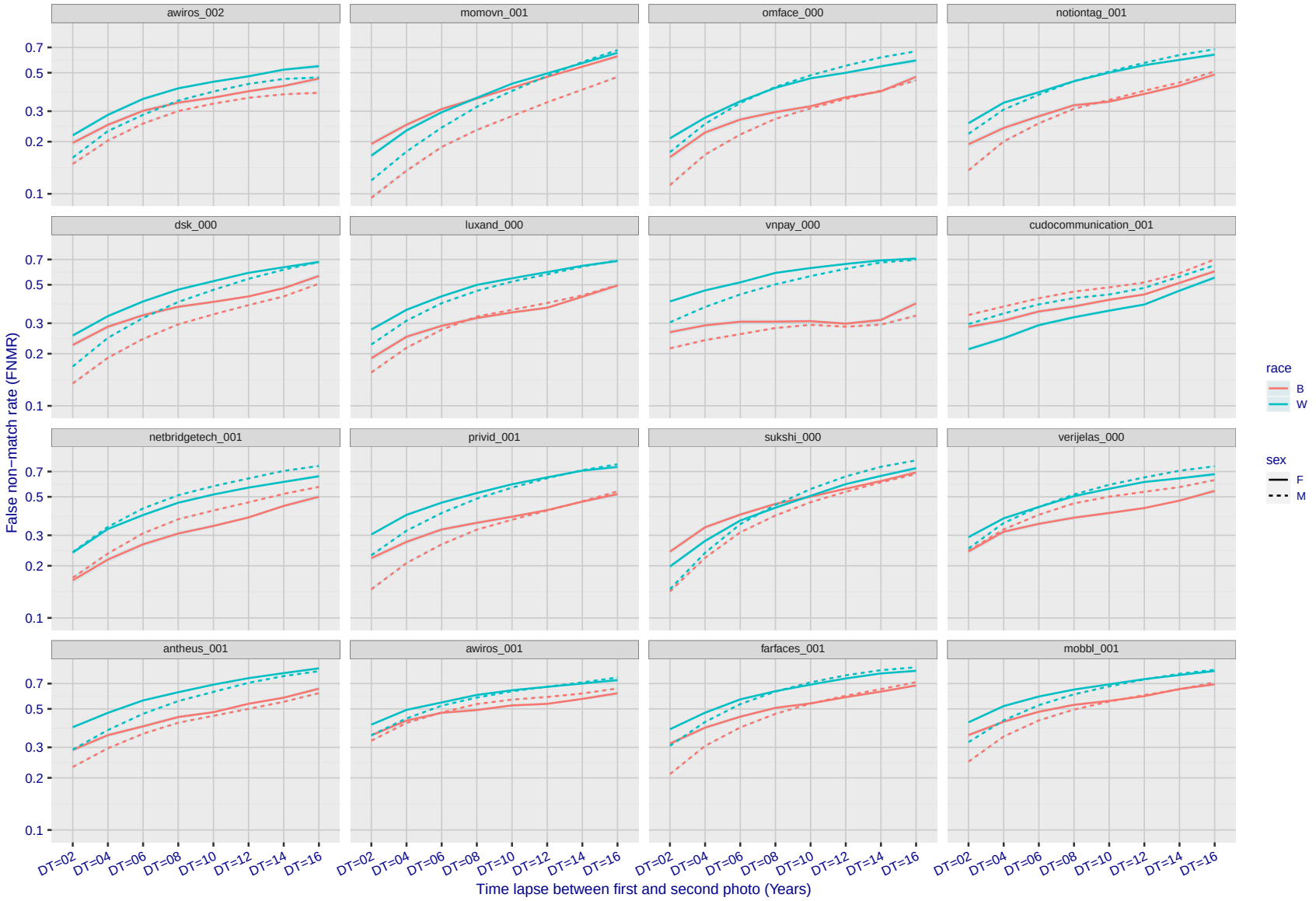

Figure 365: For the mugshot images, FNMR *as a function of elapsed time between initial enrollment and second verification images. The panels appear most accurate first, and vertical scale changes on each page. The four traces correspond to images annotated with codes for black female, black male, white female, white male. The threshold is fixed for each algorithm to give FMR = 0.00001 over all (10^8) impostor comparisons. For short time-lapses, the most accurate algorithms give very few errors (FNMR < 0.001) so that the uncertainty estimates are high.*

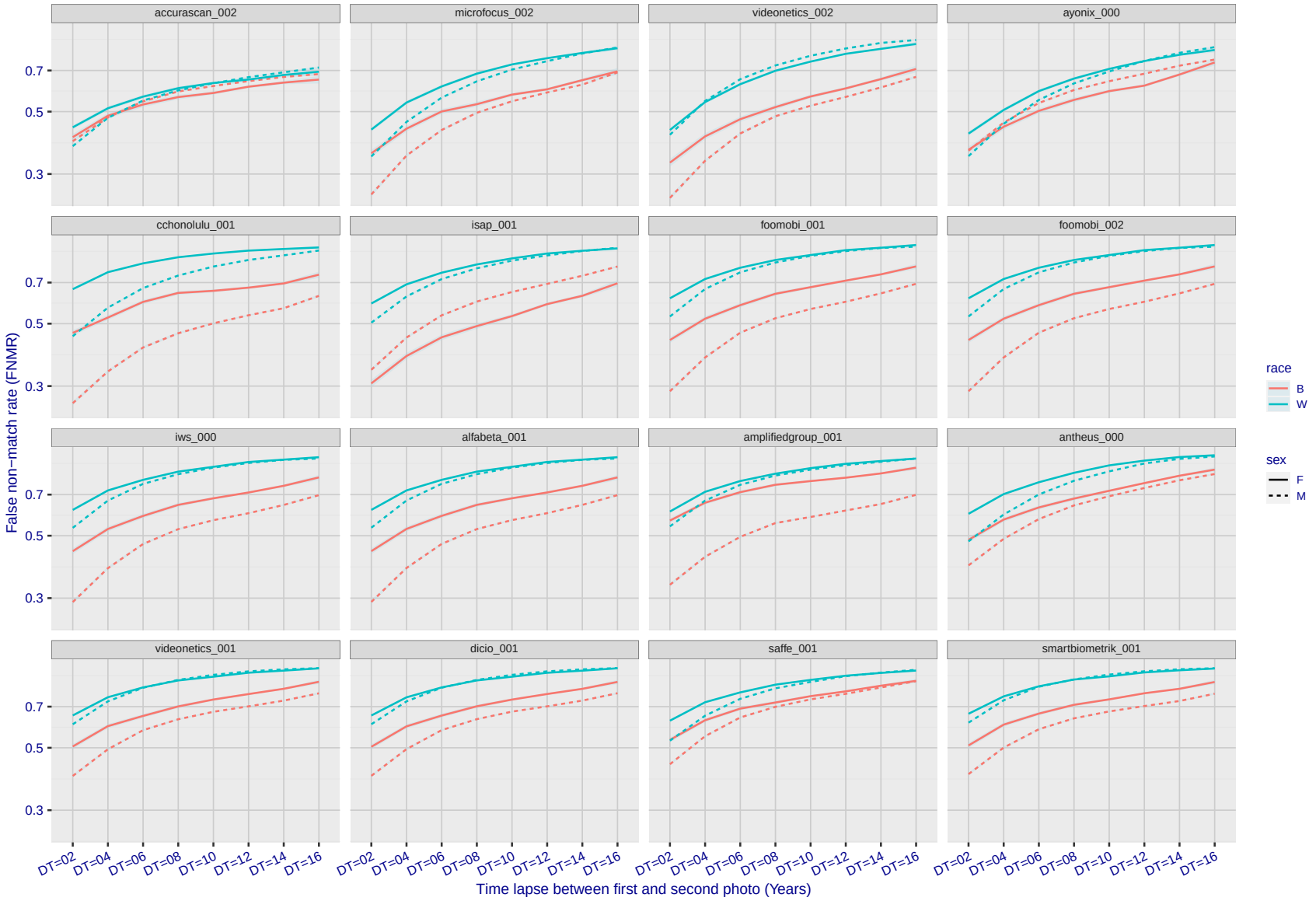

Figure 366: For the mugshot images, FNMR *as a function of elapsed time between initial enrollment and second verification images. The panels appear most accurate first, and vertical scale changes on each page. The four traces correspond to images annotated with codes for black female, black male, white female, white male. The threshold is fixed for each algorithm to give FMR = 0.00001 over all (10^8) impostor comparisons. For short time-lapses, the most accurate algorithms give very few errors (FNMR < 0.001) so that the uncertainty estimates are high.*

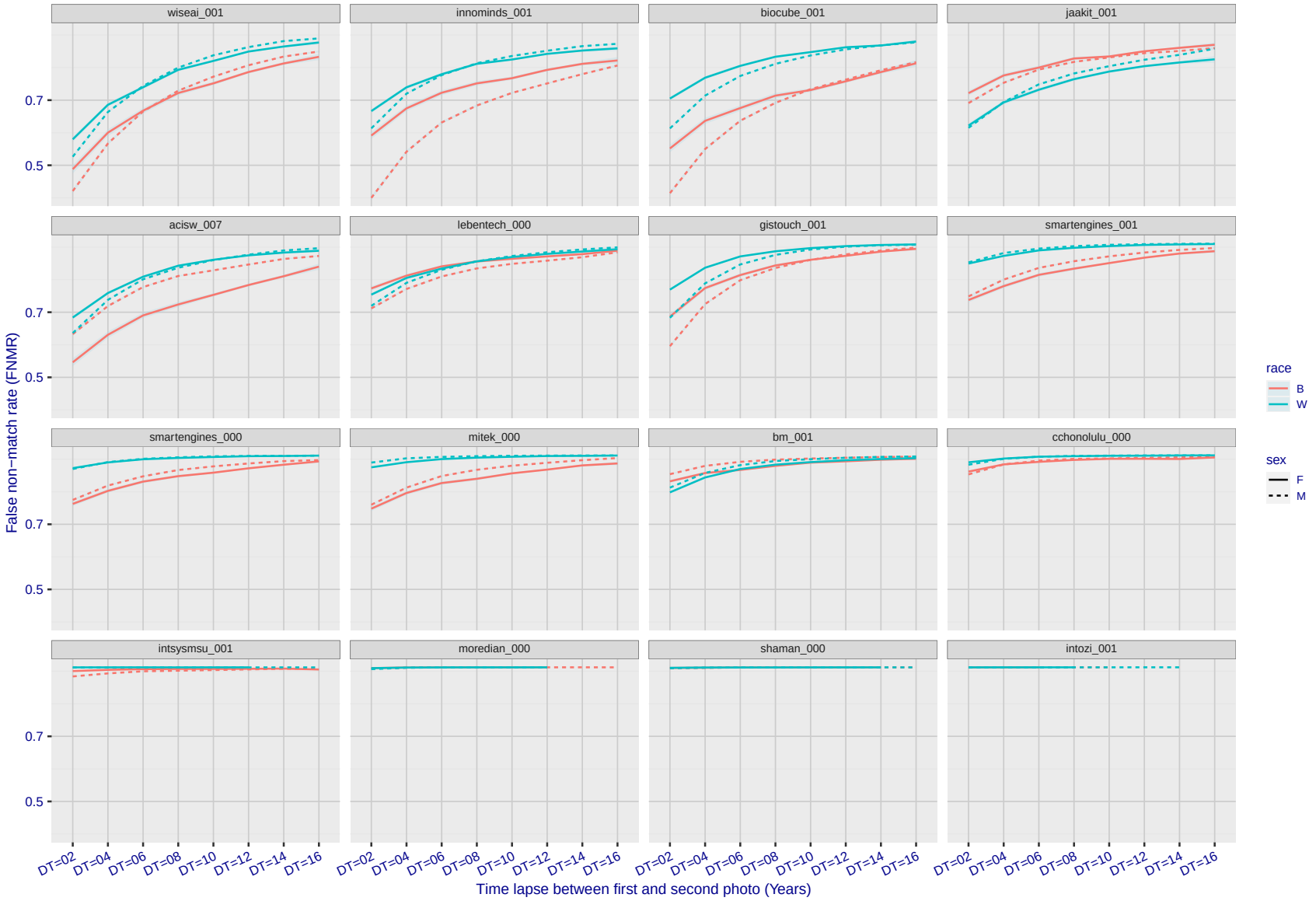

Figure 367: For the mugshot images, FNMR *as a function of elapsed time between initial enrollment and second verification images. The panels appear most accurate first, and vertical scale changes on each page. The four traces correspond to images annotated with codes for black female, black male, white female, white male. The threshold is fixed for each algorithm to give FMR = 0.00001 over all (10^8) impostor comparisons. For short time-lapses, the most accurate algorithms give very few errors (FNMR < 0.001) so that the uncertainty estimates are high.*

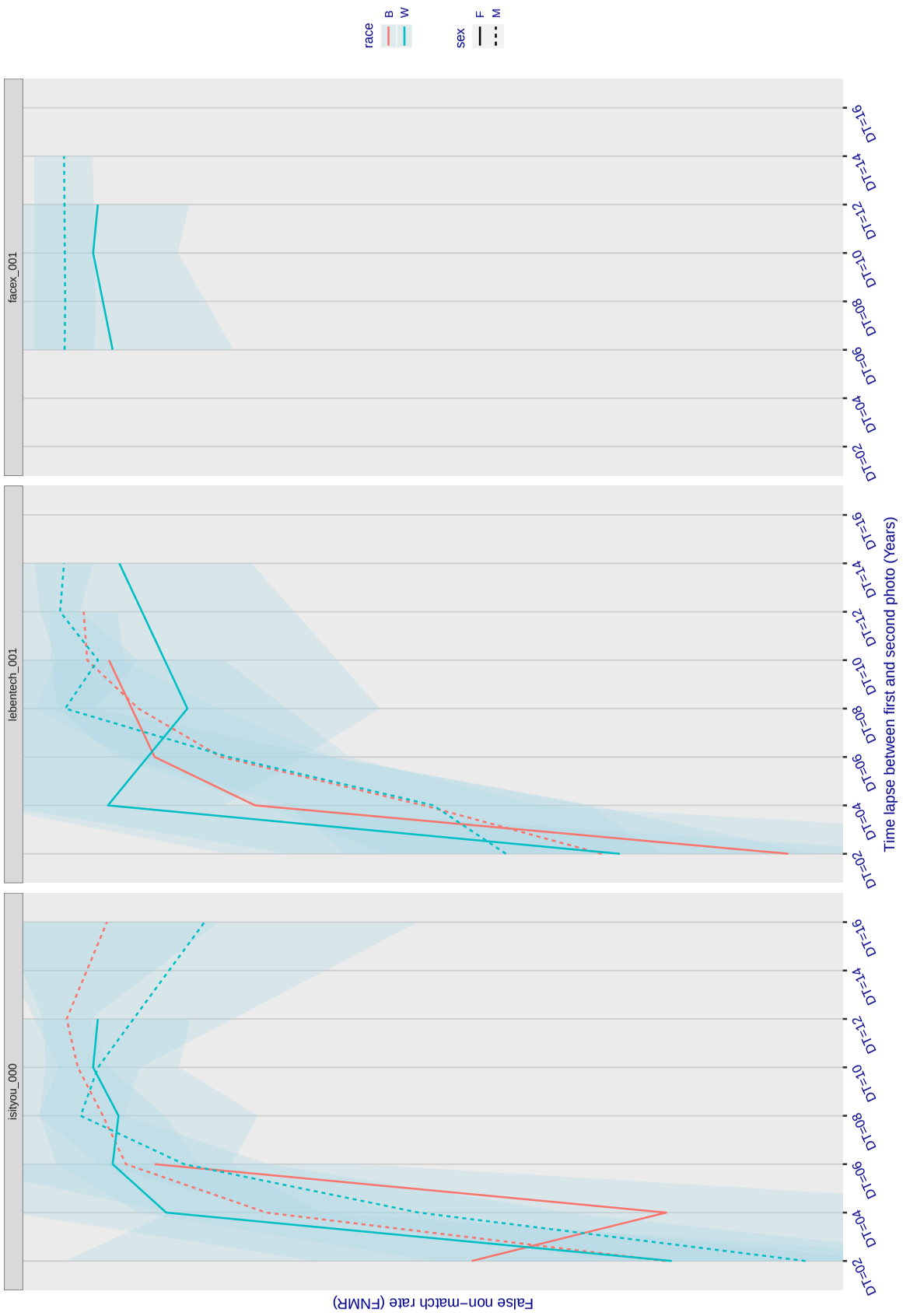

Figure 368: For the mugshot images, FNMR *as a function of elapsed time between initial enrollment and second verification images. The panels appear most accurate first, and vertical scale changes on each page. The four traces correspond to images annotated with codes for black female, black male, white female, white male. The threshold is fixed for each algorithm to give FMR = 0.00001 over all (10^8) impostor comparisons. For short time-lapses, the most accurate algorithms give very few errors (FNMR < 0.001) so that the uncertainty estimates are high.*

FNMR(T) "False non-match rate"
FMR(T) "False match rate"

3.5.3 Effect of age on genuine subjects

Background: Faces change appearance throughout life. Face recognition algorithms have previously beeen reported to give better accuracy on older individuals (See NIST IR 8009).

Goal: To quantify false non-match rates (FNMR) as a function of age, without an ageing component.

Methods: Using the visa images, which span fewer than five years, thresholds are determined that give FMR = 0.001 and 0.0001 over the entire impostor set. Then FNMR is measured over 1000 bootstrap replications of the genuine scores.

Results: For the visa images, Figure 414 shows how false non-match rates for genuine users, as a function of age group.

The notable aspects are:

- ▷ Younger subjects give considerably higher FNMR. This is likely due to rapid growth and change in facial appearance.
- ▷ FNMR trends down throughout life. The last bin, AGE $>$ 72, contains fewer than 140 mated pairs, and may be affected by small sample size.

FNMR(T) "False non-match rate"
FMR(T) "False match rate"

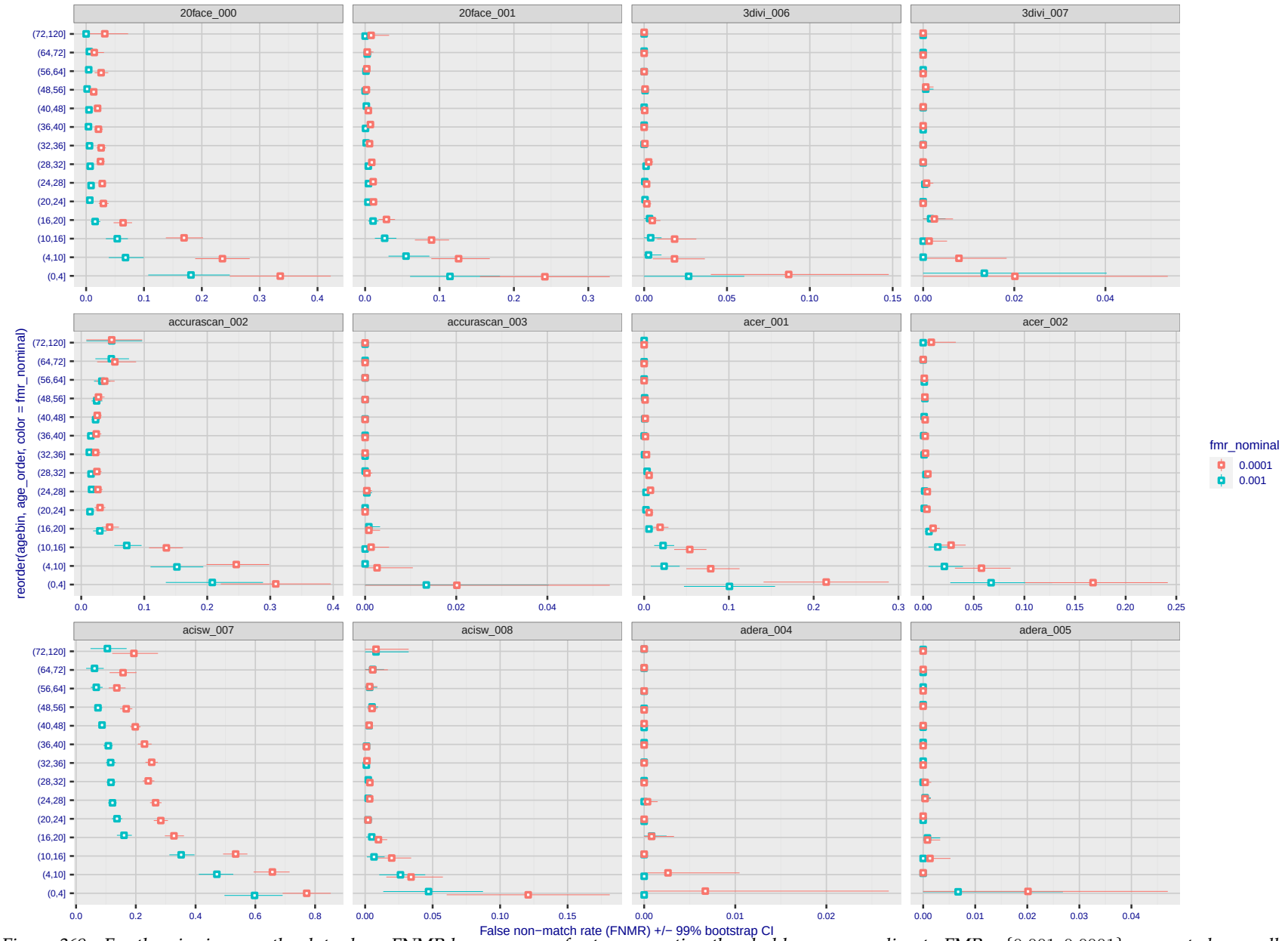

Figure 369: For the visa images, the dots show FNMR by age group for two operating thresholds corresponding to FMR = $\{0.001, 0.0001\}$ computed over all on the order of 10^{10} impostor scores. The FMR in each bin will vary also - see subsequent impostor heatmaps in sec. 3.6.2. Given a pair of face images taken at different times, we assign the comparison to the bin that is the arithmetic average of the subject's ages. This plot shows only the effect of age, not ageing. The number of comparisons in each bin is generally in the thousands, however the first and last bins are computed over 149 and 124 respectively. The error rates in some (adult) cases are zero, and in others the DET is flat so the error rates at the two thresholds are identical. The lines span 1% and 99% of boostrap replicated FNMR estimates.

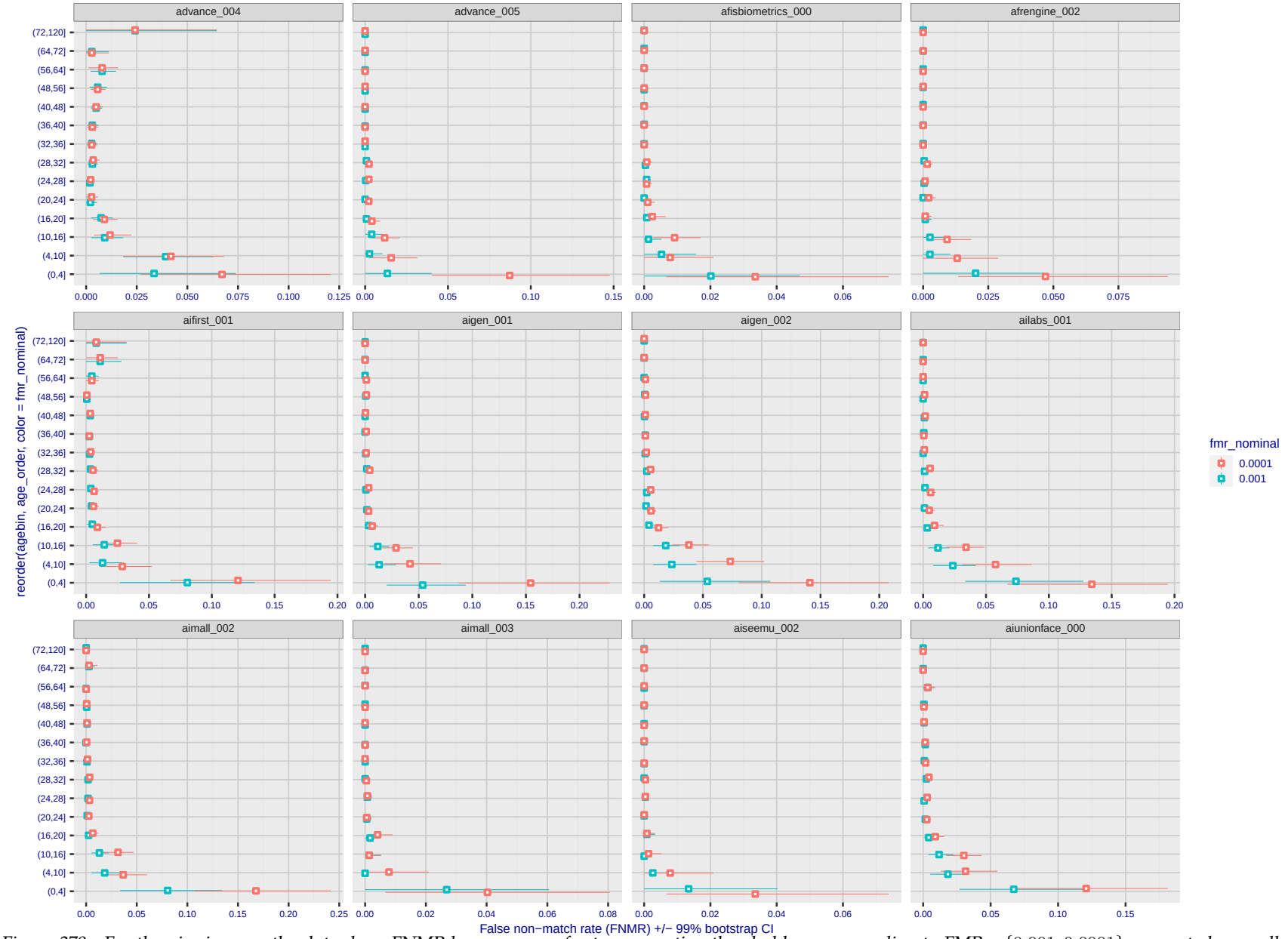

Figure 370: For the visa images, the dots show FNMR by age group for two operating thresholds corresponding to FMR = $\{0.001, 0.0001\}$ computed over all on the order of 10^{10} impostor scores. The FMR in each bin will vary also - see subsequent impostor heatmaps in sec. 3.6.2. Given a pair of face images taken at different times, we assign the comparison to the bin that is the arithmetic average of the subject's ages. This plot shows only the effect of age, not ageing. The number of comparisons in each bin is generally in the thousands, however the first and last bins are computed over 149 and 124 respectively. The error rates in some (adult) cases are zero, and in others the DET is flat so the error rates at the two thresholds are identical. The lines span 1% and 99% of boostrap replicated FNMR estimates.

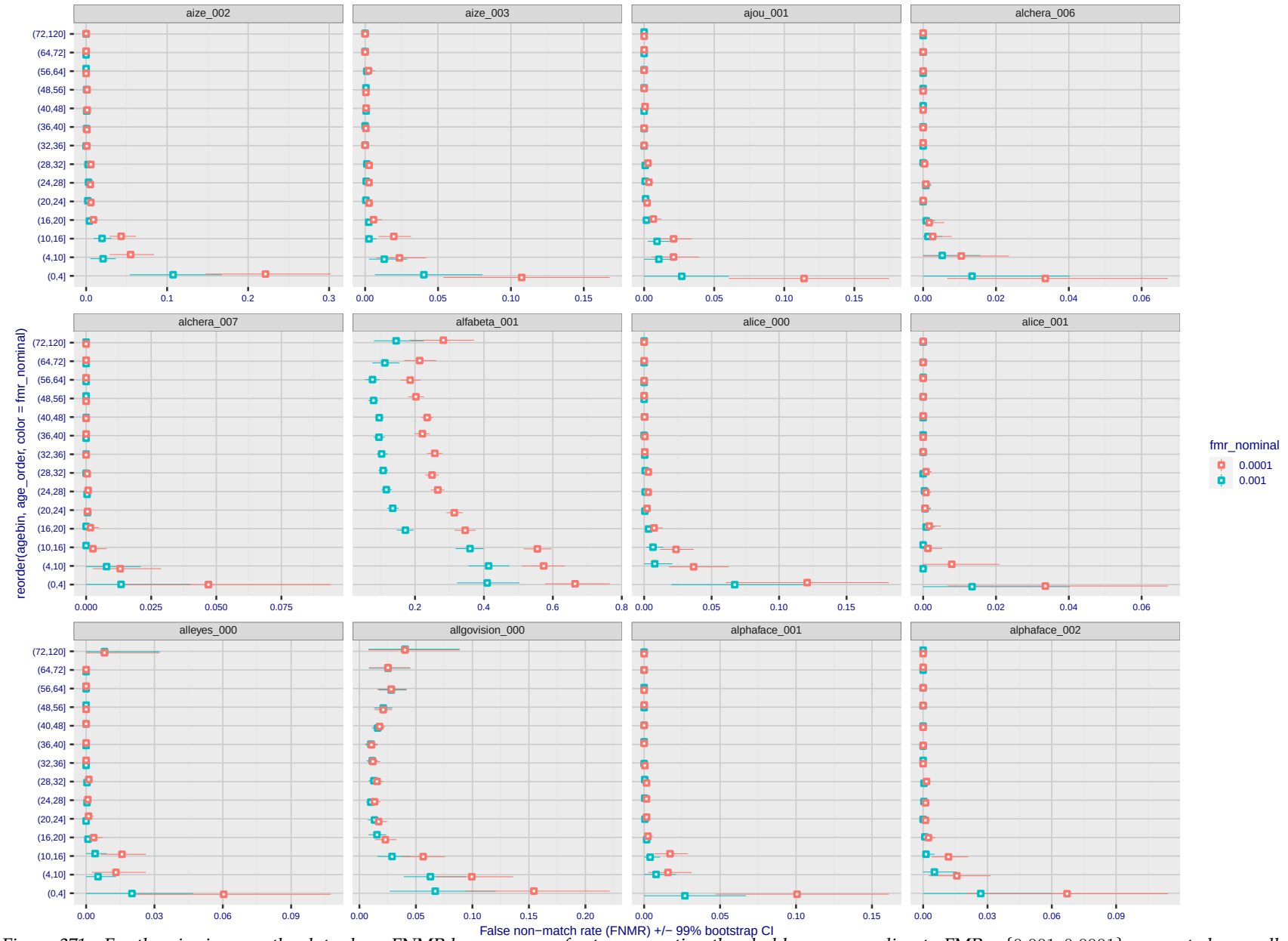

Figure 371: For the visa images, the dots show FNMR by age group for two operating thresholds corresponding to FMR = $\{0.001, 0.0001\}$ computed over all on the order of 10^{10} impostor scores. The FMR in each bin will vary also - see subsequent impostor heatmaps in sec. 3.6.2. Given a pair of face images taken at different times, we assign the comparison to the bin that is the arithmetic average of the subject's ages. This plot shows only the effect of age, not ageing. The number of comparisons in each bin is generally in the thousands, however the first and last bins are computed over 149 and 124 respectively. The error rates in some (adult) cases are zero, and in others the DET is flat so the error rates at the two thresholds are identical. The lines span 1% and 99% of boostrap replicated FNMR estimates.

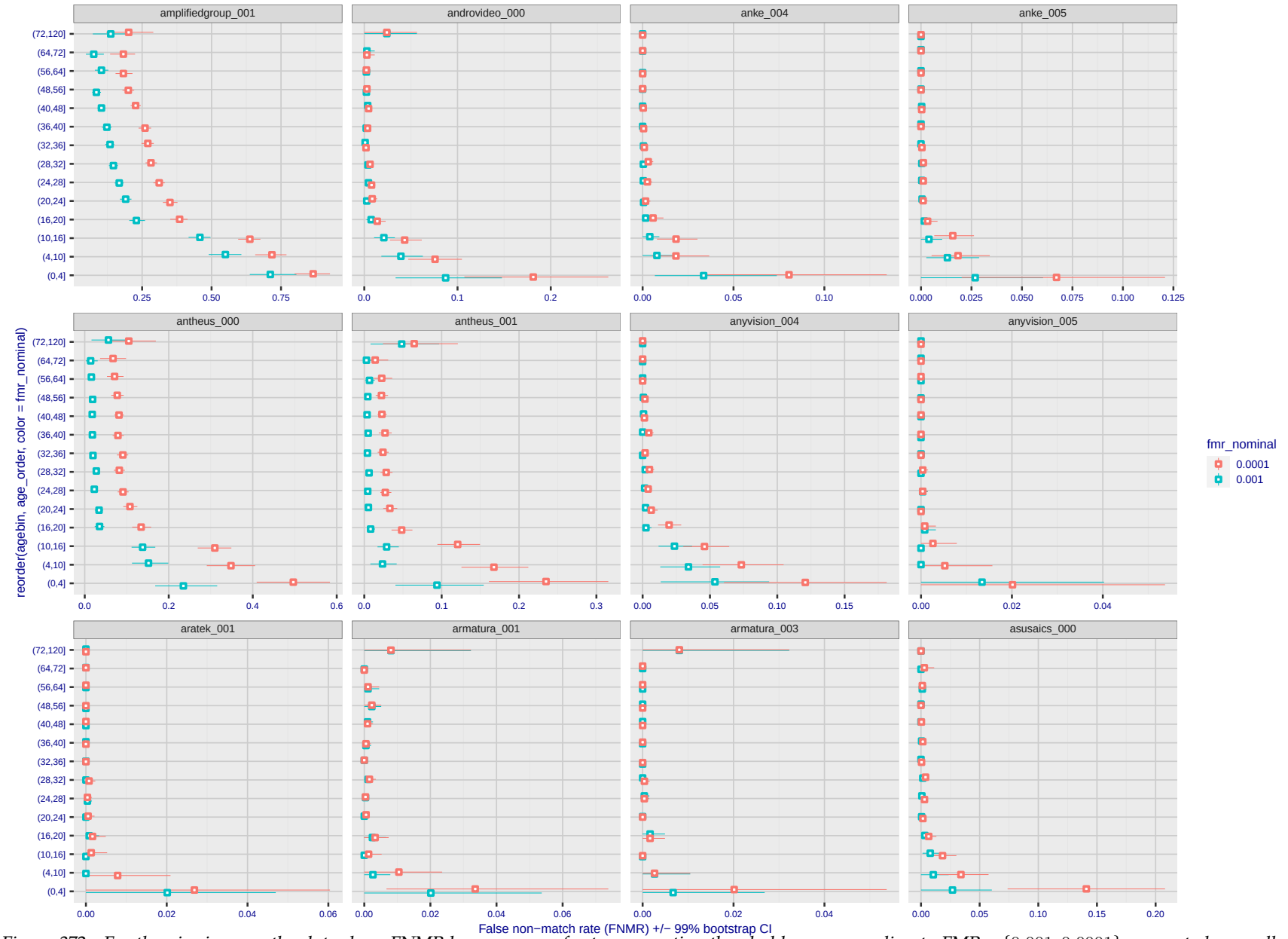

Figure 372: For the visa images, the dots show FNMR by age group for two operating thresholds corresponding to FMR = $\{0.001, 0.0001\}$ computed over all on the order of 10^{10} impostor scores. The FMR in each bin will vary also - see subsequent impostor heatmaps in sec. 3.6.2. Given a pair of face images taken at different times, we assign the comparison to the bin that is the arithmetic average of the subject's ages. This plot shows only the effect of age, not ageing. The number of comparisons in each bin is generally in the thousands, however the first and last bins are computed over 149 and 124 respectively. The error rates in some (adult) cases are zero, and in others the DET is flat so the error rates at the two thresholds are identical. The lines span 1% and 99% of boostrap replicated FNMR estimates.

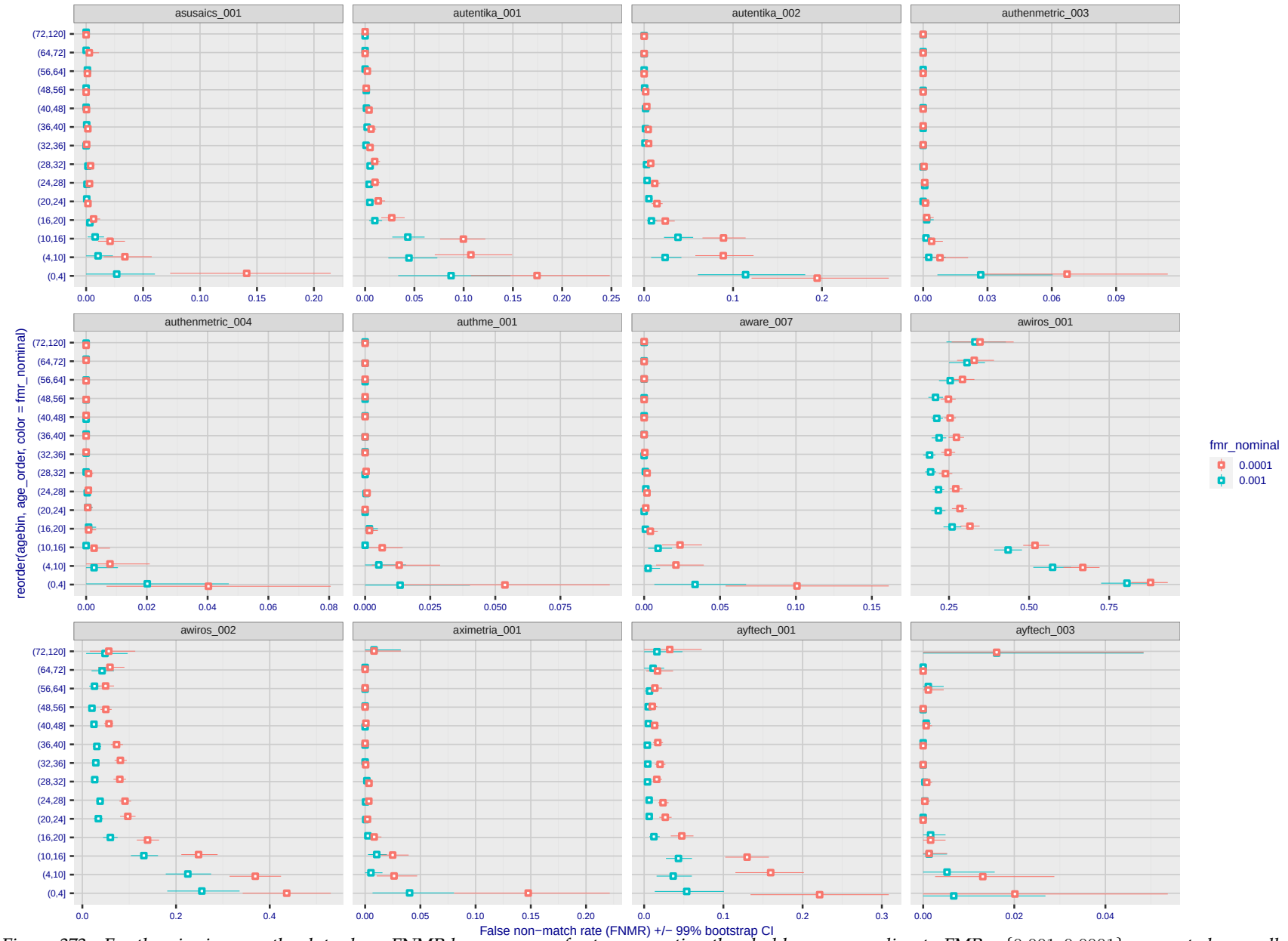

Figure 373: For the visa images, the dots show FNMR by age group for two operating thresholds corresponding to FMR = $\{0.001, 0.0001\}$ computed over all on the order of 10^{10} impostor scores. The FMR in each bin will vary also - see subsequent impostor heatmaps in sec. 3.6.2. Given a pair of face images taken at different times, we assign the comparison to the bin that is the arithmetic average of the subject's ages. This plot shows only the effect of age, not ageing. The number of comparisons in each bin is generally in the thousands, however the first and last bins are computed over 149 and 124 respectively. The error rates in some (adult) cases are zero, and in others the DET is flat so the error rates at the two thresholds are identical. The lines span 1% and 99% of boostrap replicated FNMR estimates.

Figure 374: For the visa images, the dots show FNMR by age group for two operating thresholds corresponding to FMR = $\{0.001, 0.0001\}$ computed over all on the order of 10^{10} impostor scores. The FMR in each bin will vary also - see subsequent impostor heatmaps in sec. 3.6.2. Given a pair of face images taken at different times, we assign the comparison to the bin that is the arithmetic average of the subject's ages. This plot shows only the effect of age, not ageing. The number of comparisons in each bin is generally in the thousands, however the first and last bins are computed over 149 and 124 respectively. The error rates in some (adult) cases are zero, and in others the DET is flat so the error rates at the two thresholds are identical. The lines span 1% and 99% of boostrap replicated FNMR estimates.

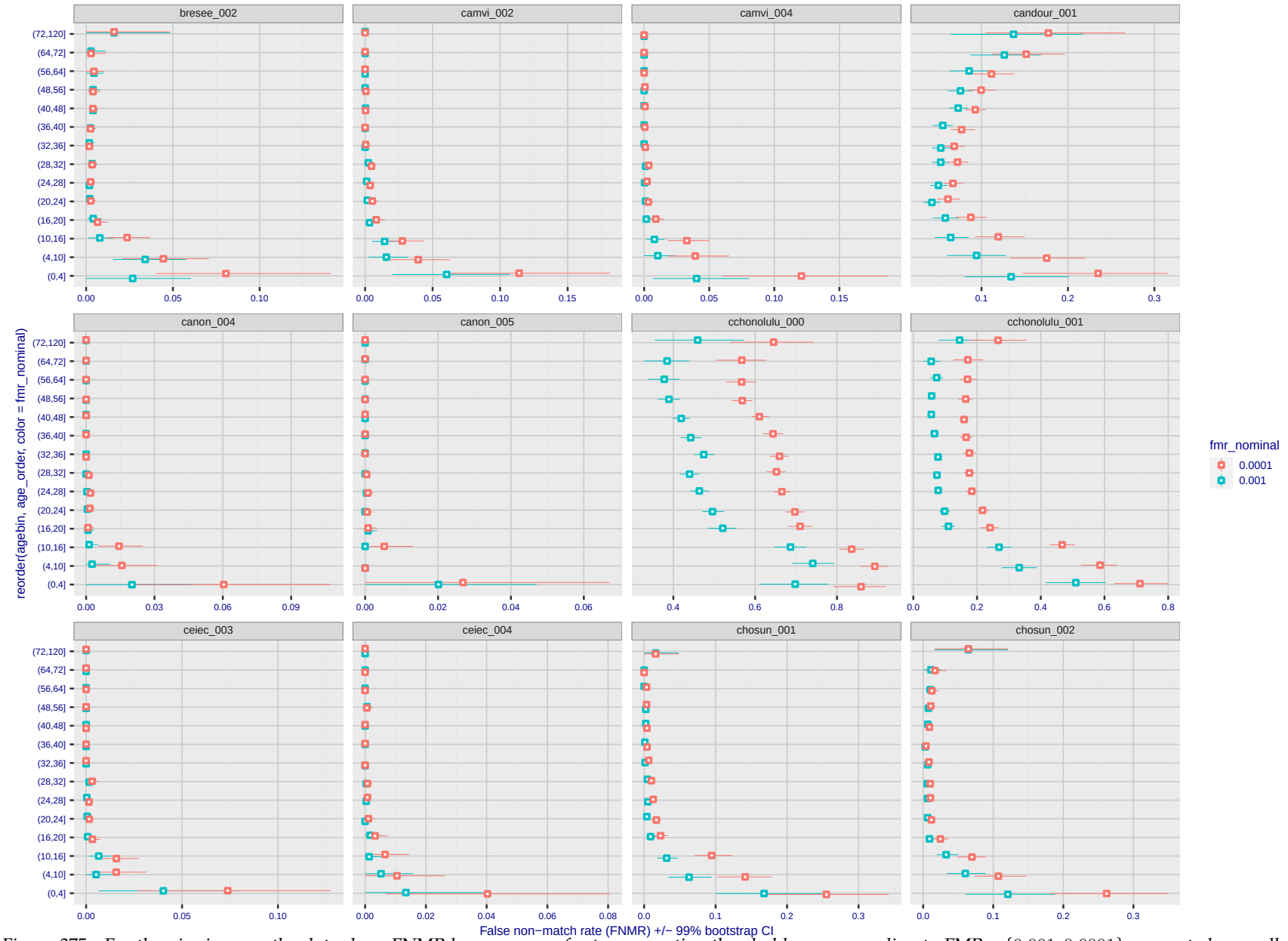

Figure 375: For the visa images, the dots show FNMR by age group for two operating thresholds corresponding to FMR = $\{0.001, 0.0001\}$ computed over all on the order of 10^{10} impostor scores. The FMR in each bin will vary also - see subsequent impostor heatmaps in sec. 3.6.2. Given a pair of face images taken at different times, we assign the comparison to the bin that is the arithmetic average of the subject's ages. This plot shows only the effect of age, not ageing. The number of comparisons in each bin is generally in the thousands, however the first and last bins are computed over 149 and 124 respectively. The error rates in some (adult) cases are zero, and in others the DET is flat so the error rates at the two thresholds are identical. The lines span 1% and 99% of boostrap replicated FNMR estimates.

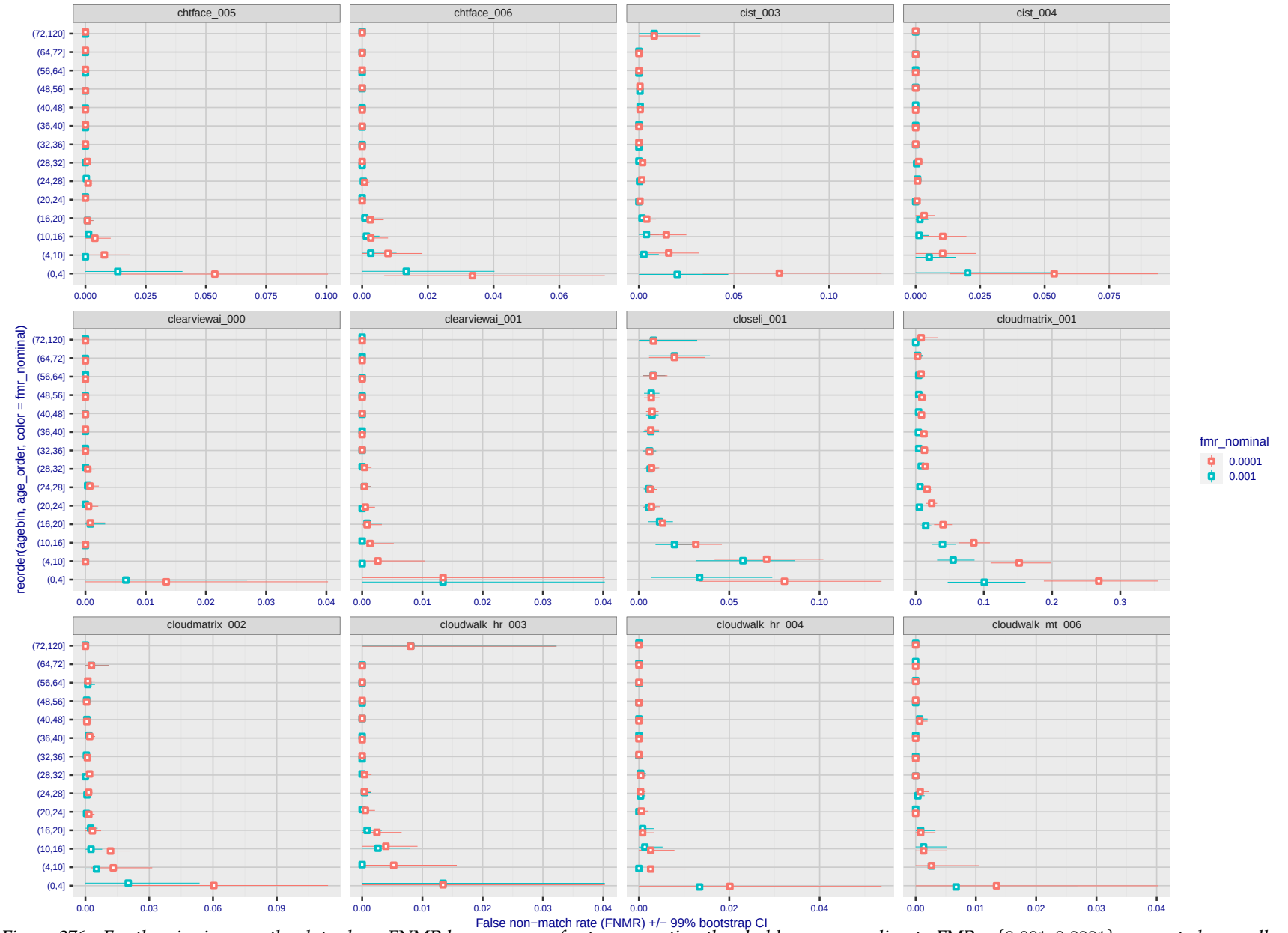

Figure 376: For the visa images, the dots show FNMR by age group for two operating thresholds corresponding to FMR = $\{0.001, 0.0001\}$ computed over all on the order of 10^{10} impostor scores. The FMR in each bin will vary also - see subsequent impostor heatmaps in sec. 3.6.2. Given a pair of face images taken at different times, we assign the comparison to the bin that is the arithmetic average of the subject's ages. This plot shows only the effect of age, not ageing. The number of comparisons in each bin is generally in the thousands, however the first and last bins are computed over 149 and 124 respectively. The error rates in some (adult) cases are zero, and in others the DET is flat so the error rates at the two thresholds are identical. The lines span 1% and 99% of boostrap replicated FNMR estimates.

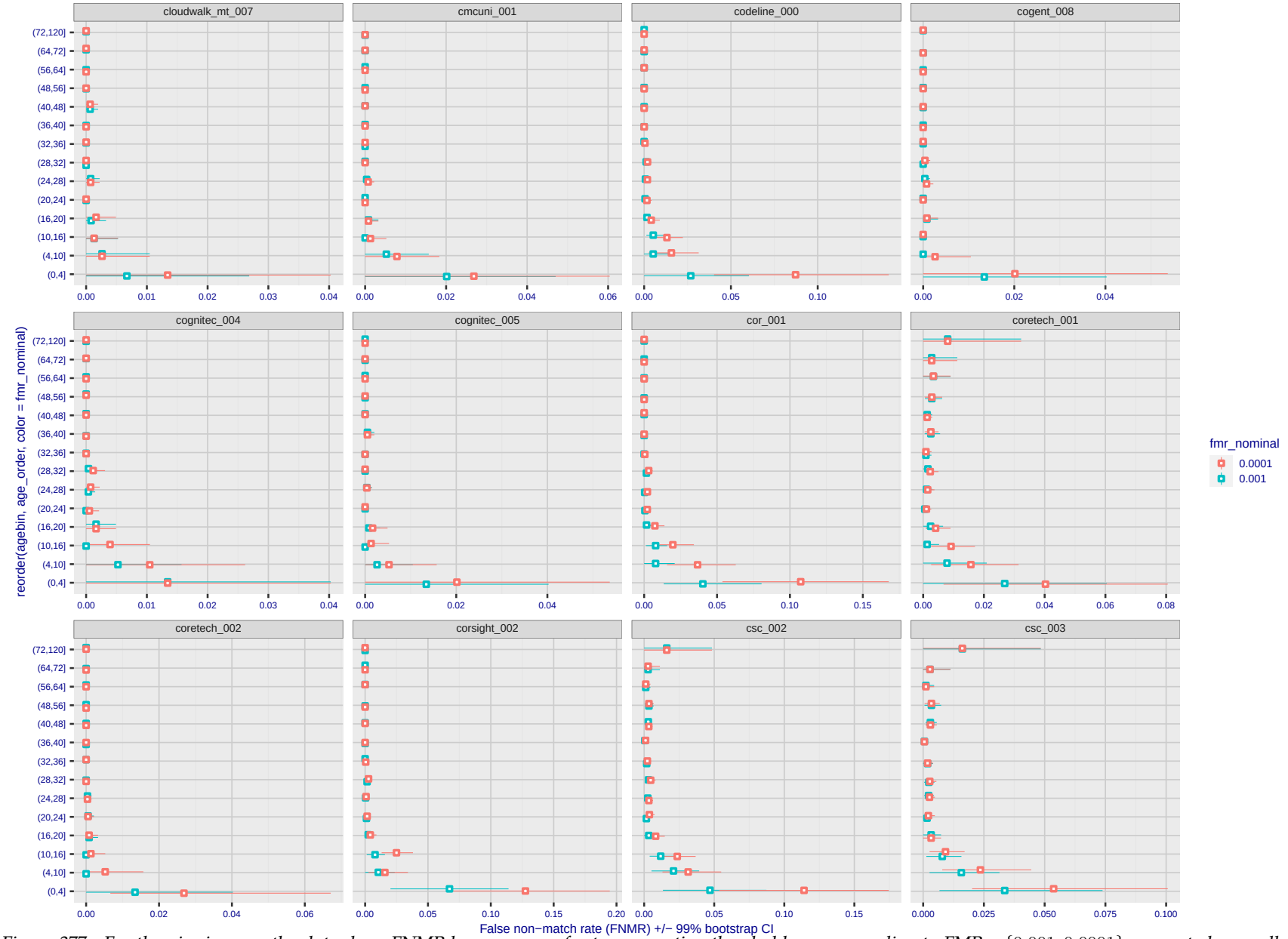

Figure 377: For the visa images, the dots show FNMR by age group for two operating thresholds corresponding to FMR = $\{0.001, 0.0001\}$ computed over all on the order of 10^{10} impostor scores. The FMR in each bin will vary also - see subsequent impostor heatmaps in sec. 3.6.2. Given a pair of face images taken at different times, we assign the comparison to the bin that is the arithmetic average of the subject's ages. This plot shows only the effect of age, not ageing. The number of comparisons in each bin is generally in the thousands, however the first and last bins are computed over 149 and 124 respectively. The error rates in some (adult) cases are zero, and in others the DET is flat so the error rates at the two thresholds are identical. The lines span 1% and 99% of boostrap replicated FNMR estimates.

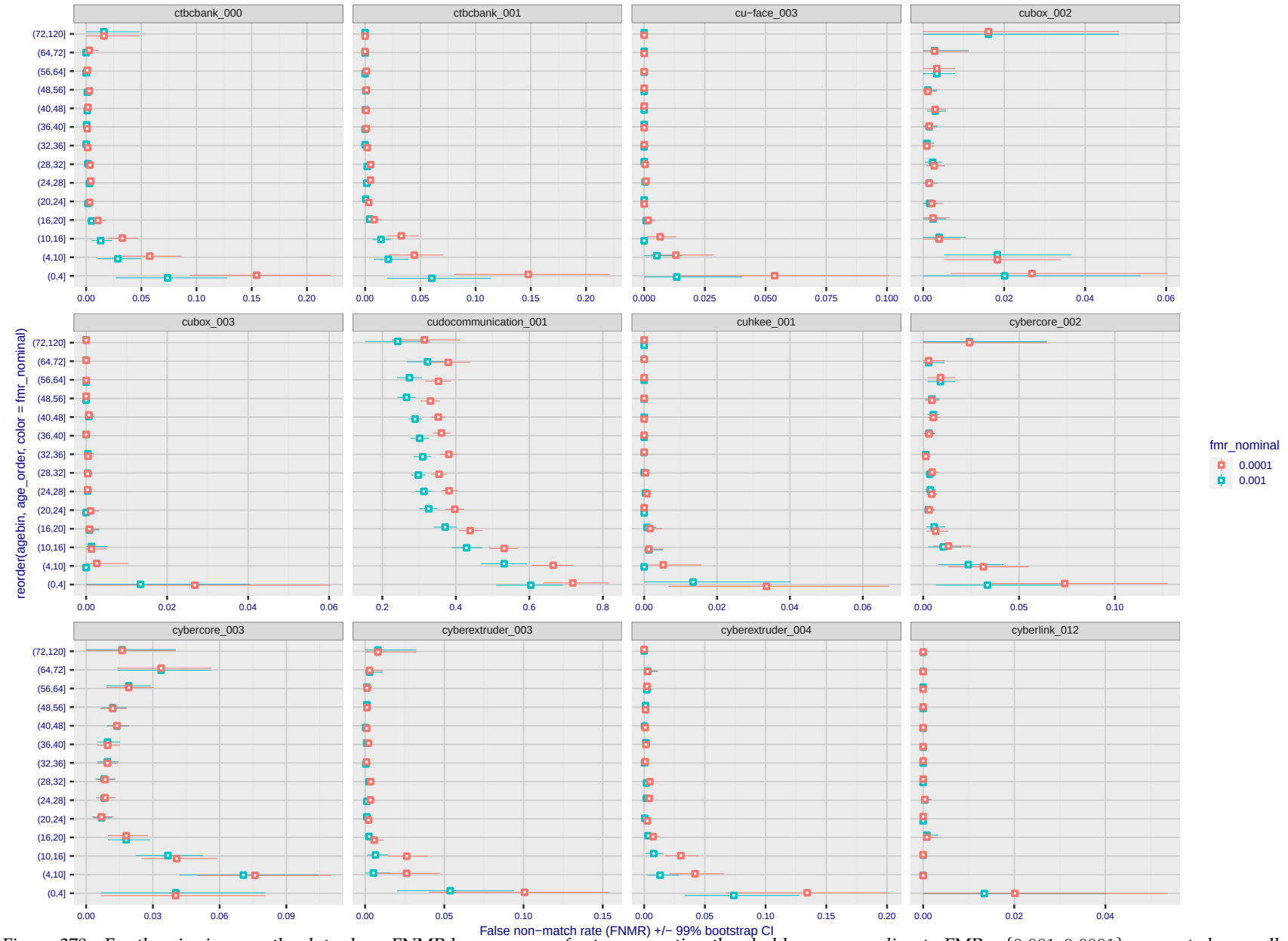

Figure 378: For the visa images, the dots show FNMR by age group for two operating thresholds corresponding to FMR = $\{0.001, 0.0001\}$ computed over all on the order of 10^{10} impostor scores. The FMR in each bin will vary also - see subsequent impostor heatmaps in sec. 3.6.2. Given a pair of face images taken at different times, we assign the comparison to the bin that is the arithmetic average of the subject's ages. This plot shows only the effect of age, not ageing. The number of comparisons in each bin is generally in the thousands, however the first and last bins are computed over 149 and 124 respectively. The error rates in some (adult) cases are zero, and in others the DET is flat so the error rates at the two thresholds are identical. The lines span 1% and 99% of boostrap replicated FNMR estimates.

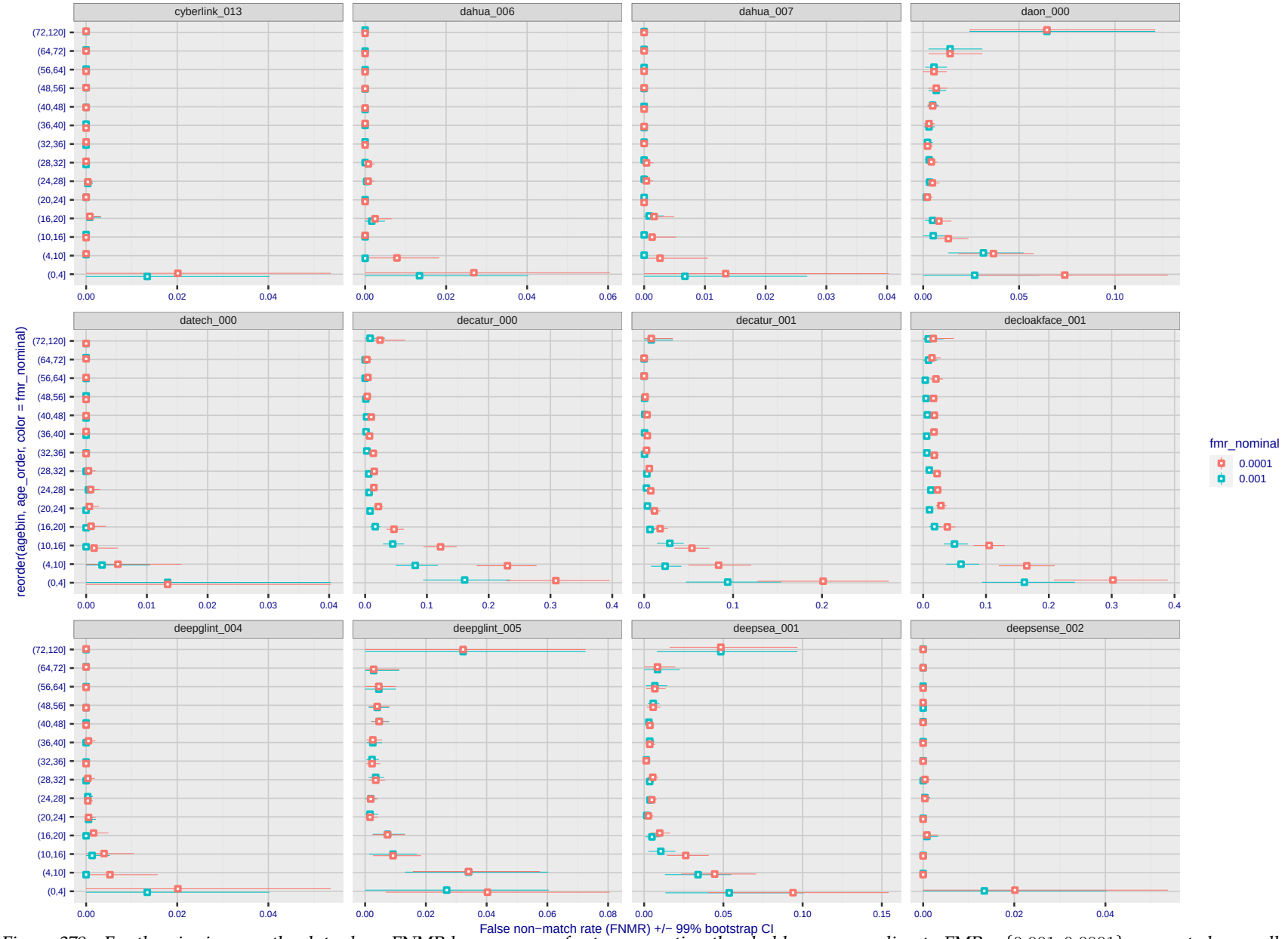

Figure 379: For the visa images, the dots show FNMR by age group for two operating thresholds corresponding to FMR = $\{0.001, 0.0001\}$ computed over all on the order of 10^{10} impostor scores. The FMR in each bin will vary also - see subsequent impostor heatmaps in sec. 3.6.2. Given a pair of face images taken at different times, we assign the comparison to the bin that is the arithmetic average of the subject's ages. This plot shows only the effect of age, not ageing. The number of comparisons in each bin is generally in the thousands, however the first and last bins are computed over 149 and 124 respectively. The error rates in some (adult) cases are zero, and in others the DET is flat so the error rates at the two thresholds are identical. The lines span 1% and 99% of boostrap replicated FNMR estimates.

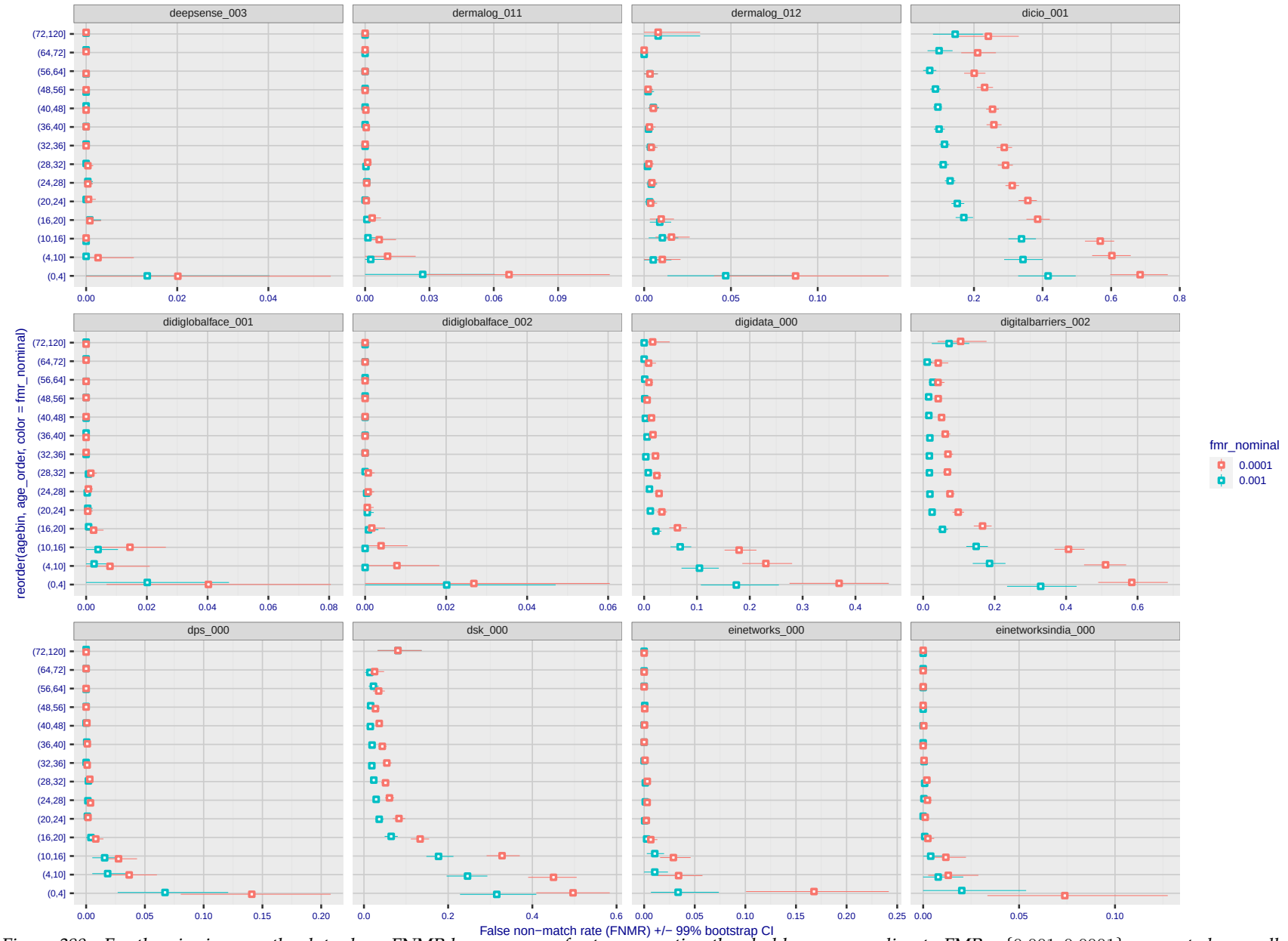

Figure 380: For the visa images, the dots show FNMR by age group for two operating thresholds corresponding to FMR = $\{0.001, 0.0001\}$ computed over all on the order of 10^{10} impostor scores. The FMR in each bin will vary also - see subsequent impostor heatmaps in sec. 3.6.2. Given a pair of face images taken at different times, we assign the comparison to the bin that is the arithmetic average of the subject's ages. This plot shows only the effect of age, not ageing. The number of comparisons in each bin is generally in the thousands, however the first and last bins are computed over 149 and 124 respectively. The error rates in some (adult) cases are zero, and in others the DET is flat so the error rates at the two thresholds are identical. The lines span 1% and 99% of boostrap replicated FNMR estimates.

Figure 381: For the visa images, the dots show FNMR by age group for two operating thresholds corresponding to FMR = $\{0.001, 0.0001\}$ computed over all on the order of 10^{10} impostor scores. The FMR in each bin will vary also - see subsequent impostor heatmaps in sec. 3.6.2. Given a pair of face images taken at different times, we assign the comparison to the bin that is the arithmetic average of the subject's ages. This plot shows only the effect of age, not ageing. The number of comparisons in each bin is generally in the thousands, however the first and last bins are computed over 149 and 124 respectively. The error rates in some (adult) cases are zero, and in others the DET is flat so the error rates at the two thresholds are identical. The lines span 1% and 99% of boostrap replicated FNMR estimates.

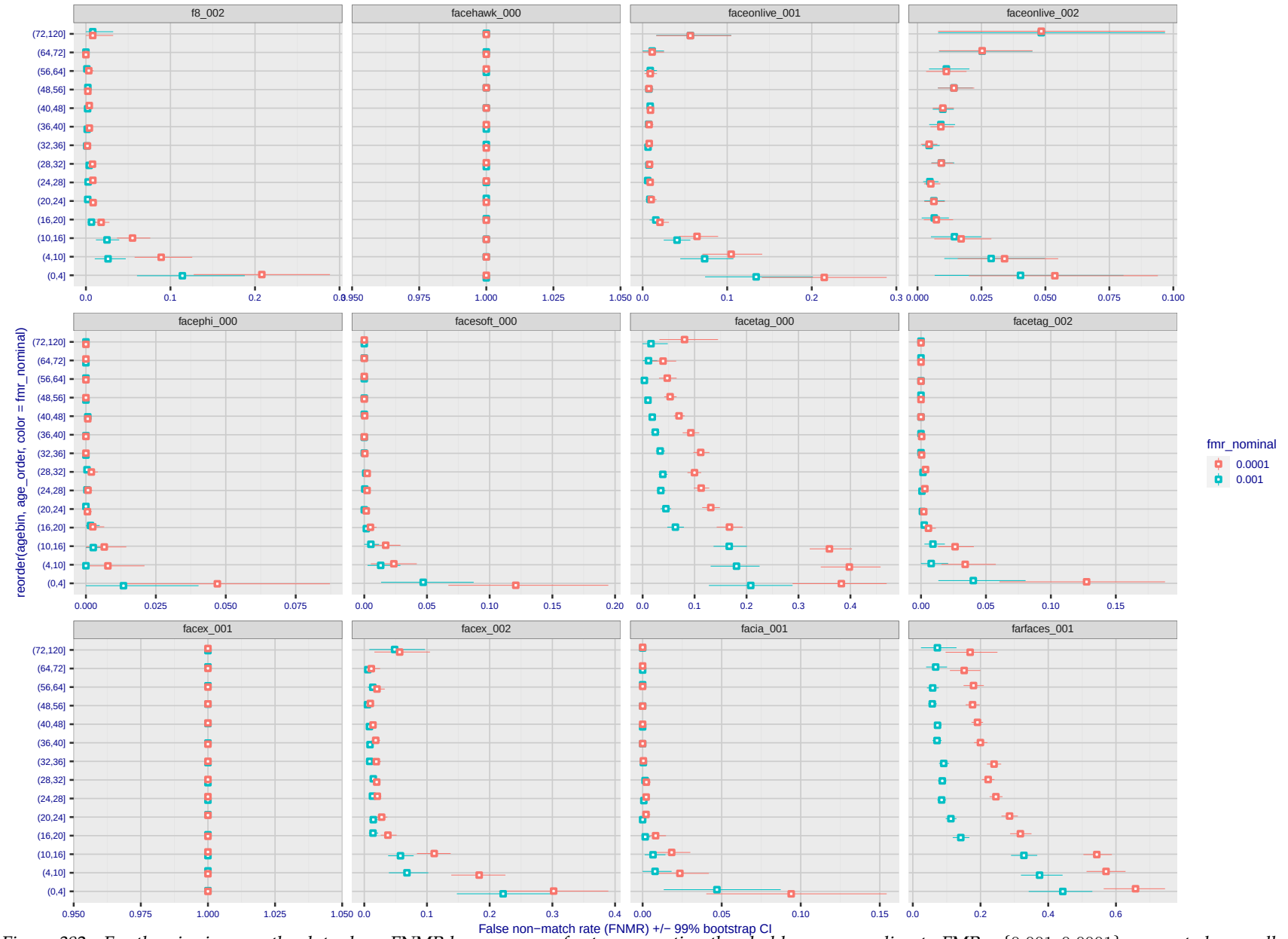

Figure 382: For the visa images, the dots show FNMR by age group for two operating thresholds corresponding to FMR = $\{0.001, 0.0001\}$ computed over all on the order of 10^{10} impostor scores. The FMR in each bin will vary also - see subsequent impostor heatmaps in sec. 3.6.2. Given a pair of face images taken at different times, we assign the comparison to the bin that is the arithmetic average of the subject's ages. This plot shows only the effect of age, not ageing. The number of comparisons in each bin is generally in the thousands, however the first and last bins are computed over 149 and 124 respectively. The error rates in some (adult) cases are zero, and in others the DET is flat so the error rates at the two thresholds are identical. The lines span 1% and 99% of boostrap replicated FNMR estimates.

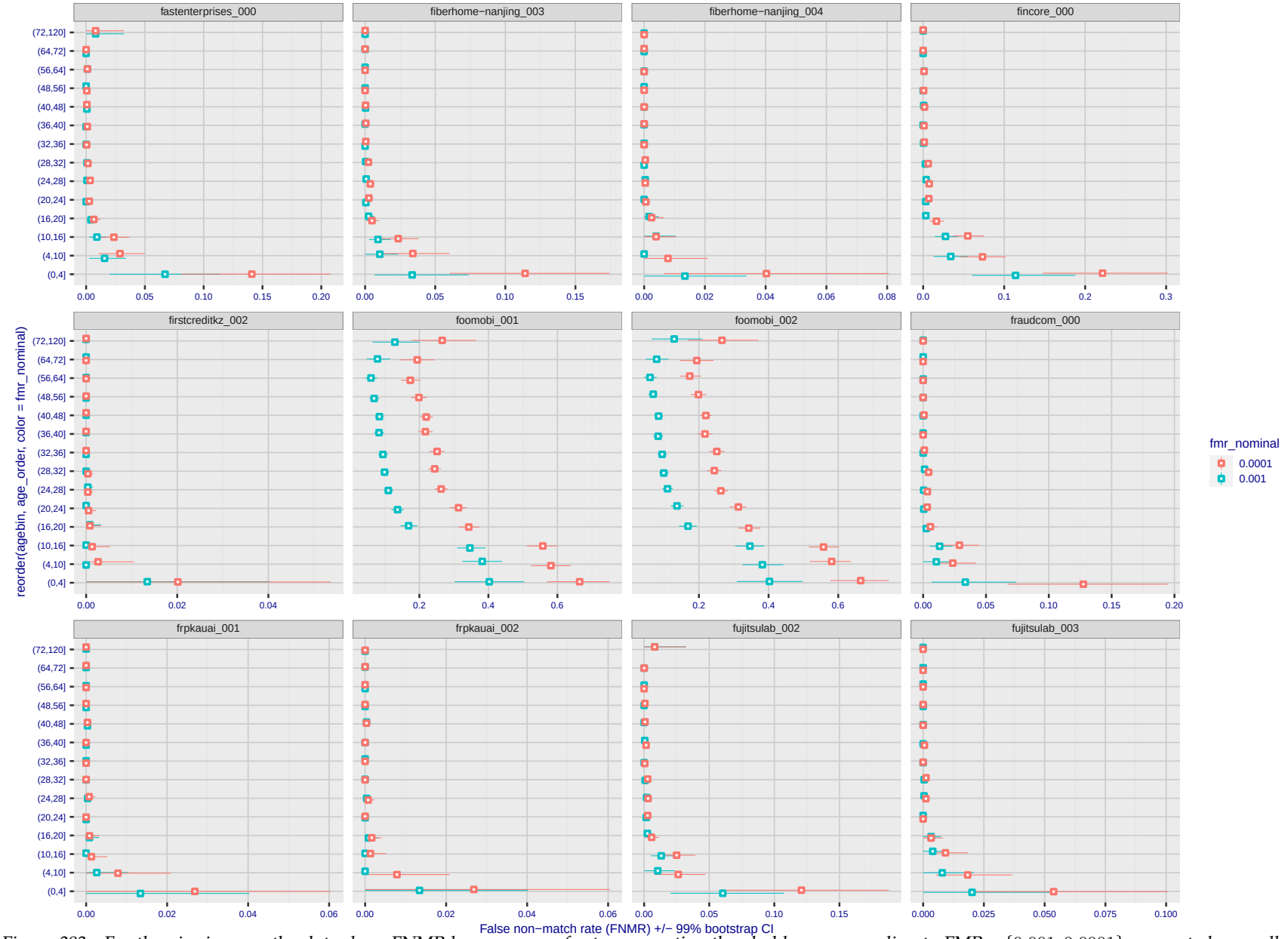

Figure 383: For the visa images, the dots show FNMR by age group for two operating thresholds corresponding to FMR = $\{0.001, 0.0001\}$ computed over all on the order of 10^{10} impostor scores. The FMR in each bin will vary also - see subsequent impostor heatmaps in sec. 3.6.2. Given a pair of face images taken at different times, we assign the comparison to the bin that is the arithmetic average of the subject's ages. This plot shows only the effect of age, not ageing. The number of comparisons in each bin is generally in the thousands, however the first and last bins are computed over 149 and 124 respectively. The error rates in some (adult) cases are zero, and in others the DET is flat so the error rates at the two thresholds are identical. The lines span 1% and 99% of boostrap replicated FNMR estimates.

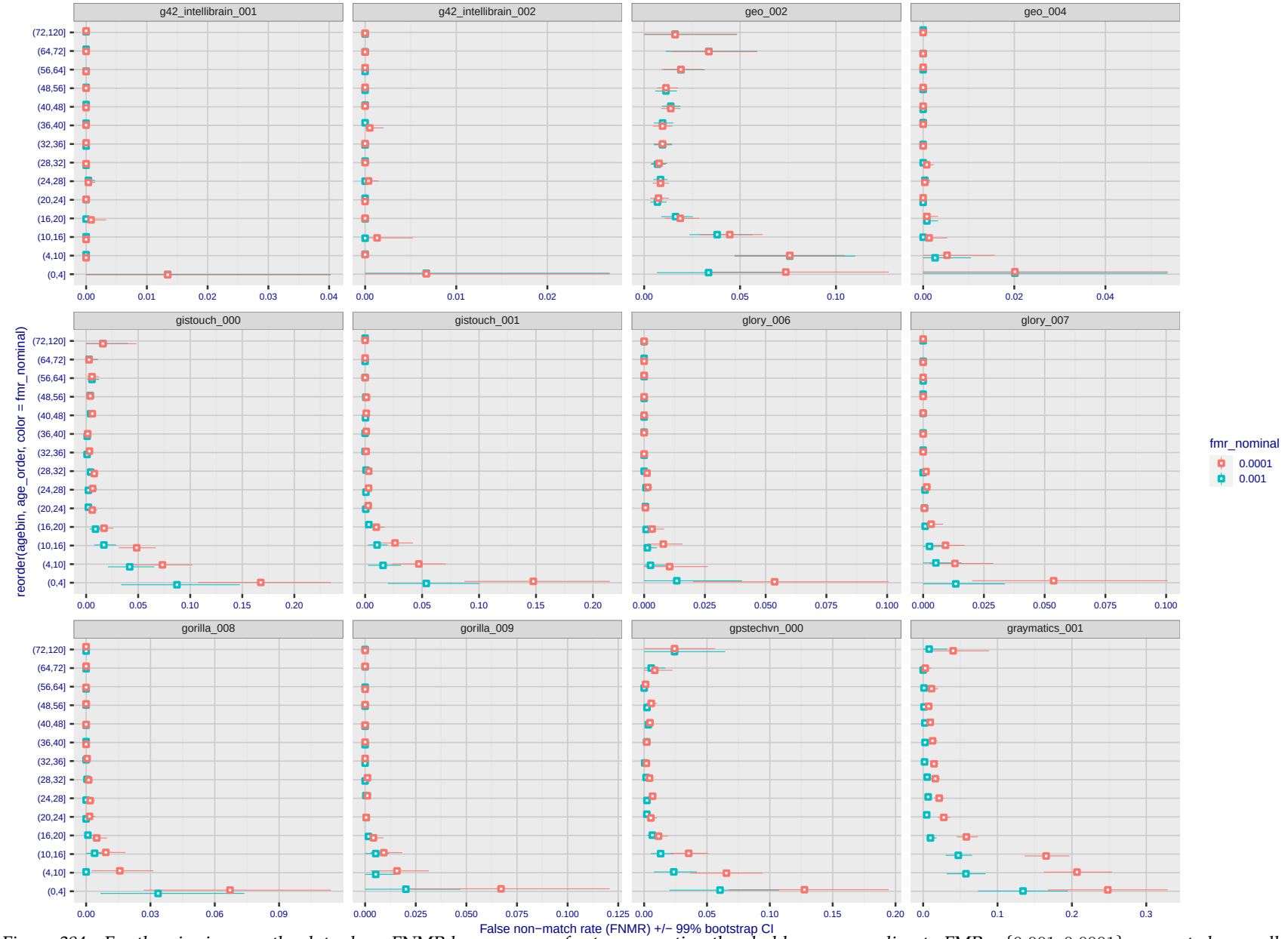

Figure 384: For the visa images, the dots show FNMR by age group for two operating thresholds corresponding to FMR = $\{0.001, 0.0001\}$ computed over all on the order of 10^{10} impostor scores. The FMR in each bin will vary also - see subsequent impostor heatmaps in sec. 3.6.2. Given a pair of face images taken at different times, we assign the comparison to the bin that is the arithmetic average of the subject's ages. This plot shows only the effect of age, not ageing. The number of comparisons in each bin is generally in the thousands, however the first and last bins are computed over 149 and 124 respectively. The error rates in some (adult) cases are zero, and in others the DET is flat so the error rates at the two thresholds are identical. The lines span 1% and 99% of boostrap replicated FNMR estimates.

Figure 385: For the visa images, the dots show FNMR by age group for two operating thresholds corresponding to FMR = $\{0.001, 0.0001\}$ computed over all on the order of 10^{10} impostor scores. The FMR in each bin will vary also - see subsequent impostor heatmaps in sec. 3.6.2. Given a pair of face images taken at different times, we assign the comparison to the bin that is the arithmetic average of the subject's ages. This plot shows only the effect of age, not ageing. The number of comparisons in each bin is generally in the thousands, however the first and last bins are computed over 149 and 124 respectively. The error rates in some (adult) cases are zero, and in others the DET is flat so the error rates at the two thresholds are identical. The lines span 1% and 99% of boostrap replicated FNMR estimates.

Figure 386: For the visa images, the dots show FNMR by age group for two operating thresholds corresponding to FMR = $\{0.001, 0.0001\}$ computed over all on the order of 10^{10} impostor scores. The FMR in each bin will vary also - see subsequent impostor heatmaps in sec. 3.6.2. Given a pair of face images taken at different times, we assign the comparison to the bin that is the arithmetic average of the subject's ages. This plot shows only the effect of age, not ageing. The number of comparisons in each bin is generally in the thousands, however the first and last bins are computed over 149 and 124 respectively. The error rates in some (adult) cases are zero, and in others the DET is flat so the error rates at the two thresholds are identical. The lines span 1% and 99% of boostrap replicated FNMR estimates.

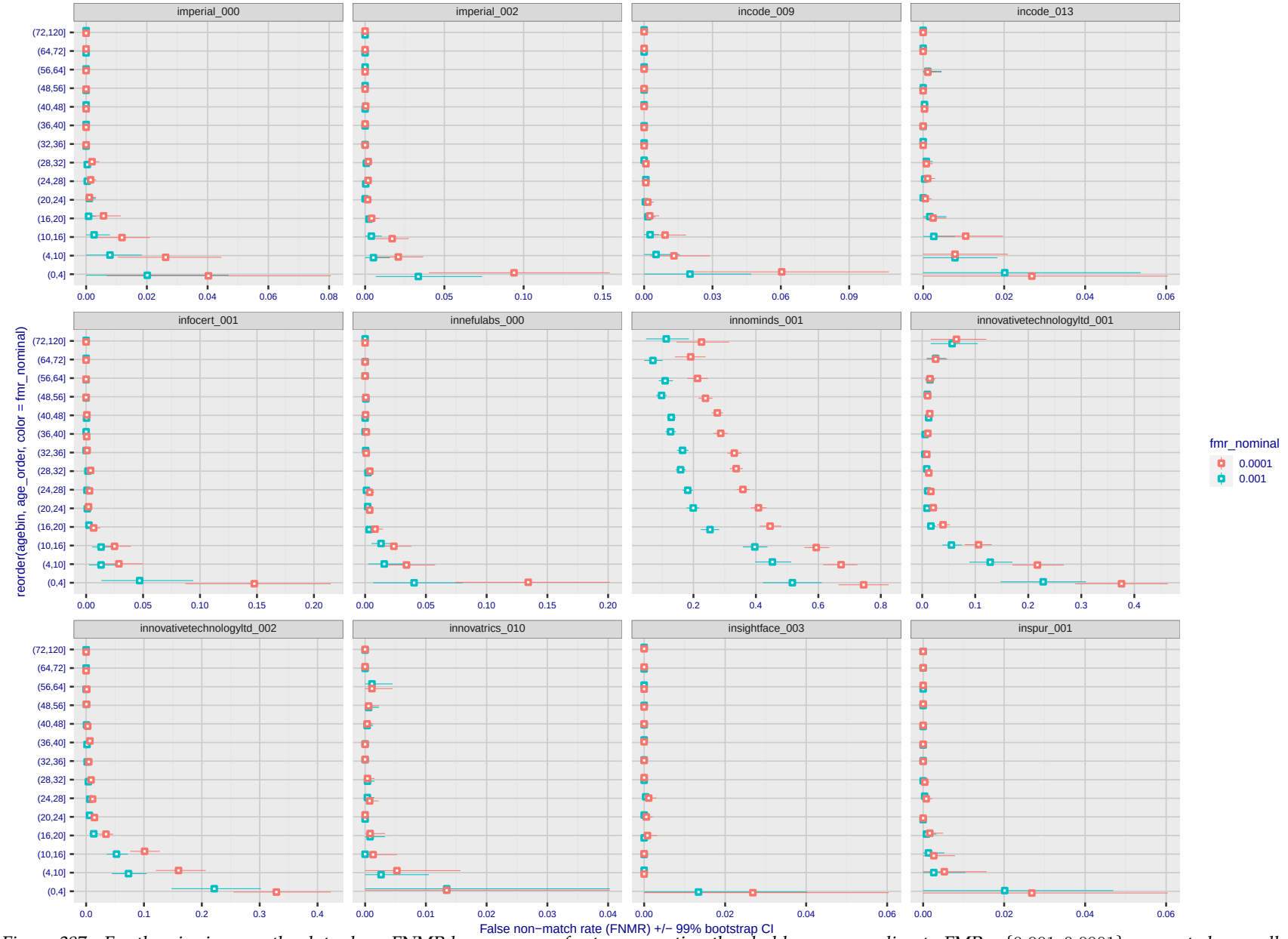

Figure 387: For the visa images, the dots show FNMR by age group for two operating thresholds corresponding to FMR = $\{0.001, 0.0001\}$ computed over all on the order of 10^{10} impostor scores. The FMR in each bin will vary also - see subsequent impostor heatmaps in sec. 3.6.2. Given a pair of face images taken at different times, we assign the comparison to the bin that is the arithmetic average of the subject's ages. This plot shows only the effect of age, not ageing. The number of comparisons in each bin is generally in the thousands, however the first and last bins are computed over 149 and 124 respectively. The error rates in some (adult) cases are zero, and in others the DET is flat so the error rates at the two thresholds are identical. The lines span 1% and 99% of boostrap replicated FNMR estimates.

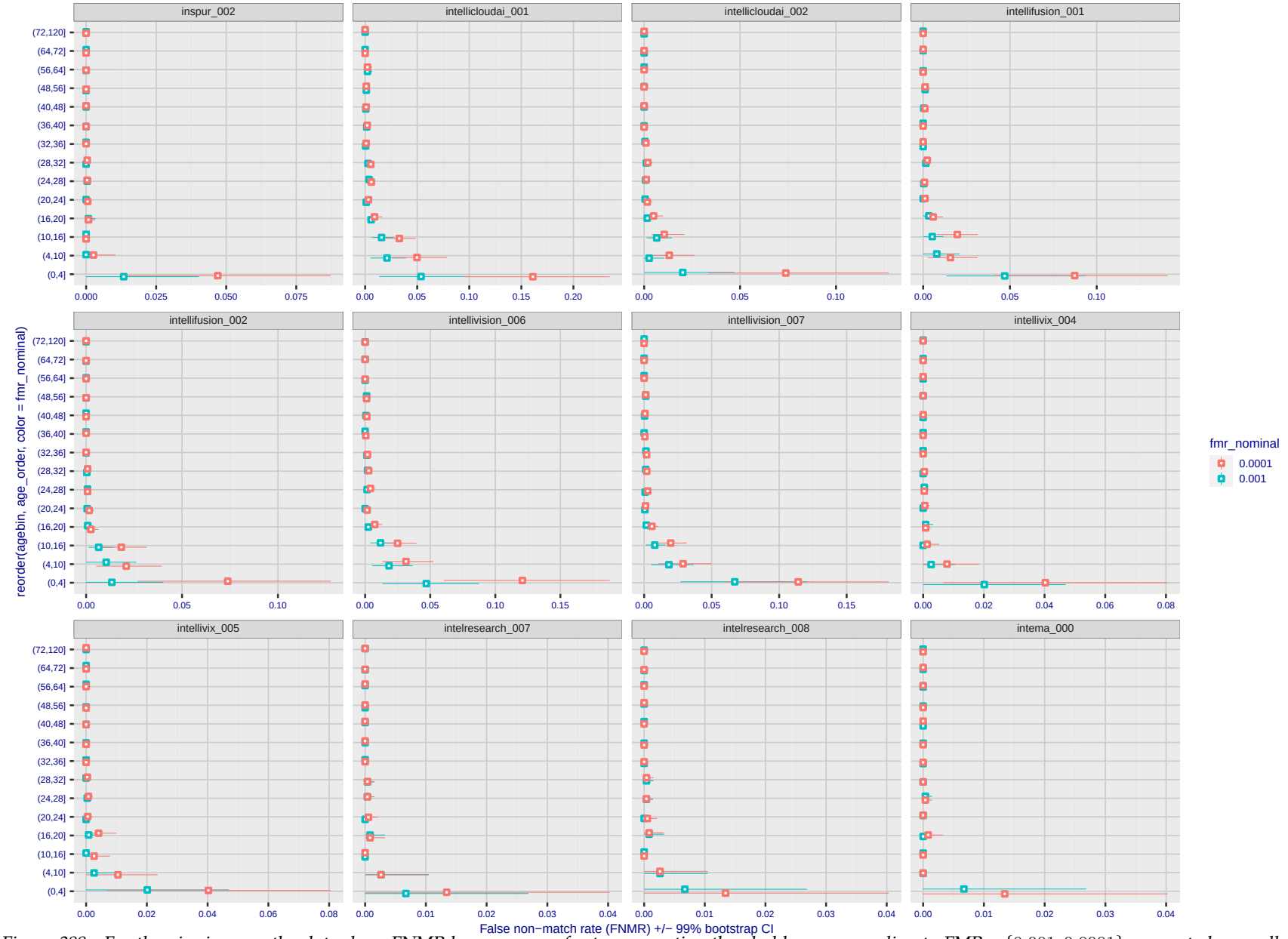

Figure 388: For the visa images, the dots show FNMR by age group for two operating thresholds corresponding to FMR = $\{0.001, 0.0001\}$ computed over all on the order of 10^{10} impostor scores. The FMR in each bin will vary also - see subsequent impostor heatmaps in sec. 3.6.2. Given a pair of face images taken at different times, we assign the comparison to the bin that is the arithmetic average of the subject's ages. This plot shows only the effect of age, not ageing. The number of comparisons in each bin is generally in the thousands, however the first and last bins are computed over 149 and 124 respectively. The error rates in some (adult) cases are zero, and in others the DET is flat so the error rates at the two thresholds are identical. The lines span 1% and 99% of boostrap replicated FNMR estimates.

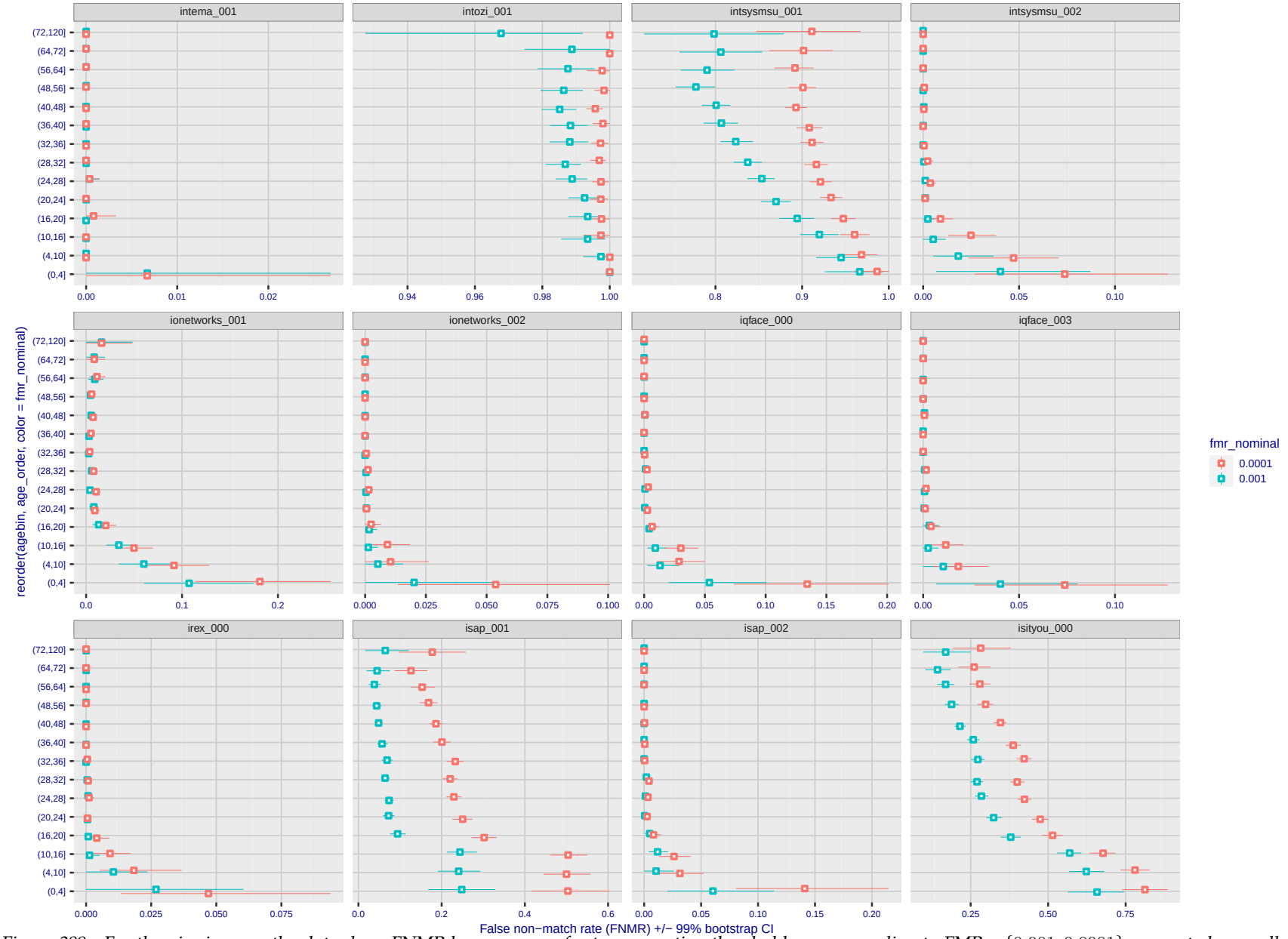

Figure 389: For the visa images, the dots show FNMR by age group for two operating thresholds corresponding to FMR = $\{0.001, 0.0001\}$ computed over all on the order of 10^{10} impostor scores. The FMR in each bin will vary also - see subsequent impostor heatmaps in sec. 3.6.2. Given a pair of face images taken at different times, we assign the comparison to the bin that is the arithmetic average of the subject's ages. This plot shows only the effect of age, not ageing. The number of comparisons in each bin is generally in the thousands, however the first and last bins are computed over 149 and 124 respectively. The error rates in some (adult) cases are zero, and in others the DET is flat so the error rates at the two thresholds are identical. The lines span 1% and 99% of boostrap replicated FNMR estimates.

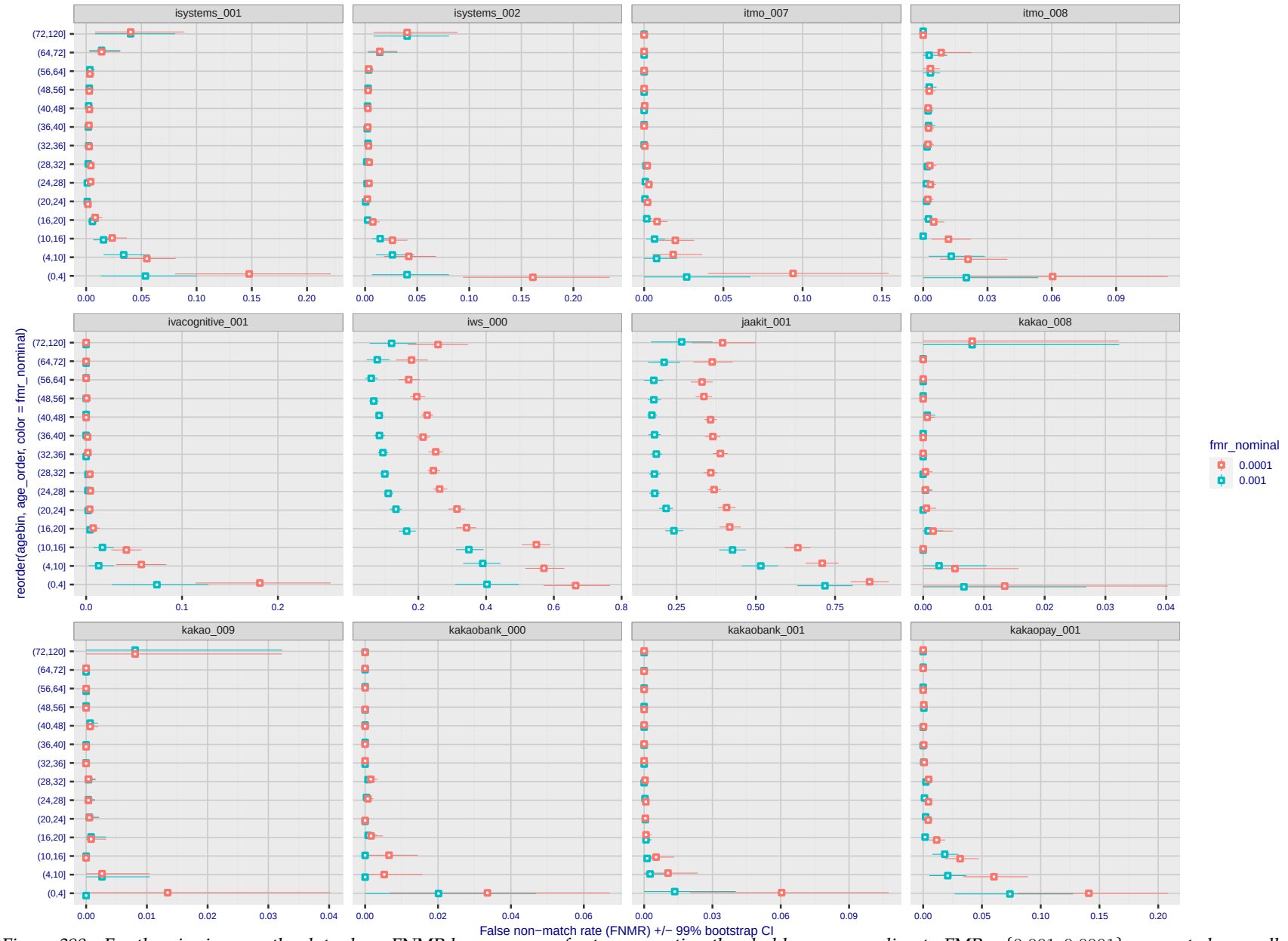

Figure 390: For the visa images, the dots show FNMR by age group for two operating thresholds corresponding to FMR = $\{0.001, 0.0001\}$ computed over all on the order of 10^{10} impostor scores. The FMR in each bin will vary also - see subsequent impostor heatmaps in sec. 3.6.2. Given a pair of face images taken at different times, we assign the comparison to the bin that is the arithmetic average of the subject's ages. This plot shows only the effect of age, not ageing. The number of comparisons in each bin is generally in the thousands, however the first and last bins are computed over 149 and 124 respectively. The error rates in some (adult) cases are zero, and in others the DET is flat so the error rates at the two thresholds are identical. The lines span 1% and 99% of boostrap replicated FNMR estimates.

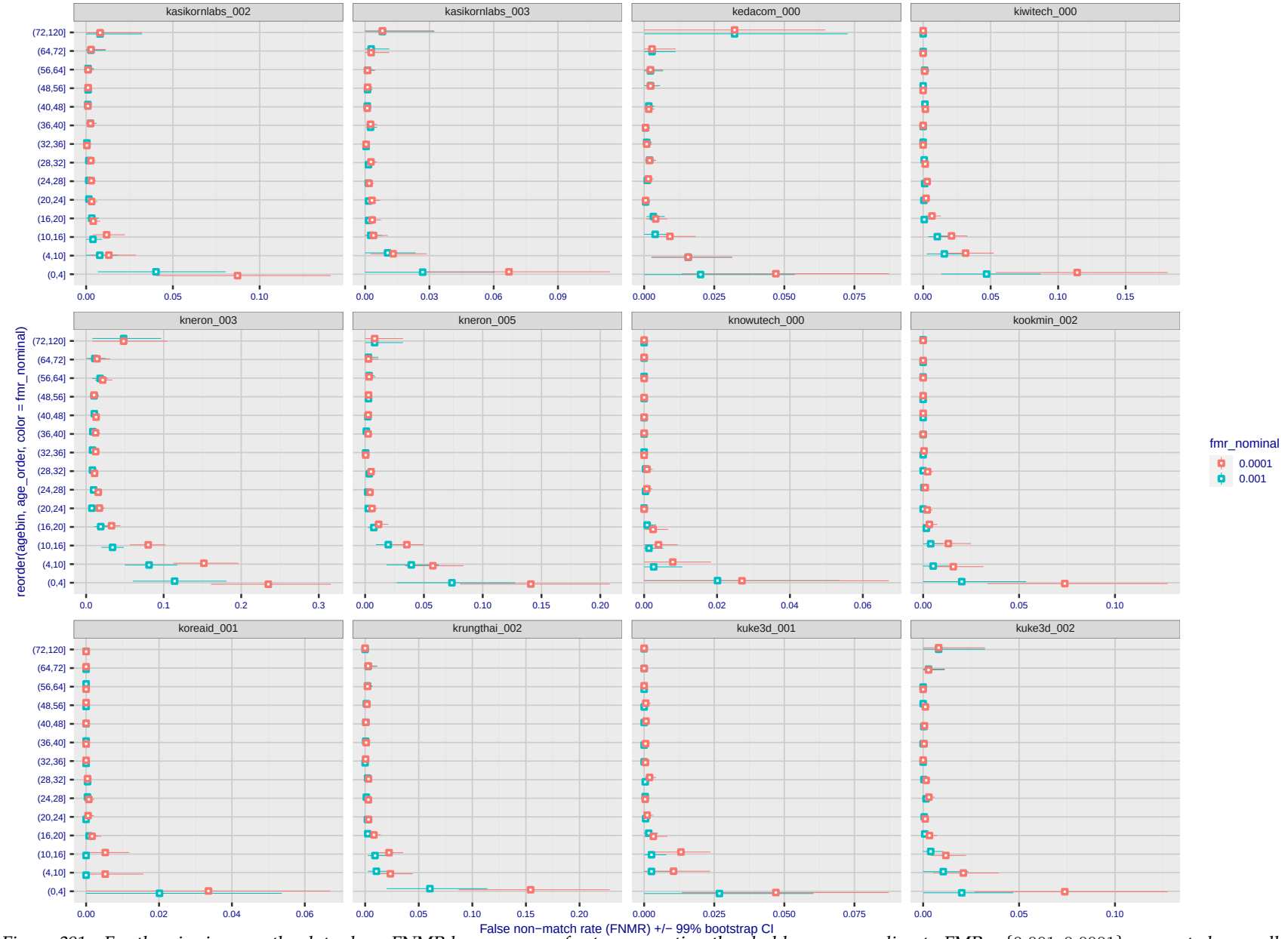

Figure 391: For the visa images, the dots show FNMR by age group for two operating thresholds corresponding to FMR = $\{0.001, 0.0001\}$ computed over all on the order of 10^{10} impostor scores. The FMR in each bin will vary also - see subsequent impostor heatmaps in sec. 3.6.2. Given a pair of face images taken at different times, we assign the comparison to the bin that is the arithmetic average of the subject's ages. This plot shows only the effect of age, not ageing. The number of comparisons in each bin is generally in the thousands, however the first and last bins are computed over 149 and 124 respectively. The error rates in some (adult) cases are zero, and in others the DET is flat so the error rates at the two thresholds are identical. The lines span 1% and 99% of boostrap replicated FNMR estimates.

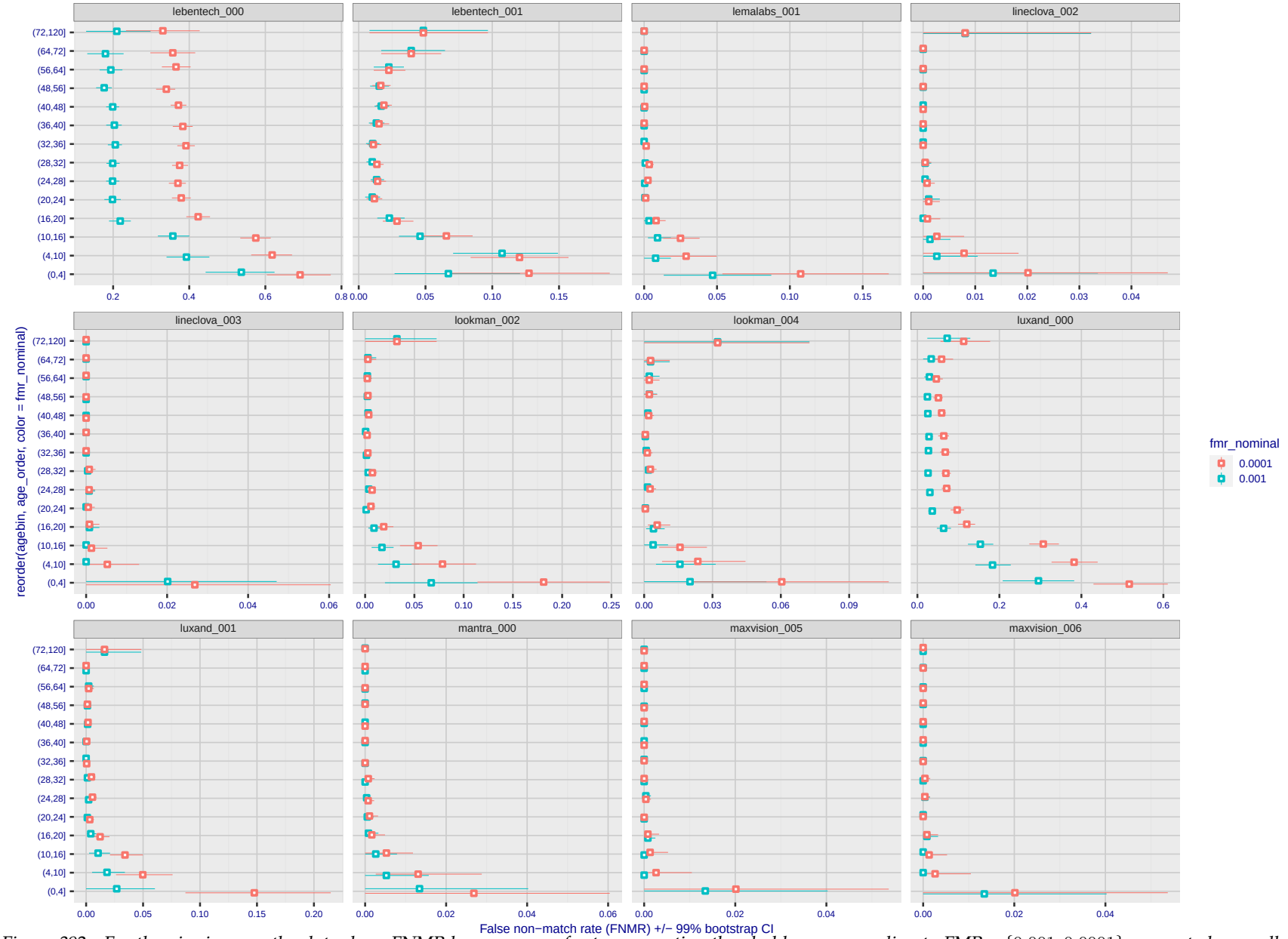

Figure 392: For the visa images, the dots show FNMR by age group for two operating thresholds corresponding to FMR = $\{0.001, 0.0001\}$ computed over all on the order of 10^{10} impostor scores. The FMR in each bin will vary also - see subsequent impostor heatmaps in sec. 3.6.2. Given a pair of face images taken at different times, we assign the comparison to the bin that is the arithmetic average of the subject's ages. This plot shows only the effect of age, not ageing. The number of comparisons in each bin is generally in the thousands, however the first and last bins are computed over 149 and 124 respectively. The error rates in some (adult) cases are zero, and in others the DET is flat so the error rates at the two thresholds are identical. The lines span 1% and 99% of boostrap replicated FNMR estimates.

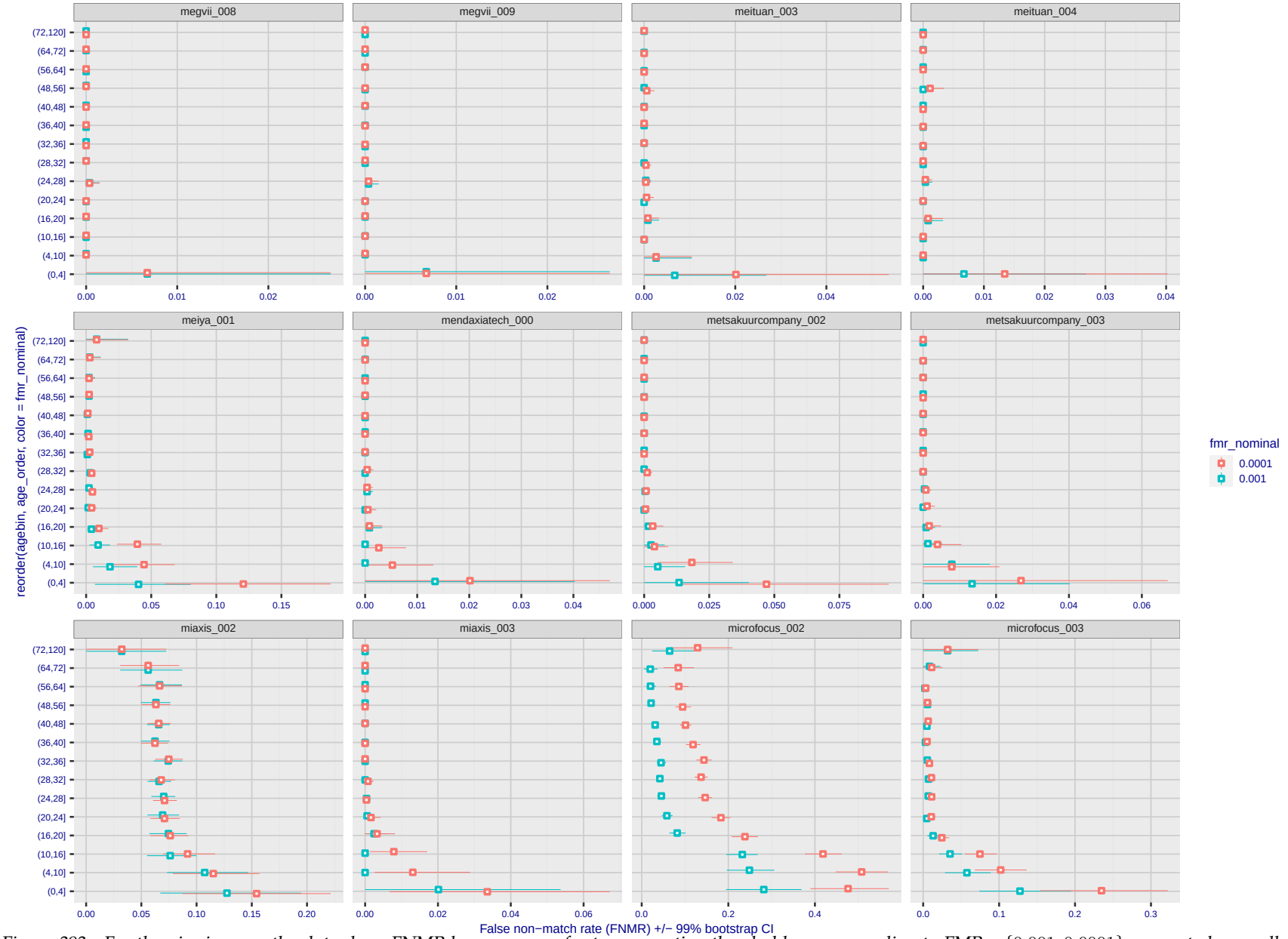

Figure 393: For the visa images, the dots show FNMR by age group for two operating thresholds corresponding to FMR = $\{0.001, 0.0001\}$ computed over all on the order of 10^{10} impostor scores. The FMR in each bin will vary also - see subsequent impostor heatmaps in sec. 3.6.2. Given a pair of face images taken at different times, we assign the comparison to the bin that is the arithmetic average of the subject's ages. This plot shows only the effect of age, not ageing. The number of comparisons in each bin is generally in the thousands, however the first and last bins are computed over 149 and 124 respectively. The error rates in some (adult) cases are zero, and in others the DET is flat so the error rates at the two thresholds are identical. The lines span 1% and 99% of boostrap replicated FNMR estimates.

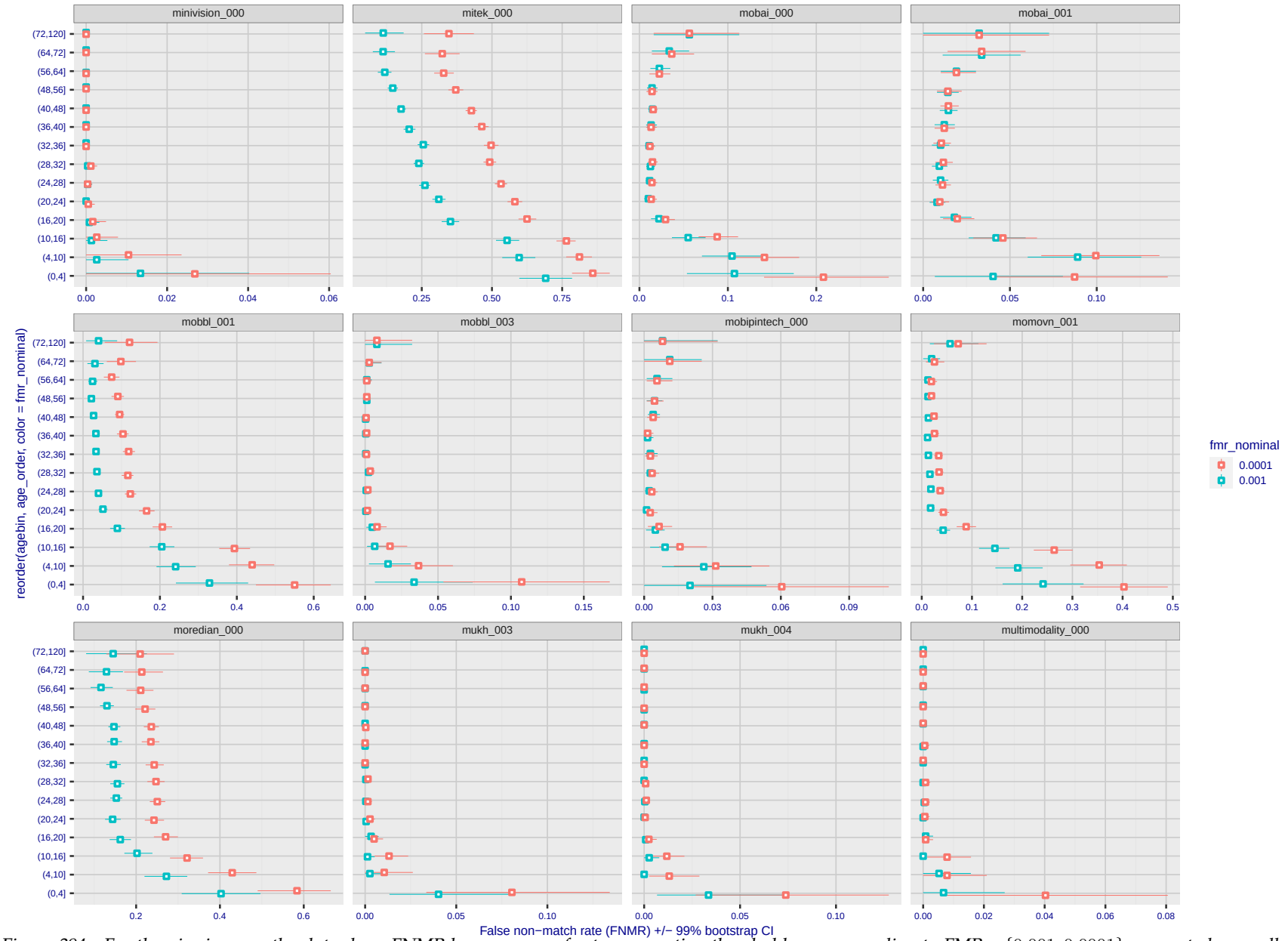

Figure 394: For the visa images, the dots show FNMR by age group for two operating thresholds corresponding to FMR = $\{0.001, 0.0001\}$ computed over all on the order of 10^{10} impostor scores. The FMR in each bin will vary also - see subsequent impostor heatmaps in sec. 3.6.2. Given a pair of face images taken at different times, we assign the comparison to the bin that is the arithmetic average of the subject's ages. This plot shows only the effect of age, not ageing. The number of comparisons in each bin is generally in the thousands, however the first and last bins are computed over 149 and 124 respectively. The error rates in some (adult) cases are zero, and in others the DET is flat so the error rates at the two thresholds are identical. The lines span 1% and 99% of boostrap replicated FNMR estimates.

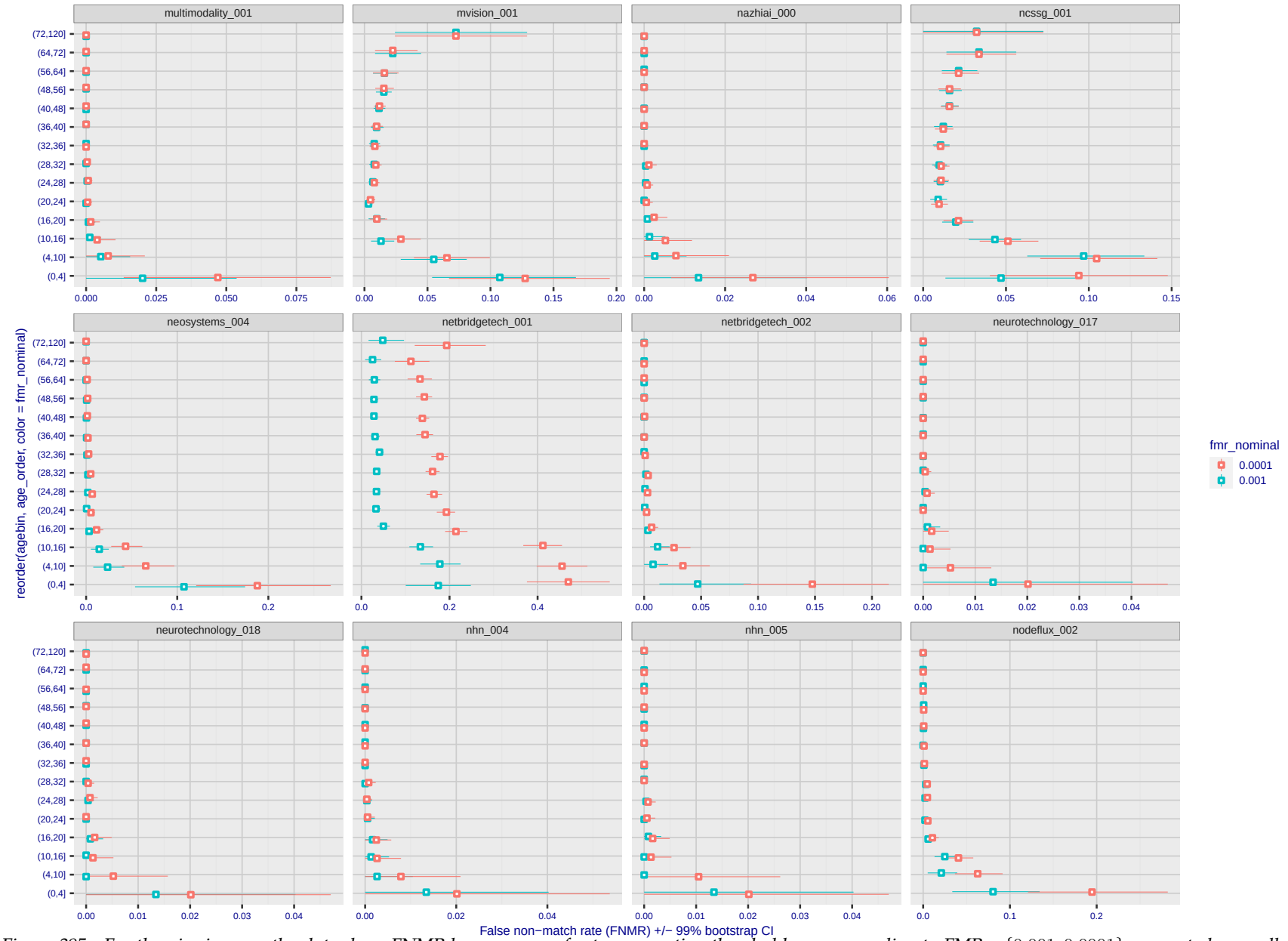

Figure 395: For the visa images, the dots show FNMR by age group for two operating thresholds corresponding to FMR = $\{0.001, 0.0001\}$ computed over all on the order of 10^{10} impostor scores. The FMR in each bin will vary also - see subsequent impostor heatmaps in sec. 3.6.2. Given a pair of face images taken at different times, we assign the comparison to the bin that is the arithmetic average of the subject's ages. This plot shows only the effect of age, not ageing. The number of comparisons in each bin is generally in the thousands, however the first and last bins are computed over 149 and 124 respectively. The error rates in some (adult) cases are zero, and in others the DET is flat so the error rates at the two thresholds are identical. The lines span 1% and 99% of boostrap replicated FNMR estimates.

Figure 396: For the visa images, the dots show FNMR by age group for two operating thresholds corresponding to FMR = $\{0.001, 0.0001\}$ computed over all on the order of 10^{10} impostor scores. The FMR in each bin will vary also - see subsequent impostor heatmaps in sec. 3.6.2. Given a pair of face images taken at different times, we assign the comparison to the bin that is the arithmetic average of the subject's ages. This plot shows only the effect of age, not ageing. The number of comparisons in each bin is generally in the thousands, however the first and last bins are computed over 149 and 124 respectively. The error rates in some (adult) cases are zero, and in others the DET is flat so the error rates at the two thresholds are identical. The lines span 1% and 99% of boostrap replicated FNMR estimates.

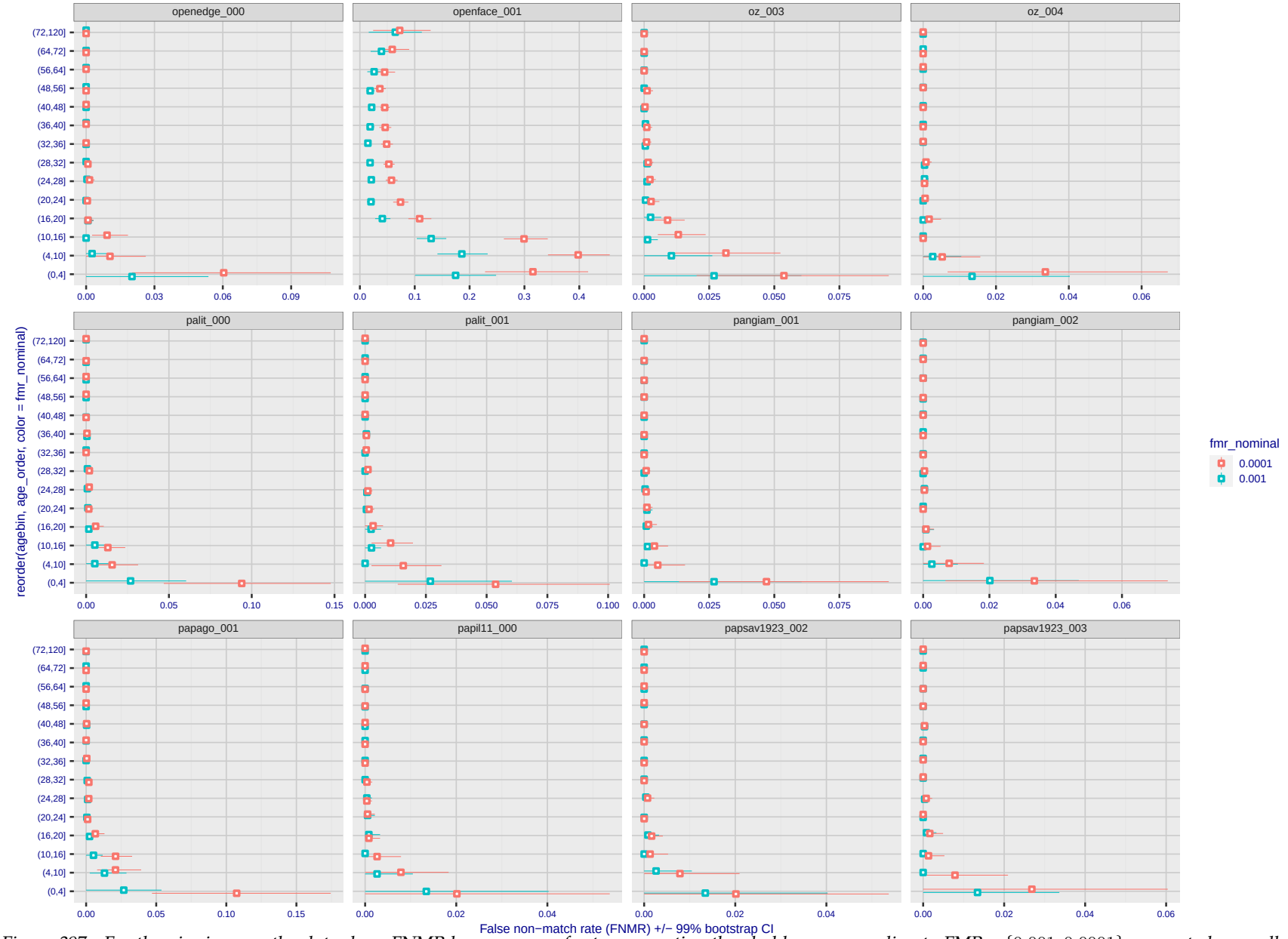

Figure 397: For the visa images, the dots show FNMR by age group for two operating thresholds corresponding to FMR = $\{0.001, 0.0001\}$ computed over all on the order of 10^{10} impostor scores. The FMR in each bin will vary also - see subsequent impostor heatmaps in sec. 3.6.2. Given a pair of face images taken at different times, we assign the comparison to the bin that is the arithmetic average of the subject's ages. This plot shows only the effect of age, not ageing. The number of comparisons in each bin is generally in the thousands, however the first and last bins are computed over 149 and 124 respectively. The error rates in some (adult) cases are zero, and in others the DET is flat so the error rates at the two thresholds are identical. The lines span 1% and 99% of boostrap replicated FNMR estimates.

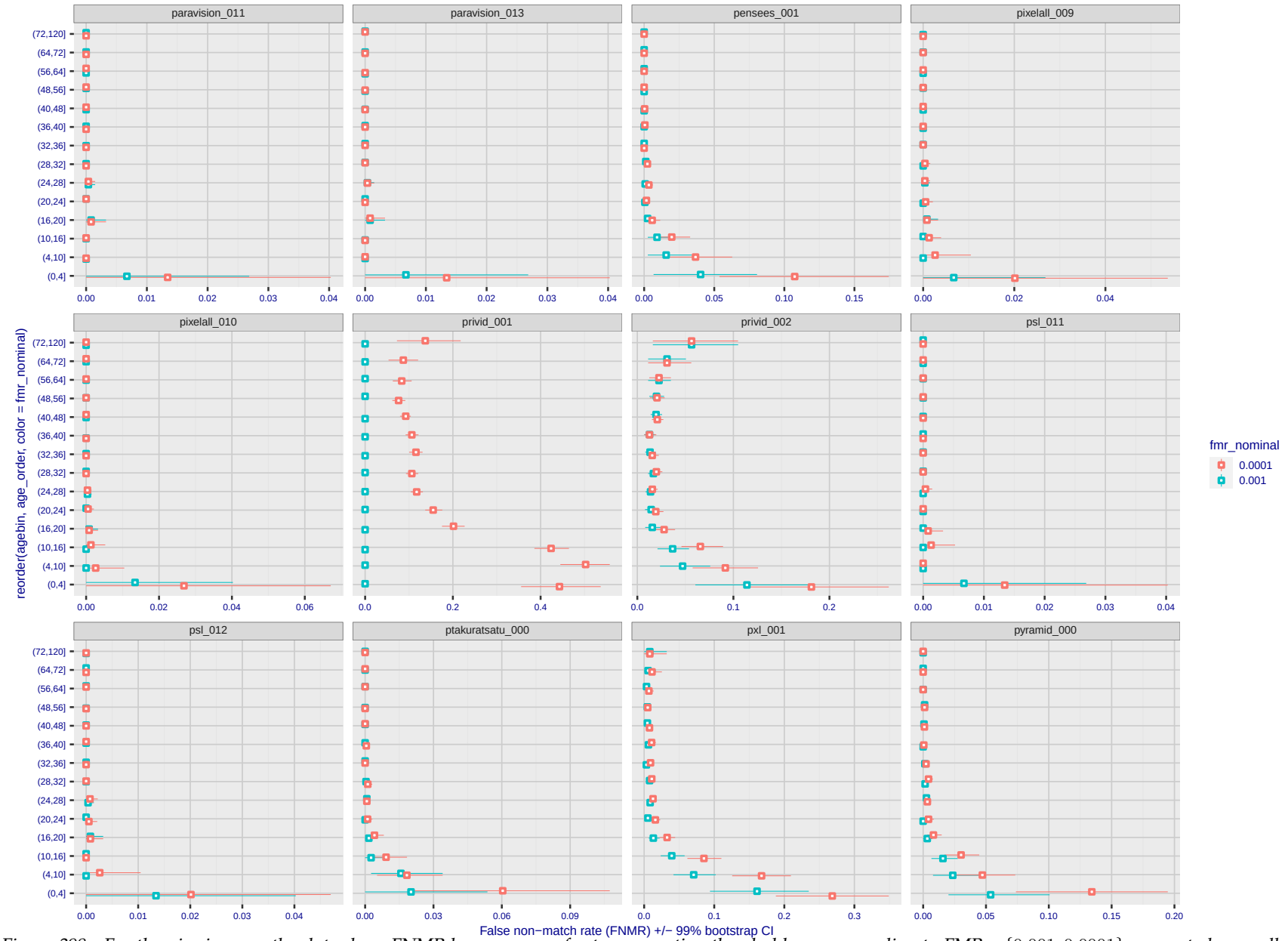

Figure 398: For the visa images, the dots show FNMR by age group for two operating thresholds corresponding to FMR = $\{0.001, 0.0001\}$ computed over all on the order of 10^{10} impostor scores. The FMR in each bin will vary also - see subsequent impostor heatmaps in sec. 3.6.2. Given a pair of face images taken at different times, we assign the comparison to the bin that is the arithmetic average of the subject's ages. This plot shows only the effect of age, not ageing. The number of comparisons in each bin is generally in the thousands, however the first and last bins are computed over 149 and 124 respectively. The error rates in some (adult) cases are zero, and in others the DET is flat so the error rates at the two thresholds are identical. The lines span 1% and 99% of boostrap replicated FNMR estimates.

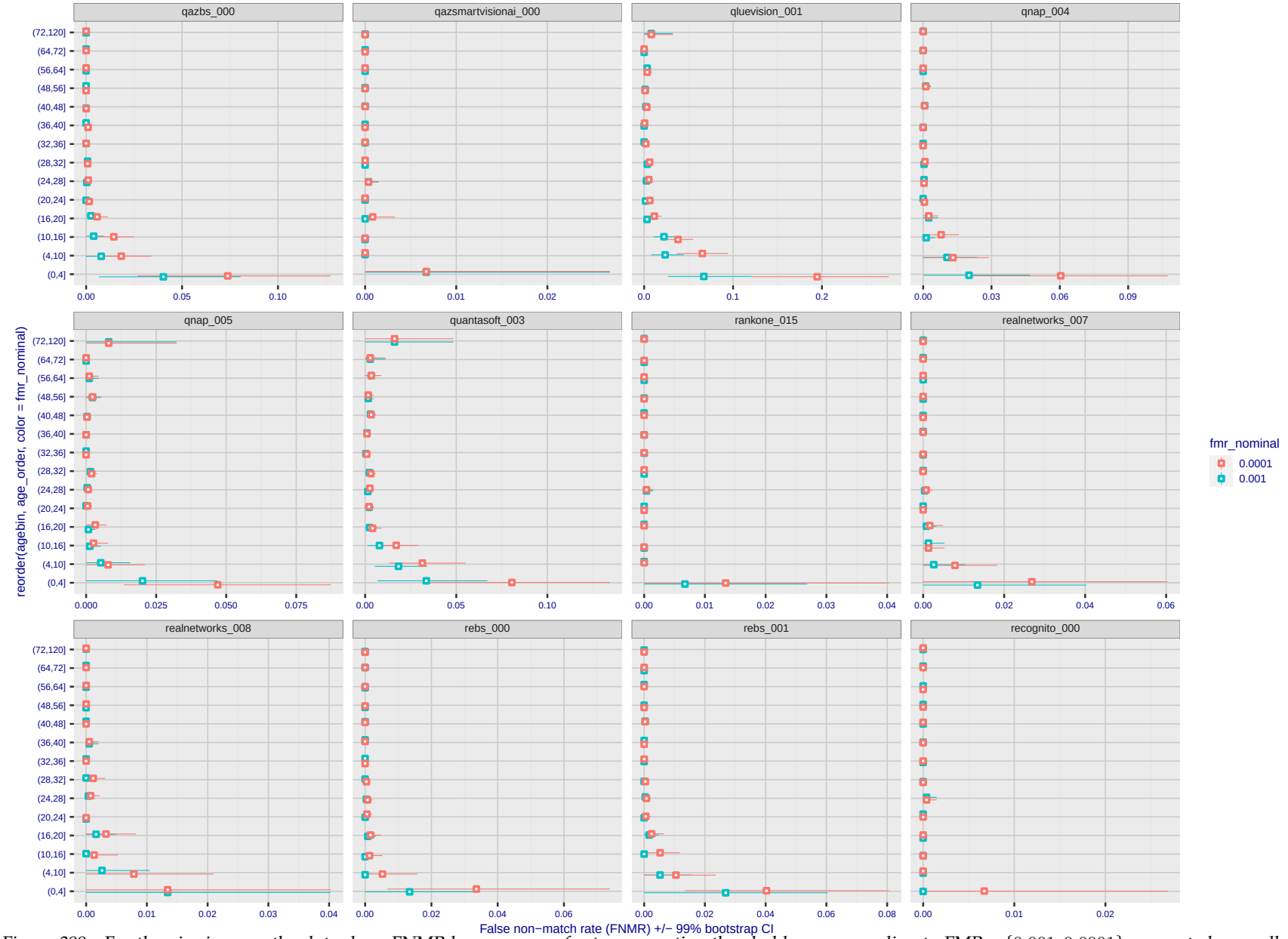

Figure 399: For the visa images, the dots show FNMR by age group for two operating thresholds corresponding to FMR = $\{0.001, 0.0001\}$ computed over all on the order of 10^{10} impostor scores. The FMR in each bin will vary also - see subsequent impostor heatmaps in sec. 3.6.2. Given a pair of face images taken at different times, we assign the comparison to the bin that is the arithmetic average of the subject's ages. This plot shows only the effect of age, not ageing. The number of comparisons in each bin is generally in the thousands, however the first and last bins are computed over 149 and 124 respectively. The error rates in some (adult) cases are zero, and in others the DET is flat so the error rates at the two thresholds are identical. The lines span 1% and 99% of boostrap replicated FNMR estimates.

Figure 400: For the visa images, the dots show FNMR by age group for two operating thresholds corresponding to FMR = $\{0.001, 0.0001\}$ computed over all on the order of 10^{10} impostor scores. The FMR in each bin will vary also - see subsequent impostor heatmaps in sec. 3.6.2. Given a pair of face images taken at different times, we assign the comparison to the bin that is the arithmetic average of the subject's ages. This plot shows only the effect of age, not ageing. The number of comparisons in each bin is generally in the thousands, however the first and last bins are computed over 149 and 124 respectively. The error rates in some (adult) cases are zero, and in others the DET is flat so the error rates at the two thresholds are identical. The lines span 1% and 99% of boostrap replicated FNMR estimates.

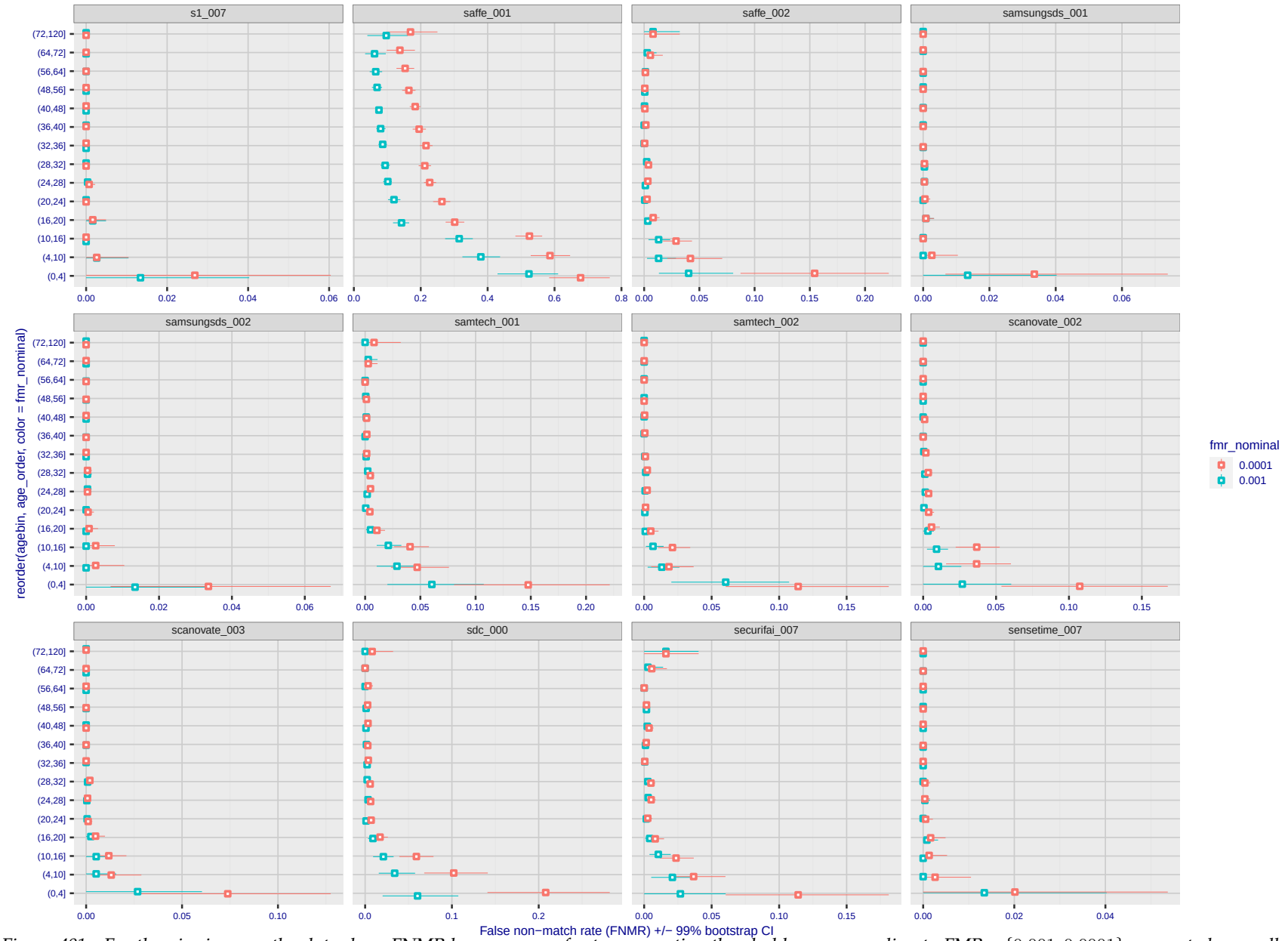

Figure 401: For the visa images, the dots show FNMR by age group for two operating thresholds corresponding to FMR = $\{0.001, 0.0001\}$ computed over all on the order of 10^{10} impostor scores. The FMR in each bin will vary also - see subsequent impostor heatmaps in sec. 3.6.2. Given a pair of face images taken at different times, we assign the comparison to the bin that is the arithmetic average of the subject's ages. This plot shows only the effect of age, not ageing. The number of comparisons in each bin is generally in the thousands, however the first and last bins are computed over 149 and 124 respectively. The error rates in some (adult) cases are zero, and in others the DET is flat so the error rates at the two thresholds are identical. The lines span 1% and 99% of boostrap replicated FNMR estimates.

Figure 402: For the visa images, the dots show FNMR by age group for two operating thresholds corresponding to FMR = $\{0.001, 0.0001\}$ computed over all on the order of 10^{10} impostor scores. The FMR in each bin will vary also - see subsequent impostor heatmaps in sec. 3.6.2. Given a pair of face images taken at different times, we assign the comparison to the bin that is the arithmetic average of the subject's ages. This plot shows only the effect of age, not ageing. The number of comparisons in each bin is generally in the thousands, however the first and last bins are computed over 149 and 124 respectively. The error rates in some (adult) cases are zero, and in others the DET is flat so the error rates at the two thresholds are identical. The lines span 1% and 99% of boostrap replicated FNMR estimates.

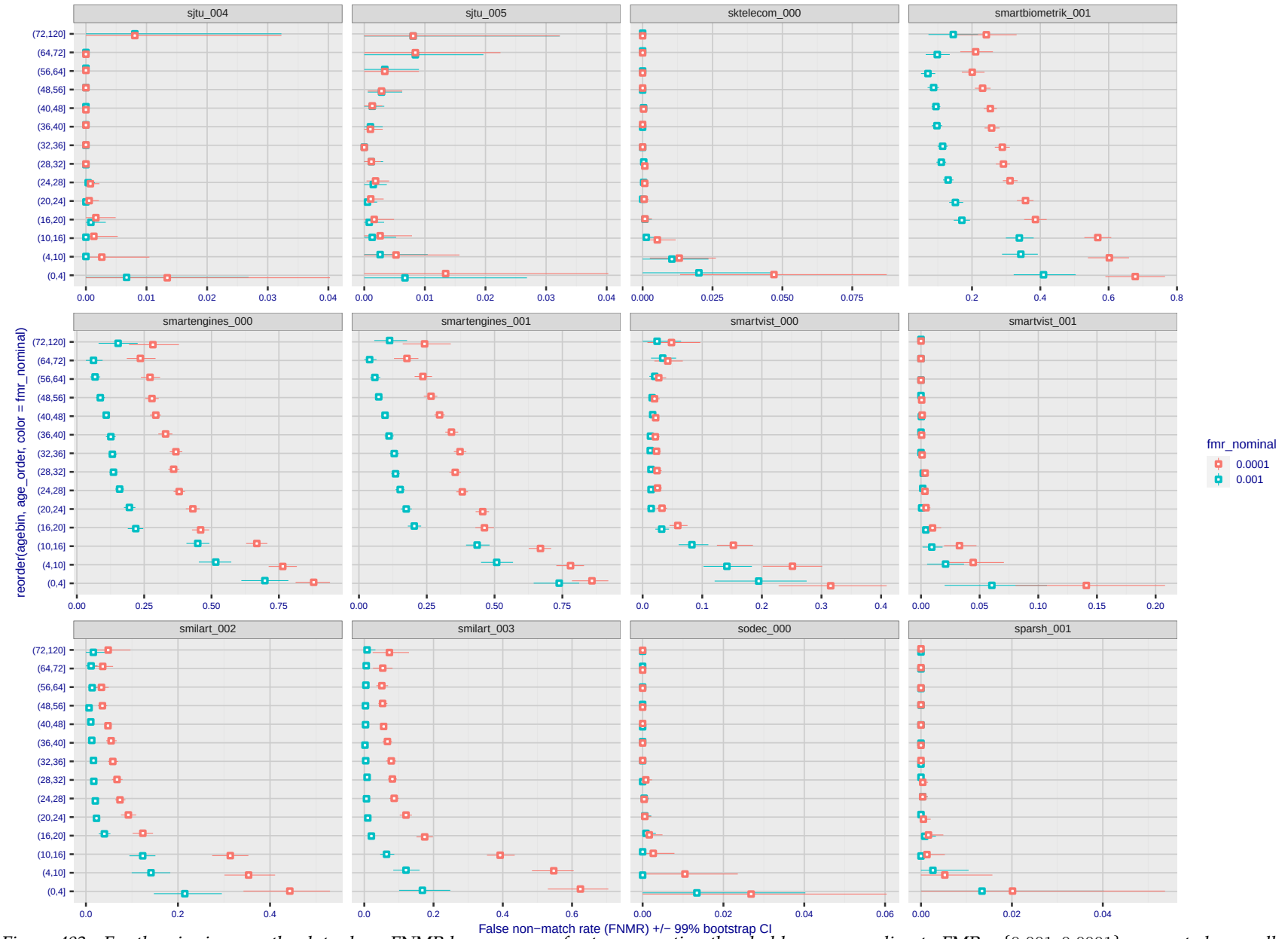

Figure 403: For the visa images, the dots show FNMR by age group for two operating thresholds corresponding to FMR = $\{0.001, 0.0001\}$ computed over all on the order of 10^{10} impostor scores. The FMR in each bin will vary also - see subsequent impostor heatmaps in sec. 3.6.2. Given a pair of face images taken at different times, we assign the comparison to the bin that is the arithmetic average of the subject's ages. This plot shows only the effect of age, not ageing. The number of comparisons in each bin is generally in the thousands, however the first and last bins are computed over 149 and 124 respectively. The error rates in some (adult) cases are zero, and in others the DET is flat so the error rates at the two thresholds are identical. The lines span 1% and 99% of boostrap replicated FNMR estimates.

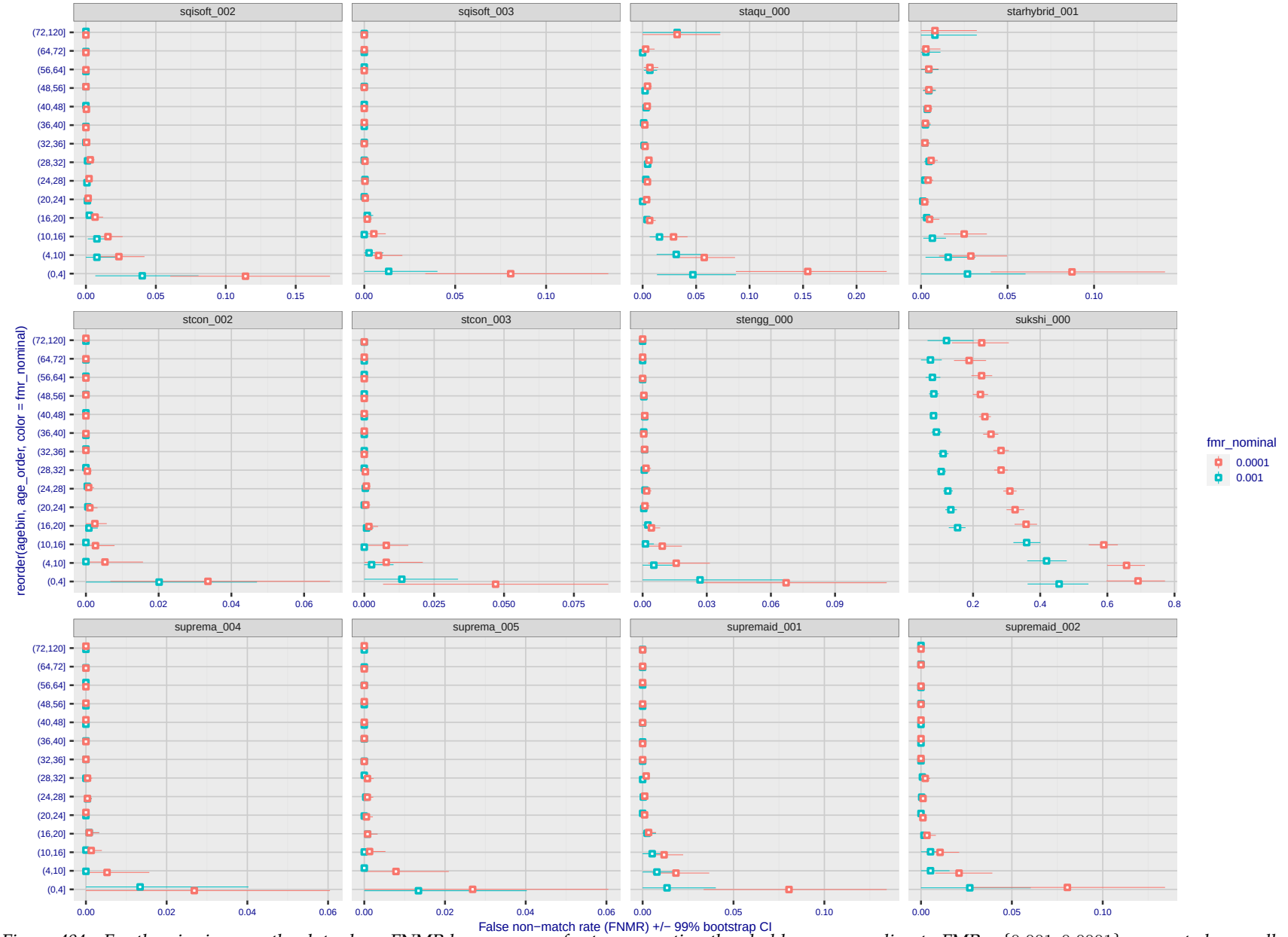

Figure 404: For the visa images, the dots show FNMR by age group for two operating thresholds corresponding to FMR = $\{0.001, 0.0001\}$ computed over all on the order of 10^{10} impostor scores. The FMR in each bin will vary also - see subsequent impostor heatmaps in sec. 3.6.2. Given a pair of face images taken at different times, we assign the comparison to the bin that is the arithmetic average of the subject's ages. This plot shows only the effect of age, not ageing. The number of comparisons in each bin is generally in the thousands, however the first and last bins are computed over 149 and 124 respectively. The error rates in some (adult) cases are zero, and in others the DET is flat so the error rates at the two thresholds are identical. The lines span 1% and 99% of boostrap replicated FNMR estimates.

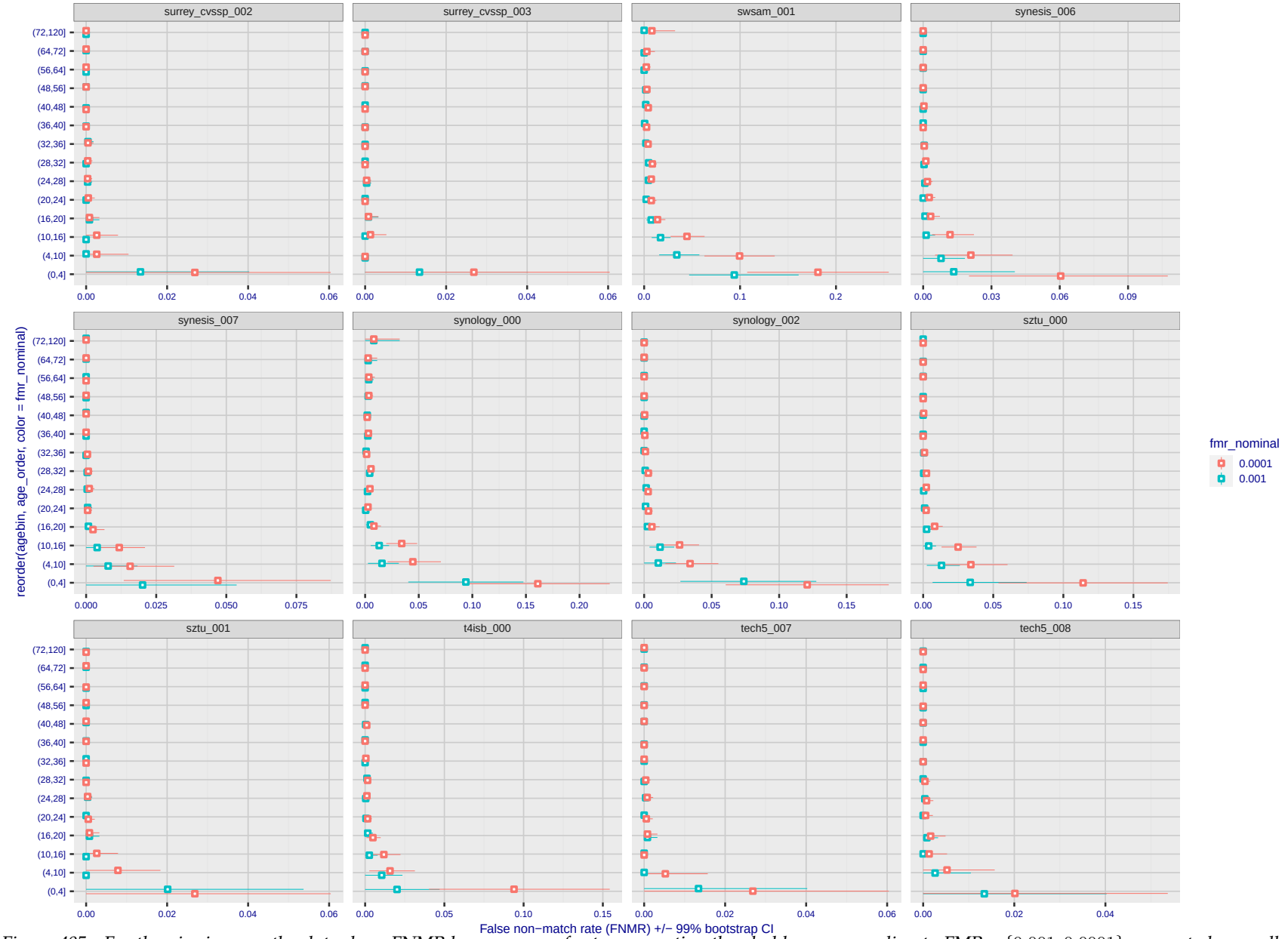

Figure 405: For the visa images, the dots show FNMR by age group for two operating thresholds corresponding to FMR = $\{0.001, 0.0001\}$ computed over all on the order of 10^{10} impostor scores. The FMR in each bin will vary also - see subsequent impostor heatmaps in sec. 3.6.2. Given a pair of face images taken at different times, we assign the comparison to the bin that is the arithmetic average of the subject's ages. This plot shows only the effect of age, not ageing. The number of comparisons in each bin is generally in the thousands, however the first and last bins are computed over 149 and 124 respectively. The error rates in some (adult) cases are zero, and in others the DET is flat so the error rates at the two thresholds are identical. The lines span 1% and 99% of boostrap replicated FNMR estimates.

Figure 406: For the visa images, the dots show FNMR by age group for two operating thresholds corresponding to FMR = $\{0.001, 0.0001\}$ computed over all on the order of 10^{10} impostor scores. The FMR in each bin will vary also - see subsequent impostor heatmaps in sec. 3.6.2. Given a pair of face images taken at different times, we assign the comparison to the bin that is the arithmetic average of the subject's ages. This plot shows only the effect of age, not ageing. The number of comparisons in each bin is generally in the thousands, however the first and last bins are computed over 149 and 124 respectively. The error rates in some (adult) cases are zero, and in others the DET is flat so the error rates at the two thresholds are identical. The lines span 1% and 99% of boostrap replicated FNMR estimates.

Figure 407: For the visa images, the dots show FNMR by age group for two operating thresholds corresponding to FMR = $\{0.001, 0.0001\}$ computed over all on the order of 10^{10} impostor scores. The FMR in each bin will vary also - see subsequent impostor heatmaps in sec. 3.6.2. Given a pair of face images taken at different times, we assign the comparison to the bin that is the arithmetic average of the subject's ages. This plot shows only the effect of age, not ageing. The number of comparisons in each bin is generally in the thousands, however the first and last bins are computed over 149 and 124 respectively. The error rates in some (adult) cases are zero, and in others the DET is flat so the error rates at the two thresholds are identical. The lines span 1% and 99% of boostrap replicated FNMR estimates.

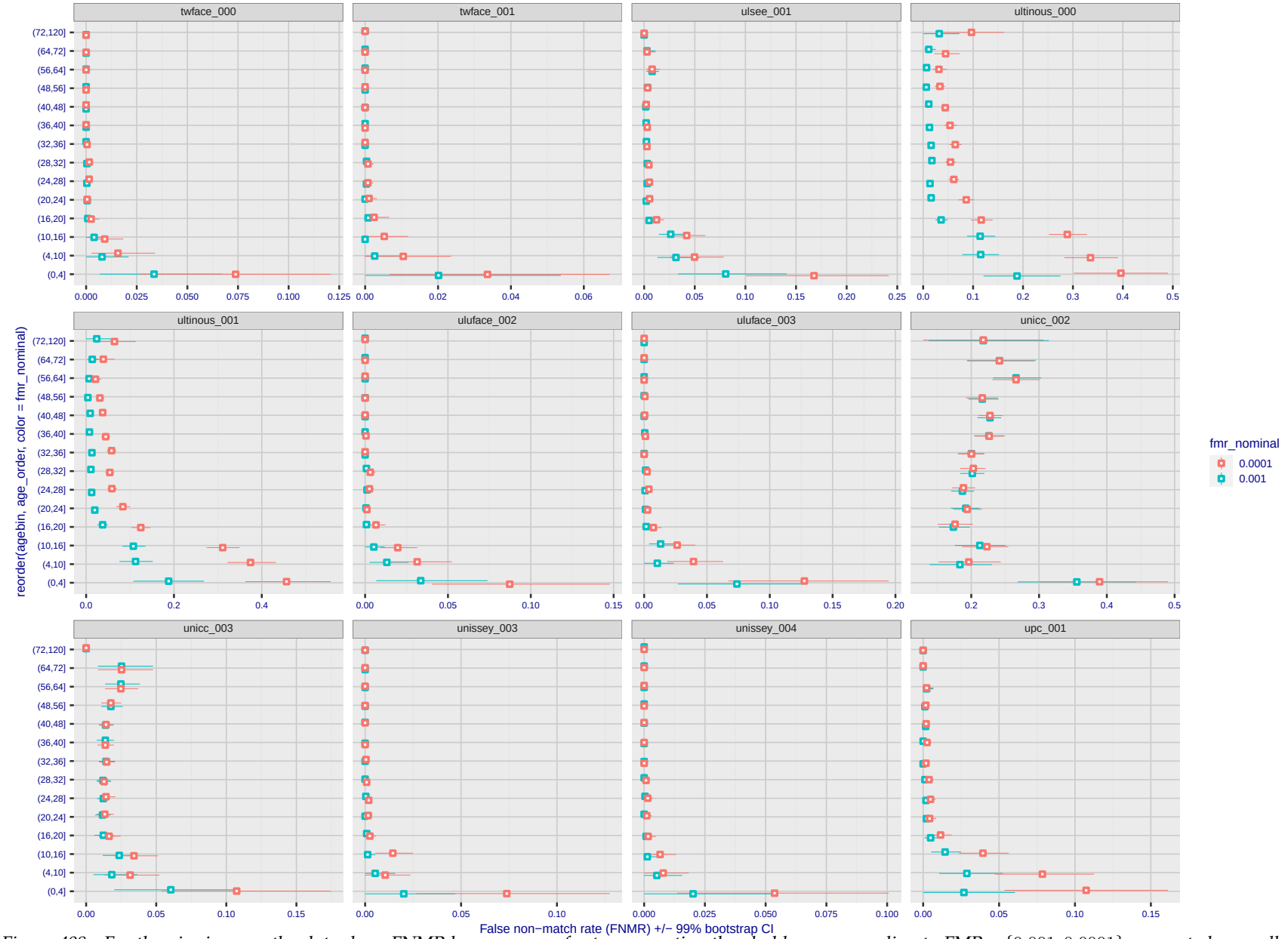

Figure 408: For the visa images, the dots show FNMR by age group for two operating thresholds corresponding to FMR = $\{0.001, 0.0001\}$ computed over all on the order of 10^{10} impostor scores. The FMR in each bin will vary also - see subsequent impostor heatmaps in sec. 3.6.2. Given a pair of face images taken at different times, we assign the comparison to the bin that is the arithmetic average of the subject's ages. This plot shows only the effect of age, not ageing. The number of comparisons in each bin is generally in the thousands, however the first and last bins are computed over 149 and 124 respectively. The error rates in some (adult) cases are zero, and in others the DET is flat so the error rates at the two thresholds are identical. The lines span 1% and 99% of boostrap replicated FNMR estimates.

Figure 409: For the visa images, the dots show FNMR by age group for two operating thresholds corresponding to FMR = $\{0.001, 0.0001\}$ computed over all on the order of 10^{10} impostor scores. The FMR in each bin will vary also - see subsequent impostor heatmaps in sec. 3.6.2. Given a pair of face images taken at different times, we assign the comparison to the bin that is the arithmetic average of the subject's ages. This plot shows only the effect of age, not ageing. The number of comparisons in each bin is generally in the thousands, however the first and last bins are computed over 149 and 124 respectively. The error rates in some (adult) cases are zero, and in others the DET is flat so the error rates at the two thresholds are identical. The lines span 1% and 99% of boostrap replicated FNMR estimates.

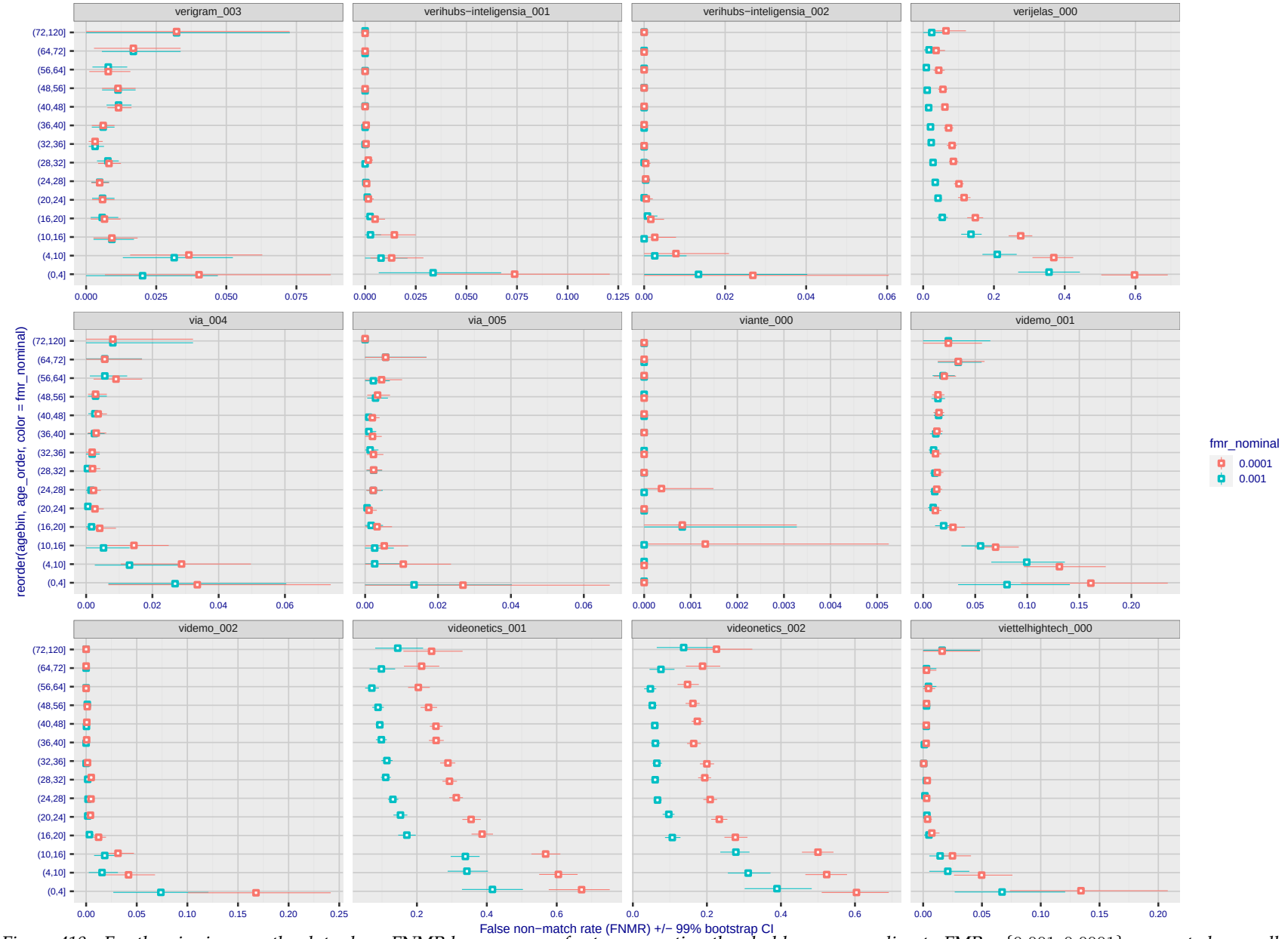

Figure 410: For the visa images, the dots show FNMR by age group for two operating thresholds corresponding to FMR = $\{0.001, 0.0001\}$ computed over all on the order of 10^{10} impostor scores. The FMR in each bin will vary also - see subsequent impostor heatmaps in sec. 3.6.2. Given a pair of face images taken at different times, we assign the comparison to the bin that is the arithmetic average of the subject's ages. This plot shows only the effect of age, not ageing. The number of comparisons in each bin is generally in the thousands, however the first and last bins are computed over 149 and 124 respectively. The error rates in some (adult) cases are zero, and in others the DET is flat so the error rates at the two thresholds are identical. The lines span 1% and 99% of boostrap replicated FNMR estimates.

Figure 411: For the visa images, the dots show FNMR by age group for two operating thresholds corresponding to FMR = $\{0.001, 0.0001\}$ computed over all on the order of 10^{10} impostor scores. The FMR in each bin will vary also - see subsequent impostor heatmaps in sec. 3.6.2. Given a pair of face images taken at different times, we assign the comparison to the bin that is the arithmetic average of the subject's ages. This plot shows only the effect of age, not ageing. The number of comparisons in each bin is generally in the thousands, however the first and last bins are computed over 149 and 124 respectively. The error rates in some (adult) cases are zero, and in others the DET is flat so the error rates at the two thresholds are identical. The lines span 1% and 99% of boostrap replicated FNMR estimates.

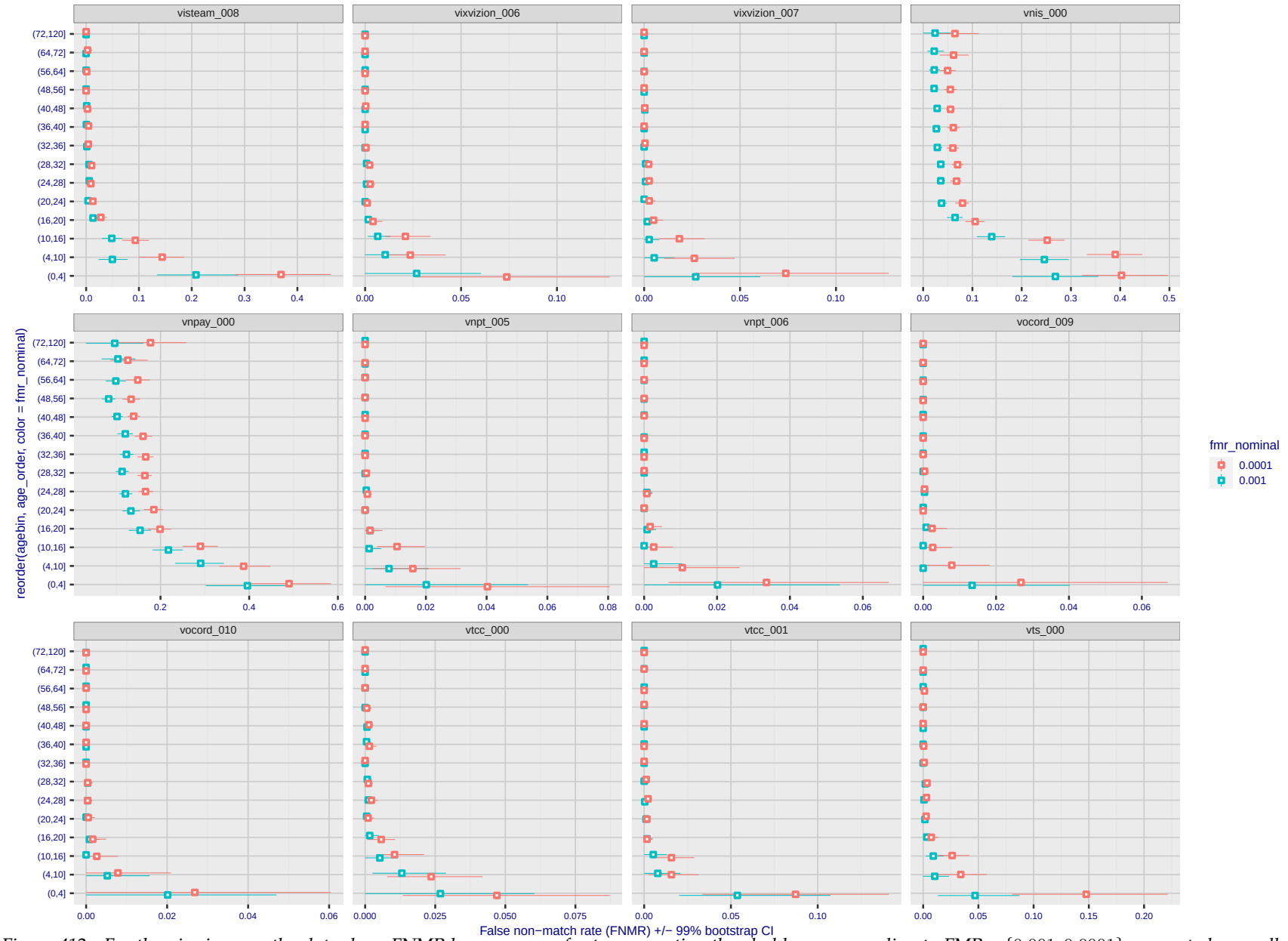

Figure 412: For the visa images, the dots show FNMR by age group for two operating thresholds corresponding to FMR = $\{0.001, 0.0001\}$ computed over all on the order of 10^{10} impostor scores. The FMR in each bin will vary also - see subsequent impostor heatmaps in sec. 3.6.2. Given a pair of face images taken at different times, we assign the comparison to the bin that is the arithmetic average of the subject's ages. This plot shows only the effect of age, not ageing. The number of comparisons in each bin is generally in the thousands, however the first and last bins are computed over 149 and 124 respectively. The error rates in some (adult) cases are zero, and in others the DET is flat so the error rates at the two thresholds are identical. The lines span 1% and 99% of boostrap replicated FNMR estimates.

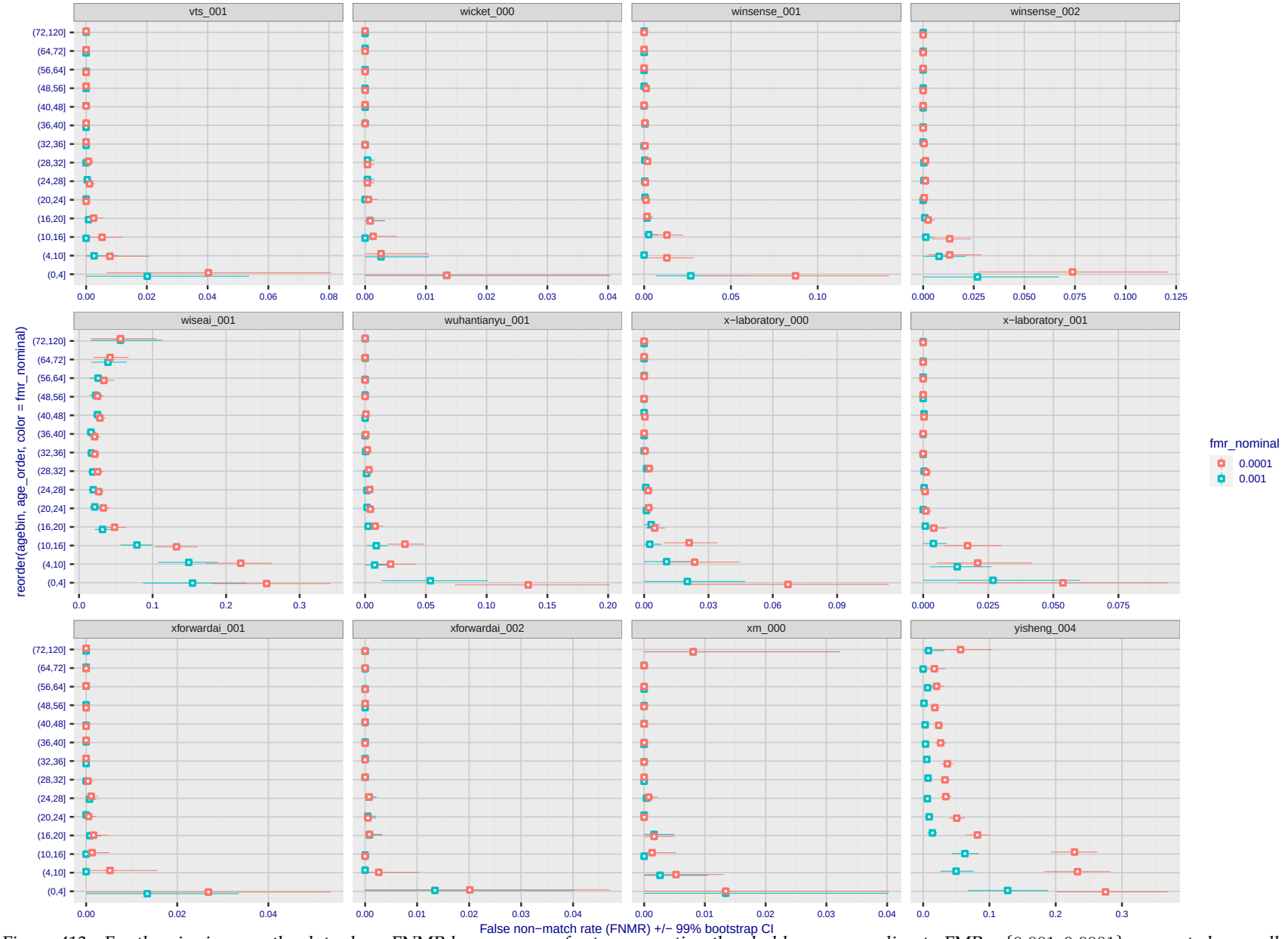

Figure 413: For the visa images, the dots show FNMR by age group for two operating thresholds corresponding to FMR = $\{0.001, 0.0001\}$ computed over all on the order of 10^{10} impostor scores. The FMR in each bin will vary also - see subsequent impostor heatmaps in sec. 3.6.2. Given a pair of face images taken at different times, we assign the comparison to the bin that is the arithmetic average of the subject's ages. This plot shows only the effect of age, not ageing. The number of comparisons in each bin is generally in the thousands, however the first and last bins are computed over 149 and 124 respectively. The error rates in some (adult) cases are zero, and in others the DET is flat so the error rates at the two thresholds are identical. The lines span 1% and 99% of boostrap replicated FNMR estimates.

Figure 414: For the visa images, the dots show FNMR by age group for two operating thresholds corresponding to FMR = $\{0.001, 0.0001\}$ computed over all on the order of 10^{10} impostor scores. The FMR in each bin will vary also - see subsequent impostor heatmaps in sec. 3.6.2. Given a pair of face images taken at different times, we assign the comparison to the bin that is the arithmetic average of the subject's ages. This plot shows only the effect of age, not ageing. The number of comparisons in each bin is generally in the thousands, however the first and last bins are computed over 149 and 124 respectively. The error rates in some (adult) cases are zero, and in others the DET is flat so the error rates at the two thresholds are identical. The lines span 1% and 99% of boostrap replicated FNMR estimates.

Caveats: None.

FNMR(T) "False non-match rate"
FMR(T) "False match rate"

3.6 Impostor distribution stability

3.6.1 Effect of birth place on the impostor distribution

Background: Facial appearance varies geographically, both in terms of skin tone, cranio-facial structure and size. This section addresses whether false match rates vary intra- and inter-regionally.

Goals:

- ▷ To show the effect of birth region of the impostor and enrollee on false match rates.
- ▷ To determine whether some algorithms give better impostor distribution stability.

Methods:

- ▷ For the visa images, NIST defined 10 regions: Sub-Saharan Africa, South Asia, Polynesia, North Africa, Middle East, Europe, East Asia, Central and South America, Central Asia, and the Caribbean.
- ▷ For the visa images, NIST mapped each country of birth to a region. There is some arbitrariness to this. For example, Egypt could reasonably be assigned to the Middle East instead of North Africa. An alternative methodology could, for example, assign the Philippines to *both* Polynesia and East Asia.
- ▷ FMR is computed for cases where all face images of impostors born in region r_2 are compared with enrolled face images of persons born in region r_1.

$$\text{FMR}(r_1, r_2, T) = \frac{\sum_{i=1}^{N_{r_1,r_2}} H(s_i - T)}{N_{r_1,r_2}} \tag{5}$$

  where the same threshold, T, is used in all cells, and H is the unit step function. The threshold is set to give FMR(T) = 0.001 over the entire set of visa image impostor comparisons.
- ▷ This analysis is then repeated by country-pair, but only for those country pairs where both have at least 1000 images available. The countries[1] appear in the axes of graphs that follow.
- ▷ The mean number of impostor scores in any cross-region bin is 33 million. The smallest number of impostor scores in any bin is 135000, for Central Asia - North Africa. While these counts are large enough to support reasonable significance, the number of individual faces is much smaller, on the order of $N^{0.5}$.
- ▷ The numbers of impostor scores in any cross-country bin is shown in Figure 415.

Results: Subsequent figures show heatmaps that use color to represent the base-10 logarithm of the false match rate. Red colors indicate high (bad) false match rates. Dark colors indicate benign false match rates. There are two series of graphs corresponding to aggregated geographical regions, and to countries. The notable observations are:

- ▷ The on-diagonal elements correspond to within-region impostors. FMR is generally above the nominal value of FMR = 0.001. Particularly there is usually higher FMR in, Sub-Saharan Africa, South Asia, and the Caribbean. Europe and Central Asia, on the other hand, usually give FMR closer to the nominal value.
- ▷ The off-diagonal elements correspond to across-region impostors. The highest FMR is produced between the Caribbean and Sub-Saharan Africa.
- ▷ Algorithms vary.

[1] These are Argentina, Australia, Brazil, Chile, China, Costa Rica, Cuba, Czech Republic, Dominican Republic, Ecuador, Egypt, El Salvador, Germany, Ghana, Great Britain, Greece, Guatamala, Haiti, Hong Kong, Honduras, Indonesia, India, Israel, Jamaica, Japan, Kenya, Korea, Lebanon, Mexico, Malaysia, Nepal, Nigeria, Peru, Philippines, Pakistan, Poland, Romania, Russia, South Africa, Saudi Arabia, Thailand, Trinidad, Turkey, Taiwan, Ukraine, Venezuela, and Vietnam.

FNMR(T) "False non-match rate"
FMR(T) "False match rate"

▷ We computed the same quantities for a global FMR = 0.0001. The effects are similar.

Caveats:

▷ The effects of variable impostor rates on one-to-many identification systems may well differ from what's implied by these one-to-one verification results. Two reasons for this are a) the enrollment galleries are usually imbalanced across countries of birth, age and sex; b) one-to-many identification algorithms often implement techniques aimed at stabilizing the impostor distribution. Further research is necessary.

▷ In principle, the effects seen in this subsection could be due to differences in the image capture process. We consider this unlikely since the effects are maintained across geography - e.g. Caribbean vs. Africa, or Japan vs. China.

FNMR(T) "False non-match rate"
FMR(T) "False match rate"

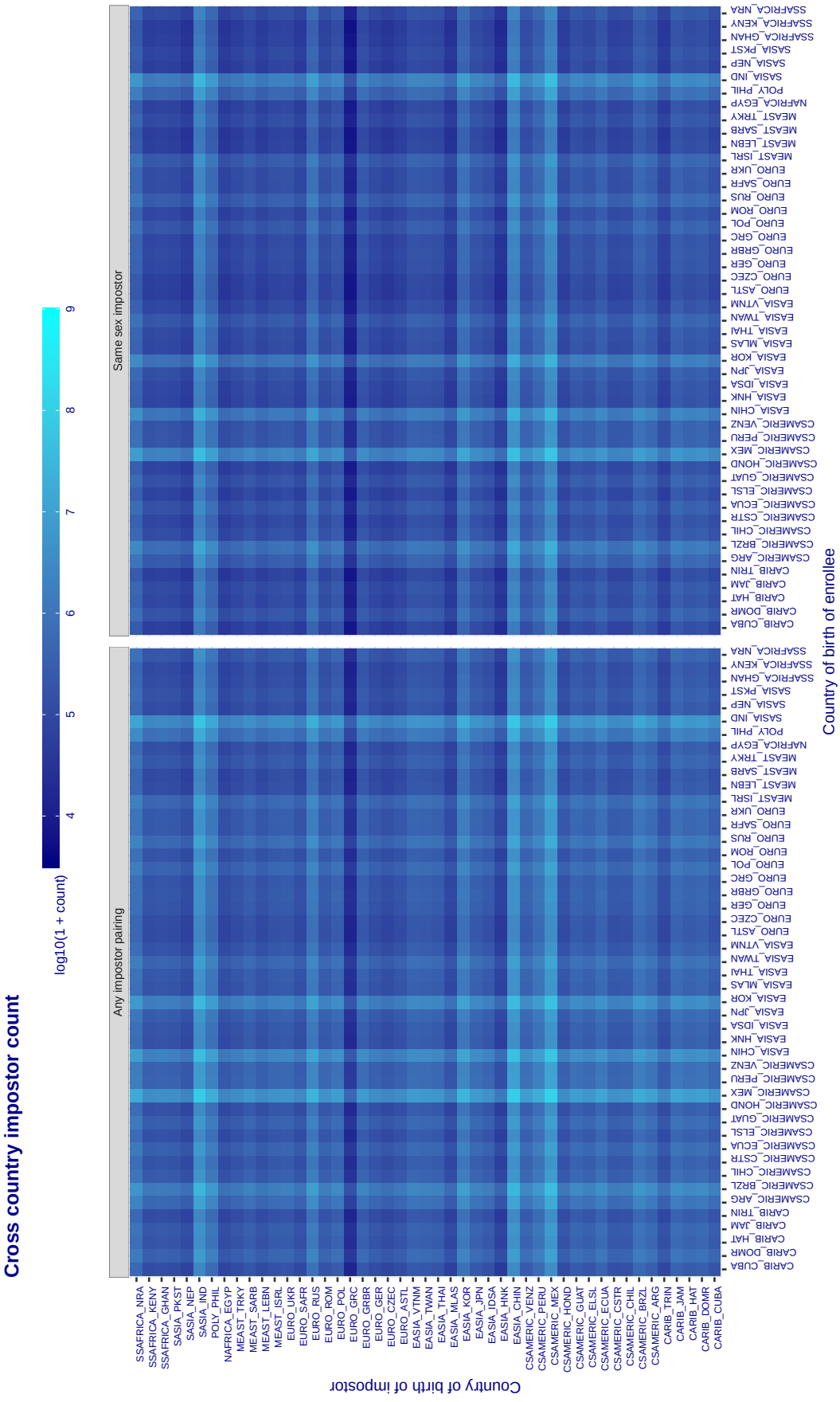

Figure 415: For visa images, the heatmap shows the count of impostor comparisons of faces from different individuals who were born in the given country pair. The FMR heatmaps themselves appear in the 1:1 report cards, for example, this one.

FNMR(T) "False non-match rate"
FMR(T) "False match rate"

3.6.2 Effect of age on impostors

Background: This section shows the effect of age on the impostor distribution. The ideal behaviour is that the age of the enrollee and the impostor would not affect impostor scores. This would support FMR stability over sub-populations.

Goals:

- ▷ To show the effect of relative ages of the impostor and enrollee on false match rates.
- ▷ To determine whether some algorithms have better impostor distribution stability.

Methods:

- ▷ Define 14 age group bins, spanning 0 to over 100 years old.
- ▷ Compute FMR over all impostor comparisons for which the subjects in the enrollee and impostor images have ages in two bins.
- ▷ Compute FMR over all impostor comparisons for which the subjects are additionally of the same sex, and born in the same geographic region.

Results:

The notable aspects are:

- ▷ Diagonal dominance: Impostors are more likely to be matched against their same age group.
- ▷ Same sex and same region impostors are more successful. On the diagonal, an impostor is more likely to succeed by posing as someone of the same sex. If $\Delta \log_{10}$ FMR $= 0.2$, then same-sex same-region FMR exceeds the all-pairs FMR by factor of $10^{0.2} = 1.6$.
- ▷ Young children impostors give elevated FMR against young children. Older adult impostor give elevated FMR against older adults. These effects are quite large, for example if $\Delta \log_{10}$ FMR $= 1.0$ larger than a 32 year old, then these groups have higher FMR by a factor of $10^1 = 10$. This would imply an FMR above 0.01 for a nominal (global) FMR = 0.001.
- ▷ Algorithms vary.
- ▷ We computed the same quantities for a global FMR = 0.0001. The effects are similar.

Note the calculations in this section include impostors paired across all countries of birth.

Accuracy Terms + Definitions

In biometrics, Type II errors occur when two samples of one person do not match – this is called a **false negative**. Correspondingly, Type I errors occur when samples from two persons do match – this is called a **false positive**. Matches are declared by a biometric system when the native comparison score from the recognition algorithm meets some **threshold**. Comparison scores can be either **similarity scores**, in which case higher values indicate that the samples are more likely to come from the same person, or **dissimilarity scores**, in which case higher values indicate different people. Similarity scores are traditionally computed by **fingerprint** and **face** recognition algorithms, while dissimilarities are used in **iris recognition**. In some cases, the dissimilarity score is a distance; this applies only when **metric** properties are obeyed. In any case, scores can be either **mate** scores, coming from a comparison of one person's samples, or **nonmate** scores, coming from comparison of different persons' samples. The words **genuine** or **authentic** are synonyms for mate, and the word **impostor** is used a synonym for nonmate. The words mate and nonmate are traditionally used in identification applications (such as law enforcement search, or background checks) while genuine and impostor are used in verification applications (such as access control).

A **error tradeoff** characteristic represents the tradeoff between Type II and Type I classification errors. For verification this plots false non-match rate (FNMR) vs. false match rate (FMR) parametrically with T.

The error tradeoff plots are often called **detection error tradeoff (DET)** characteristics or **receiver operating characteristic** (ROC). These serve the same function but differ, for example, in plotting the complement of an error rate (e.g. TMR = 1 – FNMR) and in transforming the axes most commonly using logarithms, to show multiple decades of FMR. More rarely, the function might be the inverse Gaussian function.

More detail and generality is provided in formal biometrics testing standards, see the various parts of ISO/IEC 19795 Biometrics Testing and Reporting. More terms, including and beyond those to do with accuracy, see ISO/IEC 2382-37 Information technology -- Vocabulary -- Part 37: Harmonized biometric vocabulary

FNMR(T) "False non-match rate"
FMR(T) "False match rate"

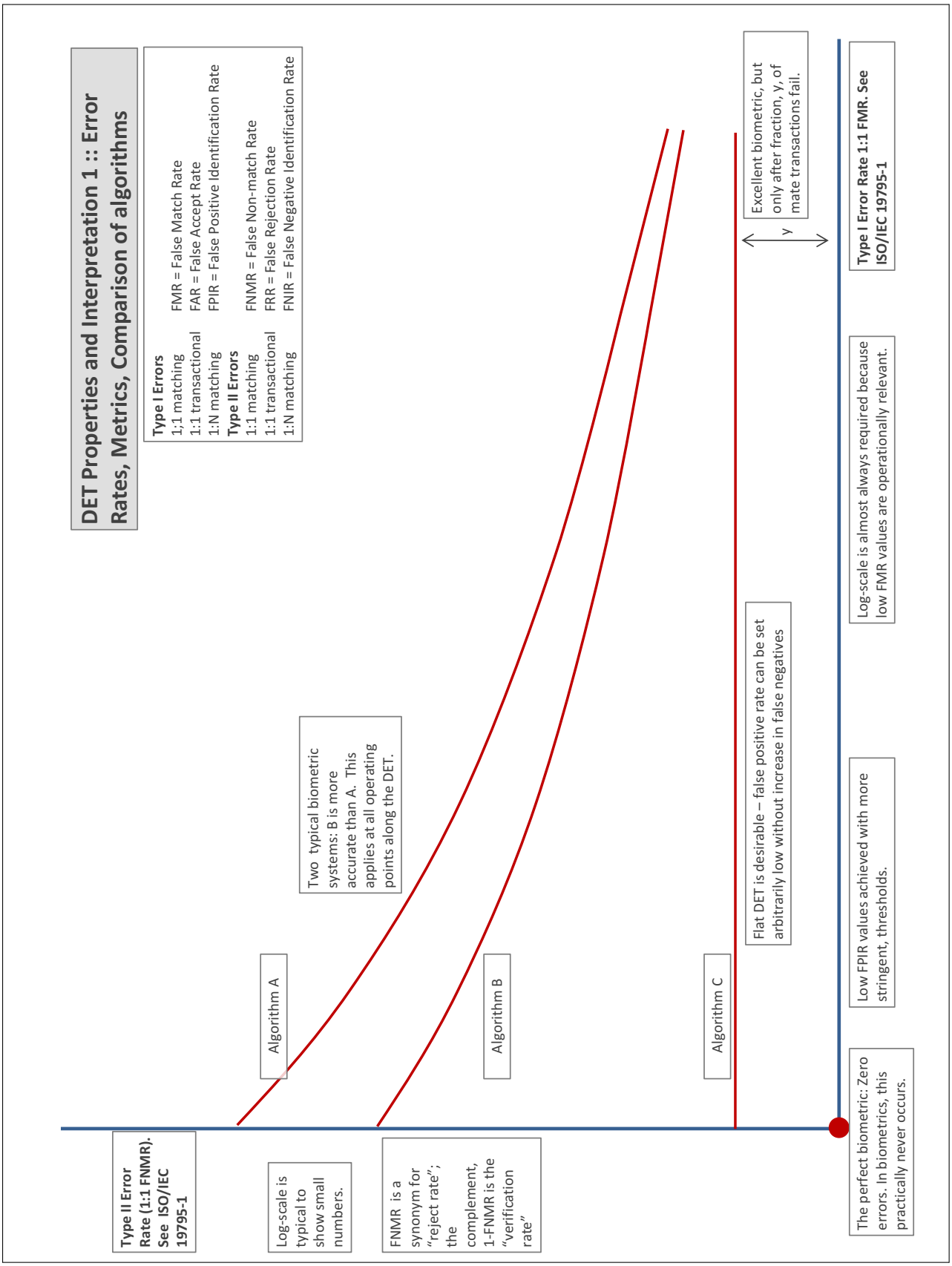

FNMR(T) "False non-match rate"
FMR(T) "False match rate"

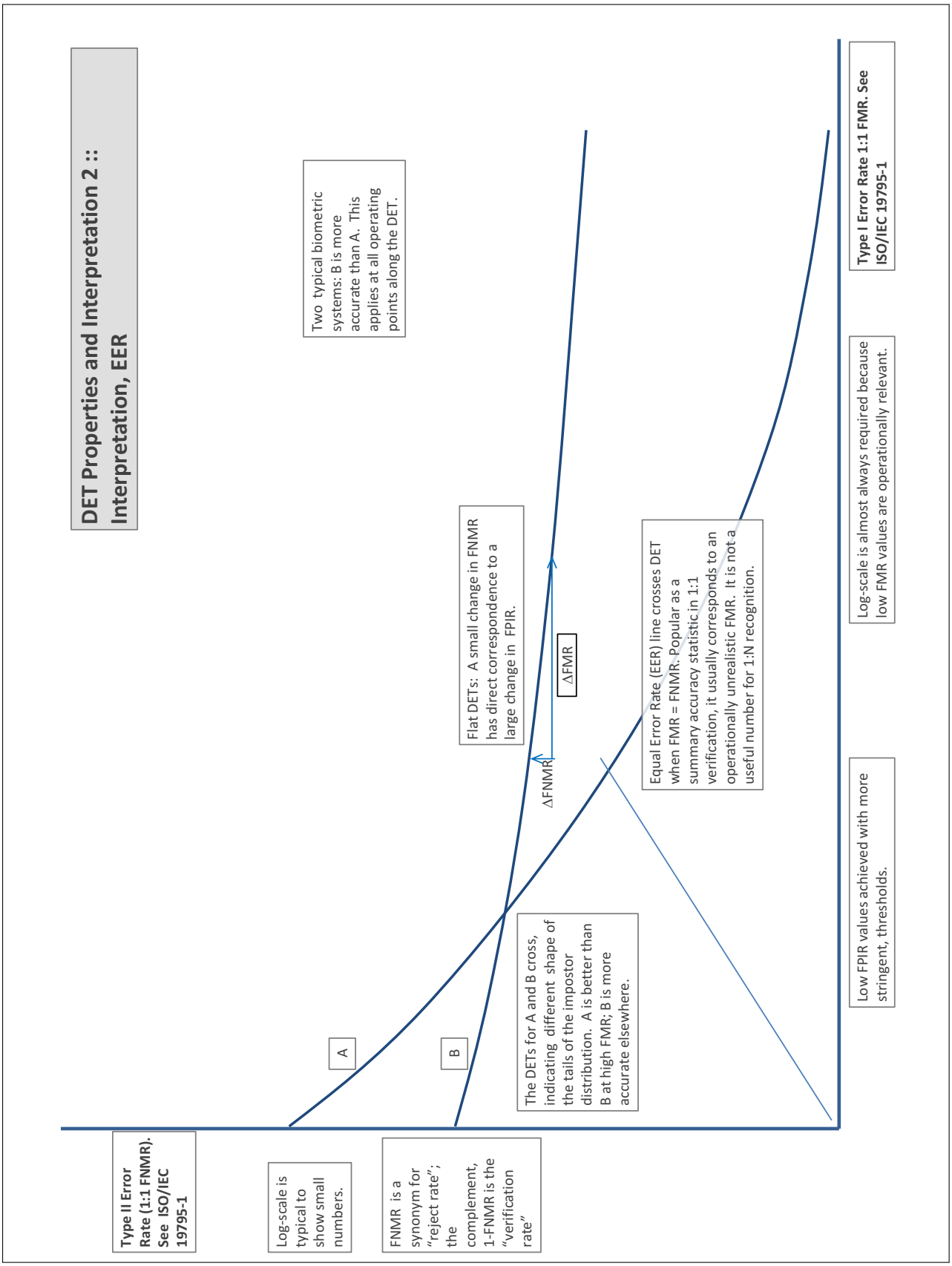

FNMR(T) "False non-match rate"
FMR(T) "False match rate"

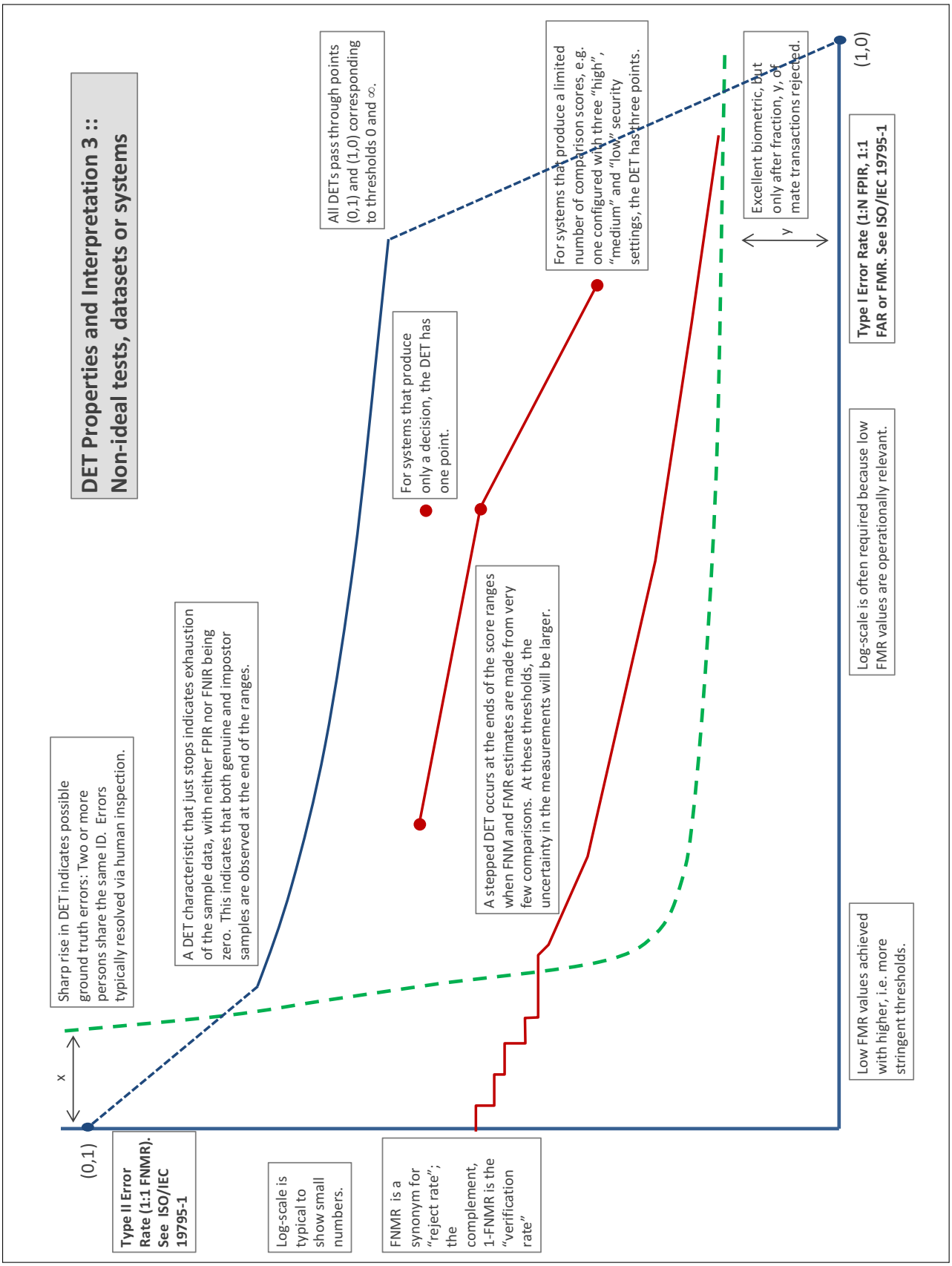

FNMR(T) "False non-match rate"
FMR(T) "False match rate"

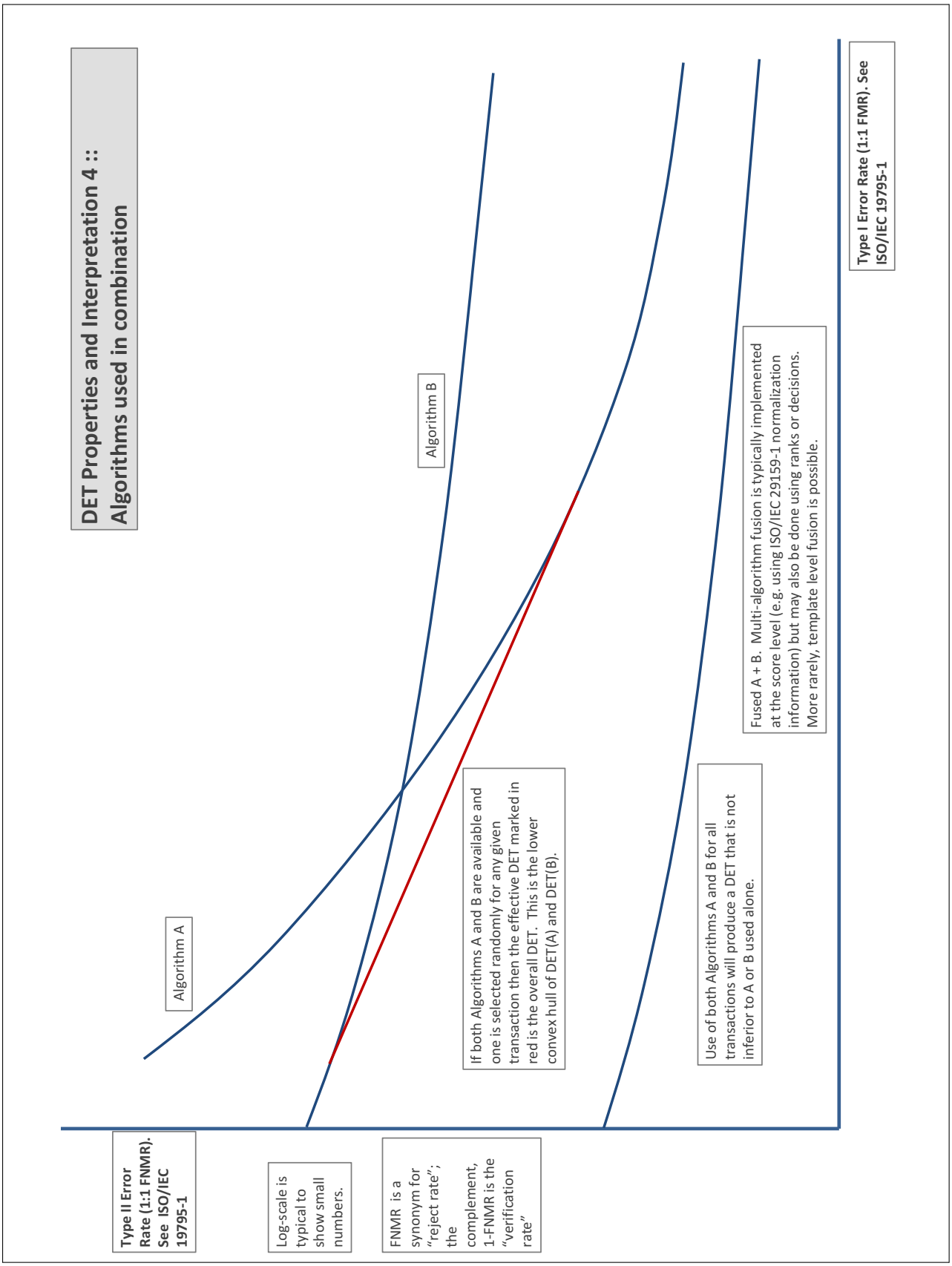

FNMR(T) "False non-match rate"
FMR(T) "False match rate"

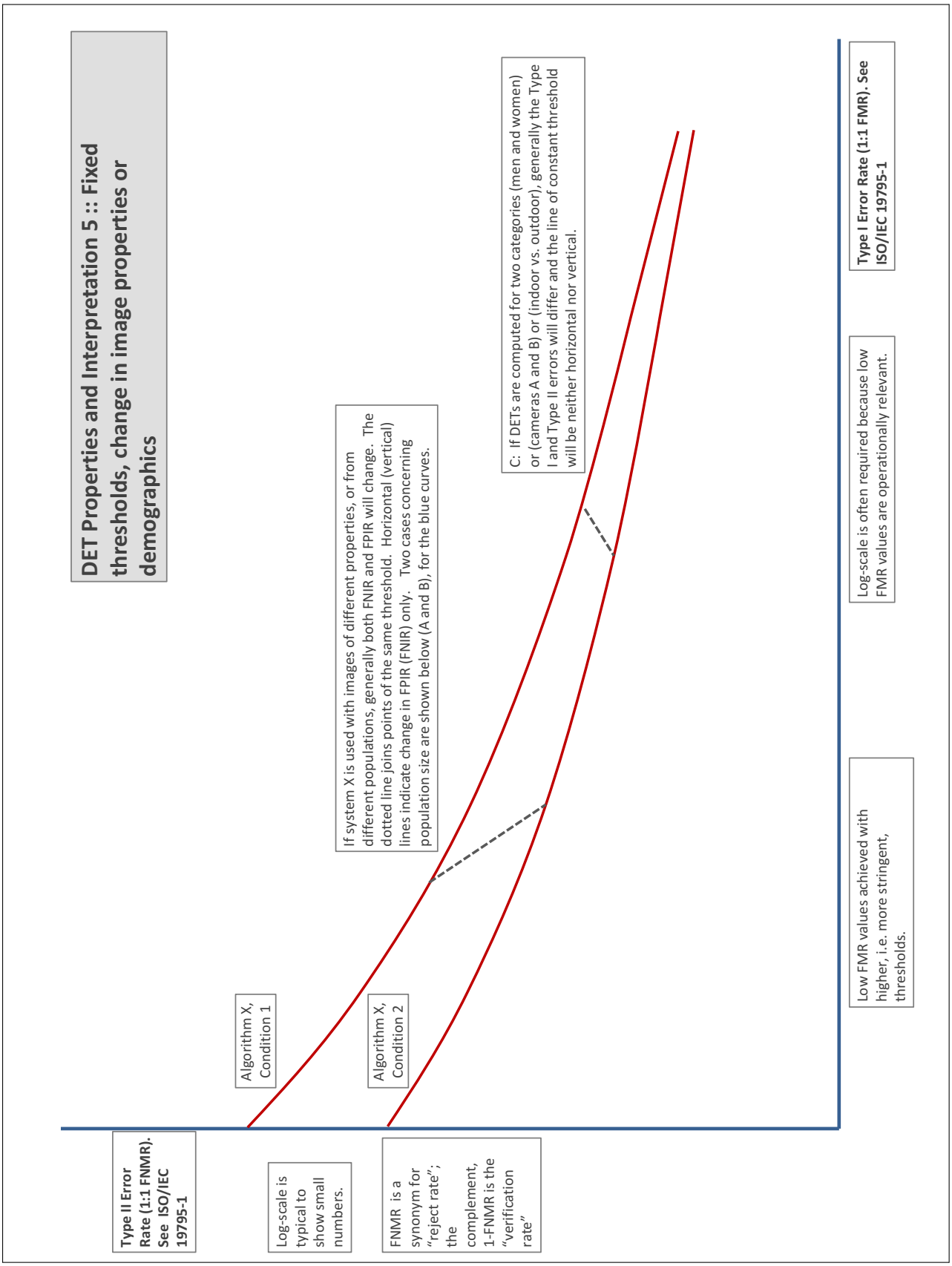

FNMR(T) "False non-match rate"
FMR(T) "False match rate"

References

[1] P. Jonathon Phillips, Amy N. Yates, Ying Hu, Carina A. Hahn, Eilidh Noyes, Kelsey Jackson, Jacqueline G. Cavazos, Géraldine Jeckeln, Rajeev Ranjan, Swami Sankaranarayanan, Jun-Cheng Chen, Carlos D. Castillo, Rama Chellappa, David White, and Alice J. O'Toole. Face recognition accuracy of forensic examiners, superrecognizers, and face recognition algorithms. *Proceedings of the National Academy of Sciences*, 115(24):6171–6176, 2018.

FNMR(T) "False non-match rate"
FMR(T) "False match rate"